First-Trimester Ultrasound

A Comprehensive Guide

Jacques S. Abramowicz
Ryan E. Longman
Editors

Second Edition

MOREMEDIA

Springer

First-Trimester Ultrasound

Jacques S. Abramowicz
Ryan E. Longman
Editors

First-Trimester Ultrasound

A Comprehensive Guide

Second Edition

Springer

Editors
Jacques S. Abramowicz
University of Chicago
Chicago, IL, USA

Ryan E. Longman
University of Chicago
Chicago, IL, USA

ISBN 978-3-031-24132-1 ISBN 978-3-031-24133-8 (eBook)
https://doi.org/10.1007/978-3-031-24133-8

© The Editor(s) (if applicable) and The Author(s), under exclusive license to Springer Nature Switzerland AG 2016, 2023
This work is subject to copyright. All rights are solely and exclusively licensed by the Publisher, whether the whole or part of the material is concerned, specifically the rights of translation, reprinting, reuse of illustrations, recitation, broadcasting, reproduction on microfilms or in any other physical way, and transmission or information storage and retrieval, electronic adaptation, computer software, or by similar or dissimilar methodology now known or hereafter developed.
The use of general descriptive names, registered names, trademarks, service marks, etc. in this publication does not imply, even in the absence of a specific statement, that such names are exempt from the relevant protective laws and regulations and therefore free for general use.
The publisher, the authors, and the editors are safe to assume that the advice and information in this book are believed to be true and accurate at the date of publication. Neither the publisher nor the authors or the editors give a warranty, expressed or implied, with respect to the material contained herein or for any errors or omissions that may have been made. The publisher remains neutral with regard to jurisdictional claims in published maps and institutional affiliations.

This Springer imprint is published by the registered company Springer Nature Switzerland AG
The registered company address is: Gewerbestrasse 11, 6330 Cham, Switzerland

Jacques S. Abramowicz: This book is dedicated to my parents, Sarah and Theo; my children, Shelly and Ory (and their spouses, Garrett and Esther); my grandchildren, Sarah, Noah, Aaron, Ariel, and Maya; and mostly to my wife, Annie, my best friend, the love of my life.

Ryan E. Longman: This book is dedicated to my wonderful children, Noa and Ethan, seeing them excel and achieve in life makes everything worth it, and to my amazing wife Gabriela, without her support I would be lost.

Foreword

The second edition of *First-Trimester Ultrasound: A Comprehensive Guide* adds significantly to the already outstanding first edition. Dr. Abramowicz and Dr. Longman have brought together additional leading experts to contribute to the book. The book is well divided into ideal chapters highlighting the various areas of importance in the first trimester. To begin with, Dr. Abramowicz, a world expert about the bioeffects of ultrasound, has provided an outstanding review of how to ensure the safety of ultrasound in early pregnancy by respecting the ALARA principle. Dr. Longman has added his expertise in genetics to ensure that the subject matter is properly covered in the appropriate places in the book.

The authors have presented superb images highlighting both normal and abnormal development in the early parts of pregnancy. The early recognition of cesarean scar pregnancy has been artistically presented by world authorities in this area. It is well-known that performing an ultrasound examination in the first trimester is the ideal time for dating a pregnancy once an embryo has been visualized. The importance of biometry is also well described. While the use of nuchal translucency has played an important role in pregnancy screening for aneuploidy, this textbook emphasizes the importance of a detailed, anatomic evaluation of the fetus in the first trimester. Recognizing structural abnormalities as shown in numerous illustrations throughout the book helps the clinician to provide better diagnosis and management for their patients and their families in these difficult situations. With the improved resolution of ultrasound equipment available today, we are making these diagnoses earlier in pregnancy.

Throughout the textbook, the contributing authors have followed the same theme throughout the chapters by providing outstanding images with very well-described findings. They have made reading the text easier while allowing for better retention of the information. What is particularly important is how the contributing authors have provided information on some of the more troubling diagnostic and treatment dilemmas in the first trimester. Their review of trophoblastic disease is one such example. The textbook is organized by organ systems which makes reading and referencing logical for the clinician. Further, they have provided excellent chapters on pelvic findings that is an essential component of the first trimester examination. Finally, the authors have provided an update on invasive procedures performed in the first trimester to use for advanced genetic studies.

In summary, this is an outstanding contribution in what might be presumed as a crowded field. This second edition of the textbook, *First-Trimester Ultrasound: A Comprehensive Guide,* will certainly make its mark among medical textbooks. The thoroughness and organized approach of the editors and authors, coupled with the addition of new contributing authors, will elevate this book among the standings. Both the editors and authors have done an outstanding job in preparing the second edition of the textbook.

David Geffen School of Medicine at UCLA
Center for Fetal Medicine
and Women's Ultrasound
Los Angeles, CA, USA

Lawrence D. Platt

Preface

The preface to the first edition of this book begins with the sentence "There is, to our knowledge, no book dedicated exclusively to the first trimester of pregnancy. The present book, authored by, arguably, the best in their field, comes to fill this void." While there may now be a few publications dealing with early pregnancy, this second edition greatly expands the previous one. The early stages of pregnancy may be the most important phases of our lives. Both normal and abnormal development are described, including failed pregnancy. A major difference in this second edition: we decided to incorporate separate chapters on the main fetal organs: brain, face and neck, heart, abdomen/gastro-intestinal system, urinary system, and limbs. As in the first edition, the pre-pregnancy period is also considered, as well as embryology notions, maternal diseases that can justify early scanning, elements of teratology, examination guidelines, multiple gestations, genetics concepts (major updates), new rules in the diagnosis of viable and ectopic gestations, gestational trophoblastic disease, invasive procedures, and gynecological incidental findings, as well as chapters on the use of Doppler and three-dimensional ultrasound. The authors, most of whom are among the world leaders in the field of obstetric and gynecologic ultrasound, were again given "literary freedom" to compose their chapters. It is safe to assume that most will not read this book cover to cover in a single session, thus each chapter is independent and will provide information about an entire and, sometimes, expanded topic while some elements may appear in multiple chapters. The book should be helpful to anyone practicing or interested in ultrasound, physicians, sonographers, nurses from several specialties and sub-specialties such as obstetrics and gynecology, maternal-fetal medicine, radiology, emergency medicine (Point-of-Care), and family medicine. We hope that this will be a reference for beginners and advanced users of this technology, students, residents, and fellows in the various health fields.

We are deeply grateful to all the authors for accepting to be part of this endeavor and to Dr. Lawrence (Larry) D. Platt for agreeing to write the foreword to the book. Thank you to all the sonographers with whom we have worked over the years and to our patients and their babies who have taught us so much.

Chicago, IL, USA Jacques S. Abramowicz
Chicago, IL, USA Ryan E. Longman

Contents

1 **Ultrasound in the First Trimester: How to Keep It Safe** 1
Jacques S. Abramowicz

2 **How to Optimize the Ultrasound Image** 21
Kathryn Mussatt and Jacques S. Abramowicz

3 **Ultrasound and Infertility** 31
A. Musa Zamah, Robyn Power, Ryan E. Longman,
and Jacques S. Abramowicz

4 **Maternal Co-morbidities and First Trimester Ultrasound Examination** 51
Elena Bronshtein and Karoline S. Puder

5 **First Trimester Embryology: An Overview** 65
Cresta W. Jones, Sabrina C. Burn, Jill Lewter, and Randall S. Kuhlmann

6 **Elements of Teratology** 77
Eran Barzilay and Gideon Koren

7 **First-Trimester Ultrasound: Practice Guidelines** 93
Roni Yoeli-Bik, Jude P. Crino, and Jacques S. Abramowicz

8 **Normal First Trimester of Pregnancy** 107
Kalesha Hack and Phyllis Glanc

9 **Screening for Fetal Chromosome Abnormalities** 139
Bryanna Cox McCathern, Ryan E. Longman,
and Jacques S. Abramowicz

10 **Threshold, Discriminatory Zone, and "The New Rules"** 151
James M. Shwayder

11 **Fetal Biometry in Early Pregnancy** 157
Lea M. Porche, Steven L. Warsof, and Alfred Z. Abuhamad

12 **The Fetal Heart in Early Pregnancy** 169
Edgar Hernandez-Andrade and Erin S. Huntley

13 **Doppler Sonography in Early Pregnancy** 197
David Mundy, Devika Maulik, and Dev Maulik

14 Three-Dimensional Ultrasound: A Role in Early Pregnancy? 219
Renato Ximenes, Rafael Peters, and Luís F. Goncalves

15 Multiple Gestations: Multiple Headaches 261
Jacques S. Abramowicz

16 First-Trimester Ultrasound: Early Pregnancy Failure 293
Timothy P. Canavan and Joan M. Mastrobattista

17 Ectopic Pregnancy and Pregnancy of Unknown Location (PUL) 319
James M. Shwayder

18 Cesarean Scar Pregnancy: A Baby Placenta Accreta 339
Ilan E. Timor-Tritsch, Ana Monteagudo, and Terry-Ann Bennett

19 The First-Trimester Fetal Head and Brain 371
Ana Monteagudo and Ilan E. Timor-Tritsch

20 Fetal Face and Neck 389
Henry O. Adekola, Sergiu Puiu, and Jacques S. Abramowicz

21 Fetal Gastrointestinal and Abdominal Wall Imaging 413
Desiree G. Fiorentino and Ryan E. Longman

22 First-Trimester Genitourinary Development and Anomalies 425
Yair J. Blumenfeld

23 Fetal Skeletal Anomalies 433
Carol B. Benson

24 First-Trimester Ultrasound in Gestational Trophoblastic Disease 445
Kevin M. Elias, Neil S. Horowitz, and Ross S. Berkowitz

25 Invasive Procedures in the First Trimester 457
Mark I. Evans, Jenifer Curtis, and Shara M. Evans

26 Sonography of Pelvic Masses Associated with Early Pregnancy 475
Catherine H. Phillips, Lavenia Carpenter, Glynis Sacks, and Arthur C. Fleischer

Index 491

Contributors

Jacques S. Abramowicz Department of Obstetrics and Gynecology, University of Chicago Medical Center, Chicago, IL, USA

Alfred Z. Abuhamad Division of Maternal-Fetal Medicine, Department of Obstetrics and Gynecology, Eastern Virginia Medical School, Norfolk, VA, USA

Henry O. Adekola Department of Maternal-Fetal Medicine, Southern Illinois University, Springfield, IL, USA

Eran Barzilay Department of Obstetrics and Gynecology, Samson Assuta Ashdod University Hospital, Ashdod, Israel

Faculty of Health Sciences, Ben-Gurion University of the Negev, Beer-Sheva, Israel

Terry-Ann Bennett Division of Obstetrical and Gynecological Ultrasound and Maternal Fetal Medicine, Department of Obstetrics and Gynecology, New York University School of Medicine, New York, NY, USA

Carol B. Benson Department of Radiology, Brigham and Women's Hospital, Boston, MA, USA

Ross S. Berkowitz New England Trophoblastic Disease Center, Donald P. Goldstein M.D. Trophoblastic Tumor Registry, Brigham and Women's Hospital and Dana-Farber Cancer Institute, Dana Farber/Brigham and Women's Cancer Center, Division of Gynecologic Oncology and the Department of Obstetrics, Gynecology and Reproductive Biology, Harvard Medical School, Boston, MA, USA

Yair J. Blumenfeld Department of Obstetrics & Gynecology, Stanford University School of Medicine, Stanford, CA, USA

Elena Bronshtein Department of Obstetrics and Gynecology, Kaiser Permanente, Fontana, CA, USA

Sabrina C. Burn Division of Maternal-Fetal Medicine, Department of Obstetrics, Gynecology and Women's Health, University of Minnesota Medical School, Minneapolis, MN, USA

Timothy P. Canavan Division of Maternal Fetal Medicine, Department of Obstetrics and Gynecology, University of Pittsburgh School of Medicine, UPMC Pinnacle, Harrisburg, PA, USA

Lavenia Carpenter Vanderbilt University Medical Center, Nashville, TN, USA

Jude P. Crino Department of Obstetrics, Gynecology and Reproductive Sciences, University of Maryland School of Medicine, Baltimore, MD, USA

Jenifer Curtis Fetal Medicine Foundation of America and Comprehensive Genetics, PC, New York, NY, USA

Kevin M. Elias New England Trophoblastic Disease Center, Donald P. Goldstein M.D. Trophoblastic Tumor Registry, Brigham and Women's Hospital and Dana-Farber Cancer Institute, Dana Farber/Brigham and Women's Cancer Center, Division of Gynecologic Oncology and the Department of Obstetrics, Gynecology and Reproductive Biology, Harvard Medical School, Boston, MA, USA

Mark I. Evans Fetal Medicine Foundation of America and Comprehensive Genetics, PC, New York, NY, USA

Department of Obstetrics & Gynecology, Icahn School of Medicine at Mt. Sinai, New York, NY, USA

Shara M. Evans Fetal Medicine Foundation of America and Comprehensive Genetics, PC, New York, NY, USA

Desiree G. Fiorentino Division of Maternal-Fetal Medicine, Department of Obstetrics & Gynecology and Women's Health, Montefiore Medical Center/ Albert Einstein College of Medicine, Bronx, NY, USA

Arthur C. Fleischer Vanderbilt University Medical Center, Nashville, TN, USA

Phyllis Glanc Department of Medical Imaging, Body Division, Sunnybrook Health Sciences Centre, Toronto, ON, Canada

Radiology, Obstetrics and Gynecology, University of Toronto, Toronto, ON, Canada

Sunnybrook Research Institute, Toronto, ON, Canada

Luís F. Goncalves Department of Radiology, Fetal Imaging, Phoenix Children's Hospital, Phoenix, AZ, USA

Radiology and Child Health, University of Arizona School of Medicine, Phoenix, AZ, USA

Radiology, Mayo Clinic, Phoenix, AZ, USA

Radiology, Creighton University, Phoenix, AZ, USA

Kalesha Hack Department of Radiology, University of Toronto, Toronto, ON, Canada

Department of Medical Imaging, Body Division, Sunnybrook Health Sciences Centre, Toronto, ON, Canada

Edgar Hernandez-Andrade Department of Obstetrics and Gynecology and Reproductive Sciences, McGovern Medical School, University of Texas, Health Science Center at Houston (UTHealth), Houston, TX, USA

Neil S. Horowitz New England Trophoblastic Disease Center, Donald P. Goldstein M.D. Trophoblastic Tumor Registry, Brigham and Women's Hospital and Dana-Farber Cancer Institute, Dana Farber/Brigham and Women's Cancer Center, Division of Gynecologic Oncology and the Department of Obstetrics, Gynecology and Reproductive Biology, Harvard Medical School, Boston, MA, USA

Erin S. Huntley Department of Obstetrics and Gynecology and Reproductive Sciences, McGovern Medical School, University of Texas, Health Science Center at Houston (UTHealth), Houston, TX, USA

Cresta W. Jones Division of Maternal-Fetal Medicine, Department of Obstetrics, Gynecology and Women's Health, University of Minnesota Medical School, Minneapolis, MN, USA

Gideon Koren Motherisk Israel, Adelson Faculty of Medicine, Ariel University, Ariel, Israel

Randall S. Kuhlmann Maternal-Fetal Medicine, ProHealth Care, Waukesha, WI, USA

Jill Lewter Division of Maternal-Fetal Medicine, Department of Obstetrics, Gynecology and Women's Health, University of Minnesota Medical School, Minneapolis, MN, USA

Ryan E. Longman Department of Obstetrics and Gynecology, University of Chicago Medical Center, Chicago, IL, USA

Department of Obstetrics and Gynecology, University of Chicago Pritzker School of Medicine, Chicago, IL, USA

Joan M. Mastrobattista Division of Maternal Fetal Medicine, Department of Obstetrics and Gynecology, Baylor College of Medicine, Houston, TX, USA

Dev Maulik Department of Obstetrics and Gynecology, UMKC School of Medicine, Kansas City, MO, USA

Devika Maulik Department of Obstetrics and Gynecology, UMKC School of Medicine, Kansas City, MO, USA

Department of Obstetrics and Gynecology, University Health-Truman Medical Center, Kansas City, MO, USA

Bryanna Cox McCathern Department of Obstetrics and Gynecology, University of Chicago Medical Center, Chicago, IL, USA

Ana Monteagudo Division of Obstetrical and Gynecological Ultrasound and Maternal Fetal Medicine, Department of Obstetrics and Gynecology, New York University School of Medicine, New York, NY, USA

Carnegie Imaging for Women, Icahn School of Medicine at Mount Sinai, New York, NY, USA

David Mundy Department of Obstetrics and Gynecology, UMKC School of Medicine, Kansas City, MO, USA

Department of Obstetrics and Gynecology, University Health-Truman Medical Center, Kansas City, MO, USA

Kathryn Mussatt Department of Obstetrics and Gynecology, University of Chicago, Chicago, IL, USA

Rafael Peters Centro Médico Bom Pastor, Igrejinha, Rio Grande do Sul, Brazil

Catherine H. Phillips Vanderbilt University Medical Center, Nashville, TN, USA

Lea M. Porche Division of Maternal-Fetal Medicine, Department of Obstetrics and Gynecology, Eastern Virginia Medical School, Norfolk, VA, USA

Robyn Power The University of Chicago, Chicago, IL, USA

Karoline S. Puder Beaumont Hospital, Royal Oak, MI, USA

Sergiu Puiu Department of Radiology and Imaging, "Nicolae Testemitanu" State University of Medicine and Pharmacy/Repromed Plus Hospital, Chisinau, Republic of Moldova

Glynis Sacks Vanderbilt University Medical Center, Nashville, TN, USA

James M. Shwayder Department of Obstetrics and Gynecology, University of Florida, Gainesville, FL, USA

Ilan E. Timor-Tritsch Division of Obstetrical and Gynecological Ultrasound and Maternal Fetal Medicine, Department of Obstetrics and Gynecology, New York University School of Medicine, New York, NY, USA

Department of OB/GYN, NYU School of Medicine, New York, NY, USA

Steven L. Warsof Division of Maternal-Fetal Medicine, Department of Obstetrics and Gynecology, Eastern Virginia Medical School, Norfolk, VA, USA

Renato Ximenes Fetal Medicine Foundation Latin America—FMFLA, São Paulo, Brazil

Roni Yoeli-Bik Department of Obstetrics and Gynecology, University of Chicago, Chicago, IL, USA

Musa Zamah The University of Chicago, Chicago, IL, USA

1

Ultrasound in the First Trimester: How to Keep It Safe

Jacques S. Abramowicz

"Ultrasound is safe… Ultrasound is not X-rays… Our machines are FDA-approved." These are statements most heard when engaging in a conversation on safety of ultrasound. This is one of the reasons cited for it becoming an essential tool in medicine. Other important bona fide aspects are the relative low cost and immediate results availability. Diagnostic ultrasound (DUS) was first described in obstetrics and gynecology by Ian Donald, in 1958 [1], and the benefits of this technology are multiple [2, 3]. In areas where prenatal care is implemented and followed, most pregnant women have 2–3 ultrasound examinations (and many more in certain countries) during their pregnancies. In early pregnancy and before (i.e., in the field of Artificial Reproductive Technologies (ART)), these include multiple serial scans of the developing follicles during ovulation induction [4] and in the earliest stages of gestation [5], for viability, for instance. Furthermore, first-trimester ultrasound for aneuploidy screening (nuchal translucency, NT) has been almost universally integrated in prenatal care as well as early anatomy survey [6, 7]. Such is the widespread enthusiasm and the generally accepted notion of safety that its use has spilled into the commercial world with mall stores offering non-medical ultrasound or "souvenir" scans, although this practice is strongly disapproved by most scientific societies. The record of safety of DUS is excellent: there are no epidemiological studies demonstrating harmful effects in human fetuses [8]. Most human epidemiological studies, however, published so far are based on information obtained with pre-1991/2 machines. Around that time, under pressure from end users and manufacturers, maintaining that higher outputs would allow for better images (an argument not necessarily proven), the US Federal Drug Administration (FDA) allowed the acoustic output of ultrasound machines for fetal use to be increased from 94 to 720 mW/cm^2, a factor of almost 8 [9, 10]. We have to ponder several important questions: Is there enough evidence to validate the use of ultrasound imaging in general and Doppler in particular in the first trimester [11] and could ultrasound have detrimental effects on the fetus in the first trimester, a time of maximal susceptibility to external factors? If there are clinical indications to perform these scans (and if there were none, there would be no raison-d'être for the two editions of this book), safety must be guaranteed by educating the end users on ways to limit the possible hazards of exposure of the follicles/ova and the fetus at early stages of gestation [2, 12].

J. S. Abramowicz (✉)
Department of Obstetrics and Gynecology, University of Chicago, Chicago, IL, USA
e-mail: jabramow@bsd.uchicago.edu

© The Author(s), under exclusive license to Springer Nature Switzerland AG 2023

J. S. Abramowicz, R. E. Longman (eds.), *First-Trimester Ultrasound*,
https://doi.org/10.1007/978-3-031-24133-8_1

Bioeffects of Ultrasound

Ultrasound is a waveform with a succession of positive and negative pressures [13]. Whenever an ultrasound beam traverses biological tissues, two major mechanisms are operative: thermal and non-thermal (also known as mechanical). This will occur *every time* ultrasound is used. As the waveform travels through tissue, it loses amplitude by absorption and scatter. With absorption, energy is converted into heat, hence a thermal effect [14], an indirect effect of the waveform. A direct effect of the passage of the waveform, secondary to the succession of positive and negative pressures is non-thermal or mechanical [15].

Thermal Effects

Human body normal core temperature is generally accepted to be 37 °C with a diurnal variation of ±0.5–1 °C [15]. Temperature in the human fetus is slightly higher than maternal body temperature by 0.3–0.5 °C during the early gestation (two first trimesters). During the third trimester, fetal temperature is higher by 0.5 °C than that of its mother. Ultrasound may cause a rise in temperature in insonated tissues [16]. This rise will be small and, most likely, clinically insignificant, *if certain precautions are respected* (as detailed below). Why is this important? Because specific structural abnormalities have been shown to be produced by increased temperature in many pregnant animal studies, as well as several controlled human studies [17], *but not by ultrasound*. Elevated maternal temperature in early gestation, secondary to viral infection, for instance, has been associated with a higher-than-expected incidence of congenital anomalies [18]. Edwards and others have demonstrated that hyperthermia is teratogenic for many animal species (such as guinea pigs, rats, monkeys, and more), including the human [17, 19]. Major anomalies observed included microcephaly, encephalocele, microphthalmia, skeletal anomalies as well as growth delay. It was suggested that a 1.5 °C temperature elevation above the normal body temperature should be considered a universal threshold [20]. The acceptance of a threshold forms the basis for the ALARA (As Low As Reasonably Achievable) principle: keep the exposure as low as possible, for the least amount of time possible, but yet enough to get adequate diagnostic images [21]. Some scientists, however, assert that *any* temperature increment for *any* period of time has *some* effect, the higher the temperature differential or the longer the temperature increment the greater the likelihood of producing an effect, i.e., there is no thermal threshold for hyperthermia-induced birth defects [22, 23]. Whether a threshold exists or not, two facts are undeniable: ultrasound has the potential to elevate the temperature of the tissues being scanned [24–27] and elevated maternal temperature, whether from illness or exposure to heat, can produce teratologic effects [17, 28–30]. Consequently, the obvious question that emerges is: can diagnostic ultrasound produce harmful/teratological temperature rise in the fetus [14, 25, 31]? Some believe that such a temperature rise is, in effect, the major operational mechanism for ultrasound bioeffects [15, 32]. For prolonged exposures, temperature elevations of up to 5 °C have been obtained [31]. The actual in situ temperature change in insonated tissues depends on the balance between heat production and heat loss. Local perfusion is a specific tissue condition that strongly influences the amount of heat loss and which very clearly diminishes the risk if present. In early pregnancy, under 6–8 weeks, there appears to be minimal maternal-fetal circulation and minimal fetal perfusion, which may potentially reduce heat dispersion [33]. Only at about weeks 10–11 does the embryonic circulation actually link up with the maternal circulation [34]. The early absence of perfusion may thus lead to some underestimation of the actual ultrasound-induced temperature in early gestation. Interestingly, this lack of perfusion, which also exists in the eye, is one reason why the spatial peak temporal average intensity (I_{SPTA}) for ophthalmic applications has been kept very low, in fact, much lower than peripheral, vascular, cardiovascular, and even obstetric scanning, despite the general increase in acoustic power that was allowed after 1992 (see Table 1.1). Specific recommendations regarding ophthalmic

Table 1.1 Changes over the years in I_{SPTA} (in mW/cm^2) in various medical applications (adapted from various sources [10, 15, 61, 175, 185])

Ultrasound clinical application	1976	1986	1991
Ophthalmic	17	17	50
Fetal, neonatal, pediatric imaging	46	94	720
Cardiac (adult)	430	430	720
Peripheral vascular	720	720	720

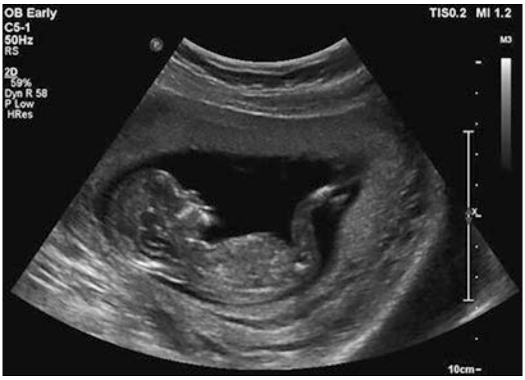

Fig. 1.1 In early pregnancy, the entire fetus is within the ultrasound beam. Gestational age of 12 weeks

scanning have been published [35]. One should note that there are some similarities in physical characteristics between the early, first-trimester embryo, and the eye: neither is perfused; they can be of similar size; and protein is present (in an increasing proportion in the fetus). At about gestational weeks 4–5, the gestational sac is about the size of the eye (2.5 cm in diameter), and by week 8, it is around 8 cm in diameter [36]. Ultrasound imaging in these early stages of gestation involves "whole body" scanning since the fetal size is less than the cross section of the beam (Fig. 1.1). An additional factor, virtually ignored clinically, is modifications of tissue temperature due to ambient maternal and fetal temperatures. Elevated maternal temperature is immediately translated into a similar increase in the fetus which may compound the ultrasound-induced heat burden [37]. On the other hand, motions (even very small) of the examiner's hand as well as the patient's breathing and body movements (in the case of obstetric ultrasound, both the mother's and the fetus') tend to spread the region being heated. However, for spectral (pulsed) Doppler studies, conditions may be different since the Doppler gate has to be kept on a specific area (blood vessel) for some amount of time (see below). As mentioned above, there is a mathematical/physical relation between temperature elevation and several beam characteristics. The elevation is proportional to the product of the wave amplitude, length of the pulse, and pulse-repetition frequency (PRF). Hence, manipulating any of these via instrument controls will alter the in situ conditions. A significant problem is that the end user will not be aware that by operating certain controls, he/she actually alters the acoustic output. Temperature increases of 1 °C are easily reached in routine scanning [38]. A general threshold of temperature elevation of 1.5–2 °C has been suggested before any evidence of developmental effect occurs [15]. An increase of 2.5 °C and above is possible with 1 h of exposure to ultrasound [15]. When using an abdominal probe, the skin surface is close to room temperature and heat is removed by air-convection but in the case of endovaginal scanning, tissues are at an average temperature of 37 °C—or possibly higher in febrile patients—and there is very little heat removal [39]. In addition, the surface of all ultrasound transducers, including endovaginal probes, self-heats [40], and particular attention is necessary during ART procedures and the first 10–12 weeks of gestation, when endovaginal scanning is often the favored method. As was concluded by the World Federation for Ultrasound in Medicine and Biology (WFUMB), exposure that produces a maximum temperature elevation of no more than 1.5 °C above normal physiological levels may be used without reservation on thermal ground [41].

Non-thermal Effects

Ultrasound bioeffects may also occur through non-thermal or mechanical processes [42, 43]. These include acoustic cavitation, *if gas bubbles are present*, as well as radiation torque and force and acoustic streaming secondary to propagation of the ultrasound waves. Included in this category are physical (shock wave) or chemical (release of free radicals) effects. Bubble cavitation seems to be the major factor in mechanical effects [44, 45], as it has been demonstrated to occur in living tissues when insonated [46, 47]. Non-thermal mechanisms have been implicated in biological effects of ultrasound in animals, such as local intestinal [48], renal [49], and pulmonary hemorrhages [50], although cavitation could not always be incriminated. Furthermore, since there does not seem to be gas bubbles in the ovarian vasculature or parenchyma, nor the fetal lungs or bowels (both organs where effects have been described in neonates or adult animals), the risk to the ovum and fetus from mechanical effect appears to be minimal [51]. However, the use of contrast agents (including agitated saline) to image the fallopian tubes or the endometrial cavity, for instance, introduces these potential cavitation foci [52]. Another described result of mechanical energy is hemolysis [53]. Again, it is evident, however, that the presence of some cavitation nuclei is necessary for hemolysis to occur. In the presence of such contrast agents, fetal red blood cells are more susceptible to lysis from ultrasound exposure in vitro [54]. In addition to the above, fetal stimulation caused by ultrasound (Doppler) insonation has been described, with no apparent relation to cavitation [55]. This effect may be secondary to radiation forces associated with ultrasound exposures. These forces were suspected at the earliest stages of ultrasound research [56] and are known to possibly stimulate auditory [57] and other sensory tissues [58]. The main effects of non-thermal damage have been demonstrated in mammalian tissues containing gas where capillary bleeding has been observed [43, 46, 59]. This potentially pertains to the neonatal lung, intestine, and as noted above, also in the presence of ultrasound microbubble contrast agents. Several non-thermal mechanisms, not related to cavitation have also been described: radiation force, acoustic streaming, modification of electrical potentials, effect on cardiac performance, and stimulation of bone repair [15]. None of these has been demonstrated in humans and no harmful effects of diagnostic ultrasound, secondary to non-thermal mechanisms have been reported in human fetuses.

The Output Display Standard (OSD)

Until 1992, acoustic outputs of clinical ultrasound machines had specific limits. For instance, the upper limit of the spatial peak temporal average intensity or I_{SPTA} (the most clinically useful intensity used to determine acoustic power of the ultrasound beam) for adult use was 720 mW/cm^2 and for fetal use, 94 mW/cm^2, which in fact, already had been increased from a previous maximum value of 46 mW/cm^2. It was assumed that higher outputs would generate better images and, thus, improve diagnostic accuracy. Hence, end users required ultrasound manufacturers to increase their machines output. Some worry, however, was expressed regarding the actual amount of energy absorbed by a human fetus during an ultrasound examination. This amount cannot be measured precisely. Not only the lack of an internal recording device is a major issue but, in addition, elements such as variations in maternal body habitus, fetal position changes, and gestational age progression render such a task impossible. To allow clinical users of ultrasound to use their instruments at higher powers than originally intended and to reflect the two major potential biological consequences of ultrasound (thermal and mechanical), the American Institute of Ultrasound in Medicine (AIUM), the National Electrical Manufacturers' Association (NEMA), and the US food and Drug Administration (FDA), with representatives from the Canadian Health Protection Branch, the National Council on Radiation Protection and Measurements (NCRP), and 14 other medical organizations, as well as representatives from the public, developed a standard related to the potential for ultrasound bioeffects [15]. The Standard for Real-Time Display of Thermal and Mechanical Indices on Diagnostic Ultrasound Equipment, generally known as the Output Display Standard or ODS, was an attempt to provide quantitative safety-related information. This information was to appear on-screen during an exam, so that the end users would be able to see how manipulation of the instrument controls during an examination causes alterations in the output and, thus, on the exposure, providing, from a clinical standpoint, a rough estimate to compare various modes of examination. Consequently, the acoustic output for fetal use, as expressed by the I_{SPTA} went from the previous value of 94–720 mW/cm^2 (Table 1.1). It is interesting to observe from the table that, for fetal imaging, the I_{SPTA} was allowed to increase by a factor of almost 16 from 1976 to the most recent values in 1992; yet, virtually all epidemiological information available regarding fetal effects predates 1992. A further remarkable fact is that intensity for ophthalmic examination was increased from the original 17–50 mW/cm^2, a value approximately 12 times lower than the present allowed maximal value for fetal scanning. Furthermore, the clinical categories included in the analysis consisted of ophthalmic, fetal (without specification of gestational age), cardiac, and peripheral vascular examinations. Pelvic imaging (abdominal or transvaginal), including, naturally, examination of ovaries in ovulation induction, is not mentioned. The indices to appear on-screen (Fig. 1.2) were the thermal index (TI), to provide some indication of potential temperature increase and the mechanical index (MI), to provide indication of potential for non-thermal (i.e., mechanical) effects [60, 61]. The TI calculation is based on the formula:

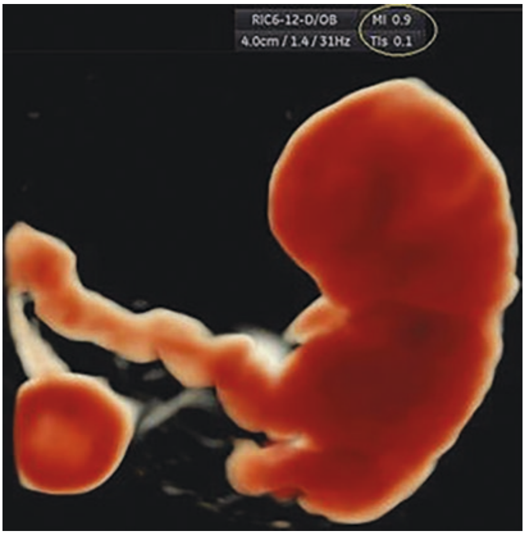

Fig. 1.2 The TI and MI acoustic indices as demonstrated on the monitor screen during routine ultrasound examination. In this picture, the MI is 0.9 and the $\mathrm{TI_S}$, 0.1

$$\mathrm{TI} = W / W_{\mathrm{deg}}$$

where W is the acoustic power while scanning and W_{deg} is the acoustic power required to achieve an increase in temperature of 1 °C under similar conditions [62]. The TI has three variants [39]: TI for soft tissue ($\mathrm{TI_S}$), to be used mostly in early pregnancy when ossification is low (as well as in ART for ovulation studies), for bones ($\mathrm{TI_B}$), to be used when the ultrasound beam impinges on bone, at or near the beam focus, such as late second and third trimesters of pregnancy and for transcranial studies ($\mathrm{TI_C}$) when the transducer is essentially against bone, mostly for examinations in adult patients. These indices were required to be displayed if equal to or over 0.4. It needs to be made very clear that *TI does not represent an actual or an assumed temperature increase*. It bears some correlation with temperature rise in degrees Celsius, but in no way allowing an estimate or a guess as to what that temperature change *actually* is in the tissue. The TI represents reasonable "worst-case" estimate of the temperature rise resulting from the exposure. It can, thus, be used to assess the potential for harm via a thermal mechanism, the higher the TI, the higher this potential. Calculations are also on the ultimate temperature reached after prolonged exposure. This time will be short (less than 5 min) with a narrow beam and good tissue perfusion, as is the case in late first trimester scanning. When bone is present, this time is very short, approximately 30 s. An important point to remember is that experimental data has clearly demonstrated that this worst-case elevation of temperature may be a gross underestimation, by as much as a factor of 2 or even 6, and, more rarely, an overestimation [15]. Furthermore, *exposure time is not part of the equation*, nor is it in the second index, the MI, which represents the potential for cavitation in tissues, but is not based on actual in situ measurements. The MI is defined as:

$$\mathrm{MI} = p / \sqrt{f}$$

It is a theoretical formulation of the ratio of the peak rarefaction pressure to the square root of the ultrasound frequency (hence, the higher the frequency, the lesser risk of mechanical effect, which is an advantage in endovaginal scanning). Both the TI and MI can and should be followed as an indication of change in output during the clinical examination. A major component of the implementation of the ODs was supposed to be education of the end user. Unfortunately, this aspect of the ODS does not seem to have succeeded as end users' knowledge of bioeffects, safety, and output indices is lacking. Both in Europe [63] and the United States [64], approximately 70% of clinicians (physicians and sonographers, including nurses who perform ultrasound) show very poor, or no knowledge of bioeffects and safety issues do not know what TI and MI represent and don't even know that these appear on-screen during clinical ultrasound examinations. This is true in several other countries [65–67] as well as among residents/fellows [68] and sonographers, regardless of their seniority [69]. Unfortunately, this doesn't seem to improve much with time [70]. Furthermore, several assumptions were made when formulating the indices, which bring questions on their clinical value [71]. Details can be found in the NCRP report 140 [15]. These indices, however, are the best mean we have, nowadays, to estimate, in real time, changes occurring in acoustic output of the instrument, although various modifications have been offered, in particular with regard to exposure time [72, 73]. There is, in fact, little information on energy output and exposure in clinical obstetrical ultrasound. Only relatively recently has it been shown that, if one considers TI and MI to be some indication of acoustic output, then the levels are low in the first [74, 75], second and third trimester [76], and even Doppler studies [77]—although higher levels of TI can be reached in this modality—as well as 3D/4D examinations [78]. It should also be noted that in some countries, the number of prenatal ultrasound examinations has reached 10 per pregnancy and it is presently unknown whether there is a cumulative dose effect to exposure [79].

Ultrasound and the Ovum

Ultrasound has permeated the field of infertility and reproductive endocrinology (see Chap. 3), from diagnosing uterine anomalies [80], following development of the follicle [81], evaluating tubal patency [82], to its use in embryo transfer [83]. A study from 1982 demonstrated premature ovulation in women who underwent ultrasound examination of the ovaries (B-mode) in the late follicular phase [84]. The authors compared patients in induced ovulation cycles, followed by ultrasound (study group) or only by hormone levels (control group). They investigated timing of follicle rupture after the onset of LH surge or administration of hCG. Rupture never occurred before the 37th hour in control patients (no ultrasound in the follicular phase). However, (premature) ovulation was observed at 26–36 h in about 50% cases in the study group (ultrasound during the previous 3 days or in the 36 h immediately following the ovulatory stimulus). This study was very concerning but has never been reproduced. Ultrasound-guided oocyte aspiration for in vitro fertilization and embryo transfer was reported in the early 1980s [85, 86]. It has now become routine [87]. There are only a few, relatively dated, studies aimed at determining the interaction between ultrasound exposure and successful fertilization. Most are, in fact, concerned with success or lack thereof of the procedure in terms of pregnancy rates and not possible bioeffects. Some researchers have reported deleterious effects of ultrasound on the menstrual cycle, particularly decrease in ovulation rates in mice [88] and premature ovulation [84], as well as reduced cumulative pregnancy rates in mice [89] and in humans [90]. Others have demonstrated no effects on the ovulation process or egg quality, including DNA and RNA synthesis [91], nor on fertilization rate and embryonic development following in vitro fertilization and embryo transfer [92]. In general, the clinically available data on ultrasound exposure of oocytes during meiosis are confusing. Some researchers reported a deleterious effect on the fertility of patients undergoing artificial insemination with a reduction in the cumulative rate of pregnancy [90]. A study of ultrasound exposure of meiotically active, preovulatory oocytes showed no differences between rats exposed to ultrasound after the LH surge and controls in terms of pregnancy rate, number of corpora lutea, implantations, pups, and mean pup and placental weights at autopsy on day 22 of pregnancy [93]. Others have claimed an increase in the success rate, allowing ultrasound monitoring of follicular growth [94], although, evidently, this is not a direct effect of ultrasound but of improved intervention timing. An attempt to clarify this was described by Mahadevan and colleagues [92]. They wanted to determine how oocytes obtained under ultrasound guidance affected the pregnancy rate. The results obtained with 3.5 MHz probes suggest that exposure of human oocytes to ultrasonic waves during the different phases of meiosis does not significantly influence the developmental potential of the in vitro fertilized embryos. Unfortunately, no researcher describes any of the relevant exposure parameters discussed earlier, except for ultrasound frequency.

Ultrasound in Early Gestation

There are many valid medical indications to perform ultrasound in early gestation [2, 95]. These are described in various parts of this book and include, among others, pregnancy location, accurate gestation dating, confirmation of viability, verification of number of fetuses, and early anatomy survey. These examinations are, generally, performed with B-mode, a mode with relatively low acoustic output. However, more recently, screening for genetic abnormalities such as nuchal translucency and early assessment of structural abnormalities are described in the literature in early (11–15 weeks) pregnancy [6, 96, 97]. While most of these are also performed with B-mode, Doppler is often used to detect blood vessels and/or to visualize and analyze cardiac valves [98], exposing the fetus to much higher energy levels (see below). One needs to keep in mind that, even with B-mode, dwell time is important since prolonged examination can result in higher exposure levels [99]. Interesting but somewhat worrying, unexplained data have been published on an increased incidence of fetal anomalies in fetuses resulting from ART [100, 101]. Some concerning effects on the chorionic villi in women who had transvaginal ultrasound during the first trimester were reported [102]. There was a time-effect relation with activation of an enzyme pathway responsible for apoptosis through a mitochondrial pathway with exposures of 20 and 30 min but not 0 (control group) or 10 min.

Fetal Susceptibility to External Insults

The growing fetus is very sensitive to external influences (see Chap. 6). This is especially true in the first 10–12 weeks of gestation [103, 104]. Known teratological agents include, for instance, certain medications or drug of abuse taken by the pregnant woman, exposure to X-rays and elevated temperature, secondary to infectious diseases [105]. Gestational age is thus a vital factor when considering possible bioeffects: milder exposure during the preimplantation period or more severe exposures during embryonic and fetal development can have similar results and can result in embryonic/fetal death and abortion or a wide range of structural and functional defects. Most at risk is the central nervous system (CNS), due to a lack of compensatory growth of undamaged neuroblasts. In experimental animals, the most common defects are of the neural tube as well as microphthalmia, cataract, and microencephaly, with associated functional and behavioral problems [17]. Other prominent defects are seen in craniofacial development, such as facial clefts [106], the skeleton [107], the body wall, teeth, and heart [108]. Hyperthermia in utero (due to maternal influenza, for instance) was long known to potentially induce structural anomalies in the fetus [109–111] but it has been described also as an environmental risk factor for psychological/behavioral disturbances [112] and, more particularly, schizophrenia [110]. It is stressed that these are not ultrasound-induced hyperthermia harmful effects. Yet, ultrasound has been shown to induce temperature increase in vivo [14, 24, 27, 32, 113–115], albeit not in humans. Subtle effects are possible, such as abnormal neuronal migration with unclear potential results [116]. One specific single specific effect has been described in various publications: a mild increase in the prevalence of non-right handedness among male children exposed to prenatal ultrasound with no other neurological, intellectual, behavioral, or physical anomalies [117–119]. Ultrasound has been implicated, in chicks who were insonated in ovo, in learning and memory disturbances [120]. A study failed to demonstrate a relation between ultrasound insonation in utero and decreased intellectual performance [121]. In mice, the etiology of symptoms similar to those seen in autism was attributed to ultrasound [122]. Extrapolation to humans is not automatic, despite the argument, by some, that the increased incidence of this condition in children over the last 20 years or so is secondary to the similar increase in the use of ultrasound in obstetrics [123]. One study reported on approximately 750 children, half with autism spectrum disorders and half without [124]. The conclusion was that ultrasound in any of the three trimesters of pregnancy could not be correlated with an increased risk of ASD. In fact, there is a serious lack of data examining the role of ultrasound in the etiology of autism while rigorously excluding other confounding factors [125]. If one, however, considers together the facts that hyperthermia is potentially harmful to the fetus and that ultrasound may under certain circumstances elevate tissue temperature, then precaution must be recommended, particularly in early gestation and especially with modes known to emit higher acoustic energy levels (such as pulsed Doppler, see below).

Is Doppler Different and Can It Have Detrimental Effects on the Fetus in the First Trimester?

Ultrasound modalities can result in either scanned or un-scanned exposure. Scanned conditions are associated with gray-scale B-mode images (the most commonly used real-time application) and Doppler images of tissue cross sections. Un-scanned conditions are used for M-mode and pulsed Doppler studies of tissue movement (such as cardiac valves) or blood velocity waveforms. This is clinically very important because for un-scanned beams, the power is limited to the area of the beam cross section, often very narrow (1 mm^2) in the focal region. For scanned beams, the acoustic power is not limited to a narrow area, but may cover large areas in the lateral direction, hence less risk of high exposure at a specific point. Furthermore, a variety of movements intervene during B-mode imaging, such as fetal body motion, observer's hand movements, and maternal breathing. During a Doppler examination, however, it is necessary to have the transducer as steady as possible. This is because, in general, blood vessels or heart valves are small in comparison to the general organ or body size being scanned and even small movements will have more undesired effects on the resulting image. As described below, the most commonly used intensity (spatial peak temporal average intensity, I_{SPTA}) associated with Doppler ultrasound is the highest of all the general-use categories, 1180 mW/cm^2 for pulsed Doppler, as opposed to 34 mW/cm^2 for B-mode, a 35-fold difference. Dwell time (duration of exposure) is also of major importance: Ziskin [126] reported that among 15,973 Doppler ultrasound examinations, the average duration was 27 min (and the longest 4 h!). A study in chicken seemed to clearly implicate Doppler [120]. Chicken eggs were insonated on day 19 of a 21-day incubation period. Exposure was to B-mode for 5 or 10 min or to pulsed Doppler for 1–5 min. Eggs were allowed to hatch with learning, and memory tests were performed in the chicks on day 2. Impairment in ability to learn or in short, medium, and long-term memory was not observed after B-mode exposure but was clearly demonstrated for those exposed to Doppler, with a dose–effect relationship. Furthermore, the chicks were still unable to learn with a second training session 5 min after completion of the initial testing**.** Hearing the fetal heartbeat is certainly a very satisfying experience for the expecting parents. Often this is accomplished by using pulsed Doppler. This is so engrained in the minds of the public that each time ultrasound is mentioned in a television series or a movie, one can hear the heartbeat in the background although the image on screen is only of a B-mode exam. In fact, using Doppler to "listen" to the fetal heart is not new [127, 128]. This should be discouraged and replaced by M-mode assessment. If Doppler is used, it is sufficient to "hear" 3–4 heart beats and thus limit the exposure [129, 130]. One of the major uses of ultrasound is the prenatal detection of fetal abnormalities. The organ most commonly affected by major genetic disorders is the heart, hence extensive research is conducted in imaging and functional assessment of the heart [131–135]. While B-mode is used to assess structure, Doppler (pulsed [spectral] and color) are the ideal techniques to examine heart function. A vast amount of literature has been published on the value of ultrasound examination of the fetal heart, using various techniques, including Doppler analysis of flow across the cardiac valves and Doppler velocimetry of various fetal vessels [136–138]. The vast majority of published reports was, until recently, on B-mode examinations around 18–20 weeks. However, several authors have demonstrated the feasibility of examining the heart much sooner in pregnancy, beginning around 10 or 11 weeks [139–142]. Doppler analysis has long been a tool to study cardiac function, although mostly in the placenta, umbilical, or uterine arteries [143]. Studies have been published of Doppler study of flow through cardiac valves, beginning at 6 weeks [144, 145]. It should be noted that it is technically extremely difficult to obtain these tracings and, thus, *very* prolonged dwell times may be necessary. Some have described performing a measurement of the heart diameter, heart rate, and inflow and outflow waveforms "after 5 weeks" [146]. No details are available on exposure levels. It should also be remembered that, at these early stages of pregnancy, fetuses measure 1–2 cm in length and are completely included in the beam, therefore generating "total body scanning" in B-mode which is necessary to position the Doppler gate. Analysis of ductus venosus flow as well as characteristics of flow across the tricuspid valve has been shown to be helpful in screening for chromosomal anomalies in the first trimester of pregnancy, as an adjunct to measurement of the nuchal translucency (NT). Waveform analysis of the ductus venosus reduces the false positive rate of the screening test [147, 148]. For example, in fetuses with increased NT but with normal karyotype, from 11 to 13 6/7 weeks, absent or reversed A-wave (atrial contraction) in the ductus venosus is associated with a three-fold increase in the likelihood of a major cardiac defect, whereas normal ductal flow is associated with a 50% reduction in the risk for such defects [149–151]. It is clear that Doppler is an important tool to study fetal health in early (and late) pregnancy [138] but appropriate precautions need to be taken to limit exposure in terms of clear indication, time, and acoustic output [152].

Acoustic Output

Based on various sources, it appears that acoustic output (as expressed by various intensities) is much higher in Doppler than in B-mode: for instance, 34 mW/cm^2 for the I_{SPTA} in B-mode versus 1080 mW/cm^2 for spectral Doppler [153, 154]. Furthermore, as demonstrated in Table 1.2, the output has increased in all modes over the years [35]. If one compares outputs (as expressed by TI and MI, a clinically easy-to-use but somewhat remote expression of output) between first and second to third trimesters, differences are not major [75] but higher TI values are obtained when switching to Doppler mode [77]. The increase in TI is, generally, small but with some

Table 1.2 Changes over the years in I_{SPTA} (in mW/cm^2), mean (and range) in various ultrasound modalities (adapted from [154])

Ultrasound modality	1991	1995	1998
B-mode	17 (0.3–177)	34 (0.3–991)	94 (4.2–600)
Pulsed Doppler	1140 (110–4520)	1659 (173–9080)	1420 (214–7500)
Color Doppler	148 (25–511)	344 (21–2050)	470 (27–2030)

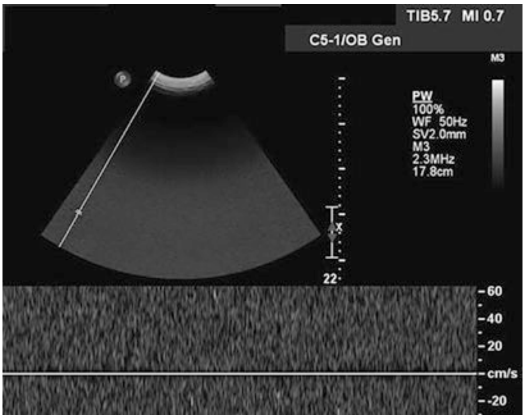

Fig. 1.3 Very high TI (5.7) may be obtained in Doppler mode (not an actual clinical examination). Note that this is a general obstetrics setting

new machines, TI's of up to 5–6 are displayed in Doppler mode (Fig. 1.3). Research has shown that excellent diagnostic images can be obtained at low outputs, as defined by the TI values of 0.5 or even 0.1 [155]. This is illustrated in Fig. 1.4. Therefore, the switch-on default should be set up such that a low acoustic output power is initiated for each new patient when starting an examination. Only if images are not satisfactory from a diagnostic standpoint, should the output be increased. Under pressure from safety committees of various societies, several ultrasound manufacturers have implemented this recommendation. Concerns about the fact that outputs are much higher in Doppler applications were expressed in three editorials [11, 156, 157]. In one of these, the authors raised the question whether research involving Doppler in the first trimester should even be considered for publication [156]. Based on these considerations, some recommend extreme caution when employing Doppler in the first trimester [158]. Furthermore, acoustic outputs, as published by the various ultrasound instruments manufacturers may not always be adequate [159] and an additional cause for concern is the increase in instruments outputs over the years [160]. Despite this, as detailed above, in recent years, there has been a major recrudescence in the usage of Doppler in very early pregnancy. Unfortunately, one of the reasons for this is the ignorance of many end users of potential bioeffects, based on the "nothing has been shown" principle. Therefore, the risk is that this will become a routine standard, secondary to the push to utilize this modality by certain individuals, not necessarily knowledgeable of potential safety issues and that inexperienced end users, wishing to imitate and adulate these "experts" will attempt to perform these exams for extremely extended periods of time at pregnancy stages which are very susceptible to external insults (Christoph Brezinka, personal communication). Indeed, as mentioned earlier, a major issue is the lack of knowledge of ultrasound clinical users on output, bioeffects, and safety, both in the USA [64] and abroad [63, 65, 66].

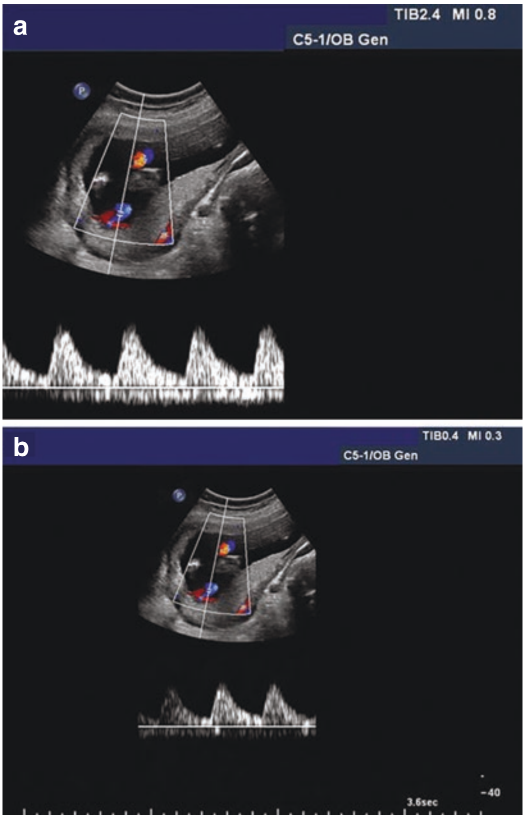

Fig. 1.4 Doppler velocimetry in the umbilical artery. Panel **a**, TI_B is 2.4; panel **b**, the TI_B is 0.4 and the image is equally diagnostic

3D/4D Ultrasound

Three-dimensional (3D) and four-dimensional (4D) ultrasound are gaining recognition in obstetrics and gynecology. In prenatal diagnosis, it adds to the detection of a wide range of anomalies, such as those involving the face, skeleton, and extremities. The usefulness in early gestation is less obvious [161]. Characteristics are short acquisition time and post-processing analysis, hence decreased exposure. As determined by TI and MI, acoustic output during 3D/4D exams does not seem excessive [78]. Figure 1.5 demonstrates low TI and MI during a 3D acquisition. The resulting reconstructed image is, obviously, a post-processing process. Sheiner et al. have shown that mean TIs during the 3D (0.27 ± 0.1) and 4D examinations (0.24 ± 0.1) were comparable to the TI during the B-mode scanning (0.28 ± 0.1; $P = 0.343$) [78]. The 3D volume acquisitions added 2.0 ± 1.8 min of actual ultrasound scanning time (i.e., not including data processing and manipulation, nor 3D displays, which are all post-processing steps). The 4D ultrasound added 2.2 ± 1.2 min to the examination time. Amount of additional scanning time needed to choose an adequate scanning plane and to acquire a diagnostic 3D volume was not noted. Attractive views of the face, for instance, have led to its popularity among pregnant women who ask for non-medically indicated ultrasound ("keepsake ultrasound"). This is often performed in nonmedical facilities, not for diagnostic purposes, but to provide images for the family photo album. The issue was addressed long ago [162] but the practice has been opposed by various authors and

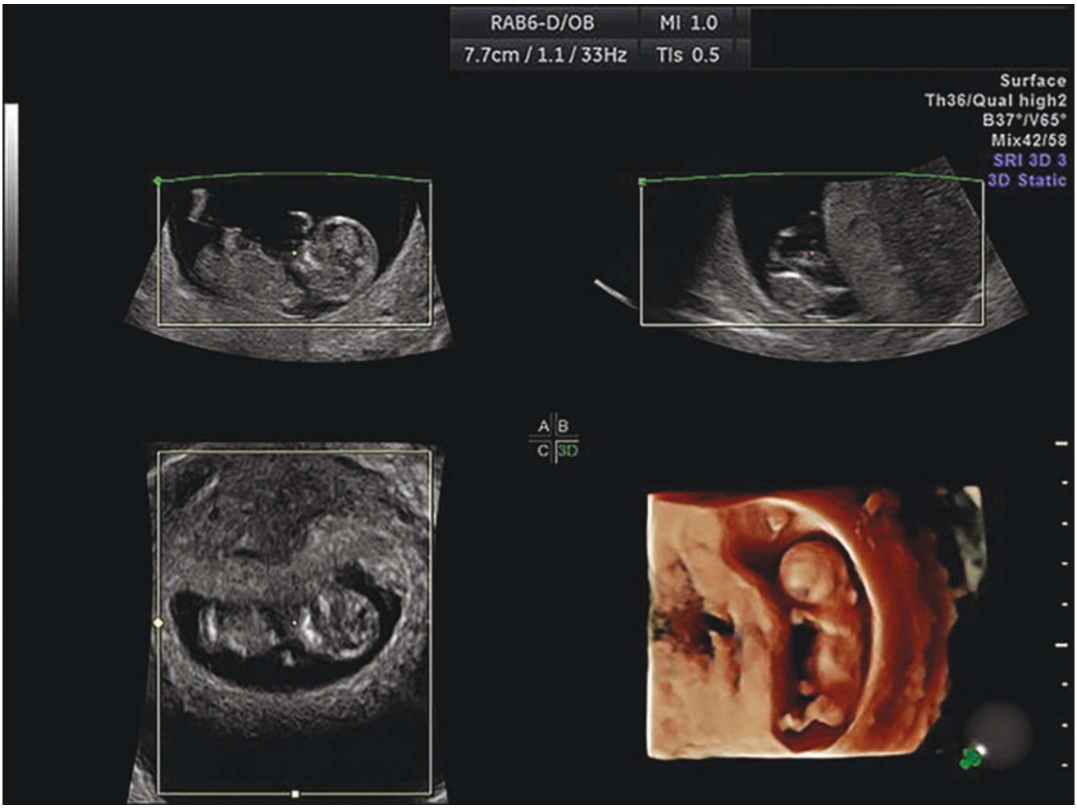

Fig. 1.5 Three-D acquisition with three orthogonal planes and reconstructed volume. The output power is determined by the acquisition plane (in general plane A), since the two other planes and the reconstructed volume are computer generated. In this acquisition, TI_S was 0.2

professional, scientific organizations [163–173], although not by all [174] and with difference of opinions on whether practitioners involved in this activity should be sanctioned [175].

Shear Wave Elastography

Shear wave elastography (SWE) is a relatively recent ultrasound technology using acoustic radiation force imaging (ARFI), to assess the elasticity or stiffness of tissues, in real time, through a quantitative color scale [176]. It has been used particularly in imaging of the breast, liver (detection of small lesions and evaluation of diffuse liver disease), prostate, and thyroid as well as in musculoskeletal ultrasound [177]. While some applications in gynecology have been described (such as assessment of uterine fibroids or cervical stiffness), the use of this modality in obstetrics is very limited and, in reality, still at the experimental stage but has been described for fetal lungs and liver, for instance [178] and placenta [179]. The issue of safety has been discussed and it appears that SWE does not have stronger effects than Doppler ultrasound [180] and that TI and MI need to be monitored during the examination, similarly to other ultrasound modalities. Caution, however, is recommended [181].

How to Limit Fetal Exposure and Safety Statements

The answer is simple: perform ultrasound only with a clear indication, keep exposure to a minimum power and time, compatible with an adequate diagnosis (application of the ALARA principle), watch the TI and, to a lesser degree, the MI on screen and do not perform examinations with new techniques “simply because you can,” if they have not been scientifically shown to afford diagnostic advantages [99, 130, 152, 182]. All this is particularly important at early gestational ages. In general, begin your exam with a low power output and increase only if necessary [182, 183]. Some scientists have clearly stated that Doppler should be avoided in the first trimester. Several ultrasound organizations, however, have publishing statements and/or guidelines specific for first trimester ultrasound, with a particular emphasis on the use of Doppler in early pregnancy. The following statement which summarizes the various guidelines is copied from the AIUM’s website and is available to the public.

> AIUM [184]: The use of Doppler ultrasound during the first trimester is currently being promoted as an aid for screening and diagnosis of some congenital abnormalities. The procedure requires considerable skill and subjects the fetus to extended periods of relatively high ultrasound exposure levels. Due to the increased acoustic output of spectral Doppler ultrasound, its use in the first trimester should be viewed with caution. Spectral Doppler imaging should only be used when there is a clear benefit/risk advantage and both the TI and examination duration are kept low. Protocols that typically involve TI values lower than 1.0 reflect minimal risk. Comparable to the World Federation for Ultrasound in Medicine and Biology/International Society of Ultrasound in Obstetrics and Gynecology statement, we recommend that:
>
> 1. All scans should begin at a displayed TI of 0.7 because the total duration of an ultrasound examination during pregnancy cannot be known in advance. Higher outputs should be used only if needed to obtain adequate images and in accordance with the as low as reasonably achievable (ALARA) principle.
> 2. Pulsed Doppler (spectral, power, and color flow imaging) ultrasound should not be used routinely.
> 3. Spectral Doppler ultrasound may be used for specific clinical indications, such as to refine risks for fetal aneuploidy, and color Doppler imaging may be useful in an early anatomic evaluation of the fetus or placenta.
> 4. When performing a Doppler ultrasound examination, the displayed TI should be less than or equal to 0.7, provided adequate images can be obtained, and the exposure time should be kept as short as possible, consistent with acquisition of needed clinical information.
> 5. When using Doppler ultrasound for research, teaching, and training purposes, the displayed TI should be less than or equal to 0.7, and the exposure time should be kept as short as possible, consistent with the purposes of the scan. Informed consent should be obtained.
> 6. In educational settings, a discussion of first-trimester pulsed or color Doppler ultrasound should be accompanied by information on safety and bioeffects (e.g., TI, exposure times, and how to reduce the output power).

7. When scanning maternal uterine arteries in the first trimester, there are unlikely to be any fetal safety implications as long as the embryo/fetus lies outside the Doppler ultrasound beam.

It should be noted that paragraphs 1–6 are common to AIUM, The European Federation of Ultrasound in Medicine and Biology (EFSUMB), the International Society of Ultrasound in Obstetrics and Gynecology (ISUOG), and the World Federation of Ultrasound in Medicine and Biology (WFUMB).

Conclusions

Ultrasound may, arguably, be the most important technology in the last 60 years in obstetrical clinical practice. Its advantages are numerous, and its use has expanded from simply measuring a biparietal diameter to three-dimensional (3D) study of the brain or heart anatomy or "real time 3D" (a.k.a. 4D) evaluation of fetal behavior. Not only is structural analysis possible but functional assessment of cardiac function is achievable with the use of Doppler applications. The fact this can be done is not a blanket permission to perform it with no control or limits, particularly in early pregnancy, a time when the fetus is very susceptible to external insults. No gross harmful bioeffects have been described in humans as a result of using DUS but indications to perform an examination should be clear and the lowest possible acoustic output power should be used, for the shortest possible time, yet compatible with accurate clinical diagnosis [21]. Clinical end users should be educated in bioeffects and in ways to keep the fetus safe.

Teaching Points

- Biological effects have been demonstrated with the use of ultrasound in animals but not in humans.
- Epidemiology data are from before 1992, when acoustic outputs were increased several folds.
- The early fetal period is a time of increased susceptibility to external factors, such as hyperthermia, a recognized teratogen, with the central nervous system (CNS) being most at risk.
- Bioeffects of ultrasound may be secondary to two major mechanisms: thermal (indirect, resulting from conversion of acoustic energy into heat) and non-thermal (also known as mechanical, direct effects caused by bubble cavitation and other mechanical phenomena).
- The Output Display Standard (ODS) is designed to give the end user an idea of exposure and includes the thermal and mechanical indices (TI and MI).
- To ensure safety of ultrasound in early pregnancy, a clear and valid indication for use should exist.
- New indications include screening for genetic disorders, ductus venosus and tricuspid Doppler and cardiac function analysis which have the potential for bioeffects, secondary to usage in early gestation, a time of increased susceptibility and/or increased acoustic power.
- To limit exposure and potential harmful effects, use ultrasound only when indicated, keep the exam as short as possible, at lowest possible output for diagnostic accuracy (ALARA principle) and keep TI and MI below 1.

References

1. Donald I, Macvicar BT. Investigation of abdominal masses by pulsed ultrasound. Lancet. 1958;1:1188–95.
2. Abramowicz JS. Benefits and risks of ultrasound in pregnancy. Semin Perinatol. 2013;37(5):295–300.
3. Abinader R, Warsof SL. Benefits and pitfalls of ultrasound in obstetrics and gynecology. Obstet Gynecol Clin N Am. 2019;46(2):367–78.
4. Baerwald AR, Walker RA, Pierson RA. Growth rates of ovarian follicles during natural menstrual cycles, oral contraception cycles, and ovarian stimulation cycles. Fertil Steril. 2009;91(2):440–9.
5. Younis JS, Jadaon JE, Haddad S, Izhaki I, Ben-Ami M. Prospective evaluation of basal stromal Doppler studies in women with good ovarian reserve and infertility undergoing in vitro fertilization-embryo

transfer treatment: patients with polycystic ovary syndrome versus ovulatory patients. Fertil Steril. 2011;95(5):1754–8.

6. Timor-Tritsch IE, Fuchs KM, Monteagudo A, D'Alton ME. Performing a fetal anatomy scan at the time of first-trimester screening. Obstet Gynecol. 2009;113(2 Pt 1):402–7.
7. Edwards L, Hui L. First and second trimester screening for fetal structural anomalies. Semin Fetal Neonatal Med. 2018;23(2):102–11.
8. Abramowicz JS, Fowlkes JB, Stratmeyer ME, Ziskin MC. Bioeffects and safety of fetal ultrasound exposure: why do we need epidemiology? In: Sheiner E, editor. Textbook of epidemiology in perinatology. New York: Nova Science Publishers, Inc.; 2010.
9. Abramowicz JS, Fowlkes JB, Skelly AC, Stratmeyer ME, Ziskin MC. Conclusions regarding epidemiology for obstetric ultrasound. J Ultrasound Med. 2008;27(4):637–44.
10. FDA. 510(k) Diagnostic ultrasound guidance update of 1991. Rockville, MD: US Food and Drug Administration; 1991.
11. Duck FA. Is it safe to use diagnostic ultrasound during the first trimester? Ultrasound Obstet Gynecol. 1999;13(6):385–8.
12. Abramowicz JS. Ultrasound in assisted reproductive technologies and the first trimester: is there a risk? Clin Obstet Gynecol. 2017;60(1):121–32.
13. Duck F. The propagation of ultrasound through tissue. In: ter Haar G, editor. The safe use of ultrasound in medical diagnosis. 3rd ed. London: The British Institute of Radiology; 2012. p. 4–18.
14. Abramowicz JS, Barnett SB, Duck FA, Edmonds PD, Hynynen KH, Ziskin MC. Fetal thermal effects of diagnostic ultrasound. J Ultrasound Med. 2008;27(4):541–59; quiz 60–3.
15. NCRP. Exposure criteria for medical diagnostic ultrasound: II. Criteria based on all known mechanisms. Report no. 140. Bethesda, MD: National Council on Radiation Protection and Measurements; 2002. Contract No.: 140.
16. Duck FA, Starritt HC. A study of the heating capabilities of diagnostic ultrasound beams. Ultrasound Med Biol. 1994;20(5):481–92.
17. Edwards MJ, Saunders RD, Shiota K. Effects of heat on embryos and foetuses. Int J Hyperthermia. 2003;19(3):295–324.
18. Botto LD, Panichello JD, Browne ML, Krikov S, Feldkamp ML, Lammer E, et al. Congenital heart defects after maternal fever. Am J Obstet Gynecol. 2014;210(4):359:e1–e11.
19. Clarren SK, Smith DW, Harvey MA, Ward RH, Myrianthopoulos NC. Hyperthermia—a prospective evaluation of a possible teratogenic agent in man. J Pediatr. 1979;95(1):81–3.
20. Edwards MJ. Hyperthermia as a teratogen: a review of experimental studies and their clinical significance. Teratog Carcinog Mutagen. 1986;6(6):563–82.
21. AIUM. AIUM As Low As Reasonably Achievable (ALARA) principle. 2014. Available from: http://www.aium.org/publications/viewStatement.aspx?id=39.
22. Miller MW, Brayman AA, Abramowicz JS. Obstetric ultrasonography: a biophysical consideration of patient safety—the "rules" have changed. Am J Obstet Gynecol. 1998;179(1):241–54.
23. Miller MW, Miller HE, Church CC. A new perspective on hyperthermia-induced birth defects: the role of activation energy and its relation to obstetric ultrasound. J Therm Biol. 2005;30:400–9.
24. Abraham V, Ziskin MC, Heyner S. Temperature elevation in the rat fetus due to ultrasound exposure. Ultrasound Med Biol. 1989;15(5):443–9.
25. Barnett SB. Can diagnostic ultrasound heat tissue and cause biological effects. In: Barnett SB, Kossoff G, editors. Safety of diagnostic ultrasound. Carnforth: Parthenon Publishing; 1998. p. 30–1.
26. Barnett SB. Routine ultrasound scanning in first trimester: what are the risks? Semin Ultrasound CT MR. 2002;23(5):387–91.
27. Nyborg WL, Steele RB. Temperature elevation in a beam of ultrasound. Ultrasound Med Biol. 1983;9(6):611–20.
28. Moretti ME, Bar-Oz B, Fried S, Koren G. Maternal hyperthermia and the risk for neural tube defects in offspring: systematic review and meta-analysis. Epidemiology. 2005;16(2):216–9.
29. Shaw GM, Todoroff K, Velie EM, Lammer EJ. Maternal illness, including fever and medication use as risk factors for neural tube defects. Teratology. 1998;57(1):1–7.
30. Dreier JW, Andersen AM, Berg-Beckhoff G. Systematic review and meta-analyses: fever in pregnancy and health impacts in the offspring. Pediatrics. 2014;133(3):e674–88.
31. Miller MW, Ziskin MC. Biological consequences of hyperthermia. Ultrasound Med Biol. 1989;15(8):707–22.
32. Miller MW, Nyborg WL, Dewey WC, Edwards MJ, Abramowicz JS, Brayman AA. Hyperthermic teratogenicity, thermal dose and diagnostic ultrasound during pregnancy: implications of new standards on tissue heating. Int J Hyperthermia. 2002;18(5):361–84.
33. Jauniaux E. Intervillous circulation in the first trimester: the phantom of the color Doppler obstetric opera. Ultrasound Obstet Gynecol. 1996;8(2):73–6.
34. Makikallio K, Tekay A, Jouppila P. Uteroplacental hemodynamics during early human pregnancy: a longitudinal study. Gynecol Obstet Investig. 2004;58(1):49–54.
35. Abramowicz JS, Adhikari S, Dickman E, Estroff JA, Harris GR, Nomura J, et al. Ocular ultrasound: review of bioeffects and safety, including fetal and point of care perspective. J Ultrasound Med. 2021; https://doi.org/10.1002/jum.15864.
36. Bottomley C, Bourne T. Dating and growth in the first trimester. Best Pract Res Clin Obstet Gynaecol. 2009;23(4):439–52.

37. Church CC, Barnett SB. Ultrasound-induced heating and its biological consequences. In: ter Haar G, editor. The safe use of ultrasound in medical diagnosis. 3rd ed. London: The British Institute of Radiology; 2012. p. 46–68.
38. O'Brien WD, Siddiqi TA. Obstetric sonography: the output display standard and ultrasound bioeffects. In: Fleischer AC, Manning FA, Jeanty P, Romero R, editors. Sonography in obstetrics and gynecology-principles and practice. 6th ed. New York: McGraw-Hill; 2001. p. 29–48.
39. Shaw A, Martin K. The acoustic output of diagnostic ultrasound scanners. In: ter Haar G, editor. The safe use of ultrasound in medical diagnosis. London: The British Institute of Radiology; 2012. p. 18–45.
40. Calvert J, Duck F, Clift S, Azaime H. Surface heating by transvaginal transducers. Ultrasound Obstet Gynecol. 2007;29(4):427–32.
41. Barnett SB. WFUMB Symposium on Safety of Ultrasound in Medicine. Conclusions and recommendations on thermal and non-thermal mechanisms for biological effects of ultrasound. Ultrasound Med Biol. 1998;24(Supplement 1):i–xvi.
42. Dalecki D. Mechanical bioeffects of ultrasound. Annu Rev Biomed Eng. 2004;6:229–48.
43. Fowlkes JB, Holland CK. Mechanical bioeffects from diagnostic ultrasound: AIUM consensus statements. American Institute of Ultrasound in Medicine. J Ultrasound Med. 2000;19(2):69–72.
44. Carstensen EL. Acoustic cavitation and the safety of diagnostic ultrasound. Ultrasound Med Biol. 1987;13(10):597–606.
45. Church CC. Spontaneous homogeneous nucleation, inertial cavitation and the safety of diagnostic ultrasound. Ultrasound Med Biol. 2002;28(10):1349–64.
46. Holland CK, Deng CX, Apfel RE, Alderman JL, Fernandez LA, Taylor KJ. Direct evidence of cavitation in vivo from diagnostic ultrasound. Ultrasound Med Biol. 1996;22(7):917–25.
47. Kimmel E. Cavitation bioeffects. Crit Rev Biomed Eng. 2006;34(2):105–61.
48. Dalecki D, Raeman CH, Child SZ, Carstensen EL. Intestinal hemorrhage from exposure to pulsed ultrasound. Ultrasound Med Biol. 1995;21(8):1067–72.
49. Wible JH Jr, Galen KP, Wojdyla JK, Hughes MS, Klibanov AL, Brandenburger GH. Microbubbles induce renal hemorrhage when exposed to diagnostic ultrasound in anesthetized rats. Ultrasound Med Biol. 2002;28(11–12):1535–46.
50. Dalecki D, Child SZ, Raeman CH, Cox C, Carstensen EL. Ultrasonically induced lung hemorrhage in young swine. Ultrasound Med Biol. 1997;23(5):777–81.
51. Stratmeyer ME, Greenleaf JF, Dalecki D, Salvesen KA. Fetal ultrasound: mechanical effects. J Ultrasound Med. 2008;27(4):597–605; quiz 6–9.
52. Bij de Vaate AJ, Brolmann HA, van der Slikke JW, Emanuel MH, Huirne JA. Gel instillation sonohysterography (GIS) and saline contrast sonohysterography (SCSH): comparison of two diagnostic techniques. Ultrasound Obstet Gynecol. 2010;35(4):486–9.
53. Dalecki D, Raeman CH, Child SZ, Cox C, Francis CW, Meltzer RS, et al. Hemolysis in vivo from exposure to pulsed ultrasound. Ultrasound Med Biol. 1997;23(2):307–13.
54. Abramowicz JS, Miller MW, Battaglia LF, Mazza S. Comparative hemolytic effectiveness of 1 MHz ultrasound on human and rabbit blood in vitro. Ultrasound Med Biol. 2003;29(6):867–73.
55. Fatemi M, Ogburn PL Jr, Greenleaf JF. Fetal stimulation by pulsed diagnostic ultrasound. J Ultrasound Med. 2001;20(8):883–9.
56. Harvey EN, Harvey EB, Loomis RW. Further observations on the effect of high frequency sound waves on living matter. Biol Bull. 1928;55:459–69.
57. Siddiqi TA, Plessinger MA, Meyer RA, Woods JR Jr. Bioeffects of diagnostic ultrasound on auditory function in the neonatal lamb. Ultrasound Med Biol. 1990;16(6):621–5.
58. Dalecki D, Child SZ, Raeman CH, Carstensen EL. Tactile perception of ultrasound. J Acoust Soc Am. 1995;97(5 Pt 1):3165–70.
59. Church CC, O'Brien WD Jr. Evaluation of the threshold for lung hemorrhage by diagnostic ultrasound and a proposed new safety index. Ultrasound Med Biol. 2007;33(5):810–8.
60. Abbott JG. Rationale and derivation of MI and TI—a review. Ultrasound Med Biol. 1999;25(3):431–41.
61. AIUM/NEMA. Standard for real-time display of thermal and mechanical acoustic output indices on diagnostic ultrasound devices. Laurel, MD and Rosslyn, VA: American Institute of Ultrasound in Medicine and the National Electrical Manufacturers' Association; 1992.
62. NCRP. Exposure criteria for medical diagnostic ultrasound: I. Criteria based on thermal mechanisms. Bethesda, MD: National Council on Radiation Protection & Measurements (NCRP); 1992.
63. Marsal K. The output display standard: has it missed its target? Ultrasound Obstet Gynecol. 2005;25(3):211–4.
64. Sheiner E, Shoham-Vardi I, Abramowicz JS. What do clinical users know regarding safety of ultrasound during pregnancy? J Ultrasound Med. 2007;26(3):319–25; quiz 26–7.
65. Akhtar W, Arain MA, Ali A, Manzar N, Sajjad Z, Memon M, et al. Ultrasound biosafety during pregnancy: what do operators know in the developing world?: national survey findings from Pakistan. J Ultrasound Med. 2011;30(7):981–5.
66. Meizner I. [What do doctors understand regarding ultrasound safety during pregnancy?]. Harefuah. 2012;151(4):234–6, 52.
67. Piscaglia F, Tewelde AG, Righini R, Gianstefani A, Calliada F, Bolondia L. Knowledge of the bio-effects of ultrasound among physicians performing clinical

ultrasonography: results of a survey conducted by the Italian Society for Ultrasound in Medicine and Biology (SIUMB). J Ultrasound. 2009;12:6–11.

68. Houston LE, Allsworth J, Macones GA. Ultrasound is safe… right?: resident and maternal-fetal medicine fellow knowledge regarding obstetric ultrasound safety. J Ultrasound Med. 2011;30(1):21–7.
69. Bagley J, Thomas K, DiGiacinto D. Safety practices of sonographers and their knowledge of the biologic effects of sonography. J Diagn Med Sonogr. 2011;27:252–61.
70. Abramowicz JS. Biosafety of sonography: still a mystery to most obstetrics (and other) providers. J Ultrasound Med. 2020;39(9):1683–5.
71. Bigelow TA, Church CC, Sandstrom K, Abbott JG, Ziskin MC, Edmonds PD, et al. The thermal index: its strengths, weaknesses, and proposed improvements. J Ultrasound Med. 2011;30(5):714–34.
72. Karagoz I, Kartal MK. A new safety parameter for diagnostic ultrasound thermal bioeffects: safe use time. J Acoust Soc Am. 2009;125(6):3601–10.
73. Ziskin MC. The thermal dose index. J Ultrasound Med. 2010;29(10):1475–9.
74. Sheiner E, Abramowicz JS. Acoustic output as measured by thermal and mechanical indices during fetal nuchal translucency ultrasound examinations. Fetal Diagn Ther. 2008;25(1):8–10.
75. Sheiner E, Shoham-Vardi I, Hussey MJ, Pombar X, Strassner HT, Freeman J, et al. First-trimester sonography: is the fetus exposed to high levels of acoustic energy? J Clin Ultrasound. 2007;35(5):245–9.
76. Sheiner E, Freeman J, Abramowicz JS. Acoustic output as measured by mechanical and thermal indices during routine obstetric ultrasound examinations. J Ultrasound Med. 2005;24(12):1665–70.
77. Sheiner E, Shoham-Vardi I, Pombar X, Hussey MJ, Strassner HT, Abramowicz JS. An increased thermal index can be achieved when performing Doppler studies in obstetric sonography. J Ultrasound Med. 2007;26(1):71–6.
78. Sheiner E, Hackmon R, Shoham-Vardi I, Pombar X, Hussey MJ, Strassner HT, et al. A comparison between acoustic output indices in 2D and 3D/4D ultrasound in obstetrics. Ultrasound Obstet Gynecol. 2007;29(3):326–8.
79. Bellieni CV, Buonocore G, Bagnoli F, Cordelli DM, Gasparre O, Calonaci F, et al. Is an excessive number of prenatal echographies a risk for fetal growth? Early Hum Dev. 2005;81(8):689–93.
80. Rackow BW. Congenital uterine anomalies. In: Stadtmauer LA, Tur-Kaspa I, editors. Ultrasound imaging in reproductive medicine. New York: Springer; 2014. p. 101–15.
81. Wiser A, Gonen O, Ghetler Y, Shavit T, Berkovitz A, Shulman A. Monitoring stimulated cycles during in vitro fertilization treatment with ultrasound only—preliminary results. Gynecol Endocrinol. 2012;28(6):429–31.
82. Vinayagam D, Ohja K. Evaluation of tubal patency (HyCoSy, Doppler). In: Stadtmauer LA, Tur-Caspa I, editors. Ultrasound imaging in reproductive medicine. New York: Springer; 2014. p. 179–87.
83. Buckett WM. A meta-analysis of ultrasound-guided versus clinical touch embryo transfer. Fertil Steril. 2003;80(4):1037–41.
84. Testart J, Thebault A, Souderes E, Frydman R. Premature ovulation after ovarian ultrasonography. Br J Obstet Gynaecol. 1982;89(9):694–700.
85. Lenz S, Lauritsen JG, Kjellow M. Collection of human oocytes for in vitro fertilisation by ultrasonically guided follicular puncture. Lancet. 1981;1(8230):1163–4.
86. Gleicher N, Friberg J, Fullan N, Giglia RV, Mayden K, Kesky T, et al. EGG retrieval for in vitro fertilisation by sonographically controlled vaginal culdocentesis. Lancet. 1983;2(8348):508–9.
87. Wongtra-Ngan S, Vutyavanich T, Brown J. Follicular flushing during oocyte retrieval in assisted reproductive techniques. Cochrane Database Syst Rev. 2010;(9):CD004634.
88. Heyner S, Abraham V, Wikarczuk ML, Ziskin MC. Effects of ultrasound on ovulation in the mouse. Gamete Res. 1989;22(3):333–8.
89. Bologne R, Demoulin A, Schaaps JP, Hustin J, Lambotte R. [Influence of ultrasonics on the fecundity of female rats]. C R Seances Soc Biol Fil. 1983;177(3):381–387.
90. Demoulin A, Bologne R, Hustin J, Lambotte R. Is ultrasound monitoring of follicular growth harmless? Ann N Y Acad Sci. 1985;442:146–52.
91. Heyner S, Abraham V, Wikarczuk ML, Ziskin MC. Effects of ultrasound on DNA and RNA synthesis in preimplantation mouse embryos. Mol Reprod Dev. 1990;25(3):209–14.
92. Mahadevan M, Chalder K, Wiseman D, Leader A, Taylor PJ. Evidence for an absence of deleterious effects of ultrasound on human oocytes. J In Vitro Fert Embryo Transf. 1987;4(5):277–80.
93. Williams SR, Rothchild I, Wesolowski D, Austin C, Speroff L. Does exposure of preovulatory oocytes to ultrasonic radiation affect reproductive performance? J In Vitro Fert Embryo Transf. 1988;5(1):18–21.
94. Kerin JF. Determination of the optimal timing of insemination in women. In: Richardson D, Joyce D, Symonds M, editors. Frozen human semen. London: Royal College of Obstetrics and Gynaecology; 1979. p. 105–32.
95. AIUM. AIUM practice guideline for the performance of obstetric ultrasound examinations. 2007. Available from: http://www.aium.org/publications/guidelines.aspx.
96. Ndumbe FM, Navti O, Chilaka VN, Konje JC. Prenatal diagnosis in the first trimester of pregnancy. Obstet Gynecol Surv. 2008;63(5):317–28.
97. Nicolaides KH. First-trimester screening for chromosomal abnormalities. Semin Perinatol. 2005;29(4):190–4.
98. Carvalho JS. Fetal heart scanning in the first trimester. Prenat Diagn. 2004;24(13):1060–7.

99. ter Haar G. Guidelines and recommendations for the safe use of diagnostic ultrasound: the user's responsibilities. In: ter Haar G, editor. The safe use of ultrasound in medical diagnosis. 3rd ed. London: British Institute of Radiology; 2012. p. 142–57.
100. Allen VM, Wilson RD, Cheung A, Genetics Committee of the Society of O, Gynaecologists of C, Reproductive Endocrinology Infertility Committee of the Society of O, et al. Pregnancy outcomes after assisted reproductive technology. J Obstet Gynaecol Can. 2006;28(3):220–50.
101. Budziszewska P, Wloch A, Rozmus-Warcholiniska W, Czuba B, Kuka-Panasiuk D, Ilski A, et al. [Heart defects and other anomalies in fetuses conceived by assisted reproduction techniques]. Ginekol Pol. 2007;78(11):865–8.
102. Zhang J, Zhou F, Song Y, Ying W, Zhang Y. Long dwell-time exposure of human chorionic villi to transvaginal ultrasound in the first trimester of pregnancy induces activation of caspase-3 and cytochrome C release. Biol Reprod. 2002;67(2):580–3.
103. Brent RL, Beckman DA, Landel CP. Clinical teratology. Curr Opin Pediatr. 1993;5(2):201–11.
104. Thorpe PG, Gilboa SM, Hernandez-Diaz S, Lind J, Cragan JD, Briggs G, et al. Medications in the first trimester of pregnancy: most common exposures and critical gaps in understanding fetal risk. Pharmacoepidemiol Drug Saf. 2013;22(9):1013–8.
105. Barzilay E, Koren G. Elements of teratology. In: Abramowicz JS, editor. First-trimester ultrasound—a comprehensive guide. New York: Springer; 2015.
106. Shahrukh Hashmi S, Gallaway MS, Waller DK, Langlois PH, Hecht JT, National Birth Defects Prevention S. Maternal fever during early pregnancy and the risk of oral clefts. Birth Defects Res. 2010;88(3):186–94.
107. Martinez-Frias ML, Garcia Mazario MJ, Caldas CF, Conejero Gallego MP, Bermejo E, Rodriguez-Pinilla E. High maternal fever during gestation and severe congenital limb disruptions. Am J Med Genet. 2001;98(2):201–3.
108. Aoyama N, Yamashina S, Poelmann RE, Gittenberger-De Groot AC, Izumi T, Soma K, et al. Conduction system abnormalities in rat embryos induced by maternal hyperthermia. Anat Rec. 2002;267(3):213–9.
109. Acs N, Banhidy F, Puho E, Czeizel AE. Maternal influenza during pregnancy and risk of congenital abnormalities in offspring. Birth Defects Res A Clin Mol Teratol. 2005;73(12):989–96.
110. Edwards MJ. Hyperthermia in utero due to maternal influenza is an environmental risk factor for schizophrenia. Congenit Anom. 2007;47(3):84–9.
111. Saxen I. The association between maternal influenza, drug consumption and oral clefts. Acta Odontol Scand. 1975;33(5):259–67.
112. Dombrowski SC, Martin RP, Huttunen MO. Association between maternal fever and psychological/behavior outcomes: a hypothesis. Birth Defects Res A Clin Mol Teratol. 2003;67(11):905–10.
113. Atkins TJ, Duck FA. Heating caused by selected pulsed Doppler and physiotherapy ultrasound beams measured using thermal test objects. Eur J Ultrasound. 2003;16(3):243–52.
114. Barnett SB. Intracranial temperature elevation from diagnostic ultrasound. Ultrasound Med Biol. 2001;27(7):883–8.
115. Horder MM, Barnett SB, Vella GJ, Edwards MJ, Wood AK. Ultrasound-induced temperature increase in guinea-pig fetal brain in utero: third-trimester gestation. Ultrasound Med Biol. 1998;24(9):1501–10.
116. Ang ESBC, Gluncic V, Duque A, Schafer ME, Rakic P. Prenatal exposure to ultrasound waves impacts neuronal migration in mice. Proc NY Acad Sci. 2006;103:12903–10.
117. Kieler H, Cnattingius S, Palmgren J, Haglund B, Axelsson O. First trimester ultrasound scans and left-handedness. Epidemiology (Cambridge, Mass.). 2002;13(3):370.
118. Salvesen KA. Ultrasound in pregnancy and non-right handedness: meta-analysis of randomized trials. Ultrasound Obstet Gynecol. 2011;38(3):267–71.
119. Salvesen KA, Vatten LJ, Eik-Nes SH, Hugdahl K, Bakketeig LS. Routine ultrasonography in utero and subsequent handedness and neurological development. BMJ (Clin Res Ed). 1993;307(6897):159–64.
120. Schneider-Kolsky ME, Ayobi Z, Lombardo P, Brown D, Kedang B, Gibbs ME. Ultrasound exposure of the foetal chick brain: effects on learning and memory. Int J Dev Neurosci. 2009;27(7):677–83.
121. Kieler H, Haglund B, Cnattingius S, Palmgren J, Axelsson O. Does prenatal sonography affect intellectual performance? Epidemiology. 2005;16(3):304–10.
122. McClintic AM, King BH, Webb SJ, Mourad PD. Mice exposed to diagnostic ultrasound in utero are less social and more active in social situations relative to controls. Autism Res. 2014;7(3):295–304.
123. Rodgers C. Questions about prenatal ultrasound and the alarming increase in autism. Midwifery Today Int Midwife. 2006;(80):16–9, 66–7.
124. Grether JK, Li SX, Yoshida CK, Croen LA. Antenatal ultrasound and risk of autism spectrum disorders. J Autism Dev Disord. 2010;40(2):238–45.
125. Abramowicz JS. Ultrasound and autism: association, link, or coincidence? J Ultrasound Med. 2012;31(8):1261–9.
126. Ziskin MC. Intrauterine effects of ultrasound: human epidemiology. Teratology. 1999;59(4):252–60.
127. Jouppila P, Piironinen O. Ultrasonic diagnosis of fetal life in early pregnancy. Obstet Gynecol. 1975;46(5):616–20.
128. Resch B, Herczeg J, Altmayer P, Sztano P. The efficiency of Doppler-technique in the first trimester of pregnancy. Ann Chir Gynaecol Fenn. 1971;60(2):85–8.
129. AIUM. AIUM Official Statement: Measurement of fetal heart rate. 2011. Available from: http://www.aium.org/publications/statements.aspx.

130. WFUMB/ISUOG. WFUMB/ISUOG statement on the safe use of Doppler ultrasound during 11-14 week scans (or earlier in pregnancy). Ultrasound Med Biol. 2013;39(3):373.
131. Zwanenburg F, Jongbloed MRM, van Geloven N, Ten Harkel ADJ, van Lith JMM, Haak MC. Assessment of human fetal cardiac autonomic nervous system development using color tissue Doppler imaging. Echocardiography (Mount Kisco, NY). 2021;38(6):974–81.
132. Zhang B, Liu H, Luo H, Li K. Automatic quality assessment for 2D fetal sonographic standard plane based on multitask learning. Medicine (Baltimore). 2021;100(4):e24427.
133. Sun L, Wang J, Su X, Chen X, Zhou Y, Zhang X, et al. Reference ranges of fetal heart function using a Modified Myocardial Performance Index: a prospective multicentre, cross-sectional study. BMJ Open. 2021;11(7):e049640.
134. Krishnan R, Deal L, Chisholm C, Cortez B, Boyle A. Concordance between obstetric anatomic ultrasound and fetal echocardiography in detecting congenital heart disease in high-risk pregnancies. J Ultrasound Med. 2021;40(10):2105–12.
135. Duta S, Veduta A, Vayna AM, Panaitescu A, Nedelea F, Peltecu G. The outcome of structural heart defects diagnosed in the first trimester of pregnancy. J Maternal Fetal Neonatal Med. 2021;34(9):1389–94.
136. Herberg U, Breuer J, Gembruch U, Willruth A. Imaging in fetal cardiology. Minerva Pediatr. 2014;66(5):453–71.
137. Turan S, Turan O, Desai A, Harman C, Baschat A. First-trimester fetal cardiac examination using spatiotemporal image correlation, tomographic ultrasound and color Doppler imaging for the diagnosis of complex congenital heart disease in high-risk patients. Ultrasound Obstet Gynecol. 2014;44:562–7.
138. Maulik D. The use of Doppler in early pregnancy. In: Abramowicz JS, editor. First-trimester ultrasound—a comprehensive guide. New York: Springer; 2015.
139. Achiron R, Rotstein Z, Lipitz S, Mashiach S, Hegesh J. First-trimester diagnosis of fetal congenital heart disease by transvaginal ultrasonography. Obstet Gynecol. 1994;84(1):69–72.
140. Carvalho JS. Screening for heart defects in the first trimester of pregnancy: food for thought. Ultrasound Obstet Gynecol. 2010;36(6):658–60.
141. DeVore GR. First-trimester fetal echocardiography: is the future now? Ultrasound Obstet Gynecol. 2002;20(1):6–8.
142. Gembruch U, Knopfle G, Chatterjee M, Bald R, Hansmann M. First-trimester diagnosis of fetal congenital heart disease by transvaginal two-dimensional and Doppler echocardiography. Obstet Gynecol. 1990;75(3 Pt 2):496–8.
143. Dillon EH, Case CQ, Ramos IM, Holland CK, Taylor KJ. Endovaginal pulsed and color Doppler in first-trimester pregnancy. Ultrasound Med Biol. 1993;19(7):517–25.
144. Leiva MC, Tolosa JE, Binotto CN, Weiner S, Huppert L, Denis AL, et al. Fetal cardiac development and hemodynamics in the first trimester. Ultrasound Obstet Gynecol. 1999;14(3):169–74.
145. Makikallio K, Jouppila P, Rasanen J. Human fetal cardiac function during the first trimester of pregnancy. Heart (British Cardiac Society). 2005;91(3):334–8.
146. Wloch A, Rozmus-Warcholinska W, Czuba B, Borowski D, Wloch S, Cnota W, et al. Doppler study of the embryonic heart in normal pregnant women. J Maternal Fetal Neonatal Med. 2007;20(7):533–9.
147. Borrell A, Grande M, Bennasar M, Borobio V, Jimenez JM, Stergiotou I, et al. First-trimester detection of major cardiac defects with the use of ductus venosus blood flow. Ultrasound Obstet Gynecol. 2013;42(1):51–7.
148. Matias A, Gomes C, Flack N, Montenegro N, Nicolaides KH. Screening for chromosomal abnormalities at 10-14 weeks: the role of ductus venosus blood flow. Ultrasound Obstet Gynecol. 1998;12(6):380–4.
149. Florjanski J, Fuchs T, Zimmer M, Homola W, Pomorski M, Blok D. The role of ductus venosus Doppler flow in the diagnosis of chromosomal abnormalities during the first trimester of pregnancy. Adv Clin Exp Med. 2013;22(3):395–401.
150. Maiz N, Valencia C, Kagan KO, Wright D, Nicolaides KH. Ductus venosus Doppler in screening for trisomies 21, 18 and 13 and Turner syndrome at 11-13 weeks of gestation. Ultrasound Obstet Gynecol. 2009;33:512–7.
151. Papatheodorou SI, Evangelou E, Makrydimas G, Ioannidis JP. First-trimester ductus venosus screening for cardiac defects: a meta-analysis. BJOG. 2011;118(12):1438–45.
152. Abramowicz JS. Fetal Doppler: how to keep it safe? Clin Obstet Gynecol. 2010;53(4):842–50.
153. Duck FA, Henderson J. Acoustic output of modern instruments: is it increasing? In: Barnett SB, Kossoff G, editors. Safety of diagnostic ultrasound. New York: The Parthenon Publishing Group; 1998. p. 15–25.
154. Shaw A, Martin K. The acoustic output of ultrasound scanners. In: ter Haar G, editor. The safe use of ultrasound in medical diagnosis. 3rd ed. London: The British Institute of Radiology; 2012. p. 18–45.
155. Sande RK, Matre K, Eide GE, Kiserud T. Ultrasound safety in early pregnancy: reduced energy setting does not compromise obstetric Doppler measurements. Ultrasound Obstet Gynecol. 2012;39(4):438–43.
156. Campbell S, Platt L. The publishing of papers on first-trimester Doppler. Ultrasound Obstet Gynecol. 1999;14(3):159–60.
157. Chervenak FA, McCullough LB. Research on the fetus using Doppler ultrasound in the first trimester: guiding ethical considerations. Ultrasound Obstet Gynecol. 1999;14(3):161.
158. ter Haar GR, Abramowicz JS, Akiyama I, Evans DH, Ziskin MC, Marsal K. Do we need to restrict the use

of Doppler ultrasound in the first trimester of pregnancy? Ultrasound Med Biol. 2013;39(3):374–80.
159. Martin K. The acoustic safety of new ultrasound technologies. Ultrasound. 2010;18:110–8.
160. Cibull SL, Harris GR, Nell DM. Trends in diagnostic ultrasound acoustic output from data reported to the US Food and Drug Administration for device indications that include fetal applications. J Ultrasound Med. 2013;32(11):1921–32.
161. Goncalves L. Three-D ultrasound-a role in early pregnancy? In: Abramowicz JS, editor. First-trimester ultrasound—a comprehensive guide. New York: Springer; 2015.
162. Furness ME. Fetal ultrasound for entertainment? Med J Aust. 1990;153(7):371.
163. Abramowicz JS, Barnett SB, Isuog W. The safe use of non-medical ultrasound: a summary of the proceedings of the joint safety symposium of ISUOG and WFUMB. Ultrasound Obstet Gynecol. 2009;33(5):617–20.
164. ACOG. American College of Obstetricians and Gynecologists (ACOG) Committee Opinion. Number 297, August 2004. Nonmedical use of obstetric ultrasonography. Obstet Gynecol. 2004;104(2):423–4.
165. AIUM. AIUM Official Statement: Keepsake fetal imaging. 2012. Available from: http://www.aium.org/publications/statements.aspx.
166. BMUS. BMUS (British Medical Ultrasound Society) Guidelines for the safe use of diagnostic ultrasound equipment. 2009. Available from: http://www.bmus.org/ultras-safety/us-safety03.asp.
167. Chudleigh T. Scanning for pleasure. Ultrasound Obstet Gynecol. 1999;14(6):369–71.
168. Rados C. FDA cautions against ultrasound ‘keepsake’ images. 2004. Available from: http://www.fda.gov/FDAC/features/2004/104_images.html.
169. Salvesen K, Lees C, Abramowicz J, Brezinka C, Ter Haar G, Marsal K. ISUOG-WFUMB statement on the non-medical use of ultrasound, 2011. Ultrasound Obstet Gynecol. 2011;38(5):608.
170. Westin S, Bakketeig LS. Unnecessary use of ultrasound in pregnancy should be avoided. Probably safe, but new evidence suggests caution. Scand J Prim Health Care. 2003;21(2):65–7.
171. WFUMB. WFUMB recommendations on non-medical use of ultrasound. Ultrasound Med Biol. 2010;36(8):1210.
172. Greene N, Platt LD. Nonmedical use of ultrasound: greater harm than good? J Ultrasound Med. 2005;24(1):123–5.
173. Chervenak FA, McCullough LB. An ethical critique of boutique fetal imaging: a case for the medicalization of fetal imaging. Am J Obstet Gynecol. 2005;192:31–3.
174. Doubilet PM. Entertainment ultrasound. J Ultrasound Med. 2005;24(2):251–3.
175. Wax JR, Cartin A, Pinette MG, Blackstone J. Nonmedical fetal ultrasound: knowledge and opinions of Maine obstetricians and radiologists. J Ultrasound Med. 2006;25(3):331–5.
176. Sigrist RMS, Liau J, Kaffas AE, Chammas MC, Willmann JK. Ultrasound elastography: review of techniques and clinical applications. Theranostics. 2017;7(5):1303–29.
177. Ozturk A, Grajo JR, Dhyani M, Anthony BW, Samir AE. Principles of ultrasound elastography. Abdom Radiol (NY). 2018;43(4):773–85.
178. Mottet N, Cochet C, Vidal C, Metz JP, Aubry S, Bourtembourg A, et al. Feasibility of two-dimensional ultrasound shear wave elastography of human fetal lungs and liver: a pilot study. Diagn Interv Imaging. 2020;101(2):69–78.
179. Simon EG, Calle S, Perrotin F, Remenieras JP. Measurement of shear wave speed dispersion in the placenta by transient elastography: a preliminary ex vivo study. PLoS One. 2018;13(4):e0194309.
180. Li C, Zhang C, Li J, Cao X, Song D. An experimental study of the potential biological effects associated with 2-D shear wave elastography on the neonatal brain. Ultrasound Med Biol. 2016;42(7):1551–9.
181. Simon EG, Calle S. Safety of elastography applied to the placenta: be careful with ultrasound radiation force. J Obstet Gynaecol Res. 2017;43(9):1509.
182. Nelson TR, Fowlkes JB, Abramowicz JS, Church CC. Ultrasound biosafety considerations for the practicing sonographer and sonologist. J Ultrasound Med. 2009;28(2):139–50.
183. Abramowicz JS, Lewin PA, Goldberg BB. Ultrasound bioeffects for the perinatologist. 2008. Available from: http://www.glowm.com/index.html?p=glowm.cml/print&articleid=204#r22.
184. AIUM. Prudent use and safety of diagnostic ultrasound in pregnancy. Laurel, MD: American Institute of Ultrasound in Medicine; 2019. Available from: https://www.aium.org/officialStatements/79?__sw_csrfToken=8004423e.
185. Carson PL, Fischella PR, Oughton TV. Ultrasonic power and intensities produced by diagnostic ultrasound equipment. Ultrasound Med Biol. 1978;3(4):341–50.

2

How to Optimize the Ultrasound Image

Kathryn Mussatt and Jacques S. Abramowicz

Introduction

Ultrasound may be the most operator-dependent imaging modality. When performing an ultrasound in the first trimester of pregnancy (as well as later), the quality of the images that the sonographer/physician is able to acquire will be key to determine the success of a complete diagnostic exam, helping to facilitate optimal antenatal care, allowing best possible maternal and fetal outcomes. Indeed, the exam is intended to demonstrate the presence of an intrauterine pregnancy, evaluate the number of fetuses, confirm viability, document accurate dating, and diagnose any abnormalities or any concerns with the pregnancy. These are addressed by various chapters of this book. Additionally, it has become more commonplace to perform early anatomical surveys at the end of the first trimester, especially for patients considered at high risk [1–3]. This alone makes the ability to perform sound ultrasound examinations in the first trimester more important than ever.

There are two types of ultrasounds performed in pregnancy, the first being the routine exam, offered to all pregnant patients regardless of risk and the second being a targeted exam based on an increased risk of fetal abnormalities or poor outcome [1, 3]. It is of utmost importance that the ultrasound examiner is both knowledgeable and capable of operating the ultrasound system in order to successfully meet this goal. In this chapter, we will outline some basic steps that any practicing examiner should be proficient in navigating to enhance imaging, thus providing the highest quality exam possible based on the circumstances.

Choosing the Best Tools

Imaging is an art. Choosing the right tools is the first step in creating a masterpiece. First trimester diagnostic examinations can be performed using a variety of transducers and techniques. The gestational age, whether presumed or known, will ultimately play a part in choosing to utilize either a transabdominal or transvaginal transducer. Most imaging is performed using 3 two-dimensional scanning modes: B-mode (brightness mode) imaging is gray scale, M-mode (motion mode) imaging for detecting fetal heart motion, and color Doppler mode. Spectral (pulsed) Doppler may have indications, but, because of a higher acoustic energy, needs to be employed with clear indications and strict precautions (Chaps. 1 and 13). It is important that the user understands the options and makes decisions based on information obtained prior to per-

K. Mussatt (✉) · J. S. Abramowicz
Department of Obstetrics and Gynecology, University of Chicago, Chicago, IL, USA
e-mail: Kathryn.Mussatt@uchicagomedicine.org; Kathryn.mussatt@uchospitals.edu

© The Author(s), under exclusive license to Springer Nature Switzerland AG 2023
J. S. Abramowicz, R. E. Longman (eds.), *First-Trimester Ultrasound*,
https://doi.org/10.1007/978-3-031-24133-8_2

forming the exam. Typically in first trimester imaging, three options are sufficient to perform the diagnostic exam; using a curved array transabdominal transducer, a high frequency linear transducer, and a high frequency transvaginal transducer. High frequency transducers provide the best images in the near field with a tradeoff for limited penetration. Conversely, low frequency transducers offer increased penetration with reduced resolution. Harmonic imaging has the ability to offer double the resolution without loss of penetration. Taking the patient's known or presumed gestational age in mind and, in addition, uterine position and maternal body habitus will allow the user to decide which transducer would be the practical starting point. It is not unusual to need to use more than one transducer to successfully complete a first trimester diagnostic exam. Most first trimester exams are performed using B-mode. M-mode (and not spectral Doppler) should be utilized for fetal cardiac motion documentation, and color Doppler may be utilized to evaluate ovarian vasculature. As a result of these new tools, we are now able to provide more information earlier than ever before, such as the ability to detect fetal anomalies or aneuploidy and increased risk of cardiac defect by assessing the nuchal translucency (NT) measurement as part of first trimester imaging [1–3].

A Systematic Approach

Advances in ultrasound systems have allowed for early, more precise diagnostic exams. There are a limited number of tools that can be utilized when imaging, so having a systematic approach to how they are chosen and optimized is critical in the journey to obtain quality images and diagnostically successful ultrasound examinations for the patients. The first step as already explained is choosing the best transducer for the exam and being willing to adjust as needed, understanding how to utilize basic knobs on the ultrasound system and the impact of each to allow optimizing image quality for every diagnostic exam. Following systematic steps, each time an exam is performed will build a routine and will help avoid mistakes or lead to incomplete examinations and improve the ability to detect fetal malformations [4].

Basic Knobology

One would never attempt to drive a car without having a basic understanding of how the different functions of the car work and a license to drive. It is no less important, as a user or "driver," to understand the basic system functions of an ultrasound machine. Knobology is the ability of a user to guide the ultrasound system to perform in a manner that will enhance the quality of imaging, thus improving the probability of a complete diagnostic exam. Users can approach this goal in two ways, allowing the ultrasound equipment to work independently by utilizing system presets and the consistent use of automatic image optimization or gaining a deep-rooted understanding of how the ultrasound system can best be used to achieve the best possible images with every exam [3, 5].

There are numerous controls on an ultrasound machine but a handful of knobs or buttons on every system are easily recognized and manipulated. Basic understanding of each will help the user maximize the system and lead to improved image quality with any ultrasound examination: gain, focus, depth, sector width, and dynamic range. In addition, most advanced systems will allow tissue harmonic imaging (THI) as well as three-dimensional (3D) ultrasound. See Table 2.1.

Table 2.1 Image optimization knobs for gray scale imaging (first trimester)

- Transducer selection
- Depth
- Sector width
- Overall gain
- TGC
- Focal zone
- Dynamic range
- Tissue harmonic imaging (THI)
- 3D imaging

Transducer Selection and the Impact of Frequency

Understanding the exam being performed and the general anatomy will allow to choose the best transducer for the job and limit incomplete or inaccurate diagnosis. First trimester exams typically range from early to late in the trimester or approximately 6–13 weeks 6 days gestation [3]. It is unlikely that a sonographer will use the same transducer for each phase of the trimester. Early gestation imaging will likely require a higher frequency transvaginal transducer in order to visualize small structures with good resolution. A curved array transabdominal transducer is, generally, better suited for later in the first trimester. On occasion, there may be the need to utilize more than one type of transducer to obtain adequate information to allow for a successful diagnostic examination. Users should be opened to utilizing multiple transducers in an effort to get optimal images for a diagnostic exam (see Fig. 2.1).

Once the transducer has been chosen, many machines will display various applications (such as abdomen, OB first trimester, OB second and third trimesters, gynecology, fetal cardiac, etc.). When choosing the application, the machine will optimize what the manufacturer believes are the optimal presets for that particular application in terms of transducer frequency adjustment, acoustic output, depth, overall gain, and dynamic range. It is, however, very important to not completely rely on these but being able to manipulate certain controls to further optimize the images.

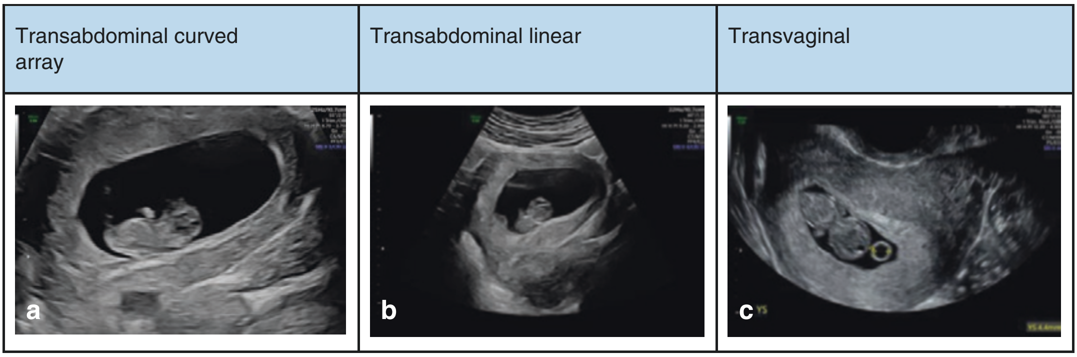

Fig. 2.1 Ultrasound images of different types of transducers on the same first trimester fetus (**a**) was obtained with a curved array transducer, (**b**) with a linear transducer and (**c**) with a transvaginal transducer

Depth

Choosing the appropriate depth setting is important and sets the tone for the entire exam. This option allows the user to make a conscious decision regarding the targeted anatomy or region of interest (ROI) to be evaluated in the first trimester examination. Depth will influence how much work (energy) the system is outputting and will have an impact on image quality. Choosing excessive depth forces the machine to display areas of no interest. Starting the exam with a high depth penetration will allow a broad overview of the anatomy but in return will reduce the overall resolution. Reducing the image window will contribute to better resolution and should be considered often. In the first trimester, there are circumstances when it is important to represent a broad overview of the anatomy [5]. For example, showing the uterine body with an intrauterine pregnancy within it will allow a diagnosis that can be confidently reported. Inappropriate choice of image depth penetration can impact the ability to definitively show that there is an intrauterine pregnancy. See examples in Figs. 2.2 and 2.3.

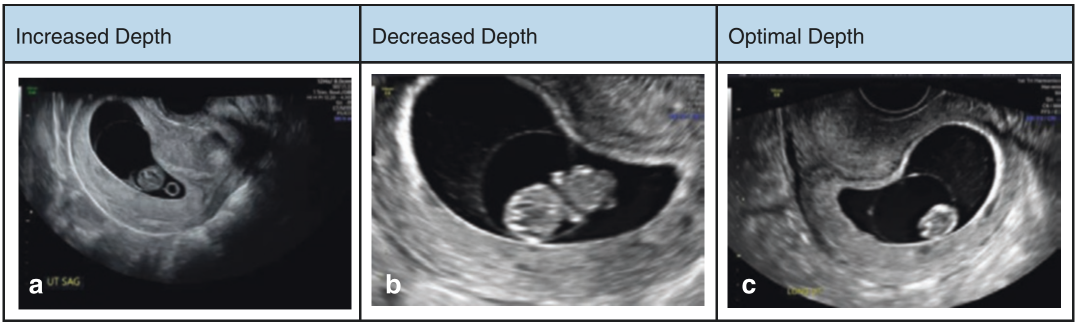

Fig. 2.2 An intrauterine pregnancy can be difficult to assess if the proper image depth is not chosen by the user. In (**a**), the depth is too profound, showing more than is intended and losing resolution on ROI as a result. In (**b**), depth is set too low which does not allow to define the complete area to compare location, etc. (**c**) Demonstrates optimal depth with good middle ground image

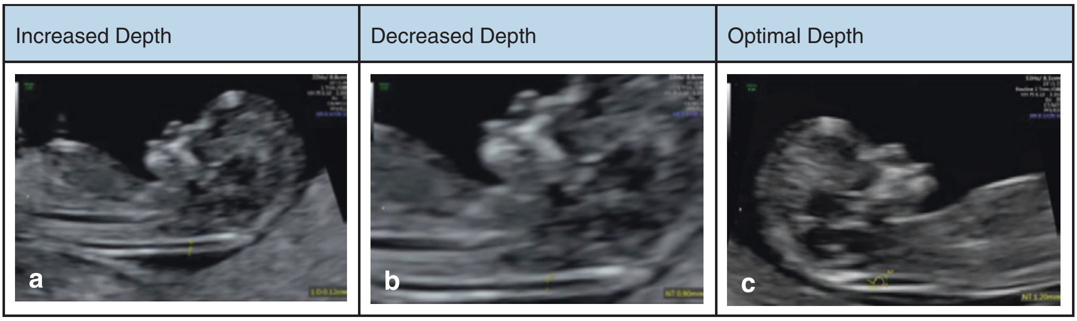

Fig. 2.3 Nuchal translucency can be difficult to assess if the proper image depth is not chosen by the user. (**a**) The depth is too profound, showing more than is intended and losing resolution on ROI as a result. In (**b**), depth is set too low which does not allow to define the complete area to compare location, etc. (**c**) Demonstrates optimal depth with good middle ground image

Sector Width

Similar to depth, having a wide sector width impacts the resolution of the image and should be reduced whenever possible to allow focus and improved detail on the ROI. This is particularly important when the user wants to point out an area of interest for the viewer. This allows focus and attention to a particular area, and there is no loss in image quality in making this choice. As mentioned, when choosing a depth, one needs to be certain that the ROI is shown from a broad view and then following with a focused image for effect.

Gain (Brightness)

Overall Gain

Overall gain is the brightness of an ultrasound image. When adjusting the overall gain, you are manually driving a change in amplitude of the entire image rather than a targeted area of the acquisition. This can be done as a pre- or post-processing step on most ultrasound systems and is typically a turn knob on your main board. See Fig. 2.4 for examples of appropriate vs inappropriate use of the overall gain. In general, gain is a post-processing step, which means the outgoing beam is not manipulated (such as increasing the intensity/power/acoustic energy with potential increased risk of bioeffects) (see Chap. 1).

Time Gain Compensation (TGC)

Adjusting brightness throughout the image depending on a specific point of attenuation is done by the means of the time gain compensation or TGC. It is, generally, a set of depth-specific slide controls, allowing changing the gain at various depths, thus permitting adjustment of echo-signals in the near field, mid field, and far field to improve axial resolution. Adjusting this is useful to compensate for absorbed or lost signals in order to better visualize a given structure. It can have a negative effect by amplifying or reducing the ultrasound signal if the user is not thoughtful about how TGC buttons are aligned when scanning. "Smart" systems will reset to the middle at the start of each exam, making any changes user dependent. It is prudent to begin each new case with the TGC's aligned in the middle and manually adjust as needed to streamline the image. See Fig. 2.5, for examples, of how to optimize the TGC. This option is typically a part of the control panel but more recently has been incorporated on many touchscreen displays.

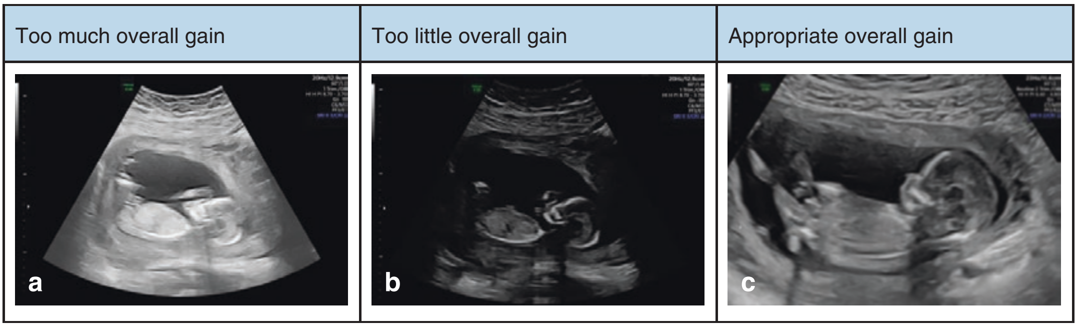
Too much overall gain

Too little overall gain

Appropriate overall gain

Fig. 2.4 The impact that overall gain has on the image is demonstrated. (**a**) Too much overall gain renders the image "too white" with loss of definition. (**b**) Overall gain is too low. Various structures cannot be distinguished. (**c**) Correct gain

TGC control panel	Too low in the near field	Too high in the far field
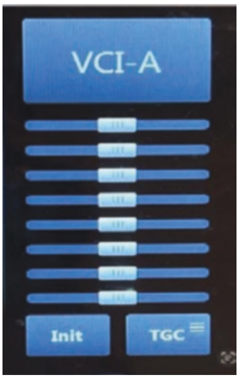	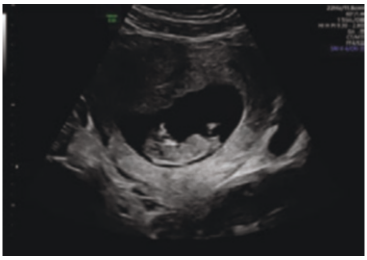	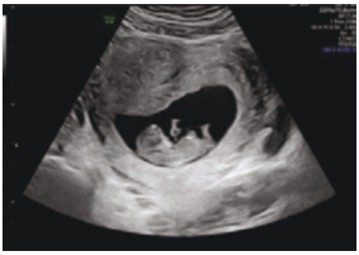

Fig. 2.5 Examples of TGC and the impact on image quality

Focus (Focal Zone)

Focus is an overlooked feature that can have a noticeable beneficial impact on the quality of the image when used properly. The focal zone represents the point where the ultrasound beam is at its narrowest and most focused point and should be carefully chosen based on what the user is attempting to optimize. Consistent use of the focal zone will improve the resolution at that particular point, thus improving image quality [5]. Starting with one focal zone and increasing if needed is the best approach to optimizing the region of interest. For optimal image enhancement, the focal zone should be just below the area of interest. See Fig. 2.6 to see how the placement of the focal zone impacts the image.

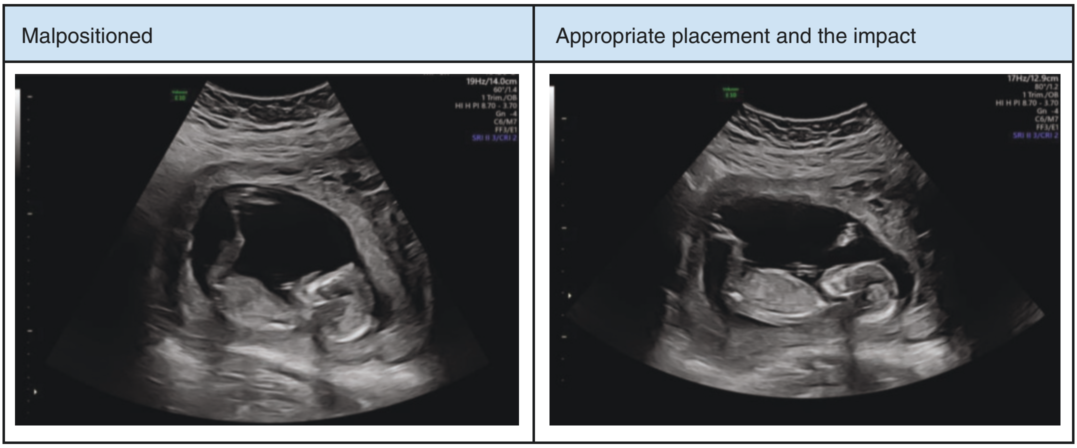

Malpositioned

Appropriate placement and the impact

Fig. 2.6 Focal zone placement direct impact on images

Dynamic Range

Determines how many shades of gray are displayed (compression) based on the controlled strength (decibels) of the ultrasound beam by throwing out the largest and the smallest signals. The ultrasound user can manipulate the image characteristics by changing the dynamic range, oftentimes part of a touch screen application. A high dynamic range will show as a wider variety of gray leading to a soft image, while a low dynamic range will show a more contrasty black and white image, leading to a very contrasty image. A high dynamic range is often the choice for soft tissue, and a low dynamic range is appropriate for vasculature [6]. See Fig. 2.7, for examples, of how adjusting the dynamic range impacts images.

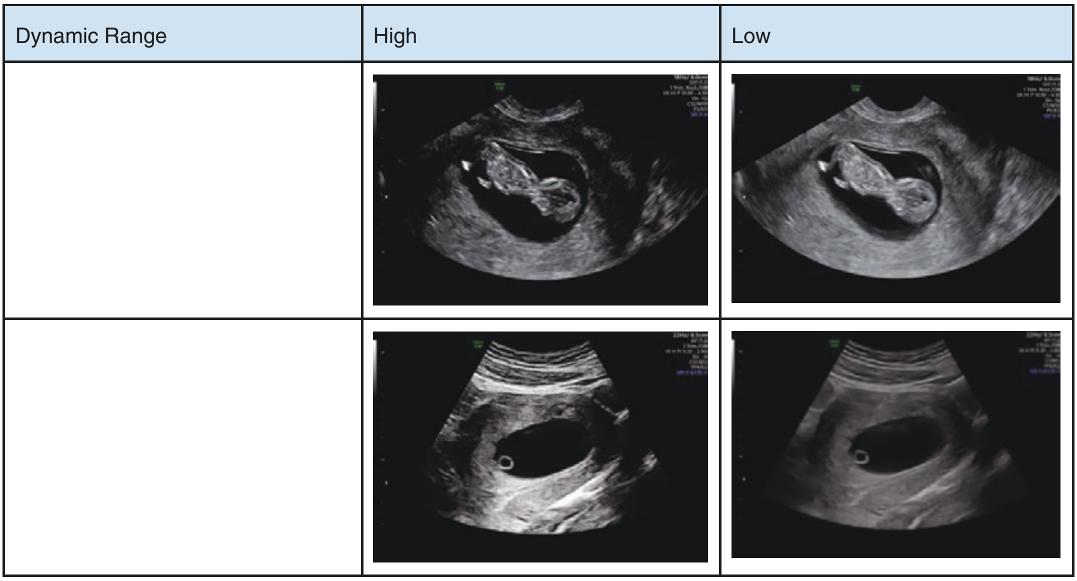

Fig. 2.7 Dynamic range impact on images

Tissue Harmonic Imaging (THI)

THI is a great tool for image optimization because it balances penetration and resolution by eliminating weak signals upon return. THI will improve resolution without the loss of penetration. See Fig. 2.8 for an example of how the use of THI can improve image quality.

Tissue Harmonic Imaging	On	Off
	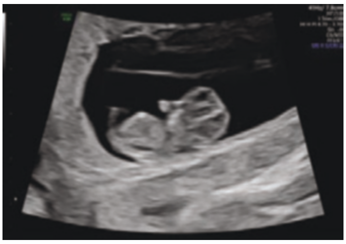	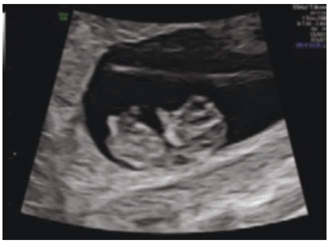

Fig. 2.8 How THI improves image quality without reducing penetration

Three-Dimensional Imaging

Utilizing 3D imaging to enhance first trimester imaging is a useful tool (see Chap. 14). Three-dimensional imaging can be used in surface mode to display the entire fetus and can identify anomalies early in pregnancy but various modes may permit visualization of internal organs. Three-dimensional volume rendering is helpful in assessing the developing embryo and fetus [1]. Figure 2.9 displays various types of 3D imaging on the same embryo.

3D Imaging			

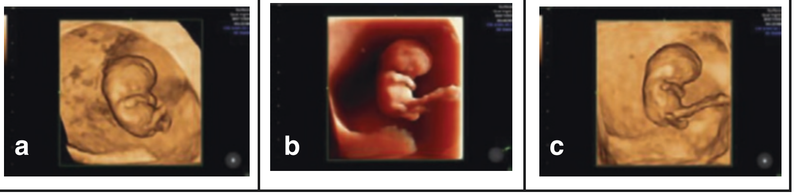

Fig. 2.9 Different types of the surface mode display 3D image effects-same embryo (**a**) 3D image of a 9 week embryo, (**b**, **c**) wide surface view of same embryo

Additional Knobs/Buttons

Freeze button: Allows stopping the scanning process and keeping an image on screen for as long as desired to observe or record.

Calipers: Allow measurements, either linear, circular or, in 3D, volumetric.

Zoom: Used for magnifying the area of interest. There are two types of zoom: read and write. Read zoom utilizes a stored image and enlarges the pixel density in that region. Write zoom increases the size of a live image and, thus, maintains the pixel density. Write zoom is preferable since it tends to produce a better-quality image.

Color Doppler: This allows visualization of movements (generally blood flowing within blood vessels). Three important knobs/buttons in color (and spectral) Doppler are the gain, the pulse repetition frequency (PRF), and the wall filter. Low PRF, high gain, low wall filter are preferred for small vessels [7].

Teaching Points

- A systematic approach to image acquisition will allow improved visualization and, hence, optimal diagnosis.
- The first step is choice of the appropriate transducer, based on exam required and clinical information.
- Choosing the depth which allows imaging of the region of interest and making sure the focal point is located just beyond that region is critical.
- Gain is a post-processing control and has no bearing on the acoustic output, thus not associated with any change in risks of bioeffects.

References

1. Abuhamad A, Chaoui R. First trimester ultrasound diagnosis of fetal abnormalities. Philadelphia: Wolters Kluwer Health; 2018.
2. Sonek J. First trimester ultrasonography in screening and detection of fetal anomalies. Am J Med Genet C Semin Med Genet. 2007;145C(1):45–61.
3. Salomon L, Alfirevic Z, Chalouhi CM, Ghi T, Kagan KO, Lau TK, et al. ISUOG Practice Guidelines: performance of first-trimester fetal ultrasound scan. Ultrasound Obstet Gynecol. 2013;41(1):102–13.
4. Grandjean H, Larroque D, Levi S. The performance of routine ultrasonographic screening of pregnancies in the Eurofetus Study. Am J Obstet Gynecol. 1999;181(2):446–54 [cited 2021 Dec 5]. Available from: https://www.sciencedirect.com/science/article/abs/pii/S0002937899705776.
5. Zander D, Hüske S, Hoffmann B, Cui X-W, Dong Y, Lim A, et al. Ultrasound image optimization ("Knobology"): B-mode. Ultrasound Int Open. 2020;6(1):E14–24. Available from: https://www.ncbi.nlm.nih.gov/pmc/articles/PMC7458857/.
6. Wiafe YA, Badu-Peprah A. The influence of ultrasound equipment knobology in abdominal sonography. London: IntechOpen; 2019. Available from: www.intechopen.com, https://www.intechopen.com/chapters/65515.
7. Löwe A, Jenssen C, Hüske S, Zander D, Ignee A, Lim A, Cui XW, Dong Y, Hoffmann B, Dietrich CF. "Knobology" in Doppler ultrasound. Med Ultrason. 2021;23(4):480–6.

Ultrasound and Infertility

3

A. Musa Zamah, Robyn Power, Ryan E. Longman,
and Jacques S. Abramowicz

Baseline Evaluation

Ultrasound is an essential component of the current evaluation of female patients affected by infertility. A systematic approach to ultrasound of the pelvis should be performed to ensure no part of the exam is omitted. The complete pelvic sonogram begins with a complete sweep through the pelvis from one side to the other side, visualizing the cervix, uterus, ovaries, adnexae, and cul-de-sac. The bladder is optimally empty during transvaginal ultrasonography, but if not, the bladder should be inspected for any abnormalities and then ask the patient to empty her bladder.

Uterus

Initial evaluation of the uterus begins with identifying the cervix at the end of the vagina and just below the bladder. The cervix should be examined for any pathology (e.g., nabothian cysts) and orientation. The cervical orientation can be helpful in directing the examiner to the rest of the uterus and help identify its location and position.

The baseline evaluation of the uterine body traditionally includes several features, comprising the overall size in standard dimensions of the uterus (length, height, width, and calculated volume), position, the sonographic appearance of the endometrium, as well as any defects of the uterus or other pathology. The uterus is typically measured in the mid-sagittal plane for the longitudinal length and the height, measured in the anterior-posterior (AP) diameter (Fig. 3.1). The length extends from the end of the cervix (external cervical os) to the top of the fundus. The transverse measurement of the uterus is also measured in the mid-corpus (Fig. 3.2).

The size of the uterus corresponds well to the overall estrogenization status, with lower and normal/elevated estrogen values correlating with smaller and larger uterine size, respectively. An enlarged uterine volume may also suggest uterine pathology such as leiomyomata or adenomyosis. The position of the uterus is also routinely recorded as a dynamic measurement. This information is important for procedures such as embryo transfer, which will be subsequently discussed; furthermore, if the uterus is noted to remain motionless on serial exams, the concern is raised for adhesive disease or an entrapped uterus.

The uterine evaluation may reveal factors that contribute to infertility or result in early pregnancy loss. Common uterine abnormalities include polyps, fibroids, intrauterine adhesions,

---

A. M. Zamah (✉) · R. Power · R. E. Longman
J. S. Abramowicz
The University of Chicago, Chicago, IL, USA
e-mail: azamah@bsd.uchicago.edu

© The Author(s), under exclusive license to Springer Nature Switzerland AG 2023

J. S. Abramowicz, R. E. Longman (eds.), *First-Trimester Ultrasound*,
https://doi.org/10.1007/978-3-031-24133-8_3

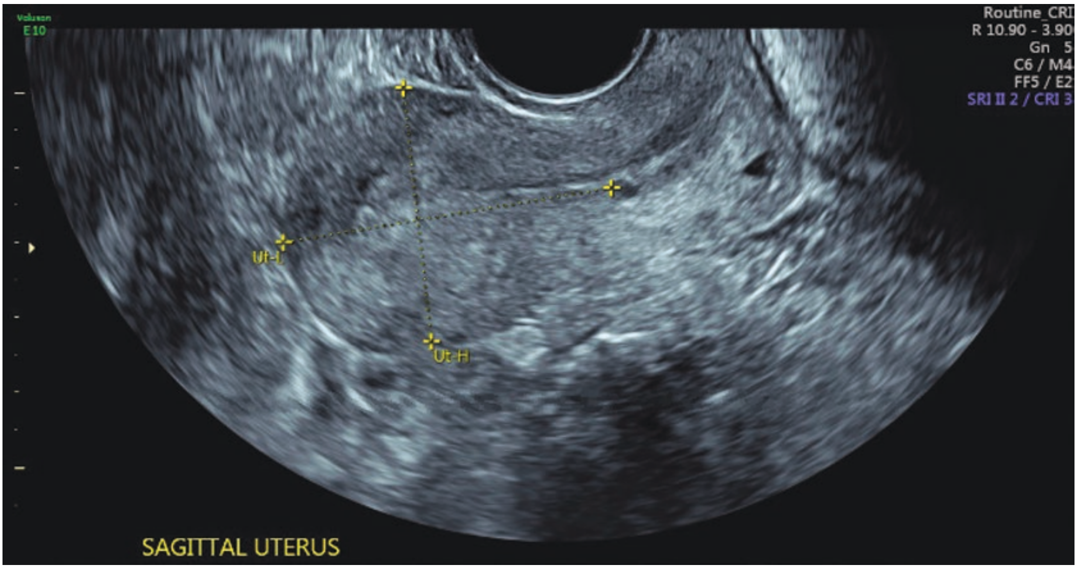
Voluson
E10
Routine_CRI
R 10.90 - 3.90
Gn 5
C6 / M4
FF5 / E2
SRI II 2 / CRI 3
Ut-L
Ut-H
SAGITTAL UTERUS

Fig. 3.1 Longitudinal length and the height, measured in the anterior-posterior (AP) diameter

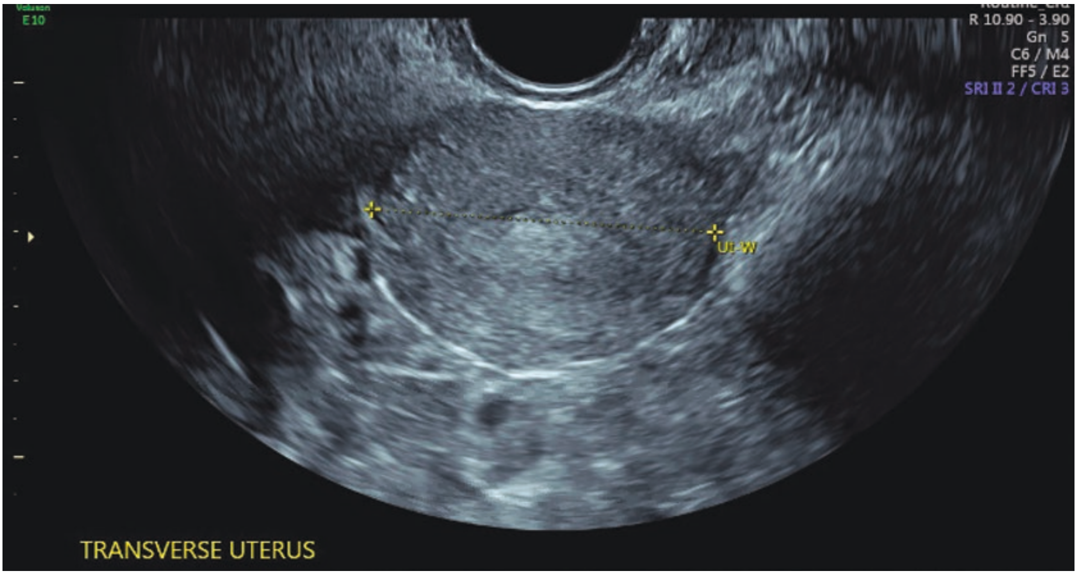
Voluson
E10
R 10.90 - 3.90
Gn 5
C6 / M4
FF5 / E2
SRI II 2 / CRI 3
Ut-W
TRANSVERSE UTERUS

Fig. 3.2 Transverse measurement of the uterus

cesarean section scars, and congenital uterine anomalies. Submucosal fibroids (Fig. 3.3) may affect fertility and reproductive outcomes, by impairing blood flow to the endometrium/myometrium, resulting in failed implantation and pregnancy loss. Surgical correction of these defects has been found to improve pregnancy outcomes. In contrast, intramural fibroids (Fig. 3.4) may also increase pregnancy loss and be associated with infertility, but which intramural myomas warrant surgical removal for fertility purposes is not well established [1]. The role of ultrasound for fibroid mapping is to, as definitively as possible, document fibroid dimensions, position, and endometrial distortion to allow for appropriate patient counseling by the care pro-

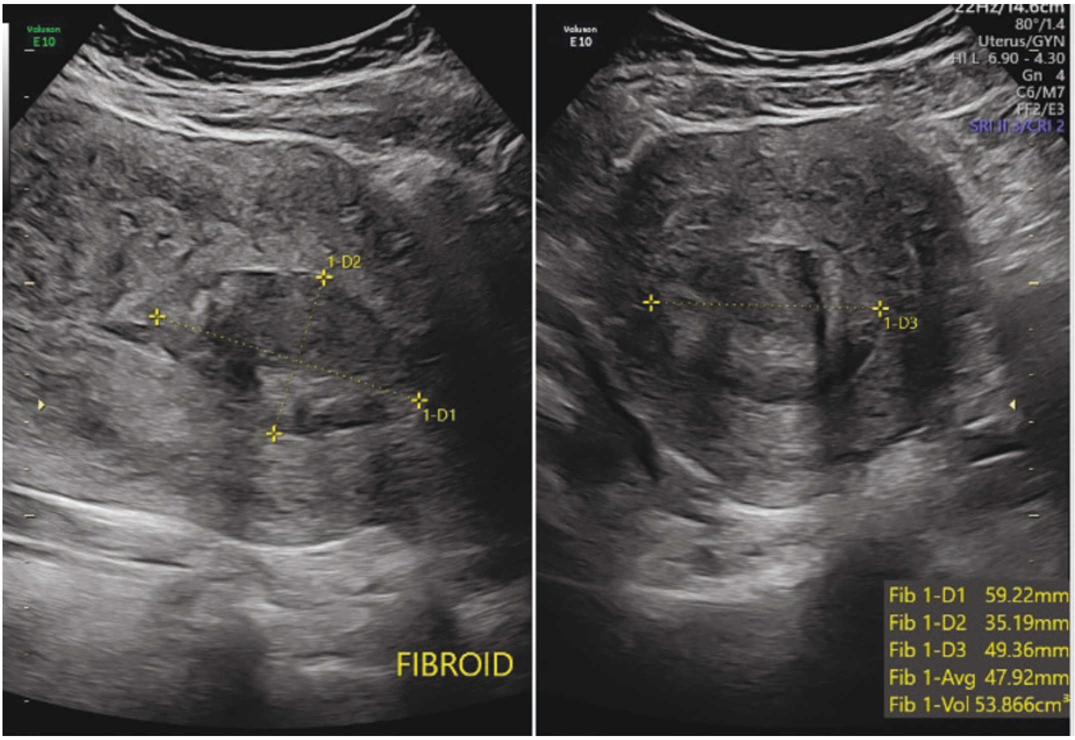
Voluson E10
1-D2
1-D1
FIBROID
Voluson E10
80°/1.4
Uterus/GYN
HI L 6.90 - 4.30
Gn 4
C6/M7
FF2/E3
SRI II 3/CRI 2
1-D3
Fib 1-D1 59.22mm
Fib 1-D2 35.19mm
Fib 1-D3 49.36mm
Fib 1-Avg 47.92mm
Fib 1-Vol 53.866cm³

Fig. 3.3 Submucosal fibroids

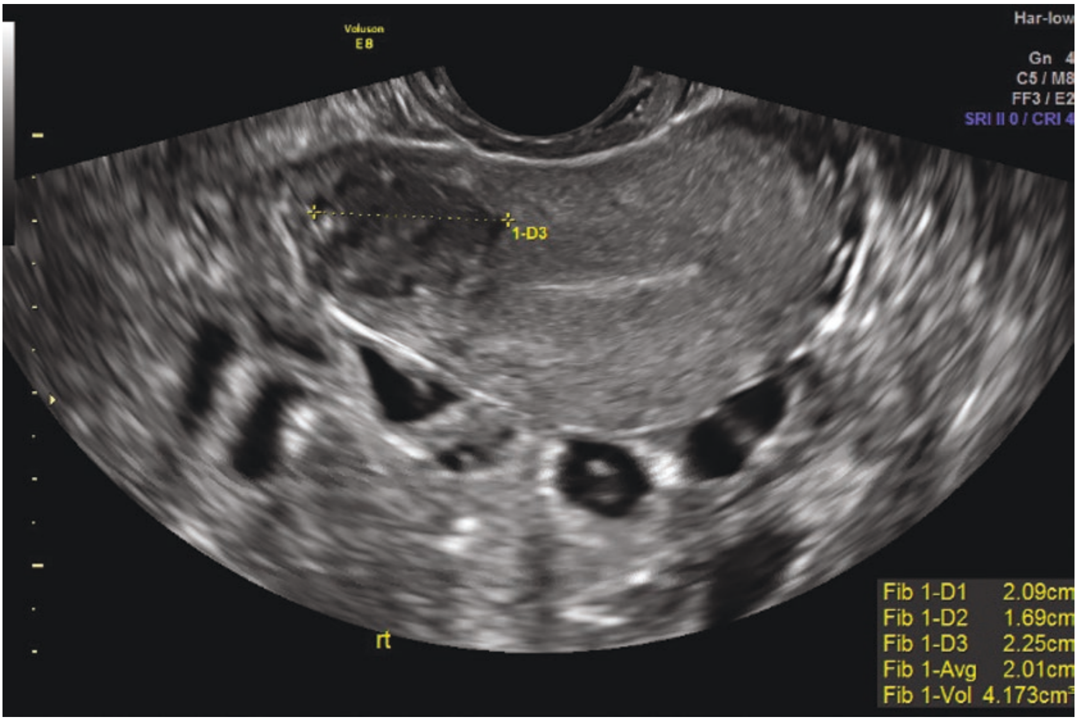
Voluson E8
Har-low
Gn 4
C5 / M8
FF3 / E2
SRI II 0 / CRI 4
1-D3
rt
Fib 1-D1 2.09cm
Fib 1-D2 1.69cm
Fib 1-D3 2.25cm
Fib 1-Avg 2.01cm
Fib 1-Vol 4.173cm³

Fig. 3.4 Intramural fibroids

vider. Some fibroids may grow large enough to impact fallopian tube architecture, making the passage of gametes into and out of the fallopian tube more difficult.

The endometrium is known to be a dynamic endocrine tissue, which responds to sex steroids to prepare to receive the developing embryo. Therefore, the endometrium is an important focus of the evaluation and treatment of the infertile patient. The overall thickness of the endometrium, when measured across the AP diameter, is correlated with the overall estrogen status and also correlates with the likelihood of embryo implantation during IVF treatment [2, 3]. The endometrial lining is expected to be very thin during the initial part of the menstrual cycle, when estrogen levels are at a nadir, and is noted to increase throughout the follicular phase and reaches a peak thickness around the time of ovulation and into the early luteal phase (Fig. 3.5). The ultrasound appearance of the estrogenized endometrium is typically described as a trilaminar appearance where there is a hyperechoic middle line visible separating each endometrial leaflet. In response to exposure to progesterone, there are physical changes in the endometrium such as changes in water content that typically result in a more uniform homogenous or isoechoic appearance of the endometrium. Unlike endometrial thickness, these patterns have not definitively correlated with pregnancy outcomes but the sonographic appearance of the endometrium is often used as a part of the clinical assessment. Pathologies of the endometrium are known to affect reproductive outcomes and are evaluated during the baseline examination. Intracavitary adhesions may be noted by an irregular or thin endometrium. Conversely, the presence of a thickened endometrial lining, on baseline ultrasound, may indicate a polyp or other defect is present within the endometrial cavity, which may need further evaluation to understand its impact on fertility. The thickness of the endometrium may also be increased with chronic anovulation or endometrial hyperplasia.

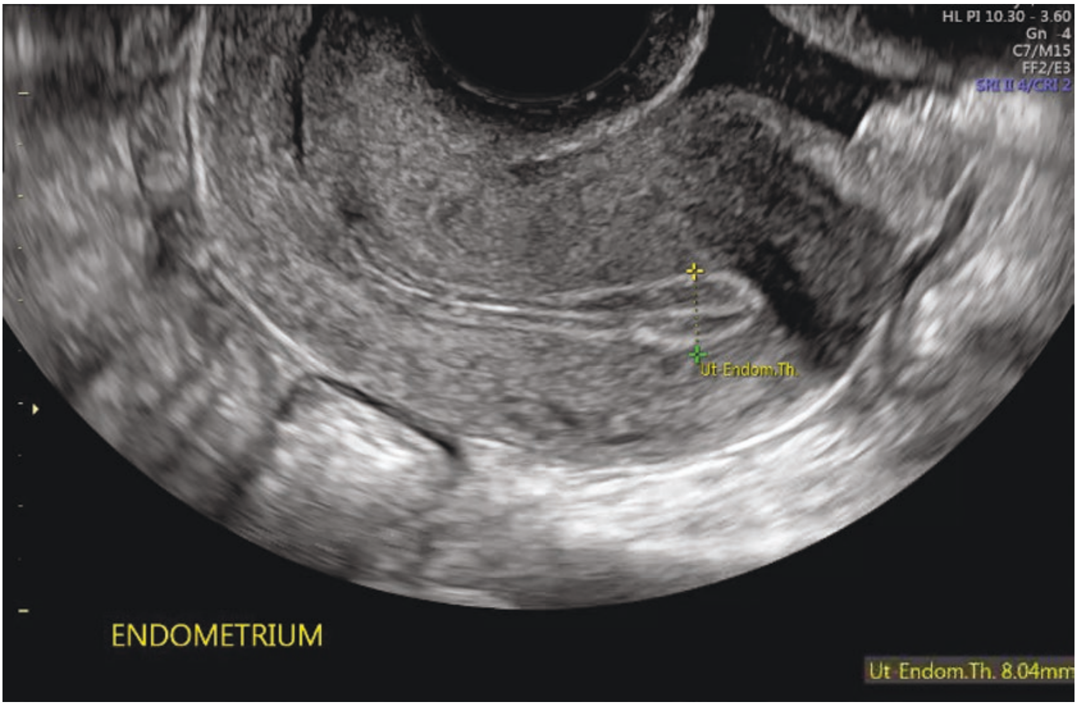

Fig. 3.5 Estrogenized endometrium–trilaminar appearance

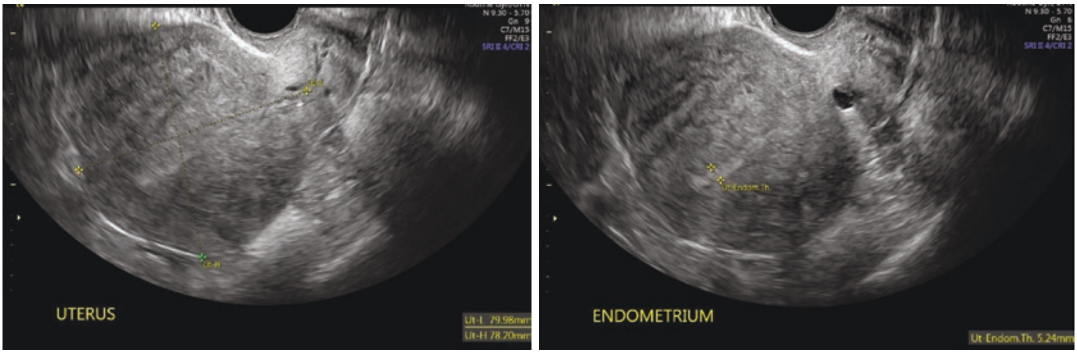

Fig. 3.6 Adenomyosis

The presence of endometrial glands and stroma located within the myometrium is termed adenomyosis. Adenomyosis is known to be clinically associated with dysmenorrhea, abnormal uterine bleeding, and pelvic pain and may co-exist with endometriosis. It is traditionally diagnosed histologically; however, several sonographic features are known to be correlated with its presence (Fig. 3.6) [4]. These include cystic areas in the myometrium as well as increased vascularity along the periphery of the uterine body and an indistinct endo-myometrial border. Because of the myometrial changes induced by adenomyosis, there is often the presence of a unique shadowing pattern in the myometrium that has been described as “venetian blinds” secondary to the shadowing produced by these defects on structures further from the ultrasound probe. In addition, one can often demonstrate asymmetry of the anterior and posterior aspects (in relation to the endometrium) of the myometrium and an overall increase in uterine volume without any identifiable discrete myometrial lesions such as myomas [5]. The presence of adenomyosis decreases reproductive outcomes after infertility treatment such as in vitro fertilization (IVF) and may also be related to an increased chance of pregnancy loss. MRI may also be used to further assess for the presence of adenomyosis when ultrasound is suspicious for this finding.

Ultrasound can be a very effective tool to assess for congenital abnormality of the uterus. Congenital uterine anomalies require 3D ultrasound or MRI to make the diagnosis, since the coronal surface of the uterus must be evaluated along with the endometrial cavity to distinguish between an arcuate uterus, a septate or subseptate uterus, and a bicornuate uterus (Fig. 3.7). This distinction is clinically very important since different Müllerian anomalies carry different reproductive risk. For example, a septum is associated with early pregnancy loss and can be hysteroscopically resected with resultant improvement in pregnancy outcomes [6]. Bicornuate uterus is associated with later pregnancy loss, as well as fetal malposition and is not typically considered for surgical correction. Arcuate uterus for most patients does not have significant reproductive risks and is typically not recommended for surgical correction. The differentiation of these pathologies can typically be very reliably assessed during 3D saline contrast sonography [7]. If there is only a plan for a pelvic sonogram, the luteal phase is the best time to perform a 3D ultrasound to assess for a congenital uterine anomaly since the endometrium will be thickened and hyperechoic and thus will act as its own contrast material. Based on the ability to identify relevant reproductive pathology, it can be considered good standard practice to perform a three-dimensional assessment of the uterus at least once for the infertile patient.

Ovaries

As part of the baseline ultrasound evaluation, both ovaries are identified, measured in three dimensions, their position described (especially if located high out of the pelvis or posterior to the

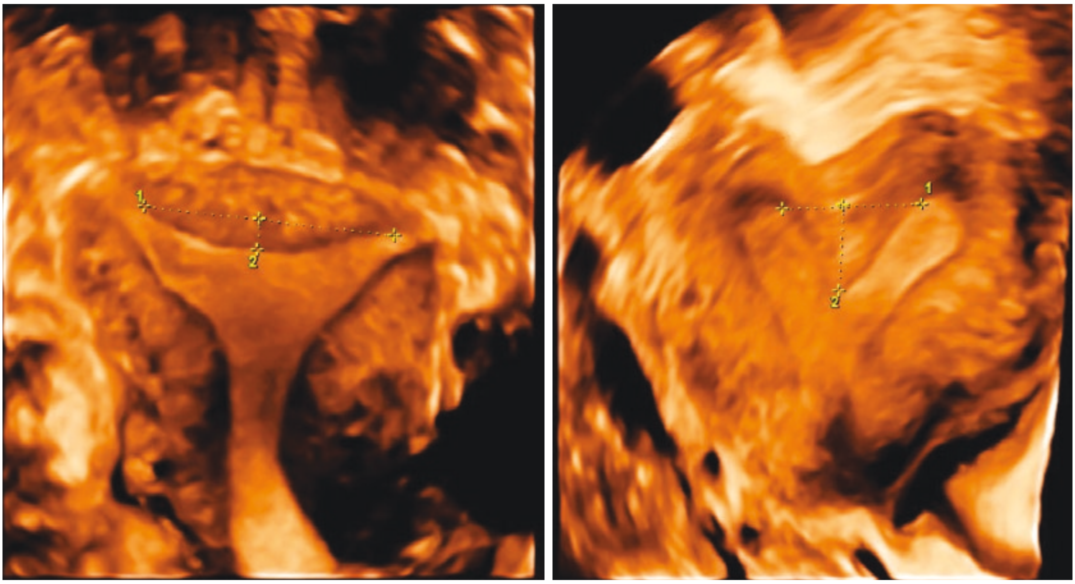

Arcuate Uterus

Septate Uterus

Fig. 3.7 Congenital uterine anomalies

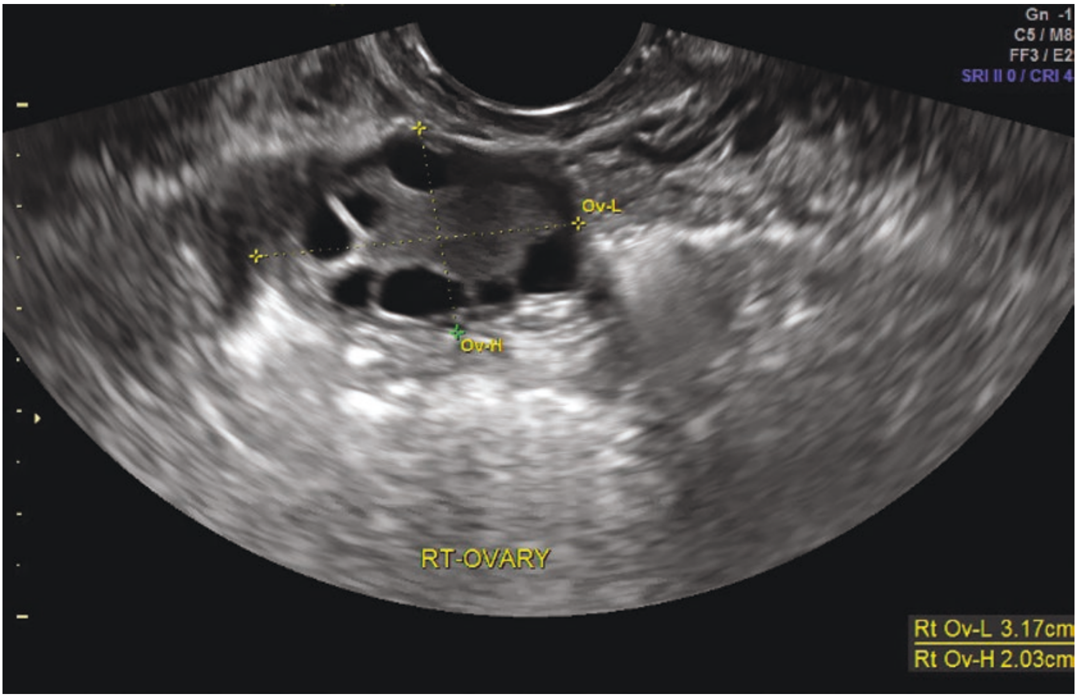
Gn -1
C5 / M8
FF3 / E2
SRI II 0 / CRI 4
Ov-L
Ov-H
RT-OVARY
Rt Ov-L 3.17cm
Rt Ov-H 2.03cm

Fig. 3.8 Ovarian measurements (H&L)

uterus), and the number of follicles (3–9 mm) in each ovary is counted (Fig. 3.8). This counting of follicles from 3 to 9 mm in size is termed an "antral follicle count" or AFC and has great importance for fertility patients. The AFC is a measure of ovarian reserve, and is one of the best

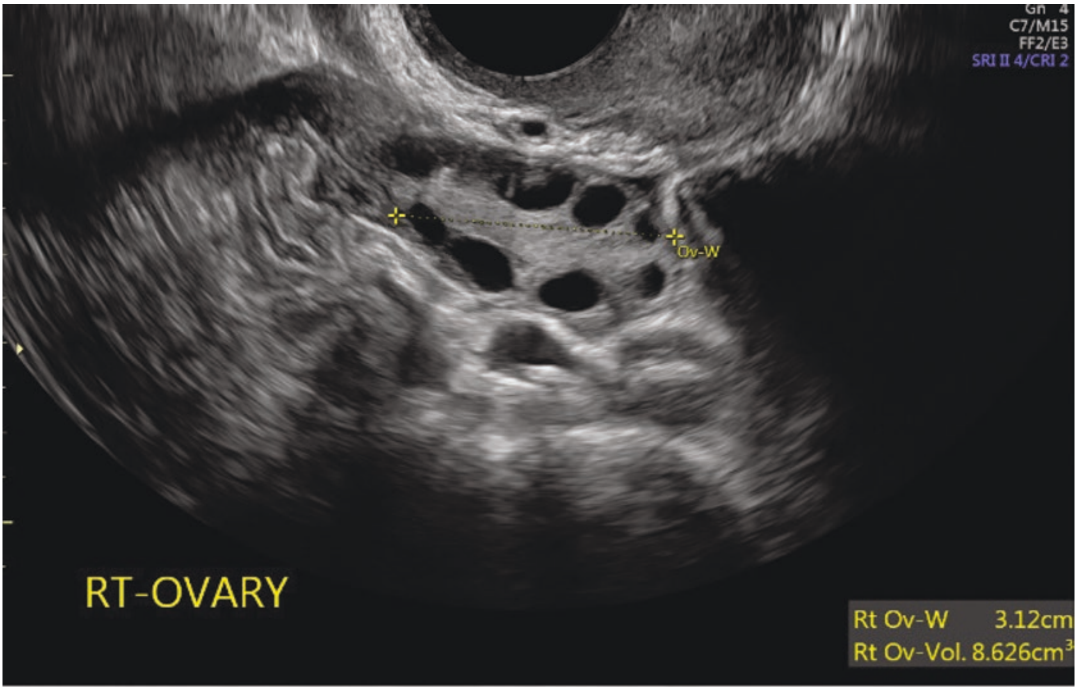

Fig. 3.9 Polycystic ovaries

estimates of the number of oocytes likely to be retrieved during an ovarian stimulation treatment cycle. AFC also correlates with risk of ovarian hyperstimulation syndrome and is useful to guide gonadotropin dosing during ART treatments [8]. A reduced antral follicle count (i.e., less than 8 total follicles in the ovaries) is a sign of diminished ovarian reserve and has negative implications for fertility treatment outcomes, particularly in older patients. Any ovarian cysts or masses are described, and further evaluation of these cysts/masses is performed with color or power Doppler.

The iliac vessels are used as a guide to find the ovaries and to determine the measurements. The length of the ovary is parallel to the length of the iliac vessel, and the height is perpendicular to this measurements. Next, an orthogonal view of the same organ is performed, and the width of the ovary is measured in this transverse view. The ovarian volume can be determined using a modified ellipsoid formula or a 3D volume. Ovarian size can be diminished by hormonal contraceptives, smoking, menopause (including premature menopause), radiation, among other disorders. An enlarged ovarian volume (>10 cm^3) and an increased number of antral follicles (>12 in a single ovary) are the basis for the sonographic appearance of polycystic ovaries as defined by the Rotterdam criteria (Fig. 3.9) [9]. More recent data have suggested that with today's higher resolution transvaginal ultrasonography, the polycystic ovary morphology be defined as greater than 19 follicles in a single ovary [10]. Given that there are two varying sonographic criteria for follicle count and polycystic ovarian morphology, we recommend reporting the follicle count and using a single standard for the assessment of polycystic ovary morphology. As expected, ovaries with cysts or masses will measure larger than normal.

In the infertility population like all reproductive age women, ultrasound is most likely to identify benign ovarian pathology when an ovarian mass is present. Physiologic or simple cysts may be commonly visualized as follicular cysts, which are anechoic with no internal debris and usually round or potentially collapsed after ovulation (Fig. 3.10). These are thin-walled with posterior enhancement, and no internal color flow with Doppler ultrasound.

Other commonly visualized cysts include hemorrhagic cysts, corpus luteum cysts, endometriomas, and mature teratomas. Hemorrhagic cysts and corpus luteum cysts can have several appearances from an initial simple cyst when the blood is still liquid to more complex cystic masses, as the blood organizes into clots, which gives the appearance of a reticular pattern of internal echoes (a lacy appearance, generally due to fibrin strands) and/or, lastly, a combination appearance (cystic and solid), with solid-appearing area with concave margins, no internal flow on color Doppler ultrasound, and fluid (Fig. 3.11). Usually the ovarian wall around a corpus luteum cyst has circumferential Doppler flow (Fig. 3.12) [11].

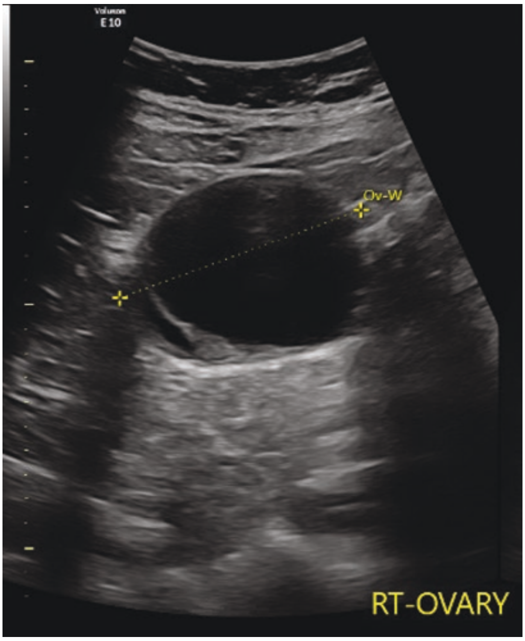

Fig. 3.10 Physiologic cyst

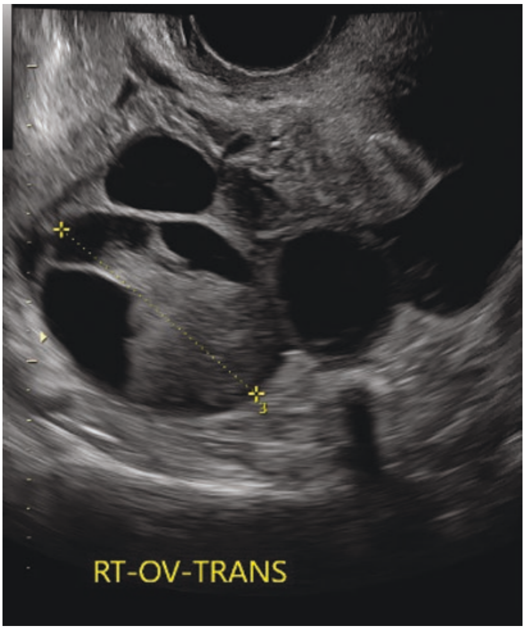

Fig. 3.11 Hemorrhagic cyst

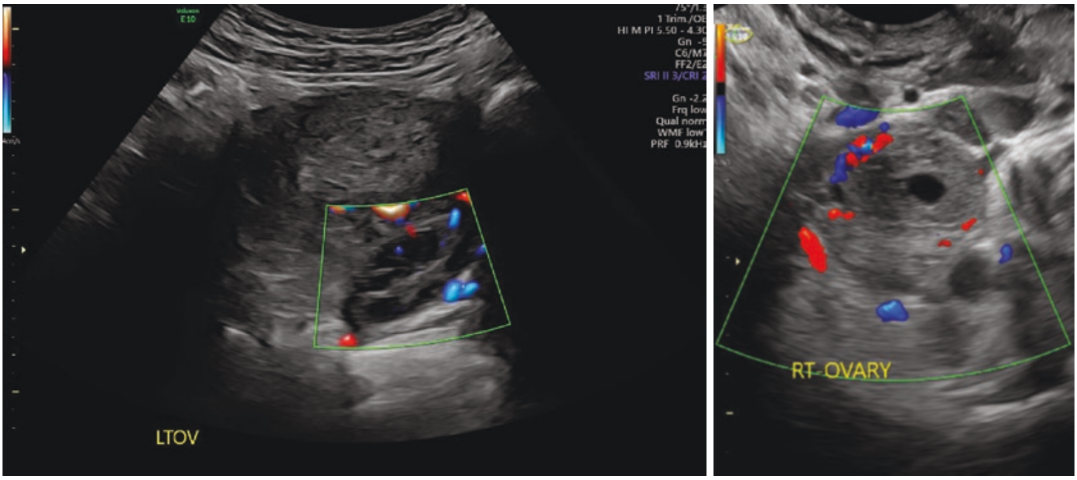

Fig. 3.12 Corpus luteum

The typical endometriomas have internal homogeneous low-level echoes, sometimes described as a “ground glass” appearance, and have no internal color Doppler flow, wall nodules, or other neoplastic features. In such masses, the additional features of multilocularity and/or tiny echogenic wall foci may occur (Fig. 3.13) [12]. Small endometriomas often do not need intervention and have not been found to definitively affect reproductive outcomes. The presence of endometriomas is an important factor for patient counseling since during transvaginal oocyte retrieval, if an endometrioma is entered with the aspiration needle, this can increase the chance of post procedure infection.

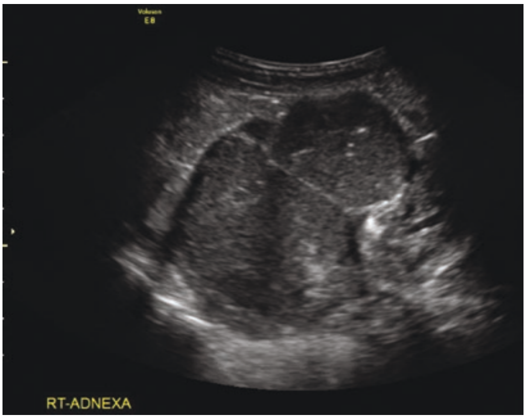

Fig. 3.13 Endometrioma

Mature cystic teratomas of the ovary (commonly known as “dermoid cysts”) can contain tissue arising from endoderm, mesoderm, and ectoderm lineages. They often contain sebaceous material, hair, and teeth and may also contain bone or virtually any other tissue type. The ultrasound appearances of dermoids consist of focal or diffuse hyperechoic components, hyperechoic lines and dots, and area of acoustic shadowing, with no internal flow on color Doppler ultrasound (Fig. 3.14). Some have a hyperechoic focus with shadowing called Rokitansky’s nodule. Color and/or power Doppler is also helpful in assessing adnexal masses. All abnormal findings need to be monitored with serial ultrasounds to determine which may warrant surgical inter-

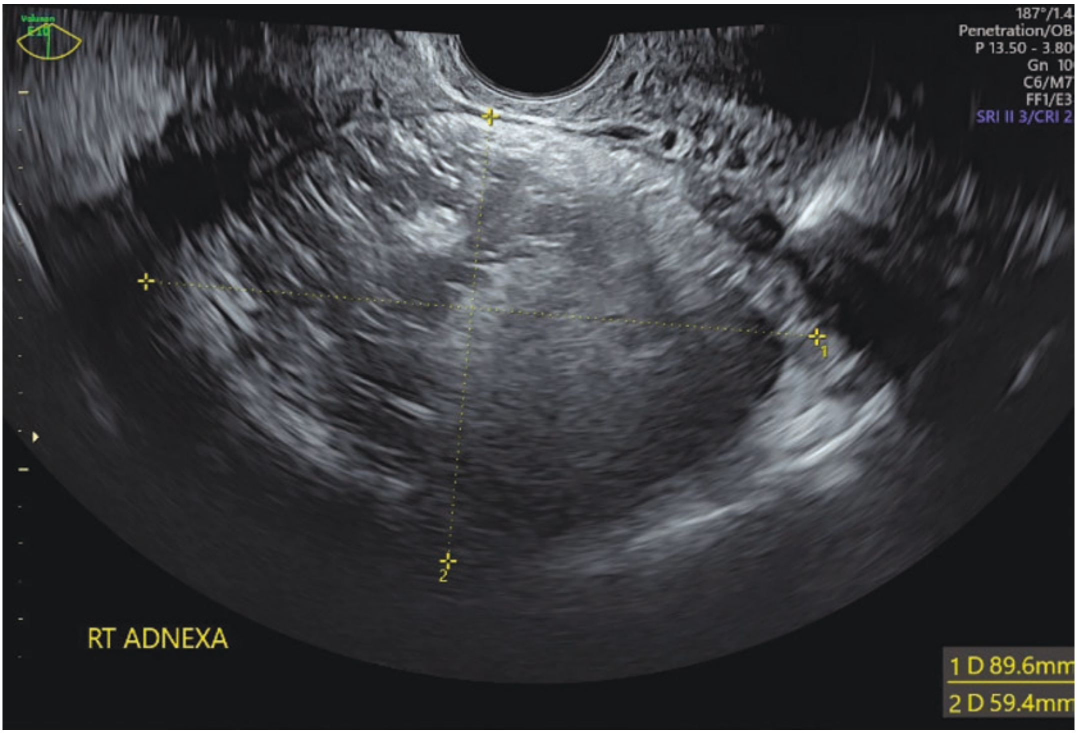

Fig. 3.14 Dermoid cyst

vention [11]. The presence of dermoids is also an important finding for counseling when patients are planning IVF oocyte retrieval. Puncture of a dermoid during the egg retrieval can result in leakage of contents resulting in peritonitis or abscess formation.

Other presentations to note include the situation of diminished ovarian reserve (DOR), where the ovaries will be much smaller and few or no antral follicles will be visualized. This finding can be supportive of a diagnosis of DOR and is relevant for fertility counseling.

Adnexa

Another critical component of the baseline ultrasound is to evaluate for any adnexal pathology. The most commonly encountered tubal findings are hydrosalpinx (Fig. 3.15) and paratubal cysts or cysts of Morgagni. Both of these findings can be confused with a dominant follicle, instead of a diseased tube, and it is important that the provider performing the ultrasound clearly assesses the location of the pathology (in, versus adjacent to, the ovary) and view the pathology in three dimensions, to ensure that optimal information is gathered from the study (Fig. 3.16). The presence of a hydrosalpinx has been shown to decrease the pregnancy rate with IVF and also increases the likelihood of ectopic pregnancy.

Miscellaneous

A variety of other findings are noted on the baseline ultrasound of the patient presenting with infertility. These may include free fluid around the ovaries or in the posterior cul-de-sac, as well as abnormalities in the bowel or surrounding structures. All abnormalities should be noted in the report.

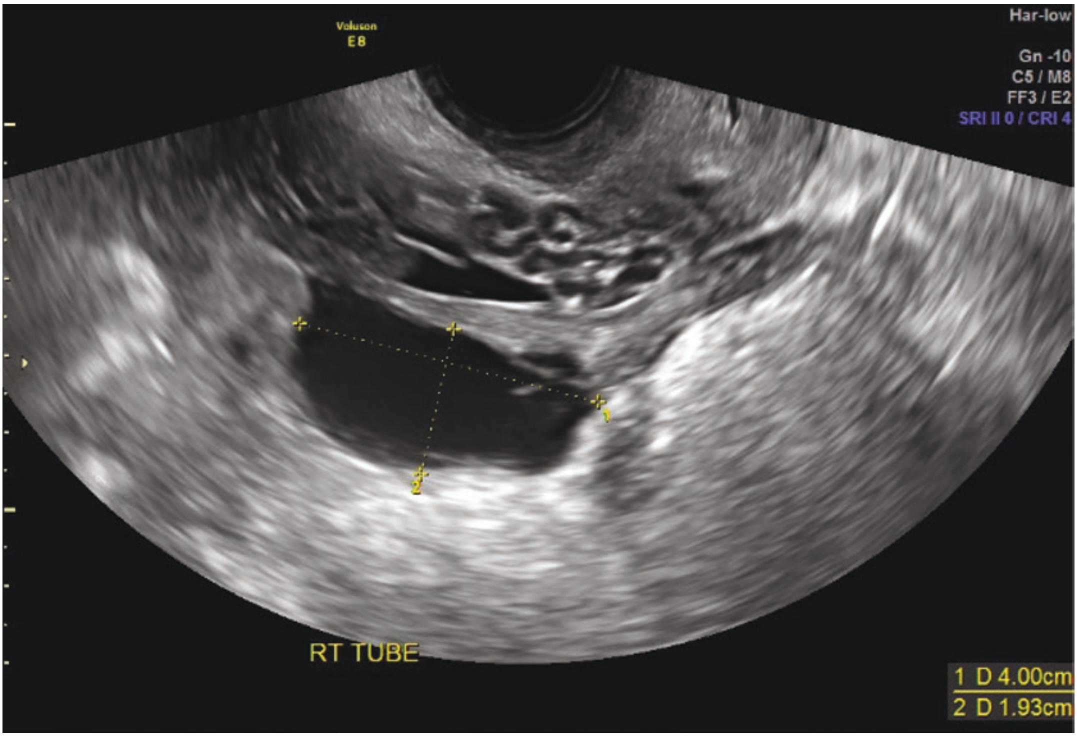

Fig. 3.15 Hydrosalpinx

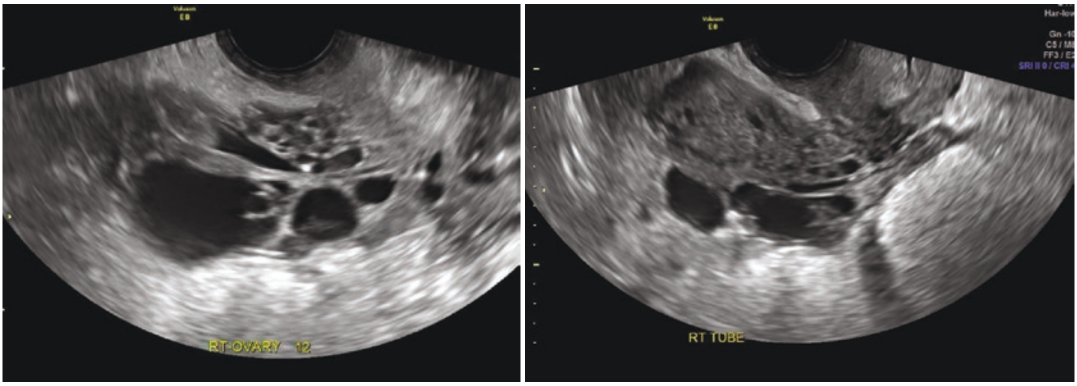

Fig. 3.16 Hydrosalpinx in three dimensions

Advanced Ultrasound Techniques and Reproductive Pathology

Ultrasound has been recently utilized as an imaging modality to diagnose deeply infiltrating endometriosis and pelvic adhesions. Both of these conditions can be a cause of infertility. Traditionally, surgery has been the gold standard methodology to diagnose both of these conditions.

Endometriomas can be reliably identified in most cases by ultrasonography due to their characteristic sonographic appearance. Classical appearance includes a persistent hypoechoic cyst within the ovary. There are atypical appearing endometriomas which are a fairly common clinical entity where the endometrioma may have a small solid component or mural nodule for example.

Deeply infiltrating endometriosis (DIE) has been proposed to be assessed via transvaginal ultrasonography. DIE is defined as lesions affecting the peritoneum that infiltrates either the retroperitoneal space or the wall of pelvic organs to a depth of at least 5 mm. The use of transvaginal sonography for this diagnosis requires specific expertise, and studies have shown varying degrees of accuracy for the diagnosis. However, this does show great promise in that there can be a high degree of sensitivity and specificity. DIE nodules typically appear as hypoechoic lesions with nodular or linear areas of peritoneal thickening with irregular borders (Fig. 3.17). Lesions on the bowel may appear to penetrate the bowel wall and distort the normal architecture [13]. Regarding the ultrasound diagnosis of DIE, the sensitivity can range from 50% to 60% with the specificity typically over 90% [14].

Pelvic adhesions can often be diagnosed by the absence of the sliding organ sign. The sliding organ sign is a dynamic ultrasound test where during the performance of the transvaginal ultrasound, the sonographer or clinician provides abdominal pressure over the adnexa to see the mobility of the ovaries (or any other structure) which can be captured with a cine loop [15]. Immobile adnexae are very often associated with the presence of pelvic adhesions. This test is also important in patients considering IVF who have ovaries in an unusual anatomic location. If the ovaries are mobile, then while the patient is under anesthesia, the clinician can often mobilize the ovaries with pressure in order to position them for safe transvaginal retrieval. If the ovaries are fixed in a difficult location to access (posterior to the uterus or high in the pelvis), then the patient can be counseled that this may increase the risk of her procedure or that abdominal oocyte retrieval may be needed (Fig. 3.18). The use of real time dynamic transvaginal ultrasound is a fairly reliable method to diagnose pelvic adhesions and cul-de-sac obliteration in the hands of a skilled operator [13].

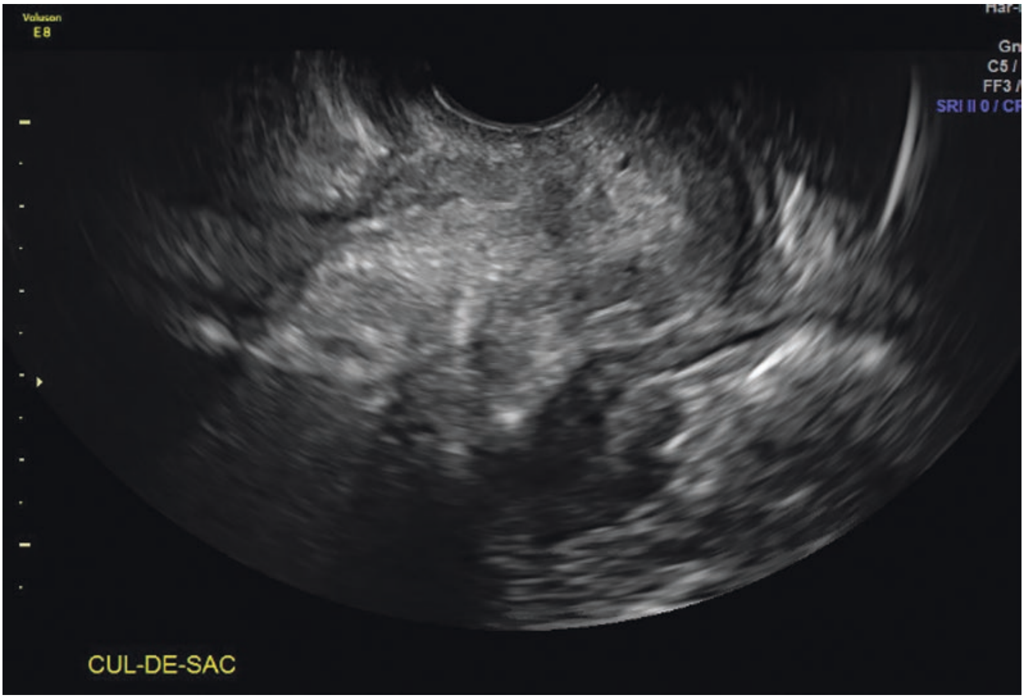
Voluson
E8
Gn
C5 /
FF3 /
SRI II 0 / CF
CUL-DE-SAC

Fig. 3.17 DIE

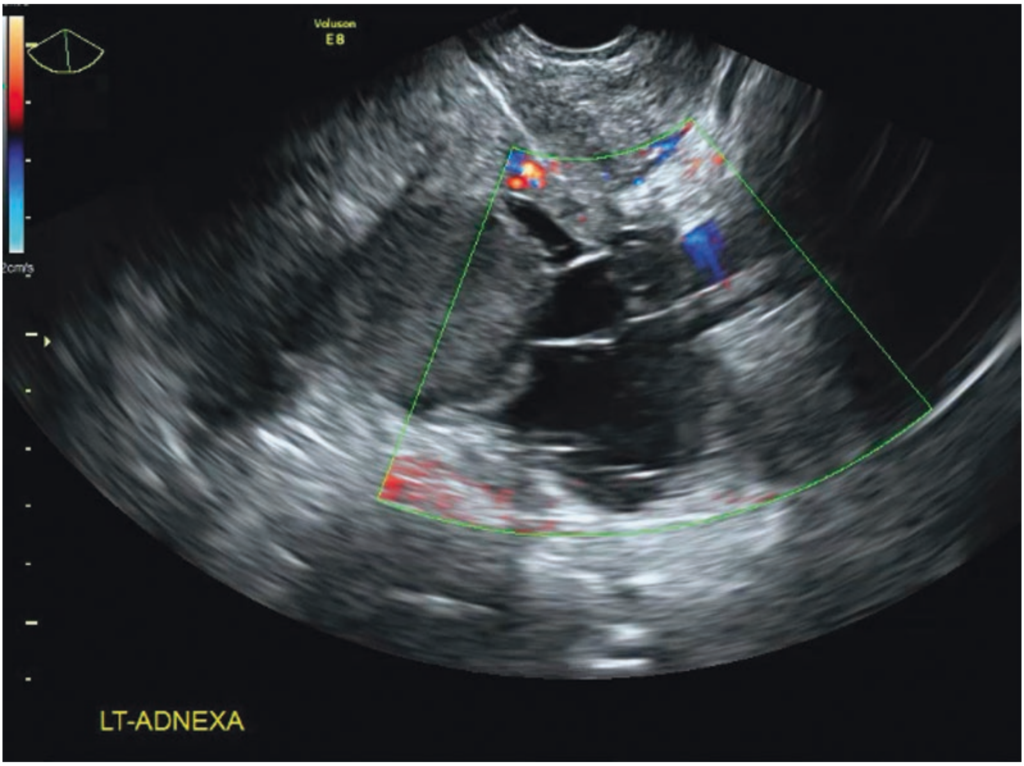
Voluson
E8
2cm/s
LT-ADNEXA

Fig. 3.18 Fixed ovaries, difficult to access

Since both endometriosis and associated pelvic adhesions can result in infertility, ultrasound is therefore potentially very helpful in determining which patients may benefit from surgery to either optimize natural fertility or assisted reproductive technology (ART) outcomes. These examples illustrate that in addition to the images captured during the ultrasound, much more clinically relevant information can be gathered during the process of active sonography.

Contrast Infusion Sonography for Uterine Cavity Assessment and Tubal Patency Assessment

The evaluation of the infertile female patient requires an assessment of the uterine cavity and an assessment of tubal patency. This information is critical in the decision of need and type of treatment offered to the patient. 3D sonohysterography is considered the gold standard imaging study for assessment of the uterine cavity.

The uterine cavity is best evaluated when the endometrium is thin and there is no chance of pregnancy (pre-ovulatory) which is typically cycle days 5–12 for most patients. The assessment of the uterine cavity is optimally performed with a 3D saline infusion sonohysterogram (SHG). Multiple studies have reported an increased sensitivity and specificity for intracavitary pathology with SHG compared to hysterosalpingogram (HSG). The SHG allows for concurrent assessment of the myometrium and endometrium which increases the accuracy of pathologic diagnosis. Being able to perform and interpret the ultrasound exam in real time is a benefit of the SHG and, unlike an HSG, this test typically also accurately identifies the structural etiology resulting in the abnormal filling defect (i.e., polyp, fibroid, adhesions). During a SHG procedure, a patient is placed in lithotomy position, vagina and cervix are prepped, and then, typically, a catheter is placed into the cervix or endometrial cavity. If a balloon is used, this balloon is then inflated to create a seal, preventing liquid from escaping the uterine cavity through the cervix. Sterile saline is then injected, and the uterine cavity is thoroughly examined in multiple planes, to detect any filling defects (Fig. 3.19), such as polyps (Fig. 3.20) or submucosal fibroid (Fig. 3.21). SHG used with color Doppler cannot only identify a filling defect, but also can in the majority of cases identify the nature of the defect (i.e., polyp, fibroid, adhesion, etc.). Other pathology which can be detected includes intrauterine adhesions/synechiae also known as Asherman syndrome (Fig. 3.22). In a population of subfertile women, SHG has been shown to be more sensitive and specific in diagnosing intracavitary pathology than HSG, and comparable to the gold standard of hysteroscopy in the detection of intrauterine abnormalities [16].

The evaluation of the uterine cavity has traditionally been performed utilizing 2D ultrasonography, with the operator examining and sweeping through the cavity in sagittal and coronal planes, to evaluate the entire uterine cavity. As stated ear-

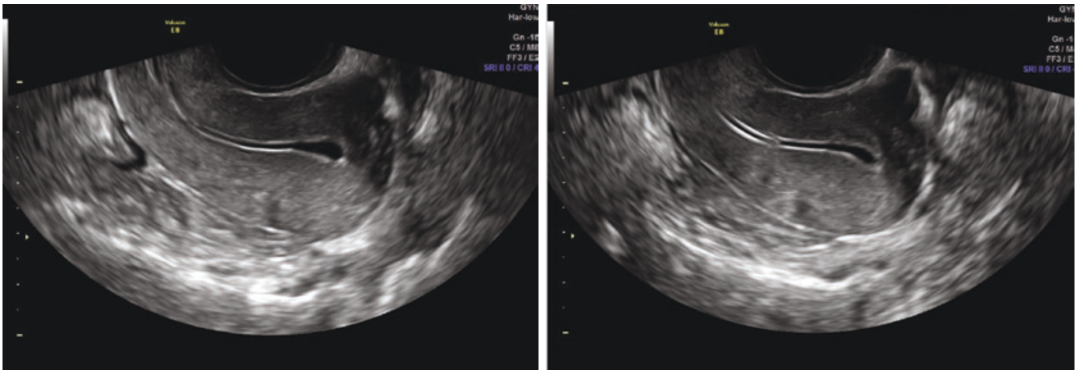

Fig. 3.19 SHG

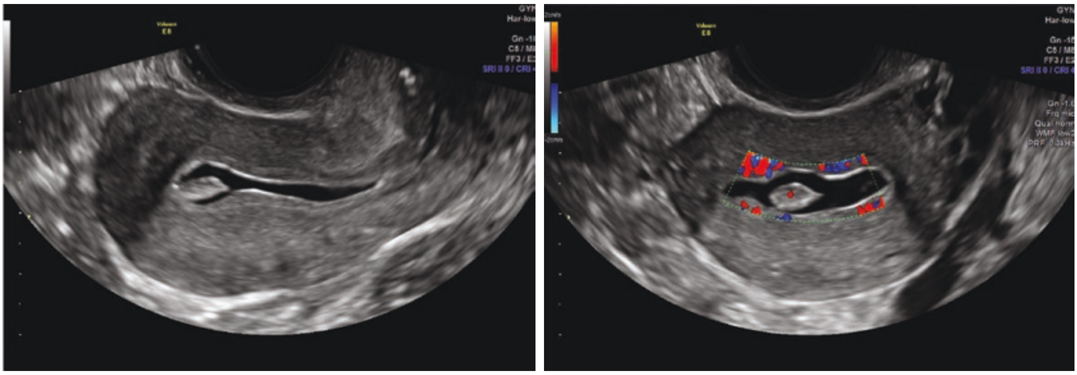

Fig. 3.20 SHG polyps

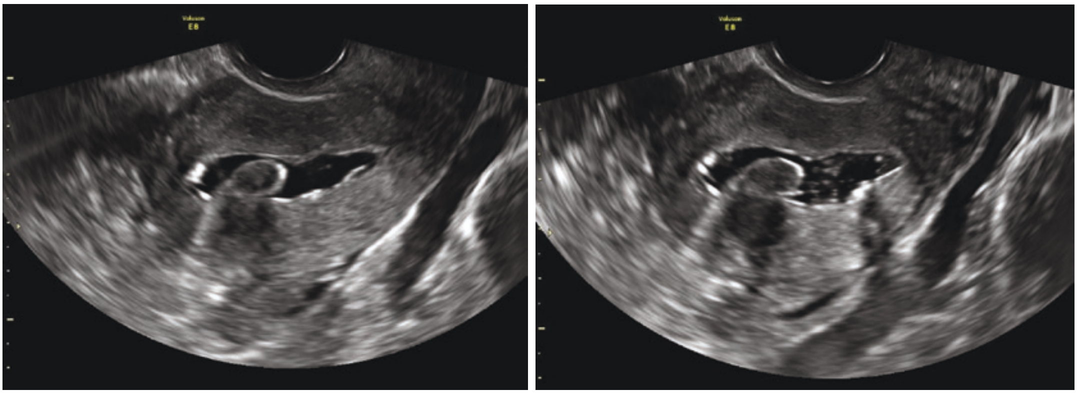

Fig. 3.21 SHG submucosal fibroid

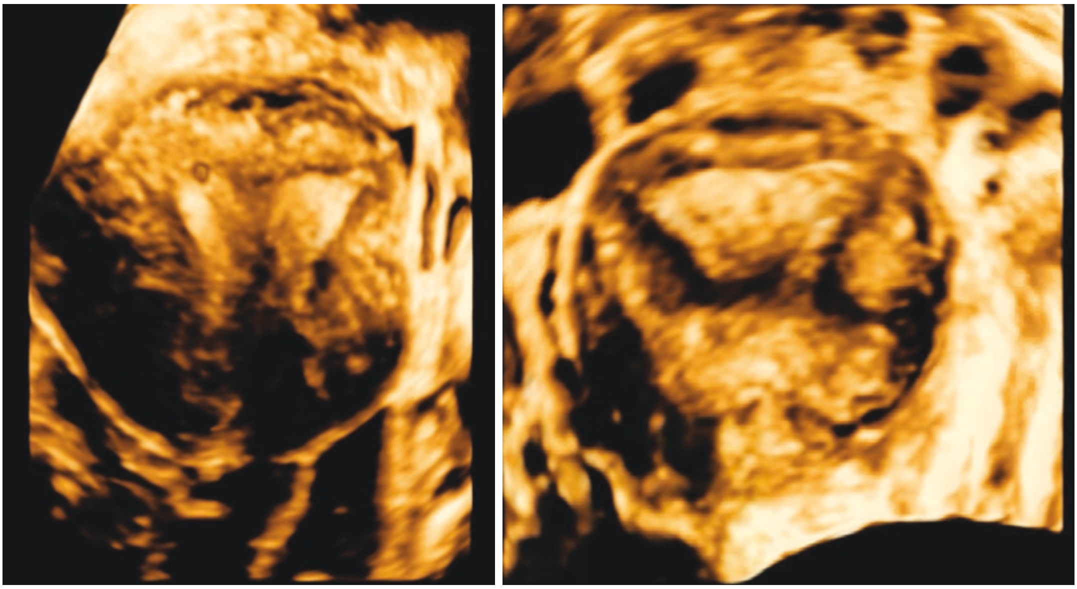

Fig. 3.22 Intrauterine synechiae

lier, there is overall a more complete assessment of the uterine cavity and contour with the use of 3D ultrasound during the SHG procedure.

Assessment of tubal patency is essential for infertility patients as a diagnostic test as well as a test to help guide fertility treatment therapies. Tubal patency evaluation has traditionally been performed as a radiographic procedure, called a hysterosalpingogram (HSG) in which contrast dye is injected through a cannula into the uterine cavity and the uterine cavity and Fallopian tubes images with fluoroscopy. More recently, ultrasound is being increasingly used for tubal patency assessment instead of hysterosalpingography (HSG). When ultrasound is used with contrast medium to assess tubal patency, the procedure is termed hysterosalpingo-contrast sonography (HyCoSy) [17]. The procedure is most commonly performed using a mixture of aerated saline as the contrast medium and can be performed before or after assessment of the uterine cavity. Utilizing a transverse view of the uterine fundus near the cornua, aerated saline can be visualized with air bubbles traversing the proximal fallopian tubes. More specifically, the cornual portion of the uterus can be identifiable as a "lemon-appearing" transverse view of the uterus. It is often apparent to see a pencil thin line going from the endometrium into the proximal tube; however, if this is not observed, then the passage of the echogenic bubbles can be visualized traversing the cornua as evidence of tubal patency (Fig. 3.23). Typically bubbles can be seen exiting both cornua if tubes are patent. Tilting of the patient's pelvis may help to assess the contralateral tube if the bubbles are preferentially flowing into one fallopian tube.

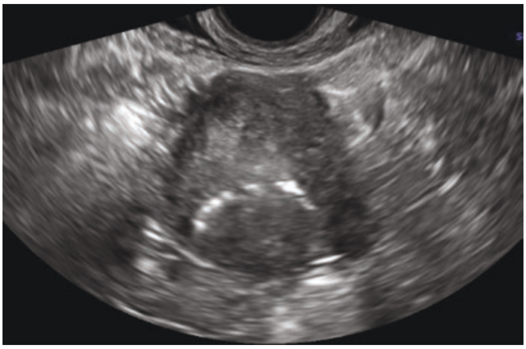

Fig. 3.23 Echogenic bubbles traversing the cornua during HyCoSy

There are a number of reasons why HyCoSy is of potential benefit for patients and clinicians. Unlike HSG, ultrasound assessment also allows for assessment of the myometrium and ovaries. Therefore, one can get a full anatomic assessment from a single imaging study as opposed to requiring two imaging studies if HSG is utilized. HSG does require low-level radiation exposure for the fluoroscopy and has increased risk of allergic reaction due to contrast/iodine allergy possibility. Furthermore, HSG typically requires access to radiologic equipment which many REI practices do not have, whereas every REI clinic will typically have multiple ultrasound machines. Ultrasound tubal assessment does have limitations, however. The main limitation is that the procedure may not be diagnostic in women with specific anatomic issues such as large uterine fibroids or if there is shadowing from other issues such as bowel gas. Also, the ability to identify tubal architecture or loculated spill is not present. For women who are at low or average risk for tubal pathology, it is very reasonable to use ultrasound contrast sonography (HyCoSy) for tubal patency assessment. It is important to not only document tubal patency, but to also assess for any hydrosalpinx during the study. The presence of a hydrosalpinx has negative implications for fertility prognosis with IVF and can be surgically treated to improve fertility outcomes [18]. There is a commercially available device (FemVue) which creates a stream of aerated saline for the purpose of HyCoSy. The contrast of the air with the saline provides an effective tool to visualize air bubbles exiting the cornua into the fallopian tubes (Fig. 3.24). One can also attempt to create a stream of aerated saline with manual agitation of a syringe partly filled with saline. The use of foam contrast instead of aerated saline may even further improve upon tubal patency assessment with ultrasonography [19]. Our practice is that for patients at high risk of tubal disease we perform hysterosalpingogram, and for the majority of patients we have found that we can effectively determine tubal patency with hysterosalpingo-contrast sonography and the use of aerated saline as the distension media.

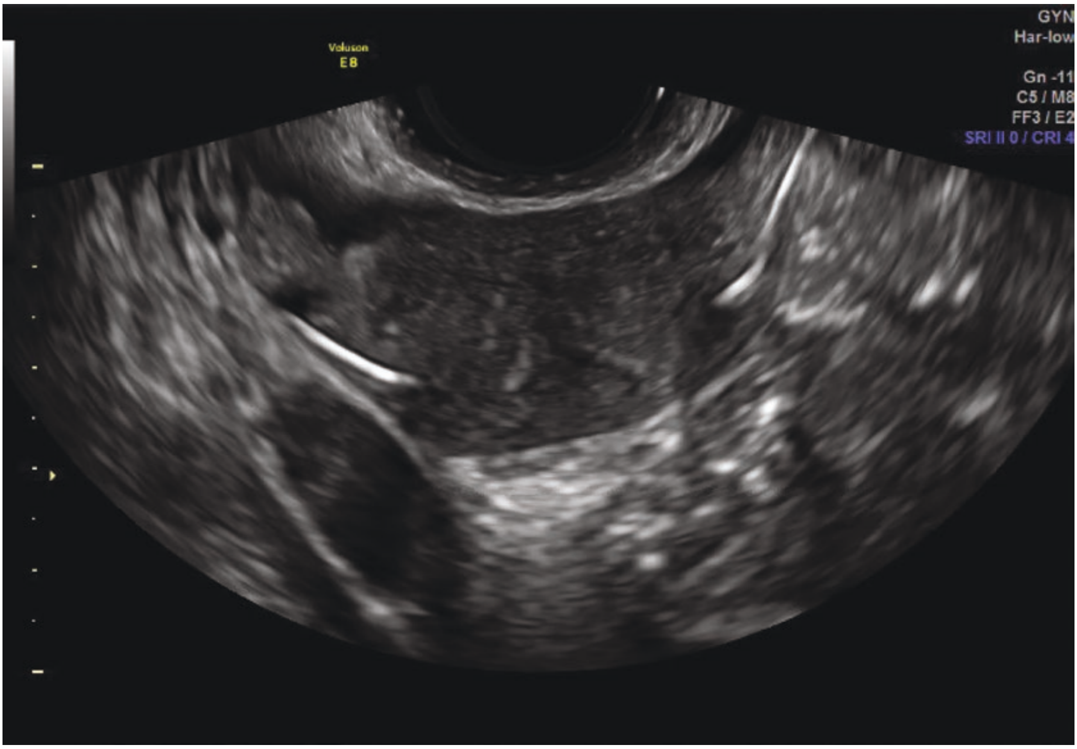

Fig. 3.24 FemVue bubbles

Follicular Monitoring Ultrasounds

In addition to the initial infertility workup, ultrasound is an integral part of infertility treatments: follicular monitoring, oocyte aspiration, and embryo transfers. Transvaginal ultrasound is the preferred modality for follicular monitoring of the infertile patient throughout treatment. Low level, oral fertility treatments do not necessarily require regular ultrasound monitoring. Mid-cycle sonographic confirmation of a dominant follicle, however, may be employed. Any treatment using gonadotropin injections for ovulation induction, or any form of in vitro fertilization (IVF), requires sonographic monitoring on a frequent basis, possibly even daily depending on the ovarian stimulation response. Ultrasound monitoring has been shown to increase the efficacy of ART and to decrease the risks of treatment such as ovarian hyperstimulation syndrome (OHSS) [20]. Ultrasound can also identify patients at increased risk during IVF, through identification of specific pathology known to increase risk such as hydrosalpinges or ovarian masses such as endometrioma or mature teratoma in the ovary, or ovaries in a challenging anatomic position. This can allow for improved patient counseling prior to treatments and appropriate risk assessment.

The primary goal of the infertility specialist is to identify optimal timing for certain key elements of fertility treatments: time of ovulation to optimize intrauterine insemination, time of follicle maturation for human chorionic gonadotropin administration, and time of optimal oocyte retrieval to facilitate aspiration of oocytes prior to ovulation. This is reliant on serial ultrasounds and the monitoring of the growth of ovarian follicles in the mid and late follicular phase, in conjunction with serum hormonal assessments.

Traditionally, 2D ultrasound was performed. In order to calculate the optimal timing for intervention, 2D measurements of follicles (typically in two orthogonal planes) were made and their mean was taken to be the true follicle diameter. However, these measurements were highly subject to variation with a trend of greater measurement errors in larger follicles as well as decreased reliability of follicular measurements with increasing number of follicles [21]. Additionally, follicles are not necessarily symmetrical in shape, thus making it difficult to determine the optimal plane in which to measure irregular shaped follicles. Thus came the advent of Sonography-based Automated Volume Count (SonoAVC), a 3D US technology, which utilizes ovarian mapping to automatically generate a set of measurements and calculate follicular volume for each follicle in the ovaries. Since its introduction, the follicular volumes measured and calculated with the automated volume count (AVC) have proven to be in accordance with true aspirated volumes, providing more accurate data than traditional 2D measurements [22].

Accurate determination of follicle maturation is essential for optimal fertility outcomes, both in oral medicated cycles (such as Clomid) and injectable gonadotropin stimulated cycles for IVF. It is well established that mean follicle diameter as measured with 2-D TVUS correlates with the likelihood of a follicle containing a mature egg as well as overall pregnancy rates [23]. Importantly, these correlations have been shown to be dependent on the size down to a 1–2 mm gradation. Therefore, accuracy of follicular measurement is important for optimal treatment outcomes. Technically, when measuring follicles with 2-D TVUS, it is recommended to measure to each follicle when it is in its sharpest focus using two orthogonal vectors, with one of the diameters measuring the follicle in its maximal diameter. Of course, not every follicle is ellipsoid and clinical judgment must be used for the measurement of irregularly shaped follicles.

Clinical decisions are typically guided by measurement of the overall follicular cohort, expressed as mean follicle diameter for each follicle measured. The calculated volume of the follicle can be converted to a composite mean diameter assuming an ellipsoid shape, and therefore the medical assessment of the stimulation cycle and physician interpretation of the data are similar to these processes with 2D follicle measurements, with potentially more accurate follicular data. Additionally, the image acquisition can be faster and allow for post image processing for follicle calculation which may improve the patient experience with follicular monitoring during fertility treatments [24]. Automated follicle monitoring with SonoAVC has the potential to replace and is encouraged to be used interchangeably with conventional 2D measurements [22].

During the mid-cycle period, the ovary typically produces a dominant follicle within cycle days 10–15. Follicular monitoring revolves around the tenet that once recruited, a stimulated ovarian follicle is expected to grow by approximately 1.5–2 mm/day once follicles reach the growing stage of 13 mm or larger, as detected by ultrasound, until full follicular maturation (typically lead follicle size 18–20 mm). Therefore, the frequency, timing, and reliable sonographic measurements from serial ultrasounds are extremely important. Ultrasound, additionally, offers a key advantage over hormonal monitoring alone, as many clinical situations introduce variability in the hormonal milieu, including peri-menopausal patients and PCOS patients with high LH levels, which may obscure ovulation predictor kits [25].

Ultrasound in ART Procedures (Oocyte Retrieval and Embryo Transfer)

Ultrasound has transformed the procedural elements of IVF within the past few decades. Initially, egg retrievals were performed via laparoscopy in operating rooms located in hospitals. The advent of high resolution transvaginal ultrasonography allowed for transvaginal oocyte retrieval which increased the safety and efficacy of follicular aspiration compared to laparoscopy or transabdominal ultrasonography guided oocyte retrieval. The improved visualization of the ovaries with transvaginal ultrasonography allows for more precise oocyte aspiration, shorter procedural times, and lower risk of complications [26]. Furthermore, the use of transvaginal sonography has therefore allowed for the practice of IVF outside of the hospital space.

Embryo transfer is the final procedure in an IVF cycle, where a catheter is inserted into the uterus and the fluid media containing the embryo is gently deposited into the uterine cavity. Originally this procedure was done based on the clinician's "feel" for catheter entry into the uterine cavity along with a previous tactile measurement of the uterine depth. The use of transabdominal ultrasound guidance has significantly improved the efficacy of the embryo transfer procedure. Today, it is standard practice to use abdominal ultrasound guidance during the embryo transfer. It has been shown that embryo deposition based on ultrasound assessment approximately 1–1.5 cm from the uterine fundus improves pregnancy rates and is considered a best practice for embryo transfer [27]. Ultrasound guidance has many potential benefits for the embryo transfer process. Ultrasound decreases the incidence of difficult embryo transfers, allows the operator to confirm optimal placement of the catheter within the uterine cavity, and decreases the likelihood that there will be fundal trauma which can result in blood in the cavity and uterine contractility, which have been shown to decrease implantation rates [28]. For some patients, transabdominal ultrasonography may be technically challenging (e.g., obesity, uterine myomas, uterine position). Studies have shown that in this setting, transvaginal ultrasound guidance for embryo transfer can achieve pregnancy rates comparable to routine cases where transabdominal ultrasonography is used [29, 30].

Conclusion

Ultrasonography is essential to the current practice of reproductive endocrinology and infertility. Ultrasound is utilized in several elements of the diagnostic testing for infertility ranging from overall assessment of pelvic anatomy, assessment of the uterine cavity and tubal patency and ovarian reserve. Ultrasound is essential for modern fertility treatments as follicular monitoring via transvaginal ultrasonography needs to be optimized in order to have optimal fertility treatment outcomes with reduced risks. The procedures of transvaginal oocyte retrieval and embryo transfer require ultrasound guidance for optimal safety and efficacy. Finally, more advanced ultrasound techniques are enabling the accurate diagnosis of endometriosis implants and pelvic adhesions and other pathologies that may be causes of infertility.

Teaching Points

- Ultrasound is an essential component of evaluation of female patients affected by infertility as well as an integral part of infertility treatments.
- Sonographic uterine evaluation helps reveal factors that contribute to infertility, subfertility, and early pregnancy loss.
- Ultrasound monitoring has been shown to increase the efficacy of ART, decrease the risks of treatment such as ovarian hyperstimulation syndrome, and identify patients at increased risk during IVF.
- Active sonography (real time dynamic TVUS) can be utilized as an imaging modality to diagnose deeply infiltrating endometriosis and pelvic adhesions, traditionally reliant on surgical diagnosis.
- SHG has been shown to be more sensitive and specific in diagnosing intracavitary pathology than HSG, and comparable to the gold standard of hysteroscopy in the detection of intrauterine abnormalities.
- Ultrasound allows for improved patient counseling prior to treatments and appropriate risk assessment.
- The advent of high resolution transvaginal ultrasonography allows for transvaginal oocyte retrieval which increases the safety and efficacy of follicular aspiration, allowing for more precise oocyte aspiration, shorter procedural times, lower risks of complications, as well as practice of IVF outside of the hospital space.
- Ultrasound guidance has many potential benefits for the embryo transfer process. It

decreases the incidence of difficult embryo transfers, allows the operator to confirm optimal placement of the catheter within the uterine cavity, and decreases the likelihood that there will be fundal trauma which has been shown to decrease implantation rates.

References

1. Somigliana E, Reschini M, Bonanni V, Busnelli A, Li Piani L, Vercellini P. Fibroids and natural fertility: a systematic review and meta-analysis. Reprod Biomed Online. 2021;43(1):100–10.
2. Liu KE, Hartman M, Hartman A, Luo ZC, Mahutte N. The impact of a thin endometrial lining on fresh and frozen-thaw IVF outcomes: an analysis of over 40 000 embryo transfers. Hum Reprod. 2018;33:1883–8.
3. Wu Y, Gao X, Lu X, Xi J, Jiang S, Sun Y, Xi X. Endometrial thickness affects the outcome of in vitro fertilization and embryo transfer in normal responders after GnRH antagonist administration. Reprod Biol Endocrinol. 2014;12:1–5.
4. Andres MP, Borrelli GM, Ribeiro J, Baracat EC, Abrão MS, Kho RM. Transvaginal ultrasound for the diagnosis of adenomyosis: systematic review and meta-analysis. J Minim Invasive Gynecol. 2018;25(2):257–64.
5. Van den Bosch T, Dueholm M, Leone FP, Valentin L, Rasmussen CK, Votino A, et al. Terms, definitions and measurements to describe sonographic features of myometrium and uterine masses: a consensus opinion from the Morphological Uterus Sonographic Assessment (MUSA) group. Ultrasound Obstet Gynecol. 2015;46:284–98.
6. Carrera M, Pérez Millan F, Alcázar JL, Alonso L, Caballero M, Carugno J, Dominguez JA, Moratalla E. Effect of hysteroscopic metroplasty on reproductive outcomes in women with septate uterus: systematic review and meta-analysis. J Minim Invasive Gynecol. 2022;29(4):465–75.
7. Cekdemir YE, Mutlu U, Acar D, Altay C, Secil M, Dogan OE. The accuracy of three-dimensional ultrasonography in the diagnosis of Müllerian duct anomalies and its concordance with magnetic resonance imaging. J Obstet Gynaecol. 2022;42(1):67–73.
8. Broer SL, Dólleman M, Opmeer BC, Fauser BC, Mol BW, Broekmans FJ. AMH and AFC as predictors of excessive response in controlled ovarian hyperstimulation: a meta-analysis. Hum Reprod Update. 2011;17(1):46–54.
9. Rotterdam ESHRE/ASRM-Sponsored PCOS Consensus Workshop Group. Revised 2003 consensus on diagnostic criteria and long-term health risks related to polycystic ovary syndrome (PCOS). Hum Reprod. 2004;19(1):41–7.
10. Dewailly D, Gronier H, Poncelet E, Robin G, Leroy M, Pigny P, Duhamel A, Catteau-Jonard S. Diagnosis of polycystic ovary syndrome (PCOS): revisiting the threshold values of follicle count on ultrasound and of the serum AMH level for the definition of polycystic ovaries. Hum Reprod. 2011;26(11):3123–9.
11. Levine D, Brown DL, Andreotti RF, Benacerraf B, Benson CB, Brewster WR, Coleman B, Depriest P, Doubilet PM, Goldstein SR, Hamper UM, Hecht JL, Horrow M, Hur HC, Marnach M, Patel MD, Platt LD, Puscheck E, Smith-Bindman R. Management of asymptomatic ovarian and other adnexal cysts imaged at US: Society of Radiologists in Ultrasound Consensus Conference Statement. Radiology. 2010;256(3):943–54.
12. Asch E, Levine D. Variations in appearance of endometriomas. J Ultrasound Med. 2007;26(8):993–1002.
13. Exacoustos C, Zupi E, Piccione E. Ultrasound imaging for ovarian and deep infiltrating endometriosis. Semin Reprod Med. 2017;35(1):5–24.
14. Guerriero S, Ajossa S, Minguez JA, Jurado M, Mais V, Melis GB, Alcazar JL. Accuracy of transvaginal ultrasound for diagnosis of deep endometriosis in uterosacral ligaments, rectovaginal septum, vagina and bladder: systematic review and meta-analysis. Ultrasound Obstet Gynecol. 2015;46(5):534–45.
15. Reid S, Condous G. Transvaginal sonographic sliding sign: accurate prediction of pouch of Douglas obliteration. Ultrasound Obstet Gynecol. 2013;41:605–7.
16. Soares SR, Barbosa dos Reis MM, Camargos AF. Diagnostic accuracy of sonohysterography, transvaginal sonography, and hysterosalpingography in patients with uterine cavity diseases. Fertil Steril. 2000;73(2):406–11.
17. Luciano DE, Exacoustos C, Luciano AA. Contrast ultrasonography for tubal patency. J Minim Invasive Gynecol. 2014;21(6):994–8. https://doi.org/10.1016/j.jmig.2014.05.017. Epub 2014 Jun 6.
18. Volodarsky-Perel A, Buckett W, Tulandi T. Treatment of hydrosalpinx in relation to IVF outcome: a systematic review and meta-analysis. Reprod Biomed Online. 2019;39(3):413–32.
19. Ludwin I, Ludwin A, Wiechec M, Nocun A, Banas T, Basta P, Pitynski K. Accuracy of hysterosalpingo-foam sonography in comparison to hysterosalpingo-contrast sonography with air/saline and to laparoscopy with dye. Hum Reprod. 2017;32(4):758–69.
20. Kwan I, Bhattacharya S, Woolner A. Monitoring of stimulated cycles in assisted reproduction (IVF and ICSI). Cochrane Database Syst Rev. 2021;4(4):CD005289. https://doi.org/10.1002/14651858.CD005289.pub4.
21. Peres Fagundes PA, Chapon R, Olsen PR, Schuster AK, Mattia MMC, Cunha-Filho JS. Evaluation of three-dimensional SonoAVC ultrasound for antral follicle count in infertile women: its agreement with conventional two-dimensional ultrasound and serum levels of anti-Müllerian hormone. Reprod Biol Endocrinol. 2017;15(1):96. https://doi.org/10.1186/s12958-017-0314-x.

22. Raine-Fenning N, Jayaprakasan K, Clewes J, Joergner I, Bonaki SD, Chamberlain S, Devlin L, Priddle H, Johnson I. SonoAVC: a novel method of automatic volume calculation. Ultrasound Obstet Gynecol. 2008;31(6):691–6. https://doi.org/10.1002/uog.5359.
23. Bessow C, Donato R, de Souza T, Chapon R, Genro V, Cunha-Filho JS. Antral follicle responsiveness assessed by follicular output RaTe(FORT) correlates with follicles diameter. J Ovarian Res. 2019;12(1):48. https://doi.org/10.1186/s13048-019-0522-4.
24. Re C, Mignini Renzini M, Rodriguez A, Dal Canto M, Buccheri M, Sacchi S, Bartolucci S, Fadini R, La Marca A. From a circle to a sphere: the ultrasound imaging of ovarian follicle with 2D and 3D technology. Gynecol Endocrinol. 2019;35(3):184–9.
25. Iyoke CA, Ugwu GO, Ezugwu FO, Ajah LO, Mba SG. The role of ultrasonography in in-vitro fertilization and embryo transfer (IVF-ET). Niger J Med. 2013;22(3):162–70.
26. Healy MW, Hill MJ, Levens ED. Optimal oocyte retrieval and embryo transfer techniques: where we are and how we got here. Semin Reprod Med. 2015;33(2):83–91.
27. Practice Committee of the American Society for Reproductive Medicine. Performing the embryo transfer: a guideline. Fertil Steril. 2017;107:882–96.
28. Schoolcraft WB. Importance of embryo transfer technique in maximizing assisted reproductive outcomes. Fertil Steril. 2016;105(4):855–60.
29. Anderson RE, Nugent NL, Gregg AT, Nunn SL, Behr BR. Transvaginal ultrasound-guided embryo transfer improves outcome in patients with previous failed in vitro fertilization cycles. Fertil Steril. 2002;77(4):769–75.
30. Larue L, Keromnes G, Massari A, Roche C, Moulin J, Gronier H, Bouret D, Cassuto NG, Ayel JP. Transvaginal ultrasound-guided embryo transfer in IVF. J Gynecol Obstet Hum Reprod. 2017;46(5):411–6.
31. Carson SA, Kallen AN. Diagnosis and management of infertility: a review. JAMA. 2021;326(1):65–76. https://doi.org/10.1001/jama.2021.4788.

4

Maternal Co-morbidities and First Trimester Ultrasound Examination

Elena Bronshtein and Karoline S. Puder

Introduction

Ultrasonography is one of the most important and useful diagnostic tools in obstetrics. It is a non-invasive, portable, quick, and safe technology. Ultrasound performed in the first trimester confirms an intrauterine pregnancy, establishes accurate dates, and is crucial in diagnosing early pregnancy failure and ectopic pregnancy. It is commonly used for risk assessment for aneuploidy, through measurement of nuchal translucency and identification of the presence or absence of the nasal bone. Moreover, ultrasound for fetal assessment of early pregnancy reduces the failure to detect multiple pregnancy by 24 weeks of gestation and is also associated with a reduction in induction of labor for post-term pregnancy [1]. Standard indications for first trimester ultrasound are shown in Table 4.1. These are addressed in detail in various chapters of this book. Several maternal conditions are known to be associated with an increased risk of fetal anomalies and may justify early or more detailed fetal anatomy survey.

Table 4.1 Standard indications for first trimester ultrasound [139]

1.	Confirmation of the presence of an intrauterine pregnancy
2.	Evaluation of a suspected ectopic pregnancy
3.	Defining the cause of vaginal bleeding
4.	Evaluation of pelvic pain
5.	Estimation of gestational (menstrual) age
6.	Diagnosis or evaluation of multiple gestations
7.	Confirmation of fetal cardiac activity
8.	Imaging as an adjunct to chorionic villus sampling, embryo transfer
9.	Localization and removal of an intrauterine device
10.	Assessing for certain fetal anomalies, such as anencephaly, in high-risk patients
11.	Evaluation of maternal pelvic masses and/or uterine abnormalities
12.	Measuring the nuchal translucency (NT) when part of a screening program for fetal aneuploidy
13.	Evaluation of a suspected hydatidiform mole

Late first trimester fetal anatomic and placental imaging are rapidly evolving. Imaging of the fetus in first trimester provides an opportunity to evaluate the structural integrity of the fetus [2]. Many anomalies that were historically diagnosed in the second trimester can be identified in the letter part of the first trimester by sonographers or sonologists [3–10]. Some malformations, such as anencephaly, alobar holoprosencephaly, ectopia cordis, body stalk abnormalities, large abdominal wall defects, megacystis, conjoined twins, molar pregnancy are usually identified [11–18].

E. Bronshtein (✉)
Department of Obstetrics and Gynecology, Kaiser Permanente, Fontana, CA, USA
e-mail: e.bronstein@kp.org

K. S. Puder
Beaumont Hospital, Royal Oak, MI, USA

© The Author(s), under exclusive license to Springer Nature Switzerland AG 2023
J. S. Abramowicz, R. E. Longman (eds.), *First-Trimester Ultrasound*,
https://doi.org/10.1007/978-3-031-24133-8_4

The development of high-frequency and high-resolution transvaginal ultrasound transducers, along with substantial improvement of the technology has resulted in the visualization of fetal anatomic structures in greater details earlier in gestation [19–30].

A recent systematic review by Karim et al. analyzed 30 studies to assess the diagnostic accuracy of ultrasound in the detection of congenital fetal anomalies before 14 weeks of gestation. The detection rate of major abnormalities in low-risk population was 46.1%; the detection of all abnormalities was 32.35%. In high-risk population, the overall detection rate was 61.18% [14].

This helps to shift the prenatal diagnosis from the standard second trimester anatomy scan into the first trimester.

Detection of abnormal findings in the first trimester increases the time available for diagnostic testing, patient counseling, and decision-making regarding the course of pregnancy. If termination of pregnancy is an option, then it is much safer in the first trimester.

On the other hand, the absence of major fetal structural malformations in the first trimester could reassure patients and reduce anxiety.

While there are some anomalies that will not be evident at a first trimester anatomy evaluation, due to the natural history of fetal malformations, and a second trimester anatomical survey remains the "gold standard," we will consider some patients who might benefit from first trimester anatomy ultrasound. Diagnostic performance of first trimester ultrasound in detecting major fetal structural abnormalities had been described as 29–78.8%, with an overall detection rate of 50% [31–33]. Scanning in the first trimester may be performed either transabdominally or transvaginally. It was demonstrated that the transvaginal approach is significantly better in visualizing the cranium, spine, stomach, kidneys, bladder, and limbs. Complete fetal anatomy surveys were achieved in 64% of transabdominal scans and 82% of transvaginal scans at 13–14 weeks of gestation [34]. Using both transabdominal and transvaginal ultrasonography, noncardiac anatomy was seen in 75% of fetuses with a crown-rump length of 45–54 mm and in 96% with a crown-rump length of more than 65 mm [35] (Figs. 4.1 and 4.2). There are no absolute contraindications to either transabdominal or transvaginal ultrasound in the first trimester, except patient refusal.

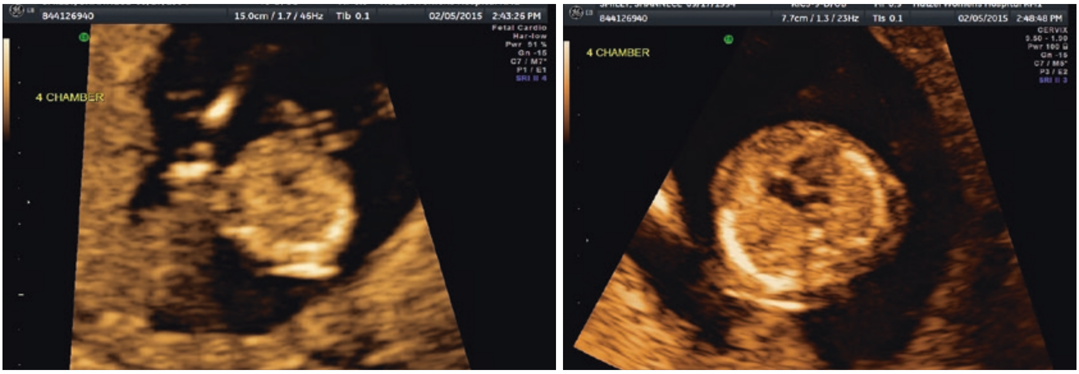

Fig. 4.1 A four-chamber view of the fetal heart at 13 weeks of gestation. Trans abdominal approach. Transvaginal approach

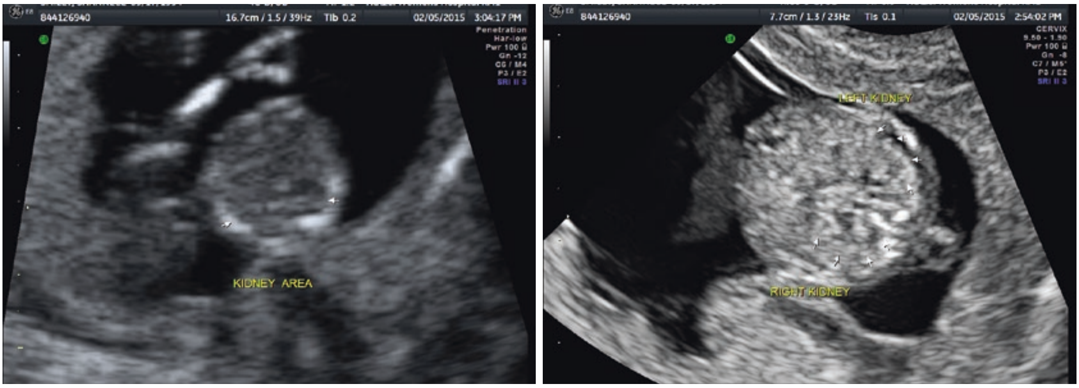

Fig. 4.2 Kidney area of the fetus at 13 weeks of gestation. Transabdominal approach. Transvaginal approach

Maternal Co-morbidities

Fetal anomalies may have various etiologies such as genetic, environmental, or multifactorial. Various maternal conditions and/or their treatment are known to be associated with structural anomalies or restricted growth. Sonographic measurements of fetal ultrasound parameters are the basis for accurate determination of gestational age and detection of fetal growth abnormalities. Crown-rump length (CRL) between 7 and 12 weeks is the most accurate parameter for first-trimester dating. First-trimester growth charts and predictive equations based on CRL instead of menstrual dating are more accurate [36]. Gestational age assessment is very important in the diagnosis of fetal conditions that involve early growth abnormalities due to conditions such as maternal hypertension, autoimmune disease, and preeclampsia. Clinical application of fetal biometry in abnormal growth is also important in cases of small- and large-for-gestational-age fetuses, chromosomal aberrations, and skeletal dysplasias.

Pregestational Diabetes

The prevalence of pregestational diabetes is observed in 1–2% of pregnancies [37–39].

Maternal pregestational diabetes is a well-known risk factor for congenital anomalies. The types of congenital anomalies in diabetic pregnancies differ from those of non-diabetic pregnancies.

The overall incidence of congenital malformations in diabetic pregnancies has been reported to be 6–13%, which is two- to four-fold greater than that of the general population [40–42]. A higher proportion of CNS abnormalities (anencephaly, encephalocele, meningomyelocele, spina bifida, and holoprosencephaly); cardiac anomalies (transposition of the great vessels, VSD, single ventricle, and hypoplastic left ventricle); and kidney anomalies [43–48] are reported. The detection rate, for CNS anomalies in the first trimester, has been reported to be as high as 100% in cases of anencephaly and encephalocele and only 18% in cases of spina bifida [32, 49], because the typical findings of "lemon sign" and "banana sign" do not appear until the end of the first trimester [50, 51].

Obesity is a well-known risk factor for and co-morbidity of diabetes. Moreover, several studies reported that women with pregestational diabetes and BMI higher than 28 kg/m^2 have a three-fold increase in the risk of congenital anomalies, and the risk further increases proportionally with BMI [52–54]. The potential role of first trimester anatomy ultrasound in the obese gravida is discussed further below.

Rates of fetal malformation appear to be similar for type 1 and type 2 diabetes [55]. It is well known that the poorer the glycemic control is periconceptionally or early in pregnancy, the greater the risk is for congenital anomalies [56, 57]. Lack of proper glycemic control during pregnancy is associated with profound fetal anomalies. Maternal hyperglycemia at the time of fertilization (defined as a glycosylated hemoglobin (HbA1c) >7.5%) has been associated with a nine-fold increase in congenital fetal anomalies and a four-fold increase in spontaneous abortion [58, 59].

Women with pregestational diabetes are advised to plan their pregnancy and optimize the glycemic control before pregnancy.

The American College of Obstetricians and Gynecologists recommend HbA1c level for pregnancy to be ≤6% before conception is attempted to decrease the risk of congenital malformations [60]. They also encourage to take at least 400 μg of folic acid daily to all women contemplating pregnancy [61], and 800 μg or 1 mg of folic acid in the presence of other risk factors for neural tube defects. However, there is not specific, prospective evidence that supports these recommendations, and the evidence suggests that folic acid is more protective against spina bifida than anencephaly and encephalocele [62]. However, unplanned pregnancies occur in 50% of all pregnancies, and the majority of women do not seek prenatal care until after embryogenesis (4–8 weeks of gestation). Thus, we should consider the evaluation of anatomy using first trimester ultrasound in a pregnancy complicated by pregestational diabetes. Although certain anomalies of the central nervous system may not be detected between 11 and 14 postmenstrual weeks, there have been case reports demonstrating the detection of congenital and major anomalies of the central nervous system using transvaginal ultrasonography in the first trimester [63].

While infants of diabetic mothers are at risk for a wide variety of malformations, one syndrome is strongly associated with diabetes. Caudal regression syndrome (Fig. 4.3) is a condition associated with hypoplasic lower extremities, caudal vertebrae, sacrum, neural tube, and urogenital organs [44, 47, 59]. Sirenomelia (the mermaid syndrome) has been described as a severe and lethal form of caudal regression sequence and characterized by a single lower extremity, absent sacrum, urogenital anomalies, and imperforate anus. The prevalence of sirenomelia has been reported to be 1–3 per 100,000. These malformations occur before the 9th pregnancy week, which has important implications in the prevention of malformations in diabetic pregnancies. The detection of sirenomelia has been described as early as 9 weeks of gestation [64].

A first trimester anatomy ultrasound may be considered in women with pregestational diabetes in order to detect NTD such as anencephaly and encephalocele, certain cardiac anomalies, and certain limb defects [25, 33].

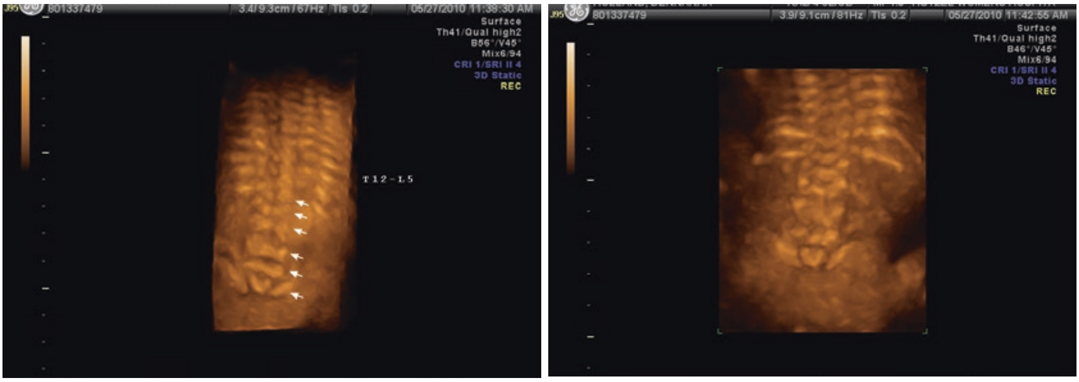

Fig. 4.3 Sacral agenesis in patient with pre-gestational diabetes

Obesity

Obesity in pregnancy, defined as maternal pre-pregnancy body mass index (BMI) of 30 kg/m^2 and extreme obesity with BMI >40 kg/m^2, is now recognized as a major syndrome in the Western world [65–67].

Based on the 2017–2018 National Health and Nutrition Examination Survey, the prevalence of obesity in the United States is 39.7% [68].

From 1999 to 2010, the prevalence of obesity increased from 28.4% to 34% in the women aged 20–39 years, with a higher prevalence in non-Hispanic black and Mexican American women [69]. From 1999–2000 through 2017–2018, the overall prevalence of obesity and severe obesity (defined as BMI greater or equal to 40) increased in United States.

Obese women are at increased risk of pregnancies affected by neural tube defects, hydrocephaly, cardiovascular, orofacial, and limb reduction anomalies [70].

It is also associated with an increased risk of congenital anomalies such as anal atresia, hypospadias, cystic kidney, pes equinovarus, omphalocele, and diaphragmatic hernia [71–75]. Thus, the ability to adequately visualize these structures at midtrimester prenatal ultrasound examination has significant clinical implications. Antenatal sonographic detection of congenital anomalies is difficult in obese patients. A patient's body mass index significantly affects the ability of the sonographer to achieve a complete anatomical survey. As maternal BMI increases, the rate of completion of anatomic surveys decreases and the number of scans required increases [76]. The detection rate of anomalous fetuses with either standard or targeted ultrasonography decreased by at least 20% in obese women compared to those with normal BMI [77].

Potential means to optimize ultrasonographic image quality in obese pregnant women include a vaginal approach [62] in the first trimester or using the maternal umbilicus as acoustic window, as well as tissue harmonic imaging [78–80].

Timor-Tritsch et al. proposed that early ultrasound examination can be effectively done with state-of-the-art equipment and in expert hands, and 13–14-week scan is more effective than an 11–12-week scan. Transvaginal scanning was significantly more useful than transabdominal as well [30].

Hendler et al. found that obesity increased the rate of sub-optimal ultrasound visualization for fetal cardiac and craniospinal structures and recognized that in these cases it may require visualization of these structures after 18–22 weeks using a transabdominal approach [81]. Gupta et al. suggested performing first–trimester fetal anatomic survey in addition to routine second trimester anatomy scan to improve the detection rate of congenital anomalies in obese patients [82]. Transvaginal sonography bypasses the maternal abdominal adipose tissue, and the late first-trimester transvaginal scan may be the only opportunity to visualize the fetal anatomy adequately in the obese pregnant patient [83].

Combining transvaginal and transabdominal approach yields the highest detection rate overall.

Maternal Conditions Associated with Congenital Heart Defects

Various teratogenic agents and maternal conditions have been implicated as the etiologic agents of CHD (see also Chap. 4). Maternal pregestational diabetes has 2–5 times the risk of CHD. Anomalies, such as transposition of the great arteries, truncus arteriosus, visceral heterotaxy, and single ventricle, are more common among offspring of diabetic mothers compared to women without diabetes [45, 84–87]. Ventricular septal defect and transposition of the great arteries are the most common cardiac defects in fetuses of diabetic mothers [84]. Establishing glycemic control before and early in pregnancy improves maternal and fetal outcomes, including reduction of CHD [88–90].

Overall, congenital heart disease (CHD) is the most common congenital anomaly, with an incidence of 6–8% of all live births, accounting for 30–45% of all congenital defects [91–93]. Prenatal diagnosis of CHD may be used to optimize care and potentially be lifesaving [94–96]. Fetal echocardiogram at 18–20 weeks gestation is a well-established method for evaluation of fetal cardiac structure and function. With improved technology, it has become feasible to obtain images of the fetal heart as early as 11 weeks gestation [28, 97]. Moreover, there is mounting evidence that an increased nuchal translucency (NT) is associated with major cardiac defects in the fetus and therefore represents an indication for specialized fetal echocardiography [98–100]. A meta-analysis showed that the use of the 99th centile (i.e., 3.5 mm) can identify around 30% of fetuses with CHD, supporting the notion that NT is the strongest predictor of CHD in the first trimester [98]. Abnormal ductus venosus (DV) blood velocity waveform (absent or reverse A-wave) in the first trimester has also been associated with increased risk for adverse perinatal outcome, in particular for chromosomal anomalies and CHD [101, 102] (Fig. 4.4). Abnormal DV blood velocity in the first trimester is an independent predictor of CHD and should constitute an indication for early echocardiography. It has been reported that the use of DV blood velocity assessment increased early detection of CHD by 11% with respect to the use of NT measurement alone [103]. The combined data from eight studies on euploid fetuses with increased NT (above the 95th centile) demonstrated abnormal DV blood velocity in 87% of fetuses with cardiac defects, compared with 19% without cardiac defects [104]. Thus, many groups have suggested the use of DV as a secondary marker to be assessed selectively in fetuses with increased NT [105–107].

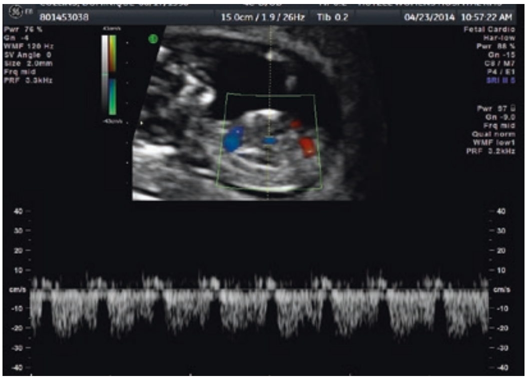

Fig. 4.4 Abnormal ductus venosus (DV) blood velocity waveform at 12 weeks of gestation

Several studies have shown that complete evaluation rate of the heart increased from 45% at 11 weeks to 90% between 12–14 weeks and 100% at 15 weeks [26, 27, 108]. The visualization of the four-chamber view and the cross-over of the pulmonary artery and aorta have been reported from 44% at 10 weeks to 100% at 13–17 weeks [26]. Transvaginal echocardiography is reported to be superior to the transabdominal approach between 10 and 13 weeks of gestation, both methods are similar at 14 weeks of gestation, and transabdominal echocardiography is more accurate than transvaginal at 15 weeks of gestation [108]. Detection of cardiac anomalies in the first trimester varies by lesion, as noted in Tables 4.2 and 4.3.

Phenylketonuria (PKU) is another metabolic disorder that is associated with CHD. Women with PKU who have elevated phenylalanine levels are at increased risk for offspring with CHD. VSD and coarctation of the aorta are most common in this population [109]. Levels exceeding 15 mg/mL are associated with a 10–15-fold increase in CHD [110]. The etiology of CHD is related not only elevated blood phenylalanine levels, but also poor protein and vitamin intake during the first trimester [111]. Diet control before conception and during pregnancy had shown reduced risk of CHD [112, 113].

Table 4.2 Cardiac lesions that may be detected in the first trimester [140]

1. Tricuspid atresia
2. Pulmonary atresia (with or without ventricular septal defect (VSD))
3. Mitral atresia
4. Aortic atresia
5. Hypoplastic left heart syndrome (aortic and mitral atresia or severe stenosis)
6. Complete transposition
7. Corrected transposition
8. Double inlet ventricle
9. Atrioventricular septal defect (large septal defects)
10. Truncus arteriosus
11. Tetralogy of Fallot
12. Large ventricular septal defects
13. Complex lesions in the setting of laterality defects

Table 4.3 Cardiac lesions that may be overlooked in the first trimester [140]

Developmental lesions
1. Mild aortic/pulmonary stenosis
2. Mild mitral/tricuspid valve abnormalities
3. Coarctation of the aorta
4. Cardiac tumors
5. Cardiomyopathies
Septal defects
1. Ventricular septal defects
2. Primum atrial septal defects
3. Atrioventricular septal defects
Others
1. Tetralogy of Fallot with normal size pulmonary arteries
2. Abnormalities of pulmonary venous return

Anticonvulsants, a class of drugs that includes phenytoin, carbamazepine, and sodium valproate, are commonly used in the treatment of epilepsy. The incidence of congenital defects is 4–10%, an approximate two- to four-fold increase compared to the general population [114–120]. Polytherapy with anti-epileptic drugs (AEDs) is associated with a higher malformation rate than monotherapy [121]. Use of certain AEDs during pregnancy increases the risk for specific congenital malformations, such as neural tube defects, cleft lip and palate, and cardiovascular malformations [122–125]. Valproic acid monotherapy, among the different regimens, has the highest risk of congenital abnormalities in offspring [94]. The use of valproate and carbamazepine is strongly associated with neural tube defects (NTDs), especially with spina bifida. The prevalence of spina bifida is approximately 1–2% with valproate exposure and 0.5% with carbamazepine [126].

Carbamazepine exposure is associated with Tetralogy of Fallot, esophageal atresia, vertebral anomalies, and multiple terminal transverse limb defects [120]. The most common cardiac anomalies reported among offspring exposed to carbamazepine are VSD, Tetralogy of Fallot, PDA, and ASD [120, 123, 127, 128]. In a light of these results, we should consider first trimester anatomy ultrasound and fetal echocardiogram for women with epilepsy on AEDs.

Alcohol abuse during pregnancy is associated with health problems to both mother and fetus.

Of the 4 million pregnancies in the US each year, 3–5% of women drink heavily throughout pregnancy [129]. The Fetal Alcohol Syndrome (FAS) is considered to be the most severe manifestation of the adverse effect of alcohol on the fetus. A diagnosis of FAS requires prenatal alcohol exposure and the following characteristics: fetal growth restriction, neurocognitive delays and/or mental retardation, and at least two facial dysmorphic features (short palpebral fissures, thin vermillion border or smooth philtrum) [130]. FAS occurs in 4–10% of children born to alcoholic mothers. CHD is reported in 25–50% of infants with FAS; ASD and VSD are the most common [131–133]. The findings suggest that prenatal alcohol exposure as a potential etiology of CHD may also be considered as an indication for performing first trimester fetal echocardiogram.

Maternal Vascular Disease

Women with hypertension, renal disease, and vascular disease have a recognized increased risk of preeclampsia, fetal growth restriction, and other adverse pregnancy outcomes. While most of these women will be candidates for low-dose aspirin therapy, identification of a particularly high-risk subset may allow more intensive surveillance and targeted interventions. Abnormal placental vascular development is a basis of common obstetrical disorders such as fetal growth restriction and preeclampsia. Uterine artery Doppler has been investigated as a predictive and diagnostic tool.

It has been reported that pregnancies with an increased risk of developing hypertensive disorders and related complications have an abnormally increased UtA-PI in early pregnancy [134, 135]. The 11–14 weeks period is characterized by an elevated UtA-PI and bilateral notching. As pregnancy progresses, UtA-PI decreases and bilateral notching is less prevalent [134, 136]. A meta-analysis involving 55,974 women has shown that first trimester uterine artery Doppler is a useful tool for predicting early-onset preeclampsia, as well as other adverse pregnancy outcomes [137]. ASA treatment initiated before 16 weeks of pregnancy may reduce the incidence of preeclampsia and its consequences in women with ultrasonographic evidence of abnormal placentation diagnosed by first trimester uterine artery Doppler studies [138].

Conclusion

First trimester ultrasound is already a common part of our obstetric armamentarium. As our patients, their co-morbidities, and the sophistication of ultrasound changes, so too may we change our approach to prenatal diagnosis. While the information presented here does not reflect current standard of care, we anticipate further evolution of condition- and exposure-based recommendations, including first trimester anatomy studies and echocardiography in selected populations.

Teaching Points

- Ultrasound performed in the first trimester confirms an intrauterine pregnancy, establishes accurate dates, pregnancy failure, and ectopic pregnancy.
- It is also used for risk assessment for aneuploidy, through measurement of nuchal translucency and identification of the presence or absence of the nasal bone.
- Complete fetal anatomy surveys can be achieved in 64% of transabdominal scans and 82% of transvaginal scans at 13–14 weeks of gestation. This helps to shift the prenatal diagnosis from the standard second trimester anatomy scan into the first trimester.
- Various maternal conditions and/or their treatment are known to be associated with structural anomalies or restricted growth. Maternal pregestational diabetes is a well-known risk factor for congenital anomalies. The overall incidence of congenital malformations in diabetic pregnancies is 6–13%, which is two- to four-fold greater than that of the general population.
- Obesity is a well-known risk factor for and co-morbidity of diabetes. Women with pregestational diabetes and BMI higher than 28 kg/m^2 have a three-fold increase in the risk of congenital anomalies, and the risk further increases proportionally with BMI.
- Congenital heart disease (CHD) is the most common congenital anomaly, with an incidence of 6–8% of all live births, accounting for 30–45% of all congenital defects. An increased nuchal translucency (NT) and/or abnormal ductus venosus (DV) blood velocity waveform are associated with major cardiac defects in the fetus. Complete evaluation rate of the heart increased from 45% at 11 weeks to 90% between 12–14 weeks and 100% at 15 weeks.
- Maternal metabolic diseases such as PKU and diabetes and exposure to certain medications such as anticonvulsants are associated with CHD. These conditions might be considered as an indication for performing first trimester fetal echocardiogram.
- First trimester uterine artery Doppler is a useful tool for predicting early-onset preeclampsia, as well as other adverse pregnancy outcomes. ASA treatment initiated before 16 weeks of pregnancy may reduce the incidence of preeclampsia and its consequences in women with ultrasonographic evidence of abnormal placentation diagnosed by first trimester uterine artery Doppler studies.

References

1. Whitworth M, Bricker L, Neilson JP, Dowswell T. Ultrasound for fetal assessment in early pregnancy. Cochrane Database Syst Rev. 2010;(4):CD007058. Epub 2010/04/16.
2. AIUM practice parameter for the performance of detailed diagnostic obstetric ultrasound examinations between 12 weeks 0 days and 13 weeks 6 days. J Ultrasound Med. 2021;40:E1–E16.
3. Timor-Tritsch IE, Monteagudo A, Waren WB. Transvaginal ultrasonographic definition of the central nervous system in the first and early second trimesters. Am J Obstet Gynecol. 1991;164:497–503.
4. Monteagudo A, Timor-Trisch IE, Sharma S. Early and simple determination of chorionic and amniotic type in multifetal gestation in the first fourteen weeks by high-frequency transvaginal ultrasonography. Am J Obstet Gynecol. 1994;170:824–9.
5. Timor-Tritsch IE, Bashin A, Monteagudo A, Arslan AA. Qualified and trained sonographers in the US can perform early fetal anatomy scans between 11 and 14 weeks. Am J Obstet Gynecol. 2004;191:1247–52.

6. Timor-Tritsch IE, Fuchs KM, Monteagudo A, D'Alton ME. Performing a fetal anatomy scan at the time of first trimester screening. Obstet Gynecol. 2009;113:402–7.
7. Souka AP, Pilalis A, Kavalakis Y, Kosmas Y, Antsaklis P, Antsaklis A. Assessment of fetal anatomy at the 11-14-week ultrasound examination. Ultrasound Obstet Gynecol. 2004;24:73–734.
8. Wan JJ, Schrimmer D, Tache V, et al. Current practice in determining amnionicity and chorionicity in multiple gestations. Prenat Diagn. 2011;31:125–30.
9. Syngelaki A, Hammami A, Bower S, Zadere V, Akolekar R, Nicolaides KH. Diagnosis of fetal non-chromosomal abnormalities on routine ultrasound examination at 11-13 weeks' gestation. Ultrasound Obstet Gynecol. 2019;54:468–76.
10. Chen FC, Bacovsky A, Entezami M, Henrich W. Nearly half of all severe fetal anomalies can be detected by first-trimester screening in experts' hands. J Perinat Med. 2019;47:619–24.
11. Iliescu D, Tudorache S, Comanescu A, et al. Improved detection rate of structural abnormalities in the first trimester using an extended examination protocol. Ultrasound Obstet Gynecol. 2013;42:300–9.
12. Rossi AC, Prefumo F. Accuracy of ultrasonography at 11-14 weeks of gestation for detection of fetal structural anomalies: systematic review. Obstet Gynecol. 2013;122:1160–7.
13. Broomley B, Shipp TD, Lyons J, Navatche RS, Grozmann Y, Benacerraf BR. Detection of fetal structural anomalies in a basic first trimester screening program for aneuploidy. J Ultrasound Med. 2014;33:1737–45.
14. Karim JN, Roberts NW, Salomon LJ, Papageorghiou AT. Systematic review of first trimester ultrasound screening for detection of fetal structural anomalies and factors that affect screening performance. Ultrasound Obstet Gynecol. 2017;50:429–41.
15. Kenkhuis MJA, Bakker M, Bardi F, et al. Effectiveness 12-13-week scan for early diagnosis of fetal congenital anomalies in the cell-free DNA era. Ultrasound Obstet Gynecol. 2018;51:463–9.
16. Becker R, Wegner RD. Detailed screening for fetal anomalies and cardiac defects at the 11-13-week scan. Ultrasound Obstet Gynecol. 2006;27:613–8.
17. D'Antonio F, Familian A, Thilaganathan B, et al. Sensitivity of first trimester ultrasound in the detection of congenital anomalies in twin pregnancies: population study and systematic review. Acta Obstet Gynecol Scand. 2016;95:1359–67.
18. Syngelaki A, Cimpoca B, Litwinska E, Akolekar R, Nicolaides KH. Diagnosis of fetal defects in twin pregnancies at routine ultrasound examination at 11-13-weeks' gestation. Ultrasound Obstet Gynecol. 2020;55:474–81.
19. Timor-Tritsch IE, Farine D, Rosen MG. A close look at early embryonic development with the high-frequency transvaginal transducer. Am J Obstet Gynecol. 1988;159(3):676–81. Epub 1988/09/01.
20. Timor-Tritsch IE, Monteagudo A, Peisner DB. High-frequency transvaginal sonographic examination for the potential malformation assessment of the 9-week to 14-week fetus. J Clin Ultrasound. 1992;20(4):231–8. Epub 1992/05/01.
21. Lasser DM, Peisner DB, Vollebergh J, Timor-Tritsch I. First-trimester fetal biometry using transvaginal sonography. Ultrasound Obstet Gynecol. 1993;3(2):104–8. Epub 1993/03/01.
22. den Hollander NS, Wessels MW, Niermeijer MF, Los FJ, Wladimiroff JW. Early fetal anomaly scanning in a population at increased risk of abnormalities. Ultrasound Obstet Gynecol. 2002;19(6):570–4. Epub 2002/06/06.
23. Michailidis GD, Papageorgiou P, Economides DL. Assessment of fetal anatomy in the first trimester using two- and three-dimensional ultrasound. Br J Radiol. 2002;75(891):215–9. Epub 2002/04/05.
24. Hernadi L, Torocsik M. Screening for fetal anomalies in the 12th week of pregnancy by transvaginal sonography in an unselected population. Prenat Diagn. 1997;17(8):753–9. Epub 1997/08/01.
25. Whitlow BJ, Economides DL. The optimal gestational age to examine fetal anatomy and measure nuchal translucency in the first trimester. Ultrasound Obstet Gynecol. 1998;11(4):258–61. Epub 1998/06/10.
26. Gembruch U, Shi C, Smrcek JM. Biometry of the fetal heart between 10 and 17 weeks of gestation. Fetal Diagn Ther. 2000;15(1):20–31. Epub 2000/03/08.
27. Haak MC, Twisk JW, Van Vugt JM. How successful is fetal echocardiographic examination in the first trimester of pregnancy? Ultrasound Obstet Gynecol. 2002;20(1):9–13. Epub 2002/07/09.
28. Johnson P, Sharland G, Maxwell D, Allan L. The role of transvaginal sonography in the early detection of congenital heart disease. Ultrasound Obstet Gynecol. 1992;2(4):248–51. Epub 1992/07/01.
29. Dolkart LA, Reimers FT. Transvaginal fetal echocardiography in early pregnancy: normative data. Am J Obstet Gynecol. 1991;165(3):688–91. Epub 1991/09/01.
30. Timor-Tritsch IE, Bashiri A, Monteagudo A, Arslan AA. Qualified and trained sonographers in the US can perform early fetal anatomy scans between 11 and 14 weeks. Am J Obstet Gynecol. 2004;191(4):1247–52. Epub 2004/10/28.
31. Borrell A, Robinson JN, Santolaya-Forgas J. Clinical value of the 11- to 13+6-week sonogram for detection of congenital malformations: a review. Am J Perinatol. 2011;28(2):117–24. Epub 2010/08/12.
32. Grande M, Arigita M, Borobio V, Jimenez JM, Fernandez S, Borrell A. First-trimester detection of structural abnormalities and the role of aneuploidy markers. Ultrasound Obstet Gynecol. 2012;39(2):157–63. Epub 2011/08/17.
33. Syngelaki A, Chelemen T, Dagklis T, Allan L, Nicolaides KH. Challenges in the diagnosis of fetal non-chromosomal abnormalities at 11-13 weeks. Prenat Diagn. 2011;31(1):90–102. Epub 2011/01/07.
34. Ebrashy A, El Kateb A, Momtaz M, El Sheikhah A, Aboulghar MM, Ibrahim M, et al. 13-14-week fetal anatomy scan: a 5-year prospective study.

Ultrasound Obstet Gynecol. 2010;35(3):292–6. Epub 2010/03/06.

35. Souka AP, Pilalis A, Kavalakis Y, Kosmas Y, Antsaklis P, Antsaklis A. Assessment of fetal anatomy at the 11-14-week ultrasound examination. Ultrasound Obstet Gynecol. 2004;24(7):730–4. Epub 2004/12/09.
36. Salomon LJ, Bernard JP, Duyme M, Dorion A, Ville Y. Revisiting first-trimester fetal biometry. Ultrasound Obstet Gynecol. 2003;22(1):63–6. Epub 2003/07/15.
37. Peterson C, Grosse SD, Li R, Sharma AJ, Razzaghi H, Herman WH, et al. Preventable health and cost burden of adverse birth outcomes associated with pregestational diabetes in the United States. Am J Obstet Gynecol. 2015;212:74.e1–9.
38. Lawrence JM, Contreras R, Chen W, Sacks DA. Trends in the prevalence of preexisting diabetes and gestational diabetes mellitus among racially/ethnically diverse population of pregnant women, 1999-2005. Diabetes Care. 2008;31:899–904.
39. Britton LE, Hussey JM, Crandell JL, Berry DC, Brooks JL, Bryant AG. Racial/ethnic disparities in diabetes diagnosis and glycemic control among women reproductive age. J Womens Health. 2018; https://doi.org/10.1089/jwh.2017.6845.
40. Naeye RL. Infants of diabetic mothers: a quantitative, morphologic study. Pediatrics. 1965;35:980–8. Epub 1965/06/01.
41. Soler NG, Soler SM, Malins JM. Neonatal morbidity among infants of diabetic mothers. Diabetes Care. 1978;1(6):340–50. Epub 1978/11/01.
42. Mills JL. Malformations in infants of diabetic mothers. Teratology 25:385–94. 1982. Birth Defects Res A Clin Mol Teratol. 2010;88(10):769–78. Epub 2010/10/26.
43. Ramos-Arroyo MA, Rodriguez-Pinilla E, Cordero JF. Maternal diabetes: the risk for specific birth defects. Eur J Epidemiol. 1992;8(4):503–8. Epub 1992/07/01.
44. Becerra JE, Khoury MJ, Cordero JF, Erickson JD. Diabetes mellitus during pregnancy and the risks for specific birth defects: a population-based case-control study. Pediatrics. 1990;85(1):1–9. Epub 1990/01/01.
45. Lisowski LA, Verheijen PM, Copel JA, Kleinman CS, Wassink S, Visser GH, et al. Congenital heart disease in pregnancies complicated by maternal diabetes mellitus. An international clinical collaboration, literature review, and meta-analysis. Herz. 2010;35(1):19–26. Epub 2010/02/09.
46. Kucera J. Rate and type of congenital anomalies among offspring of diabetic women. J Reprod Med. 1971;7(2):73–82. Epub 1971/08/01.
47. Schwartz R, Teramo KA. Effects of diabetic pregnancy on the fetus and newborn. Semin Perinatol. 2000;24(2):120–35. Epub 2000/05/11.
48. Garne E, Loane M, Dolk H, Barisic I, Addor MC, Arriola L, et al. Spectrum of congenital anomalies in pregnancies with pregestational diabetes. Birth Defects Res A Clin Mol Teratol. 2012;94(3):134–40. Epub 2012/03/01.
49. Taipale P, Ammala M, Salonen R, Hiilesmaa V. Two-stage ultrasonography in screening for fetal anomalies at 13-14 and 18-22 weeks of gestation. Acta Obstet Gynecol Scand. 2004;83(12):1141–6. Epub 2004/11/19.
50. Sebire NJ, Noble PL, Thorpe-Beeston JG, Snijders RJ, Nicolaides KH. Presence of the ‘lemon’ sign in fetuses with spina bifida at the 10-14-week scan. Ultrasound Obstet Gynecol. 1997;10(6):403–5. Epub 1998/02/26.
51. Nicolaides KH, Campbell S, Gabbe SG, Guidetti R. Ultrasound screening for spina bifida: cranial and cerebellar signs. Lancet. 1986;2(8498):72–4. Epub 1986/07/12.
52. Cedergren MI, Kallen BA. Maternal obesity and infant heart defects. Obes Res. 2003;11(9):1065–71. Epub 2003/09/16.
53. Moore LL, Singer MR, Bradlee ML, Rothman KJ, Milunsky A. A prospective study of the risk of congenital defects associated with maternal obesity and diabetes mellitus. Epidemiology. 2000;11(6):689–94. Epub 2000/10/31.
54. Martinez-Frias ML, Frias JP, Bermejo E, Rodriguez-Pinilla E, Prieto L, Frias JL. Pre-gestational maternal body mass index predicts an increased risk of congenital malformations in infants of mothers with gestational diabetes. Diabet Med. 2005;22(6):775–81. Epub 2005/05/25.
55. Towner D, Kjos SL, Leung B, Montoro MM, Xiang A, Mestman JH, et al. Congenital malformations in pregnancies complicated by NIDDM. Diabetes Care. 1995;18(11):1446–51. Epub 1995/11/01.
56. Aberg A, Westbom L, Kallen B. Congenital malformations among infants whose mothers had gestational diabetes or preexisting diabetes. Early Hum Dev. 2001;61(2):85–95. Epub 2001/02/27.
57. Sheffield JS, Butler-Koster EL, Casey BM, McIntire DD, Leveno KJ. Maternal diabetes mellitus and infant malformations. Obstet Gynecol. 2002;100(5 Pt 1):925–30. Epub 2002/11/09.
58. Rosenn B, Miodovnik M, Combs CA, Khoury J, Siddiqi TA. Glycemic thresholds for spontaneous abortion and congenital malformations in insulin-dependent diabetes mellitus. Obstet Gynecol. 1994;84(4):515–20. Epub 1994/10/01.
59. Greene MF. Spontaneous abortions and major malformations in women with diabetes mellitus. Semin Reprod Endocrinol. 1999;17(2):127–36. Epub 1999/10/21.
60. American College of Obstetricians and Gynecologists. Pregestational diabetes mellitus. Practice Bulletin No. 201. Obstet Gynecol. 2018;132:e228–47.
61. American College of Obstetricians and Gynecologists. Neural tube defects. Practice Bulletin No. 187. Obstet Gynecol. 2017;130:e279–90.
62. De Wals P, Tairou F, Van Allen MI, Uh SH, Lowry RB, Sibbald B, et al. Reduction in neural-tube

defects after folic acid fortification in Canada. N Engl J Med. 2007;357(2):135–42. Epub 2007/07/13.
63. Timor-Tritsch IE, Monteagudo A, Warren WB. Transvaginal ultrasonographic definition of the central nervous system in the first and early second trimesters. Am J Obstet Gynecol. 1991;164(2):497–503. Epub 1991/02/01.
64. Schiesser M, Holzgreve W, Lapaire O, Willi N, Luthi H, Lopez R, et al. Sirenomelia, the mermaid syndrome—detection in the first trimester. Prenat Diagn. 2003;23(6):493–5. Epub 2003/06/19.
65. National Institutes of Health. Clinical guidelines on the identification, evaluation, and treatment of overweight and obesity in adults—the evidence report. Obes Res. 1998;6(Suppl 2):51S–209S. Epub 1998/11/14.
66. Mokdad AH, Serdula MK, Dietz WH, Bowman BA, Marks JS, Koplan JP. The spread of the obesity epidemic in the United States, 1991-1998. JAMA. 1999;282(16):1519–22. Epub 1999/11/05.
67. Gross T, Sokol RJ, King KC. Obesity in pregnancy: risks and outcome. Obstet Gynecol. 1980;56(4):446–50. Epub 1980/10/01.
68. Hales CM, Carroll MD, Fryar CD, Ogden CL. Prevalence of obesity and severe obesity among adults: United States 2017–2018. NCHS Data Brief. 2020;360:1–8.
69. Flegal KM, Carroll MD, Ogden CL, Curtin LR. Prevalence and trends in obesity among US adults, 1999–2008. JAMA. 2010;303:235–41.
70. Stothard KJ, Tennant PW, Bell R, Rankin J. Maternal overweight and obesity and the risk of congenital anomalies: systematic review and meta-analysis. JAMA. 2009;301:636–50.
71. Ogden CL, Carroll MD, Kit BK, Flegal KM. Prevalence of obesity in the United States, 2009-2010. NCHS Data Brief. 2012;82:1–8. Epub 2012/05/24.
72. Hendricks KA, Nuno OM, Suarez L, Larsen R. Effects of hyperinsulinemia and obesity on risk of neural tube defects among Mexican Americans. Epidemiology. 2001;12(6):630–5. Epub 2001/10/27.
73. Mikhail LN, Walker CK, Mittendorf R. Association between maternal obesity and fetal cardiac malformations in African Americans. J Natl Med Assoc. 2002;94(8):695–700. Epub 2002/08/03.
74. Queisser-Luft A, Kieninger-Baum D, Menger H, Stolz G, Schlaefer K, Merz E. [Does maternal obesity increase the risk of fetal abnormalities? Analysis of 20,248 newborn infants of the Mainz Birth Register for detecting congenital abnormalities]. Ultraschall Med. 1998;19(1):40–4. Epub 1998/05/13. Erhoht mutterliche Adipositas das Risiko fur kindliche Fehlbildungen? Analyse von 20,248 Neugeborenen des Mainzer Geburtenregisters zur Erfassung angeborener Fehlbildungen.
75. Blomberg MI, Kallen B. Maternal obesity and morbid obesity: the risk for birth defects in the offspring. Birth Defects Res A Clin Mol Teratol. 2010;88(1):35–40. Epub 2009/08/28.
76. Thornburg LL, Miles K, Ho M, Pressman EK. Fetal anatomic evaluation in the overweight and obese gravida. Ultrasound Obstet Gynecol. 2009;33(6):670–5. Epub 2009/05/30.
77. Dashe JS, McIntire DD, Twickler DM. Effect of maternal obesity on the ultrasound detection of anomalous fetuses. Obstet Gynecol. 2009;113(5):1001–7. Epub 2009/04/23.
78. Reddy UM, Abuhamad AZ, Levine D, Saade GR. Fetal imaging: executive summary of a joint Eunice Kennedy Shriver National Institute of Child Health and Human Development, Society of Maternal-Fetal Medicine, American Institute Ultrasound in Medicine, American College of Ob and Gyn, American College of Radiology, Society of Radiologists in Ultrasound fetal imaging Workshop. J Ultrasound Med. 2014;33:745–57.
79. Weichert J, Hartge DR. Obstetrical sonography in obese women. J Clin Ultrasound. 2011;39:209–16.
80. Davidoff A, Reuter K, Karellas A, et al. Maternal umbilicus: ultrasound window to the gravid uterus. J Clin Ultrasound. 1994;22:263–7.
81. Hendler I, Blackwell SC, Bujold E, Treadwell MC, Wolfe HM, Sokol RJ, et al. The impact of maternal obesity on midtrimester sonographic visualization of fetal cardiac and craniospinal structures. Int J Obes Relat Metab Disord. 2004;28(12):1607–11. Epub 2004/08/11.
82. Gupta S, Timor-Tritsch IE, Oh C, Chervenak J, Monteagudo A. Early second-trimester sonography to improve the fetal anatomic survey in obese patients. J Ultrasound Med. 2014;33(9):1579–83. Epub 2014/08/27.
83. Timor-Tritsch IE. Transvaginal sonographic evaluation of fetal anatomy at 14 to 16 weeks. Why is this technique not attractive in the United States? J Ultrasound Med. 2001;20(7):705–9. Epub 2001/07/11.
84. Rowland TW, Hubbell JP Jr, Nadas AS. Congenital heart disease in infants of diabetic mothers. J Pediatr. 1973;83(5):815–20. Epub 1973/11/01.
85. Erickson JD. Risk factors for birth defects: data from the Atlanta Birth Defects Case-Control Study. Teratology. 1991;43(1):41–51. Epub 1991/01/01.
86. Correa A, Gilboa SM, Botto LD, Moore CA, Hobbs CA, Cleves MA, et al. Lack of periconceptional vitamins or supplements that contain folic acid and diabetes mellitus-associated birth defects. Am J Obstet Gynecol. 2012;206(3):218.e1–13. Epub 2012/01/31.
87. Correa A, Gilboa SM, Besser LM, Botto LD, Moore CA, Hobbs CA, et al. Diabetes mellitus and birth defects. Am J Obstet Gynecol. 2008;199(3):237.e1–9. Epub 2008/08/05.
88. Ray JG, O'Brien TE, Chan WS. Preconception care and the risk of congenital anomalies in the offspring of women with diabetes mellitus: a meta-analysis. QJM. 2001;94(8):435–44. Epub 2001/08/09.
89. Wahabi HA, Alzeidan RA, Bawazeer GA, Alansari LA, Esmaeil SA. Preconception care for diabetic

women for improving maternal and fetal outcomes: a systematic review and meta-analysis. BMC Pregnancy Childbirth. 2010;10:63. Epub 2010/10/16.

90. Balsells M, Garcia-Patterson A, Gich I, Corcoy R. Maternal and fetal outcome in women with type 2 versus type 1 diabetes mellitus: a systematic review and metaanalysis. J Clin Endocrinol Metab. 2009;94(11):4284–91. Epub 2009/10/08.
91. Hoffman JI, Kaplan S. The incidence of congenital heart disease. J Am Coll Cardiol. 2002;39(12):1890–900. Epub 2002/06/27.
92. Garne E, Stoll C, Clementi M. Evaluation of prenatal diagnosis of congenital heart diseases by ultrasound: experience from 20 European registries. Ultrasound Obstet Gynecol. 2001;17(5):386–91. Epub 2001/06/02.
93. Hoffman JI. Congenital heart disease: incidence and inheritance. Pediatr Clin N Am. 1990;37(1):25–43. Epub 1990/02/01.
94. Wan AW, Jevremovic A, Selamet Tierney ES, McCrindle BW, Dunn E, Manlhiot C, et al. Comparison of impact of prenatal versus postnatal diagnosis of congenitally corrected transposition of the great arteries. Am J Cardiol. 2009;104(9):1276–9. Epub 2009/10/21.
95. Tworetzky W, McElhinney DB, Reddy VM, Brook MM, Hanley FL, Silverman NH. Improved surgical outcome after fetal diagnosis of hypoplastic left heart syndrome. Circulation. 2001;103(9):1269–73. Epub 2001/03/10.
96. Lagopoulos ME, Manlhiot C, McCrindle BW, Jaeggi ET, Friedberg MK, Nield LE. Impact of prenatal diagnosis and anatomical subtype on outcome in double outlet right ventricle. Am Heart J. 2010;160(4):692–700. Epub 2010/10/12.
97. Gembruch U, Knopfle G, Chatterjee M, Bald R, Hansmann M. First-trimester diagnosis of fetal congenital heart disease by transvaginal two-dimensional and Doppler echocardiography. Obstet Gynecol. 1990;75(3 Pt 2):496–8. Epub 1990/03/01.
98. Makrydimas G, Sotiriadis A, Ioannidis JP. Screening performance of first-trimester nuchal translucency for major cardiac defects: a meta-analysis. Am J Obstet Gynecol. 2003;189(5):1330–5. Epub 2003/11/25.
99. Muller MA, Clur SA, Timmerman E, Bilardo CM. Nuchal translucency measurement and congenital heart defects: modest association in low-risk pregnancies. Prenat Diagn. 2007;27(2):164–9. Epub 2007/01/24.
100. Clur SA, Ottenkamp J, Bilardo CM. The nuchal translucency and the fetal heart: a literature eview. Prenat Diagn. 2009;29(8):739–48. Epub 2009/04/29.
101. Montenegro N, Matias A, Areias JC. Ductus venosus blood flow evaluation: its importance in the screening of chromosomal abnormalities. Am J Obstet Gynecol. 1999;181(4):1042–3. Epub 1999/10/16.
102. Matias A, Gomes C, Flack N, Montenegro N, Nicolaides KH. Screening for chromosomal abnormalities at 10-14 weeks: the role of ductus venosus blood flow. Ultrasound Obstet Gynecol. 1998;12(6):380–4. Epub 1999/01/26.
103. Martinez JM, Comas M, Borrell A, Bennasar M, Gomez O, Puerto B, et al. Abnormal first-trimester ductus venosus blood flow: a marker of cardiac defects in fetuses with normal karyotype and nuchal translucency. Ultrasound Obstet Gynecol. 2010;35(3):267–72. Epub 2010/01/07.
104. Maiz N, Nicolaides KH. Ductus venosus in the first trimester: contribution to screening of chromosomal, cardiac defects and monochorionic twin complications. Fetal Diagn Ther. 2010;28(2):65–71. Epub 2010/06/24.
105. Bilardo CM, Muller MA, Zikulnig L, Schipper M, Hecher K. Ductus venosus studies in fetuses at high risk for chromosomal or heart abnormalities: relationship with nuchal translucency measurement and fetal outcome. Ultrasound Obstet Gynecol. 2001;17(4):288–94. Epub 2001/05/08.
106. Favre R, Cherif Y, Kohler M, Kohler A, Hunsinger MC, Bouffet N, et al. The role of fetal nuchal translucency and ductus venosus Doppler at 11-14 weeks of gestation in the detection of major congenital heart defects. Ultrasound Obstet Gynecol. 2003;21(3):239–43. Epub 2003/04/01.
107. Maiz N, Plasencia W, Dagklis T, Faros E, Nicolaides K. Ductus venosus Doppler in fetuses with cardiac defects and increased nuchal translucency thickness. Ultrasound Obstet Gynecol. 2008;31(3):256–60. Epub 2008/03/01.
108. Smrcek JM, Berg C, Geipel A, Fimmers R, Diedrich K, Gembruch U. Early fetal echocardiography: heart biometry and visualization of cardiac structures between 10 and 15 weeks' gestation. J Ultrasound Med. 2006;25(2):173–82; quiz 83–5. Epub 2006/01/28.
109. Platt LD, Koch R, Hanley WB, Levy HL, Matalon R, Rouse B, et al. The international study of pregnancy outcome in women with maternal phenylketonuria: report of a 12-year study. Am J Obstet Gynecol. 2000;182(2):326–33. Epub 2000/02/29.
110. Lenke RR, Levy HL. Maternal phenylketonuria and hyperphenylalaninemia. An international survey of the outcome of untreated and treated pregnancies. N Engl J Med. 1980;303(21):1202–8. Epub 1980/11/20.
111. Koch R, Friedman E, Azen C, Hanley W, Levy H, Matalon R, et al. The International Collaborative Study of Maternal Phenylketonuria: status report 1998. Eur J Pediatr. 2000;159(Suppl 2):S156–60. Epub 2000/10/24.
112. Matalon KM, Acosta PB, Azen C. Role of nutrition in pregnancy with phenylketonuria and birth defects. Pediatrics. 2003;112(6 Pt 2):1534–6. Epub 2003/12/05.
113. Michals-Matalon K, Platt LD, Acosta PP, Azen C, Walla CA. Nutrient intake and congenital heart defects in maternal phenylketonuria. Am J Obstet Gynecol. 2002;187(2):441–4. Epub 2002/08/24.

114. Tomson T, Battino D, Bonizzoni E, Craig J, Lindhout D, Sabers A, et al. Dose-dependent risk of malformations with antiepileptic drugs: an analysis of data from the EURAP epilepsy and pregnancy registry. Lancet Neurol. 2011;10(7):609–17. Epub 2011/06/10.
115. Holmes LB, Harvey EA, Coull BA, Huntington KB, Khoshbin S, Hayes AM, et al. The teratogenicity of anticonvulsant drugs. N Engl J Med. 2001;344(15):1132–8. Epub 2001/04/12.
116. Samren EB, van Duijn CM, Koch S, Hiilesmaa VK, Klepel H, Bardy AH, et al. Maternal use of antiepileptic drugs and the risk of major congenital malformations: a joint European prospective study of human teratogenesis associated with maternal epilepsy. Epilepsia. 1997;38(9):981–90. Epub 1998/05/14.
117. Samren EB, van Duijn CM, Christiaens GC, Hofman A, Lindhout D. Antiepileptic drug regimens and major congenital abnormalities in the offspring. Ann Neurol. 1999;46(5):739–46. Epub 1999/11/30.
118. Canger R, Battino D, Canevini MP, Fumarola C, Guidolin L, Vignoli A, et al. Malformations in offspring of women with epilepsy: a prospective study. Epilepsia. 1999;40(9):1231–6. Epub 1999/09/16.
119. Kaneko S, Battino D, Andermann E, Wada K, Kan R, Takeda A, et al. Congenital malformations due to antiepileptic drugs. Epilepsy Res. 1999;33(2–3):145–58. Epub 1999/03/27.
120. Holmes LB. The teratogenicity of anticonvulsant drugs: a progress report. J Med Genet. 2002;39(4):245–7. Epub 2002/04/16.
121. Holmes LB, Mittendorf R, Shen A, Smith CR, Hernandez-Diaz S. Fetal effects of anticonvulsant polytherapies: different risks from different drug combinations. Arch Neurol. 2011;68(10):1275–81. Epub 2011/06/15.
122. Barrett C, Richens A. Epilepsy and pregnancy: report of an Epilepsy Research Foundation Workshop. Epilepsy Res. 2003;52(3):147–87. Epub 2003/01/22.
123. Matalon S, Schechtman S, Goldzweig G, Ornoy A. The teratogenic effect of carbamazepine: a meta-analysis of 1255 exposures. Reprod Toxicol. 2002;16(1):9–17. Epub 2002/04/06.
124. Arpino C, Brescianini S, Robert E, Castilla EE, Cocchi G, Cornel MC, et al. Teratogenic effects of antiepileptic drugs: use of an International Database on Malformations and Drug Exposure (MADRE). Epilepsia. 2000;41(11):1436–43. Epub 2000/11/15.
125. Lindhout D, Omtzigt JG. Teratogenic effects of antiepileptic drugs: implications for the management of epilepsy in women of childbearing age. Epilepsia. 1994;35(Suppl 4):S19–28. Epub 1994/01/01.
126. Jentink J, Dolk H, Loane MA, Morris JK, Wellesley D, Garne E, et al. Intrauterine exposure to carbamazepine and specific congenital malformations: systematic review and case-control study. BMJ. 2010;341:c6581. Epub 2010/12/04.
127. Janz D. Are antiepileptic drugs harmful when taken during pregnancy? J Perinat Med. 1994;22(5):367–77. Epub 1994/01/01.
128. Thomas SV, Ajaykumar B, Sindhu K, Francis E, Namboodiri N, Sivasankaran S, et al. Cardiac malformations are increased in infants of mothers with epilepsy. Pediatr Cardiol. 2008;29(3):604–8. Epub 2008/01/12.
129. Floyd RL, Sidhu JS. Monitoring prenatal alcohol exposure. Am J Med Genet C Semin Med Genet. 2004;127C(1):3–9. Epub 2004/04/20.
130. Hoyme HE, May PA, Kalberg WO, Kodituwakku P, Gossage JP, Trujillo PM, et al. A practical clinical approach to diagnosis of fetal alcohol spectrum disorders: clarification of the 1996 institute of medicine criteria. Pediatrics. 2005;115(1):39–47. Epub 2005/01/05.
131. Jones KL, Smith DW, Ulleland CN, Streissguth P. Pattern of malformation in offspring of chronic alcoholic mothers. Lancet. 1973;1(7815):1267–71. Epub 1973/06/09.
132. Clarren SK, Smith DW. The fetal alcohol syndrome. N Engl J Med. 1978;298(19):1063–7. Epub 1978/05/11.
133. Burd L, Deal E, Rios R, Adickes E, Wynne J, Klug MG. Congenital heart defects and fetal alcohol spectrum disorders. Congenit Heart Dis. 2007;2(4):250–5. Epub 2008/04/02.
134. Gomez O, Martinez JM, Figueras F, Del Rio M, Borobio V, Puerto B, et al. Uterine artery Doppler at 11-14 weeks of gestation to screen for hypertensive disorders and associated complications in an unselected population. Ultrasound Obstet Gynecol. 2005;26(5):490–4. Epub 2005/09/27.
135. Prefumo F, Guven M, Ganapathy R, Thilaganathan B. The longitudinal variation in uterine artery blood flow pattern in relation to birth weight. Obstet Gynecol. 2004;103(4):764–8. Epub 2004/03/31.
136. Gomez O, Figueras F, Martinez JM, del Rio M, Palacio M, Eixarch E, et al. Sequential changes in uterine artery blood flow pattern between the first and second trimesters of gestation in relation to pregnancy outcome. Ultrasound Obstet Gynecol. 2006;28(6):802–8. Epub 2006/10/26.
137. Velauthar L, Plana MN, Kalidindi M, Zamora J, Thilaganathan B, Illanes SE, et al. First-trimester uterine artery Doppler and adverse pregnancy outcome: a meta-analysis involving 55,974 women. Ultrasound Obstet Gynecol. 2014;43(5):500–7. Epub 2013/12/18.
138. Bujold E, Morency AM, Roberge S, Lacasse Y, Forest JC, Giguere Y. Acetylsalicylic acid for the prevention of preeclampsia and intra-uterine growth restriction in women with abnormal uterine artery Doppler: a systematic review and meta-analysis. J Obstet Gynaecol Can. 2009;31(9):818–26. Epub 2009/11/28.
139. AIUM practice guideline for the performance of obstetric ultrasound examinations. J Ultrasound Med. 2013;32(6):1083–101. Epub 2013/05/30.
140. Carvalho JS. Fetal heart scanning in the first trimester. Prenat Diagn. 2004;24(13):1060–7. Epub 2004/12/23.

5

First Trimester Embryology: An Overview

Cresta W. Jones, Sabrina C. Burn, Jill Lewter, and Randall S. Kuhlmann

Introduction

Normal human development is a continuum. In particular, the first trimester of pregnancy is a period of rapid change from a fertilized egg to an embryo with a clearly recognizable human form. Interruptions in this process can result in abnormal development and congenital fetal anomalies. These anomalies can be the result of a variety of etiologic factors (Table 5.1) [1]. Up to 3% of human pregnancies are complicated by congenital abnormalities and it is anticipated that the majority of these abnormalities can be identified by prenatal ultrasound as early as the first trimester. The purpose of this chapter is to provide the clinician or sonographer with a basic understanding of embryonic and fetal development in the first trimester. Knowledge of normal and abnormal human embryology is critical to adequate evaluation of the first trimester fetus, whether normal or with anatomical abnormalities.

Table 5.1 Causes of malformations in the fetus/infant[a]

Chromosomal	10.0%
Single gene	3.0%
Familial	14.5%
Multifactorial	23.0%
Teratogens	3.2%
Uterine anomalies	2.5%
Twinning	0.4%
Unknown	

[a] Based on data from Ref. [1]

Signaling Pathways Identified for Embryologic Development

Embryonic development in the first trimester is complex and extensive. A small number of totipotent stem cells are responsible for cellular differentiation and organ formation. It is important to be aware that these complex processes are controlled by *cell signaling* pathways, which guide development both by the location of their expression and by the specific time at which they are actively expressed in the embryo and its surrounding tissues. Detailed information on signaling pathways is beyond the scope of this chapter but are well described in other texts [2–6].

Development of the Bilaminar Embryo (Weeks 1–2)

After successful fertilization, the resulting zygote quickly undergoes cleavage and progresses

---

C. W. Jones (✉) · S. C. Burn · J. Lewter
Division of Maternal-Fetal Medicine, Department of Obstetrics, Gynecology and Women's Health, University of Minnesota Medical School, Minneapolis, MN, USA
e-mail: JONESC@UMN.EDU; BURN@UMN.EDU; Jill.Lewter@fairview.org

R. S. Kuhlmann
Maternal-Fetal Medicine, ProHealth Care, Waukesha, WI, USA
e-mail: randall.kuhlmann@phci.org

© The Author(s), under exclusive license to Springer Nature Switzerland AG 2023
J. S. Abramowicz, R. E. Longman (eds.), *First-Trimester Ultrasound*,
https://doi.org/10.1007/978-3-031-24133-8_5

through the morula stage. The morula, a solid ball of dividing cells, will separate into an inner cell mass (the embryoblast or future embryo) and an outer cell mass (the trophoblastic component of the placenta).

The embryoblast further differentiates into a bilaminar embryonic disc, consisting of dorsal epiblast and ventral hypoblast. This occurs around day 14 post-fertilization, around the time of implantation [6].

Embryonic Weeks 3–4

During the 3rd week of life (i.e., 5 weeks after the last menstrual period), the dorsal epiblast goes on to develop an elongated primitive streak, which marks the start of gastrulation or conversion into the trilaminar embryonic disc, comprised of the three critical germ layers in the human embryo—ectoderm, mesoderm, and endoderm [7, 8]. From these three layers, all fetal tissues and organs will develop (Fig. 5.1).

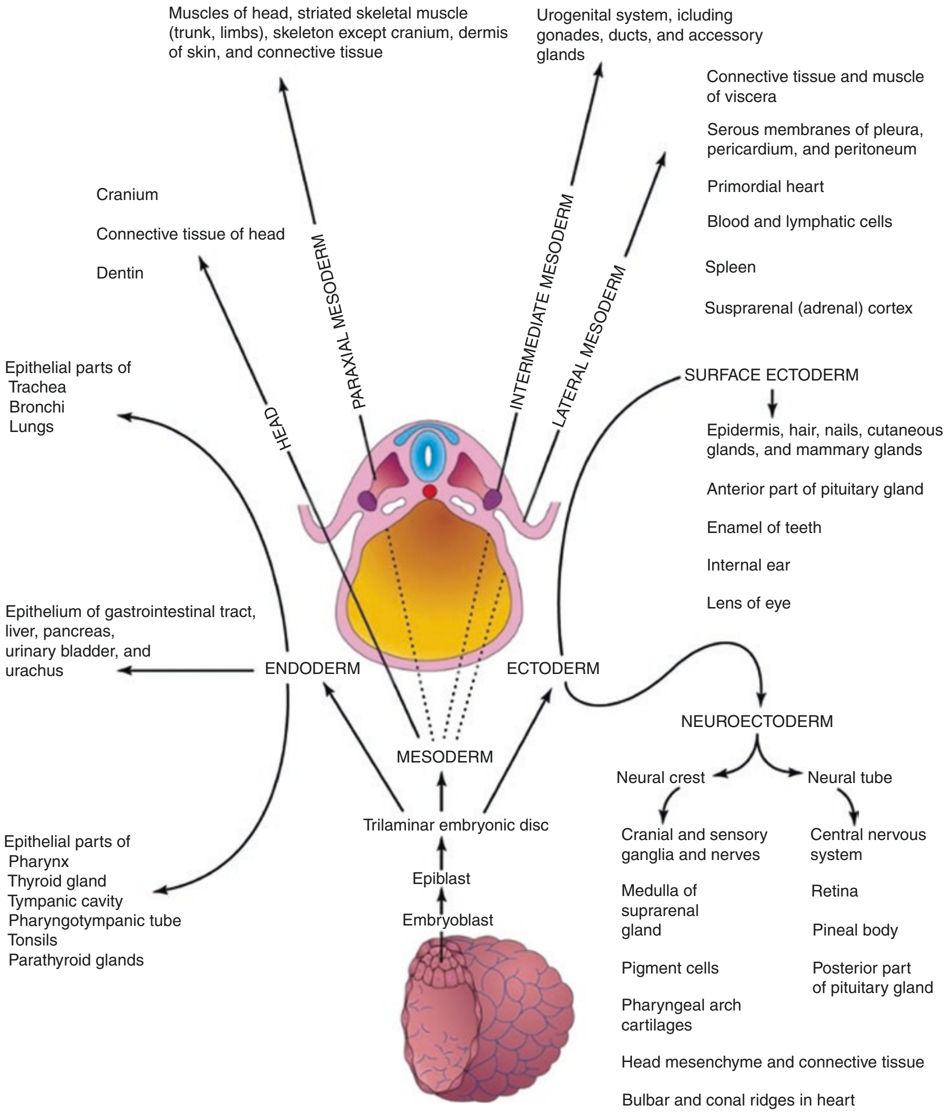
Muscles of head, striated skeletal muscle (trunk, limbs), skeleton except cranium, dermis of skin, and connective tissue
Urogenital system, icluding gonades, ducts, and accessory glands
Connective tissue and muscle of viscera
Serous membranes of pleura, pericardium, and peritoneum
Primordial heart
Blood and lymphatic cells
Spleen
Susprarenal (adrenal) cortex
Cranium
Connective tissue of head
Dentin
PARAXIAL MESODERM
INTERMEDIATE MESODERM
LATERAL MESODERM
HEAD
Epithelial parts of Trachea Bronchi Lungs
SURFACE ECTODERM
Epidermis, hair, nails, cutaneous glands, and mammary glands
Anterior part of pituitary gland
Enamel of teeth
Internal ear
Lens of eye
Epithelium of gastrointestinal tract, liver, pancreas, urinary bladder, and urachus
ENDODERM
ECTODERM
NEUROECTODERM
MESODERM
Neural crest
Neural tube
Trilaminar embryonic disc
Cranial and sensory ganglia and nerves
Central nervous system
Epithelial parts of Pharynx Thyroid gland Tympanic cavity Pharyngotympanic tube Tonsils Parathyroid glands
Epiblast
Embryoblast
Medulla of suprarenal gland
Retina
Pineal body
Pigment cells
Posterior part of pituitary gland
Pharyngeal arch cartilages
Head mesenchyme and connective tissue
Bulbar and conal ridges in heart

Fig. 5.1 Schematic of the derivatives of the three germ layers of the trilaminar embryonic disc: ectoderm, endoderm, and mesoderm. (This figure was published in The Developing Human: Clinically Oriented Embryology, 11th ed., Moore KL, Persaud TVN, Torchia MG, page 70, copyright Elsevier 2020)

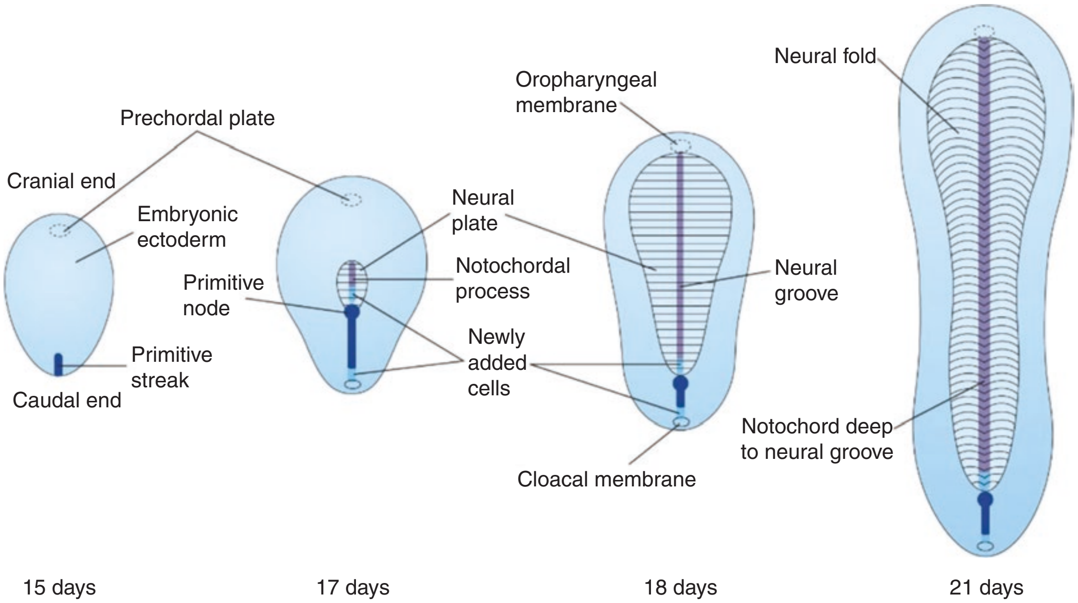

Fig. 5.2 Development of the primitive streak and notochord. The embryo begins to lengthen and change shape in the 3rd embryonic week. The primitive streak lengthens by adding cells at its caudal end, while the notochord lengthens by migration of cells from the primitive node. This process is the embryonic basis of the central nervous system. (This figure was published in The Developing Human: Clinically Oriented Embryology, 11th ed., Moore KL, Persaud TVN, Torchia MG, page 51, copyright Elsevier 2020)

The mesoderm also aids in the orientation of extraembryonic components such as the amniotic cavity, yolk sac, and the primary umbilical vesicle. In addition, gastrulation marks the beginning of morphogenesis, which is the shaping of an organism by the differentiation of cells, tissues, organs, and organ systems [9].

As the primitive streak develops (Fig. 5.2), it gives rise to the primitive node. This is critical for the development of mesenchyme, an embryonic tissue which will go on to serve as the progenitor for many supporting tissues of the fetus. Although the totipotent cells of the primitive streak typically regress by week 4 of embryonic development, remnants are believed to lead to the formation of a unique fetal tumor, the sacrococcygeal teratoma [10]. Newly formed mesenchyme cells will migrate through the streak and become a chord of tissue known as the notochord. The notochord determines the axis of the embryo and becomes a rod-like support for further axial development. Through notable signaling pathways that include sonic hedgehog (Shh) and bone morphogenetic proteins (BMPs), the notochord and the overlying neural tube will orchestrate the establishment of the axial musculoskeletal system as well as the development and segmentation of the central nervous system [11]. In addition, the paraxial mesoderm (mesoderm located on each side of the developing neural tube) divides into intermediate and lateral mesoderm, which gives rise to the components of the musculoskeletal system and the urinary tract [6].

Formation of the Neural Tube

This vital component of embryonic development begins during the 4th embryologic week. As the notochord develops, signaling pathways support the formation of the neural plate, which will give rise to the brain and spinal cord. The neural plate becomes a groove and folds in a process known as neurulation [12]. Fusion of the neural groove into a neural tube occurs in a zipper-like fashion, beginning in the middle and progressing in both cranial and caudal directions. Failure to fuse at any site in the process is known as a neural tube defect, which can range from small defects that are functionally unim-

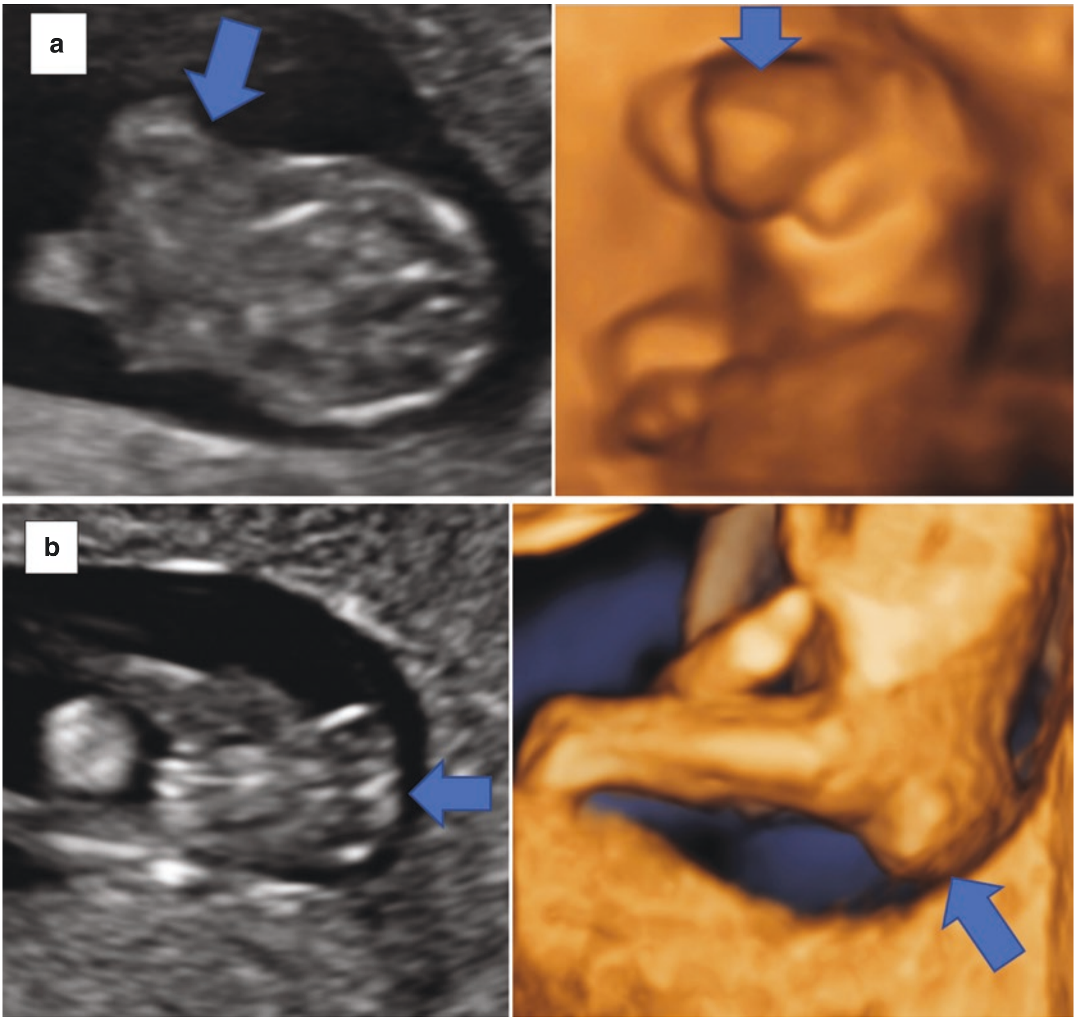

Fig. 5.3 (**a**) Ultrasound images (2D left, 3D right) at 11 weeks gestation with acrania, resulting from failure of the rostral neuropore to close. This results in the absence of a skull or cranium. Prolonged exposure of the fetal brain (blue arrows) to amniotic fluid can eventually lead to the destruction and degeneration of the brain or anencephaly. (**b**) Ultrasound images (2D left,3D right) at 14 weeks gestation of a sacral neural tube defect (blue arrows). This results from failure of the neural tube to close at the 5-6th week of gestation. (Courtesy of Dr. Cresta Jones, Division of Maternal Fetal Medicine, University of Minnesota, Minneapolis, MN)

portant (spina bifida occulta) to severe defects located at the cranial tube (acrania and anencephaly) (Fig. 5.3a) or further caudally (spina bifida) (Fig. 5.3b) [13].

Formation of the Fetal Brain

The fetal brain begins to develop from the most cranial portion of the neural tube during the 3rd embryologic week. Three primary brain vesicles (forebrain, midbrain, and hindbrain) will further divide into five secondary brain vesicles during the 5th embryonic week. Abnormalities in brain division and migration can result in abnormalities, which have the potential to cause significant challenges for normal neonatal neurodevelopmental outcomes.

Neural crest cells can be found alongside both sides of the neural tube. These cells are critical to normal development, as they migrate throughout the embryo to give rise to components of the heart, head, and face, and to ganglia of the spine and autonomic nervous system, pigment cells, adrenal glands, and the medulla [14]. Abnormal development or migration of neural crest cells is believed to influence the development of disorders such as neurofibromatosis and CHARGE association [15].

Embryonic Weeks 5–8

After the formation of the neural tube, the embryo enters a period in which many major body structures are developed. This period extends from the 5th to 8th week of embryonic development (7–10 postmenstrual weeks) [6]. This critical phase of development is the time at which the conceptus is most vulnerable to abnormal development due to teratogen exposure. Unfortunately, it is also a time at which many pregnant people might not yet be aware that they are pregnant, and thus exposure to environmental teratogens may be increased.

Individual organ systems and structures, as formed during the first trimester, will next be addressed individually.

Development of the Embryonic Cavities and Diaphragm

The primordium or the earliest recognizable body cavities is called intraembryonic coelom and is divided into individual cavities during the 4th and 5th embryonic weeks. These cavities include one pericardial cavity, two pericardioperitoneal cavities, and one peritoneal cavity. As the fetus begins to develop and fold cranially, the heart and pericardial cavity are located near the developing foregut and remain in direct communication with the paired pericardioperitoneal cavities [6]. As development continues, the peritoneal cavity becomes isolated, while the remaining cavities fuse and expand to establish separate pleural and peritoneal cavities, which will contribute to the creation of the diaphragm. Development of the diaphragm is dependent on the coordinated development of four separate components: the pleuroperitoneal membranes, the mesentery of the developing esophagus, the muscular ingrowth from the lateral body wall, and the septum transversum, an outgrowth of the dorsal body wall [16]. Defects in any of these components can result in a congenital diaphragmatic hernia (CDH) (Fig. 5.4). The most common cause of a CDH is the abnormal formation or fusion of the pleuroperitoneal membranes with the other components of the diaphragm and occurs on the left side of the fetus in 90% of cases [17].

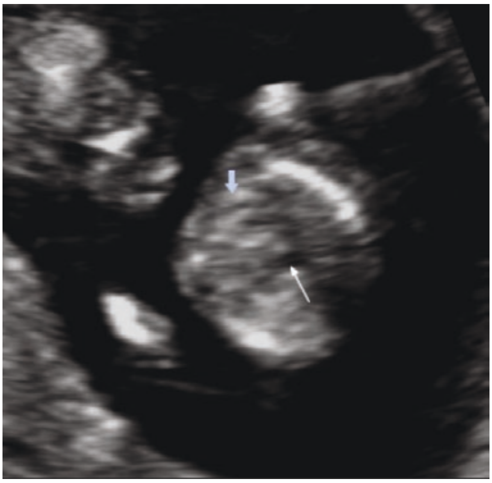

Fig. 5.4 Ultrasound image at 11 weeks with a congenital diaphragmatic hernia. The white arrow identified the fetal stomach in the chest, alongside the fetal heart (gray arrow). This results from a developmental defect of the diaphragm, with abdominal contents migrated into the fetal chest. (Courtesy of Dr. Cresta Jones, Division of Maternal Fetal Medicine, University of Minnesota, Minneapolis, MN)

Development of the Fetal Face

The development of the fetal face begins with embryonic primordia around the primordial fetal mouth or stomodeum. Facial development is dependent on the formation of five structures: a frontonasal prominence and paired maxillary and mandibular prominences. Appropriate migration and fusion are essential for normal facial and palate development [18]. Abnormalities in these processes can result in cleft lip and palate or more severe clefting of the fetal face. Clefting can also be associated with other midline anomalies such as holoprosencephaly (Fig. 5.5), often due to inappropriate signaling which prevents normal component migration and fusion. Such facial hypoplasia is often seen in trisomy 13.

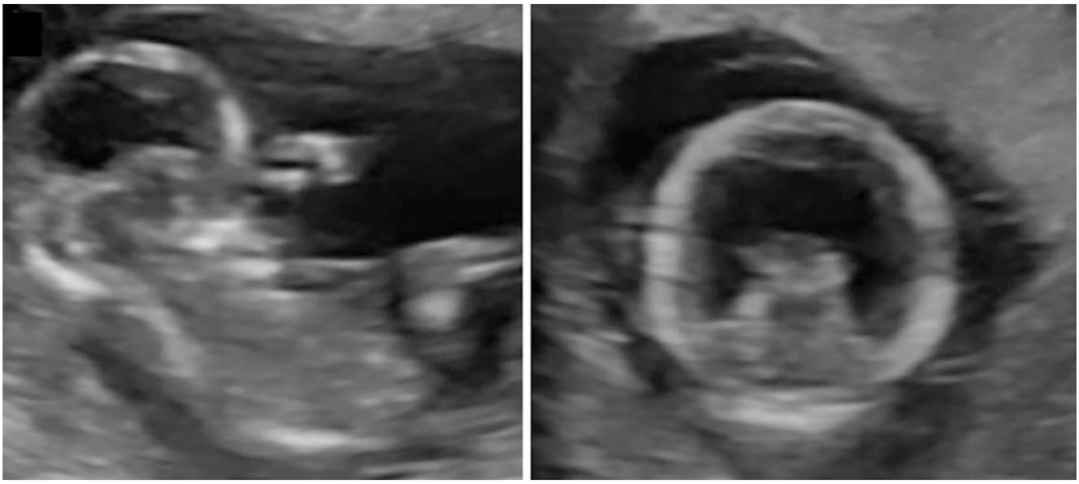

Fig. 5.5 Ultrasound images at 13 weeks gestation demonstrating the midline developmental defect of the embryonic forebrain called holoprosencephaly. This defect results in incomplete development of essential brain structures and is also associated with midline facial clefs. (Courtesy of Dr. Cresta Jones, Division of Maternal Fetal Medicine, University of Minnesota, Minneapolis, MN)

Development of the Respiratory System

The respiratory system also begins to develop during the 4th embryonic week, as the respiratory diverticulum buds from the primitive foregut. Subsequent migration of splanchnic mesoderm over the diverticulum results in the development of respiratory buds, which will further divide and differentiate over the course of fetal development and after birth. An important step in the respiratory system formation is the separation of the foregut and the esophagus from the trachea, through the development of tracheoesophageal folds. These folds will fuse to form the tracheoesophageal septum. Inappropriate or incomplete development of this septum can result in various types of tracheoesophageal fistulas (TEF). TEF is associated with incomplete formation of the esophagus in 85% of cases (esophageal atresia) [6] and can lead to an ultrasound finding of excess amniotic fluid, also known as polyhydramnios, and is secondary to the fetus' inability to swallow appropriately [19].

Development of the Gastrointestinal Tract

The primordial gut tube begins to form in the 4th embryonic week as a portion of the yolk sac is incorporated into the embryo as it folds. Cell proliferation will initially obliterate the lumen of the tube, which will then recanalize and differentiate into foregut, midgut, and hindgut components [6]. Incomplete recanalization can result in areas of stenotic or atretic intestine [20]. The foregut is divided into the trachea and esophagus as addressed in the prior section. Additional components of the foregut include the stomach, which will dilate and rotate to its normal physiologic location in the left upper quadrant, as well as the liver and duodenum [21].

At approximately the 6th embryonic week, the midgut forms a U-shaped loop, which will herniate through the umbilical ring of the embryo, causing physiologic gut herniation (Fig. 5.6a), which is a normal step in embryonic development. The loop will rotate 270° and then return to the abdomen by embryonic week 11. Abnormalities in hernia reduction can result in persistent bowel herniation into a sac at the umbilical cord insertion into the fetal abdomen, known as an omphalocele (Fig. 5.6b). Omphalocele is associated with an increased risk of fetal aneuploidy [22]. This contrasts with gastroschisis (Fig. 5.6c) which is defined by a defect located to the right of the umbilicus. Subsequently, the bowel and other structures can herniate through this defect. The speculated etiologies for

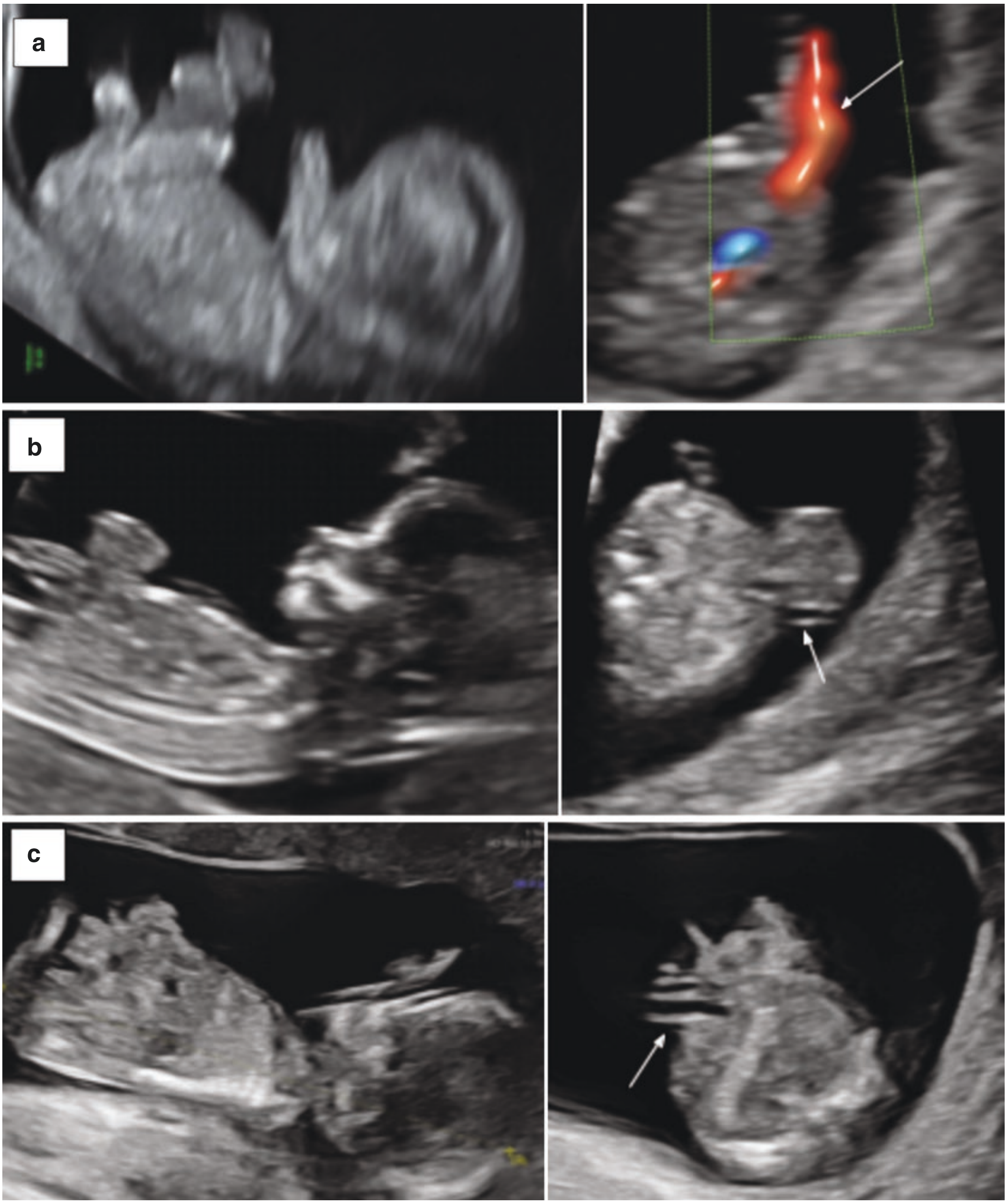

Fig. 5.6 Physiologic gut herniation and midline abdominal wall defects. (**a**) Ultrasound images at 9 weeks gestation with physiologic gut herniation, which occurs between 7 and 12 weeks. In the transverse plane (image on right), the gut is visualized directly alongside the umbilical cord vessel (arrow). (**b**) Ultrasound images at 13 weeks gestation with omphalocele. In the transverse (image on right) the herniation is central with the umbilical cord (arrow) inserted in the hernia sac. An omphalocele is frequently associated with other congenital anomalies. (**c**) Ultrasound images at 13 weeks gestation with gastroschisis. In the transverse plane (image on right), the umbilical cord (arrow) is located to the left of the herniated bowel. Gastroschisis is rarely associated with other congenital anomalies. (Courtesy of Dr. Cresta Jones, Division of Maternal Fetal Medicine, University of Minnesota, Minneapolis, MN)

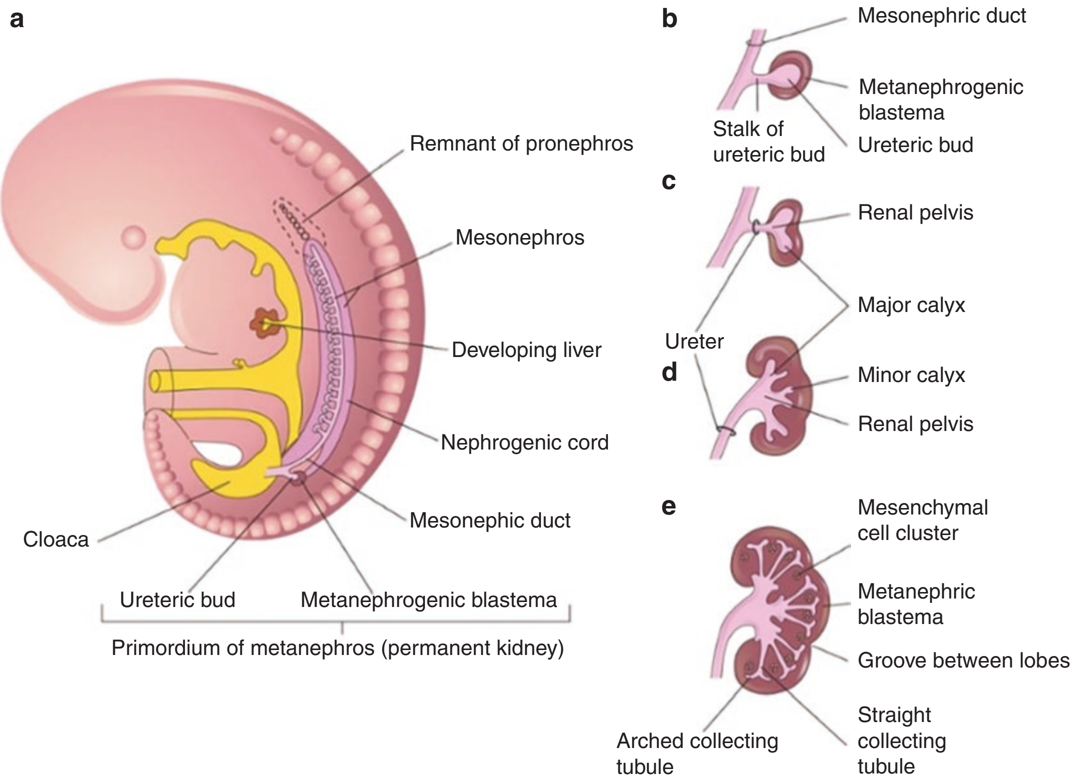
a
Remnant of pronephros
Mesonephros
Developing liver
Nephrogenic cord
Mesonephic duct
Cloaca
Ureteric bud
Metanephrogenic blastema
Primordium of metanephros (permanent kidney)
b
Mesonephric duct
Metanephrogenic blastema
Stalk of ureteric bud
Ureteric bud
c
Renal pelvis
Major calyx
Ureter
d
Minor calyx
Renal pelvis
e
Mesenchymal cell cluster
Metanephric blastema
Groove between lobes
Arched collecting tubule
Straight collecting tubule

Fig. 5.7 Development of the permanent kidney. (**a**) Five week human embryo showing the developing metanephros and ureteric bud. (**b–e**) Successive stages in the development of ureteric bud (5th to 8th weeks). (This figure was published in The Developing Human: Clinically Oriented Embryology, 11th ed., Moore KL, Persaud TVN, Torchia MG, page 228, copyright Elsevier 2020)

this defect include the agenesis of the right omphalomesenteric artery, or the early disappearance of the right umbilical vein resulting in non-fusion of the lateral folds of the embryo [6]. Gastroschisis is typically not associated with an increased risk of fetal genetic abnormalities [23].

Development of the Urogenital System

The fetal renal system progresses through three separate functioning kidney structures [6]. All three originate primarily from the intermediate mesoderm, which develops into the nephrogenic cord. The initial fetal renal structure, the pronephros, disappears by week 5 of embryonic life. It is replaced by the mesonephros and mesonephros (Wolffian) duct, which also plays a critical role in the development of the male reproductive system. At 10 embryonic weeks, the permanent renal structure, the metanephros, is formed and functional. It develops from an outgrowth of the mesonephros (ureteric bud), and this bud induces the formation of the metanephros (Fig. 5.7). Lack of development of the ureteric bud will result in absence of permanent fetal kidneys, or renal agenesis. This anomaly can be lethal if bilateral and is identified by a lack of amniotic fluid, also known as anhydramnios, typically identified in the second trimester of pregnancy [24].

Highlights of Cardiac Development

Highlights of cardiac development are reviewed in the section. A detailed review of the development of the human heart is beyond the scope of this chapter, due to the level of complexity of its formation.

Early Cardiac Development

The cardiovascular system is the first organ system to begin functioning at 3–4 weeks of embryonic age. It is primarily derived from splanchnic mesoderm, paraxial and lateral mesoderm, and pharyngeal mesoderm, but also involves the migration of neural crest cells [6]. Paired angiogenic cords, formed from the cardiogenic mesoderm, undergo fusion and canalization to form a simple tube, the initial heart structure. Blood begins flowing through the cardiac tube at approximately 4 weeks of embryonic age. The outside of the single tube becomes the myocardium, and the inside of the tube becomes the endocardium. The epicardium (visceral pericardium) is derived from mesothelial cell proliferation from the external surface of the sinus venosus, which is a predecessor of the cardiac atria [25]. Folding of the head results in a heart location, which is ventral to the foregut and caudal to the developing mouth.

After the formation of a single cardiac tube, partitioning of the heart begins at the end of the 4th embryonic week and continues into the 9th week [6]. The developing heart begins to bend and constrict, resulting in the formation of five segmental primitive heart dilations: the truncus arteriosus, bulbus cordis, primitive ventricle, primitive atrium, and sinus venosus. The truncus arteriosus gives rise to the precursors of the aorta and pulmonary trunk, the bulbus cordis and primitive ventricle given risk to the ventricles, and the primitive atrium and sinus venosus given rise to the atria and the coronary sinus. Dextral (right-handed) cardiac looping is also initiated during this period and is believed to primarily occur during embryonic weeks 5–7 [25]. The process results in a U-shaped loop and determines the normal axis of the heart (Fig. 5.8).

When the heart tube loops left, rather than right, the heart is displaced and its great vessels are reversed, creating a mirror image of the normal heart structure, called dextrocardia. Dextrocardia

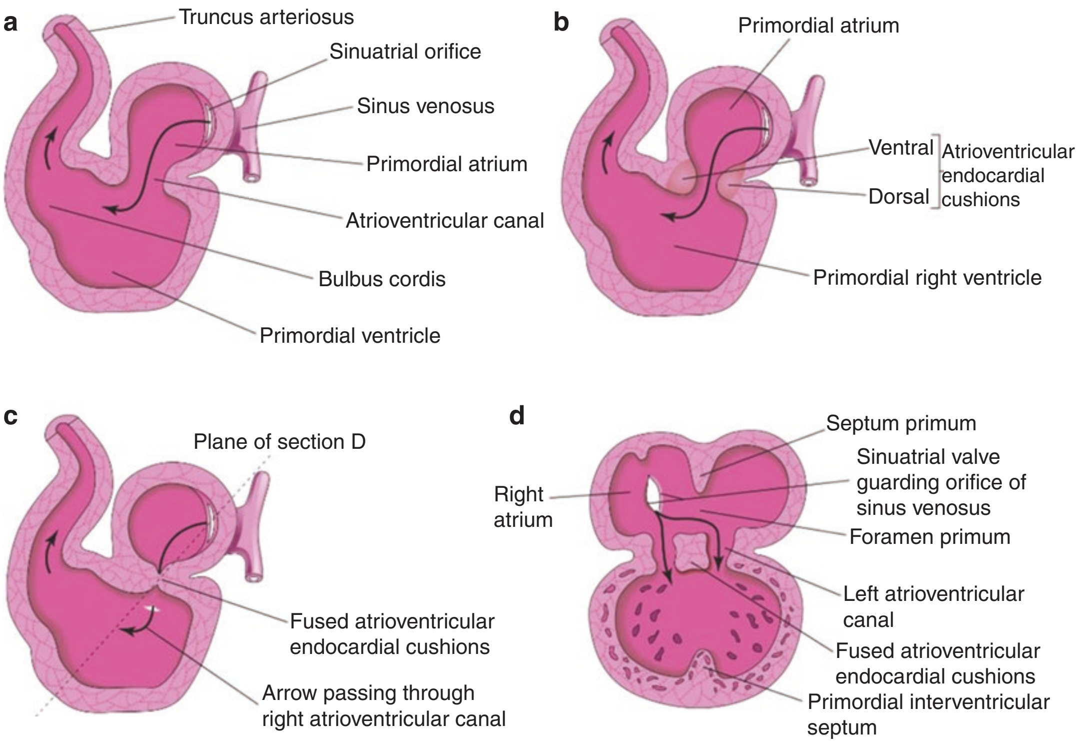
a
Truncus arteriosus
Sinuatrial orifice
Sinus venosus
Primordial atrium
Atrioventricular canal
Bulbus cordis
Primordial ventricle
b
Primordial atrium
Ventral
Dorsal
Atrioventricular endocardial cushions
Primordial right ventricle
c
Plane of section D
Fused atrioventricular endocardial cushions
Arrow passing through right atrioventricular canal
d
Right atrium
Septum primum
Sinuatrial valve guarding orifice of sinus venosus
Foramen primum
Left atrioventricular canal
Fused atrioventricular endocardial cushions
Primordial interventricular septum

Fig. 5.8 (**a**, **b**) Sagittal sections of the heart during the 4th and 5th weeks, illustrating blood flow and division of the atrioventricular canal. (**c**) Fusion of the atrioventricular endocardial cushions. (**d**) Coronal section of the plane shown in (**c**). (This figure was published in The Developing Human: Clinically Oriented Embryology, 11th ed., Moore KL, Persaud TVN, Torchia MG, page 273, copyright Elsevier 2020) can be associated in some cases with an increased risk of severe cardiac abnormalities [26].

Cardiac Septae Formation and Valvular Development

Multiple separate cell migration and signaling pathway processes are involved in the development of appropriate cardiac septae.

Atrioventricular (AV) Septum

The AV endocardial cushions develop from a specialized extracellular matrix (cardiac jelly) within the walls of the AV canal. These cushions move toward each other and eventually fuse to form the AV septum with separation of a common AV canal into left and right AV canals. The cushions then function as the precursor to AV valves until further differentiation occurs, resulting in definitive valve structures. Inductive signals from the myocardium of the AV canal cause epithelial-mesenchymal transformation, which changes the endocardial cushions and ultimately contributes to the development of the definitive AV valves and membranous septum of the heart [26].

Numerous cardiac anomalies are attributable to the abnormal development of the endocardial cushions. Failure of cushion fusion is responsible for a persistent common AV canal, in which there is no true septal division of the heart, and a single common AV valve in place of the tricuspid and mitral valves (Fig. 5.9). Inadequate amounts of cushion are also believed to be associated with abnormal development of the tricuspid valve, including abnormal location (Ebstein's anomaly) or congenital absence of the valve, the results of which can have devastating consequences for long-term cardiac function [26].

Atrial Septum

Partitioning of the atria begins at the end of the 4th embryonic week [6]. The right and left atria are created by fusion of the two septae, the septum primum and the septum secundum. The septum primum has an initial foramen or hole, termed the foramen primum, and subsequently develops the foramen secundum. As the septum secundum develops, an incomplete septation occurs resulting in the foramen ovale [27]. The inferior aspect of the septum primum becomes the flap (valve) of the foramen ovale, which should fuse anatomically shortly after birth. Excessive resorption of either the septum primum or septum secundum results in an atrial septal defect or persistent foramen ovale, which are among the most common congenital heart abnormalities. The female to male ratio for atrial septal defects is 3:1 [28].

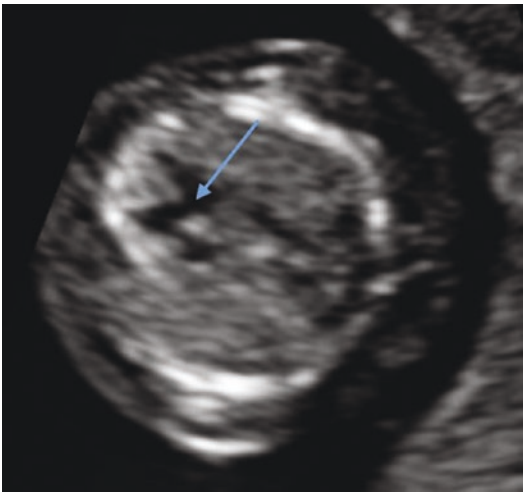

Fig. 5.9 US image at 12 weeks gestation of a transverse view through a persistent common atrioventricular canal defect (arrow). This is complication of abnormal endocardial cushion development. (Courtesy of Dr. Cresta Jones, Division of Maternal Fetal Medicine, University of Minnesota, Minneapolis, MN)

Ventricular Septum

Partitioning of the ventricles also involves septation, accomplished by fusion of the muscular portion of the interventricular (IV) septum with the membranous area of the septum [6]. Until the 7th embryonic week, a defect is noted in the IV septum between the free edge of the muscular portion and the lower component of the AV cushions. Closure of the defect typically occurs at the end of the 7th week and involves fusion of the membranous portion of the IV septum with the muscular component [27]. Failure of this closure to occur results in ventricular septal defects (VSDs), which are the most common form of congenital heart disease, making up approximately 25% of cases [29]. Typically, the defect results from failure of the membranous portion of the septum to close, although defects in other locations do occur. Many small VSDs close during embryonic and fetal development, although larger defects can result in cardiac dysfunction and require postnatal surgical management.

Aorticopulmonary (AP) Septum

The septation of the truncus arteriosus and bulbus cordis is critical to normal cardiac development as well as to normal outflow through the pulmonary trunk and the aorta. This occurs during the 5th embryonic week [6]. The AP septum is believed to be formed by mesenchyme derived from migrating neural crest cells, which invade the truncus arteriosus and bulbus cordis [27]. As the cells migrate, they develop in a spiral fashion, fusing to form the AP septum and separating the pulmonary and aortic outflow tracts. Membranous tissue from the interventricular septum also fuses with the aorticopulmonary septum, resulting in a normal anatomic relationship, where the pulmonary artery arises from the right ventricle and the aorta arises from the left ventricle. If neural crest cell migration does not proceed appropriately, the AP septum may not develop properly. This includes a condition called truncus arteriosus, which results from limited development of the AP septum, with only one large vessel leaving the heart. Abnormal or absent spiraling of the septum can cause transposition of each vessel from its appropriate ventricular outflow, called transposition of the great arteries. Unequal division of the truncus arteriosus is also believed to contribute to the development of Tetralogy of Fallot, in which pulmonary artery stenosis, ventricular septal defect, overriding aorta, and right ventricular hypertrophy occur together [26].

Development of the Lymphatic System

Development of the lymphatic system begins at the end of the 6th embryonic week after the cardiovascular system has developed [30]. It develops with a process like that for fetal blood vessels, with a series of small lymphatic tubes joining to form a lymphatic network. Lymphatic drainage encompasses six primary lymph sacs and many lymph nodes. Draining occurs first from the cranial and caudal aspects of the embryo and then primarily into the right lymphatic duct. A small measurable area filled with lymphatic fluid is typically seen behind the fetal neck at 10–14 weeks gestation and is known as the nuchal translucency (Fig. 5.10a). Abnormalities in lymphatic drainage, due to a blocked or malformed lymphatic sac or channel, may cause a thickened nuchal translucency (Fig. 5.10b) or even larger swellings around the fetal neck known as cystic hygroma (Fig. 5.10c). The presence of a cystic hygroma is associated with an increased risk of fetal genetic abnormalities, cardiac malformations, and other fetal developmental problems [31, 32].

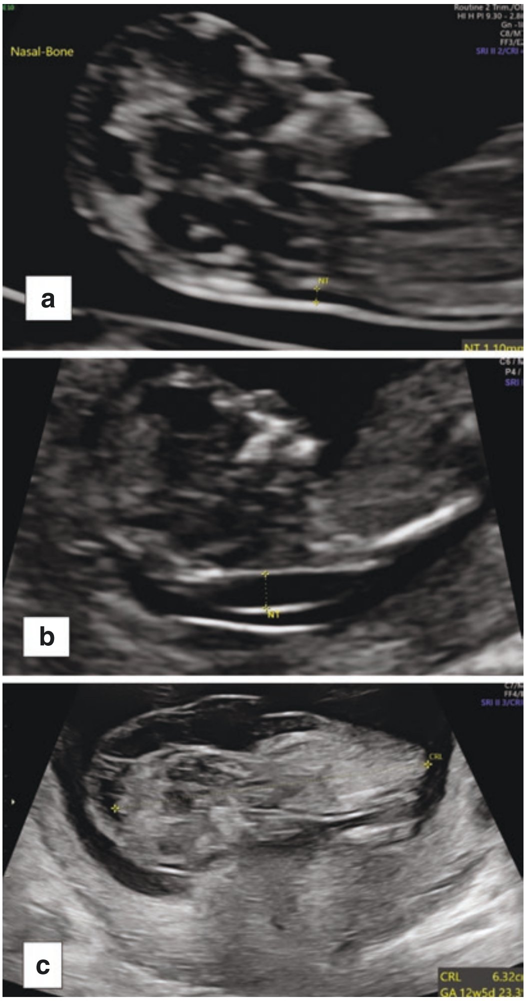

Fig. 5.10 First trimester images of nuchal translucency and related abnormalities. (**a**) Ultrasound image at 12 weeks gestation with a normal nuchal translucency. (**b**) Ultrasound image at 13 weeks gestation with a thickened nuchal translucency. (**c**) Ultrasound image at 12 weeks gestation with a cystic hygroma. (Courtesy of Dr. Cresta Jones, Division of Maternal Fetal Medicine, University of Minnesota, Minneapolis, MN)

Summary

The human embryo undergoes remarkable development in the first trimester of pregnancy, progressing from several cells to an organism with clear organ structure and function. This formation is in large part affected by a complex system of embryonic cell signaling and the fetus' surrounding environment. Abnormalities in signaling function and cell migration, including those resulting from first trimester teratogen exposure or genetic abnormalities can have long-term complications for the developing fetus and newborn.

References

1. Nelson K, Holmes LB. Malformation due to presumed spontaneous mutations in newborn infants. N Engl J Med. 1989;320(1):19–23.
2. Clark E. Time and space in segmentation. Interface Focus. 2021;11(3):20200049.
3. Valcourt JR, Huang RE, Kundu S, Venkatasubramanian D, Kingston RE, Ramanathan S. Modulating mesoendoderm competence during human germ layer differentiation. Cell Rep. 2021;37(6):109990.
4. Dutta D. Signaling pathways dictating pluripotency in embryonic stem cells. Int J Dev Biol. 2013;57(9–10):667–75.
5. Huang G, Ye S, Zhou X, Liu D, Ying Q. Molecular basis of embryonic stem cell self-renewal: from signaling pathways to pluripotency network. Cell Mol Life Sci. 2015;72(9):1741–57.
6. Moore KL, Persaud TVN, Torchia MG. The developing human: clinically oriented embryology. 11th ed. Edinburgh: Elsevier; 2020.
7. Downs KM. Enigmatic primitive streak: prevailing notions and challenges concerning the body axis of mammals. BioEssays. 2009;31(8):892–902.
8. Schauer A, Heisenberg C. Reassembling gastrulation. Dev Biol. 2021;474:71–31.
9. Wang Y, Minarsky A, Penner R, Soule C, Morozova N. Model of morphogenesis. J Comput Biol. 2020;27(9):1373–83.
10. Phi JH. Sacrococcygeal teratoma: a tumor at the center of embryogenesis. J Korean Neurosurg Soc. 2021;64(3):406–13.
11. Wymeersch FJ, Wilson V, Tsakiridis A. Understanding axial progenitor biology *in vivo* and *in vitro*. Development. 2021;148(4):dev180612.
12. Kuwar Chhetri P, Das JM. Neuroanatomy, neural tube development and states. In: StatPearls. Treasure Island, FL: StatPearls Publishing; 2021.
13. Wolujewicz P, Steele JW, Kaltschmidt JA, Finnell RH, Ross ME. Unraveling the complex genetics of neural tube defects: from biological models to human genomics and back. Genesis. 2021;59(11):e23459.
14. Gandhi S, Bronner ME. Seq your destiny: neural crest fate determination in the genomic era. Annu Rev Genet. 2021;55:349–76.
15. Takahashi Y, Sipp D, Enomoto H. Tissue interactions in neural crest development and disease. Science. 2013;341(6148):860–3.
16. Sefton EM, Gallardo M, Kardon G. Developmental origin and morphogenesis of the diaphragm, an essential mammalian muscle. Dev Biol. 2018;440(2):64–73.
17. Mehollin-Ray AR. Congenital diaphragmatic hernia. Pediatr Radiol. 2020;50(13):1855–71.
18. Andresen C, Matias A, Merz E. Fetal face: the whole picture. Ultraschall Med. 2012;33(5):431–40.
19. Varela P, Torre M, Schweiger C, Nakamura H. Congenital tracheal malformations. Pediatr Surg Int. 2018;34(7):701–13.
20. Dadhwal V, Kochhar S, Mittal S, Kumar S, Agarwal S, Arora V, Barua A. Fetal gastrointestinal malformations. Indian J Pediatr. 2001;68(1):27–30.
21. Adams AD, Stover S, Rac MW. Omphalocele—what should we tell the prospective parents? Prenat Diagn. 2021;41(4):486–96.
22. Bhat V, Moront M, Bhandari V. Gastroschisis: a state-of-the-art review. Children (Basel). 2020;7(12):302.
23. Huber C, Shazly SA, Blumenfeld YJ, Jelin E, Ruano R. Update on the prenatal diagnosis and outcomes of fetal bilateral renal agenesis. Obstet Gynecol Surv. 2019;74(5):298–302.
24. Hernandez-Andrade E, Patwardhan M, Cruz-Lemini M, Luewan S. Early evaluation of the fetal heart. Fetal Diagn Ther. 2017;42(3):161–73.
25. Mandrycky CJ, Williams NP, Batalov I, El-Nachef D, de Bakker BS, Davis J, Kim DH, DeForest CA, Zheng Y, Stevens KR, Sniadecki NJ. Engineering heart morphogenesis. Trends Biotechnol. 2020;38(8):835–45.
26. Lambert TE, Kuller J, Small M, Rhee E, Barker P. Abnormalities of fetal situs: an overview and literature review. Obstet Gynecol Surv. 2016;71(1):33–8.
27. Calkoen EE, Hazekamp MG, Blom NA, Elders BB, Gittenberger-de Groot AC, Haak MC, Bartelings MM, Roest AA, Jongbloed MR. Atrioventricular septal defect: from embryonic development to long-term follow-up. Int J Cardiol. 2016;202:784–95.
28. Das BB. Patent foramen ovale in fetal life, infancy and childhood. Med Sci (Basel). 2020;8(3):25.
29. Ahmed I, Anjum F. Atrioventricular septal defect. In: StatPearls. Treasure Island, FL: StatPearls Publishing; 2021.
30. Hutson MR, Kirby ML. Model systems for the study of heart development and disease. Cardiac neural crest and conotruncal malformations. Semin Cell Dev Biol. 2007;18(1):101–10.
31. Karl TR, Stocker C. Tetralogy of Fallot and its variants. Pediatr Crit Care Med. 2016;17(8 Suppl 1):S330–6.
32. Yang Y, Oliver G. Development of the mammalian lymphatic vasculature. J Clin Invest. 2014;124(3):888–97.

6

Elements of Teratology

Eran Barzilay and Gideon Koren

Definition

A teratogen is defined as any agent that can produce an adverse fetal outcome, including congenital anomaly, miscarriage, intrauterine growth restriction, stillbirth, prematurity, or long-term developmental delay [1, 2]. Environmental factors that have a teratogenic potential include drugs, chemicals, infections, and physical factors (such as radiation).

Perception of Teratogenic Risk

Birth defects are not a rare phenomenon, and in most cases are not related to environmental agents [1]. A baseline risk for malformation of 1–3% is a useful reference frame for evaluating the teratogenic risk of environmental exposures [3, 4]. Before thalidomide was recognized as a teratogen, the placenta was perceived to serve as a barrier that protected the developing embryo from any maternal exposure [2]. This perception may explain the fact that years had passed before thalidomide was recognized as a teratogen, despite a high rate of malformations and their characteristic pattern [5, 6]. The thalidomide disaster shifted the perception of risk to the other extreme, to a point that physicians and patients alike consider every drug as potentially harmful for the embryo [7]. Recent studies have shown that women exposed to agents not known to be teratogenic assigned themselves an unrealistically higher risk for major malformations and were more likely to terminate their pregnancy [7, 8]. Overestimation of teratogenic risk, aside from effecting decisions regarding pregnancy termination, may also prompt women to discontinue vital drug treatment and thereby endanger both their and their offspring's health.

An example for how erroneous perception of risk can affect medical practice is the withdrawal of bendectin from the market worldwide. Bendectin (a combination of vitamin B6 and doxylamine) was voluntarily removed from market by its manufacturer in 1983 due to multiple liability suits and a steep increase in insurance premiums. This happened despite the fact that an FDA investigation did not find an association between bendectin and birth defects. Following bendectin's withdrawal, admissions for excessive vomiting in pregnancy per thousand live births rose by 50% in 1984 [9]. Another example for the possible detrimental effects of overestimation of teratogenic risk is the panic that followed the

---

E. Barzilay (✉)
Department of Obstetrics and Gynecology, Samson Assuta Ashdod University Hospital, Ashdod, Israel

Faculty of Health Sciences, Ben-Gurion University of the Negev, Beer-Sheva, Israel

G. Koren
Motherisk Israel, Adelson Faculty of Medicine, Ariel University, Ariel, Israel

© The Author(s), under exclusive license to Springer Nature Switzerland AG 2023
J. S. Abramowicz, R. E. Longman (eds.), *First-Trimester Ultrasound*,
https://doi.org/10.1007/978-3-031-24133-8_6

Chernobyl nuclear accident in 1986. A study from Greece estimated that 2500 otherwise wanted pregnancies were terminated due to perceived radiation risk, despite the fact that radiation levels in Athens were within normal levels [10]. Furthermore, according to the International Atomic Energy Agency, an estimated 100,000–200,000 desired pregnancies were aborted in Western Europe because physicians advised patients that the radiation from Chernobyl posed a significant health risk to unborn children [11].

Teratogens

The baseline risk for major fetal malformations is estimated at 1–3% [3, 4]. In most cases, the cause of the malformation is unknown. In 20–25%, the malformation is caused by genetic factors and in 8–11% they are attributed to environmental factors [4]. Environmental factors that have been associated with congenital malformations include exposure to chemical and drugs, maternal disease, infection, and exposure to radiation.

Drugs in Pregnancy

Prescription drugs are used in more than 50% of pregnancies [12, 13]. Considering non-prescription drugs and drugs of abuse, the prevalence of exposure to drugs in pregnancy is probably much higher. Nevertheless, only a few drugs (Table 6.1) have been proven to be teratogenic in humans [2]. In most cases, the sensitive period for fetal development is in the first trimester. However, some drugs have been shown to affect the fetus in later pregnancy. For example, tetracycline exposure after 25 weeks might result in staining of teeth and possibly affect bone growth [14], third trimester exposure to non-steroidal anti-inflammatory drugs has been associated with premature constriction of the ductus arteriosus and oligohydramnios [15, 16], and late exposure to ACE inhibitors has been associated with fetal and neonatal death, renal abnormalities, oligohydramnios, fetal skull ossification defects, and patent ductus arteriosus [17].

Table 6.1 Drugs considered as teratogens

Drug	Teratogenic effects
Alcohol	Fetal alcohol syndrome, growth retardation, neurological abnormality, developmental delay, intellectual impairment, microcephaly, micro-ophthalmia, short palpebral fissures, poorly developed philtrum, thin upper lip and/or flattening of maxillary area, congenital heart defects, neural tube defects, renal abnormalities, cleft palate.
Aminopterin	A “clover-leaf” skull, large head, swept-back hair, low-set ears, prominent eyes, wide nasal bridge, meningoencephalocele, anencephaly, brachycephaly, hydrocephaly, delayed calvarial ossification, craniosynostosis, ocular hypertelorism, micrognathia, oral clefts, limb anomalies, neural tube defects.
Benzodiazepines	Oral clefts (conflicting results).
Carbamazepine	Neural tube defects.
Carbon monoxide	Stillbirth, growth retardation, and severe neurological sequelae. Possibly also VSD and pulmonic stenosis.
Cocaine	Stillbirth, placental abruption, prematurity, low birth weight, microcephaly, intraventricular hemorrhage, and developmental difficulties. An association with urinary tract anomalies was suggested.
Corticosteroids	Cleft palate (conflicting results), fetal growth impairment.
Diethylstilbestrol	Abnormal urogenital tract development, increased risk of vaginal clear cell carcinoma.
Lithium	Ebstein’s anomaly, other cardiac malformations.
Methotrexate	Intrauterine growth restriction, dysmorphic facial features, digital anomalies, limb, ear, skeletal, genital, skull, chin, central nervous system, spinal, cardiac, gastrointestinal defects and oral clefts.
Methyl mercury, mercury sulfide	Fetal Minamata disease (microcephaly, seizures, ataxia, cognitive impairment, and cerebral palsy).
Misoprostol	Moebius sequence (paralysis of the sixth and seventh cranial nerves).

Table 6.1 (continued)

Drug	Teratogenic effects
Mycophenolate mofetil	Microtia, auditory canal atresia, cleft lip and palate, micrognathia, hypertelorism, ocular coloboma, short fingers, and hypoplastic nails.
PCB	Dark brown pigmentation of the skin and the mucous membrane, gingival hyperplasia, exophthalmic edematous eye, dentition at birth, abnormal calcification of the skull, rocker bottom feet, and low birth weight.
Penicillamine	Cutis laxa and inguinal hernia (conflicting results).
Phenobarbital	Cardiac defects and cleft palate.
Phenytoin	Broad nasal bridge, metopic ridging, microcephaly, cleft lip/palate, ptosis, variable degrees of hypoplasia of the distal phalanges.
Retinoids	Microtia/anotia, micrognathia, thymic, CNS, and cardiac defects.
Thalidomide	Limb reduction defects, cardiac defects, facial hemangiomata, esophageal and duodenal atresia, renal defects, microtia, and anotia.
Valproic acid	Spina bifida, atrial septal defect, cleft palate, hypospadias, polydactyly, and craniosynostosis.
Warfarin	Skeletal defects (nasal hypoplasia, stippled epiphysis), growth restriction, CNS damage, eye defects, and hearing loss.

A list of drugs considered as teratogens and the main teratogenic effects that were associated with first trimester exposure to these drugs

Moreover, because the fetal brain continues to develop throughout pregnancy, late effects of chemicals such as alcohol and tobacco smoke have been documented.

Alcohol

Ethanol (alcohol) consumption during pregnancy has been associated with a variety of birth anomalies, many of which can be demonstrated by ultrasound, as well as neurocognitive impairment.

Diagnosis of Fetal Alcohol Spectrum disorder (FASD) requires:

1. Prenatal and/or postnatal growth restriction (weight, length, and/or head circumference below the 10th centile).
2. Central nervous system involvement (signs of neurological abnormality, developmental delay, behavioral effects, or intellectual impairment).
3. Characteristic facial dysmorphology with at least two of these three signs:
   (a) Microcephaly
   (b) Micro-ophthalmia and/or short palpebral fissures
   (c) Poorly developed philtrum, thin upper lip, and/or flattening of maxillary area

Structural malformations other than those of the face are sometime associated with FASD, including congenital heart defects, neural tube defects, renal abnormalities, cleft palate, and minor malformations such as strabismus, unusual palmar creases, and poorly formed ears. Full expression of the fetal alcohol syndrome generally occurs with chronic ingestion of at least 2 g/kg/day of alcohol. A conservative estimation of malformation risk for women consuming more than 2 g/kg/day during the first trimester is a two- to three-fold increase in risk. It is possible that minor effects would be caused by smaller amounts of alcohol, however, a safe amount of alcohol consumption in pregnancy has not been determined [18–22].

Aminopterin

Aminopterin is a folic acid antagonist closely related to methotrexate. It has been used in the 1950s as an anticancer drug and to induce abortions. Exposure to aminopterin in the first trimester has been associated with a "clover-leaf" skull with a large head, swept-back hair, low-set ears, prominent eyes and wide nasal bridge, as well as meningoencephalocele, anencephaly, brachycephaly, hydrocephaly, short stature, delayed calvarial ossification, craniosynostosis, ocular hypertelorism, micrognathia, oral clefts, limb anomalies, and neural tube defects. The critical period of exposure appears to be the 6th to 8th week of gestation [23–27]. Most of these malformations such as anencephaly or micrognathia are recognizable by ultrasound, often in early gestation.

Benzodiazepines

Based on meta-analysis of case-control studies, benzodiazepines may increase the risk for oral cleft. Data in the literature, however, show conflicting results. Pooled data from cohort studies showed no association between fetal exposure to benzodiazepines and the risk of major malformations or oral cleft. On the basis of pooled data from case-control studies, however, there was a significant increased risk for major malformations or oral cleft alone [28]. The absolute increase in risk for oral clefts, if it exists, appears to be very low (incidence of oral clefts in the general population is about 1 in 1000) [29, 30]. Oral clefts should be recognized with ultrasound examination of the fetal face.

Carbamazepine

Exposure to carbamazepine monotherapy in utero increases the risk of NTD to a higher rate than the general population but less than that associated with valproic acid. The risk of NTD has been estimated to increase from a baseline of about 0.1% to 0.2–1% [31–37]. Fetal spine examination is part of any routine ultrasound anatomy study.

Carbon Monoxide Poisoning

Mild carbon monoxide poisoning was not associated with increased fetal risk, but adverse fetal outcomes were noted with severe maternal toxicity, including a high risk of stillbirth, growth restriction, and severe neurological sequelae (mental retardation, seizures, spasticity). An association with VSD and pulmonic stenosis was also suggested. The relative risk for birth defects in cases of carbon monoxide poisoning is unknown. Most adverse effects were observed when toxicity was severe enough to cause maternal symptoms [38–40].

Cocaine

Studies on the effect of cocaine exposure in pregnancy frequently suffer from methodological drawbacks that make the results difficult to interpret. Most women who abuse cocaine are polydrug abusers, use alcohol, smoke and have other risk factors for poor pregnancy outcome including poor nutrition, high gravidity, and lack of prenatal care. Cocaine use in pregnancy has been associated with an increased risk for stillbirth, placental abruption, prematurity, lower birth weight, and microcephaly compared to nonexposed infants. Associations with intraventricular hemorrhage, developmental difficulties, and SIDS have also been suggested. There is disagreement on whether cocaine use increases the risk of structural malformations, although some studies show an increase in urinary tract anomalies [41–46].

Corticosteroids

Corticosteroids have been consistently shown to produce cleft palate in animals. Human studies have shown conflicting results. A possible association with oral clefts cannot be excluded. Glucocorticoids are associated with fetal growth impairment. The absolute increase in risk for oral clefts, if it exists, appears to be low (baseline 0.1%) [47–53]. Oral clefts can be observed during examination of the fetal face.

Diethylstilbestrol (DES)

DES has been associated with abnormal urogenital tract development and an increased risk of vaginal clear cell carcinoma. Vaginal adenosis was reported in up to 50% of offspring, and the incidence of preterm deliveries was reported as 11–39% [54, 55].

Lithium

Lithium exposure during the first trimester is associated with an increased risk of major malformations [56]. Lithium use has been associated with cardiac malformations in general and specifically with Ebstein's anomaly. Early information regarding teratogenic risk of lithium was derived from retrospective reports with a high risk of bias. More recent studies indicate that the risk is much lower. Risk for Ebstein's anomaly after first trimester exposure has been estimated as 0.05–0.1% [57–59]. This cardiac anomaly has specific components (displacement of the septal and posterior leaflets of the tricuspid valve toward the apex of the right ventricle of the heart, resulting in the typical appearance with a large right atrium and a small right ventricle) that can be observed in a simple four-chamber view of the heart (see Chap. 12).

Methotrexate

Methotrexate is a folic acid antagonist closely related to aminopterin. Several reports of exposure to single high-dose methotrexate, in cases of failed termination of pregnancy or misdiagnosis of ectopic pregnancy, have demonstrated a variety of anomalies. The anomalies noted on prenatal ultrasonography and/or at birth included intrauterine growth restriction, dysmorphic facial features, digital anomalies, limb, ear, skeletal, genital, skull, chin, central nervous system, spinal, cardiac, gastrointestinal defects, and oral clefts. A recent prospective observational study of pregnancy outcome in women taking methotrexate (up to 30 mg/week) for rheumatic disease demonstrated that among women exposed to methotrexate post conception (188) 42.5% had spontaneous abortions and the risk of major birth defects was elevated (6.6%, odds ratio 3.1, 95% CI 1.03–9.5). The observed malformations included gastroschisis, scoliosis, CCAM, cardiac malformation, renal malformations, limb defects, holoprosencephaly, and megabladder. Women planning a pregnancy after methotrexate therapy should be counseled to use contraception and folate supplementation during therapy and for a period of 3 months after stopping the drug [23, 25, 26, 60–66].

Methyl Mercury, Mercury Sulfide

Exposure to high levels of organic mercury in utero may cause fetal Minamata disease,[1] manifested by microcephaly, seizures, ataxia, cognitive impairment, and cerebral palsy. Relative risk has not been established, however, 13/220 babies born in Minamata at time of contamination suffered from severe disease [67–69].

Misoprostol

Exposure to misoprostol is associated with Moebius sequence (paralysis of the sixth and seventh cranial nerves). Association with other malformations, such as limb reduction defects, abnormalities of frontal and temporal bones in the skull, has been suggested but not confirmed. Odds ratio for Moebius sequence was reported to be 25.32 (95% CI 11.11–57.66). However, the true risk is less than 1–2%. Odds ratio for limb reduction was estimated to be 11.86 (95% CI 4.86–28.9).

Mycophenolate Mofetil (CellCept)

This is a medication used for prophylaxis of organ rejection. Exposure to mycophenolate mofetil has been associated with birth defects including microtia, auditory canal atresia, cleft lip and palate, micrognathia, hypertelorism, ocular coloboma, short fingers, and hypoplastic nails [70]. A higher incidence of structural malformations was seen with mycophenolate mofetil exposures during pregnancy compared to the overall kidney transplant recipient population [71]. The risk for birth defect following first trimester exposure to mycophenolate mofetil has been reported as 26% [71, 72].

Polychlorinated Biphenyls

Exposure to high levels of polychlorinated biphenyls (PCB) has been reported in cases of accidental human exposure to rice oil contaminated with PCBs. Exposure to high levels of PCBs is associated with dark brown pigmentation of the skin and the mucous membrane, gingival hyperplasia, exophthalmic edematous eye, dentition at birth, abnormal calcification of the skull, rocker bottom feet, and low birth weight [73].

Penicillamine

Data regarding exposure to penicillamine are conflicting. However, there may be an association with cutis laxa and inguinal hernia. Hypothyroidism was also suggested to be associated with penicillamine exposure [74, 75].

Phenobarbital

Phenobarbital use may be associated with cardiac defects and cleft palates. According to some reports, there is 6–20% risk for malformation. Other reports did not find an increase in risk. A study of 250 cases of monotherapy exposure reported that the risk for major malformation was not greater than other anticonvulsant monotherapies [37, 76–79].

---

[1] Named after the city of Minamata in Japan where, in 1956, methylmercury was released in the industrial wastewater from a chemical factory that resulted in mercury poisoning and cat, dog, pig and human deaths as well as fetal malformations.

Phenytoin

A pattern of malformations has been associated with in utero phenytoin exposure, referred to as fetal hydantoin syndrome. The pattern of malformation includes craniofacial abnormalities such as broad nasal bridge, metopic ridging, microcephaly, cleft lip/palate and ptosis, as well as variable degrees of hypoplasia and ossification of the distal phalanges. The risk of teratogenicity with phenytoin exposure in the first trimester was defined as 10%. However, subsequent reports have found a lower risk for malformations, and the relative risk was estimated to be about 2–3 [32, 37, 80, 81].

Systemic Retinoids

Use of systemic retinoids such as isotretinoin in pregnancy is associated with an increased risk for malformations. The most common anomalies include microtia/anotia, micrognathia, thymic hypoplasia, aplasia or ectopic location, CNS, and cardiac defects (VSD, tetralogy of Fallot and transposition of the great vessels), most of which are recognizable by ultrasound. Due to a relatively long half-life, a waiting period of at least 1 month is recommended by some authors before considering pregnancy, while others recommended a 3-months waiting period. The risk for malformations with exposure to isotretinoin after conception was estimated to be 35%. Furthermore, 43% of exposed to isotretinoin were found to have a subnormal IQ (<85) [82, 83].

Thalidomide

Thalidomide was a medication used in pregnancy as an anxiolytic and sleep medicine. While it was effective, it resulted in the birth of infants with severe limb anomalies (phocomelia). This has been described as the cause of the largest iatrogenic medical disaster in history with huge numbers (over 10,000) of severe birth defects in children [84]. In addition to limb reduction defects, use of Thalidomide during the first trimester is associated with cardiac defects, facial hemangiomata, esophageal and duodenal atresia, renal defects, microtia, and anotia. The risk was estimated to be 20–30% when exposure occurs between gestational weeks 5 and 7 [5, 6].

Valproic Acid

Use of valproic acid in pregnancy is associated with an increased risk for major malformation [37]. The specific malformations found in association with valproic acid are spina bifida, atrial septal defect, cleft palate, hypospadias, polydactyly, and craniosynostosis. The highest relative risk compared with no use of antiepileptic drugs was for spina bifida (relative risk of 12). Relative risk for the other conditions was 2–7. Exposure to monotherapy with valproic acid was associated with a relative risk of 2.6 for major malformation (95% CI 2.11–3.17) when compared to monotherapy with other antiepileptic drugs, 3.2 (95% CI 2.2–4.6) when compared to untreated epileptic patients and 3.77 (95% CI 2.18–6.52) when compared to healthy controls. The risk for malformations appears to be dose dependent. Absolute risk for spina bifida is usually quoted as 1–2%. A more recent study had an absolute risk of 0.6% for spina bifida [85–88]. Detailed ultrasound anatomy survey is indicated in mothers who received this medication.

Warfarin

Exposure to warfarin between 6 and 12 weeks of gestation has been associated with skeletal defects (such as nasal hypoplasia and stippled epiphysis), intrauterine growth restriction, CNS damage, eye defects, and hearing loss. Exposure after the first trimester might increase the risk of CNS defects, perhaps due to microhemorrhages. The absolute risk is not clear. One review sited a 6.4% risk for congenital anomalies [89–92].

Infections

Maternal infections during pregnancy are very common and, in most cases, do not interfere with fetal development. However, there are some pathogens, including bacteria, viruses, and parasites that may lead to fetal death, birth defects, and long-term sequelae.

Cytomegalovirus

Cytomegalovirus (CMV) is one of the most common causes of intrauterine infection [93, 94]. CMV can pass from mother to fetus through the placenta or during a vaginal delivery. Fetal CMV infection is mostly associated with maternal primary CMV infection during pregnancy. However, fetal CMV infection has been reported in recurrent infection as well, albeit with a much lower risk [95, 96]. Transmission of the virus from the mother to the fetus occurs more frequently in more advanced gestational age, but the risk for permanent sequelae is higher if transmission to the fetus occurred in the first trimester [97]. The estimated risk of transmission in cases of maternal primary CMV infection is 30–40% [98]. Birth abnormalities, including microcephaly, ventriculomegaly, intracranial calcifications, jaundice, and deafness, are apparent in about 10% of infants born with congenital CMV infection. The cranial ultrasound findings have been extensively described in the literature [99]. Most of the symptomatic infants will suffer from sequelae such as sensorineural hearing loss and learning disabilities, and the most severe cases will have a high mortality rate [93, 95]. The asymptomatic cases (about 90% of children born with congenital CMV) may develop progressive sensorineural hearing loss at a frequency of 13–15%. In cases of recurrent infection, only 0.2–1% of infants will be infected [98]. Of these, less than 1% will show symptoms at birth, and 10% of the asymptomatic newborns may experience hearing loss later in life.

Parvovirus B19

Approximately 50% of pregnant women are believed to be immune to B19. In cases of maternal infection during pregnancy, vertical transmission has been reported as 25–33% [100, 101]. Parvovirus does not seem to increase the risk for birth defects. However, fetal infection has been associated with fetal hydrops and death, mostly with infection before 20 weeks. The estimated risk for fetal death, if maternal infection occurs before 20 weeks gestation, is 1–9%. If maternal infection occurs after 20 weeks gestation, the risk of hydrops is estimated to be 1% [102].

Rubella

Due to widespread childhood vaccination, rubella infections rarely occur nowadays. Rubella in pregnancy may infect the fetus, producing congenital malformations, miscarriage, or fetal death [103, 104]. The main defects associated with congenital rubella infection are cataracts, glaucoma, heart defects, deafness, pigmentary retinopathy, microcephaly, developmental delay, and radiolucent bone disease. Infants with congenital rubella syndrome usually present with more than one of these signs or symptoms. More than half of the patients will have three or more defects. Hearing impairment is the most frequently reported clinical manifestation and is most likely to present as a single defect [103–105]. Almost all birth defects caused by rubella are associated with infections in the first 16 weeks. However, later infection has been associated with growth restriction, and cases of deafness and pulmonary artery stenosis have been reported [105]. Congenital rubella survivors have an increased risk for type I diabetes, thyroid dysfunction, and progressive rubella panencephalitis [105, 106]. In cases of maternal rubella infection during the first trimester, the risk of malformation may be as high as 90%.

Toxoplasma gondii

The overall maternal-fetal transmission rate in cases of maternal toxoplasmosis in pregnancy was reported to be about 30%. The risk of transmission to the fetus increases with gestational age from 6% at 13 weeks to 72% at 36 weeks. However, fetuses infected in early pregnancy are much more likely to show clinical signs of infection [107]. Symptoms of congenital toxoplasmosis present at birth can include a maculopapular rash, generalized lymphadenopathy, hepatomegaly, splenomegaly, jaundice, and/or thrombocytopenia. However, 70–90% of infants with congenital infection are asymptomatic at birth and sequelae can develop months or even years later. Up to 85% will develop chorioretinitis, 20–75% will have some form of developmental delay and 10–30% will have moderate hearing loss [108–110].

Treponema pallidum

Treponema pallidum, the agent responsible for syphilis, can infect the fetus at 14 weeks gestation, and possibly earlier. The risk for fetal infection increases with gestational age. In cases of fetal infection, 40–50% of the fetuses will die in utero while 30–40% will be born with signs of congenital syphilis [111]. Signs of congenital syphilis may include hydrops fetalis, an unexpectedly large placenta, intractable diaper rash, jaundice, hepatosplenomegaly, and anemia. Hepatosplenomegaly has been reported in almost 90% of all such babies, and jaundice in 33% of these neonates. The jaundice may be caused by syphilitic hepatitis or by hemolytic components of the disease [112]. Generalized lymphadenopathy usually occurs in association with hepatosplenomegaly and has been described in 50% of the patients. In one study of 9 patients with congenital syphilis, 8 had evidence of anemia, 4 had evidence of thrombocytopenia, and 6 had jaundice [113].

Varicella

Varicella zoster virus infection (chickenpox) is a very common childhood infection which is usually mild in children, but can be more serious in newborn babies and adults. Pregnant women in the third trimester are at higher risk for more severe disease including varicella pneumonia [114]. Fetal infection has been associated with a syndrome of congenital anomalies. Features of the congenital varicella embryopathy include skin lesions and hypopigmentation, eye defects (cataracts, microphthalmia, chorioretinitis), neurologic abnormalities (microcephaly, mental retardation, cortical atrophy), limb and muscle hypoplasia, gastrointestinal reflux, urinary tract malformations, intrauterine growth restriction, developmental delay, and cardiovascular malformations [114, 115]. Based on the case reports and larger studies, it is now believed that the sensitive period for fetal effects is from 0 to 20 weeks of pregnancy, although there are case reports of clinical embryopathy after maternal infection at up to 28 weeks of gestation [116]. The risk for congenital varicella embryopathy in cases of maternal infection before 20 weeks gestation ranges from less than 1% [116–118] to 3% [119]. Maternal infection in the third trimester does not cause malformation, however it can cause severe neonatal varicella and herpes zoster in the infant. There seems to be an increase in neonatal varicella severity when maternal rash appears 7 days before to 7 days after delivery, with most severe cases when rash appeared in the mother from 4 days before and up to 2 days after delivery [116].

Zika

Zika virus infection during pregnancy or shortly before conception has been shown to detrimentally effect the developing fetus and has been a source of concern especially during the 2015–2016 Zika epidemic [120]. Zika infection during pregnancy has been linked to pregnancy loss [121, 122]. However, the hallmark of intrauterine fetal infection is the fetal brain disruption sequence culmination in microcephaly and anomalies of the shape of the skull with redundancy of scalp [123–127]. In addition to microcephaly, fetal brain anomalies such as ventriculomegaly or hydrocephalus, lissencephaly, agyria, and dystrophic calcifications have been reported in association with fetal Zika virus infection [123, 125, 126]. Features relating to immobility were also reported, including malposition of foot, hand contractures, and arthrogryposis [126, 127]. The risk of affected fetus in cases of maternal infection is unclear, and reports range from as low as 1% [124] to as high as 42% [128, 129]. Infection during the first trimester has been reported to be associated with a higher risk of fetal damage [130]. Most of the Zika-associated anomalies, such as microcephaly, ventriculomegaly, lissencephaly, agyria, calcifications, and limb contractures, are recognizable by ultrasound.

COVID-19

Severe acute respiratory syndrome coronavirus 2 (SARS-CoV-2) infection has been reported to increase the risk of stillbirth compared to women without COVID-19, with a relative risk of 1.9 [131]. The risk of vertical transmission was suggested to be low and unrelated to severity of maternal disease [132, 133]. Nevertheless, several reports of proven intrauterine transmission of SARS-CoV-2 demonstrated chronic histiocytic intervillositis and syncytiotrophoblast necrosis in the placental tissue, possibly contributing to fetal loss [134, 135]. Malformations caused by SARS-CoV-2 infection have not been described.

Physical Factors

Ionizing Radiation

High levels of ionizing radiation have been shown to interfere with fetal development. Exposure to high levels of ionizing radiation has been associated with fetal death, growth restriction, microcephaly, organ aplasia and hypoplasia, oral clefts, cataracts, CNS malformations, and mental retardation [136–139]. In very early pregnancy, especially in the preimplantation period of the pregnancy, the embryo is mainly sensitive to the lethal effect of radiation [140]. During early organogenesis, the embryo is also sensitive to the growth-restricting and teratogenic effects of radiation [141], while during the early fetal period, the effects are mainly on fetal growth and CNS development [142]. Exposure to ionizing radiation is very common and is frequently associated with medical procedures [143]. While radiation exposure in pregnancy is a cause for much anxiety, in most cases, such as chest and dental X-rays, exposure to ionizing radiation in various diagnostic imaging tests is much below the 5 rad threshold, which is the commonly accepted safe level of exposure in pregnancy.

Non-ionizing Radiation

Exposure to electromagnetic fields is very common. Exposure to non-ionizing radiation can theoretically pose a risk of thermal damage, especially to the eyes (because they cannot dissipate heat efficiently). The nonthermal effects have not been clearly demonstrated. However, there is currently no indication that this type of radiation can produce malignancy or mutations [144].

Ultrasound Waves

Studies on diagnostic ultrasound have not found any measurable effect on the fetus, and the fetal anomaly rate was comparable to the general population [145]. No effect was demonstrated on Apgar scores, gestational age, head circumference, birth weight, length, congenital abnormalities, neonatal infection, and congenital infection. At 7–12 years of age, there was no effect on hearing, visual acuity, and color vision, cognitive function, or behavior [146, 147]. Furthermore, diagnostic ultrasound was not found to increase the risk of childhood malignancy up to 6 years [148]. On the other hand, therapeutic ultrasound involves higher intensity and may produce deep tissue heating. Studies in rats showed a lower weight but no fetal damage [149]. However, because of the potential of hyperthermia to induce birth defects, it is advised to avoid therapeutic ultrasound during pregnancy [144]. See Chap. 1.

Summary

Only a handful of drugs and other exposures have proven to be teratogenic in human. However, women tend to overestimate teratogenic risk. In many cases, overestimation of risk may cause women to discontinue essential medications or alternatively to terminate wanted pregnancies. Evidence-based teratogen risk counseling is therefore needed to promote evidence-based rather than fear-based decision-making.

Teaching Points

- In every pregnancy, regardless of maternal diseases or environmental exposures, there is a 1–3% risk of major malformation.
- Only a handful of drugs and other environmental exposures have been proven to be teratogenic.

- For most teratogens, there is a typical pattern of malformations, commonly recognizable by ultrasound.
- Women tend to overestimate teratogenic risk and may act according to this misperception by discontinuing essential medications or terminating a wanted pregnancy.
- Evidence-based teratogen risk counseling is needed to promote evidence-based rather than fear-based decision-making.

References

1. Moore KL, Persaud TVN, Torchia MG. The developing human: clinically oriented embryology. 8th ed. Philadelphia, PA: Saunders/Elsevier; 2008. p. xiv, 522 p.
2. Koren G, Pastuszak A, Ito S. Drugs in pregnancy. N Engl J Med. 1998;338(16):1128–37. Epub 1998/04/17.
3. Heinonen OP, Slone D, Shapiro S. Birth defects and drugs in pregnancy. Littleton, MA: Publishing Sciences Group; 1977. p. xi, 516 p.
4. Nava-Ocampo AA, Koren G. Human teratogens and evidence-based teratogen risk counseling: the Motherisk approach. Clin Obstet Gynecol. 2007;50(1):123–31. Epub 2007/02/17.
5. Newman CG. Teratogen update: clinical aspects of thalidomide embryopathy—a continuing preoccupation. Teratology. 1985;32(1):133–44. Epub 1985/08/01.
6. Smithells RW. Defects and disabilities of thalidomide children. Br Med J. 1973;1(5848):269–72. Epub 1973/02/03.
7. Koren G, Bologa M, Long D, Feldman Y, Shear NH. Perception of teratogenic risk by pregnant women exposed to drugs and chemicals during the first trimester. Am J Obstet Gynecol. 1989;160(5 Pt 1):1190–4. Epub 1989/05/01.
8. Walfisch A, Sermer C, Matok I, Einarson A, Koren G. Perception of teratogenic risk and the rated likelihood of pregnancy termination: association with maternal depression. Can J Psychiatry. 2011;56(12):761–7. Epub 2011/12/14.
9. Neutel CI, Johansen HL. Measuring drug effectiveness by default: the case of Bendectin. Can J Public Health. 1995;86(1):66–70. Epub 1995/01/01.
10. Trichopoulos D, Zavitsanos X, Koutis C, Drogari P, Proukakis C, Petridou E. The victims of chernobyl in Greece: induced abortions after the accident. Br Med J (Clin Res Ed). 1987;295(6606):1100. Epub 1987/10/31
11. Ketchum LE. Lessons of Chernobyl: SNM members try to decontaminate world threatened by fallout. Part II. J Nucl Med. 1987;28(6):933–42. Epub 1987/06/01.
12. Andrade SE, Gurwitz JH, Davis RL, Chan KA, Finkelstein JA, Fortman K, et al. Prescription drug use in pregnancy. Am J Obstet Gynecol. 2004;191(2):398–407. Epub 2004/09/03.
13. Engeland A, Bramness JG, Daltveit AK, Ronning M, Skurtveit S, Furu K. Prescription drug use among fathers and mothers before and during pregnancy. A population-based cohort study of 106,000 pregnancies in Norway 2004-2006. Br J Clin Pharmacol. 2008;65(5):653–60. Epub 2008/02/26.
14. Kutscher AH, Zegarelli EV, Tovell HM, Hochberg B, Hauptman J. Discoloration of deciduous teeth induced by administration of tetracycline antepartum. Am J Obstet Gynecol. 1966;96(2):291–2. Epub 1966/09/15.
15. Hendricks SK, Smith JR, Moore DE, Brown ZA. Oligohydramnios associated with prostaglandin synthetase inhibitors in preterm labour. Br J Obstet Gynaecol. 1990;97(4):312–6. Epub 1990/04/01.
16. Levin DL. Effects of inhibition of prostaglandin synthesis on fetal development, oxygenation, and the fetal circulation. Semin Perinatol. 1980;4(1):35–44. Epub 1980/01/01.
17. Cunniff C, Jones KL, Phillipson J, Benirschke K, Short S, Wujek J. Oligohydramnios sequence and renal tubular malformation associated with maternal enalapril use. Am J Obstet Gynecol. 1990;162(1):187–9. Epub 1990/01/01.
18. Chudley AE, Conry J, Cook JL, Loock C, Rosales T, LeBlanc N. Fetal alcohol spectrum disorder: Canadian guidelines for diagnosis. CMAJ Can Med Assoc J. 2005;172(5 Suppl):S1–S21. Epub 2005/03/02.
19. Graham JM Jr, Hanson JW, Darby BL, Barr HM, Streissguth AP. Independent dysmorphology evaluations at birth and 4 years of age for children exposed to varying amounts of alcohol in utero. Pediatrics. 1988;81(6):772–8. Epub 1988/06/01.
20. Mills JL, Graubard BI. Is moderate drinking during pregnancy associated with an increased risk for malformations? Pediatrics. 1987;80(3):309–14. Epub 1987/09/01.
21. Sampson PD, Streissguth AP, Bookstein FL, Little RE, Clarren SK, Dehaene P, et al. Incidence of fetal alcohol syndrome and prevalence of alcohol-related neurodevelopmental disorder. Teratology. 1997;56(5):317–26. Epub 1998/02/06.
22. Meyer KA, Werler MM, Hayes C, Mitchell AA. Low maternal alcohol consumption during pregnancy and oral clefts in offspring: the Slone Birth Defects Study. Birth Defects Res A Clin Mol Teratol. 2003;67(7):509–14. Epub 2003/10/21.
23. Hyoun SC, Obican SG, Scialli AR. Teratogen update: methotrexate. Birth Defects Res A Clin Mol Teratol. 2012;94(4):187–207. Epub 2012/03/22.
24. Thiersch JB. Therapeutic abortions with a folic acid antagonist, 4-aminopteroylglutamic acid (4-amino P.G.A) administered by the oral route. Am J Obstet Gynecol. 1952;63(6):1298–304. Epub 1952/06/01.

25. Feldkamp M, Carey JC. Clinical teratology counseling and consultation case report: low dose methotrexate exposure in the early weeks of pregnancy. Teratology. 1993;47(6):533–9. Epub 1993/06/01.
26. Warkany J. Aminopterin and methotrexate: folic acid deficiency. Teratology. 1978;17(3):353–7. Epub 1978/06/01.
27. Del Campo M, Kosaki K, Bennett FC, Jones KL. Developmental delay in fetal aminopterin/methotrexate syndrome. Teratology. 1999;60(1):10–2. Epub 1999/07/21.
28. Enato E, Moretti M, Koren G. The fetal safety of benzodiazepines: an updated meta-analysis. J Obstet Gynaecol Can. 2011;33(1):46–8. Epub 2011/01/29.
29. Dolovich LR, Addis A, Vaillancourt JM, Power JD, Koren G, Einarson TR. Benzodiazepine use in pregnancy and major malformations or oral cleft: meta-analysis of cohort and case-control studies. BMJ. 1998;317(7162):839–43. Epub 1998/09/25.
30. Bergman U, Rosa FW, Baum C, Wiholm BE, Faich GA. Effects of exposure to benzodiazepine during fetal life. Lancet. 1992;340(8821):694–6. Epub 1992/09/19.
31. Kaaja E, Kaaja R, Hiilesmaa V. Major malformations in offspring of women with epilepsy. Neurology. 2003;60(4):575–9. Epub 2003/02/26.
32. Artama M, Auvinen A, Raudaskoski T, Isojarvi I, Isojarvi J. Antiepileptic drug use of women with epilepsy and congenital malformations in offspring. Neurology. 2005;64(11):1874–8. Epub 2005/06/16.
33. Morrow J, Russell A, Guthrie E, Parsons L, Robertson I, Waddell R, et al. Malformation risks of antiepileptic drugs in pregnancy: a prospective study from the UK Epilepsy and Pregnancy Register. J Neurol Neurosurg Psychiatry. 2006;77(2):193–8. Epub 2005/09/15.
34. Wide K, Winbladh B, Kallen B. Major malformations in infants exposed to antiepileptic drugs in utero, with emphasis on carbamazepine and valproic acid: a nation-wide, population-based register study. Acta Paediatr. 2004;93(2):174–6. Epub 2004/03/30.
35. Meador KJ, Baker GA, Finnell RH, Kalayjian LA, Liporace JD, Loring DW, et al. In utero antiepileptic drug exposure: fetal death and malformations. Neurology. 2006;67(3):407–12. Epub 2006/08/09.
36. Jentink J, Dolk H, Loane MA, Morris JK, Wellesley D, Garne E, et al. Intrauterine exposure to carbamazepine and specific congenital malformations: systematic review and case-control study. BMJ. 2010;341:c6581. Epub 2010/12/04.
37. Tomson T, Battino D, Bonizzoni E, Craig J, Lindhout D, Perucca E, et al. Comparative risk of major congenital malformations with eight different antiepileptic drugs: a prospective cohort study of the EURAP registry. Lancet Neurol. 2018;17(6):530–8. Epub 2018/04/24.
38. Koren G, Sharav T, Pastuszak A, Garrettson LK, Hill K, Samson I, et al. A multicenter, prospective study of fetal outcome following accidental carbon monoxide poisoning in pregnancy. Reprod Toxicol. 1991;5(5):397–403. Epub 1991/01/01.
39. Dadvand P, Rankin J, Rushton S, Pless-Mulloli T. Ambient air pollution and congenital heart disease: a register-based study. Environ Res. 2011;111(3):435–41. Epub 2011/02/19.
40. Ritz B, Yu F, Fruin S, Chapa G, Shaw GM, Harris JA. Ambient air pollution and risk of birth defects in Southern California. Am J Epidemiol. 2002;155(1):17–25. Epub 2002/01/05.
41. Chavez GF, Mulinare J, Cordero JF. Maternal cocaine use during early pregnancy as a risk factor for congenital urogenital anomalies. JAMA. 1989;262(6):795–8. Epub 1989/08/11.
42. Frank DA, Zuckerman BS, Amaro H, Aboagye K, Bauchner H, Cabral H, et al. Cocaine use during pregnancy: prevalence and correlates. Pediatrics. 1988;82(6):888–95. Epub 1988/12/01.
43. Bingol N, Fuchs M, Diaz V, Stone RK, Gromisch DS. Teratogenicity of cocaine in humans. J Pediatr. 1987;110(1):93–6. Epub 1987/01/01.
44. Nulman I, Rovet J, Altmann D, Bradley C, Einarson T, Koren G. Neurodevelopment of adopted children exposed in utero to cocaine. CMAJ Can Med Assoc J. 1994;151(11):1591–7. Epub 1994/12/01.
45. Kliegman RM, Madura D, Kiwi R, Eisenberg I, Yamashita T. Relation of maternal cocaine use to the risks of prematurity and low birth weight. J Pediatr. 1994;124(5 Pt 1):751–6. Epub 1994/05/01.
46. Chasnoff IJ, Burns WJ, Schnoll SH, Burns KA. Cocaine use in pregnancy. N Engl J Med. 1985;313(11):666–9. Epub 1985/09/12.
47. Rodriguez-Pinilla E, Martinez-Frias ML. Corticosteroids during pregnancy and oral clefts: a case-control study. Teratology. 1998;58(1):2–5. Epub 1998/08/12.
48. Robert E, Vollset SE, Botto L, Lancaster PA, Merlob P, Mastroiacovo P, et al. Malformation surveillance and maternal drug exposure: the MADRE project. Int J Risk Saf Med. 1994;6(2):75–118. Epub 1994/01/01.
49. Czeizel AE, Rockenbauer M. Population-based case-control study of teratogenic potential of corticosteroids. Teratology. 1997;56(5):335–40. Epub 1998/02/06.
50. Fraser FC, Sajoo A. Teratogenic potential of corticosteroids in humans. Teratology. 1995;51(1):45–6. Epub 1995/01/01.
51. Carmichael SL, Shaw GM. Maternal corticosteroid use and risk of selected congenital anomalies. Am J Med Genet. 1999;86(3):242–4. Epub 1999/09/14.
52. Park-Wyllie L, Mazzotta P, Pastuszak A, Moretti ME, Beique L, Hunnisett L, et al. Birth defects after maternal exposure to corticosteroids: prospective cohort study and meta-analysis of epidemiological studies. Teratology. 2000;62(6):385–92. Epub 2000/11/25.
53. Rayburn WF. Glucocorticoid therapy for rheumatic diseases: maternal, fetal, and breast-feeding consid-

erations. Am J Reprod Immunol. 1992;28(3-4):138–40. Epub 1992/10/01.

54. Orr JW Jr, Shingleton HM, Gore H, Austin JM Jr, Hatch KD, Soong SJ. Cervical intraepithelial neoplasia associated with exposure to diethylstilbestrol in utero: a clinical and pathologic study. Obstet Gynecol. 1981;58(1):75–82. Epub 1981/07/01.
55. Barnes AB, Colton T, Gundersen J, Noller KL, Tilley BC, Strama T, et al. Fertility and outcome of pregnancy in women exposed in utero to diethylstilbestrol. N Engl J Med. 1980;302(11):609–13. Epub 1980/03/13.
56. Munk-Olsen T, Liu X, Viktorin A, Brown HK, Di Florio A, D'Onofrio BM, et al. Maternal and infant outcomes associated with lithium use in pregnancy: an international collaborative meta-analysis of six cohort studies. Lancet Psychiatry. 2018;5(8):644–52. Epub 2018/06/23.
57. Diav-Citrin O, Shechtman S, Tahover E, Finkel-Pekarsky V, Arnon J, Kennedy D, et al. Pregnancy outcome following in utero exposure to lithium: a prospective, comparative, observational study. Am J Psychiatry. 2014;171(7):785–94. Epub 2014/05/02.
58. Cohen LS, Friedman JM, Jefferson JW, Johnson EM, Weiner ML. A reevaluation of risk of in utero exposure to lithium. JAMA. 1994;271(2):146–50. Epub 1994/01/12.
59. Jacobson SJ, Jones K, Johnson K, Ceolin L, Kaur P, Sahn D, et al. Prospective multicentre study of pregnancy outcome after lithium exposure during first trimester. Lancet. 1992;339(8792):530–3. Epub 1992/02/29.
60. Weber-Schoendorfer C, Chambers C, Wacker E, Beghin D, Bernard N, Shechtman S, et al. Pregnancy outcome after methotrexate treatment for rheumatic disease prior to or during early pregnancy: a prospective multicenter cohort study. Arthritis Rheumatol. 2014;66(5):1101–10. Epub 2014/01/29.
61. Chapa JB, Hibbard JU, Weber EM, Abramowicz JS, Verp MS. Prenatal diagnosis of methotrexate embryopathy. Obstet Gynecol. 2003;101(5 Pt 2):1104–7. Epub 2003/05/10.
62. Adam MP, Manning MA, Beck AE, Kwan A, Enns GM, Clericuzio C, et al. Methotrexate/misoprostol embryopathy: report of four cases resulting from failed medical abortion. Am J Med Genet A. 2003;123A(1):72–8. Epub 2003/10/14.
63. Yedlinsky NT, Morgan FC, Whitecar PW. Anomalies associated with failed methotrexate and misoprostol termination. Obstet Gynecol. 2005;105(5 Pt 2):1203–5. Epub 2005/05/03.
64. Usta IM, Nassar AH, Yunis KA, Abu-Musa AA. Methotrexate embryopathy after therapy for misdiagnosed ectopic pregnancy. Int J Gynaecol Obstet. 2007;99(3):253–5. Epub 2007/09/25.
65. Wheeler M, O'Meara P, Stanford M. Fetal methotrexate and misoprostol exposure: the past revisited. Teratology. 2002;66(2):73–6. Epub 2002/09/05.
66. Poggi SH, Ghidini A. Importance of timing of gestational exposure to methotrexate for its teratogenic effects when used in setting of misdiagnosis of ectopic pregnancy. Fertil Steril. 2011;96(3):669–71. Epub 2011/07/08.
67. Harada M. Congenital Minamata disease: intrauterine methylmercury poisoning. Teratology. 1978;18(2):285–8. Epub 1978/10/01.
68. Amin-Zaki L, Majeed MA, Greenwood MR, Elhassani SB, Clarkson TW, Doherty RA. Methylmercury poisoning in the Iraqi suckling infant: a longitudinal study over five years. J Appl Toxicol. 1981;1(4):210–4. Epub 1981/08/01.
69. Marsh DO, Myers GJ, Clarkson TW, Amin-Zaki L, Tikriti S, Majeed MA. Fetal methylmercury poisoning: clinical and toxicological data on 29 cases. Ann Neurol. 1980;7(4):348–53. Epub 1980/04/01.
70. Merlob P, Stahl B, Klinger G. Tetrada of the possible mycophenolate mofetil embryopathy: a review. Reprod Toxicol. 2009;28(1):105–8. Epub 2009/06/06.
71. Sifontis NM, Coscia LA, Constantinescu S, Lavelanet AF, Moritz MJ, Armenti VT. Pregnancy outcomes in solid organ transplant recipients with exposure to mycophenolate mofetil or sirolimus. Transplantation. 2006;82(12):1698–702. Epub 2007/01/02.
72. Hoeltzenbein M, Elefant E, Vial T, Finkel-Pekarsky V, Stephens S, Clementi M, et al. Teratogenicity of mycophenolate confirmed in a prospective study of the European Network of Teratology Information Services. Am J Med Genet A. 2012;158A(3):588–96. Epub 2012/02/10.
73. Yamashita F, Hayashi M. Fetal PCB syndrome: clinical features, intrauterine growth retardation and possible alteration in calcium metabolism. Environ Health Perspect. 1985;59:41–5. Epub 1985/02/01.
74. Rosa FW. Teratogen update: penicillamine. Teratology. 1986;33(1):127–31. Epub 1986/02/01.
75. Hanukoglu A, Curiel B, Berkowitz D, Levine A, Sack J, Lorberboym M. Hypothyroidism and dyshormonogenesis induced by D-penicillamine in children with Wilson's disease and healthy infants born to a mother with Wilson's disease. J Pediatr. 2008;153(6):864–6. Epub 2008/11/19.
76. Bertollini R, Kallen B, Mastroiacovo P, Robert E. Anticonvulsant drugs in monotherapy. Effect on the fetus. Eur J Epidemiol. 1987;3(2):164–71. Epub 1987/06/01.
77. Kjaer D, Horvath-Puho E, Christensen J, Vestergaard M, Czeizel AE, Sorensen HT, et al. Use of phenytoin, phenobarbital, or diazepam during pregnancy and risk of congenital abnormalities: a case-time-control study. Pharmacoepidemiol Drug Saf. 2007;16(2):181–8. Epub 2006/08/31.
78. Arpino C, Brescianini S, Robert E, Castilla EE, Cocchi G, Cornel MC, et al. Teratogenic effects of antiepileptic drugs: use of an International Database on Malformations and Drug Exposure (MADRE). Epilepsia. 2000;41(11):1436–43. Epub 2000/11/15.
79. Waters CH, Belai Y, Gott PS, Shen P, De Giorgio CM. Outcomes of pregnancy associated with antiep-

ileptic drugs. Arch Neurol. 1994;51(3):250–3. Epub 1994/03/01.

80. Smith DW. Teratogenicity of anticonvulsive medications. Am J Dis Child. 1977;131(12):1337–9. Epub 1977/12/01.
81. Harden CL, Meador KJ, Pennell PB, Hauser WA, Gronseth GS, French JA, et al. Management issues for women with epilepsy-Focus on pregnancy (an evidence-based review): II. Teratogenesis and perinatal outcomes: Report of the Quality Standards Subcommittee and Therapeutics and Technology Subcommittee of the American Academy of Neurology and the American Epilepsy Society. Epilepsia. 2009;50(5):1237–46. Epub 2009/06/10.
82. Berard A, Azoulay L, Koren G, Blais L, Perreault S, Oraichi D. Isotretinoin, pregnancies, abortions and birth defects: a population-based perspective. Br J Clin Pharmacol. 2007;63(2):196–205. Epub 2007/01/12.
83. Lammer EJ, Chen DT, Hoar RM, Agnish ND, Benke PJ, Braun JT, et al. Retinoic acid embryopathy. N Engl J Med. 1985;313(14):837–41. Epub 1985/10/03.
84. Vargesson N. Thalidomide-induced teratogenesis: history and mechanisms. Birth Defects Res C Embryo Today. 2015;105(2):140–56. Epub 2015/06/06.
85. Samren EB, van Duijn CM, Koch S, Hiilesmaa VK, Klepel H, Bardy AH, et al. Maternal use of antiepileptic drugs and the risk of major congenital malformations: a joint European prospective study of human teratogenesis associated with maternal epilepsy. Epilepsia. 1997;38(9):981–90. Epub 1998/05/14.
86. Valproic acid and spina bifida: a preliminary report—France. MMWR Morb Mortal Wkly Rep. 1982;31(42):565–6. Epub 1982/10/29.
87. Valproate: a new cause of birth defects—report from Italy and follow-up from France. MMWR Morb Mortal Wkly Rep. 1983;32(33):438–9. Epub 1983/08/26.
88. Jentink J, Loane MA, Dolk H, Barisic I, Garne E, Morris JK, et al. Valproic acid monotherapy in pregnancy and major congenital malformations. N Engl J Med. 2010;362(23):2185–93. Epub 2010/06/19.
89. Hall JG, Pauli RM, Wilson KM. Maternal and fetal sequelae of anticoagulation during pregnancy. Am J Med. 1980;68(1):122–40. Epub 1980/01/01.
90. Iturbe-Alessio I, Fonseca MC, Mutchinik O, Santos MA, Zajarias A, Salazar E. Risks of anticoagulant therapy in pregnant women with artificial heart valves. N Engl J Med. 1986;315(22):1390–3. Epub 1986/11/27.
91. Ville Y, Jenkins E, Shearer MJ, Hemley H, Vasey DP, Layton M, et al. Fetal intraventricular haemorrhage and maternal warfarin. Lancet. 1993;341(8854):1211. Epub 1993/05/08.
92. Chan WS, Anand S, Ginsberg JS. Anticoagulation of pregnant women with mechanical heart valves: a systematic review of the literature. Arch Intern Med. 2000;160(2):191–6. Epub 2000/01/27.
93. Raynor BD. Cytomegalovirus infection in pregnancy. Semin Perinatol. 1993;17(6):394–402. Epub 1993/12/01.
94. Leruez-Ville M, Ville Y. Fetal cytomegalovirus infection. Best Pract Res Clin Obstet Gynaecol. 2017;38:97–107. Epub 2016/12/08.
95. Brown HL, Abernathy MP. Cytomegalovirus infection. Semin Perinatol. 1998;22(4):260–6. Epub 1998/09/17.
96. Hedrick J. The effects of human parvovirus B19 and cytomegalovirus during pregnancy. J Perinat Neonatal Nurs. 1996;10(2):30–9. Epub 1996/09/01.
97. Bodeus M, Hubinont C, Goubau P. Increased risk of cytomegalovirus transmission in utero during late gestation. Obstet Gynecol. 1999;93(5 Pt 1):658–60. Epub 2000/07/27.
98. Fowler KB, Stagno S, Pass RF, Britt WJ, Boll TJ, Alford CA. The outcome of congenital cytomegalovirus infection in relation to maternal antibody status. N Engl J Med. 1992;326(10):663–7. Epub 1992/03/05.
99. Malinger G, Lev D, Zahalka N, Ben Aroia Z, Watemberg N, Kidron D, et al. Fetal cytomegalovirus infection of the brain: the spectrum of sonographic findings. AJNR Am J Neuroradiol. 2003;24(1):28–32. Epub 2003/01/21.
100. Gratacos E, Torres PJ, Vidal J, Antolin E, Costa J. Jimenez de Anta MT, et al. The incidence of human parvovirus B19 infection during pregnancy and its impact on perinatal outcome. J Infect Dis. 1995;171(5):1360–3. Epub 1995/05/01.
101. Prospective study of human parvovirus (B19) infection in pregnancy. Public Health Laboratory Service Working Party on Fifth Disease. BMJ. 1990;300(6733):1166–70. Epub 1990/05/05.
102. Markenson GR, Yancey MK. Parvovirus B19 infections in pregnancy. Semin Perinatol. 1998;22(4):309–17. Epub 1998/09/17
103. Control and prevention of rubella: evaluation and management of suspected outbreaks, rubella in pregnant women, and surveillance for congenital rubella syndrome. MMWR Recomm Rep. 2001;50(RR-12):1–23. Epub 2001/07/28.
104. Reef SE, Plotkin S, Cordero JF, Katz M, Cooper L, Schwartz B, et al. Preparing for elimination of congenital Rubella syndrome (CRS): summary of a workshop on CRS elimination in the United States. Clin Infect Dis. 2000;31(1):85–95. Epub 2000/07/29.
105. Webster WS. Teratogen update: congenital rubella. Teratology. 1998;58(1):13–23. Epub 1998/08/12.
106. McIntosh ED, Menser MA. A fifty-year follow-up of congenital rubella. Lancet. 1992;340(8816):414–5. Epub 1992/08/15.
107. Dunn D, Wallon M, Peyron F, Petersen E, Peckham C, Gilbert R. Mother-to-child transmission of toxoplasmosis: risk estimates for clinical counselling. Lancet. 1999;353(9167):1829–33. Epub 1999/06/08.

108. McAuley J, Boyer KM, Patel D, Mets M, Swisher C, Roizen N, et al. Early and longitudinal evaluations of treated infants and children and untreated historical patients with congenital toxoplasmosis: the Chicago Collaborative Treatment Trial. Clin Infect Dis. 1994;18(1):38–72. Epub 1994/01/01.
109. Koppe JG, Loewer-Sieger DH, de Roever-Bonnet H. Results of 20-year follow-up of congenital toxoplasmosis. Lancet. 1986;1(8475):254–6. Epub 1986/02/01.
110. Wilson CB, Remington JS, Stagno S, Reynolds DW. Development of adverse sequelae in children born with subclinical congenital Toxoplasma infection. Pediatrics. 1980;66(5):767–74. Epub 1980/11/01.
111. Goldenberg RL, Thompson C. The infectious origins of stillbirth. Am J Obstet Gynecol. 2003;189(3):861–73. Epub 2003/10/04.
112. Saxoni F, Lapaanis P, Pantelakis SN. Congenital syphilis: a description of 18 cases and re-examination of an old but ever-present disease. Clin Pediatr. 1967;6(12):687–91. Epub 1967/12/01.
113. Whitaker JA, Sartain P, Shaheedy M. Hematological aspects of congenital syphilis. J Pediatr. 1965;66:629–36. Epub 1965/03/01.
114. Smith CK, Arvin AM. Varicella in the fetus and newborn. Semin Fetal Neonatal Med. 2009;14(4):209–17. Epub 2008/12/23.
115. Ahn KH, Park YJ, Hong SC, Lee EH, Lee JS, Oh MJ, et al. Congenital varicella syndrome: a systematic review. J Obstet Gynaecol. 2016;36(5):563–6. Epub 2016/03/12.
116. Tan MP, Koren G. Chickenpox in pregnancy: revisited. Reprod Toxicol. 2006;21(4):410–20. Epub 2005/06/28.
117. Sanchez MA, Bello-Munoz JC, Cebrecos I, Sanz TH, Martinez JS, Moratonas EC, et al. The prevalence of congenital varicella syndrome after a maternal infection, but before 20 weeks of pregnancy: a prospective cohort study. J Maternal Fetal Neonatal Med. 2011;24(2):341–7. Epub 2010/07/31.
118. Harger JH, Ernest JM, Thurnau GR, Moawad A, Thom E, Landon MB, et al. Frequency of congenital varicella syndrome in a prospective cohort of 347 pregnant women. Obstet Gynecol. 2002;100(2):260–5. Epub 2002/08/02.
119. Gilbert GL. Chickenpox during pregnancy. BMJ. 1993;306(6885):1079–80. Epub 1993/04/24.
120. Leone T, Coast E, Correa S, Wenham C. Web-based searching for abortion information during health emergencies: a case study of Brazil during the 2015/2016 Zika outbreak. Sex Reprod Health Matters. 2021;29(1):1883804. Epub 2021/02/19.
121. Sarno M, Sacramento GA, Khouri R, do Rosario MS, Costa F, Archanjo G, et al. Zika virus infection and stillbirths: a case of hydrops fetalis, hydranencephaly and fetal demise. PLoS Negl Trop Dis. 2016;10(2):e0004517. Epub 2016/02/26.
122. van der Eijk AA, van Genderen PJ, Verdijk RM, Reusken CB, Mogling R, van Kampen JJ, et al. Miscarriage associated with Zika virus infection. N Engl J Med. 2016;375(10):1002–4. Epub 2016/07/28.
123. Mlakar J, Korva M, Tul N, Popovic M, Poljsak-Prijatelj M, Mraz J, et al. Zika virus associated with microcephaly. N Engl J Med. 2016;374(10):951–8. Epub 2016/02/11.
124. Cauchemez S, Besnard M, Bompard P, Dub T, Guillemette-Artur P, Eyrolle-Guignot D, et al. Association between Zika virus and microcephaly in French Polynesia, 2013-15: a retrospective study. Lancet. 2016;387(10033):2125–32. Epub 2016/03/20.
125. de Araujo TVB, Rodrigues LC, de Alencar Ximenes RA, de Barros M-FD, Montarroyos UR, de Melo APL, et al. Association between Zika virus infection and microcephaly in Brazil, January to May, 2016: preliminary report of a case-control study. Lancet Infect Dis. 2016;16(12):1356–63. Epub 2016/09/20.
126. Moore CA, Staples JE, Dobyns WB, Pessoa A, Ventura CV, Fonseca EB, et al. Characterizing the pattern of anomalies in congenital Zika syndrome for pediatric clinicians. JAMA Pediatr. 2017;171(3):288–95. Epub 2016/11/05.
127. Del Campo M, Feitosa IM, Ribeiro EM, Horovitz DD, Pessoa AL, Franca GV, et al. The phenotypic spectrum of congenital Zika syndrome. Am J Med Genet A. 2017;173(4):841–57. Epub 2017/03/23.
128. Hoen B, Schaub B, Funk AL, Ardillon V, Boullard M, Cabie A, et al. Pregnancy outcomes after ZIKV infection in French Territories in the Americas. N Engl J Med. 2018;378(11):985–94. Epub 2018/03/15.
129. Brasil P, Pereira JP Jr, Moreira ME, Ribeiro Nogueira RM, Damasceno L, Wakimoto M, et al. Zika Virus Infection in Pregnant Women in Rio de Janeiro. N Engl J Med. 2016;375(24):2321–34. Epub 2016/03/05.
130. Souza JP, Meio M, de Andrade LM, Figueiredo MR, Gomes Junior SC, Pereira Junior JP, et al. Adverse fetal and neonatal outcomes in pregnancies with confirmed Zika Virus infection in Rio de Janeiro, Brazil: a cohort study. PLoS Negl Trop Dis. 2021;15(1):e0008893. Epub 2021/01/05.
131. DeSisto CL, Wallace B, Simeone RM, Polen K, Ko JY, Meaney-Delman D, et al. Risk for stillbirth among women with and without COVID-19 at delivery hospitalization—United States, March 2020-September 2021. MMWR Morb Mortal Wkly Rep. 2021;70(47):1640–5. Epub 2021/11/25.
132. Bellos I, Pandita A, Panza R. Maternal and perinatal outcomes in pregnant women infected by SARS-CoV-2: A meta-analysis. Eur J Obstet Gynecol Reprod Biol. 2021;256:194–204. Epub 2020/11/28.
133. Juan J, Gil MM, Rong Z, Zhang Y, Yang H, Poon LC. Effect of coronavirus disease 2019 (COVID-19) on maternal, perinatal and neonatal outcome: systematic review. Ultrasound Obstet Gynecol. 2020;56(1):15–27. Epub 2020/05/21.

134. Schwartz DA, Baldewijns M, Benachi A, Bugatti M, Collins RRJ, De Luca D, et al. Chronic histiocytic intervillositis with trophoblast necrosis is a risk factor associated with placental infection from coronavirus disease 2019 (COVID-19) and intrauterine maternal-fetal severe acute respiratory syndrome coronavirus 2 (SARS-CoV-2) transmission in liveborn and stillborn infants. Arch Pathol Lab Med. 2021;145(5):517–28. Epub 2021/01/05.
135. Ganor Paz Y, Shiloh S, Brosh-Nissimov T, Grupel D, Sorek N, Kustin T, et al. The association between SARS-CoV-2 infection and late pregnancy loss. Int J Gynaecol Obstet. 2021. Epub 2021/11/16.
136. Dekaban AS. Abnormalities in children exposed to x-radiation during various stages of gestation: tentative timetable of radiation injury to the human fetus. I. J Nucl Med. 1968;9(9):471–7. Epub 1968/09/01.
137. Miller RW. Delayed radiation effects in atomic-bomb survivors. Major observations by the Atomic Bomb Casualty Commission are evaluated. Science. 1969;166(3905):569–74. Epub 1969/10/31.
138. Plummer G. Anomalies occurring in children exposed in utero to the atomic bomb in Hiroshima. Pediatrics. 1952;10(6):687–93. Epub 1952/12/01.
139. Wood JW, Johnson KG, Omori Y. In utero exposure to the Hiroshima atomic bomb. An evaluation of head size and mental retardation: twenty years later. Pediatrics. 1967;39(3):385–92. Epub 1967/03/01.
140. Jankowski CB. Radiation and pregnancy. Putting the risks in proportion. Am J Nurs. 1986;86(3):260–5. Epub 1986/03/01.
141. Lione A. Ionizing radiation and human reproduction. Reprod Toxicol. 1987;1(1):3–16. Epub 1987/01/01.
142. Russell LB, Russell WL. An analysis of the changing radiation response of the developing mouse embryo. J Cell Physiol Suppl. 1954;43(Suppl. 1):103–49. Epub 1954/05/01.
143. Rowley KA, Hill SJ, Watkins RA, Moores BM. An investigation into the levels of radiation exposure in diagnostic examinations involving fluoroscopy. Br J Radiol. 1987;60(710):167–73. Epub 1987/02/01.
144. Koren G. Medication safety in pregnancy and breastfeeding. New York: McGraw-Hill, Health Professions Division; 2007. p. xv, 623 p.
145. Hellman LM, Duffus GM, Donald I, Sunden B. Safety of diagnostic ultrasound in obstetrics. Lancet. 1970;1(7657):1133–4. Epub 1970/05/30.
146. Scheidt PC, Stanley F, Bryla DA. One-year follow-up of infants exposed to ultrasound in utero. Am J Obstet Gynecol. 1978;131(7):743–8. Epub 1978/08/01.
147. Stark CR, Orleans M, Haverkamp AD, Murphy J. Short- and long-term risks after exposure to diagnostic ultrasound in utero. Obstet Gynecol. 1984;63(2):194–200. Epub 1984/02/01.
148. Wilson MK. Obstetric ultrasound and childhood malignancies. Radiography. 1985;51(600):319–20. Epub 1985/11/01.
149. Smith DP, Graham JB, Prystowsky JB, Dalkin BL, Nemcek AA Jr. The effects of ultrasound-guided shock waves during early pregnancy in Sprague-Dawley rats. J Urol. 1992;147(1):231–4. Epub 1992/01/11.

7

First-Trimester Ultrasound: Practice Guidelines

Roni Yoeli-Bik, Jude P. Crino,
and Jacques S. Abramowicz

Guidelines and recommendations for the performance of first-trimester ultrasound have been developed and published by several societies and organizations, including the American College of Obstetricians and Gynecologists (ACOG), American College of Radiology (ACR), American Institute of Ultrasound in Medicine (AIUM), Australasian Society for Ultrasound in Medicine (ASUM), Hong Kong College of Obstetricians and Gynecologists (HKCOG), International Society of Ultrasound in Obstetrics and Gynecology (ISUOG), National Institute of Child Health and Human Development (NICHD), Society for Maternal-Fetal Medicine (SMFM), Society of Obstetricians and Gynecologists of Canada (SOGC), Society for Reproductive Endocrinology and Infertility (SREI), and Society of Radiologists in Ultrasound (SRU) [1–16].

These guidelines and recommendations have been published in various printed and online formats. Several of these organizations have published collaborative guidelines. This chapter summarizes the key components of the current guidelines and recommendations for the first-trimester ultrasound. Not all concepts are covered in each guideline, and pertinent differences between the published guidelines are described.

Equipment

The first-trimester scans should be conducted with real-time scanners using a transabdominal or transvaginal approach. The choice of transducer frequency is a trade-off between beam penetration and resolution. With modern ultrasound machines, in most patients, abdominal transducers (≥3 MHz) will allow sufficient penetration while providing adequate resolution [1]. During early pregnancy, a transvaginal ultrasound may provide superior resolution, as compared to a transabdominal scan, while still allowing sufficient penetration [1]. If the transabdominal approach is limited by maternal factors (such as increased body mass index, retroverted uterus, or uterine fibroids) or when an anomaly is suspected, using transvaginal transducers with frequencies of 5–12 MHz will enhance the detection rates of structural malformations [9]. The SOGC guidelines specify the use of both low frequency (2–5 MHz) and mid-frequency (4–9 MHz) for the transabdominal approach and high frequency (9–12 MHz) for the transvaginal approach [7]. The ISUOG guidelines list minimum capabilities of the required equipment for sonographic assessment, including real-

---

R. Yoeli-Bik · J. S. Abramowicz
Department of Obstetrics and Gynecology, University of Chicago, Chicago, IL, USA

J. P. Crino (✉)
Department of Obstetrics, Gynecology and Reproductive Sciences, University of Maryland School of Medicine, Baltimore, MD, USA
e-mail: Jcrino1@alumni.jh.edu

© The Author(s), under exclusive license to Springer Nature Switzerland AG 2023
J. S. Abramowicz, R. E. Longman (eds.), *First-Trimester Ultrasound*,
https://doi.org/10.1007/978-3-031-24133-8_7

time gray-scale two-dimensional ultrasound machines, with options for color and spectral Doppler functions, and M-mode, including transabdominal and transvaginal ultrasound transducers, adjustable acoustic power output controls (including output display standard [ODS, see below]), freeze frame and zoom capabilities, electronic calipers for measurements, and ability to store and print the images [4].

Safety[1]

Diagnostic ultrasound is generally considered safe and has been used clinically in obstetrics for over 50 years. However, it is a form of energy that affects the tissues it traverses (bioeffects) [10]. The two major effects are: (a) direct effect, caused by the alternation of positive and negative pressures (mechanical effects); (b) indirect effect, resulting from the heating of the tissues, secondary to the transformation of the acoustic energy into heat (thermal effects). Two real-time on-screen indices allow the end user to make assumptions regarding the potential risk: the mechanical index (MI) and the thermal index (TI) [10]. These two indices constitute the Output Display Standard (ODS) which should be available in real-time on the screen and monitored by the examiner for potential bioeffects. A thermal index for soft tissue (TIS) should be used before 10 weeks of gestation, and a thermal index for bone (TIB) should be used subsequently when bone ossification occurs [1, 9, 10]. SOGC guidelines suggest keeping the thermal and mechanical indices below 1.0 [7], compared to the AIUM guidelines that recommend keeping TI less than or equal to 0.7 [9, 17]. Fetal exposure times should be minimized, especially with Doppler modalities that produce greater energy output, using the shortest scan times and lowest possible power output to obtain diagnostic imaging, following the "as low as reasonably achievable" (ALARA) principle. In the first-trimester ultrasound scan, the Doppler ultrasound should only be used if clinically indicated while carefully monitoring for TI below 1.0 and the shortest exam time (5–10 min) [4, 5]. Identifying fetal cardiac activity can be done using the 2D B-mode ultrasound [2, 4, 17]. ISUOG guidelines suggest verifying and recording the fetal heart rate with either M-mode or spectral Doppler [4], compared to the ACOG practice bulletin and AIUM's official statement that both recommend obtaining the fetal heart rate using M-mode and not Doppler due to its higher energy output [2, 17].

Indications and Timing of First-Trimester Ultrasound

The first trimester is defined as a gestational age of up to 14 + 0 weeks of gestation. Ultrasound imaging of the fetus in the first trimester has been widely incorporated into prenatal care. It promotes accurate dating, optimal assessment of amnionicity and chorionicity in multiple-gestation pregnancies, and an opportunity to assess the structural integrity of the fetus.

The most comprehensive lists of indications for the first-trimester scan are published in the collaborative AIUM/ACR/ACOG/SMFM/SRU guidelines and SOGC guidelines [1, 8] (Table 7.1).

Table 7.1 Indications for first trimester ultrasound examination (up to 13 + 6 weeks of gestation)

Confirmation of intrauterine pregnancy
Confirmation of cardiac activity
Estimation of gestational age
Evaluation of multiple-gestation pregnancies (including chorionicity and amnionicity)
Measurement of the nuchal translucency (as part of a fetal aneuploidy screening)
Assessment for fetal anomalies
Visual guidance as a part of chorionic villus sampling or embryo transfer or prophylactic cervical cerclage placement
Evaluation of a suspected ectopic pregnancy or threatened abortion
Prior to pregnancy termination
Evaluation of suspected gestational trophoblastic disease
Localization or removal of an intrauterine device
Evaluation of vaginal bleeding, pelvic pain, pelvic masses, or uterine abnormalities
As part of the first-trimester combined screening test for pre-eclampsia

Modified from references [1] and [8]

---

[1] See also Chap. 1

Table 7.2 Indications for detailed sonographic assessment for women at increased risk for fetal or placental abnormalities (At 12 + 0 to 13 + 6 weeks of gestation)

Pregnancy conceived via in vitro fertilization
Twin or high-order multiple-gestation pregnancies
Previous fetus or child with a congenital, genetic, or chromosomal anomaly
Suspected or known fetal abnormality detected by ultrasound, enlarged nuchal translucency, or positive aneuploidy screening test results
Maternal age (above 35 years), pregestational diabetes, maternal body mass index (>30 kg/m^2), or teratogens exposure
Placental implantation covering the internal cervical os or at the cesarean scar site

Modified from reference [9]

For some indications and purposes, specific timing is required for the ultrasound exam. In women with unreliable last menstrual period (LMP), an assessment of the gestational age is more accurate when performed earlier in the first trimester using the crown-rump length (CRL). But, in asymptomatic women with a known and reliable LMP, it remains controversial whether to offer routine early first-trimester scans to confirm an ongoing early pregnancy. If an earlier scan has not been performed, SOGC and ISUOG guidelines recommend the first-trimester scan at 11–14 weeks of gestation [4, 7, 8]. For women at increased risk for fetal or placental abnormalities (Table 7.2), an indication-driven examination should be performed in the late first trimester when organogenesis has occurred (between 12 + 0 and 13 + 6 weeks of gestation) [9].

Content of the Examination

Components of a standard first-trimester examination are assessment of viability and pregnancy location, fetal number, measurements, and determination of gestational age. Fetal anatomy and aneuploidy screening may be appropriate for some patients. Assessment of other intrauterine and extrauterine structures is recommended. First-trimester prenatal pre-eclampsia screening is feasible.

Assessment of Viability[2]

Usually, the term "viability" implies the ability to live independently outside the uterus. However, from an ultrasound perspective, the term is used to describe the presence of an embryo with cardiac activity at the time of the examination. Heartbeat is typically seen as early as 5–6 weeks of gestation, once the embryonic heart tube starts to beat [4, 11]. An alternative definition proposed by the SRU is a pregnancy that can potentially result in a liveborn baby [15, 16]. This definition was introduced after women with viable intrauterine pregnancies in the early first trimester were incorrectly diagnosed with pregnancy failure (nonviable intrauterine or ectopic pregnancy). Those false-positive diagnoses may prompt interventions leading to embryonic demise or congenital anomalies [15, 16]. In 2012, to minimize and avoid the possibility of harming a potentially viable intrauterine pregnancy, the SRU published uniform terminology and guidelines to assess pregnancies of uncertain viability (Tables 7.3 and 7.4) [16]. The possibility of incorrect dating should always be considered, especially when there is no pain or bleeding. In a hemodynamically stable woman with findings suspicious for pregnancy failure (Table 7.4), monitoring of maternal serum human chorionic gonadotropin (β-hCG) level and a repeat ultrasound scan is recommended after an additional 7–10 days [13, 16]. Notably, a single measurement of β-hCG,

Table 7.3 Terminology for viability of early pregnancy

Terminology	Explanation
Viable pregnancy	A pregnancy that can potentially result in a liveborn baby
Nonviable pregnancy	A pregnancy that cannot possibly result in a liveborn baby (ectopic pregnancy, failed intrauterine pregnancy)
Intrauterine pregnancy of uncertain viability	Visualization of an intrauterine gestational sac with no embryonic heartbeat and no findings of definite pregnancy failure
Pregnancy of unknown location	A positive urine or serum pregnancy test and absence of intrauterine pregnancy or ectopic pregnancy

Modified from reference [16]

---

[2] See also Chap. 10

regardless of its value, does not reliably distinguish between intrauterine and ectopic pregnancy, irrespective of viability [16].

Table 7.4 Transvaginal ultrasound assessment of intrauterine pregnancy of uncertain viability

Diagnosis of pregnancy failure
Crown-rump length ≥ 7 mm and no heartbeat
Mean sac diameter ≥ 25 mm and no embryo
Absence of an embryo with a heartbeat more than 2 weeks after visualizing a gestational sac without a yolk sac
Absence of an embryo with a heartbeat more than 11 days after visualizing a gestational sac and a yolk sac
Findings suspicious for pregnancy failure
Crown-rump length of <7 mm and no heartbeat
Mean sac diameter of 16–24 mm and no embryo
Absence of an embryo with a heartbeat 7–13 days after visualizing a gestational sac without a yolk sac
Absence of an embryo with a heartbeat 7–10 days after visualizing a gestational sac with a yolk sac
Absence of an embryo ≥6 weeks after the last menstrual period
Empty amnion
Yolk sac > 7 mm
Small gestational sac compared to the size of the embryo (less than 5 mm difference)

Modified from reference [16]

Pregnancy Location

The location of the pregnancy should be determined and documented. A definitive diagnosis of intrauterine pregnancy can be made when an intrauterine gestational sac containing a yolk sac or an embryo is visualized [1]. The gestational sac should be entirely bounded by the myometrium [4]. In the early stage of intrauterine pregnancy, a small and eccentric intrauterine fluid collection with an echogenic rim can be seen before the yolk sac or embryo. In the absence of sonographic signs of ectopic pregnancy, this fluid collection is highly likely to represent an intrauterine gestational sac. The mean sac diameter (MSD) is the average of three orthogonal measurements of the fluid-filled space within the gestational sac (Fig. 7.1), and it

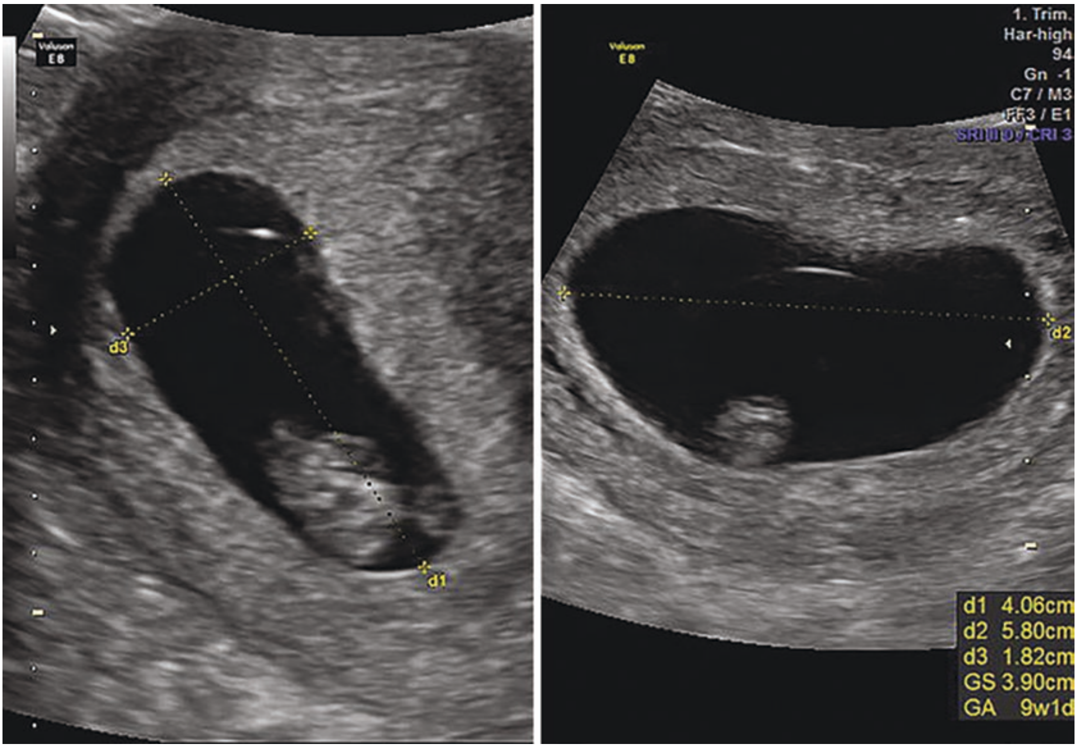

Fig. 7.1 Measurement of the mean gestational sac diameter in three orthogonal planes at 9 weeks of gestation

helps to assess pregnancy development (at MSD above 25 mm, an embryo should be visualized) [16]. In pregnancies of undetermined location (Table 7.3), follow-up sonography and serial determination of β-hCG levels are appropriate[3] [1, 10, 11, 13].

Fetal Number

Although the visualization of multiple sacs early in the first trimester is suspicious for multiple gestations, the actual diagnosis requires the visualization of multiple embryos. The first trimester is the optimal time to determine chorionicity and amnionicity, which are essential for managing multi-fetal pregnancies. The presence of separate sacs, the thickness of the intervening membrane, and the shape of its junction with the placenta should be assessed [7, 11] (Fig. 7.2). Chorionicity is most reliably determined before 14 weeks of gestation by evaluating the insertion of the amniotic membrane into the placenta and by identifying the T-sign in monochorionic twins or the λ-sign (also known as twin peak) in dichorionic twins [7, 13]. This sign gradually disappears with advancing gestation and might not be observable after the second trimester [13]. Amnionicity and chorionicity should be listed in the ultrasound report[4].

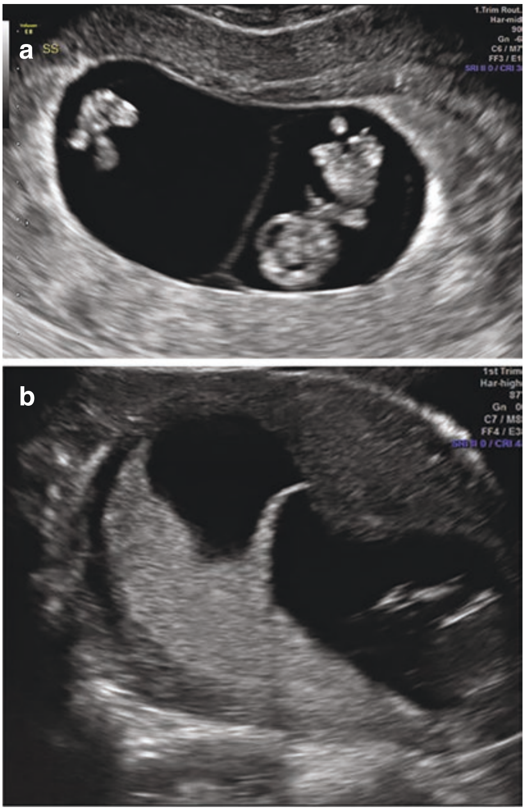

Fig. 7.2 (**a**) Monochorionic twin pregnancy at 9 weeks of gestation. Note the thin intervening membrane with no placental tissue. (**b**) Dichorionic twin pregnancy at 12 weeks of gestation. Note the thick intervening membrane with placental tissue ("twin peak" sign)

Measurements and Determination of Gestational Age[5]

Gestational age refers to menstrual age and represents post-conception (post-fertilization) age plus 14 days. First-trimester measurement of the crown-rump length (CRL), especially between 7 and 12 weeks of gestation, is the most accurate method to establish or confirm gestational age, with an accuracy of ±5–7 days [8]. The variability in predicting menstrual age by CRL is 8% [9]. Besides pregnancies conceived by assisted reproductive technology (in which the timing of conception is precisely known), CRL measurements should be used in all pregnancies to estimate the gestational age [4, 7]. The CRL is the maximum length of the entire embryo or fetus measured as a straight line in a true midsagittal plane, ideally with the embryo or fetus oriented horizontally on the screen (Fig. 7.3). It should be routinely measured using a transabdominal or transvaginal approach. At earlier gestations, the embryo is typically hyper-flexed, and the actual measurement reflects the neck-rump length, yet is still called CRL. The CRL measurement in the later first trimester may be affected by the fetal position and image magnification, and care should be taken to ensure that the fetus is not flexed (Fig. 7.4). Detailed technical requirements are

---

[3] See also Chap. 10

[4] See also Chap. 15

[5] See also Chap. 11

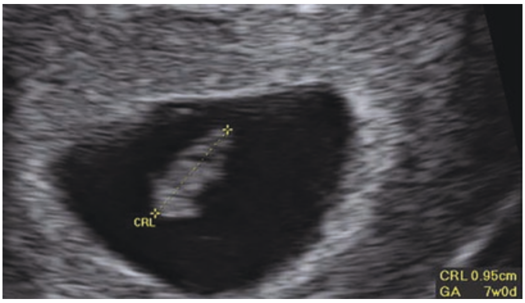

Fig. 7.3 Measurement of the crown-rump length at 7 weeks of gestation

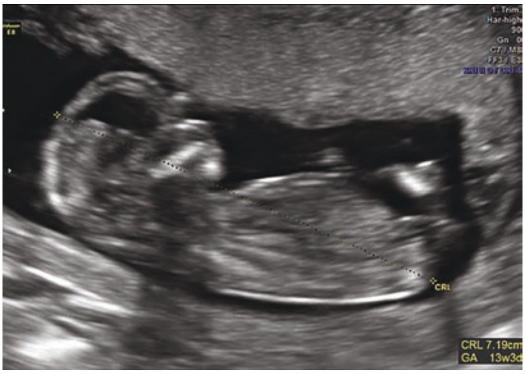

Fig. 7.4 Measurement of the crown-rump length at 13 weeks of gestation. Note the fluid between the fetal chin and chest, confirming that the fetus is not flexed

summarized in the practice parameter published by AIUM and in ISUOG guidelines [4, 9].

Discrepancies between ultrasound dating and last menstrual period (LMP) dating that support re-dating based on CRL measurement is more than 5 days at ≤8 + 6/7 weeks and more than 7 days from 9 + 0/7 weeks to 13 + 6/7 weeks of gestation [1–3, 9]. In cases where several first-trimester sonographic examinations have been performed, SOGC guidelines suggest using the earliest exam after 7 weeks of gestation or after a CRL above 10 mm was measured to estimate the delivery date (considering the image quality) [7]. ISUOG guidelines recommend assessing the gestational age based on the best quality CRL measurement between 45 and 84 mm [4]. Beyond the first trimester, or when the CRL is measured more than 84 mm, a variety of sonographic parameters, such as biparietal diameter (BPD), head circumference (HC), abdominal circumference (AC), and femoral diaphysis length (FL), can be used to estimate gestational age (the AC is the least reliable) [7]. Significant discrepancies between gestational age and fetal biometry measurements may suggest a fetal growth abnormality and can reveal early expression of severe pathologies. The threshold values for follow-up procedures should be decided following local protocols to avoid an excessive rate of false-positive findings and unnecessary follow-ups [4]. The pregnancy should not be redated after an accurate earlier scan has been performed since the earlier measurement is the most reliable [1]. Systematic measures of the cephalic, abdominal, and femoral biometry will also enable the assessment of anatomical landmarks [4]. Further details about the technical requirements for these measurements are documented in several guidelines [1, 4, 9].

In spontaneously conceived high-order multiple-gestation pregnancies, gestational age should be estimated between 11 and 13 + 6/7 weeks of gestation [7]. While it is controversial which CRL to use for a twin pregnancy, the most common practice is to use the larger CRL to minimize the risk of missing growth failure [7, 11].

Assessment of Fetal Anatomy

Advances in ultrasound technology in recent years have allowed many anomalies historically diagnosed in the second trimester to be identified earlier in pregnancy [9], with an estimation that approximately 40–66% of fetal anomalies can be identified during this time window [7]. The advantages of the first-trimester anatomy scan are well known, as detailed in several chapters of this book, including early reassurance for most women and early detection of many major anomalies that may lead to earlier genetic diagnosis, prenatal counseling, and decision-making. A standardized systematic protocol for the sonographic examination will enable a higher detection rate of structural anomalies in early pregnancy [4]. Limitations include the need for an experienced examiner and debatable economic benefits due to the uncertain clinical significance of some findings. The detailed anatomy scan requires advanced training, knowledge,

Table 7.5 Milestone of normal early pregnancy development and fetal structures that may be visualized using high-resolution ultrasound equipment

Week 0	Last menstrual period
Week 2	Conception occurs
Week 4.5–5	Gestational sac appears
Week 5–5.5	Yolk sac appears
Week 5–6	Embryo appears, cardiac pulsation
Week 6.5–7	Amniotic membrane appears
Week 7–8	Spine develops
Week 8	Head and trunk, four limb buds appear
Week 8–10	Rhombencephalon (hindbrain) develops
Week 10	Heart rate increases with the gestational age (up to 10 weeks; mean 171 bpm)
Week 11	Cranial bone ossification, spine, four-chamber heart, stomach, hands and feet, physiologic midgut herniation is present up to 11 weeks
Week 12	Bladder (with a longitudinal diameter < 7 mm), kidneys, normal insertion of the umbilical cord (should be documented after 12 weeks), vertebral bodies ossification
Week 10–14	Heart rate decreases (mean 156 bpm)

Modified from references [4], [11], and [15]

imaging skills, and the ability to effectively communicate the findings to the patients and the referring physician [9]. Of note, false-positive and false-negative results may occur (as in any other screening modality). Developmental milestones and anatomical structures that may be visualized during the first trimester are listed in Table 7.5.

Published guidelines differ on the recommendation of fetal anatomy assessment in the first trimester. ISUOG guidelines suggest the most detailed anatomy scan and separate the first-trimester scan into minimum requirements (e.g., visualizing the four-chamber heart at the axial view, identifying the stomach) (Table 7.6) and a more advanced detailed examination for anatomical structures that may be visualized (e.g., cisterna magna, upper lip) [4]. Conversely, HKCOG guidelines state that a routine first-trimester ultrasound examination to screen for fetal abnormalities is only recommended in highly specialized centers or research settings [14]. AIUM guidelines recommend an indication-driven late sonographic examination between 12 + 0 and 13 + 6 weeks of gestation for women at increased risk for fetal or placental abnormalities (Table 7.2) [9]. Certain anomalies, such as microcephaly and callosal agenesis, can only be visualized during a second-trimester ultrasound scan [6, 7, 9]. In the absence of specific indication (such as estimating gestational age in patients of uncertain menstrual dating, confirming viability, or as part of screening for aneuploidy), ACOG guidelines suggest that the optimal timing for a single ultrasound examination for the evaluation of fetal anatomy is at 18–22 weeks of gestation [2].

Table 7.6 Minimum requirements for the basic first-trimester anatomy assessment (between 11 + 0 and 14 + 0 weeks of gestation)

General and Biometry	Fetal number (in multiple-gestation pregnancies—assessment of chorionicity and amnionicity) Crown-rump length and biparietal diameter
Head and brain	Cranial bones ossification and shape Symmetrical hemispheres and midline falx Choroid-plexus-filled ventricles
Neck	Nuchal translucency thickness
Chest and heart	Heart position inside the chest Regular heart rhythm
Abdomen	Stomach visible in the left upper quadrant Intact abdominal wall Bladder not dilated
Extremities	Four limbs each with three segments Normal orientation of the hands and feet
Placenta	Normal echotexture
Additional components	Uterine morphology Adnexa assessment

Modified from reference [4]

Fetal Aneuploidy Assessment[6]

The first-trimester screening for chromosomal abnormalities includes two approaches: combined screening of maternal history with serum biochemistry with sonographic measurements of nuchal translucency (NT), or cell-free DNA

---

[6] See also Chap. 9

(cfDNA) testing. Most guidelines recommend that all women be offered the option of aneuploidy screening or diagnostic testing for fetal genetic disorders, regardless of maternal age, risk factors, or previous preimplantation genetic testing. Though the guidelines differ regarding the choice of screening strategies, that also depends on the available resources. ISUOG guidelines review the different screening methods' performances, including the detection and false-positive rates [4]. Pretest and posttest counseling should be provided to all women to facilitate informed decision-making [4, 6].

The first approach, the combined screening, includes maternal history (such as age and history of aneuploidy), maternal serum biochemistry (β-hCG and PAPP-A), and sonographic NT measurements. The NT refers to the fluid-filled space on the dorsal aspect of the fetal neck. This is the subcutaneous area between the skin and the soft tissues overlying the cervical spine. The accurate assessment of the NT is essential, and the standardized measurements should be done only by specialized examiners with continuous training and certification (such as the program suggested by the Fetal Medicine Foundation) [18]. An increased NT is independently associated with fetal aneuploidy or major structural malformations (such as cardiac anomalies) and should prompt a discussion about the risk, even if the aneuploidy risk is low based on the combined screening [4, 6, 7]. SOGC guidelines recommend offering NT measurements to all patients as part of the aneuploidy screening examination [7]. ISUOG guidelines recommend routine sonographic assessment of the NT thickness in all patients, independent of whether it is used as part of an aneuploidy screening test [4]. ASUM guidelines however recommend NT evaluation only at the request of the referring health practitioner [11]. For women at increased risk (Table 7.2), the AIUM practice parameter suggests regular assessment of the fetal neck for abnormal fluid collection or masses and subjective evaluation of the NT thickness [9]. A precise measurement of the NT thickness should be done when it appears thickened or as part of an aneuploidy screening protocol [9].

The first-trimester sonographic evaluation may include additional ultrasound markers, such as the fetal nasal bone, tricuspid flow, and ductus venosus flow, potentially improving the screening performance [4, 7]. Reliably evaluating these markers requires advanced sonographic skills; therefore, there is only limited uptake into the clinical practice [4] Currently, these measurements are not routinely recommended by SOGC [7], and as isolated sonographic markers, these findings have limited utility[7] [6].

The second approach, the cell-free DNA (cfDNA) analysis from maternal blood, was introduced in 2011 as an additional approach for screening [6, 19, 20]. The cfDNA is also known as noninvasive prenatal screening (NIPS) or noninvasive prenatal testing (NIPT). The test can be done at 9–10 weeks of gestation through the term [6, 19, 20]. The fetal component of cfDNA (known as the fetal fraction) is derived from placental trophoblasts released into the maternal circulation. It comprises approximately 3–13% of the total cfDNA in maternal blood. The cfDNA is affected by various factors such as gestational age, maternal body mass index, maternal medication, and maternal malignancy [6]. The cfDNA is the only screening test to detect fetal sex and sex chromosomal aneuploidies [6]. The ACOG and SMFM guidelines elaborate on the interpretation of the test results (which are affected by the prevalence and the type of studied disorder) and the role of ultrasound in women who undergo cfDNA testing [6, 19]. ACOG guidelines encourage pursuing one approach but recommend a baseline sonogram assessment, as some ultrasound findings may affect the appropriateness and timing of cfDNA testing and the ability to interpret the test results [6]. ISUOG guidelines do not recommend the cfDNA as a single test without the performance of the first-trimester sonographic scan [4].

---

[7] See also Chap. 9

In high-order multiple-gestation pregnancies, both approaches (the combined screening and cfDNA screening) are less accurate, and the complex analysis of the risk and benefits of the screening options should be discussed with the patients [6]. A positive test result should prompt further evaluation, including genetic and maternal-fetal medicine consultations and reviewing options for diagnostic testing (such as chorionic villus sampling [CVS] or amniocentesis) [6]. Due to the low effectiveness of these screening methods, sonographic screening alone may be relied upon; further sonographic markers, such as nasal bone, tricuspid flow, and ductus venosus flow, can be used to improve diagnostic performance [6, 7].

Other Intrauterine and Extrauterine Structures

There is a consensus that the uterus, cervix, adnexa, and cul-de-sac region should be examined. Pathologic findings such as abnormalities of uterine morphology and adnexal masses should be surveyed and documented. The echotexture of the placenta should also be evaluated [4, 9]. There is no role in assessing placenta previa at this stage [4, 7] since the diagnosis is overestimated [10]. Patients with a history of cesarean delivery should be examined for scar pregnancy and placenta accreta spectrum (PAS), which may result in significant complications [4, 7, 9]. Patients with these prenatal diagnoses will benefit from a referral to a specialized center [4, 7, 9]. The most common early sonographic sign of PAS is low anterior implantation of the gestational sac or the placenta near or in the scar niche[8] [4].

First-Trimester Screening for Pre-Eclampsia

Traditionally, pre-eclampsia (PE) screening was mainly based on maternal risk factors, such as advanced maternal age, nulliparity, previous history of PE, presence of diabetes mellitus, and more. These screening protocols however had poor detection rates. Alternative patient-specific approaches that combine biophysical and biochemical measurements have shown improved predictions. The most established method for first-trimester prenatal PE screening is the combined test that includes the a priori risk derived from maternal characteristics and medical history with mean arterial blood pressure measurements, uterine artery pulsatility index (UtA-PI), and serum analytes (Placental Growth Factor [PLGF]; or Pregnancy-Associated Plasma Protein A [PAPP-A] when PLGF is not available) [4, 21, 22]. This multifactorial approach has been prospectively validated in large multicenter cohorts and incorporated into ISUOG guidelines as the recommended screening option for all women with singleton pregnancies [4]. The UtA-PI measurements should be obtained during the first-trimester sonographic scan by examiners who have completed appropriate training and certification (such as that provided by the Fetal Medicine Foundation [FMF]) [4, 8, 22]. The risk calculator is available free of charge on the FMF website [21].

In low resources practices, a two-stage screening strategy for PE is recommended: first, a routine screening by maternal factors and blood pressure measurements should be performed in all women; then, in the second stage, further assessment with UtA-PI and PLGF should be evaluated in a subgroup of women with a higher risk based on the routine assessment [4, 22]. Notably, the first-trimester combined test for PE can be used for screening also in twin pregnancies [22].

---

[8] See also Chap. 18

Universal screening to identify women at increased risk for PE has great potential to improve patients' care because early treatment with low-dose aspirin and calcium supplements or replacements (in women with low calcium intake) is known to improve pregnancy outcomes [4, 7]. The International Federation of Gynecology and Obstetrics (FIGO) published a pragmatic guide for the first-trimester screening and prevention of PE [22, 23].

Documentation

Recommendation for the standardized documentation of ultrasound examinations is suggested by AIUM guidelines [24]. There should be a permanent record of the sonographic scans and their reports. Appropriately labeled relevant images should be recorded in a retrievable format. A signed official interpretation (final report) of the findings should be included in the patient's medical record and is the definitive documentation of the study. The final reports should be available within 24 h of the examination or, for nonemergent cases, by the next business day. Specific documentation requirements will vary depending on the type of exam, indication, findings, and whether any associated procedures were performed. In certain circumstances, such as if the examination results are unexpected or require urgent intervention, communication should occur directly between the interpreting physician and the patient's healthcare provider, and this should be documented in the report. Communication should occur promptly in accordance with the patient's clinical condition and the ultrasound findings.

Training Guidelines

ISUOG has published recommendations for basic training in obstetric and gynecologic ultrasound [25]. Formal basic teaching should include three steps: theoretical training, practical training, and examination. Theoretical training is primarily didactic and should cover physics principles, the basics of diagnostic ultrasound, and clinical concepts. This is followed by practical training with formal supervision, which should include a method of confirming that the sonographic scans were performed and documented in a standardized way. The examination should assess theoretical knowledge and may be complemented by a practical exam [25]. ISUOG education committee suggests a minimum of 100 h of supervised scanning to enable certification of a trainee in the ultrasound [25]. Those supervised scanning hours should include a minimum of 100 obstetric scans covering a broad spectrum of obstetric conditions and a minimum of 100 gynecological examinations, including early pregnancy complications [25].

The European Federation of Societies for Ultrasound in Medicine and Biology (EFSUMB) also published guidelines for minimum training recommendations for medical ultrasound, including obstetrics and gynecology [26, 27]. It includes standards for theoretical knowledge, practical skills, and curriculums by levels of expertise. Level 1 competence should be obtained by physicians performing unsupervised obstetrics ultrasound scans [26, 27]. Level 1 theoretical knowledge required a minimum of 30 h of theoretical course followed by an exam. For practical skills, a minimum of 500 supervised ultrasound scan examinations over 3–4 months is recommended. However, these skills may be acquired at different rates, and an assessment of competence should be performed at the endpoint. To maintain level 1 competence in obstetric ultrasound, a minimum of 500 ultrasound examinations per year is required [26, 27]. Level 2 would be gained after subspecialty training, including a theoretical course and exam, participation in at least 30 supervised clinic sessions and a minimum of 800 examinations. To maintain level 2 competence, a minimum of 400 obstetric ultrasound examinations per year is required [26, 27]. Level 3 practitioners are experts who spend most of their time performing obstetrics ultrasound examinations and/or conducting research, development, and teaching [26, 27].

AIUM has published training guidelines for physicians who evaluate and interpret diagnostic obstetric ultrasound examinations [28]. According to the guidelines, a physician should be involved with performing, evaluating, interpreting, and reporting a minimum of 300 diagnostic obstetric ultrasound scan examinations during an approved training program. For physicians who did not receive ultrasound training during residency or fellowship, a minimum of 50 AMA PRA Category 1 Credits dedicated to diagnostic obstetric ultrasound and involvement with at least 300 diagnostic scans under the supervision of a qualified physician within 36 months is recommended [28]. To maintain competence in obstetric ultrasound, a minimum of 170 diagnostic obstetric ultrasound examinations per year is recommended [28]. AIUM published further guidelines for physicians who evaluate and interpret diagnostic detailed fetal anatomic ultrasound scans [29].

Quality Assurance

Quality assurance is an essential component of obstetric imaging [30]. One of the first steps in guaranteeing these is accreditation. The ACR and the AIUM have a process to accredit ultrasound practices in the United States [30, 31]. There are specific requirements for accreditation in various specialties, specifically, Standard Obstetric (all trimesters or trimester-specific) and Standard Obstetric with an Adjunct in Detailed Fetal Anatomic Ultrasound Examinations [31, 32]. Receiving accreditation demonstrates that a practice meets minimal standards and guidelines for safety and quality. Specific components of the obstetrics ultrasound examination (such as the assessment of NT) require additional training and a continuous quality assurance and certification process.

Cleaning and Preparing Transducers

AIUM has published guidelines for preparing ultrasound transducers between patients, including specific procedures for cleaning and disinfection [33]. External probes that only come into contact with clean, intact skin require a low-level disinfection process with cleaning after each use. Preparation of internal probes requires routine mandatory high-level disinfection and a high-quality single-use transducer cover during each examination. Variable rates of leakage have been reported with both condoms and commercially available covers, and therefore high-level disinfection of the probe is required after each use. Protective barriers, such as medical gloves and condoms, are regulated by an acceptable quality level (AQL). Interestingly, condoms have a better AQL as compared to standard examination gloves and even as compared to surgical gloves. Users should be aware of latex sensitivity issues and have non-latex-containing barriers available.

As a result of the SARS-CoV-2 outbreak, several guidelines were published by AIUM, ISUOG, and the World Federation for Ultrasound in Medicine and Biology (WFUMB) [33–36]. The guidelines mention that for external and interventional procedures, low-level disinfection is effective. In addition, if possible, the recommendation is to use a dedicated system (scanner and transducers) for COVID-19, positive or suspected patients.

Teaching Points

- Several societies and organizations have developed and published guidelines and recommendations for the performance of the first-trimester ultrasound scan. The first-trimester sonographic scan promotes accurate dating, optimal assessment of amnionicity and chorionicity in multiple-gestation pregnancies, and an opportunity to assess the structural integrity of the fetus.
- The first-trimester ultrasound examination should be conducted with real-time scanners using a transabdominal or transvaginal approach. Components of a standard basic first-trimester examination are assessing viability and pregnancy location, fetal number, measurements, determination of gestational age, and assessment of other intrauterine and extrauterine structures. Fetal anatomy and fetal aneuploidy screening may be appropriate for some patients. First-trimester combined test for pre-eclampsia is feasible.

- The output display standard, a real-time on-screen display of the MI and TI, should be visible and monitored. The exposure time should be minimized under the "as low as reasonably achievable" (ALARA) principle.
- A definitive diagnosis of intrauterine pregnancy can be made when an intrauterine gestational sac containing a yolk sac or an embryo is visualized. Heartbeat is typically seen as early as 5–6 weeks of gestation.
- Findings diagnostic of pregnancy failure include a CRL measurement of ≥7 mm and no heartbeat, MSD of ≥25 mm and no embryo, absence of an embryo with a heartbeat more than 2 weeks after visualizing a gestational sac without a yolk sac, and absence of an embryo with a heartbeat more than 11 days after visualizing a gestational sac with a yolk sac. When there are findings suspicious of pregnancy failure, the possibility of incorrect dating should always be considered; a repeat scan after an additional 7–10 days is recommended in clinically stable women.
- Gestational age assessment is most accurate when done early in the first trimester, and CRL is the most accurate measurement. Discrepancies between ultrasound dating and LMP dating that support re-dating based on CRL measurement are more than 5 days at ≤8 + 6/7 weeks and more than 7 days from 9 + 0/7 weeks to 13 + 6/7 weeks.
- The first-trimester screening for chromosomal abnormalities includes two approaches: combined screening of maternal history (such as age and history of aneuploidy) with maternal serum biochemistry (β-hCG and PAPP-A), and sonographic measurements of nuchal translucency (NT); or cell-free DNA (cfDNA) testing.
- The most established method for first-trimester prenatal PE screening is the combined test that includes the a priori risk derived from maternal characteristics and medical history with mean arterial blood pressure measurements, uterine artery pulsatility index (UtA-PI), and serum analytes (PLGF; or PAPP-A when PLGF is not available).
- The record of the ultrasound examination and its interpretation should be permanently saved.
- The formal basic ultrasound training should include three steps: theoretical training, practical training, and examination. Quality assurance is an essential component of obstetric imaging.
- External probes that only come into contact with clean, intact skin require a low-level disinfection process with cleaning after each use. Preparation of internal probes requires routine mandatory high-level disinfection and a high-quality single-use transducer cover during each examination. Due to COVID-19, new cleaning and preparation recommendations were published. For external and interventional procedures, low-level disinfection is effective. In addition, if possible, a dedicated system (scanner and transducers) for COVID-19, positive or suspected patients is recommended.

References

1. AIUM-ACR-ACOG-SMFM-SRU practice parameter for the performance of standard diagnostic obstetric ultrasound examinations. J Ultrasound Med. 2018;37(11):E13–24.
2. American Institute of Ultrasound in Medicine. AIUM Committee on Practice Bulletins—Obstetrics Practice bulletin no. 175: ultrasound in pregnancy. Obstet Gynecol. 2016;128(6):e241–e56.
3. American College of Obstetricians and Gynecologists. ACOG Committee opinion No 700: methods for estimating the due date. American College of Obstetricians and Gynecologists. Obstet Gynecol. 2017;129(5):e150–e4.
4. Bilardo CM, Chaoui R, Hyett JA, Kagan KO, Karim JN, Papageorghiou AT, et al. ISUOG practice guidelines (updated): performance of 11-14-week ultrasound scan. Ultrasound Obstet Gynecol. 2023;61(1):127–43.
5. Bhide A, Acharya G, Baschat A, Bilardo CM, Brezinka C, Cafici D, et al. ISUOG practice guidelines (updated): use of Doppler velocimetry in obstetrics. Ultrasound Obstet Gynecol. 2021;58(2):331–9.
6. Rose NC, Kaimal AJ, Dugoff L, Norton ME. American College of Obstetricians and Gynecologists' committee on practice bulletins—obstetrics committee on genetics Society for Maternal-Fetal Medicine Screening for Fetal chromosomal abnormalities. Screening for Fetal chromosomal abnormalities:

practice bulletin No. 226. Obstet Gynecol. 2020;136(4):e48–69.
7. Simula N, Brown R, Butt K, Morency AM, Demers S, Grigoriu A, et al. Committee Opinion No. 418: the complete 11-14 week prenatal sonographic examination. J Obstet Gynaecol Can. 2021;43(8):1013–21.
8. Van den Hof MC, Smithies M, Nevo O, Oullet A. No. 375-clinical practice guideline on the use of first trimester ultrasound. J Obstet Gynaecol Can. 2019;41(3):388–95.
9. American Institute of Ultrasound in Medicine. AIUM practice parameter for the performance of detailed diagnostic obstetric ultrasound examinations between 12 weeks 0 days and 13 weeks 6 days. J Ultrasound Med. 2021;40(5):E1–E16.
10. Reddy UM, Abuhamad AZ, Levine D, Saade GR, Fetal Imaging Workshop Invited Participants. Fetal imaging: executive summary of a joint Eunice Kennedy Shriver National Institute of Child Health and Human Development, Society for Maternal-Fetal Medicine, American Institute of Ultrasound in Medicine, American College of Obstetricians and Gynecologists, American College of Radiology, Society for Pediatric Radiology, and Society of Radiologists in ultrasound fetal imaging workshop. Am J Obstet Gynecol. 2014;210(5):387–97.
11. Mizia K, Campbell Westerway S, Robertson M, Parry E, Paoletti D, Perry D, et al. Guidelines for the performance of the first trimester ultrasound. Australas J Ultrasound Med. 2018;21(3):179–82.
12. Mizia K, Campbell Westerway S, Robertson M, Parry E, Paoletti D, Perry D, et al. Erratum to "guidelines for the performance of the first trimester ultrasound". Australas J Ultrasound Med. 2021;24(3):181.
13. The Hong Kong College of Obstetricians and Gynaecologists. Guidelines for first trimester ultrasound examination: part I. 2004. https://www.hkcog.org.hk/hkcog/pages_4_81.html. Accessed 20 May 2022.
14. The Hong Kong College of Obstetricians and Gynaecologists. Guidelines for first trimester ultrasound examination: part II. 2004. https://www.hkcog.org.hk/hkcog/pages_4_81.html. Accessed 20 May 2022.
15. Rodgers SK, Chang C, DeBardeleben JT, Horrow MM. Normal and abnormal US findings in early first-trimester pregnancy: review of the Society of Radiologists in ultrasound 2012 consensus panel recommendations. Radiographics. 2015;35(7):2135–48.
16. Doubilet PM, Benson CB, Bourne T, Blaivas M, Barnhart KT, Benacerraf BR, et al. Society of radiologists in ultrasound multispecialty panel on early first trimester diagnosis of miscarriage and exclusion of a viable intrauterine pregnancy. Diagnostic criteria for nonviable pregnancy early in the first trimester. N Engl J Med. 2013;369(15):1443–51.
17. American Institute of Ultrasound in Medicine. AIUM official statement: prudent use and safety of diagnostic ultrasound in pregnancy (Approved 05-19-2020). https://www.aium.org/officialStatements/79. Accessed 20 May 2022.
18. The Fetal Medicine Foundation. Nuchal translucency scan. https://fetalmedicine.org/fmf-certification-2/nuchal-translucency-scan. Accessed 30 May 2022.
19. Norton ME, Biggio JR, Kuller JA, Blackwell SC. Society for Maternal-Fetal Medicine. The role of ultrasound in women who undergo cell-free DNA screening. Am J Obstet Gynecol. 2017;216(3):B2–7.
20. Gregg AR, Skotko BG, Benkendorf JL, Monaghan KG, Bajaj K, Best RG, et al. Noninvasive prenatal screening for fetal aneuploidy, 2016 update: a position statement of the American College of Medical Genetics and Genomics. Genet Med. 2016;18(10):1056–65.
21. The Fetal Medicine Foundation. Preeclampsia screening. https://fetalmedicine.org/fmf-certification-2/preeclampsia-screening-1. Accessed 30 May 2022.
22. Poon LC, Shennan A, Hyett JA, Kapur A, Hadar E, Divakar H, et al. The International Federation of Gynecology and Obstetrics (FIGO) initiative on pre-eclampsia: a pragmatic guide for first-trimester screening and prevention. Int J Gynaecol Obstet. 2019;145(Suppl 1):1–33.
23. Poon LC, Shennan A, Hyett JA, Kapur A, Hadar E, Divakar H, et al. Erratum to the International Federation of Gynecology and Obstetrics (FIGO) initiative on pre-eclampsia: a pragmatic guide for first-trimester screening and prevention. Int J Gynaecol Obstet. 2019;146(3):390–1. [Int J Gynecol Obstet 2019; 145 Suppl. 1 :1–33].
24. American Institute of Ultrasound in Medicine. AIUM practice parameter for documentation of an ultrasound examination. J Ultrasound Med. 2020;39(1):E1–4.
25. ISUOG education committee recommendations for basic training in obstetric and gynecological ultrasound. Ultrasound Obstet Gynecol. 2014;43(1):113–6.
26. European federation of societies for ultrasound in medicine and biology. Minimum training recommendations. https://efsumb.org/minimum-training-recommendations/. Accessed 1 Feb 2023.
27. Education and practical standards committee, European Federation of Societies for ultrasound in medicine biology. Minimum training recommendations for the practice of medical ultrasound. Ultraschall Med. 2006;27(1):79–105.
28. American Institute of Ultrasound in Medicine. AIUM training guidelines for physicians who evaluate and interpret diagnostic obstetric ultrasound examinations (Revised 10-31-2015). https://www.aium.org/official-Statements/59. Accessed 20 May 2022.
29. American Institute of Ultrasound in Medicine. AIUM training guidelines for physicians who evaluate and interpret diagnostic detailed fetal anatomic ultrasound examinations including assessments between 12 weeks 0 days and 13 weeks 6 days (Revised 06-16-2020). https://www.aium.org/resources/ptguidelines.aspx. Accessed 20 May 2022.
30. Holt R, Abramowicz JS. Quality and safety of obstetric practices using new modalities–ultrasound, MR, and CT. Clin Obstet Gynecol. 2017;60(3):546–61.

31. American College of Radiology (ACR). ACR ultrasound accreditation program requirements. exam requirements: obstetrical ultrasound (Revised 11-10-2022). https://accreditationsupport.acr.org/support/solutions/folders/11000012186. Accessed 5 Feb 2023.
32. American Institute of Ultrasound in Medicine. AIUM. practice parameter for the performance of obstetric ultrasound examinations. https://www.aium.org/accreditation/accreditation.aspx. Accessed 22 June 2022.
33. American Institute of Ultrasound in Medicine. AIUM. guidelines for cleaning and preparing external and internal use ultrasound transducers and equipment between patients as well as safe handling and use of ultrasound coupling gel (Revised 12-05-2022). https://www.aium.org/officialStatements/57. Accessed 20 Jan 2023.
34. Poon LC, Abramowicz JS, Dall'Asta A, Sande R, Ter Haar G, Marsal K, et al. ISUOG safety committee position statement on safe performance of obstetric and gynecological scans and equipment cleaning in context of COVID-19. Ultrasound Obstet Gynecol. 2020;55(5):709–12.
35. Abramowicz JS, Basseal JM, Brezinka C, Dall'Asta A, Deng J, Harrison G, et al. ISUOG safety committee position statement on use of personal protective equipment and hazard mitigation in relation to SARS-CoV-2 for practitioners undertaking obstetric and gynecological ultrasound. Ultrasound Obstet Gynecol. 2020;55(6):886–91.
36. Abramowicz JS, Basseal JM. World Federation for Ultrasound in medicine and biology position statement: how to perform a safe ultrasound examination and clean equipment in the context of COVID-19. Ultrasound Med Biol. 2020;46(7):1821–6.

8

Normal First Trimester of Pregnancy

Kalesha Hack and Phyllis Glanc

Introduction

The first trimester conventionally refers to the stage of pregnancy occurring prior to 14 weeks gestational age (GA). First trimester ultrasound may be used to refer to all scans performed prior to the 14 week mark [1] or to scans occurring between confirmation of an intrauterine pregnancy and 13+6 weeks gestation [2]. With the advent of highly sensitive home pregnancy tests, more women are presenting for a dating ultrasound before ultrasound is able to show confirmatory evidence of an early intrauterine pregnancy [3]. For this reason, we have chosen to include a discussion of all ultrasounds performed in a woman with a positive β-subunit of human chorionic gonadotropin (β-hCG) pregnancy test prior to 14 weeks in this chapter.

All dates in this chapter are referred to in menstrual age which, hereafter, will be considered synonymous with GA. GA is defined as the conceptual age + 2 weeks. Pregnancy dating can also be described based on timing of conception, known as the conceptual age or embryonic age, where day 1 refers to fertilization. This dating method may be used by assisted reproductive technology specialists.

There are several important stages in early pregnancy development that occur before they can be resolved by current commercial ultrasound technology.[1] Fertilization typically takes place around day 14 of the menstrual cycle when the sperm and mature ovum unite to form a zygote in the outer portion of the fallopian tube. Initially, the zygote undergoes rapid cellular division and migrates toward the uterus. Implantation typically is complete by 10 days post-fertilization and, in a normal pregnancy, occurs within the central portion of the uterine cavity. The embryo begins to flatten out and form a bilaminar disc that lies between the amniotic cavity and exocoelomic cavity. The primitive yolk sac develops at 9 days post-fertilization, however, it is not visible sonographically.

The primitive yolk sac subsequently breaks off and is extruded, around 4 weeks GA, to form

K. Hack (✉)
Department of Radiology, University of Toronto,
Toronto, ON, Canada

Department of Medical Imaging, Body Division,
Sunnybrook Health Sciences Centre,
Toronto, ON, Canada
e-mail: Kalesha.hack@sunnybrook.ca

P. Glanc
Department of Medical Imaging, Body Division,
Sunnybrook Health Sciences Centre,
Toronto, ON, Canada

Radiology, Obstetrics and Gynecology, University of
Toronto, Toronto, ON, Canada

Sunnybrook Research Institute, Toronto, ON, Canada
e-mail: phyllis.glanc@sunnybrook.ca

---

[1] See also Chap. 5.

© The Author(s), under exclusive license to Springer Nature Switzerland AG 2023
J. S. Abramowicz, R. E. Longman (eds.), *First-Trimester Ultrasound*,
https://doi.org/10.1007/978-3-031-24133-8_8

the secondary yolk sac which can be seen at early ultrasound. Subsequent use of the term yolk sac in this chapter refers to the secondary yolk sac. In the 5th gestational week, gastrulation occurs and results in the formation of the three germ cells layers: ectoderm, mesoderm, and endoderm, each giving rise to different organ systems. Closure of the neural tube is generally completed by the end of the 6th week. The developing heart begins to form in week 5 of the pregnancy. Development of the internal and external organs occurs during the first 8–10 weeks of pregnancy, known as the *embryonic period* or *organogenesis*. Recent advances in 3D imaging techniques have enabled detailed images of the developing embryo to be obtained and correlated to embryonic anatomy sections and micro-CT images increasing the body of knowledge of early normal and abnormal imaging appearances [4]. Prior to the end of the 10th week, the developing pregnancy is referred to as an *embryo*. After this time, once the organogenesis phase is completed, the term *fetus* is used.

Gestational Sac

The earliest sonographically visible evidence of an intrauterine pregnancy is the appearance of an intrauterine gestational sac [1, 5, 6]. With modern high-frequency transvaginal transducers, the gestational sac can first be seen as early as 4 weeks 1 day gestation and is typically seen around 4.5–5 weeks at which time it measures 2–3 mm [7–10]. The gestational sac is a round or ovoid fluid-filled structure identified within the central echogenic portion of the uterus, i.e., the decidualized endometrium. On closer inspection, one can identify that the sac is eccentrically located within the decidua, as opposed to in the endometrial cavity itself and has a peripheral echogenic rim (Fig. 8.1a).

An important distinction in early pregnancy ultrasound is the ability to differentiate a true intrauterine gestational sac, before the yolk sac or embryo is seen, from an intrauterine fluid collection such as a subendometrial cyst, decidual cyst, or fluid collection in the setting of an ectopic pregnancy. Careful interrogation will demonstrate that subendometrial cysts are external to the decidualized endometrium (Fig. 8.2). A decidual cyst is also a benign finding but is more challenging to distinguish from an early IUP. The key distinction will depend on the relationship of the early IUP, which should abut the interstitial line of the collapsed endometrial cavity (Fig. 8.1b), whereas the decidual cyst may not be anatomically related to the collapsed endometrial cavity. Decidual cysts also typically have a thinner wall and may be multiple. In cases where there is doubt, follow-up imaging will demonstrate appropriate growth of the early intrauterine gestational sac, with development of a yolk sac to confirm an early IUP.

It is equally important to ensure the "cyst" is not actually within the endometrial cavity. In most cases, fluid within the endometrial cavity can be distinguished from fluid outside of the endometrial cavity on the basis of shape, location, and contents. Whereas endometrial cavity fluid collections may be angular, complex with internal echogenic debris, or elongated, conforming to the uterine cavity, the early gestational sac will be anechoic and typically rounded or ovoid [11]. In cases where there is uncertainty, the differential diagnosis will include a pregnancy of unknown location or intracavitary fluid collection, accompanying early pregnancy loss.

It has been shown that intrauterine fluid, commonly referred to as a "pseudogestational sac," in the setting of ectopic pregnancy occurs much less frequently than previously thought and may be seen in only around 10% of ectopic pregnancies [12, 13]. Doubilet et al. reported in an editorial on pregnancy of unknown location that given the relatively low incidence of ectopic pregnancy (approximately 2%) and low likelihood of intrauterine fluid with an ectopic pregnancy, the probability that any intrauterine fluid collection in a woman with a positive pregnancy test represents a gestational sac is 99.5% [14]. This led to a change in thinking with respect to early pregnancy such that, **in the absence of sonographic evidence of ectopic pregnancy, any fluid col-**

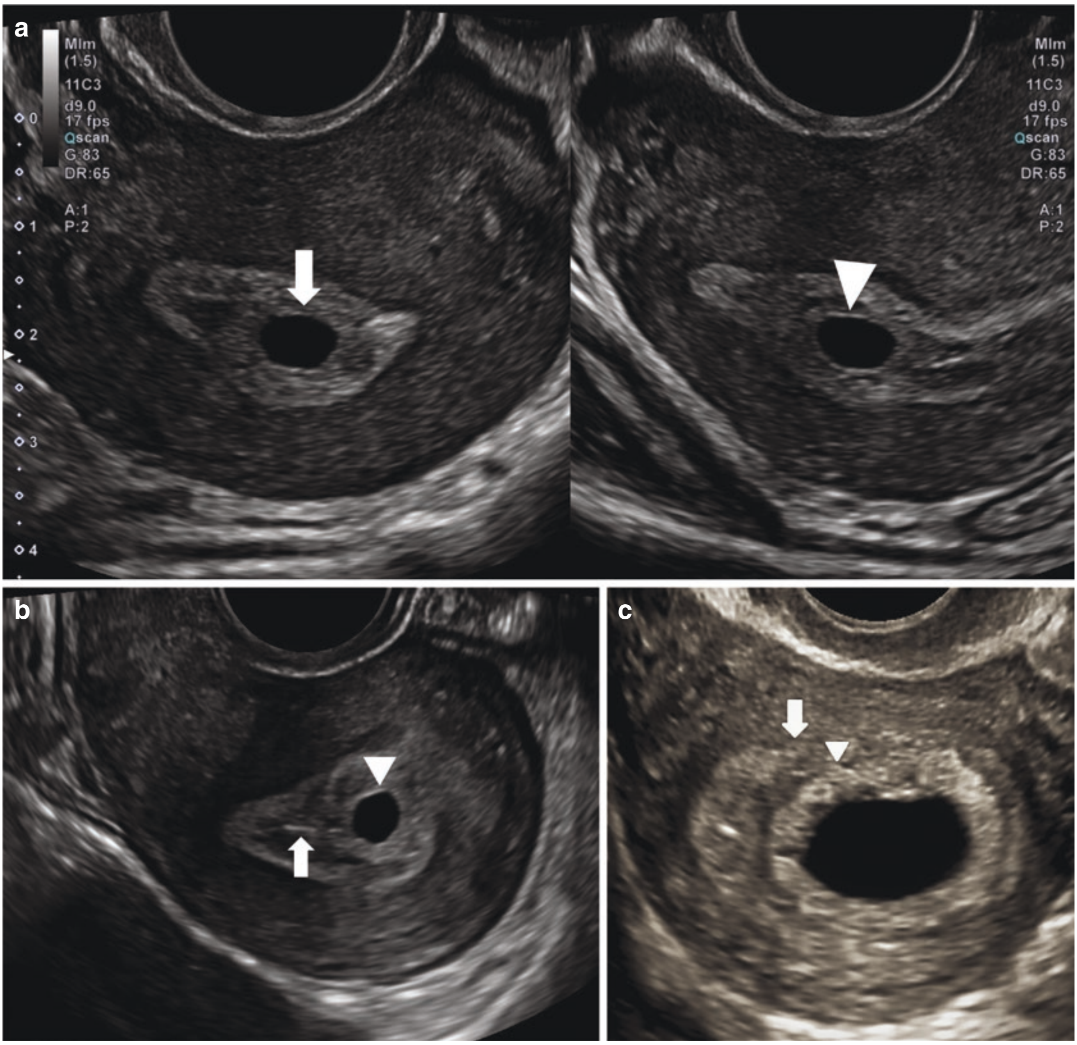

Fig. 8.1 Normal early gestational sac: (**a**) 5 weeks 2 days transvaginal transverse and sagittal images showing an oval intrauterine fluid collection (white arrow) eccentrically located within the endometrial cavity in a woman with a positive serum B-hCG. Note the faint surrounding echogenic rim (white arrowhead) typical of an early gestational sac. Although there is no yolk sac or fetal pole identified, findings should be reported as an early intrauterine pregnancy of unknown viability. (**b**) 5 weeks 2 days transverse sagittal image shows an eccentric round fluid collection with an echogenic rim (white arrowhead) adjacent to the thin echogenic line (white arrow) of the collapsed endometrial cavity demonstrating the "intradecidual sign." (**c**) 6 weeks 5 days transvaginal transverse image showing an intrauterine fluid collection surrounded by two concentric echogenic rings (white arrowhead inner and white arrow outer) forming the so-called double sac sign

lection with curved edges in a woman with a positive pregnancy test should be thought of as an early intrauterine gestational sac [14]. In a study of 649 women presenting with a positive β-hCG and an intrauterine sac-like structure without a yolk sac or embryo on ultrasound, none of the intrauterine fluid collections represented a pseudogestational sac [15]. In the setting of a suspected early intrauterine pregnancy, follow-up imaging can be obtained, to confirm subsequent appearance of embryonic structures including a yolk sac and an embryo with cardiac activity. The role of follow-up β-hCG serology in this setting will be discussed separately.

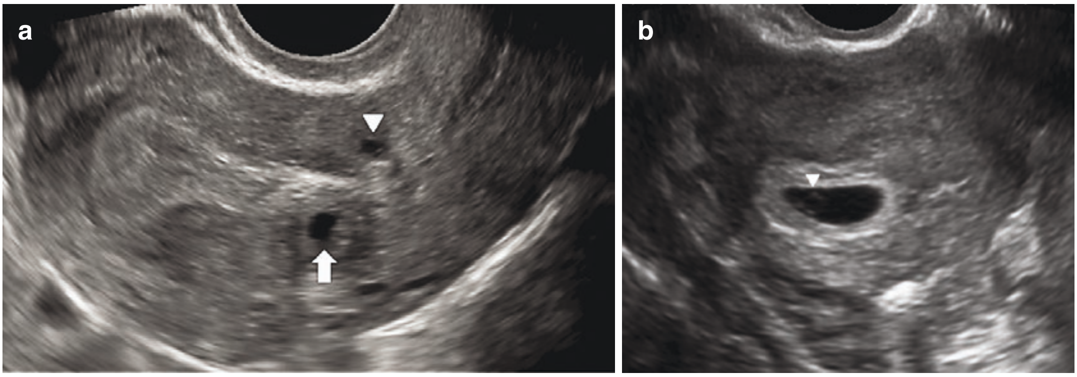

Fig. 8.2 Subendometrial cysts in a patient with a positive pregnancy test and unknown dates, transvaginal images: (**a**) Sagittal image of the uterus showing two round fluid collections outside of the echogenic endometrial cavity (arrow and arrowhead). These can be identified as decidual cysts due to their location outside of the endometrial cavity. Note that these cysts also demonstrate a thin imperceptible wall in contrast to the echogenic rim typically seen around an early gestational age. No intrauterine gestational sac is identified. (**b**) Transverse image from follow-up study 9 days later shows an intrauterine gestational sac with visible yolk sac (arrowhead) confirming an intrauterine pregnancy

The **double sac sign (DSS)** and **intradecidual sign (IDS)** have historically been described as useful in differentiating a true IUP from a non-gestational intrauterine fluid collection [16, 17]. The DDS, first described in 1982, refers to the appearance of two echogenic rings around the gestational sac felt to represent the inner and outer layers of the decidua, the decidua capsularis and decidua basalis (Fig. 8.1c) [17]. The IDS, initially described in 1986, refers to a fluid collection with an echogenic rim in an eccentric location on one side of the uterine cavity (Fig. 8.1b) [16]. Both of these signs were initially described on transabdominal ultrasound and considered to be early reliable signs of an IUP with the DSS seen in 77% of the initial study population with an IUP and the IDS seen in 92% [14, 16, 17]. Currently, with the advent of high resolution, high-frequency transvaginal transducers, subsequent studies have shown that in normal IUP the DSS may be absent in 50–60% and the IDS absent in up to 50% [14, 18, 19]. With improvements in technology, it is no longer infrequent that the yolk sac is visible prior to DSS and IDS and, consequently, these signs are now felt to be of limited utility. The absence of a DSS or IDS should not be used to exclude one [20] and similarly should not be interpreted as a poor prognostic factor. In 2020, Phillips et al. reported that the likelihood of an early intrauterine gestational sac progressing to a live pregnancy by the end of the first trimester was better in women when an intradecidual sign was present (46% vs 35%), however, neither the intradecidual sign or double sac sign proved to be of clinical value in predicting the outcome of an early pregnancy [15].

Measurement of the Gestational Sac[2]

Measurements of the gestational sac can be obtained and used to estimate gestational age and predict appearance of normal embryonic structures. The mean sac diameter (MSD) is obtained by averaging the transverse, sagittal, and anteroposterior dimensions of the gestational sac and can be correlated with expected GA and with β-hCG levels (Fig. 8.3). There is variability in gestational sac size measurements between different observers. In a study of 54 patients by Pexsters et al. [21] interobserver

---

[2] See also Chap. 9.

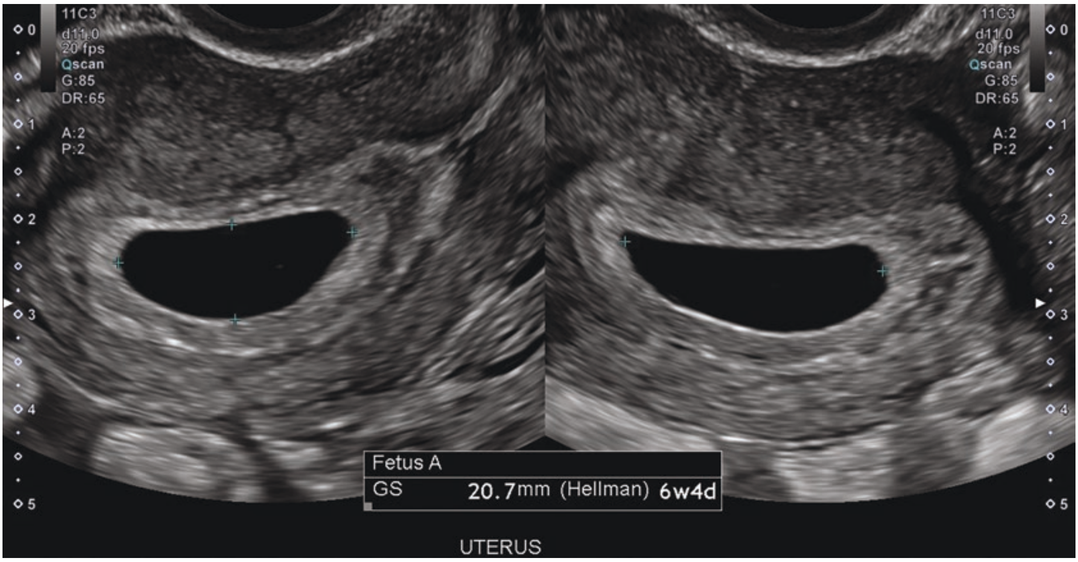

Fig. 8.3 Mean sac diameter: 6 weeks 4 days transvaginal sagittal and transverse images of the uterus measuring the gestational sac in three orthogonal dimensions which are averaged to obtain the mean sac diameter (MSD). Care should be taken to place calipers directly on the white line around the sac to ensure accurate measurements

variability for MSD was reported as being up to ±19%. Expected rate of growth of the gestational sac has previously been reported as approximately 1 mm/day [8]. However, in a study of 359 women, Abdallah et al. [22] found overlap in MSD growth rate in viable and nonviable early IUP and were unable to define a rate of gestational sac size that can be considered normal in early pregnancy [22]. A small gestational sac with less than 5 mm difference between crown rump length and gestational sac length has been referred to as first trimester oligohydramnios and considered to be associated with poor outcome [23]. However, this has only been examined in a small population and as an isolated finding likely warrants follow-up imaging (Fig. 8.4). It is important to note that in addition to growth, the shape of the gestational sac may change on serial ultrasound from a round to more irregular appearance. This may be the result of maternal factors such as uterine contractions, over-filled bladder, fibroids, or subchorionic hematomas and should not necessarily be interpreted as a sign of an impending loss (Fig. 8.5).

Mean Sac Diameter and Viability

Much attention has been given to the maximum size at which an empty gestational sac, i.e., a sac without a visible yolk sac or embryo, can be considered normal. While a yolk sac is usually seen with a MSD >8 mm, the MSD at which a yolk sac and embryo can be sonographically detected is variable and caution should be exercised if using MSD to determine viability [24]. Historically, the upper limit at which an empty gestational sac was considered a normal early pregnancy finding was a transvaginally measured MSD between 16 and 20 mm [25, 26]. However, several recent studies have shown that a small percentage of viable pregnancies may exist with empty sac size up to 18–19 mm [27, 28] and given interobserver variability in sac size measurement, **an empty gestational sac should be considered a potentially normal early pregnancy finding up to a MSD of 25 mm on transvaginal ultrasound** [22, 25, 26, 28, 29] (Fig. 8.6). This is discussed further in Chap. 10 which refers to new discriminatory criteria for defining early viability. One caveat of using more stringent criteria to diagnose early

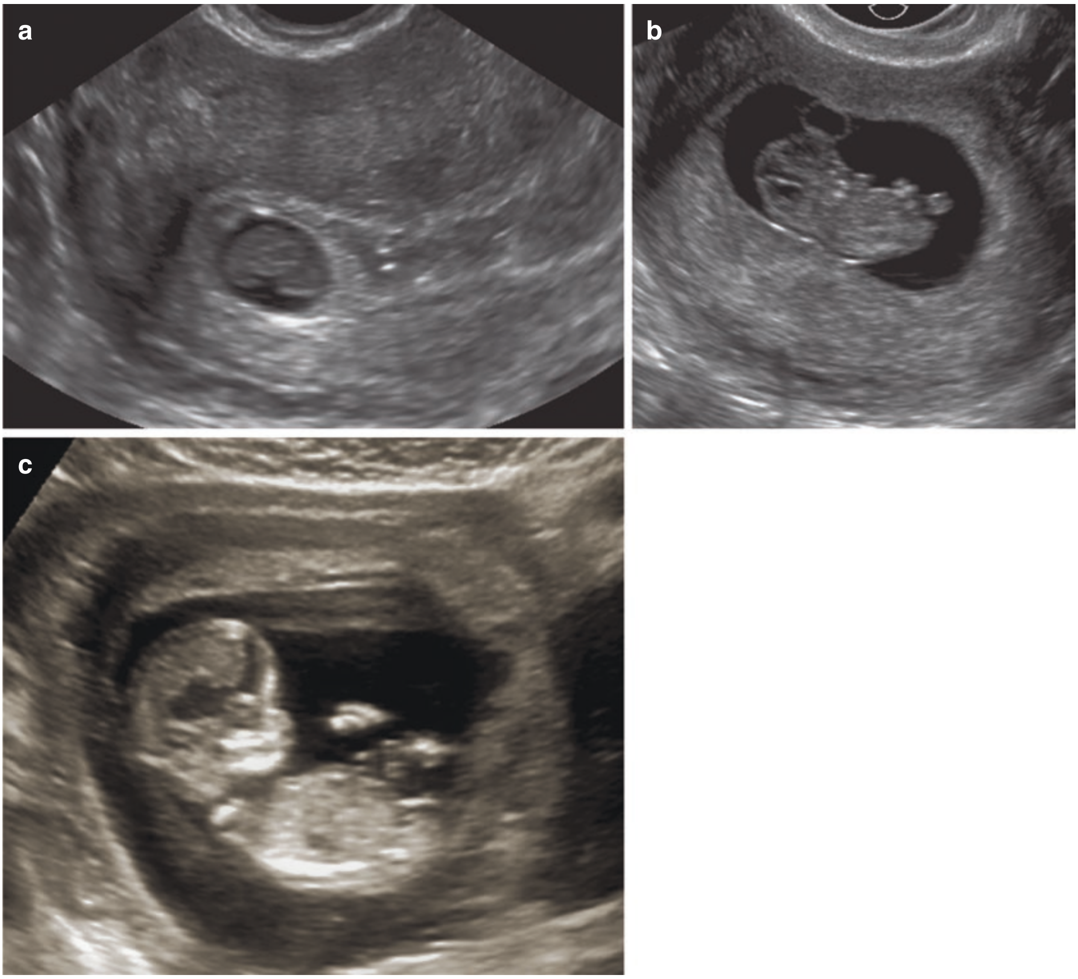

Fig. 8.4 First trimester oligohydramnios: (**a**) 7 weeks 4 days transvaginal image showing small sac size (MSD 12.4 mm) for CRL (8.1 mm) in keeping with "first-trimester oligohydramnios." (**b**) 8 weeks 1 day transvaginal follow-up scan shows live embryo with persistent discordant GS size. (**c**) 12 weeks 0 days transabdominal image shows live fetus with interval growth of both sac and fetus; however, sac continues to be small

pregnancy loss is that it may cause delayed diagnosis in patients who wish to have expedited treatment for various reasons. In such cases, it may be reasonable to apply a lower threshold such as a MSD ≥21 mm or CRL ≥6 mm when measurements are close to threshold and patients wish to proceed with urgent management. Detection of peritrophoblastic flow demonstrating high velocity and low impedance around the gestational sac is a normal finding that has been described as an aid in confirming a very early intrauterine pregnancy [30]. However, caution is recommended in the use of color and, particularly, spectral Doppler imaging in early pregnancy, due to increased power output and potential risk to developing pregnancy [9, 31].

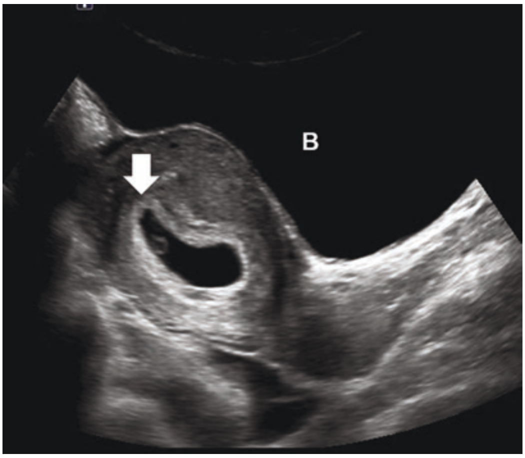

Fig. 8.5 Eccentric appearance of gestational sac: 6 weeks 2 days transabdominal sagittal image shows an intrauterine gestational sac with yolk sac confirming an intrauterine pregnancy. The superior aspect of the sac has a pointed appearance due to compression by the over-filled maternal bladder (B). This should not be presumed to be an abnormal finding or worrisome for a subsequent pregnancy loss

Gestational Sac Appearance and β-hCG in Early Pregnancy

A gestational sac is usually visible in an intrauterine pregnancy when the β-hCG level is between 1000 and 2000 mIU/mL [5]. Historically, much attention has been paid to the concept of a discriminatory β-hCG level above which an intrauterine gestational sac should always be seen in a normal IUP. This number was initially around 2000 mIU/mL; however, it is now recognized that there is considerable overlap of β-hCG levels in viable IUP, nonviable IUP, and ectopic pregnancy [32, 33]. Doubilet et al. have reported that, in rare instances, even with an absent gestational sac on transvaginal ultrasound and β-hCG level >4000 mIU/mL, follow-up ultrasound can show a normal pregnancy [32]. Practically speaking, it is unlikely to have a normal IUP develop when no gestational sac is seen with a β-hCG level >3000 mIU/mL. This can-

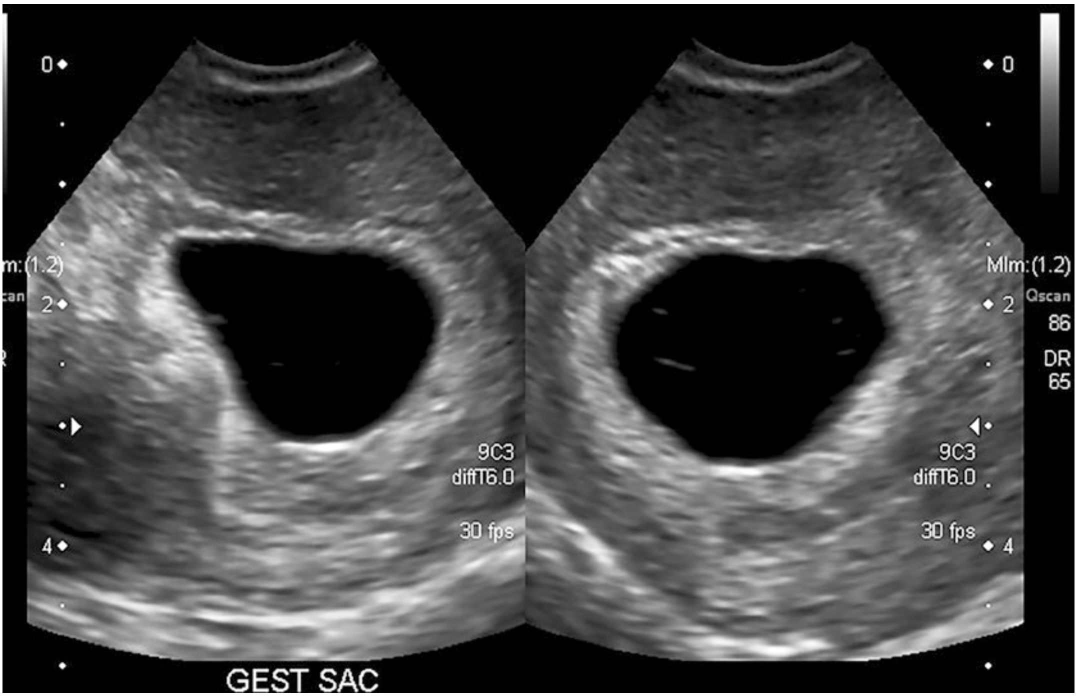

Fig. 8.6 Empty gestational sac: 7 weeks 0 days transvaginal sagittal and transverse images show an intrauterine gestational sac with MSD 19.5 mm. No yolk sac or fetal pole is identified. These findings are suspicious but not diagnostic for early pregnancy loss as the MSD is <25 mm. Findings should be reported as an early intrauterine pregnancy of unknown viability and follow-up scan performed

not, however, be considered diagnostic criteria for early pregnancy loss with 100% specificity. Consequently, the use of a single discriminatory β-hCG level to guide management in the setting of pregnancy of unknown location (PUL) is not recommended [32, 34]. There is emerging evidence that the incremental increase in serum β-hCG over 48 h, expressed as a ratio, may be a useful predictor of IUP when ultrasound findings are inconclusive [35–37]. β-hCG levels obtained 48 h apart should typically double, i.e., increase 100%. Various thresholds can be used to achieve greater diagnostic certainty with a rise of <67% predictive of an abnormal outcome with 95% certainty and a rise of ≤35% predictive of an abnormal pregnancy with 99.9% certainty [38–40]. Bignardi et al. [35] have reported that a β-hCG ratio >2.0 is suggestive of a viable IUP with sensitivity of 77%, specificity of 96%, and a positive predictive value of 87%. However, the use of β-hCG ratio as a predictor of viability in the setting of early pregnancy is not routine practice in all centers.

Yolk Sac

The appearance of the yolk sac provides the first *definitive* confirmation of an intrauterine pregnancy. **Although visualization of an intrauterine gestational sac with an echogenic rim is likely to represent an IUP, it is not as accurate at confirming an IUP as detection of the yolk sac.**

The yolk sac can first be visualized within the gestational sac at approximately 5.5 weeks gestation [1, 6, 9, 41] as a thin echogenic circular ring within the gestational sac on transvaginal scanning. It is usually visible by the time the MSD reaches 8 mm. If the yolk sac is not identified by this stage, a careful interrogation of the gestational sac with image optimization may assist in the ability to detect it. These may include narrowing the sector width, image zoom, appropriate placement of the focal zone, choice of a higher frequency, or other vendor specific post-processing settings (Fig. 8.7).

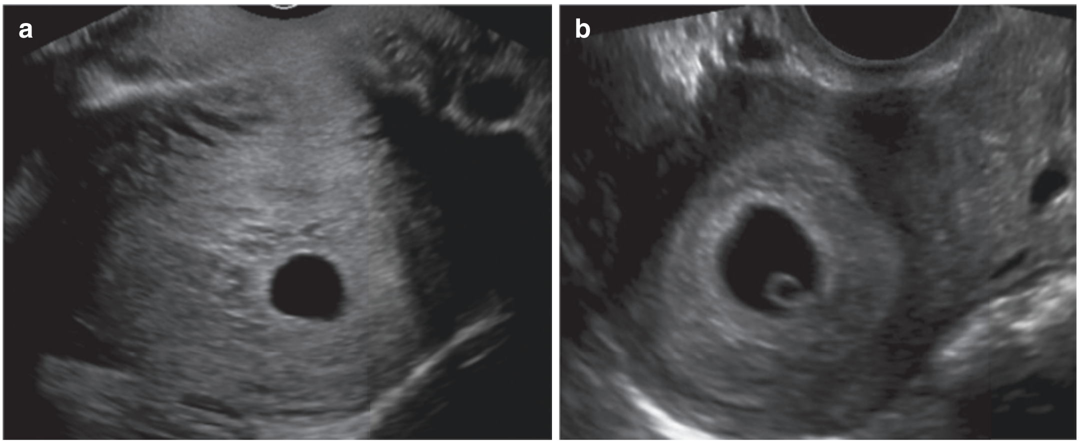

Fig. 8.7 Normal yolk sac: (**a**) 6 weeks 1 day transvaginal transverse images show an apparently empty gestational sac. (**b**) Same patient as above with transvaginal transverse image with narrow sector width is able to detect a circular echogenic ring representing the yolk sac thus confirming an early IUP. (**c**) 5 weeks 3 day transvaginal images show a very small circular echogenic ring (white arrow) within the gestational sac representing a normal yolk sac and confirming an IUP. This patient also has a small subchorionic hematoma at the posterior aspect of the gestational sac (white arrowhead)

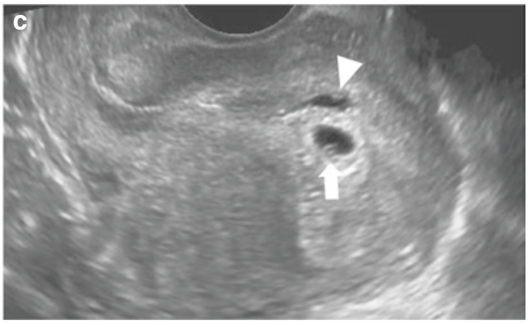

Fig. 8.7 (continued)

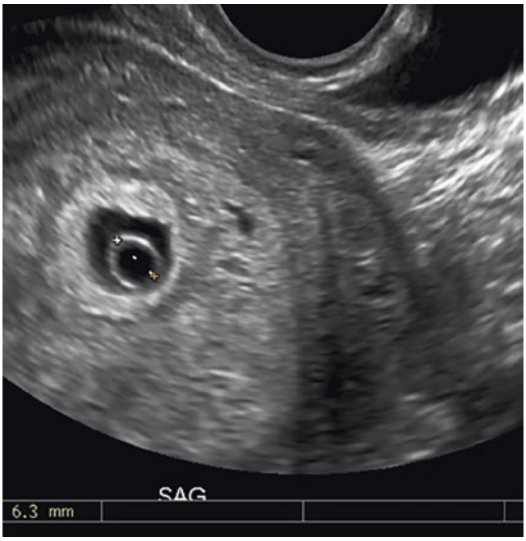

Fig. 8.8 Enlarged yolk sac: 5 weeks 6 days transvaginal sagittal image shows an enlarged yolk sac measuring 6 mm

Normal yolk sac measurement between 5 and 10 weeks GA is around 5 mm [9]. An enlarged yolk sac greater than 5 mm may be associated with poor pregnancy outcome. As an isolated finding, however, it cannot be considered definitely abnormal (Fig. 8.8) [42]. Typically, the yolk sac will gradually decrease in size after the 10th week of gestation and usually disappears by the end of the first trimester.

Embryo

The embryo is first visualized alongside the yolk sac at approximately 6 weeks gestation. Initially, it appears as a featureless linear echogenic structure without discernible limb buds and with no distinct cranial or caudal end (Fig. 8.9a). At this stage, a quantitative assessment of the embryo is achieved by obtaining the longest length measurement. Once the crown and rump are distinguishable, it is ideal to acquire the crown rump length (CRL) which is defined as the longest length excluding the limbs and yolk sac (Fig. 8.9b). The CRL can be measured on transabdominal or transvaginal. The ideal plane of measurement is midsagittal, with the embryo or fetus in a neutral position. Presence of fluid between the fetal chin and chest can be used as a sign to ensure that the fetus is not hyperflexed [2]. In practical terms, prior to 7 weeks gestation, measurement is actually of the longest length of the embryo that can be seen, but, after 7 weeks, a concerted effort should be made to measure the embryo in the midsagittal plane, excluding the yolk sac [43]). The smallest detectable embryo transvaginally has a CRL of 1–2 mm. Normograms are available to correlate CRL with gestational age [44–47]. A 2014 publication by Papageorghiou et al. established a CRL chart for pregnancy dating, based on a multi-center international trial, thereby providing an international standard for evaluating CRL linear growth in the first trimester [48].

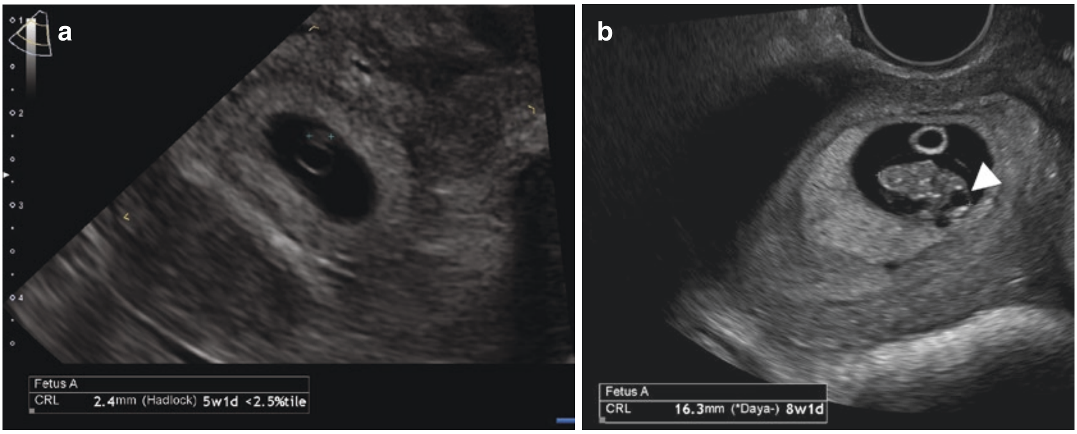

Fig. 8.9 Early embryo and crown rump length: (**a**) 5 weeks 1 day transvaginal image showing yolk sac and a 2 mm embryo. At this stage, the embryo has no discernible features and the longest length is measured to obtain the crown rump length (CRL). (**b**) 8 weeks 1 day transvaginal images showing a single embryo with CRL 16.3 mm. Note the clearly visible rhombencephalon (white arrowhead) identifying the fetal cranium as distinct from the caudal end. Calipers must be carefully placed to exclude yolk sac and flexed limbs

Embryonic and Fetal Cardiac Activity

Embryonic cardiac activity (ECA) is usually visible as soon as the embryo is detectable and can be seen with a CRL as small as 1 mm [5]. **Although ECA is virtually universally identified by CRL of 4–5 mm, the absence of ECA cannot be considered abnormal until the embryo reaches 7 mm** [25, 26]. This number is chosen to achieve as close to 100% specificity as possible for diagnosing early pregnancy loss based on absence of embryonic cardiac activity while taking into account the potential ±15% interobserver variability in CRL measurement [49].

Embryonic cardiac activity is documented using motion mode (M mode) to determine a heart rate (Fig. 8.10). ECA is considered normal if greater than 100 beats per minute (bpm). Doubilet et al. [50] suggested a lower limit of normal embryonic heart rate of 100 bpm up to 6.2 weeks gestation and 120 bpm between 6.3 and 7 weeks. Embryonic heart rates <100 bpm were thought to be associated with an increased risk of demise. In a 2018 meta-analysis on prediction of miscarriage in women with viable intrauterine pregnancy up to 15+6 weeks, fetal bradycardia had a sensitivity of 68% and specificity of 98% and likelihood ratio of 32 in predicting pregnancy loss [51]. Sensitivity and specificity greatly increased if vaginal bleeding was also present. In this study, a cut-off of ≤100 bpm showed the best predictive value for miscarriage. However, there is also data from a review of early first trimester pregnancies with slow embryonic heart rate revealing that this may not necessarily be a poor prognostic factor [50, 52, 53]. High embryonic heart rate in early pregnancy has been defined by Benson et al. [54] as >135 bpm before 6.3 weeks and >155 bpm between 6.3 and 7 weeks. This, generally has a good prognosis with high likelihood of normal outcome.

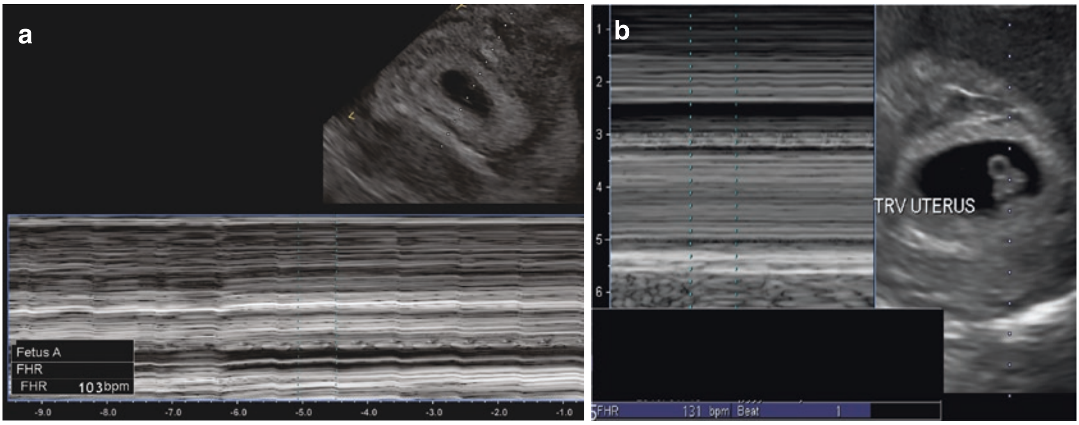

Fig. 8.10 M mode of embryonic cardiac activity: (**a**) 5 weeks 1 day transvaginal image showing embryonic cardiac activity detected with M mode in an embryo with CRL 2 mm. Note that even at this small size, ECA can be clearly demonstrated although its absence is not considered an abnormal finding until the embryo has reached a CRL of 7 mm. (**b**) 6 weeks 6 days transvaginal image where they embryo is more clearly visualized with FHR 131 bpm as detected with M mode

Multiple Gestations and Chorionicity[3]

Globally twins are approximately 1–3% of all pregnancies [55]. Twin rates have doubled between 1980 and 2009 from 18.9 to 33.2 per 1000 births [56]. In some areas of the US, the prevalence of multiple gestations is as high as 1 in 30 pregnancies. This is thought to be related to a combination of assisted reproductive technologies and increasing maternal age. Two-thirds of twin pregnancies are dizygotic, and one-third are monozygotic. The rate of intrapartum complications including pregnancy loss due to twin-twin transfusion syndrome or selective fetal growth restriction is far greater in monochorionic twins [57]. For optimal care, monochorionic pregnancies should be identified as early as possible to allow for closer surveillance and early detection of these conditions. **Assignment of chorionicity is therefore a mandatory and vital component of first trimester ultrasound with multiple gestations.** However, surprisingly in a review by Wan et al., only 44% of pregnancies referred to a tertiary care center had accurate diagnosis of amnionicity and chorionicity [58]. It is therefore important that practitioners be familiar with signs used to assess amnionicity and chorionicity in the first trimester.

The best time to determine chorionicity is prior to 14 weeks gestational age [57]. The classic features to determine a dichorionic gestation include two separate gestational sacs or placental masses, a thick inter-twin membrane in association with the lambda (λ) sign and different fetal genders. The λ sign refers to a triangular shaped projection of tissue which extends into the inter-twin membrane and is synonymous with the "twin-peak" sign (Fig. 8.11). With respect to triplet pregnancies, the upsilon zone representing the interface of the three amniotic membranes has been identified as useful to assign chorionicity in triplet pregnancies (Fig. 8.12) [59]. A recent study of 55 triplet pregnancies showed that the upsilon zone was identifiable in 95% of scans and demonstrated interobserver agreement of 100% [60].

Prior to 10 weeks the presence of two distinct, separated gestational sacs will confirm a dichorionic-diamniotic (DCDA) pregnancy. After 10 weeks, the most reliable signs for assessing chorionicity are a combination of placental number and the λ sign [57] given that gender cannot be reliably determined prior to 12 weeks. In a

---

[3] See also Chap. 14.

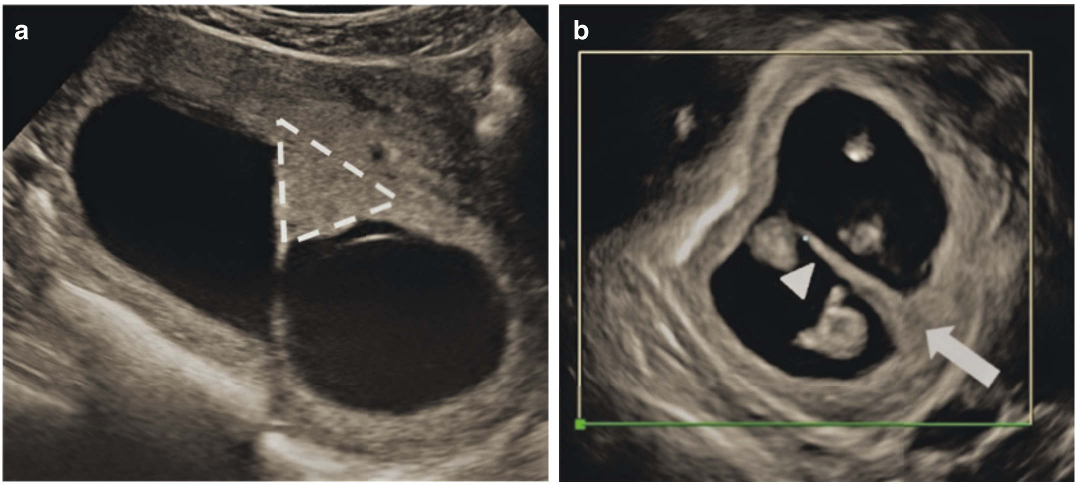

Fig. 8.11 Lambda sign in 11 weeks 3 days dichorionic twin gestation: (**a**) Transabdominal image showing triangular shaped tissue projecting into the inter-twin membrane (white outline) representing the lambda sign. (**b**) 3D representation showing the lambda sign (arrow) and thick inter-twin membrane (arrowhead)

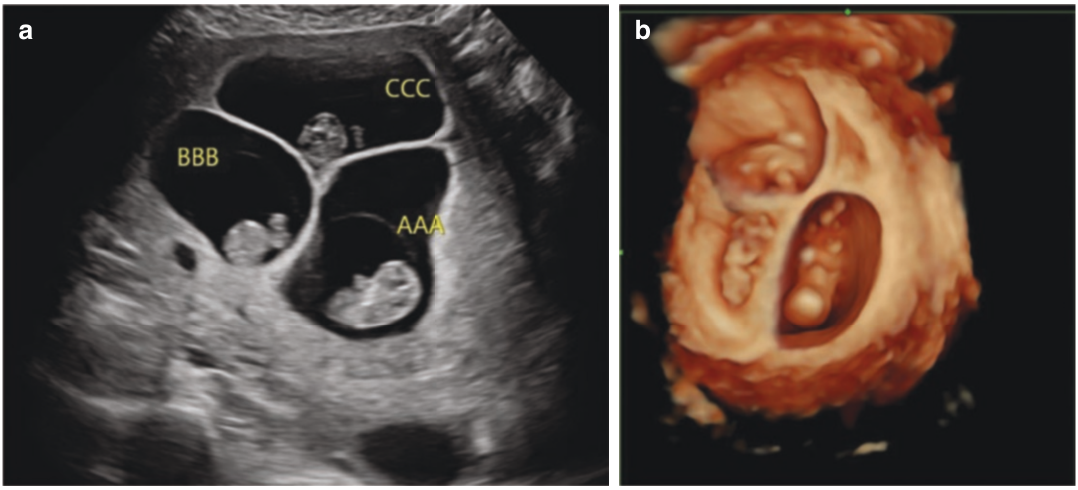

Fig. 8.12 Upsilon zone in triplet gestation 9 weeks 4 days: (**a**) Transabdominal images showing "upsilon zone" which demonstrates thick inter-fetal membranes and their intersections in a trichorionic triamniotic (TCTA) first trimester pregnancy. (**b**) 3D representation of upsilon zone showing thick inter-fetal membranes in a TCTA pregnancy at 9 weeks

study of 648 twin pregnancies, the number of placental masses and the presence of either the T or λ sign is virtually 100% accurate for determining chorionicity between 11 and 14 weeks [57]. A study by Bora et al. suggests that evaluation for chorionicity at 7–9 weeks had very high agreement with the 11–14 week scan and can be attempted; however, challenges were noted with respect to differentiating monochorionic monoamniotic pregnancies from monochorionic diamniotic pregnancies as the appearance of the inter-twin membrane may be delayed [61].

With respect to differentiating monoamniotic from diamniotic pregnancies, it is important to recognize that the temporal development of the yolk sac and the amnion is variable [62]. The appearance of the amniotic sac can be as late as 8–10 weeks with the thin membranes making it

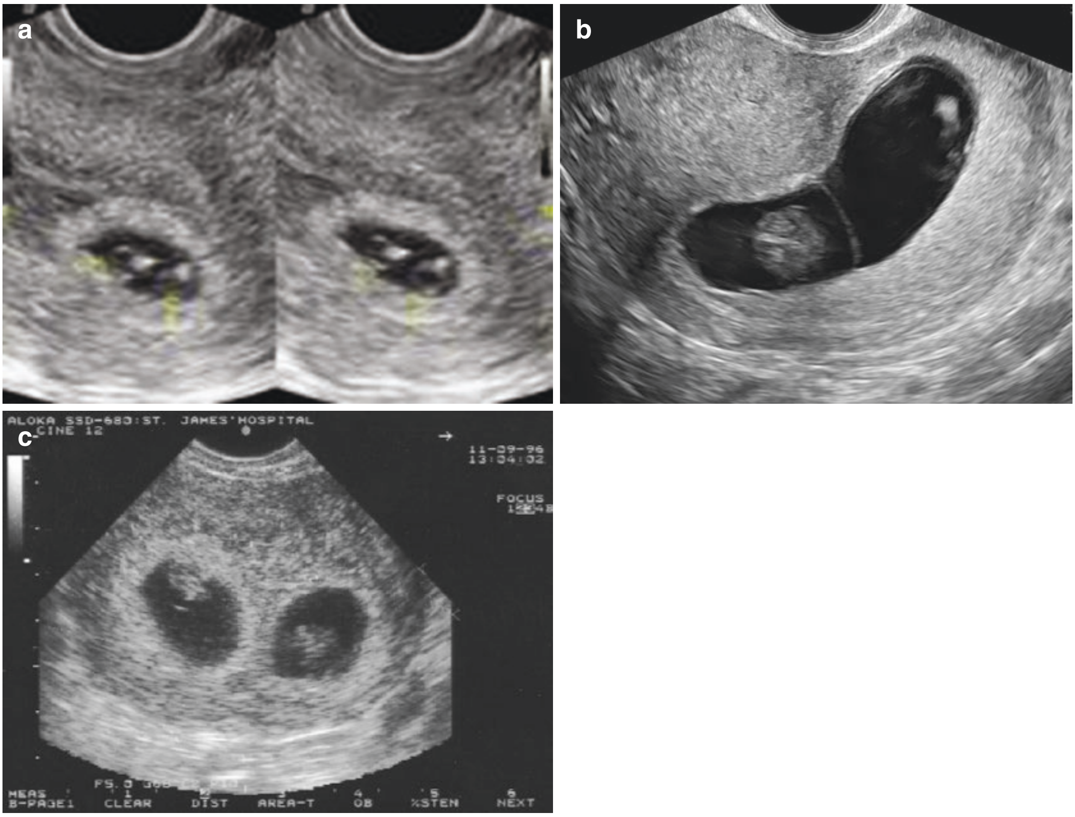

Fig. 8.13 Early monochorionic diamniotic twin pregnancy: (**a**) 8 weeks 0 days transvaginal transverse image showing two yolk sacs in keeping with twin gestation. No clear dividing membrane is seen. (**b**) Follow-up scan at 13 weeks showing thin inter-twin membrane and T-sign confirming monochorionic diamniotic twin pregnancy. (**c**) 3D representation of MCDA twins at 8 weeks

challenging to identify, even with the higher resolution of transvaginal ultrasound (Fig. 8.13). In the setting of multifetal pregnancies, the number of yolk sacs was previously thought to be a reliable way to assign amnionicity; however, it is less reliable than once presumed [62, 63]. While the presence of two yolk sacs is highly predictive of a diamniotic pregnancy and is seen in approximately 85% of monochorionic diamniotic (MCDA) twins, the presence of only one yolk sac can be seen with both monoamniotic and diamniotic twin pregnancies [62]. On rare occasion, a monochorionic monoamniotic twin pregnancy may present with two yolk sacs. If uncertain that a membrane is present separating the fetuses, it is prudent to repeat the test 1–2 weeks later. Alternatively, direct visualization of umbilical cord entanglement may provide early confirmation of the monoamniotic status of a twin gestation.

Heterotopic Pregnancy

Prior to the more widespread use of assisted reproductive techniques (ART), the presence of an intrauterine gestational sac with a yolk sac was felt to virtually exclude the diagnosis of ectopic pregnancy. Nonetheless, heterotopic pregnancy can occur where an ectopic pregnancy coincides with an otherwise normal IUP. The estimated incidence of this occurrence is between 1 in 8000 and 1 in 30,000 (Fig. 8.14) [64]. The incidence may be higher in gestations after

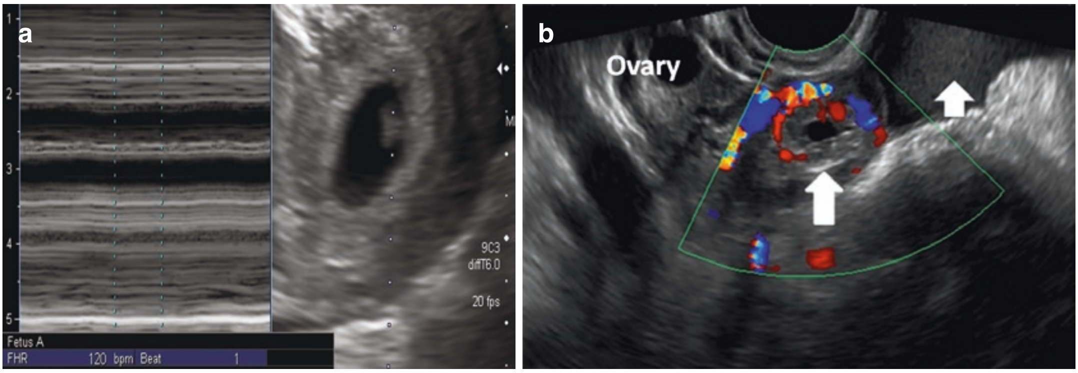

Fig. 8.14 Heterotopic pregnancy: (**a**) 6 weeks 5 days transvaginal image showing live intrauterine pregnancy. (**b**) Transvaginal sagittal image of right adnexa showing a hypoechoic mass (long arrow) with peripheral vascularity separate from the normal ovary with follicles which is seen at the upper margin of the image. Complex free fluid is seen in the pelvis (short arrow) representing hemorrhagic fluid

assisted fertility [65] and has been estimated as high as 1 in 100 in this population [45]. Thus, in patients who have undergone ART, despite the presence of an IUP, a thorough interrogation of the adnexae is recommended, to rule out a heterotopic pregnancy.

Early Pregnancy Dating

One of the indications of first trimester ultrasound is to confirm dating of pregnancy. Accurate pregnancy dating is critical to prenatal management for a variety of reasons including: to prevent preterm induction of supposed postdates pregnancies, to determine viability in the setting of premature delivery, to interpret growth patterns, to optimize prenatal screening for aneuploidy, and to appropriately time diagnostic interventions such as chorionic villus sampling and amniocentesis [66, 67]. Evidence has shown early ultrasound dating of pregnancy to be more accurate at predicting the expected due date than menstrual history [2, 68, 69]. Pregnancy dating is most accurate in the first trimester and can be determined using MSD, CRL, or fetal biometry. MSD can be used for dating when the embryo is not seen but shows greater variability in predicting GA compared to CRL [70] and should not be used when an embryo is visible. **The most accurate estimation of gestational age is achieved in the first trimester by using the CRL somewhere between 8 and 13+6 weeks [47, 67, 71, 72].** At earlier gestations, the relatively small size of the embryo may lead to more significant measurement error. The reported accuracy of the CRL measurement for dating is within 3–8 days [8], with the most accurate results reported when CRL measures [73] between 7 and 60 mm [46, 47, 71]. CRL continues to be the most reliable predictor of gestational age until 12–14 weeks, when CRL and biometry begin to achieve similar accuracy [74–77]. Based on current recommendations by the International Society of Ultrasound in Obstetrics and Gynecology (ISUOG), CRL is recommended for dating until the embryo measures 84 mm. Beyond 84 mm, the use of head circumference has been shown to be slightly more accurate than BPD [2]. Given the increased accuracy of ultrasound for pregnancy dating and the clinical importance of accurate dating, it has been suggested that a first trimester dating ultrasound be performed in all pregnancies [73, 78–81]. Dating of the pregnancy may be performed concurrently with the 11–14 week nuchal translucency scan.

Thresholds for Assessing Viability

The criteria for assessing viability of pregnancy early in the first trimester including thresholds for establishing a sonographic diagnosis of early pregnancy loss will be discussed further in a separate. These values have been chosen to include almost all normal pregnancies in an effort to "do no harm" and prevent the small risk of erroneously reporting early pregnancy loss in the setting of a viable pregnancy.

The criteria, which are based on transvaginal ultrasound assessment, have increased the thresholds at which nonvisualization of ECA and embryonic structures may be considered normal and are summarized as follows:

- Absence of cardiac activity in an embryo <7 mm _may be normal_.
- Absence of an embryo with a MSD < 25 mm _may be normal_.

Follow-up in 1 week's time is recommended in the above two scenarios.

Nuchal Translucency Evaluation[4]

Assessment of nuchal translucency is routinely offered in many countries, including the United States, as a component of prenatal screening and when combined with maternal age and maternal serum biochemistry (β-hCG and pregnancy associated plasma protein-A [PAPP-A]) can be an effective method of screening for chromosomal abnormalities [82]. Even in the setting of a normal noninvasive cell-free DNA test for aneuploidy, 11 to 13+6 week ultrasound including nuchal translucency assessment is recommended to assess for structural anomalies which may not be associated with a detectable chromosomal abnormality [83]. Nuchal translucency (NT) refers to the sonolucent area posterior to the fetal neck. For the purpose of prenatal screening, the NT should be assessed between 11 and 13+6 weeks gestational age, when the embryo measures between 45 and 84 mm by transabdominal ultrasound technique. The NT should be seen transabdominally in about 80% of cases [82]. Transvaginal assessment of the NT can be attempted if visualization is inadequate by transabdominal approach; however, it is more challenging due to limited ability to maneuver the probe to obtain a true midline sagittal image. If the NT is not adequately seen transabdominally, our routine is to either bring the patient back later the same day or on a subsequent day, rather than perform a transvaginal study. However, many centers will prefer to proceed to a transvaginal examination immediately following an unsuccessful transabdominal NT evaluation.

Criteria for NT Measurement

Accurate measurement of nuchal translucency is required to optimize results of screening tests. Both the American Institute of Ultrasound in Medicine (AIUM) and ISUOG have published guidelines outlining proper technique for NT measurement [2, 6]. The NT should be evaluated in the midsagittal plane of the face, defined by visualization of the echogenic tip of the nose and rectangular shape of the palate [2]. The fetus should be in a neutral position, neither hyperflexed nor extended. The image should be magnified, such that the fetal head and upper thorax fill the screen. Margins of the NT edges must be clear enough for proper placement of calipers which should be placed directly on the edges of the NT. Equipment used should allow for precise measurement up to 0.1 mm. The amnion should be seen as a separate echogenic line from the NT (Fig. 8.15). The NT should be measured at the

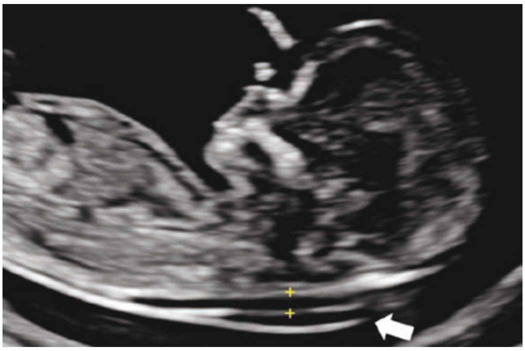

Fig. 8.15 Nuchal translucency at 12 weeks 6 days: transabdominal sagittal midline image showing normal nuchal translucency (between yellow calipers). The thin echogenic line of the amnion can be seen as separate from the NT

widest space and, if multiple measurements meeting the criteria are obtained, the largest measurement should be used for risk assessment. It is important that individuals who perform a NT evaluation have undergone training and are associated with an appropriate quality assurance program.

---

[4] See also Chaps. 8 and 9.

Significance of Elevated NT Measurement

Normal nuchal translucency is defined as a measurement less than 3 mm, if the 95th percentile is used or 3.5 mm, if the 99th percentile is chosen [82]. Nuchal translucency increases with increasing gestational age, and higher measurements are associated with greater risk of abnormality [84]. When combined with maternal age and serology (including PAPP-A and maternal serum β-hCG), NT thickness successfully identified 89% of fetuses with trisomy 21, with a false positive rate of 5% [82]. Elevated nuchal translucency can also be associated with other chromosomal abnormalities, including trisomy 13, 18 and Turner's syndrome [82]. Even in normal karyotype fetuses, an elevated NT confers a greater risk of fetal structural anomalies, most commonly congenital heart anomalies [85]. The prevalence of congenital heart disease with an NT >95th percentile is 1/48 and is 1/19 with NT >99th percentile [85]. A meta-analysis of 2271 singleton euploid fetuses, with NT >3 mm at 10–14 weeks, reported structural anomalies in 10.6% and genetic syndromes and single-gene disorders in 15% [86]. The prevalence of abnormal outcome was shown to increase with increasing NT measurements.

It is important to note, however, when counselling patients, that not all elevated NT pregnancies are necessarily associated with congenital or structural anomalies. In one report, 90% of pregnancies with NT measurement below 4.5 mm and normal karyotype resulted in healthy live births [82]. Normal outcome was seen in 80% of pregnancies with NT between 4.5 and 6.4 mm and 45% of pregnancies with NT greater than 6.5 mm [87]. In the previously described meta-analysis evaluating outcome of elevated NT above 3 mm, chromosomally normal fetuses had a 68% overall chance of normal outcome. Long-term neurodevelopmental outcomes have also been evaluated in children who had an increased fetal NT and normal karyotype. In a systematic review of 17 studies and 2458 patients, there was no significant difference in the rate of neurodevelopmental delay in this group, when compared to the general population. Nonetheless, further large-scale prospective studies are needed to predict neurodevelopmental outcome in this population with greater certainty [88].

Recommendations in the setting of increased NT include detailed early anatomic assessment to look for structural anomalies, fetal echocardiography, and discussion regarding cell-free DNA analysis and/or invasive diagnostic testing such as chorionic villus sampling and amniocentesis.

Assessment of the Nasal Bone During the NT Evaluation

Evaluation for presence or absence of the nasal bone can be performed at the time of NT scan [82, 89, 90]. Nasal bone ossification first becomes apparent at a crown rump length of approximately 42 mm [90] or 11 weeks gestation and nasal bone length progressively increases with gestation. Assessment for presence of the nasal bone is performed in the midsagittal plane and, as for NT measurement, requires strict adherence to proper technique and operator experience to be reliable. The nasal bone appears as an echogenic line parallel to and thicker than the echogenic skin line overlying the nasal bridge. It is best seen when the footplate of the transducer is parallel to the long axis of the nasal bone. The two parallel lines of the nasal bone and skin line comprise the "equal sign" (Fig. 8.16). The nasal bone is considered absent if the deeper line is not present. Nasal bone assessment appears to be more difficult than NT assessment. Nevertheless, there are reports that, with adequate training and experience, assessment for presence or absence of nasal bone can be performed with success in up to 99% of fetuses [91].

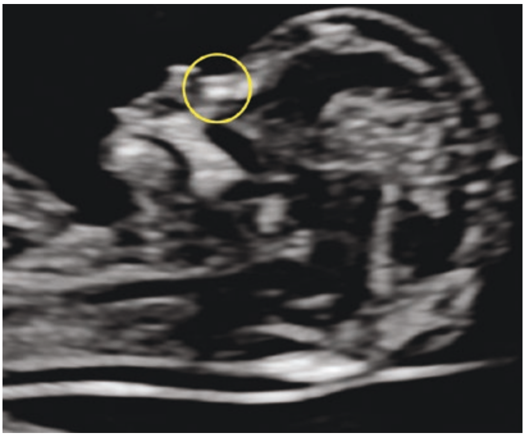

Fig. 8.16 Nasal bone at 12 weeks 5 days. Transabdominal sagittal midline image shows the nasal bone as an echogenic line posterior to the skin line resulting in two parallel echogenic lines often referred to as the "equal sign" (yellow circle)

Significance of Absent Nasal Bone

As mentioned, an absent nasal bone is seen more frequently in trisomy 21 as compared to the general population. In a study of over 21,000 fetuses between 11 and 14 weeks, absence of the nasal bone was noted in 62% of fetuses with trisomy 21 as compared to 0.6% of unaffected fetuses [91]. Absence of nasal bone has been shown to be an independent finding with respect to serum β-hCG and PAPP-A and can, therefore, be added to routine combined prenatal screening for trisomy 21 [90]. When combined with routine NT screening and serum β-hCG and PAPP-A, addition of nasal bone presence may decrease the false positive rate for trisomy 21 from 5% to 2.5% [90]. Absence of the nasal bone has also been reported in approximately 55% of fetuses with trisomy 18, 35% of trisomy 13, and 10% of Turner's syndrome [92].

However, it is important to be aware that an absent or hypoplastic nasal bone does not necessarily imply pathology and can be a normal variant. The prevalence of absent nasal bone decreases with gestational age and absence of the nasal bone prior to a crown rump length of 42 mm should not be considered abnormal. If there is question of nasal bone absence between 11 and 12 weeks, a repeat scan can be obtained to ensure that lack of visualization represents true absence, as opposed to late ossification. Additionally, there is ethnic variation in presence and size of the nasal bone, and an absent nasal bone may be more prevalent in certain ethnic groups, particularly African and Asian populations. A prospective study of nearly 4000 fetuses reported prevalence of absent nasal bone to be 5.8% in patients of African origin, 3.4% in patients of Asian origin, and 2.6% in patients of Caucasian origin [93].

In some instances, the nasal bone may be present but seen to be shortened or hypoplastic. Nasal bone length has not been shown to be a useful first trimester measurement for screening of trisomy 21 [90].

Screening for Neural Tube Defects at the Time of the NT Evaluation

Neural tube defect with open spina bifida is a relatively uncommon condition affecting approximately 1 in 2000 fetuses [94]. Traditionally open spina bifida was diagnosed via a combination of alpha-fetoprotein from maternal serum or amniocentesis and second trimester ultrasound evaluations. With the move to first trimester screening and earlier anatomic ultrasound evaluations, a number of investigators have proposed parameters to assess for these conditions in the first trimester.

Open spina bifida may be accompanied by sonographically visible changes in the posterior fossa at the time of the NT evaluation [95–97]. In these cases, the combination of CSF leakage with a gradual shift of the brainstem toward the occipital bone may result in obliteration of the intracranial translucency or developing fourth ventricle and thickening of the brainstem as it prolapses caudally.

The developing fourth ventricle can be identified as an intracranial translucency (IT) or fluid containing space which is parallel to the nuchal translucency in the midsagittal plane at 11–14 weeks. The IT borders are defined anteriorly by the posterior border of the brain stem and posteriorly by the anterior border choroid plexus

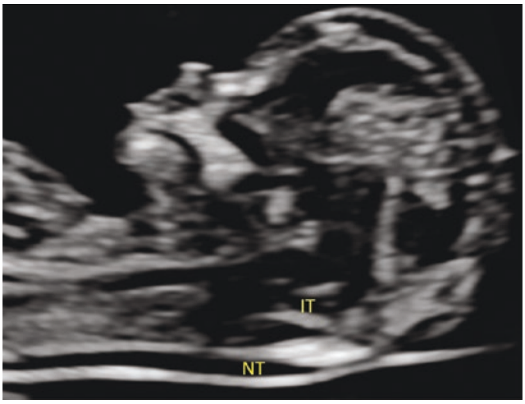

Fig. 8.17 Intracranial translucency 12 weeks 6 days. Transabdominal image showing normal intracranial translucency (IT) anterior to the nuchal transluency (NT). The anterior border of the IT is the brainstem and the posterior border is the choroid plexus

(Fig. 8.17). The IT may be absent in cases of open spina bifida and can be assessed between 11 and 14 weeks at the time of NT screening. Initially, it was felt that IT evaluation would be a simple addition to routine NT evaluation given that the structures to be evaluated are in the same plane. However, on further evaluation, IT measurement may be more technically challenging than previously thought [98]. It is currently not routine practice in all centers [95–97].

Measurement of the thickness of the brainstem (BS) and the vertical distance between the brainstem anteriorly and occipital bone posteriorly (BSOB) can be obtained between 11 and 14 weeks using the same imaging plane at the NT evaluation (Fig. 8.18). The ratio of the BS/BSOB can be evaluated and is ≤1 in normal fetuses [97]. In cases of open spina bifida, the BS diameter is greater (>95th percentile) and the BSOB is decreased (<5th percentile) resulting in an increased BS/BSOB ratio >1 [97, 99]. This is related to the cerebrospinal fluid leakage and development of the Arnold-Chiari II malformation, with a gradual shift of the posterior brain toward the occipital bone. Several studies [95–97] have showed that evaluation of the posterior fossa may be a useful marker for open spina bifida in the first trimester. It is recommended that a targeted ultrasound of the fetus spine, with transvaginal technique, be performed in order to evaluate directly for open spina bifida, in particular when the IT, BS-BSOB ratio, or BPD findings are suspicious or abnormal. This is not yet, however, routine practice.

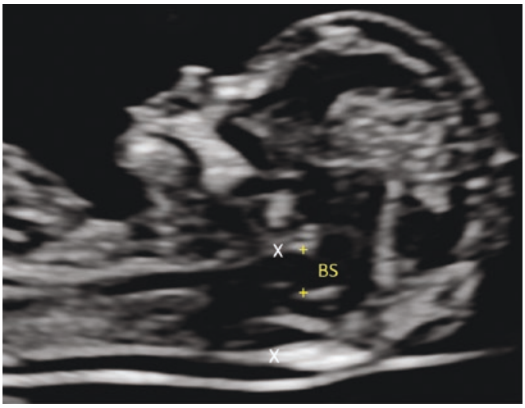

Fig. 8.18 Brainstem to brainstem-occipital bone ratio 12 weeks 6 days. Transabdominal image showing measurement of the brainstem (yellows calipers) and the brainstem to occipital bone distance (white x). Although the brainstem and brainstem to occipital bone measurements are obtained in the same plane as the nuchal translucency, it is not routine practice to measure these structures in all fetuses

These posterior fossa measurements have proven to be challenging and require a high degree of expertise to perform. As such, more recently simpler methods have been described to assist with this challenging diagnosis. Firstly, it has been demonstrated that the BPD will measure below the 5th percentile in fetuses affected with open spina bifida [100] and may ultimately prove to be the simplest way to assess for coexistent posterior fossa abnormalities associated with the Arnold-Chiari malformation. There are also two new signs that have been described which are based on simple pattern recognition of the effects of CSF leakage via an open spine bifida which are visible in the axial plane without requiring specific measurements. The “dry brain” size which compared the size of the choroid plexus to the fetal head is measured in the same plane as the BPD [101]. The “crash sign” represents posterior displacement of the mesencephalon which is compressed against the occipital bone in the axial view, likened to the appearance of a car crashing into a wall [102].

Normal First Trimester Anatomical Assessment

Formation of most major internal and external organs is complete by the end of the 10th week of gestation during the stage of pregnancy commonly referred to as organogenesis. Assessment of fetal anatomy can, therefore, be performed in the first trimester, provided that the fetus is large enough to allow visualization of structures with sufficient resolution for diagnostic evaluation, and that organ development be advanced enough that normal developmental stages can be differentiated from pathology. The performance of a first trimester anatomy scan has become more mainstream practice in many centers, as new high-frequency transducers, as well as increased use and patient acceptability of transvaginal scanning have enabled better visualization of smaller fetal structures, at earlier gestational ages. It is important, however, to be aware that first trimester anatomy evaluation is a specialized examination that requires an in-depth understanding of embryology and a high level of technical expertise, particularly with transvaginal techniques and unique scan planes that may be required to visualize some structures. Advantages of first trimester anatomy assessment include earlier detection of anomalies, earlier patient reassurance in high-risk settings with normal anatomy, and potential for better visualization in certain populations, specifically maternal obesity and patients with abdominal scar tissue from prior surgeries. Some disadvantages include increased cost to the medical system, potential to misdiagnose normal developmental structures for pathology, and potential to miss diagnoses that do not present until later in pregnancy. Evaluation of first trimester transvaginal anatomy is generally reserved for high-risk women, including those with elevated NT, inherited conditions associated with fetal anomalies, previous pregnancy with an anomaly, and maternal hazardous exposure or infection.

Several studies have investigated the feasibility and detection rates of performing first trimester anatomy for anomalies [103–105]. Braithwaite et al. [105] reported that complete first trimester anatomic survey was attainable in 95% of fetuses with transvaginal scanning only required in 20%. A subsequent study of 2876 patients by Ebrashy et al. [106] reported that a complete anatomical survey was obtained in 64% of patients using transabdominal approach only and in 82% using combination of transabdominal and transvaginal scanning. In their study, transvaginal images were particularly useful to evaluate the cranium, spine, stomach, kidneys, bladder, upper and lower extremities. They reported highest rates of nonvisualization for fetal heart and kidneys. Whitlow and Economides found that visualization of first trimester anatomy improved with increasing gestational age and reported 98% visualization at 13 weeks [107]. Monteagudo and Timor-Trisch [108] also support that visualization of first trimester anatomy, while possible at 12 weeks, is optimally performed closer to 13 weeks.

Detection rate of anomalies at first trimester scanning between 11 and 14 weeks has been reported as between 18% and 68% [106, 109]. In a 2014 retrospective cohort of 9692 nuchal translucency scans performed without a dedicated anatomical survey protocol, 41% of major anomalies confirmed on second trimester scan were diagnosed at the time of the first trimester NT scan [110]. A similar detection rate of 45% was found in a 2018 study of 5534 women including 297 at higher risk for a fetal anomaly [109]. In a prospective study of over 100,000 singleton pregnancies, 28% of all anomalies were detected. In this study, anomalies were categorized into those always detectable, those sometimes detectable and those never detectable [111]. This study highlighted an important consideration that the overall detection rate of anomalies in the first trimester may be less relevant than the detection rate specifically for those anomalies that *can* be diagnosed at an earlier gestation, as some anomalies may not develop or be detectable until later in gestation and thus are never detectable at early scan. It is important to note that performing a complete first trimester anatomical survey does not obviate the need for routine anatomical assessment at the 18–22 week stage to assess for such conditions. A systematic approach should be used keeping in mind that some structures seen at the 18–22 scan may not be fully developed in the first trimester. Various protocols have been suggested with respect to what should be included in first trimester anatomy assessment [112]. In one of the largest prospective studies, including over 45,000 NT evaluations, Syngelaki et al. concluded that certain abnormalities should always be detected during this time period. Specifically they recommended the following conditions should not be missed during a routine NT evaluation: acrania or exencephaly; alobar holoprosencephaly; omphalocele; gastroschisis; megacystis; and body stalk anomaly [113].

In 2013, ISUOG published practice guidelines for first trimester stating that the purpose of the study also includes the detection of gross fetal malformations [72]. The 2013 guidelines from the AIUM state "embryonic/fetal anatomy appropriate for the first trimester should be assessed" [6]. As the 11–14 week ultrasound becomes routine practice in more and more centers, it will become more important for ultrasound practitioners to familiarize themselves with the normal embryology and development of the fetus in the first trimester in order to distinguish normal anatomy from pathology at progressive gestational ages.

Fetal Brain in the First Trimester

Early brain development begins in the 6th week of gestation before formation of the neural tube, with division of the neural groove into three distinct parts: the prosencephalon or *forebrain*, the mesencephalon or *midbrain,* and the rhombencephalon or *hindbrain*. One of the earliest structures to be visualized, at around 7 weeks, is the rhombencephalon. This appears as a cystic area in the posterior brain which should not be mistaken for pathology such as a posterior fossa cyst (Fig. 8.19). At 8–9 weeks gestation, the choroid plexus begins to develop, initially in the fourth ventricle and, subsequently, in the lateral ventricles. At this stage, the cerebral hemispheres can be delineated, as well as the diencephalon and rhombencephalon. The telencephalon and diencephalon are divisions of the forebrain and give rise to the lateral ventricles and third ventricle, respectively. The metencephalon and myelencephalon are formed from the rhombencephalon. With new high-frequency 2D and 3D transvaginal technology, detailed images of the developing fetal brain and ventricular system can be obtained in the first trimester including images depicting the primary brain structures including the telencephalon, diencephalon, mesencephalon, metencephalon, and myelencephalon (Fig. 8.20). The lateral ventricles initially appear as small cystic structures and become more identifiable toward the end of the first trimester, when they are filled by the echogenic choroid plexuses. At 9–10 weeks of gestation, the falx cerebri first becomes apparent and cranial ossification begins. These structures are more readily identifiable, however, closer to 11 weeks gestation and are important landmarks to identify, in order to exclude early diagnosis of anencephaly and alobar holoprosencephaly (Fig. 8.21). Cranial ossification should be seen by the end of the 11th week. It is best visualized in the axial and coronal planes in the frontal region, and may not be visible in the midsagittal plane, typically used for NT assessment (Fig. 8.22).

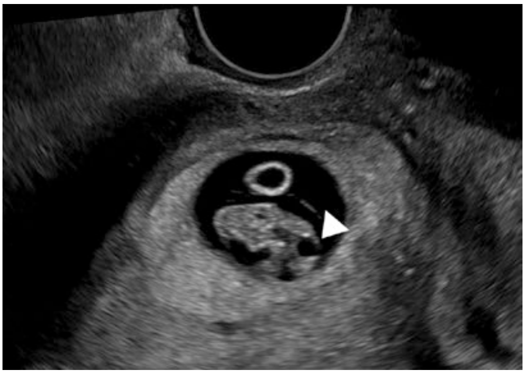

Fig. 8.19 Rhombencephalon 8 week 1 day transvaginal transverse images showing embryo with cystic rhombencephalon in the posterior head (arrowhead). This is a normal findings and should not be mistaken for a pathologic entity such as a posterior fossa cyst or hydrocephalus

The cerebral hemispheres are symmetrical, separated by the interhemispheric fissure and the falx cerebri. The fetal brain has a smooth appearance at this gestation, with sulci and gyri devel-

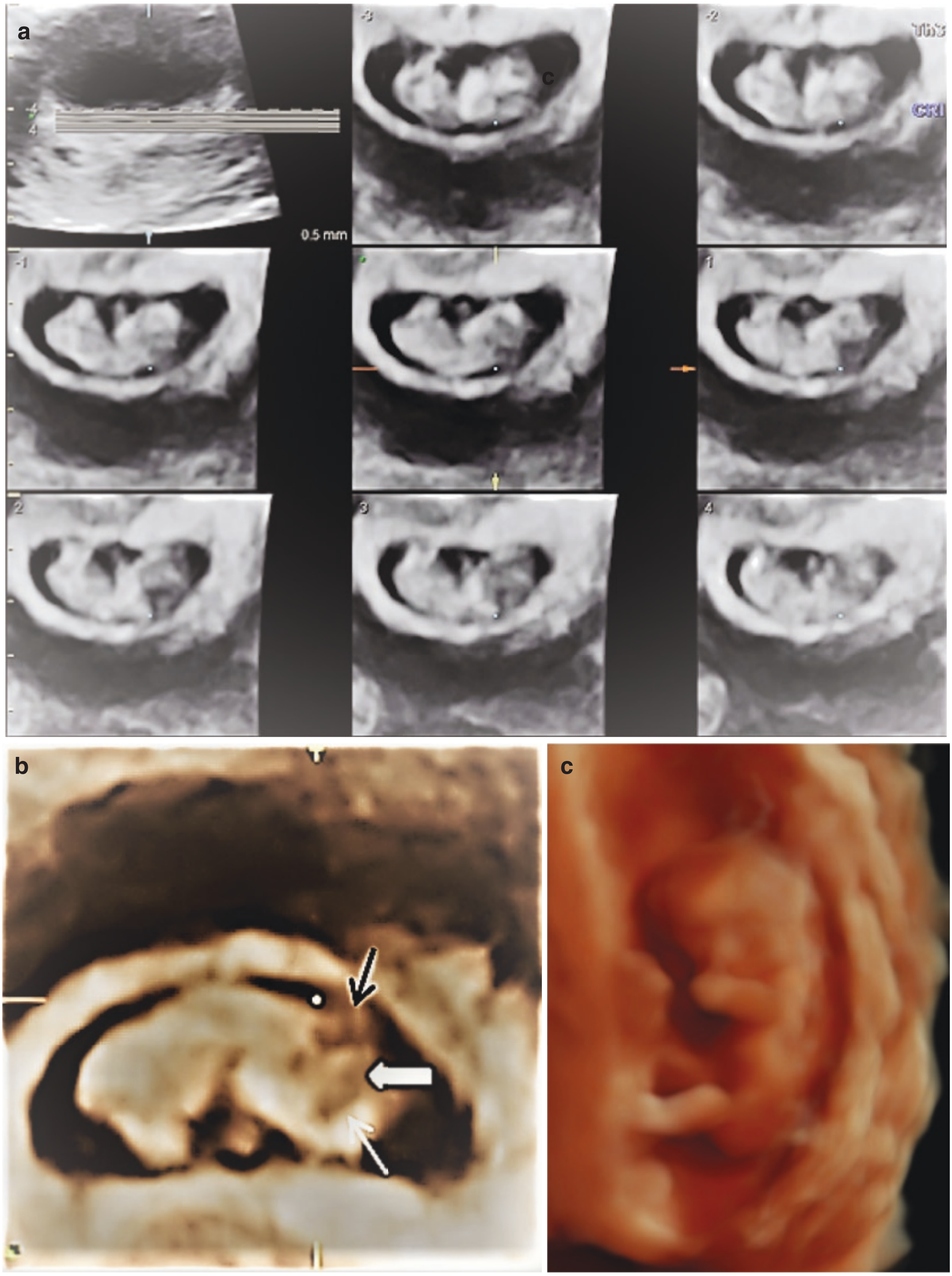

Fig. 8.20 3D Brain at 9 weeks 4 days transabdominal 3D images showing: (**a**) Serial slicing technique through the 3D volume of the embryo. (**b**) Selected 3D sliced image showing early cystic spaces in the cranium representing the developing diencephalon (thin white arrow), mesencephalon (thick white arrow), and metencephalon/myelencephalon (black arrow). (**c**) 3D surface rendered image of the embryo

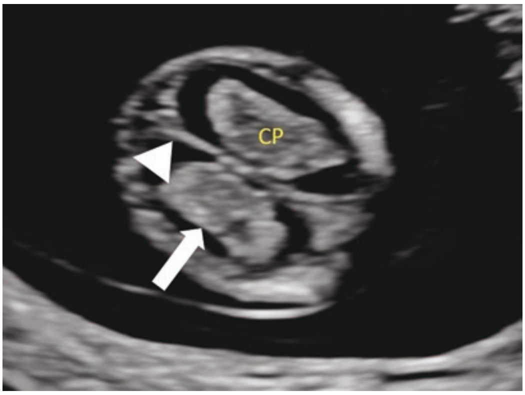

Fig. 8.21 Normal choroid plexus and falx at 12 weeks 6 days on transabdominal images of the fetal head showing bilateral symmetrical echogenic choroid plexuses (CP) which fill the lateral ventricles. White arrow denotes border of the lateral ventricle. The falx cerebri (white arrowhead) divides the cranium at the level of the choroid plexus resulting in a symmetric appearance of the brain

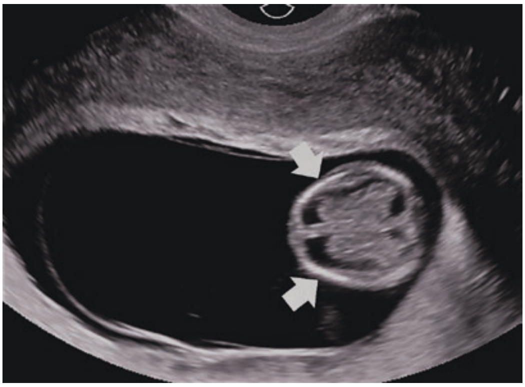

Fig. 8.22 Cranial bone ossification at 12 weeks 3 days transvaginal image of the fetal head shows bilateral normal frontal bone ossification (white arrows)

oping later in the second and third trimester. The cerebral mantle is a thin rim of tissue, seen around the hypoechoic, large lateral ventricles, filled with choroid plexus and occupying most of the cranium at this stage. The posterior fossa structures are not fully developed by the end of the first trimester. The cerebellum and upper vermis can be seen, but the lower vermis is incomplete and persistent communication between the fourth ventricle and cisterna magna is a normal finding at this stage (Fig. 8.23). Structures such as the cavum septum pellucidum and corpus callosum are not yet developed and should be re-assessed at a later point in the pregnancy.

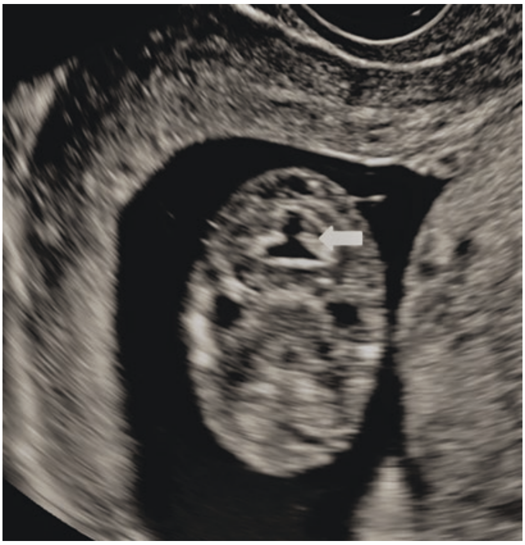

Fig. 8.23 Posterior fossa at 12 weeks 3 days transvaginal image showing normal communication of the fourth ventricle and cisterna magna (white arrow) due to incomplete development of the cerebellar vermis

Face

Structures that can be assessed include the orbits, lens, profile, and nasal bone (Fig. 8.24). The soft tissue structures of the nose and lips are more challenging. Nevertheless, the diagnosis of cleft lip/palate, in particular when bilateral, can be made at this time. Examination in the coronal plane of the retronasal triangle (Fig. 8.25), formed by the two front processes of the maxilla and the primary palate, has been described as a potential way to facilitate detection of cleft palate in the first trimester [114].

Thorax

The lungs appear as echogenic structures in the developing thoracic cavity and should be symmetric. The diaphragm (black arrow) can be seen as an intact structure separating the echogenic lungs from intra-abdominal contents, specifically the stomach and liver (Fig. 8.26).

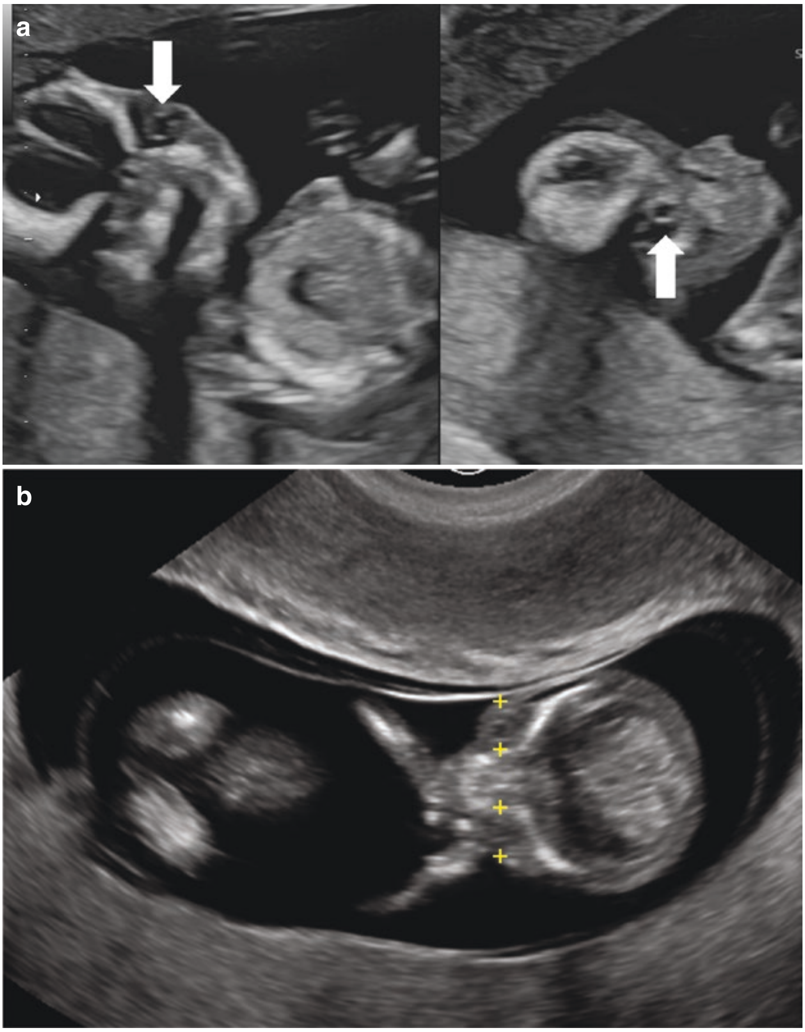

Fig. 8.24 Normal orbits and lenses: (**a**) At 13 weeks 4 days transabdominal image showing fetal lenses. (**b**) At 12 weeks 3 days transvaginal semi-coronal image showing normal inter-orbital distance (yellow calipers)

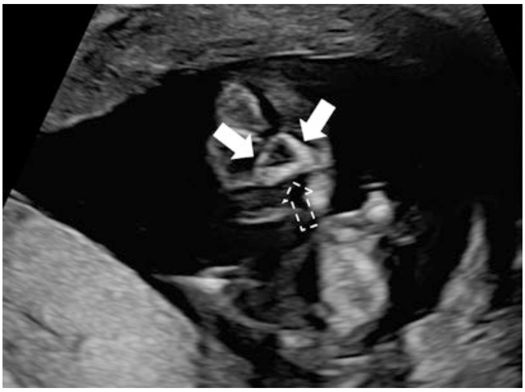

Fig. 8.25 Retronasal triangle at 13 weeks 4 days. Transabdominal coronal image showing the complete retronasal triangle comprised of the two frontal processes of the maxilla (solid white arrows) and the primary palate inferiorly (dashed white arrow)

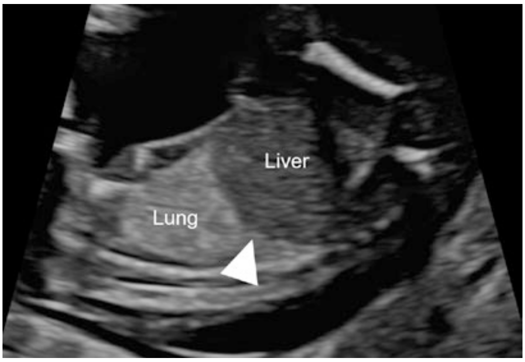

Fig. 8.26 Fetal chest and diaphragm at 13 weeks 1 day. Transabdominal image showing echogenic fetal lungs separated by intact diaphragm (white arrowhead) from the more hypoechoic liver inferiorly

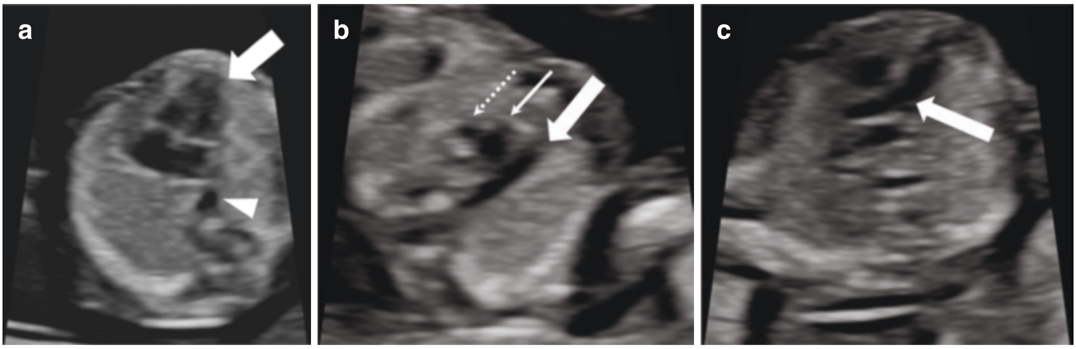

Fig. 8.27 Fetal heart at 13 weeks 4 days. Transabdominal axial images of the fetal chest showing: (**a**) Four-chamber view of the heart demonstrates symmetric cardiac chambers. The apex of the heart (arrow) and the aorta (arrowhead) are to the left of the fetal spine. (**b**) Right ventricular outflow tract (white arrow). Also shown are the aorta (thin white arrow) and SVC (white dashed arrow). (**c**) Left ventricular outflow tract (white arrow)

Fetal Heart in the First Trimester[5]

Development of the fetal heart begins during the 4th week of gestation and the beating heart can be detected sonographically as early as 5 weeks. Heart position can be documented to confirm situs solitus. Normal cardiac structures that can be identified during the first trimester include the four-chamber view which should show symmetry of the atria and ventricles with the cardiac apex directed to the left (Fig. 8.27a). While the four-chamber view may be seen in as many 85% of 11 week fetuses, it is visualized in almost all fetuses by the 13th week of gestation [115]. The cardiac outflow tracts are fully developed and may be visible toward the end of the first trimester (Fig. 8.27b, c), although assessment of these structures may be more technically challenging. There are several studies that now describe first trimester detection of cardiac anomalies as well as early fetal echocardiography [116]. In a systematic review and meta-analysis of first trimester detection of heart anomalies, 767/1445 (53%) of anomalies identified in low-risk patients were detected on first trimester scan [117]. At present, detailed fetal echocardiography is not routine practice in low risks patients. However, a simple screening tool that may be useful is evaluation of the cardiac axis. The cardiac axis can be measured on the four-chamber view of the fetal heart as the angle between a line transecting the thorax in anterior-posterior dimension and a line along the long axis of the heart with normal defined is between 30° and 60° (Fig. 8.28). In a case-control study of 197 fetuses with congenital heart defects, 2/3 of fetuses with cardiac anomalies had an abnormal cardiac axis in the first trimester [118]. While abnormal cardiac axis may not provide a spe-

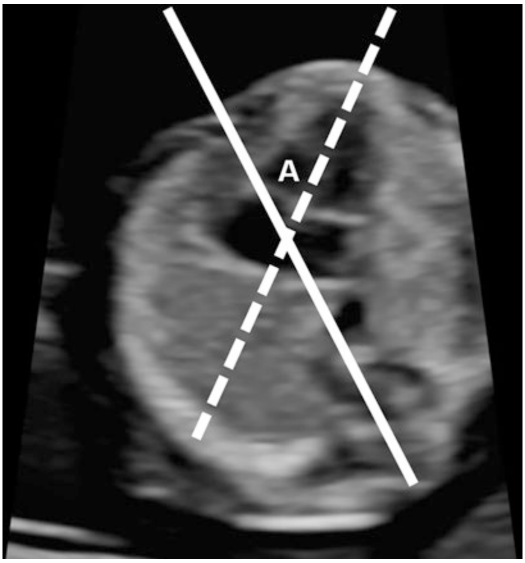

Fig. 8.28 Cardiac axis at 13 weeks 4 days. Transabdominal axial image of the fetal chest at the level of the four-chamber view. The cardiac axis is the angle (A) measured between a line bisecting the fetal chest in anterior-posterior dimension (solid line) and a line drawn along the inter-ventricular septum (dashed line)

cific diagnosis, this may be a useful screen to identify fetuses who may be at increased risk and require more careful evaluation.

---

[5] See also Chap. 11.

Fetal Kidneys and Urinary Tract System in the First Trimester

The fetal kidneys are sonographically detectable by the 9th week of gestation (Fig. 8.29). The fetal bladder is not reliably visualized until later in the first trimester at around 12 weeks (Fig. 8.30). By 13 weeks gestation, the bladder can be seen in up to 98% of cases and kidneys in up to 99% [119]. Documentation of these structures is important, as urine production does not begin until the 12th or 13th week, and secondary signs of renal agenesis or dysfunction, such as oligohydramnios, may not manifest until later in pregnancy after 16 weeks gestation.

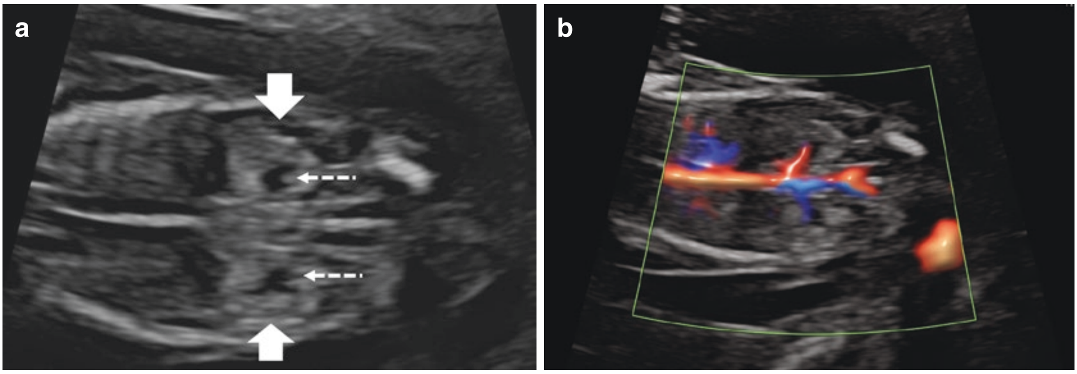

Fig. 8.29 Fetal kidneys at 13 weeks 1 day: (**a**) Transabdominal coronal image of the fetal abdomen demonstrates bilateral kidneys seen as echogenic ovoid structures in a paraspinal location (solid arrows) with central anechoic fluid within the renal pelvis (dashed arrow). The presence of fluid in the renal pelvis helps confirm the structure as a fetal kidney rather than collapsed bowel within the renal fossa. (**b**) Transabdominal coronal image with color Doppler demonstrating bilateral renal arteries arising from the aorta to supply the fetal kidneys

Fig. 8.30 Fetal bladder at 12 weeks 0 days. Transabdominal image showing fetal bladder (**b**) with 2 umbilical arteries coursing adjacent to bladder walls

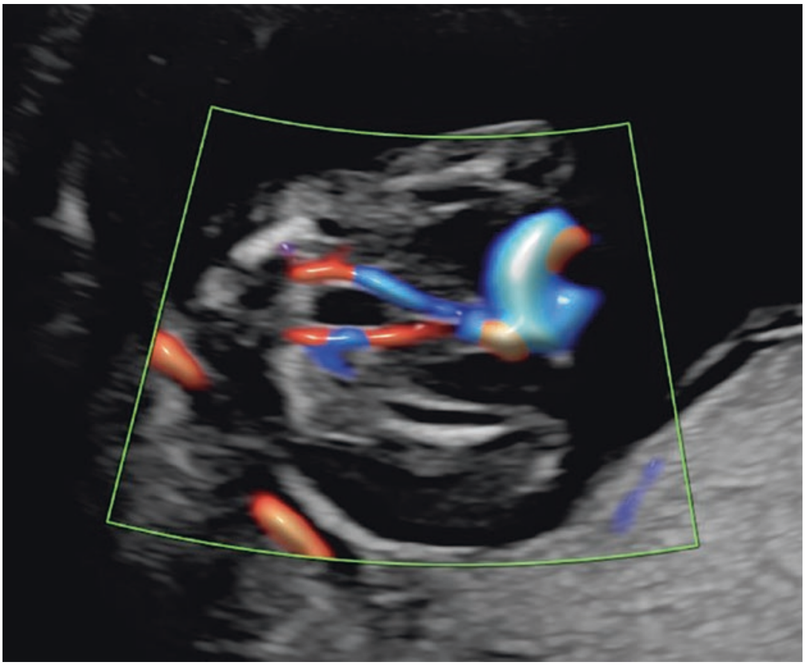

The normal urinary bladder should measure less than 7 mm in midsagittal dimension at the time of the NT evaluation [119]. When it is greater than 16 mm, the majority of fetuses will have a poor outcome. In the 7–15 mm range, in the euploid group, the majority (>90%) will have a normal outcome [120]. It is felt that this euploid group with transient megacystis may be related to a delay in autonomic innervation of the smooth muscle of the bladder wall. An initial follow-up in 2 weeks is a reasonable approach in this intermediate group.

Fetal Gastrointestinal Tract in the First Trimester

In the embryonic period, the midgut herniates into the umbilical cord at the start of the 8th weeks and, following a 90° rotation, returns to the abdominal cavity by the end of the 12th week. Although normal physiological midgut herniation should measure less than 10 mm prior to 10 weeks and should resolve by 12 weeks, there remains some variability in timing of when the midgut fully returns to the abdomen and herniated bowel may still be present at 12 weeks in up to 20% of fetuses. If midgut herniation is still suspected at 12 weeks, follow-up imaging is recommended to ensure complete return of the herniated bowel into the abdominal cavity. The normal appearance of herniated bowel is an echogenic mass in the central cord, which progressively decreases in size toward the 9th and 10th week [113]. The liver should never be present within the herniated contents. The fetal stomach can be visualized as a fluid-filled structure in the upper abdomen by 12–13 weeks [105]. Absence of the stomach at sonography may be seen in cases of esophageal atresia; however, serial scans documenting persistent nonvisualization of the stomach are required to make this diagnosis.

Abdominal Wall and Umbilical Cord

Normal cord insertion, centrally within the abdomen, can be routinely documented after 12 weeks, following the return of the small bowel into the abdominal cavity. Number of cord vessels can be assessed and normal appearance of two arteries and one vein can be seen, either on gray scale in cross-section, or by using color Doppler to show two arteries adjacent to the urinary bladder. Umbilical cord cysts can be seen and may be associated with chromosomal abnormalities. However, these can also be a normal variant and may resolve on subsequent imaging.

Fetal Skeleton in the First Trimester

Limb buds start to form as early as the 4th week of gestation. They are first identified at ultrasound, however, between 8 and 9 weeks gestation. Ossification of the long bones of the skeletal system can be seen at around 10 weeks. Distal ossification of the phalanges is present by 11 weeks gestation. It is important to document the presence of four limbs, with each limb demonstrating three segments (Fig. 8.31). In normal development, the ratio between upper extremity and lower extremity long bones should approximate 1.0. Disproportionate length of either upper or lower extremities can indicate an underlying skeletal dysplasia and warrants further assessment. Biometry of long bones can be performed with accuracy after 11 weeks and published normograms are available for reference [121].

Assessment of Fetal Genitalia in the First Trimester

In early pregnancy, the genital tubercle is identical in size in male and female fetuses. Accurate sonographic sex determination based on external genitalia can be performed between 12 and 14 weeks [122]. Gender determination at this stage is based upon orientation of the genital tubercle, as seen in the midsagittal plane. The angle of the genital tubercle to a horizontal line through the lumbosacral skin surface is measured. Male gender is assigned if the angle is greater than 30° and female gender if the angle is less than 10° (Fig. 8.32). Gender assignment is considered indeterminate if the angle is between 10°

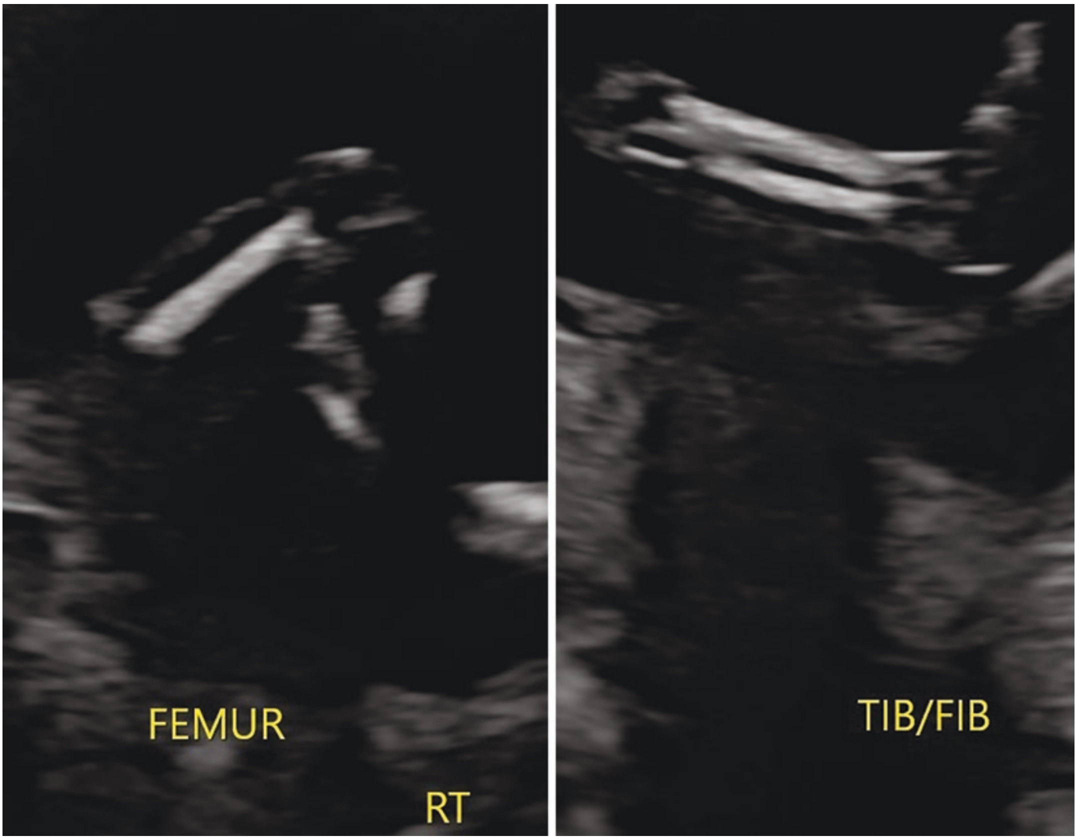

Fig. 8.31 Lower extremity at 13 weeks. Transabdominal image showing three segments of lower extremity (femur, tibia/fibula, and foot)

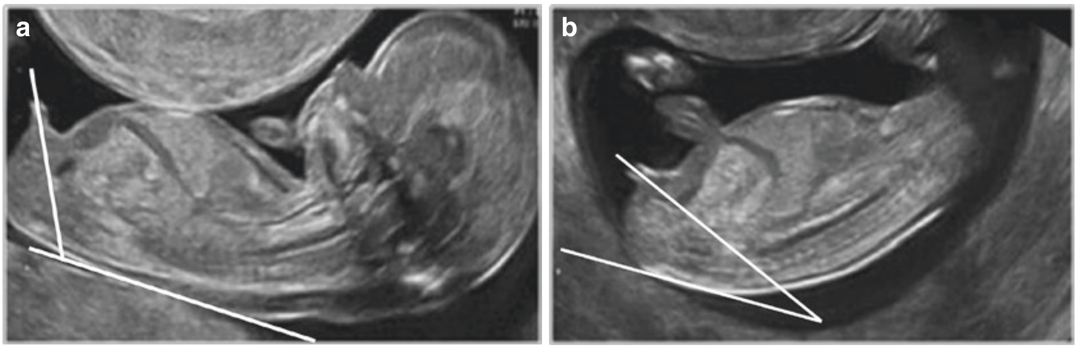

Fig. 8.32 Genital tubercle 12 weeks transvaginal images: (**a**) Vertical orientation of genital tubercle (>30° angulation) in male fetus. (**b**) More horizontal orientation of genital tubercle (<10° angulation) in female fetus

and 30°. Accuracy of gender assignment in higher in male fetuses and accuracy increases with increasing gestational age, with near 100% reliable gender identification possible at 13+6 weeks. Early assignment of fetal gender may be useful in decision-making with regard to invasive testing, such as CVS, in patients at increased risk of sex-linked disorders [123]. It should be noted that fetal sex determination using cell-free fetal DNA in maternal plasma is increasingly performed in pregnancies at increased risk of X-linked genetic disorders or congenital adrenal hyperplasia. Early reporting of fetal gender is controversial as it may facilitate the practice of sex selection.

Assessment of Spine

Longitudinal and axial views can demonstrate normal alignment and integrity of the overlying skin, in particular toward the end of first trimester. Detailed spine assessment is recommended when the BPD measurements are less than the 5th percentile or a posterior fossa abnormality is suspected [100].

Role of Three-Dimensional (3D) and Four-Dimensional (4D) Ultrasound

Three-dimensional and 4D ultrasound are not part of the routine first trimester care evaluation. Their role remains an area for further research.[6]

Conclusion

In summary, the main goal of a first trimester ultrasound is to provide information which can be used to optimize antenatal care. The establishment of a viable intrauterine pregnancy, accurate dating, and assessment of the fetal number, chorionicity, and amnionicity are crucial components of an early pregnancy evaluation. Evaluation of the nuchal translucency is now routine practice in many centers and, when combined with maternal serology, is useful in assessing aneuploidy risk. Even in the setting of a normal cell-free DNA test excluding fetal aneuploidy, early ultrasound assessment for nuchal translucency and fetal anatomy are of value for detecting structural abnormalities. There is an increasing movement toward a systematic structured and detailed anatomic evaluation of the fetus in the first trimester. Transvaginal ultrasound provides an opportunity for evaluation of the developing embryo as early as 8–9 weeks and is an area of future research interest. It is, therefore, increasingly important to be familiar with the developmental stages of the embryo and fetus at various stages in the first trimester.

Teaching Points

- Without sonographic evidence of ectopic pregnancy, any fluid collection with curved margins in a woman with a positive pregnancy test should be considered an early intrauterine gestational sac.
- The most accurate sonographic sign for confirmation of an IUP is visualization of the yolk sac.
- An empty gestational sac should be considered a potentially normal early pregnancy finding up to a MSD of 25 mm on transvaginal ultrasound.
- The absence of embryonic cardiac activity should be considered a potentially normal finding up to a measured embryo length of 7 mm.
- Assignment of chorionicity is a mandatory and vital component of first trimester ultrasound with multiple gestations.
- The most accurate estimation of gestational age is achieved in the first trimester by using the CRL between 8 and 13+6 weeks.
- Assessment of nuchal translucency, especially when combined with maternal age and maternal serum biochemistry, can be an effective method of screening for chromosomal abnormalities.
- In euploid fetuses, borderline or mild elevated nuchal translucency may be associated with a normal outcome.
- It is important for practitioners to be familiar with normal anatomy at various gestational ages in the first trimester.

References

1. Van den Hof MC, Smithies M, Nevo O, Oullet A. No. 375-Clinical practice guideline on the use of first trimester ultrasound. J Obstet Gynaecol Can. 2019;41(3): 388–95. https://doi.org/10.1016/j.jogc.2018.09.020.
2. Salomon LJ, et al. ISUOG practice guidelines: performance of first-trimester fetal ultrasound scan. Ultrasound Obstet Gynecol. 2013;41(1):102–13.
3. Bottomley C, Van Belle V, Mukri F, Kirk E, Van Huffel S, Timmerman D, et al. The optimal timing of an ultrasound scan to assess the location and viability of an early pregnancy. Hum Reprod. 2009;24(8):1811–7.
4. Benoit B, et al. Three-dimensional sonoembryology. J Perinat Med. 2002;30:63–73.

---

[6] See also Chap. 13.

5. Doubilet PM, Benson C, Bourne T, Blaivas M. Diagnostic criteria for nonviable pregnancy early in the first trimester. Ultrasound Q. 2014;30:3–9.
6. American Institute of Ultrasound in Medicine. AIUM practice guideline for the performance of obstetric ultrasound examinations. J Ultrasound Med. 2013;32(6):1083–101.
7. Timor-Trisch IE, Bar-Yam Y, Elgali S, Rottem S. The technique of TVS sonography with the use of 6.5 MHz probe. Am J Obstet Gynecol. 1988;158:1019–24.
8. Butt K, Lim KI. Guideline No. 388-Determination of gestational age by ultrasound. J Obstet Gynaecol Can. 2019;41(10):1497–507. https://doi.org/10.1016/j.jogc.2019.04.010.
9. Rumack CM, Wilson SR, Charboneau JW, Levine D. Diagnostic ultrasound, vol. 2. 4th ed. Philadelphia, PA: Elsevier; 2011.
10. Doubilet PM. Ultrasound evaluation of the first trimester. Radiol Clin N Am. 2014;52(6):1191–9.
11. Benson CB, Doubilet P, Peters HE, Frates MC. Intrauterine fluid with ectopic pregnancy: a reappraisal. J Ultrasound Med. 2013;32(3):389–93.
12. Hill LM, Kislak S, Martin JG. Transvaginal sonographic detection of the pseudogestational sac associated with ectopic pregnancy. Obstet Gynecol. 1990;75:986–8.
13. Fleischer AC, Pennell R, MS MK, Worrell JA, Keefe B, Herbert CM, et al. Ectopic pregnancy: features at transvaginal sonography. Radiology. 1990;174:375–8.
14. Doubilet PM, Benson C. First, do no harm... to early pregnancies. J Ultrasound Med. 2010;29:685–9.
15. Phillips CH, et al. “Pseudogestational Sac” and other 1980s-era concepts in early first-trimester ultrasound: are they still relevant today? J Ultrasound Med. 2020;39(8):1547–51.
16. Yeh HC, Goodman J, Carr L, et al. Intradecidual sign: a US criterion of early intrauterine pregnancy. Radiology. 1986;161:463–7.
17. Bradley WG, Fiske C, Filly RA. The double sac sign of early intrauterine pregnancy: use in exclusion of ectopic pregnancy. Radiology. 1982;143:223–6.
18. Chiang G, Levine D, Swire M, McNamara A, Mehta T. The intradecidual sign: is it reliable for diagnosis of early intrauterine pregnancy? AJR. 2004;183:725–31.
19. Parvey HR, Dubinsky T, Johnston DA, Maklad NF. The chorionic rim and low-impedance intrauterine arterial flow in the diagnosis of early intrauterine pregnancy: evaluation of efficacy. AJR. 1996;167:1479–85.
20. Doubilet PM, Benson C. Double sac sign and intradecidual sign in early pregnancy. J Ultrasound Med. 2013;32:1207–14.
21. Pexters A, Luts J, van Schoubroek D, et al. Clinical implications of intra- and interobserver reproducibility of transvaginal sonographic measurement of gestational sac and crown-rump length at 6-9 weeks’ gestation. Ultrasound Obstet Gynecol. 2011;38:510–5.
22. Abdallah Y, et al. Limitations of current definitions of miscarriage using mean gestational sac diameter and crown-rump length measurements: a multicenter observational study. Ultrasound Obstet Gynecol. 2011;38(5):497–502.
23. Bromley B, Harlow B, Laboda LA, Benacerraf BR. Small sac size in the first trimester: a predictor of poor fetal outcome. Radiology. 1991;178:375.
24. Levi VS, Lyons E, Zheng XH, Lindsay DJ, Jolt SC. Endovaginal US: demonstration of cardiac activity in embryos of less than 5.0 mm in crown-rump length. Radiology. 1990;176:71–4.
25. Doubilet PM, et al. Diagnostic criteria for nonviable pregnancy early in the first trimester. N Engl J Med. 2013;369(15):1443–51.
26. Bourne T, Bottomley C. When is a pregnancy nonviable and what criteria should be used to define miscarriage. Fertil Steril. 2012;98(5):1091–6.
27. Elson J, Salim R, Tailor A, Benerjee S, Zosmer N, Jurkovic D. Prediction of early pregnancy viability in the absence of an ultrasonically detectable embryo. Ultrasound Obstet Gynecol. 2003;21:57–61.
28. Bottomley C, Van Belle V, Pexsters A, Papageorghiou AT, Mukri F, Kirk E, et al. A model and scoring system to predict outcome of intrauterine pregnancies of uncertain viability. Ultrasound Obstet Gynecol. 2011;37(5):588–95.
29. Bickhaus J, Perry E, Schust D. Re-examining sonographic cut-off values for diagnosing early pregnancy loss. Gynecol Obstet (Sunnyvale). 2013;3(1):141.
30. Emerson DS, Cartier M, Altieri LA, et al. Diagnostic efficacy of endovaginal color Doppler flow imaging in an ectopic pregnancy screening program. Radiology. 1992;183:413–20.
31. Abramowicz JS, Kossoff G, Marsal K, Ter Haar G. Safety Statement, 2000 (reconfirmed 2003). International Society of Ultrasound in Obstetrics and Gynecology (ISUOG). Ultrasound Obstet Gynecol. 2003;21(1):100.
32. Doubilet PM, Benson C. Further evidence against the reliability of the human chorionic gonadotropin discriminatory level. J Ultrasound Med. 2011;30:1637–42.
33. Seeber BE. What serial hCG can tell you, and cannot tell you, about an early pregnancy. Fertil Steril. 2012;98(5):1074–7.
34. Condous G, Kirk E, Lu C, Van Huffel C, Gevaert S, De Moor O, et al. Diagnostic accuracy of varying discriminatory zones for the prediction of ectopic pregnancy in women with a pregnancy of unknown location. Ultrasound Obstet Gynecol. 2005;26:770–5.
35. Bignardi T, Condous G, Alhamdan D, Kirk E, Calster B, Van Huffel S, et al. The hCG ratio can predict the ultimate viability of the intrauterine pregnancies of uncertain viability in the pregnancy

of unknown location population. Hum Reprod. 2008;23(9):1964–7.

36. Bignardi T, Condous G, Kirk E, Van Calster B, Van Huffel S, Timmerman D, et al. Viability of intrauterine pregnancy in women with pregnancy of unknown location: prediction using human chorionic gonadotropin ratio vs progesterone. Ultrasound Obstet Gynecol. 2010;35:656–61.
37. Condous G, Kirk E, Van Calster C, Van Huffel B, Timmerman S, Bourne DT. There is no role for uterine curettage in the contemporary diagnostic workup of women with a pregnancy of unknown location. Hum Reprod. 2006;21:2706–10.
38. Barnhart KT, Simhan H, Kamelle SA. Diagnostic accuracy of ultrasound above and below the beta-hCG discriminatory zone. Obstet Gynecol. 1999;94(4):583–7.
39. Carusi D. Pregnancy of unknown location: evaluation and management. In: Seminars in perinatology. Elsevier. 2019.
40. Connolly A, et al. Reevaluation of discriminatory and threshold levels for serum β-hCG in early pregnancy. Obstet Gynecol. 2013;121(1):65–70.
41. Yeh HC. Sonographic signs of early pregnancy. Crit Rev Diagn Imaging. 1988;28(3):181–211.
42. Berdahl DM, Blaine J, Van Voorhis B, Dokras A. Detection of enlarged yolk sac on early ultrasound is associated with adverse pregnancy outcomes. Fertil Steril. 2010;94(4):1535–7.
43. Sauerbrei E, Cooperberg P, Poland BJ. Ultrasound demonstration of the normal fetal yolk sac. J Clin Ultrasound. 1980;8:217–20.
44. Robinson HP, Fleming J. A critical evaluation of sonar “crown-rump length” measurements. Br J Obstet Gynaecol. 1975;82:702–10.
45. Tal J, Haddad S, Gordon N, Timoro-Tritsch I. Heterotopic pregnancy after ovulation induction and assisted reproductive technologies: a literature review from 1971 to 1993. Fertil Steril. 1996;66(1):1–12.
46. Daya S. Accuracy of gestational age estimation by means of fetal crown-rump length measurements. Am J Obstet Gynecol. 1993;168:903–8.
47. Hadlock FP, Shah Y, Kanon OJ, Lindsey JV. Fetal crown-rump length: reevaluation of relation to menstrual age (5-18 weeks) with high-resolution real-time US. Radiology. 1992;182:501–5.
48. Papageorghiou AT, Kennedy S, Salomon LJ, Ohuma EO, Cheikh Ismail L, Barros FC, et al. International standards for early fetal size and pregnancy dating based on ultrasound measurement of crown-rump length in the first trimester of pregnancy. Ultrasound Obstet Gynecol. 2014;44(6):641–8.
49. Pexsters A, Luts J, Van Schoubroek D, Bottomley C, Van Calster B, Van Huffel S, et al. Clinical implications of intra- and interobserver reproducibility of transvaginal sonographic measurement of gestational sac and crown-rump length at 6-9 weeks’ gestation. Ultrasound Obstet Gynecol. 2010;38:510–5.
50. Doubilet PM, Benson C. Embryonic heart rate in the early first trimester: what rate is normal? J Ultrasound Med. 1995;14(6):431–4.
51. Pillai RN, et al. Prediction of miscarriage in women with viable intrauterine pregnancy—a systematic review and diagnostic accuracy meta-analysis. Eur J Obstet Gynecol Reprod Biol. 2018;220:122–31.
52. Benson CB, Doubilet P. Slow embryonic heart rate in early first trimester: indicator of poor pregnancy outcome. Radiology. 1994;192(2):343–4.
53. Arleo EK, Troiano R. Outcome of early first-trimester pregnancies (<6.1 weeks) with slow embryonic heart rate. AJR. 2011;197:252–5.
54. Doubilet PM, Benson C, Chow JS. Outcome of pregnancies with rapid embryonic heart rates in the early first trimester. Am J Roentgenol. 2000;175(1):67–9.
55. Martin JA, Hamilton B, Sutton PD, Ventura SJ, Menacker F, Munson ML. Births: final data for 2003. Natl Vital Stat Rep. 2005;54:1–116.
56. Martin JA, Hamilton B, MJK O. In: U.D.o.H.a.H. Services, editor. Three decades of twin births in the United States, 1980–2009. Hyattsville, MD: National Center for Health Statistics; 2012.
57. Dias T, Arcangeli T, Bhide A, Napolitano R, Mahsud-Dornan S, Thilaganathan B. First-trimester ultrasound determination of chorionicity in twin pregnancy. Ultrasound Obstet Gynecol. 2011;38:530–2.
58. Wan JJ, Schrimmer D, Tache V, Quinn K, Yvette Lacoursiere D, James G, et al. Current practices in determining amnionicity and chorionicity in multiple gestations. Prenat Diagn. 2011;31(1):125–30.
59. Sepulveda W, et al. Prenatal determination of chorionicity in triplet pregnancy by ultrasonographic examination of the ipsilon zone. Obstet Gynecol. 1996;88(5):855–8.
60. Stratulat V, et al. Validation of upsilon (Y) zone as pathognomonic ultrasound landmark for chorionicity and amnionicity in triplet pregnancy at any gestational age. Ultrasound Obstet Gynecol. 2021;57(3):501–3.
61. Bora S, et al. Reliability of transvaginal ultrasonography at 7–9 weeks’ gestation in the determination of chorionicity and amnionicity in twin pregnancies. Ultrasound Obstet Gynecol. 2008;32(5):618–21.
62. Shen O, Samueloff A, Beller U, Rabinowitz R. Number of yolk sacs does not predict amnionicity in early first-trimester monochorionic multiple gestations. Ultrasound Obstet Gynecol. 2006;27:53–5.
63. Bromley B, Benacerraf B. Using the number of yolk sacs to determine amnionicity in early first trimester monochorionic twins. J Ultrasound Med. 1995;14(6):415–9.
64. Kamath MS, Aleyamma T, Muthukumar K, Kumar RM, George K. A rare case report: ovarian heterotopic pregnancy after in vitro fertilization. Fertil Steril. 2010;94(5):1910–1.
65. Maruotti GM, Sarno L, Morlando M, Sirico A, Martinelli P. Heterotopic pregnancy: it is really a

rare event? The importance to exclude it not only after in vitro fertilization but also in case of spontaneous conception. Fertil Steril. 2010;94(3):e49.

66. Kalish RB, Chervenak F. Sonographic determination of gestational age. Ultrasound Rev Obstet Gynecol. 2005;5:254–8.
67. Bottomley C, Bourne T. Dating and growth in the first trimester. Best Pract Res Clin Obstet Gynaecol. 2009;23:439–52.
68. Gardosi J. Dating of pregnancy: time to forget the last menstrual period. Ultrasound Obstet Gynecol. 1997;9:367–8.
69. Gardosi J, Geirsson R. Routine ultrasound is the method of choice for dating pregnancy. Br J Obstet Gynaecol. 1998;105:933–6.
70. Robinson HP, Sweet EM, Adam A. The accuracy of radiological estimates of gestational age using early fetal crown-rump length measurements by ultrasound as a basis for comparison. Br J Obstet Gynaecol. 1979;86:525–8.
71. Piantelli G, Sacchini C, Coltri A, Ludovici G, Paita Y, Gramellini D. Ultrasound dating-curve analysis in the assessment of gestational age. Clin Exp Obstet Gynecol. 1994;2:108–18.
72. Salomon LJ, Alfirevic Z, Bilardo CM, Chalouhi GE, Ghi T, Kagan KO, et al. ISUOG practice guidelines: performance of first-trimester fetal ultrasound scan. Ultrasound Obstet Gynecol. 2013;41(1):102–13.
73. Caughey AB, Nicholson J, Washington AE. First- vs second-trimester ultrasound: the effect on pregnancy dating and perinatal outcomes. Am J Obstet Gynecol. 2008;198:703–5.
74. Saltved S, Almström H, Kublickas M. Ultrasound dating at 12-14 or 15-20 weeks of gestation? A prospective cross-validation of established dating formulae in a population of in-vitro fertilized pregnancies randomized to early or late dating scan. Ultrasound Obstet Gynecol. 2004;24:42–50.
75. Sladkevicius P, Saltvedt S, Almstrom H, Kublickas M, Grunewald C, Valentin L, et al. Ultrasound dating at 12-14 weeks of gestation. A prospective cross-validation of established dating formulae in in-vitro fertilized pregnancies. Ultrasound Obstet Gynecol. 2005;26:504–11.
76. Wu FS, Hwu Y, Lee RK, Li SH, Sun FJ, Lin MH, et al. First trimester ultrasound estimation of gestational age in pregnancies conceived after in vitro fertilization. Eur J Obstet Gynecol Reprod Biol. 2012;160:151–5.
77. Chalouhi GE, Bernard J, Benoist G, Nasr B, Ville Y, Salomon LJ. A comparison of first trimester measurements for prediction of delivery date. J Matern Fetal Neonatal Med. 2011;24:51–7.
78. Blondel B, Morin I, Platt RW, Kramer MS, Usher R, Breart G. Algorithms for combining menstrual and ultrasound estimates of gestational age: consequences for rates of preterm and postterm birth. BJOG. 2002;109:718–20.
79. Taipale P, Hiilesmaa V. Predicting delivery date by ultrasound and last menstrual period in early gestation. Obstet Gynecol. 2001;97:189–94.
80. Harrington DJ, MacKenzie I, Thompson K, Fleminger M, Greenwood C. Does a first trimester dating scan using crown rump length measurement reduce the rate of induction of labour for prolonged pregnancy? An uncompleted randomised controlled trial of 463 women. BJOG. 2006;113:171–6.
81. Bennett KA, Crane JMG, O'Shea P, Lacelle J, Hutchens D, Copel JA. First-trimester ultrasound screening is effective in reducing postterm labor induction rates: a randomized controlled trial. Am J Obstet Gynecol. 2004;190:1077–81.
82. Nicolaides KH. Screening for fetal aneuploidies at 11 to 13 weeks. Prenat Diagn. 2004;31(1):7–15.
83. Salomon L, et al. ISUOG updated consensus statement on the impact of cfDNA aneuploidy testing on screening policies and prenatal ultrasound practice. Ultrasound Obstet Gynecol. 2017;49(6):815–6.
84. Nicholaides KH, Heath V, Liao AW. The 11-14 week scan. Baillieres Clin Obstet Gynaecol. 2000;14(4):581–94.
85. Sotiriadis A, Papatheodorou S, Eleftheriades M, Makrydimas G. Nuchal translucency and major congenital heart defects in fetuses with normal karyotype: a meta-analysis. Ultrasound Obstet Gynecol. 2013;42:383–9.
86. Bilardo CM, Timmerman E, Pajkrt E, van Maarle M. Increased nuchal translucency in euploid fetuses—what should we be telling the parents? Prenat Diagn. 2010;30(2):93–102.
87. Souka AP, Snijders RJ, Novakov A, et al. Defects and syndromes in chromosomally normal fetuses with increased nuchal translucency thickness at 10-14 weeks of gestation. Ultrasound Obstet Gynecol. 1998;11:391–400.
88. Sotiriadis A, Papatheodorou S, Makrydimas G. Neurodevelopmental outcome of fetuses with increased nuchal translucency and apparently normal prenatal and/or postnatal assessment: a systematic review. Ultrasound Obstet Gynecol. 2012;39:10–9.
89. Cicero S, Curcio P, Papageorghiou A, Sonek J, Nicolaides KH. Absence of nasal bone in fetuses with trisomy 21 at 11-14 weeks of gestation: an observational study. Lancet. 2001;358:1665–7.
90. Sonek JD, Cicero S, Neiger R, Nicholaides KH. Nasal bone assessment in prenatal screening for trisomy 21. Am J Obstet Gynecol. 2006;195:1219–30.
91. Cicero S, Avgidou K, Rembouskos G, Kafan KO, Nicolaides KH. Nasal bone in first-trimester screening for trisomy 21. Am J Obstet Gynecol. 2006;195(1):109–14.
92. Cicero S, Rembouskos G, Vandercruys H, Hogg M, Nicolaides KH. Likelihood ratio for Trisomy 21 in fetuses with absent nasal bone at 11-14 week scan. Ultrasound Obstet Gynecol. 2004;23:218–23.
93. Prefumo F, Sairam S, Bhide A, Penna L, Hollis B, Thilaganathan B. Maternal ethnic origin and fetal

nasal bones at 11-14 weeks of gestation. BJOG. 2004;111:109–12.

94. Sebire NJ, Spencer K, Noble PL, Hughes K, Nicolaides KH. Maternal serum alpha-fetoprotein in fetal neural tube and abdominal wall defects at 10 to 14 weeks of gestation. BJOG. 1997;104(7):849–51.
95. Chaoui R, Nicolaides KH. From nuchal translucency to intracranial translucency: towards the early detection of spina bifida. Ultrasound Obstet Gynecol. 2010;35(2):133.
96. Chaoui R, Benoit B, Mitkowska-Wozniak H, Heling KS, Nicolaides KH. Assessment of intracranial translucency (IT) in the detection of spina bifida at the 11-13 week scan. Ultrasound Obstet Gynecol. 2009;34:249–52.
97. Lachmann R, Chaoui R, Moratalla J, Picciaarelli G, Nicolaides KH. Posterior brain in fetuses with open spina bifida at 11 to 13 weeks. Prenat Diagn. 2011;31:103–6.
98. Fong KW, Toi A, Okun N, Al-Shami E, Menezes RJ. Retrospective review of diagnostic performance of intracranial translucency in detection of open spina bifida at the 11-13 week scan. Ultrasound Obstet Gynecol. 2011;38(6):630–4.
99. Iliescu D, Comănescu A, Antsaklis P, Tudorache S, Ghilusi M, Comenscu V, et al. Neuroimaging parameters in early open spina bifida detection. Further benefit in first trimester screening? Romanian J Morphol Embryol. 2011;52(3):809–17.
100. Bernard JP, Cuckle HS, Stirnemann JJ, Salomon LJ, Ville Y. Screening for fetal spina bifida by ultrasound examination in the first trimester of pregnancy using fetal biparietal diameter. Am J Obstet Gynecol. 2012;207(4):306.e1–5.
101. Chaoui R, et al. Ratio of fetal choroid plexus to head size: simple sonographic marker of open spina bifida at 11–13 weeks' gestation. Ultrasound Obstet Gynecol. 2020;55(1):81–6.
102. Ushakov F, et al. Crash sign: new first-trimester sonographic marker of spina bifida. Ultrasound Obstet Gynecol. 2019;54(6):740–5.
103. Rossi AC, Prefumo F. Accuracy of ultrasonography at 11-14 weeks of gestation for detection of fetal structural anomalies. Obstet Gynecol. 2013;122(6):1160–7.
104. Timor-Tritsch IE, Fuchs KM, Monteagudo A, D'Alton ME. Performing a fetal anatomy scan at the time of first trimester screening. Obstet Gynecol. 2009;113(2):402–7.
105. Braithwaite JM, Armstrong MA, Economides DL. Assessment of fetal anatomy at 12 to 13 weeks of gestational by transabdominal and transvaginal sonography. Br J Obstet Gynaecol. 1996;103:82–5.
106. Ebrashy A, El Kateb A, Momtaz M, El Sheikhah A, Aboulghar MM, Ibrahim M, Saad M. 13-14 week fetal anatomy scan: a 5-year prospective study. Ultrasound Obstet Gynecol. 2010;35(3):292–6.
107. Whitlow BJ, Economides DL. The optimal gestational age to examine fetal anatomy and measure nuchal translucency in the first trimester. Ultrasound Obstet Gynecol. 1998;11(4):258–61.
108. Monteagudo A, Timor-Tritsch IE. First trimester anatomy: pushing the limits. What can we see now? Curr Opin Obstet Gynecol. 2003;15:131–41.
109. Kenkhuis M, et al. Effectiveness of 12–13-week scan for early diagnosis of fetal congenital anomalies in the cell-free DNA era. Ultrasound Obstet Gynecol. 2018;51(4):463–9.
110. Bromley B, et al. Detection of fetal structural anomalies in a basic first-trimester screening program for aneuploidy. J Ultrasound Med. 2014;33(10):1737–45.
111. Syngelaki A, et al. Diagnosis of fetal non-chromosomal abnormalities on routine ultrasound examination at 11–13 weeks' gestation. Ultrasound Obstet Gynecol. 2019;54(4):468–76.
112. Donnelly JC, Malone FD. Early fetal anatomical sonography. Best Pract Res Clin Obstet Gynaecol. 2012;26:561–73.
113. Syngelaki A, Chelemen T, Dagklis T, Allan L, Nicolaides KH. Challenges in the diagnosis of fetal non-chromosomal abnormalities at 11-13 weeks. Prenat Diagn. 2011;31(1):90–102.
114. Sepulveda W, et al. Retronasal triangle: a sonographic landmark for the screening of cleft palate in the first trimester. Ultrasound Obstet Gynecol. 2010;35(1):7–13.
115. Haak MC, Twisk JWR, JMG VV. How successful is fetal echocardiographic examination in the first trimester of pregnancy? Ultrasound Obstet Gynecol. 2002;20:9–13.
116. Yu D, Sui L, Zhang N. Performance of first-trimester fetal echocardiography in diagnosing fetal heart defects: meta-analysis and systematic review. J Ultrasound Med. 2020;39(3):471–80.
117. Karim J, et al. First-trimester ultrasound detection of fetal heart anomalies: systematic review and meta-analysis. Ultrasound Obstet Gynecol. 2022;59(1):11–25.
118. Sinkovskaya ES, et al. Fetal cardiac axis and congenital heart defects in early gestation. Obstet Gynecol. 2015;125(2):453–60.
119. Liao AW, Sebire NJ, Geerts L, Cicero S, Nicolaides KH. Megacystis at 10-14 weeks of gestation: chromosomal defects and outcome according to bladder length. Ultrasound Obstet Gynecol. 2003;21:338–41.
120. Kagan KO, Staboulidou I, Syngelaki A, Cruz J, Nicolaides KH. The 11-13 week scan: diagnosis and outcome of holoprosencephaly, exomphalos and megacystis. Ultrasound Obstet Gynecol. 2010;36(1):10–4.
121. Exacoustos C, Rosati P, Rizzo G, Arduini D. Ultrasound measurements of fetal limb bones. Ultrasound Obstet Gynecol. 1991;1(5):325–30.
122. Efrat Z, Perri T, Ramati E, Tugendreich D, Meizner I. Fetal gender assignment by first-trimester ultrasound. Ultrasound Obstet Gynecol. 2006;27:619–21.
123. Chitayat D, Glanc P. Diagnostic approach in prenatally detected genital abnormalities. Ultrasound Obstet Gynecol. 2010;35:637–46.

9

Screening for Fetal Chromosome Abnormalities

Bryanna Cox McCathern, Ryan E. Longman, and Jacques S. Abramowicz

Introduction

Chromosome abnormalities are present in 1/170 live births. The most common type of chromosome abnormality is aneuploidy, which refers to the presence of an extra (trisomy) or missing (monosomy) chromosome from the normal 46 chromosomes present in humans [1].

The most common of all chromosome abnormalities is Down syndrome, caused by trisomy of chromosome 21. Down syndrome is characterized by intellectual disability, distinctive facial features, and an increased risk for structural anomalies. The next two most common trisomies are trisomy 18, also referred to as Edward syndrome and trisomy 13, also known at Patau syndrome. Trisomy 18 and trisomy 13 are characterized by multiple structural malformations, intellectual disabilities, and high mortality rates in the first year of life [1, 2]. The only viable monosomy, Monosomy X or Turner syndrome, occurs in females and results in ovarian failure and short stature with normal cognitive development [1, 2].

In addition to aneuploidy, there can be the presence of 46 chromosomes with one (or more) chromosomes having a deletion or duplication of genetic material. These are referred to as copy number variants (CNVs). Copy number variants that result in an early-onset syndromic disorder are present in 1/270 live births [3]. The most common pathogenic CNV, 22q11.2 deletion syndrome, also known as velocardiofacial syndrome (VCFS) or DiGeorge syndrome, is present in 1/4000 newborns and is associated with cardiac defects, palatal abnormalities, immune deficiencies, and learning difficulties [4]. CNVs can be detected through the use of chromosome microarray, which is able to detect small CNVs that are below the level of resolution of a karyotype [5].

Aneuploidy screening is designed to provide an accurate risk assessment for the probability of having a fetus with a chromosome abnormality [6, 7] and diagnostic testing, such as amniocentesis and chorionic villus sampling, are available to determine with certainty if a fetus is affected with a chromosome abnormality; each procedure is associated with a small risk of pregnancy loss above the background risk of ~1/500 when performed at experienced centers [8]. When diagnostic testing for aneuploidy is performed, a chromosome microarray can be performed to detect pathogenic copy number variants [5, 8].

Aneuploidy screening and diagnostic testing for chromosome abnormalities have been a part

---

B. C. McCathern (✉) · R. E. Longman
J. S. Abramowicz
Department of Obstetrics and Gynecology, University of Chicago Medical Center, Chicago, IL, USA
e-mail: Bryanna.mccathern@uchospitals.edu; relongman@bsd.uchicago.edu; jabramowicz@bsd.uchicago.edu

© The Author(s), under exclusive license to Springer Nature Switzerland AG 2023
J. S. Abramowicz, R. E. Longman (eds.), *First-Trimester Ultrasound*,
https://doi.org/10.1007/978-3-031-24133-8_9

of routine prenatal care since the 1980s [6], and multiple professional organizations recommend that screening and diagnostic testing for chromosome abnormalities should be offered to all pregnant women [7, 9, 10]. Pregnant patients may use the results of aneuploidy screening to make a decision regarding whether to pursue diagnostic prenatal genetic testing.

Aneuploidy screening results should be interpreted in light of a patient's obstetrical and family history. For some patients, diagnostic testing may be recommended when ultrasound anomalies are present or based on family history indications [8].

Pregnant patients should receive pre- and post-test counseling prior to accepting or declining aneuploidy screening and diagnostic genetic testing [7, 9, 10].

Biochemical and Ultrasound Screening for Aneuploidy

Historical Approaches

As early as the 1960s, maternal age was recognized as a risk factor for fetal aneuploidy. Rates of chromosome abnormalities at different maternal ages were published in the 1980s to aid in genetic counseling for these conditions, especially given the uptake in prenatal diagnosis due to improved safety and efficacy of invasive prenatal diagnosis [1, 6].

Historically, women over 35 years of age at term were considered "high-risk" for chromosome aneuploidy and were offered invasive prenatal diagnosis via fetal karyotyping following amniocentesis beginning in the 1960s. In the 1980s, chorionic villus sampling became an option for first trimester diagnostic testing. Age 35 was selected as the cut-off, in part, due to the oft-quoted 1 in 200 risk of complications with the amniocentesis; the risk of aneuploidy was felt to be approximately equal or greater than the procedural risk (Table 9.1). The cost-effectiveness and utility of this approach were questioned, particularly in light of the procedure-related pregnancy loss rate [11].

Table 9.1 Estimates of rates of chromosome abnormalities in live born infants[a]

Age of mother at term (years)	Risk for trisomy 21 (Down syndrome) (%)		Total risk for any chromosome abnormality (%)[b]	
20	1/1667	0.06	1/526	0.2
21	1/1429	0.07	1/526	0.2
22	1/1429	0.07	1/500	0.2
23	1/1429	0.07	1/500	0.2
24	1/1250	0.08	1/476	0.2
25	1/1250	0.08	1/476	0.2
26	1/1176	0.09	1/476	0.2
27	1/1111	0.09	1/455	0.2
28	1/1053	0.09	1/435	0.2
29	1/1000	0.1	1/417	0.2
30	1/952	0.11	1/384	0.3
31	1/909	0.11	1/384	0.3
32	1/769	0.13	1/323	0.3
33	1/625	0.16	1/286	0.3
34	1/500	0.2	1/238	0.4
35	1/385	0.26	1/192	0.5
36	1/294	0.34	1/156	0.6
37	1/227	0.44	1/127	0.8
38	1/175	0.57	1/102	1.0
39	1/137	0.73	1/83	1.2
40	1/106	0.94	1/66	1.5
41	1/82	1.2	1/53	1.9
42	1/64	1.6	1/42	2.4
43	1/50	2.0	1/33	3.0
44	1/38	2.6	1/26	3.8
45	1/30	3.3	1/21	4.8
46	1/23	4.3	1/16	6.3
47	1/18	5.6	1/13	7.7
48	1/14	7.1	1/10	10.0
49	1/11	9.1	1/8	12.5

[a] Adapted from Hook (1981) and Hook et al. (1983)

[b] Excludes 45,X and 47,XXX

As use of microarray technology has increased, it is known that the risk for any pregnant woman to have a child with a CNV that results in an early-onset syndromic disorder is 1/270 [3]. The risk of having a child with a pathogenic CNV is not influenced by maternal age. Fetal risks for a CNV should be incorporated into patient counseling.

Second Trimester Maternal Serum Biochemical Screening

Second trimester biochemical maternal serum screening started with the finding that low maternal serum alpha-fetoprotein (MS-AFP) was associated with an increased risk of Down syndrome [12]. Maternal serum screening for aneuploidy then expanded to include multiple additional markers: human chorionic gonadotropin (hCG), unconjugated estriol (uE3), and dimeric inhibin A (DIA). The quadruple ("Quad") screen provided additional parameters by which to estimate a woman's risk of fetal aneuploidy in a given pregnancy, with higher sensitivity than age alone (approximately 80% for Down syndrome at a 5% false-positive rate) [13]. The "pattern" of high or low levels (as calculated by the multiple of the median, or MoM) of these analytes combined with maternal age, weight, gestational age (ideally confirmed by ultrasound biometry), and ancestry is used to calculate a risk for fetal Down syndrome, trisomy 18, and open neural tube defects.

Although no uniformly accepted practice exists, it has been suggested in multiple studies that unexplained extreme values of second trimester analytes can be associated with an increased risk for adverse antenatal outcomes such as fetal growth restriction and stillbirth, and therefore should prompt investigation and increased antenatal surveillance [7, 14, 15].

First-Trimester Maternal Serum Biochemical Screening

In an effort to perform risk assessment for aneuploidy at an earlier gestational age, first trimester markers for aneuploidy were investigated. Previously used second trimester markers were explored for utility in the first trimester, but only hCG was found to be informative; elevated hCG is associated with an increased risk for Down syndrome. PAPP-A, another product of the placenta, is found in low levels in maternal serum of affected pregnancies. Low levels of both analytes are concerning for trisomy 18. Taken together, these two markers had a 65% detection rate at a 5% false-positive rate for Down syndrome; however, second trimester maternal serum screening had a higher detection rate. Therefore, additional markers were needed to improve first trimester screening [16].

First Trimester Ultrasound Markers for Chromosome and Genetic Anomalies

Nuchal translucency (NT), a measurement of the thickness of the subcutaneous fluid at the back of the neck of the fetus in the late first trimester, was observed to be increased in fetuses with Down syndrome. Stringent, efficacious, and standardized methods for measurement of the fetal NT were developed in the early 1990s [17]. NT alone was found to have a ~75% detection rate and a ~5% false-positive rate for Down syndrome [18]. Kagan and colleagues found that 19.2% of pregnancies with NT >3.4 mm had an abnormal fetal karyotype [19]. Furthermore, the incidence of chromosome abnormalities increased with NT thickness, from approximately 7% with an NT of 3.4 mm (95th percentile for crown-rump length) to 75% for an NT ≥8.5 mm.

In addition to aneuploidy, increased NT has been associated with an increased risk for CNVs. In a systematic review and meta-analysis of cases with a NT ≥3.5 mm and a normal karyotype, microarray analysis revealed a pathogenic CNV in 4.0% of cases of isolated increased NT and 7.0% when additional ultrasound anomalies were present [20].

Increased NT has also been associated with an increased risk for Noonan syndrome, an autosomal dominant disorder characterized by dysmorphic facies, short stature, congenital heart defects, and developmental delay of variable degree [21]. The rate of Noonan syndrome is ~10% in fetuses with an NT ≥3.5 mm that have a normal karyotype and CMA [22, 23]. If the patient elects for an amniocentesis or chorionic villus sampling for diagnostic testing of chromosome abnormalities due to an increased NT, prenatal diagnosis for Noonan syndrome can be accomplished from the fetal tissue obtained if the chromosome studies are normal.

First trimester screening using a combination of NT measurement and maternal serum analytes has a Down syndrome detection rate of ~85% with a false-positive rate of 5% and a trisomy 18 detection rate of 90% with a 1–2% screen positive rate [13]. A first trimester screen has the benefit of delivering results in the first trimester of pregnancy.

Integrated and Sequential Screening

In an effort to further improve detection rates and lower false-positive rates, various aneuploidy screening tests have been developed that utilize first and second trimester screening methods. Integrated screen uses first trimester screening (NT and PAPP-A) with second trimester screen analytes. Integrated screening has a 94% detection rate for Down syndrome and 91–96% detection rate for trisomy 18 with a 5% screen positive rate [10, 24].

Contingent or sequential screening first involves NT and PAPP-A to calculate a risk for Down syndrome and trisomy 18. If the risk for Down syndrome or trisomy 18 is elevated based on these two measurements, an increased risk report is generated and the screening test is complete. If the aneuploidy risk is not elevated based on these measurements, then a blood draw for second trimester analytes is recommended and a final report combining first and second trimester results is generated. This allows for the higher detection rate that is obtained with integrated screening while also allowing those women with the highest risk for aneuploidy to have a risk assessment in the first trimester [10, 25].

A drawback to integrated and sequential screening is that most patients who undergo screening must have two blood draws at specific gestational ages. If the second trimester blood draw is missed, then only limited aneuploidy risk information is available.

Cell Free DNA Screening for Aneuploidy

In 1997, Lo and colleagues first reported on the presence of fetal DNA in maternal serum [26]. During pregnancy, DNA fragments are released from the placental trophoblasts into the maternal circulation [27]. The percentage of circulating cell free DNA that is placental in origin is known as the fetal fraction, and comprises approximately 3–13% of the total circulating cell free DNA [28]. The fetal fraction increases during the first trimester and is felt to be at a sufficient quantity to perform cell free DNA screening at 10 weeks gestation [29].

There are two basic molecular approaches to performing cell free DNA screening (also referred to as non-invasive prenatal testing or non-invasive prenatal screening). In the whole genome sequencing method, the cell free DNA molecules are sequenced and then mapped to the chromosome of origin. If a higher number of cell free DNA molecules are identified than expected from the chromosomes of interest, then the fetus may have an extra copy of that chromosome and an increased risk for aneuploidy is reported. In the single nucleotide polymorphism (SNP) method, SNPs on the chromosomes of interest are sequenced and the ratios between heterozygous SNP alleles are compared with those of other chromosomes. A skewing of the ratios suggests fetal aneuploidy [28].

When first introduced to clinical practice, cell free DNA screening was recommended for women designated as being at increased risk for having a fetus with aneuploidy based on age, previous screening results, or abnormal ultrasound findings. A meta-analysis by the U.K. National Screening Committee on the performance of cell free DNA screening in high-risk women found a sensitivity and specificity of 97% and 99.7% for trisomy 21, 93% and 99.7% for trisomy 18, and 95% and 99.9% for trisomy 13 [30].

Since that time the performance of cell free DNA screen has been studied in the average risk population and findings were similar to the high risk population. A meta-analysis performed by Gil et al. in 2017 found detection rates of 99.7% for Down syndrome, 97.9% for trisomy 18, and 99.0% for trisomy 13 with a combined false-positive rate of 0.12% [31].

Screening for sex chromosome aneuploidies (45,X; 47,XXX; 47,XXY, and 47,XYY) can be performed, and the results are reported by most clinical laboratories in the United States. The meta-analysis performed by Gil determined that the number of reported cases of sex chromosome abnormalities was too small for accurate assessment of screening performance [31]. Several studies have reported higher false-positive rates for sex chromosome aneuploidies compared to autosomal aneuploidy. The positive predictive value, which is the probability that a positive result is a true positive, is reported to be 20–30% for Monosomy X, and between 50–80% for the other sex chromosome aneuploidies [32, 33]. One reason for the poorer performance of cell free DNA screening for sex chromosome aneuploidies may be maternal sex chromosome abnormalities. One study performed a microarray analysis on 86 pregnant women who had a screen positive result for a sex chromosome aneuploidy and found 21 abnormal maternal sex chromosomes, including 12 sex chromosome aneuploidies and 9 with an X-chromosome copy number variant [34].

Despite high sensitivity and specificity, cell free DNA is a screening test. False positives and false negatives do occur. The cell free "fetal" DNA in the maternal blood is actually placental in origin. Experience with chorionic villus sampling has found that 1–2% of placentas can have a different chromosome make-up than the fetus. Most often observed is mosaicism for a normal cell line and a cell line with an aneuploidy in the placenta, with a chromosomally normal fetus [2]. This is referred to as confined placental mosaicism (CPM). If CPM is present for chromosomes 21, 18, 13 or X, the screen may indicate an increased risk. False positives can also occur due to true fetal mosaicism or maternal chromosome abnormality. False negative results are less common but may arise from low fetal fraction or triploidy [28]. For these reasons, any screen positive result should be confirmed with diagnostic testing (chorionic villus sampling or amniocentesis) before any irreversible action such as pregnancy termination is pursued. Also, if the suspicion for aneuploidy is high, diagnostic testing should be offered despite a negative cell free DNA screen [7, 9].

Approximately 3% of cell free DNA screens fail to return a result. The most common reason for a test failure is low fetal fraction (typically <3%). There are a number of etiologies for low fetal fraction, including early gestational age, high maternal weight, in vitro fertilization, Lovenox use, and chromosome abnormalities [28]. A study by Norton et al. included a study population of 16,329 women with singleton gestations that underwent cell free DNA screening, and 488 (3.0%) had a lack of results on cell free DNA testing. In the group with no results, there were 13 chromosome abnormalities, to give a prevalence of aneuploidy of 1/38 in this group compared to 1/236 in the overall cohort [35]. When there is a cell free DNA test failure, it is recommended that the woman be offered diagnostic testing due to the increased risk for a chromosome abnormality. A redraw of the cell free DNA screen can be considered. The chance of obtaining a result is ~80% with a repeat specimen [36].

A rare result that can occur from cell free DNA screening that bears mention is a high risk for multiple aneuploidies and/or high risk for autosomal monosomy. An initial study reported some cases of maternal malignancy when the cell free DNA screen and fetal karyotype are discordant, and the risk for malignancy was increased when multiple aneuploidies or monosomies were identified [37]. A retrospective analysis of 113,415 cell free DNA screens identified 138 (0.12%) reported as a single autosomal monosomy, single trisomy with a sex chromosome aneuploidy or with multiple aneuploidies. In the 67 cases where fetal or neonatal karyotype was available, 24% were fully or partially concordant with the cell free DNA screen results, 6% had aneuploidy of a reference chromosome, and 70% (47 cases) had normal fetal chromosomes. In these 47 cases, five had maternal malignancies reported [38]. Some experts have proposed a protocol for evaluation of patients with more than one aneuploidy detected on cell free DNA screen [39], and genetic counseling and maternal fetal medicine consultation are recommended.

See Table 9.2 for a review of current aneuploidy screens.

Table 9.2 Aneuploidy screening tests [10, 13, 24, 31]

Screening method	Detection rate Trisomy 21 (%)	Detection rate Trisomy 18 (%)	Procedure	Gestational age range for screening (weeks)	Advantages	Limitations
First trimester screening (NT + blood analytes)	78–91	91–96	Nuchal translucency ultrasound and blood analytes (PAPP-A and hCG)	10–13 6/7	Available in first trimester, single point in time test	NT required, lower detection rate than combined or cell free DNA
Integrated screening	94–96	91–96	PAPP-A and NT in the trimester, second trimester blood draw for measurement of AFP, uE3, hCG, and DIA. Results available after second trimester blood draw.	Part 1—10–13 6/7 Part 2—15–21 6/7	Higher detection rate	NT required, no results until the second trimester, two samples needed
Contingent/sequential screening	91–95	91–96	PAPP-A and NT in first trimester, risk reported if elevated. Second trimester blood drawn if first part of screen is low risk	Part 1—10–13 6/7 Part 2—15–21 6/7	Maintains high detection rate while allowing highest risk patients results in the first trimester	NT required, most patients do not receive results until the second trimester, two samples needed.
Multiple marker serum screening (quad screen)	75–83	60–70	Blood draw for measurement of AFP, uE3, hCG, and DIA	15–21 6/7	Available for women who present to care after the first trimester, single test, no NT required	Lower detection rate than other available screening tests
Cell free DNA Screen	>99	>97	Blood draw for analysis of cell free DNA	≥10 0/7	Highest detection rate, available in the first trimester, no NT required	~3% test failure rate, results can be abnormal due to maternal chromosome abnormality or malignancy.

Aneuploidy Screening in Multiple Gestations

Aneuploidy screening in twin gestations has lower sensitivity and specificity in twin gestations compared to singletons.

A meta-analysis on first trimester screening in twin gestations found a Down syndrome detection rate of ~90% with a false-positive rate of 5% [40].

There is limited data on the performance of cell free DNA screening in twin gestations, given both the smaller number of twin gestations and that initial validation studies excluded multiple gestations. A meta-analysis on cell free DNA screening in twin gestations found a detection rate of 99.0% and a false-positive rate of 0.02%. The number of pregnancies affected with trisomies 18 and 13 is too small for accurate assessment of screening performance [41].

There is an increased risk for test failure in twin gestations compared to singletons due to low fetal fraction. The chance to obtain a result with a redraw in twin gestations is ~60% [42]. If a patient has two cell free DNA screen failures, a third draw is not recommended and other aneuploidy screening options should be explored.

Serum based screening for triplet and other higher order multiples is not available. Nuchal translucency ultrasound without blood analyte testing can be offered.

In cases of a vanishing twin or twin demise, serum based aneuploidy screening can return inaccurate results and should not be performed [7]. Nuchal translucency ultrasound without blood analyte testing can be offered. Diagnostic testing for chromosome abnormalities should be offered.

Current Status of Aneuploidy Screening

Professional organizations have endorsed that all pregnant women who desire aneuploidy screening should have the option of cell free DNA screening [7, 9, 43].

Appropriate pre- and post-test counseling is essential in respecting patient's autonomy. Pre-test counseling should include a discussion of the difference between screening and diagnostic testing, the conditions included on the screening test, and the follow-up that would be offered if an increased risk is identified. Patients with a family history of a genetic condition or with many questions about prenatal genetic screening and diagnostic testing may benefit from genetic counseling [7, 10, 43].

If after appropriate counseling, a pregnant patient elects for aneuploidy screening, cell free DNA screen should be made available given that it has the highest detection rate of currently available aneuploidy screens with lower false-positive rates.

Nuchal Translucency Ultrasound in the Era of Cell Free DNA Screening

Given the high sensitivity and specificity for cell free DNA screening for aneuploidy, cell free DNA screen is increasingly being used as a first tier screening test for all pregnant patients. Given this, investigators have asked: Is there clinical utility in NT ultrasound for pregnant patients who are pursuing a cell free DNA screen?

Reiff et al. looked at 1739 women who had a low-risk cell free DNA screen and an ultrasound at 11–14 weeks gestation to determine how often there was an unexpected finding on ultrasound. An unexpected finding was identified in 60/1739 cases (3.5%). Unexpected findings included an increased NT, cystic hygroma, unexpected multiple gestation, and fetal demise [44].

A second multicenter study from the Netherlands [45] looked at the outcomes of pregnancies that had a NT exceeding the 95th percentiles for gestational age and to investigate what abnormalities would have been missed if cell free DNA screening was used as a first-tier test. A total of 1901 pregnancies met criteria. In this group, 43% of the pregnancies had at least one abnormality, and 34% of these abnormalities, including single gene disorders, pathogenic CNVs, and structural abnormalities, would have been missed if cell free DNA screening has been performed without an NT ultrasound (see Table 9.3) [45]. Other groups have suggested that using a higher cut-off (>99th percentile or NT >3.5 mm) to define an increased NT is superior to detecting fetuses with atypical chromosome abnormalities and lowering the number of false positives [46].

In the Netherlands study, of the 38 fetuses diagnosed with single gene disorders about half had Noonan syndrome or related disorders (referred to collectively as RASopathies); the remainder of fetuses each had a different disorder, illustrating the non-specific nature of increased NT and the difficulty of prenatal diagnosis for single gene disorders with this finding. Whole exome sequencing (WES), which involves sequencing of the coding region of the genome, has been demonstrated to have a high diagnostic yield (~25%) in the pediatric population with children suspected of having a genetic disorder with normal microarray results [47]. Application of this technology in pregnancies with structural abnormalities on ultrasound has found a diagnostic yield of ~10% when one malformation is present and ~35% when two or more abnormalities is

Table 9.3 Congenital abnormalities and increased nuchal translucency

NT	All fetuses with increased NT (%)	All abnormal fetuses	Trisomy 21, 18, or 13	Atypical chromosome abnormalities (incl CNVs)	Single gene disorder	Structural malformation
>95th–99th percentile	894 (47)	190 (21.3)	112 (12.5)	20 (2.2)	5 (0.6)	53 (5.9)
>99th percentile (≥3.5 mm)	1007 (53)	624 (62)	344 (34)	122 (12.1)	33 (3.3)	125 (12.4)
Total	1901	814 (43)	456 (23.9)	104 (14.3)	38 (2.0)	178 (9.3)

Adapted from Bardi et al. Is there still a role for nuchal translucency measurement in the changing paradigm of first trimester screening? Prenat diagn. 2020 Jan;40(2):197–205

present [48, 49]. Limited information exists regarding the diagnostic yield based on the specific malformation present. Kelly et al. (2021) reviewed 6 studies of prenatal whole exome sequencing and found that of 242 fetuses with an indication of isolated NT ≥3.5 mm, a total of 9 (3.7%) received a diagnosis [50]. Given the complexity of prenatal WES testing, adequate pre- and post-test counseling by a genetics professional such as a genetic counselor or medical geneticist is recommended [51].

Professional organizations have offered opinions on the utility of NT ultrasound when cell free DNA screening is performed. The American College of Obstetrics and Gynecology opines that nuchal translucency ultrasound for aneuploidy risk assessment is not necessary when cell free DNA screening is being performed, but that ultrasound prior to screening can be beneficial to confirm viability and gestational age and determine if multiple is present. Any patient with an increased NT should be offered genetic counseling and diagnostic testing [7, 9]. The International Society for Ultrasound in Obstetrics and Gynecology recommends that all women should be offered first trimester ultrasound that includes NT measurement regardless of whether they intend to undergo cell free DNA screening [52].

Future Applications of Cell Free DNA Testing

In addition to screening for common aneuploidies, most commercial laboratories also offer screening for common pathogenic CNVs, including 22q11.2 deletion (DiGeorge syndrome), 15q11.2-q13 (Prader-Willi/Angelman syndrome), 1p36 deletion, 4p16.3-4p16.2 (Wolf-Hirschhorn syndrome), and 5p15.3-5p15.1 (Cri du Chat syndrome). Some laboratories are also offering screening for pathogenic CNVs across the genome.

A recent systematic review and meta-analysis were performed to assess the performance of cell free DNA screening for pathogenic CNVs. Their review included 474,189 screened pregnancies with 210 that had an increased risk for a CNV. They found a positive predictive value of 40% with an overall false-positive rate of <0.1%. Importantly, none of the studies performed systematic confirmatory analysis in cases that did not undergo prenatal diagnostic genetic testing, therefore the detection rate and negative predictive value of such screening are unknown [53]. Given a lack of data on performance, professional societies do not recommend performing screening for CNVs with cell free DNA screening for aneuploidy [7, 9, 43]. If a woman desires information on whether her fetus has a pathogenic CNV diagnostic testing with microarray analysis is available.

Techniques to perform prenatal diagnosis of single gene disorders for fetuses known to be a 25% risk have been developed and are clinically available in the United States at a limited number of laboratories [54, 55]. This may be referred to as non-invasive prenatal diagnosis (NIPD). However, given limited information on test performance, it is recommended that results of NIPD be confirmed by prenatal diagnostic genetic testing before irreversible active such as pregnancy termination is undertaken. Pre or postnatal confirmation of the NIPD test results should be performed.

Summary

Prenatal screening for aneuploidy, to provide patients with an individualized risk assessment to have a child with a chromosome aneuploidy, has been available since the 1980s. Since the introduction of prenatal aneuploidy screening into prenatal care, new screening tests have been developed with higher detection rates and the ability to be performed in the first trimester. The introduction of cell free DNA screening to prenatal care in 2012, a single point of care blood test that can be performed in the first trimester, has been shown to have very high sensitivity and specificity with low false-positive rates and has revolutionized prenatal screening. Most women with a singleton gestation are appropriate candidates for cell free DNA screening. Nuchal translucency measurement for aneuploidy risk assessment is less valuable in the era of cell free DNA screening, given that cell free DNA screen is superior in detecting fetuses with aneuploidy. However, nuchal translucency ultrasound can remain useful to screen pregnancies that are not candidates for cell free DNA testing. First trimester ultrasound also has the benefit of verifying gestational age and the presence of fetal anomalies which may affect when screening is performed, or diagnostic genetic testing is recommended. Methods to detect rare chromosome disorders and single gene disorders through cell free DNA analysis are being developed and may be available in the future.

Teaching Points

- Multiple methods of aneuploidy screening exist. For women with uncomplicated singleton gestations who desire aneuploidy screening, cell free DNA screening should be offered as a first-tier test, as it has the highest detection rates with the lowest false-positive rate of the available aneuploidy screens.
- Cell free DNA screening is not diagnostic. Any increased risk result should be confirmed with diagnostic testing, prenatally or after delivery, based on patient preferences.
- Approximately 3% of cell free DNA screens fail to produce a result, the failure to produce a result is associated with an increased risk for chromosome abnormalities. Genetic counseling and diagnostic testing should be offered.
- Cell free DNA screening can be performed in twin gestations, however data on performance is limited and the risk of a no-call result is increased.
- First trimester ultrasound is beneficial, including nuchal translucency assessment when available, even if cell free DNA screening is performed, as it can provide dating information and identify patients with an increased risk for atypical chromosome abnormalities and single gene disorders that may benefit from diagnostic prenatal genetic testing.
- Cell free DNA screening for copy number variants is not recommended as data on its performance is not available. Diagnostic testing with microarray analysis is available for women who desire to know if their fetus has a pathogenic copy number variant.

References

1. Nussbaum R, McInnes R, Willard H. Principles of clinical cytogenetics and genome analysis. 8th ed. Philadelphia, PA: Elsevier; 2016.
2. McKinlay Gardner R, Amor D. Gardner and Sutherland's chromosome abnormalities and genetic counseling. 5th ed. New York: Oxford University Press; 2018.
3. Srebniak MI, Joosten M, Knapen MFCM, et al. Frequency of submicroscopic chromosomal aberrations in pregnancies without increased risk for structural chromosomal aberrations: systematic review and meta-analysis. Ultrasound Obstet Gynecol. 2018;51(4):445–52. https://doi.org/10.1002/uog.17533.
4. McDonald-McGinn DM, Hain HS, Emanuel BS, et al. 22q11.2 Deletion syndrome. 1999 Sep 23 [Updated 2020 Feb 27]. In: Adam MP, Ardinger HH, Pagon RA, et al., editors. GeneReviews®. Seattle, WA: University of Washington; 1993–2021. Available from: https://www.ncbi.nlm.nih.gov/books/NBK1523/.

5. Society for Maternal-Fetal Medicine (SMFM), Dugoff L, Norton ME, Kuller JA. The use of chromosomal microarray for prenatal diagnosis. Am J Obstet Gynecol. 2016;215(4):B2–9. https://doi.org/10.1016/j.ajog.2016.07.016.
6. Dashe JS. Aneuploidy screening in pregnancy. Obstet Gynecol. 2016;128(1):181–94. https://doi.org/10.1097/AOG.0000000000001385.
7. ACOG Practice Bulletin: Clinical management guidelines for obstetrician-gynecologists screening for fetal chromosomal abnormalities; 2020.
8. Practice Bulletin No. 162: Prenatal diagnostic testing for genetic disorders. Obstet Gynecol. 2016;127(5):e108–22. https://doi.org/10.1097/AOG.0000000000001405.
9. Benn P, Borell A, Chiu R, et al. Position statement from the Aneuploidy Screening Committee on behalf of the Board of the International Society for Prenatal Diagnosis. Prenat Diagn. 2013;33(7):622–9. https://doi.org/10.1002/pd.4139.
10. Wilson KL, Czerwinski JL, Hoskovec JM, et al. NSGC practice guideline: prenatal screening and diagnostic testing options for chromosome aneuploidy. J Genet Couns. 2013;22(1):4–15. https://doi.org/10.1007/s10897-012-9545-3.
11. Drugan A. Advanced maternal age and prenatal diagnosis: it's time for individual assessment of genetic risks. Israel Med Assoc J. 2005;7(2):99–102.
12. Merkatz IR, Nitowsky HM, Macri JN, Johnson WE. An association between low maternal serum alpha-fetoprotein and fetal chromosomal abnormalities. Am J Obstet Gynecol. 1984;148(7):886–94. https://doi.org/10.1016/0002-9378(84)90530-1.
13. Malone FD, Canick JA, Ball RH, et al. First-trimester or second-trimester screening, or both, for Down's syndrome. N Engl J Med. 2005;353(19):2001–11. https://doi.org/10.1056/NEJMoa043693.
14. Dugoff L, Society for Maternal–Fetal Medicine. First- and second-trimester maternal serum markers for aneuploidy and adverse obstetric outcomes. Obstet Gynecol. 2010;115(5):1052–61. https://doi.org/10.1097/AOG.0b013e3181da93da.
15. McPherson E, Thomas GD, Manlick C, et al. Extreme values of maternal serum analytes in second trimester screening: looking beyond trisomy and NTD's. J Genet Couns. 2011;20(4):396–403. https://doi.org/10.1007/s10897-011-9364-y.
16. Saller DN, Canick JA. Current methods of prenatal screening for Down syndrome and other fetal abnormalities. Clin Obstet Gynecol. 2008;51(1):24–36. https://doi.org/10.1097/GRF.0b013e318160f274.
17. Nicolaides KH, Azar G, Byrne D, Mansur C, Marks K. Fetal nuchal translucency: ultrasound screening for chromosomal defects in first trimester of pregnancy. BMJ (Clin Res Ed). 1992;304(6831):867–9. https://doi.org/10.1136/bmj.304.6831.867.
18. Nicolaides KH. Nuchal translucency and other first-trimester sonographic markers of chromosomal abnormalities. Am J Obstet Gynecol. 2004;191(1):45–67. https://doi.org/10.1016/j.ajog.2004.03.090.
19. Kagan KO, Avgidou K, Molina FS, Gajewska K, Nicolaides KH. Relation between increased fetal nuchal translucency thickness and chromosomal defects. Obstet Gynecol. 2006;107(1):6–10. https://doi.org/10.1097/01.AOG.0000191301.63871.c6.
20. Grande M, Jansen FAR, Blumenfeld YJ, et al. Genomic microarray in fetuses with increased nuchal translucency and normal karyotype: a systematic review and meta-analysis. Ultrasound Obstet Gynecol. 2015;46(6):650–8. https://doi.org/10.1002/uog.14880.
21. Allanson JE, Roberts AE. Noonan syndrome. 2001 Nov 15 [Updated 2019 Aug 8]. In: Adam MP, Ardinger HH, Pagon RA, et al., editors. GeneReviews®. Seattle, WA: University of Washington; 1993–2021. Available from: https://www.ncbi.nlm.nih.gov/books/NBK1124/.
22. Ali MM, Chasen ST, Norton ME. Testing for Noonan syndrome after increased nuchal translucency. Prenat Diagn. 2017;37(8):750–3. https://doi.org/10.1002/pd.5076.
23. Croonen EA, Nillesen WM, Stuurman KE, et al. Prenatal diagnostic testing of the Noonan syndrome genes in fetuses with abnormal ultrasound findings. Eur J Human Genet. 2013;21(9):936–42. https://doi.org/10.1038/ejhg.2012.285.
24. Wald NJ, Watt HC, Hackshaw AK. Integrated screening for Down's syndrome based on tests performed during the first and second trimesters. N Engl J Med. 1999;341(7):461–7. https://doi.org/10.1056/NEJM199908123410701.
25. Baer RJ, Flessel MC, Jelliffe-Pawlowski LL, et al. Detection rates for aneuploidy by first-trimester and sequential screening. Obstet Gynecol. 2015;126(4):753–9. https://doi.org/10.1097/AOG.0000000000001040.
26. Lo YM, Corbetta N, Chamberlain PF, et al. Presence of fetal DNA in maternal plasma and serum. Lancet (London, England). 1997;350(9076):485–7. https://doi.org/10.1016/S0140-6736(97)02174-0.
27. Alberry M, Maddocks D, Jones M, et al. Free fetal DNA in maternal plasma in anembryonic pregnancies: confirmation that the origin is the trophoblast. Prenat Diagn. 2007;27(5):415–8. https://doi.org/10.1002/pd.1700.
28. Bianchi DW, Chiu RWK. Sequencing of circulating cell-free DNA during pregnancy. N Engl J Med. 2018;379(5):464–73. https://doi.org/10.1056/NEJMra1705345.
29. Lo YM, Tein MS, Lau TK, et al. Quantitative analysis of fetal DNA in maternal plasma and serum: implications for noninvasive prenatal diagnosis. Am J Hum Genet. 1998;62(4):768–75. https://doi.org/10.1086/301800.
30. Taylor-Phillips S, Freeman K, Geppert J, et al. Accuracy of non-invasive prenatal testing using

cell-free DNA for detection of Down, Edwards and Patau syndromes: a systematic review and meta-analysis. BMJ Open. 2016;6(1):e010002. https://doi.org/10.1136/bmjopen-2015-010002.

31. Gil MM, Accurti V, Santacruz B, Plana MN, Nicolaides KH. Analysis of cell-free DNA in maternal blood in screening for aneuploidies: updated meta-analysis. Ultrasound Obstet Gynecol. 2017;50(3):302–14. https://doi.org/10.1002/uog.17484.
32. Wang Y, Li S, Wang W, et al. Cell-free DNA screening for sex chromosome aneuploidies by non-invasive prenatal testing in maternal plasma. Mol Cytogenet. 2020;13(1) https://doi.org/10.1186/s13039-020-0478-5.
33. Lüthgens K, Grati FR, Sinzel M, Häbig K, Kagan KO. Confirmation rate of cell free DNA screening for sex chromosomal abnormalities according to the method of confirmatory testing. Prenat Diagn. 2021;41(10):1258–63. https://doi.org/10.1002/pd.5814.
34. Zhang B, Zhou Q, Chen Y, et al. High false-positive non-invasive prenatal screening results for sex chromosome abnormalities: Are maternal factors the culprit? Prenat Diagn. 2020;40(4):463–9. https://doi.org/10.1002/pd.5529.
35. Norton ME, Jacobsson B, Swamy GK, et al. Cell-free DNA analysis for noninvasive examination of trisomy. N Engl J Med. 2015;372(17):1589–97. https://doi.org/10.1056/NEJMoa1407349.
36. Palomaki GE, Kloza EM. Prenatal cell-free DNA screening test failures: a systematic review of failure rates, risks of Down syndrome, and impact of repeat testing. Genet Med. 2018;20(11):1312–23. https://doi.org/10.1038/gim.2018.22.
37. Bianchi DW, Chudova D, Sehnert AJ, et al. Noninvasive prenatal testing and incidental detection of occult maternal malignancies. J Am Med Assoc. 2015;314(2):162–9. https://doi.org/10.1001/jama.2015.7120.
38. Snyder HL, Curnow KJ, Bhatt S, Bianchi DW. Follow-up of multiple aneuploidies and single monosomies detected by noninvasive prenatal testing: Implications for management and counseling. Prenat Diagn. 2016;36(3):203–9. https://doi.org/10.1002/pd.4778.
39. Carlson LM, Hardisty E, Coombs CC, Vora NL. Maternal malignancy evaluation after discordant cell-free DNA results. Obstet Gynecol. 2018;131(3):464–8. https://doi.org/10.1097/AOG.0000000000002474.
40. Prats P, Rodríguez I, Comas C, Puerto B. Systematic review of screening for trisomy 21 in twin pregnancies in first trimester combining nuchal translucency and biochemical markers: a meta-analysis. Prenat Diagn. 2014;34(11):1077–83. https://doi.org/10.1002/pd.4431.
41. Judah H, Gil MM, Syngelaki A, et al. Cell-free DNA testing of maternal blood in screening for trisomies in twin pregnancy: updated cohort study at 10–14 weeks and meta-analysis. Ultrasound Obstet Gynecol. 2021;58(2):178–89. https://doi.org/10.1002/uog.23648.
42. Palomaki GE, Chiu RWK, Pertile MD, et al. International Society for Prenatal Diagnosis Position Statement: cell free (cf)DNA screening for Down syndrome in multiple pregnancies. Prenat Diagn. 2021;41(10):1222–32. https://doi.org/10.1002/pd.5832.
43. Gregg AR, Skotko BG, Benkendorf JL, et al. Noninvasive prenatal screening for fetal aneuploidy, 2016 update: a position statement of the American College of Medical Genetics and Genomics. Genet Med. 2016;18(10):1056–65. https://doi.org/10.1038/gim.2016.97.
44. Reiff ES, Little SE, Dobson L, Wilkins-Haug L, Bromley B. What is the role of the 11- to 14-week ultrasound in women with negative cell-free DNA screening for aneuploidy? Prenat Diagn. 2016;36(3):260–5. https://doi.org/10.1002/pd.4774.
45. Bardi F, Bosschieter P, Verheij J, et al. Is there still a role for nuchal translucency measurement in the changing paradigm of first trimester screening? Prenat Diagn. 2020;40(2):197–205. https://doi.org/10.1002/pd.5590.
46. Hui L, Pynaker C, Bonacquisto L, et al. Reexamining the optimal nuchal translucency cutoff for diagnostic testing in the cell-free DNA and microarray era: results from the Victorian Perinatal Record Linkage study. Am J Obstet Gynecol. 2021;225(5):527.e1–527.e12. https://doi.org/10.1016/j.ajog.2021.03.050.
47. Yang Y, Muzny DM, Xia F, et al. Molecular findings among patients referred for clinical whole-exome sequencing. JAMA. 2014;312(18):1870. https://doi.org/10.1001/jama.2014.14601.
48. Lord J, McMullan DJ, Eberhardt RY, et al. Prenatal exome sequencing analysis in fetal structural anomalies detected by ultrasonography (PAGE): a cohort study. Lancet (London, England). 2019;393(10173):747–57. https://doi.org/10.1016/S0140-6736(18)31940-8.
49. Petrovski S, Aggarwal V, Giordano JL, et al. Whole-exome sequencing in the evaluation of fetal structural anomalies: a prospective cohort study. Lancet (London, England). 2019;393(10173):758–67. https://doi.org/10.1016/S0140-6736(18)32042-7.
50. Kelley J, McGillivray G, Meagher S, Hui L. Increased nuchal translucency after low-risk noninvasive prenatal testing: What should we tell prospective parents? Prenat Diagn. 2021;41(10):1305–15. https://doi.org/10.1002/pd.6024.
51. Monaghan KG, Leach NT, Pekarek D, Prasad P, Rose NC, ACMG Professional Practice and Guidelines Committee. The use of fetal exome sequencing in prenatal diagnosis: a points to consider document of the American College of Medical Genetics and Genomics (ACMG). Genet Med. 2020;22(4):675–80. https://doi.org/10.1038/s41436-019-0731-7.

52. Salomon LJ, Alfirevic Z, Audibert F, et al. ISUOG updated consensus statement on the impact of cfDNA aneuploidy testing on screening policies and prenatal ultrasound practice. Ultrasound Obstet Gynecol. 2017;49(6):815–6. https://doi.org/10.1002/uog.17483.
53. Familiari A, Boito S, Rembouskos G, et al. Cell-free DNA analysis of maternal blood in prenatal screening for chromosomal microdeletions and microduplications: a systematic review. Prenat Diagn. 2021;41(10):1324–31. https://doi.org/10.1002/pd.5928.
54. Hayward J, Chitty LS. Beyond screening for chromosomal abnormalities: advances in non-invasive diagnosis of single gene disorders and fetal exome sequencing. Semin Fetal Neonatal Med. 2018;23(2):94–101. https://doi.org/10.1016/j.siny.2017.12.002.
55. Chiu EKL, Hui WWI, Chiu RWK. cfDNA screening and diagnosis of monogenic disorders—where are we heading? Prenat Diagn. 2018;38(1):52–8. https://doi.org/10.1002/pd.5207.

10

Threshold, Discriminatory Zone, and "The New Rules"

James M. Shwayder

Abbreviations

CRL	Crown-rump length
hCG	Human chorionic gonadotropin
IUP	Intrauterine pregnancy
mIU/mL	Milli-international units per milliliter
MSD	Mean sac diameter
TVS	Transvaginal sonography

Introduction

Early pregnancy evaluation markedly improved with the introduction of transvaginal sonography (TVS). Our understanding of early pregnancy growth has increased with improved resolution and imaging capabilities. As a result, a reevaluation of the threshold levels, the discriminatory zone, and determination of early pregnancy failure has occurred, with dramatic changes in our recommendations.

Threshold Value

The threshold value is the lowest hCG level at which a normal intrauterine pregnancy (IUP) can be detected. Connolly et al. reevaluated the threshold value in a 2013 manuscript [1]. Previously, threshold values had been reported in the 500–1000 mIU/mL range. Connolly reported a 99% probability of detecting a gestational sac at 390 mIU/mL (Fig. 10.1). Thus, the diagnosis of an IUP can be made earlier than previously assumed. However, this refined capability depends on the sophistication of the ultrasound equipment, the transducer frequency, uterine position and morphology, a patient's body habitus, and the operators experience and ability. Modern ultrasound equipment has higher frequency vaginal probes that detect very early pregnancies. However, a mid-plane, or axial uterus, or one with numerous myomas may make visualization quite difficult. Body habitus may also impact the ability to adequately visualize the pelvic anatomy. If an ultrasound study does not resolve or clarify the clinical situation, referral to an expert sonographer/sonologist with more sophisticated equipment is often of value. Finally, caution is warranted, as these guidelines do not apply to patients with multiple gestations. This is particularly pertinent in patients who have undergone assisted reproduction, since the incidence of twins or higher-degree multiple gestation is increased in this group.

J. M. Shwayder (✉)
Department of Obstetrics and Gynecology, University of Florida, Gainesville, FL, USA
e-mail: jshwayder@ufl.edu

© The Author(s), under exclusive license to Springer Nature Switzerland AG 2023
J. S. Abramowicz, R. E. Longman (eds.), *First-Trimester Ultrasound*,
https://doi.org/10.1007/978-3-031-24133-8_10

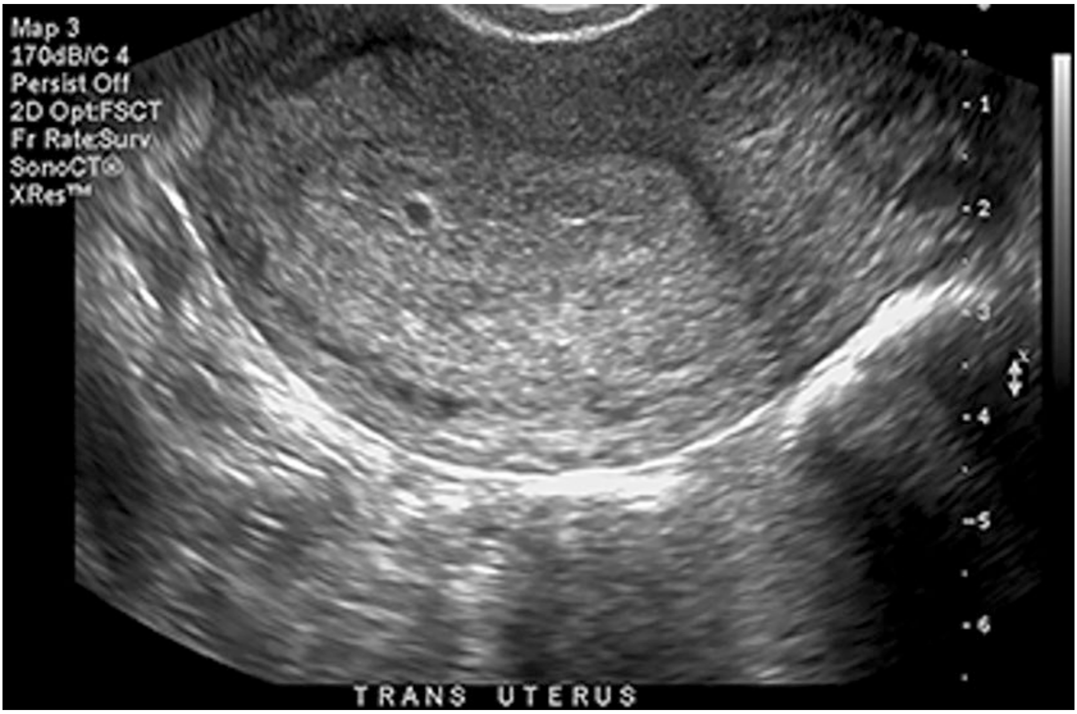

Fig. 10.1 Early gestational sac with hCG = 420 mIU/mL

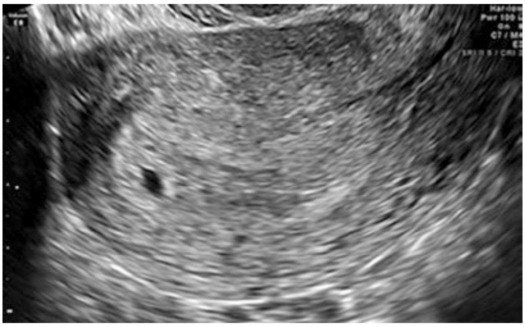

Fig. 10.2 Gestational sac finally visualized when the hCG =1570 mIU/mL

Discriminatory Value

The discriminatory value is that level of hCG above which all normal intrauterine pregnancies should be visualized. An early study, using transabdominal ultrasound, advocated a level of 6500 mIU/mL [2]. Clearly, the introduction of transvaginal sonography revolutionized early pregnancy assessment. In 1987, relatively early in the use of TVS, Nyberg et al. reported that the discriminatory level was 1800 mIU/mL (Third International Standard) [3]. As equipment improved the general consensus was that the discriminatory level was between 1000 and 1500 mIU/mL in most centers. This level has become progressively more important with the adoption of medical management of ectopic pregnancy. Unfortunately, early IUPs have been treated with methotrexate, being erroneously diagnosed as an ectopic pregnancy based on the lack of an intrauterine gestational sac when the hCG is above the discriminatory value. This clearly has both medical and legal implications [4]. The reliance on the previous discriminatory values was contested in a paper by Doubilet and Benson in 2011 [5]. This retrospective review assessed the hCG level in 202 patients evaluated over 10 years, who had a TVS and β-hCG on the same day, no visualized intrauterine fluid collection on their initial study, yet subsequently found to have an intrauterine pregnancy, with embryonic fetal cardiac activity. They found that 10.4% of such pregnancies had an hCG >1500 mIU/mL, with 4.5% having an hCG above 2000 mIU/mL (Fig. 10.2). This challenged the medical community to reevaluate our current hCG discriminatory level. Connolly et al., in 2013, reported on 651 patients with known intrauterine pregnancies who had a TVS and β-hCG within 6 hours of each other. They evaluated the initial ultrasound findings which were visualized 99% of the time, correlated with the hCG level (Table 10.1). They determined that the discriminatory value was 3510 mIU/mL, much higher than previously advocated. It is estimated that women with an hCG above 2000 mIU/ML and no visualized gestational sac are more likely to have a nonviable intrauterine pregnancy (65%) than an ectopic pregnancy (33%), with the remainder (2%) being viable intrauterine pregnancies. Thus, in a patient with a pregnancy of unknown location [6], with an hCG level over 2000 mIU/mL and who is hemodynamically stable, observation and follow-up are recommended until the clinical diagnosis is clarified (Fig. 10.3) [7, 8].

Table 10.1 Threshold and discriminatory values in 99% of intrauterine pregnancies [1]

hCG (mIU/mL)	Gestational sac	Yolk sac	Embryo
Threshold value	390	1094	1394
Discriminatory value	3510	17,716	47,685

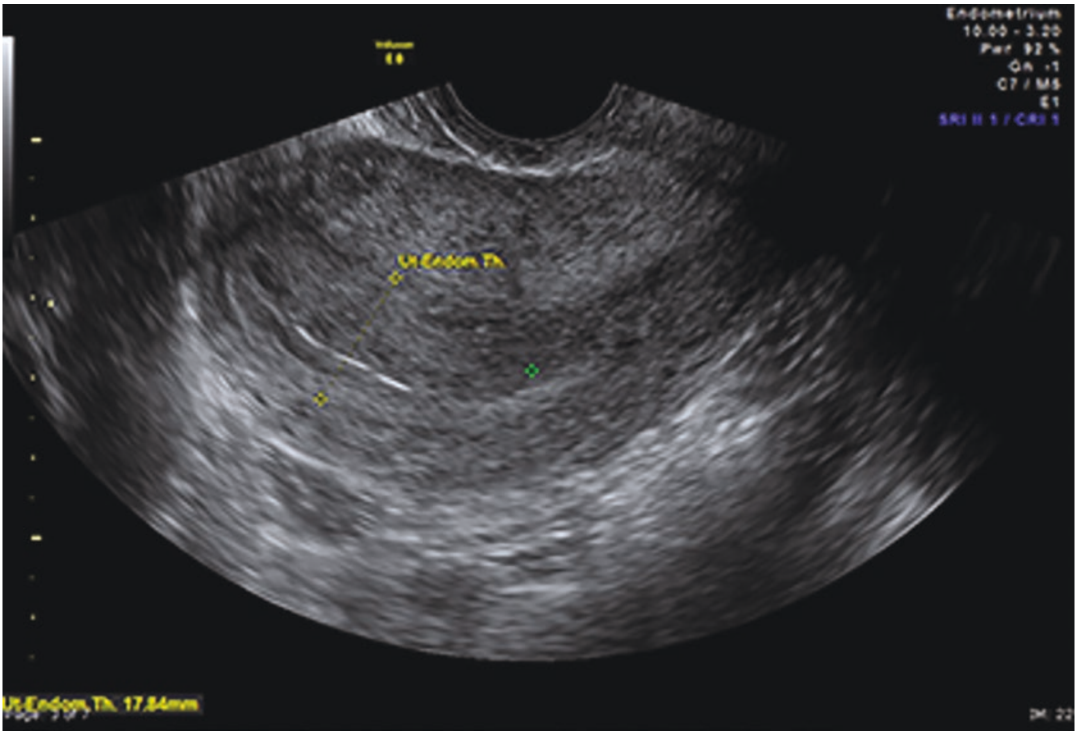

Fig. 10.3 Pregnancy of unknown location with an hCG = 3810 mIU/mL. Patient ultimately had an IUP with a twin gestation

The “New Rules” Regarding Early Pregnancy Failure

Several developmental milestones are observed in normal intrauterine pregnancy, including an intrauterine sac at 5 weeks; a yolk sac at 5.5 weeks, and an embryonic pole and fetal heart activity at 6–6.5 weeks of gestation [9, 10]. Early pregnancy failure was felt to be present when these milestones were not met. However, there is significant inter- and intraobserver variability (±18.78%) in measuring the mean sac diameter, and the crown-rump length [11]. As a result, there are recognized limitations of our current definitions of a non-viable pregnancy based on ultrasound evaluation [12]. Abdallah et al. evaluated 1060 women with a diagnosis of an intrauterine pregnancy of unknown viability, of which 473 (44.6%) remained viable and (55.4%) non-viable by the 11–14-week scan. There was a 4.4% false-positive rate for a non-viable pregnancy using the traditional cut off for mean sac diameter (MSD) of 16 mm. This rate dropped to 0.5% using 20 mm, with no false positives when a MSD of ≥21 mm was used. Considering the inherent variability identified, these authors recommended a discriminatory MSD ≥25 mm, a level where no false positives would be encountered (Fig. 10.4).

The lack of fetal cardiac activity with a crown-rump length (CRL) = 4 or 5 mm had a false-positive rate of 8.3%. There were no false-positive results using a CRL cutoff of 5.3 mm. However, considering the identified variability, they recommended using a CRL ≥7 mm as the discriminatory size for determining a non-viable pregnancy (Fig. 10.5). The authors recommended observation with a repeat ultrasound in ~7 days in hemodynamically stable patients not warranting the more stringent cutoffs identified by their study.

In 2013, a multispecialty panel on early first trimester pregnancy diagnosis was convened to review the literature and make further recom-

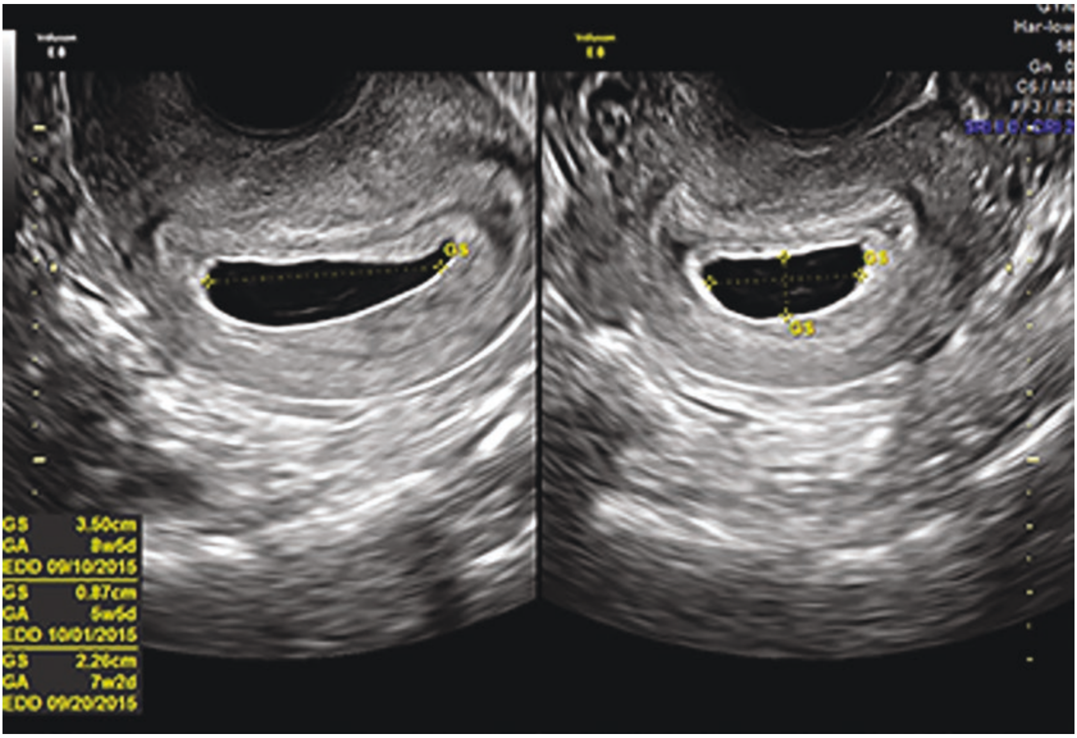

Fig. 10.4 Anembryonic pregnancy with a gestational sac with a mean average diameter of 2.2 cm. No yolk sac or embryo was identified 14 days later

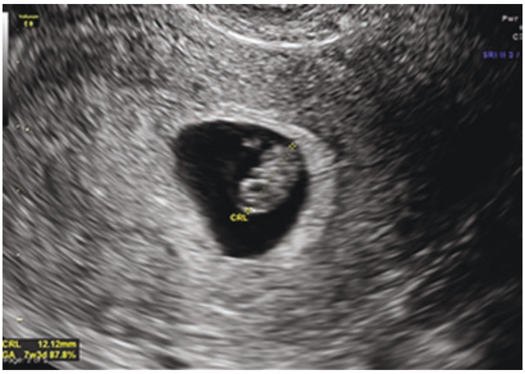

Fig. 10.5 Non-viable pregnancy. CRL = 12.12 mm with no cardiac activity on initial evaluation

Table 10.2 Ultrasound findings *diagnostic* of pregnancy failure [7]

- Crown-rump length of ≥7 mm without cardiac activity
- Mean sac diameter of ≥25 mm without an embryo
- Absence of embryonic cardiac activity ≥11 days after an ultrasound showing a gestational sac with a yolk sac
- Absence of embryonic cardiac activity ≥14 days after an ultrasound showing a gestational sac without a yolk sac

mendations [7]. This panel's goal was to virtually eliminate false-positive results for early pregnancy failure, thus preventing intervention in early viable intrauterine pregnancies. They had similar findings as Abdallah's, recommending cutoffs of ≥2.5 cm for MSD without an embryo, and a crown-rump length ≥7.0 mm without embryonic cardiac activity for defining a non-viable pregnancy. In addition, ultrasound findings diagnostic for pregnancy failure included the absence of an embryo with cardiac activity ≥11 days after demonstrating a gestational sac with a yolk sac, or ≥14 days after demonstrating a gestational sac without a yolk sac (Table 10.2) (Fig. 10.6). They also established criteria that were suspicious, but not diagnostic, of a failed pregnancy (Table 10.3).

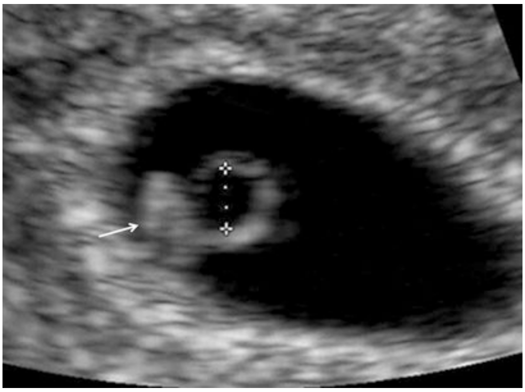

Fig. 10.6 Embryo (arrow) with cardiac activity visualized 10 days. After visualizing a yolk sac with no embryo

Table 10.3 Ultrasound findings *suspicious* for pregnancy failure [7]

- Crown-rump length of <7 mm without cardiac activity
- Mean sac diameter of 16–24 mm without an embryo
- Absence of embryonic cardiac activity 7–10 days after an ultrasound showing a gestational sac with a yolk sac
- Absence of embryonic cardiac activity 7–13 days after an ultrasound showing a gestational sac without a yolk sac
- Absence of an embryo >6 weeks after a sure last menstrual period
- Empty amnion with no visible embryo
- Enlarged yolk sac (>7 mm)
- Small gestational sac in relation to the size of the embryo
  - Defined as <5 mm difference between the MSD and the CRL

Conclusion

Transvaginal sonography has remarkably improved our assessment of early pregnancy. Recent studies have altered our understanding of the ultrasound findings associated with early intrauterine pregnancies, as well as early pregnancy failure. Adopting these revised guidelines will reduce inappropriate treatment of early intrauterine pregnancies with methotrexate and avoid intervening on early intrauterine pregnancies destined for viability.

Teaching Points

- The threshold hCG value for initial visualization of an intrauterine pregnancy ranges between 390 and 1000 mIU/mL.
- The discriminatory value (that level where all intrauterine pregnancies should have an identifiable gestational sac) in identifying an intrauterine pregnancy is higher than previously advocated. The discriminatory level of hCG in diagnosing an intrauterine pregnancy is as high as 3500 mIU/mL.
- The discriminatory level of hCG is higher with multiple pregnancies. Thus, one should exercise additional caution in patients who have undergone assisted reproduction to conceive.
- Findings that confirm pregnancy failure include
  - An embryo with a crown-rump length ≥7 mm and NO cardiac activity.
  - A mean sac diameter of ≥25 mm with NO embryo.
  - Absence of an embryo with a heartbeat ≥2 weeks after an ultrasound revealed a gestational sac without a yolk sac.
  - Absence of an embryo with a heartbeat ≥11 days after an ultrasound revealed a gestational sac with a yolk sac.

References

1. Connolly A, Ryan DH, Stuebe AM, Wolfe HM. Reevaluation of discriminatory and threshold levels for serum β-hCG in early pregnancy. Obstet Gynecol. 2013;121(1):65–70. https://doi.org/10.1097/AOG.0b013e318278f421.
2. Kadar N, DeVore G, Romero R. Discriminatory hCG zone: its use in the sonographic evaluation for ectopic pregnancy. Obstet Gynecol. 1981;58(2):156–61.
3. Nyberg DA, Mack LA, Laing FC, Patten RM. Distinguishing normal from abnormal gestational sac growth in early pregnancy. J Ultrasound Med. 1987;6(1):23–7.
4. Shwayder JM. Waiting for the tide to change: reducing risk in the turbulent sea of liability. Obstet Gynecol. 2010;116(1):8–15.
5. Doubilet PM, Benson CB. Further evidence against the reliability of the human chorionic gonadotropin discriminatory level. J Ultrasound Med. 2011;30(12):1637–42.
6. Barnhart K, van Mello NM, Bourne T, Kirk E, Van Calster B, Bottomley C, et al. Pregnancy of unknown location: a consensus statement of nomenclature, definitions, and outcome. Fertil Steril. 2011;95(3):857–66.
7. Doubilet PM, Benson CB, Bourne T, Blaivas M. Diagnostic criteria for nonviable pregnancy early in the first trimester. N Engl J Med. 2013;15:1443–51.
8. Barbieri RL. Stop using the hCG discriminatory zone of 1,500 to 2,000 mIU/mL to guide intervention during early pregnancy. OBG Manag. 2015;27(1):8–12.
9. Goldstein I, Zimmer E, Tamir A, Peretz B, Paldi E. Evaluation of normal gestational sac growth: appearance of embryonic heartbeat and embryo body movements using the transvaginal technique. Obstet Gynecol. 1991;77(6):885–8.
10. Goldstein SR. Early pregnancy: normal and abnormal. Semin Reprod Med. 2008;26:277–84.
11. Pexsters A, Luts J, Van Schoubroeck D, Bottomley C, Van Calster B, Van Huffel S, et al. Clinical implications of intra- and interobserver reproducibility of transvaginal sonographic measurement of gestational sac and crown-rump length at 6–9 weeks' gestation. Ultrasound Obstet Gynecol. 2011;38(5):510–5.
12. Abdallah Y, Daemen A, Kirk E, Pexsters A, Naji O, Stalder C, et al. Limitations of current definitions of miscarriage using mean gestational sac diameter and crown–rump length measurements: a multicenter observational study. Ultrasound Obstet Gynecol. 2011;38(5):497–502.

Fetal Biometry in Early Pregnancy

11

Lea M. Porche, Steven L. Warsof,
and Alfred Z. Abuhamad

Introduction

Fetal biometry, morphometric measurements of the fetus and gestational structures, has routinely been utilized in the second trimester for the determination of gestational age, estimation of abnormalities in fetal growth and weight, and determining normal and abnormal fetal anatomy. With improvements in ultrasound technology, biometry in the first trimester has become a more accurate and useful tool. Many structures can be measured in the first trimester and are now able to give clues regarding pregnancy location, viability, gestational age, chorionicity in multiple gestations, and the risk of aneuploidy. In this chapter, we will review the assessment of these structures and their significance in the first trimester.[1]

Biometry

Gestational Sac

As the earliest sonographic evidence of intrauterine pregnancy, the gestational sac (GS) can be seen as early as 4 weeks of gestation, just days after the first missed menses [1]. The GS can also be used in early pregnancy for assessment of dating [2]. When seen at 4 weeks, the gestational sac is about 2–3 mm in diameter and in this early phase grows rapidly at a rate of about 1 mm per day [3] (Table 11.1).

One measurement that has been used with high accuracy is the mean sac diameter (MSD). This measurement is obtained by taking the average of the measurements of the GS in three orthogonal planes: coronal, sagittal, and transverse [1]. The MSD is useful early in the first trimester, but loses accuracy for gestational dating when it becomes greater than 14 mm at which time the fetal pole should become visible. When measuring the dimensions of the GS, calipers should be placed on its borders and care should be taken to avoid including the surrounding decidual tissue (Fig. 11.1) [4].

---

[1] See also Chap. 8

L. M. Porche (✉) · S. L. Warsof · A. Z. Abuhamad
Division of Maternal-Fetal Medicine, Department of Obstetrics and Gynecology, Eastern Virginia Medical School, Norfolk, VA, USA
e-mail: porchelm@evms.edu; warsofsl@evms.edu; abuhamaz@evms.edu

© The Author(s), under exclusive license to Springer Nature Switzerland AG 2023
J. S. Abramowicz, R. E. Longman (eds.), *First-Trimester Ultrasound*,
https://doi.org/10.1007/978-3-031-24133-8_11

Table 11.1 Relation between mean sac diameter (MSD) and menstrual age

Mean sac diameter (mm)	Predicted age range (weeks) = 95% CI
2	5.0 (4.5–5.5)
3	5.1 (4.6–5.6)
4	5.2 (4.8–5.7)
5	5.4 (4.9–5.8)
6	5.5 (5.0–6.0)
7	5.6 (5.1–6.1)
9	5.9 (5.4–6.3)
10	6.0 (5.5–6.5)
11	6.1 (5.6–6.6)
12	6.2 (5.8–6.7)
13	6.4 (5.9–6.8)
14	6.5 (6.0–7.0)
15	6.6 (6.2–7.1)
16	6.7 (6.3–7.2)
17	6.9 (6.4–7.3)
18	7.0 (6.5–7.5)
19	7.1 (6.6–7.6)
20	7.3 (6.8–7.7)
21	7.4 (6.9–7.8)
22	7.5 (7.0–8.0)
23	7.6 (7.2–8.1)
24	7.8 (7.3–8.3)

Adapted from Daya S, Wood S, Ward S, et al.: Early pregnancy assessment with transvaginal ultrasound scanning. Can Med Assoc J 144:441, 1991

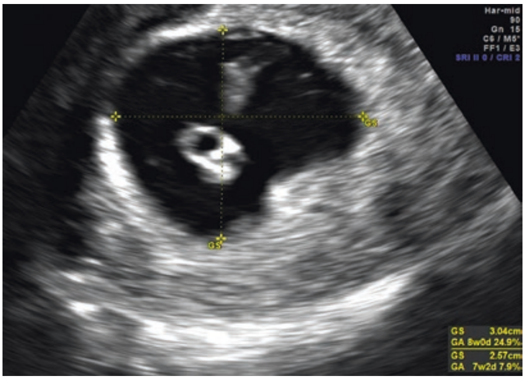

Fig. 11.1 The fetal pole and yolk sac can be seen within this gestational sac. Caliper measurements are taken in the coronal and transverse planes. A third measurement will be taken in the sagittal plane to complete the three required measurements. The fetal crown-rump length will be used for the most accurate dating

Caution must be exercised in differentiating a true gestational sac from a pseudosac or a small intrauterine fluid or blood collection, both of which can be associated with ectopic or failed pregnancies (Fig. 11.2) [1]. A true GS should typically be located eccentrically within the endometrial cavity due to it being embedded within the decidual layer [1]. There should also be evidence of "double ring" sign, which refers to two echogenic rings surrounding the gestational sac. These rings represent the chorionic cavity with its associated villi and the surrounding developing decidua (Fig. 11.3) [5]. If eccentric location of the GS with a double ring sign is not seen in a woman with a positive pregnancy test, a viable intrauterine pregnancy cannot be excluded,

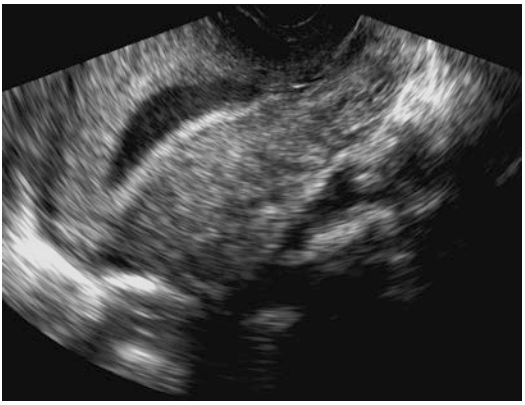

Fig. 11.2 This fluid collection within the uterus is as "pseudo sac" in the setting of an abdominal pregnancy. Note the central location and absence of two echogenic rings. These characteristics help to distinguish this from a true gestational sac associated with viable intrauterine pregnancy

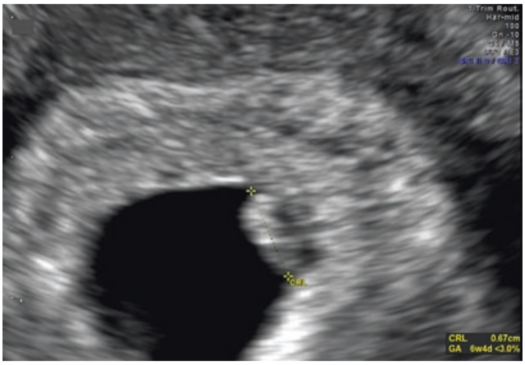

Fig. 11.3 "Double ring sign." The gestational sac can be seen with the yolk sac within (measurement calipers on the yolk sac). The two echogenic rings surrounding the gestational sac are clear in this image

but these findings should raise suspicion for abnormal or extrauterine pregnancy, and close clinical follow-up is indicated [6].

Yolk Sac

The yolk sac (YS) first appears within the GS at 5 weeks of gestation and is frequently the first identifiable structure within the GS [1, 7, 8]. Functioning as the first nutritional and metabolic support to the developing embryo prior to establishment of the placenta, it also offers ultrasonographic confirmation of intrauterine pregnancy [9] (Fig. 11.4).

While usually apparent by week 5 of gestation, the YS may not be visible until later when the MSD is closer to 8 mm [7]. It is connected to the embryo by the vitelline duct. When the amnion forms around the fetus, the YS is then seen as an extra-amniotic structure. The YS progresses in size to a usual maximum of 6 mm around 10 weeks, and then regresses until it is absorbed between the amnion and chorion by the completion of week 12–13 [10]. Measurement of the YS should be performed by placing the calipers on the innermost border of the echogenic rim [11].

Nomograms relating YS size with gestational age have been developed [12] but due to marked variation in normal pregnancies, YS diameter should not be used a primary means of pregnancy dating [10].

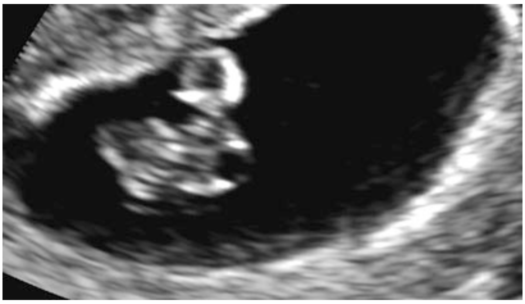

Fig. 11.4 Normal yolk sac. The yolk sac (above) can be seen in close proximity to the fetal pole (below). The hypoechoic developing rhombencephalon can be seen at the right end of the fetal pole

As mentioned previously, the YS offers confirmation of an intrauterine pregnancy, and may even help to indicate amnionicity in multiple gestations, as the number of YSs should correlate with the number of amniotic sacs if the embryos are viable, although it has been reported where this is not true in a small number of cases [8]. This can be particularly important in higher order multiple gestations.

Marked variation in the size and shape of the YS can be noted. These variations may be of clinical significance. A small or large YS (<3 mm prior to 6–10 weeks and >7 mm prior to 9 weeks) may be suspicious for an abnormally developing pregnancy. These cases should be followed up with repeat ultrasound evaluation to confirm progression of the pregnancy [1]. Absence of the YS or embryo in the presence of a MSD of ≥25 mm is diagnostic of a failed pregnancy with specificity and positive predictive value approaching 100% [12]. Echogenic, irregularly shaped or persistent YS, particularly after 12 weeks gestation, is of uncertain significance [13].

Crown-Rump Length

The fetal pole is first visible by transvaginal ultrasound at 5 weeks gestation with cardiac activity notable by 6–6.5 weeks gestation [1]. It is important to note that fetal heart rates can be slower than anticipated in these very early pregnancies, but should be within the normal range of 110–160 beats per minute by 8 weeks gestation.

The first true fetal biometric measurement possible is the crown-rump length (CRL). By definition, the CRL is not actually measured from the fetal crown to its rump, but instead the longest linear dimension from the cephalic to the caudal end of the embryo with the fetus in neutral position (Fig. 11.5). In early gestation, between 6 and 9 weeks, there is little difference between these measurements, but beyond this point, there can be a significant discrepancy.

Obtaining the CRL should be done in a standardized fashion to increase the accuracy of the measurement. A midsagittal section of the embryo should be captured, and the image maxi-

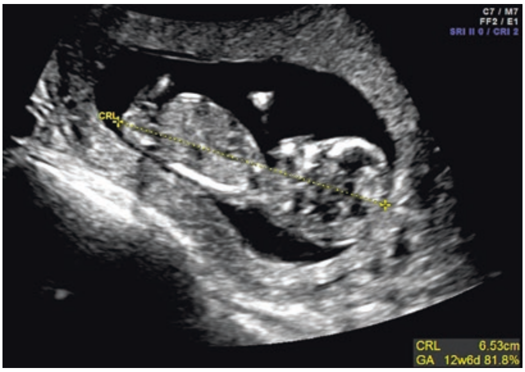

Fig. 11.5 Crown-rump length: Here the calipers are placed at the cephalic and caudal ends of the fetus. This fetus appears to be slightly flexed at the time of measurement

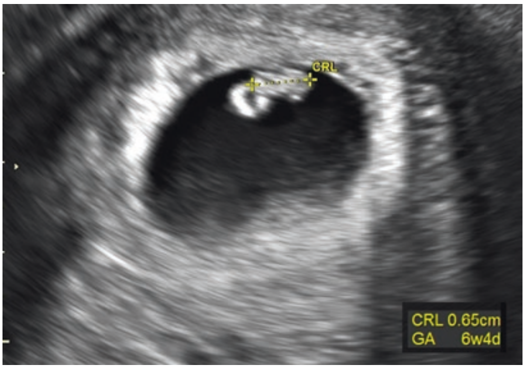

Fig. 11.6 Crown-rump length: This early crown-rump length measurement demonstrates the difficulty in identifying cephalic and caudal ends of the embryo at this early gestational age. Here, the greatest longitudinal measurement is obtained. The yolk sac can be seen in close proximity to the fetal pole

mized to fill the majority of the screen. Care should be taken to attempt capturing this image with the embryo in neutral position, avoiding hyperflexion or extension. The two ends of the embryo should be well defined, and the caliper function on the ultrasound machine used to capture the measurement. In extremely early gestations, the cephalic and caudal ends of the fetus may not be distinguishable. In this scenario, the greatest longitudinal measurement should be obtained [14] (Fig. 11.6).

The primary importance of the CRL measurement is in pregnancy dating. Of the first to pursue the biometric measurement of the fetal pole was Dr. Hugh Robinson who worked with Professor Ian Donald at The Queen Mother's Hospital in Glasgow, Scotland. In early 1970s, he published works that gave validity to the use of ultrasound in the measurement of the early fetal pole. In one study, he evaluated women between 6 and 14 weeks gestation with regular cycles and known last menstrual periods by B-mode transabdominal ultrasound techniques [15]. He plotted his measurements against menstrual age, and in those with missed abortion, against the physical measurement of the conceptus after delivery. He noted a high degree of correlation between ultrasound measurements and menstrual age in both groups. Despite the most rudimentary of ultrasound equipment, his meticulous measurements have stood the test of time and are still used over 50 years later. Hence, first-trimester ultrasound with measurement of CRL is still considered the most reliable method of pregnancy dating with known and unknown last menstrual period. More recently, the accuracy of transvaginal ultrasound as a means for pregnancy dating was confirmed in a study by Pexters et al. showing that in 54 patients, CRL and MSD measurements showed high inter- and intra-observer correlation and were highly reproducible [16].

Many studies have been completed in different populations to assess the ability to generalize these initial nomograms. One such study was performed by Papageorghiou et al. in 8 geographically different countries. Data from 4265 women were included to determine an equation that would be generalizable to multiple populations [17]. Many nomograms for CRL have been developed over the years. Based on the population, prediction equations can differ significantly. For example, the CRL curves developed by Robinson and Pexsters differ at very early gestations, but are very similar after approximately 8 weeks. Most published CRL curves differ very little from the measurement published by Dr. Robinson in 1973 (Tables 11.2 and 11.3).

Measurement of CRL can routinely be completed via transvaginal ultrasound by 6 weeks of gestation. When measured between weeks 7 and 10, CRL is proven to be accurate within 3 days of actual gestational age [15, 18]. However between

Table 11.2 Gestational age estimation by Crown-Rump Length—Robinson (CRL)

Fetal CRL (mm)	Gestational age (weeks + days)
5	6 + 0
10	7 + 1
15	7 + 6
20	8 + 4
25	9 + 2
30	9 + 6
35	10 + 2
40	10 + 6
45	11 + 2
50	11 + 5
55	12 + 1
60	12 + 3
65	12 + 6
70	13 + 1
75	13 + 4
80	13 + 6
85	14 + 1
Formula	GA (days) = 8.052 × (CRL × 1.037)1/2 + 23.73

Adapted from Robinson HP, Fleming JE. A critical evaluation of sonar "crown-rump length" measurements. Br J Obstet Gynaecol 1975; 82:702–10

Table 11.3 Gestational age estimation by Crown-Rump Length (CRL)—Pexsters

Mean CRL (mm)	Gestational age (weeks + days)
0.4	5 + 5
1.1	5 + 6
1.9	6 + 0
2.7	6 + 1
3.5	6 + 2
4.3	6 + 3
5.2	6 + 4
6.1	6 + 5
7.0	6 + 6
8.0	7 + 0
8.9	7 + 1
9.9	7 + 2
10.9	7 + 3
12.0	7 + 4
13.1	7 + 5
14.2	7 + 6
15.3	8 + 0
16.4	8 + 1
17.6	8 + 2
18.8	8 + 3
20.0	8 + 4
21.2	8 + 5
22.5	8 + 6
23.8	9 + 0
25.1	9 + 1
26.4	9 + 2
27.8	9 + 3
29.2	9 + 4
30.6	9 + 5
32.0	9 + 6
33.5	10 + 0
35.0	10 + 1
36.5	10 + 2
38.1	10 + 3
39.6	10 + 4
41.2	10 + 5
42.8	10 + 6
44.5	11 + 0
46.1	11 + 1
47.8	11 + 2
49.5	11 + 3
51.3	11 + 4
53.0	11 + 5
54.8	11 + 6
56.6	12 + 0
58.5	12 + 1
60.3	12 + 2
62.2	12 + 3
64.1	12 + 4
66.1	12 + 5
68.0	12 + 6
70.0	13 + 0
72.0	13 + 1
74.0	13 + 2
76.1	13 + 3
78.2	13 + 4
80.3	13 + 5
82.4	13 + 6
84.6	14 + 0

Adapted from Pexsters, et al. New crown-rump length curve based on over 3500 pregnancies. Ultrasound Obstet Gynecol 2010; 35: 650–655

10 and 14 weeks, the accuracy decreases slightly to a margin of ±5 days [19], and with the addition of just one more week, the accuracy at 15 weeks gestation is as wide as ±8 days [20]. This reinforces the fact that for the most accurate pregnancy dating, CRL should be measured between 7 and 10 weeks of gestation. Of note, once the CRL measures beyond 84 mm (about 14 weeks gestation), the biparietal diameter (BPD) has

Table 11.4 Guidelines for redating pregnancy based on ultrasound in first trimester

Gestational age range (weeks + days)	Method of measurement	Discrepancy between ultrasound dating and LMP dating that supports redating
≤13 + 6	CRL	
• ≤8 + 6 • 9 + 0 to 13 + 6		More than 5 days More than 7 days
14 + 0 to 15 + 6	BPD, HC, AC, FL	More than 7 days
16 + 0 to 21 + 6	BPD, HC, AC, FL	More than 10 days

Adapted from ACOG Committee Opinion 611: Method for Estimating Due Date, October 2014

been proven to be more accurate in pregnancy dating [15]. While many complex formulas have been determined, an easy formula to correlate gestational age with CRL from 7 to 14 weeks gestation is

$$\mathrm{GA}(\mathrm{weeks}) = 6.5 + \mathrm{CRL}(\mathrm{cm})$$

When assigning a due date for early pregnancy, the American College of Obstetricians and Gynecologist (ACOG) has published criteria regarding what degree of discrepancy warrants a change in assigned due date. In the first trimester prior to 9 weeks gestation, the due date should be reassigned if the discrepancy between the ultrasound and menstrual dating is ±5 days. Between 9 and 15+6 weeks, dating should be reassigned based on a discrepancy of ±7 days [21, 22] (Table 11.4).

Nuchal Translucency

The importance of the nuchal translucency (NT) measurement in fetal medicine was first recognized by the pioneering work of Professor Kypros Nicolaides, MD in the mid-1990s at King's College Hospital in London, UK. Measurement of the nuchal translucency is now recommended as an option for patients as a part of first trimester screening for aneuploidy [23]. One element of the first trimester screening exam, the NT measurement is combined with levels of maternal serum beta human chorionic gonadotropin (beta HCG) and pregnancy-associated plasma protein-A (PAPP-A) [24]. These parameters together with maternal age give a patient-specific risk for trisomy 21 and 18. For trisomy 21, the detection rate is 85% with a 5% false positive rate, which is higher than the detection rate in the second trimester using multiple maternal serum markers alone [25].

The NT is a hypoechoic structure located under the skin on the posterior fetal neck that represents fluid collection in that space [1] (Fig. 11.7). This structure can be identified and measured in all normal pregnancies, but the measurement is increased in cases of fetal aneuploidy, other genetic conditions, or congenital heart disease. In monochorionic twins, intertwin discrepancies in the NT measurement have been associated with early evidence of twin-twin transfusion syndrome [26].

There are multiple theories regarding the etiology of increased NT measurements. In trisomy 21, dermal collagen has more hydrophilic properties, trapping fluid in the subcutaneous tissues [3]. In Turner syndrome, dysplastic lymphatics are credited with obstruction of the normal flow of fluid out of this space. Abnormal lymphatic drainage can also arise in the absence of Turner syndrome leading to increased NT, enlarged jugular venous sacs, and subsequent increase in venous pressure that can be detected as decreased

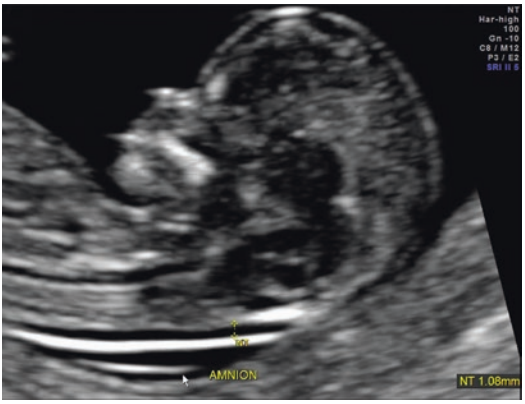

Fig. 11.7 Normal NT Measurement: Here a normal NT measurement can be seen with all criteria met. Note the amnion that is clearly seen as separate from the posterior margin of the nuchal fluid collection

or absent flow in the ductus venosus [27, 28]. Finally, it has been seen that an enlarged NT can be associated with congenital cardiac disease, especially ventricular septal defects. It is postulated that endothelial dysfunction is responsible for the appearance of these two abnormalities together. Importantly, it has not been proven that an enlarged NT measurement is a sign of cardiac failure and it should not be considered a marker for hydrops [29] (Fig. 11.8).

Similarly, a cystic hygroma arises from obstruction of lymphatic flow into the venous system, often leading to concomitant distention of the jugular venous sacs. Depending on the size of the cystic hygroma, it may be difficult to differentiate from an enlarged NT. While an enlarged NT is usually confined to the cervical region, cystic hygromas are usually larger and extend beyond the neck. They also often contain septations that make their appearance differ from that of an enlarged NT [30] (Fig. 11.9a, b). Care should be taken not to confuse posterior neural tube defects, such as a posterior encephalocele, with a cystic hygroma, as they can be similar in appearance [27].

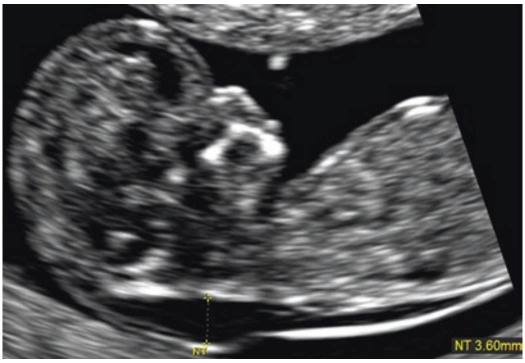

Fig. 11.8 Enlarged NT measurement: The enlarged NT can be well seen in this image. Note that the measurement is taken at the largest portion of the fluid collection

The differential diagnosis for conditions associated with an enlarged NT can be seen in Table 11.5. Enlargement of the NT measurement is defined in most settings as an NT measurement above the 95th percentile for gestational age or ≥3 mm [23].

Accurate acquisition of the NT measurement is of great importance. In fact, no other ultrasound measurement requires the same degree of precision needed for accurate assessment of aneuploidy risk. The measurement should be obtained between 11 and 13+6 week gestation which is equivalent to a CRL of 45–84 mm [14]. Images can be obtained transvaginally or transabdominally using a high-resolution ultrasound machine. A magnified midsagittal section through the head and upper torso must be obtained and captured with the fetus in neutral position. The echogenic tip of the fetal nose is an indicator that one is imaging through this midsagittal plane. The amnion, which has not yet fused with the chorion at this gestational age, should be visualized to ensure that the measure-

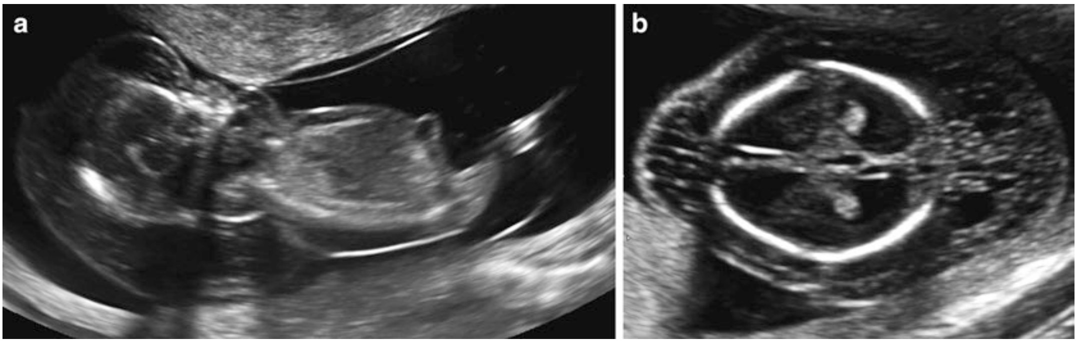

Fig. 11.9 (**a**) Cystic hygroma: Sagittal view of a fetus with a cystic hygroma. This fluid collection is not confined to the posterior cervical region, but instead extends cephalad to the face and caudad to the sacrum and legs. In this image, the fetal head is on the left, and the legs and pelvis are to the right. (**b**) Cystic hygroma: An axial view of the same cystic hygroma. The bones of the calvarium can be seen with surrounding increase in soft tissue and fluid. Posteriorly (right), fluid pockets, and septations can be seen

Table 11.5 Differential diagnosis for enlarged nuchal translucency (NT)

Aneuploidy
• Trisomy 21
• Trisomy 13
• Trisomy 18
• Monosomy X
• Triploidy
Structural anomalies
• Cardiac defects
• Diaphragmatic hernia
• Renal anomalies
• Body stalk disruption
• Abdominal wall defects
Genetic Syndromes[a]
• Noonan syndrome
• Roberts syndrome
• Cornelia de Lange syndrome
• Congenital adrenal hyperplasia
• Spinal muscular atrophy
• DiGeorge syndrome
• Smith-Lemli-Opitz syndrome
• Various skeletal dysplasias
Increased risk of twin-to twin transfusion syndrome

Adapted from Simpson LL. First trimester cystic hygroma and increased nuchal translucency, UpToDate 2014

[a] Not a comprehensive list

ment is only of the NT and does not include intraamniotic fluid. The calipers should be placed on the inner margins of the thickest portion of the NT and this is where the measurement should be obtained. If multiple adequate images are obtained, the largest measurement should be used for determination of risk, not an average of the measurements [14]. The criteria needed to obtain an accurate NT are shown in Table 11.6. With such extensive criteria, it is possible that a NT measurement cannot always be obtained. Some limiting factors are fetal position and maternal body habitus. If the NT cannot be obtained and first trimester screening cannot be completed, the patient should be offered alternative risk assessment for aneuploidy commensurate with her clinical scenario.

It is also important that a practice seeking to perform NT measurements is adequately equipped to acquire accurate images and to manage any abnormalities diagnosed. High-resolution ultrasound equipment should be available for use. Special training, certification, and maintenance of certification for those obtaining and interpreting the image are also required. Finally, appropriate counseling and follow-up strategies should be in place to address abnormal results [14].

Table 11.6 Guidelines for measurement of nuchal translucency (NT)

• Margins of NT clear enough for proper caliper placement
• Fetus in midsagittal plane
• Image magnified to be filled with fetal head, neck, and upper thorax
• Fetal neck in neutral position
• Amnion must be seen separate from the NT
• Calipers must be used for measurement
• Calipers must be placed on the inner border of the nuchal line space with none of the horizontal crossbar protruding into the space
• Calipers placed perpendicular to the long axis of the fetus
• Measurement obtained at the widest space of the NT

Adapted from the AIUM Practice Guideline for the performance of Obstetric Ultrasound Examinations, 2013

Follow-up of high-risk first trimester screening is of utmost importance in patient management. Genetic counseling should be made available so that patients can explore all available options for genetic testing. Those wanting a low stakes but more definitive assessment of their risk can undergo a second screening test by evaluation of maternal cell-free DNA that yields a sensitivity of 99% with a false positive rate of 1%. Cell-free DNA has replaced NT measurement for the sole purpose of aneuploidy screening in many populations, but does not diminish the additional information gained by the assessment of the NT. Early in the first trimester prior to fusion of the chorion and amnion, the most common diagnostic test that is offered is chorionic villus sampling for direct evaluation of karyotype. Comparative genetic hybridization (CGH) studies can also be done to identify subchromosomal abnormalities at the same time. Later in the early second trimester, once the amnion and chorion have fused, amniocentesis can be performed to obtain fetal cells for karyotype and CGH. If aneuploidy is unable to be ruled out with diagnostic testing, close ultrasound surveillance should be undertaken with detailed anatomic survey and fetal echocardiography in the second trimester [3]. Details on aneuploidy screening are available in Chap. 9.

Nasal Bone

The absence of the nasal bone (NB) is considered a soft marker for aneuploidy. A soft marker is a sonographic finding that in and of itself is not clinically significant, but can be associated with a fetal condition. It is not considered diagnostic of said fetal condition [31]. In the midsagittal plane, the NB is seen as a bright line of greater echogenicity than the skin (Fig. 11.10). The presence of the NB is best assessed at a CRL between 65 and 84 mm correlating to a gestational age of 13 to 13+5 weeks [32]. Criteria for measurement of the nasal bone can be seen in Table 11.7.

A hypoplastic or absent NB has been associated with trisomy 21. One publication reviewed over 35,000 NB examinations from 9 different studies and showed that the NB was absent in 65% of fetuses with trisomy 21 but only in 0.8% of chromosomally normal fetuses [33]. In the second trimester, this marker becomes less predictive with absent NB seen in 30–40% of fetuses with trisomy 21 and 0.3–0.7% of chromosomally normal fetuses [34].

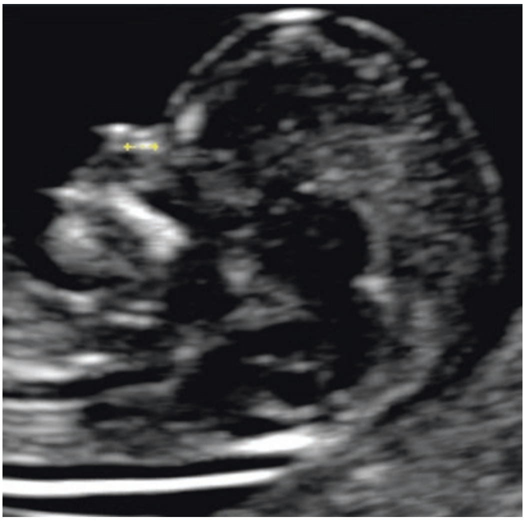

Fig. 11.10 Nasal bone: The hyperechoic nasal tip and skin can be seen with a normal nasal bone noted underneath. The angle of insonation is correct in this image. Note the additional landmark of the rectangular hard palate seen inferior to the nasal bone

Table 11.7 Guidelines for measurement of nasal bone NB

- Measured from 11 to 13+6 weeks gestation
- Fetal head, neck, and thorax should occupy the entire image
- Measured in the midsagittal view
  - Echogenic tip of nose should be seen
  - Third and fourth ventricle seen
  - Rectangular palate should be seen
- Angle of insonation ~45° to fetal profile
- Brightness of NB equal to or greater than overlying skin

Adapted from The Fetal Medicine Foundation, www.fetalmedicine.org

Different methods of reporting observations of the NB yield different results. Some report the NB categorically as “present” or “absent” while others measure it and report whether it is hypoplastic. Absent NB in the second trimester was seen in 30–40% of fetuses with trisomy 21 and 0.3–0.7% of chromosomally normal fetuses. By considering NB hypoplasia or absent nasal bone as a single category, the finding was seen in 50–60% of fetuses with trisomy 21 and 6–7% of chromosomally normal fetuses [34]. Other ways to report hypoplasia of the NB include an absolute cutoff of <2.5 mm, gestational age-related cutoff of <2.5th or <5th percentile, a ratio of BPD/NB length or multiples of the median for gestational age with <0.75 MoM being the cutoff for abnormal NB measurement [35, 36].

It is noteworthy that there is natural variation in the appearance of the NB. Absence of the NB at or before 13 weeks gestation can be a result of delayed ossification instead of absence or hypoplasia [37]. Similarly, ethnic variations exist in the presence and size of the nasal bone. In a study by Cicero et al., the likelihood ratio for trisomy 21 with an absent NB was higher in Caucasian women than in Afro-Caribbean women (likelihood ration of 31 vs. 9) [38]. These variations reinforce that assessment of the NB should not be used in isolation for diagnosis of trisomy 21. On the contrary, it has been used in combination with first trimester serum screening and NT measurement to increase the detection of trisomy 21 to 90% improved compared to the 85% of first trimester combined screening alone [39].

Other Biometric Measurements

Four other biometric measurements are used in the second trimester to estimate gestational age or fetal weight. These measurements include the biparietal diameter (BPD), head circumference (HC), abdominal circumference (AC), and femur length (FL). The combination of these four measurements for dating and estimation of fetal weight is usually begun starting at 14 weeks gestation, but there is some utility in measuring these parameters in the first trimester.

The measurement of BPD can be useful in the later portions of the first trimester when CRL measurements may be less accurate [18]. This decrease in the accuracy of the CRL may be due to normal changes in embryonic and fetal posture that can distort the CRL measurement. Head circumference can similarly be used in this scenario [40].

A BPD that is inconsistent with expected size may also be an indicator of fetal anomaly. Two studies have reported that small BPD values less than the 5th to 10th percentile may be associated with subsequent diagnosis of open spina bifida [41, 42].

By 10 weeks gestation, the femur can be identified and measured. Its measurement is usually accurate within 1 week of the fetus's true gestational age before 20 weeks gestation [40]. This makes it an ideal parameter for quick estimation of gestational age, but care must be taken in order to obtain an accurate measurement. One should be able to see the femoral head or greater trochanter proximally and the femoral condyle distally, and measurement should only include the ossified portion of the bone [43]. This measurement should not be taken in isolation, as it is known that there are some normal variations between ethnic groups. A FL less than the 5th percentile may also be a marker of aneuploidy (such as in trisomy 21) or an early indicator of fetal skeletal dysplasia or early growth restriction [44, 45].

Conclusion

Fetal biometry in the first trimester is important, as it is our first evaluation regarding the health of a pregnancy. It can give clues regarding risk of fetal anomalies and aneuploidy. Understanding normal and abnormal measurements allows the clinician to accurately evaluate aberrations of early pregnancy and to counsel patients about physiologic and pathologic findings.

Teaching Points

- The gestational sac is the earliest ultrasound finding of an intrauterine pregnancy.
- First trimester ultrasound evaluation is useful in identification of ectopic pregnancies.
- Failure of appropriate growth of GS and CRL is associated with early pregnancy failure.
- First trimester measurement of the CRL is the most accurate ultrasound method of determining gestational age and EDC.
- Measurement of the nuchal translucency from 10 to 14 weeks gestation in combination with serum markers can be used for risk assessment for fetal aneuploidy.

References

1. Abuhamad A, editor. Ultrasound in obstetrics and gynecology: a practical approach. Thieme; 2014.
2. American Institute of Ultrasound in Medicine. AIUM practice guideline for the performance of obstetric ultrasound examinations. 2018 [Nov 4 2021]. http://www.aium.org/resources/guidelines/obstetric.pdf.
3. Simpson L. First trimester cystic hygroma and increased nuchal translucency. Waltham, MA: Up To Date; 2014. [Updated Dec 30 2014; cited 2015 Jan 22 2015].
4. Laing FC, Frates MC. Sonographic determination of menstrual age. In: Callen PW, editor. Ultrasonography in obstetrics and gynecology. 4th ed. Philadelphia, PA: WB Saunders Co.; 2000.
5. Bradley WG, Fiske CE, Filly RA. The double sac sign of early intrauterine pregnancy: use in exclusion of ectopic pregnancy. Radiology. 1982;143(1):223–6.
6. Doubilet PM, Benson CB. Double sac sign and intradecidual sign in early pregnancy: interobserver reliability and frequency of occurrence. J Ultrasound Med. 2013;32(7):1207–14.
7. Bree RL, Edwards M, Bohm-Velez M, Beyler S, Roberts J, Mendelson EB. Transvaginal sonogra-

phy in the evaluation of normal early pregnancy: correlation with HCG level. AJR Am J Roentgenol. 1989;153(1):75–9.

8. Tan S, Pektas MK, Arslan H. Sonographic evaluation of the yolk sac. J Ultrasound Med. 2012;31(1):87–95.
9. Makikallio K, Tekay A, Jouppila P. Yolk sac and umbilicoplacental hemodynamics during early human embryonic development. Ultrasound Obstet Gynecol. 1999;14(3):175–9.
10. Stampone C, Nicotra M, Muttinelli C, Cosmi EV. Transvaginal sonography of the yolk sac in normal and abnormal pregnancy. J Clin Ultrasound. 1996;24(1):3–9.
11. Jauniaux E, Jurkovic D, Henriet Y, Rodesch F, Hustin J. Development of the secondary human yolk sac: correlation of sonographic and anatomical features. Hum Reprod. 1991;6(8):1160–6.
12. Doubilet PM, Benson CB, Bourne T, Blaivas M, Society of Radiologists in Ultrasound Multispecialty Panel on Early First Trimester Diagnosis of Miscarriage and Exclusion of a Viable Intrauterine Pregnancy, et al. Diagnostic criteria for nonviable pregnancy early in the first trimester. N Engl J Med. 2013;369(15):1443–51.
13. Tan S, Ipek A, Pektas MK, Arifoglu M, Teber MA, Karaoglanoglu M. Irregular yolk sac shape: is it really associated with an increased risk of spontaneous abortion? J Ultrasound Med. 2011;30(1):31–6.
14. Salomon LJ, Alfirevic Z, Bilardo CM, Chalouhi GE, Ghi T, Kagan KO, et al. ISUOG practice guidelines: performance of first-trimester fetal ultrasound scan. Ultrasound Obstet Gynecol. 2013;41(1):102–13.
15. Robinson HP. Sonar measurement of fetal crown-rump length as means of assessing maturity in first trimester of pregnancy. Br Med J. 1973;4(5883):28–31.
16. Pexsters A, Luts J, Van Schoubroeck D, Bottomley C, Van Calster B, Van Huffel S, et al. Clinical implications of intra- and interobserver reproducibility of transvaginal sonographic measurement of gestational sac and crown-rump length at 6–9 weeks' gestation. Ultrasound Obstet Gynecol. 2011;38(5):510–5.
17. Papageorghiou AT, Kennedy SH, Salomon LJ, Ohuma EO, Cheikh Ismail L, Barros FC, et al. International standards for early fetal size and pregnancy dating based on ultrasound measurement of crown-rump length in the first trimester of pregnancy. Ultrasound Obstet Gynecol. 2014;44(6):641–8.
18. Goldstein SR, Wolfson R. Endovaginal ultrasonographic measurement of early embryonic size as a means of assessing gestational age. J Ultrasound Med. 1994;13(1):27–31.
19. MacGregor SN, Tamura RK, Sabbagha RE, Minogue JP, Gibson ME, Hoffman DI. Underestimation of gestational age by conventional crown-rump length dating curves. Obstet Gynecol. 1987;70(3 Pt 1):344–8.
20. Hadlock FP, Shah YP, Kanon DJ, Lindsey JV. Fetal crown-rump length: reevaluation of relation to menstrual age (5–18 weeks) with high-resolution real-time US. Radiology. 1992;182(2):501–5.
21. American College of Obstetricians and gynecologists. Committee Opinion No. 611. Method for estimating due date. Obstet Gynecol. 2014;124(4):863–6.
22. Reddy UM, Abuhamad AZ, Levine D, Saade GR, Fetal Imaging Workshop Invited Participants. Fetal imaging: executive summary of a joint Eunice Kennedy Shriver National Institute of Child Health and Human Development, Society for Maternal-Fetal Medicine, American Institute of Ultrasound in Medicine, American College of Obstetricians and Gynecologists, American College of Radiology, Society for Pediatric Radiology, and Society of Radiologists in Ultrasound Fetal Imaging Workshop. J Ultrasound Med. 2014;33(5):745–57.
23. Nicolaides KH, Azar G, Byrne D, Mansur C, Marks K. Fetal nuchal translucency: ultrasound screening for chromosomal defects in first trimester of pregnancy. BMJ. 1992;304(6831):867–9.
24. Reddy UM, Mennuti MT. Incorporating first-trimester Down syndrome studies into prenatal screening: executive summary of the National Institute of Child Health and Human Development workshop. Obstet Gynecol. 2006;107(1):167–73.
25. Wald NJ, Hackshaw AK. Combining ultrasound and biochemistry in first-trimester screening for Down's syndrome. Prenat Diagn. 1997;17(9):821–9.
26. Cleary-Goldman J, D'Alton ME, Berkowitz RL. Prenatal diagnosis and multiple pregnancy. Semin Perinatol. 2005;29(5):312–20.
27. Bekker MN, Haak MC, Rekoert-Hollander M, Twisk J, Van Vugt JM. Increased nuchal translucency and distended jugular lymphatic sacs on first-trimester ultrasound. Ultrasound Obstet Gynecol. 2005;25(3):239–45.
28. Haak MC, Twisk JW, Bartelings MM, Gittenberger-de Groot AC, van Vugt JM. Ductus venosus flow velocities in relation to the cardiac defects in first-trimester fetuses with enlarged nuchal translucency. Am J Obstet Gynecol. 2003;188(3):727–33.
29. Haak MC, Twisk JW, Bartelings MM, Gittenberger-de Groot AC, van Vugt JM. First-trimester fetuses with increased nuchal translucency do not show altered intracardiac flow velocities. Ultrasound Obstet Gynecol. 2005;25(3):246–52.
30. Malone FD, Ball RH, Nyberg DA, Comstock CH, Saade GR, Berkowitz RL, et al. First-trimester septated cystic hygroma: prevalence, natural history, and pediatric outcome. Obstet Gynecol. 2005;106(2):288–94.
31. Morris JK, Wald NJ, Watt HC. Fetal loss in Down syndrome pregnancies. Prenat Diagn. 1999;19(2):142–5.
32. Ville Y. What is the role of fetal nasal bone examination in the assessment of risk for trisomy 21 in clinical practice? Am J Obstet Gynecol. 2006;195(1):1–3.
33. Rosen T, D'Alton ME, Platt LD, Wapner R, Nuchal Translucency Oversight Committee Maternal Fetal Medicine Foundation. First-trimester ultrasound assessment of the nasal bone to screen for aneuploidy. Obstet Gynecol. 2007;110(2 Pt 1):399–404.

34. Moreno-Cid M, Rubio-Lorente A, Rodriguez MJ, Bueno-Pacheco G, Tenias JM, Roman-Ortiz C, et al. Systematic review and meta-analysis of performance of second-trimester nasal bone assessment in detection of fetuses with Down syndrome. Ultrasound Obstet Gynecol. 2014;43(3):247–53.
35. Cicero S, Sonek JD, McKenna DS, Croom CS, Johnson L, Nicolaides KH. Nasal bone hypoplasia in trisomy 21 at 15–22 weeks' gestation. Ultrasound Obstet Gynecol. 2003;21(1):15–8.
36. Odibo AO, Sehdev HM, Stamilio DM, Cahill A, Dunn L, Macones GA. Defining nasal bone hypoplasia in second-trimester Down syndrome screening: does the use of multiples of the median improve screening efficacy? Am J Obstet Gynecol. 2007;197(4):361.e1–4.
37. Benacerraf B. Sonographic findings associated with fetal aneuploidy. Waltham, MA: Up To Date; 2014. [updated Sep 10 2014; cited 2015 Jan 22 2015]
38. Cicero S, Rembouskos G, Vandecruys H, Hogg M, Nicolaides KH. Likelihood ratio for trisomy 21 in fetuses with absent nasal bone at the 11–14-week scan. Ultrasound Obstet Gynecol. 2004;23(3):218–23.
39. Cicero S, Avgidou K, Rembouskos G, Kagan KO, Nicolaides KH. Nasal bone in first-trimester screening for trisomy 21. Am J Obstet Gynecol. 2006;195(1):109–14.
40. Filly RA. Sonographic determination of menstrual age. In: Callen PW, editor. Ultrasonography in obstetrics and gynecology. 4th ed. Philadelphia, PA: WB Saunders Co.; 2000.
41. Karl K, Benoit B, Entezami M, Heling KS, Chaoui R. Small biparietal diameter in fetuses with spina bifida on 11–13-week and mid-gestation ultrasound. Ultrasound Obstet Gynecol. 2012;40(2):140–4.
42. Khalil A, Coates A, Papageorghiou A, Bhide A, Thilaganathan B. Biparietal diameter at 11–13 weeks' gestation in fetuses with open spina bifida. Ultrasound Obstet Gynecol. 2013;42(4):409–15.
43. Goldstein RB, Filly RA, Simpson G. Pitfalls in femur length measurements. J Ultrasound Med. 1987;6(4):203–7.
44. Papageorghiou AT, Fratelli N, Leslie K, Bhide A, Thilaganathan B. Outcome of fetuses with antenatally diagnosed short femur. Ultrasound Obstet Gynecol. 2008;31(5):507–11.
45. Weisz B, David AL, Chitty L, Peebles D, Pandya P, Patel P, et al. Association of isolated short femur in the mid-trimester fetus with perinatal outcome. Ultrasound Obstet Gynecol. 2008;31(5):512–6.

The Fetal Heart in Early Pregnancy

12

Edgar Hernandez-Andrade and Erin S. Huntley

Introduction

Congenital heart defects (CHD) are the most frequent fetal anomalies during pregnancy [1, 2]. The prevalence of CHDs can be estimated at 8–12 per 1000 live births with some minor variations in relation to the types of cardiac defects [3]. CHDs are more frequently seen in fetuses with chromosomal and other congenital anomalies [4]. Major CHDs increase the risk of perinatal death and can be identified before birth, whereas minor CHDs may not increase the risk of mortality but are difficult to diagnose prenatally. Minor cardiac defects are usually undiagnosed unless clinical manifestations are present after birth [5]. Some cardiac anomalies evolve during pregnancy and became more apparent in later stages of pregnancy [6, 7], while others, as muscular interventricular septal defects, may resolve before delivery [8]. All these factors have an impact in the different detection rates reported in the literature.

First trimester ultrasound was originally proposed as a screening test to identify fetuses at risk of chromosomal anomalies by identification of indirect ultrasound markers [9]. This approach has changed in recent years as noninvasive prenatal testing (NIPT), or quantification of cell-free fetal DNA in maternal blood, has become the gold standard to identify fetuses at risk of aneuploidies [10]. These advances have challenged the utility of sonographic markers such as the nuchal translucency (NT) [11]; however, an increased NT is still the most important marker for congenital heart defects in the first trimester of pregnancy [12].[1] In addition, better ultrasound systems and more experienced operators have improved the evaluation of the fetus, making first trimester ultrasound a reliable method for early identification of fetal cardiac anomalies and providing more time for confirmation tests and for parental counseling. First trimester ultrasound does not replace the anatomy scan at 20–22 weeks but offers a good opportunity to identify major cardiac anomalies.

First trimester ultrasound can be an advantage for pregnant women with a high body mass index (BMI). It has been reported that among women with BMI ≥30, adequate visualization of the fetal cardiac structures in the second trimester of pregnancy can be achieved in only 50% of cases as compared to 87–90% in women with normal BMI (18–25) [13]. Early fetal evaluation combining TAU and TVU may be a valid alternative in these patients. Even in women with BMI >25,

E. Hernandez-Andrade (✉) · E. S. Huntley
Department of Obstetrics and Gynecology and Reproductive Sciences, McGovern Medical School, University of Texas, Health Science Center at Houston (UTHealth), Houston, TX, USA
e-mail: Edgar.A.HernandezAndrade@uth.tmc.edu; Erin.S.Huntley@uth.tmc.edu

---

[1] See also Chap. 9.

© The Author(s), under exclusive license to Springer Nature Switzerland AG 2023
J. S. Abramowicz, R. E. Longman (eds.), *First-Trimester Ultrasound*,
https://doi.org/10.1007/978-3-031-24133-8_12

the combination of TAU and TVU seems to provide a more complete evaluation of the fetal heart at 13 weeks than TAU alone at 16 weeks of gestation [14]. In general, it has been estimated that approximately 7–10% of all pregnant women, and about 40–50% with high BMI, require TVU to complete the fetal cardiac examination during the first trimester ultrasound scan [15].

Basic Description of Cardiac Development[2]

Formation of the fetal heart begins at around the 23–25th day of gestation when the embryo is 2 mm long and it is completed when the embryonic length is 15 mm, at approximately day 46 of gestation. Some structures, such as the atrioventricular septum, complete their development later in pregnancy. The fetal heart starts contracting at approximately 23 days of gestation. Four main processes occur during cardiac development (Fig. 12.1): (1) formation of the cardiac tube, (2) looping of the heart, (3) formation of the conotruncus, and (4) septation. In each of these processes, specific cardiac defects can originate [16–19].

At the 23–25th days of gestation (2 mm embryo), clusters of angiogenic cells called blood islands create a vascular plexus in the anterior segment of the embryo. These clusters generate two primitive cardiac tubes which will later fuse,

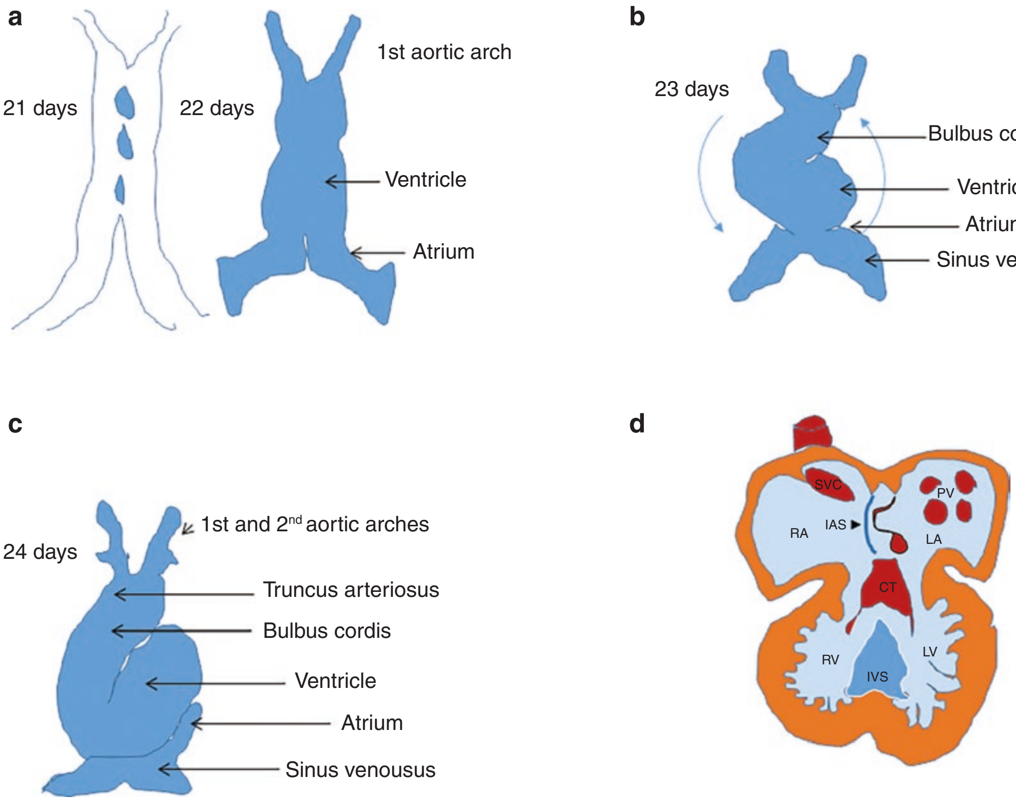
a
21 days
22 days
1st aortic arch
Ventricle
Atrium
b
23 days
Bulbus cordis
Ventricle
Atrium
Sinus venosus
c
24 days
1st and 2nd aortic arches
Truncus arteriosus
Bulbus cordis
Ventricle
Atrium
Sinus venousus
d
SVC
PV
RA
IAS
LA
CT
RV
LV
IVS

Fig. 12.1 Four main processes during cardiac development: (**a**) formation of the cardiac tube, (**b**) looping of the heart, (**c**) formation of the conotruncus, and (**d**) septation. *CT* Conotruncus, *IVS* interventriclar septum, *IAS* interauricular septum, *LA* left atrium, *LV* left ventricle, *PV* pulmonary veins, *RA* right atrium, *RV* right ventricle, *SVC* superior vena cava

forming the bulboventricular tube (Fig. 12.1a). The primitive ventricles and the outflow tracts originate from this structure. At this stage, the aortic sac and aortic arches begin to develop and cardiac looping is initiated through a process of bending of the cardiac tube toward the anterior and right parts of the embryo (Fig. 12.1b). One of the main cardiac defects originating at this stage is transposition of the great arteries.

---

[2] See also Chap. 5.

On gestational day 28 (3 mm embryo), the early embryonic ventricle originates from the diverticula located near the left ventro-lateral border of the cardiac tube. These diverticula penetrate the myocardium, increasing its thickness and creating multiple trabeculae forming the primitive left ventricle. The bulbus cordis splits into three sections: the proximal third forms the primitive right ventricle; the middle third forms the conus cordis and the outflow portions of the ventricles; and the terminal third forms the aortic and pulmonary roots or primitive truncus arteriosus (Fig. 12.1c). The formation of the primitive atria, the septum primum, septum secundum, as well as the process of septation begins at this stage. Cardiac defects that can develop during this period are single ventricle, double inlet and double outlet right ventricle, atrial septal and truncus arteriosus.

On gestational days 29–30 (4–5 mm embryo), the sinus venosus and the sinus cordis are formed, and the external shape of the heart resembles a four-chamber structure. Cardiac defects that can occur during this period are persistent left superior vena cava, Tetralogy of Fallot, and ventricular septal defects.

On gestational days 30–32 (5–6 mm embryo), the atrioventricular canal, the pulmonary veins and septation of the truncus arteriosus are formed (Fig. 12.1d). Cardiac defects developing during this period are anomalous pulmonary venous return, persistent atrioventricular canal, ventricular septal and aortico-pulmonary defects, and persistent truncus arteriosus.

Formation of the arterial valves begins on gestational day 36 (9 mm embryo), and of the atrioventricular valves on days 39–40 (10–12 mm embryo). Cardiac defects occurring during this period are bicuspid arterial valves, absent arterial valves, tricuspid valve atresia, and Ebstein's anomaly. The development of the aortic arch is completed by approximately the 46th day of gestation (17 mm embryo). Cardiac defects that may develop during this period are double aortic arch, interrupted aortic arch, right aortic arch, and coarctation of the aorta. At the time of the first trimester ultrasound when the embryonic length is >45 mm, all cardiac structures are already formed.

Why Do We Have to Scan the Fetal Heart Early in Pregnancy?

Early evaluation of the fetal heart can be performed in selected pregnant women with high risk for CHD characterized by family or obstetric history of congenital heart defects [20, 21], uncontrolled diabetes [22], under medication, i.e., anticonvulsants [23], monochorionic twin pregnancies [24], in pregnancies from assisted reproductive techniques [25]; and in fetuses with indirect markers of congenital heart defects, e.g., increased nuchal translucency [26–28], abnormal ductus venous waveform [29–32], tricuspid regurgitation [33], or cystic hygroma [34, 35]; and fetuses with any other structural defect [36, 37] (Table 12.1). Fetal cardiac evaluation can also be part of the routine anatomy scan performed to all pregnant women undergoing an ultrasound scan at 11 to 13+6 weeks of gestation. Protocols and methods may differ when evaluating either group; however, to achieve a successful evaluation in a basic or in an extended cardiac scan, operators experience, the use of a standard protocol, and good quality imaging are essential.

Table 12.1 Risk factors associated with the presence of congenital heart defects (CHD)

Indication	Association with cardiac defects
Non-cardiac major structural anomalies [114]	21%
Previous history of congenital heart defects [20]	8.7%
Maternal exposure to anticonvulsants [23]	7.8%
Abnormal ductus venosus waveform [115]	7.5%
Increased nuchal translucency [116]	7%
Monochorionic twins [24]	5.5% (9.3% in cases with TTS)
Tricuspid regurgitation [33]	5.1%
Aberrant right subclavian artery [82]	5.1%
Consanguinity [117]	4.4%
Assisted Reproductive Technologies [118]	4.3%

Operator Experience and Route of Ultrasound Examination

Experienced operators can identify most cardiac anomalies in the first trimester scan, but confirmation is always required by a pediatric cardiologist with extensive experience in fetal heart imaging [38]. A minimum number of 180 first trimester fetal cardiac evaluations are needed to reach enough expertise to obtain good quality cardiac images in at least 80% of all scans [39]. Chen and colleagues [40] showed that most of major cardiac anomalies and nearly half of all fetal cardiac defects can be detected in low-risk pregnant women by highly trained maternal-fetal experts. They evaluated 10,294 pregnant women with singleton pregnancies, 129 had cardiac anomalies, 50% of them were diagnosed in the first trimester of pregnancy. The highest detection rates were for hypoplastic left heart (100%), truncus arteriosus (100%), atrioventricular septal defect (100%), and complex cardiac defects (93%); moderate detection rates for transposition of the great arteries (75%), coarctation (67%), and Tetralogy of Fallot (62.5%); and a low detection rate for ventricular septal defects (20%). Similar results were described by Hutchinson et al. [41] showing that experienced operators can visualize the four-chamber view in 98% of cases, the aortic and ductal arches in 91% of cases, and outflow tracts in 72% of pregnant women at 12 weeks of gestation using gray scale and color Doppler imaging. Rasiah and colleagues [42] reported that despite TVU providing better quality images than TAU, training and experience of the operators, and the use of high-quality ultrasound (US) systems can lead to similar detection rates using only TAU. They performed a systematic review and identified ten good quality studies showing a pooled sensitivity of 85% (95% CI, 78–90%), specificity of 99% (95% CI, 98–100%), positive LR of 59.6 (95% CI, 26.5–133.6), and negative LR 0.25 (95% CI, 0.1–0.6) for congenital heart defects.

When Is the Optimal Time to Perform Early Fetal Cardiac Evaluation?

Visualization of cardiac images improves with gestational age (Table 12.2, Fig. 12.2). Despite having good quality images at 11 weeks (Figs. 12.3 and 12.4) and 12 weeks (Fig. 12.5), examining the heart at 13 weeks is probably the best (Fig. 12.6). Haak et al. [43] reported that at 11 weeks, successful evaluation of the heart can be achieved in about 20% of fetuses, whereas at 13 weeks, the success rate increases to 92%. Smrcek et al. [44] studied fetuses from 10 to 15 weeks of gestation and evaluated the following cardiac planes: four-chamber view, three-vessel view, origin and crossing of the great arteries, aortic and ductal arches, superior and inferior vena cava, and at least two pulmonary veins. They were able to identify all structures in 80% of fetuses between 12 and 14 weeks, and in 100% of fetuses at 15 weeks of gestation. The authors reported an increment in the detection rate of cardiac defects from 67% at 10 weeks to 100% at 15 weeks of gestation. They mentioned that between 10 and 13 weeks, TVU was better than TAU; between 12 and 14 weeks both TAU and TVU had a similar detection rate; and from 15 weeks of gestation onwards TAU was better.

Table 12.2 Visualization of fetal cardiac structures during the early ultrasound fetal cardiac examination between 11 and 13+6 weeks of gestation

	10 weeks	11 weeks	12 weeks	13 weeks	13+6 weeks
Four-chamber view	Yes	Yes	Yes	Yes	Yes
Outflow tracts	–	–	Yes	Yes	Yes
Aortic and ductal arches	–	–	Yes	Yes	Yes
Both cava veins	–	–	Yes	Yes	Yes
Pulmonary veins	–	–	–	Yes	Yes

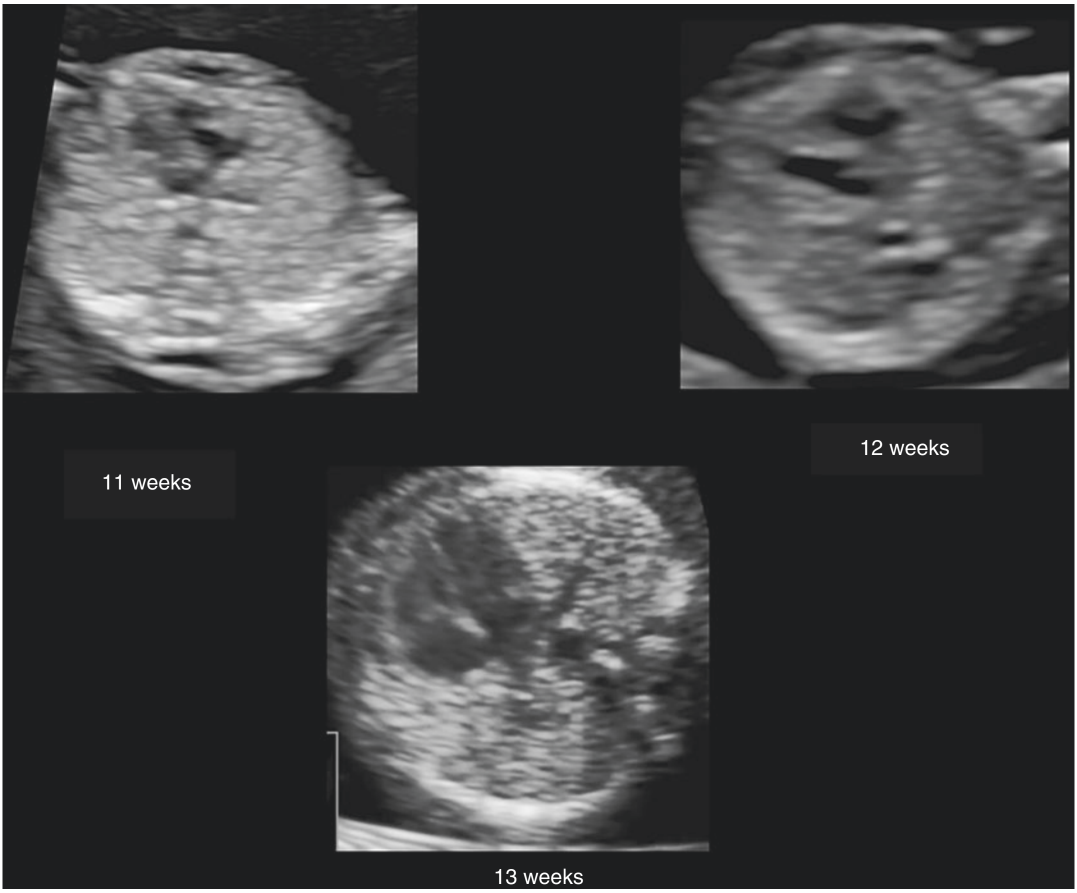

Fig. 12.2 The four-chamber view at 11, 12, and 13 weeks of gestation

The authors mentioned that complementary use of color directional Doppler or power Doppler and not limiting the scanning time can improve the optimal visualization of the fetal heart.

Vimpelli et al. [45] evaluated the feasibility of performing fetal cardiac examination at different weeks during the first trimester of pregnancy. The authors aimed to obtain the following planes: four-chamber, longitudinal views of the aorta and pulmonary trunks, crossing of the great arteries, and both aortic and ductal arches. They reported that visualization of all structures varied from 43% at 11 weeks to 62% at 13+6 weeks. The four-chamber view was obtained in 74% of cases at 13 weeks. McAuliffe et al. [46] evaluated a high-risk group of 160 women defined by previous history of congenital heart disease, increased nuchal translucency, or presence of a non-cardiac malformation during the NT scan. The author’s protocol included the following cardiac parameters: four-

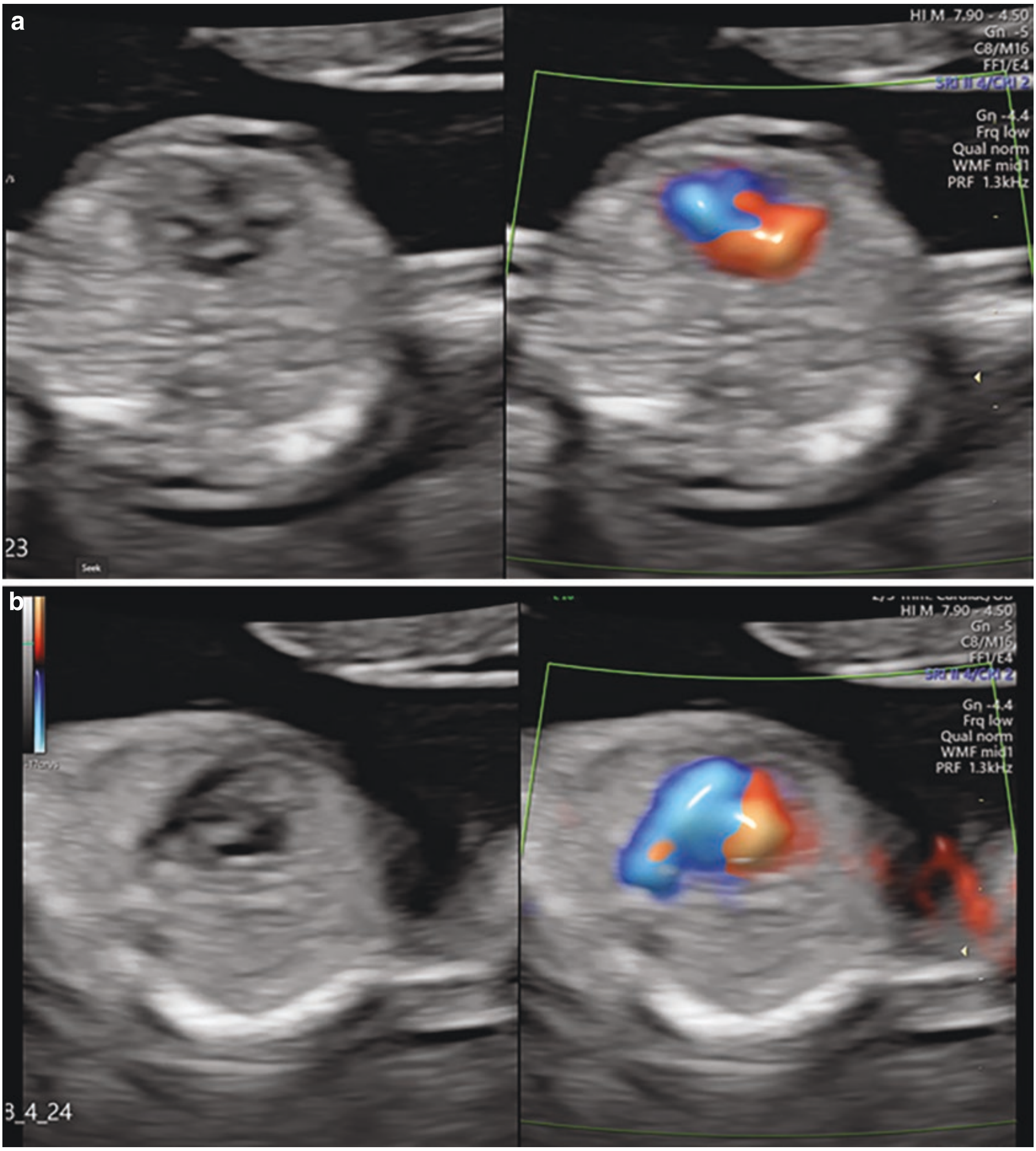

Fig. 12.3 Gray scale and directional power Doppler of the left (**a**) and right (**b**) ventricular outflows at 11 weeks of gestation

chamber view, symmetry of the cardiac chambers, atrioventricular valves, outflow tracts, crossing of the great arteries, and when possible, the ductal and aortic arches. The mean gestational age at examination was 13 weeks when the four-chamber view was seen in 100% of fetuses, the tricuspid and mitral valves in 96%, the outflow tracts in 95%, the aortic and ductal arches in 45%, and the pulmonary veins in 16% of all fetuses. Marques Carvalho et al. [47] explored the feasibility of obtaining the four-chamber view and outflow tracts with TVU in early pregnancy. They obtained the three planes in 37% of fetuses at 11 weeks of gestation, and in 85% of fetuses at 12 weeks of gestation; at 14 weeks, the three planes were obtained in all fetuses.

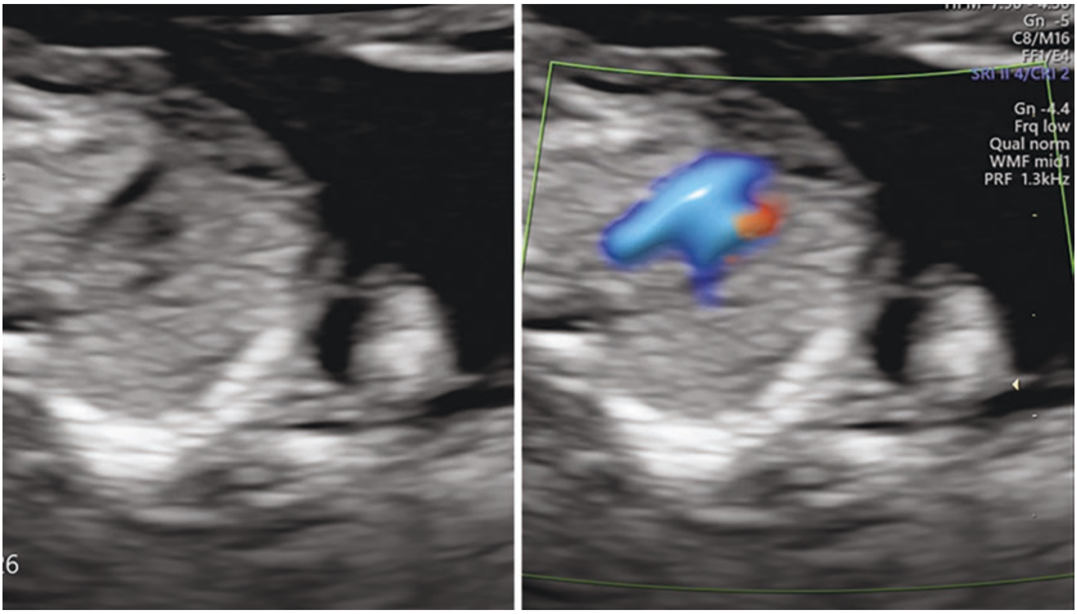
Gn -5
C8/M16
FF1/E4
SRI II 4/CRI 2
Gn -4.4
Frq low
Qual norm
WMF mid1
PRF 1.3kHz

Fig. 12.4 Three-vessel view at 11 weeks of gestation

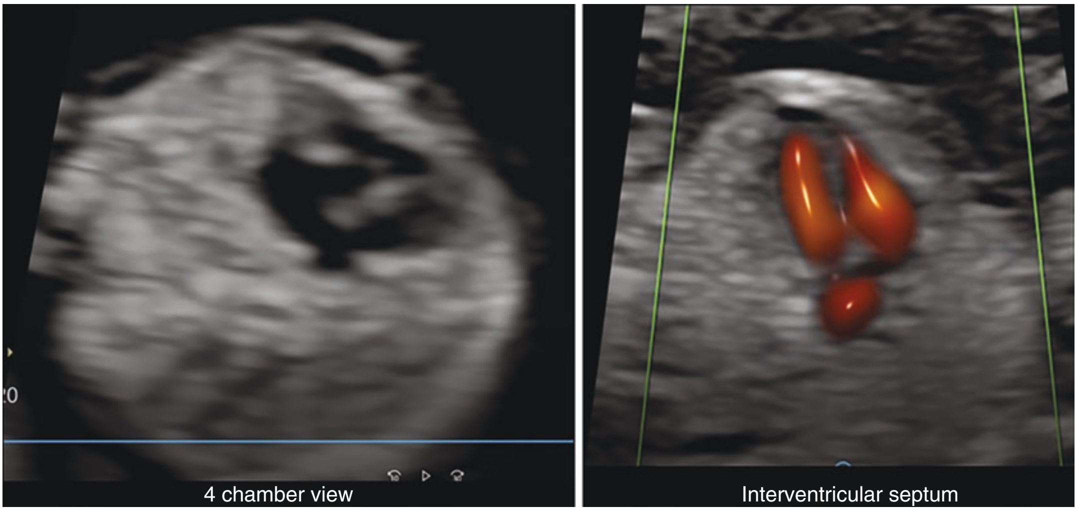
4 chamber view

Interventricular septum

Fig. 12.5 Four-chamber view and interventricular septum using gray scale and color directional Doppler at 12 weeks

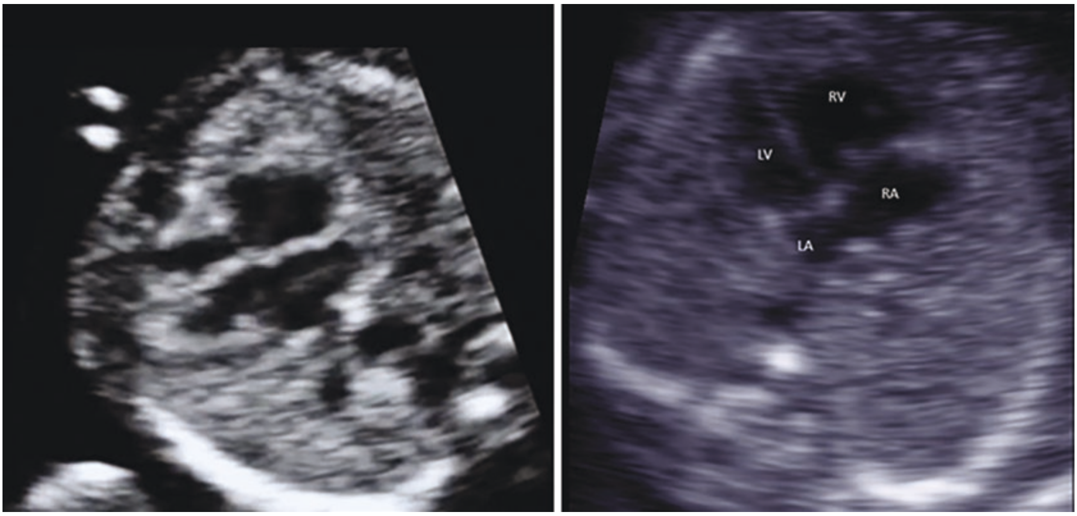

Fig. 12.6 Four-chamber views obtained at 13+0 to 13+6 weeks of gestation. *LA* left atrium, *LV* left ventricle, *RA* right atrium, *RV* right ventricle

Practical Recommendations

The ultrasound settings should be adjusted prior fetal cardiac examination, and the ALARA (As Low As Reasonable Achievable) principle must be followed for limiting fetal exposure to gray scale and Doppler ultrasound [48, 49]. Thermal and mechanic indices should always be maintained <1.0 [50]. Allowance of enough time for scanning as determined by operators experience to obtain good quality images is ideal. High frequency transducers are the best option for fetal cardiac evaluation [51]. Linear transabdominal probes emitting at 5–9 MHz might be preferred at 12–13 weeks of gestation, whereas transvaginal probes emitting at 9–12 MHz might be preferable at 11–12 weeks of gestation. Adjustment of ultrasound settings should include high frame rate (≥80 frames/s), increased contrast, high resolution, a single acoustic focal zone, and a narrow image field. Depth adjustment and magnification should also be employed when possible. Harmonic imaging can be used to improve image quality, particularly for patients with increased BMI.

What Constitutes a Cardiac Scan in the First Trimester?

Identification of the cardiac views—A cross-sectional plane of the fetal thorax with the heart in an apical projection and the fetal spine in the lower part of the ultrasound screen is the optimal image for cardiac examination. The four-chamber view (Fig. 12.6), crossing of the big arteries, and three-vessel view can be obtained from this view by performing a slow sweep toward the fetal head and maintaining cross-sectional images of the studied planes (Fig. 12.7a). The two outflow tracts can be visualized by rotating the ultrasound probe clockwise or anticlockwise from the four-chamber view (Fig. 12.7b, c). By rotating the probe 90° from the four-chamber view, a sagittal plane of the thorax is obtained, and by gently moving the ultrasound probe from side to side, the aortic and ductal arches, and inferior and superior vena cava can be observed (Fig. 12.8). Color directional Doppler might be helpful in assessing the integrity of the interventricular septum, to visualize the crossing of the great arteries, and to document the direction of flow in the aortic arch (Fig. 12.9).

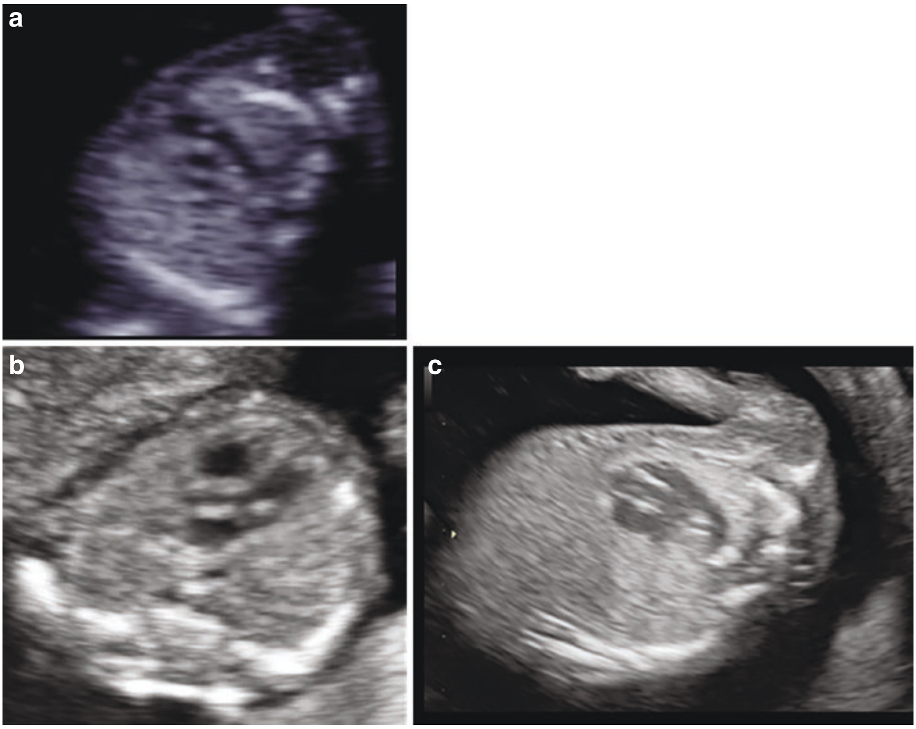

Fig. 12.7 (**a**) Three-vessel view (3-VV); (**b**) left and right (**c**) outflow tracts at 13 weeks of gestation

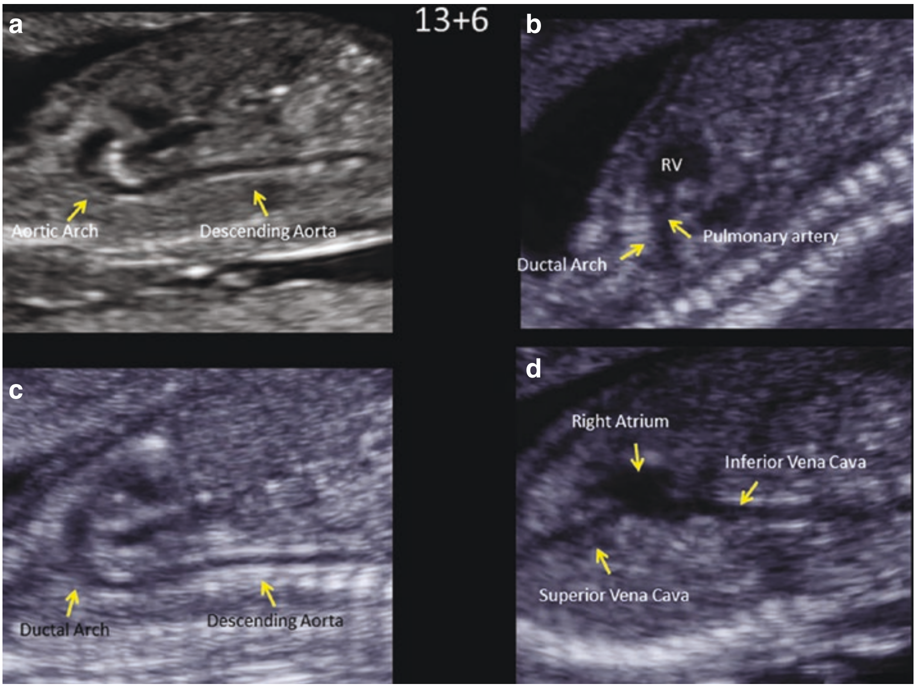
a
13+6
b
Aortic Arch
Descending Aorta
RV
Pulmonary artery
Ductal Arch
c
d
Right Atrium
Inferior Vena Cava
Superior Vena Cava
Ductal Arch
Descending Aorta

Fig. 12.8 Sagittal images of the aortic (**a**) and ductal (**b**, **c**) arches, and the superior and inferior vena cava (**d**) at 13 weeks and 6 days of gestation

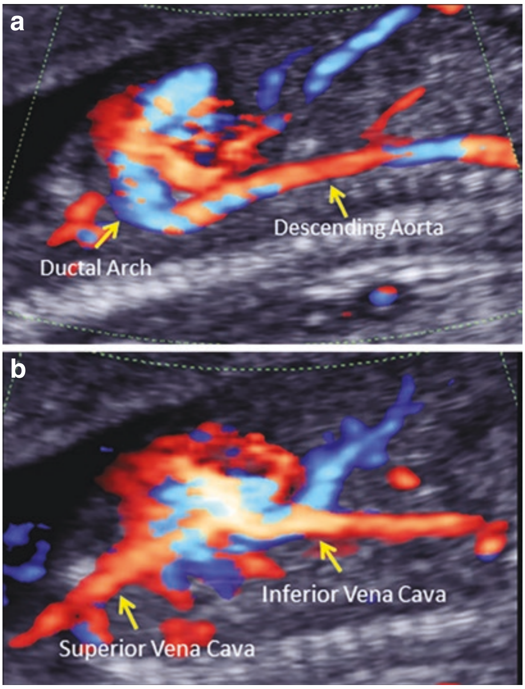

Fig. 12.9 Sagittal images of the ductal arch (**a**) and the superior and inferior vena cava (**b**) at 13 wees and 6 days of gestation using gray scale and directional color Doppler

Color Doppler

The use of color Doppler either directional or power improves the evaluation of the fetal heart and characterization of normal or abnormal cardiac anatomy [13, 52]. It provides great information in the evaluation of the four-chamber view, three-vessel view (3-VV), and the three-vessel trachea view (3-VTV) images [53–55]. Wiechec et al. [56] reported different filling patterns in the cardiac ventricles identified using color Doppler in 1084 fetuses with postnatal or autopsy data. They classified color images obtained in the four-chamber view in four different patterns (1) biventricular function with clear septum (normal heart but also seen in transposition of the great arteries, double outflow right ventricle, atrioventricular septal defect (AVSD), ventricular septal defect (VSD), and right aortic arch); (2) differences in color image in one of the ventricles (coarctation and Ebstein's anomaly); (3) separation only in the distal part of the septum (AVSD); (4) color in only one ventricle (hypoplastic left ventricle syndrome [HLHS], univentricular heart). In 3-VTV, six different color patterns were also described. They reported sensitivity of 43% only when the four-chamber view was evaluated, 71.4% when only the 3-VTV was evaluated, and 88.6% when both images were included.

Prefumo et al. [57] reported two cases of cardiac diverticula with large pericardial effusions in which Color flow and Doppler demonstrated bidirectional flow into a saccular dilatation at the ventricular apex filling the pericardial space in both cases. Gottschalk et al. [58] reported a detection rate of 25% of cases with absent pulmonary valve syndrome in the first trimester of pregnancy. The diagnosis was done using color Doppler techniques by presence of rudimentary or dysplastic pulmonary valve leaflets with bidirectional blood flow in the pulmonary trunk.

Alternatives for an Early Cardiac Scan

In many centers, the basic examination of the fetal heart in the first trimester of pregnancy includes the four-chamber view, NT measurement, and ductus venosus Doppler waveform as markers for cardiac defects [30, 59]. Different alternatives for a more complete fetal cardiac scan have been proposed. Carvalho et al. [60] suggested that the routine examination of the fetal heart at 11 to 13+6 weeks should include visceral situs, cardiac position (axis), normal and symmetric four-chamber view, two separate atrioventricular valves, normal outflow tracts, two great arteries of similar size, and evidence of aortic and ductal arches. The authors mentioned that septal defects cannot be completely excluded and that evolving cardiac lesions might not be visible in early pregnancy. Krapp et al. [61] reported that during the 11 to 13+6 week scan, the four-chamber view could be visualized in 96% of fetuses, the left ventricular outflow tract in 97%, the 3-VV view in 98%, and the aortic arch in 72% of fetuses, whereas the pulmonary veins were observed in only 23% of cases. Yagel et al. [62] proposed the following planes for fetal heart examination: upper abdomen, four-chamber view, five-chamber view, bifurcation of the pulmonary artery, 3-VTV, and the short axis of the right ventricle. TVU was suggested to be better than TAU for detailed examination of the fetal heart. The authors reported that all proposed cardiac planes were obtained in 98% of fetuses at 11–12 weeks, and in 100% of fetuses at 13–15 weeks of gestation. They reached 64% detection rate for CHD when the cardiac examination was performed before 15 weeks of gestation and an extra 17% detection when the heart was re-evaluated at 20–24 weeks, with an overall detection rate of 85% for CHD. Khalil et al. [63] proposed the following steps for cardiac evaluation in the first trimester: assessment of the fetal position, orientation of the fetal heart, visualization of the four-chamber view, assessment of the tricuspid valve and tricuspid regurgitation, visualization of the outflow tracts, and identification of the aortic and pulmonary arches. Abu-Rustum et al. [64] reported the following success rate for visualization of the cardiac structures during an early fetal cardiac scan: four-chamber view (100%), presence/absence of tricuspid regurgitation (100%), crossing of the great vessels (90%), bifurcation of the pulmonary artery (81%), 3-VV (55%), aortic arch (76%), superior and inferior vena cava (65%), and ductus venosus (99%). They also suggested that operators should perform a minimum of 70 fetal heart examinations at 11 to 13+6 weeks to gain reliable experience for obtaining the proposed anatomical planes with an allocated time of up to 10 min for fetal cardiac evaluation.

Including the 3-VV, 3-VTV, and Outflow Tracts in the Fetal Cardiac Evaluation in the First Trimester of Pregnancy

Quarello et al. [65] reported their results in screening using a simplified fetal echocardiography including nuchal translucency, four-chamber view, and 3-VTV. The combined use of color and gray scale allowed the following planes to be visualized: two atrioventricular and separate filling flow patterns, two separate atrioventricular filling flow patterns from atria to the apex of the ventricles, and convergence of the two filling flow patterns (V-shaped) in the upper part of the thorax. Another proposal for extended cardiac scan included seven views using gray scale and color Doppler modalities: abdominal situs, four-chamber view, left and right outflow tracts, 3-VTV, and ductal and aortic arches view [66]. High experienced operators applying this protocol in high-risk population achieved a detection rate of 94.9% and specificity of 96.9% for CHD. For most major cardiac defects, the detection rate was above 75% but for ventricular septal defects they only achieved a 20% detection.

By adding the 3-VTV view, De Robertis et al. [67] reported 57 major cardiac defects (0.1%) confirmed after birth when evaluating 5343 low-risk pregnant women in the first trimester of pregnancy. The 3-VTV was obtained in 94% of all fetuses; a cardiac anomaly was suspected in 22 fetuses based on the 3-VTV and conformed in 21 cases. The detection rate improved to 75.6% when the 3-VTV was added to the standard cardiac examination. The most frequent anomalies were Tetralogy of Fallot, coarctation, transposition of the great arteries, right aortic arch, AVSD, and aortic and pulmonary stenosis.

Lafouge et al. [68] reported a right aortic arch and ductus arteriosus in the first trimester identified by the presence of a mirror image-like appearance of the main vessels in a 3-VTV.

Bravo-Valenzuela et al. [69] reported two important markers for suspicion of early diagnosis of transposition of the great arteries: presence of only two vessels in the 3-VV and reversed curvature of the aorta emerging from the right ventricle. The authors reported that all cases with confirmed transposition of the great arteries ($n = 6$) had those two findings.

Dmitrovic et al. [70] proposed an extended examination of the heart including: four-chamber, left ventricle outflow tract (LVOT), descending aorta, heart size, cardiac axis, atrial size, identification of right and left atrioventricular valves crossing of the great arteries 3-VV, 3-VTV, two great arteries of equal diameter, V configuration of the aortic and ductal arch, ductus venosus, diastolic filling of the left ventricle, tricuspid regurgitation, and forward flow in both arches. They evaluated 2643 (2010 low risk and 633 high risk) fetuses and reported a prevalence of 4.2% ($n = 111$) of cardiac anomalies, 1.8% (36/2010) in the low-risk group and 11.8% (75/633) in the high-risk group. They used TAU and TVU and showing 79% detection rate with 10% false positive rate (FPR) for CHD. Similarly, Duta et al. [71] performed an extended cardiac evaluation in the first trimester in 7597 pregnant women including cardiac position, abdominal situs, four-chamber view, outflow tracts, 3-VTV, heart position, orientation and size of the heart chambers, the crux, the offsetting of the atrioventricular valves, and assessed ventricular filling by color Doppler mapping. The aorta, pulmonary artery, 3-VTV, and subclavian artery were visualized only with the contribution of color Doppler. They reported 39 cardiac defects with a detection rate of 76.9% and a FPR of 10%. The most frequently diagnosed defects were Tetralogy of Fallot, coarctation, hypoplastic left heart, and AVSD. Using an extended cardiac scan, a 62.5% detection rate with 1.5% false positive rate and a positive predictive value of 56% was achieved [72]. The success rate for obtaining the 3-VV improved from 47% at 11 weeks to 97.3% at 13 weeks, the aortic root from 47% at 11 weeks to 92% at 13 weeks, and the longitudinal axis of the aorta from 28% at 11 weeks to 92% at 13 weeks. Adding the 3-VV and 3-VTV as part of the routine examination of the fetal heart in the first trimester of pregnancy has been supported by other authors [73].

Indirect Markers for Early Fetal Cardiac Evaluation

Nuchal Translucency and Ductus Venosus

Borrell et al. [29] reported that among fetuses with congenital heart disease identified at 11–14 weeks, 40% had increased nuchal translucency (Fig. 12.10a), and 39% reversed atrial flow in the ductus venosus (Fig. 12.10b). Clur et al. [74] showed that among fetuses with normal chromosomes but increased nuchal translucency and abnormal ductus venous, 63% had cardiac defects. The authors also suggested that analysis of the pulsatility index of the ductus venosus instead of presence/absence of atrial flow might improve to 70% the detection rate of fetal cardiac anomalies. Other researchers have confirmed the association between abnormal ductus venosus and cardiac defects [75]. In a study from Finland [76], the authors evaluated 31,144 births including 170 congenital heart defects. They reported a significant increase in NT in the group with cardiac anomalies. They showed that using a NT cut-off value of 1.8 mm, 36.7% of major cardiac anomalies can be detected; using a NT cut-off value corresponding to the 99th percentile (2.4 mm approx.), 24.1% of major cardiac anomalies could be identified, and using a defined NT cut-off value of 3.0 mm, a detection rate of 17.7% could be achieved. The authors concluded that using a NT threshold of 1.8 mm, a large proportion of normal fetuses will be considered at risk (18.5% FPR); however, with a high NT (3.5 mm) a low detection rate (1/5 major cardiac anomalies) would be achieved; therefore, a NT value of 2.0 mm may provide the best predictor with a detection rate of 25.3% at a FPR of 3.3%.

Tricuspid Regurgitation

Pereira et al. [33] studied 85 euploid fetuses with major congenital heart defects and found an increased NT (>95th percentile) in 35.3%, tricuspid regurgitation in 32.9% (Fig. 12.10c), and reversed A wave in the ductus venosus in 28.2% of them during first trimester ultrasound. In fact, any one of these ultrasound markers was observed in 57.6% of fetuses with cardiac defects and in 8% of structurally normal fetuses. They concluded that these three markers improved the performance of screening for congenital heart defects in the first trimester. Presence of tricuspid regurgitation (TR) has a detection rate of 31.2% of cardiac anomalies in low-risk population and 53.4% detection rate in high-risk population.

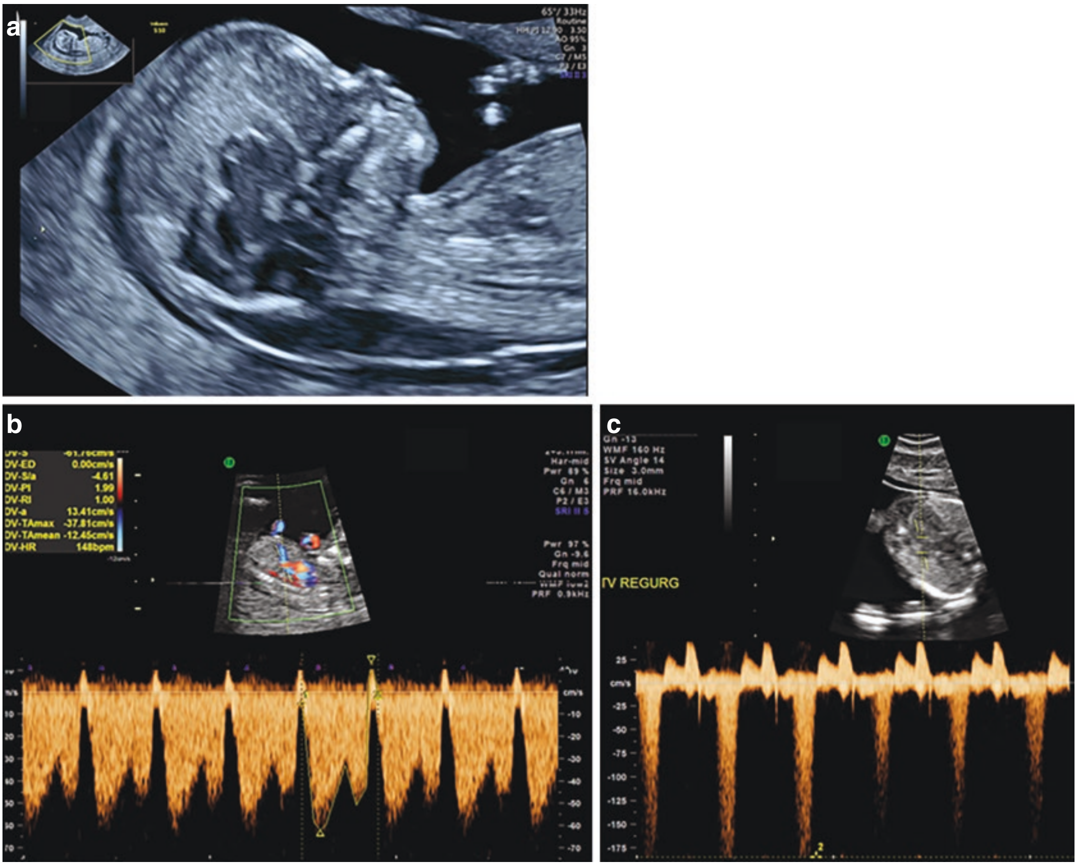

Fig. 12.10 Indirect sonographic markers of congenital heart defects. (**a**) Increased nuchal translucency; (**b**) reversed atrial flow in the ductus venosus; (**c**) tricuspid regurgitation. (Image courtesy of Dr. Rogelio Cruz Martinez)

Fetuses with tricuspid regurgitation and increased NT had an association 9.6 times higher for cardiac anomalies than fetuses without TR [77].

Cardiac Axis

The complex process of cardiac looping during embryonic development is demonstrated by the cardiac axis being fairly midline at 8 weeks and then gradually levo-rotating by 12 weeks after which it stabilizes at the end of the first trimester (Fig. 12.11a). Fetuses with cardiac defects might show an abnormal deviation of the cardiac axis in relation to gestational age. Mc Brien et al. [78] studied the normal variation in the fetal cardiac axis between 8 and 15 weeks of gestation and reported that the cardiac axis is orientated more to the midline of the thorax in early gestation, and then rotates to the left with advancing gestation. The authors noted that the cardiac axis changed from 39° at 11 weeks to 50° at 14 weeks. Sinskovskaya et al. [79] reported a normal variation in the cardiac axis from 34.5° at 11 weeks to 56.8° at 13+6 weeks of gestation, and that an abnormal cardiac axis in early gestation can be associated with coarctation of the aorta, Ebstein's anomaly, transposition of the great arteries, and heterotaxy. The same group compared 197 cases with cardiac defects and 394 structurally normal fetuses at 11–14 weeks [80]. The authors reported that 74.1% ($n = 129$) of fetuses with cardiac defects had an abnormal axis, 110 with left deviation (increased angle) and 19 with right deviation (smaller angle). After excluding cases with chromosomal anomalies, the cardiac axis was abnor-

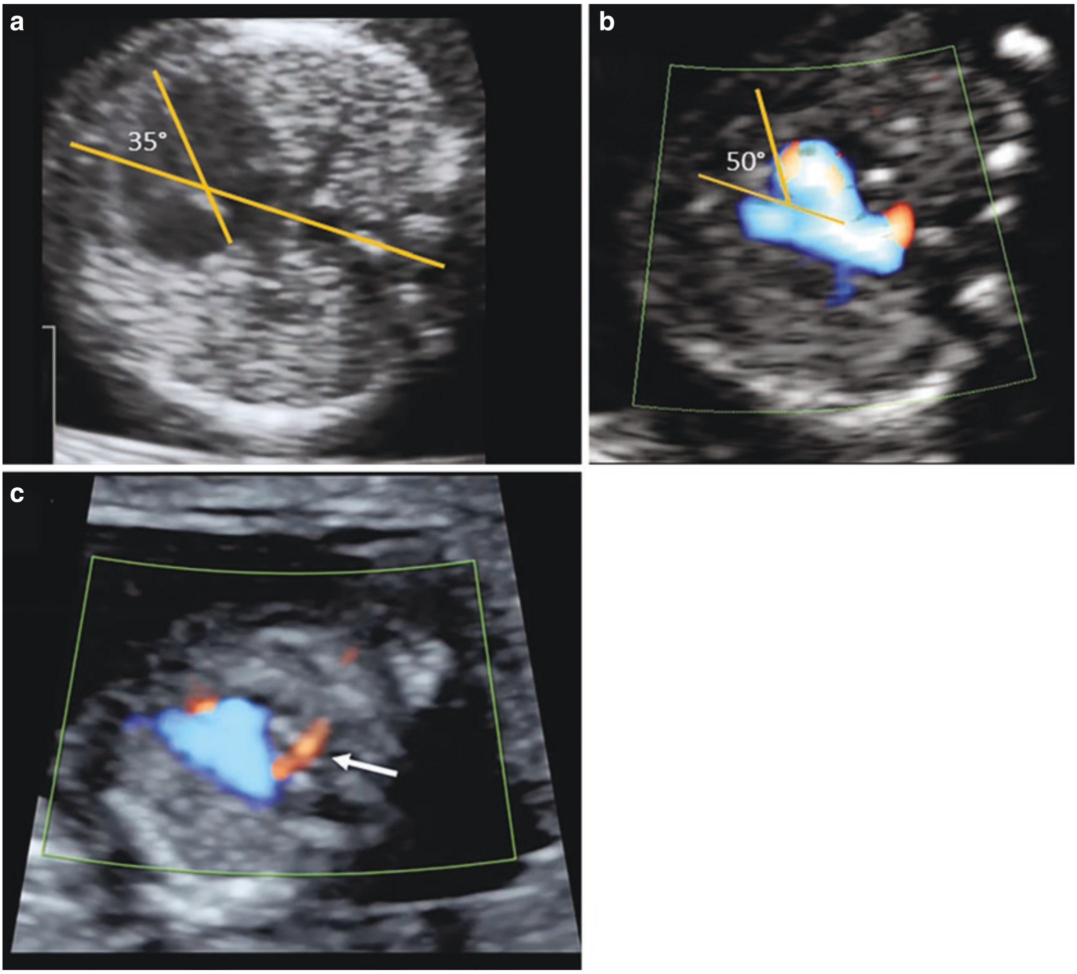

Fig. 12.11 (**a**) Cardiac axis; (**b**) "V" axis; (**c**) aberrant right subclavian artery. (Images **b** and **c**, courtesy of Dr. Rogelio Cruz Martinez)

mal in 75.6% of fetuses with cardiac anomalies. The authors also reported that in normal fetuses, the cardiac axis does not change between 11 and 14 weeks maintaining a mean value of 45°, and a 95th percentile value corresponding to 60°. The authors conclude that an abnormal cardiac axis during first trimester ultrasound should be considered an indication for fetal echocardiogram.

In addition to the cardiac axis, measuring the "V axis" (angle between the aorta and pulmonary artery) may improve identification of fetuses at risk of cardiac defects (Fig. 12.11b). Zheng et al. [81] reported a normal V angle of 20°–40°, corresponding to the 2.5th and 97.5th percentiles, respectively. The authors showed that 66.7% of fetuses with major cardiac anomalies had an abnormal V axis (<30° in hypoplastic left heart, >40° in atrioventricular septal defect). They reported that an abnormal cardiac axis or an abnormal "V axis" was observed in 28/30 (93.3%) of fetuses with cardiac defects.

Aberrant Right Subclavian Artery (ARSA)

Rembuskos et al. [82] suggested an association between an Aberrant Right Subclavian Artery (ARSA) and fetal cardiac defects (Fig. 12.11c). The authors studied 4,566 fetuses and identified

89 fetuses with ARSA, and of them, 12 fetuses had a chromosomal anomaly. The prevalence of fetal cardiac defects in chromosomally normal fetuses with ARSA was 4/77 (5.1%), including Tetralogy of Fallot (*n* = 1), aberrant umbilical vein (*n* = 1), and tricuspid atresia (*n* = 2). The authors suggested that early fetal echocardiography is indicated in the presence of ARSA.

Heart-to-Chest Ratio

Although the size of the fetal heart increases with gestational age, the mean heart-to-chest area ratio of 0.20 (SD 0.04) is maintained between 11 and 14 weeks [83]. The cardiothoracic ratio in early gestation may contribute in the diagnosis of anemic fetuses due to Hemoglobin Bart's Disease [84].

Detection of Cardiac Anomalies in All Fetuses Undergoing First Trimester Ultrasound

The reported prenatal detection for all cardiac anomalies ranges from 25% to 50% and for major cardiac anomalies from 60% to 100% [15, 85–88] (Table 12.3). Variations in detection rate are related to four important factors: (1) targeted population either high or low-risk, or both, (2) the protocol for cardiac evaluation either basic or extended, (3) training and expertise of the operators, and (4) confirmation by a pediatric cardiologist in the prenatal or postnatal periods.

Syngelaki et al. [89] in a large study including 100,997 women evaluated between 11 and 13+6 weeks in singleton gestations by TAU (with 2–3% of cases requiring TVU) reported a prevalence of cardiac defects (major and minor) of 0.38% (*n* = 389), and an overall detection rate of 30% (117/389). When classified by anomaly, >90% of tricuspid or pulmonary atresia, hypoplastic left heart syndrome and atrioventricular septal defects were detected, 60% for complex cardiac defects and left atrial isomerism, 30–40% for Tetralogy of Fallot and arches anomalies, and 15% for transposition of the great arteries, and right aortic arch. The authors also reported that aortic and pulmonary stenosis, common trunk, ventricular septal defects, arrhythmias, rhabdomyoma, and ventricular aneurisms were diagnosed either in the second trimester or at birth. They concluded that many anomalies can be detected in the first trimester, but it varies according to the type of defect; therefore, additional scans in the second and third trimesters of pregnancy are still needed. The same group [90] evaluated twin pregnancies in the first trimester (*n* = 6,366; 4,979 dichorionic and 1,387 monochorionic) and reported a similar prevalence of cardiac defects in dichorionic twins as compared to singletons (1/262 vs 1/260), and a higher prevalence in monochorionic twins (1/139). Detection rate in dichorionic twins was 28.9% (11/38) and 15% (3/20) in monochorionic twins. A similar

Table 12.3 Studies published between 2015 and 2022 on the detection rate of congenital heart defects when the fetus is evaluated at 11–14 weeks of gestation (from the highest to the lowest sample size)

Study	Total (*n*)	Scan route	GA (weeks)	Prevalence of CHD [*n* (%)]	First trimester detection rate [*n* (%)]
Karim [94]	328,214	TA/TV	11–14	1925 (0.6)	1105 (57%)
Singelaki [89]	100,997	TA/TV	11 to 13+6	389 (0.38)	119 (30%)
Minella [59]	93,209	TA/TV	11–13	211 (0.23)	113 (56%)
Jorgensen [96]	86,121	TA/TV	11–14	408 (0.47)	87 (21.3%)
Yu [93]	26,201	TA/TV	11–13	448 (1.7)	336 (75%)
Bardi [11]	13,417	TA/TV	11 to 13+6	21 (0.16)	4 (19%)
Chen [40]	10,294	TA/?	11 to 13+6	129 (1.2)	66 (51%)
Duta [71]	6912	TA/TV	11–14	39 (0.56)	30 (76%)

CHD congenital heart defects, *GA* gestational age, *TA* transabdominal, *TV* transvaginal detection rate of cardiac defects in twin pregnancies (20%) was reported by D'Antonio et al. [91].

In a study from the United Kingdom [59], the authors included 93,209 women evaluated in the first trimester with no signs of chromosomal anomalies. Major cardiac defects were observed in 211 cases (0.23%), and 53.6% (113) were diagnosed at 11+0 to 13+6 weeks/days. Their protocol included transverse section of the thorax, use of color Doppler to assess the four-chamber view, blood flow across the tricuspid valve, outflow tracts, and ductus venosus. The authors reported than in 36.5% of all major cardiac anomalies, an increased NT, tricuspid regurgitation, or an abnormal ductus venosus Doppler waveform were observed. They reported a detection rate >60% for tricuspid or pulmonary atresia, polyvalvular dysplasia, hypoplastic left heart, atrioventricular septal defects, and left atrial isomerism. Additionally, they found a moderate detection rate of 30–40% for Tetralogy of Fallot and arch anomalies, and a low detection rate (<25%) for tricuspid valve anomalies and transposition of the great arteries. No cases with aortic or pulmonary stenosis, or common arterial trunk were identified.

There are differences in the type of defects diagnosed in the first and second trimesters of pregnancy. Jicinska et al. [92] described defects mainly seen in the first trimester: hypoplastic left heart, atrioventricular septal defects, disproportion of the great vessels (coarctation), and pulmonary atresia. Among these defects, 65% had another major anatomical anomaly and/or a chromosomal defect, and only 33.1% were isolated defects. In the second trimester (n = 344), the most frequent defects were atrioventricular septal defects, transposition of the great arteries, coarctation, and hypoplastic left heart syndrome. Isolated defects were observed in 67.4% of fetuses, whereas in 32.6% of cases, other anomalies were detected. The authors showed that severe CHDs with associated anomalies were more frequently diagnosed in the first trimester.

In a recent meta-analysis, Yu et al. [93] included 18 studies published between 1993 and 2017 with a total of 26,201 low- and high-risk fetuses evaluated in the first trimester of pregnancy. The authors reported a pooled sensitivity for major and minor cardiac defects of 75% (95% CI 70–79), (336/448), and specificity of 99%. From the 112 missed cases, 60 had minor cardiac anomalies and 52 major cardiac anomalies.

Another recent meta-analysis included 63 studies from 1998 to 2020 with a total of 328,214 screened fetuses [94]. Low-risk fetuses (306,872) had a prevalence of major cardiac defects (0.41%) from where 767 were correctly identified with a pooled sensitivity of 55.8% and specificity of 99.8%. In the high-risk population including 21,342 fetuses, 480 were found with major cardiac defects (prevalence 1.3%), 67% of them (n = 338) were identified in the first trimester. The authors reported an increase in detection rate when a more detailed examination was performed, in particular with the addition of the outflow tracts and color Doppler. A similar report [95] in low-risk pregnant women detected >67% of major cardiac anomalies, 50% of them diagnosed during the first trimester scan.

In Denmark, among women undergoing first and second trimester screening, researchers reported their experience in detection of cardiac anomalies in 86,121 low-risk pregnancies from 2008 to 2010 [96]. The prevalence of heart defects changed in relation to the exclusion criteria, finally including 408 fetuses with cardiac anomalies (135 major) evaluated in the first trimester of pregnancy. They reported 21.3% detection rate for all anomalies, and 47.4% for major cardiac defects. Smrcek et al. [97] studied 2,165 low and high-risk fetuses using the combination of fundamental 2-D ultrasound imaging and color directional Doppler. They reported a detection rate for congenital heart defects of 63.0% (29/46), whereas nine more fetuses (19.5%) were diagnosed during the second trimester ultrasound scan with a total detection rate of 82.6%. The authors mentioned that cardiac defects that tend to progress—such as myocardial hypertrophy, ventricular hypoplasia, fibroelastosis, and coarctation of the aorta—might not be identified at 11–14 weeks. Among fetuses with an abnormal cardiac examination, 32.2% had an increased nuchal translucency and 51.2% an abnormal ductus venosus.

It can be concluded that when all pregnant women are evaluated in the first trimester of pregnancy, a detection rate between 20% and 50% for all fetal cardiac anomalies can be achieved, 70% detection for major cardiac anomalies, and <20% for minor cardiac anomalies (Figs. 12.12, 12.13, 12.14, 12.15, 12.16, and 12.17).

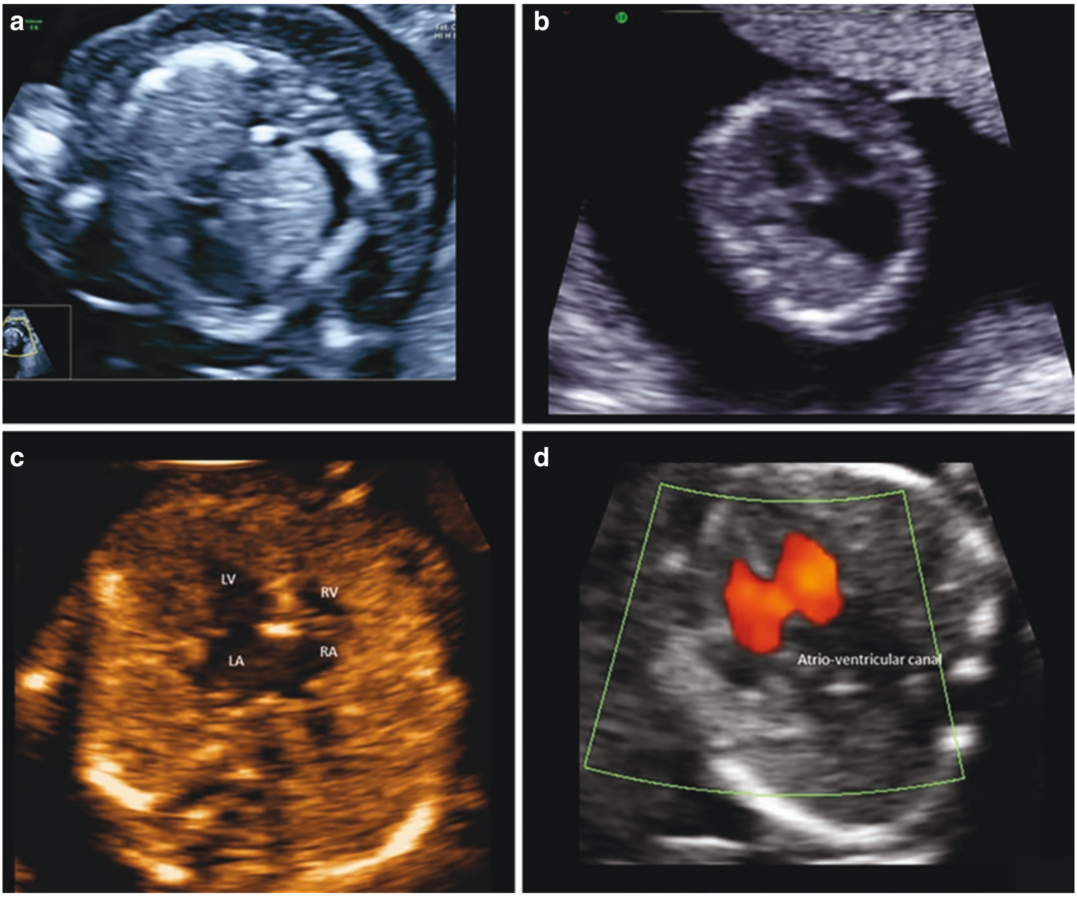

Fig. 12.12 Abnormal four-chamber views: (**a**) single ventricle with one atrioventricular valve; (**b**) dilatation of the right atrium due to pulmonary stenosis; (**c**) severely small right ventricle and increased thickness of the left ventricular walls; (**d**) atrioventricular septal defect. (Image **a** courtesy of Dr. Rogelio Cruz Martinez)

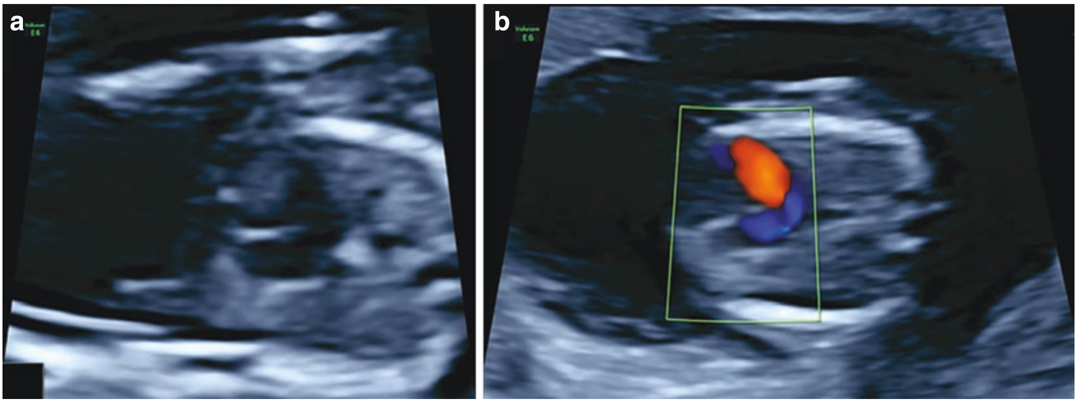

Fig. 12.13 Four-chamber view in a 13 weeks fetus showing (**a**) hyperechogenic right atrioventricular valve. (**b**) Color Doppler demonstrates lack of blood flow from the right atrium to the right ventricle. (Image courtesy of Dr. Rogelio Cruz Martinez)

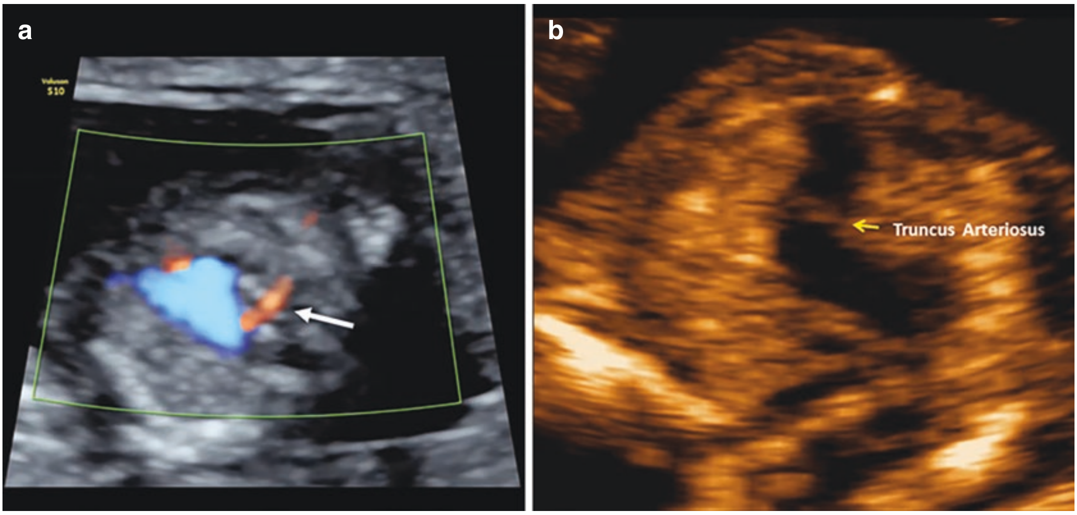

Fig. 12.14 Aberrant right subclavian artery (**a**), and truncus arteriosus (**b**). (Image **a** courtesy of Dr. Rogelio Cruz Martinez)

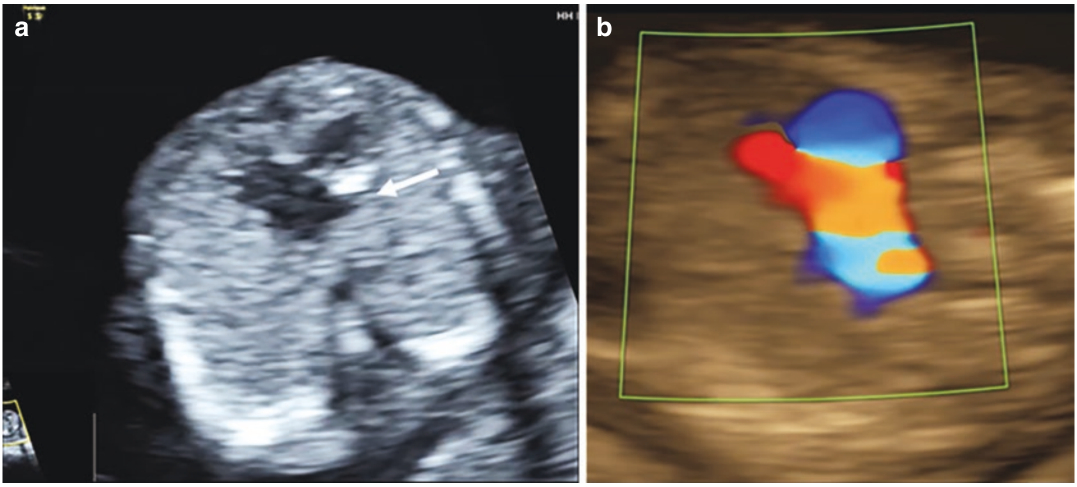

Fig. 12.15 Single ventricle at 11 weeks of gestation (**a**) gray scale image; (**b**) color Doppler ultrasound. (Image courtesy of Dr. Rogelio Cruz Martinez)

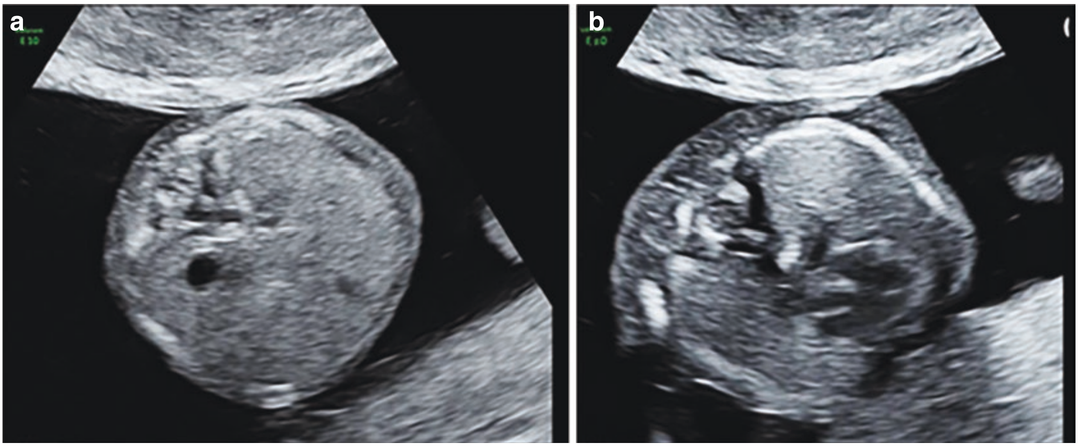

Fig. 12.16 Fetal echocardiography in a 12 weeks fetus with heterotaxy: (**a**) the stomach is on the right side; (**b**) levocardia and large interventricular septal defect; (**c**) three-vessel and trachea view showing a single vessel arising from the hearth on the right side of the fetal trachea (right aortic arch), and a persistent left superior vena cava on the left of the aortic arch. (Image courtesy of Dr. Rogelio Cruz Martinez)

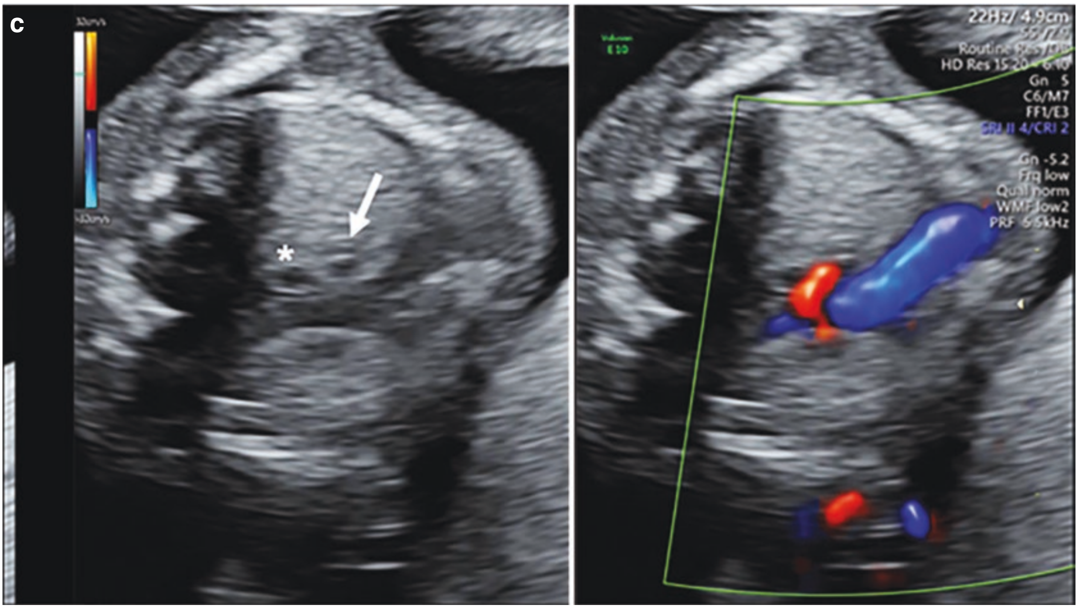

Fig. 12.16 (continued)

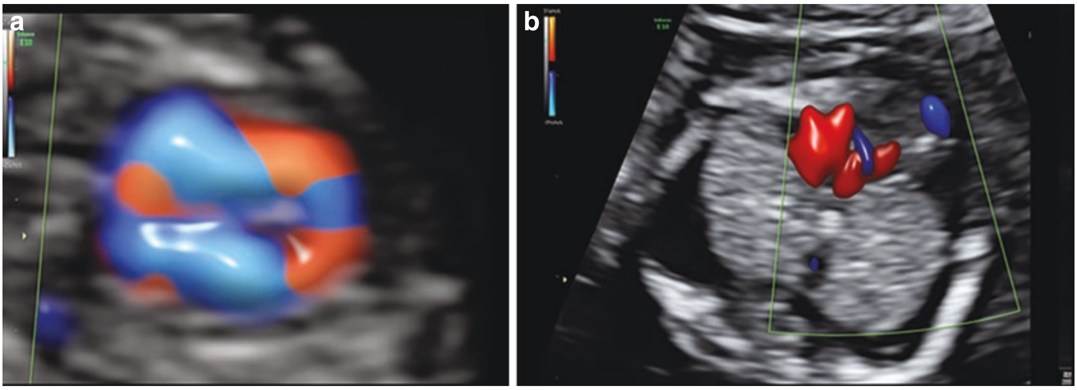

Fig. 12.17 Interventricular septal defects: (**a**) muscular apical; (**b**) perimembranous (fetus with pleural effusions). (Image courtesy of Dr. Rogelio Cruz Martinez)

High-Risk Population

In high-risk pregnant women with at least one risk factor associated with fetal congenital heart defects, Turan et al. [98] proposed the use of a standardized early fetal heart assessment performed by experienced operators using gray scale and power Doppler ultrasound in the four-chamber, outflow tract relationship (OTR), and transverse arches views reaching 93.2% sensitivity and 99.9% specificity for detection of major cardiac anomalies (70/1,024) (6.8%). Volpe et al. [99] reported their experience in cardiac evaluation in 870 high-risk women for CHD in the first and second trimesters of pregnancy referred due to increased NT, history of cardiac defects, or extracardiac anomalies. An abnormal cardiac evaluation was observed in 68 fetuses (7.8%) and confirmed in 36 (52%) at the second trimester scan. Among the 32 remaining fetuses, in 26 diagnosis changed in the second trimester. Persico et al. [100] evaluated the fetal heart in 855 pregnant women undergoing chorionic villus sampling due to presence of ultrasound markers, or altered maternal biomarkers of fetal chromosomal anomalies. They reported 100 cases in which a cardiac defect was suspected (54% major and 46% minor). The authors showed 93.1% detection rate of cardiac anomalies using TAU and a high association between congenital heart defects and increased nuchal translucency and tricuspid regurgitation.

Carvallo et al. [101] reported the diagnostic performance of targeted cardiac examination in 230 high-risk pregnant women for fetal cardiac defects (increased NT, family history of congenital heart disease, abnormal findings during the routine US scan) at the end of the first and early second trimesters of pregnancy. The following structures were visualized: visceral situs solitus, normal cardiac position, normal four-chamber view, two separate atrioventricular valves, normal aortic and pulmonary outflow tracts, two great arteries of similar size, and visualization of the aortic and ductal arches. An abnormal cardiac evaluation was observed in 21 of 199 fetuses, and in 10 fetuses the cardiac scan was not completed. The authors reported a 96% diagnostic accuracy of early fetal echocardiography, and a high association between increased nuchal translucency, chromosomal anomalies and cardiac defects.

Becker et al. [102] evaluated 3,094 fetuses referred due to an abnormal US examination or increased nuchal translucency, and reported a 2.8% prevalence of CHD ($n = 86$) with 84.2% of them detected during the first trimester scan. The cardiac evaluation included visualization of the four-chamber view, outflow tracts, and pulmonary and aortic valves. They reported that fetuses with nuchal translucency >2.5 mm had a 9.8% prevalence of heart defects, whereas fetuses with a nuchal translucency <2.5 mm had a prevalence of 0.3%.

Complementary Ultrasound Techniques

Fundamental 2-D imaging and color Doppler are the cornerstones for fetal cardiac evaluation; however, M-mode ultrasound might contribute in the diagnosis of septal defects and cardiac arrhythmias [8, 103]. Baschat et al. [104] evaluated four fetuses referred due to an increased nuchal translucency and bradycardia. Fetal heart block was diagnosed using M-mode ultrasound, and a congenital heart defect was present in all four fetuses; three had heterotaxy confirmed on autopsy.

4D-Spatio-Temporal Imaging Correlation (STIC)

4D-STIC (Figs. 12.12, 12.13, 12.14, 12.15, 12.16, 12.17 and 12.18) can be applied for off-line evaluation of the fetal heart either by the same or by different operators to confirm/exclude congenital heart defects. Tudorache et al. [105] reported an adequate visualization of cardiac planes in about 78% of cases and a good to excellent agreement in defining cardiac planes using STIC volumes. Similar results were shown by Turan et al. [106] who reported a good agreement in images obtained with gray scale 2D ultrasound with those obtained using STIC to define specific planes for cardiac evaluation.

Espinoza et al. [107] obtained STIC volumes from 17 normal fetuses and 16 fetuses with congenital heart defects. The STIC volumes were evaluated by operators blinded to the clinical diagnosis. The results showed 79% sensitivity and 90% specificity for identification of fetal cardiac defects. The authors concluded that acquisition of cardiac STIC volumes and evaluation by an expert in fetal heart can be used to confirm/exclude the presence of a cardiac defect. Lima et al. [108] explored the combined value of color Doppler ultrasound and STIC volume analysis in the identification of the basic planes for first tri-

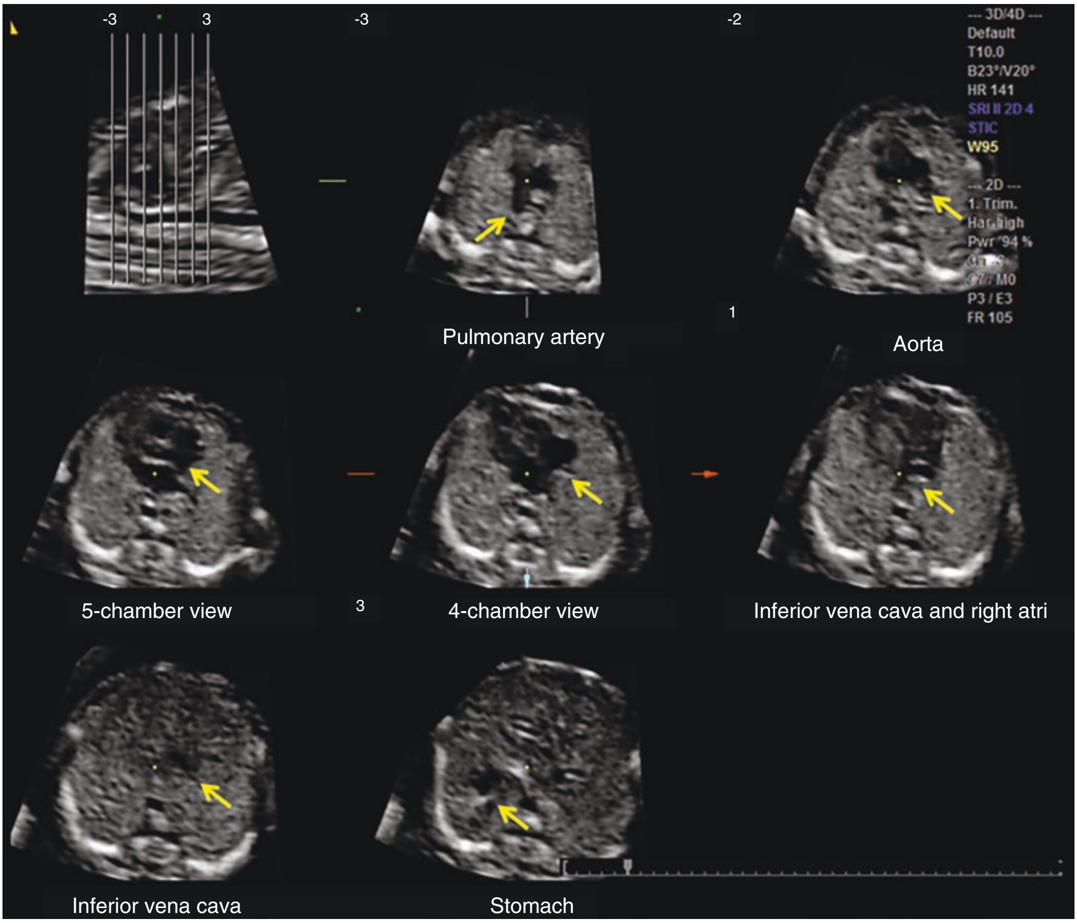
-3
3
-3
-2
--- 3D/4D ---
Default
T10.0
B23°/V20°
HR 141
SRI II 2D 4
STIC
W95
--- 2D ---
1. Trim.
Har/high
Pwr 94 %
P3 / E3
FR 105
1
Pulmonary artery
Aorta
5-chamber view
3
4-chamber view
Inferior vena cava and right atri
Inferior vena cava
Stomach

Fig. 12.18 Spatiotemporal imaging correlation (STIC) at 14 weeks of gestation. From a sagittal plane where the ductal arch and descending aorta can be visualized, seven cross-sectional planes are generated using tomographic ultrasound imaging (TUI)

mester fetal cardiac examination. The authors reported that this combination allowed identification of most of fetal cardiac planes in 90.6% of women from STIC volumes obtained either using TAU or TVU.

Evaluation of the Cardiac Function in Early Pregnancy

The evaluation of the fetal cardiac function in early pregnancies might be a complementary method for improving the identification of congenital heart defects.

In normal fetuses in the first trimester, Clur et al. [74] reported discrepancies in E/A ratios, outflow velocities, stroke volume, and cardiac output between the two cardiac ventricles, with a predominant function of the right ventricle. Ninno et al. [109] evaluated the tricuspid valve at 11 to 13+6 weeks and showed an increment in the E velocity and in the E/A ratios, and mild changes in the A velocity as gestation progresses. Rozmus-Warcholinska et al. [83] described normal values for fetal cardiac function parameters obtained between 11 and 13+6 weeks of gestation. The authors reported stable myocardial performance index (MPI) values during this gestational period with mild differences between the left and right ventricles. There was an increment in the E/A ratio and in the E velocity but no changes in the A velocity. Turan et al. [110] reported a high association between abnormal fetal cardiac function parameters in early pregnancy and maternal hyperglycemia in women with pregestational diabetes. The authors showed reduced left E/A ratio, prolongation of the isovolumetric relaxation time in both ventricles, reduction in the isovolumetric contraction time in the left ventricle and prolonged MPI in the two ventricles in diabetic women with poor glycemic control.

Cardiac strain can be evaluated in the first trimester of pregnancy. Chelliah et al. [111] reported that strain values can be obtained in 68% of fetuses at 12–14 weeks of gestation from an apical image of the four-chamber view; however, only in half, an adequate endocardial tracking was achieved with moderate to poor agreement between operators. The results showed similar peak systolic longitudinal strain in the left and right ventricles.

Precautions When Evaluating Fetuses at 11 to 13+6 Weeks?

Despite the high detection rate reported by several groups, mainly for major cardiac anomalies, not all cardiac defects can be identified at the 11 to 13+6 weeks scan (Table 12.4). Gardiner et al. [112] suggested caution when defining cardiac anomalies in the first trimester of pregnancy due to the risk of false positive cases in which parents might decide to terminate the pregnancy in a structurally normal fetus. The authors mentioned that based on morphologic information provided by High-Resolution Episcopic Microscopy (HREM), growth of the atrioventricular septum occurs later in the first trimester of pregnancy and offset of the mitral and tricuspid valves might not be visualized before 14 weeks of gestation in a structurally normal fetus. The authors concluded that there is a risk of incorrect diagnoses of atrioventricular septal defects in early pregnancy. Volpe et al. [99] evaluated the contribution of the first and second trimester echocardiography in the diagnosis of CHD and reported that a considerable proportion of cases considered as normal in the first trimester examination might develop cardiac defects at later stages of pregnancy. They also mentioned that a high percentage of fetuses with an abnormal cardiac examination might actually have a structurally normal heart.

Table 12.4 Congenital heart defects that can be identified during the early ultrasound fetal cardiac examination at 11 to 13+6 weeks of gestation

Cardiac defects with the highest detection rate in the first trimester	Atrioventricular septal defect Hypoplastic left heart Tricuspid and pulmonary atresia
Cardiac defects with a moderate detection rate	Coarctation Tetralogy of Fallot Truncus arteriosus Transposition
Cardiac defects unlikely to be diagnosed	Ventricular septal defects Ebstein's anomaly Mild aortic and pulmonary stenosis Cardiac tumors Myocardial hypertrophy Fibroelastosis Abnormal pulmonary venous return
	Aortic pulmonary stenosis

Safety

Guidelines of the International Society of Ultrasound in Obstetrics and Gynecology recommend maintaining the thermal index (TI) <1.0 during Doppler examination at 11 to 13+6 weeks [49, 113]. They suggest that the main reason for advocating the ALARA principle in the first trimester of pregnancy is the unknown effect of Doppler ultrasound during embryogenesis [113]. Nemescu et al. [50] assessed the safety of first trimester fetal echocardiography by measuring the thermal index (TI) and mechanical index (MI) generated during 399 examinations. Although there was an increase in TI values from gray scale to color flow and power Doppler studies, these values were always lower than 0.5. Satisfactory Doppler images were obtained using these settings.

Teaching Points

- When all pregnant women are evaluated between 11 and 14 weeks of gestation, a detection rate of 20–50% for all fetal cardiac anomalies (70% major, and <20% minor cardiac anomalies) can be achieved.
- Evaluation of the fetal heart at 11–14 weeks of gestation is indicated in pregnant women with history of cardiac defects, diabetes, under medication, with monochorionic twins and from assisted reproductive techniques; and in fetuses with increased nuchal translucency, tricuspid regurgitation, reversed atrial flow in the ductus venosus, aberrant right subclavian artery, abnormal cardiac axis, hydrops, or any other fetal structural defect.
- Experience and training of ultrasound operators are the most important factors for early identification of fetal cardiac defects; highly trained operators achieve a better detection rate. Good quality ultrasound imaging greatly contributes.
- Gray scale imaging and color Doppler are the cornerstones for fetal cardiac evaluation and additional techniques, i.e., M-mode, and 3D and 4D ultrasound, may also contribute in improving the detection rate of congenital heart defects in early pregnancy.
- Prior to 12 weeks of gestation, transvaginal ultrasound provides adequate images for cardiac examination; from 13 weeks onwards, fetal cardiac evaluation can be reliably performed with transabdominal ultrasound.
- The four-chamber is the most important ultrasound view to identify a normal or abnormal heart. When adding the outflow tracts, the 3-vessel, and 3-vessel and trachea views, the detection of cardiac anomalies can be improved.

References

1. Hoffman JI, Kaplan S. The incidence of congenital heart disease. J Am Coll Cardiol. 2002;39(12):1890–900.
2. CDC. Congenital heart defects (CHDs). 2022. https://www.cdc.gov/ncbddd/heartdefects/data.html.
3. Hoffman J. The global burden of congenital heart disease. Cardiovasc J Afr. 2013;24(4):141–5.
4. Cai M, Huang H, Su L, Lin N, Wu X, Xie X, et al. Fetal congenital heart disease: associated anomalies, identification of genetic anomalies by single-nucleotide polymorphism array analysis, and postnatal outcome. Medicine (Baltimore). 2018;97(50):e13617.
5. Jaeggi E, Ohman A. Fetal and neonatal arrhythmias. Clin Perinatol. 2016;43(1):99–112.
6. Makikallio K, McElhinney DB, Levine JC, Marx GR, Colan SD, Marshall AC, et al. Fetal aortic valve stenosis and the evolution of hypoplastic left heart syndrome: patient selection for fetal intervention. Circulation. 2006;113(11):1401–5.
7. Kailin JA, Santos AB, Yilmaz Furtun B, Sexson Tejtel SK, Lantin-Hermoso R. Isolated coarctation of the aorta in the fetus: a diagnostic challenge. Echocardiography. 2017;34(12):1768–75.
8. Bahtiyar MO, Dulay AT, Weeks BP, Friedman AH, Copel JA. Prenatal course of isolated muscular ventricular septal defects diagnosed only by color Doppler sonography: single-institution experience. J Ultrasound Med. 2008;27(5):715–20.
9. Nicolaides KH, Azar G, Byrne D, Mansur C, Marks K. Fetal nuchal translucency: ultrasound screening for chromosomal defects in first trimester of pregnancy. BMJ. 1992;304(6831):867–9.
10. Rose NC, Barrie ES, Malinowski J, Jenkins GP, McClain MR, LaGrave D, et al. Systematic evidence-based review: the application of noninvasive prenatal screening using cell-free DNA in general-risk pregnancies. Genet Med. 2022;24:1379–91.
11. Bardi F, Bosschieter P, Verheij J, Go A, Haak M, Bekker M, et al. Is there still a role for nuchal translucency measurement in the changing paradigm of first trimester screening? Prenat Diagn. 2020;40(2):197–205.
12. Mogra R, Alabbad N, Hyett J. Increased nuchal translucency and congenital heart disease. Early Hum Dev. 2012;88(5):261–7.
13. Inocencio G, Rodrigues S, Braga A, Rodrigues MC. Is it worth to evaluate the fetal heart with color doppler scan at 11 to 13+6 weeks? Ultrasound Q. 2015;31(3):175–9.
14. Garcia Delgado R, Garcia Rodriguez R, Ortega Cardenes I, Gonzalez Martin JM, De Luis Alvarado M, Segura Gonzalez J, et al. Feasibility and accuracy of early fetal echocardiography performed at 13(+0)-13(+6) weeks in a population with low and high body mass index: a prospective study. Reprod Sci. 2021;28(8):2270–7.
15. Volpe P, Ubaldo P, Volpe N, Campobasso G, De Robertis V, Tempesta A, et al. Fetal cardiac evaluation at 11-14 weeks by experienced obstetricians in a low-risk population. Prenat Diagn. 2011;31(11):1054–61.

16. Kirby M, Waldo K. Cardiac morphogenesis. In: Yagel S, Silverman, N.H, Gembruch U. Fetal cardiology. London: Martin Dunitz; 2003. p. 1–9.
17. del Monte-Nieto G, Harvey RP. Embryology of the heart. In: Salavastru C, Murrell DF, Otton J, editors. Skin and heart. Switzerland: Springer; 2021. p. 11–33.
18. Martinsen B, Lohr J. Cardiac Development in: Paul A. Iaisso, Editor Handbook of Cardiac Anatomy, Physiology, and Devices. Humana Press 2005, New Jersey, USA; pp 15–24.
19. Van Mierop H, Kutsche LM. Embryology of the heart. In: Hurst J, editor. The heart. New York: McGraw-Hill; 1986. p. 3–16.
20. Hoffman JI. Congenital heart disease: incidence and inheritance. Pediatr Clin N Am. 1990;37(1):25–43.
21. Fung A, Manlhiot C, Naik S, Rosenberg H, Smythe J, Lougheed J, et al. Impact of prenatal risk factors on congenital heart disease in the current era. J Am Heart Assoc. 2013;2(3):e000064.
22. Helle E, Priest JR. Maternal obesity and diabetes mellitus as risk factors for congenital heart disease in the offspring. J Am Heart Assoc. 2020;9(8):e011541.
23. Thomas SV, Ajaykumar B, Sindhu K, Francis E, Namboodiri N, Sivasankaran S, et al. Cardiac malformations are increased in infants of mothers with epilepsy. Pediatr Cardiol. 2008;29(3):604–8.
24. Springer S, Mlczoch E, Krampl-Bettelheim E, Mailath-Pokorny M, Ulm B, Worda C, et al. Congenital heart disease in monochorionic twins with and without twin-to-twin transfusion syndrome. Prenat Diagn. 2014;34(10):994–9.
25. Tararbit K, Lelong N, Thieulin AC, Houyel L, Bonnet D, Goffinet F, et al. The risk for four specific congenital heart defects associated with assisted reproductive techniques: a population-based evaluation. Hum Reprod. 2013;28(2):367–74.
26. Sairam S, Carvalho JS. Early fetal echocardiography and anomaly scan in fetuses with increased nuchal translucency. Early Hum Dev. 2012;88(5):269–72.
27. Hyett J, Perdu M, Sharland G, Snijders R, Nicolaides KH. Using fetal nuchal translucency to screen for major congenital cardiac defects at 10-14 weeks of gestation: population based cohort study. BMJ. 1999;318(7176):81–5.
28. Bahado-Singh RO, Wapner R, Thom E, Zachary J, Platt L, Mahoney MJ, et al. Elevated first-trimester nuchal translucency increases the risk of congenital heart defects. Am J Obstet Gynecol. 2005;192(5):1357–61.
29. Borrell A, Grande M, Bennasar M, Borobio V, Jimenez JM, Stergiotou I, et al. First-trimester detection of major cardiac defects with the use of ductus venosus blood flow. Ultrasound Obstet Gynecol. 2013;42(1):51–7.
30. Maiz N, Nicolaides KH. Ductus venosus in the first trimester: contribution to screening of chromosomal, cardiac defects and monochorionic twin complications. Fetal Diagn Ther. 2010;28(2):65–71.
31. Chelemen T, Syngelaki A, Maiz N, Allan L, Nicolaides KH. Contribution of ductus venosus Doppler in first-trimester screening for major cardiac defects. Fetal Diagn Ther. 2011;29(2):127–34.
32. Matias A, Huggon I, Areias JC, Montenegro N, Nicolaides KH. Cardiac defects in chromosomally normal fetuses with abnormal ductus venosus blood flow at 10-14 weeks. Ultrasound Obstet Gynecol. 1999;14(5):307–10.
33. Pereira S, Ganapathy R, Syngelaki A, Maiz N, Nicolaides KH. Contribution of fetal tricuspid regurgitation in first-trimester screening for major cardiac defects. Obstet Gynecol. 2011;117(6):1384–91.
34. Sananes N, Guigue V, Kohler M, Bouffet N, Cancellier M, Hornecker F, et al. Nuchal translucency and cystic hygroma colli in screening for fetal major congenital heart defects in a series of 12,910 euploid pregnancies. Ultrasound Obstet Gynecol. 2010;35(3):273–9.
35. Hsieh YY, Lee CC, Chang CC, Tsai HD, Hsu TY, Tsai CH. Prenatal sonographic diagnosis of Cantrell's pentalogy with cystic hygroma in the first trimester. J Clin Ultrasound. 1998;26(8):409–12.
36. Weiner Z, Lorber A, Shalev E. Diagnosis of congenital cardiac defects between 11 and 14 weeks' gestation in high-risk patients. J Ultrasound Med. 2002;21(1):23–9.
37. Gibbin C, Touch S, Broth RE, Berghella V. Abdominal wall defects and congenital heart disease. Ultrasound Obstet Gynecol. 2003;21(4):334–7.
38. Allan L. Screening the fetal heart. Ultrasound Obstet Gynecol. 2006;28(1):5–7.
39. Nemescu D, Onofriescu M. Factors affecting the feasibility of routine first-trimester fetal echocardiography. J Ultrasound Med. 2015;34(1):161–6.
40. Chen FC, Bacovsky A, Entezami M, Henrich W. Nearly half of all severe fetal anomalies can be detected by first-trimester screening in experts' hands. J Perinat Med. 2019;47(6):619–24.
41. Hutchinson D, McBrien A, Howley L, Yamamoto Y, Sekar P, Motan T, et al. First-trimester fetal echocardiography: identification of cardiac structures for screening from 6 to 13 weeks' gestational age. J Am Soc Echocardiogr. 2017;30(8):763–72.
42. Rasiah SV, Publicover M, Ewer AK, Khan KS, Kilby MD, Zamora J. A systematic review of the accuracy of first-trimester ultrasound examination for detecting major congenital heart disease. Ultrasound Obstet Gynecol. 2006;28(1):110–6.
43. Haak MC, Twisk JW, Van Vugt JM. How successful is fetal echocardiographic examination in the first trimester of pregnancy? Ultrasound Obstet Gynecol. 2002;20(1):9–13.
44. Smrcek JM, Berg C, Geipel A, Fimmers R, Diedrich K, Gembruch U. Early fetal echocardiography: heart biometry and visualization of cardiac structures between 10 and 15 weeks' gestation. J Ultrasound Med. 2006;25(2):173–82; quiz 83–5.
45. Vimpelli T, Huhtala H, Acharya G. Fetal echocardiography during routine first-trimester screening: a

feasibility study in an unselected population. Prenat Diagn. 2006;26(5):475–82.

46. McAuliffe FM, Trines J, Nield LE, Chitayat D, Jaeggi E, Hornberger LK. Early fetal echocardiography—a reliable prenatal diagnosis tool. Am J Obstet Gynecol. 2005;193(3 Pt 2):1253–9.
47. Marques Carvalho SR, Mendes MC, Poli Neto OB, Berezowski AT. First trimester fetal echocardiography. Gynecol Obstet Investig. 2008;65(3):162–8.
48. Bly S, Van den Hof MC, Diagnostic Imaging Committee SoO, Gynaecologists of C. Obstetric ultrasound biological effects and safety. J Obstet Gynaecol Can. 2005;27(6):572–80.
49. Salvesen K, Abramowicz J, Ter Haar G, Miloro P, Sinkovskaya E, Dall'Asta A, et al. ISUOG statement on the safe use of Doppler for fetal ultrasound examination in the first 13 + 6 weeks of pregnancy (updated). Ultrasound Obstet Gynecol. 2021;57(6):1020.
50. Nemescu D, Berescu A. Acoustic output measured by thermal and mechanical indices during fetal echocardiography at the time of the first trimester scan. Ultrasound Med Biol. 2015;41(1):35–9.
51. Bellotti M, Fesslova V, De Gasperi C, Rognoni G, Bee V, Zucca I, et al. Reliability of the first-trimester cardiac scan by ultrasound-trained obstetricians with high-frequency transabdominal probes in fetuses with increased nuchal translucency. Ultrasound Obstet Gynecol. 2010;36(3):272–8.
52. Jabak S, Vigneswaran TV, Charakida M, Kasapoglu T, de Jesus CJ, Simpson JM, et al. Initial experience of superb microvascular imaging for key cardiac views in foetal assessment before 15 weeks gestation. Fetal Diagn Ther. 2020;47(4):268–76.
53. Pasternok M, Nocun A, Knafel A, Grzesiak M, Orzechowski M, Konarska K, et al. "Y Sign" at the level of the 3-vessel and trachea view: an effective fetal marker of aortic dextroposition anomalies in the first trimester. J Ultrasound Med. 2018;37(8):1869–80.
54. Yang SH, Li XQ, Yang ZJ, Tian XX, Wei HW. Persistent truncus arteriosus with absent semilunar valve in first trimester. J Med Ultrason (2001). 2019;46(2):273–5.
55. Yu R, Li SL, Luo GY, Wen HX, Ouyang SY, Chen CY, et al. First-trimester echocardiographic features and perinatal outcomes in fetuses with congenital absence of the aortic valve. J Ultrasound Med. 2016;35(4):739–45.
56. Wiechec M, Knafel A, Nocun A. Prenatal detection of congenital heart defects at the 11- to 13-week scan using a simple color Doppler protocol including the 4-chamber and 3-vessel and trachea views. J Ultrasound Med. 2015;34(4):585–94.
57. Prefumo F, Bhide A, Thilaganathan B, Carvalho JS. Fetal congenital cardiac diverticulum with pericardial effusion: two cases with different presentations in the first trimester of pregnancy. Ultrasound Obstet Gynecol. 2005;25(4):405–8.
58. Gottschalk I, Jehle C, Herberg U, Breuer J, Brockmeier K, Bennink G, et al. Prenatal diagnosis of absent pulmonary valve syndrome from first trimester onwards: novel insights into pathophysiology, associated conditions and outcome. Ultrasound Obstet Gynecol. 2017;49(5):637–42.
59. Minnella GP, Crupano FM, Syngelaki A, Zidere V, Akolekar R, Nicolaides KH. Diagnosis of major heart defects by routine first-trimester ultrasound examination: association with increased nuchal translucency, tricuspid regurgitation and abnormal flow in ductus venosus. Ultrasound Obstet Gynecol. 2020;55(5):637–44.
60. Carvalho JS. Fetal heart scanning in the first trimester. Prenat Diagn. 2004;24(13):1060–7.
61. Krapp M, Ludwig A, Axt-Fliedner R, Kreiselmaier P. First trimester fetal echocardiography: which planes and defects can be displayed during the daily routine in a prenatal medicine unit? Ultraschall Med. 2011;32(4):362–6.
62. Yagel S, Cohen SM, Messing B. First and early second trimester fetal heart screening. Curr Opin Obstet Gynecol. 2007;19(2):183–90.
63. Khalil A, Nicolaides KH. Fetal heart defects: potential and pitfalls of first-trimester detection. Semin Fetal Neonatal Med. 2013;18(5):251–60.
64. Abu-Rustum RS, Ziade MF, Abu-Rustum SE. Learning curve and factors influencing the feasibility of performing fetal echocardiography at the time of the first-trimester scan. J Ultrasound Med. 2011;30(5):695–700.
65. Quarello E, Lafouge A, Fries N, Salomon LJ. Basic heart: a feasibility study of first-trimester systematic simplified fetal echocardiography. Ultrasound Obstet Gynecol. 2016; https://doi.org/10.1002/uog.15866.
66. Ye B, Wu Y, Chen J, Yang Y, Niu J, Wang H, et al. The diagnostic value of the early extended fetal heart examination at 13 to 14 weeks gestational age in a high-risk population. Transl Pediatr. 2021;10(11):2907–20.
67. De Robertis V, Rembouskos G, Fanelli T, Volpe G, Muto B, Volpe P. The three-vessel and trachea view (3-VTV) in the first trimester of pregnancy: an additional tool in screening for congenital heart defects (CHD) in an unselected population. Prenat Diagn. 2017;37(7):693–8.
68. Lafouge A, Quarello E. Right aortic arch and ductus arteriosus: a case diagnosed during the first trimester of pregnancy. Diagn Interv Imaging. 2014;95(9):877–9.
69. Bravo-Valenzuela NJ, Peixoto AB, Araujo Junior E, Da Silva CF, Meagher S. The reverse boomerang sign: a marker for first-trimester transposition of great arteries. J Matern Fetal Neonatal Med. 2019;32(4):677–80.
70. Dmitrovic A, Jeremic K, Babic UM, Perovic M, Mihailovic T, Opric D, et al. Early fetal heart ultrasonography as additional indicator for chromosomopathies. Clin Exp Obstet Gynecol. 2016;43(2):245–9.

71. Duta S, Veduta A, Vayna AM, Panaitescu A, Nedelea F, Peltecu G. The outcome of structural heart defects diagnosed in the first trimester of pregnancy. J Matern Fetal Neonatal Med. 2021;34(9):1389–94.
72. Ebrashy A, Aboulghar M, Elhodiby M, El-Dessouky SH, Elsirgany S, Gaafar HM, et al. Fetal heart examination at the time of 13 weeks scan: a 5 years' prospective study. J Perinat Med. 2019;47(8):871–8.
73. Springhall EA, Rolnik DL, Reddy M, Ganesan S, Maxfield M, Ramkrishna J, et al. How to perform a sonographic morphological assessment of the fetus at 11-14 weeks of gestation. Australas J Ultrasound Med. 2018;21(3):125–37.
74. Clur SA, Oude Rengerink K, Mol BW, Ottenkamp J, Bilardo CM. Fetal cardiac function between 11 and 35 weeks' gestation and nuchal translucency thickness. Ultrasound Obstet Gynecol. 2011;37(1):48–56.
75. Wagner P, Eberle K, Sonek J, Berg C, Gembruch U, Hoopmann M, et al. First-trimester ductus venosus velocity ratio as a marker of major cardiac defects. Ultrasound Obstet Gynecol. 2019;53(5):663–8.
76. Alanen J, Leskinen M, Sairanen M, Korpimaki T, Kouru H, Gissler M, et al. Fetal nuchal translucency in severe congenital heart defects: experiences in Northern Finland. J Matern Fetal Neonatal Med. 2019;32(9):1454–60.
77. Scala C, Morlando M, Familiari A, Leone Roberti Maggiore U, Ferrero S, D'Antonio F, et al. Fetal tricuspid regurgitation in the first trimester as a screening marker for congenital heart defects: systematic review and meta-analysis. Fetal Diagn Ther. 2017;42(1):1–8.
78. McBrien A, Howley L, Yamamoto Y, Hutchinson D, Hirose A, Sekar P, et al. Changes in fetal cardiac axis between 8 and 15 weeks' gestation. Ultrasound Obstet Gynecol. 2013;42(6):653–8.
79. Sinkovskaya E, Horton S, Berkley EM, Cooper JK, Indika S, Abuhamad A. Defining the fetal cardiac axis between 11 + 0 and 14 + 6 weeks of gestation: experience with 100 consecutive pregnancies. Ultrasound Obstet Gynecol. 2010;36(6):676–81.
80. Sinkovskaya ES, Chaoui R, Karl K, Andreeva E, Zhuchenko L, Abuhamad AZ. Fetal cardiac axis and congenital heart defects in early gestation. Obstet Gynecol. 2015;125(2):453–60.
81. Zheng MM, Tang HR, Zhang Y, Ru T, Li J, Xu BY, et al. Contribution of the fetal cardiac axis and V-sign angle in first-trimester screening for major cardiac defects. J Ultrasound Med. 2019;38(5):1179–87.
82. Rembouskos G, Passamonti U, De Robertis V, Tempesta A, Campobasso G, Volpe G, et al. Aberrant right subclavian artery (ARSA) in unselected population at first and second trimester ultrasonography. Prenat Diagn. 2012;32(10):968–75.
83. Rozmus-Warcholinska W, Wloch A, Acharya G, Cnota W, Czuba B, Sodowski K, et al. Reference values for variables of fetal cardiocirculatory dynamics at 11-14 weeks of gestation. Ultrasound Obstet Gynecol. 2010;35(5):540–7.
84. Wanapirak C, Sirichotiyakul S, Luewan S, Srisupundit K, Tongprasert F, Tongsong T. Appearance of abnormal cardiothoracic ratio of fetuses with hemoglobin Bart's disease: life table analysis. Ultraschall Med. 2017;38(5):544–8.
85. Iliescu D, Tudorache S, Comanescu A, Antsaklis P, Cotarcea S, Novac L, et al. Improved detection rate of structural abnormalities in the first trimester using an extended examination protocol. Ultrasound Obstet Gynecol. 2013;42(3):300–9.
86. Rossi AC, Prefumo F. Accuracy of ultrasonography at 11-14 weeks of gestation for detection of fetal structural anomalies: a systematic review. Obstet Gynecol. 2013;122(6):1160–7.
87. Eleftheriades M, Tsapakis E, Sotiriadis A, Manolakos E, Hassiakos D, Botsis D. Detection of congenital heart defects throughout pregnancy; impact of first trimester ultrasound screening for cardiac abnormalities. J Maternal Fetal Neonatal Med. 2012;25(12):2546–50.
88. van Velzen CL, Ket JCF, van de Ven PM, Blom NA, Haak MC. Systematic review and meta-analysis of the performance of second-trimester screening for prenatal detection of congenital heart defects. Int J Gynaecol Obstet. 2018;140(2):137–45.
89. Syngelaki A, Hammami A, Bower S, Zidere V, Akolekar R, Nicolaides KH. Diagnosis of fetal nonchromosomal abnormalities on routine ultrasound examination at 11-13 weeks' gestation. Ultrasound Obstet Gynecol. 2019;54(4):468–76.
90. Syngelaki A, Cimpoca B, Litwinska E, Akolekar R, Nicolaides KH. Diagnosis of fetal defects in twin pregnancies at routine 11-13-week ultrasound examination. Ultrasound Obstet Gynecol. 2020;55(4):474–81.
91. D'Antonio F, Familiari A, Thilaganathan B, Papageorghiou AT, Manzoli L, Khalil A, et al. Sensitivity of first-trimester ultrasound in the detection of congenital anomalies in twin pregnancies: population study and systematic review. Acta Obstet Gynecol Scand. 2016;95(12):1359–67.
92. Jicinska H, Vlasin P, Jicinsky M, Grochova I, Tomek V, Volaufova J, et al. Does first-trimester screening modify the natural history of congenital heart disease? Analysis of outcome of regional cardiac screening at 2 different time periods. Circulation. 2017;135(11):1045–55.
93. Yu D, Sui L, Zhang N. Performance of first-trimester fetal echocardiography in diagnosing fetal heart defects: meta-analysis and systematic review. J Ultrasound Med. 2020;39(3):471–80.
94. Karim JN, Bradburn E, Roberts N, Papageorghiou AT, study A. First-trimester ultrasound detection of fetal heart anomalies: systematic review and meta-analysis. Ultrasound Obstet Gynecol. 2022;59(1):11–25.
95. Karadzov Orlic N, Egic A, Damnjanovic-Pazin B, Lukic R, Joksic I, Mikovic Z. Screening performance of congenital heart defects in first trimester using simple cardiac scan, nuchal translucency, abnormal

ductus venosus blood flow and tricuspid regurgitation. Congenit Heart Dis. 2019;14(6):1094–101.

96. Jorgensen DE, Vejlstrup N, Jorgensen C, Maroun LL, Steensberg J, Hessellund A, et al. Prenatal detection of congenital heart disease in a low risk population undergoing first and second trimester screening. Prenat Diagn. 2015;35(4):325–30.
97. Smrcek JM, Berg C, Geipel A, Fimmers R, Axt-Fliedner R, Diedrich K, et al. Detection rate of early fetal echocardiography and in utero development of congenital heart defects. J Ultrasound Med. 2006;25(2):187–96.
98. Turan S, Asoglu MR, Ozdemir H, Seger L, Turan OM. Accuracy of the standardized early fetal heart assessment in excluding major congenital heart defects in high-risk population: a single-center experience. J Ultrasound Med. 2022;41(4):961–9.
99. Volpe P, De Robertis V, Campobasso G, Tempesta A, Volpe G, Rembouskos G. Diagnosis of congenital heart disease by early and second-trimester fetal echocardiography. J Ultrasound Med. 2012;31(4):563–8.
100. Persico N, Moratalla J, Lombardi CM, Zidere V, Allan L, Nicolaides KH. Fetal echocardiography at 11-13 weeks by transabdominal high-frequency ultrasound. Ultrasound Obstet Gynecol. 2011;37(3):296–301.
101. Carvalho JS, Moscoso G, Tekay A, Campbell S, Thilaganathan B, Shinebourne EA. Clinical impact of first and early second trimester fetal echocardiography on high risk pregnancies. Heart. 2004;90(8):921–6.
102. Becker R, Wegner RD. Detailed screening for fetal anomalies and cardiac defects at the 11-13-week scan. Ultrasound Obstet Gynecol. 2006;27(6):613–8.
103. Detterich JA, Pruetz J, Sklansky MS. Color M-mode sonography for evaluation of fetal arrhythmias. J Ultrasound Med. 2012;31(10):1681–8.
104. Baschat AA, Gembruch U, Knopfle G, Hansmann M. First-trimester fetal heart block: a marker for cardiac anomaly. Ultrasound Obstet Gynecol. 1999;14(5):311–4.
105. Tudorache S, Cara M, Iliescu DG, Novac L, Cernea N. First trimester two- and four-dimensional cardiac scan: intra- and interobserver agreement, comparison between methods and benefits of color Doppler technique. Ultrasound Obstet Gynecol. 2013;42(6):659–68.
106. Turan S, Turan OM, Desai A, Harman CR, Baschat AA. First-trimester fetal cardiac examination using spatiotemporal image correlation, tomographic ultrasound and color Doppler imaging for the diagnosis of complex congenital heart disease in high-risk patients. Ultrasound Obstet Gynecol. 2014;44(5):562–7.
107. Espinoza J, Lee W, Vinals F, Martinez JM, Bennasar M, Rizzo G, et al. Collaborative study of 4-dimensional fetal echocardiography in the first trimester of pregnancy. J Ultrasound Med. 2014;33(6):1079–84.
108. Lima AI, Araujo Junior E, Martins WP, Nardozza LM, Moron AF, Pares DB. Assessment of the fetal heart at 12-14 weeks of pregnancy using B-mode, color Doppler, and spatiotemporal image correlation via abdominal and vaginal ultrasonography. Pediatr Cardiol. 2013;34(7):1577–82.
109. Ninno MA, Liao AW, Lamberty CO, Miguelez J, Zugaib M. Fetal tricuspid valve Doppler at 11-13 weeks and 6 days: reference values and reproducibility. Prenat Diagn. 2010;30(8):790–4.
110. Turan S, Turan OM, Miller J, Harman C, Reece EA, Baschat AA. Decreased fetal cardiac performance in the first trimester correlates with hyperglycemia in pregestational maternal diabetes. Ultrasound Obstet Gynecol. 2011;38(3):325–31.
111. Chelliah A, Dham N, Frank LH, Donofrio M, Krishnan A. Myocardial strain can be measured from first trimester fetal echocardiography using velocity vector imaging. Prenat Diagn. 2016;36(5):483–8.
112. Gardiner HM. First-trimester fetal echocardiography: routine practice or research tool? Ultrasound Obstet Gynecol. 2013;42(6):611–2.
113. Salvesen K, Lees C, Abramowicz J, Brezinka C, Ter Haar G, Marsal K, et al. ISUOG statement on the safe use of Doppler in the 11 to 13 +6-week fetal ultrasound examination. Ultrasound Obstet Gynecol. 2011;37(6):628.
114. Groves R, Sunderajan L, Khan AR, Parikh D, Brain J, Samuel M. Congenital anomalies are commonly associated with exomphalos minor. J Pediatr Surg. 2006;41(2):358–61.
115. Martinez JM, Comas M, Borrell A, Bennasar M, Gomez O, Puerto B, et al. Abnormal first-trimester ductus venosus blood flow: a marker of cardiac defects in fetuses with normal karyotype and nuchal translucency. Ultrasound Obstet Gynecol. 2010;35(3):267–72.
116. Ghi T, Huggon IC, Zosmer N, Nicolaides KH. Incidence of major structural cardiac defects associated with increased nuchal translucency but normal karyotype. Ultrasound Obstet Gynecol. 2001;18(6):610–4.
117. Badaruddoza, Afzal M, Akhtaruzzaman. Inbreeding and congenital heart diseases in a north Indian population. Clin Genet. 1994;45(6):288–91.
118. Tararbit K, Houyel L, Bonnet D, De Vigan C, Lelong N, Goffinet F, et al. Risk of congenital heart defects associated with assisted reproductive technologies: a population-based evaluation. Eur Heart J. 2011;32(4):500–8.

13

Doppler Sonography in Early Pregnancy

David Mundy, Devika Maulik, and Dev Maulik

Introduction

Doppler sonography was introduced into obstetrical practice in the 1980s and has revolutionized fetal and maternal investigations [1, 2]. Spectral and color Doppler ultrasound provide noninvasively hemodynamic information [3] and have broad clinical applications, including high-risk fetal surveillance and fetal echocardiography [4, 5].

Although Doppler ultrasound investigations frequently target the second and third trimesters of pregnancy, first-trimester Doppler insonation of fetal and maternal circulations has also proven beneficial for risk assessment. Current first-trimester applications include Doppler assessment of the fetal ductus venosus, tricuspid valve, and maternal uterine artery flow. This chapter reviews these applications, specifically addressing the following:

1. Ductus venosus Doppler during the first trimester and its applications in screening for aneuploidy and congenital heart disease.
2. Tricuspid Doppler flow assessment and its applications in screening for aneuploidy and congenital heart disease.
3. Doppler of the uterine artery in predicting subsequent development of preeclampsia.
4. Doppler of the placental implantation site for early detection of placenta accreta spectrum.

Doppler Sonography of the Ductus Venosus

Anatomy and Hemodynamics

The ductus venosus is a venous shunt that preferentially streams oxygenated blood from the placenta, via the umbilical vein, to the fetal heart and brain. Although traditionally depicted as an anatomically contiguous vascular structure with the umbilical vein, more recent autopsy dissections in 14–19-week fetuses demonstrated that the umbilical vein ends in the portal sinus. The portal sinus is a venous confluence that gives rise to the ductus venosus and the right and left portal veins [6] (Fig. 13.1).

The ductus venosus is a conical branchless structure with a narrow proximal inlet, called the isthmus, and a broad distal outlet that joins the portal sinus. This configuration increases blood flow velocity, propelling it to the foramen ovale and onto the left atrium. There is a com-

---

D. Mundy · D. Maulik
Department of Obstetrics and Gynecology, UMKC School of Medicine, Kansas City, MO, USA

Department of Obstetrics and Gynecology, University Health-Truman Medical Center, Kansas City, MO, USA
e-mail: mundyd@umkc.edu; maulikde@umkc.edu

D. Maulik (✉)
Department of Obstetrics and Gynecology, UMKC School of Medicine, Kansas City, MO, USA
e-mail: Dev.Maulik@uhkc.org

© The Author(s), under exclusive license to Springer Nature Switzerland AG 2023
J. S. Abramowicz, R. E. Longman (eds.), *First-Trimester Ultrasound*,
https://doi.org/10.1007/978-3-031-24133-8_13

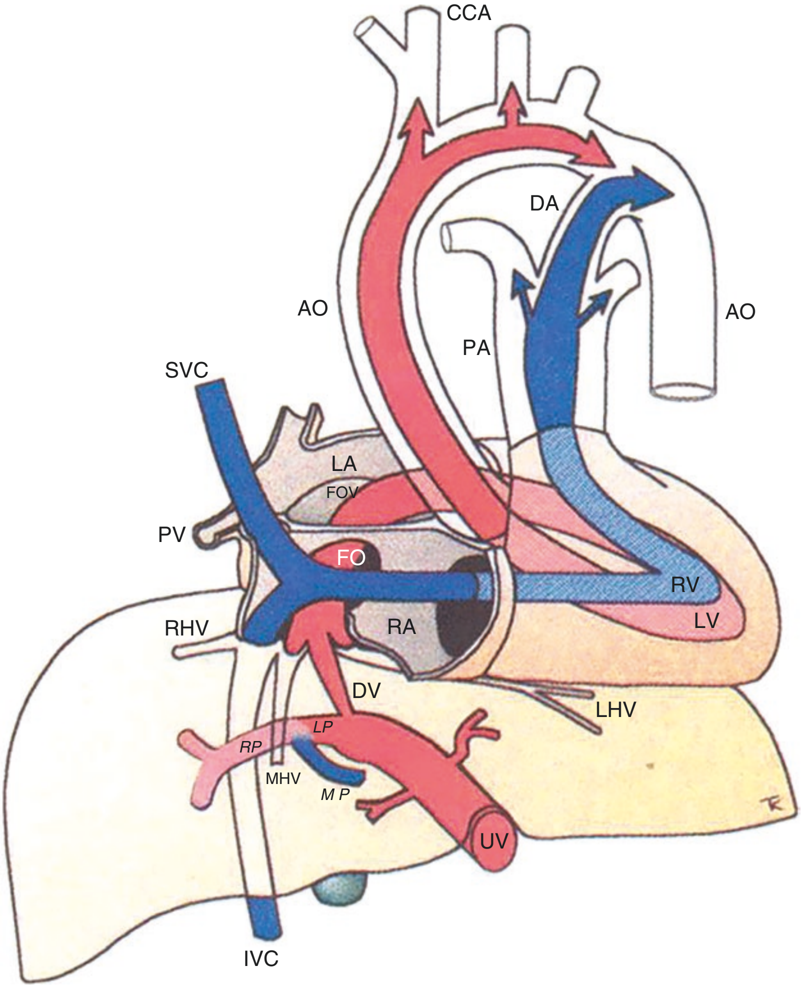

Fig. 13.1 The fetal circulatory pathways show the three shunts: ductus arteriosus (DA), ductus venosus (DV), and the foramen ovale (FO). The via sinistra (red) directs blood from the umbilical vein (UV) through the DV and FO to the left atrium (LA), left ventricle (LV), and ascending aorta (AO), thus supplying the coronary and cerebral circuit with well-oxygenated blood before joining with the via dextra (blue) in the descending AO. The via dextra receives deoxygenated blood from the abdominal inferior vena cava (IVC) and superior vena cava (SVC) directed to the right atrium (RA), right ventricle (RV), pulmonary trunk (PA), bypassing the pulmonary circuit through the DA. Splanchnic blood from the main portal stem (MP) is directed to the right liver lobe after blending with umbilical blood that reaches the right portal branch (RP) through the left branch (LP). *CCA* common carotid arteries, *FOV* foramen ovale valve, *LHV* left hepatic vein, *MHV* medial hepatic vein, *PV* pulmonary vein. (With kind permission from: Kiserud T, Rasmussen S, Skulstad S. Blood flow and the degree of shunting through the ductus venosus in the human fetus. Am J Obstet Gynecol. 2000;182(1 Pt 1):147–53. doi: https://doi.org/10.1016/s0002-9378(00)70504-7. PMID: 10649170)

plex interrelationship between the umbilical vein, ductus venosus, and hepatic-portal circulations that maintain vital organ perfusion. Under pathological conditions, such as fetal growth restriction, oxygen and nutrient delivery to the heart and brain is supported by increasing the ductus venosus blood flow at the cost of perfusion of the liver [7].

The ductus venosus was first identified in the sixteenth century, but Doppler sonography has only recently revealed its importance in fetal circulatory physiology and pathology [8].

Utilizing two-dimensional, color Doppler, and pulsed spectral Doppler sonography, Kiserud and colleagues studied the ductus venosus flow longitudinally in normal pregnancies from 18 weeks to term and noted an increase in the mean peak velocity throughout gestation. They also reported reversed flow during atrial systole in two cases with fetal cardiac disease.

Over the last two decades, numerous investigators demonstrated the value of ductus venosus Doppler in understanding circulatory pathophysiology and its predictive utility in complicated pregnancies, especially with fetal growth restriction [9]. Subsequent studies have reported the potential of ductus venosus Doppler in prenatal risk assessment for aneuploidy and congenital cardiac disease in the first trimester of pregnancy, addressed in this review.[1] A detailed discussion of the ductus venosus is beyond the scope of this chapter, but Kiserud has comprehensively reviewed the topic elsewhere [10, 11].

Doppler Imaging Technique for the Ductus Venosus

The optimal imaging technique for Doppler interrogation of the ductus venosus has been well described [12]. The ultrasound modalities include two-dimensional, color flow Doppler, and spectral Doppler imaging. The essential steps are as follows.

The high-pass filter is set as low as permitted by the device, usually about 50 Hz, and a Doppler frequency range is selected adequate to accommodate peak velocities without aliasing. The acoustic power output (the mechanical and thermal indices) should be as low as feasible to achieve reasonable image quality [13]. The anterior sagittal fetal plane is optimal for imaging the ductus (Fig. 13.2). However, a posterior sagittal plane may also be helpful. These approaches promote viewing the ductus venosus in the long axis, displaying aliased high-velocity color flow at the isthmus, and enabling optimal pulsed spectral Doppler interrogation with a minimal insonation angle. In difficult fetal positions, an oblique cross-sectional view may be the only choice; however, this will limit imaging at an optimal angle.

The fetal image should be large enough to include just abdomen and thorax in early pregnancy, which minimizes measurement errors related to small size. The sample volume is adjusted to include only the target vein to avoid collecting signals from other veins in proximity, such as the umbilical vein, the hepatic vein, or the inferior vena cava. The imaging is performed when the fetus is at rest, without body movements, breathing, or hiccups.

Ductus Venosus Doppler Waveforms

In normal pregnancies, blood flow in the ductus venosus is directed toward the fetal heart. The Doppler waveform is triphasic with two peaks and a trough reflecting the phases of the fetal cardiac cycle (see Fig. 13.2). The first peak, the S wave, is the highest velocity during the ventricular systole. The second peak, termed the D wave, is the highest velocity during the ventricular diastole and is lower than the S wave. The trough, called the a-wave, is the lowest velocity of the Doppler waveform corresponding to the minimum velocity during the atrial contraction. The Doppler waveforms from the ductus venosus are analyzed quantitatively or qualitatively.

The quantitative assessment is based on actual velocity values, which require an optimal insonation angle and angle correction. However, various pulsatility indices obviate the need for angle correction. In all measurements, the maximum frequency shift envelope of the waveform is utilized (see Fig. 13.2).

The qualitative assessment constitutes the most relevant and frequently used approach in clinical practice and comprised of the visual assessment of the a-wave, which is related to atrial contraction. A zero or negative waveform indicates an increased end-diastolic filling pressure in the right heart (Fig. 13.3).

---

[1] See also Chap. 12.

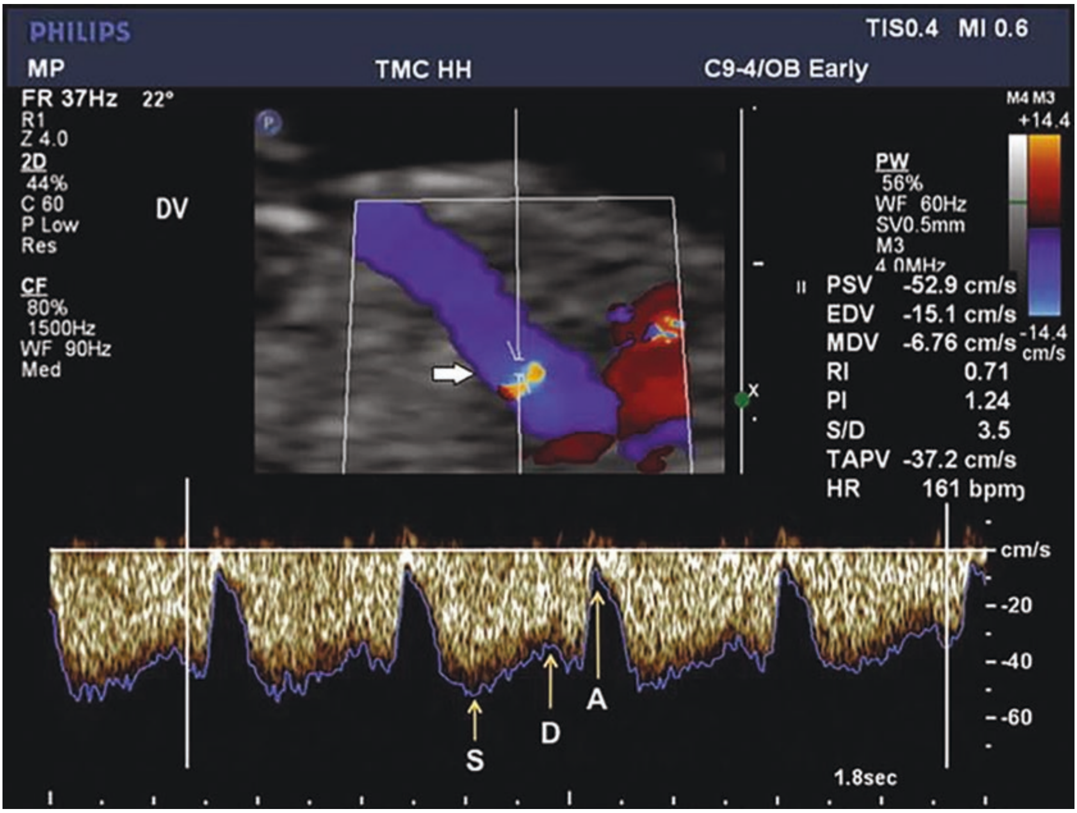
PHILIPS
TIS0.4 MI 0.6
MP
TMC HH
C9-4/OB Early
FR 37Hz 22°
R1
Z 4.0
2D
44%
C 60
P Low
Res
CF
80%
1500Hz
WF 90Hz
Med
DV
PW
56%
WF 60Hz
SV0.5mm
M3
4.0MHz
M4 M3
+14.4
-14.4 cm/s
PSV -52.9 cm/s
EDV -15.1 cm/s
MDV -6.76 cm/s
RI 0.71
PI 1.24
S/D 3.5
TAPV -37.2 cm/s
HR 161 bpm
cm/s
-20
-40
-60
S
D
A
1.8sec

Fig. 13.2 Doppler ultrasound imaging of ductus venosus flow in the sagittal plane at 12 weeks' gestation in color Doppler and spectral Doppler modes. The upper panel shows a color Doppler flow pattern with lighter color area related to high velocity, which guides the placement of the Doppler sample volume (horizontal arrow). The flow is away from the transducer, as indicated by the color map. The lower panel depicts the triphasic spectral waveforms from the ductus. S, peak systolic velocity; D, peak diastolic velocity; A, lowest peak velocity due to atrial contraction

Factors Affecting the Ductus Venosus Waveform

In early pregnancy, blood flow velocity in the ductus venosus increases with gestational age, and the increase is present throughout the fetal cardiac cycle. In a cross-sectional study of 262 normal singleton fetuses between 8 and 20 weeks' gestation, van Splunder and associates noted a significant nonlinear rise in S, D, and time-averaged peak velocity (Vta) but a significant decline in the pulsatility index for veins (PIV) [14]. The Vta increased almost fourfold. Prefumo and colleagues measured the ductus venosus velocity parameters between 10 and 14 weeks in 201 normal fetuses in a cross-sectional study [15]. During this period, the mean S wave increased from 27 to 33.6 cm/s, the mean a-wave from 5.9 to 7.8 cm/s, and the time-averaged peak velocity from 19.4 to 25.3 cm/s. These increases level off beyond the first half of pregnancy. The reference ranges for this study's ductus venosus Doppler velocity components are depicted in Figs. 13.4, 13.5, 13.6, and 13.7.

Fetal breathing movements produce intrathoracic pressure fluctuations, leading to changes in the venous pressure dynamics. Breathing-induced pressure gradients of up to 22 mmHg across the ductus venosus have been estimated in fetuses during 18–40 weeks of pregnancy utilizing the Bernoulli equation [16], which is the rationale for not assessing the ductus venosus Doppler

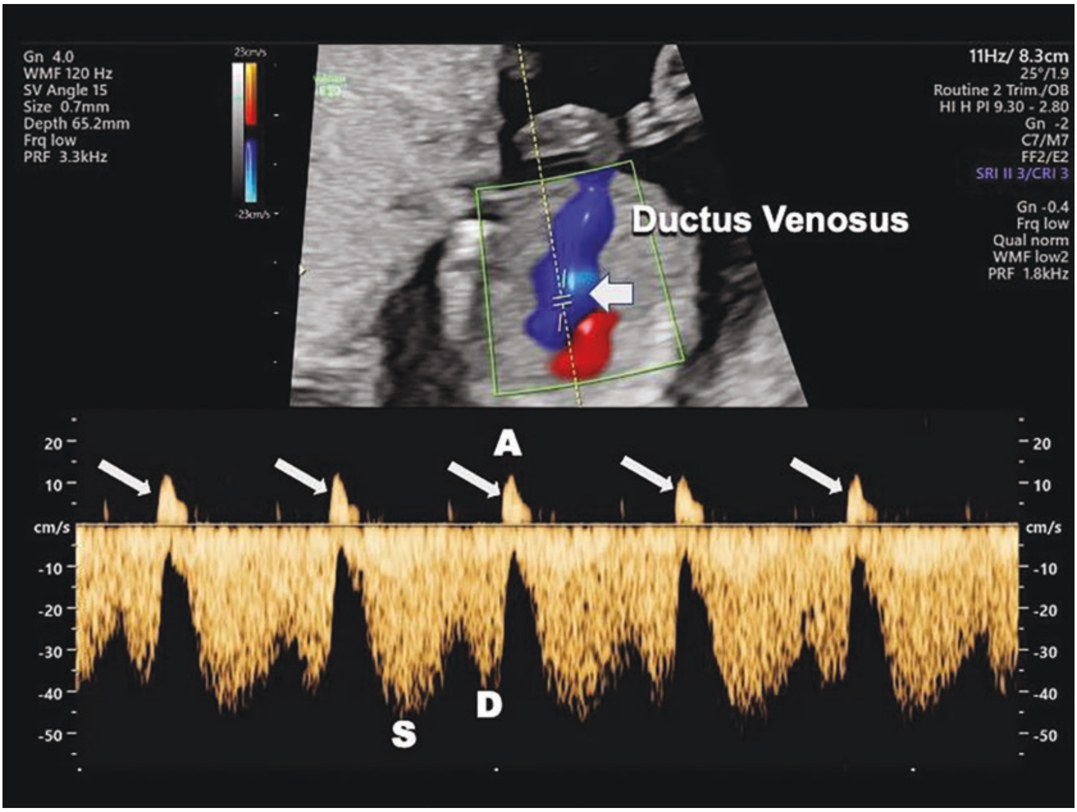
Gn 4.0
WMF 120 Hz
SV Angle 15
Size 0.7mm
Depth 65.2mm
Frq low
PRF 3.3kHz
23cm/s
-23cm/s
11Hz/ 8.3cm
25°/1.9
Routine 2 Trim./OB
HI H PI 9.30 - 2.80
Gn -2
C7/M7
FF2/E2
SRI II 3/CRI 3
Gn -0.4
Frq low
Qual norm
WMF low2
PRF 1.8kHz
Ductus Venosus
A
S
D
20
10
cm/s
-10
-20
-30
-40
-50

Fig. 13.3 Reversal of flow in the ductus venosus is depicted in color Doppler directed spectral Doppler display. The upper panel, in the oblique axial plane, shows the color Doppler flow in the ductus, and the lower panel the spectral display. The oblique arrows indicate the reversal of flow. The horizontal arrow shows the placement of the Doppler sample volume

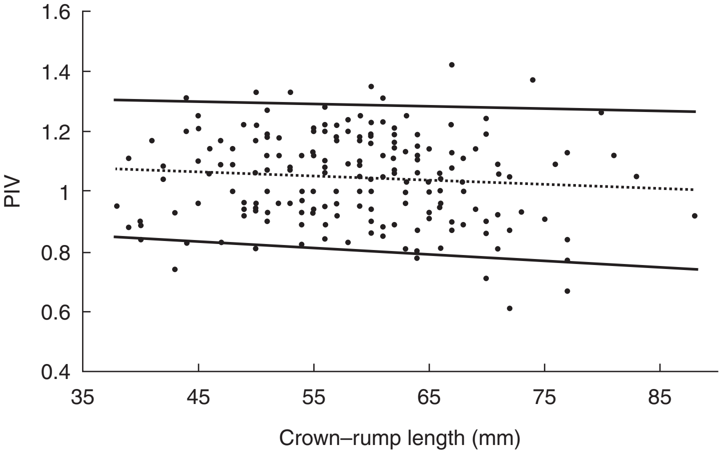

Fig. 13.4 Ductus venosus pulsatility index for veins (PIV) measurements according to crown-rump length in 198 fetuses presented with 5th, 50th, and 95th centiles. The equation for the 50th centile is $y = -0.0014x + 1.1279$ and for the standard deviation is SD = $0.0004x + 0.1233$. (Reprinted from Prefumo F, Risso D, Venturini PL, De Biasio P. Reference values for ductus venosus Doppler flow measurements at 10–14 weeks of gestation. Ultrasound Obstet Gynecol. 2002;20(1):42–6, with permission from John Wiley & Sons)

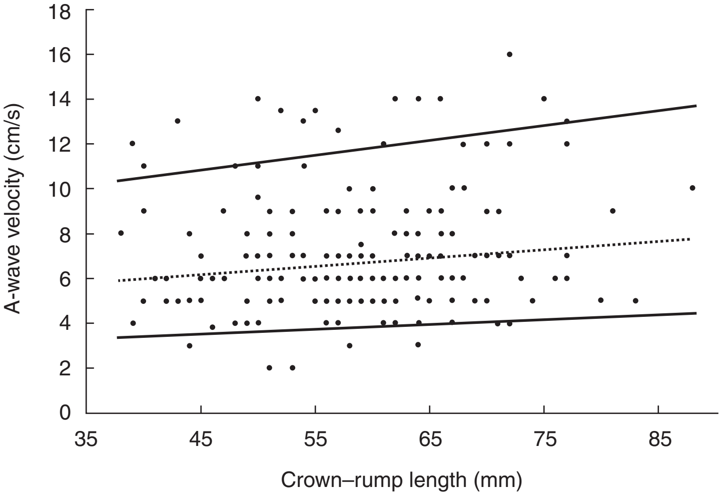

Fig. 13.5 Ductus venosus A-wave velocity measurements according to crown-rump length in 198 fetuses presented with 5th, 50th, and 95th centiles. The equation for the 50th centile is $y = 0.1304x + 22.083$ and for the standard deviation is $SD = 0.0448x + 4.862$. (Reprinted from Prefumo F, Risso D, Venturini PL, De Biasio P. Reference values for ductus venosus Doppler flow measurements at 10–14 weeks of gestation. Ultrasound Obstet Gynecol. 2002;20(1):42–6, with permission from John Wiley & Sons)

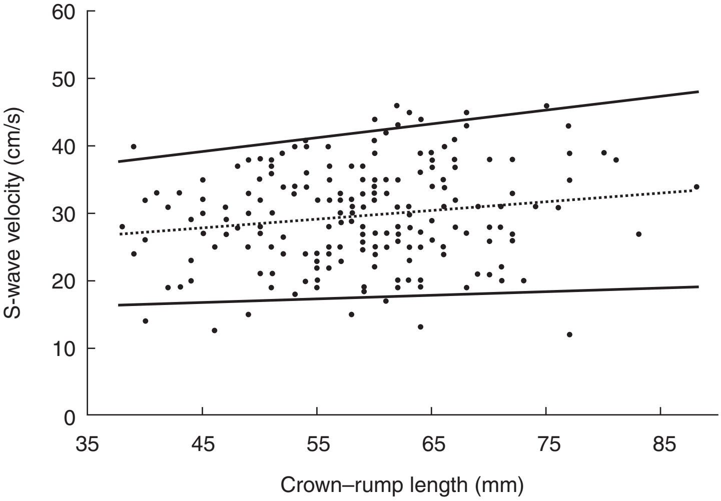

Fig. 13.6 Ductus venosus S-wave velocity measurements according to crown-rump length in 198 fetuses presented with 5th, 50th, and 95th centiles. Log10 transformation was performed for data analysis; data are displayed after antilog transformation. The equation for the 50th centile is $y = 100.0024x + 0.679$, and the standard deviation is $SD = 100.1492$. (Reprinted from Prefumo F, Risso D, Venturini PL, De Biasio P. Reference values for ductus venosus Doppler flow measurements at 10–14 weeks of gestation. Ultrasound Obstet Gynecol. 2002;20(1):42–6, with permission from John Wiley & Sons)

hemodynamics during fetal breathing. Breathing movements in early gestation are not regular and become more frequent as the fetus approaches mid-gestation [17]. Fetal movements will also affect the Doppler shift.

Fetal heart rate affects ductus venosus Doppler waveform. Bradycardia allows an increased venous return and atrial filling, leading to an enhanced atrial contraction and an enhanced a-wave. In a sheep model, Gudmundsson and

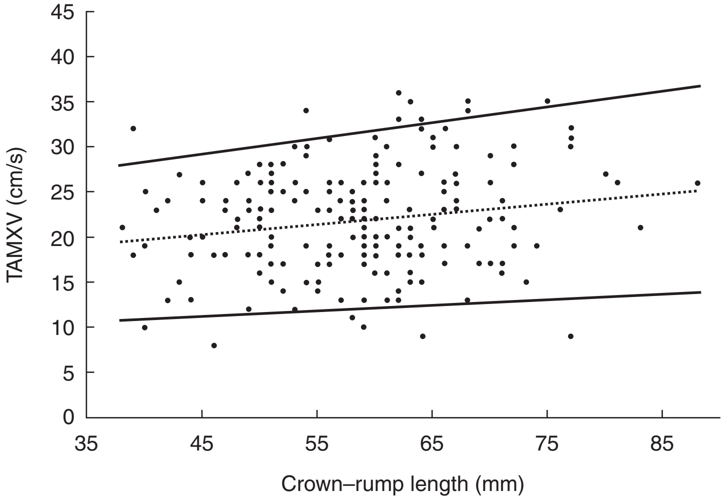

Fig. 13.7 Ductus venosus time-averaged maximum velocity (TAMXV) measurements according to crown-rump length in 198 fetuses presented with 5th, 50th, and 95th centiles. The equation for the 50th centile is $y = 0.1174x + 14.95$ and for the standard deviation is SD = $0.0342x + 3.9375$. (Reprinted from Prefumo F, Risso D, Venturini PL, De Biasio P. Reference values for ductus venosus Doppler flow measurements at 10–14 weeks of gestation. Ultrasound Obstet Gynecol. 2002;20(1):42–6, with permission from John Wiley & Sons)

coworkers noted changes in ductus venosus velocity waveform directly related to fetal bradycardia consequent to fetal hypoxemia [18]. Any increase in fetal myocardial compliance will lead to changes in the ductal waveform. Thus, hypoxia, acidosis, or intrathoracic lesions such as pleural effusion compressing the heart will lower cardiac compliance, leading to augmented a-waves [10, 19]. Blood viscosity also modifies venous Doppler waveforms, seen in fetal anemia. Lam and co-investigators reported significant increase in S, a-wave, and Vta in nonhydropic fetuses between 12 and 13 weeks with homozygous alpha thalassemia-1 [20], attributed to lower blood viscosity in anemia and hypoxia.

Ductus Venosus Doppler in First-Trimester Aneuploidy Screen

The most frequent and significant utilization of ductus venosus Doppler in the first trimester of pregnancy is for aneuploidy screening. Various investigators have demonstrated its efficacy, with or without the nuchal translucency and biomarkers. Selected reports are discussed below and summarized in Table 13.1 [21–30].

Borrell and colleagues reported Doppler velocimetry of the ductus venosus before performing invasive diagnostic procedures for trisomy 21 in 534 consecutive fetuses of 10–18 weeks of gestation [21]. Trisomy 21 was present in 11 fetuses, eight of whom had venous pulsatility index >95th centile, and three had the a-wave below 5th centile. Matias and coworkers performed Doppler velocimetry of the ductus venosus in 486 consecutive singleton pregnancies between 10 and 14 weeks, just before fetal karyotyping [22]. Of the 63 fetuses with a chromosomal anomaly, 57 (90.5%) had reverse or absent a-wave. Abnormal ductus venosus Doppler indices were observed in 13 (3.1%) of the 423 euploid fetuses. Multivariate regression analysis demonstrated that only the abnormal a-wave showed significant independent discrimination between the euploid and the aneuploid cases.

Maiz and colleagues performed a combined first-trimester screening test in a cohort of about 20,000 singleton pregnancies, examining variables including maternal age, fetal nuchal

Table 13.1 Reported abnormal ductus venosus Doppler in fetal aneuploidy in the first trimester of pregnancy

First author (reference)	Date	Total patients	Euploid cases	Aneuploid cases	Abnormal DVD aneuploid cases (%)	Abnormal DVD in euploid fetuses (%)
Matias [22]	1998	486	423	63	90.5	3.07
Antolin [23]	2001	924	911	13	77.0	4.28
Murta [24]	2002	372	343	29	89.7	2.04
Zoppi [25]	2002	325	292	33	69.7	13.0
Borrell [26][a]	2003	3382	3289	93	64.5	4.93
Toyama [27]	2004	1097	1075	22	68.2	6.42
Prefumo [28]	2005	572	497	47[b]	[c]	5.23
Maiz [29]	2009	19,800	19,614	186	64.0	3.17
Florjański [30]	2013	1526	1480	46	63.0	7.43
Totals		28,484	27,924	532	69.9	3.89

DVD ductus venosus Doppler

[a] Forty cases were defined as euploid cases due to being either placental mosaicism or a balanced translocation

[b] Only trisomy 21 cases

[c] Data were not reported, given that not all aneuploid cases in this study had DVD findings reported

translucency thickness, fetal heart rate, serum free beta human chorionic gonadotropin, pregnancy-associated plasma protein-A (PAPP-A), and the ductus venosus Doppler [29]. The a-wave was reversed in 66–75% of aneuploid but only 3.2% of euploid fetuses. Universal inclusion of the first-trimester ductus venosus Doppler would detect 96%, 92%, 100%, and 100% of trisomies 21, 18, 13, and Turner syndrome, respectively, at a false-positive rate of 3%. Similar detection rates were achieved in a two-step strategy with a false-positive rate of 2.6%, necessitating ductus venosus Doppler in only 15% of the total population.

Most fetuses with abnormal ductus venosus Doppler are euploid, and not all fetuses with aneuploidy will have abnormal findings. Table 13.1 summarizes several first-trimester ductus venosus Doppler studies demonstrating abnormal Doppler findings in 70% of aneuploid fetuses but only in 4% of the euploid fetuses.

Prenatal noninvasive risk assessment for chromosomal abnormalities during early gestation involves multiple modalities, such as the sonographic assessment of nuchal translucency and measurement of multiple analytes. The efficacy of incorporating the ductus venosus Doppler into these algorithms is discussed later.

Ductus Venosus Doppler Screening for Congenital Heart Disease

Ductus venosus Doppler waveforms reflect fetal central hemodynamics, especially in the right heart. We expect that effect of functional and anatomical abnormalities will alter this waveform. This hypothesis prompted many to explore its screening potential for the early detection of fetal cardiac disease.

Matias and coworkers performed Doppler velocimetry of the ductus venosus in 200 singleton fetuses with increased nuchal translucency, at 10–14 weeks' gestation, immediately before fetal karyotyping [22]. The results suggested that in euploid fetuses with increased nuchal translucency, the presence of abnormal ductus venosus blood flow recognized those with significant cardiac defects.

In a study involving over 41,000 euploid fetuses, the reversal of ductus venosus a-wave was observed in about 28% of the fetuses with cardiac anomalies and about 2% of the fetuses with no cardiac anomalies [31]. The authors estimated that comprehensive fetal echocardiography would detect approximately 39% of major cardiac defects, at an overall false-positive rate of about 3%, in cases with nuchal translucency above the 99th centile and those with reversed a-wave, independent of the nuchal translucency measurement.

These findings were confirmed by Borrell and associates, who studied the efficacy of various first-trimester ultrasound screening strategies for the recognition of major cardiac malformations in euploid fetuses [32]. The sonographic methods included fetal nuchal translucency and Doppler indices of the ductus venosus. When ultrasound findings were abnormal, early echocardiography was recommended. Fetal cardiac status was verified by fetal echocardiography in the second and third trimester, neonatal assessment, or autopsy. Of the 37 euploid fetuses with a major cardiac malformation, the nuchal translucency was above the 99th centile in 27% of cases, and the ductus venosus a-wave was absent or reversed in 39% of the fetuses. The authors noted a 47% detection rate of major heart defects, with a false-positive rate of about 3%.

These and other investigations suggest a role for ductus venosus Doppler for the early identification of fetuses at a higher risk of CHD. Early fetal echocardiography can be challenging and may not eliminate the need for a comprehensive ultrasound examination in mid-pregnancy. However, Zidere and associates recently demonstrated that, in expert hands, early ultrasound might achieve a high degree of accuracy [33].

More recently, the value of nuchal translucency (NT), ductus venosus Doppler, and tricuspid Doppler measurements in detecting significant CHD in the first trimester was further explored by Minella et al., who conducted a retrospective analysis of prospectively collected routine ultrasound information from over 93,000 singleton gestations between 11 and 13 weeks [34]. Those with known aneuploidy or malformations were excluded. Reversal of ductus venosus a-wave was associated with a detection rate of 27.5% with a false-positive rate of 1.8%. The use of NT measurement, tricuspid regurgitation, or reversal of the ductus venosus a-wave was associated with over 50% cases of major CHD. This is further discussed below.

Doppler Investigation of Tricuspid Flow in the First Trimester

Over the recent years, there has been a wider use of Doppler echocardiography for assessing fetal cardiac function in early pregnancy. Of the various aspects of fetal cardiac function, the tricuspid flow patterns have received the most attention, especially regarding its association with congenital cardiac malformations and aneuploidy.

Doppler Insonation Technique

The Doppler echocardiographic modalities used for assessing tricuspid flow include a two-dimensional image of the fetal heart, used to direct spectral Doppler interrogation. It is beyond the scope of this review to discuss the technique in detail. The principles are essentially the same as in later gestation [5]; however, Huggon and associates have addressed the specific technical issues related to first-trimester use [35]. An apical or a basal four-chamber view is preferred, aligning the Doppler beam with the atrioventricular flow, allowing an insonation angle below 30°. The high-pass filter is set at the lowest level allowed by the device and the power output as low as feasible. Color Doppler mode will show reversed flow depicting regurgitation. Color M-mode has the advantage of providing more accurate temporal resolution, but color modes are not routinely used for the first-trimester screening because of their inconsistency in depicting intracardiac flow in early gestation. In common practice, two-dimensional B mode imaging is utilized to place the Doppler sample volume across the tricuspid valves.

Tricuspid Flow Pattern

Spectral Doppler insonation of the atrioventricular flow reveals a biphasic flow pattern, reflecting the contributions of ventricular relaxation and atrial contractions to the Doppler flow veloc-

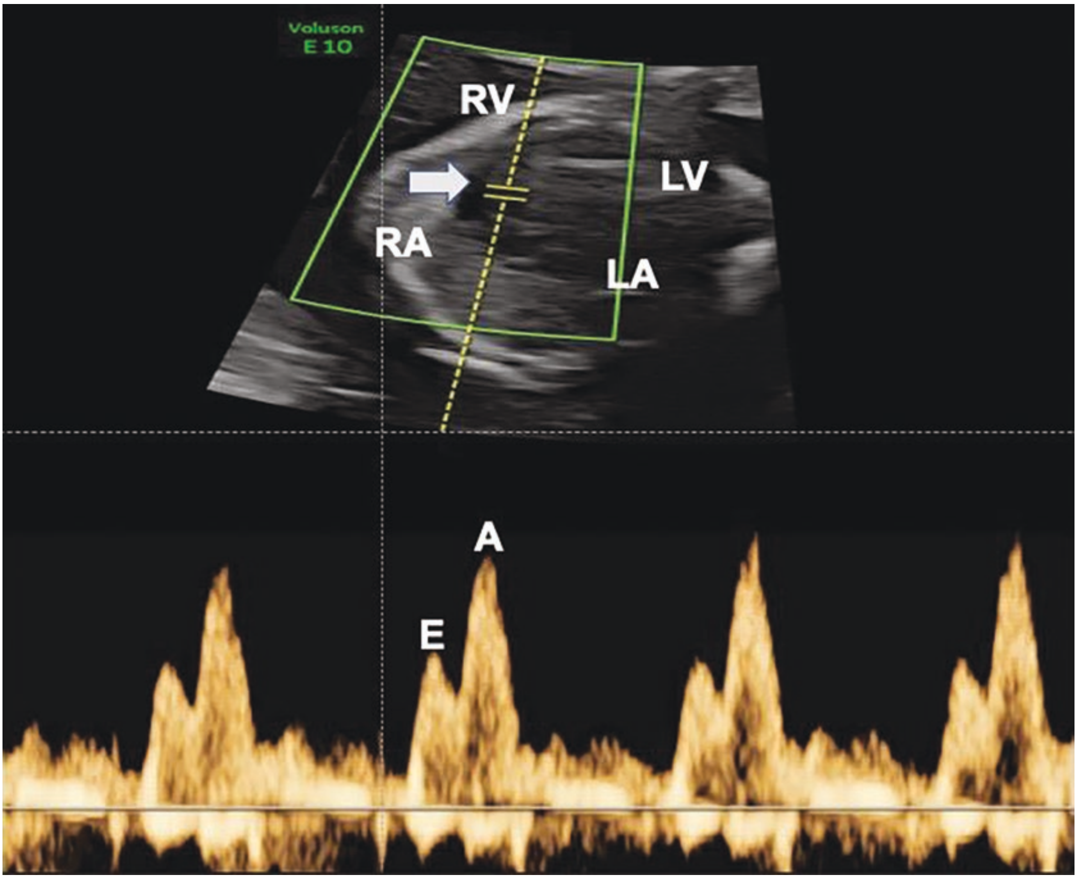

Fig. 13.8 Doppler imaging of the tricuspid flow in the first trimester of pregnancy is depicted here. The upper panel shows two-dimensional echocardiography of an apical four-chamber view of the fetal heart at 13 weeks' gestation. The horizontal arrow indicates the Doppler sampling location. Note the optimal alignment of the ultrasound beam path with the flow direction (vertical white line). The Doppler spectral display of the biphasic blood flow velocities across the tricuspid orifice is shown in the lower panel. E, peak flow velocity during ventricular diastole; A, peak flow velocity during the atrial systole; RA, right atrium; RV, right ventricle; LA, left atrium; LV, left ventricle; SP, spine

ity waveforms (Fig. 13.8). The first peak, called the E-wave, represents the peak flow velocity due to the atrial systole. The second peak, A-wave, is the peak flow velocity caused by the ventricular diastole. In the right heart, the A-wave is substantially greater than the E-wave, whereas, in the left heart, the waves are less discrepant (mitral valve). These patterns reflect physiologically lower compliance of the right ventricle compared to the left. Neonates and infants demonstrate a similar pattern.

Tricuspid Regurgitation

Normal atrioventricular flow is unidirectional, from the atrium to the ventricle. Reversal of this pattern indicates tricuspid incompetence, with the flow regurgitating from the right ventricle to the right atrium (Fig. 13.9). In the fetus, however, this finding is not always pathological. Utilizing color Doppler, Maulik et al. noted mild tricuspid regurgitation in normal fetuses in mid-pregnancy [36]. Others have extensively demonstrated this.

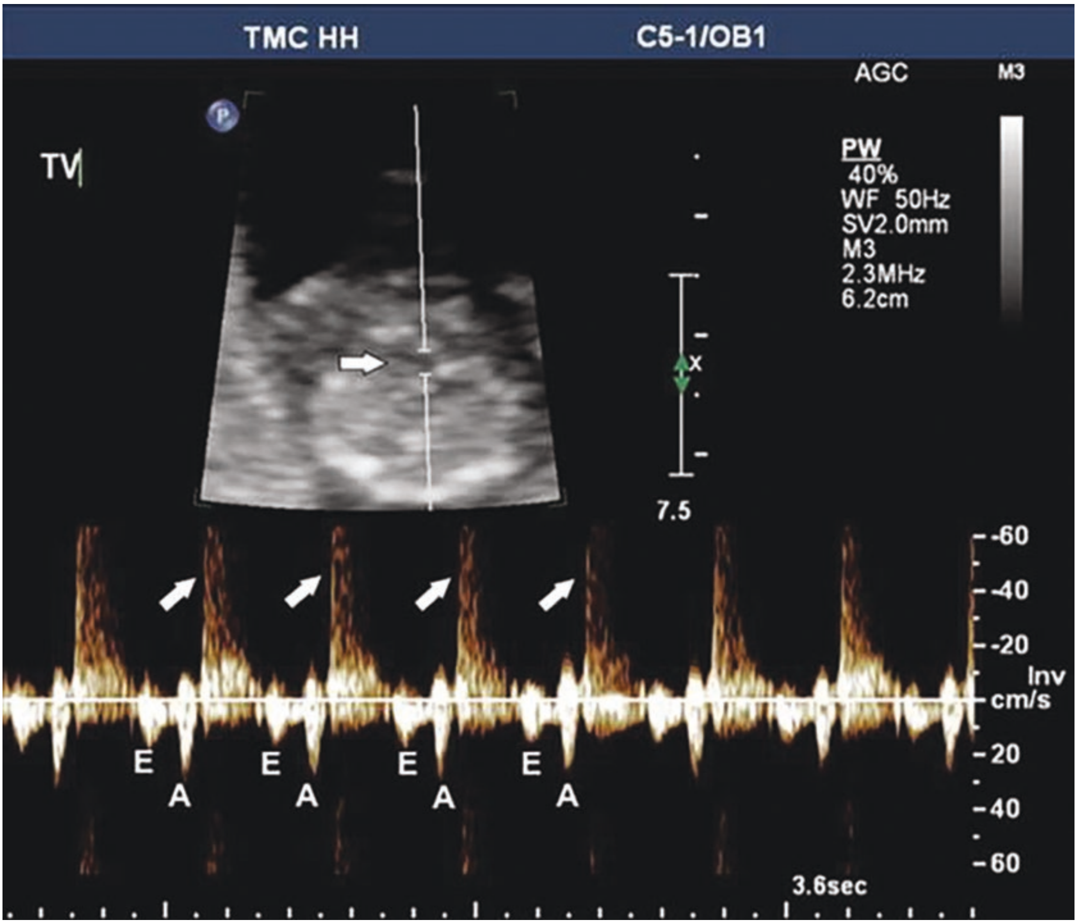

Fig. 13.9 The sonogram illustrates tricuspid regurgitation in a first-trimester fetus. The upper panel shows the placement of the Doppler sample volume. E, peak flow velocity during ventricular diastole; A, peak flow velocity during the atrial systole. The upward oblique arrows indicate the high-velocity regurgitant flow jets from the right ventricle to the right atrium. Note aliasing of the flow jets due to their high velocity

For example, utilizing color Doppler and color M-mode, Gembruch et al. demonstrated a 6% prevalence of tricuspid regurgitation in a cross-sectional study of 289 normal singleton fetuses [37]. Makikallio and associates utilized Doppler echocardiography to characterize fetal cardiac function in 16 uncomplicated pregnancies between 6 and 10 weeks [38]. They noted that the atrioventricular flow was initially monophasic and became biphasic after 9+ weeks and that regurgitant atrioventricular flow was typical after 10 weeks. The isovolumetric relaxation time significantly increased from 6 to 7 weeks, indicating progressive maturation of fetal cardiac diastolic function.

Tricuspid Doppler Screening for Aneuploidy and Congenital Heart Disease

Rizzo and colleagues performed Doppler echocardiography in 20–23-week euploid fetuses with an elevated nuchal translucency, but without any major malformations to investigate cardiac function. They observed that the ratios between the E-wave and A-wave and the ratios between the E-wave and time velocity integral were significantly decreased at both the mitral and tricuspid valves, suggesting diastolic dysfunction [39].

Lopes and colleagues performed echocardiography in 275 fetuses with increased nuchal translucency between 12 and 16 weeks' gestation [40]. Subsequent follow-ups included fetal and neonatal echocardiography, chromosomal analyses, and autopsy. Structural malformations were detected in 37 (14%) and functional abnormalities in 24 (9%) fetuses. Of the latter group, 2 (8.3%) had isolated tricuspid regurgitation and trisomy 21.

Falcon and coworkers comprehensively addressed the role of tricuspid regurgitation in prenatal diagnosis in 1557 fetuses at 11+0 to 13+6 weeks' gestation [41]. The authors successfully performed a Doppler assessment of tricuspid flow in 98.8% of cases and observed tricuspid regurgitation in 4.4% of the euploid fetuses. In contrast, fetuses with trisomy 21 and 18 had a substantially higher occurrence of regurgitation (67.5%, 33.3%, respectively). Moreover, trained sonographers could reliably assess tricuspid regurgitation during the first trimester.

In the study by Minnella et al. as discussed previously, Doppler demonstration of tricuspid regurgitation showed a detection rate of 28.9% for any significant CHD with a false-positive rate of 1.2%. The use of NT measurement, Doppler of tricuspid flow, or ductus venosus flow allowed the detection of over 55% cases of major CHD [34]. The potential impact of cell-free DNA testing may potentially affect the wide use of multimodal ultrasound screening, which is further discussed below.

Biophysical, Biochemical, and Molecular Screening in Early Pregnancy[2]

With the availability of multiple first-trimester screening tests, including the fetal Doppler and the rapid adoption of cell-free DNA testing, it is critical to determine the most effective approach for first-trimester aneuploidy screening. The advent of molecular blood tests may eventually replace personnel-intensive procedures such as nuchal translucency and fetal Doppler measurements. Only a few studies have comprehensively assessed which approach provides the optimal yet cost-effective care.

Nicolaides prospectively analyzed data to determine the effectiveness of a contingent screening approach for trisomy 21 that combined maternal age, first-trimester biomarkers, and cell-free DNA testing in 93,545 singleton pregnancies [42]. The authors observed that a detection rate of 98% of fetuses with trisomy 21, with an overall chorionic villous sampling rate <0.5%, might be accomplished by offering cell-free DNA testing to about 36%, 21%, and 11% of cases identified by first-line screening, using the combined test alone, the combined test with the addition of serum placental growth factor (PlGF) and alpha-fetoprotein (AFP), and the combined test with the addition of PIGF, AFP, and ductus venosus Doppler pulsatility index for veins, respectively.

Although cost-effective strategies were not explicitly analyzed, the authors observed that the existing protocols that include biomarkers, biophysical modalities including venous Doppler, and cell-free DNA in selected cases would reduce the need for chorionic villous sampling, with a high detection rate and a low false-positive rate. Although universal cell-free DNA testing would have an even higher detection rate, the cost may substantially increase. Other complex factors influence the efficacy and economy of the various screening approaches, which require more focused scrutiny.

Doppler Ultrasound Imaging of the Uterine Artery in the First Trimester

In the 1980s, Doppler sonography of the uterine artery ushered in exciting opportunities to investigate uteroplacental circulation [43]. The uteroplacental circulation undergoes enormous changes to fulfill fetal requirements, including the early transformation of the spiral endometrial arteries and remodeling of the placental intervillous space into large conduits of low impedance flow. Specialized trophoblastic cells invade and replace the intima and media of these arteries to cause this change [44]. This process starts in early pregnancy and extends to the myometrial course of these arteries by the middle of the second trimester.

---

[2] See also Chap. 9.

These vascular changes are reflected in the uterine artery Doppler waveforms. Failure of this remodeling process is associated with the subsequent development of preeclampsia and fetal growth restriction [45, 46]. Uterine artery Doppler has the potential for prediction and prognostication for these pregnancy complications. Early investigators used continuous-wave Doppler probes, but this blind approach was soon replaced by pulsed Doppler interrogation guided by color Doppler imaging [47–49].

Doppler Imaging Technique for the Uterine Artery

The uterine arteries can be interrogated either transabdominally or transvaginally in the first trimester. In the transabdominal approach, the paracervical site at the internal os level is preferred over the iliac crossover site as it is easier to obtain [50]. In a prospective longitudinal study of fetuses at 11–13 and 21–22 weeks of gestation, Lefebvre and colleagues successfully obtained adequate Doppler signals from both the uterine arteries in all the cases at the paracervical site at the os level, but only in about 60% of the cases at the iliac crossover site [51]. Using color Doppler, the uterus and the cervix are imaged in a midsagittal plane at the level of the internal os. Lateral manipulation of the transducer reveals the ascending branch of the uterine artery, which is sampled to obtain the uterine artery spectral Doppler signals.

The transducer is placed in the anterior fornix and manipulated laterally in the transvaginal approach. The color Doppler image reveals the uterine artery, and pulsed Doppler interrogation is performed. The angle of insonation should be less than 30°, the frequency range should accommodate the peak velocities without aliasing, the high-pass filter should be set at the lowest possible level, and the power setting should be at the lowest level providing adequate image quality.

Uterine Artery Doppler Waveform

In early pregnancy, the uterine artery Doppler waveform demonstrates a rapid acceleration and deceleration of the flow velocity during systole, followed by an early diastolic deceleration known as the diastolic notch, and a slight rise in the late diastole (Fig. 13.10). Factors that influence the waveform include gestational age, maternal heart rate, placental location, and the location of the measurement in the uterine artery system.

The pulsatility of the waveform declines rapidly between 14 and 16 weeks of pregnancy, then slowly until about 26 weeks, stabilizing until the end of pregnancy [43]. A more recent study reported a decline until 34 weeks [52]. These changes reflect the profound reduction in uteroplacental circulatory impedance during early pregnancy, consequent to the dramatic transformation of the spiral endometrial arteries by the invasion of specialized trophoblastic cells.

The effect of maternal heart rate on the diastolic run-off time modifies the waveform and its pulsatility. A higher rate will shorten the diastolic run-off time, leading to decreased pulsatility. In comparison, a lower rate will lengthen the diastolic run-off time, increasing pulsatility. Uterine artery waveforms from the ipsilateral placental site show a lower pulsatility than those from the contralateral side [53]. Finally, pulsatility declines as the Doppler sampling site is moved from upstream to downstream in the uteroplacental arterial system [46]. Thus, Doppler waveforms from the spiral arteries show significantly lower pulsatility than those from the main uterine artery, reflecting the progressive decline in circulatory impedance down the arterial tree.

The pulsatility of the uterine artery waveforms is analyzed utilizing the Doppler frequency shift’s maximum frequency shift envelope (see Fig. 13.10). The standard indices are calculated, including the pulsatility index, resistance index, and systolic-diastolic ratio. A high Doppler index is associated with adverse pregnancy outcomes, especially the development of preeclampsia and/or fetal growth restriction. Transient decelerations, called notches, have been described during

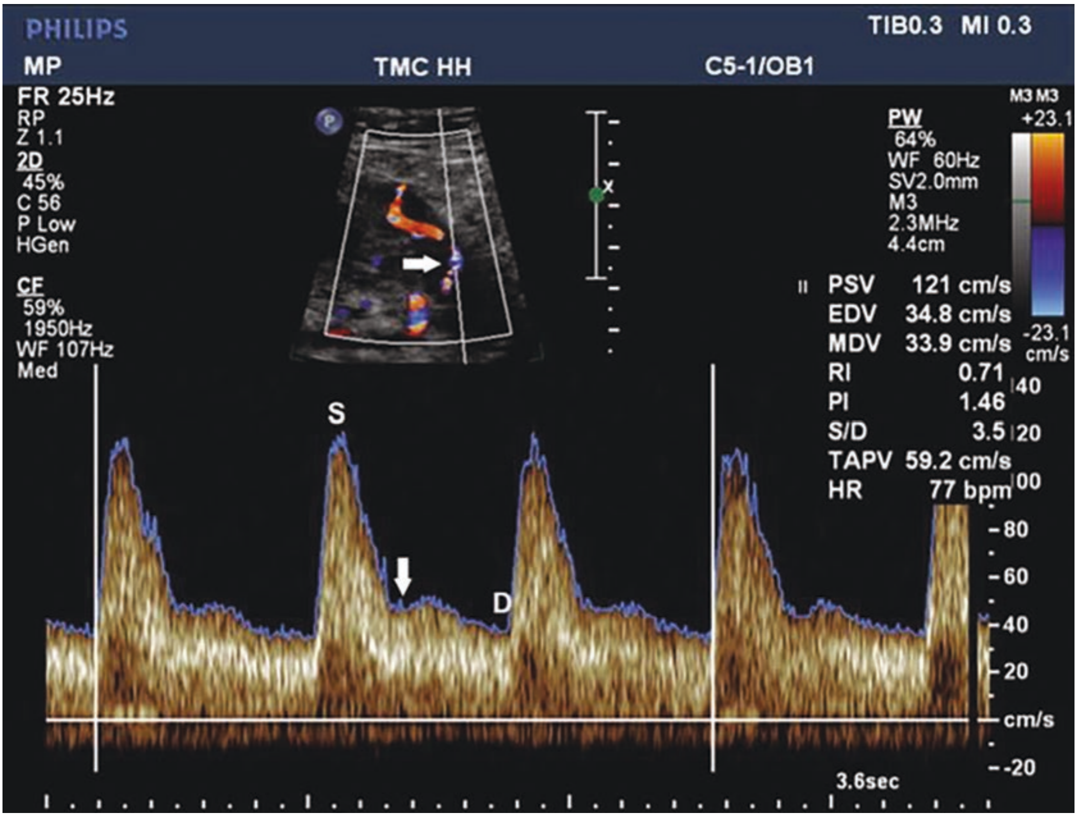
PHILIPS
TIB0.3 MI 0.3
MP
TMC HH
C5-1/OB1
FR 25Hz
RP
Z 1.1
2D
45%
C 56
P Low
HGen
CF
59%
1950Hz
WF 107Hz
Med
M3 M3
+23.1
PW
64%
WF 60Hz
SV2.0mm
M3
2.3MHz
4.4cm
PSV 121 cm/s
EDV 34.8 cm/s
MDV 33.9 cm/s
-23.1 cm/s
RI 0.71
PI 1.46
S/D 3.5
TAPV 59.2 cm/s
HR 77 bpm
S
D
140
120
100
80
60
40
20
cm/s
-20
3.6sec

Fig. 13.10 The figure shows uterine artery Doppler waveforms in the first trimester of pregnancy. The upper panel shows color Doppler flow in the ascending branch of the uterine artery. The horizontal arrow indicates the site of Doppler sampling. The lower panel depicts the spectral Doppler waveforms. The blue margin of the waveform shows the peak velocity envelope through the maternal cardiac cycle. S, the peak systolic velocity; D, the end-diastolic velocity. The vertical down arrow indicates the diastolic notch

the systolic or the diastolic phase [54–56]. Such a notch implies a high impedance in the uterine circulation. Gomez and coworkers noted bilateral notches declined from 49% of the waveforms at 11 weeks to 14% at 22 weeks; however, their persistence beyond mid-gestation was associated with adverse outcomes [52].

Clinical Applications of the Uterine Artery Doppler

High pulsatility indices and persistent notch in the uterine artery Doppler have been associated with subsequent preeclampsia, fetal growth restriction, and adverse perinatal outcomes [48, 49]. Recent reports have been variably consistent.

In a study involving 3324 consecutive singleton pregnancies, Martin and associates studied the efficacy of uterine artery Doppler, between 11 and 14 weeks of gestation, to predict subsequent development of preeclampsia and fetal growth restriction [57]. Preeclampsia developed in about 2% and fetal growth restriction in about 10% of the cases. The sensitivity of a mean pulsatility index >2.35 was only 12% for isolated fetal growth restriction and 27.0% for preeclampsia with or without coexisting fetal growth restriction. However, the sensitivity for these complications requiring delivery before 32 weeks of gestation was 60% for preeclampsia and 28% for fetal growth restriction. Gomez and associates reported that the persistence of abnormal Doppler findings, such as bilateral notch and elevated pulsatility index into the second trimester, increased adverse outcomes [52]. The highest risk was noted in those with persistent abnormal pulsatility indices (OR, 10.7; 95% CI, 3.7–30.9). Conversely, in a prospective study involving a Scandinavian population, with a prior risk for developing hypertension in pregnancy, Skrastad and colleagues observed only modest efficacy of a first-trimester protocol that combined maternal attributes, mean arterial pressure, uterine artery pulsatility index, PAPP-A, and PIGF [58].

In a systematic review of 74 studies of preeclampsia, with a total population of almost 80,000 patients, Cnossen and associates noted that an elevated uterine pulsatility index with notching carried a positive likelihood ratio of 21 in high-risk and 7.5 in low-risk mothers for developing preeclampsia [59]. For fetal growth restriction, a review of 61 studies with a population of over 41,000 low-risk women showed a positive likelihood ratio of 14.6 for developing severe growth restriction. Uterine artery Doppler was more predictive when performed in the second versus first trimester.

Others, however, could not corroborate the predictive efficacy of the first-trimester uterine artery Doppler. Audibert and associates did not observe any further improvement in the predictive efficacy when the uterine artery Doppler results were combined with biomarkers for the development of preeclampsia [60]. In a prospective cohort study of patients presenting for first-trimester aneuploidy screening between 11 and 14 weeks gestation, Goetzinger and others observed that, for a fixed false-positive rate of 10%, A-disintegrin and metalloprotease 12, PAPP-A, and uterine artery Doppler pulsatility index, in combination with maternal attributes, identified 50%, 48%, and 52% of patients who subsequently developed preeclampsia, respectively. Their combination did not enhance predictive efficiency [61]. More recently, the addition of maternal ophthalmic artery peak systolic velocity ratio may further enhance the first-trimester uterine artery Doppler detection rate of preeclampsia. A prospective observational study on 4066 pregnancies found the addition of the ophthalmic artery Doppler to first-trimester uterine artery assessment, mean arterial pressure, and maternal risk factors improved the detection rate of preterm preeclampsia from 65.9% to 70.6% [62].

Numerous studies have addressed the efficacy of early pregnancy uterine artery Doppler for predicting pregnancy complications. In a meta-analysis involving 18 studies and 55,974 women, Velauthar and associates investigated the efficacy of abnormal uterine artery Doppler for predicting preeclampsia and fetal growth restriction [63]. For early-onset preeclampsia, the sensitivity and specificity were 47.8% (95% confidence interval: 39.0–56.8) and 92.1% (95% CI: 88.6–94.6), and for early-onset fetal growth restriction they were 39.2% (95% CI: 26.3–53.8) and 93.1% (95% CI: 90.6–95.0), respectively. For any preeclampsia and fetal growth restriction, the sensitivities were 26.4% (95% CI: 22.5–30.8) and 15.4% (95% CI:12.4–18.9), respectively, and the specificities were 93.4% (95% CI: 90.4–95.5%) and 93.3% (95% CI: 90.9–95.1), respectively. The numbers of women with abnormal Doppler needed to treat with aspirin to prevent one case of early-onset preeclampsia were 173 and 421 for background risks varying between 1% and 0.4%, respectively. The authors recommended aspirin in low-risk pregnancies with abnormal uterine artery Dopplers to prevent certain pregnancy complications.

However, any such recommendation must be based on the evidence of the effectiveness of early pregnancy aspirin prophylaxis. There have been several randomized clinical trials addressing this issue. Yet, none of the studies had sufficient power. In a meta-analysis of 42 randomized controlled trials of the effectiveness of low-dose aspirin prophylaxis involving 27,222 women, Roberge and associates noted a significant reduction in adverse perinatal outcomes when the prophylactic therapy was initiated at or before 16 weeks of gestation [64]. The selection criteria for treatment included clinical risk factors such as nulliparity and chronic hypertension, and abnormal uterine artery Doppler. Initiation of aspirin at or before 16 weeks' gestation, compared to after 16 weeks, was associated with a 53% decrease in preeclampsia and an 82%

decrease in severe preeclampsia. Moreover, statistically significant declines in perinatal mortality, fetal growth restriction, and preterm births were also observed. This study provides an evidence-based justification for initiating low-dose aspirin before 16 weeks in women at risk for preeclampsia or other related adverse outcomes.

Of note, there were no differences in the outcomes, regardless of whether the patients were selected based on risk assessment or abnormal uterine artery Doppler. This intriguing study suggests the need for further investigations with an adequate sample size and appropriate study design. The most recent Cochrane review on the uteroplacental Doppler came to a similar conclusion and suggested more research [65].

Uterine artery Doppler in the first trimester of pregnancy has modest to moderate efficacy in identifying women destined to develop preeclampsia. It may also predict other adverse outcomes, including stillbirth, fetal growth restriction, and preterm labor. There is evidence of its effectiveness in improving the pregnancy outcome if low-dose aspirin prophylaxis is used before 16 completed weeks of gestation. The intervention is less effective if aspirin is used after 16 weeks' gestation. However, it is uncertain whether the addition of the uterine artery Doppler to clinical risk assessment improves the latter's predictive efficacy for implementing early aspirin prophylaxis.

Doppler of the Placental Implantation Site for Early Detection of Placental Accreta Spectrum[3]

The placenta accreta spectrum (PAS) is characterized by abnormal placenta invasion through the decidual myometrial junction into the myometrium and adjacent tissue. The heterogeneity of terminology to describe abnormally adherent placentas has made changes in prevalence over time challenging to assess. PAS encompasses placenta accreta, placenta increta, placenta percreta, morbidly adherent placenta, and invasive placentation. These conditions are associated with massive obstetrical hemorrhage with corresponding increases in fetal and maternal morbidity and mortality. Cook et al. estimated a population prevalence of PAS of 1.7/10,000. These risks jumped to 4.1% in women with one prior Cesarean delivery and to 13.3% after two or more cesarean deliveries [66].

The early diagnosis and management of PAS are critical, primarily because of increasing cesarean delivery rates. Other factors accelerating risks include placenta previa, placenta uterine anomalies, leiomyomata, prior uterine surgery, in vitro fertilization, and age greater than 35 [67]. In 2021, the Society for Maternal-Fetal Medicine (SMFM) issued a consensus report defining ultrasound markers, a systematic approach to examining pregnancies at risk for PAS, and recommended protocols for early and late first-trimester ultrasound examinations [68].

Doppler Imaging Technique

The techniques for first-trimester ultrasound diagnosis of PAS have been described in the SMFM review and are briefly summarized here. Transvaginal ultrasound is recommended in early pregnancy, and transabdominal ultrasound may be performed when appropriate. Detailed evaluation of the uterus in the midsagittal plane is performed to document the gestational sac (up to 8 6/7 weeks of gestation) and/or the placental location (up to 13 6/7 weeks of gestation). Documentation should include reference to the position of the sac and/or placenta relative to the bladder, cesarean scar (if present), and internal cervical os. Color Doppler imaging is performed using a low-velocity scale, low wall filter, and high gain to maximize detection of flow (adjusting as needed for body habitus and other clinical factors). The shape of gestational sac (up to 8 6/7 weeks of gestation) is performed. Imaging should be performed with a partially filled maternal bladder. The area of interest should be magnified so that it occupies at least half of the ultrasound image with the focal zone at an appropriate depth.

---

[3] See also Chap. 18.

First Trimester Ultrasound Markers

Several first-trimester PAS ultrasound markers have been identified and are divided into early first trimester (6–9 weeks) and late first trimester (10–14 weeks).

Early first trimester:

In patients having one or more prior cesarean sections, cesarean scar pregnancy (CSP) is characterized by the implantation of the gestational sac in the lower uterine segment proximal to or within the cesarean scar and abnormal color Doppler vascularity (Fig. 13.11a, b).

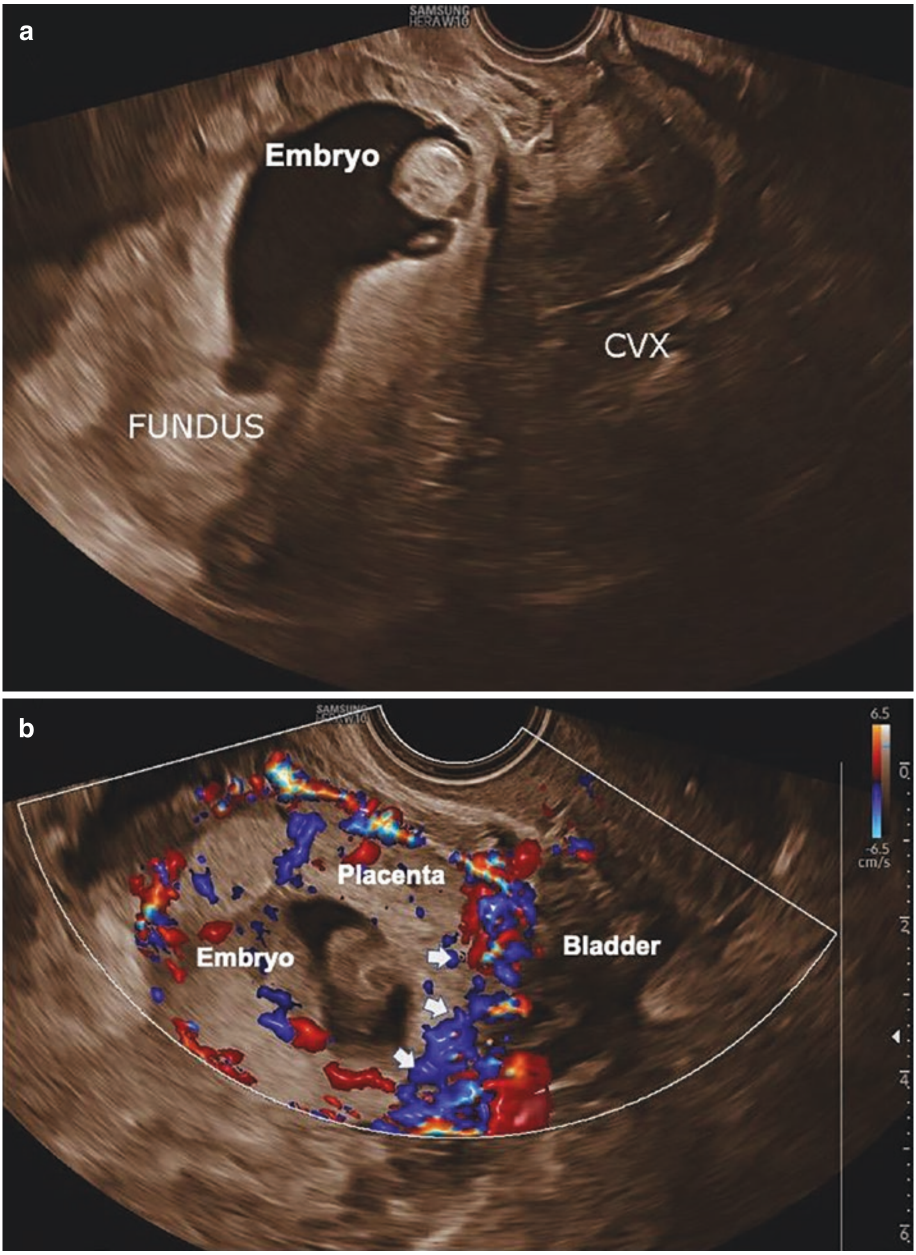
a
SAMSUNG HERA W10
Embryo
CVX
FUNDUS
b
SAMSUNG HERA W10
6.5
-6.5
cm/s
Placenta
Embryo
Bladder
0
2
4
6

Fig. 13.11 (**a**) Transvaginal sonography showing low implantation of the gestation in the uterine cavity at 11 weeks' gestation. (**b**) Transvaginal sonography showing anterior placentation and increased vascularity and lacunae (white arrows) in the lower part

In CSP, the risks of placental tissue extending into the scar and the need for hysterectomy are high. The histopathology of CSP and PAS is indistinguishable. In a retrospective study of prenatally diagnosed PAS confirmed at delivery, all had low implantation of the gestational sac. A case-control study by Abinader et al. examined women with PAS who had first trimester ultrasounds with low implantation pregnancies, and found that controls had fewer lacunae with a median of 1 versus 5 in cases, had smaller lacunae, and had different patterns on color Doppler. Lacunar swirling was only seen in women with PAS, with swirling in 10/12 women using grayscale and 12/12 with color Doppler. The presence of an abnormal uteroplacental interface was only seen in cases [69].

Late first trimester:

There is a tendency toward fundal gestational sac growth throughout pregnancy. In a study of women having a histopathological diagnosis of PAS at delivery, 28% were identified with low implantation of the gestational sac between 11 and 14 weeks. In a meta-analysis evaluating first-trimester detection of PAS, D'Antonio et al. identified a gestational sac proximal to the uterine scar in 82% of women but with a sensitivity of only 44% [70]. Other markers traditionally described in the second and third trimesters were also identified in the late first trimester. Color Doppler is particularly effective in identifying placental lacunar feeding vessels, subplacental hypervascularity, hypervascularity of the uterovesical space, intraplacental hypervascularity, and bridging vessels. Multiple concurrent markers increase the diagnostic accuracy [71].

Teaching Points

- First-trimester Doppler of fetal and uterine circulation improves the risk assessment for fetal aneuploidy, congenital heart defects, and subsequent development of preeclampsia.
- Effective Doppler sonography in early pregnancy requires appropriate technical training and adhering to the best available evidence.
- First-trimester Doppler of the ductus venosus identifies fetuses at a higher risk of aneuploidy and congenital heart defects.
- The most relevant and frequently utilized attribute of the ductus venosus Doppler is the absence or reversal of the a-wave.
- Abnormal ductus venosus Doppler is encountered in approximately 70% of the aneuploid fetuses. The ductus venosus a-wave is absent or reversed in approximately 40% of the fetuses with major cardiac defects.
- First-trimester Doppler assessment of the tricuspid flow enhances the predictive accuracy of early pregnancy aneuploidy screening.
- The presence of tricuspid regurgitation in early pregnancy identifies fetuses at a higher risk of congenital heart defects. It is seen in 67% of trisomy 21 fetuses but only in 4% of euploid fetuses.
- The addition of first-trimester fetal ultrasound screening to the biomarkers and selective use of cell-free DNA testing may substantially improve the aneuploidy detection rate and reduce the need for chorionic villous sampling.
- First-trimester uterine artery Doppler identifies pregnancies at a higher risk of developing preeclampsia and other adverse outcomes.
- Maternal prophylaxis with low-dose aspirin before 16 weeks of gestation reduces subsequent preeclampsia. It is uncertain whether adding uterine artery Doppler to clinical risk assessment improves the predictive accuracy for implementing early aspirin prophylaxis.
- Early and late first-trimester ultrasound incorporating color Doppler assists in the early recognition of PAS.

Acknowledgments We appreciate the superb assistance of our lead sonographer Maria Pinon, ARDMS.

References

1. Stuart B, Drumm J, FitzGerald DE, Duignan NM. Fetal blood velocity waveforms in normal pregnancy. Br J Obstet Gynaecol. 1980;87(9):780–5.

2. Maulik D, Saini VD, Nanda NC, Rosenzweig MS. Doppler evaluation of fetal hemodynamics. Ultrasound Med Biol. 1982;8(6):705–10.
3. Maulik D. Hemodynamic interpretation of the arterial Doppler waveform. Ultrasound Obstet Gynecol. 1993;3(3):219–27.
4. Maulik D, Mundy D, Heitmann E, Maulik D. Evidence-based approach to umbilical artery Doppler fetal surveillance in high-risk pregnancies: an update. Clin Obstet Gynecol. 2010;53:869–78.
5. Maulik D, Nanda NC, Saini VD. Fetal Doppler echocardiography: methods and characterization of normal and abnormal hemodynamics. Am J Cardiol. 1984;53(4):572–8.
6. Mavrides E, Moscoso G, Carvalho JS, Campbell S, Thilaganathan B. The anatomy of the umbilical, portal and hepatic venous system in the human fetus at 14-19 weeks of gestation. Ultrasound Obstet Gynecol. 2001;18(6):598–604.
7. Kessler J, Rasmussen S, Godfrey K, Hanson M, Kiserud T. Fetal growth restriction is associated with prioritization of umbilical blood flow to the left hepatic lobe at the expense of the right lobe. Pediatr Res. 2009;66(1):113–7.
8. Kiserud T, Eik-Nes SH, Blaas H-G, Hellevik LR. Ultrasonographic velocimetry of the fetal ductus venosus. Lancet. 1991;338(8780):1412–4.
9. Baschat AA. Ductus venosus Doppler for fetal surveillance in high-risk pregnancies. Clin Obstet Gynecol. 2010;53(4):858–68.
10. Kiserud T, Kessler J. Venous hemodynamics. In: Maulik D, Lees C, editors. Doppler ultrasound in obstetrics and gynecology. 3rd ed. New York: Springer; 2022.
11. Kiserud T. Physiology of the fetal circulation. Semin Fetal Neonatal Med. 2005;10(6):493–503.
12. Kiserud T, Kessler J. Ductus venosus. In: Maulik D, Lees C, editors. Doppler ultrasound in obstetrics and gynecology. 3rd ed. New York: Springer; 2022.
13. Nelson TR, Fowlkes JB, Abramowicz JS, Church CC. Ultrasound biosafety considerations for the practicing sonographer and sonologist. J Ultrasound Med. 2009;28(2):139–50.
14. Van Splunder P, Huisman TW, DeRidder MA, Wladimiroff JW. Fetal venous and arterial flow velocity wave forms between eight and twenty weeks of gestation. Pediatr Res. 1996;40(1):158–62.
15. Prefumo F, Risso D, Venturini PL, De Biasio P. Reference values for ductus venosus Doppler flow measurements at 10-14 weeks of gestation. Ultrasound Obstet Gynecol. 2002;20(1):42–6.
16. Kiserud T, Hellevik LR, Eik-Nes SH, Angelsen BA, Blaas HG. Estimation of the pressure gradient across the fetal ductus venosus based on Doppler velocimetry. Ultrasound Med Biol. 1994;20(3):225–32.
17. de Vries JI, Visser GH, Prechtl HF. The emergence of fetal behaviour. II. Quantitative aspects. Early Hum Dev. 1985;12(2):99–120.
18. Gudmundsson S, Gunnarsson GO, Hokegard KH, Ingemarsson J, Kjellmer I. Venous Doppler velocimetry in relationship to central venous pressure and heart rate during hypoxia in the ovine fetus. J Perinat Med. 1999;27(2):81–90.
19. Bhide A, Acharya G, Bilardo CM, Brezinka C, Cafici D, Hernandez-Andrade E, et al. ISUOG practice guidelines: use of Doppler ultrasonography in obstetrics. Ultrasound Obstet Gynecol. 2013;41(2):233–9.
20. Lam YH, Tang MH, Tse HY. Ductus venosus Doppler study in fetuses with homozygous alpha-thalassemia-1 at 12 to 13 weeks of gestation. Ultrasound Obstet Gynecol. 2001;7(1):30–3.
21. Borrell A, Antolin E, Costa D, Farre MT, Martinez JM, Fortuny A. Abnormal ductus venosus blood flow in trisomy 21 fetuses during early pregnancy. Am J Obstet Gynecol. 1998;179(6 Pt 1):1612–7.
22. Matias A, Gomes C, Flack N, Montenegro N, Nikolaides KH. Screening for chromosomal defects at 11-14 weeks: the role of ductus venosus blood flow. Ultrasound Obstet Gynecol. 1998;12(6):380–4.
23. Antolin E, Comas C, Torrents M, Munoz A, Figueras F, Echevarria M, et al. The role of ductus venosus blood flow assessment in screening for chromosomal abnormalities at 10–16 weeks of gestation. Ultrasound Obstet Gynecol. 2001;17(4):295–300.
24. Murta CG, Moron AF, Avila MA, Weiner CP. Application of ductus venosus Doppler velocimetry for the detection of fetal aneuploidy in the first trimester of pregnancy. Fetal Diagn Ther. 2002;17(5):308–14.
25. Zoppi MA, Putzolu M, Ibba RM, Floris M, Monni G. First trimester ductus venosus velocimetry in relation to nuchal translucency thickness and fetal karyotype. Fetal Diagn Ther. 2002;17(1):52–7.
26. Borrell A, Martinez JM, Seres A, Borobio V, Cararach V, Fortuny A. Ductus venosus assessment at the time of nuchal translucency measurement in the detection of fetal aneuploidy. Prenat Diagn. 2003;23(11):921–6.
27. Toyama JM, Brizot ML, Liao AW, Lopes LM, Nomura RM, Saldanha FA, et al. Ductus venosus blood flow assessment at 11 to 14 weeks of gestation and fetal outcome. Ultrasound Obstet Gynecol. 2004;23(4):341–5.
28. Prefumo F, Sethna F, Sairam S, Bhide A, Thilaganathan B. First trimester ductus venosus, nasal bones, and Down syndrome in a high-risk population. Obstet Gynecol. 2005;105(6):1348–54.
29. Maiz N, Valencia C, Kagan KO, Wright D, Nicolaides KH. Ductus venosus Doppler in screening for trisomies 21, 18 and 13 and Turner syndrome at 11-13 weeks of gestation. Ultrasound Obstet Gynecol. 2009;33(5):512–7.
30. Florjański J, Fuchs T, Zimmer M, Homola W, Pomorski M, Blok D. The role of ductus venosus Doppler flow in the diagnosis of chromosomal abnormalities during the first trimester of pregnancy. Adv. Clin Exp Med. 2013;22(3):395–401.
31. Chelemen T, Syngelaki A, Maiz N, Allan L, Nicolaides KH. Contribution of ductus venosus Doppler in first-trimester screening for major cardiac defects. Fetal Diagn Ther. 2011;29(2):127–34.

32. Borrell A, Grande M, Bennasar M, Borobio V, Jimenez JM, Stergiotou I, et al. First-trimester detection of major cardiac defects with the use of ductus venosus blood flow. Ultrasound Obstet Gynecol. 2013;42(1):51–7.
33. Zidere V, Bellsham-Revell H, Persico N, Allan LD. Comparison of echocardiographic findings in fetuses at less than 15 weeks' gestation with later cardiac evaluation. Ultrasound Obstet Gynecol. 2013;42(6):679–86.
34. Minnella GP, Crupano FM, Syngelaki A, Zidere V, Akolekar R, Nicolaides KH. Diagnosis of major heart defects by routine first-trimester ultrasound examination: association with increased nuchal translucency, tricuspid regurgitation and abnormal flow in ductus venosus. Ultrasound Obstet Gynecol. 2020;55(5):637–44.
35. Huggon IC, DeFigueiredo DB, Allan LD. Tricuspid regurgitation in the diagnosis of chromosomal anomalies in the fetus at 11–14 weeks of gestation. Heart. 2003;89:1071–3.
36. Maulik D, Nanda NC, Hsiung MC, Youngblood JP. Doppler color flow mapping of the fetal heart. Angiology. 1986;37(9):628–32.
37. Gembruch U, Smrcek JM. The prevalence and clinical significance of tricuspid valve regurgitation in normally grown fetuses and those with intrauterine growth retardation. Ultrasound Obstet Gynecol. 1997;9(6):374–82.
38. Makikallio K, Jouppila P, Rasanen J. Human fetal cardiac function during the first trimester of pregnancy. Heart. 2005;91:334–8.
39. Rizzo G, Muscatello A, Angelini E, Capponi A. Abnormal cardiac function in fetuses with increased nuchal translucency. Ultrasound Obstet Gynecol. 2003;21(6):539–42.
40. Lopes LM, Brizot ML, Lopes MA, Ayello VD, Schultz R, Zugaib M. Structural and functional cardiac abnormalities identified prior to 16 weeks' gestation in fetuses with increased nuchal translucency. Ultrasound Obstet Gynecol. 2003;22(5):470–8.
41. Falcon O, Faiola S, Huggon I, Allan L, Nicolaides KH. Fetal tricuspid regurgitation at the 11+0 to 13+6-week scan: association with chromosomal defects and reproducibility of the method. Ultrasound Obstet Gynecol. 2006;27(6):609–12.
42. Nicolaides KH, Wright D, Poon LC, Syngelaki A, Gil MM. First-trimester contingent screening for trisomy 21 by biomarkers and maternal blood cell-free DNA testing. Ultrasound Obstet Gynecol. 2013;42(1):41–50.
43. Schulman H, Fleischer A, Farmakides G, Bracero L, Rochelson B, Grunfeld L. Development of uterine artery compliance in pregnancy as detected by Doppler ultrasound. Am J Obstet Gynecol. 1986;55(5):1031–6.
44. Pijnenborg R, Bland JM, Robertson WB, Brosens I. Uteroplacental arterial changes related to interstitial trophoblast migration in early human pregnancy. Placenta. 1983;4(4):397–413.
45. Brosens IA, Robertson WB, Dixon HG. The role of the spiral arteries in the pathogenesis of preeclampsia. Obstet Gynecol Annu. 1972;1:117–91.
46. Lyall F, Robson SC, Bulmer JN. Spiral artery remodeling and trophoblast invasion in preeclampsia and fetal growth restriction: relationship to clinical outcome. Hypertension. 2013;62(6):1046–54.
47. Jurkovic D, Jauniaux E, Kurjak A, Hustin J, Campbell S, Nicolaides KH. Transvaginal color Doppler assessment of the uteroplacental circulation in early pregnancy. Obstet Gynecol. 1991;77(3):365–9.
48. Guzman ER, Kontopoulos E, Zalud I. Doppler velocimetry of the uteroplacental circulation. In: Maulik D, Zalud I, editors. Doppler ultrasound in obstetrics and gynecology. 2nd ed. New York: Springer; 2005. p. 227–42.
49. Thaler I, Amin A. Doppler velocimetry of the uteroplacental circulation in early pregnancy. In: Maulik D, Zalud I, editors. Doppler ultrasound in obstetrics and gynecology. 2nd ed. New York: Springer; 2005. p. 255–75.
50. Khalil A, Nicolaides KH. How to record uterine artery Doppler in the first trimester. Ultrasound Obstet Gynecol. 2013;42(4):478–9.
51. Lefebvre J, Demers S, Bujold E, Nicolaides KH, Girard M, Brassard N, et al. Comparison of two different sites of measurement for transabdominal uterine artery Doppler velocimetry at 11-13 weeks. Ultrasound Obstet Gynecol. 2012;40(3):288–92.
52. Gomez O, Figueras F, Martinez JM, del Rio M, Palacio M, Eixarch E, et al. Sequential changes in uterine artery blood flow pattern between the first and second trimesters of gestation in relation to pregnancy outcome. Ultrasound Obstet Gynecol. 2006;28(6):802–8.
53. Kofinas A, Penry M, Greiss F, Meis PJ, Nelson LH. The effect of placental location on uterine artery flow velocity waveforms. Am J Obstet Gynecol. 1988;159(6):1504–8.
54. Campbell S, Bewley S, Cohen-Overbrook T. Investigation of the uteroplacental circulation by Doppler ultrasound. Semin Perinatol. 1987;11(4):362–8.
55. Fleischer A, Schulman H, Farmakides G, Bracero L, Grunfeld L, Rochelson B, et al. Uterine artery Doppler velocimetry in pregnant women with hypertension. Am J Obstet Gynecol. 1986;154(4):806–13.
56. Thaler I, Weiner Z, Itskovitz J. Systolic or diastolic notch in uterine artery blood flow velocity waveforms in hypertensive pregnant patients: relationship to outcome. Obstet Gynecol. 1992;80(2):277–82.
57. Martin AM, Bindra R, Curcio P, Cicero S, Nicolaides KH. Screening for preeclampsia and fetal growth restriction by uterine artery Doppler at 11-14 weeks of gestation. Ultrasound Obstet Gynecol. 2001;18(6):583–6.
58. Skrastad RB, Hov GG, Blaas HG, Romundstad PR, Salvesen K. A prospective study of screening for hypertensive disorders of pregnancy at 11-13 weeks in a Scandinavian population. Acta Obstet Gynecol Scand. 2014;93(12):1238–47.

59. Cnossen JS, Morris RK, ter Riet G, Mol BW, van der Post JA, Coomarasamy A, et al. Use of uterine artery Doppler ultrasonography to predict preeclampsia and intrauterine growth restriction: a systematic review and bivariable meta-analysis. CMAJ. 2008;178(6):701–11.
60. Audibert F, Boucoiran I, An N, Aleksandrov N, Delvin E, Bujold E, et al. Screening for preeclampsia using first-trimester serum markers and uterine artery Doppler in nulliparous women. Am J Obstet Gynecol. 2010;203(4):383.e1–8.
61. Goetzinger KR, Zhong Y, Cahill AG, Odibo L, Macones GA, Odibo AO. Efficiency of first-trimester uterine artery Doppler, a-disintegrin and metalloprotease 12, pregnancy-associated plasma protein a, and maternal characteristics in the prediction of preeclampsia. J Ultrasound Med. 2013;32(9):1593–600.
62. Gana N, Sarno M, Vieira N, Wright A, Charakida M, Nicolaides KH. Ophthalmic artery Doppler at 11-13 weeks' gestation in prediction of pre-eclampsia. Ultrasound Obstet Gynecol. 2022;59(6):731–6.
63. Velauthar L, Plana MN, Kalidindi M, Zamora J, Thilaganathan B, Illanes SE, et al. First-trimester uterine artery Doppler and adverse pregnancy outcome: a meta-analysis involving 55,974 women. Ultrasound Obstet Gynecol. 2014;43(5):500–7.
64. Roberge S, Nicolaides KH, Demers S, Villa P, Bujold E. Prevention of perinatal death and adverse perinatal outcome using low-dose aspirin: a meta-analysis. Ultrasound Obstet Gynecol. 2013;41(5):491–9.
65. Stampalija T, Gyte GML, Alfirevic Z. Utero-placental Doppler ultrasound for improving pregnancy outcome. Cochrane Database Syst Rev. 2010;9:CD008363.
66. Cook JR, Jarvis S, Knight M, Dhanjal MK. Multiple repeat caesarean section in the UK: incidence and consequences to mother and child. A national, prospective, cohort study. BJOG Int J Obstet Gynaecol. 2013;120(1):85–91.
67. Fitzpatrick KE, et al. Incidence and risk factors for placenta accreta/increta/percreta in the UK: a National case-control. PLoS One. 2012;7(12):e52893.
68. Shainker SA, Coleman B, Timor-Tritsch IE, Bhide A, Bromley B, Cahill AG, Gandhi M, Hecht JL, Johnson KM, Levine D, Mastrobattista J. Special Report of the Society for Maternal-Fetal Medicine Placenta Accreta Spectrum Ultrasound Marker Task Force: Consensus on definition of markers and approach to the ultrasound examination in pregnancies at risk for placenta accreta spectrum. Am J Obstet Gynecol. 2021;224(1):B2–14.
69. Abinader RR, Macdisi N, El Moudden I, Abuhamad A. First-trimester ultrasound diagnostic features of placenta accreta spectrum in low-implantation pregnancy. Ultrasound Obstet Gynecol. 2022 Apr;59(4):457–64.
70. D'Antonio F, et al. First-trimester detection of abnormally invasive placenta in high-risk women: systematic review and meta-analysis. Ultrasound Obstet Gynecol. 2018;51:176–83.
71. Calì G, Timor-Tritsch IE, Palacios-Jaraquemada J, et al. Changes in ultrasonography indicators of abnormally invasive placenta during pregnancy. Int J Gynaecol Obstet. 2018;140:319–25.

14

Three-Dimensional Ultrasound: A Role in Early Pregnancy?

Renato Ximenes, Rafael Peters,
and Luís F. Goncalves

Abbreviations

2D US	Two-dimensional ultrasonography
3D US	Three-dimensional ultrasonography
4D US	Four-dimensional ultrasonography
STIC	Spatiotemporal image correlation

Introduction

Although the second-trimester "18–22-week" scan is the standard of care for fetal anatomical evaluation, technological progress in ultrasound (US) equipment and high frequency transvaginal transducers made detailed assessment of the first trimester fetus a reality [1–9]. High-quality first trimester ultrasonography represents the first opportunity to understand embryonic development and to identify congenital structural anomalies, usually those at the most severe end of the spectrum [8, 10–13]. When major and/or lethal anomalies are diagnosed, benefits include the possibility of early genetic testing and counseling and a wide range of management options that may not be available later. If pregnancy termination is a consideration, the procedure can be performed safer during the first or early second trimesters [11].

This chapter reviews the role of three-dimensional (3D) US as an adjunctive imaging modality to two-dimensional ultrasound (2D) US for first trimester evaluation of embryonic development and early diagnosis of congenital structural anomalies. The reader is reminded that knowledge of normal embryonic and fetal development, congenital anomalies, as well as operator experience, are all likely to have a higher impact on the quality of ultrasonographic examinations performed in the first trimester than the availability of high-resolution US systems equipped with state-of-the-art 3D technology.

Instrumentation

3D US can be performed using mechanical or matrix array transducers. First trimester prenatal diagnosis of congenital anomalies is ideally performed using high frequency transvaginal probes.

R. Ximenes
Fetal Medicine Foundation Latin America—FMFLA, Campinas, São Paulo, Brazil

R. Peters
Centro Médico Bom Pastor, Igrejinha, Rio Grande do Sul, Brazil

L. F. Goncalves (✉)
Department of Radiology, Fetal Imaging, Phoenix Children's Hospital, Phoenix, AZ, USA

Radiology and Child Health, University of Arizona School of Medicine, Phoenix, AZ, USA

Radiology, Mayo Clinic, Phoenix, AZ, USA

Radiology, Creighton University, Phoenix, AZ, USA
e-mail: lgoncalves@phoenixchildrens.com

© The Author(s), under exclusive license to Springer Nature Switzerland AG 2023
J. S. Abramowicz, R. E. Longman (eds.), *First-Trimester Ultrasound*,
https://doi.org/10.1007/978-3-031-24133-8_14

If evaluation of the fetal heart is desired, color Doppler is strongly advised, as its use is associated with increased detection rates for congenital heart disease (CHD) in the first trimester [11, 14–16]. In addition, volumetric imaging can be performed using four-dimensional (4D) spatio-temporal image correlation (STIC) technology, which allows evaluation of both cardiac anatomy and contractility (Fig. 14.1) [17–20]. The use of transducers with the highest possible frequency is advised in order to maximize spatial resolution (Fig. 14.2).

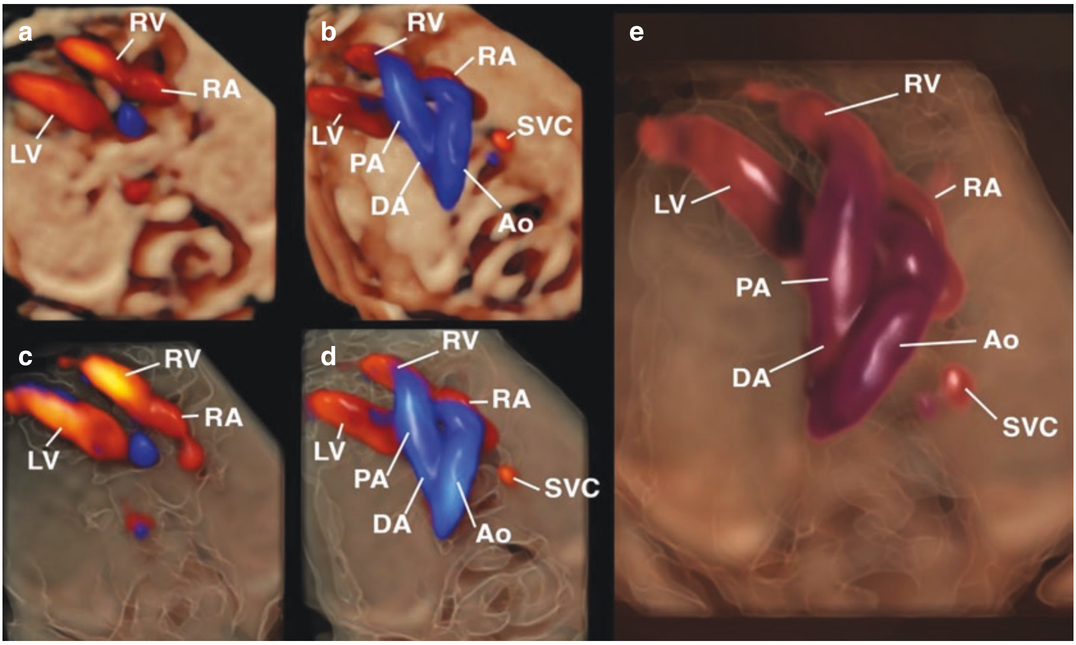

Fig. 14.1 Several examples of volumetric images of the fetal heart at 12 weeks obtained with STIC technology. HDLive flow (**a**) and HD live silhouette mode (**c**) rendered images of the four-chamber view showing right and left atrioventricular connections. HDLive flow (**b**), HDLive silhouette mode (**d**), and monochromatic HDLive silhouette mode (**e**) images of the three-vessel and trachea view showing the pulmonary artery/ductus arteriosus, transverse arch of the aorta and superior vena cava. *LV* left ventricle, *RV* right ventricle, *RA* right atrium, *PA* pulmonary artery, *DA* ductus arteriosus, *SVC* superior vena cava, *Ao* aorta. (Courtesy Prof. Rabih Chaoui)

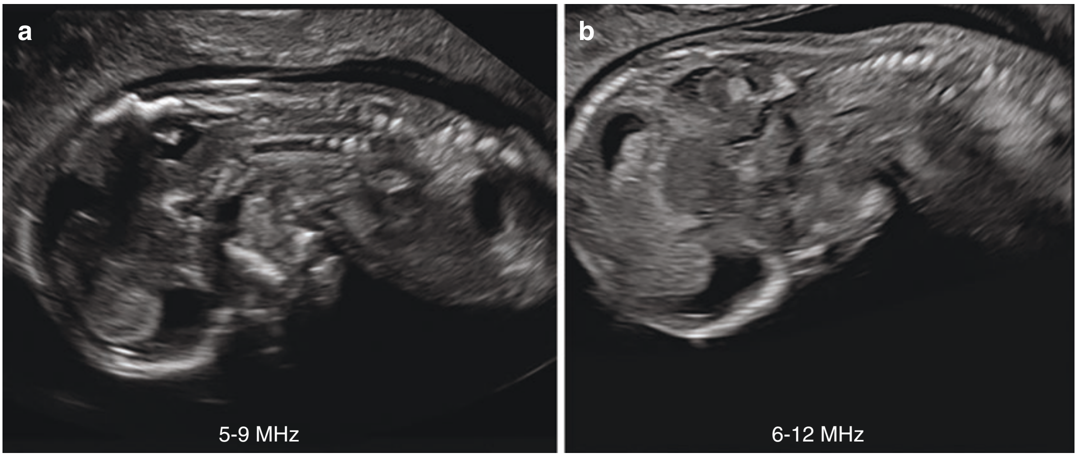

Fig. 14.2 Comparison of image resolution in the same 11-week embryo examined by transvaginal 5–9 MHz (**a**) and 6–12 MHz probes (**b**). Note the higher resolution achieved with the higher frequency probe

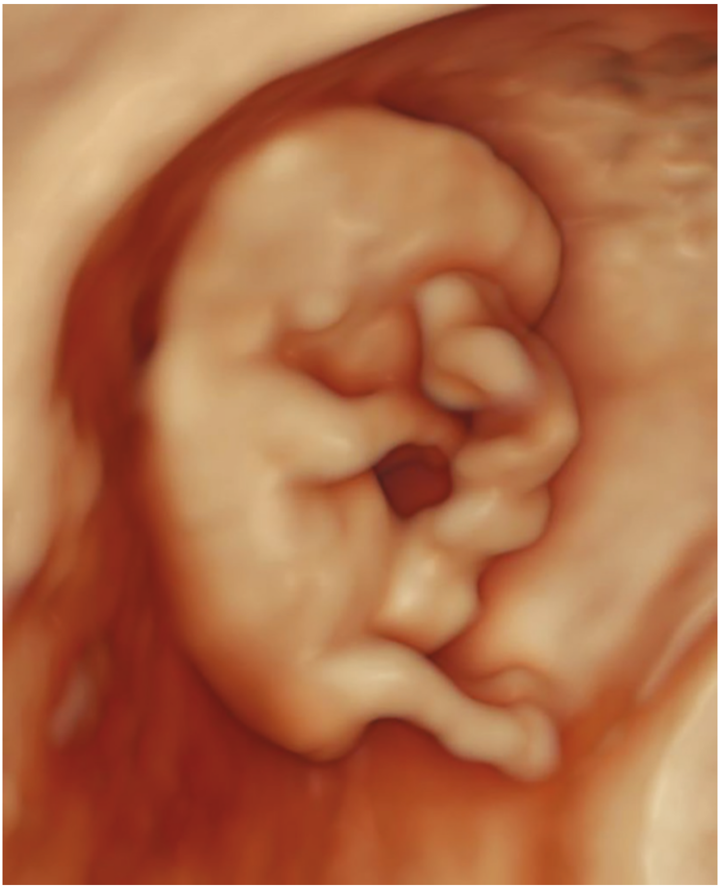

Fig. 14.3 3D rendered HDLive image of a 9–10-week embryo (crown-rump length 30 mm)

Novel 3D rendering methodologies that use an adjustable light source coupled with software that calculates the propagation of light through surface structures in relation to the light direction (HDLive—General Electric Medical System, Zipf, Austria; TrueVue—Philips Healthcare, Bothell, Washington, USA) allow the generation of realistic 3D and 4D images of human embryos, propelling the field of sonoembryology (Fig. 14.3) [21–24].

Ideal Gestational Age to Perform the Exam

The first trimester examination can be performed in two distinct periods:

- Early first trimester scan (sonoembryology), from 4 weeks to 10 weeks and 6 days or up to a crown-rump length (CRL) of 44 mm.
- Early anatomical scan, performed from 11 to 14 weeks or with a CRL ranging between 44 and 84 mm.

The main objectives of the "early first trimester scan" are to evaluate the presence, size, location, and number of gestational sacs (GS), confirm viability, establish the number of viable embryos, and establish an accurate gestational age. As gestational age advances, gross embryonic anatomy can be evaluated, and congenital anomalies identified.

Over the past three decades, several studies have shown the importance of first trimester prenatal diagnosis by US. Nicolaides et al. [25] established the "11–14 week scan" in 1992 by standardizing the criteria to measure nuchal translucency (NT) as a marker for aneuploidy and subsequently for CHD. More recently, the NT examination has been extended to include a detailed survey for fetal anomalies, in addition to early fetal echocardiography if the NT is increased above 99° centile, resulting in a high detection rate of congenital anomalies [11, 12, 16, 26]. Visualization rates for fetal cardiac structures are higher after 12 weeks compared to 11 weeks, and even better after 13 weeks, when the aortic root can be more consistently demonstrated [27]. The tradeoff is the upper CRL limit of 84 mm to measure the NT [9]. Therefore, careful scheduling of the examination is advised so that both NT measurement and early morphological evaluation can be performed at the same visit. Please note that a high detection rate for fetal anomalies, including congenital heart disease, has also been reported with the use of transvaginal ultrasonography by expert sonologists performing such exams between 14 and 17 weeks of gestation [13, 28].

What Can Be Confidently Imaged?

Much of what can be confidently imaged in the first trimester comes from work performed with 2D US. Table 14.1 provides a list of anatomical structures that may be assessed during the 11–14 weeks scan, as recommended by ISUOG [9]. The reader is encouraged to attempt to image structures marked as optional as well, and to push his/her limits beyond the guidelines. For example, with good technique and adequate equipment, the outflow tracts of the fetal heart can be imaged early, and early diagnosis of conotruncal anomalies is possible [5, 14, 29, 30].

Table 14.1 Suggested anatomical assessment at 11 to 13+6 weeks (ISUOG—International Society of Ultrasound in Obstetrics and Gynecology—guidelines)

Organ/anatomical area	Present and/or normal?
Head	Present
	Cranial bones
	Midline falx
	Choroid-plexus-filled ventricles
Neck	Normal appearance
	Nuchal translucency thickness (if accepted after informed consent and trained/certified operator available)[a]
Face	Eyes with lens[a]
	Nasal bone[a]
	Normal profile/mandible[a]
	Intact lips[a]
Spine	Vertebrae (longitudinal and axial)[a]
	Intact overlying skin[a]
Chest	Symmetrical lung fields
	No effusions or masses
Heart	Cardiac regular activity
	Four symmetrical chambers[a]
Abdomen	Stomach present in left upper quadrant
	Bladder[a]
	Kidneys[a]
Abdominal wall	Normal cord insertion
	No umbilical defects
Extremities	Four limbs each with three segments
	Hands and feet with normal orientation[a]
Placenta	Size and texture
Cord	Three-vessel cord[a]

Adapted with permission from Salomon et al. ISUOG practice guidelines: performance of first-trimester fetal ultrasound scan. Ultrasound Obstet Gynecol 2013;41:102–113 [9]

[a] Optional structures

Sonoembryology

Sonoembryology is the term used to describe detailed assessment of the embryo in vivo by high-resolution transvaginal US [31–33]. Initial publications on sonoembryology relied on images obtained by 2D US. Since the original work describing the use of a specially designed high-resolution 3D transvaginal probe for reconstruction of small embryonic structures by Blaas et al. [34] in 1995, several investigators have reported on the use 3D US for volumetric measurements [35, 36], assessment of normal embryonic and fetal development [21, 37–43], as well as early prenatal diagnosis of congenital anomalies [40, 44–52].

The best studied organ has been the embryonic brain, with initial studies focusing on volumetry and anatomy of cerebral brain vesicles [34, 35, 53]. As shown below, exquisite 3D US images of the early CNS can be obtained between 5 and 12 weeks using commercially available equipment [40].

4 to 5 Weeks

The intrauterine gestational sac (GS) can be identified as early as 4 weeks and 2 days (Fig. 14.4). At this stage, the trilaminar embryo consisting of endoderm, mesoderm, and ectoderm cannot be visualized by US [54].

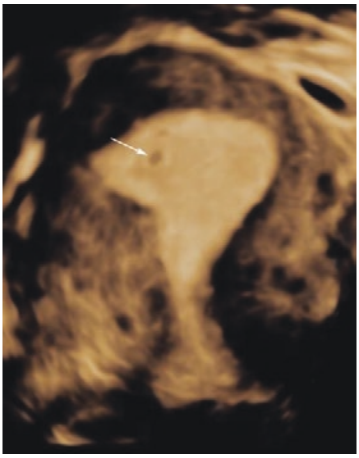

Fig. 14.4 Coronal 3D-rendered image of the uterus showing intrauterine implantation of a 2.5 mm GS (arrow)

Figure 14.5 shows a series of representative images summarizing the evolution of normal singleton pregnancies from 5 to 12 weeks as seen by 3D US.

5 to 6 Weeks

The yolk sac (YS) is the next visualizable embryological structure, usually when the GS reaches a diameter of approximately 10 mm. The 5-week embryo measures between 2 and 5 mm and can be identified when the GS diameter is greater than 18 mm. At this gestational age, when the YS and embryo are seen at the same time, they should be seen in close apposition to each other (Fig. 14.6). Embryos with a CRL of 5 mm or more seen by transvaginal US should have detectable cardiac activity. Closure of the rostral and caudal neuropores takes place during the 5th week and the five major subdivisions of the developing brain are already present; however, these structures cannot be resolved sonographically, even with the use of high frequency 3D transducers.

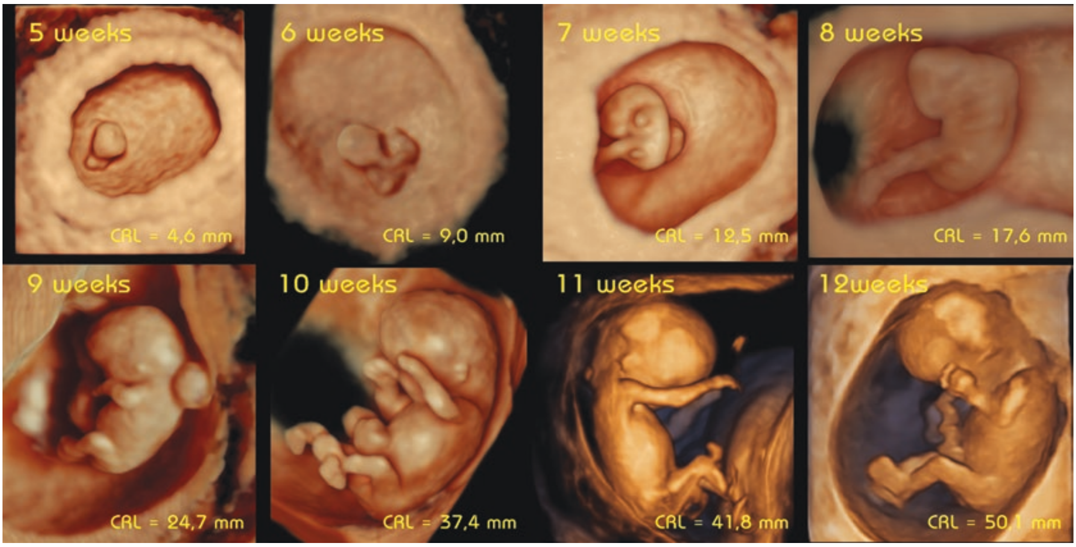

Fig. 14.5 Embryonic (5–10 weeks) and fetal (11–12 weeks) development as seen by 3D US

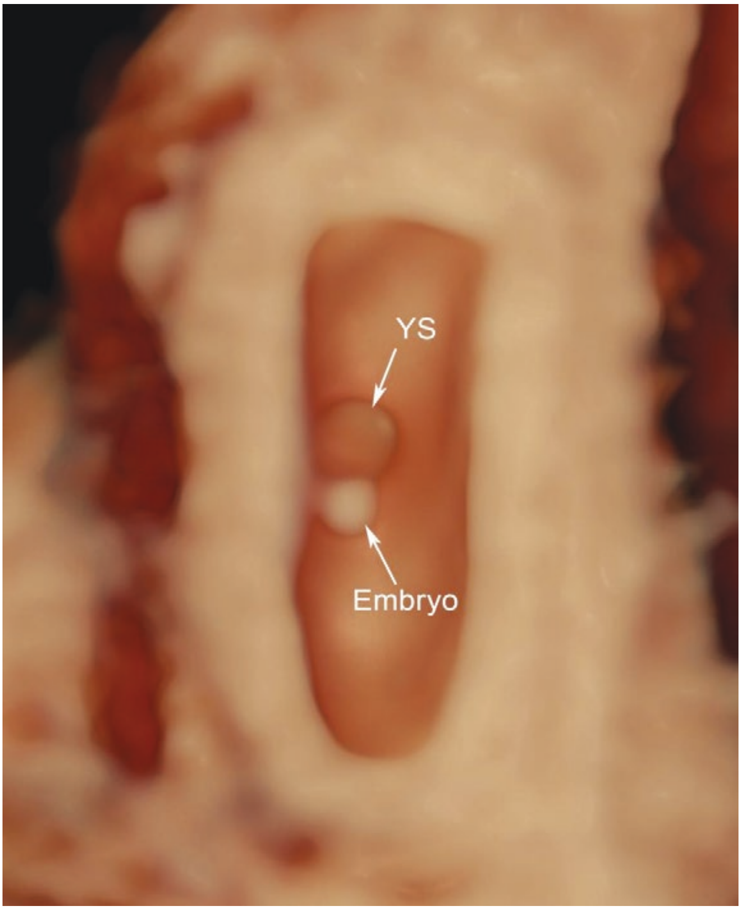

Fig. 14.6 3D Rendered HDLive image of a 5-week pregnancy showing a normal yolk sac (YS) and embryo in close apposition to each other

6 to 7 Weeks

During the 6th week, the embryo measures between 5 and 9 mm, the heartbeat is evident and must be seen in all intrauterine pregnancies [55]. The five main subdivisions of the brain and the pontine flexure can be seen with high-resolution transducers as a small closed anechoic tube (Fig. 14.7) [56]. The embryo is located within the amniotic sac and the YS resides within the extra-coelomic space.

7 to 8 Weeks

At this stage, the morphology of the early CNS as a closed liquid tube facilitates its study by US, especially with the help of 3D and even more with the Silhouette mode that contrasts the abrupt interfaces between the anechoic fluid and the hyperechogenic membrane. At 7–8 weeks of gestation, the embryo measures 8–15 mm and the telencephalon, early lateral ventricles, diencephalon, mesencephalon, a prominent fourth ventricle, and myelencephalon can be identified [57, 58]. The heart is prominent and conspicuous, the head forms a 90° angle with the trunk, the upper and lower limb buds are present, and the umbilical cord contains a physiological hernia. The YS and vitelline duct can also be easily identified (Figs. 14.8 and 14.9) [58].

8 to 9 Weeks

At this stage, the embryo measures between 14 and 21 mm in length (Fig. 14.10) and begins to have more recognizable human features second-

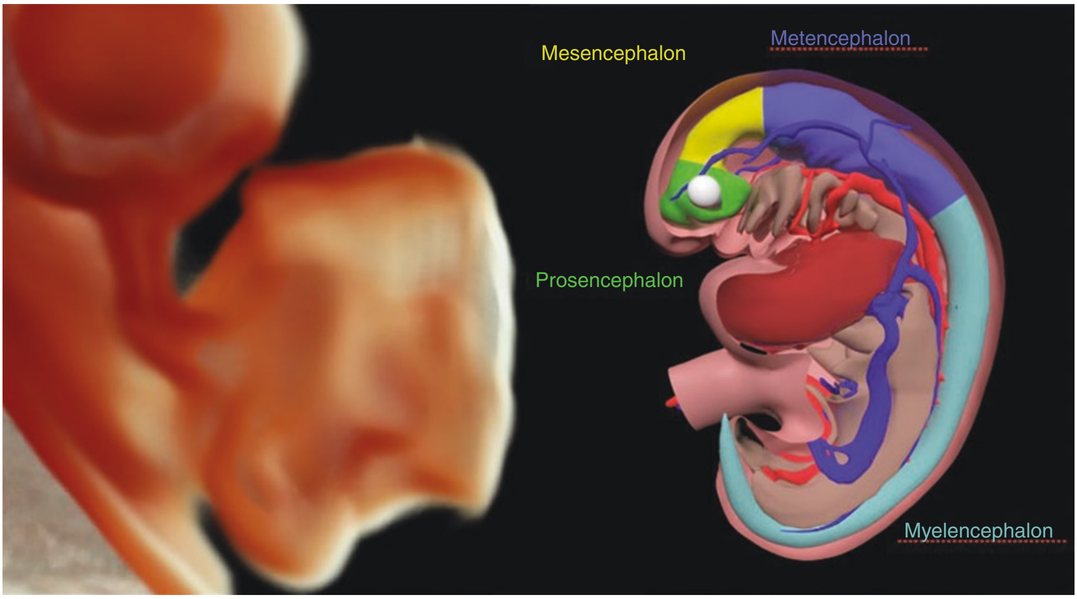

Fig. 14.7 3D HDLive with Silhouette mode of a 7.2 mm embryo compared to a 3D model based of the same CRL. (The 3D model was produced by Drs. Renato Ximenes and Rafael Peters using Blender software (https://blender.org))

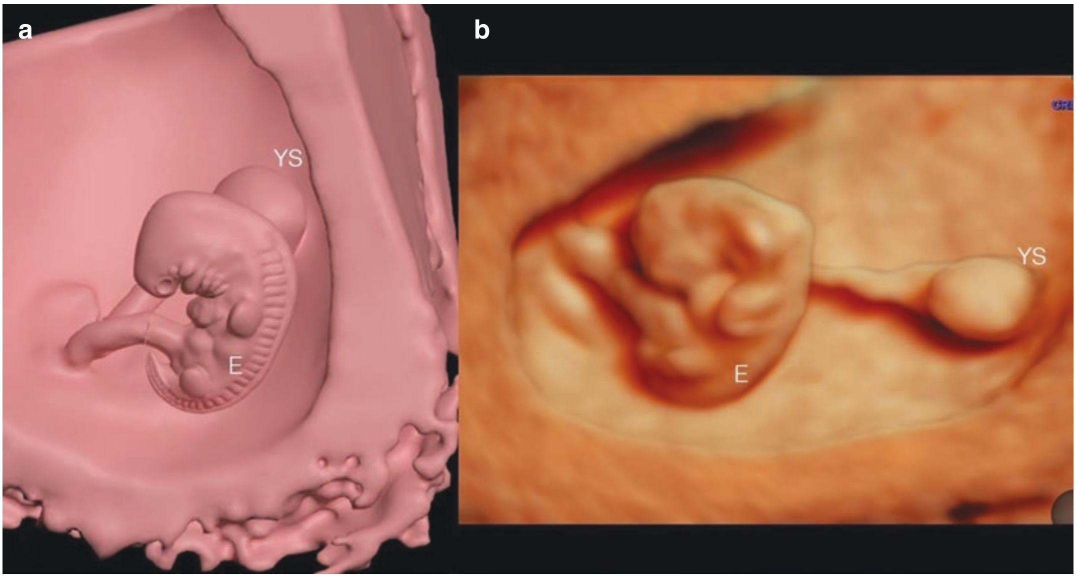

Fig. 14.8 (**a**) 3D model of a 7–8-week embryo; (**b**) 3D rendered HDLive mode image of an embryo with a CRL of 17.0 mm. (The 3D model was produced by Drs. Renato Ximenes and Rafael Peters using Blender software (https://blender.org))

ary to the development of the face, elongation of the limbs, and formation of the fingers and toes [23]. The trunk straightens, and the degree of head flexion decreases during this period. The lateral ventricles with their respective choroid plexuses and the aqueduct of Sylvius can be identified [57]. The fourth ventricle and choroid plexus form an evident fold.

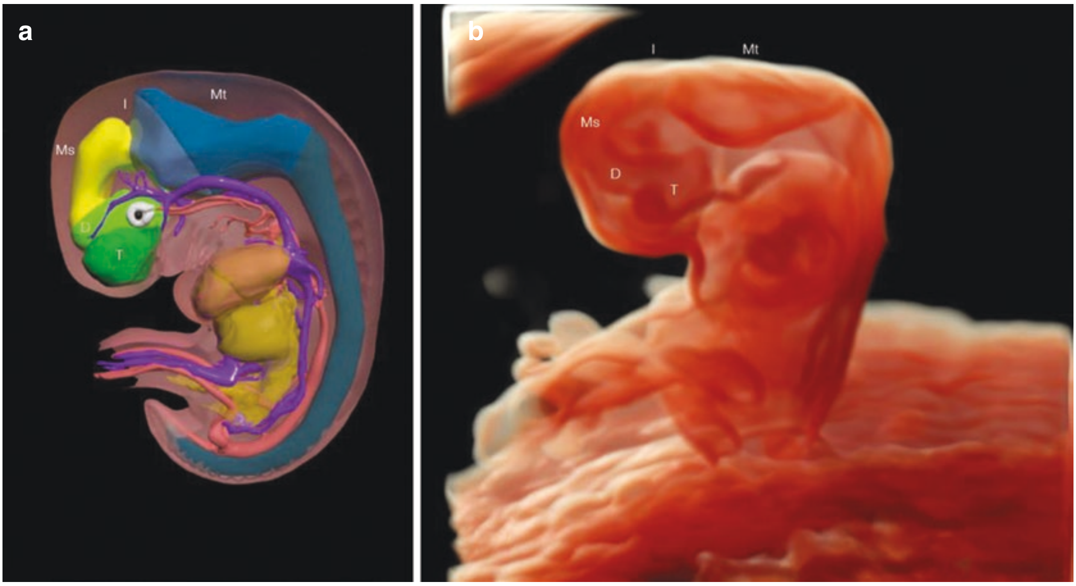
a
Mt
I
Ms
D
T
b
I
Mt
Ms
D
T

Fig. 14.9 (**a**) 3D model of a 7–8-week embryo illustrating the cerebral vesicles; (**b**) contrast with the corresponding 3D silhouette mode high-resolution image of a 17 mm embryo. *T* telencephalon (forebrain), *D* diencephalon (forebrain), *MS* mesencephalon (midbrain), *I* isthmus, *MT* metencephalon (rhombencephalon). (The 3D model was produced by Drs. Renato Ximenes and Rafael Peters using Blender software (https://blender.org))

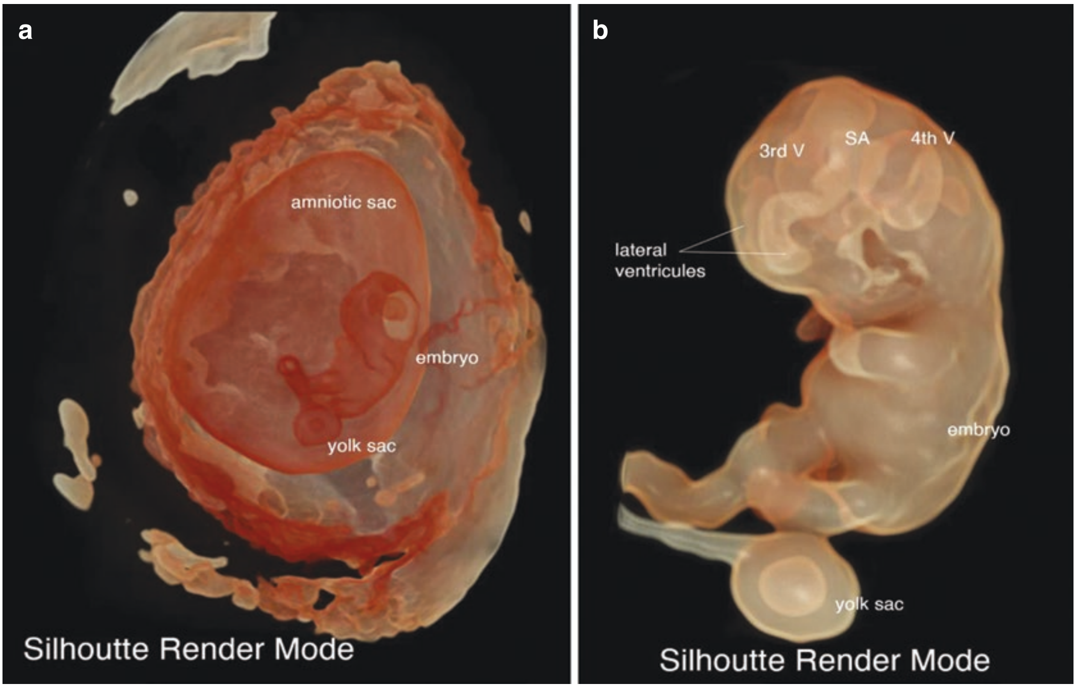
a
amniotic sac
embryo
yolk sac
Silhoutte Render Mode
b
3rd V
SA
4th V
lateral ventricules
embryo
yolk sac
Silhoutte Render Mode

Fig. 14.10 (**a**) 3D rendered view using Silhouette mode of an 8–9-week embryo (CRL 21 mm) located within its amniotic sac. (**b**) Magnified view of the same embryo showing the lateral ventricles, third ventricle, aqueduct of Sylvius and fourth ventricle

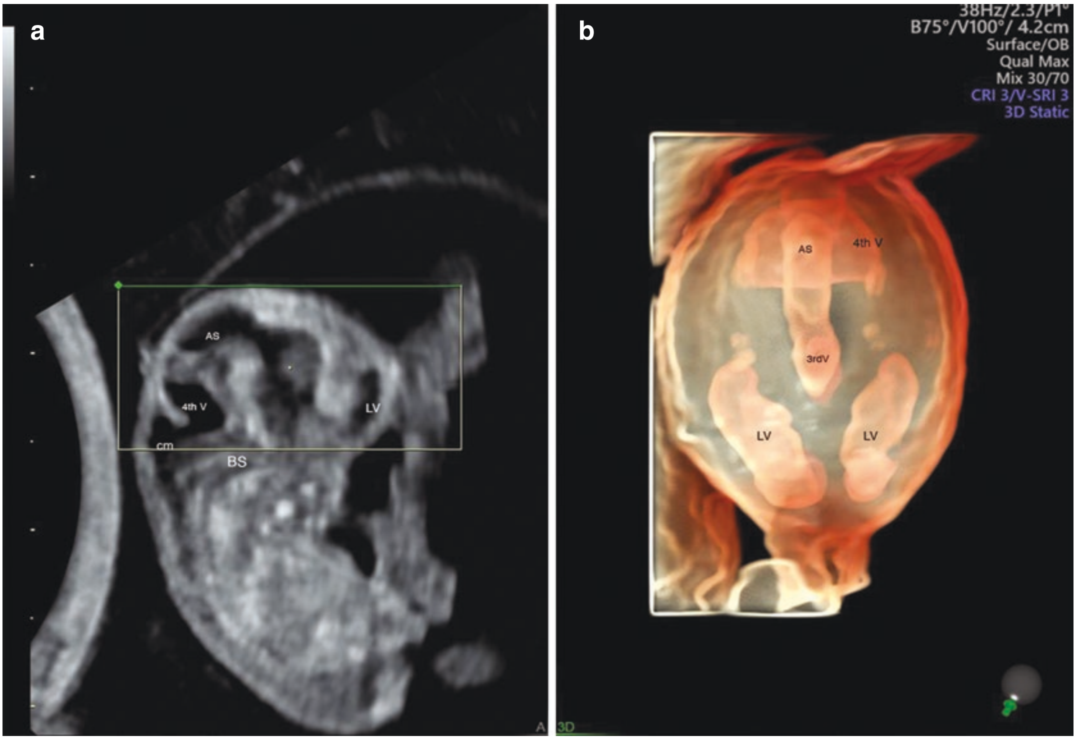

Fig. 14.11 (**a**) High-resolution sagittal view of a 21 mm embryo showing early development of the CNS. (**b**) Corresponding 3D rendered view of the cerebral vesicles using the Silhouette mode. The volume dataset is viewed from the top using the region of interest outlined on (**a**). *BS* brain stem, *CM* cisterna magna, *4th V* fourth ventricle, *AS* aqueduct of Sylvius, *3rd V* third ventricle, *LV* lateral ventricles

9 to 10 Weeks

This is the last week of the embryonic period since at 10 weeks, when the CRL measures about 30 mm, the embryo is called a fetus. At this stage, the early CNS is more conspicuous and easier to image, and it is possible to demonstrate complete separation of the hemispheres, the size and shape of the choroid plexuses, the integrity of the early calvarium, the third ventricle, the aqueduct of Sylvius, and the fourth ventricle (Fig. 14.11) [59]. The head is rounder, the trunk is further elongated, the limbs are longer and turned inwards, the fingers and toes can be identified, and the umbilical cord demonstrates physiological intestinal herniation [60, 61].

Congenital Anomalies That May Be Diagnosed During the Embryonic Period

Several case reports and series have illustrated how 3D US helped with specific diagnoses in the embryonic period [45–48, 62–65]. Among the most interesting are the early detection of a case of spina bifida at 9 weeks with exquisite detail of the defect demonstrated by 3D surface rendered images of the embryonic torso (Fig. 14.12) [46, 63–65], confident diagnoses of cyclopia [47], and proboscis [47, 48] by 3D multiplanar reconstruction at 9 2/7 weeks [47] and 10 6/7 weeks [48] in association with alobar holoprosencephaly, digital casts of the abnormal ventricular system in

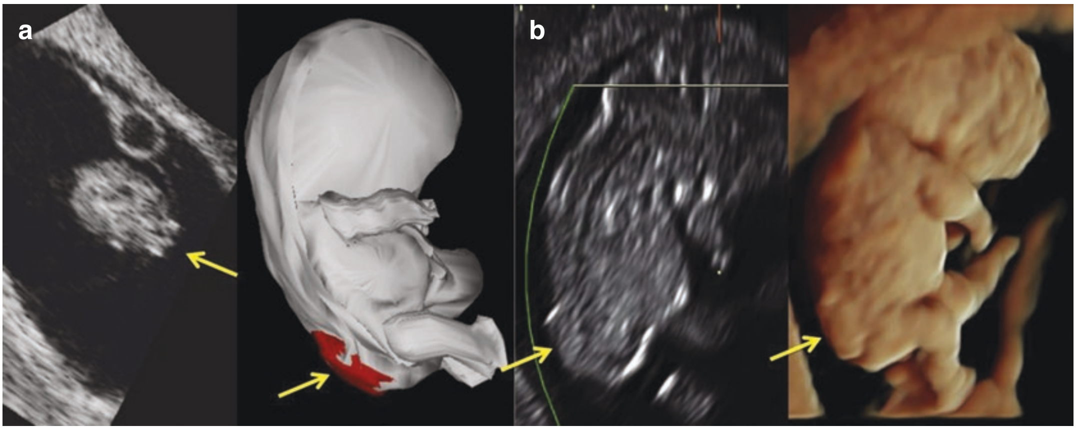

Fig. 14.12 Very early diagnosis of spina bifida by 2DUS and 3DUS at 9 weeks last menstrual period-based gestational weeks. (**a**) Crown-rump length 22 mm. *Left*: horizontal section through the embryonic abdomen. *Right*: three-dimensional geometric reconstruction obtained through manual segmentations; the elevated spinal defect was segmented separately and colored *red*. The *arrows* point at the spinal defect; (**b**) crown-rump length 25 mm. *Left*: sagittal section through the embryonic spine. *Right*: three-dimensional surface rendering clearly showing the myelomeningocele at the embryo's back. The *arrows* point at the spinal defect. (Reprinted from Best Practice & Research Clinical Obstetrics & Gynaecology, 28, Blaas HK, Detection of structural abnormalities in the first trimester using ultrasound, 341–53, Copyright 2014, with permission from Elsevier)

cases of holoprosencephaly as early as 9 2/7 weeks, and conjoined twins at 9 [52] and 10 weeks [62]. In the following paragraphs, we will illustrate a few prenatal diagnoses of congenital anomalies performed with 3D US during the embryonic period.

Body-Stalk Anomaly

Body-stalk anomaly (BSA) is a lethal severe abdominal wall defect characterized by a short umbilical cord associated with evisceration of abdominal and, in some cases, thoracic organs. The estimated incidence is 1/14,000–1/31,000. The condition is associated with scoliosis and anal atresia in most cases. Limb defects may or may not be present. BSA is also known as limb body wall complex or short umbilical cord syndrome [66, 67]. Most cases can be diagnosed during the first trimester, and prenatal diagnosis has been reported as early as 9 weeks [66]. Figure 14.13 shows a case of BSA diagnosed at 9 weeks using transvaginal 3D US. The patient was referred to our center by an obstetrician who noted that the heart was beating eccentrically to the main longitudinal axis of the embryo during a routine transabdominal US performed in the office.

Fetal Edema in Early Pregnancy

Early nuchal edema has been defined as increased edema in the region of the fetal neck >2.2 mm in embryos with a CRL <44 mm (Fig. 14.14). Ramkrishna et al. [68] studied 104 embryos with a CRL of 28–44 mm and nuchal edema identified before cell-free DNA non-invasive prenatal testing (NIPT) was performed. Nuchal edema was isolated in 40 cases (38.5%) and associated with generalized edema in 64 cases (61.5%). Chromosomal anomalies occurred in 10% of the embryos with isolated nuchal edema and 25% of those with generalized edema. The incidence of structural anomalies with normal karyotype was 3.8%. Miscarriage occurred in 3.8%. Nuchal edema resolved at the time of the 11–14 weeks scan in 81.9%. Embryos with early nuchal edema should undergo individualized genetic counseling and testing and followed by careful anatomical evaluation at 11–14 weeks.

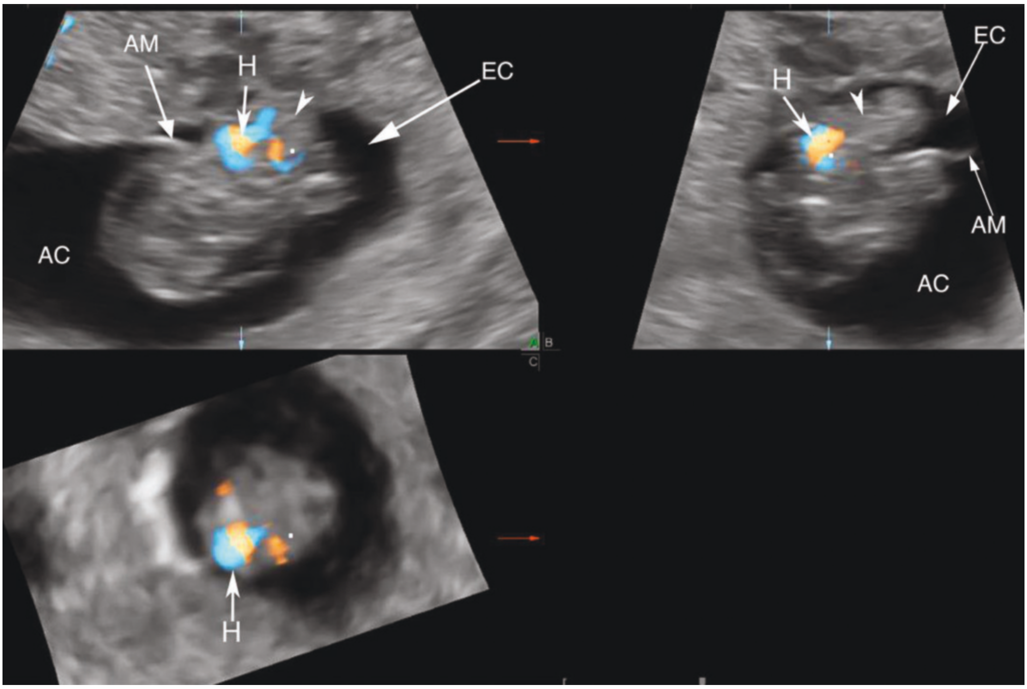
AM
H
EC
AC
H
EC
AM
AC
A
B
C
H

Fig. 14.13 Body-stalk anomaly diagnosed by transvaginal 3D US at 9 weeks. Multiplanar display image shows the fetal torso (arrowhead), including the heart (H), located outside of the embryonic body and in the extracelomic space (EC). Note the amniotic membrane (AM) separating the amniotic cavity (AC) from the EC

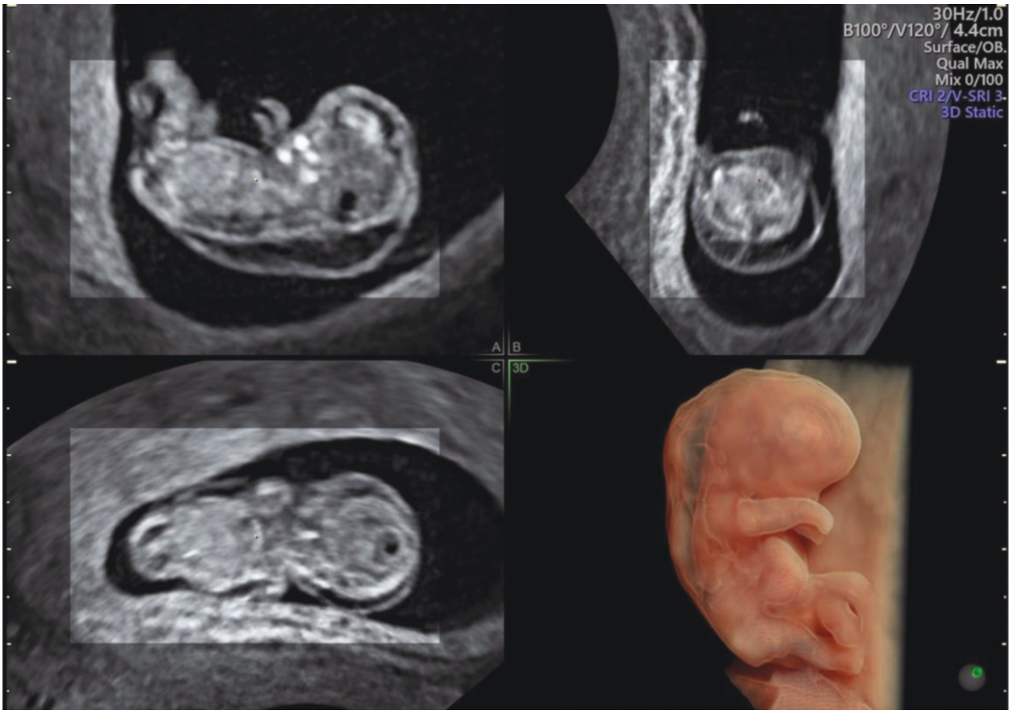
30Hz/1.0
B100°/V120°/ 4.4cm
Surface/OB.
Qual Max
Mix 0/100
CRI 2/V-SRI 3
3D Static
A
B
C
3D

Fig. 14.14 31.2 mm embryo with nuchal edema and a final diagnosis of trisomy 18

Acrania-Exencephaly-Anencephaly Sequence

Fetal cranial ossification starts after 9 weeks but is not complete until 10–11 weeks. Acrania presents as lack of ossification of the calvarium associated with exposure of the bilateral early brain parenchyma to amniotic fluid, giving the appearance of a mushroom ("mushroom" sign) (Fig. 14.15). Since in acrania the early cerebral tissue is not protected by meninges and cranial bones, continuous exposure to amniotic fluid causes progressive tissue damage and evolution to exencephaly and anencephaly [69, 70]. Given that early ossification of the calvarium is not identifiable until 11 weeks, it is prudent to re-examine patients at that time to confirm the diagnosis.

Holoprosencephaly

Holoprosencephaly (HPE) arises from failure of the prosencephalon to cleave during early embryonic life, resulting in wide range of ventricular fusion and facial defects, classified into four main categories, namely lobar, semilobar, alobar, and interhemispheric variant (syntelencephaly) forms (Fig. 14.16). Alobar HPE is the most severe form,

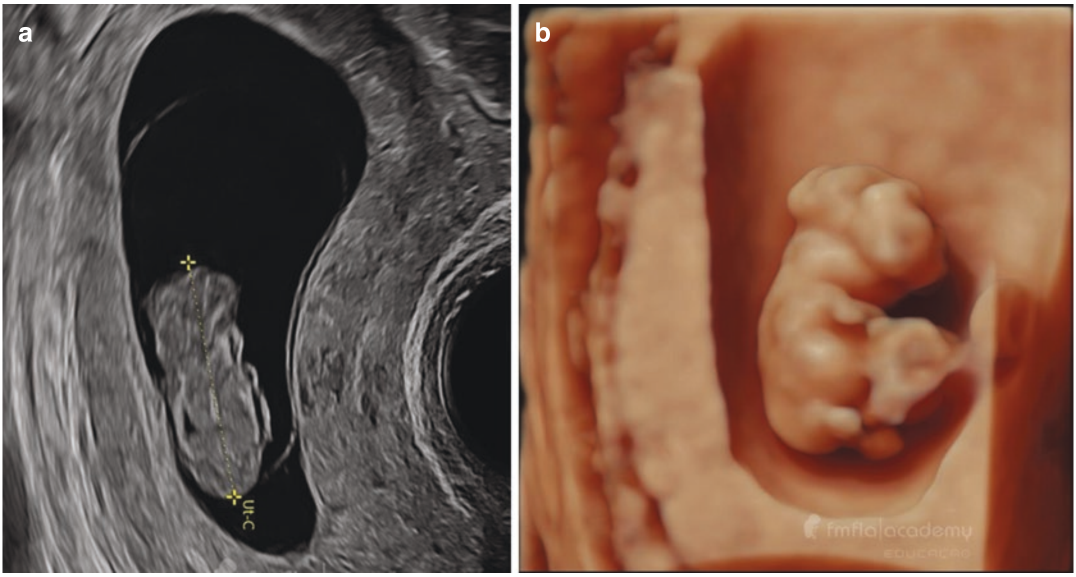

Fig. 14.15 (**a**) 2D coronal image of a 9-week embryo showing developing brain parenchyma exposed to amniotic fluid with no intervening bone. (**b**) 3D-rendered HDLive view of the embryo showing the "mushroom" sign

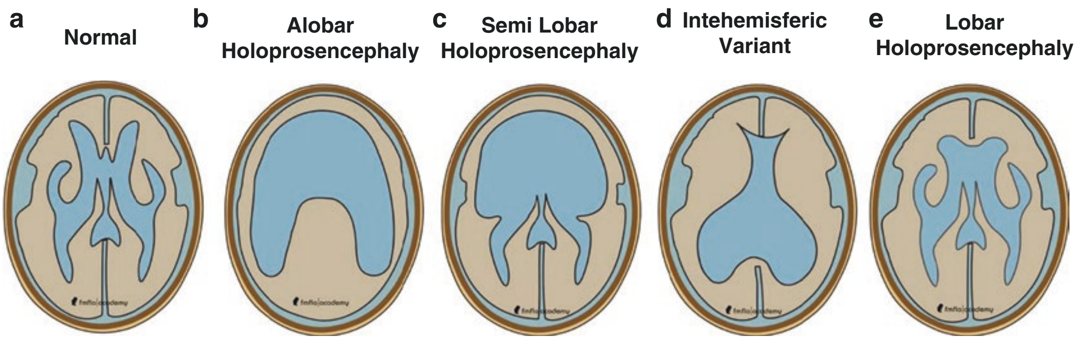

Fig. 14.16 (**a**) Normal; (**b**) most severe form—alobar holoprosencephaly; (**c**) semilobar holoprosencephaly; (**d**) interhemispheric variant; and (**e**) lobar holoprosencephaly

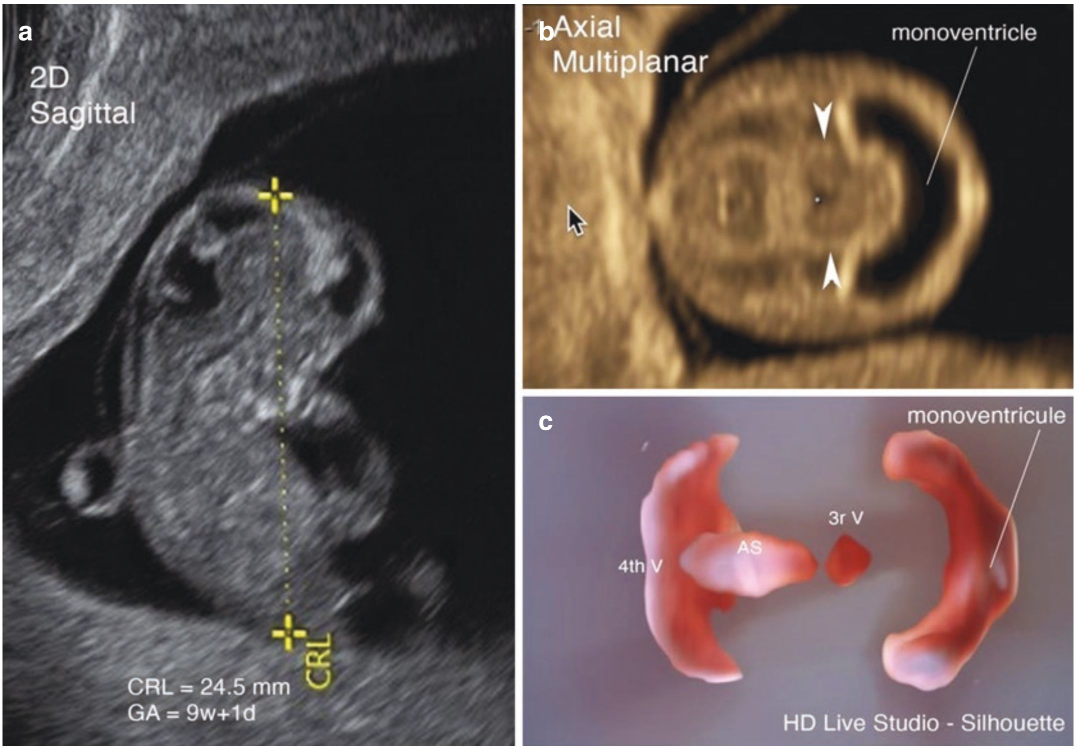

Fig. 14.17 (**a**) 2D sagittal plane of a 24.5 mm embryo (9 weeks and 1 day). No obvious abnormalities are identified in this plane. (**b**) Axial view shows a large anechoic area in the anterior aspect of the brain, consistent with a monoventricular cavity. Fusion of the thalami is also noted (arrowheads); (**c**) 3D rendered HDLive view of the early ventricular system using Silhouette mode shows the anterior monoventricle, the third ventricle, the aqueduct of Sylvius (AS), and the fourth ventricle

characterized by monoventricle, fused thalami, absent corpus callosum, absent interhemispheric fissure, absent cavum septi pellucidi, absent third ventricle, neurohypophysis and olfactory bulbs, and severe facial malformations including proboscis, mononostril, and orbit/ocular anomalies ranging from hypotelorism to cyclopia. Early prenatal diagnosis has been reported multiple times and it is consensual that it can be performed before 10 weeks [47–49, 71]. Figure 14.17 illustrates prenatal diagnosis of alobar holoprosencephaly at 9 weeks and day by 3D US.

Early Pleural Effusion

The pleuropericardial folds develop into the pleural and pericardial cavities around 8 weeks. Therefore, it is not possible to distinguish pericardial from pleural fluid collections before 8 weeks. Hashimoto et al. [72] reported on the outcome of 14 embryos diagnosed with bilateral pleural effusion between 8 and 10 weeks, 12 of which (86%) miscarried by 14 weeks. Karyotype was abnormal in 82%, and the most prevalent aneuploidy was 45, X0. Figure 14.18 shows early

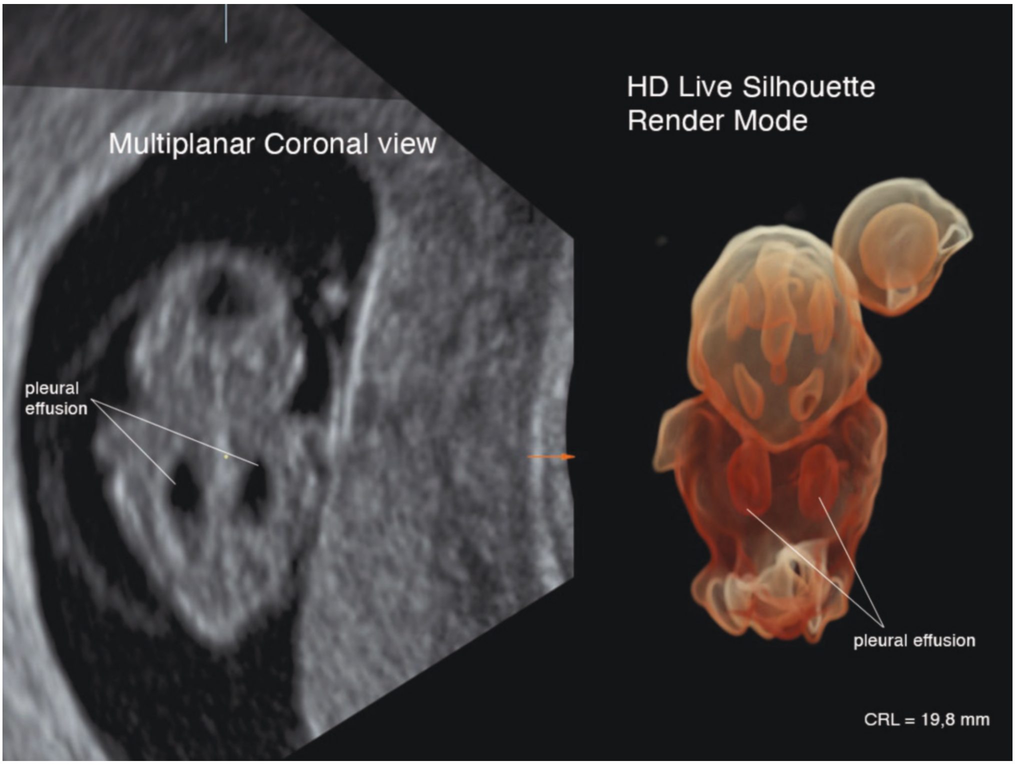

Fig. 14.18 19.8 mm embryo (8–9 weeks) presenting with bilateral pleural effusions demonstrated by the multiplanar coronal view (right) and 3D rendered HD Live Silhouette mode (left)

bilateral pleural effusions at 8 weeks by transvaginal 2D and 3D US. The embryo miscarried within 2 weeks of the examination.

Additional Potential Benefits of 3D US During Early Pregnancy

Chorionic Bump

A chorionic bump is defined as a focal area of bulging choriodecidual tissue into the GS, typically located within the thickest part of the developing placenta [73]. The estimated prevalence is 0.4–0.7% [74]. The etiology is incompletely elucidated, with sonographic findings and histopathological analysis suggesting that the chorionic bump might be a hematoma, which has been consistently supported by sonographic findings and histopathological analysis [75]. In a systematic review, Arleo et al. [74] reported that in pregnancies complicated by a chorionic bump and otherwise normal GS, YS, and embryo with documented cardiac activity, the live birth rate was estimated at 83%. An example of a chorionic bump in a viable 7-week intrauterine pregnancy is shown on Fig. 14.19.

Determination of Chorionicity and Amnionicity in Multiple Pregnancies

3D US can aid in the determination of chorionicity and amnionicity in multiple pregnancies

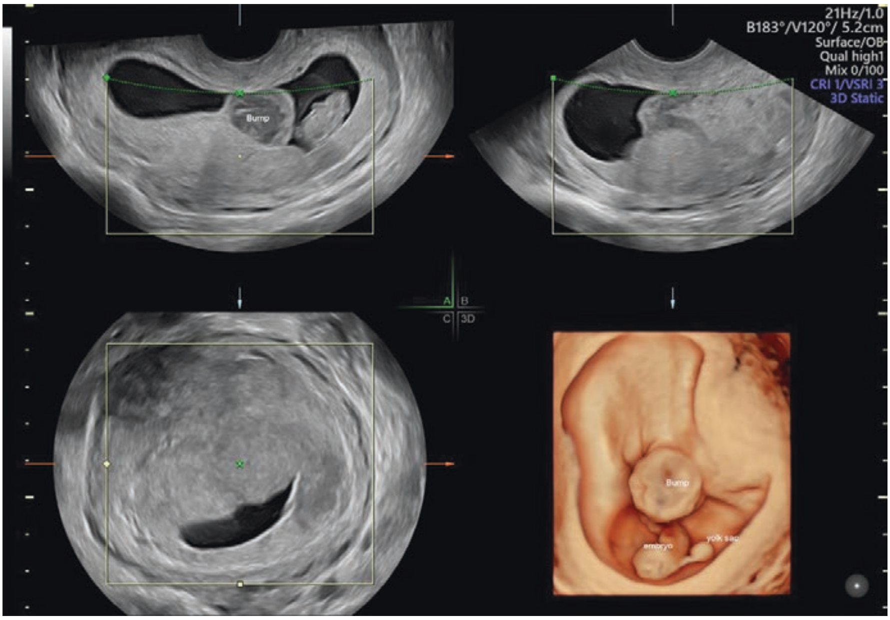
21Hz/1.0
B183°/V120°/ 5.2cm
Surface/OB
Qual high1
Mix 0/100
CRI 1/VSRI 3
3D Static
Bump
A B
C 3D
Bump
embryo
yolk sac

Fig. 14.19 Multiplanar (panels **a**, **b,** and **c**) and 3D rendered (3D) views of a 7-week intrauterine pregnancy, showing the position, size, and proportionality of a chorionic bump in relationship to the GS, embryo, and YS

Fig. 14.20 Monochorionic-diamniotic triplets. 3D rendered view of the uterus using HDLive silhouette mode. The image shows a single developing placental mass (P) and two separate gestational sacs (GS1 and GS2). Gestational sac 2 has two separate embryos (E2 and E3) with no intervening amniotic membrane

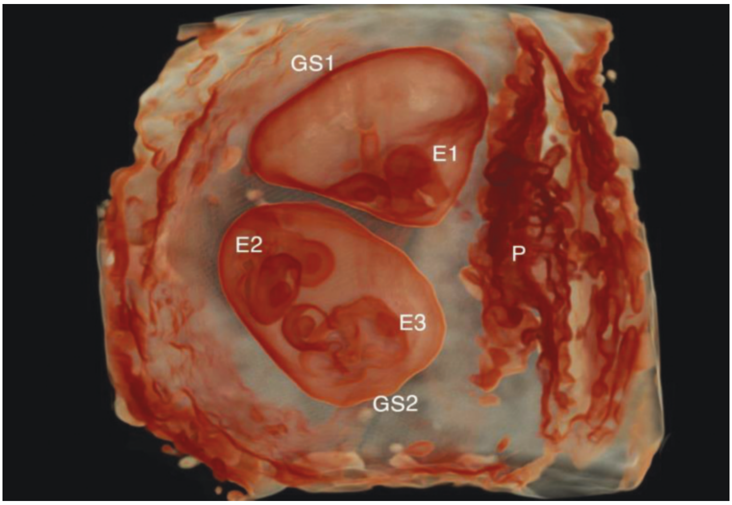
GS1
E1
E2
P
E3
GS2

(Figs. 14.20 and 14.21), keeping in mind that precise diagnosis of amnionicity in monochorionic placentation is only possible after 7 weeks of gestational age.

Differences in size between gestational sac diameters and/or CRLs in twin pregnancies can also be easily appreciate with the use of 3D US (Fig. 14.22). An intertwin discordance in CRL >19% between 7+0 and 9+6 weeks predicts subsequent single fetal loss at 11–14 weeks with 87.2% sensitivity (95% CI 79.7–92.9%) and 95% specificity (95% CI 93.8–96.3%) [76].

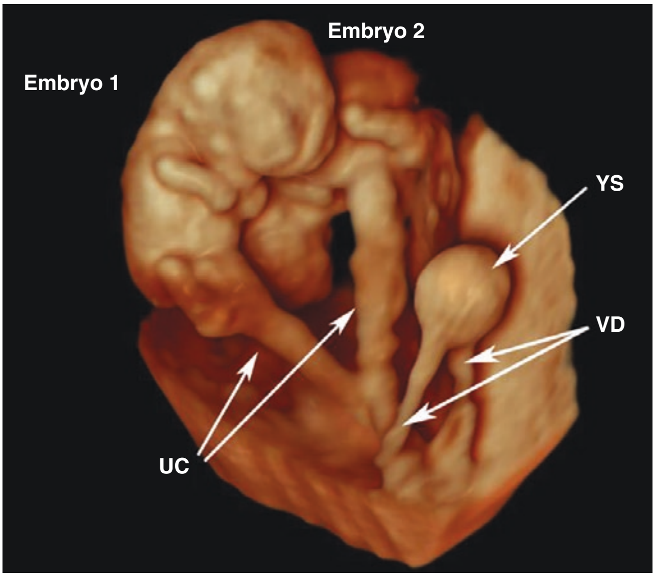

Fig. 14.21 Monochorionic-monoamniotic twins at 9 weeks. 3D rendered view using HDLive shows two separate umbilical cords converging to the placenta with no intervening amniotic membrane. In addition, two separate vitelline ducts (VD) converge to a single yolk sac (YS). A single yolk sac is a frequent finding in monochorionic-monoamniotic twins

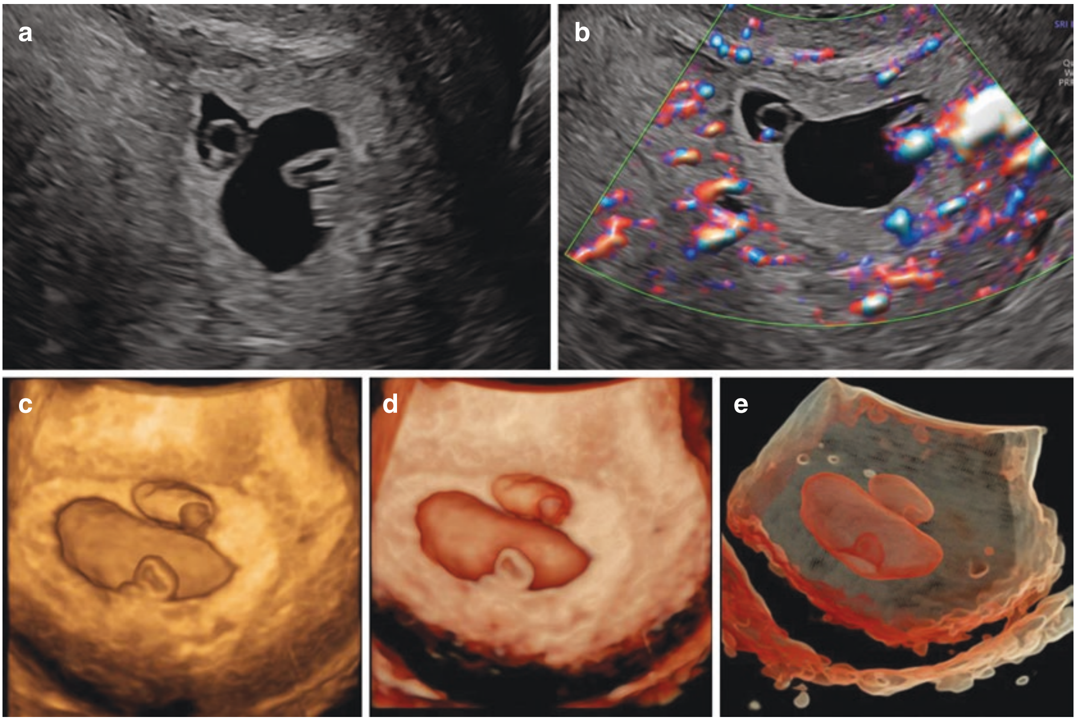

Fig. 14.22 Differences between gestational sac diameter and embryos in a twin pregnancy seen under different presentations. (**a**) Gray scale; (**b**) power Doppler; (**c**) 3D surface mode; (**d**) 3D HDLive; (**e**) 3D Silhouette mode

Anomalies Diagnosable During the 11–14 Weeks Scan

It is well established that an increased nuchal translucency identified during the 11–14-week scan is associated not only with an increased risk of chromosomal and structural anomalies, but also with congenital heart disease (CHD) [77–79]. Although this has been the initial impetus to routinely scan a fetus between 11 and 14 weeks, mounting evidence supports that a more comprehensive examination at this time yields a wealth of additional information that can impact pregnancy management [80], including identification of 40–66% of fetal anomalies in various organ systems [12, 14–16, 81, 82], establishing amnionicity and chorionicity for multiple pregnancies [83], and providing an opportunity for early screening for preeclampsia [84].

3D US can enhance the 11–14-week scan by allowing the possibility of obtaining multiple planes of an anatomical structure from a single 3D volume dataset. The elevation plane, which is perpendicular to the direction of the sound beam, is impossible to obtain using conventional 2D US. This capability can be particularly advantageous during the first trimester, when manipulation of the vaginal probe is restricted and, therefore, the obtainable planes of section are limited [32]. Another potential benefit, provided that it can be proved beyond doubt that offline analysis of volume datasets has at least the same level of accuracy as real-time analysis of 2D US images, is that embryonic exposure to ultrasound can be reduced, since volume acquisition takes only a few seconds and image processing and analysis can be performed offline [17].

In this section of the chapter, we will review congenital structural anomalies that have been identified during the 11–14-week scan with the aid of 3D US imaging.

Central Nervous System

Expert neurosonography with 2D and 3D US at 11–14 weeks combines the knowledge of the fetal anatomy and sonoembryology to detect the early brain abnormalities, which are otherwise commonly diagnosed later in gestation. A standardized protocol for the 11–14 weeks neurosonography includes the systematic evaluation of specific intracranial markers for structural abnormalities to maximize early diagnosis of congenital brain anomalies. Using such approach, most cases of acrania, alobar holoprosencephaly, and cephalocele can be detected; however, several other CNS abnormalities are likely to remain undiagnosed until the second and third trimester. Examples of anomalies that can be missed by a first trimester scan include vermian hypoplasia, agenesis of the corpus callosum, and abnormalities of neuronal migration (e.g., lissencephaly, polymicrogyria, gray matter heterotopia) [7, 10, 12, 14, 30, 85–88].

Sagittal View

A midline sagittal view of the fetus can be obtained with 2D US or 3D US when 2D is not technically feasible. Besides being the correct plane to measure the CRL, this view contains a wealth of information, as shown in Fig. 14.23. In the midline sagittal view, the thalamus (T) is seen as a hypoechoic round-shaped structure, followed caudally by the brainstem (BS), which includes the mesencephalon (M), pons (P), and medulla oblongata (Mo) (Fig. 14.21b). The BS has a typical "S" shape. Posteriorly to the BS and within the posterior fossa, it is possible to visualize the fourth ventricle (which has also been named "intracranial translucency" when seen during the 11–14-week scan) [89] and cisterna magna (CM) forming three parallel anechoic spaces between the sphenoid and occipital bones [90]. Details of this view are further explored in Figs. 14.24 and 14.25.

Axial Views

Volume datasets of the fetal brain acquired with 3D US can be evaluated with the multiplanar display method to demonstrate the following standardized axial views: (**a**) falx view, (**b**) third ventricle view, (**c**) aqueduct of Sylvius view, and (**d**) fourth ventricle view (Figs. 14.26, 14.27, 14.28, 14.29 and 14.30).

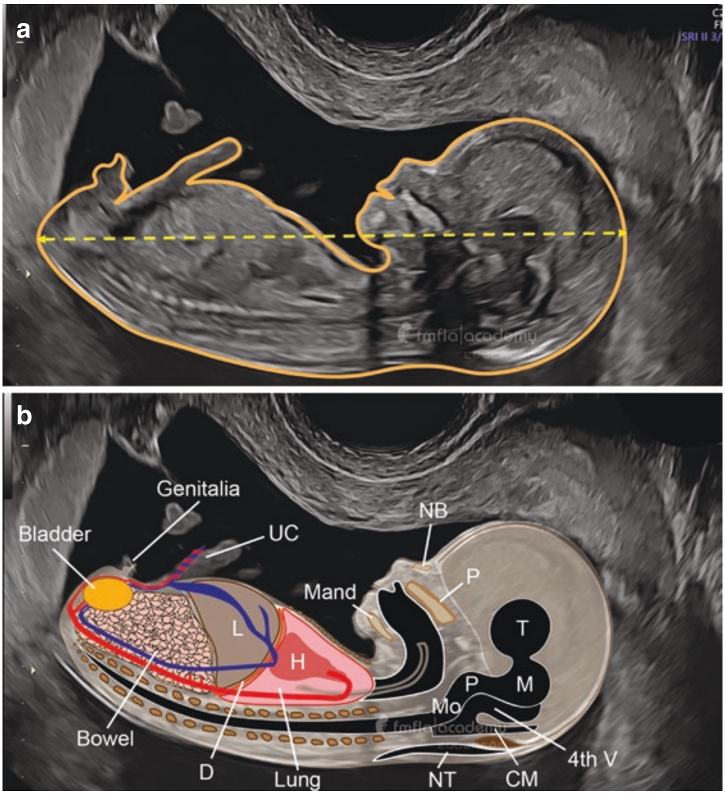
a
SRI II 3/
fmf|a|academy
b
Genitalia
Bladder
UC
NB
P
Mand
L
T
H
P
M
Mo
Bowel
4th V
D
Lung
NT
CM

Fig. 14.23 Sagittal view of a 12–13-week fetus. (**a**) Dotted double arrow shows the correct plane and caliper placement for measurement of the CRL. (**b**) A wealth of anatomical information can be obtained from the midline sagittal view including visualization of the thalamus (T), midbrain (M), pons (P), medulla oblongata (Mo), fourth ventricle (4th V), cisterna magna (CM), nuchal translucency (NT), nasal bone (NB), palate (P), mandible (Mand), heart (H), lung, diaphragm (D), liver (L), umbilical cord (UC), genitalia, bladder, and bowel

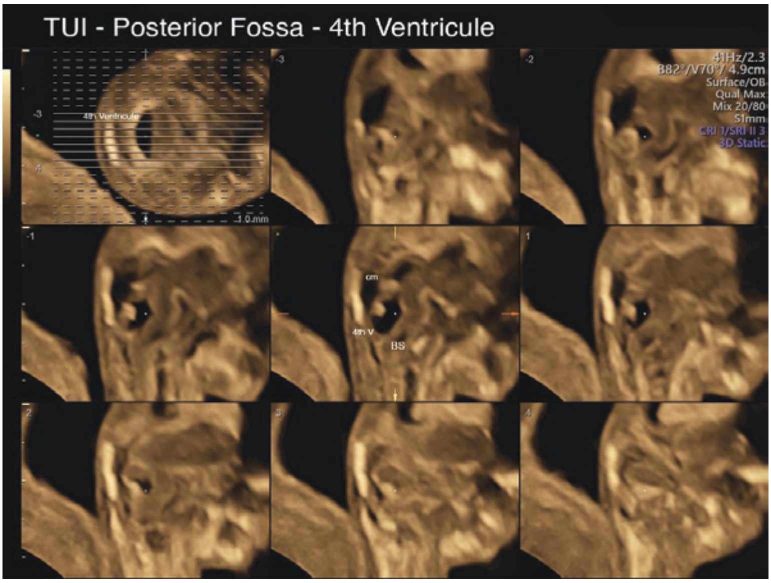
TUI - Posterior Fossa - 4th Ventricule
4th Ventricule
1.0 mm
-3
-2
-1
1
2
3
4
41Hz/2.3
B82°/V70°/ 4.9cm
Surface/OB
Qual Max
Mix 20/80
51mm
CRI 1/SRI II 3
3D Static
cm
4th V
BS

Fig. 14.24 Tomographic ultrasound images (TUI) of the posterior fossa in the sagittal plane. The planes of section are shown in the axial view of the posterior fossa (right upper corner panel). The sagittal midline is shown in the center panel. Please note that the brain stem (BS), which comprises the mesencephalon, pons, and medulla oblongata, has a typical "S" shape and is located ventrally to the fourth ventricle (4th V, a.k.a. "intracranial translucency") and cisterna magna (CM)

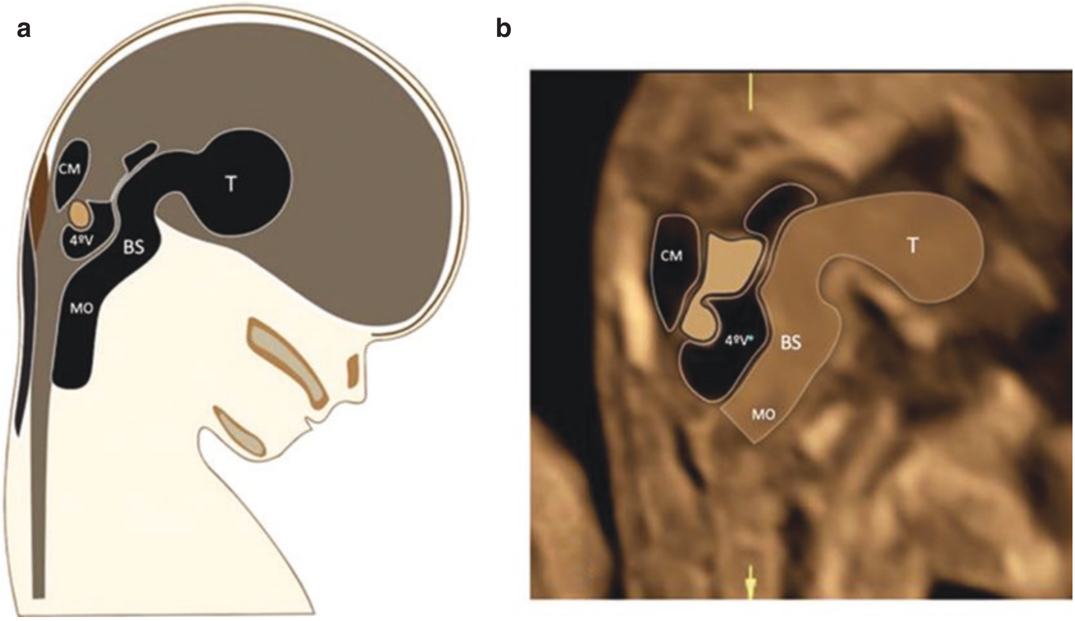
a
b
CM
T
4ºV
BS
MO
CM
T
4ºV
BS
MO

Fig. 14.25 Drawing (**a**) and annotated (**b**) US image of the posterior fossa as seen on the sagittal plane. *T* thalamus, *BS* brain stem, *Mo* medulla oblongata, *4th V* fourth ventricle, *CM* cisterna magna

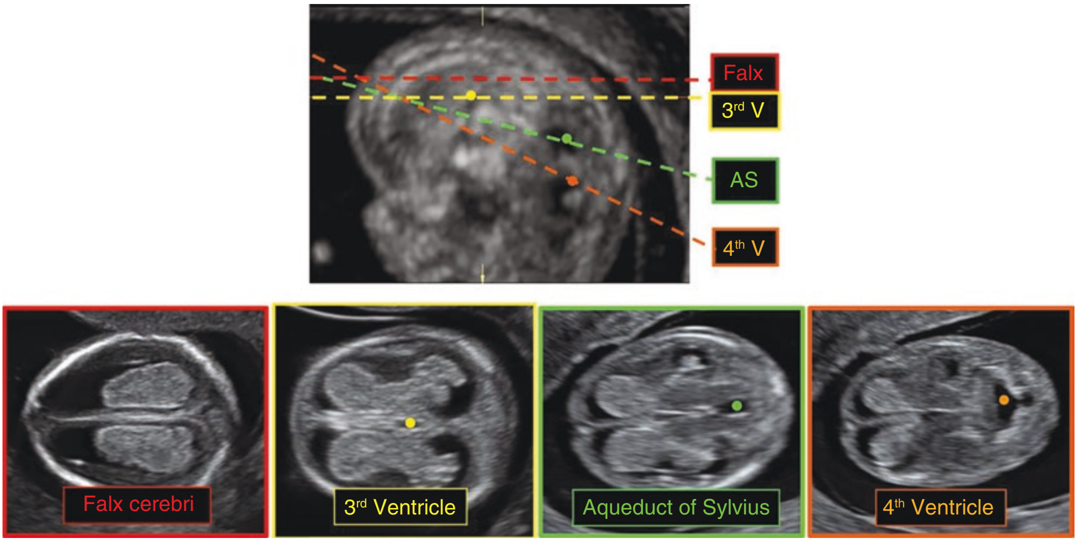
Falx
3rd V
AS
4th V
Falx cerebri
3rd Ventricle
Aqueduct of Sylvius
4th Ventricle

Fig. 14.26 Systematic evaluation of the early fetal brain at 11–14 weeks using 4 axial planes with the specific levels shown in the top sagittal view: falx cerebri view (red), third ventricle view (yellow), aqueduct of Sylvius view (green), and fourth ventricle view (orange)

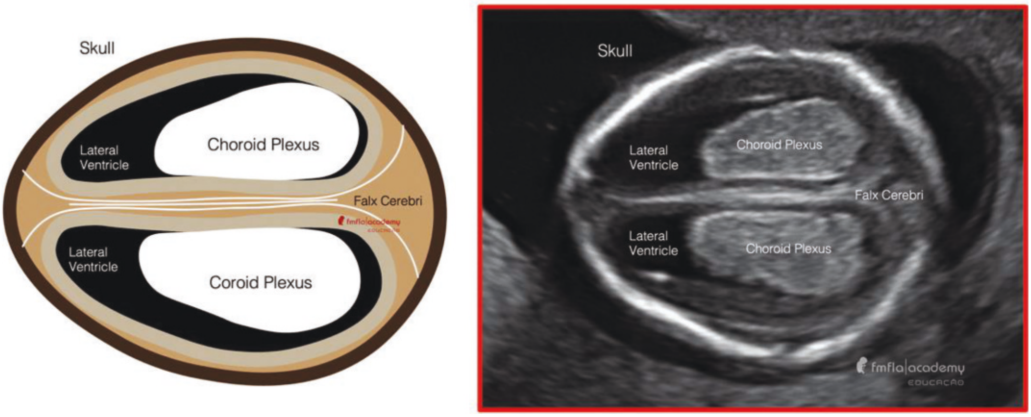
Skull
Lateral Ventricle
Choroid Plexus
Falx Cerebri
Lateral Ventricle
Coroid Plexus
Skull
Lateral Ventricle
Choroid Plexus
Falx Cerebri
Lateral Ventricle
Choroid Plexus

Fig. 14.27 Falx cerebri view

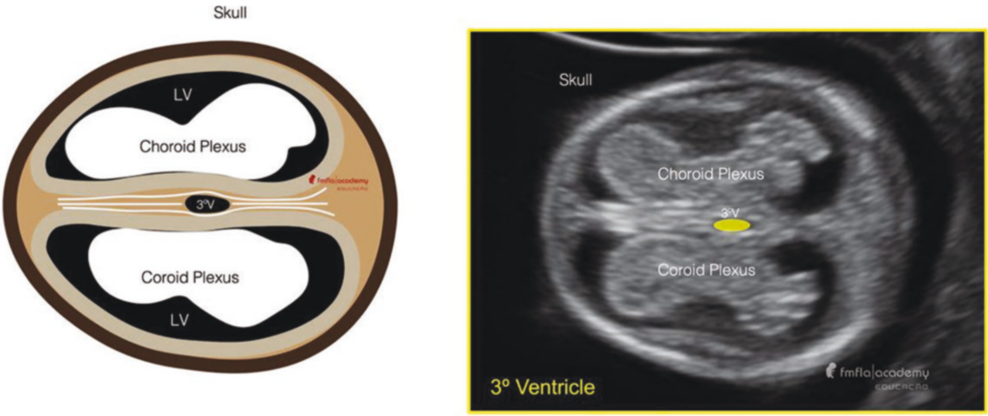
Skull
LV
Choroid Plexus
3ºV
Coroid Plexus
LV
Skull
Choroid Plexus
3ºV
Coroid Plexus
3º Ventricle

Fig. 14.28 Third ventricle view. The third ventricle plane shows the integrity and echogenicity of the skull, the choroid plexuses ("butterfly" sign), and the third ventricle. It also allows a qualitative assessment of the amount of fluid at the lateral ventricles in relation to the size of the choroid plexuses

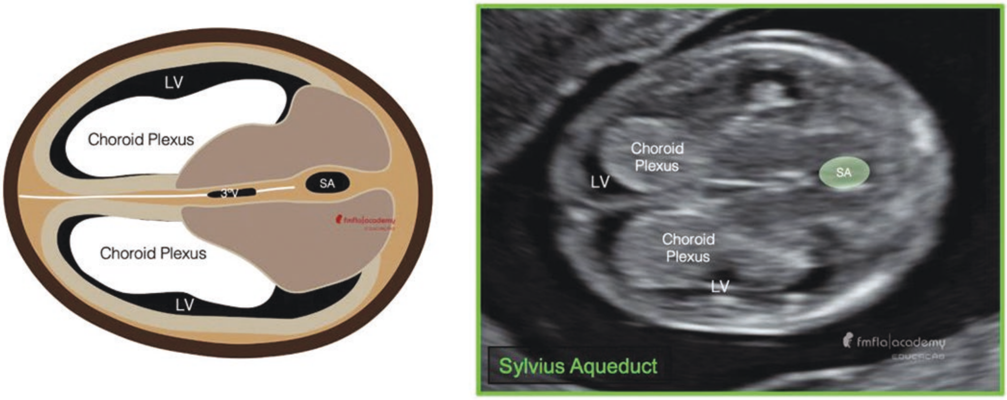
LV
Choroid Plexus
3ºV
SA
Choroid Plexus
LV
Choroid Plexus
LV
SA
Choroid Plexus
LV
Sylvius Aqueduct

Fig. 14.29 Aqueduct of Sylvius view. The aqueduct Sylvius view is an oblique plane that traverses the frontal horns of the lateral ventricles, third ventricle, and posterior fossa, showing the lateral ventricles and their respective choroid plexuses, the third ventricle, and the aqueduct of Sylvius. The size and position of the aqueduct are important when screening for open spinal dysraphism

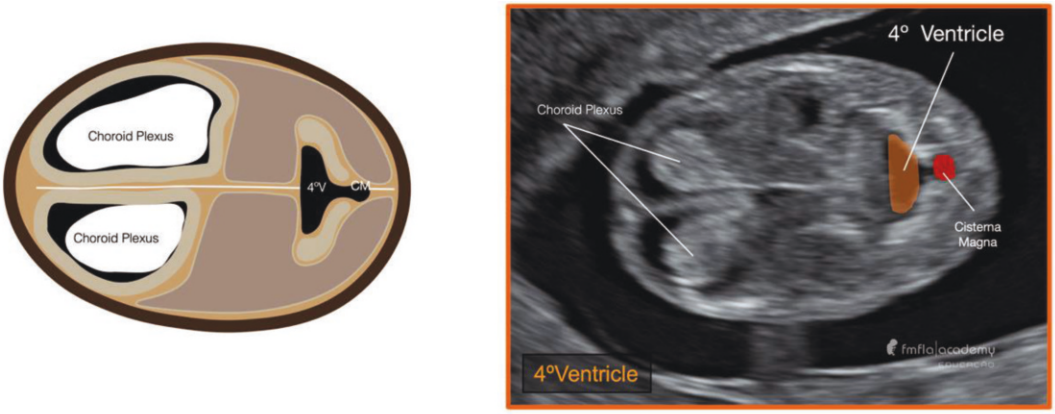

Fig. 14.30 Posterior fossa view—fourth ventricle

Table 14.2 Direct and indirect signs of CNS anomalies as seen during a first trimester scan

Malformation	Ultrasound direct signs	Ultrasound indirect signs
Acrania	Absent skull Deformity of brain (“mushroom” sign)	
Encephalocele	Brain herniation	
Ventriculomegaly	Increased ventricular size	
Open spina bifida	U-shaped spine Myelomeningocele	Small IT or fourth ventricle Absent cisterna magna BPD <5th percentile
Holoprosencephaly	Fused frontal horns Monoventricle	Fused metopic suture Non-visualization of the butterfly sign
Agenesis of the corpus callosum	No direct sign	Non-visualization of the pericallosal artery Abnormal midbrain/falx diameter ratio
Dandy-Walker malformation	Enlarged posterior fossa	Enlarged fourth ventricle BSOB diameter >95%

BPD biparietal diameter, *BSOB* brain stem-occipital bone diameter (distance between the posterior border of the brain stem and inner border of the occipital bone), *IT* intracranial translucency

Table 14.2 shows direct and indirect ultrasonographic signs that can be identified in these views for early diagnosis of CNS anomalies.

Acrania–Exencephaly–Anencephaly Sequence

According to the “Performance of First-Trimester Fetal Ultrasound Scan” practice guidelines issued by the International Society of Ultrasound in Obstetrics and Gynecology (ISUOG) in 2013 [9], mineralization of the calvarium should be demonstrated in axial and coronal views from 11 weeks’ gestation. Thus, acrania–exencephaly–anencephaly sequence can be suspected earlier during the embryonic period as shown in Fig. 14.15 and confidently diagnosed during the 11–14 weeks scan (Fig. 14.31).

Holoprosencephaly

As seen previously, HPE is among the CNS abnormalities that can be diagnosed as early as 9 weeks (Fig. 14.17). Sepulveda et al. [91] have shown that failure to identify the “butterfly” sign of the choroid plexus at 11–14 weeks must be considered a warning sign of alobar HPE (Fig. 14.32). At this time, associated anomalies such as extreme hypotelorism, cyclopia, and proboscis may also be diagnosed using 3D rendering techniques (Fig. 14.33).

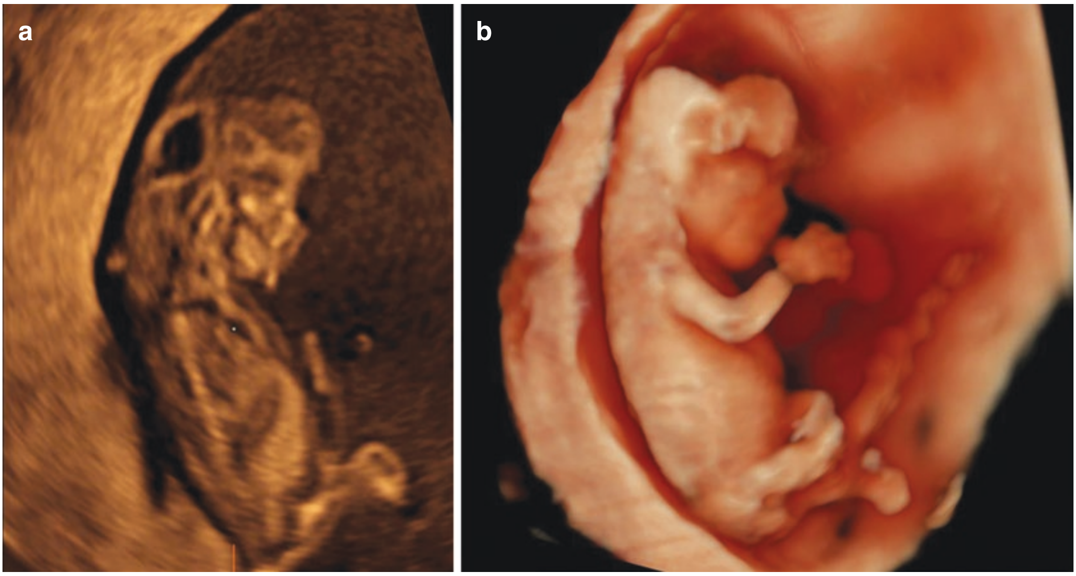

Fig. 14.31 2D (**a**) and 3D rendered view using HDLive (**b**) of a 12-week fetus with acrania–exencephaly–anencephaly sequence. Note the absence of the cranial vault and exposure of the rudimentary fetal brain to the amniotic fluid

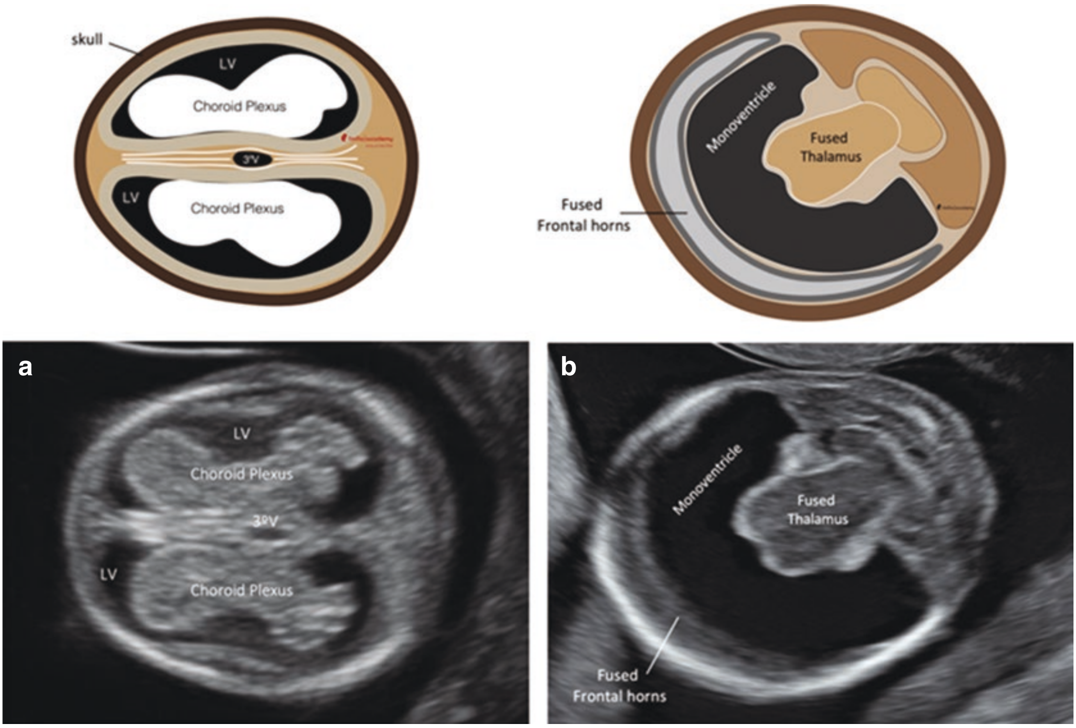
skull
LV
Choroid Plexus
3ºV
LV
Choroid Plexus
Monoventricle
Fused
Thalamus
Fused
Frontal horns
a
LV
Choroid Plexus
3ºV
LV
Choroid Plexus
b
Monoventricle
Fused
Thalamus
Fused
Frontal horns

Fig. 14.32 (**a**) Choroid plexus plane showing the "butterfly" sign and third ventricle. (**b**): Fused frontal horns (monoventricle) and fused thalamus. *LV* lateral ventricle, *3rd V* third ventricle

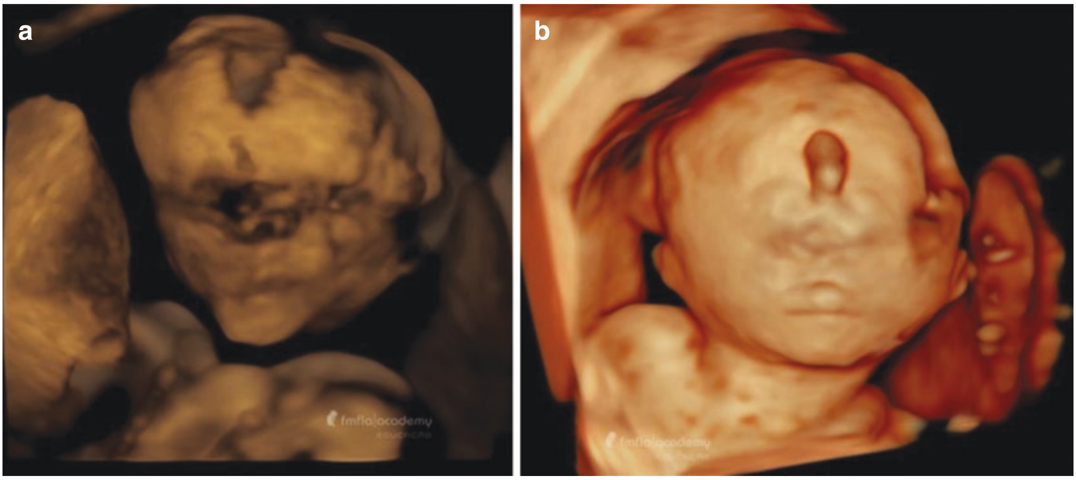

Fig. 14.33 (**a**) 3D rendered view of the fetal face using maximum intensity projection ("skeleton" mode) shows premature close of the metopic suture and extreme hypotelorism. (**b**) 3D rendered view using HDLive shows the proboscis and arrhinia to greater advantage

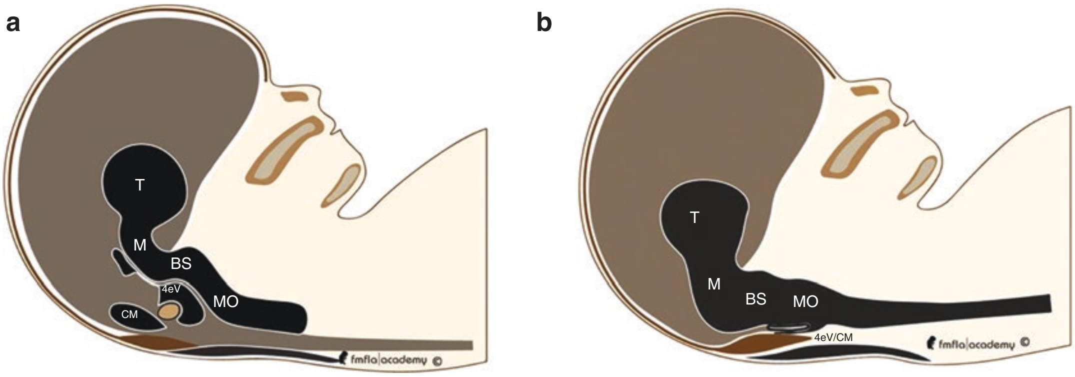

Fig. 14.34 (**a**) Diagram depicting the midline sagittal plane of the fetal face showing the normal fourth ventricle (4th V) presenting as an intracranial translucency (IT) located between the posterior aspect of the brain stem and choroid plexus. (**b**) Failure to visualize the IT as seen in cases of spina bifida (see details in Fig. 14.35). *T* thalamus, *M* mesencephalon, *BS* brain stem, *MO* medulla oblongata, *CM* cisterna magna

Open Spinal Dysraphism (Spina Bifida)

Prenatal diagnosis of spina bifida is usually performed during the second trimester examination, when well-established screening signs such as the "lemon-shaped" head and "banana-shaped" cerebellum which are thought to occur as a consequence of caudal displacement of the hindbrain secondary to the Chiari-II malformation have been shown to be both sensitive and specific for the diagnosis [92].

During the 11–14-week scan, using the same sagittal plane used to measure the NT to assess the nasal bone while screening for aneuploidies, it is possible to evaluate the fourth ventricle as a marker for spina bifida. The fourth ventricle, as seen between 11 and 14 weeks, has been termed "intracranial translucency" (IT) (Figs. 14.23, 14.24, 14.25, and 14.34a). Failure to visualize the IT during the 11–14-week scan (Figs. 14.34b and 14.35) is a positive screening sign for open spina bifida, and dedicated examination of the fetal spine is warranted [89].

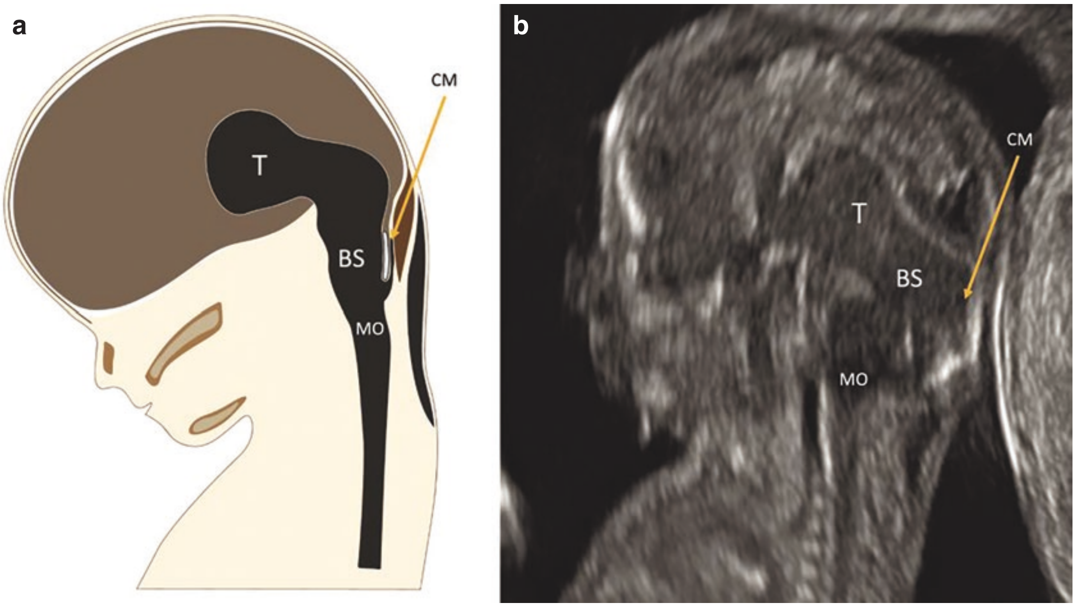

Fig. 14.35 (**a**) Diagram and (**b**) sagittal 3D US view using multiplanar display of the posterior fossa, showing caudal and inferior displacement of the brain resulting in compression of the fourth ventricle (intracranial translucency) and enlargement of the brainstem (BS). *T* thalamus, *MO* medulla oblongata, *CM* cisterna magna

Cervical Spina Bifida

Cervical spina bifida (CEB) is a rare condition that represents 3–4% of all cases of spina bifida. Anatomically, the defect is characterized by a "cyst within a cyst." The outer cyst is in continuity with the subarachnoid space (meningocele), is composed of arachnoid and fibrous tissue, and is covered by skin. The inner cyst is in continuity with a distended central canal (Figs. 14.36 and 14.37) [93].

Figure 14.38 illustrates the main differential diagnoses for CEB, which are encephalocele and cystic hygroma.

Face

Cleft Lip and Palate

Cleft lip and palate (CLP) is a common congenital defect that can be either isolated or associated with a wide range of chromosomal abnormalities and genetic syndromes. While most cases of CLP are not detected during the 11–14 weeks scan, Syngelaki et al. [82] reported a detection rate of 35% of cleft lip and 14% of cases of cleft lip during routine examinations, improvement may be achieved by adhering to a standardized 3D US protocol that analyzes early facial anatomy in the sagittal, coronal, and axial planes using the multiplanar display method. For example, using a standard mid-sagittal view of the fetal face at 11–14 weeks gestation, detection of a maxillary gap (Figs. 14.39 and 14.40) should prompt a detailed examination of the fetal face as Chaoui et al. have reported a maxillary gap in 96% of cases of CLP with additional abnormalities, 65% of fetuses with isolated CLP, but also 7% of normal fetuses [94].

Figure 14.41 shows a 3D rendered view of the face of a fetus examined at 13 weeks and 1 day diagnosed with cleft lip and palate.

Low-Set Ear in Early Fetuses Examined at 11–14 Weeks

Low-set ear is identified when the helix is situated below a horizontal plane traced from the outer canthus of the eye to the back to the occiput. Since the helix of the ear and skull bone are not in the same plane, identification of ear position is, at a minimum, difficult by 2D US. Volumetric 3D

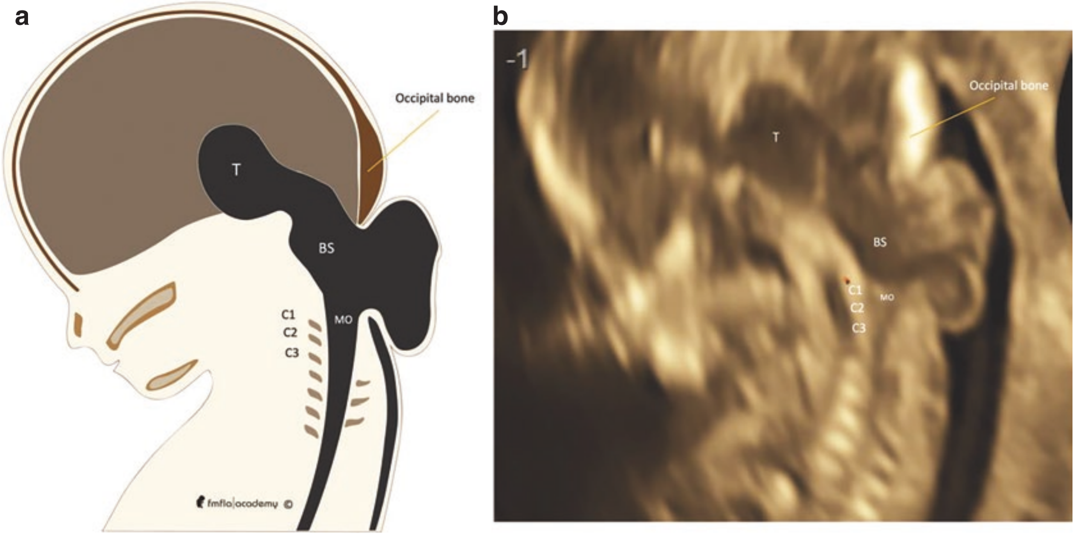

Fig. 14.36 Cervical spina bifida. (**a**) Diagram and (**b**) 3D multiplanar sagittal view of a 12-weeks and 5 days fetus in the mid-sagittal plane. A large cervical spinal dysraphism is seen with herniated cystic contents covered by skin. Note also associated dorsal and caudal displacement of the thalamus and brain stem which are partially protruding through the defect. *T* thalamus, *BS* brain stem, *MO* medulla oblongata

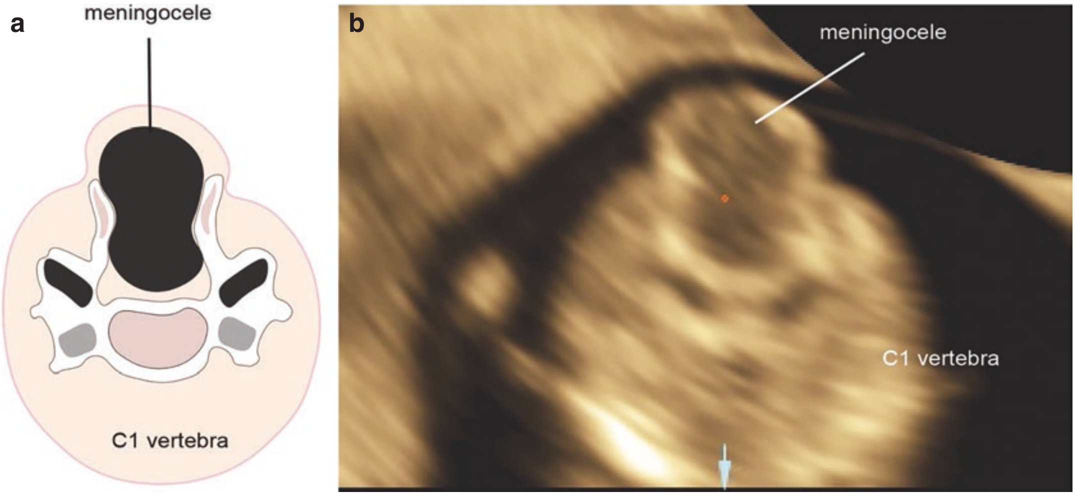

Fig. 14.37 Cervical spina bifida. (**a**) Diagram and (**b**) 3D multiplanar axial view of a 12-weeks and 5 days fetus at the level of C1. Note the splaying of the posterior lamina of C1 with herniation of meninges and CSF (meningocele) covered by skin

rendered views of the side of the fetal head can display the eye, helix, and cranium at the same time and, therefore, can reliably identify ear position (Fig. 14.42). In a study of 3559 fetuses examined by 3D US between 11 and 14 weeks, Pooh et al. [95] were able to determine ear position in 3559 cases (99.9%). There were 123 cases of low-set ear (3.46%) and, out of the 81 who underwent genetic testing, chromosomal anomalies were identified in 26 (32%). These included 11 cases of 18, 10 cases of trisomy 21, 3 cases of trisomy 13, and 1 case each of monosomy X and

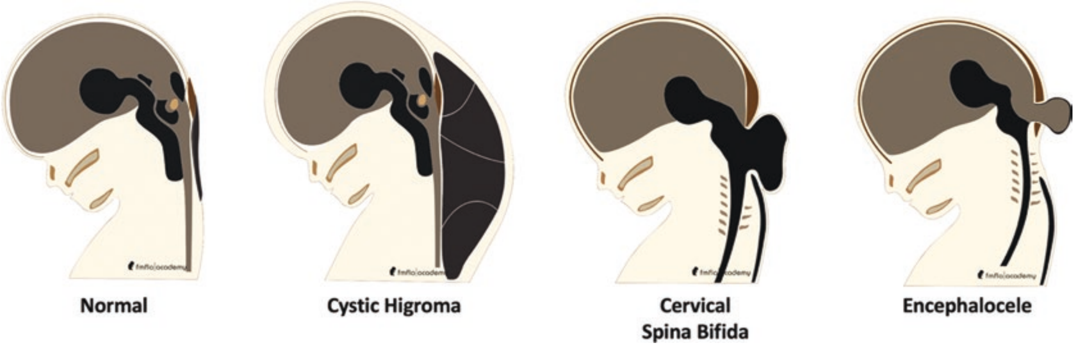
fmfla|academy
Normal
Cystic Higroma
Cervical
Spina Bifida
Encephalocele

Fig. 14.38 Differential diagnoses for cervical spina bifida

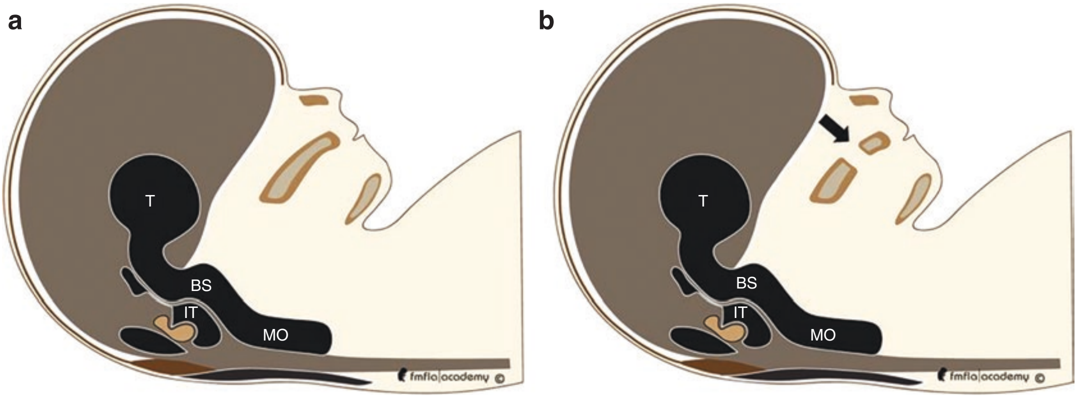
a
b
T
BS
IT
MO
fmfla|academy ©

Fig. 14.39 Diagram depicting the standard mid-sagittal view of the fetal face used routinely at 11–14 weeks, showing the palate in a normal fetus (**a**) and a maxillary gap (black arrow) commonly seen in fetuses with cleft lip and palate (**b**)

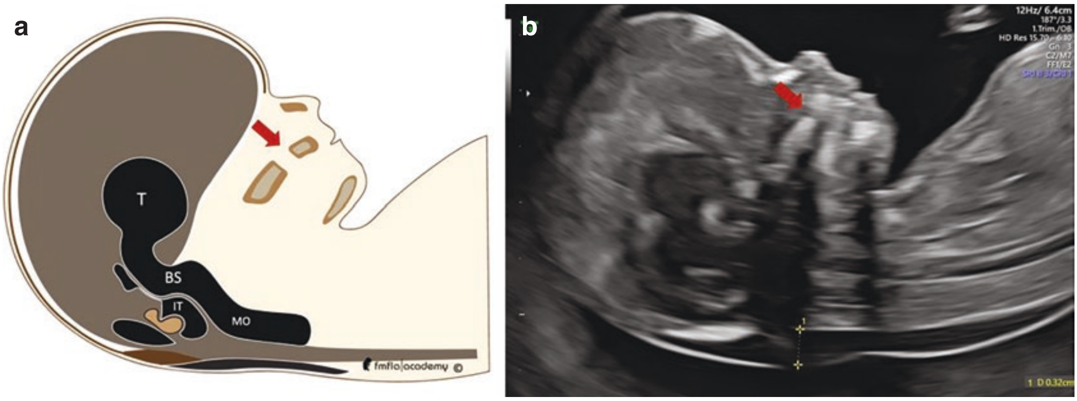
a
T
BS
IT
MO
fmfla|academy ©
b
12Hz/ 6.4cm
187°/3.3
1.Trim./OB
Gn 3
C2/M7
FF1/E2
1 D 0.32cm

Fig. 14.40 Diagram (**a**) and mid-sagittal view of the fetal face of a 12 weeks and 5 days fetus (**b**) showing the maxillary gap sign (red arrow)

partial deletion of chromosome 4. Thus, identification a low-set ear should prompt detailed fetal evaluation and genetic counseling.

Micrognathia

Micrognathia is a common craniofacial deformity characterized by mandibular hypoplasia and

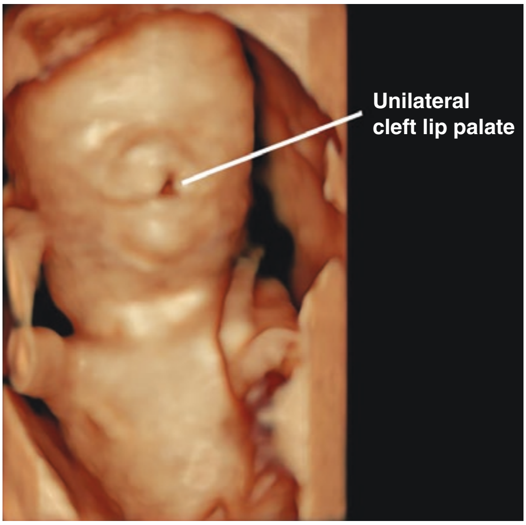

Fig. 14.41 HDLive 3D rendered image of the fetal face at 13 week and 1 day showing a unilateral cleft lip and palate

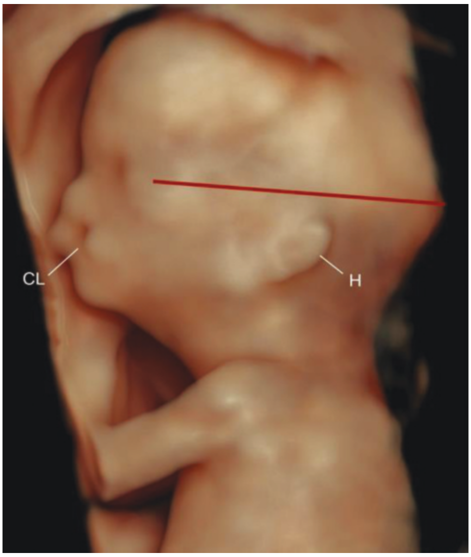

Fig. 14.42 3D rendered lateral view of the fetal cranium using HDLive mode. A low-set ear identified with the helix of the ear (H) is located bellow a plane the extends from the outer canthus of the eye to the occiput (red line). Also note the cleft lip (CL) that can be identified in the same view

retrognathia. The condition is commonly associated with syndromic conditions. In a recent study proposing a genetic-phenotypic classification syndrome micrognathia, 325 genes and 172 syndromes were found to be associated with micrognathia, with pathogenic genes divided into 4 main groups according to function: cellular processes and structures, cell metabolism, cartilage and bone development, and neuromuscular function [96]. A large postnatal series spanning a period of 28 years highlights the most common syndromic conditions in children presenting for postnatal treatment for micrognathia. Among 266 patients, the majority (n = 148) had oculo-auriculo-vertebral (OAV) spectrum, followed by 52 with mandibulofacial dysostosis, 31 with Pierre Robin sequence, 17 with miscellaneous syndromes, and 18 patients with isolated mandibular hypoplasia [97]. Evaluation for micrognathia in the first trimester relies on identification of an absent mandibular gap in the retronasal triangle (Figs. 14.43 and 14.44) [98, 99].

Heart

The knowledge that an increased NT between 11 and 14 weeks is associated not only with an increased risk of aneuploidies but also with CHD [79] prompted many investigators to evaluate the capability of early fetal echocardiography for the early diagnosis of heart defects [14, 15, 29]. Early examination of the fetal heart can be performed with the aid of color Doppler as shown in Fig. 14.45. A meta-analysis of 63 studies including 328,262 fetuses with known postnatal outcome found that first-trimester echocardiography had a sensitivity of 55.8% (95% CI 45.87–65.50%) and a specificity of 99.98% (95% CI 9997–99.99%) to detect CHD in a non-high-risk population, and a sensitivity of 67.74% (95% CI 55.24–79.06%) and a specificity of 99.75% (95% CI 99.47–99.92%) in fetuses at high-risk for CHD [100].

A handful of studies evaluated first trimester examination of the fetal heart using volumetric imaging obtained with spatiotemporal image correlation (STIC) [17–19, 101]. Studies addressing visualization rates of standard anatomical planes found that a complete examination is possible after 12 weeks and that the capability of obtaining diagnostic images correlates with high-quality initial gray-scale images, use of a transvaginal probe for volume acquisition and the addition of color Doppler (Figs. 14.1, 14.46, and 14.47) [17–19, 102–104].

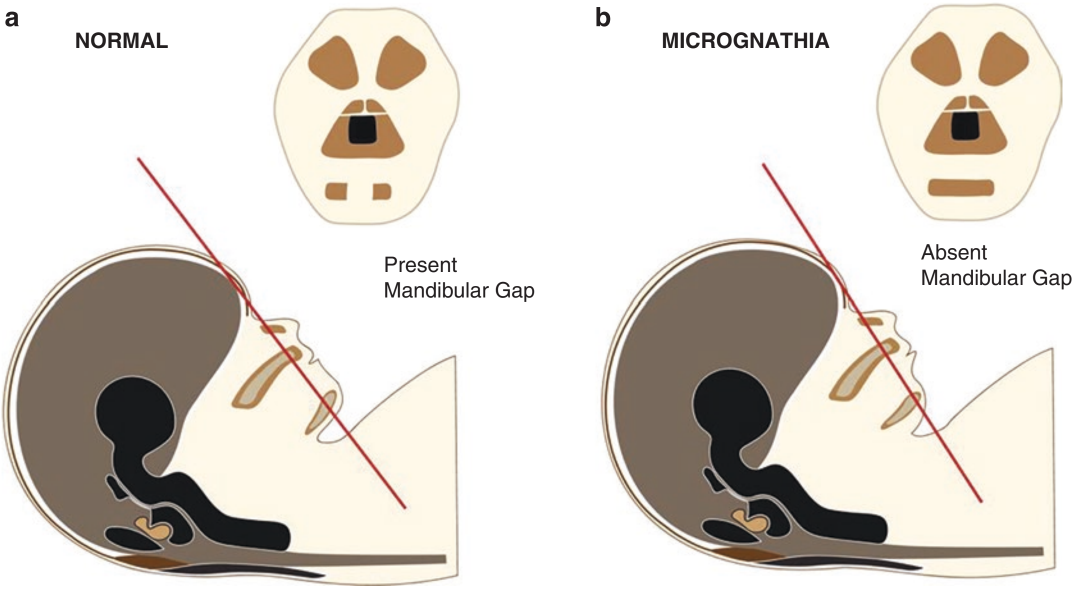
a
NORMAL
Present
Mandibular Gap
b
MICROGNATHIA
Absent
Mandibular Gap

Fig. 14.43 Diagrams illustrating the plane of section to visualize the retronasal triangle. Note the presence of a gap in the center of the mandible (mandibular gap) which is seen in normal pregnancies (**a**). The mandibular gap is not present in fetuses with micrognathia. Instead, a bony structure representing the receding chin is identified (**b**)

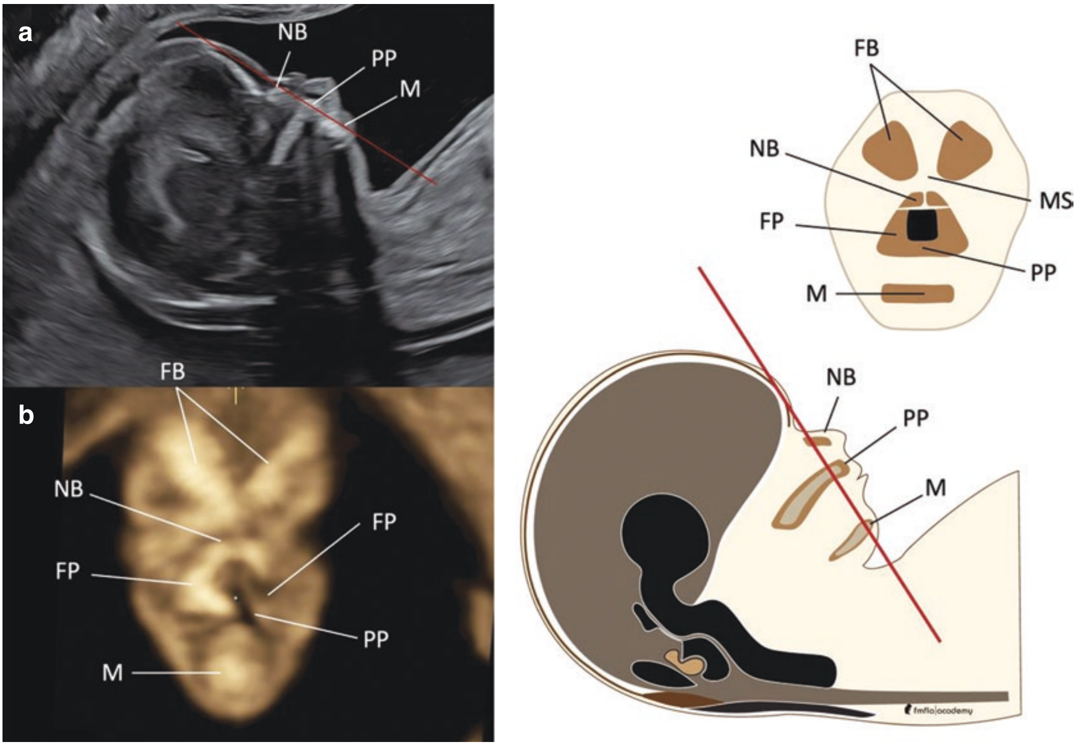
a
NB
PP
M
FB
b
NB
FP
FP
PP
M
FB
NB
MS
FP
PP
M
NB
PP
M

Fig. 14.44 (**a**) 2D Fetal profile at 13 weeks +1 days in a fetus with micrognathia. (**b**) Multiplanar coronal view through a plane illustrated by the red line on (**a**) shows the retronasal triangle in a case with associated unilateral cleft clip and palate. Note the absent frontal process of the maxilla and cleft through the primary palate on the left side. *FB* frontal bones, *MS* metopic suture, *NB* nasal bone, *FP* frontal process of the maxilla, *PP* primary palate

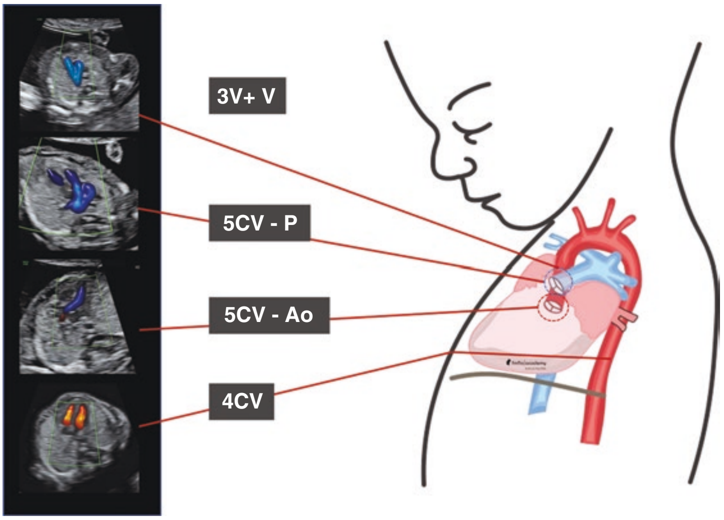
3V+ V
5CV - P
5CV - Ao
4CV

Fig. 14.45 Planes of section for examination of the fetal heart during the 11–14-week scan. The use of high-quality color Doppler enhances the ability to diagnose CHD. *4CV* four-chamber view, *5CV-Ao* five-chamber/aorta view, *5CV-P* five-chamber/pulmonary artery view, *3Vt V* three-vessel and trachea view

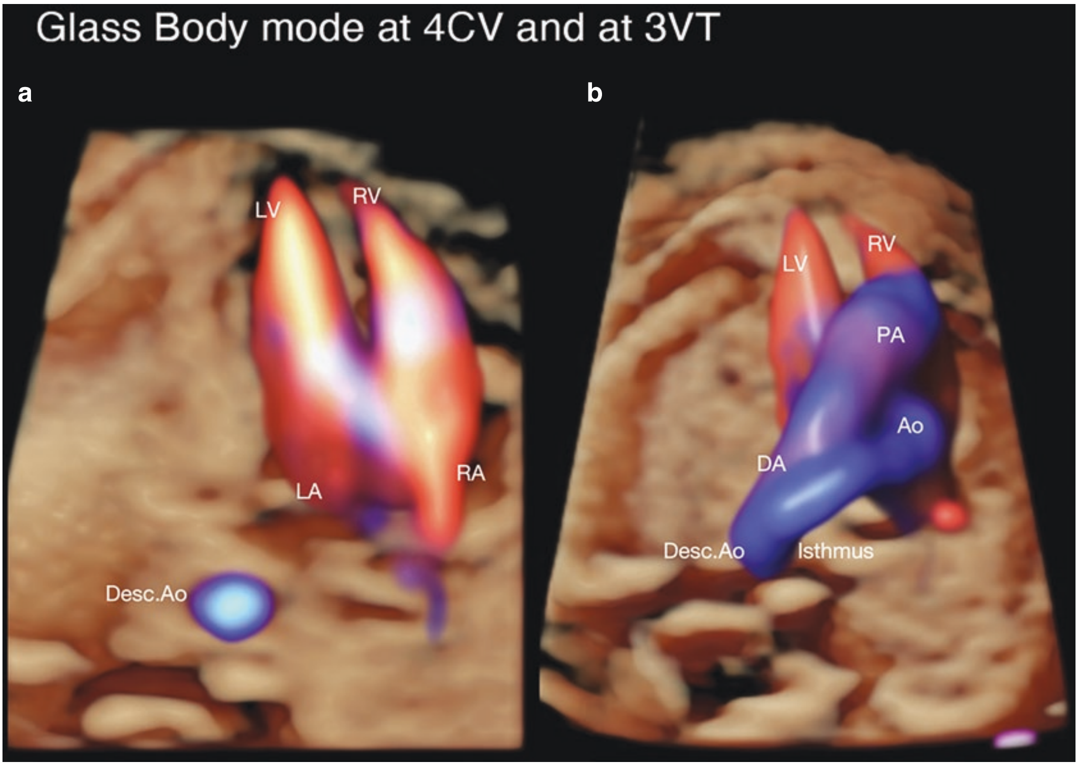
Glass Body mode at 4CV and at 3VT
a
LV
RV
LA
RA
Desc.Ao
b
RV
LV
PA
Ao
DA
Desc.Ao
Isthmus

Fig. 14.46 (**a**) Glass body mode at the 4-chamber view (4CV) showing the inflow of the left and right chambers; (**b**) 3VT glass body mode combines information from multiple planes (4CV, outflow tracts and three-vessel and trachea view (3VT)) in a single image, allowing simultaneous visualization of the anatomical relationships between the ventricular chambers (RV and LV), aorta (Ao), pulmonary artery (PA), and ductus arteriosus (DA). (Image courtesy Prof. Rabih Chaoui)

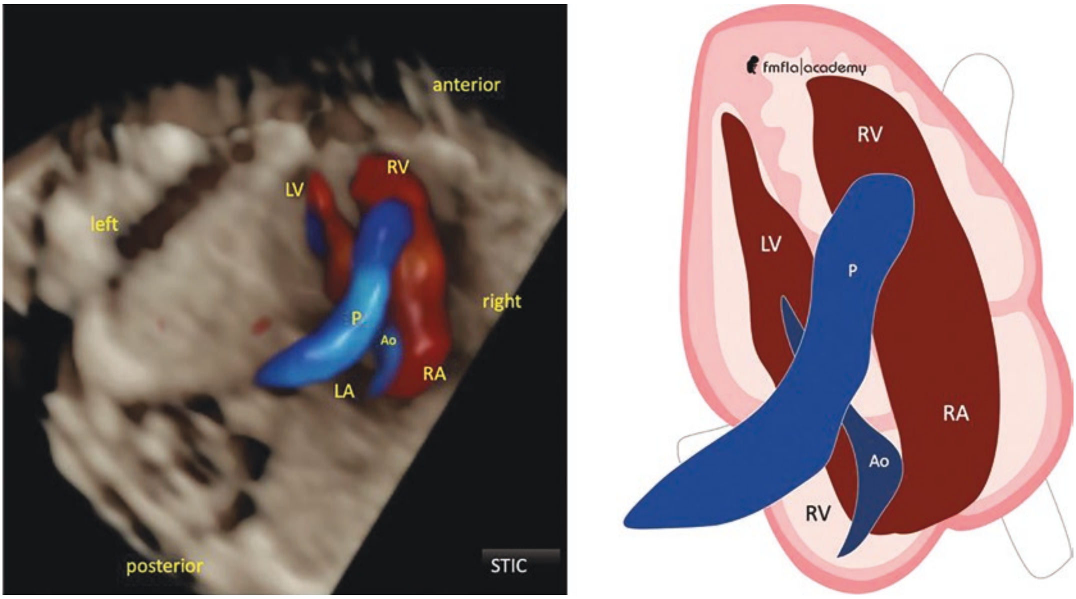

Fig. 14.47 4D Rendered view of the fetal heart acquired with STIC and color Doppler at 13 weeks and 1 day (left) and corresponding diagram (right) show small left cardiac chambers compared to the right and a hypoplastic aorta in a case of early diagnosis of hypoplastic left heart syndrome (HLHS). *LV* left ventricle, *RV* right ventricle, *LA* left atrium, *RA* right atrium, *Ao* aorta, *P* pulmonary artery

Espinoza et al. [20] conducted a multicentric study in which 4 international centers with expertise in first trimester 4D fetal echocardiography were asked to examine 4D volume datasets of normal ($n = 17$) and abnormal fetuses ($n = 16$) without prior knowledge of clinical indications or results of the 2DUS examination. The median (range) accuracy, sensitivity, and specificity as well as the positive and negative likelihood ratios, for the identification of fetuses with congenital heart defects were 79% (95% CI 77%–83%), 90% (95% CI 70%–96%), 59% (95% CI 58%–93%), 2.35 (95% CI 2.05–9.80), and 0.18 (95% CI 0.08–0.32), respectively. The study showed that experienced examiners can use volume datasets to diagnose congenital heart disease with reasonable sensitivity between 11 and 15 weeks; however, the specificity of 59% was somewhat disappointing. In a subsequent study of 152 fetuses who had volume datasets of the fetal heart acquired with STIC and color Doppler and visualized using a tomographic imaging display, Turan et al. [104] reported 91% sensitivity and 100% specificity for the diagnosis of CHD, with 85% of the anomalies visualized in the four-chamber view plane and the remainder seen in planes depicting the outflow tracts with color Doppler. In the only study that compared the effectiveness of 4DUS using STIC with transvaginal 2DUS for diagnosis of congenital heart disease, which included 121 fetuses examined by 2DUS and 115 fetuses examined by 2DUS and 4DUS with STIC, the diagnostic accuracy and area under the receiver-operating characteristics (ROC) curve were significantly higher for 2DUS (diagnostic accuracy: 2DUS 94.2% vs. 4DUS with STIC 88.7%; area under the ROC curve: 2DUS 0.912 vs. 4DUS with STIC 0.818, $p < 0.05$) [18].

Thorax and Abdomen

Evaluation of the position of thoracic and abdominal organs as well as early demonstration of the integrity of the diaphragm is possible with first trimester 3D US (Figs. 14.48, 14.49, 14.50, and 14.51). Examples of prenatal diagnosis of omphalocele (Fig. 14.52), gastroschisis (Fig. 14.53).

Urinary Tract

Below we present a few cases of congenital anomalies of the urinary tract diagnosed with first trimester 3D US.

Patent Urachus with Bladder Prolapse

Persistent urachal anomalies are rare congenital lesions of the urinary tract. The spectrum of described urachal anomalies includes urachal cysts or sinus, bladder diverticulum, and a patent urachus. A patent urachus represents that a complete connection between the bladder and the umbilical cord is a very rare anomaly with an incidence of 3/1,000,000 live births, being three times more frequent in males than in females [105]. Figure 14.54 shows early 3D US diagnosis of a bladder prolapse through a patent urachus to the umbilical cord which is on the spectrum of urachal anomalies (Fig. 14.55).

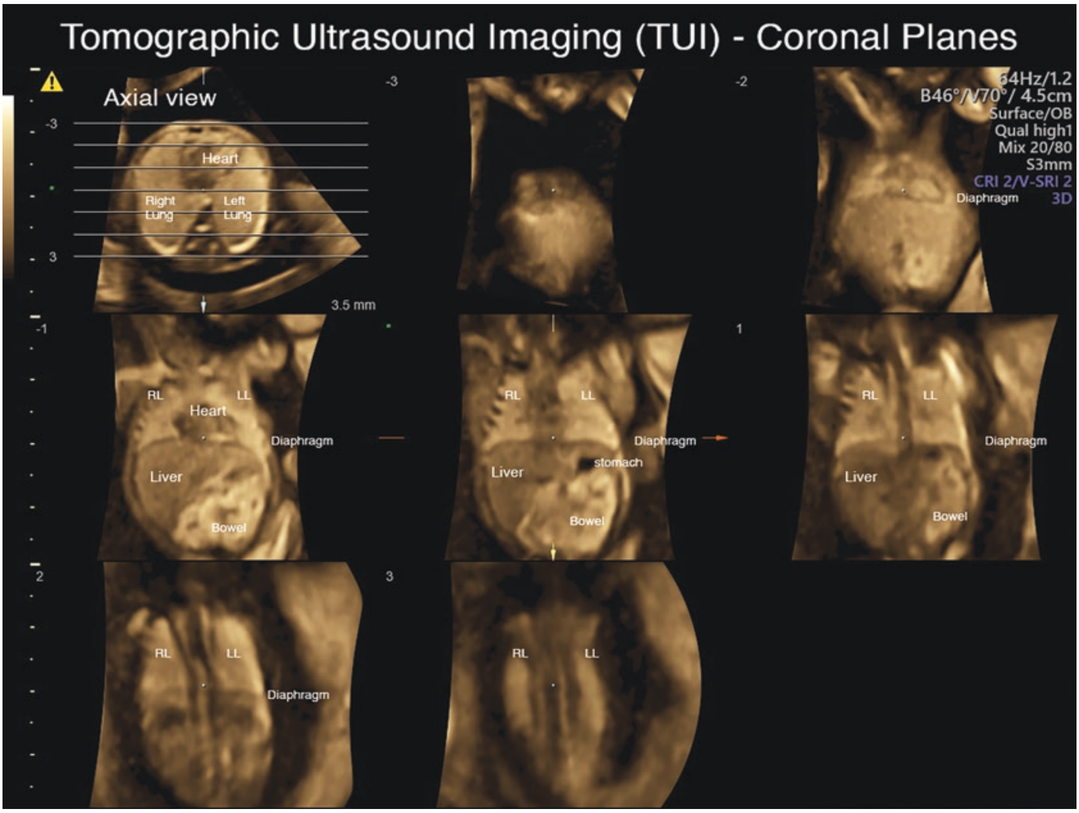
Tomographic Ultrasound Imaging (TUI) - Coronal Planes
Axial view
Heart
Right Lung
Left Lung
3.5 mm
-3
-2
-1
1
2
3
64Hz/1.2
B46°/V70°/ 4.5cm
Surface/OB
Qual high1
Mix 20/80
S3mm
CRI 2/V-SRI 2
3D
Diaphragm
RL
LL
Heart
Liver
Bowel
stomach

Fig. 14.48 Tomographic ultrasound imaging (TUI) in coronal planes covering the entire chest and abdomen using 3 mm-thick slices, demonstrating integrity of the diaphragm and position of the various organs in the thorax and abdomen. *RL* right lung, *LL* left lung

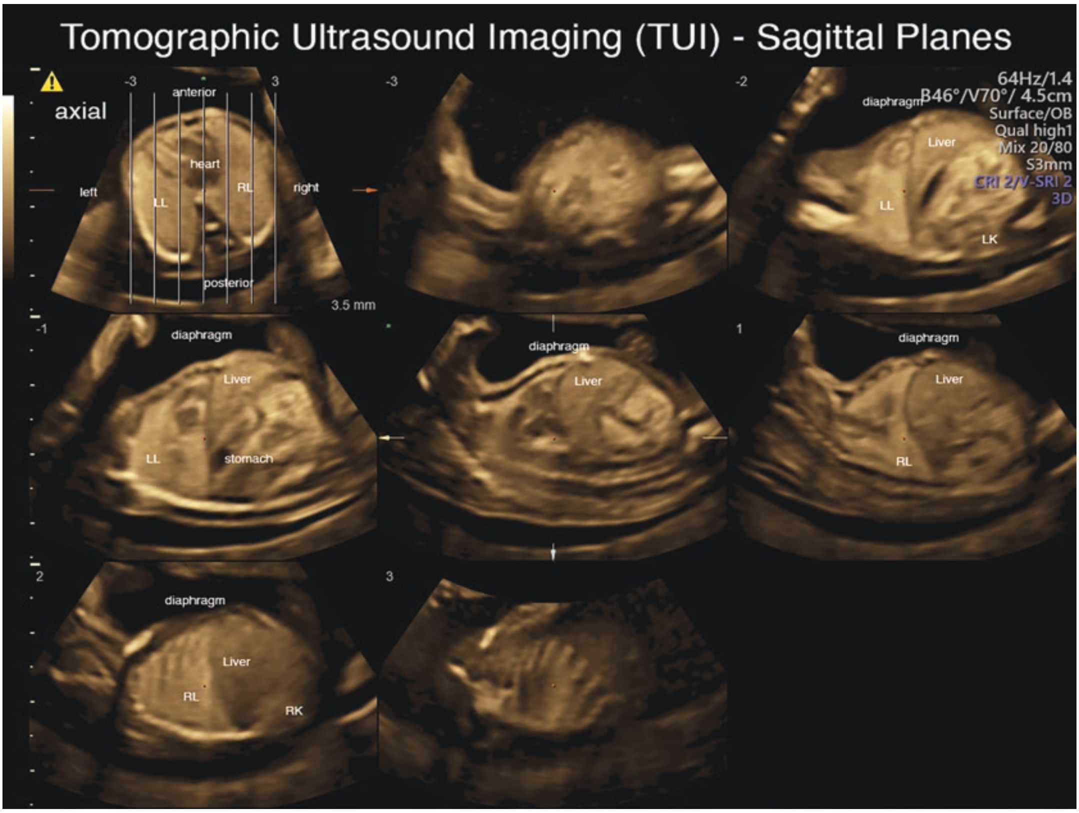
Tomographic Ultrasound Imaging (TUI) - Sagittal Planes
axial
-3
3
anterior
heart
left
LL
RL
right
posterior
3.5 mm
-3
-2
diaphragm
64Hz/1.4
B46°/V70°/ 4.5cm
Surface/OB
Qual high1
Mix 20/80
S3mm
CRI 2/V-SRI 2
3D
Liver
LL
LK
-1
diaphragm
Liver
LL
stomach
diaphragm
Liver
1
diaphragm
Liver
RL
2
diaphragm
Liver
RL
RK
3

Fig. 14.49 Tomographic ultrasound imaging (TUI) in the sagittal planes covering the entire chest and abdomen using 3 mm-thick slices, demonstrating integrity of the diaphragm and position of the various organs in the thorax and abdomen. *RL* right lung, *LL* left lung

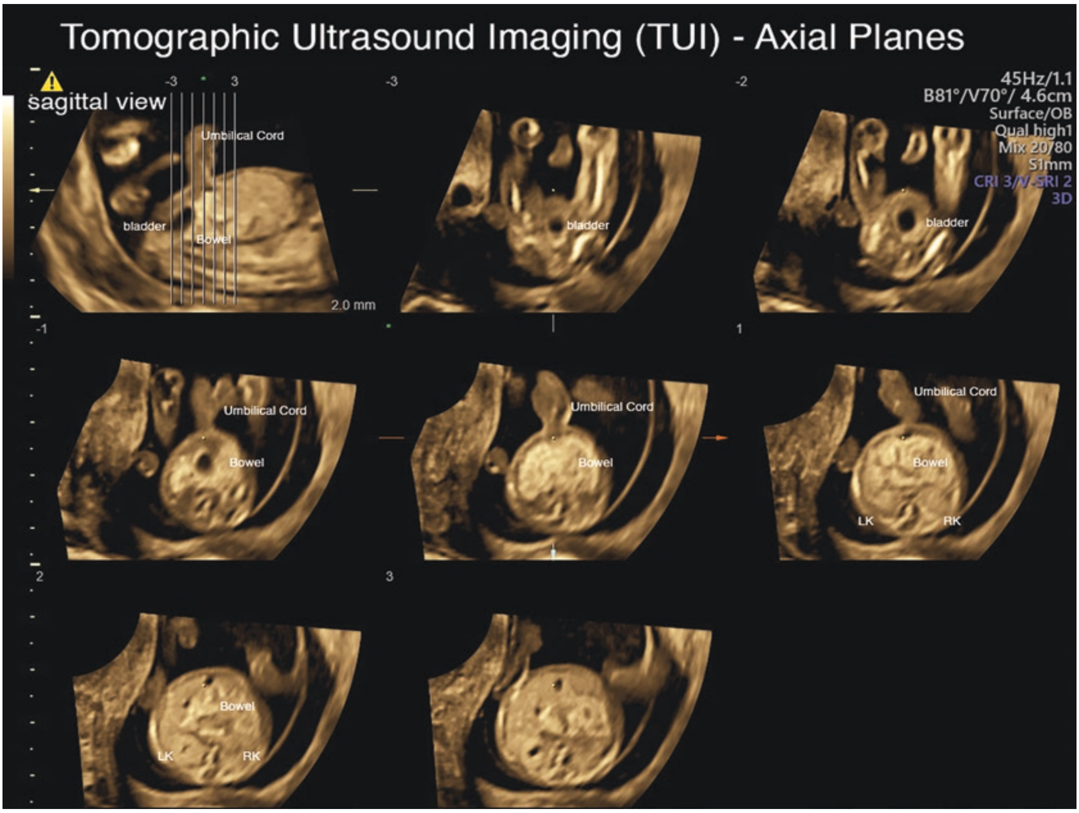
Tomographic Ultrasound Imaging (TUI) - Axial Planes
sagittal view
-3
3
Umbilical Cord
bladder
Bowel
2.0 mm
-3
bladder
-2
bladder
45Hz/1.1
B81°/V70°/ 4.6cm
Surface/OB
Qual high1
Mix 20/80
S1mm
CRI 3/V-SRI 2
3D
-1
Umbilical Cord
Bowel
Umbilical Cord
Bowel
1
Umbilical Cord
Bowel
LK
RK
2
Bowel
LK
RK
3

Fig. 14.50 Tomographic ultrasound imaging (TUI) in axial planes covering the entire abdomen using 3 mm-thick slices, demonstrating umbilical cord insertion, bladder, and kidneys

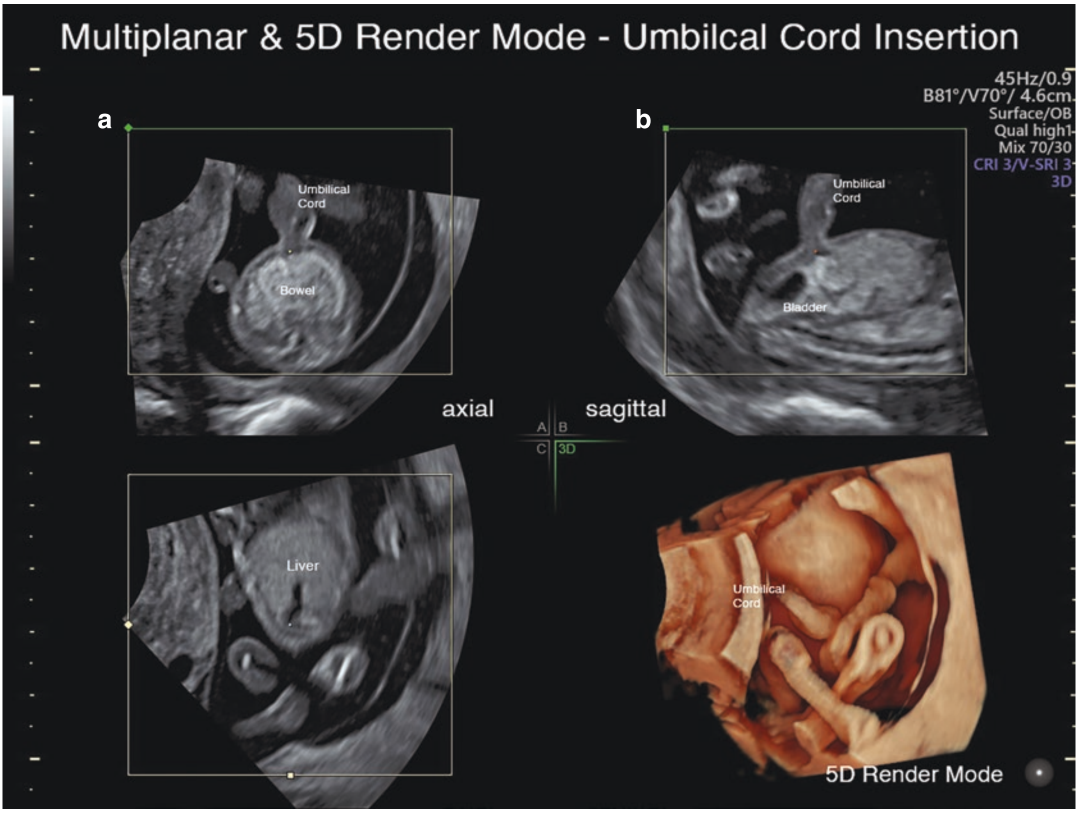
Multiplanar & 5D Render Mode - Umbilcal Cord Insertion
45Hz/0.9
B81°/V70°/ 4.6cm
Surface/OB
Qual high1
Mix 70/30
CRI 3/V-SRI 3
3D
a
b
Umbilical Cord
Bowel
Umbilical Cord
Bladder
axial
sagittal
A
B
C
3D
Liver
Umbilical Cord
5D Render Mode

Fig. 14.51 Multiplanar and 3D HDLive image of the umbilical cord insertion as seen in axial (panel **a**), sagittal (panel **b**), and 3D rendered views (panel **3D**)

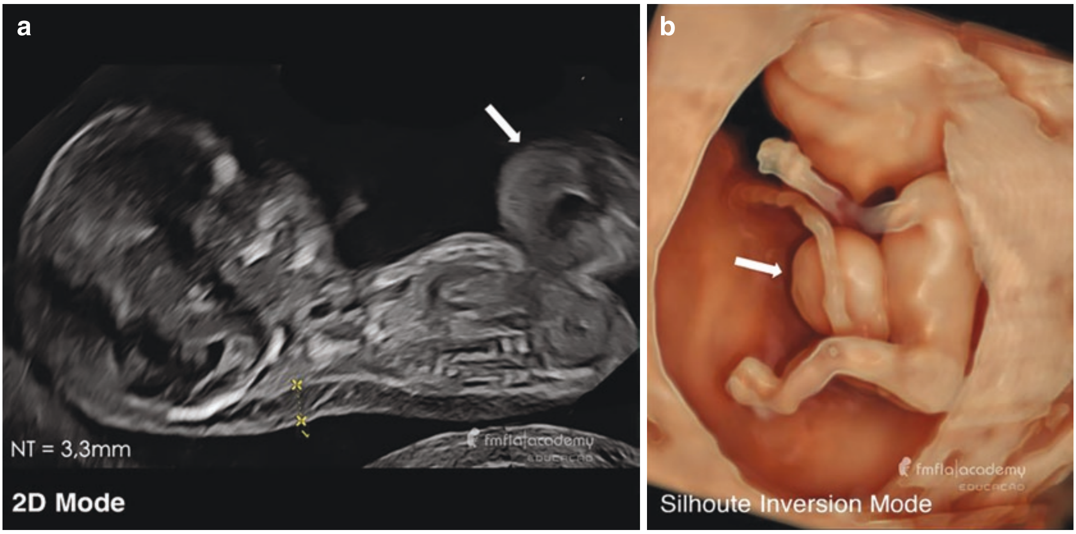
a
b
NT = 3,3mm
2D Mode
fmflaacademy
Silhoute Inversion Mode

Fig. 14.52 Prenatal diagnosis of omphalocele at 12 weeks. (**a**) sagittal plane showing the extruded abdominal organs (arrow). (**b**) 3D rendered view using HDLive mode shows the omphalocele (arrow). Note the insertion of the umbilical cord into the inferolateral aspect of the omphalocele

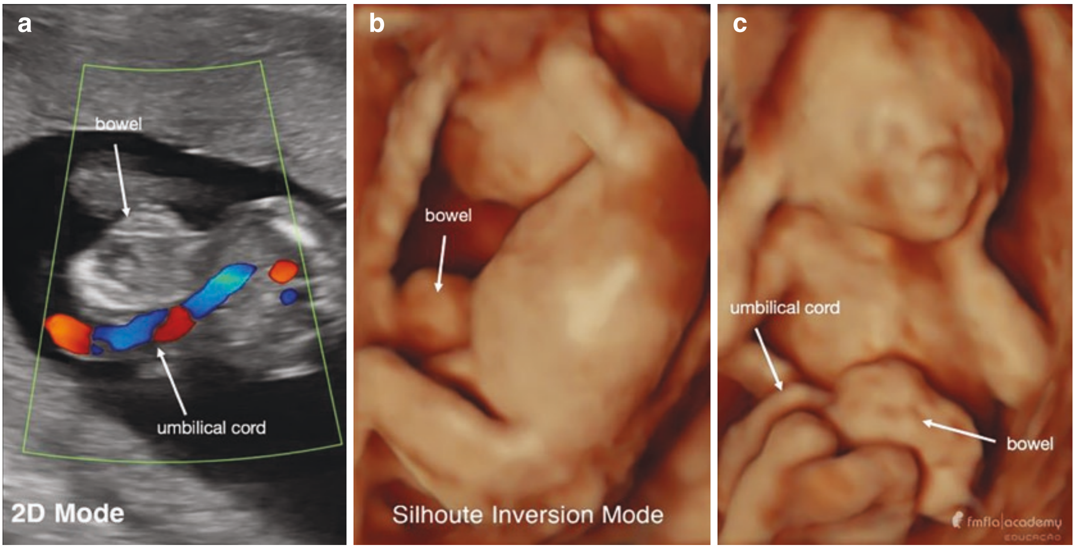
a
bowel
umbilical cord
2D Mode
b
bowel
Silhoute Inversion Mode
c
umbilical cord
bowel
fmfla academy

Fig. 14.53 Prenatal diagnosis of gastroschisis in a 13-weeks fetus. (**a**) 2D US image shows extruded bowel and the paraumbilical umbilical cord insertion. 3D rendered images using Silhouette inversion mode show the extruded bowel loops in the lateral and frontal views (**b**, **c**) and the paraumbilical cord insertion on (**c**)

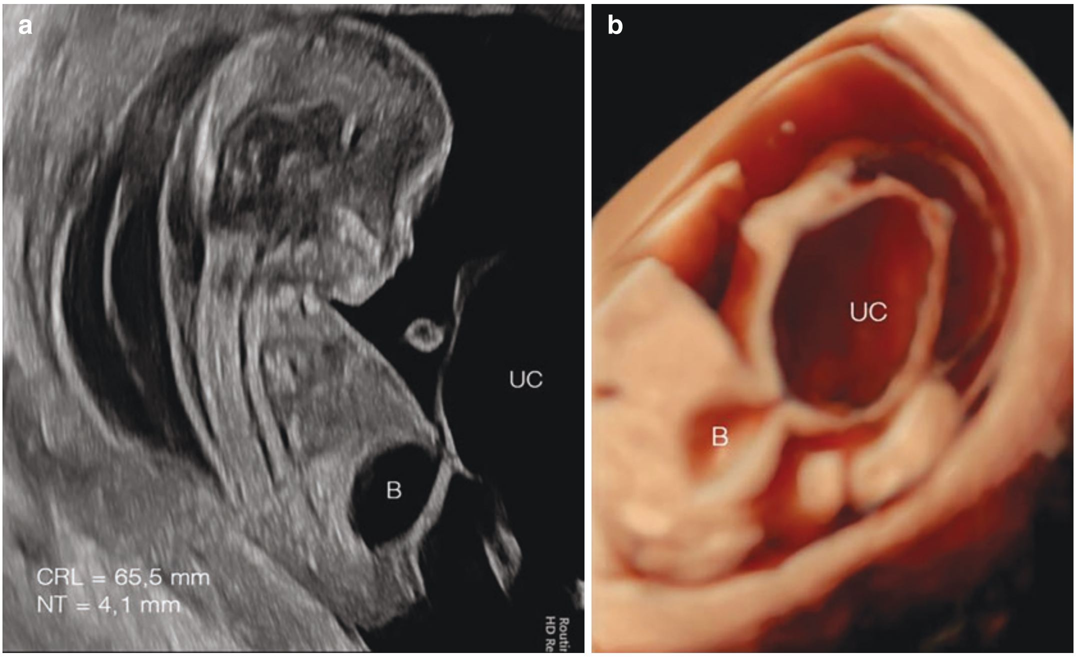
a
UC
B
CRL = 65,5 mm
NT = 4,1 mm
b
UC
B

Fig. 14.54 3D US of a 12-weeks fetus with a bladder prolapse to the umbilical cord, an anomaly within the spectrum of urachal anomalies. (**a**) Sagittal view of the multiplanar display mode. (**b**) 3D rendered view using HDLive. *B* bladder, *UC* umbilical cord

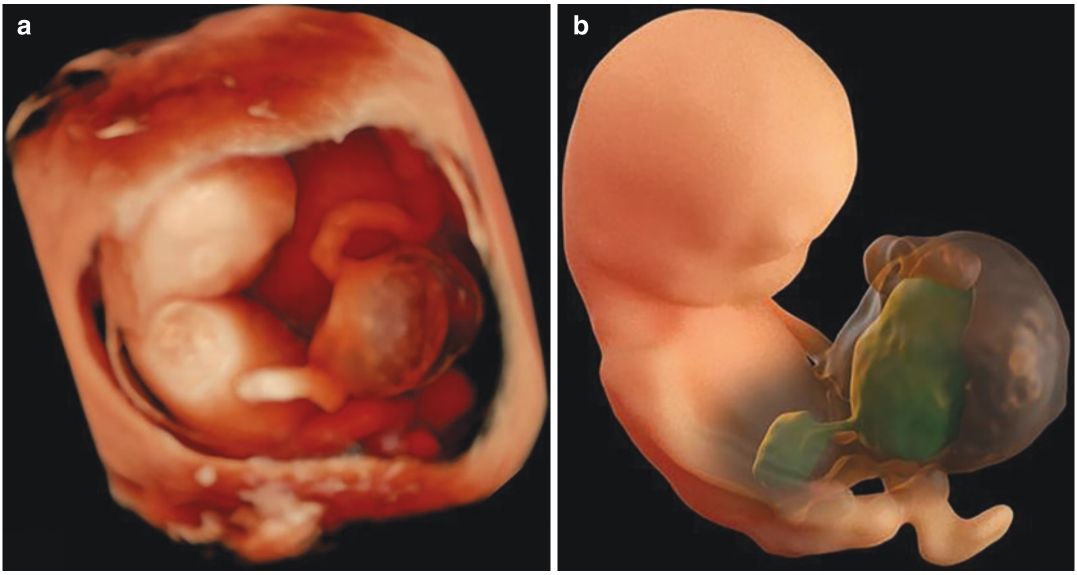

Fig. 14.55 3D US of a 12-weeks fetus with a bladder prolapse to the umbilical cord, an anomaly within the spectrum of urachal anomalies. (**a**) 3D rendered view using the Silhouette mode. (**b**) 3D computer model of the fetus. (The 3D model was produced by Drs. Renato Ximenes and Rafael Peters using Blender software (https://blender.org))

Conclusion

3DUS is an attractive technology for early evaluation of the human fetus, with several anomalies, usually major, correctly diagnosed by the method, as documented in the literature and illustrated by the images in this chapter.

Teaching Points

- High-resolution images of the embryo and early fetus can be obtained with transvaginal ultrasonography.
- Several studies demonstrate that early diagnosis of major congenital anomalies is possible by high-resolution transvaginal ultrasonography; however, early ultrasonography is not sufficient to diagnose a significant number of anomalies that may manifest only in the second or third trimesters.
- High-resolution 3D imaging of the embryo and early fetus can be obtained using transvaginal probes equipped with 3D and 4D technology, facilitating understanding of embryonic anatomy in vivo (sonoembryology).

References

1. Rottem S, Bronshtein M, Thaler I, Brandes JM. First trimester transvaginal sonographic diagnosis of fetal anomalies. Lancet. 1989;1(8635):444–5. http://www.ncbi.nlm.nih.gov/pubmed/2563825.
2. Rottem S, Bronshtein M. Transvaginal sonographic diagnosis of congenital anomalies between 9 weeks and 16 weeks, menstrual age. J Clin Ultrasound. 1990;18(4):307–14. http://www.ncbi.nlm.nih.gov/pubmed/2160998.
3. Achiron R, Tadmor O. Screening for fetal anomalies during the first trimester of pregnancy: transvaginal versus transabdominal sonography. Ultrasound Obstet Gynecol. 1991;1(3):186–91. https://doi.org/10.1046/j.1469-0705.1991.01030186.x.
4. Timor-Tritsch IE, Monteagudo A, Peisner DB. High-frequency transvaginal sonographic examination for the potential malformation assessment of the 9-week to 14-week fetus. J Clin Ultrasound. 1992;20(4):231–8. http://www.ncbi.nlm.nih.gov/pubmed/1315796.
5. Achiron R, Weissman A, Rotstein Z, Lipitz S, Mashiach S, Hegesh J. Transvaginal echocardiographic examination of the fetal heart between 13 and 15 weeks' gestation in a low-risk population. J Ultrasound Med. 1994;13(10):783–9. http://www.ncbi.nlm.nih.gov/pubmed/7823340.
6. Souka AP, Pilalis A, Kavalakis Y, Kosmas Y, Antsaklis P, Antsaklis A. Assessment of fetal anat-

omy at the 11-14-week ultrasound examination. Ultrasound Obstet Gynecol. 2004;24(7):730–4. https://doi.org/10.1002/uog.1775.

7. Ebrashy A, El Kateb A, Momtaz M, et al. 13-14-week fetal anatomy scan: a 5-year prospective study. Ultrasound Obstet Gynecol. 2010;35(3):292–6. https://doi.org/10.1002/uog.7444.
8. Katorza E, Achiron R. Early pregnancy scanning for fetal anomalies—the new standard? Clin Obstet Gynecol. 2012;55(1):199–216. https://doi.org/10.1097/GRF.0b013e3182446ae9.
9. Salomon LJ, Alfirevic Z, Bilardo CM, et al. ISUOG practice guidelines: performance of first-trimester fetal ultrasound scan. Ultrasound Obstet Gynecol. 2013;41(1):102–13. https://doi.org/10.1002/uog.12342.
10. Guariglia L, Rosati P. Transvaginal sonographic detection of embryonic-fetal abnormalities in early pregnancy. Obstet Gynecol. 2000;96(3):328–32. http://www.ncbi.nlm.nih.gov/pubmed/10960620.
11. Iliescu D, Tudorache S, Comanescu A, et al. Improved detection rate of structural abnormalities in the first trimester using an extended examination protocol. Ultrasound Obstet Gynecol. 2013;42(3):300–9. https://doi.org/10.1002/uog.12489.
12. Bromley B, Shipp TD, Lyons J, Navathe RS, Groszmann Y, Benacerraf BR. Detection of fetal structural anomalies in a basic first-trimester screening program for aneuploidy. J Ultrasound Med. 2014;33(10):1737–45. https://doi.org/10.7863/ultra.33.10.1737.
13. Bronshtein M, Solt I, Blumenfeld Z. [The advantages of early midtrimester targeted fetal systematic organ screening for the detection of fetal anomalies—will a global change start in Israel?]. Harefuah. 2014;153(6):320–324, 368. http://www.ncbi.nlm.nih.gov/pubmed/25095602.
14. Becker R, Wegner RD. Detailed screening for fetal anomalies and cardiac defects at the 11-13-week scan. Ultrasound Obstet Gynecol. 2006;27(6):613–8. https://doi.org/10.1002/uog.2709.
15. Lombardi CM, Bellotti M, Fesslova V, Cappellini A. Fetal echocardiography at the time of the nuchal translucency scan. Ultrasound Obstet Gynecol. 2007;29(3):249–57. https://doi.org/10.1002/uog.3948.
16. Persico N, Moratalla J, Lombardi CM, Zidere V, Allan L, Nicolaides KH. Fetal echocardiography at 11-13 weeks by transabdominal high-frequency ultrasound. Ultrasound Obstet Gynecol. 2011;37(3):296–301. https://doi.org/10.1002/uog.8934.
17. Vinals F, Ascenzo R, Naveas R, Huggon I, Giuliano A. Fetal echocardiography at 11 + 0 to 13 + 6 weeks using four-dimensional spatiotemporal image correlation telemedicine via an Internet link: a pilot study. Ultrasound Obstet Gynecol. 2008;31(6):633–8. https://doi.org/10.1002/uog.5350.
18. Bennasar M, Martinez JM, Olivella A, et al. Feasibility and accuracy of fetal echocardiography using four-dimensional spatiotemporal image correlation technology before 16 weeks' gestation. Ultrasound Obstet Gynecol. 2009;33(6):645–51. https://doi.org/10.1002/uog.6374.
19. Votino C, Cos T, Abu-Rustum R, et al. Use of spatiotemporal image correlation at 11-14 weeks' gestation. Ultrasound Obstet Gynecol. 2013;42(6):669–78. https://doi.org/10.1002/uog.12548.
20. Espinoza J, Lee W, Vinals F, et al. Collaborative study of 4-dimensional fetal echocardiography in the first trimester of pregnancy. J Ultrasound Med. 2014;33(6):1079–84. https://doi.org/10.7863/ultra.33.6.1079.
21. Pooh RK, Kurjak A. Novel application of three-dimensional HDlive imaging in prenatal diagnosis from the first trimester. J Perinat Med. 2014; https://doi.org/10.1515/jpm-2014-0157.
22. Castro PT, Werner H, Araujo JE. First-trimester diagnosis of conjoined twins in a multifetal pregnancy after assisted reproduction technique using HDlive rendering. J Ultrasound. 2017;20(1):85–6. https://doi.org/10.1007/s40477-016-0235-0.
23. Popovici R, Pristavu A, Sava A. Three dimensional ultrasound and hdlive technology as possible tools in teaching embryology. Clin Anat. 2017;30(7):953–7. https://doi.org/10.1002/ca.22963.
24. Hata T, Koyanagi A, Kawahara T, et al. HDlive Flow Silhouette with spatiotemporal image correlation for assessment of fetal cardiac structures at 12 to 14 + 6 weeks of gestation. J Perinat Med. 2022;50(3):313–8. https://doi.org/10.1515/jpm-2021-0252.
25. Nicolaides KH, Azar G, Byrne D, Mansur C, Marks K. Fetal nuchal translucency: ultrasound screening for chromosomal defects in first trimester of pregnancy. BMJ. 1992;304(6831):867–9. https://doi.org/10.1136/bmj.304.6831.867.
26. Goldstein I, Weizman B, Nizar K, Weiner Z. The nuchal translucency examination leading to early diagnosis of structural fetal anomalies. Early Hum Dev. 2014;90(2):87–91. https://doi.org/10.1016/j.earlhumdev.2013.12.008.
27. Haak MC, van Vugt JM. Echocardiography in early pregnancy: review of literature. J Ultrasound Med. 2003;22(3):271–80. http://www.ncbi.nlm.nih.gov/pubmed/12636327.
28. Bronshtein M, Zimmer EZ. The sonographic approach to the detection of fetal cardiac anomalies in early pregnancy. Ultrasound Obstet Gynecol. 2002;19(4):360–5. https://doi.org/10.1046/j.1469-0705.2002.00682.x.
29. Achiron R, Rotstein Z, Lipitz S, Mashiach S, Hegesh J. First-trimester diagnosis of fetal congenital heart disease by transvaginal ultrasonography. Obstet Gynecol. 1994;84(1):69–72. http://www.ncbi.nlm.nih.gov/pubmed/8008327.
30. Yagel S, Weissman A, Rotstein Z, et al. Congenital heart defects: natural course and in utero development. Circulation. 1997;96(2):550–5. http://www.ncbi.nlm.nih.gov/pubmed/9244224.
31. Timor-Tritsch IE, Farine D, Rosen MG. A close look at early embryonic development with the high-

frequency transvaginal transducer. Am J Obstet Gynecol. 1988;159(3):676–81. http://www.ncbi.nlm.nih.gov/pubmed/3048101.

32. Timor-Tritsch IE, Peisner DB, Raju S. Sonoembryology: an organ-oriented approach using a high-frequency vaginal probe. J Clin Ultrasound. 1990;18(4):286–98. http://www.ncbi.nlm.nih.gov/pubmed/2160995.
33. Takeuchi H. Transvaginal ultrasound in the first trimester of pregnancy. Early Hum Dev. 1992;29(1–3):381–4. http://www.ncbi.nlm.nih.gov/pubmed/1396272.
34. Blaas HG, Eik-Nes SH, Kiserud T, Berg S, Angelsen B, Olstad B. Three-dimensional imaging of the brain cavities in human embryos. Ultrasound Obstet Gynecol. 1995;5(4):228–32. https://doi.org/10.1046/j.1469-0705.1995.05040228.x.
35. Blaas HG, Eik-Nes SH, Berg S, Torp H. In-vivo three-dimensional ultrasound reconstructions of embryos and early fetuses. Lancet. 1998;352(9135):1182–6. https://doi.org/10.1016/S0140-6736(98)03227-9.
36. Blaas HG, Taipale P, Torp H, Eik-Nes SH. Three-dimensional ultrasound volume calculations of human embryos and young fetuses: a study on the volumetry of compound structures and its reproducibility. Ultrasound Obstet Gynecol. 2006;27(6):640–6. https://doi.org/10.1002/uog.2794.
37. Benoit B, Hafner T, Kurjak A, Kupesic S, Bekavac I, Bozek T. Three-dimensional sonoembryology. J Perinat Med. 2002;30(1):63–73. https://doi.org/10.1515/JPM.2002.009.
38. Pooh RK, Pooh KH. The assessment of fetal brain morphology and circulation by transvaginal 3D sonography and power Doppler. J Perinat Med. 2002;30(1):48–56. https://doi.org/10.1515/JPM.2002.007.
39. Zanforlin Filho SM, Araujo Junior E, Guiaraes Filho HA, Pires CR, Nardozza LM, Moron AF. Sonoembryology by three-dimensional ultrasonography: pictorial essay. Arch Gynecol Obstet. 2007;276(2):197–200. https://doi.org/10.1007/s00404-007-0330-8.
40. Kim MS, Jeanty P, Turner C, Benoit B. Three-dimensional sonographic evaluations of embryonic brain development. J Ultrasound Med. 2008;27(1):119–24. http://www.ncbi.nlm.nih.gov/pubmed/18096737.
41. Atanasova D, Markov D, Pavlova E, Markov P, Ivanov S. [Three-dimensional sonoembryology—myth or reality]. Akush Ginekol. 2010;49(6):26–30. http://www.ncbi.nlm.nih.gov/pubmed/21427872.
42. Pooh RK, Shiota K, Kurjak A. Imaging of the human embryo with magnetic resonance imaging microscopy and high-resolution transvaginal 3-dimensional sonography: human embryology in the 21st century. Am J Obstet Gynecol. 2011;204(1):77:e1–16. https://doi.org/10.1016/j.ajog.2010.07.028.
43. Pooh RK. Neurosonoembryology by three-dimensional ultrasound. Semin Fetal Neonatal Med. 2012;17(5):261–8. https://doi.org/10.1016/j.siny.2012.05.008.
44. Bonilla-Musoles F, Raga F, Osborne NG, Blanes J. Use of three-dimensional ultrasonography for the study of normal and pathologic morphology of the human embryo and fetus: preliminary report. J Ultrasound Med. 1995;14(10):757–65. http://www.ncbi.nlm.nih.gov/pubmed/8544243.
45. Blaas HG, Eik-Nes SH. First-trimester diagnosis of fetal malformations. In: Rodeck C, Whittle M, editors. Fetal medicine: basic science and clinical practice. London: Harcourt Brace; 1999. p. 581–97.
46. Blaas HG, Eik-Nes SH, Isaksen CV. The detection of spina bifida before 10 gestational weeks using two- and three-dimensional ultrasound. Ultrasound Obstet Gynecol. 2000;16(1):25–9. https://doi.org/10.1046/j.1469-0705.2000.00149.x.
47. Blaas HG, Eik-Nes SH, Vainio T, Isaksen CV. Alobar holoprosencephaly at 9 weeks gestational age visualized by two- and three-dimensional ultrasound. Ultrasound Obstet Gynecol. 2000;15(1):62–5. https://doi.org/10.1046/j.1469-0705.2000.00005.x.
48. Tonni G, Ventura A, Centini G, De Felice C. First trimester three-dimensional transvaginal imaging of alobar holoprosencephaly associated with proboscis and hypotelorism (ethmocephaly) in a 46, XX fetus. Congenit Anom. 2008;48(1):51–5. https://doi.org/10.1111/j.1741-4520.2007.00171.x.
49. Timor-Tritsch IE, Monteagudo A, Santos R. Three-dimensional inversion rendering in the first- and early second-trimester fetal brain: its use in holoprosencephaly. Ultrasound Obstet Gynecol. 2008;32(6):744–50. https://doi.org/10.1002/uog.6245.
50. Blaas HG, Eik-Nes SH. Sonoembryology and early prenatal diagnosis of neural anomalies. Prenat Diagn. 2009;29(4):312–25. https://doi.org/10.1002/pd.2170.
51. Dane B, Dane C, Aksoy F, Yayla M. Semilobar holoprosencephaly with associated cyclopia and radial aplasia: first trimester diagnosis by means of integrating 2D-3D ultrasound. Arch Gynecol Obstet. 2009;280(4):647–51. https://doi.org/10.1007/s00404-009-0975-6.
52. Bromley B, Shipp TD, Benacerraf BR. Structural anomalies in early embryonic death: a 3-dimensional pictorial essay. J Ultrasound Med. 2010;29(3):445–53. http://www.ncbi.nlm.nih.gov/pubmed/20194939.
53. Blaas HG, Eik-Nes SH, Kiserud T, Hellevik LR. Early development of the hindbrain: a longitudinal ultrasound study from 7 to 12 weeks of gestation. Ultrasound Obstet Gynecol. 1995;5(3):151–60. https://doi.org/10.1046/j.1469-0705.1995.05030151.x.
54. Fleischer A, Rebele E. Transvaginal sonography of early (first trimester) intrauterine pregnancy. In: Fleischer A, Toy E, Manning F, Abramowicz J, Goncalves L, Timor-Tritsch IE, editors. Fleischer's sonography in obstetrics & gynecology. 8th ed. New York: McGraw-Hill; 2018. p. 45–80.
55. Doubilet PM, Benson CB, Bourne T, et al. Diagnostic criteria for nonviable pregnancy early in the first

trimester. N Engl J Med. 2013;369(15):1443–51. https://doi.org/10.1056/NEJMra1302417.
56. O'Rahilly R, Müller F, Wiley I. The embryonic human brain : an atlas of developmental stages. 3rd ed. Hoboken, NJ: Wiley-Liss; 2006.
57. Pooh RK. Sonoembryology by 3D HDlive silhouette ultrasound—what is added by the "see-through fashion"? J Perinat Med. 2016;44(2):139–48. https://doi.org/10.1515/jpm-2016-0008.
58. Yamada S, Samtani RR, Lee ES, et al. Developmental atlas of the early first trimester human embryo. Dev Dyn. 2010;239(6):1585–95. https://doi.org/10.1002/dvdy.22316.
59. Shiraishi N, Katayama A, Nakashima T, et al. Morphology and morphometry of the human embryonic brain: a three-dimensional analysis. NeuroImage. 2015;115:96–103. https://doi.org/10.1016/j.neuroimage.2015.04.044.
60. Pooh RK, Kurjak A. Novel application of three-dimensional HDlive imaging in prenatal diagnosis from the first trimester. J Perinat Med. 2015;43(2):147–58. https://doi.org/10.1515/jpm-2014-0157.
61. O'Rahilly R, Muller F. Developmental stages in human embryos: revised and new measurements. Cells Tissues Organs. 2010;192(2):73–84. https://doi.org/10.1159/000289817.
62. Maymon R, Halperin R, Weinraub Z, Herman A, Schneider D. Three-dimensional transvaginal sonography of conjoined twins at 10 weeks: a case report. Ultrasound Obstet Gynecol. 1998;11(4):292–4. https://doi.org/10.1046/j.1469-0705.1998.11040292.x.
63. Kurjak A, Pooh RK, Merce LT, Carrera JM, Salihagic-Kadic A, Andonotopo W. Structural and functional early human development assessed by three-dimensional and four-dimensional sonography. Fertil Steril. 2005;84(5):1285–99. https://doi.org/10.1016/j.fertnstert.2005.03.084.
64. Forest CP, Goodman D, Hahn RG. Meningomyelocele: early detection using 3-dimensional ultrasound imaging in the family medicine center. J Am Board Fam Med. 2010;23(2):270–2. https://doi.org/10.3122/jabfm.2010.02.090226.
65. Blaas HG. Detection of structural abnormalities in the first trimester using ultrasound. Best Pract Res Clin Obstet Gynaecol. 2014;28(3):341–53. https://doi.org/10.1016/j.bpobgyn.2013.11.004.
66. Quijano FE, Rey MM, Echeverry M, Axt-Fliedner R. Body stalk anomaly in a 9-week pregnancy. Case Rep Obstet Gynecol. 2014;2014:357285. https://doi.org/10.1155/2014/357285.
67. Yang Y, Wang H, Wang Z, Pan X, Chen Y. First trimester diagnosis of body stalk anomaly complicated by ectopia cordis. J Int Med Res. 2020;48(12):300060520980210. https://doi.org/10.1177/0300060520980210.
68. Ramkrishna J, Menezes M, Humnabadkar K, et al. Outcomes following the detection of fetal edema in early pregnancy prior to non-invasive prenatal testing. Prenat Diagn. 2021;41(2):241–7. https://doi.org/10.1002/pd.5847.
69. Cafici D, Sepulveda W. First-trimester echogenic amniotic fluid in the acrania-anencephaly sequence. J Ultrasound Med. 2003;22(10):1075–9; quiz 1080–1. https://doi.org/10.7863/jum.2003.22.10.1075.
70. Timor-Tritsch IE, Greenebaum E, Monteagudo A, Baxi L. Exencephaly-anencephaly sequence: proof by ultrasound imaging and amniotic fluid cytology. J Matern Fetal Med. 1996;5(4):182–5. https://doi.org/10.1002/(SICI)1520-6661(199607/08)5:4<182::AID-MFM4>3.0.CO;2-G.
71. Sepulveda W, Dezerega V, Be C. First-trimester sonographic diagnosis of holoprosencephaly: value of the "butterfly" sign. J Ultrasound Med. 2004;23(6):761–5; quiz 766–7. https://doi.org/10.7863/jum.2004.23.6.761.
72. Hashimoto K, Shimizu T, Fukuda M, et al. Pregnancy outcome of embryonic/fetal pleural effusion in the first trimester. J Ultrasound Med. 2003;22(5):501–5. https://doi.org/10.7863/jum.2003.22.5.501.
73. Harris RD, Couto C, Karpovsky C, Porter MM, Ouhilal S. The chorionic bump: a first-trimester pregnancy sonographic finding associated with a guarded prognosis. J Ultrasound Med. 2006;25(6):757–63. https://doi.org/10.7863/jum.2006.25.6.757.
74. Arleo EK, Dunning A, Troiano RN. Chorionic bump in pregnant patients and associated live birth rate: a systematic review and meta-analysis. J Ultrasound Med. 2015;34(4):553–7. https://doi.org/10.7863/ultra.34.4.553.
75. Baalmann CG, Galgano SJ, Pietryga JA, Novak L, Robbin ML. A case of a chorionic bump: new sonographic-histopathologic findings with review of the literature. J Ultrasound Med. 2017;36(9):1968–70. https://doi.org/10.1002/jum.14240.
76. D'Antonio F, Khalil A, Mantovani E, Thilaganathan B. Southwest Thames Obstetric Research C. Embryonic growth discordance and early fetal loss: the STORK multiple pregnancy cohort and systematic review. Hum Reprod. 2013;28(10):2621–7. https://doi.org/10.1093/humrep/det277.
77. Snijders RJ, Noble P, Sebire N, Souka A, Nicolaides KH. UK multicentre project on assessment of risk of trisomy 21 by maternal age and fetal nuchal-translucency thickness at 10-14 weeks of gestation. Fetal Medicine Foundation First Trimester Screening Group. Lancet. 1998;352(9125):343–6. https://doi.org/10.1016/s0140-6736(97)11280-6.
78. Souka AP, Snijders RJ, Novakov A, Soares W, Nicolaides KH. Defects and syndromes in chromosomally normal fetuses with increased nuchal translucency thickness at 10-14 weeks of gestation. Ultrasound Obstet Gynecol. 1998;11(6):391–400. https://doi.org/10.1046/j.1469-0705.1998.11060391.x.
79. Hyett J, Perdu M, Sharland G, Snijders R, Nicolaides KH. Using fetal nuchal translucency to screen for major congenital cardiac defects at 10-14 weeks

of gestation: population based cohort study. BMJ. 1999;318(7176):81–5. https://doi.org/10.1136/bmj.318.7176.81.

80. Simula N, Brown R, Butt K, et al. Committee Opinion No. 418: The complete 11-14 week prenatal sonographic examination. J Obstet Gynaecol Can. 2021;43(8):1013–21. https://doi.org/10.1016/j.jogc.2021.05.004.
81. Karim JN, Roberts NW, Salomon LJ, Papageorghiou AT. Systematic review of first-trimester ultrasound screening for detection of fetal structural anomalies and factors that affect screening performance. Ultrasound Obstet Gynecol. 2017;50(4):429–41. https://doi.org/10.1002/uog.17246.
82. Syngelaki A, Hammami A, Bower S, Zidere V, Akolekar R, Nicolaides KH. Diagnosis of fetal non-chromosomal abnormalities on routine ultrasound examination at 11-13 weeks' gestation. Ultrasound Obstet Gynecol. 2019;54(4):468–76. https://doi.org/10.1002/uog.20844.
83. Dias T, Arcangeli T, Bhide A, Napolitano R, Mahsud-Dornan S, Thilaganathan B. First-trimester ultrasound determination of chorionicity in twin pregnancy. Ultrasound Obstet Gynecol. 2011;38(5):530–2. https://doi.org/10.1002/uog.8956.
84. Rolnik DL, Wright D, Poon LC, et al. Aspirin versus placebo in pregnancies at high risk for preterm preeclampsia. N Engl J Med. 2017;377(7):613–22. https://doi.org/10.1056/NEJMoa1704559.
85. Yagel S, Achiron R, Ron M, Revel A, Anteby E. Transvaginal ultrasonography at early pregnancy cannot be used alone for targeted organ ultrasonographic examination in a high-risk population. Am J Obstet Gynecol. 1995;172(3):971–5. http://www.ncbi.nlm.nih.gov/pubmed/7892892.
86. Hernadi L, Torocsik M. Screening for fetal anomalies in the 12th week of pregnancy by transvaginal sonography in an unselected population. Prenat Diagn. 1997;17(8):753–9. http://www.ncbi.nlm.nih.gov/pubmed/9267899.
87. D'Ottavio G, Mandruzzato G, Meir YJ, et al. Comparisons of first and second trimester screening for fetal anomalies. Ann N Y Acad Sci. 1998;847:200–9. http://www.ncbi.nlm.nih.gov/pubmed/9668713.
88. Comas Gabriel C, Galindo A, Martinez JM, et al. Early prenatal diagnosis of major cardiac anomalies in a high-risk population. Prenat Diagn. 2002;22(7):586–93. https://doi.org/10.1002/pd.372.
89. Chaoui R, Benoit B, Mitkowska-Wozniak H, Heling KS, Nicolaides KH. Assessment of intracranial translucency (IT) in the detection of spina bifida at the 11-13-week scan. Ultrasound Obstet Gynecol. 2009;34(3):249–52. https://doi.org/10.1002/uog.7329.
90. Volpe N, Dall'Asta A, Di Pasquo E, Frusca T, Ghi T. First-trimester fetal neurosonography: technique and diagnostic potential. Ultrasound Obstet Gynecol. 2021;57(2):204–14. https://doi.org/10.1002/uog.23149.
91. Sepulveda W, Wong AE. First trimester screening for holoprosencephaly with choroid plexus morphology ('butterfly' sign) and biparietal diameter. Prenat Diagn. 2013;33(13):1233–7. https://doi.org/10.1002/pd.4235.
92. Van den Hof MC, Nicolaides KH, Campbell J, Campbell S. Evaluation of the lemon and banana signs in one hundred thirty fetuses with open spina bifida. Am J Obstet Gynecol. 1990;162(2):322–7. https://doi.org/10.1016/0002-9378(90)90378-k.
93. Andronikou S, Wieselthaler N, Fieggen AG. Cervical spina bifida cystica: MRI differentiation of the subtypes in children. Childs Nerv Syst. 2006;22(4):379–84. https://doi.org/10.1007/s00381-005-1165-x.
94. Chaoui R, Orosz G, Heling KS, Sarut-Lopez A, Nicolaides KH. Maxillary gap at 11-13 weeks' gestation: marker of cleft lip and palate. Ultrasound Obstet Gynecol. 2015;46(6):665–9. https://doi.org/10.1002/uog.15675.
95. Pooh KH, Nakamura CT, Kawakami K, Inoue K. Low-set ear in fetuses with CRL 45-84mm detected by 3D ultrasound. Ultrasound Obstet Gynecol. 2014;44(S1):79(Abstract) (in English). https://doi.org/10.1002/uog.13691.
96. Chen Q, Zhao Y, Qian Y, Lu C, Shen G, Dai J. A genetic-phenotypic classification for syndromic micrognathia. J Hum Genet. 2019;64(9):875–83. https://doi.org/10.1038/s10038-019-0630-4.
97. Singh DJ, Bartlett SP. Congenital mandibular hypoplasia: analysis and classification. J Craniofac Surg. 2005;16(2):291–300. https://doi.org/10.1097/00001665-200503000-00017.
98. Sepulveda W, Wong AE, Vinals F, Andreeva E, Adzehova N, Martinez-Ten P. Absent mandibular gap in the retronasal triangle view: a clue to the diagnosis of micrognathia in the first trimester. Ultrasound Obstet Gynecol. 2012;39(2):152–6. https://doi.org/10.1002/uog.10121.
99. Sepulveda W, Wong AE, Martinez-Ten P, Perez-Pedregosa J. Retronasal triangle: a sonographic landmark for the screening of cleft palate in the first trimester. Ultrasound Obstet Gynecol. 2010;35(1):7–13. https://doi.org/10.1002/uog.7484.
100. Karim JN, Bradburn E, Roberts N, Papageorghiou AT, ACCEPTS Study. First-trimester ultrasound detection of fetal heart anomalies: systematic review and meta-analysis. Ultrasound Obstet Gynecol. 2022;59(1):11–25. https://doi.org/10.1002/uog.23740.
101. Gindes L, Matsui H, Achiron R, Mohun T, Ho SY, Gardiner H. Comparison of ex-vivo high-resolution episcopic microscopy with in-vivo four-dimensional high-resolution transvaginal sonography of the first-trimester fetal heart. Ultrasound Obstet Gynecol. 2012;39(2):196–202. https://doi.org/10.1002/uog.9068.
102. Lima AI, Araujo Junior E, Martins WP, Nardozza LM, Moron AF, Pares DB. Assessment of the fetal heart at 12-14 weeks of pregnancy using B-mode, color Doppler, and spatiotemporal image correla-

tion via abdominal and vaginal ultrasonography. Pediatr Cardiol. 2013;34(7):1577–82. https://doi.org/10.1007/s00246-013-0686-4.

103. Tudorache S, Cara M, Iliescu DG, Novac L, Cernea N. First trimester two- and four-dimensional cardiac scan: intra- and interobserver agreement, comparison between methods and benefits of color Doppler technique. Ultrasound Obstet Gynecol. 2013;42(6):659–68. https://doi.org/10.1002/uog.12459.
104. Turan S, Turan OM, Desai A, Harman CR, Baschat AA. First-trimester fetal cardiac examination using spatiotemporal image correlation, tomographic ultrasound and color Doppler imaging for the diagnosis of complex congenital heart disease in high-risk patients. Ultrasound Obstet Gynecol. 2014;44(5):562–7. https://doi.org/10.1002/uog.13341.
105. Parada Villavicencio C, Adam SZ, Nikolaidis P, Yaghmai V, Miller FH. Imaging of the urachus: anomalies, complications, and mimics. Radiographics. 2016;36(7):2049–63. https://doi.org/10.1148/rg.2016160062.

Multiple Gestations: Multiple Headaches

15

Jacques S. Abramowicz

Introduction

Multiple gestations are often a surprise. When diagnosed, all involved become concerned, future parents and caregivers alike, which explains the title of this chapter. Although the general fertility rate declined for nearly all races as did the twin, triplet, and higher order multiple birth rates in 2019 compared with 2018 [1], the incidence of multiple births has risen in the last 30 years and comprise today 3% of all live births in the United States [2] and in the United Kingdom [3]. This rise is principally due to the introduction and increasing use of assisted reproduction techniques (ART), specifically in vitro fertilization (IVF) with almost a quarter of these procedures resulting in multiple gestations (mostly twins), when successful [4, 5]. Another factor is the shift in the women age demographics with maternal advancing age an etiologic factor both by the increased rate of spontaneous multiple gestations with one-fourth to one-third of the increase in multiple gestations explained solely by the increase in maternal age [6], as well as the need for ART in this population [7]. Twins have, traditionally been classified as dizygotic (DZ), commonly referred to as "non-identical" or "fraternal" or monozygotic (MZ), also called "identical." Genetics have provided new insights that seem to revolutionize our thinking of the twinning phenomenon: there are non-identical MZ twins, there are intermediate forms rather than pure di- or monozygosity and MZ twins may not happen by chance alone [8, 9]. An unchanged fact over the years is that these multiple pregnancies are at increased risks of complications, both maternal and fetal/neonatal [10]. Maternal morbidity—such as miscarriages [11], diabetes [12], hypertensive disorders [13], including preeclampsia [14], preterm labor [15], preterm premature rupture of membranes [16], placental abruption, operative delivery [17], and postpartum hemorrhage [18]—and mortality are greatly increased [19]. The fetuses, in turn, have a much higher rate of spontaneous abortions, genetic anomalies, growth restriction, stillbirth, preterm deliveries (50% of twins, with 67% of multiple pregnancies with gestational age [GA] below 28 weeks compared to 26% of single pregnancies [20]), as well as specific complications in the case of monochorionicity, such as twin-to-twin transfusion syndrome [21]. While multiple pregnancies result in 3% of live births, they encompass 10–15% of perinatal death [22] and a much higher prevalence of complications [23]. Among babies born with low birth weight, 23% are twins. Up to 25% of most NICU census are the results of multiple gestations, and the expenditure for twins is six

J. S. Abramowicz (✉)
Department of Obstetrics and Gynecology, University of Chicago, Chicago, IL, USA
e-mail: jabramowicz@bsd.uchicago.edu

© The Author(s), under exclusive license to Springer Nature Switzerland AG 2023
J. S. Abramowicz, R. E. Longman (eds.), *First-Trimester Ultrasound*,
https://doi.org/10.1007/978-3-031-24133-8_15

times that for a singleton newborn [24, 25]. This, naturally, is even higher for higher degree multiple gestations [26, 27]. In an analysis of 11,061,599 singleton, 297,622 twin, and 15,375 triplet gestations, the prospective risk of fetal death at 24 weeks was 0.28 per 1000, 0.92 per 1000, and 1.30 per 1000, respectively [27]. Furthermore, 4.6–10% of all cerebral palsy cases occur in twins which is more than four times the observed frequency in the general population [28]. The rate of multiple birth in the populations increased from 1.9% in 1980 to 2.4% in 1990, and the proportion of multiples among CP infants increased from 4.6% in 1976 to 10% in 1990. Multiples have a four times higher rate of CP than singletons (7.6 vs. 1.8 per 1000 live births, relative risk [RR] 4.36; 95% confidence interval [CI] 3.76–4.97) overall [25, 29]. It is interesting to note that the risk is not related to preterm birth only. A threefold increase in CP is found in neonates from multiple versus singleton pregnancies [30]. These complications become even more prevalent in higher order multiple gestations such as triplets, quadruplets, or higher [22, 31].

Embryology

A major reason for the recent increase in multiple pregnancies is ART and the use of fertility-enhancing treatments. In the United States, twin births increased from about 1/50 infants in 1980 to 1/30 infants in 2009 [32]. Similar trends have been described in multiple reports from other parts of the world [33]. The two commonly cited reasons are that ovulation inducing agents increase the likelihood of more than one ovulation (Fig. 15.1) and multiple embryos are transferred in in vitro fertilization (IVF), all resulting in DZ twins [34]. This has led various societies, involved with reproductive endocrinology and infertility, to regularize the optimal number of embryos to transfer [35]. It appears, however, that the risk of embryo cleavage, resulting in monozygotic twins, is also increased in IVF [36, 37]. Genetic factors, rather than the procedure itself, are suspected to be the basis for this occurrence [37].

Embryological development of the fetus is addressed in detail in Chap. 2 of this book. Multiple gestations can be the result of a single

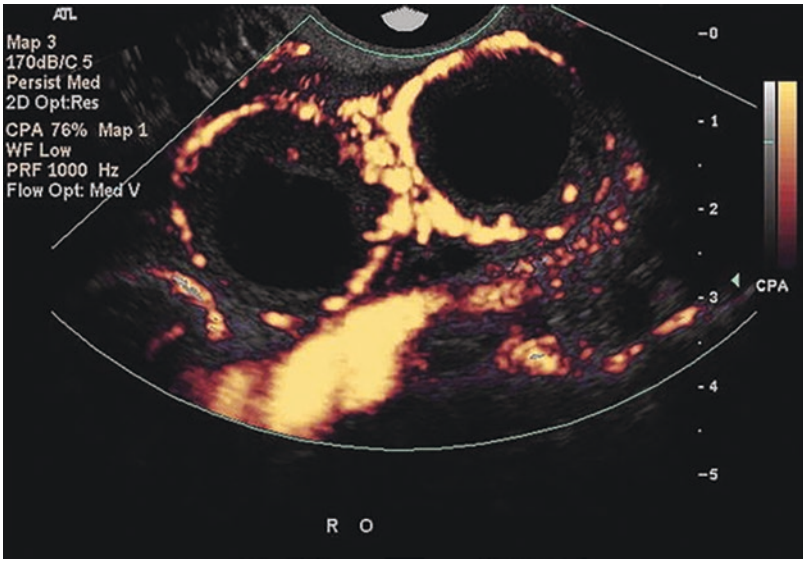

Fig. 15.1 Multiple corpora lutei. This is indicative of multiple follicular ovulation. Multiple corpora lutei can be a sign of a dizygotic pregnancy; however, it is also frequently seen with the use of fertility-enhancing medications

oocyte being fertilized by a single spermatozoon with splitting of the resulting zygote at various times (monozygotic [MZ] twins) or multiple oocytes (two or more), each fertilized by its own spermatozoon, resulting in two or more zygotes (dizygotic twins [DZ], or higher degree multiples). Dizygotic twins are more common (70%) and are also known as “fraternal twins” since, genetically, the two zygotes that resulted are as different as two regular siblings (e.g., opposite genders). The incidence of DZ twins increases with maternal age, parity, ovulation induction, and they are more common in some families, with mothers of DZ twins reporting significantly more female family members with DZ twins than mothers of monozygotic twins. Maternal factors such as genetic/family history, advanced age, and increased parity are known to increase the risk of DZ twins [38, 39]. New findings indicate some women may have a genetic predilection to conceive twins, specifically insertion/deletions and missense alterations in the growth differentiation factor 9 (GDF9) sequence in mothers of twins [40, 41]. Rates of DZ twins have a geographical variation with some countries/continents such as South and South East Asia as well as Latin America exhibiting low prevalence, e.g., six to nine twin sets per thousand births [42], and rates being much more common in some ethnicities, such as in Nigeria, where the Yoruba have the highest rate of twinning in the world, at 45–50 twin sets per 1000 live births, possibly due to high consumption of a specific type of yam containing a natural phytoestrogen [43]. Dizygotic twins will always be dichorionic diamniotic (DCDA). Monozygotic twins are known as “identical twins” since they originate from a single zygote and are thus genetically identical (with exceptions, see below). They comprise 30% of twins and their incidence is sporadic, with no family predilection and with a rate similar throughout the world (1:250 pregnancies). In MZ twins, the time of splitting will determine placentation, chorionicity and amnionicity (see below, section “Placentation”). The prevalence of females compared to males increases progressively from a relatively equal prevalence in singletons to a clear preponderance in conjoined twins.

Diagnosis

Before the development of ultrasound, twins were often diagnosed at birth, after the delivery of one neonate. In fact, a multiple gestation was clinically suspected in only 25–50%. In the famous Routine Antenatal Diagnostic Imaging with Ultrasound Study (RADIUS), 38% of twins were recognized after 26 weeks and 13% were not diagnosed until delivery [44]. In the Helsinki ultrasound trial, 25% twins were not recognized until 21 weeks [45]. These two studies, however, were not about first trimester ultrasound but rather about scanning at mid-trimester (16–24 weeks). The diagnosis should be obtainable, with ultrasound, from very early in gestation. When ultrasound is performed for an indication (e.g., the uterus is larger than expected), the accuracy is about 75%. When ultrasound is performed routinely, this climbs to 90% [46], with better outcomes in women known to carry multiple gestations [47]. The first ultrasound indication of a multiple gestation may be the presence of multiple corpora lutei (see Fig. 15.1). While routine ultrasound is still not the official rule, as recommended in low risk pregnancies by the American College of Obstetricians and Gynecologists (ACOG), the American College of Radiology (ACR), or the American Institute of Ultrasound in Medicine (AIUM), the advantages of a policy of routine scanning in the first trimester include, among others, the early detection of multiple gestations, allowing for early determination of chorionicity and amnionicity [48, 49]. Another clear advantage is accurate assessment of gestational age (GA). When ultrasound is ordered “to date” the pregnancy, in cases of unknown or unclear last menstrual period, fetal biometry is used to determine GA. In twins, however, there may be growth discordancy, for instance, with one twin measuring 1 week more than the other. The published literature does not provide evidence-based data on whether dating should be based on the smaller twin, the larger or an average. It is important, however, to avoid missing early growth restriction in one twin, thus the majority will date the pregnancy based on biometry of the larger twin [50] . An important consideration is whether growth nomograms for singleton gestations can be used for twins or higher order gestations [51, 52]. It appears that during the first trimester, there are no major differences in fetal biometry between singleton or multiple pregnancies among fetuses with no abnormalities [50]. Hence, crown-rump -length (CRL) curves published for singletons may be used in the assessment of twins and triplets [53, 54]. Furthermore, there is no difference in placental mass between singletons, monochorionic (MC) and dichorionic (DC) twins and trichorionic triplets between 11 and 13 6/7 weeks [55]. Growth curves for singletons may be used in the assessment of biometry in twins until approximately 34 weeks GA [56]. For triplets, the upper limit may be lower, e.g., 25 weeks [57].

Placentation

Determining the number of chorionic sacs is important because prognosis is much better in DC than MC twin pregnancies [58]. Mortality (stillbirth, perinatal and neonatal death) is three to four times higher in MC twins [59–64]. The major reason is the presence of vascular anastomoses between the two placental circulations [65–68]. They are at risk of twin-to-twin transfusion syndrome or TTTS [69–72], twin anemia polycythemia syndrome or TAPS [73–75], twin reversed arterial perfusion or TRAP syndrome [76–78], unequal placental sharing with discordant twin growth or selective intrauterine fetal growth restriction [79], and, if also monoamniotic (MA), cord entanglement [80–82] with the added risk of demise of one twin and embolization of thromboplastin from the demised fetus to the healthy twin [83]. Additionally, there is the risk of conjoining, an event occurring in 1/50,000 births [84] and can be diagnosed as early as 8 weeks gestation [85]. Mortality is 8–10% in DCDA, 25% in MCDA, 50–60% in MCMA, and perhaps 90% in conjoined twins [86–88] with fetal loss under 24 weeks, 1.8% in DC twins, and 12% in MC twins [58].

As described above, approximately 70% of twins delivered and conceived naturally, result from the fertilization of two independent oocytes, i.e., dizygotic (DZ) twins; the remaining 30% are the result of the division of a single zygote, i.e., monozygotic (MZ) twins. Interestingly, the rate of MZ twins is three times higher in pregnancies conceived with the help of ART, compared to spontaneous conceptions [89, 90]. If the division of the zygote occurs at the two-cells stage (0–4 days), before the morula stage, this results in two morulas, two blastocysts, two chorions, and two amnions (dichorionic diamniotic or DCDA placentation), about one-third of monozygotic twins. In about two-thirds of monozygotic twins, the split occurs after the morula stage (4–7 days) and the single morula split will result in MCDA placentation. If it occurs at 7–14 days, the embryonic disc was already formed and the result will be two embryos in the same sac (MCMA). If after day 13–14, conjoined twins will result. A combination of both may also exist, when one of two dizygotic twins splits, in a monozygotic fashion, resulting, in various combinations of chorionicity and amnionicity. Placental examination will provide important information on placental factors leading to the twinning process in complicated twin pregnancies [91], although, this is, naturally a post-delivery assessment and not a first trimester ultrasound examination.

Ultrasound plays an important, if not the major, role in the diagnosis of multiple gestations and, in particular, the determination of chorionicity and amnionicity early in pregnancy [48, 92–104]. Various algorithms themes can be used, based on what is the known (or assumed) gestational age [105–107]. With appropriate training, reproducibility of the results has been shown to be excellent [108]. Both the chorionicity and amnionicity should always be recorded and reported when performing early ultrasound scans in multiple pregnancies [109].

Diagnosis of Chorionicity and Amnionicity

From 4 to 6 weeks, the number of sacs determine the chorionicity: two sacs means twins are DC (Fig. 15.2).

From 6 to 8 weeks, if the number of sacs is the same as the number of yolk sacs and the number of fetuses, this is a DCDA pregnancy. If the pregnancy is MC, two fetuses will be visualized within the sac and the number of yolk sacs will help distinguish between DA and MA placentation. Observing two yolk sacs or two clear amniotic cavities (Fig. 15.3) allows one to make the diagnosis of diamniotic twins [103]. Visualization of two fetal poles with a single yolk sac is diagnostic of monoamnionicity (Fig. 15.4). Once the membranes can be visualized, ultrasound imaging can distinguish between MC and DC twin pregnancies with more than 90% accuracy [104]. The "twin peak," also called lambda sign, at the level of the attachment of the chorionic membranes to the placenta is formed by projection of the trophoblast from a fused dichorionic placenta between the layers of the membranes and indicates a DC twin pregnancy (Fig. 15.5), with 100% accuracy, while the "T sign" at the site where the thin intertwin membrane composed of two amnions with no chorions leaves the placenta at a 90° angle (Fig. 15.6) indicates a monochorionic diamniotic (MCDA) twin pregnancy [110, 111]. In a study of 55 cases, sensitivity of the twin-peak sign for dichorionicity was 94%, specificity 88%, positive predictive value 97%, and negative predictive value 78% [112]. In another study of 506 DC and 154 MC twin pregnancies, between 11 and 14 weeks of gestation, use of the twin-peak and T signs and the number of placentas had sensitivity of 100% specificity of 99.8% for monochorionicity, with only one DC pregnancy incorrectly assigned as MC [113].

From 8 to 14 weeks, the number of placental masses and/or the lambda or T sign can be assessed, as above, but at that stage, membrane thickness can also be analyzed [98, 114]. A dichorionic membrane is typically well defined and easy to visualize with ultrasound. It consists of four layers (i.e., two layers of both amnion and chorion), and its width will be greater than 2 mm (Fig. 15.7). The presence of a thick dividing membrane indicated a dichorionic diamniotic gestation in 38 (90%) of 42 cases in which it

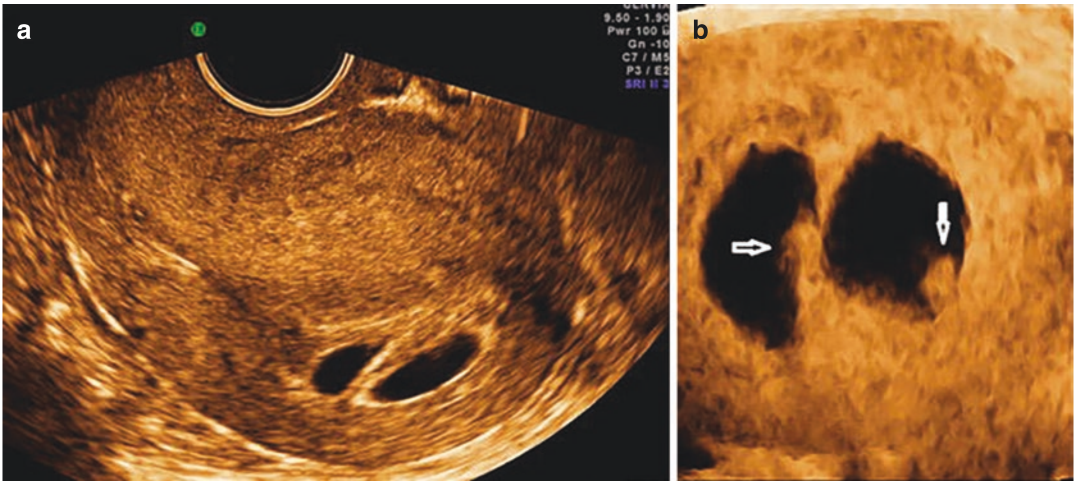

Fig. 15.2 Dichorionic diamniotic twins, 5 weeks. (**a**) In this retroverted uterus, two separate sacs are distinguished at 5 weeks. (**b**) 3D image a few days later demonstrates the presence of two fetal poles (arrows)

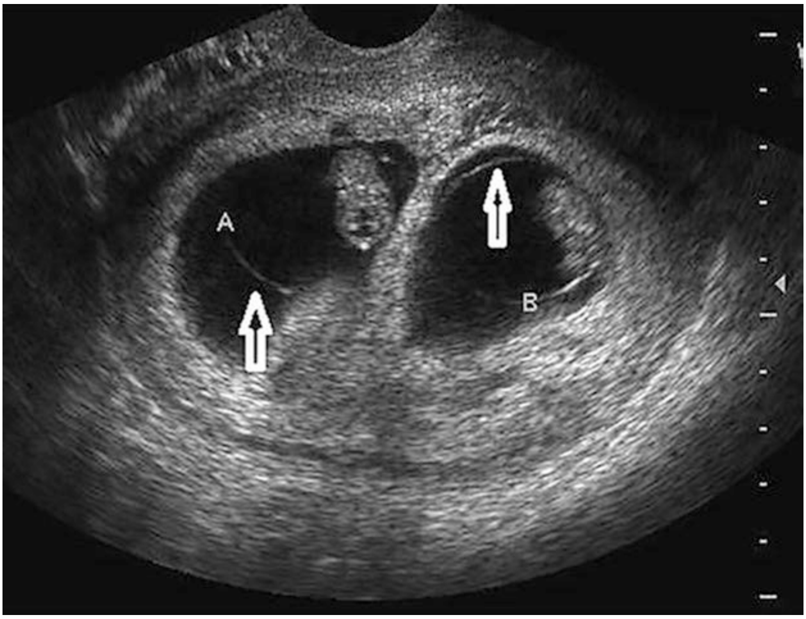

Fig. 15.3 Diamniotic twins. Two clearly separate amniotic cavities are distinguished. Amniotic membranes are marked by arrows

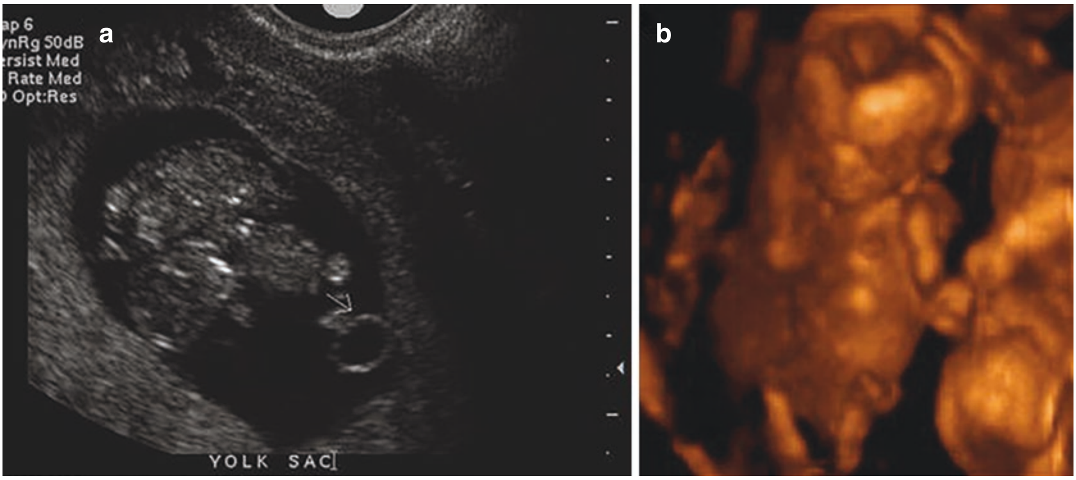

Fig. 15.4 Monoamniotic twins, 6 weeks. (**a**) Two fetal poles and only one yolk sac are demonstrated (arrow). (**b**) At 10 weeks, three-dimensional ultrasound demonstrates both twins in a single sac, with no intervening membrane

was identified [115]. The number of dividing membranes can also, occasionally, be counted: four means DCDA (Fig. 15.8), two means MCDA [106].

For women presenting **after 14 weeks 0 days**, all of the above features should be used and, in addition, evaluation of fetal gender, since discordancy would, obviously, signify dizygosity. In the second and third trimesters, membrane thickness is much less useful [114].

If transabdominal views are poor because of elevated BMI or retroverted uterus, transvaginal ultrasound is recommended. In a study by Bora and colleagues [116], chorionicity and amnionicity were documented in 67 viable twin pregnancies at both 7–9 and 11–14 weeks' gestation.

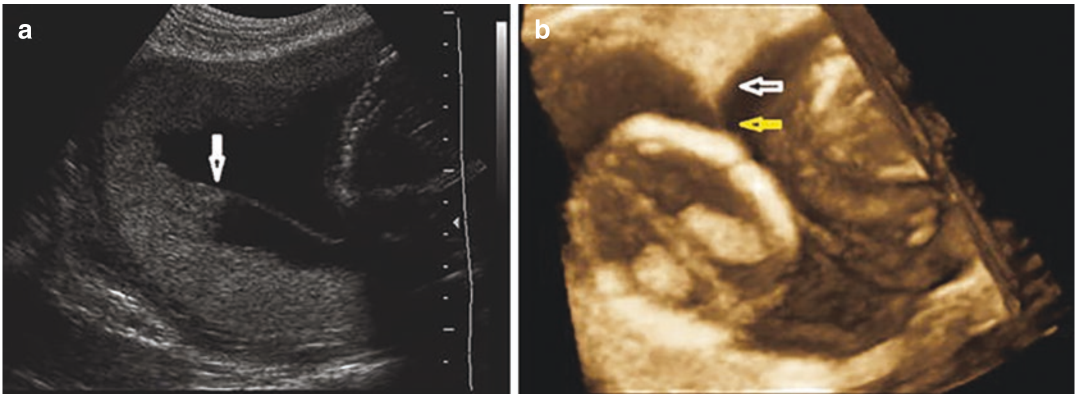

Fig. 15.5 Twin-peak or lambda sign. Two-dimensional B-mode (**a**) and three-dimensional (**b**) ultrasound of a dichorionic diamniotic pregnancy. The white arrows point to where the "peak" is formed from the two placentas abutting. The intertwin membrane (yellow arrow) appears thin. If the lambda sign was absent, accurately determination of chorionicity would be challenging

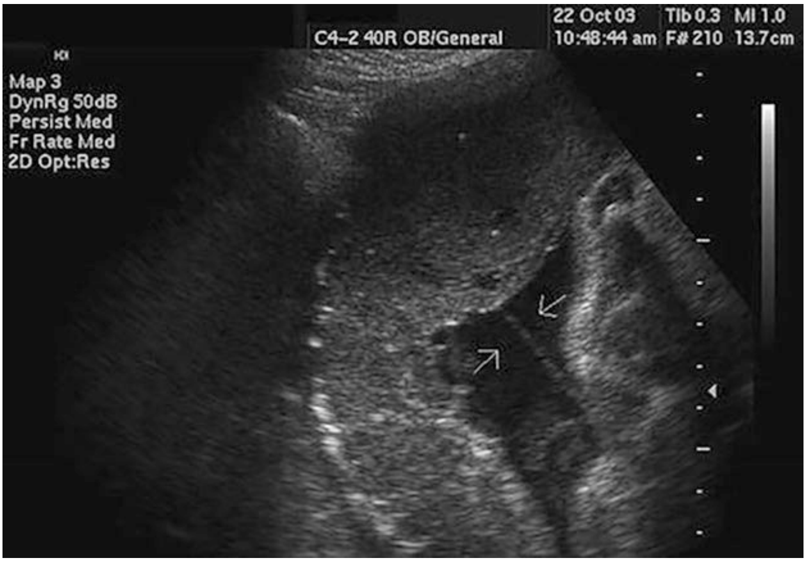

Fig. 15.6 T sign. The arrows point to a thin membrane, connecting to the placenta at a right angle, forming the letter T. This is diagnostic for a monochorionic placentation

There was agreement in the chorionicity and amnionicity reported at each of the two scans in 65 out of 67 (97%) cases. Of the DCDA pregnancies reported at 7–9 weeks, 53 out of 54 (98%) were confirmed at the 11- to 14-week scan and 1 (2%) was found to be MCDA. At birth, however, these twins were of different sex, confirming DCDA twins as initially diagnosed at 7–9 weeks. Of the 12 pregnancies diagnosed as MCDA at 7–9 weeks, all were found to be MCDA at the 11- to 14-week scan. In the (rare) case when chorionicity cannot be established, management should be based on the assumption that the gestation is monochorionic, until proved otherwise. After ultrasound diagnosis and characterization of twins, the risk of spontaneous loss of both fetuses before 22 weeks of gestation is significantly higher in MC than in DC pregnancies, and is sig-

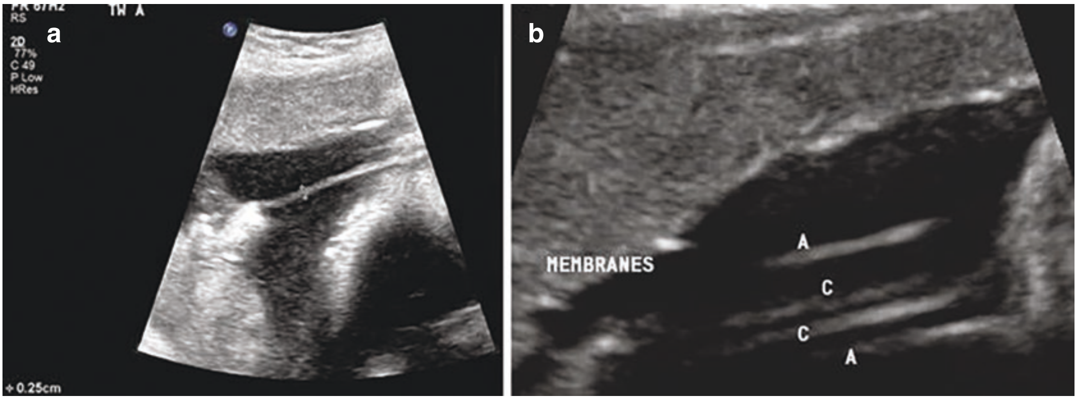

Fig. 15.7 Dichorionic diamniotic membrane. (**a**) Membrane measures more than 2 mm in width. (**b**) Four layers (two chorionic and two amniotic membranes) can be visualized

Fig. 15.8 Monochorionic diamniotic membrane. The membrane is thin (1.4 mm) and elusive

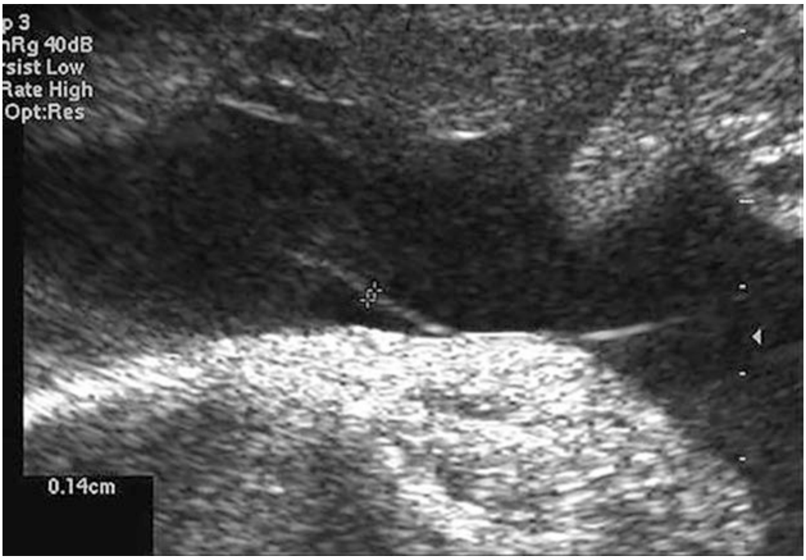

nificantly higher in MCMA pregnancies than in MCDA pregnancies [117]. Hence, no ultrasound report on twins should be considered finalized without details of the type of placentation. Another sign has been described in triplet pregnancy: the ipsilon zone, the junction of the three interfetal membranes with 100% success in determining chorionicity in 19 sets of triplets [118].

Another important role for ultrasound in multiple gestation is observation of the umbilical cord insertions in the placenta. Abnormal cord insertions such as marginal and velamentous insertions are much more frequent in multiple gestation (Fig. 15.9). In addition, single umbilical artery is also much more frequent in twins [119, 120].

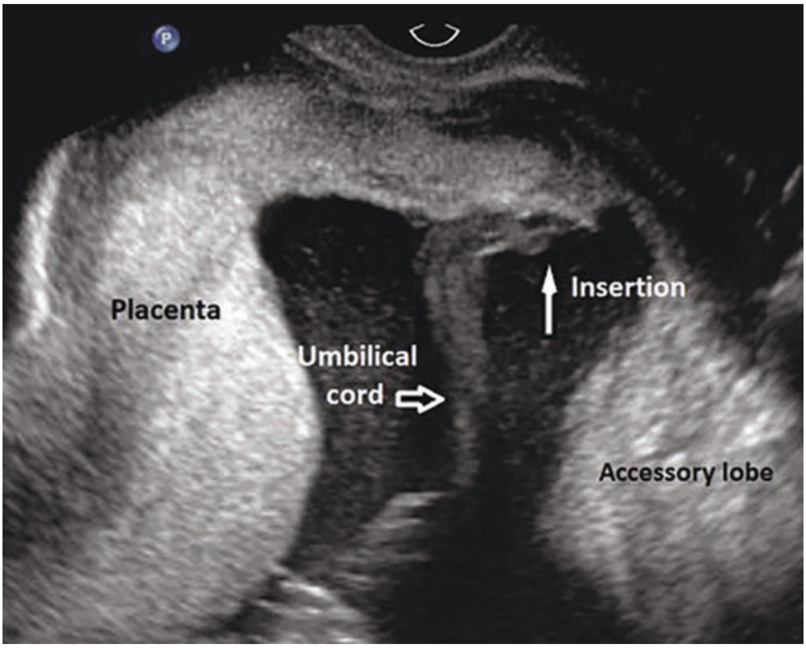

Fig. 15.9 Velamentous insertion of the cord in a twin pregnancy

Complications

Several complications are unique to multiple gestations: vanishing twin, death of one fetus, discordant fetal growth, discordance for genetic/structural anomaly, and partial mole. Some will only be found in monochorionic gestations (TTTS, TAPS, TRAP) while conjoined twins and cord entanglement are specific for MCMA gestations, which have been called "the most precarious of twin pregnancies" [121].

Vanishing Twin

This refers to a phenomenon, first described by ultrasound in 1982 [122], where, after documentation of multiple fetal heart activity, one embryo may not be visualized in a subsequent ultrasound. In fact, among gestations that start as twins, approximately one-third will ultimately result in singletons and about 10% will result in no fetuses. Multiple pregnancies may constitute more than 12% of all natural conceptions, of which only about 2% survive to term as twins and about 12% result in single births [123]. In pregnancies diagnosed as twins prior to 7 weeks of gestation spontaneous reduction of one or more gestational sacs and or embryos occurred before the 12th week of gestation in 36% of twin, 53% of triplet, and 65% of quadruplet pregnancies [124]. As evident from the above numbers, the phenomenon is even more common in higher order multiples [125], occurring in up to 50% of triplet pregnancies with a triplets delivery rate of 47.4% among 38 pregnancies diagnosed around 7 weeks with triplets, whereas 31.6% delivered twins, 18.4% delivered singletons, and only one patient miscarried all three cases [126]. The ultrasound diagnosis includes complete disappearance of a previously clearly demonstrated gestational sac and/or embryo or sonographic findings, indicating a failed pregnancy: sac smaller than expected, with irregular margins, crescent as opposed to sphere shaped or incomplete trophoblastic ring [126] (Fig. 15.10). Despite the fact that some patients will have vaginal bleeding, prognosis for continuation of a pregnancy in which the vanishing twin phenomenon occurred is excellent, regardless of the type of chorionic placentation. Birth weight, however, is lower for survivors of the vanishing twin syndrome [127]. One of the problems when this occurs is that serum aneuploidy screening may be affected with elevated

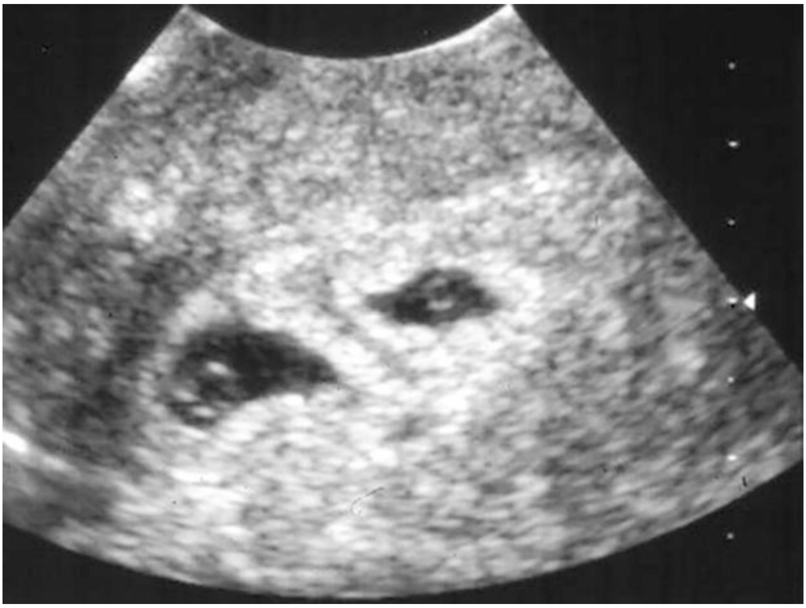

Fig. 15.10 Vanishing twin. One sac is much smaller and contains a very small yolk sac. If scanned at a later date, this would probably be missed

levels of several analytes [128]. In a recent study of 174 pregnancies with a vanishing twin, compared with control pregnancies, pregnancy-associated plasma protein A (PAPP-A) increased by 21% ($p = 0.0026$), alpha-fetoprotein (AFP) increased by 10% ($p < 0.0001$), and dimeric inhibin A (DIA) increased by 13% ($p = 0.0470$) in pregnancies with a vanishing twin. Unconjugated oestriol and total human chorionic gonadotrophin were not significantly changed in these pregnancies [129]. Errors may also occur with noninvasive cell-free fetal DNA testing, specifically with sex determination [130]. Death of one fetus is somewhat similar to the vanishing twin phenomenon but generally occurring later in pregnancy [131]. Single fetal demise occurs in 3.7–6.8% of all twin pregnancies and considerably increases the complication rate in the co-twin including fetal loss, premature delivery, and end-organ damage [83, 132]. In a large review of the literature, Ong and colleagues determined that following the death of one twin, the risk of a DC and MC co-twin demise was 4% and 12%, respectively. The risk of neurological abnormality in the surviving DC and MC co-twin was 1% and 18%, respectively. The odds of MC co-twins intrauterine death was six times that of DC twins [131]. The issue of neurological damage in the surviving twin is particularly relevant to parents and clinicians. When death of one of a set of MC twins occurs, the surviving twin is at risk of major morbidity and mortality. This is thought to be due to exposure to thromboplastin, originating in the dead fetus circulation and reaching the surviving twin placental vascular connections and causing thromboembolic phenomena in various organs, particularly the brain [133] and DIC. Anomalies most commonly described in the literature all seem to involve some vascular accident component and include porencephalic cyst, hydranencephaly, microcephaly, intestinal atresia, gastroschisis, limb amputation, and aplasia cutis [134]. Another possible mechanism is hypovolemic-related hypotension, secondary to extensive blood loss from the surviving twin into the lower resistance circulation of the deceased twin. Fetus papyraceus is a rare condition with intrauterine demise of one twin [135]. The estimated frequency is 1:12,000 live births with an incidence of 1:184 to 1:200 twin pregnancies [136] but may occur more commonly in higher order gestations. Water content and amniotic fluid of the dead twin are reabsorbed, and the fetus is compressed and mummified, resembling Egyptian parchment paper, hence the name. It is incorporated into the placenta of the surviving twin and is retained for various periods of time, including until delivery (preterm or term) of the surviving twin when it can be looked for in the placenta, after delivery [137].

Growth Restriction and Differential Growth

In the first and second trimesters, the growth rate of normal twins is not significantly different from that of singletons. Differences are more pronounced in the third trimester [138]. Size discordance between twins, particularly at an early gestational age, is an independent risk factor for adverse neonatal outcomes [139–141]. Any etiology of restricted growth in singletons may affect both twins equally or one, rather than the other, a condition designated as differential growth. Generally, in these cases, one twin is appropriate for GA (AGA) and one is small for GA (SGA). If the differential growth is secondary to one fetus being AGA and the other large for GA (LGA), this is not associated with major complications (at least until labor and delivery). The two major mechanisms for differential growth are placental specific dysfunction and genetic factors. In DZ twins, the SGA twin is often simply constitutionally small and different from his/her co-twin as two siblings might be. Another possible etiology is velamentous insertion of the cord of the small fetus since, as mentioned earlier, this entity is more common in multiple gestations [120] and is known to possibly be associated with intrauterine growth restriction [142], maybe due to disadvantageous competition for nutrients [143, 144]. In addition, both fetuses may be SGA for placental or genetic reasons. In early pregnancy differential growth may be detected by a difference in crown-rump length (CRL). This trend may start very early [145, 146]. A smaller than expected CRL is more commonly associated with chromosomal anomalies than a normal CRL [145, 147–150]. Aneuploidy by chorionic villus sampling was 4.3% in a group of singletons with smaller than expected CRL and 1.7% in controls ($p < 0.004$) among 3194 chorionic villus sampling procedures, with 277 (8.7%) fetuses with CRL smaller than expected by at least 7 days [145]. This association was demonstrated in a study of 159 twin pregnancies. Crown-rump length discordance of more than 10% was associated with a significantly higher incidence of fetal anomalies (22.2% vs. 2.8%; $p = 0.01$) [150]. Other outcomes, such as fetal loss, are also worse with a 10% discordance or more [148, 151], even in euploid fetuses [152, 153]. In a large metanalysis of 17 studies, twin pregnancies with CRL discordance ≥10% were at significantly higher risk of perinatal loss (RR = 2.80), fetal loss at ≥24 weeks (RR = 4.07), BW discordance (RR = 2.24), and preterm delivery at <34 weeks (RR = 1.49) but not of fetal loss at <24 weeks [154]. Before 8 weeks, more than 3-mm difference is associated with 50% risk of demise of smaller twin [155]. Such discordant growth is not always associated with poor outcome [69], and prediction of outcome based on this difference is less than optimal [156] but intertwin CRL difference greater than 10% increases the risk for discordant fetal growth or TTTS while CRL difference of less than 10% carries an excellent prognosis in terms of perinatal outcome [157]. Growth discrepancy may also be found when both fetuses are AGA but one is significantly smaller than the other [158]. The risk for adverse perinatal outcomes in these cases exists for monochorionic, but not dichorionic, twins [158]. Later in pregnancy (second and third trimesters), various definitions are used: estimated weight of one twin below the 10th percentile, abdominal circumference difference, or growth discordance in estimated twin weights greater than 25% . This aspect is beyond the scope of this book.

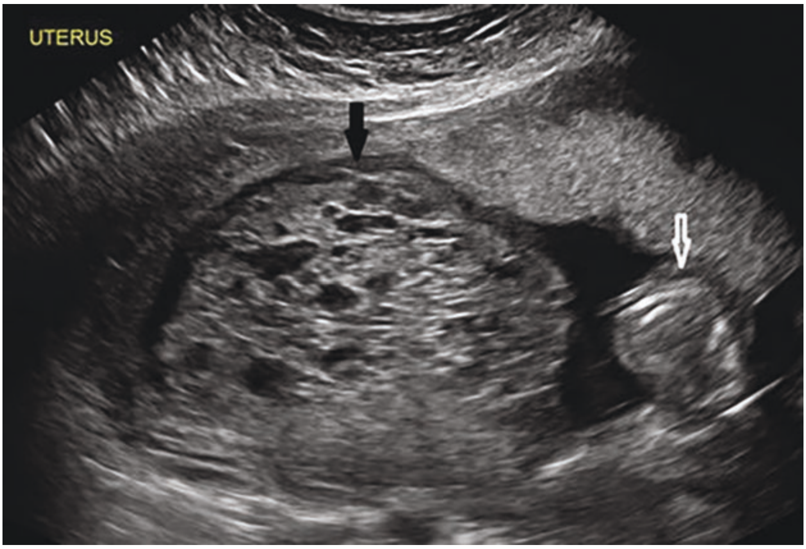

Fig. 15.11 Concomitant mole. Typical appearance of the placenta (black arrow). Fetal parts can be distinguished on the right (white arrow)

Discordance for Genetic/Structural Anomaly

See below, Screening for Genetic and Morphologic Abnormalities.

Complete Hydatidiform Mole and Coexisting Fetus

This is another rare "twinning" event with a normal fetus developing in the presence of a complete hydatidiform mole [159]. The incidence is 1:20,000 to 1:100,000 pregnancies [160] (Fig. 15.11). If the pregnancy is maintained, management is complicated and women should be followed in a high-risk obstetrics unit. Risks include fetal loss, preeclampsia, and persistent gestational trophoblastic disease in over one-third of the cases [161, 162] but delivery of a healthy baby is not impossible, in approximately 50% of cases [163].

Complications Specific for MC Twins

There is, often, unequal sharing of the placenta, which may cause grave problems: discordant fetal growth with IUGR, metabolic compromise, and death [164]. In addition, chronic unidirectional blood shunting through placental vascular anastomoses may occur and result in TTTS or twin reverse arterial perfusion [TRAP] and death. Furthermore, for MCMA twins, additional risks include conjoined twinning and cord entanglement. Risk of cerebral injury and subsequent cerebral palsy is seven times higher than in DC, most likely secondary to vascular anastomoses. If TTTS is present, this risk climbs to 21% [165]. After single intrauterine demise, it is up to 18% [165–167]. The etiology of all these complications is type of zygote and placentation which, obviously, originate very early in pregnancy. The diagnosis, however, is, generally, made later in pregnancy. An extensive description of these conditions is, therefore, beyond the scope of this book, specifically concerning surveillance and management.

Twin-to-Twin Transfusion Syndrome (TTTS)

Twin-to-twin transfusion syndrome is one of the most serious complications of monochorionic multiple gestations that occurs in 10–15% of MCDA twin pregnancies [72, 168]. It is associated with a high risk of fetal/neonatal morbidity and mortality, close to 100% if not diagnosed and managed [70]. Surviving fetuses are at risk of severe cardiac, neurologic, and developmental disorders. The diagnosis of TTTS requires two criteria: (1) the presence of a MCDA pregnancy and (2) the presence of oligohydramnios (defined as a maximal vertical pocket of <2 cm) in one sac, and of polyhydramnios (a maximal vertical pocket of >8 cm) in the other sac [72]. Typically this syndrome is suspected when discordant fetal size is present, associated with polyhydramnios in the larger twin and oligohydramnios in the smaller twin of a MCDA pregnancy (Fig. 15.12). Changes in amniotic fluid volume are often the first sign although CRL and nuchal translucency (NT) differences can also be seen, early in gestation [169, 170]. First trimester abnormal Doppler velocity in the ductus venosus (absent or reversed a-wave) has been associated with increased risks of chromosomal abnormalities, cardiac defects, and fetal deaths [171, 172] (Fig. 15.13). Differences in ductus venosus Doppler waveforms between twins have also been described as an early warning sign for subsequent develop-

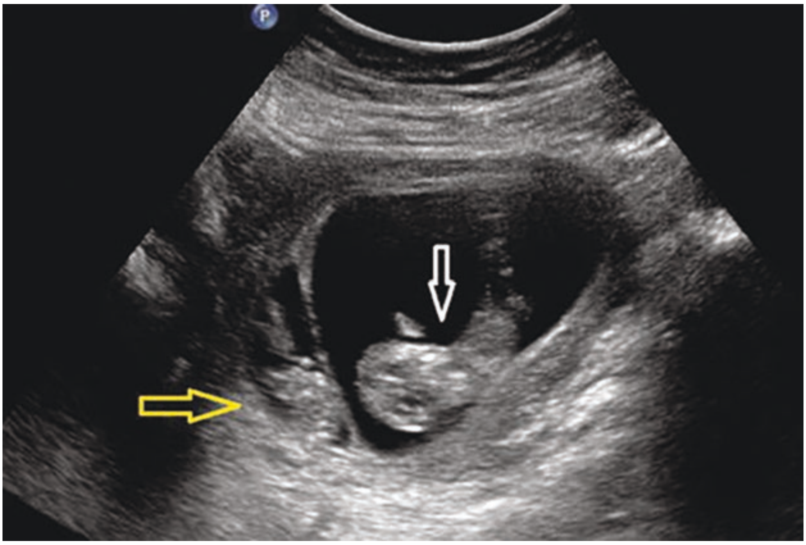

Fig. 15.12 Early signs of TTTS, 10 weeks. Clear difference in size and amount of amniotic fluid between donor (yellow arrow) and recipient (white arrow)

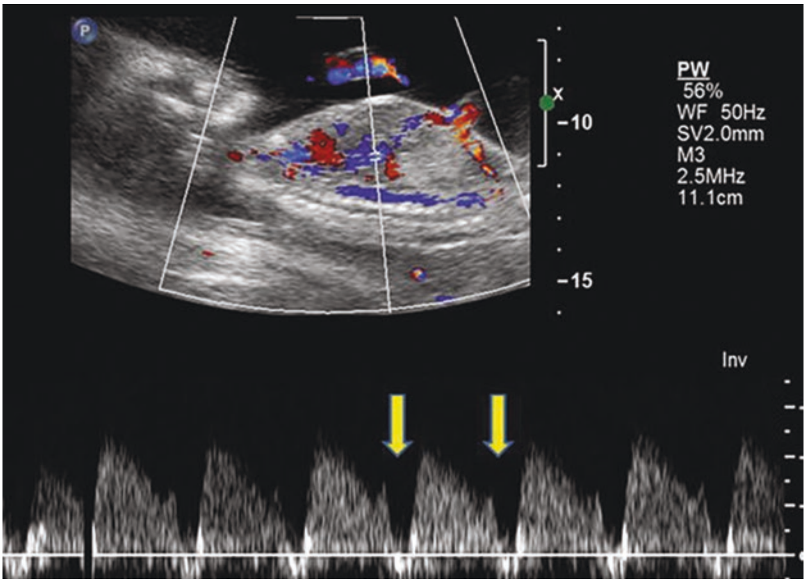

Fig. 15.13 Ductus venosus Doppler velocimetry in TTTS. Reversed a-wave is evident (arrow). This is a sign of cardiac failure in the recipient

ment of TTTS [170]. The etiology is unbalanced vascular anastomoses between the two placentae, either arteriovenous (AV), arterio-arterial (AA), venoarterial (VA), or venovenous (VV). While AA and VV anastomoses are on the surface of the placenta, AV and VA are deeper in the placental substance. Connections between the two circulations exist in virtually all MC placentation but TTTS develops in only 10–15%, secondary to hemodynamic imbalance, a phenomenon that is not entirely explained [173]. In 150 pairs of MCDA twins, TTTS occurred predominantly in the presence of AV-anastomoses without compensating superficial AA-anastomoses ($p = 0.005$) and occurred more frequently in the presence of velamentous cord insertion [67]. There is relative hypovolemia in the smaller twin (donor) who releases vasopressin and renin-angiotensin, resulting in oligohydramnios. If this is extreme, the amniotic membrane becomes tightly adherent to the fetal body, resulting in an immobilized “stuck twin.” The other twin (recipient) becomes hypervolemic, which results in release of atrial natriuretic peptide (ANP) from the enlarged heart as well as brain natriuretic peptide (BNP). Release of these (natriuretic) hormones results in polyuria and polyhydramnios. In the recipient twin, hypervolemia and increased levels of renin and angiotensin (coming from the donor twin through transplacental crossing) result in cardiomegaly, hypertrophy, particularly of the right side and cardiomyopathy. Diastolic myocardial dysfunction occurs early in the pathophysiology of TTTS [171] and together with cerebroplacental redistribution precede findings of overt cardiomyopathy [174]. Further deterioration occurs secondary to venous hypertension with development of hydrops. During the second trimester, Quintero’s stages are often used to describe the severity of the condition [175].

Twin Anemia Polycythemia Syndrome (TAPS)

TAPS is a form of TTTS, characterized by large intertwin hemoglobin differences in the absence of amniotic fluid discordances, as opposed to twin oligo-polyhydramnios sequence or TOPS [176]. It may occur spontaneously in up to 5% of monochorionic twins and may also develop after incomplete laser treatment in TTTS cases [177]. The etiology is probably few, minuscule AV placental anastomoses (diameter <1 mm) with a slow blood transfusion from donor to recipient, leading gradually to very high hemoglobin (Hb) levels in one twin and very low levels in the second one [177]. Diagnosis may be arrived at by finding discordance in fetal middle cerebral artery peak systolic velocity (MCA-PSV) measurements [178]. Perinatal outcome is difficult to evaluate, since the literature contains mainly case reports and small series. Outcomes vary according to severity and may range from double intrauterine fetal demise to two healthy neonates without major morbidity at birth, besides large intertwin Hb differences. Severe anemia can be seen at birth in the donor, requiring blood transfusion, and severe polycythemia in the recipient, requiring partial exchange transfusion. Cases of severe cerebral injury in TAPS have also been described but outcome seems to be much better than in classic TTTS. In 19 pairs of twins affected by TAPS, matched to 38 pairs of non-affected twins, neonatal mortality and morbidity rates were similar to controls [179].

Twin Reversed Arterial Perfusion (TRAP) Syndrome

This is a very severe form of TTTS complication occurring with monochorionic placentation, due to unidirectional arterio-arterial placental anastomosis. It can be diagnosed in the first trimester [177]. It affects about 1% of MC twins, with a prevalence is 1:35,000 births. There are two theories to explain the phenomenon, both resulting in artery-to-artery anastomosis between the umbilical arteries of both twins. One theory states that the primary event is a teratological accident with severe abnormal development of the fetal heart, resulting in absence of the structure (hence “acardiac”). The vascular anastomoses are felt to be secondary. According to the second explanation, the primary event is the development of anastomoses and reversed deoxygenated blood perfusion from the donor (pump) fetus to the acardiac (recipient) twin, as demonstrable by Doppler studies [178, 180] (Fig. 15.14). This is responsible for secondary fetal cardiac hypoplasia [181] and amorphic development of one twin with poor formation of the head, trunk, and upper extremities but occasionally recognizable spine and lower extremities. The lower part of the body extracts the remainder of the oxygen, allowing for some development of the lower limbs, while the remainder of the body gets none. Acardiac twins often demonstrate a two-vessel cord and polyhydramnios. A somewhat older classification includes acardius amorphous, the least differentiated, appearing as a heterogenous mass, acardiac acephalus, the most common form of acardia, where the fetus lacks a head, thorax, and upper extremities (see Fig. 15.14), as well as acardius acormus and acardius anceps, the most developed form, with a head, thorax, and abdominal organs but no heart. All acardiac twins may originate in the acardius anceps which evolves into the others because of poor oxygen supply to the remainder of the fetus. TRAP occurs in both MCMA and MCDA twin pregnancies. The overall pregnancy loss rate is estimated at 50%, due to high output cardiac failure in the pump twin and preterm delivery [182]. Prognosis can be ascertained by calculating the ratio of the acardiac weight to pump twin estimated weight. The weight of the acardiac twin is calculated by the formula: weight (g) = 1.2 × (longest dimension (cm))^2 − 1.7 × longest dimension (cm) [183]. If the ratio is above 70%, this indicates dire prognosis, as do signs of congestive heart failure (such as non-immune hydrops) in the pump twin. Various treatment modalities have been described: cord occlusion (by embolization, cord ligation, laser coagulation, bipolar diathermy, and monopolar diathermy) and intrafetal ablation (by alcohol, monopolar diathermy, interstitial laser, and radiofrequency) with intrafetal ablation appearing to provide the best results [183].

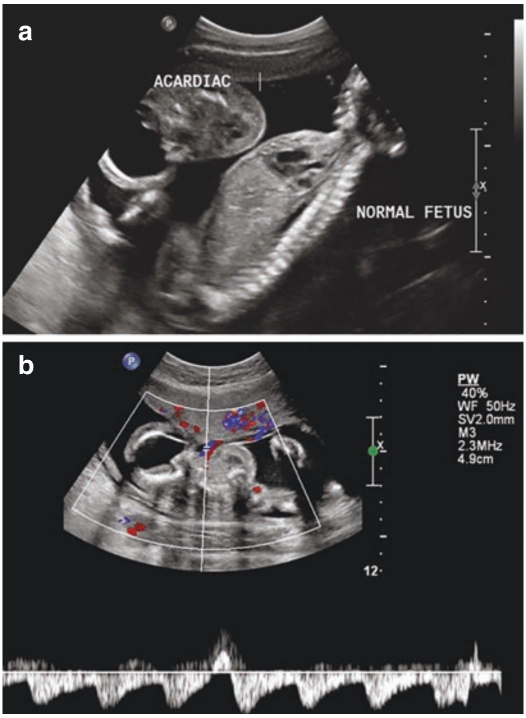

Fig. 15.14 TRAP sequence. (**a**) The acardiac twin is in the upper part of the image, as marked. Some vague anatomy can be recognized. (**b**) Doppler velocimetry demonstrates flow away from the transducer in the umbilical artery of the acardiac twin, i.e., reversed, from the placenta toward the fetal body

Conjoined Twins

Twinning occurs in approximately 1 of every 87 live births. One-third of these are monozygotic twins, and about 1% of monozygotic twins are conjoined. Conjoined twins represent a rare entity with estimates ranging from 1 in 75,000 to 1 in 250,000 deliveries [184, 185]. In the United States, the incidence is 1 per 33,000–165,000 births and 1 per 200,000 live births [186]. Conjoined twins are MCMA with the diagnosis usually made in the second trimester, although early, first trimester diagnosis is also feasible [187–190]. They are more common among females than males (3:1 in live born), and in nonwhites than whites [187]. For unclear reasons, it seems to be more common in Indian and African population. Stillbirth rate is very high (40–60%). More cases are being reported now because of the routine use of ultrasound in early pregnancy [184, 187]. Conjoined twins may be symmetrical with two well-developed bodies or asymmetrical where one is normally developed and the second is incomplete, for example, twin reversed arterial perfusion or TRAP (previously called acardiac twin) or parasitic twin or fetus in fetu, a very rare condition where a monozygotic, MCDA abnormal twin with rudimentary anatomy is contained within a host twin [191].

Classification of conjoined twins is according to site of union [186]. The most common types are the following:

1. Thoraco-omphalopagus (joined at chest or abdomen or both), 75% (Fig. 15.15). Thoracopagus generally shares a heart (Fig. 15.16), which renders separation to save both twins virtually impossible.
2. Pygopagus (joined at the buttocks), 18%.
3. Ischiopagus (joined at the ischium), 6%.
4. Craniopagus (linked at the cranium), 2–5%.

Management, outcomes and post-natal issues are beyond the scope of this book [192, 193].

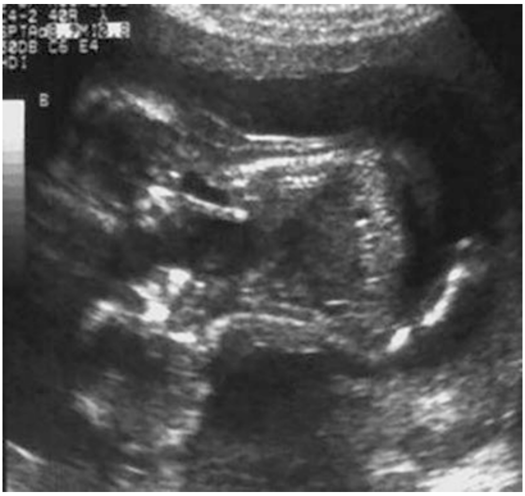

Fig. 15.15 Conjoined twins, 13 weeks. This is a typical thoraco-omphalopagus, the most common type, with joining at the thorax and abdomen levels

Cord Entanglement

This complication of MZ twins (designed as uniovular) was already described (not by ultrasound!) in 1952 [194]. It may begin early in the pregnancy, as soon as fetal (nonvoluntary) movements are initiated, around 7–8 weeks GA [195]. Major risks include intermittent cord compression which may result in neurological damage although a direct cause-effect relation is hard to prove [81] and complete occlusion with fetal demise [196]. Ultrasound is very useful to detect this condition [80], specifically with the use of spectral and color Doppler. Color Doppler demonstrates a complex vascular mass [197, 198] (Fig. 15.17). Three-D ultrasound can also be used to demonstrate the entanglement [199, 200]. There are several Doppler waveform characteristic of entanglement: persistent absent end-diastolic velocity in the umbilical artery [201] and pulsatile, high velocity waveform, with absent diastolic in the umbilical vein [202]. A notch in the umbilical artery before the entanglement region indicating downstream elevated resistance was described as a specific sign associated with bad prognosis [203, 204], although more recent studies seem to indicate that the presence of an umbilical artery notch in cases of cord entanglement, without other signs of fetal deterioration, is not indicative of an adverse perinatal outcome [205]. The previously cited dire prognosis may, in fact, be less dire than originally described [206, 207]. In a study of 114 monoamniotic twin sets (228 fetuses) with documented cord entanglement at delivery, cord entanglement itself did not contribute to prenatal morbidity and mortality [207]. In another report, umbilical cord entanglement was present in all 18 sets of monoamniotic twins when it was systematically evaluated by ultrasound and color Doppler [86]. Perinatal mortality was mainly a consequence of conjoined twins, TRAP, discordant anomaly, and spontaneous miscarriage before 20 weeks' gestation.

Fig. 15.16 Conjoined twins, 8 weeks. Color Doppler confirms conjoined twins with one heart

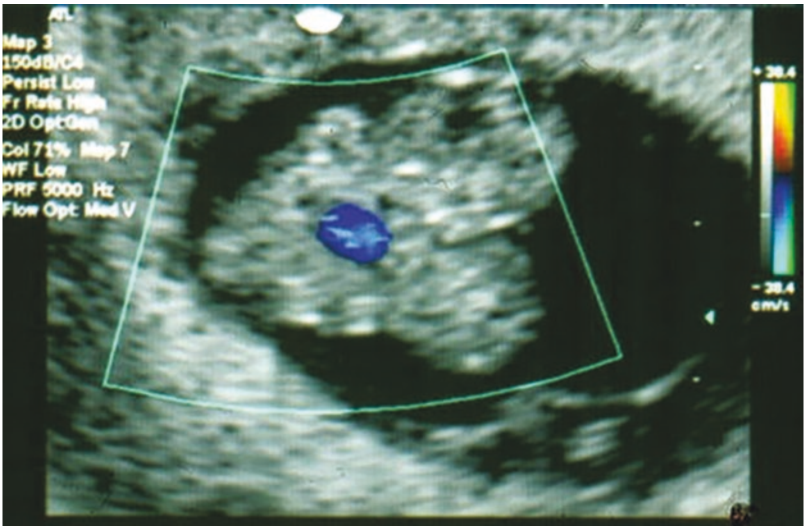

Fig. 15.17 Cord entanglement in monoamniotic twins. In this color Doppler image, a mass containing both cord is appreciated. The gestation is not in the first trimester but in the early second trimester

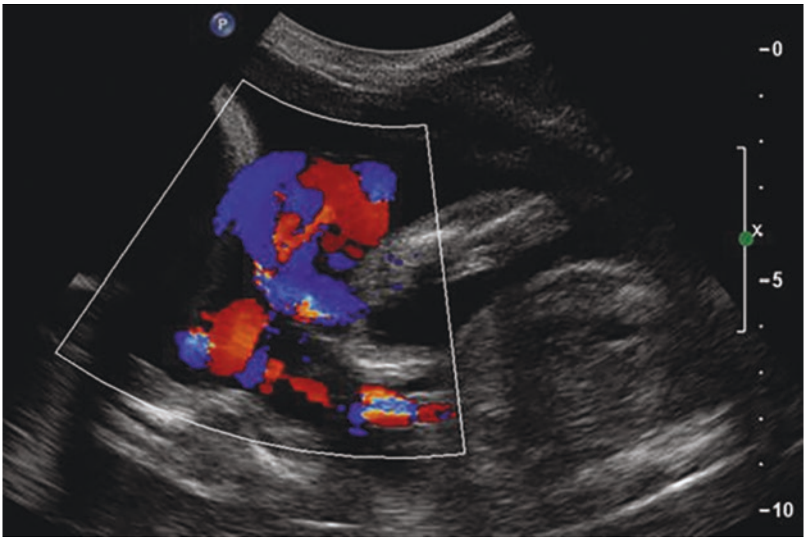

Screening for Genetic and Morphologic Abnormalities[1]

Twins represent a complex problem for genetic testing [208, 209]. Twins are at increased risk for genetic anomalies, as clearly documented in a study of 5.4 million births, from 14 European countries, of which 3% were multiple [210]. The risk of karyotypic anomalies is different between monozygotic and dizygotic twins. For MZ twins, the age-related risk to simultaneously be abnormal is the same as in a singleton gestation, although, from a maternal standpoint, the risk to the pregnancy to have one affected fetus is twice the risk of a singleton in cases of twins, three times in the case of triplets, etc. For dizygotic twins, however, the risk of one being affected is similar to a singleton but the risk of both being affected is much lower. In fact, it is the square of the risk of a singleton: for instance, if the age-related risk of the mother is 1:250, the risk of both twins, if dizygotic, to be affected is

---

[1] See also Chap. 9.

1:250 × 1:250 or 1:62,500 [210]. Screening for trisomy 21 in multiple gestations is complicated [211, 212]. Local prevalence of aneuploidy in twins needs to be taken into account for all calculations of risk [213]. Serum screening alone is of limited value because a high value may indicate elevated risk but with no determination of which or how many fetuses are affected, since it is possible that an unaffected co-twin may "mask" the abnormal serum results of an affected one and the fact that for DZ or MZ twins the interpretation may need to be different [214–216]. Specific references may need to be utilized [217]. An acceptable screening test for aneuploidy in the first trimester twin pregnancy includes fetal nuchal translucency, combined with maternal age. Structural (as opposed to maternal serum) first trimester markers (including NT, nasal bone, tricuspid valve flow, and ductus venosus waveform) may be helpful in risk assessment for aneuploidy as they are independent measurements for each fetus, regardless of chorionicity [[172]. Nuchal translucency (NT) screening is effective and is an excellent modality (when cell-free fetal DNA is not available, see below) for twin pregnancies [218]. When screening is done by nuchal translucency and maternal age, a pregnancy-specific risk should be calculated in MC twins. In DC twins, a fetus-specific risk is calculated [219]. Among twins, NT alone has a 69% trisomy 21 detection rate [220]. Screening with first trimester serum analytes, combined with nuchal translucency (also known as First Screen) may also be considered. It decreases the false-positive rate. In a 2014 systematic review of first trimester combined risk assessment (nuchal translucency and maternal serum analytes) in twin pregnancies, the combined test had a pooled sensitivity for detection of Down syndrome of 89% and a pooled specificity of 95% [220]. In DC twins, sensitivity and specificity were 86% and 95%, respectively, and in MC twins, the sensitivity and specificity were 87% and 95% [220]. Integrated screening with first screen and second trimester serum screening is an option. Naturally, in addition to trisomy 21, increased nuchal translucency is a marker for other aneuploidies, congenital malformations, and a sign of early development of TTTS [69, 170]. First trimester combined NT and serum biochemistry has a 72% DS detection rate, and an integrated screen will have an 80% DS detection rate at a 5% FPR [220]. The issue of "vanishing twin" (see below) is specifically problematic since early loss of one or more embryos of a multiple gestation may affect analyte levels [221]. In known cases, NT screening may be the preferred option. When screening is done by nuchal translucency and maternal age, a pregnancy-specific risk should be calculated in MC twins. In DC twins, a fetus-specific risk is calculated [217]. Noninvasive DNA screening (NIDS, also called noninvasive prenatal diagnosis [NIPD], noninvasive prenatal screening [NIPS], or noninvasive prenatal testing [NIPT]) offers special challenges in multiple gestations [222]. Some laboratories that perform noninvasive DNA screening (NIDS) with MPS methodology offer testing for twin gestations after it has been validated for twins [223]. Testing for monozygotic twins is expected to perform similarly to a singleton gestation, although testing in dizygotic twin and higher order multiple gestations is complicated by the fact that the per-fetus fetal fraction may be lower [224]. In fact, the nonreportable rate is higher (7.4%) than that for singleton pregnancies (2%). Additionally, if one fetus is euploid while the other is aneuploid, there is a dilution of the cell-free fetal DNA from the aneuploidy fetus resulting in decreased detection rates compared to singleton gestations. Based solely on NIDS results, it is impossible to determine which twin is abnormal. Therefore, invasive testing (CVS or amniocentesis) is required to distinguish which twin is affected. Several false-positive results have been reported with biological basis, such as confined placental mosaicism (CPM), maternal chromosome abnormality, and vanishing twin. Additional unexpected information such as undiagnosed molar pregnancy or vanishing twin may be detected by some NIDS methods [225].

The incidence of congenital anomalies is much higher in MZ twins, in fact three to five times higher than in DZ twins [226, 227].

Although this has been party correlated with assisted reproductive technologies [228], there seems to also be a direct relation with the twinning phenomenon itself, whether spontaneous or induced with a common etiology for both the MZ twinning and the early sequence of the malformation [229]. Most common structural anomalies in twins include anencephaly, facial clefts, holoprosencephaly, VATER association (vertebral defects, imperforate anus, esophageal fistula with tracheoesophageal fistula, radial and renal dysplasia), exstrophy of the cloaca malformation sequence, and sacrococcygeal teratoma, all of which should be recognized early by detailed ultrasound anatomy scan and most of them, if not all, in early (late first trimester) scan [230]. In a large study by Glinianaia and colleagues [227], 2329 twin pregnancies (4658 twins) and 147,655 singletons were compared. The rate of congenital anomalies in twins was 405.8 per 10,000 twins versus 238.2 per 10,000 singletons (rate ratios [RR] = 1.7, 95% confidence interval [CI] 1.5–2.0). In twins with known chorionicity (84.8% of all twins), the prevalence of congenital anomalies in MC twins (633.6 per 10,000) was nearly twice that in DC (343.7 per 10,000; RR = 1.8, 95% CI 1.3–2.5). There was an increased rate of congenital anomalies for all major types of anomalies in twin compared with singleton pregnancies, except chromosomal abnormalities. Monozygosity, specifically MCDA twinning, seems be an independent factor for an increase in congenital heart disease (CHD) with a 9.18 relative risk increase in one report of 40 fetuses with CHDs among 830 fetuses from MCDA twin gestations [231]. Congenital heart disease, however, is also more common in DZ twins than in singleton [232]. Thus, fetal echocardiography is indicated in all wins. In a study of 844 pairs of twins, the prevalence of major congenital malformations was 2.7% for MZ twins, 1.0% for DZ twins, and 0.6% for singletons. The concordance rate of major congenital malformations was 18% for MZ twins, but no DZ pair was concordant for any major congenital malformation [232].

Are monozygotic twins "really" identical? They are very similar but genetically, most often, not "exactly" the same [233–235]. In fact, hundreds (360 by one estimate) of genetic differences may occur very early in fetal life [236]. Parallel sequencing (ultra-deep next generation sequencing) has allowed identification of several genetic variations (e.g., single nucleotide polymorphism and copy number variations). These may be due to post-fertilization events, such as chromosomal mosaicism, skewed X-inactivation, imprinting mechanisms, as well as DNA point mutations or copy errors, taking place early after blastocyst splitting [234]. There are also genetic differences due to mutations which may occur later in life as well as epigenetic[2] modifications, due to environmental factors [237, 238]. Another phenomenon explaining a difference in the karyotype of two MCMA twins is heterokaryotypia: a discordance in karyotype due to either an early postzygotic chromosomal rescue in one fetus or a mitotic error that leads to one trisomic fetus with a normal co-twin [239]. A curious condition is superfecundation by two different fathers with presence of "fake dizygotic twins" [240, 241]. Discordance for a congenital anomaly is extremely problematic, from a moral, ethic, religious, philosophical and, often, medical standpoints [242, 243]. Until intrauterine therapy is effective and safe (it may already be for a very small number of anomalies), the options include expectant management [244], termination of the entire pregnancy, or selective feticide [244–247]. Selective termination of an anomalous DC twin is relatively safe with intravascular injection of potassium chloride or digoxin, although there is some increased risk of miscarriage or preterm delivery [248, 249]. In monochorionic twins, selective feticide needs to result in complete separation of the circulations [250, 251] and is, thus, best accomplished by sealing one umbilical cord with ligation [252], bipolar coagulation [253, 254], radiofrequency [255, 256], or laser ablation [250].

---

[2] Epigenetics: level of activity of any particular gene (i.e., switched on, off, or partially switched on or off).

Maternal Complications

As described in the introduction, maternal morbidity (and mortality) is increased in multiple pregnancies. Multiple pregnancy is the most powerful predictive factor for adverse maternal, obstetrical, and perinatal outcomes [257]. Pregnancy induces physiological stress to the maternal body, and multiple gestations provide even additional strain and nutritional demands [258]. Most of the complications do not become clinically apparent in the first trimester but later in pregnancy, such as preeclampsia and diabetes [259], although some level of prediction may ascertain in the first trimester [260, 261]. Among women with 684 twin and 2946 singleton gestations enrolled in multicenter trials, rates for both gestational hypertension and preeclampsia were significantly higher among women with twin gestations than among those with singleton gestations. Furthermore, adverse neonatal outcomes were more frequent in women with twin pregnancies and hypertensive complications [19, 262]. In a study of over 23,000 women, 553 of whom had twins, after adjusting for age, race/ethnicity, body mass index, maximal systolic and diastolic blood pressure, smoking and parity, multiple regression analysis showed that twin pregnancy was associated with an approximately twofold increase in the risk for developing gestational diabetes. The risk was highest among African-American and young women [263]. Thromboembolic disorders are major causes of morbidity and mortality in the pregnant patient. Contributing factors are increased blood coagulability [264], elevated BMI, maternal age above 35 and, specifically, multiple gestation with an incidence rate of 6.3/10,000 year in singletons versus 18.2/10,000 year among women with multiple pregnancies [265]. Other complications more common in women carrying multiple gestations, most likely secondary to increased levels of various hormones, in particular βHCG, include hyperemesis gravidarum [266]—although this is not universally accepted as a more frequent complication in multiple pregnancies [267]—iron deficiency anemia [268], intrahepatic cholestasis of pregnancy [269], and pruritic urticarial papules and plaques of pregnancy or PUPPP [270]. This is the most common specific dermatosis of pregnancy, with an incidence is 1/160 to 1/300 pregnancies [270]. The majority of patients are nulliparous and PUPPP is 8- to 12-fold more common in women with multiple gestations, possibly due to increased hormones levels, as stated above, or increased abdominal distension [271]. An additional complication is acute fatty liver. This is a rare condition, usually of the third trimester, complicating approximately 1 in 10,000 singleton gestations [272] but, of all the published cases, 14% have been reported in twin gestations [273]. The rate seems to be 7% in triplet pregnancies [274]. An important factor to consider is the influence of maternal conditions on the fetus (see Chap. 4). This has taken front stage with the coronavirus 2 (SARS-CoV-2) pandemic. Transplacental transmission of the infection, however, seems improbable [275].

Higher Order Multiple Gestations

These pregnancies (triplets, quadruplets, etc.) are at extremely high risk of complications [276]. The classic teachings are that the prevalence for triplets is 1:90^2 and 1:90^3 for quadruplets. Numbers have greatly changed with the introduction of ART [277–279]. Classification is based on chorionicity and amnionicity [280, 281] (Figs. 15.18 and 15.19). In a study of 49 consecutive sets of triplets, including 18 sets of spontaneously conceived triplet pregnancies and 31 sets resulting from ART, the rate of MZ twin pairs was 48% among spontaneously conceived triplet pregnancies; 30% of DC triplet pregnancies were MZ and 70% DZ; 20% of trichorionic (TC) triplet pregnancies were DZ and 80% trizygotic (TZ). For triplet pregnancies conceived using ART, the rate of MZ twin pairs was 6.5%; 100% of DC triplet pregnancies were DZ; 4% of TC triplet pregnancies were DZ and 96% TZ [282]. Early complications, such as genetic anomalies, growth discordancy, TTTS, are similar to twin pregnancies, depending on placentation, although, naturally, much more challenging from a management standpoint [278,

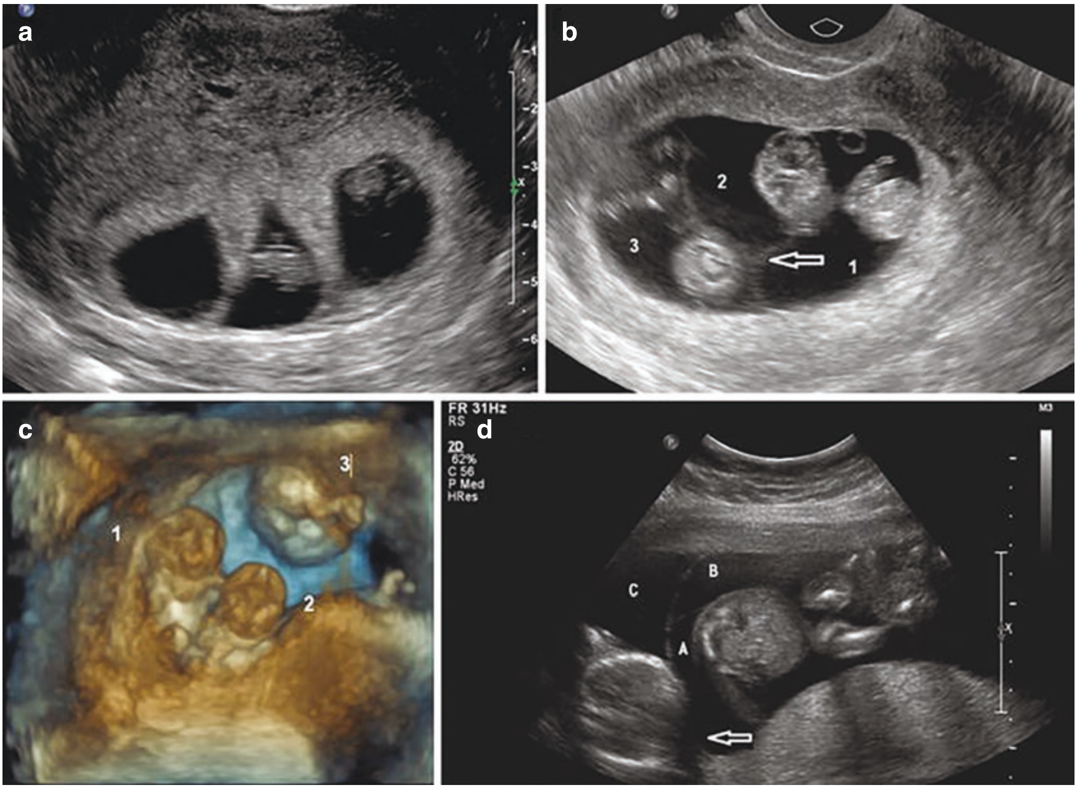

Fig. 15.18 Triplets. (**a**) Early first trimester trichorionic triplet pregnancy. (**b**) The ipsilon sign (arrow) allows diagnosis of trichorionic pregnancy. (**c**) 3D view of triplet pregnancy. Although two "lower" fetuses appear to be in one sac, the pregnancy is trichorionic, as demonstrated by the ipsilon sign. (**d**) Dichorionic triplets. Triplets A and B share a chorionic sac but are in separate amniotic sacs. Triplet C is in its own chorionic and amniotic sac. The arrow points to the twin-peak sign. This confirms that triplet C is in its own chorionic and amniotic sac

Fig. 15.19 Quadruplet pregnancy. Four distinct gestational sacs are demonstrated, with what appears to be thick separations between them. This represents quadra-chorionic-quadra-amniotic placentation, in a patient who underwent ovulation induction

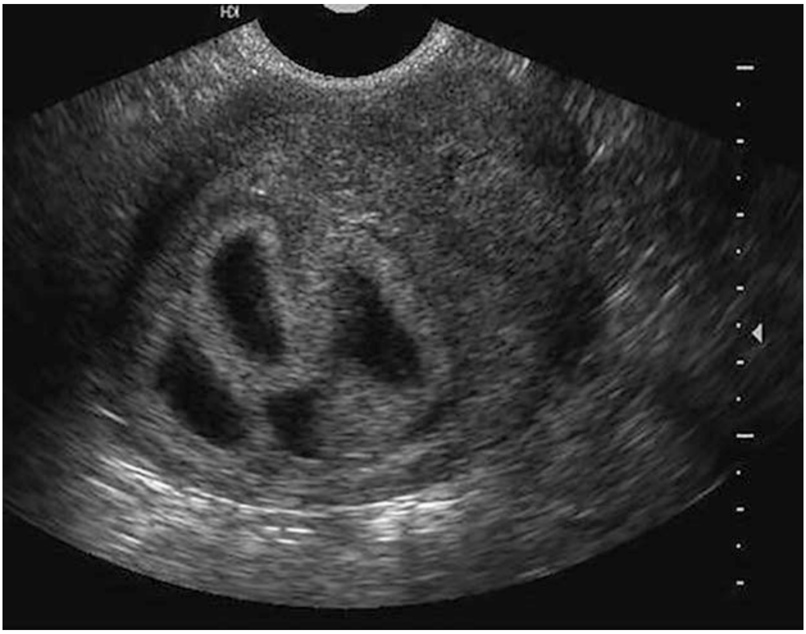

282, 283]. Incidence of congenital anomalies is not increased, compared to twins [279]. The complications are mostly later in pregnancy. In a study of 316,696 twin, 12,193 triplet, and 778 quadruplet pregnancies, compared with mothers of twins, mothers of triplets and quadruplets were more likely to be diagnosed with preterm premature rupture of membranes, (AORs, 1.53, 1.74, respectively), pregnancy-associated hypertension (AORs, 1.22, 1.27), and excessive bleeding (AORs, 1.50, 2.22), to be delivered by cesarean section (AORs, 6.55, 7.38) at <29 weeks of gestation (AORs, 3.76, 7.96), and to have one or more infants die (AORs, 3.02, 4.07). The rate of maternal complications is also increased compared to twin pregnancies where it is already increased compared to singletons. In a retrospective study of 57 triplet gestations, preterm labor occurred in 86.0%, anemia in 58.1%, preeclampsia in 33.3%, preterm premature rupture of the membranes in 17.5%, postpartum hemorrhage in 12.3%, and HELLP (hemolysis, elevated liver enzymes, and low platelets) syndrome in 10.5% [284].

Invasive Diagnostic/Therapeutic Procedures in Twins

This is addressed in detail in Chap. 25 of this book.

Teaching Points

- Multiple births comprise today 3% of all live births in the United States.
- Dizygotic form 70% of twin pregnancies and monozygotic, 30%.
- Determination of placentation (chorionicity and amnionicity) should always be attempted when performing an ultrasound and should be reported.
- All twins are at increased risk for genetic anomalies.
- Vanishing twin, death of one fetus, discordant fetal growth, discordance for genetic/structural anomaly, and partial mole are complications unique to twin pregnancies.
- Complications specific for monochorionic twins are TTTS and its variants and (TTTS, TAPS, TRAP) as well as conjoined twins and cord entanglement in monoamniotic twins.
- Maternal complications are common in women carrying multiple gestations, such as preeclampsia, gestational diabetes, thromboembolic disorders, cholestasis of pregnancy, and acute fatty liver, as well as being exposed to a much higher risk of operative delivery.
- Classification of high order multiple gestations (triplets and above) are by placentation, similar to twin gestations.

References

1. Martin JA, Hamilton BE, Osterman MJK, Driscoll AK. Births: final data for 2019. Natl Vital Stat Rep. 2021;70(2):1–51.
2. Martin JA, Hamilton BE, Osterman MJ, Curtin SC, Matthews TJ. Births: final data for 2013. Natl Vital Stat Rep. 2015;64(1):1–65.
3. National Institute for Care and Excellence (NICE) Guideline (NG 137): Twin and triplet pregnancy. London, UK; 2019.
4. Reynolds MA, Schieve LA, Martin JA, Jeng G, Macaluso M. Trends in multiple births conceived using assisted reproductive technology, United States, 1997–2000. Pediatrics. 2003;111(5 Pt 2):1159–62.
5. Vahratian A, Schieve LA, Reynolds MA, Jeng G. Live-birth rates and multiple-birth risk of assisted reproductive technology pregnancies conceived using thawed embryos, USA 1999–2000. Hum Reprod. 2003;18(7):1442–8.
6. Blondel B, Kaminski M. The increase in multiple births and its consequences on perinatal health. J Gynecol Obstet Biol Reprod (Paris). 2002;31(8):725–40.
7. Oleszczuk JJ, Keith LG, Oleszczuk AK. The paradox of old maternal age in multiple pregnancies. Obstet Gynecol Clin N Am. 2005;32(1):69–80, ix.
8. Shur N. The genetics of twinning: from splitting eggs to breaking paradigms. Am J Med Genet C Semin Med Genet. 2009;151c(2):105–9.
9. Boomsma DI. The genetics of human DZ twinning. Twin Res Hum Genet. 2020;23(2):74–6.
10. Duffy CR. Multifetal gestations and associated perinatal risks. NeoReviews. 2021;22(11):e734–e46.
11. Joo JG, Csaba A, Szigeti Z, Rigo J Jr. Spontaneous abortion in multiple pregnancy: focus on fetal pathology. Pathol Res Pract. 2012;208(8):458–61.
12. Roach VJ, Lau TK, Wilson D, Rogers MS. The incidence of gestational diabetes in multiple pregnancy. Aust N Z J Obstet Gynaecol. 1998;38(1):56–7.
13. Krotz S, Fajardo J, Ghandi S, Patel A, Keith LG. Hypertensive disease in twin pregnancies: a review. Twin Res. 2002;5(1):8–14.

14. Mastrobattista JM, Skupski DW, Monga M, Blanco JD, August P. The rate of severe preeclampsia is increased in triplet as compared to twin gestations. Am J Perinatol. 1997;14(5):263–5.
15. Elliott JP. Preterm labor in twins and high-order multiples. Clin Perinatol. 2007;34(4):599–609, vii.
16. von Dadelszen P, Kives S, Delisle MF, Wilson RD, Joy R, Ainsworth L, et al. The association between early membrane rupture, latency, clinical chorioamnionitis, neonatal infection, and adverse perinatal outcomes in twin pregnancies complicated by preterm prelabour rupture of membranes. Twin Res. 2003;6(4):257–62.
17. Sentilhes L, Bouhours AC, Biquard F, Gillard P, Descamps P, Kayem G. Delivery of twins. Gynecol Obstetr Fertilite. 2009;37(5):432–41.
18. Suzuki S, Kikuchi F, Ouchi N, Nagayama C, Nakagawa M, Inde Y, et al. Risk factors for postpartum hemorrhage after vaginal delivery of twins. J Nippon Med School. 2007;74(6):414–7.
19. American College of Obstetricians and Gynecologists' Committee on Practice Bulletins-Obstetrics and Society for Maternal-Fetal Medicine. Multifetal gestations: twin, triplet, and higher-order multifetal pregnancies: ACOG Practice Bulletin, Number 231. Obstet Gynecol. 2021;137(6):e145–e62.
20. Garne E, Andersen HJ. The impact of multiple pregnancies and malformations on perinatal mortality. J Perinat Med. 2004;32(3):215–9.
21. Quintero RA. Twin-twin transfusion syndrome. Clin Perinatol. 2003;30(3):591–600.
22. Alexander GR, Slay Wingate M, Salihu H, Kirby RS. Fetal and neonatal mortality risks of multiple births. Obstet Gynecol Clin N Am. 2005;32(1):1–16, vii.
23. Wang SS, Revels J, Dubinsky TJ. Double trouble: complications in twin pregnancies. Ultrasound Q. 2020;36(3):240–6.
24. Luke B, Bigger HR, Leurgans S, Sietsema D. The cost of prematurity: a case-control study of twins vs singletons. Am J Public Health. 1996;86(6):809–14.
25. Ananth CV, Joseph Ks K, Smulian JC. Trends in twin neonatal mortality rates in the United States, 1989 through 1999: influence of birth registration and obstetric intervention. Am J Obstet Gynecol. 2004;190(5):1313–21.
26. Chelmow D, Penzias AS, Kaufman G, Cetrulo C. Costs of triplet pregnancy. Am J Obstet Gynecol. 1995;172(2 Pt 1):677–82.
27. Kahn B, Lumey LH, Zybert PA, Lorenz JM, Cleary-Goldman J, D'Alton ME, et al. Prospective risk of fetal death in singleton, twin, and triplet gestations: implications for practice. Obstet Gynecol. 2003;102(4):685–92.
28. Yokoyama Y, Shimizu T, Hayakawa K. Incidence of handicaps in multiple births and associated factors. Acta Genet Med Gemellol. 1995;44(2):81–91.
29. Topp M, Huusom LD, Langhoff-Roos J, Delhumeau C, Hutton JL, Dolk H, et al. Multiple birth and cerebral palsy in Europe: a multicenter study. Acta Obstet Gynecol Scand. 2004;83(6):548–53.
30. Grether JK, Nelson KB, Cummins SK. Twinning and cerebral palsy: experience in four northern California counties, births 1983 through 1985. Pediatrics. 1993;92(6):854–8.
31. Yokoyama Y, Shimizu T, Hayakawa K. Prevalence of cerebral palsy in twins, triplets and quadruplets. Int J Epidemiol. 1995;24(5):943–8.
32. Martin JA, Hamilton BE, Osterman MJ. Three decades of twin births in the United States, 1980–2009. NCHS Data Brief. 2012;80:1–8.
33. Scholten I, Chambers GM, van Loendersloot L, van der Veen F, Repping S, Gianotten J, et al. Impact of assisted reproductive technology on the incidence of multiple-gestation infants: a population perspective. Fertil Steril. 2015;103(1):179–83.
34. Sunderam S, Kissin DM, Crawford SB, Folger SG, Jamieson DJ, Barfield WD. Assisted reproductive technology surveillance—United States, 2011. MMWR Surveill Summ. 2014;63(10):1–28.
35. Pandian Z, Marjoribanks J, Ozturk O, Serour G, Bhattacharya S. Number of embryos for transfer following in vitro fertilisation or intra-cytoplasmic sperm injection. Cochrane Database Syst Rev. 2013;7:Cd003416.
36. Knopman JM, Krey LC, Oh C, Lee J, McCaffrey C, Noyes N. What makes them split? Identifying risk factors that lead to monozygotic twins after in vitro fertilization. Fertil Steril. 2014;102(1):82–9.
37. Sobek A Jr, Zborilova B, Prochazka M, Silhanova E, Koutna O, Klaskova E, et al. High incidence of monozygotic twinning after assisted reproduction is related to genetic information, but not to assisted reproduction technology itself. Fertil Steril. 2015;103(3):756–60.
38. Hoekstra C, Zhao ZZ, Lambalk CB, Willemsen G, Martin NG, Boomsma DI, et al. Dizygotic twinning. Hum Reprod Update. 2008;14(1):37–47.
39. Hoekstra C, Willemsen G, van Beijsterveldt TC, Montgomery GW, Boomsma DI. Familial twinning and fertility in Dutch mothers of twins. Am J Med Genet A. 2008;146A(24):3147–56.
40. Palmer JS, Zhao ZZ, Hoekstra C, Hayward NK, Webb PM, Whiteman DC, et al. Novel variants in growth differentiation factor 9 in mothers of dizygotic twins. J Clin Endocrinol Metab. 2006;91(11):4713–6.
41. Montgomery GW, Zondervan KT, Nyholt DR. The future for genetic studies in reproduction. Mol Hum Reprod. 2014;20(1):1–14.
42. Smits J, Monden C. Twinning across the Developing World. PLoS One. 2011;6(9):e25239.
43. Segal NL. Art for twins: Yoruba artists and their statues/twin research studies: twins' education and conceptions; diurnal preference; inherited eye diseases; ultrasound counseling when twins are conjoined/popular twin reports: twin sisters (the film); rare pregnancy; diet test; French twins reared apart and reunited. Twin Res Hum Genet. 2014;17(3):215–21.

44. Ewigman BG, Crane JP, Frigoletto FD, LeFevre ML, Bain RP, McNellis D. Effect of prenatal ultrasound screening on perinatal outcome. RADIUS Study Group. N Engl J Med. 1993;329(12):821–7.
45. Saari-Kemppainen A, Karjalainen O, Ylostalo P, Heinonen OP. Ultrasound screening and perinatal mortality: controlled trial of systematic one-stage screening in pregnancy. The Helsinki Ultrasound Trial. Lancet. 1990;336(8712):387–91.
46. Chasen ST, Chervenak FA. What is the relationship between the universal use of ultrasound, the rate of detection of twins, and outcome differences? Clin Obstet Gynecol. 1998;41(1):66–77.
47. Hughey MJ, Olive DL. Routine ultrasound scanning for the detection and management of twin pregnancies. J Reprod Med. 1985;30(5):427–30.
48. Abramowicz JS. Benefits and risks of ultrasound in pregnancy. Semin Perinatol. 2013;37(5):295–300.
49. Reddy UM, Abuhamad AZ, Levine D, Saade GR, Fetal Imaging Workshop Invited Participants. Fetal imaging: executive summary of a joint Eunice Kennedy Shriver National Institute of Child Health and Human Development, Society for Maternal-Fetal Medicine, American Institute of Ultrasound in Medicine, American College of Obstetricians and Gynecologists, American College of Radiology, Society for Pediatric Radiology, and Society of Radiologists in Ultrasound Fetal Imaging Workshop. J Ultrasound Med. 2014;33(5):745–57.
50. Morin L, Lim K, Diagnostic Imaging Committee; Special Contributor; Genetics Committee; Maternal Fetal Medicine Committee. Ultrasound in twin pregnancies. J Obstet Gynaecol Can. 2011;33(6):643–56.
51. Blickstein I. Normal and abnormal growth of multiples. Semin Neonatol. 2002;7(3):177–85.
52. Hiersch L, Okby R, Freeman H, Rosen H, Nevo O, Barrett J, et al. Differences in fetal growth patterns between twins and singletons. J Matern Fetal Neonatal Med. 2020;33(15):2546–55.
53. Martins WP, Nastri CO, Barra DA, Navarro PA, Mauad Filho F, Ferriani RA. Fetal volume and crown-rump length from 7 to 10 weeks of gestational age in singletons and twins. Eur J Obstet Gynecol Reprod Biol. 2009;145(1):32–5.
54. Dias T, Mahsud-Dornan S, Thilaganathan B, Papageorghiou A, Bhide A. First-trimester ultrasound dating of twin pregnancy: are singleton charts reliable? BJOG. 2010;117(8):979–84.
55. Wegrzyn P, Fabio C, Peralta A, Faro C, Borenstein M, Nicolaides KH. Placental volume in twin and triplet pregnancies measured by three-dimensional ultrasound at 11 + 0 to 13 + 6 weeks of gestation. Ultrasound Obstet Gynecol. 2006;27(6):647–51.
56. Senoo M, Okamura K, Murotsuki J, Yaegashi N, Uehara S, Yajima A. Growth pattern of twins of different chorionicity evaluated by sonographic biometry. Obstet Gynecol. 2000;95(5):656–61.
57. Shushan A, Mordel N, Zajicek G, Lewin A, Schenker JG, Sadovsky E. A comparison of sonographic growth curves of triplet and twin fetuses. Am J Perinatol. 1993;10(5):388–91.
58. Sebire NJ, Snijders RJ, Hughes K, Sepulveda W, Nicolaides KH. The hidden mortality of monochorionic twin pregnancies. Br J Obstet Gynaecol. 1997;104(10):1203–7.
59. D'Antonio F, Khalil A, Dias T, Thilaganathan B, Southwest Thames Obstetric Research Collaborative (STORK). Early fetal loss in monochorionic and dichorionic twin pregnancies: analysis of the Southwest Thames Obstetric Research Collaborative (STORK) multiple pregnancy cohort. Ultrasound Obstet Gynecol. 2013;41(6):632–6.
60. El Kateb A, Nasr B, Nassar M, Bernard JP, Ville Y. First-trimester ultrasound examination and the outcome of monochorionic twin pregnancies. Prenat Diagn. 2007;27(10):922–5.
61. Ghalili A, McLennan A, Pedersen L, Kesby G, Hyett J. Outcomes of monochorionic diamniotic twin pregnancies: a comparison of assisted and spontaneous conceptions. Aust N Z J Obstet Gynaecol. 2013;53(5):437–42.
62. Lopriore E, Stroeken H, Sueters M, Meerman RJ, Walther F, Vandenbussche F. Term perinatal mortality and morbidity in monochorionic and dichorionic twin pregnancies: a retrospective study. Acta Obstet Gynecol Scand. 2008;87(5):541–5.
63. Matijevic R, Solak M, Kalogjera N, Kurjak A. Monochorionic twin pregnancy: retrospective analysis of predicted pregnancy outcome. Croat Med J. 2003;44(6):734–9.
64. Van Mieghem T, Abbasi N, Shinar S, Keunen J, Seaward G, Windrim R, et al. Monochorionic monoamniotic twin pregnancies. Am J Obstet Gynecol MFM. 2022;4(2S):100520.
65. Denbow ML, Blomley MJ, Cosgrove DO, Fisk NM. Ultrasound microbubble contrast angiography in monochorionic twin fetuses. Lancet. 1997;349(9054):773.
66. Hack KE, van Gemert MJ, Lopriore E, Schaap AH, Eggink AJ, Elias SG, et al. Placental characteristics of monoamniotic twin pregnancies in relation to perinatal outcome. Placenta. 2009;30(1):62–5.
67. Lewi L, Gucciardo L, Huber A, Jani J, Van Mieghem T, Done E, et al. Clinical outcome and placental characteristics of monochorionic diamniotic twin pairs with early- and late-onset discordant growth. Am J Obstet Gynecol. 2008;199(5):511.e1–7.
68. Obladen M. Unequal but monozygous: a history of twin-twin transfusion syndrome. J Perinat Med. 2010;38(2):121–8.
69. Allaf MB, Vintzileos AM, Chavez MR, Wax JA, Ravangard SF, Figueroa R, et al. First-trimester sonographic prediction of obstetric and neonatal outcomes in monochorionic diamniotic twin pregnancies. J Ultrasound Med. 2014;33(1):135–40.
70. Diehl W, Diemert A, Hecher K. Twin-twin transfusion syndrome: treatment and outcome. Best Pract Res Clin Obstet Gynaecol. 2014;28(2):227–38.

71. Giconi SS. Twin-to-twin transfusion syndrome: a case study. Adv Neonatal Care. 2013;13(1):31–7.
72. Simpson LL. Twin-twin transfusion syndrome. Am J Obstet Gynecol. 2013;208(1):3–18.
73. Degenhardt J, Enzensberger C, Tenzer A, Kawecki A, Kohl T, Axt-Fliedner R. Management of complicated monochorionic twin pregnancies. Z Geburtshilfe Neonatol. 2015;219(1):22–7.
74. Rossi AC, Prefumo F. Perinatal outcomes of twin anemia-polycythemia sequence: a systematic review. J Obstet Gynaecol Can. 2014;36(8):701–7.
75. Van Winden KR, Quintero RA, Kontopoulos EV, Korst LM, Llanes A, Chmait RH. Pre-operative twin anemia/polycythemia in the setting of twin-twin transfusion syndrome (TTTS). Fetal Diagn Ther. 2015;37(4):274–80.
76. Hartge DR, Weichert J. Prenatal diagnosis and outcome of multiple pregnancies with reversed arterial perfusion (TRAP-sequence). Arch Gynecol Obstet. 2012;286(1):81–8.
77. Prasad RH, Prasad TR, Kumar KD. TRAP sequence - an interesting entity in twins. J Clin Imaging Sci. 2012;2:56.
78. Tavares de Sousa M, Glosemeyer P, Diemert A, Bamberg C, Hecher K. First-trimester intervention in twin reversed arterial perfusion sequence. Ultrasound Obstet Gynecol. 2020;55(1):47–9.
79. Curado J, Sileo F, Bhide A, Thilaganathan B, Khalil A. Early- and late-onset selective fetal growth restriction in monochorionic diamniotic twin pregnancy: natural history and diagnostic criteria. Ultrasound Obstet Gynecol. 2020;55(5):661–6.
80. Panaitescu AM, Gica N, Botezatu R, Cimpoca B, Veduta A, Peltecu G, et al. Early ultrasound identification of cord entanglement in monochorionic monoamniotic twin pregnancy. Diagnostics (Basel). 2021;11(3):520.
81. Zollner U, Rehn M, Heuer S, Morr AK, Dietl J. Umbilical cord entanglement in monoamniotic twins. Ultrasound Obstet Gynecol. 2012;40(1):121–2.
82. Dias T, Mahsud-Dornan S, Bhide A, Papageorghiou AT, Thilaganathan B. Cord entanglement and perinatal outcome in monoamniotic twin pregnancies. Ultrasound Obstet Gynecol. 2010;35(2):201–4.
83. Blickstein I, Perlman S. Single fetal death in twin gestations. J Perinat Med. 2013;41(1):65–9.
84. Kaufman MH. The embryology of conjoined twins. Childs Nervous Syst. 2004;20(8–9):508–25.
85. Liang XW, Cai YY, Yang YZ, Chen ZY. Early ultrasound diagnosis of conjoined twins at eight weeks of pregnancy: a case report. World J Clin Cases. 2020;8(21):5389–93.
86. Farah N, Hogan J, Johnson S, Stuart B, Daly S. Prospective risk of fetal death in uncomplicated monochorionic twins. Acta Obstet Gynecol Scand. 2012;91(3):382–5.
87. D'Antonio F, Khalil A, Dias T, Thilaganathan B. Early fetal loss in monochorionic and dichorionic twin pregnancies: analysis of the Southwest Thames Obstetric Research Collaborative (STORK) multiple pregnancy cohort. Ultrasound Obstet Gynecol. 2013;41(6):632–6.
88. Prefumo F, Fichera A, Pagani G, Marella D, Valcamonico A, Frusca T. The natural history of monoamniotic twin pregnancies: a case series and systematic review of the literature. Prenat Diagn. 2015;35(3):274–80.
89. Alhamdan D, Bora S, Condous G. Diagnosing twins in early pregnancy. Best Pract Res Clin Obstet Gynaecol. 2009;23(4):453–61.
90. Aston KI, Peterson CM, Carrell DT. Monozygotic twinning associated with assisted reproductive technologies: a review. Reproduction. 2008;136(4):377–86.
91. Fitzgerald B. Histopathological examination of the placenta in twin pregnancies. APMIS. 2018;126(7):626–37.
92. Arabin B, van Eyck J. The role of ultrasound in multiple pregnancy. Twin Res. 2001;4(3):141–5.
93. Ayala Mendez JA, Jimenez Solis G, Fernandez Martinez LR, Lopez Rangel JA. Determination by ultrasound of chorionicity in twin pregnancy. Ginecol Obstet Mex. 1997;65:111–3.
94. Benson CB, Doubilet PM. Sonography of multiple gestations. Radiol Clin N Am. 1990;28(1):149–61.
95. Blane CE, DiPietro MA, Johnson MZ, White SJ, Louwsma GI, Hamman JE. Sonographic detection of monoamniotic twins. J Clin Ultrasound. 1987;15(6):394–6.
96. Bracero LA, Byrne DW. Ultrasound determination of chorionicity and perinatal outcome in twin pregnancies using dividing membrane thickness. Gynecol Obstet Investig. 2003;55(1):50–7.
97. Carroll SG, Soothill PW, Abdel-Fattah SA, Porter H, Montague I, Kyle PM. Prediction of chorionicity in twin pregnancies at 10–14 weeks of gestation. BJOG. 2002;109(2):182–6.
98. Cheung A, Wan M, Collins RJ. Differentiation of monochorionic and dichorionic twin placentas by antenatal ultrasonic evaluation. Aust N Z J Obstet Gynaecol. 1990;30(2):134–6.
99. D'Antonio F, Bhide A. Early pregnancy assessment in multiple pregnancies. Best Pract Res Clin Obstet Gynaecol. 2014;28(2):201–14.
100. Egan JF, Borgida AF. Multiple gestations: the importance of ultrasound. Obstet Gynecol Clin N Am. 2004;31(1):141–58.
101. Hubinont C, Santolaya-Forgas J. A systematic approach to first-trimester ultrasound assessment of twins. Am J Perinatol. 2010;27(8):595–8.
102. Kurtz AB, Wapner RJ, Mata J, Johnson A, Morgan P. Twin pregnancies: accuracy of first-trimester abdominal US in predicting chorionicity and amnionicity. Radiology. 1992;185(3):759–62.
103. Monteagudo A, Timor-Tritsch IE, Sharma S. Early and simple determination of chorionic and amniotic type in multifetal gestations in the first fourteen weeks by high-frequency transvaginal ultrasonography. Am J Obstet Gynecol. 1994;170(3):824–9.

104. Tong S, Vollenhoven B, Meagher S. Determining zygosity in early pregnancy by ultrasound. Ultrasound Obstet Gynecol. 2004;23(1):36–7.
105. Devlieger RG, Demeyere T, Deprest JA, Van Schoubroeck D, Witters I, Timmerman D, et al. Ultrasound determination of chorionicity in twin pregnancy: accuracy and operator experience. Twin Res. 2001;4(4):223–6.
106. Levy R, Arfi JS, Mirlesse V, Jacob D. Ultrasonic diagnosis of chorionicity in multiple pregnancies. Gynecol Obstet Fertil. 2003;31(11):960–3.
107. Shetty A, Smith AP. The sonographic diagnosis of chorionicity. Prenat Diagn. 2005;25(9):735–9.
108. Bromley B, Benacerraf B. Using the number of yolk sacs to determine amnionicity in early first trimester monochorionic twins. J Ultrasound Med. 1995;14(6):415–9.
109. Constantine S, Wilkinson C. Double trouble: the importance of reporting chorionicity and amnionicity in twin pregnancy ultrasound reports. J Med Imaging Radiat Oncol. 2015;59(1):66–9.
110. Sepulveda W, Sebire NJ, Hughes K, Odibo A, Nicolaides KH. The lambda sign at 10–14 weeks of gestation as a predictor of chorionicity in twin pregnancies. Ultrasound Obstet Gynecol. 1996;7(6):421–3.
111. Wood SL, St Onge R, Connors G, Elliot PD. Evaluation of the twin peak or lambda sign in determining chorionicity in multiple pregnancy. Obstet Gynecol. 1996;88(1):6–9.
112. Dias T, Arcangeli T, Bhide A, Napolitano R, Mahsud-Dornan S, Thilaganathan B. First-trimester ultrasound determination of chorionicity in twin pregnancy. Ultrasound Obstet Gynecol. 2011;38(5):530–2.
113. Hertzberg BS, Kurtz AB, Choi HY, Kaczmarczyk JM, Warren W, Wapner RJ, et al. Significance of membrane thickness in the sonographic evaluation of twin gestations. AJR Am J Roentgenol. 1987;148(1):151–3.
114. Stagiannis KD, Sepulveda W, Southwell D, Price DA, Fisk NM. Ultrasonographic measurement of the dividing membrane in twin pregnancy during the second and third trimesters: a reproducibility study. Am J Obstet Gynecol. 1995;173(5):1546–50.
115. Vayssiere C, Benoist G, Blondel B, Deruelle P, Favre R, Gallot D, et al. Twin pregnancies: guidelines for clinical practice from the French College of Gynaecologists and Obstetricians (CNGOF). Eur J Obstet Gynecol Reprod Biol. 2011;156(1):12–7.
116. Bora SA, Papageorghiou AT, Bottomley C, Kirk E, Bourne T. Reliability of transvaginal ultrasonography at 7–9 weeks' gestation in the determination of chorionicity and amnionicity in twin pregnancies. Ultrasound Obstet Gynecol. 2008;32(5):618–21.
117. Fisk NM, Bryan E. Routine prenatal determination of chorionicity in multiple gestation: a plea to the obstetrician. Br J Obstet Gynaecol. 1993;100(11):975–7.
118. Sepulveda W, Sebire NJ, Odibo A, Psarra A, Nicolaides KH. Prenatal determination of chorionicity in triplet pregnancy by ultrasonographic examination of the ipsilon zone. Obstet Gynecol. 1996;88(5):855–8.
119. Benirschke K. The biology of the twinning process: how placentation influences outcome. Semin Perinatol. 1995;19(5):342–50.
120. Victoria A, Mora G, Arias F. Perinatal outcome, placental pathology, and severity of discordance in monochorionic and dichorionic twins. Obstet Gynecol. 2001;97(2):310–5.
121. Dorum A, Nesheim BI. Monochorionic monoamniotic twins—the most precarious of twin pregnancies. Acta Obstet Gynecol Scand. 1991;70(4–5):381–3.
122. Landy HJ, Keith L, Keith D. The vanishing twin. Acta Genet Med Gemellol. 1982;31(3–4):179–94.
123. Boklage CE. Survival probability of human conceptions from fertilization to term. Int J Fertil. 1990;35(2):75, 9-80, 1-94.
124. Goldman GA, Dicker D, Feldberg D, Ashkenazi J, Yeshaya A, Goldman JA. The vanishing fetus. A report of 17 cases of triplets and quadruplets. J Perinat Med. 1989;17(2):157–62.
125. Manzur A, Goldsman MP, Stone SC, Frederick JL, Balmaceda JP, Asch RH. Outcome of triplet pregnancies after assisted reproductive techniques: how frequent are the vanishing embryos? Fertil Steril. 1995;63(2):252–7.
126. Landy HJ, Keith LG. The vanishing twin: a review. Hum Reprod Update. 1998;4(2):177–83.
127. Shebl O, Ebner T, Sommergruber M, Sir A, Tews G. Birth weight is lower for survivors of the vanishing twin syndrome: a case-control study. Fertil Steril. 2008;90(2):310–4.
128. Chaveeva P, Wright A, Syngelaki A, Konstantinidou L, Wright D, Nicolaides KH. First-trimester screening for trisomies in pregnancies with vanishing twin. Ultrasound Obstet Gynecol. 2020;55(3):326–31.
129. Huang T, Boucher K, Aul R, Rashid S, Meschino WS. First and second trimester maternal serum markers in pregnancies with a vanishing twin. Prenat Diagn. 2015;35(1):90–6.
130. Vlkova B, Hodosy J. Vanishing twin as a potential source of bias in non-invasive fetal sex determination: a case report. J Obstet Gynaecol Res. 2014;40(4):1128–31.
131. Ong SS, Zamora J, Khan KS, Kilby MD. Prognosis for the co-twin following single-twin death: a systematic review. BJOG. 2006;113(9):992–8.
132. Shek NW, Hillman SC, Kilby MD. Single-twin demise: pregnancy outcome. Best Pract Res Clin Obstet Gynaecol. 2014;28(2):249–63.
133. Bejar R, Vigliocco G, Gramajo H, Solana C, Benirschke K, Berry C, et al. Antenatal origin of neurologic damage in newborn infants. II. Multiple gestations. Am J Obstet Gynecol. 1990;162(5):1230–6.
134. Pharoah PO, Glinianaia SV, Rankin J. Congenital anomalies in multiple births after early loss of a conceptus. Hum Reprod. 2009;24(3):726–31.
135. Posner AC, Klein MA. Fetus papyraceus: recognition and significance. Obstet Gynecol. 1954;3(1):106–10.

136. Jauniaux E, Elkhazen N, Vanrysselberge M, Leroy F. Anatomo-clinical aspects of papyraceus fetus syndrome. J Gynecol Obstet Biol Reprod (Paris). 1988;17(5):653–9.
137. Nevermann L, Hartge R, Rehder H, Schumann K, Stolp W. Particularly small foetus papyraceus after full pregnancy period (author's transl). Z Geburtshilfe Perinatol. 1981;185(3):187–91.
138. Xia YQ, Lyu SP, Zhang J, Chen YT, Gao L, Zhao AD, et al. Development of fetal growth charts in twins stratified by chorionicity and mode of conception: a retrospective cohort study in China. Chin Med J. 2021;134(15):1819–27.
139. Hiersch L, Barrett J, Aviram A, Mei-Dan E, Yoon EW, Zaltz A, et al. Patterns of discordant growth and adverse neonatal outcomes in twins. Am J Obstet Gynecol. 2021;225(2):187.e1–e14.
140. Ashwal E, Hiersch L, Berger H, Aviram A, Zaltz A, Kingdom J, et al. Pathologic basis for the definition of discordant growth in dichorionic twins. Fetal Diagn Ther. 2021;48(4):279–87.
141. Litwinska E, Syngelaki A, Cimpoca B, Sapantzoglou I, Nicolaides KH. Intertwin discordance in fetal size at 11–13 weeks' gestation and pregnancy outcome. Ultrasound Obstet Gynecol. 2020;55(2):189–97.
142. Costa-Castro T, De Villiers S, Montenegro N, Severo M, Oepkes D, Matias A, et al. Velamentous cord insertion in monochorionic twins with or without twin-twin transfusion syndrome: does it matter? Placenta. 2013;34(11):1053–8.
143. Hanley ML, Ananth CV, Shen-Schwarz S, Smulian JC, Lai YL, Vintzileos AM. Placental cord insertion and birth weight discordancy in twin gestations. Obstet Gynecol. 2002;99(3):477–82.
144. Kent EM, Breathnach FM, Gillan JE, McAuliffe FM, Geary MP, Daly S, et al. Placental cord insertion and birthweight discordance in twin pregnancies: results of the national prospective ESPRiT Study. Am J Obstet Gynecol. 2011;205(4):376.e1–7.
145. Drugan A, Johnson MP, Isada NB, Holzgreve W, Zador IE, Dombrowski MP, et al. The smaller than expected first-trimester fetus is at increased risk for chromosome anomalies. Am J Obstet Gynecol. 1992;167(6):1525–8.
146. Li X, Xuan Y, Wang J, Wang L, Papageorghiou AT, Wu Q. Crown-rump length discordance, increased nuchal translucency, and detection of fetal structural anomalies in twin pregnancies in the first trimester: 5 years of experience in a tertiary hospital in China. J Ultrasound Med. 2021; https://doi.org/10.1002/jum.15784.
147. Bhide A, Sankaran S, Sairam S, Papageorghiou AT, Thilaganathan B. Relationship of intertwin crown-rump length discrepancy to chorionicity, fetal demise and birth-weight discordance. Ultrasound Obstet Gynecol. 2009;34(2):131–5.
148. Bora SA, Bourne T, Bottomley C, Kirk E, Papageorghiou AT. Twin growth discrepancy in early pregnancy. Ultrasound Obstet Gynecol. 2009;34(1):38–42.
149. Harper LM, Roehl KA, Odibo AO, Cahill AG. First-trimester growth discordance and adverse pregnancy outcome in dichorionic twins. Ultrasound Obstet Gynecol. 2013;41(6):627–31.
150. Kalish RB, Gupta M, Perni SC, Berman S, Chasen ST. Clinical significance of first trimester crown-rump length disparity in dichorionic twin gestations. Am J Obstet Gynecol. 2004;191(4):1437–40.
151. Khalil A. Re: Crown-rump length discordance in the first trimester: a predictor of adverse outcome in twin pregnancies? M. L. Johansen, A. Oldenburg, S. Rosthoj, J. C. Maxild, L. Rode and A. Tabor. Ultrasound Obstet Gynecol 2014; 43: 277–283. Ultrasound Obstet Gynecol. 2014;43(3):245–6.
152. Fareeduddin R, Williams J III, Solt I, Mirocha JM, Kim MJ, Rotmensch S. Discordance of first-trimester crown-rump length is a predictor of adverse outcomes in structurally normal euploid dichorionic twins. J Ultrasound Med. 2010;29(10):1439–43.
153. Papaioannou GI, Syngelaki A, Maiz N, Ross JA, Nicolaides KH. Prediction of outcome in dichorionic twin pregnancies at 6–10 weeks' gestation. Am J Obstet Gynecol. 2011;205(4):348.e1–5.
154. D'Antonio F, Khalil A, Pagani G, Papageorghiou AT, Bhide A, Thilaganathan B. Crown-rump length discordance and adverse perinatal outcome in twin pregnancies: systematic review and meta-analysis. Ultrasound Obstet Gynecol. 2014;44(2):138–46.
155. Dickey RP, Olar TT, Taylor SN, Curole DN, Rye PH, Matulich EM, et al. Incidence and significance of unequal gestational sac diameter or embryo crown-rump length in twin pregnancy. Hum Reprod. 1992;7(8):1170–2.
156. Johansen ML, Oldenburg A, Rosthoj S, Cohn Maxild J, Rode L, Tabor A. Crown-rump length discordance in the first trimester: a predictor of adverse outcome in twin pregnancies? Ultrasound Obstet Gynecol. 2014;43(3):277–83.
157. Tai J, Grobman WA. The association of crown-rump length discordance in twin gestations with adverse perinatal outcomes. Am J Obstet Gynecol. 2007;197(4):369.e1–4.
158. Harper LM, Weis MA, Odibo AO, Roehl KA, Macones GA, Cahill AG. Significance of growth discordance in appropriately grown twins. Am J Obstet Gynecol. 2013;208(5):393.e1–5.
159. Kutuk MS, Ozgun MT, Dolanbay M, Batukan C, Uludag S, Basbug M. Sonographic findings and perinatal outcome of multiple pregnancies associating a complete hydatiform mole and a live fetus: a case series. J Clin Ultrasound. 2014;42(8):465–71.
160. Arsene E, Clouqueur E, Stichelbout M, Devisme L, Vaast P, Subtil D. Twin pregnancy with complete mole and coexisting fetus: reach fetal viability is possible. J Gynecol Obstet Biol Reprod (Paris). 2015;44(9):887–90.
161. Piura B, Rabinovich A, Hershkovitz R, Maor E, Mazor M. Twin pregnancy with a complete hydatidiform mole and surviving co-existent fetus. Arch Gynecol Obstet. 2008;278(4):377–82.

162. Wee L, Jauniaux E. Prenatal diagnosis and management of twin pregnancies complicated by a co-existing molar pregnancy. Prenat Diagn. 2005;25(9):772–6.
163. Sebire NJ, Foskett M, Paradinas FJ, Fisher RA, Francis RJ, Short D, et al. Outcome of twin pregnancies with complete hydatidiform mole and healthy co-twin. Lancet. 2002;359(9324):2165–6.
164. Lopriore E, Slaghekke F, Vandenbussche FP, Middeldorp JM, Walther FJ, Oepkes D. Cerebral injury in monochorionic twins with selective intrauterine growth restriction and/or birthweight discordance. Am J Obstet Gynecol. 2008;199(6):628.e1–5.
165. Mogra R, Saaid R, Tooher J, Pedersen L, Kesby G, Hyett J. Prospective validation of first-trimester ultrasound characteristics as predictive tools for twin-twin transfusion syndrome and selective intrauterine growth restriction in monochorionic diamniotic twin pregnancies. Fetal Diagn Ther. 2020;47(4):321–7.
166. Pharoah PO. Twins and cerebral palsy. Acta Paediatr Suppl. 2001;90(436):6–10.
167. Sherer DM. Adverse perinatal outcome of twin pregnancies according to chorionicity: review of the literature. Am J Perinatol. 2001;18(1):23–37.
168. Fisk NM, Bajoria R, Wigglesworth J. Twin-twin transfusion syndrome. N Engl J Med. 1995;333(6):388; author reply 388–9.
169. Fratelli N, Prefumo F, Fichera A, Valcamonico A, Marella D, Frusca T. Nuchal translucency thickness and crown rump length discordance for the prediction of outcome in monochorionic diamniotic pregnancies. Early Hum Dev. 2011;87(1):27–30.
170. Matias A, Montenegro N, Areias JC. Anticipating twin-twin transfusion syndrome in monochorionic twin pregnancy. Is there a role for nuchal translucency and ductus venosus blood flow evaluation at 11–14 weeks? Twin Res. 2000;3(2):65–70.
171. Bensouda B, Fouron JC, Raboisson MJ, Lamoureux J, Lachance C, Leduc L. Relevance of measuring diastolic time intervals in the ductus venosus during the early stages of twin-twin transfusion syndrome. Ultrasound Obstet Gynecol. 2007;30(7):983–7.
172. Maiz N, Staboulidou I, Leal AM, Minekawa R, Nicolaides KH. Ductus venosus Doppler at 11 to 13 weeks of gestation in the prediction of outcome in twin pregnancies. Obstet Gynecol. 2009;113(4):860–5.
173. Bamberg C, Hecher K. Update on twin-to-twin transfusion syndrome. Best Pract Res Clin Obstet Gynaecol. 2019;58:55–65.
174. Votava-Smith JK, Habli M, Cnota JF, Divanovic A, Polzin W, Lim FY, et al. Diastolic dysfunction and cerebrovascular redistribution precede overt recipient twin cardiomyopathy in early-stage twin-twin transfusion syndrome. J Am Soc Echocardiogr. 2015;28(5):533–40.
175. Quintero RA, Morales WJ, Allen MH, Bornick PW, Johnson PK, Kruger M. Staging of twin-twin transfusion syndrome. J Perinatol. 1999;19(8 Pt 1):550–5.
176. Slaghekke F, Kist WJ, Oepkes D, Pasman SA, Middeldorp JM, Klumper FJ, et al. Twin anemia-polycythemia sequence: diagnostic criteria, classification, perinatal management and outcome. Fetal Diagn Ther. 2010;27(4):181–90.
177. Kamitomo M, Kouno S, Ibuka K, Oku S, Sueyoshi K, Maeda T, et al. First-trimester findings associated with twin reversed arterial perfusion sequence. Fetal Diagn Ther. 2004;19(2):187–90.
178. Schwarzler P, Ville Y, Moscosco G, Tennstedt C, Bollmann R, Chaoui R. Diagnosis of twin reversed arterial perfusion sequence in the first trimester by transvaginal color Doppler ultrasound. Ultrasound Obstet Gynecol. 1999;13(2):143–6.
179. Slaghekke F, Kist WJ, Oepkes D, Middeldorp JM, Klumper FJ, Vandenbussche FP, et al. TAPS and TOPS: two distinct forms of feto-fetal transfusion in monochorionic twins. Z Geburtshilfe Neonatol. 2009;213(6):248–54.
180. Bornstein E, Monteagudo A, Dong R, Schwartz N, Timor-Tritsch IE. Detection of twin reversed arterial perfusion sequence at the time of first-trimester screening: the added value of 3-dimensional volume and color Doppler sonography. J Ultrasound Med. 2008;27(7):1105–9.
181. Coulam CB, Wright G. First trimester diagnosis of acardiac twins. Early Pregnancy. 2000;4(4):261–70.
182. Moore TR, Gale S, Benirschke K. Perinatal outcome of forty-nine pregnancies complicated by acardiac twinning. Am J Obstet Gynecol. 1990;163(3):907–12.
183. Tan TY, Sepulveda W. Acardiac twin: a systematic review of minimally invasive treatment modalities. Ultrasound Obstet Gynecol. 2003;22(4):409–19.
184. Brizot ML, Liao AW, Lopes LM, Okumura M, Marques MS, Krebs V, et al. Conjoined twins pregnancies: experience with 36 cases from a single center. Prenat Diagn. 2011;31(12):1120–5.
185. Afzal AR, Montero FJ. Conjoined twins. Treasure Island, FL: StatPearls; 2021.
186. Edmonds LD, Layde PM. Conjoined twins in the united states, 1970–1977. Teratology. 1982;25(3):301–8.
187. Baken L, Rousian M, Kompanje EJ, Koning AH, van der Spek PJ, Steegers EA, et al. Diagnostic techniques and criteria for first-trimester conjoined twin documentation: a review of the literature illustrated by three recent cases. Obstet Gynecol Surv. 2013;68(11):743–52.
188. Lam YH, Sin SY, Lam C, Lee CP, Tang MH, Tse HY. Prenatal sonographic diagnosis of conjoined twins in the first trimester: two case reports. Ultrasound Obstet Gynecol. 1998;11(4):289–91.
189. Pajkrt E, Jauniaux E. First-trimester diagnosis of conjoined twins. Prenat Diagn. 2005;25(9):820–6.
190. Sherer DM, Dalloul M, Kheyman M, Zigalo A, Nader I, Sokolovski M, et al. Transvaginal color Doppler imaging diagnosis of thoracopagus conjoined twins at 7 weeks' gestation. J Ultrasound Med. 2006;25(11):1485–7.

191. Brand A, Alves MC, Saraiva C, Loio P, Goulao J, Malta J, et al. Fetus in fetu—diagnostic criteria and differential diagnosis—a case report and literature review. J Pediatr Surg. 2004;39(4):616–8.
192. Jackson OA, Low DW, LaRossa D. Conjoined twin separation: lessons learned. Plast Reconstr Surg. 2012;129(4):956–63.
193. Kobylarz K. History of treatment of conjoined twins. Anaesthesiol Intens Ther. 2014;46(2):116–23.
194. Vermelin H, Facq J. Fetal death in the fourth month by entanglement of the umbilical cords in a case of uniovular twins. Bull Fed Soc Gynecol Obstet Lang Fr. 1952;4(4):755–6.
195. Overton TG, Denbow ML, Duncan KR, Fisk NM. First-trimester cord entanglement in monoamniotic twins. Ultrasound Obstet Gynecol. 1999;13(2):140–2.
196. Hod M, Merlob P, Friedman S, Ovadia J. Single intrauterine fetal death in monoamniotic twins due to cord entanglement. Clin Exp Obstet Gynecol. 1988;15(3):63–5.
197. Belfort MA, Moise KJ Jr, Kirshon B, Saade G. The use of color flow Doppler ultrasonography to diagnose umbilical cord entanglement in monoamniotic twin gestations. Am J Obstet Gynecol. 1993;168(2):601–4.
198. Sherer DM, Sokolovski M, Haratz-Rubinstein N. Diagnosis of umbilical cord entanglement of monoamniotic twins by first-trimester color Doppler imaging. J Ultrasound Med. 2002;21(11):1307–9.
199. Hanaoka U, Tenkumo C, Ito M, Mori N, Tanaka H, Hata T. Three-dimensional surface-rendered imaging of cord entanglement in monoamniotic twins. Arch Gynecol Obstet. 2012;286(4):1091–2.
200. Henrich W, Tutschek B. Cord entanglement in monoamniotic twins: 2D and 3D colour Doppler studies. Ultraschall Med. 2008;29(Suppl 5):271–2.
201. Rosemond RL, Hinds NE. Persistent abnormal umbilical cord Doppler velocimetry in a monoamniotic twin with cord entanglement. J Ultrasound Med. 1998;17(5):337–8.
202. Kofinas AD, Penry M, Hatjis CG. Umbilical vessel flow velocity waveforms in cord entanglement in a monoamnionic multiple gestation. A case report. J Reprod Med. 1991;36(4):314–6.
203. Abuhamad AZ, Mari G, Copel JA, Cantwell CJ, Evans AT. Umbilical artery flow velocity waveforms in monoamniotic twins with cord entanglement. Obstet Gynecol. 1995;86(4 Pt 2):674–7.
204. Hugon-Rodin J, Guilbert JB, Baron X, Camus E. Notching of the umbilical artery waveform associated with cord entanglement in a monoamniotic twin pregnancy. J Matern Fetal Neonatal Med. 2013;26(15):1559–61.
205. Aurioles-Garibay A, Hernandez-Andrade E, Romero R, Garcia M, Qureshi F, Jacques SM, et al. Presence of an umbilical artery notch in monochorionic/monoamniotic twins. Fetal Diagn Ther. 2014;36(4):305–11.
206. Lewi L. Cord entanglement in monoamniotic twins: does it really matter? Ultrasound Obstet Gynecol. 2010;35(2):139–41.
207. Rossi AC, Prefumo F. Impact of cord entanglement on perinatal outcome of monoamniotic twins: a systematic review of the literature. Ultrasound Obstet Gynecol. 2013;41(2):131–5.
208. Hopkins MK, Dugoff L. Screening for aneuploidy in twins. Am J Obstet Gynecol MFM. 2021;4(2S):100499.
209. Bender W, Dugoff L. Screening for aneuploidy in multiple gestations: the challenges and options. Obstet Gynecol Clin N Am. 2018;45(1):41–53.
210. Boyle B, McConkey R, Garne E, Loane M, Addor MC, Bakker MK, et al. Trends in the prevalence, risk and pregnancy outcome of multiple births with congenital anomaly: a registry-based study in 14 European countries 1984–2007. BJOG. 2013;120(6):707–16.
211. Audibert F, Gagnon A, Genetics Committee of the Society of Obstetricians and Gynaecologists of Canada; Prenatal Diagnosis Committee of the Canadian College of Medical Geneticists. Prenatal screening for and diagnosis of aneuploidy in twin pregnancies. J Obstet Gynaecol Can. 2011;33(7):754–67.
212. Matias A, Montenegro N, Blickstein I. Down syndrome screening in multiple pregnancies. Obstet Gynecol Clin N Am. 2005;32(1):81–96. ix
213. Boyle B, Morris JK, McConkey R, Garne E, Loane M, Addor MC, et al. Prevalence and risk of Down syndrome in monozygotic and dizygotic multiple pregnancies in Europe: implications for prenatal screening. BJOG. 2014;121(7):809–19; discussion 20.
214. Linskens IH, Spreeuwenberg MD, Blankenstein MA, van Vugt JM. Early first-trimester free beta-hCG and PAPP-A serum distributions in monochorionic and dichorionic twins. Prenat Diagn. 2009;29(1):74–8.
215. Prats P, Rodriguez I, Nicolau J, Comas C. Early first-trimester free-beta-hCG and PAPP-A serum distributions in monochorionic and dichorionic twins. Prenat Diagn. 2012;32(1):64–9.
216. Spencer K, Kagan KO, Nicolaides KH. Screening for trisomy 21 in twin pregnancies in the first trimester: an update of the impact of chorionicity on maternal serum markers. Prenat Diagn. 2008;28(1):49–52.
217. Madsen HN, Ball S, Wright D, Torring N, Petersen OB, Nicolaides KH, et al. A reassessment of biochemical marker distributions in trisomy 21-affected and unaffected twin pregnancies in the first trimester. Ultrasound Obstet Gynecol. 2011;37(1):38–47.
218. Cimpoca B, Syngelaki A, Litwinska E, Muzaferovic A, Nicolaides KH. Increased nuchal translucency at 11–13 weeks' gestation and outcome in twin pregnancy. Ultrasound Obstet Gynecol. 2020;55(3):318–25.
219. Ben-Ami I, Maymon R, Svirsky R, Cuckle H, Jauniaux E. Down syndrome screening in assisted

conception twins: an iatrogenic medical challenge. Obstet Gynecol Surv. 2013;68(11):764–73.

220. Prats P, Rodriguez I, Comas C, Puerto B. Systematic review of screening for trisomy 21 in twin pregnancies in first trimester combining nuchal translucency and biochemical markers: a meta-analysis. Prenat Diagn. 2014;34(11):1077–83.
221. Spencer K, Staboulidou I, Nicolaides KH. First trimester aneuploidy screening in the presence of a vanishing twin: implications for maternal serum markers. Prenat Diagn. 2010;30(3):235–40.
222. Galeva S, Gil MM, Konstantinidou L, Akolekar R, Nicolaides KH. First-trimester screening for trisomies by cfDNA testing of maternal blood in singleton and twin pregnancies: factors affecting test failure. Ultrasound Obstet Gynecol. 2019;53(6):804–9.
223. Le Conte G, Letourneau A, Jani J, Kleinfinger P, Lohmann L, Costa JM, et al. Cell-free fetal DNA analysis in maternal plasma as a screening test for trisomy 21 in twin pregnancies. Gynecol Obstet Fertil Senol. 2018;46(7–8):580–6.
224. del Mar GM, Quezada MS, Bregant B, Syngelaki A, Nicolaides KH. Cell-free DNA analysis for trisomy risk assessment in first-trimester twin pregnancies. Fetal Diagn Ther. 2014;35(3):204–11.
225. Curnow KJ, Wilkins-Haug L, Ryan A, Kirkizlar E, Stosic M, Hall MP, et al. Detection of triploid, molar, and vanishing twin pregnancies by a single-nucleotide polymorphism-based noninvasive prenatal test. Am J Obstet Gynecol. 2015;212(1):79.e1–9.
226. Campbell KH, Copel JA, Ozan Bahtiyar M. Congenital heart defects in twin gestations. Minerva Ginecol. 2009;61(3):239–44.
227. Glinianaia SV, Rankin J, Wright C. Congenital anomalies in twins: a register-based study. Hum Reprod. 2008;23(6):1306–11.
228. Allen VM, Wilson RD, Cheung A, Genetics Committee; Reproductive Endocrinology and Infertility Committee. Pregnancy outcomes after assisted reproductive technology. J Obstet Gynaecol Can. 2006;28(3):220–33.
229. Schinzel AA, Smith DW, Miller JR. Monozygotic twinning and structural defects. J Pediatr. 1979;95(6):921–30.
230. Syngelaki A, Cimpoca B, Litwinska E, Akolekar R, Nicolaides KH. Diagnosis of fetal defects in twin pregnancies at routine 11–13-week ultrasound examination. Ultrasound Obstet Gynecol. 2020;55(4):474–81.
231. Bahtiyar MO, Dulay AT, Weeks BP, Friedman AH, Copel JA. Prevalence of congenital heart defects in monochorionic/diamniotic twin gestations: a systematic literature review. J Ultrasound Med. 2007;26(11):1491–8.
232. Chen CJ, Wang CJ, Yu MW, Lee TK. Perinatal mortality and prevalence of major congenital malformations of twins in Taipei city. Acta Genet Med Gemellol. 1992;41(2–3):197–203.
233. Machin G. Non-identical monozygotic twins, intermediate twin types, zygosity testing, and the non-random nature of monozygotic twinning: a review. Am J Med Genet C Semin Med Genet. 2009;151C(2):110–27.
234. Silva S, Martins Y, Matias A, Blickstein I. Why are monozygotic twins different? J Perinat Med. 2011;39(2):195–202.
235. Zwijnenburg PJ, Meijers-Heijboer H, Boomsma DI. Identical but not the same: the value of discordant monozygotic twins in genetic research. Am J Med Genet B Neuropsychiatr Genet. 2010;153B(6):1134–49.
236. Turrina S, Bortoletto E, Giannini G, De Leo D. Monozygotic twins: identical or distinguishable for science and law? Med Sci Law. 2021;61(1_Suppl):62–6.
237. Czyz W, Morahan JM, Ebers GC, Ramagopalan SV. Genetic, environmental and stochastic factors in monozygotic twin discordance with a focus on epigenetic differences. BMC Med. 2012;10:93.
238. Singh SM, Murphy B, O'Reilly R. Epigenetic contributors to the discordance of monozygotic twins. Clin Genet. 2002;62(2):97–103.
239. Cheng PJ, Shaw SW, Shih JC, Soong YK. Monozygotic twins discordant for monosomy 21 detected by first-trimester nuchal translucency screening. Obstet Gynecol. 2006;107(2 Pt 2):538–41.
240. Silver IA, Nedelec JL, Segal NL, Lonergan H. Heteropaternal siblings misclassified as dizygotic twins: a potential biasing factor for heritability estimates? Behav Genet. 2021;51(2):137–43.
241. Segal NL, Nedelec JL. Heteropaternal twinning: Unique case of opposite-sex twins with different fathers. Forensic Sci Int. 2021;327:110948.
242. Berkowitz RL. Ethical issues involving multifetal pregnancies. Mt Sinai J Med. 1998;65(3):185–90; discussion 215–23.
243. Malhotra A, Menahem S, Shekleton P, Gillam L. Medical and ethical considerations in twin pregnancies discordant for serious cardiac disease. J Perinatol. 2009;29(10):662–7.
244. Linskens IH, Elburg RM, Oepkes D, Vugt JM, Haak MC. Expectant management in twin pregnancies with discordant structural fetal anomalies. Twin Res Hum Genet. 2011;14(3):283–9.
245. Rodeck CH, Mibashan RS, Abramowicz J, Campbell S. Selective feticide of the affected twin by fetoscopic air embolism. Prenat Diagn. 1982;2(3):189–94.
246. Rustico MA, Baietti MG, Coviello D, Orlandi E, Nicolini U. Managing twins discordant for fetal anomaly. Prenat Diagn. 2005;25(9):766–71.
247. Stewart KS, Johnson MP, Quintero RA, Evans MI. Congenital abnormalities in twins: selective termination. Curr Opin Obstet Gynecol. 1997;9(2):136–9.
248. Alvarado EA, Pacheco RP, Alderete FG, Luis JA, de la Cruz AA, Quintana LO. Selective termination in dichorionic twins discordant for congenital defect. Eur J Obstet Gynecol Reprod Biol. 2012;161(1):8–11.

249. Evans MI, Goldberg JD, Horenstein J, Wapner RJ, Ayoub MA, Stone J, et al. Selective termination for structural, chromosomal, and mendelian anomalies: international experience. Am J Obstet Gynecol. 1999;181(4):893–7.
250. Challis D, Gratacos E, Deprest JA. Cord occlusion techniques for selective termination in monochorionic twins. J Perinat Med. 1999;27(5):327–38.
251. Rossi AC, D'Addario V. Umbilical cord occlusion for selective feticide in complicated monochorionic twins: a systematic review of literature. Am J Obstet Gynecol. 2009;200(2):123–9.
252. Quintero RA, Romero R, Reich H, Goncalves L, Johnson MP, Carreno C, et al. In utero percutaneous umbilical cord ligation in the management of complicated monochorionic multiple gestations. Ultrasound Obstet Gynecol. 1996;8(1):16–22.
253. Lewi L, Gratacos E, Ortibus E, Van Schoubroeck D, Carreras E, Higueras T, et al. Pregnancy and infant outcome of 80 consecutive cord coagulations in complicated monochorionic multiple pregnancies. Am J Obstet Gynecol. 2006;194(3):782–9.
254. Robyr R, Yamamoto M, Ville Y. Selective feticide in complicated monochorionic twin pregnancies using ultrasound-guided bipolar cord coagulation. BJOG. 2005;112(10):1344–8.
255. Paramasivam G, Wimalasundera R, Wiechec M, Zhang E, Saeed F, Kumar S. Radiofrequency ablation for selective reduction in complex monochorionic pregnancies. BJOG. 2010;117(10):1294–8.
256. Rahimi-Sharbaf F, Ghaemi M, Nassr AA, Shamshirsaz AA, Shirazi M. Radiofrequency ablation for selective fetal reduction in complicated monochorionic twins; comparing the outcomes according to the indications. BMC Pregnancy Childbirth. 2021;21(1):189.
257. Okun N, Sierra S, Genetics Committee; Special Contributors. Pregnancy outcomes after assisted human reproduction. J Obstet Gynaecol Can. 2014;36(1):64–83.
258. Luke B. Nutrition in multiple gestations. Clin Perinatol. 2005;32(2):403–29, vii.
259. Buhling KJ, Henrich W, Starr E, Lubke M, Bertram S, Siebert G, et al. Risk for gestational diabetes and hypertension for women with twin pregnancy compared to singleton pregnancy. Arch Gynecol Obstet. 2003;269(1):33–6.
260. Benkő Z, Wright A, Rehal A, Cimpoca B, Syngelaki A, Delgado JL, et al. Prediction of pre-eclampsia in twin pregnancy by maternal factors and biomarkers at 11–13 weeks' gestation: data from EVENTS trial. Ultrasound Obstet Gynecol. 2021;57(2):257–65.
261. Svirsky R, Maymon R, Melcer Y, Klog E, Cuckle H. First and second trimester maternal serum inhibin A levels in twins with pre-eclampsia. Prenat Diagn. 2016;36(11):1071–4.
262. Sibai BM, Hauth J, Caritis S, Lindheimer MD, MacPherson C, Klebanoff M, et al. Hypertensive disorders in twin versus singleton gestations. National Institute of Child Health and Human Development Network of Maternal-Fetal Medicine Units. Am J Obstet Gynecol. 2000;182(4):938–42.
263. Rauh-Hain JA, Rana S, Tamez H, Wang A, Cohen B, Cohen A, et al. Risk for developing gestational diabetes in women with twin pregnancies. J Matern Fetal Neonatal Med. 2009;22(4):293–9.
264. Bar J, Blickstein D, Hod M, Bar-Hava I, Ben-Rafael Z, Rahmany-Babai J, et al. Increased D-dimer levels in twin gestation. Thromb Res. 2000;98(6):485–9.
265. Virkus RA, Lokkegaard E, Lidegaard O, Langhoff-Roos J, Nielsen AK, Rothman KJ, et al. Risk factors for venous thromboembolism in 1.3 million pregnancies: a nationwide prospective cohort. PLoS One. 2014;9(5):e96495.
266. Derbent AU, Yanik FF, Simavli S, Atasoy L, Urun E, Kuscu UE, et al. First trimester maternal serum PAPP-A and free beta-HCG levels in hyperemesis gravidarum. Prenat Diagn. 2011;31(5):450–3.
267. McCarthy FP, Lutomski JE, Greene RA. Hyperemesis gravidarum: current perspectives. Int J Womens Health. 2014;6:719–25.
268. Hall MH, Campbell DM, Davidson RJ. Anaemia in twin pregnancy. Acta Genet Med Gemellol. 1979;28(4):279–82.
269. Rioseco AJ, Ivankovic MB, Manzur A, Hamed F, Kato SR, Parer JT, et al. Intrahepatic cholestasis of pregnancy: a retrospective case-control study of perinatal outcome. Am J Obstet Gynecol. 1994;170(3):890–5.
270. Ohel I, Levy A, Silberstein T, Holcberg G, Sheiner E. Pregnancy outcome of patients with pruritic urticarial papules and plaques of pregnancy. J Matern Fetal Neonatal Med. 2006;19(5):305–8.
271. Elling SV, McKenna P, Powell FC. Pruritic urticarial papules and plaques of pregnancy in twin and triplet pregnancies. J Eur Acad Dermatol Venereol. 2000;14(5):378–81.
272. Simpson KR, Moore KS, LaMartina MH. Acute fatty liver of pregnancy. J Obstet Gynecol Neonatal Nurs. 1993;22(3):213–9.
273. Dey M, Reema K. Acute fatty liver of pregnancy. N Am J Med Sci. 2012;4(11):611–2.
274. Nishida R, Morikawa M, Yamada T, Akaishi R, Yamada T, Minakami H. Liver dysfunction in triplet pregnancies: relation to antenatal changes in antithrombin activity and platelet count. J Obstet Gynaecol Res. 2014;40(12):2177–83.
275. Mok T, Contreras D, Chmait RH, Goldstein J, Pluym ID, Tabsh K, et al. Complicated monochorionic-diamniotic twins in a pregnant woman with COVID-19 in the second trimester. Am J Perinatol. 2021;38(7):747–52.
276. Luke B, Brown MB. Maternal morbidity and infant death in twin vs triplet and quadruplet pregnancies. Am J Obstet Gynecol. 2008;198(4):401.e1–10.
277. Elliott JP. High-order multiple gestations. Semin Perinatol. 2005;29(5):305–11.
278. Ron-El R, Mor Z, Weinraub Z, Schreyer P, Bukovsky I, Dolphin Z, et al. Triplet, quadruplet and quintuplet

pregnancies. Management and outcome. Acta Obstet Gynecol Scand. 1992;71(5):347–50.

279. Seoud MA, Toner JP, Kruithoff C, Muasher SJ. Outcome of twin, triplet, and quadruplet in vitro fertilization pregnancies: the Norfolk experience. Fertil Steril. 1992;57(4):825–34.
280. Guilherme R, Drunat S, Delezoide AL, Oury JF, Luton D. Zygosity and chorionicity in triplet pregnancies: new data. Hum Reprod. 2009;24(1):100–5.
281. Peress DA, Peaceman AM, Yee LM. Evaluation of trichorionic versus dichorionic triplet gestations from 2005 to 2016 in a large, referral maternity center. Am J Perinatol. 2017;34(6):599–605.
282. Adegbite AL, Ward BS, Bajoria R. Perinatal outcome of quadruplet pregnancies in relation to chorionicity. J Perinatol. 2007;27(1):15–21.
283. Gonen R, Heyman E, Asztalos EV, Ohlsson A, Pitson LC, Shennan AT, et al. The outcome of triplet, quadruplet, and quintuplet pregnancies managed in a perinatal unit: obstetric, neonatal, and follow-up data. Am J Obstet Gynecol. 1990;162(2):454–9.
284. Albrecht JL, Tomich PG. The maternal and neonatal outcome of triplet gestations. Am J Obstet Gynecol. 1996;174(5):1551–6.

16

First-Trimester Ultrasound: Early Pregnancy Failure

Timothy P. Canavan and Joan M. Mastrobattista

Introduction

Ultrasound imaging introduced almost four decades ago opened up a visual window for pregnancy inspection. With the development of higher-frequency endovaginal probes, sonologists were able to study the progression of first-trimester pregnancies in great detail. Markers of successful pregnancy as well as signs of pregnancy failure were defined. In this chapter, current medical evidence relating to imaging and diagnosis of first-trimester pregnancy failure is reviewed. We emphasize that no single finding can substitute for clinical judgment when examining and interpreting available data. Most pregnancy failures present with more than a single sonographic or biochemical finding.

Definitions

- **First-trimester pregnancy failure** (pregnancy failure): lack of sonographic evidence of present or expected viability
- **Threatened abortion**: vaginal bleeding in a viable pregnancy up to 20 weeks gestation in the presence of a long, closed cervix
- **Completed abortion**: complete passage of the embryo, amnion and chorion
- **"Missed abortion"**: it is terminology not currently recommended since it does not adequately describe the pathophysiologic events [1]
- **Anembryonic pregnancy**: an abnormal pregnancy composed of a gestational sac without evidence of an embryo when one is expected
- **Embryonic demise**: presence of an embryo without cardiac activity when cardiac activity is expected

Risk Factors for Failure

Numerous risk factors are associated with first-trimester pregnancy loss; however, 40–50% of losses are unexplained. Medical risk factors for pregnancy loss are listed in Table 16.1. Clinical factors associated with an increased risk for pregnancy failure include increased age at first menses, lower beta human chorionic gonadotropin (β-hCG) levels, lower progesterone levels, and vaginal bleeding [2–4]. Demographic character-

T. P. Canavan (✉)
Division of Maternal Fetal Medicine, Department of Obstetrics and Gynecology, University of Pittsburgh School of Medicine, UPMC Pinnacle,
Harrisburg, PA, USA
e-mail: canavan@upmc.edu

J. M. Mastrobattista
Division of Maternal Fetal Medicine, Department of Obstetrics and Gynecology, Baylor College of Medicine, Houston, TX, USA
e-mail: mastroba@bcm.edu

© The Author(s), under exclusive license to Springer Nature Switzerland AG 2023
J. S. Abramowicz, R. E. Longman (eds.), *First-Trimester Ultrasound*,
https://doi.org/10.1007/978-3-031-24133-8_16

Table 16.1 Medical risk factors associated with first-trimester pregnancy failure

Known etiologies	Possible etiologies
Parental chromosomal abnormality	Environmental exposures
Untreated hypothyroidism	Heritable and/or acquired thrombophilias
Uncontrolled diabetes mellitus	Infection
Septated congenital uterine anomaly	Maternal alcoholism
Asherman's syndrome	Polycystic ovarian syndrome
Antiphospholipid syndrome	

istics that have been linked to pregnancy failure include advanced maternal age, cigarette smoking, and a history of pregnancy loss. Stern and associates prospectively followed 83 pregnancies from 4 to 12 weeks of gestation and found that women with at least two prior spontaneous abortions were almost four times more likely to have a pregnancy failure after documentation of cardiac activity at 6 weeks compared to subjects without a history of recurrent pregnancy loss [5].

Chemical Evidence of Pregnancy Failure

There is very little evidence to support biochemical screening for pregnancy viability. Studies evaluating pregnancy-associated plasma protein A (PAPP-A), estriol, α-fetoprotein, and inhibin A did not find statistical association with a change in these markers and early pregnancy loss. However, β-hCG and progesterone levels may have a direct relationship with early pregnancy maturation. Several studies have reported a mathematical relationship between rising β-hCG levels and "normal" pregnancy maturation. Kadar and associates reported that a 66% rise in the β-hCG level in 48 h is associated with a normal intrauterine pregnancy [6]. However, significant weaknesses are noted in the study sample size and methodology rendering this conclusion unreliable. The study was based on only 20 patients who were sampled inconsistently at 1- to 5-day intervals, and the 48-h interval was determined after lowering the confidence interval to 85%. A more recent study by Barnhart and associates found β-hCG increased by 24% in 1 day and 53% by 2 days; however, their sampling interval was also inconsistent, varying between 1 and 7 days, raising concerns about the reproducibility of their results [7]. Although the trend of a rising β-hCG titer may not reliably predict a viable pregnancy, a low β-hCG titer with an "empty" gestational sac should raise concern for pregnancy failure [8]. Low progesterone levels have also been associated with an increased risk for pregnancy failure [3, 9]. This association increases significantly as progesterone levels fall below 30 nmol/L [3]. The association of pregnancy failure is strongest when correlating a woman's age and gestational sac size. Failure increases with advancing maternal age and increased sac size [3].

Multiple studies have attempted to determine a level of β-hCG at which a normal intrauterine pregnancy should be identified on ultrasound, frequently referred to as the discriminatory level. By transvaginal ultrasound (TVS), this discriminatory level was determined to be 1000 mIU/mL by some authors to 2000 mIU/mL by others [10]. This discriminatory level is defined as the threshold between an abnormal (spontaneous abortion or ectopic) and a normal intrauterine pregnancy. Doubilet and Benson reported the highest β-hCG that proceeded visualization of an intrauterine pregnancy by TVS and an eventual term live newborn as 4336 mIU/mL. They concluded that the β-hCG discriminatory level should not be used solely to determine first-trimester pregnancy management [10]. Therefore, a β-hCG discriminatory level is not a reliable marker for predicting pregnancy failure or an abnormal pregnancy.

Ultrasound Characteristics of Early Pregnancy

Events in early pregnancy follow a predictable sequence as documented by transvaginal sonography (see Chap. 7 for details). A gestational sac is the first identifiable sonographic sign of pregnancy at approximately 5 weeks from the last menstrual period. The gestational sac is a small cystic structure, eccentrically located within the uterine cavity as a result of implantation within the endometrial lining. The sac is circular and well defined without any visible contents. By 5 weeks, 3 days, a yolk sac can be visualized as a round structure, usually eccentrically located. An embryo is first noted adjacent to the yolk sac around 6 week's gestation. At this point, a fetal heart rate may be visualized. The embryo continues to increase in size and slowly takes on a more fetal form as it approaches 10 weeks of gestation with the crown-rump length increasing approximately 1 mm/day.

Imaging of the Early Pregnancy

The appearance and location of a first-trimester pregnancy are best imaged using a high-frequency transvaginal probe. With the transvaginal approach, the ultrasound probe is in close proximity to the pregnancy, allowing for excellent resolution. High-resolution imaging provides the necessary detail to visualize an early yolk sac, visualize and measure cardiac activity (by M-mode), and obtain an accurate crown-rump length measurement at an early gestational age. A transvaginal exam does not require a full bladder and in addition allows for an assessment of the adnexa and ovaries.

Ultrasound Evidence of Pregnancy Failure

Gestational Sac

The location and appearance of the gestational sac provide vital clues as to the likelihood of pregnancy failure. On initial sonographic evaluation, the location of the gestational sac is important to document and helps determine future viability and risk for pregnancy loss, as well as maternal morbidity, specifically from obstetrical hemorrhage if ectopic. The relationship of the sac to the cornual regions and to the cervix or prior uterine scar should be documented.

Location

Gestational sacs located in the extremes (cornua or cervix) of the uterine cavity will tend to be abnormal and either fail or need to be removed due to their risk for rupture and hemorrhage. Implantation in the cornual regions requires close observation with serial examinations. Those implanted on the cavity side of the tubal ostia, referred to as subcornual, will tend to grow into the uterine cavity and proceed normally (Fig. 16.1a, b). Those within the interstitial portion of the tube will be cornual ectopic pregnancies and need additional therapy (Fig. 16.2). Implantations close to or in the endocervical canal tend to fail due to the poor vascular infrastructure; however, some will persist, becoming cervical ectopic pregnancies (Fig. 16.3). Cervical ectopic pregnancies will eventually rupture and/or hemorrhage risking significant maternal morbidity. Identification of the gestational sac low within the uterine cavity is associated with an increased risk for failure. Nyberg and coworkers assessed gestational sac location. They reported that when a gestational sac is located within the lower uterine segment, the risk for pregnancy failure is increased with a sensitivity and positive predictive value (PPV) of 20% and 94% [11].

Appearance

The first sign of pregnancy identified by ultrasound is the gestational sac which is a round, anechoic cystic structure with an echogenic wall eccentrically located within the endometrial lining (Fig. 16.4a). The sac is usually identified when it reaches 2–3 mm in size in the fourth week of gestation. Gestational sac size is reported as a mean sac diameter (an average of the sagittal, transverse, and anteroposterior diameters of the sac). The appearance and size of the sac are important sonographic predictors of early pregnancy failure.

A centrally located cystic structure with a thin wall usually represents pseudogestational sac, a fluid collection within the uterine cavity, rather than a gestational sac (Fig. 16.4b). A pseudogestational sac can be seen when the pregnancy is located outside of the uterine cavity as with a tubal or cervical ectopic pregnancy. It tends to be

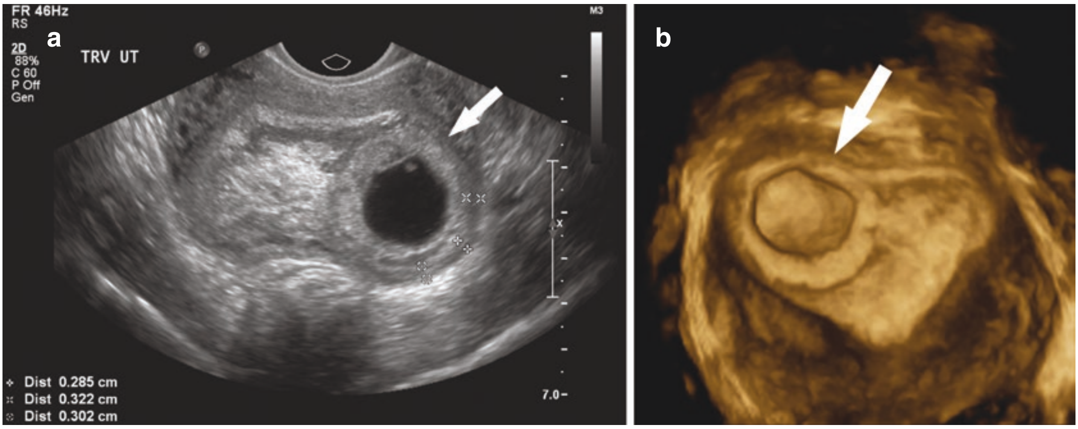

Fig. 16.1 (**a**) Subcornual implantation. A transvaginal, axial, fundal image of a subcorneal implantation of a 5 week 0 day gestational sac is depicted. (**b**) Subcornual implantation. In this 3D-rendered transverse image of the same pregnancy depicted in (**a**), the subcornual implantation is identified by the arrow

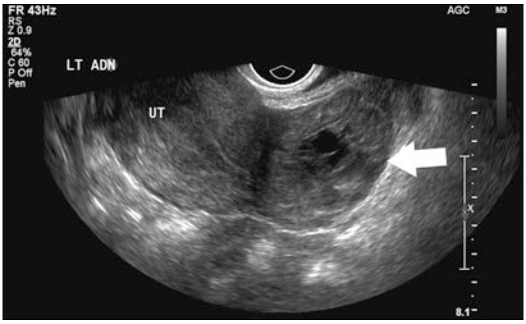

Fig. 16.2 Ectopic pregnancy. A cornual ectopic pregnancy (arrow) at 6 week 3 day is shown in this transverse image of the right uterine cornua

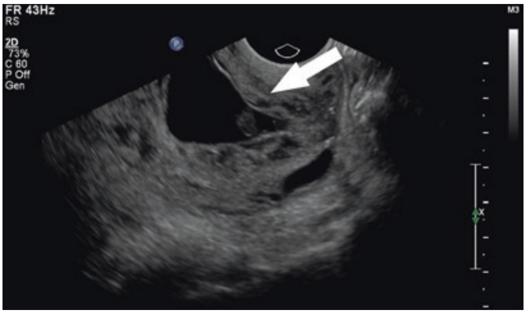

Fig. 16.3 Cervical ectopic pregnancy. A 7 week 6 day cervical ectopic pregnancy is depicted by the arrow in this midsagittal view of the cervix

"tear drop"-shaped and lacks the expected echogenic rim of a gestational sac and may contain debris. If a pseudogestational sac is suspected, further imaging is necessary to identify a possible ectopic pregnancy.

Although there is little research to predict outcome, gestational sacs that appear collapsed or contain a significant amount of debris are at high risk for pregnancy failure (Fig. 16.4c). These pregnancies may be anembryonic or may represent a recent embryonic demise. The debris may be the result of a recent hemorrhage. Careful examination of the sac for evidence of a yolk sac and/or embryo is required since the debris may mask these structures.

Nyberg and associates analyzed the appearance of the gestational sac in 168 subjects and found that a thin decidual reaction (≤2 mm), a weakly echogenic decidual reaction, and an irregular sac contour had a PPV for pregnancy failure of 96%, 98%, and 97%, respectively [11]. Moreover, the authors' report that a gestational sac located in the lower uterine segment has a PPV of 94% for pregnancy failure (Fig. 16.5). A distorted gestational sac shape had the highest PPV for pregnancy failure at 100%. Although the PPV was high, the sensitivity of these findings was low, ranging from 10% for a distorted shape to 53% for a weak echogenic decidual reaction (Fig. 16.6).

Several investigators have noted that the early gestational sac forms a cystic echogenic complex which expands into the uterine cavity and is outlined by the echogenic decidual tissue. This

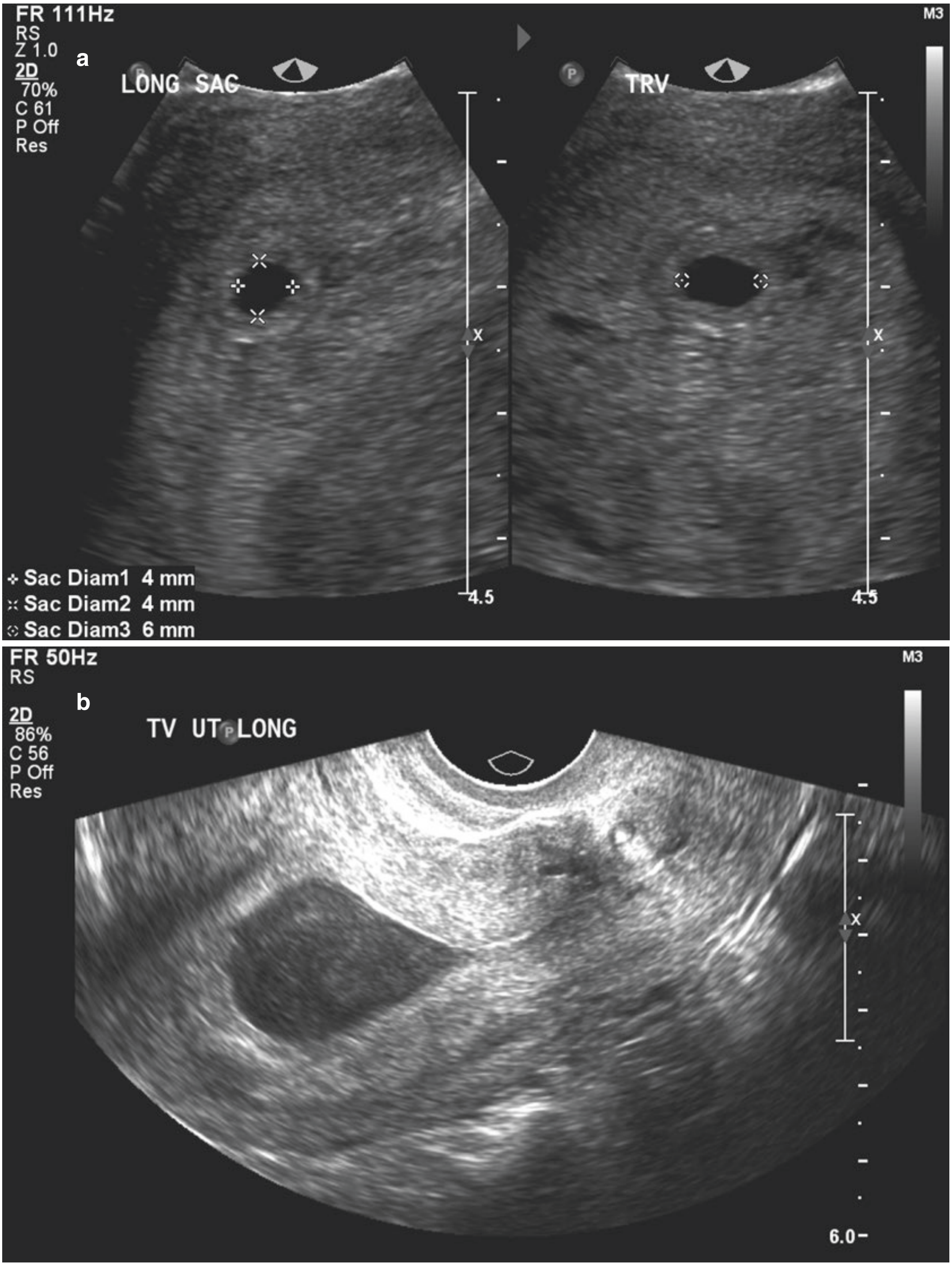
a
FR 111Hz
RS
Z 1.0
2D
70%
C 61
P Off
Res
LONG SAC
TRV
M3
4.5
4.5
Sac Diam1 4 mm
Sac Diam2 4 mm
Sac Diam3 6 mm
b
FR 50Hz
RS
2D
86%
C 56
P Off
Res
TV UT LONG
M3
6.0

Fig. 16.4 Early gestational sacs. (**a**) A normal 4 week 1 day gestational sac is shown in the longitudinal and axial transvaginal images. Note the "donut"-shaped ring around the gestational sac known as a double decidual sac sign. (**b**) Transvaginal, midsagittal image of a pregnancy pseudosac within the uterine cavity is depicted with an ectopic pregnancy (not shown) at 5 weeks 2 days gestation. (**c**) Longitudinal and transverse images of an abnormal "tear drop"—shaped gestational sac with an abnormal-appearing yolk sac at 5 weeks 5 days gestation

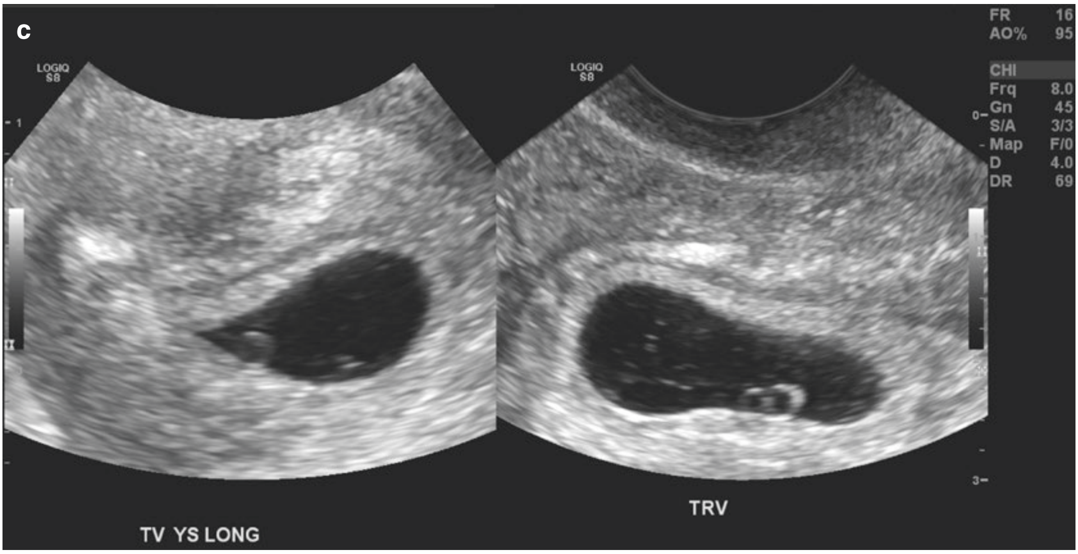

Fig. 16.4 (continued)

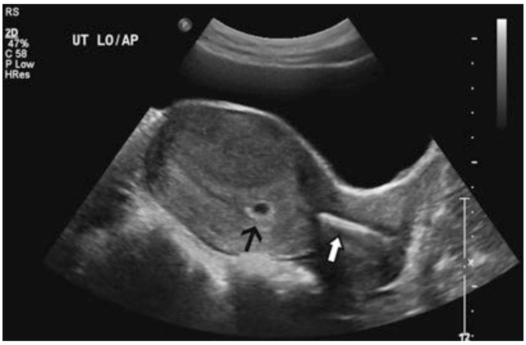

Fig. 16.5 Abnormally positioned gestational sac. This is a midsagittal, transabdominal image of a 5 week 0 day gestational sac implanted in the lower uterine segment portion (solid black arrow) of the uterine cavity with an intrauterine contraceptive device in the endocervical canal (white arrow)

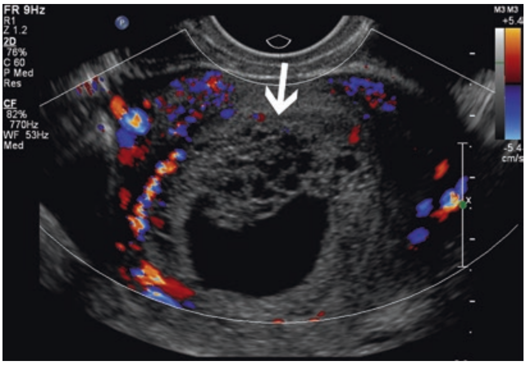

Fig. 16.6 Irregular gestational sac. A transvaginal, axial image is shown depicting an irregular 7 week 5 day gestational sac in a failed pregnancy found to be triploidy by karyotype. Note the cystic (hydropic) placenta (arrow) sometimes seen in triploidy

sonographic appearance has been referred to as the double decidual sac sign (DDS), and studies have advocated the absence of this sign as a predictor of pregnancy failure (see Fig. 16.4a). Nyberg and associates found that the absence of the DDS has a PPV of pregnancy failure of 94%. Bradley and colleagues reported the utility of the DDS in differentiating an ectopic pregnancy from an early intrauterine pregnancy but found that the DDS was a poor predictor for pregnancy failure [11, 12]. Doubilet and Benson describe poor interobserver agreement for the presence of a DDS ($\kappa = 0.24$) and note that first-trimester outcome was unrelated to the presence of a DDS [13].

Yeh and associates described another early sonographic sign of pregnancy. They reported that the early gestational sac is implanted within thickened decidua on one side of the uterine cavity, and the combination of these sonographic findings was coined the intradecidual sign (IDS) [14] (Fig. 16.7). The IDS was identified in 92%

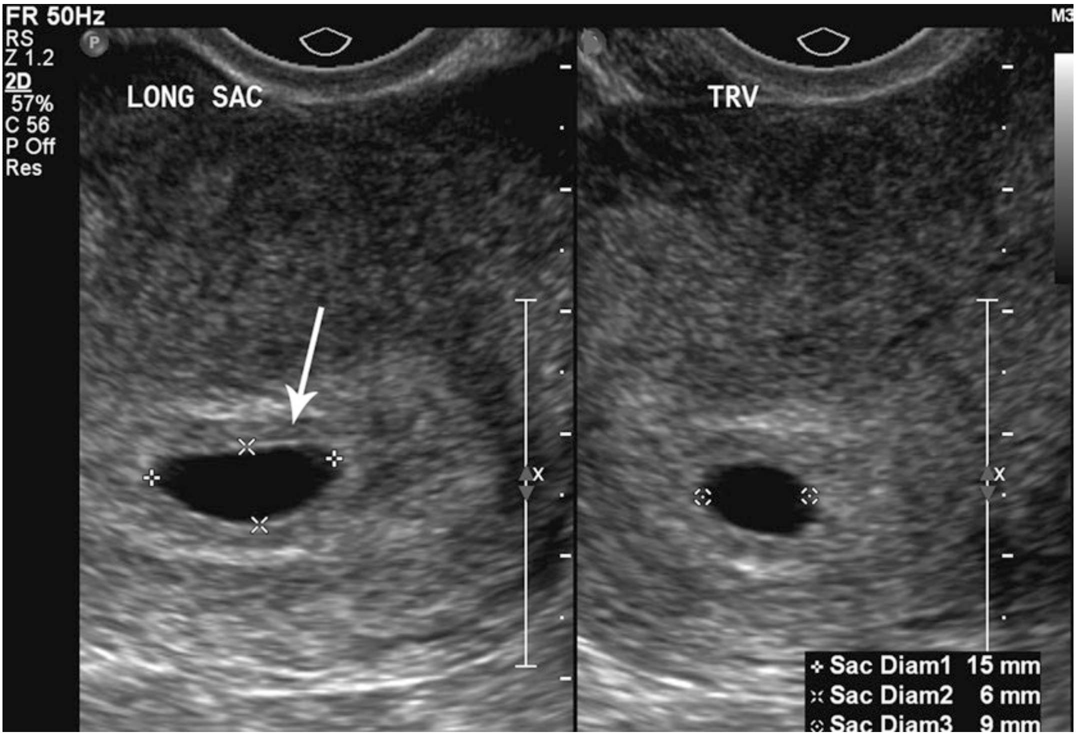

Fig. 16.7 Intradecidual sign. A transvaginal, axial image of a 5 week 1 day gestational sac with an intradecidual sign (arrow) is shown

of intrauterine pregnancies as early as 25 days of gestation, yielding a sensitivity and specificity of 92% and 100%. Laing and associates found the IDS to have a sensitivity and specificity of 34–66% and 55–73% to predict an intrauterine pregnancy, respectively, with poor interobserver agreement [15]. The overall accuracy for predicting an intrauterine pregnancy was only 45%. Chaing and colleagues revisited the utility of an IDS for determination of an intrauterine pregnancy and found more favorable sensitivity, specificity, accuracy, and interobserver agreement (kappa statistic) of 70%, 100%, 75%, and 0.79%, respectively [16]. Doubilet and Benson also investigated the IDS as a sign of a viable intrauterine pregnancy and found poor interobserver agreement with a kappa statistic of 0.23. They found no statistically significant relationship between the presence of an IDS and viability at the end of the first trimester [13]. Based on the present literature, the DDS and IDS are often not visualized or are difficult to discern, and the ultimate pregnancy outcome seems unrelated to the presence of these two findings. Given the poor agreement among investigators, these signs do not appear predictive of pregnancy success or failure.

Size/Growth

The most predictive criterion for identifying a failed pregnancy is the presence of a large gestational sac for expected age that does not contain an embryo. Several studies have investigated a critical value for the minimal mean sac diameter above which a normal embryo should reliably be identified by TVS. Initial studies suggested a cut-off of 16 mm but were based on small numbers [17]. Other studies identified empty gestational sacs with a mean sac diameter between 17 and 21 mm that subsequently were found to be viable pregnancies [18, 19]. Pexsters and associates found the interobserver error in the measurement of the mean sac diameter to be ±19% [20]. Considering the results of these studies, a 21-mm mean sac diameter by one observer could be as high as 25 mm as measured by a second observer. Therefore, a mean gestational sac diameter of 25 mm, in the absence of an embryo, would be the best diagnostic cutoff for a failed pregnancy (Fig. 16.8).

A normal gestational sac grows approximately 1 mm per day during the first trimester (Fig. 16.9) [21]. However, predicting pregnancy failure by subnormal sac growth is not reliable [22]. Usual timing of early pregnancy events (±0.5 weeks) includes visualization of the gestational sac by 4.5 weeks, yolk sac by 5.5 weeks, and an embryo with cardiac activity by 6 weeks, but variation exists. A single examination at 6 weeks that does not demonstrate an embryo with cardiac activity is not diagnostic of pregnancy failure especially if the pregnancy is dated by the menstrual cycle, which is frequently unreliable. A second examination is recommended to confirm pregnancy failure. Once a gestational sac is visualized within the uterus, an embryo with cardiac activity should be identified sonographically within 14 days. If a gestational sac and yolk sac are visualized, an embryo with cardiac activity should be seen within 11 days [23, 24]. Failure to meet these milestones would be suggestive of pregnancy failure.

Prognosis of a Gestational Sac

The identification of a gestational sac within the uterine cavity does not confirm pregnancy viability but starts the process of determining viability. Doubilet et al. assessed 590 very early pregnancies to develop a logistic regression viability prediction model and found that the mean sac diameter (MSD), patient's age, hCG rise, and vaginal bleeding correlate with first-trimester pregnancy outcome [25]. The hCG rise was considered when 2 values were available before the ultrasound and the first measured less than 5000 mIU/mL. The rise was considered appropri-

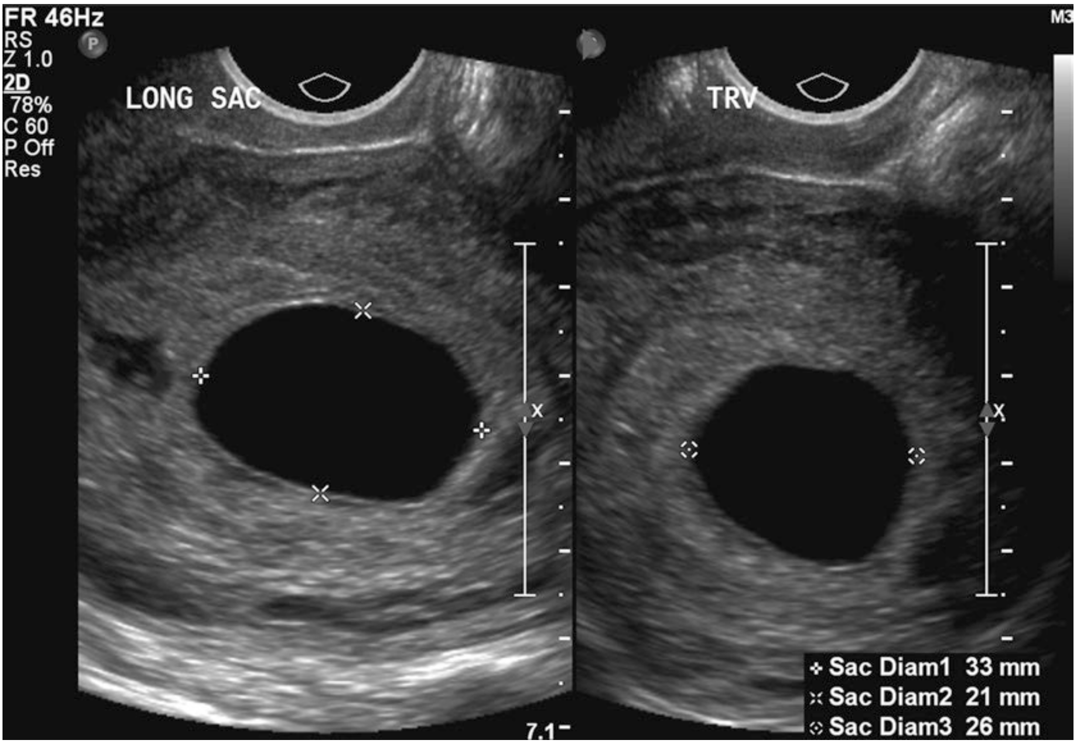

Fig. 16.8 Large, empty gestational sac. This is a transvaginal, axial image of an empty 7 week 5 day gestational sac with a mean sac diameter of 27 mm, indicating a failed pregnancy

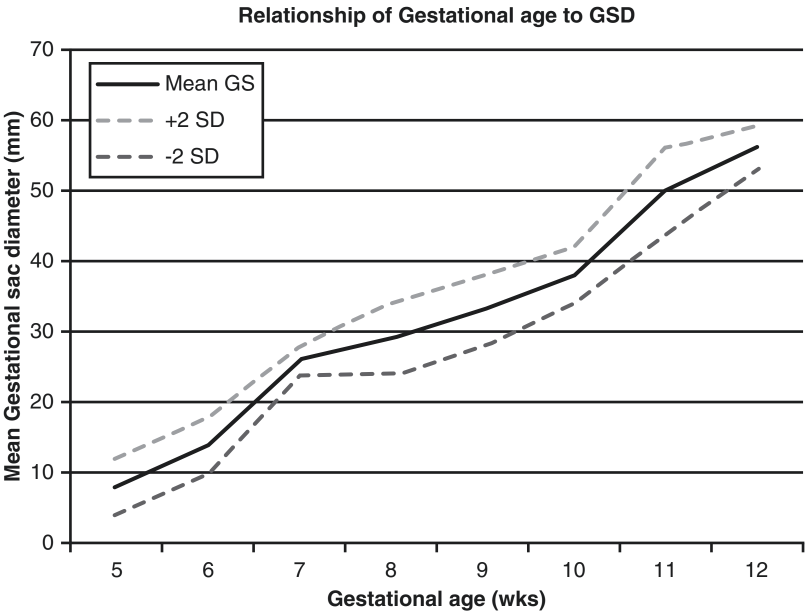

Fig. 16.9 Graph depicts the mean gestational sac diameter in mm ± 2 standard deviations compared to the gestational age in weeks created with data from [24]

ate when the value was noted to double within 2 days; otherwise, it was considered suboptimal. Vaginal bleeding was either present or absent. The probability of a good first-trimester outcome, P, is $e^X/1 + e^X$ where X is defined as:

-1.90 (MSD) $-$ 0.102 (age) $-$ 1.281 (VB) + 1.380 (hCG appropriate) $-$ 2.017 (hCG not appropriate) + 4.383 with VB (vaginal bleeding) = 1 for yes and 0 = no; hCG = 0 if not available. Doubilet and associates provide an online calculator at https://tinyurl.com/Prognosis-PD for the probability of a good first-trimester pregnancy outcome.

Amnion

The amniotic cavity is a space between the cytotrophoblast and the embryonic disc, which is lined by amnion cells. The amnion is usually visualized near the same time as the embryo (approximately 6.5 weeks). During the early first trimester (6.5–10 weeks), the diameter of the amniotic cavity is approximately equal to the embryonic crown-rump length (amniotic diameter = 1.1 × CRL − 0.07) [26]. A small or nonvisualized embryo in a well-formed amniotic cavity is suggestive of a failed pregnancy. Horrow found that a CRL/amniotic cavity difference greater than 0.48 cm (0.86 ± 0.38 cm) was associated with pregnancy failure. McKenna and associates reported that an "empty amnion" (defined as a visible amnion without an embryo) was always associated with pregnancy failure (Fig. 16.10) [27]. Yegul and colleagues described that a visible amnion with an identifiable embryo (less than 5.4 mm) without cardiac activity was associated with pregnancy failure. This finding was referred to as the "expanded amnion sign," and in their analysis, this sign had a PPV of 100% [28]. A further study by this group found that visualization of an amniotic cavity without evidence of an embryo (referred to as the "empty amnion sign"), confirmed pregnancy failure regardless of the gestational sac size with a PPV of 100% [29].

Placenta/Chorionic Frondosum

The chorion is formed from mesoderm and trophoblasts and becomes the wall of the chorionic cavity. The chorionic cavity is the anechoic fluid collection in which the embryo, amnion, and yolk sac are suspended and grow, and is measured as the "gestational sac." The cavity is even-

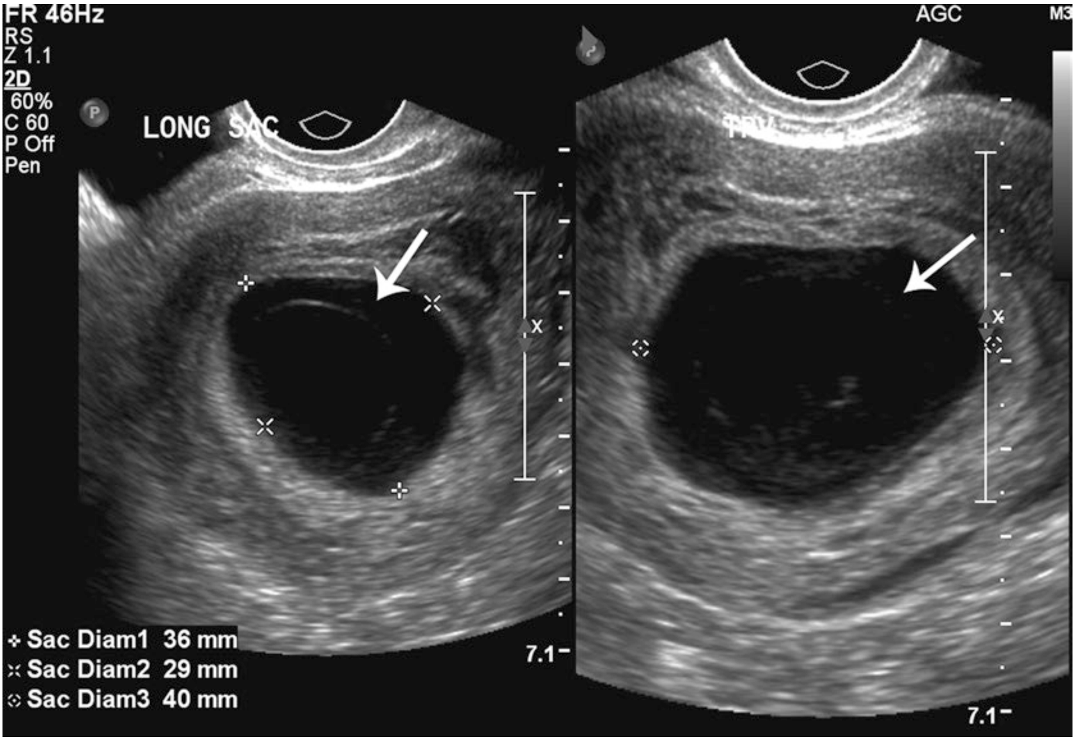

Fig. 16.10 Empty amnion. An empty amnion at 6 weeks 6 days gestation is shown (arrows) in this transvaginal, axial view of the uterus

tually obliterated by the expanding amnion, resulting in the single amniotic cavity.

The most significant concern for the chorion is hematoma formation. Bleeding during the first trimester of pregnancy is one of the most common obstetrical complications, occurring in approximately 14% of all pregnancies [30]. This bleeding can result in hematoma formation of the subchorion. Multiple studies have linked subchorionic hematomas (SCH) with both early and late adverse pregnancy outcomes. The definition of a hematoma is not always clearly defined, but the majority of investigators recognize a hematoma as a crescent-shaped, hypoechoic fluid collection behind the fetal membranes and/or the placenta. Hematomas may be subchorionic (between the chorion and myometrium) or retroplacental (behind the placenta) and frequently become filled with debris as they age [31, 32] (Fig. 16.11a, b).

Vaginal Bleeding

Falco and associates followed 270 pregnant women with vaginal bleeding between 5 and 12 weeks of gestation and found that 17% developed SCHs. Pregnancy failure ranged from 6% to 84%, depending on the presence of other factors such as the gestational sac CRL difference, menstrual sonographic age difference, and the embryonic heart rate [2]. They found that the fetal heart rate was the most powerful predictor of pregnancy outcome in their linear regression model, with a low heart rate (less than 1.2 SDs which is 94 beats per minute at 6 weeks gestation to 124 beats per minute at 10 weeks gestation) increasing the risk for pregnancy failure. Borlum et al. followed 380 women with vaginal bleeding and found an 11.3% increased pregnancy loss rate in the presence of a Scheme [33]. Schauberger and colleagues found that 14% of women with a con-

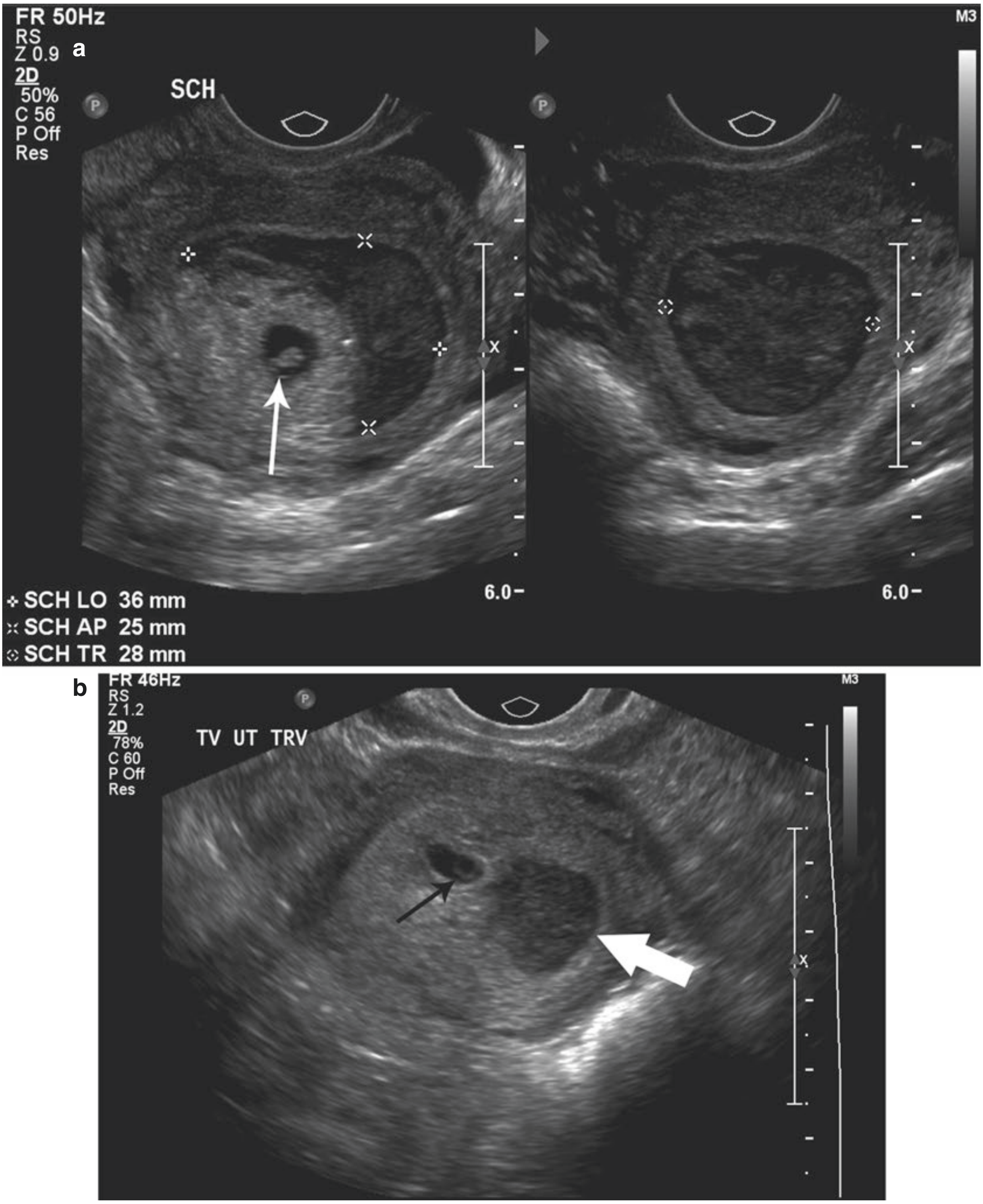
a
FR 50Hz
RS
Z 0.9
2D
50%
C 56
P Off
Res
SCH
M3
6.0
6.0
SCH LO 36 mm
SCH AP 25 mm
SCH TR 28 mm
b
FR 46Hz
RS
Z 1.2
2D
78%
C 60
P Off
Res
TV UT TRV
M3

Fig. 16.11 (**a**) Subchorionic hematoma. A large subchorionic hematoma is denoted by calipers in this transvaginal, axial image at 5 weeks 5 days gestation, showing an early embryonic pole (arrow). (**b**) Subchorionic hematoma. This transvaginal, axial image shows a subchorionic hematoma (thick white arrow) in a 5 week 0 day gestation with a normal-appearing yolk sac (thin black arrow) firmed viable pregnancy by ultrasound performed for vaginal bleeding experienced pregnancy failure by 20 weeks gestation [34]. Additional studies in women with first-trimester vaginal bleeding have reported similar results of both early pregnancy failure and pregnancy loss up to 20 weeks gestation [35].

Hematoma

Multiple studies have investigated the risk of pregnancy loss after the identification of a SCH and the findings are mixed. Additionally, there is crossover between women with first-trimester vaginal bleeding and those in which hematoma formation is actually confirmed by ultrasound. Comparison of these studies is limited by the varied methodologies and study design limitations (small sample size, lack of a control group, limited description, and analysis of patient characteristics and publication bias) [36, 37]. The rate of SCH ranged from 0.5% to 20% in these studies, and while studies by Pedersen et al. and Stabile et al. found no association of SCH to pregnancy failure, other studies by Borlum et al. and Maso et al. found at least a twofold increased risk [33, 35, 38, 39]. Most studies did not find any statistical relationship between the hematoma volume and adverse outcome; however, Maso et al. found that the overall risk for spontaneous abortion was 2.4 times higher when the hematoma was identified before 9 weeks of gestation [35]. One of the largest studies by Ball and coworkers evaluated 238 subjects with a SCH and found a 2.8-fold increased risk of spontaneous abortion (a loss before 20 weeks gestation) [32]. In those subjects with a SCH, vaginal bleeding increased the risk of spontaneous abortion compared to subjects without vaginal bleeding but findings did not reach statistical significance ($p = 0.057$) [32]. A systematic review and meta-analysis by Tuuli and coworkers calculated a 2.2-fold increased risk of spontaneous abortion in the presence of a Scheme [36]. Based on these findings, it is reasonable to assume that a SCH is associated with a twofold increased risk for pregnancy failure.

Chorionic Bump

Harris and colleagues studied the association of a round avascular mass extending from the choriodecidual surface into the gestational sac described as a chorionic bump, with first-trimester pregnancy outcome [40] (Fig. 16.12a, b). They hypothesized that chorionic bumps represent choriodecidual hemorrhages and reported that the chorionic bump was associated with a fourfold increased risk for pregnancy loss, mostly in the first trimester. Sana et al. performed a retrospective case-controlled trial and found that a chorionic bump identified in the first trimester had approximately double the risk of pregnancy loss compared to matched controls. Neither study found a statistically significant relationship between the size or location of the chorionic bump and the risk of pregnancy loss [41].

Vascular Pattern

Once a gestational sac is visualized, uteroplacental circulation can be identified in most viable pregnancies (Fig. 16.13). Moving echoes within the 8- to 11-week placenta detected by gray scale imaging is noted more frequently in those with pregnancy failure compared to viable pregnancies (88–100% vs. 36–60%, $p < 0.01–0.001$) [42]. In women with pregnancy failure, the placenta tends to have a mottled appearance due to numerous centrally located venous lakes (Fig. 16.14). Wherry and colleagues found that low-resistance arterial endometrial blood flow is associated with trophoblastic tissue but could not discriminate between a viable pregnancy and pregnancy failure [43]. Jaffe et al. prospectively followed color Doppler interrogation of the decidual spiral arteries and the intervillous space in 100 women at 7–12 weeks gestation and recorded pregnancy outcomes [44]. Thirteen women had pregnancy failure in the first trimester and six had second trimester medical complications including hypertension, preeclampsia, and diabetes. Abnormal color Doppler imaging was defined as active blood flow in the intervillous space and a resistive index >0.55 in the spiral arteries. A reassessment of their data targeting

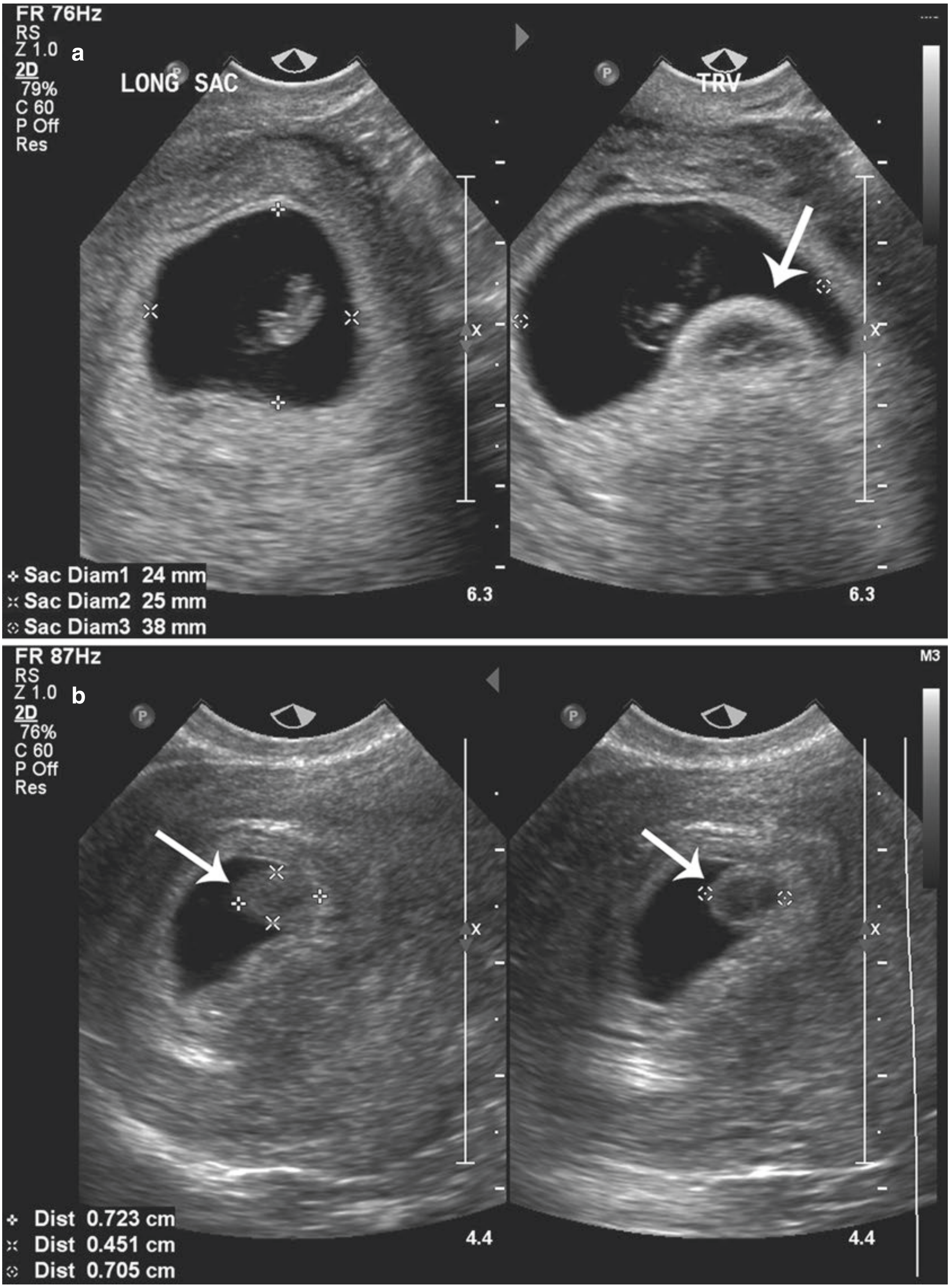
FR 76Hz
RS
Z 1.0
2D
79%
C 60
P Off
Res
a
LONG SAC
TRV
Sac Diam1 24 mm
Sac Diam2 25 mm
Sac Diam3 38 mm
6.3
6.3
FR 87Hz
RS
Z 1.0
2D
76%
C 60
P Off
Res
b
M3
Dist 0.723 cm
Dist 0.451 cm
Dist 0.705 cm
4.4
4.4

Fig. 16.12 (**a**) Chorionic bump. A chorionic bump (arrow) is visualized in the right longitudinal image of this 8 week 0 day gestational sac with an embryonic pole. (**b**) Chorionic bump. A chorionic bump (arrows) is measured in these transvaginal, axial, and longitudinal images of a 5 week 0 day gestational sac

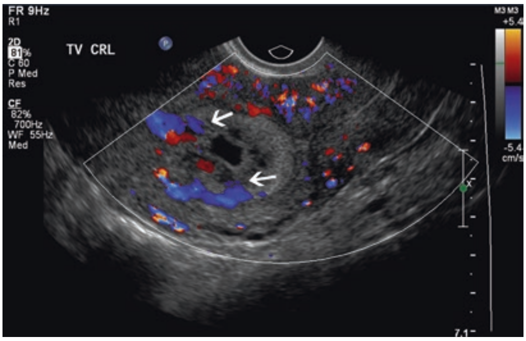

Fig. 16.13 Intervillous vascular flow. Color Doppler highlights the intervillous vascular flow (arrow) in this 5 week 6 day failed pregnancy

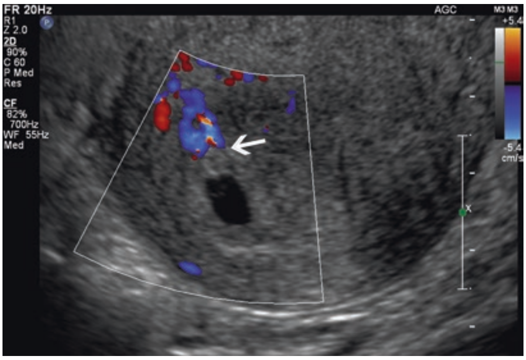

Fig. 16.14 Peritrophoblastic vascular flow. This image shows normal peritrophoblastic flow (arrow) in a 4 week 6 day pregnancy

first-trimester failure yielded a sensitivity, specificity, PPV and NPV of 92%, 82%, 43%, and 99%, respectively. These findings suggest that color Doppler may be helpful in predicting pregnancy failure but should not be used alone as diagnostic.

Yolk Sac

The primary yolk sac regresses by week 2 or 3 of pregnancy and is no longer visible by ultrasound. The secondary yolk sac (YS) is the earliest embryonic landmark visualized by ultrasound; it is usually identified by about the 5.5 weeks when the gestational sac is about 8–10 mm (Fig. 16.15). However, in occasional normal pregnancies, the YS may not be visualized until a gestational sac size of 20 mm [19]. The yolk sac is a circular structure with a hyperechoic wall and measures approximately 3–5 mm. It increases in size steadily up to 8–11 weeks gestation and disappears by 12 weeks (Fig. 16.16). Identification of the YS confirms that an intrauterine fluid collection is a gestational sac even before the appearance of the embryo. Since the YS is continuous with the embryo, amnion, and connecting stalk in the early first trimester, it will typically be found close to the wall of the gestational sac.

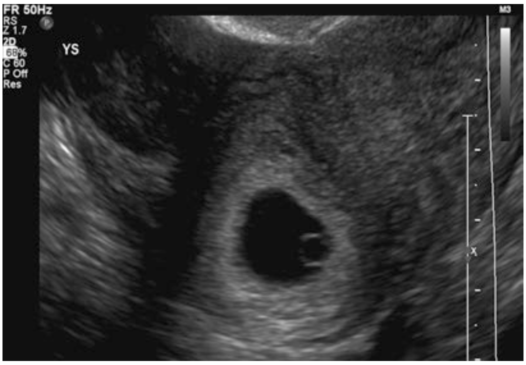

Fig. 16.15 Normal gestational sac and yolk sac. A normal 5 week 6 day gestational sac and yolk sac are shown in this parasagittal, transvaginal image

Appearance

The description of an abnormal or deformed YS varies slightly by study, but the majority of investigators describe an abnormal YS as having any of the following: an irregular (non-circular) shape, wrinkled margins, indented walls, collapsed walls, thick echogenic walls, doubled (appearance of 2 or more YS) or containing echogenic spots or bands (see Figs. 16.4c and 16.17a, b). An echogenic YS, with an echogenic central portion rather than anechoic has not been considered abnormal. Only one study described adverse outcomes in pregnancies with an echogenic YS, but several others report this finding in normal pregnancies [45]. Echogenic yolk sacs should be differentiated from a calcified YS in which acoustic shadowing is demonstrated. Calcified yolk sacs are usually indicative of a loss of fetal cardiac activity before 12 weeks of gestation [46].

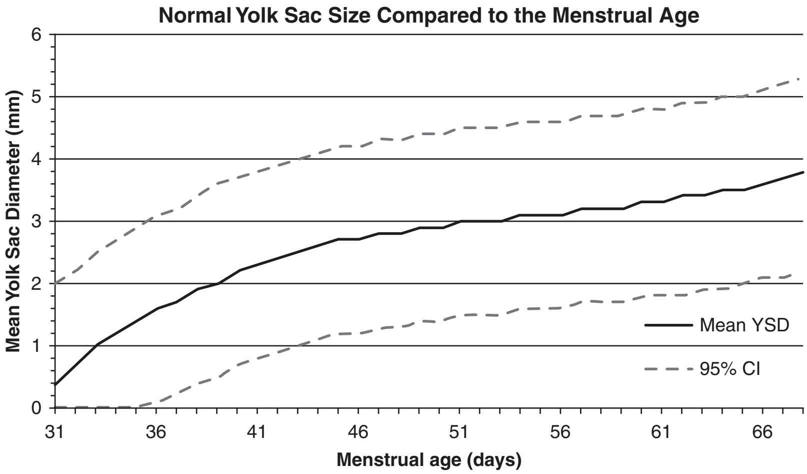

Fig. 16.16 Graph compares a normal yolk sac size in mm ± 2 standard deviations with the crown-rump length in mm using data from [46]. (Reprinted with permission from Lindsay DJ, Lovett IS, Lyons EA, et al. Yolk sac diameter and shape at endovaginal US: predictors of pregnancy outcome in the first trimester. *Radiology* 1992; 183: 115–118)

Studies on the risk of pregnancy loss associated with abnormal-appearing YS are mixed. Lindsay and Cho and their associates both found an increased risk of pregnancy loss with abnormal-appearing YSs, but both studies followed only a small number of affected pregnancies (7 and 5, respectively) [47, 48]. Kucuk et al. followed 19 women with an abnormal-appearing YS and found increased pregnancy loss with a sensitivity and PPV of 29% and 47% [49]. More recently, Tan and colleagues followed 31 women with abnormal-appearing YSs and found no statistical association with pregnancy failure [45]. In many studies that identified abnormal-appearing YSs, an embryo with cardiac activity continued normally to term. This raises concern that an abnormal YS is not consistently associated with pregnancy failure [45, 47, 50]. Therefore, an abnormal YS is, at best, a weak predictor of pregnancy failure.

An absent YS in the presence of an embryo has been associated with pregnancy loss in multiple studies [47, 48]. In pregnancies with an enlarged yolk sac, an increased risk of pregnancy loss has been reported, but in many of these studies, normal pregnancies resulted (Fig. 16.17a, b). Berdahl et al. followed 80 women with a YS diameter ≥5 mm and found a threefold increased risk of pregnancy loss compared to those with normal-sized yolk sacs [51]. Lindsay et al. found that an enlarged YS (greater than 2 standard deviations based on the gestational sac size) has a sensitivity and PPV for pregnancy loss of 15.6% and 60.0%, respectively [47]. Chama and coworkers found that a YS diameter more or less than 2 standard deviations from the mean, predicted pregnancy failure with a sensitivity, specificity, and PPV of 91.4%, 66.0%, and 88.8%, respectively [52]. Lindsay et al. identified an association of a small YS (less than 2 SD based on the gestational sac size) with pregnancy loss, with a sensitivity and PPV of 15.6% and 44.4% [46]. However, a large yolk sac when identified with a viable embryo can exist in a normal pregnancy [48]. Based on these studies, a YS diameter greater than 2 standard deviations from the mean, in the absence of an embryo, would suggest pregnancy failure.

The presence of a YS within a gestational sac is reassuring; however, in the absence of an embryo, future viability is uncertain. Abdallah and associates followed 1060 pregnancies prospectively for viability. In the subgroup of pregnancies with a YS but without an embryo, the false-positive rate (FPR) to diagnose pregnancy failure was 2.6% at a gestational sac diameter of 16 mm and 0.4% at a cutoff of 20 mm, with no false positives when the gestational sac was ≥21 mm. Given the interobserver error, a cutoff of ≥25 mm was recommended to diagnose pregnancy failure when a YS is seen without an embryo [18].

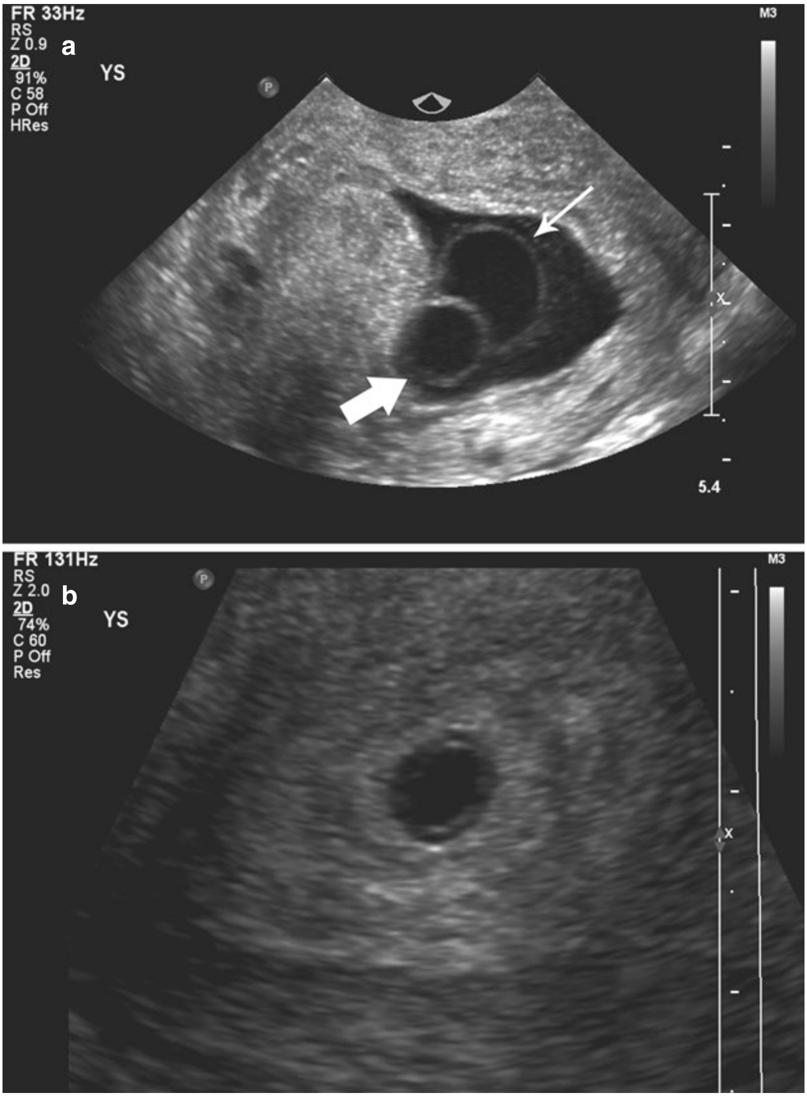

Fig. 16.17 (**a**) Large yolk sac. A large yolk sac (thick arrow) is seen compressing an empty amnion (thin arrow) at 6 weeks 1 day gestation in this transvaginal, midsagittal image. (**b**) Large yolk sac. A large yolk sac is visualized, filling the chorionic cavity in this axial, transvaginal image of a 4 week 1 day gestation

Embryo

Observation of the location, appearance and activity of the embryo can provide clues to inevitable pregnancy failure. Abnormalities of embryonic size and growth have been closely linked with pregnancy failure.

Embryonic Motion

Embryonic motion can be visualized early in gestation by TVS and tends to be rapid jerking motions due to immaturity of the embryonic nervous system [24]. Goldstein et al. reported identification of embryonic body movements starting at 8 weeks gestation, with a sensitivity and PPV of 100% and 94.3% [24].

Location

The embryo is first identified sonographically as a thickening along the YS. As the embryo grows, it assumes a C-shape and it begins to distance itself from the yolk sac, usually at around 55 days of gestation. The yolk sac maintains a thin connection to the embryo through the yolk stalk which is occasionally visualized by TVS. The yolk stalk detaches from the midgut loop at the end of the sixth week of gestation (CRL of 8 mm) allowing the yolk sac to separate from the embryo. This separation continues until approximately the 10th to 12th week of gestation when the YS begins to solidify and assumes a position between the amnion and chorion [53]. A loss of these anatomic relationships raises concern for potential pregnancy failure.

Filly and associates, in a retrospective review of the yolk stalk in embryos of 5 mm or less without cardiac activity, reported that premature separation of the embryo from the YS (evidence that the yolk stalk had developed—the "yolk stalk sign") was suggestive of an embryonic demise with a PPV of 100% [54]. They theorized that visualization of the yolk stalk is not expected until a CRL of 8 mm when cardiac activity is expected. Hence, the lack of cardiac activity is further evidence of embryonic demise.

Appearance

The embryo has a classic appearance as it grows from a thickening along the YS into a fetus with recognizable head and limbs. Initial visualization of the embryo on TVS occurs when it reaches 2–3 mm in size and has the appearance of a straight echogenicity along the YS wall (Fig. 16.18). At about day 21, the embryo develops a C-shape as the caudal neuropore elongates. At 24 days, a heart bulge can be seen, and by day 28, the embryo is 4 mm in length and limb buds appear. Distinct limbs may be visualized at about day 35 when the embryo measures 8 mm. A visible crown-rump length is not identified until about 49 days with the embryo measuring 18 mm [53].

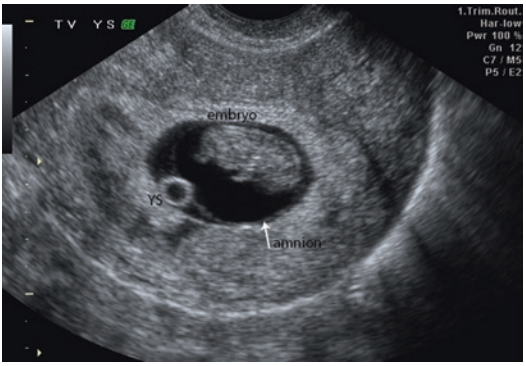

Fig. 16.18 Normal orientation of yolk sac, embryo, and amnion. This transvaginal, axial image of the normal orientation of the yolk sac (YS), embryonic pole (CRL), and amnion are depicted

There is no rigorous research assessing pregnancy outcomes in the absence of the above landmarks, but they may provide guidance clinically. A straight-appearing 4-mm embryo should raise concern for possible pregnancy failure, especially in the absence of cardiac activity prompting a follow-up exam. TVS has the potential to image the shape of the embryo, and this information can be used with other findings. Further study is ongoing, especially in the use of three-dimensional imaging, to evaluate the embryonic appearance and assess risk for pregnancy failure.

Size/Growth Rate

Multiple investigators have assessed embryo size compared to menstrual age in normal pregnancies and from this developed nomograms and regression formulas for embryonic growth. On average, these studies have supported a normal embryo growth rate of approximately 1 mm/day [55] (Fig. 16.19). A study by Bottomly et al. assessed embryonic growth and concluded that embryo growth is not linear, and their study questioned the reliability of an absolute growth rate for determining fetal viability [56]. Reljic found that when the CRL was greater than 2 standard deviations below the mean for expected gestational age, and ≤18 mm, there was a 6.5-fold increased risk of pregnancy failure compared to those at or above the mean. The risk of pregnancy failure increased as the discrepancy increased [57]. Reljic did not find a similar association when the CRL was >18 mm. A study by Stern and associates evaluating pregnancy failure after documentation of an embryonic heart rate (EHR) found that sonographic gestational age by CRL lagged by more than 0.6 weeks behind menstrual dates in 86% of women studied [5]. Mukri et al. prospectively monitored the embryo/fetal growth in 292 pregnant women and found that there was a statistically significant difference between the gestational age by CRL compared to expected gestational age by LMP in pregnancies that ended in a demise by 11–14 weeks [58]. Sixty-one per-

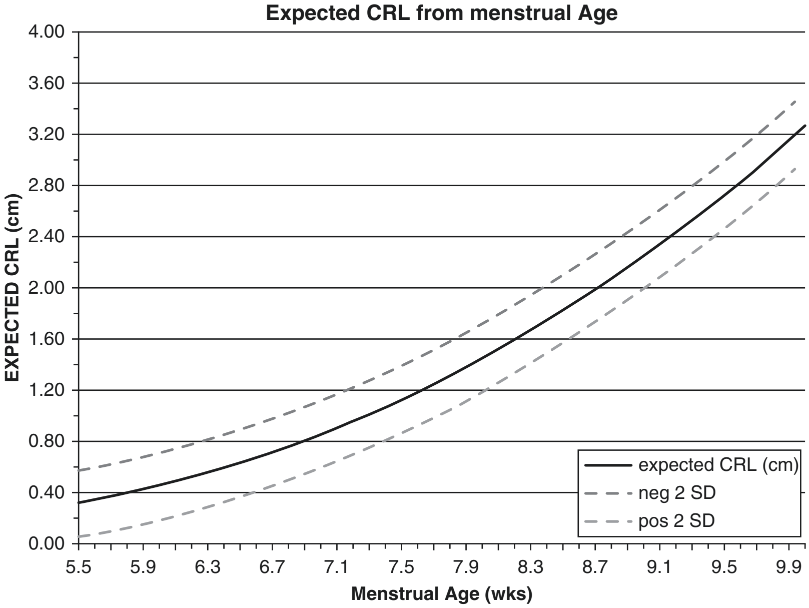

Fig. 16.19 The expected crown-rump length (CRL) in cm ± 2 standard deviation is compared to the menstrual age in weeks in this graph created with data from [54]

cent of the pregnancies that failed had CRLs that were more than 2 standard deviations below the mean; there was a direct relationship between an increasing discrepancy and the risk of pregnancy failure. At a threshold of 2 standard deviations below the mean, the sensitivity and PPV for pregnancy loss were 61% and 31%.

Numerous investigators have extensively evaluated a threshold CRL to definitively confirm an embryonic demise in the absence of cardiac activity. It is critically important to apply a threshold that provides accuracy and reliable reassurance to patients and takes into account interobserver error. Abdullah and associates in a prospective study evaluating CRL measurements in the absence of cardiac activity determined false-positive rates in diagnosing pregnancy failure as 8.3% using a CRL of 4.0 mm or 5.0 mm with no false positives found when using a CRL of ≥5.3 mm [22]. Accounting for inter- and intra-observer variation, a threshold CRL of ≥7 mm is recommended to diagnose pregnancy failure, when cardiac activity is not visualized.

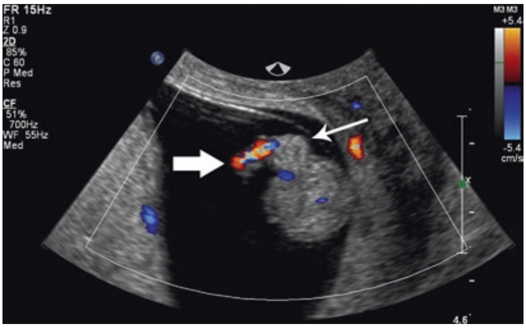

Fig. 16.20 Physiologic gut herniation. A physiologic herniation of fetal bowel (thin arrow) into the umbilical cord (thick arrow) is visualized in this transvaginal, mid-sagittal image of a 10 week 0 day fetus. This herniation was not seen at a 14 week follow-up exam

Anatomy

Anatomic structural anomalies are now detected in the first trimester with increasing frequency (also see Chap. 19). An anomaly does not necessary predicate a pregnancy failure, but certain anatomic abnormalities may be associated with aneuploidy, which increases the risk of pregnancy failure. The sonologist should exercise caution, as there are developmental changes in the embryonic and early fetal periods that can be misinterpreted as anomalies (Figs. 16.20, 16.21 and 16.22). Table 16.2 lists some of the common first-trimester ultrasound pitfalls. Anomalies visualized in the first trimester are listed in Table 16.3 (Figs. 16.23, 16.24, 16.25, 16.26, and 16.27).

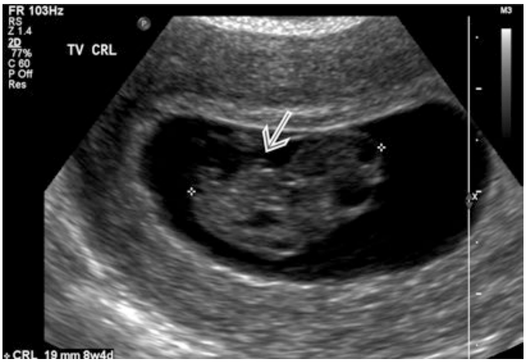

Fig. 16.21 Embryonic heart bump. The embryonic heart is noted as a "bump" (see arrow) in the mid torso of this normal 8 week 5 day embryo as seen in this transvaginal, axial image

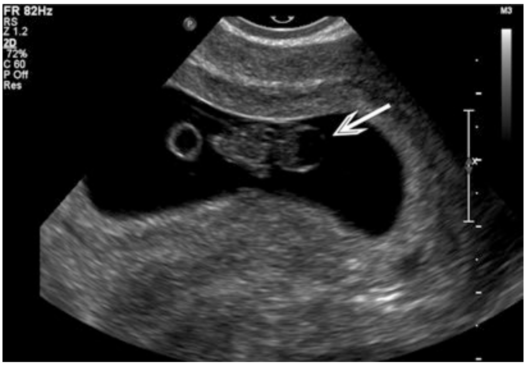

Fig. 16.22 Prominent rhombencephalon. Transvaginal, axial image of a normal 9 week 3 day fetus showing a prominent rhombencephalon mistaken for possible hydrocephalus. An 18-week fetal anatomy survey revealed normal intracranial anatomy

Table 16.2 Developmental pitfalls on first-trimester ultrasound

Ultrasound finding	Suspected anomaly	Normal embryonic development
Cystic space in the posterior cranium	Dandy walker malformation, hydrocephalus	Normal rhombencephalon
Mass at the fetal umbilical cord insertion	Omphalocele	Physiologic herniation of the fetal bowel
Embryonic heart seen as a mass on the chest	Ectopic cordis	In the early embryo, the heart is normally an anterior chest bump

Table 16.3 Anomalies identified on first-trimester ultrasound

Anencephaly
Bladder outlet obstruction/megacystis
Conjoined twins
Cystic hygroma
Encephalocele
Gastroschisis
Holoprosencephaly
Limb body wall complex

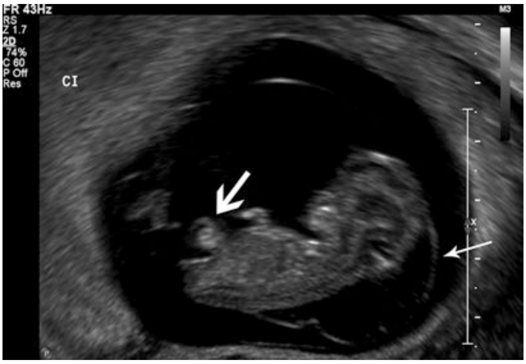

Fig. 16.23 Omphalocele. An omphalocele (thick arrow) is noted with a thickened nuchal translucency (thin arrow) in this transvaginal, axial image of an 11 week 4 day fetus

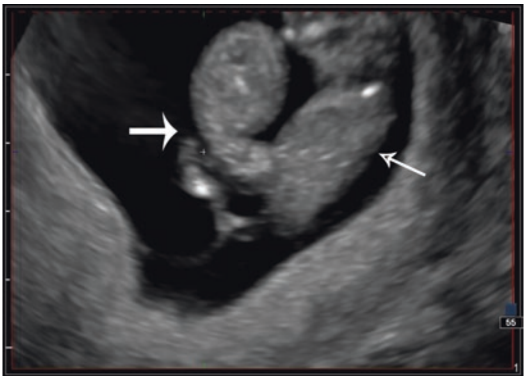

Fig. 16.24 Conjoined twins. The thin arrow depicts fetus A and the thick arrow fetus B in this transvaginal, midsagittal image of omphalopagus conjoined twins at 11 weeks 0 days gestation

Embryonic Heart Rate

The EHR increases with gestational age, ranging from 90 to 113 beats per minute (bpm) at 6 weeks gestation to a plateau of 140–170 bpm at about

9 weeks gestation [59]. Figure 16.28 depicts the mean EHR with ±2 standard deviations plotted against the crown-rump length for normal pregnancies [60, 61].

Multiple studies have determined that a low EHR, less than 85–100 bpm at a gestational age below 8 weeks gestation, is associated with pregnancy loss [59, 63]. The largest prospective study by Stefos and associates evaluated 2164 women and identified a threshold EHR of 85 bpm for predicting pregnancy loss at less than 6 weeks 3 days gestation. The threshold increased to 125 bpm between 7 weeks 4 days and 8 weeks 0 days [62]. With increasing gestational age, studies report an increase in the threshold EHR. Of note, the risk for pregnancy loss increases as the EHR decreases, especially between 6 and 9 weeks gestation [62, 64, 65]. A slow EHR (<90 bpm) when observed at 6–7 weeks gestation carries a risk of first-trimester pregnancy loss of about 25% in several studies even in cases where the EHR is in the normal range at an 8-week follow-up exam [64, 65]. An increased EHR (greater than 2 standard deviations above the mean) has not been associated with pregnancy loss [64].

Aneuploidy has been linked to abnormal fetal heart rates (FHR) [66–68]. Liao and associates retrospectively evaluated 25,000 women who

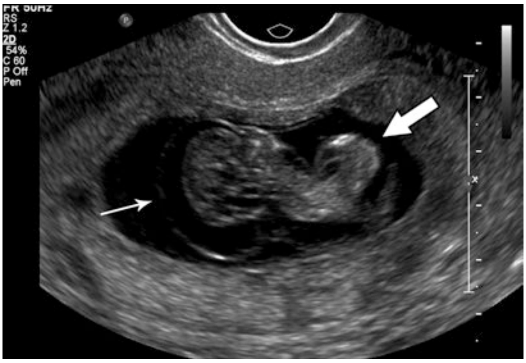

Fig. 16.25 Thoraco-abdominal wall defect. Transvaginal, axial image of an 11 week fetus showing a defect in the thoraco-abdominal wall (thick arrow) with the heart and bowel contents herniating from the fetus. A thickened nuchal translucency (thin arrow) is also noted

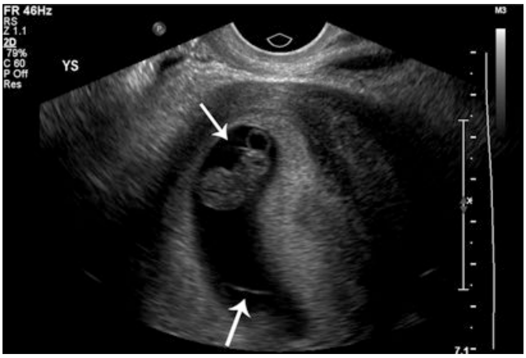

Fig. 16.27 Large amnion with abnormal-appearing fetus. A 9 week 4 day abnormal-appearing fetus with an enlarged amnion (arrows) is visualized by transvaginal imaging in the axial plane. Cardiac activity is not visualized when cardiac activity was previously demonstrated. The fetal karyotype was 45 X

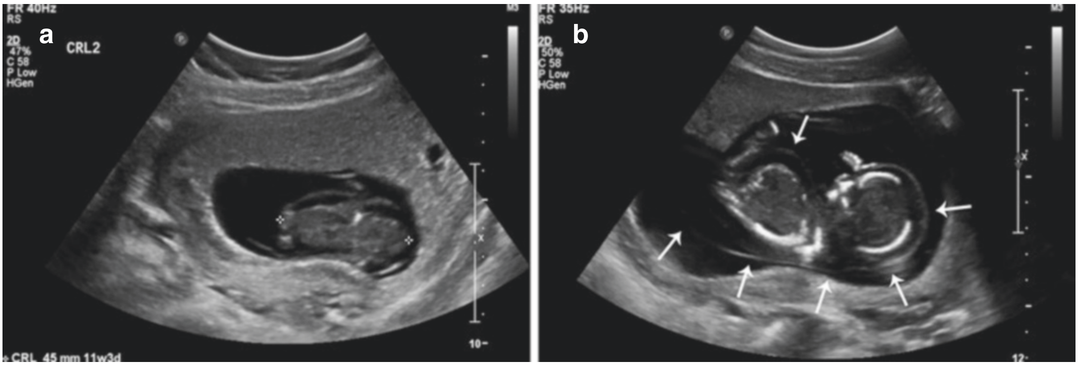

Fig. 16.26 (**a**) Fetal anasarca. This transvaginal, axial image shows an 11 week 6 day fetal demise (calipers) with anasarca found to be triploidy by karyotype. (**b**) Fetal anasarca. A 13 week 6 day fetal demise with anasarca (arrows) is visualized in this transvaginal, longitudinal image also showing a thickened nuchal translucency. A karyotype of the products of conception revealed trisomy 13

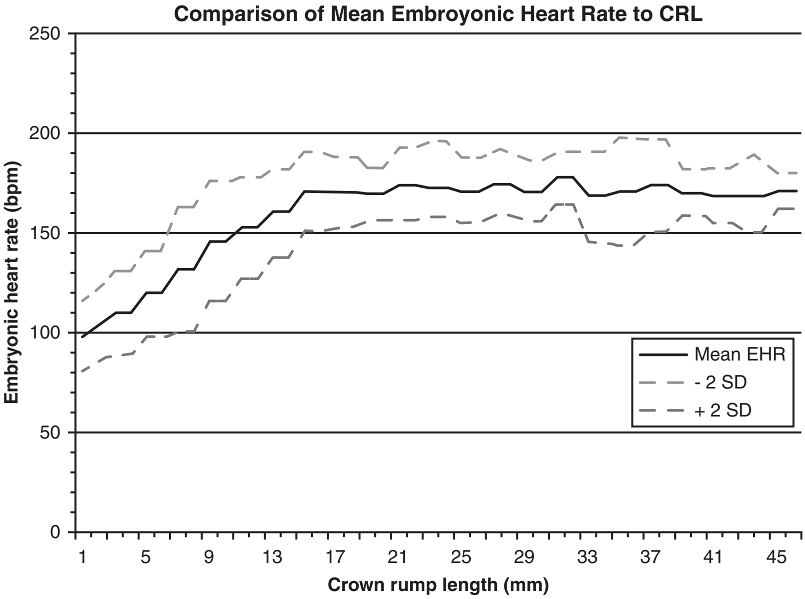

Fig. 16.28 The graph illustrates the comparison of the embryonic heart rate in bpm ± 2 standard deviations to the crown-rump length in mm created with data from [59, 60]

underwent first-trimester screening and found that fetuses with trisomy 21, trisomy 13, and Turner syndrome had an increased probability of a FHR greater than 2 standard deviations above the mean (9.7%, 67.4%, and 52.2%, respectively), while fetuses with trisomy 18 and triploidy had an increased probability of a decreased FHR more than 2 standard deviations below the mean (18.7% and 30.0%, respectively) [68].

Retained Products of Conception

Retained products of conception (RPOC) are the persistence of placental and/or fetal tissue in the uterus, following a miscarriage, termination of pregnancy, or delivery. It complicates 1% of pregnancies and is most common after medical termination of pregnancy and second trimester miscarriage. The most common patient complaints associated with RPOC are vaginal bleeding, pelvic pain, and/or fever. Abbasi and colleagues found that vaginal bleeding had the highest sensitivity and specificity for RPOC of 93% and 50%, respectively [69].

Ultrasound Evaluation

Clinical evaluation for RPOC is inaccurate, therefore, TVUS is frequently chosen for definitive evaluation. Sadan et al. reported that the presence of hyper- or hypoechoic material within the uterine cavity or an endometrial lining thicker than 8 mm had a PPV of 71% for histologically confirmed RPOC [70]. Durfee and associates found that an endometrial mass was the most sensitive and specific sonographic feature of RPOC (79% and 89%, respectively), with a PPV of 59% [71] (Fig. 16.29). An endometrial lining greater than 10 mm, as an isolated finding, had low sensitivity and specificity and was detected more frequently in patients without RPOC. Durfee et al. also found that complex fluid alone, identified within the uterine cavity, was a poor predictor of RPOC, and the absence of sonographic findings had a NPV for RPOC of 100% [71].

Color Doppler Imaging

Color Doppler mapping of the uterine cavity is advocated to further evaluate the uterine cavity for RPOC (Fig. 16.30). Durfee and associates found that blood flow in the endometrium had a

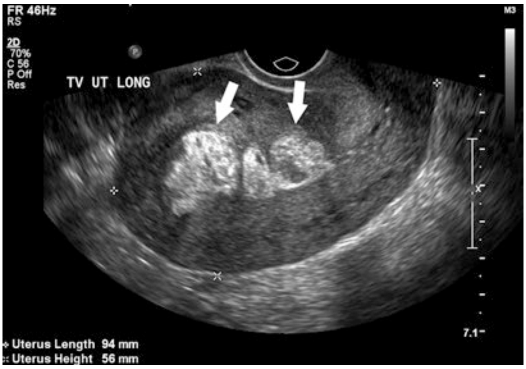

Fig. 16.29 This is a longitudinal transvaginal image of a 39-year-old woman who presented to the emergency room complaining of vaginal bleeding and pelvic pain at 10 weeks 5 days pregnant. A previously identified gestational sac and fetus are not seen. The arrows identify echogenic masses within the uterine cavity

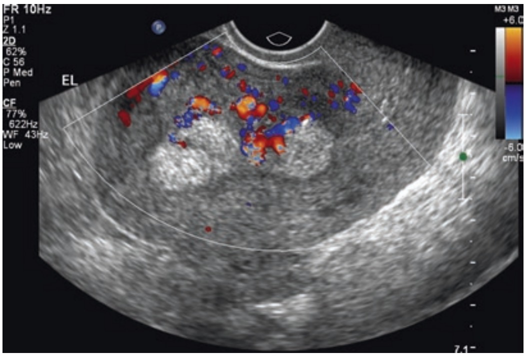

Fig. 16.30 A longitudinal, transvaginal, color Doppler image is depicted of the same patient described in Fig. 16.29. Vascular flow is demonstrated within the echogenic masses. The pathology from a dilatation and curettage revealed retained products of conception

PPV of 75% for the presence of RPOC, but a NPV of 46%. They concluded that color Doppler imaging was not helpful for predicting RPOC [71]. Kamaya et al. graded the endometrial vascularity, in women referred for suspected RPOC, by color Doppler imaging. The endometrium was graded from type 0, no detectable vascularity, to type 3, marked vascularity [72]. They found that detectable vascularity of any type (1–3) had a high likelihood of RPOC, with a PPV of 96%. All women with types 2 and 3 vascularity were found to have RPOC, while type 0 vascularity did not exclude RPOC. These findings suggest that color Doppler mapping of the uterine cavity can improve the sensitivity and PPV for predicting RPOC.

Recurrent Pregnancy Loss

Recurrent pregnancy loss (RPL) is most commonly defined as two or more failed pregnancies, which have been documented by ultrasound or histopathological examination [73]. It occurs in less than 5% of women, with 1% having three or more pregnancy losses. There are multiple suspected etiologies, with cytogenetic (2–5%), antiphospholipid syndrome (8–42%), and anatomic anomalies (1.8–37.6%) comprising the majority of causes. Congenital uterine anomalies are present in 12.6% of women with RPL and can be characterized by 3-D ultrasound imaging. The highest rates of RPL are present in women with congenital uterine anomalies: septate (44%), bicornuate (36%), and arcuate (26%) uteri [73]. Despite these findings, a definitive diagnosis for RPL is determined in only 50% of patients. The mechanisms of RPL are not completely understood and research is ongoing.

In the absence of a definitive etiology, treatment is very limited. However, Brigham and associates reported that despite three consecutive miscarriages, 70% of women with idiopathic RPL conceived and 55% went on to have fetal survival beyond 24 weeks gestation [74]. No statistical difference in outcome between women with two and those with three previous losses was found. In addition, 78% of miscarriages in women with recurrent losses were identified between 6 and 8 weeks of gestation, and in 89%, cardiac activity was never visualized [74]. Cardiac activity at 8 weeks was associated with a 98% chance of successful pregnancy that increased to 99.4% when cardiac activity was demonstrated at 10 weeks gestation.

Summary

Ultrasound assessment of the first-trimester pregnancy has dramatically improved the diagnostic capabilities of clinicians over the past four decades. Once a hidden, mysterious part of pregnancy, the first trimester is now open to investigation and examination. Imaging the stages of embryonic and fetal development provides the clinician with valuable information which can be used to screen for aneuploidy, evaluate for anomalies and identify markers of fetal viability. The best predictors of pregnancy failure are the absence of an embryo once the mean gestational sac size reaches 25 mm and the absence of cardiac activity once the embryo is ≥7 mm. These thresholds are justifiably conservative but allow us to reassure our patients with confidence of the sonographic diagnosis of pregnancy failure.

Teaching Points

- The β-hCG discriminatory level to visibly confirm an intrauterine pregnancy by transvaginal ultrasound is 4000 mIU/mL.
- An empty gestational sac with a mean sac diameter of ≥25 mm is considered anembryonic.
- An embryo without cardiac activity at a crown-rump length of ≥7 mm would be considered an embryonic demise.
- In the presence of a gestational sac only, patient age, MSD, hCG rise and vaginal bleeding correlate with first-trimester outcome.
- A fetal heart rate <90 bpm at >6 weeks gestation is concerning for impending pregnancy failure.
- A gestational sac or embryo that does not grow 1 mm/day over 7–10 days is concerning for pregnancy failure.
- Absence of a viable embryo ≥2 weeks after identification of a gestational sac without a yolk sac is anembryonic.
- Absence of a viable embryo ≥11 days after identification of a gestational sac with a yolk sac is anembryonic.
- Sixty percent of spontaneous abortions at <12 weeks gestation are due to chromosomal defects.
- The diagnosis of retained products of conception can be suspected when hyperechoic or hypoechoic material is visualized within the uterine cavity or the endometrial lining is thicker than 8–10 mm, although the positive predictive value is less than optimal. Color Doppler may be helpful in these situations.
- A definitive etiology for recurrent pregnancy loss is determined in only 50% of patients and, in the absence of a conclusive diagnosis, treatment is very limited.

References

1. Pridjian G, Moawad AH. Missed abortion: still appropriate terminology? Am J Obstet Gynecol. 1989;161(2):261–2. Epub 1989/08/01
2. Falco P, Zagonari S, Gabrielli S, Bevini M, Pilu G, Bovicelli L. Sonography of pregnancies with first-trimester bleeding and a small intrauterine gestational sac without a demonstrable embryo. Ultrasound Obstet Gynecol. 2003;21(1):62–5. Epub 2003/01/16
3. Elson J, Salim R, Tailor A, Banerjee S, Zosmer N, Jurkovic D. Prediction of early pregnancy viability in the absence of an ultrasonically detectable embryo. Ultrasound Obstet Gynecol. 2003;21(1):57–61. Epub 2003/01/16
4. Nyberg DA, Filly RA. Predicting pregnancy failure in 'empty' gestational sacs. Ultrasound Obstet Gynecol. 2003;21(1):9–12. Epub 2003/01/16
5. Stern JJ, Coulam CB. Mechanism of recurrent spontaneous abortion. I. Ultrasonographic findings. Am J Obstet Gynecol. 1992;166(6 Pt 1):1844–50; discussion 50–2. Epub 1992/06/01
6. Kadar N, Caldwell BV, Romero R. A method of screening for ectopic pregnancy and its indications. Obstet Gynecol. 1981;58(2):162–6. Epub 1981/08/01
7. Barnhart KT, Sammel MD, Rinaudo PF, Zhou L, Hummel AC, Guo W. Symptomatic patients with an early viable intrauterine pregnancy: HCG curves redefined. Obstet Gynecol. 2004;104(1):50–5. Epub 2004/07/02
8. Nyberg DA, Filly RA, Filho DL, Laing FC, Mahony BS. Abnormal pregnancy: early diagnosis by US and serum chorionic gonadotropin levels. Radiology. 1986;158(2):393–6. Epub 1986/02/01
9. Hahlin M, Sjoblom P, Lindblom B. Combined use of progesterone and human chorionic gonadotropin determinations for differential diagnosis of very early pregnancy. Fertil Steril. 1991;55(3):492–6. Epub 1991/03/01
10. Doubilet PM, Benson CB. Further evidence against the reliability of the human chorionic gonadotropin discriminatory level. J Ultrasound Med. 2011;30(12):1637–42. Epub 2011/11/30

11. Nyberg DA, Laing FC, Filly RA. Threatened abortion: sonographic distinction of normal and abnormal gestation sacs. Radiology. 1986;158(2):397–400. Epub 1986/02/01
12. Bradley WG, Fiske CE, Filly RA. The double sac sign of early intrauterine pregnancy: use in exclusion of ectopic pregnancy. Radiology. 1982;143(1):223–6. Epub 1982/04/01
13. Doubilet PM, Benson CB. Double sac sign and intradecidual sign in early pregnancy: interobserver reliability and frequency of occurrence. J Ultrasound Med. 2013;32(7):1207–14. Epub 2013/06/28
14. Yeh HC, Goodman JD, Carr L, Rabinowitz JG. Intradecidual sign: a US criterion of early intrauterine pregnancy. Radiology. 1986;161(2):463–7. Epub 1986/11/01
15. Laing FC, Brown DL, Price JF, Teeger S, Wong ML. Intradecidual sign: is it effective in diagnosis of an early intrauterine pregnancy? Radiology. 1997;204(3):655–60. Epub 1997/09/01
16. Chiang G, Levine D, Swire M, McNamara A, Mehta T. The intradecidual sign: is it reliable for diagnosis of early intrauterine pregnancy? AJR Am J Roentgenol. 2004;183(3):725–31. Epub 2004/08/31
17. Doubilet PM, Benson CB, Bourne T, Blaivas M, Barnhart KT, Benacerraf BR, et al. Diagnostic criteria for nonviable pregnancy early in the first trimester. N Engl J Med. 2013;369(15):1443–51. Epub 2013/10/11
18. Abdallah Y, Daemen A, Kirk E, Pexsters A, Naji O, Stalder C, et al. Limitations of current definitions of miscarriage using mean gestational sac diameter and crown-rump length measurements: a multicenter observational study. Ultrasound Obstet Gynecol. 2011;38(5):497–502. Epub 2011/10/15
19. Rowling SE, Coleman BG, Langer JE, Arger PH, Nisenbaum HL, Horii SC. First-trimester US parameters of failed pregnancy. Radiology. 1997;203(1):211–7. Epub 1997/04/01
20. Pexsters A, Luts J, Van Schoubroeck D, Bottomley C, Van Calster B, Van Huffel S, et al. Clinical implications of intra- and interobserver reproducibility of transvaginal sonographic measurement of gestational sac and crown-rump length at 6–9 weeks' gestation. Ultrasound Obstet Gynecol. 2011;38(5):510–5. Epub 2010/11/16
21. Nyberg DA, Filly RA, Mahony BS, Monroe S, Laing FC, Jeffrey RB Jr. Early gestation: correlation of HCG levels and sonographic identification. AJR Am J Roentgenol. 1985;144(5):951–4. Epub 1985/05/01
22. Abdallah Y, Daemen A, Guha S, Syed S, Naji O, Pexsters A, et al. Gestational sac and embryonic growth are not useful as criteria to define miscarriage: a multicenter observational study. Ultrasound Obstet Gynecol. 2011;38(5):503–9. Epub 2011/08/23
23. Bree RL, Edwards M, Bohm-Velez M, Beyler S, Roberts J, Mendelson EB. Transvaginal sonography in the evaluation of normal early pregnancy: correlation with HCG level. AJR Am J Roentgenol. 1989;153(1):75–9. Epub 1989/07/01
24. Goldstein I, Zimmer EA, Tamir A, Peretz BA, Paldi E. Evaluation of normal gestational sac growth: appearance of embryonic heartbeat and embryo body movements using the transvaginal technique. Obstet Gynecol. 1991;77(6):885–8. Epub 1991/06/01
25. Doubilet PM, Phillips CH, Durfee SM, Benson CB. First trimester prognosis when an early gestational sac seen on ultrasound imaging. J Ultrasound Med. 2021;40:541–50.
26. Horrow MM. Enlarged amniotic cavity: a new sonographic sign of early embryonic death. AJR Am J Roentgenol. 1992;158(2):359–62. Epub 1992/02/01
27. McKenna KM, Feldstein VA, Goldstein RB, Filly RA. The empty amnion: a sign of early pregnancy failure. J Ultrasound Med. 1995;14(2):117–21. Epub 1995/02/01
28. Yegul NT, Filly RA. The expanded amnion sign: evidence of early embryonic death. J Ultrasound Med. 2009;28(10):1331–5. Epub 2009/09/26
29. Yegul NT, Filly RA. Further observations on the empty "amnion sign". J Clin Ultrasound. 2010;38(3):113–7. Epub 2010/02/04
30. Weiss JL, Malone FD, Vidaver J, Ball RH, Nyberg DA, Comstock CH, et al. Threatened abortion: a risk factor for poor pregnancy outcome, a population-based screening study. Am J Obstet Gynecol. 2004;190(3):745–50. Epub 2004/03/26
31. Nagy S, Bush M, Stone J, Lapinski RH, Gardo S. Clinical significance of subchorionic and retroplacental hematomas detected in the first trimester of pregnancy. Obstet Gynecol. 2003;102(1):94–100. Epub 2003/07/10
32. Ball RH, Ade CM, Schoenborn JA, Crane JP. The clinical significance of ultransonographically detected subchorionic hemorrhages. Am J Obstet Gynecol. 1996;174(3):996–1002. Epub 1996/03/01
33. Borlum KG, Thomsen A, Clausen I, Eriksen G. Long-term prognosis of pregnancies in women with intrauterine hematomas. Obstet Gynecol. 1989;74(2):231–3. Epub 1989/08/01
34. Schauberger CW, Mathiason MA, Rooney BL. Ultrasound assessment of first-trimester bleeding. Obstet Gynecol. 2005;105(2):333–8. Epub 2005/02/03
35. Maso G, D'Ottavio G, De Seta F, Sartore A, Piccoli M, Mandruzzato G. First-trimester intrauterine hematoma and outcome of pregnancy. Obstet Gynecol. 2005;105(2):339–44. Epub 2005/02/03
36. Tuuli MG, Norman SM, Odibo AO, Macones GA, Cahill AG. Perinatal outcomes in women with subchorionic hematoma: a systematic review and meta-analysis. Obstet Gynecol. 2011;117(5):1205–12. Epub 2011/04/22
37. Pearlstone M, Baxi L. Subchorionic hematoma: a review. Obstet Gynecol Surv. 1993;48(2):65–8. Epub 1993/02/01
38. Pedersen JF, Mantoni M. Prevalence and significance of subchorionic hemorrhage in threatened abortion: a sonographic study. AJR Am J Roentgenol. 1990;154(3):535–7. Epub 1990/03/01

39. Stabile I, Campbell S, Grudzinskas JG. Threatened miscarriage and intrauterine hematomas. Sonographic and biochemical studies. J Ultrasound Med. 1989;8(6):289–92. Epub 1989/06/01
40. Harris RD, Couto C, Karpovsky C, Porter MM, Ouhilal S. The chorionic bump: a first-trimester pregnancy sonographic finding associated with a guarded prognosis. J Ultrasound Med. 2006;25(6):757–63. Epub 2006/05/30
41. Sana Y, Appiah A, Davison A, Nicolaides KH, Johns J, Ross JA. Clinical significance of first-trimester chorionic bumps: a matched case-control study. Ultrasound Obstet Gynecol. 2013;42(5):585–9. Epub 2013/06/05
42. Jauniaux E, Greenwold N, Hempstock J, Burton GJ. Comparison of ultrasonographic and Doppler mapping of the intervillous circulation in normal and abnormal early pregnancies. Fertil Steril. 2003;79(1):100–6. Epub 2003/01/14
43. Wherry KL, Dubinsky TJ, Waitches GM, Richardson ML, Reed S. Low-resistance endometrial arterial flow in the exclusion of ectopic pregnancy revisited. J Ultrasound Med. 2001;20(4):335–42. Epub 2001/04/24
44. Jaffe R, Dorgan A, Abramowicz JS. Color Doppler imaging of the uteroplacental circulation in the first trimester: value in predicting pregnancy failure or complication. AJR Am J Roentgenol. 1995;164(5):1255–8. Epub 1995/05/01
45. Tan S, Ipek A, Pektas MK, Arifoglu M, Teber MA, Karaoglanoglu M. Irregular yolk sac shape: is it really associated with an increased risk of spontaneous abortion? J Ultrasound Med. 2011;30(1):31–6. Epub 2011/01/05
46. Harris RD, Vincent LM, Askin FB. Yolk sac calcification: a sonographic finding associated with intrauterine embryonic demise in the first trimester. Radiology. 1988;166(1 Pt 1):109–10. Epub 1988/01/01
47. Lindsay DJ, Lovett IS, Lyons EA, Levi CS, Zheng XH, Holt SC, et al. Yolk sac diameter and shape at endovaginal US: predictors of pregnancy outcome in the first trimester. Radiology. 1992;183(1):115–8. Epub 1992/04/01
48. Cho FN, Chen SN, Tai MH, Yang TL. The quality and size of yolk sac in early pregnancy loss. Aust N Z J Obstet Gynaecol. 2006;46(5):413–8. Epub 2006/09/07
49. Kucuk T, Duru NK, Yenen MC, Dede M, Ergun A, Baser I. Yolk sac size and shape as predictors of poor pregnancy outcome. J Perinat Med. 1999;27(4):316–20. Epub 1999/11/24
50. Ferrazzi E, Brambati B, Lanzani A, Oldrini A, Stripparo L, Guerneri S, et al. The yolk sac in early pregnancy failure. Am J Obstet Gynecol. 1988;158(1):137–42. Epub 1988/01/01
51. Berdahl DM, Blaine J, Van Voorhis B, Dokras A. Detection of enlarged yolk sac on early ultrasound is associated with adverse pregnancy outcomes. Fertil Steril. 2010;94(4):1535–7. Epub 2010/02/16
52. Chama CM, Marupa JY, Obed JY. The value of the secondary yolk sac in predicting pregnancy outcome. J Obstet Gynaecol. 2005;25(3):245–7. Epub 2005/09/09
53. Moore KL, Persaud TVN. The developing human: clinically oriented embryology. 7th ed. Philadelphia: Saunders; 2003.
54. Filly MR, Callen PW, Yegul NT, Filly RA. The yolk stalk sign: evidence of death in small embryos without heartbeats. J Ultrasound Med. 2010;29(2):237–41. Epub 2010/01/28
55. Hadlock FP, Shah YP, Kanon DJ, Lindsey JV. Fetal crown-rump length: reevaluation of relation to menstrual age (5–18 weeks) with high-resolution real-time US. Radiology. 1992;182(2):501–5. Epub 1992/02/01
56. Bottomley C, Daemen A, Mukri F, Papageorghiou AT, Kirk E, Pexsters A, et al. Functional linear discriminant analysis: a new longitudinal approach to the assessment of embryonic growth. Hum Reprod. 2009;24(2):278–83. Epub 2008/11/04
57. Reljic M. The significance of crown-rump length measurement for predicting adverse pregnancy outcome of threatened abortion. Ultrasound Obstet Gynecol. 2001;17(6):510–2. Epub 2001/06/26
58. Mukri F, Bourne T, Bottomley C, Schoeb C, Kirk E, Papageorghiou AT. Evidence of early first-trimester growth restriction in pregnancies that subsequently end in miscarriage. BJOG. 2008;115(10):1273–8. Epub 2008/08/22
59. Benson CB, Doubilet PM. Slow embryonic heart rate in early first trimester: indicator of poor pregnancy outcome. Radiology. 1994;192(2):343–4. Epub 1994/08/01
60. Achiron R, Tadmor O, Mashiach S. Heart rate as a predictor of first-trimester spontaneous abortion after ultrasound-proven viability. Obstet Gynecol. 1991;78(3 Pt 1):330–4. Epub 1991/09/01
61. Papaioannou GI, Syngelaki A, Poon LC, Ross JA, Nicolaides KH. Normal ranges of embryonic length, embryonic heart rate, gestational sac diameter and yolk sac diameter at 6–10 weeks. Fetal Diagn Ther. 2010;28(4):207–19. Epub 2010/09/18
62. Stefos TI, Lolis DE, Sotiriadis AJ, Ziakas GV. Embryonic heart rate in early pregnancy. J Clin Ultrasound. 1998;26(1):33–6. Epub 1998/02/25
63. Chittacharoen A, Herabutya Y. Slow fetal heart rate may predict pregnancy outcome in first-trimester threatened abortion. Fertil Steril. 2004;82(1):227–9. Epub 2004/07/09
64. Doubilet PM, Benson CB, Chow JS. Long-term prognosis of pregnancies complicated by slow embryonic heart rates in the early first trimester. J Ultrasound Med. 1999;18(8):537–41. Epub 1999/08/14
65. Doubilet PM, Benson CB. Outcome of first-trimester pregnancies with slow embryonic heart rate at 6–7 weeks gestation and normal heart rate by 8 weeks at US. Radiology. 2005;236(2):643–6. Epub 2005/07/05
66. Oztekin D, Oztekin O, Aydal FI, Tinar S, Adibelli ZH. Embryonic heart rate as a prognostic factor for chromosomal abnormalities. J Ultrasound Med. 2009;28(5):609–14. Epub 2009/04/25

67. Hyett JA, Noble PL, Snijders RJ, Montenegro N, Nicolaides KH. Fetal heart rate in trisomy 21 and other chromosomal abnormalities at 10–14 weeks of gestation. Ultrasound Obstet Gynecol. 1996;7(4):239–44. Epub 1996/04/01
68. Liao AW, Snijders R, Geerts L, Spencer K, Nicolaides KH. Fetal heart rate in chromosomally abnormal fetuses. Ultrasound Obstet Gynecol. 2000;16(7):610–3. Epub 2001/02/13
69. Abbasi S, Jamal A, Eslamian L, Marsousi V. Role of clinical and ultrasound findings in the diagnosis of retained products of conception. Ultrasound Obstet Gynecol. 2008;32(5):704–7.
70. Sadan O, Golan A, Girtler O, Lurie S, Debby A, Sagiv R, et al. Role of sonography in the diagnosis of retained products of conception. J Ultrasound Med. 2004;23(3):371.
71. Durfee SM, Frates MC, Luong A, Benson CB. The sonographic and color Doppler features of retained products of conception. J Ultrasound Med. 2005;24:1181–6.
72. Kamaya A, Petrovitch I, Chen B, Frederick CE, Jeffrey RB. Retained products of conception: spectrum of color Doppler findings. J Ultrasound Med. 2009;28(8):1031–41.
73. Practice Committee of the American Society for Reproductive Medicine. Evaluation and treatment of recurrent pregnancy loss: a committee opinion. Fertil Steril. 2012;98(5):1103–11.
74. Brigham SA, Conlon C, Farquharson RG. A longitudinal study of pregnancy outcome following idiopathic recurrent miscarriage. Hum Reprod. 1999;14(11):2868–71.

17

Ectopic Pregnancy and Pregnancy of Unknown Location (PUL)

James M. Shwayder

Introduction

Ectopic pregnancy (EP) represents 1–2% of pregnancies [1]. They have a risk of rupture, hemorrhage, and tubal damage, which can lead to decreased future fertility and even death. The most common presenting symptoms suggesting an EP are abdominal pain or vaginal bleeding. Advances in ultrasound technology allow the detection of ectopic pregnancies in their earliest state, allowing treatment alternatives, e.g., observation, medical therapy, or surgical treatment, with reduced morbidity and mortality. However, immediate diagnosis is not always accomplished. Thus, a systematic approach to patients with a possible EP is required to avoid interruption or mistreatment of an intrauterine pregnancy (IUP), timely diagnosis of an EP, and appropriate management with pregnancy failure. This chapter reviews such an approach emphasizing the value of various diagnostic tests.

Pregnancy of Unknown Location

Pregnancy of unknown location (PUL) describes a situation in patients with a positive pregnancy test when transvaginal ultrasound (TVS) fails to identify a pregnancy's location, either intrauterine or extrauterine. In patients with a positive urinary pregnancy test, the location of a pregnancy is usually confirmed in more than 90% of cases [2]. The remainder are categorized as a PUL [3]. In 2011, Barnhart et al. reviewed the consensus nomenclature associated with early pregnancy evaluation, categorizing such pregnancies into the following descriptive areas [4]:

- Definite ectopic pregnancy
- Probable ectopic pregnancy
- Pregnancy of unknown location
- Probable intrauterine pregnancy
- Definite intrauterine pregnancy

The earliest sign of pregnancy is the finding of a saclike structure, regardless of the location. The finding of such a structure in the uterus is considered a probable IUP. This same finding in the adnexa is consistent with a probable EP. The finding of a yolk sac within a gestational sac definitively diagnoses a pregnancy, regardless of the location. The finding of a gestational sac with a yolk sac in the uterus is consistent with a definite IUP, while this same finding outside of the uterus definitely diagnoses an EP. A PUL exists when there are no signs of either an IUP or an EP, representing ~10% of cases [5]. Expectant management with follow-up TVS and serial human chorionic gonadotropin (hCG) levels will lead to the diagnosis of a visualized IUP (34.3%), a visu-

---

J. M. Shwayder (✉)
Department of Obstetrics and Gynecology, University of Florida, Gainesville, FL, USA
e-mail: jshwayder@ufl.edu

© The Author(s), under exclusive license to Springer Nature Switzerland AG 2023

J. S. Abramowicz, R. E. Longman (eds.), *First-Trimester Ultrasound*,
https://doi.org/10.1007/978-3-031-24133-8_17

alized EP (8.7%), or a resolved PUL in 56.9% of these patients [5]. Thus, patients who are clinically stable with a PUL warrant expectant management [3]. A small number of patients will remain with a PUL, which can be treated medically, surgically, or with a diagnostic dilatation and curettage, or observed for spontaneous resolution [4].

A consensus regarding follow-up surveillance of patients with a PUL is still evolving. Individualized surveillance based on risk factors could lead to more accurate diagnosis and reduced cost. Barnhart et al. retrospectively assessed specific clinical factors to determine the frequency and immediacy of follow-up for patients with a PUL [6]. They created a scoring system to triage women into various risk groups. Those at age "extremes" were assigned increasing risk scores: age <18 received a +1 and age >38 assigned a +3. Prior EP increased a patient's risk, with those having one prior EP assigned +2, whereas those with two or more prior EP assigned +3. Patients with bleeding were assigned +4. Patients with a prior miscarriage or with an hCG >2000 mIU/mL were assigned −1. A patient's risk for a nonviable gestation was stratified into negligible risk (−2 to −1), intermediate risk (0 to +4), and high risk (equal to or greater than +5) based on the total score. Based on their risk stratification, patients received surveillance as follows:

- Low-acuity surveillance: "send home" with follow-up in 4–7 days
- Standard surveillance: "monitor" with repeat hCG in 2 days
- High-acuity surveillance: "intervention" including uterine evacuation, laparoscopy, or surveillance in 24 h, depending on the patient's clinical status

Overall, the proposed scoring system had a >90% specificity. Thus, clinical signs and symptoms of a woman with PUL may help optimize surveillance plans.

Condous et al. developed a logistic regression model using serial hCG and progesterone levels, drawn 48 h apart, to predict the outcome of PULs [5]. An hCG increase of >66% was predictive of an IUP with a positive predictive value (PPV) of 96.5%. A serum progesterone of <20 mmol/L predicted a failing PUL with a PPV of >95%. In summary, the change in hCG outperformed serum progesterone change in predicting the location and outcome of a PUL.

One can postulate that combining the results of these two studies would improve our surveillance of patients with PUL. Specifically, individualized risk assessment, correlated with serial hCG levels and complemented with ultrasound and, in select cases, serum progesterone, will help determine the ultimate outcome of PULs.

A more recent large, multicenter study evaluated a two-step strategy (2ST) to assess the outcome in a PUL [7]. The final pregnancy outcome was defined as a failed PUL (FPUL), an intrauterine pregnancy (IUP), or an EP (which also included persistent PUL [PPUL]). Step 1 included a serum progesterone and beta-hCG (BhCG) level on presentation. An initial progesterone level of ≤2 nmol/L identified PULs of low risk of EP, with a follow-up urine pregnancy test recommended in 2 weeks to confirm a negative result. In step 2, those patients with a progesterone >2 nmol/L had the initial BhCG compared to a second BhCG obtained 48 h later, and a BhCG ratio was calculated (BhCG at 48 h/BhCG at 0 h). A BhCG ratio between 0.87 and 1.66 was classified as having a high risk of an EP, defined as a risk ≥5% of an EP. If the ratio was <0.87, the PUL was classified as low risk of an EP, most likely a failed PUL (FPUL). If the BhCG ratio was >1.66, the PUL was classified as low risk for EP, most likely an IUP (Table 17.1). The two-step strategy classified 16% of PUL as "low risk" based on a progesterone <2 nmol/L, eliminating the need for a second visit in 1 in 6 cases of PUL. In step 1, 7 of 407 patients (1.7%) initially classified as "low risk" were ultimately diagnosed with an EP. In step 2, 8 of 1038 patients (0.8%) classified as "low risk" ultimately had an EP. None of the cases resulted in a ruptured EP or significant clinical harm. Of 901 women classified as "high risk" in step 2, 275 (30.5%) had an EP. Thus, 85.9% of EP were correctly classified as "high risk."

Table 17.1 Outcomes of a two-step strategy for pregnancy of unknown location [7]

		#		FPUL		IUP		EP	
Criteria		2625	%	#	%	#	%	#	%
Step 1	$P \le 2$ nmol/L	407	15.5	386	94.8	14	3.4	7	1.7
Excluded from additional analysis	Outcome known <48 h	62	2.7						
	Protocol deviation	217	9.5						
Step 2	BhCG ratio	1989	87.7						
Low risk, FPUL	<0.87	727	37.5	685	94.2	40	5.5	2	0.3
Low risk, IUP	>1.66	311	16.0	0	0	305	98.1	6	1.9
High risk, EP	0.87–1.66	901	46.5	200	22.2	426	47.3	275	30.5

FPUL failed pregnancy of unknown location, *IUP* intrauterine pregnancy, EP ectopic pregnancy
BhCG ratio: <0.87: high risk for EP, 0.87–1.66: low risk, probable FPUL, >1.66: low risk, probable IUP

A recent multicenter study by the same group analyzed various protocols in cases of PUL [8]. The study compared the probability of a PUL being a failing PUL, an IUP, or an EP (including persistent PUL) based on different strategies: (1) simple BhCG cutoffs; (2) the initial BhCG and BhCG ratio (M4 protocol); (3) the initial BhCG, the BhCG ratio, with or without an initial serum progesterone (M6P or M6PN protocols); and (4) a two-step approach (2ST), only obtaining and calculating a BhCG ratio if the initial serum progesterone was >2 nmol/L. Patients with a progesterone ≤2 nmol/L were deemed low risk for EP, requiring only a follow-up urine hCG in 2 weeks to confirm a negative result. The authors concluded that the M6P approach is the best prediction model for PUL. However, the 2ST made PUL management more efficient with little loss of performance. The authors recommended using M6P and its incorporation into a two-step strategy (2ST) for PUL triage.

A recently published trial evaluated active versus expectant management in 255 hemodynamically stable patients with persisting PUL [9]. A persisting PUL was described as a pattern of serial hCG levels that suggests neither an ongoing pregnancy nor one undergoing spontaneous resolution. Empiric management consisted of close surveillance with serial hCG levels every 4–7 days. Active management included uterine evacuation with methotrexate as needed, or empiric methotrexate. Patients undergoing uterine evacuation had an hCG the day after the procedure. Those whose hCG did not decline at least 15% were treated with methotrexate, following a two-dose protocol of two intramuscular doses of 50 mg/m^2 given 3 days apart [10]. The two-dose protocol was also used for the empiric methotrexate treatment group. This trial found that a higher percentage of women had successful resolution of pregnancy with active management than expectant management (51.5% vs. 36.0%). There was no significant difference in resolution between the two active management groups (empiric methotrexate vs. uterine evacuation [54.9% vs. 48.3%]), although the median time to resolution was 6 days shorter for patients treated with uterine evacuation. Further, patients undergoing active management were less likely to undergo unscheduled surgery (12.7% vs. 26.7%). Five women in the study were diagnosed with a ruptured ectopic pregnancy, two undergoing expectant management and three undergoing active management. All were treated successfully with laparoscopy. Of note, one participant in the expectant management group ultimately had a normal intrauterine pregnancy, despite abnormally rising serial hCG levels initially: 7% in 2 days (86 mIU/mL and 92 mIU/mL) and 24% over 4 days (92 mIU/mL and 107 mIU/mL). Subsequently, her hCG levels rose normally. The etiology of this slow rise in very early pregnancy was not clear.

Human Chorionic Gonadotropin (hCG) Dynamics

Human chorionic gonadotropin (hCG) can be qualitatively assessed resulting in a positive or negative result. However, measuring the quantitative hCG level in the blood is quite useful if the initial pregnancy evaluation is inconclusive. One can follow serial hCG levels, using the rationale that abnormally rising levels are more consistent with either an EP or a failed IUP. Older studies determined that the 2-day rise of hCG in a normal pregnancy is at least 66% [11]. A 2004 study determined that the 2-day rise in hCG (normal pregnancy) ranged between 1.53 and 3.28 times, with a median of 2.24 times [12]. The premise is that an ectopic pregnancy will have an inadequate rise in the hCG level over 2 days, as only 21% of EPs will have a rise of 53% or more [13]. In 2016, Barnhart et al. found differences in the rate of hCG rise based on the initial hCG levels. The predicted hCG minimal rise was 49% when the hCG was less than 1500 mIU/mL, 40% with a level of 1500–3000 mIU/mL, and 33% when the initial level was greater than 3000 mIU/mL [14]. Further, they determined that hCG levels rise faster in African American women.

An often overlooked finding of one early study was that 15% of normal pregnancies had abnormal hCG increases [11]. Thus, abnormally rising hCG levels are not necessarily diagnostic of an ectopic pregnancy, only highly suggestive. Thus, one should exercise caution when evaluating the rise in hCG. Abnormal increases in hCG values should raise one's index of suspicion for an ectopic pregnancy or an abnormal intrauterine pregnancy. TVS is valuable, regardless of hCG increase, to determine the location and status of the pregnancy.

Threshold and Discriminatory Levels of hCG

Threshold Level

The threshold level is the lowest level of hCG at which a normal intrauterine pregnancy can be detected, typically visualizing an early gestational sac. Older studies proposed a threshold value of 1000 mIU/mL [15]. However, advances in ultrasound technology have improved our imaging capabilities. Thus, more recent studies indicate that the threshold level may be as low as 390 mIU/mL [16].

Discriminatory Level

The discriminatory level is that level of hCG above which all normal (singleton) intrauterine pregnancies should be seen. This level typically ranged between 1000 and 1500 mIU/mL in most laboratories. The discriminatory level or value, however, has undergone revision, based on two key studies. Doubilet and Benson reviewed a decade of experience in patients with TVS and hCG done on the same day [17]. They identified those patients whose initial TVS did not visualize an intrauterine fluid collection, with embryonic or fetal cardiac activity found on subsequent ultrasound studies. They demonstrated that slightly more than 10% of patients with an IUP that was ultimately diagnosed had an initial hCG ≥1500 mIU/mL (5.9% with levels of 1500–1999 mIU/mL; 4.5% >2000 mIU/mL) (Table 17.2). Connolly et al. performed a similar study including patients who had a TVS and hCG within 6 h of each other. They tabulated the levels associated with 99% of IUPs. In this study, the discriminatory level was 3510 mIU/mL (Table 17.3). The current recommendation with an inconclusive ultrasound, assuming that the patient is hemodynamically stable, is to follow the patient until the hCG level is at least 3000–3500 mIU/mL before declaring that an IUP is not visualized. This would defer medical intervention, such as methotrexate, until the diagnosis is

Table 17.2 Evidence against the hCG discriminatory level [17]

hCG (mIU/mL) 3rd–4th International Standard	# (202)	%
<1000	162	80.2
1000–1499	19	9.4
1500–1999	12	5.9
≥2000	9	4.5

Table 17.3 Reevaluation of the threshold and discriminatory levels [16]

hCG (mIU/mL)	Gestational sac	Yolk sac	Embryo
Threshold level	390	1094	1394
Discriminatory level	3510	17,716	47,685

clarified. This recommendation will largely avoid the inadvertent treatment of an IUP with methotrexate, with resultant fetal anomalies or fetal loss [18]. These hCG levels and recommendations pertain only to singleton pregnancies (see Chap. 10). Multiple gestations often have much higher hCG levels before identifying the intrauterine gestations. Thus, caution is advised in patients who have undergone assisted reproduction.

Endometrial Findings in Ectopic Pregnancy

Endometrial Thickness

When a gestational sac or yolk sac is not visualized, endometrial thickness may be helpful in assessing the location of a pregnancy. Spandorfer and Barnhart reviewed the ultrasound-measured endometrial thickness in patients with an hCG below the discriminatory level. In general, an IUP had a mean endometrial thickness that was greater than an EP or a spontaneous miscarriage (13.42 mm vs. 5.95 mm vs. 9.28 mm, respectively) [19]. In their study, an endometrial thickness ≤8 mm was associated with an abnormal pregnancy in 97% of cases. A more recent study found no statistical difference in the endometrial thickness in patients with an IUP (12.24 ± 6.0 mm), a spontaneous miscarriage (10.19 ± 6.0 mm), or an ectopic pregnancy (9.56 ± 4.87 mm), noting the trend for an IUP having a thicker endometrium [20]. They further found that 99% of ectopic pregnancies had an endometrial thickness of less than 21 mm. Thus, they concluded that the lack of identifying a gestational sac with an endometrial thickness >21 mm is more commonly associated with an IUP. When evaluating early pregnancy, a thicker endometrium may be more commonly associated with an IUP, while a thinner endometrium is more common with an EP (Figs. 17.1 and 17.2).

Intrauterine Fluid

The characteristics and shape of the intrauterine fluid in early pregnancy help determine a pregnancy's location. Benson et al. determined that no intrauterine fluid was present in 83.4% of patients with an EP (191 of 229) [21]. Furthermore, 86.8% of those patients with an EP and intrauterine fluid (33 of 38) also had an adnexal mass. In most of these patients (31 of 38, or 81.6%), the fluid that was present tended to follow the contour of the endometrial cavity (Fig. 17.3). A smaller number (7 of 38, or 18.4%)

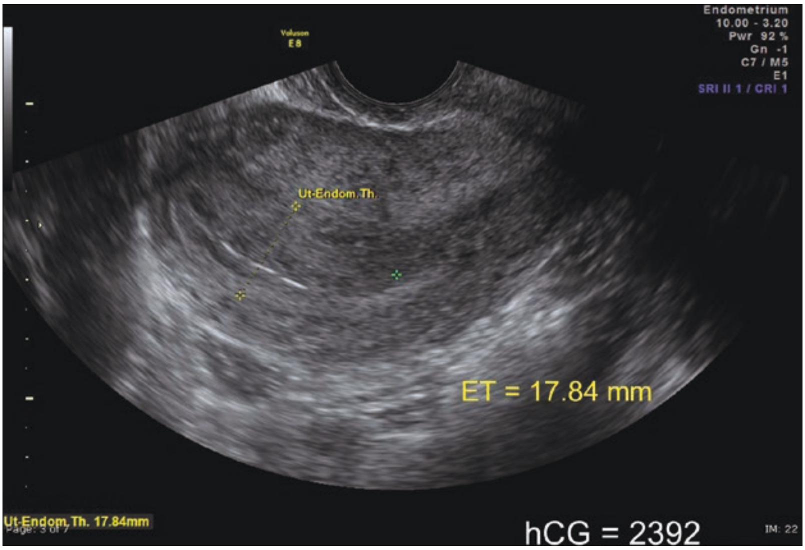

Fig. 17.1 Thicker endometrium (17.84 mm) in an early intrauterine pregnancy

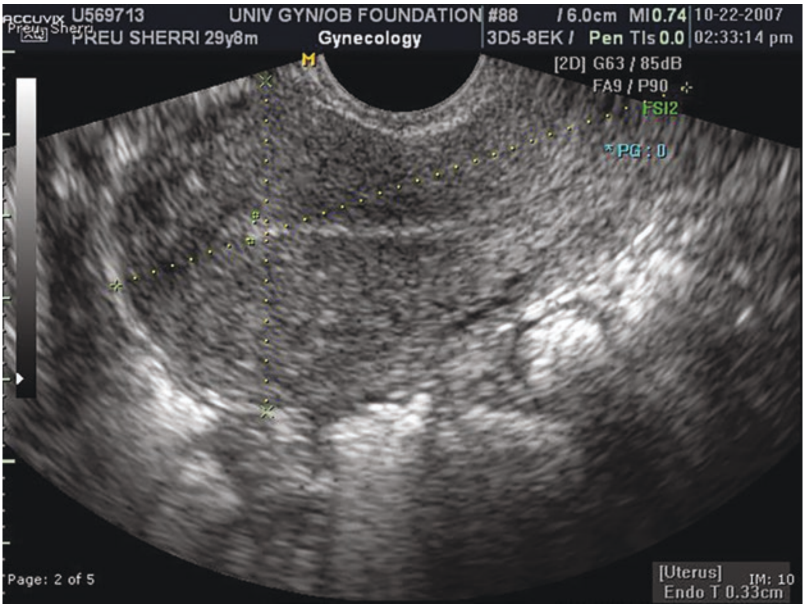

UNIV GYN/OB FOUNDATION
Gynecology
10-22-2007
Page: 2 of 5
[Uterus]
Endo T 0.33cm

Fig. 17.2 Thin endometrium (3.3 mm) associated with an ectopic pregnancy

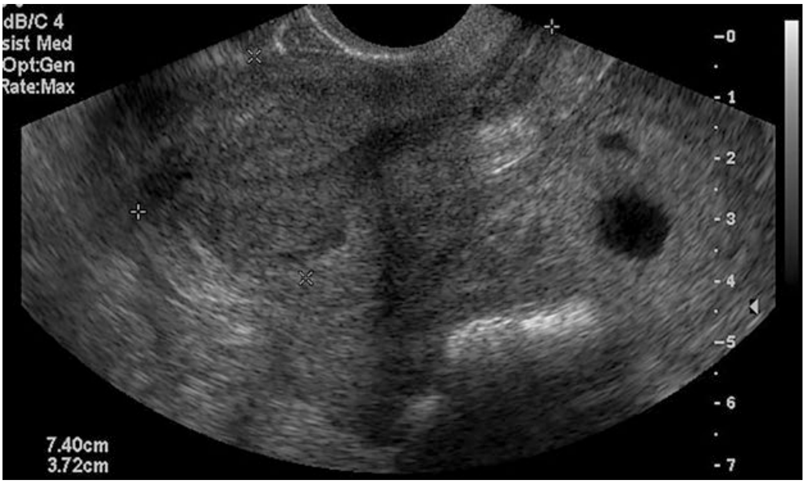

7.40cm
3.72cm

Fig. 17.3 Intrauterine fluid with low-level echoes following the endometrial contour in patient with an ectopic pregnancy

had a smooth-walled, cyst-like structure within the uterus. Such a cystic fluid collection can mimic an IUP. The differentiation is that the gestational sac of an IUP burrows into the decidua and is located slightly eccentrically (Fig. 17.4). One of the most important findings of this study was that a smooth-walled anechoic intrauterine cystic structure with no identified adnexal mass is associated with an IUP in 99.8% of patients (Fig. 17.5).

Fig. 17.4 Gestational sac located in the posterior endometrium in an early intrauterine pregnancy

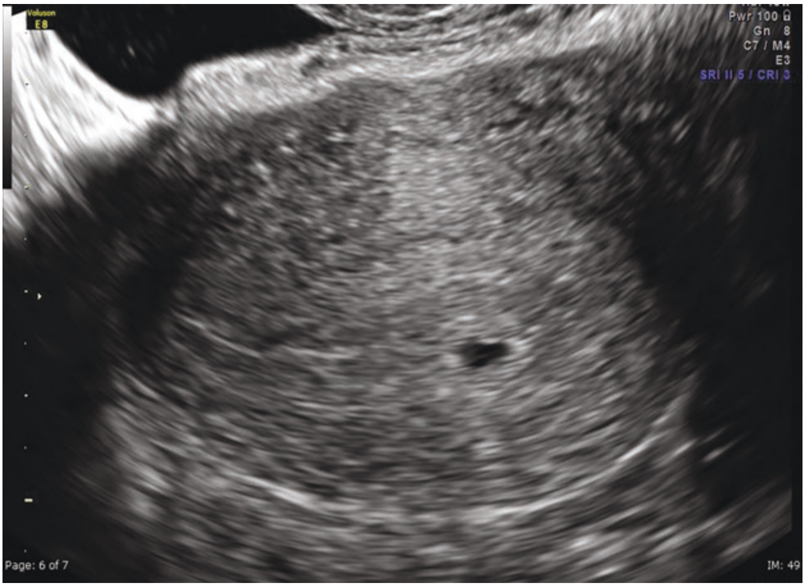
Voluson
E8
Pwr 100
Gn 8
C7 / M4
E3
SRI II 5 / CRI 3
Page: 6 of 7
IM: 49

Fig. 17.5 Smooth-walled anechoic sac in a patient with an early IUP

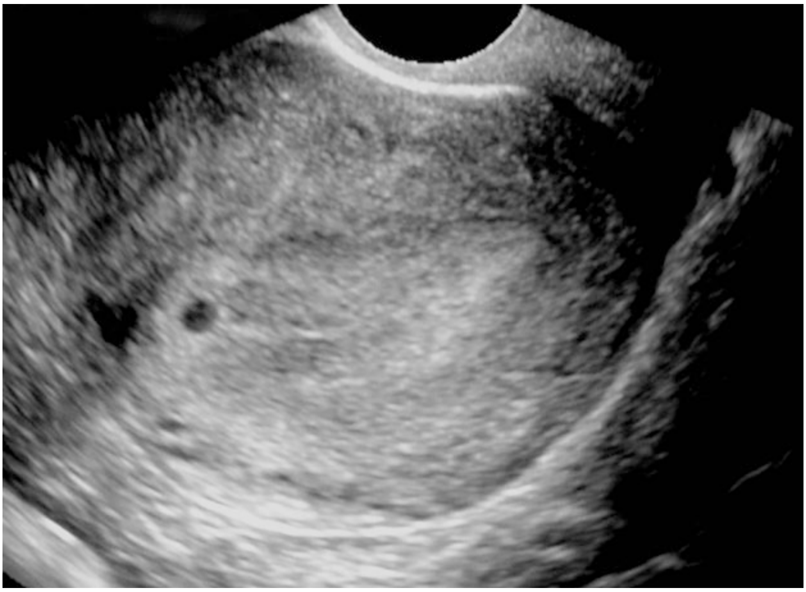

Adnexal Findings in Ectopic Pregnancy

In 1994, Brown and Doubilet reviewed 10 studies with over 2000 patients with suspected EP to determine the adnexal findings associated with an ectopic pregnancy [22]. All ectopic pregnancies were surgically confirmed. They determined the following four categories of adnexal findings associated with ectopic pregnancies:

1. An adnexal embryo with a heartbeat (Fig. 17.6)
2. An adnexal mass with a yolk sac and no embryonic cardiac activity (Fig. 17.7)
3. An adnexal mass with a central anechoic area with a hyperechoic ring ("tubal ring" or the "bagel sign") (Fig. 17.8)
4. Any adnexal mass, other than a simple cyst or an intraovarian lesion (Fig. 17.9)

The first two findings are diagnostic of an EP. The likelihood of an ectopic pregnancy with a tubal ring is 95%. The likelihood of an ectopic pregnancy with any complex or solid adnexal mass that is not intraovarian is 92% (Table 17.4). Such adnexal findings are present in almost 95% of EP with each finding being visualized in 7.4%, 8.3%, 24.7%, and 54.1% (respectively) of EP [23].

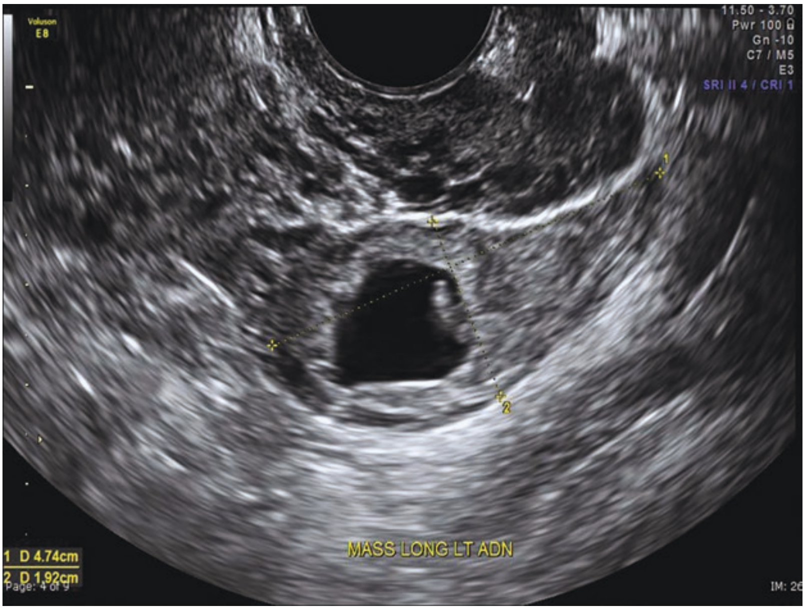

Fig. 17.6 Adnexal embryo with FHR = 172, which is diagnostic of an ectopic pregnancy

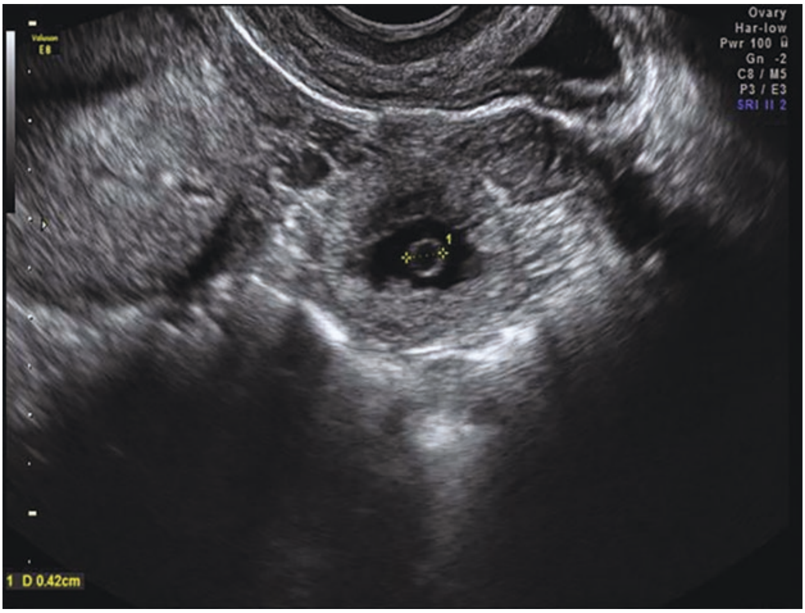
Voluson
E8
Ovary
Har-low
Pwr 100
Gn -2
C8 / M5
P3 / E3
SRI II 2
1
1 D 0.42cm

Fig. 17.7 Adnexal mass with a yolk sac, which is diagnostic of an ectopic pregnancy

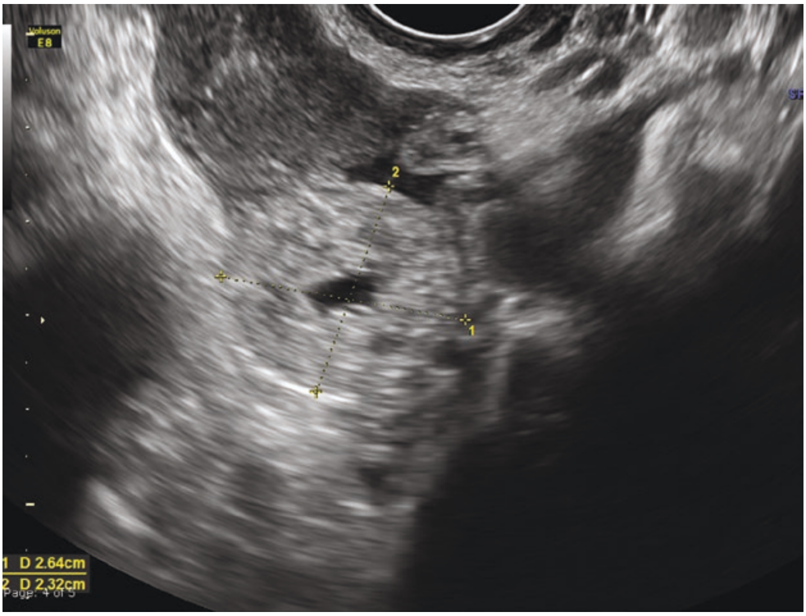
Voluson
E8
2
1
1 D 2.64cm
2 D 2.32cm
Page: 4 of 5

Fig. 17.8 "Tubal ring," or so-called bagel sign in an ectopic pregnancy

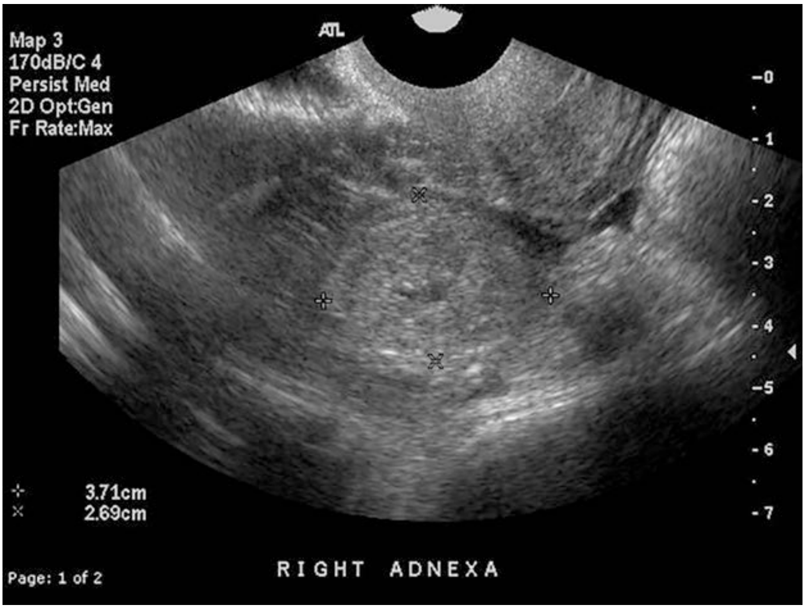

Fig. 17.9 Adnexal mass separate from the ovary in an ectopic pregnancy

Table 17.4 Adnexal criteria for ectopic pregnancy[22, 23]

Adnexal finding on TVS	Likelihood of ectopic (%) [22]	Frequency of findings (%) [23]
Extrauterine embryo with cardiac activity	100	7.4
Adnexal mass with yolk sac without embryonic cardiac activity	100	8.3
Adnexal mass with central anechoic area and hyperechoic rim ("tubal ring")	95	24.7
Any complex or solid adnexal mass other than a simple cyst or intraovarian lesion	92	54.1

Workup for Ectopic Pregnancy

This chapter reviews the hCG and ultrasound findings in ectopic pregnancy. The order in which one performs various tests, including serum progesterone, in patients with suspected EP was evaluated by Garcia and Barnhart in a 2001 paper [24]. The order of these tests included the following:

- Ultrasound followed by quantitative hCG if the ultrasound findings were inconclusive
- Quantitative hCG followed by ultrasound, when the hCG was > threshold value
- Progesterone followed by ultrasound and, if inconclusive, then quantitative hCG
- Progesterone followed by quantitative hCG and, when > threshold value, then ultrasound
- Ultrasound followed by repeat ultrasound
- Clinical examination only

They applied these algorithms to a theoretical cohort of 10,000 patients determining the number of ultrasounds, blood draws, dilatation and curettages, and laparoscopies performed. They then predicted the costs of the various strategies and their effectiveness in diagnosing EPs (Table 17.5). Ultimately, they recommended either of the first two strategies; as the progesterone methods missed more ectopic pregnancies, the ultrasound only strategy was too costly and the clinical exam-only

Table 17.5 Six strategies for diagnosing ectopic pregnancy [24]

Strategy	Days to Dx	Blood draws/10,000	Total charge per patient	Missed EP per 10,000	Interrupted IUP per 10,000
Ultrasound → hCG	1.46	5227	$1958	0	70
hCG → ultrasound	1.66	14,375	$1842	0	122
P → ultrasound → hCG	1.25	12,108	$1692	24	25
P → hCG → ultrasound	1.26	15,000	$1569	24	39
Ultrasound → ultrasound	1.21	0	$2486	0	121
Clinical exam only	1.0	0	$0	940	0

method too ineffective. Of note, although serum progesterone may be helpful in predicting the viability of a pregnancy [25], the Garcia study confirmed the findings of others that progesterone lacks adequate sensitivity in distinguishing ectopic and intrauterine pregnancies [26–28].

An Argument for Ultrasound First, Tubal Rupture Below the Threshold Level

The Connolly study previously discussed determined that the threshold level of hCG should be lowered to 390 mIU/mL [16]. Prior to this study, many practitioners deferred ultrasound until the hCG level was ≥1000 mIU/mL. However, an early study by Saxon et al. demonstrated that 50% of ruptured EPs had an hCG ≤999 mIU/mL [29]. This finding was confirmed by the 2014 report of Frates et al. also demonstrating that 41.2% of ruptured EPs had an hCG <1000 mIU/mL. Thus, in patients with suspected EP, performing ultrasound first has value in identifying a definite IUP, EP, or a significant hemoperitoneum (Fig. 17.10). Not visualizing a significant hemoperitoneum allows a more conservative evaluation of such patients while assuring patient safety.

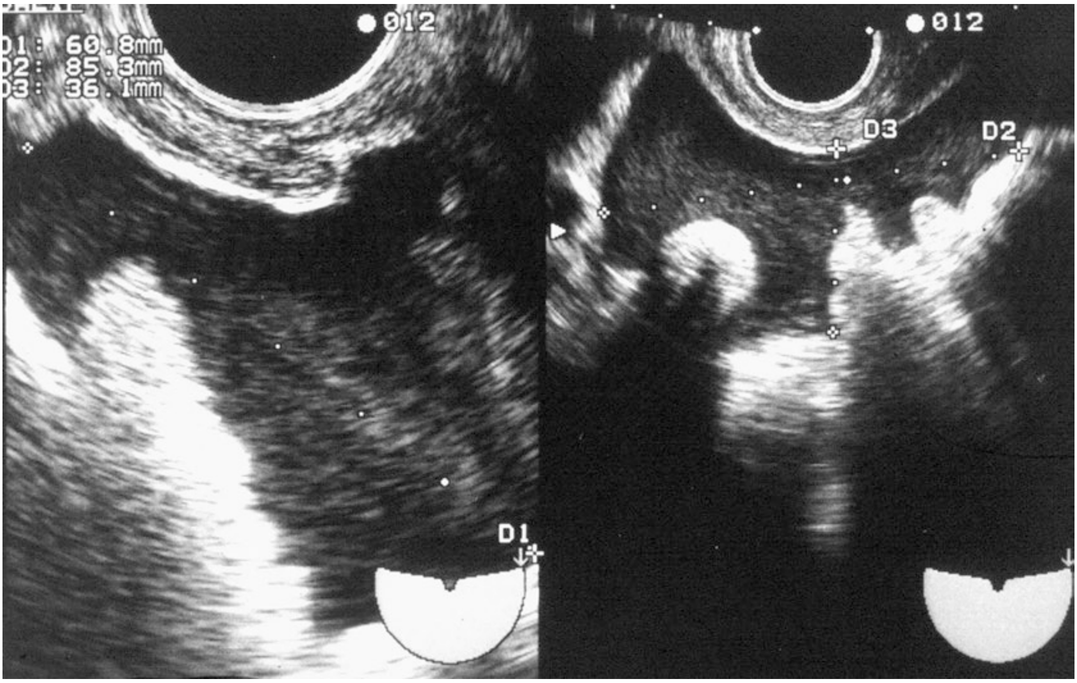

Fig. 17.10 Significant hemoperitoneum identified in a patient with an hCG = 465 mIU/mL

Spontaneous Resolution of Pregnancy

The use of ultrasound for initial patient evaluation can result in identifying adnexal masses that are highly suggestive of an EP, in association with hCG levels that are below the threshold level (Fig. 17.11). Clinicians often feel obligated to treat patients for fear of rupture of an EP. Frates et al. determined that, regardless of the four adnexal findings noted in the prior section, there was no significant difference in the rate of tubal rupture, which ranged from 17.6% to 28.4% [23]. They found that the most sensitive ultrasound finding of rupture was a moderate to large amount of free fluid. Thus, in a hemodynamically stable patient, there is no need for urgent intervention if there is either no or only a small amount of fluid in the cul-de-sac or abdomen. Korhonen et al. observed patients who had decreasing or stable hCG levels, an adnexal mass less than 4 cm in size, and no embryonic cardiac activity [30]. They found that the rate of spontaneous resolution of a suspected or definite EP was 88% when the initial hCG was less than 200 mIU/mL and 25% when the initial hCG was over 2000 mIU/mL. It must be emphasized that the hCG levels were stable or decreasing in these patients. However, this study demonstrated that observation is a reasonable option in well-selected patients meeting the criteria for spontaneous resolution of their EP.

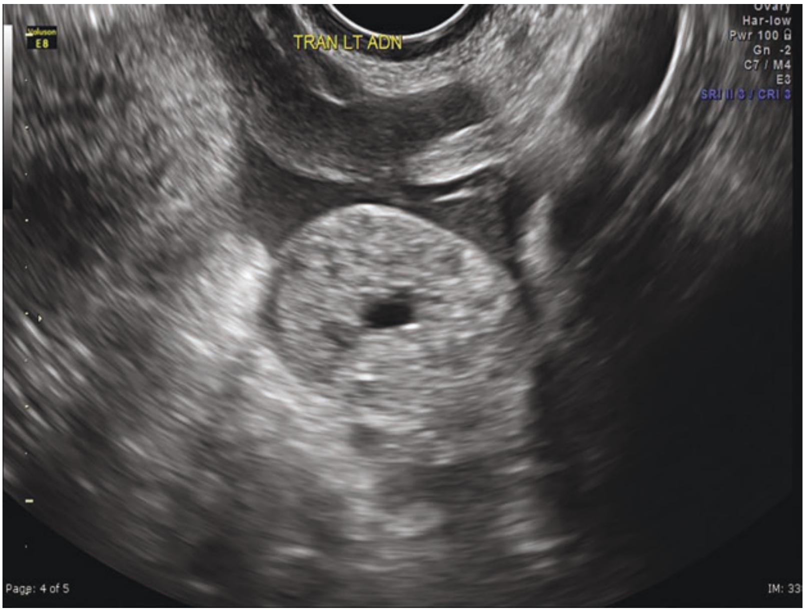

Fig. 17.11 "Tubal ring" consistent with an ectopic pregnancy in a patient with an hCG = 78 mIU/mL

Unusual Ectopic Pregnancies

Heterotopic Pregnancy

The presence of an EP in combination with an IUP is designated a heterotopic pregnancy (Fig. 17.12). The rate of such pregnancies with spontaneous conception may be as low as 1 in 30,000. However, the increased use of assisted reproductive technology has led to an increased incidence of heterotopic pregnancy, perhaps as high as 1 in 110 [31, 32]. One must establish a routine of performing a thorough evaluation of all patients to avoid missing a concomitant EP when a definite IUP is identified.

Interstitial Pregnancy

Interstitial pregnancies are those pregnancies located within the interstitial portion of the fallopian tube and lateral to the endometrial cavity, accounting for 2–4% of all ectopic pregnancies [33]. Three-dimensional (3D) multiplanar reconstruction of the coronal plane is incredibly valuable in localizing such pregnancies (Fig. 17.13). These pregnancies are defined by the ultrasound findings of an empty uterine cavity and a chorionic sac >1 cm from the lateral edge of the uterine cavity (the endometrium), with a thin (<5 mm) layer of myometrium surrounding the chorionic

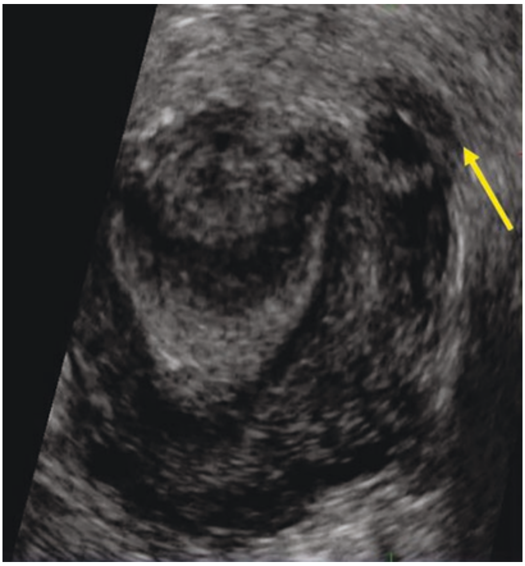

Fig. 17.13 Interstitial pregnancy identified on the 3D coronal view

Fig. 17.12 Heterotopic pregnancy with both an intrauterine pregnancy and a tubal pregnancy

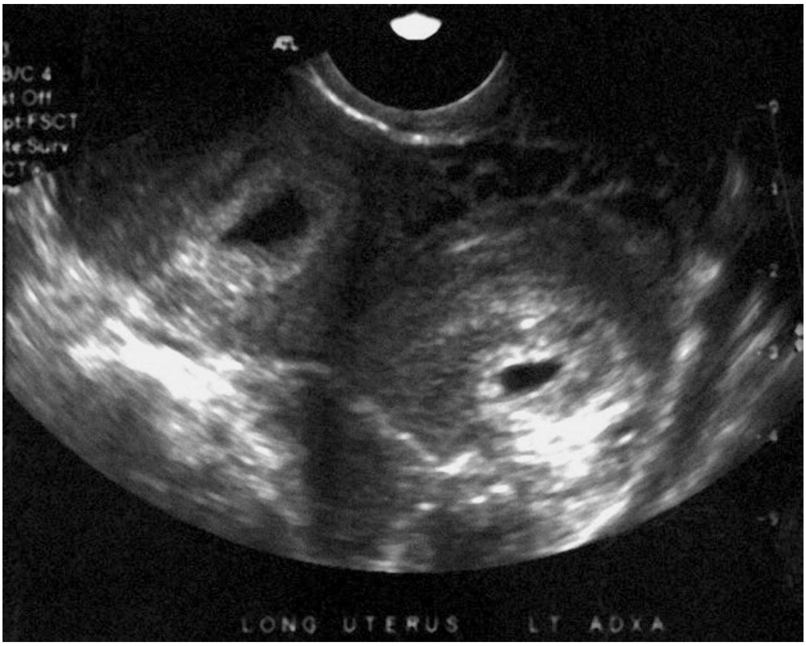

sac [34]. Unfortunately, interstitial pregnancies have also been erroneously referred to as cornual pregnancies.

Cornual Pregnancy

A cornual pregnancy previously referred to the implantation of a pregnancy in one of the cornua of a bicornuate, septate, or subseptate uterus [35]. However, such pregnancies are in fact intrauterine. Baltarowich advocated for reserving the term “cornual pregnancy” when implantation occurs in a rudimentary horn attached to a unicornuate uterus, whether communicating or not [33] (Fig. 17.14). Again, 3D ultrasound can be helpful in diagnosing such pregnancies. Although there are few reports of progression into the third trimester, most cornual pregnancies ultimately rupture with fetal demise and potentially fatal maternal hemorrhage.

Angular Pregnancies

Angular pregnancies refer to the eccentric implantation of an IUP in the cornual area of a normally shaped uterus. Specific criteria for diagnosing an angular pregnancy were offered by Jansen and Elliott in 1981 [36]. These include the following:

- Painful asymmetric uterine enlargement
- Directly observed lateral distension of the uterus, with or without rupture, accompanied by displacement of the round ligament reflection laterally
- Retention of the placenta in the uterine angle

Angular pregnancies may carry to term, or at least viability, with more conservative management options available. TVS, particularly using 3D with its coronal views (Fig. 17.15), has remarkably clarified the diagnosis of these eccentrically located pregnancies, as it offers the ability to detect any uterine anomalies and define the specific implantation site of a pregnancy. Thus, diagnostic criteria are now based on ultrasound rather than surgical pathology. Correct designation is imperative for proper communication of the ultrasound findings.

Ovarian Pregnancy

Ovarian pregnancies are rare with 0.15–3% of EP occurring in the ovary [37, 38]. The diagnosis includes an empty uterine cavity with a gestational sac, yolk sac, fetal cardiac activity, or embryo visualized in the ovary [39] (Fig. 17.16). The ultrasound criteria for diagnosing an ovarian EP are (1) a wide echogenic ring with an internal

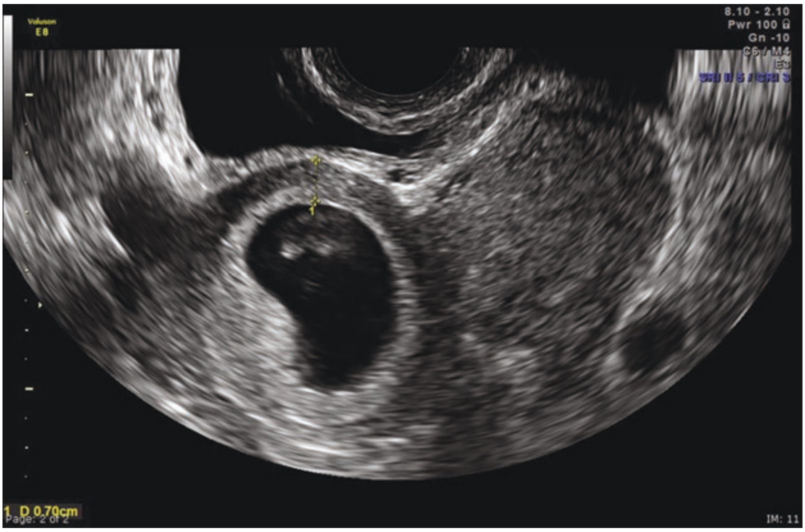

Fig. 17.14 Cornual pregnancy with pregnancy in a non-communicating uterine horn

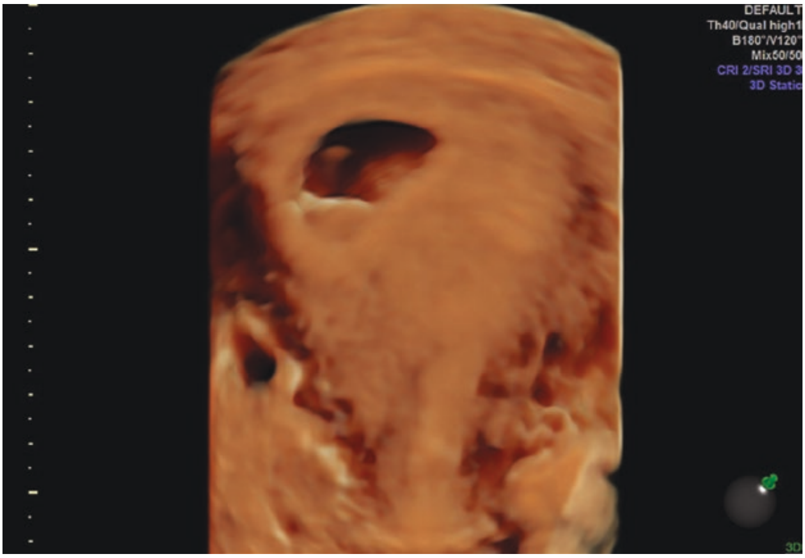
DEFAULT
Th40/Qual high1
B180°/V120°
Mix50/50
CRI 2/SRI 3D 3
3D Static
3D

Fig. 17.15 Angular pregnancy that progressed to a full-term delivery

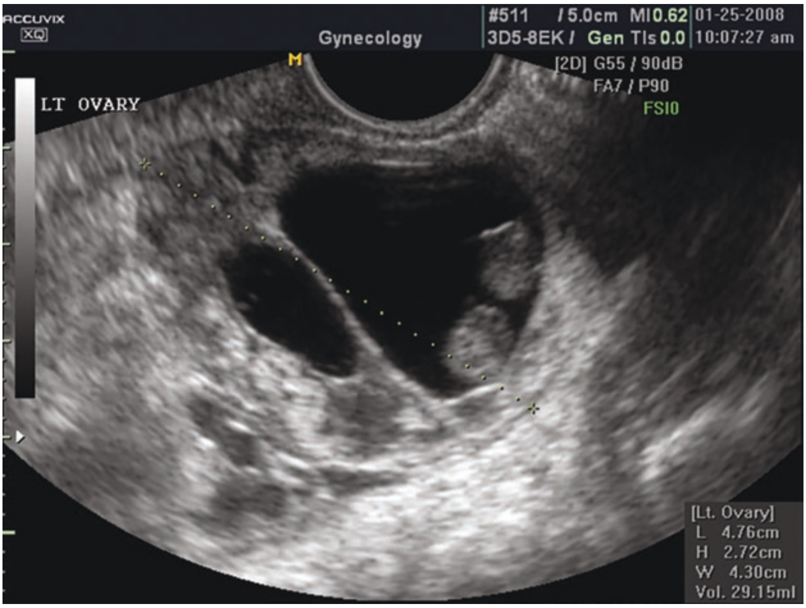
ACCUVIX
XQ
Gynecology
#511 / 5.0cm MI 0.62
3D5-8EK / Gen TIs 0.0
01-25-2008
10:07:27 am
M
[2D] G55 / 90dB
FA7 / P90
FSI0
LT OVARY
[Lt. Ovary]
L 4.76cm
H 2.72cm
W 4.30cm
Vol. 29.15ml

Fig. 17.16 Ovarian pregnancy with nonviable embryo identified in a gestational sac within the ovary

echolucent area and (2) a yolk sac or fetal heart motion in the ovary [39]. The diagnosis is confirmed histologically by the Spiegelberg criteria as follows [40]:

- The gestation occupies a normal position of the ovary.
- The gestational sac, and thus the ovary, must be attached to the uterus by the ovarian ligament.
- Ovarian tissue is histologically proven in the wall of the gestational sac.
- The fallopian tube on the affected side must be intact.

Abdominal Pregnancy

Abdominal pregnancies are quite rare. However, there is significant maternal and perinatal mortality and morbidity encountered with such pregnancies. This is due to the implantation that occurs outside of the uterus, anywhere in the abdomen. Mortality is markedly higher when attachment occurs to the liver or spleen [41]. The diagnosis is often made later in pregnancy, as the pregnancy has the ability to expand in the abdomen. Studdiford's criteria for appropriate diagnosis include the following [42]:

- The fallopian tubes and ovaries are normal.
- There is no abnormal connection, e.g., fistula, between the uterus and the abdominal cavity.
- The pregnancy is related solely to the peritoneal surface without signs of prior tubal rupture.

Diagnosis requires demonstration of an empty uterus, often normal in appearance, with the fetus contained within a gestational sac, which is separate from the uterus and cervix [43] (Fig. 17.17).

Cervical Pregnancy

Cervical pregnancy has an incidence of 1:1000 to 1:16,000 [44]. Diagnosis requires the demonstration of a gestational sac with a yolk sac or embryo in the endocervix, with an "empty" uterine cavity (Fig. 17.18a, b). If the pregnancy implants higher, near the uterine cavity, it is called a cervico-isthmic pregnancy [45]. Previously, diagnosis of a cervical pregnancy was confirmed histologically with Rubin's criteria applied to the surgical specimen. These criteria include the following [46]:

- Cervical glands are opposite to the trophoblastic tissue.
- The trophoblastic attachment is below the entrance of the uterine vessels to the uterus or the anterior peritoneal reflection.
- Fetal elements are absent from the uterine corpus.

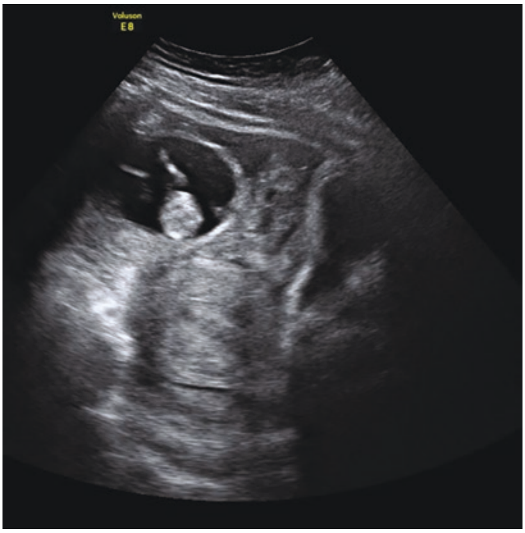

Fig. 17.17 Abdominal pregnancy on transabdominal ultrasound. Note the "empty" uterus

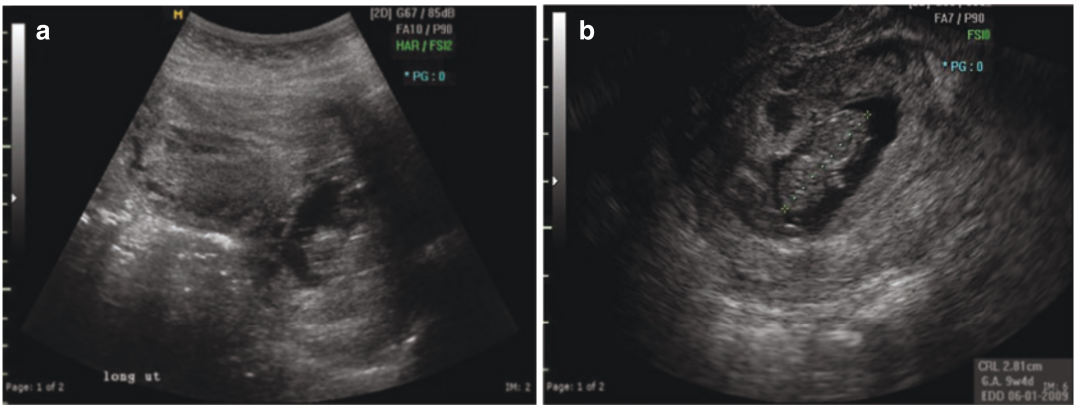

Fig. 17.18 (**a**) Cervical pregnancy with an embryo visualized in the endocervix-abdominal study. (**b**) Cervical pregnancy with an embryo visualized in the endocervix-vaginal study

Current treatment is more conservative often with direct injection of methotrexate or potassium chloride (KCl), uterine artery embolization, or more conservative surgical approaches [44]. Thus, Rubin's criteria cannot be applied to pregnancies treated without hysterectomy.

Cesarean Scar Pregnancies

These pregnancies are increasing in frequency. Timor-Tritsch, who has published extensively on the topic [47], will discuss cesarean scar pregnancies in a subsequent chapter (see Chap. 18).

Summary

Ectopic pregnancy continues to be a challenging and critical diagnosis, as conservative medical and surgical treatment options rely on early diagnosis. Ultrasound remains the mainstay in diagnosis in coordination with other laboratory tests, particularly quantitative hCG and, in select patients, serum progesterone. Clinical care algorithms are appropriate when ultrasound fails to determine the pregnancy location, the so-called pregnancy of unknown location. In hemodynamically stable patients, such algorithms allow appropriate follow-up until one determines the pregnancy location and its viability status. An established examination protocol is crucial in evaluating patients with suspected ectopic pregnancy, to assure proper diagnosis of pregnancies implanted in unusual locations. Strict adherence to such protocols and algorithms allows timely and accurate diagnosis, with appropriate and patient-specific treatment options.

Teaching Points

- Patients with pregnancies of unknown location who are hemodynamically stable can be managed expectantly as most are ultimately diagnosed as a viable or failed intrauterine pregnancy.
- In patients whose hCG is below the discriminatory level, a thin endometrium, ≤8 mm, is associated with an abnormal pregnancy in 97% of patients.
- In early pregnancy, a cystic structure within the endometrium, in the absence of an adnexal mass, is associated with an intrauterine pregnancy in >99% of patients.
- A yolk sac or embryo with or without a heartbeat in the adnexa is diagnostic of an ectopic pregnancy.
- Ultrasound is justified prior to obtaining a quantitative hCG, as almost 50% of ruptured ectopic pregnancies have hCG levels <1000 mIU/mL.
- Observation is appropriate in hemodynamically stable patients, as spontaneous resolution of ectopic pregnancy occurs in 25–88% of patients.
- There are specific criteria for the diagnosis of ectopic pregnancies in unusual locations.

References

1. Barnhart KT. Clinical practice. Ectopic pregnancy. N Engl J Med. 2009;361:379–87.
2. Kirk E, Papageorghiou A, Condous G, Tan L, Bora S, Bourne T. The diagnostic effectiveness of an initial transvaginal scan in detecting ectopic pregnancy. Hum Reprod. 2007;22:2824–8.
3. Condous G, Timmerman D, Goldstein S, Valentin L, Jurkovic D, Bourne T. Pregnancies of unknown location: consensus statement. Ultrasound Obstet Gynecol. 2006;28:121–2.
4. Barnhart K, van Mello NM, Bourne T, Kirk E, Van Calster B, Bottomley C, et al. Pregnancy of unknown location: a consensus statement of nomenclature, definitions, and outcome. Fertil Steril. 2011;95(3):857–66.
5. Condous G, Kirk E, Lu C, Van Huffel S, Gevaert O, De Moor B, et al. Diagnostic accuracy of varying discriminatory zones for the prediction of ectopic pregnancy in women with a pregnancy of unknown location. Ultrasound Obstet Gynecol. 2005;26(7):770–5.
6. Barnhart KT, Sammel MD, Takacs P, Chung K, Morse CB, O'Flynn OK, et al. Validation of a clinical risk scoring system, based solely on clinical presentation, for the management of pregnancy of unknown location. Fertil Steril. 2013;99(1):193–8.
7. Bobdiwala S, Christodoulou E, Farren J, Mitchell-Jones N, Kyriacou C, Al-Memar M, et al. Triaging women with pregnancy of unknown location using two-step protocol including M6 model: clinical implementation study. Ultrasound Obstet Gynecol. 2020;55(1):105–14.

8. Christodoulou E, Bobdiwala S, Kyriacou C, Farren J, Mitchell-Jones N, Ayim F, et al. External validation of models to predict the outcome of pregnancies of unknown location: a multicentre cohort study. BJOG. 2021;128(3):552–62.
9. Barnhart KT, Hansen KR, Stephenson MD, Usadi R, Steiner AZ, Cedars MI, et al. Effect of an active vs expectant management strategy on successful resolution of pregnancy among patients with a persisting pregnancy of unknown location. The ACT or NOT randomized clinical trial. Fertil Steril. 2021;326(5):390–400.
10. Barnhart K, Hummel AC, Sammel MD, Menon S, Jain J, Chakhtoura N. Use of "2-dose" regimen of methotrexate to treat ectopic pregnancy. Fertil Steril. 2007;87(2):250–6.
11. Kadar N, DeVore G, Romero R. Discriminatory hCG zone: its use in the sonographic evaluation for ectopic pregnancy. Obstet Gynecol. 1981;58(2):156–61.
12. Barnhart K, Sammel MD, Rinaudo PF, Zhou L, Hummel A, Guo W. Symptomatic patients with an early viable intrauterine pregnancy: hCG curves redefined. Obstet Gynecol. 2004;104:50–5.
13. Silva C, Sammel MD, Zhou L, Gracia C, Hummel AC, Barnhart K. Human chorionic gonadotropin profile for women with ectopic pregnancy. Obstet Gynecol. 2006;107(3):605–10.
14. Barnhart KT, Wensheng G, Cary M, Morse CB, Chung K, Takacs P, et al. Differences in serum human chorionic gonadotropin rise in early pregnancy by race and value at presentation. Obstet Gyencol. 2016;128(3):504–11.
15. Goldstein S, Snyder JR, Watson C, Danon M. Very early pregnancy detection with endovaginal ultrasound. Obstet Gyencol. 1988;72:200–4.
16. Connolly A, Ryan DH, Stuebe AM, Wolfe HM. Reevaluation of discriminatory and threshold levels for serum β-hCG in early pregnancy. Obstet Gynecol. 2013;121(1):65–70. https://doi.org/10.1097/AOG.0b013e318278f421.
17. Doubilet PM, Benson CB. Further evidence against the reliability of the human chorionic gonadotropin discriminatory level. J Ultrasound Med. 2011;30(12):1637–42.
18. Shwayder JM. Waiting for the tide to change: reducing risk in the turbulent sea of liability. Obstet Gynecol. 2010;116(1):8–15.
19. Spandorfer S, Barnhart K. Endometrial stripe thickness as a predictor of ectopic pregnancy. Fertil Steril. 1996;66(3):474–7.
20. Seeber BE, Sammel M, Zhou L, Hummel A, Barnhart KT. Endometrial stripe thickness and pregnancy outcome in first-trimester pregnancies with bleeding, pain or both. J Reprod Med. 2007;52(9):757–61.
21. Benson CB, Doubilet PM, Peters HE, Frates MC. Intrauterine fluid with ectopic pregnancy: a reappraisal. J Ultrasound Med. 2013;32:389–93.
22. Brown DL, Doubilet PM. Transvaginal sonography for diagnosing ectopic pregnancy: positivity criteria and performance characteristics. J Ultrasound Med. 1994;13(4):259–66.
23. Frates MC, Doubilet PM, Peters HE, Benson CB. Adnexal sonographic findings in ectopic pregnancy and their correlation with tubal rupture and human chorionic gonadotropin levels. J Ultrasound Med. 2014;33(4):697–703.
24. Garcia CR, Barnhart KT. Diagnosing ectopic pregnancy: decision analysis comparing six strategies. Obstet Gynecol. 2001;97(3):464–70.
25. El Bishry G, Ganta S. The role of single serum progesterone measurement in conjunction with βhCG in the management of suspected ectopic pregnancy. J Obstet Gynaecol. 2008;28(4):413–7.
26. Mol BWJ, van der Veen F, Bossuyt PMM. Implementation of probabilistic decision rules improves the predictive values of algorithms in the diagnostic management of ectopic pregnancy. Hum Reprod. 1999;14(11):2855–62.
27. Stovall TG, Ling FW. Single-dose methotrexate: an expanded clinical trial. Am J Obstet Gynecol. 1993;168:1759–65.
28. Mol BW, Lijmer JG, Ankum WM, van der Veen F, Bossuyt PM. The accuracy of single serum progesterone measurement in the diagnosis of ectopic pregnancy: a meta-analysis. Hum Reprod. 1998;13(11):3220–7.
29. Saxon D, Falcone T, Mascha EJ, Marino T, Yao M, Tulandi T. A study of ruptured tubal ectopic pregnancy. Obstet Gynecol. 1997;90(1):46–9.
30. Korhonen J, Stenman UH, Ylöstalo P. Serum human chorionic gonadotropin dynamics during spontaneous resolution of ectopic pregnancy. Fertil Steril. 1994;61:632–6.
31. Clayton HB, et al. Ectopic pregnancy risk with assisted reproductive technology procedures. Obstet Gynecol. 2006;107:598–604.
32. Kirk E, Bottomley C, Bourne T. Diagnosing ectopic pregnancy and current concepts in the management of pregnancy of unknown location. Hum Reprod Update. 2013;20(2):250–61.
33. Baltarowich OH. The term "cornual pregnancy" should be abandoned. J Ultrasound Med. 2017;36:1081–7.
34. Timor-Tritsch IE, Monteagudo A, Matera C, Veit CR. Sonographic evolution of cornual pregnancies treated without surgery. Obstet Gynecol. 1992;79(6):1044–9.
35. Arleo EK, DeFilippis EM. Cornual, interstitial, and angular pregnancies: clarifying the terms and a

review of the literature. Clin Imaging. 2014;38(6): 763–70.
36. Jansen RPS, Elliott PM. Angular intrauterine pregnancy. Obstet Gynecol. 1981;58(2):167–75.
37. Nwanodi O, Khulpateea N. The preoperative diagnosis of primary ovarian pregnancy. J Natl Med Assoc. 2006;989(5):796–8.
38. Einenkel J, Baier D, Horn L, Alexander H. Laparoscopic therapy of an intact primary ovarian pregnancy with ovarian hyperstimulation syndrome. Hum Reprod. 2000;15:2037–40.
39. Comstock C, Huston K, Lee W. The ultrasonographic appearance of ovarian ectopic pregnancies. Obstet Gyencol. 2005;105(1):42–5.
40. Plotti F, Di Giovanni A, Oliva C, Battaglia F, Plotti G. Bilateral ovarian pregnancy after intrauterine insemination and controlled ovarian stimulation. Fertil Steril. 2008;90(5):2015.e3–5.
41. Yagil Y, Beck-Razi N, Amit A, Kerner H, Gaitini D. Splenic pregnancy: the role of abdominal imaging. J Ultrasound Med. 2007;26(11):1629–32.
42. Studdiford W. Primary peritoneal pregnancy. Am J Obstet Gynecol. 1942;44:487–91.
43. Roberts R, Dickinson J, Leung Y, Charles A. Advanced abdominal pregnancy: still an occurrence in modern medicine. Aust N Z J Obstet Gynaecol. 2005;45:518–21.
44. Vela G, Tulandi T. Cervical pregnancy: the importance of early diagnosis and treatment. J Minim Invas Gynecol. 2007;14(4):481–4.
45. Avery DM, Wells MA, Harper DM. Cervico-isthmic corporeal pregnancy with delivery at term: a review of the literature with a case report. Obstet Gynecol Surv. 2009;64(5):335–44.
46. Dixit N, Venkatesan S. Cervical pregnancy: an uncommon ectopic pregnancy. Med J Armed Forces India. 2008;64(2):183–4.
47. Timor-Tritsch IE, Monteagudo A. Unforeseen consequences of the increasing rate of cesarean deliveries: early placenta accreta and cesarean scar pregnancy. A review. Am J Obstet Gynecol. 2012;207(1):14–29.

18

Cesarean Scar Pregnancy: A Baby Placenta Accreta

Ilan E. Timor-Tritsch, Ana Monteagudo,
and Terry-Ann Bennett

Introduction/Terminology

Before discussing epidemiology, it is important to touch upon the diagnostic issues and management of cesarean scar pregnancy (CSP). The terms and names used to define this entity and special form of early pregnancy are often referred to as "cesarean ectopic pregnancy," "cesarean scar ectopic," or "cesarean delivery scar pregnancy." Other terms may also include the word "ectopic." In fact, there is a heated discussion among societies and interested professional groups about the subject of whether CSP is a form of intrauterine pregnancy or is it, by definition, an ectopic gestation. Recently in an opinion article, convincing arguments were voiced to discourage all clinicians to use the term "cesarean ectopic pregnancy" and employ what we consider the anatomically as well as clinically correct term: CSP [1].

In fact, there are three main reasons to avoid using the term "ectopic." First, CSP is **well within the uterine cavity**. The placenta at times (but not always) is squeezed into the niche or dehiscence created by the cesarean delivery in the lower segment of the uterus or at the level of the internal os. If untreated, the gestational sac and the embryo/fetus will develop within the uterine cavity, which is within the well-defined and widely accepted anatomic boundaries of the uterus. Second, a CSP can lead to a live offspring as opposed to any kind of true ectopic pregnancy, which rarely, if ever, results in a viable neonate. Last, treatments devised for true ectopic pregnancies and applied for a CSP may not work or may even cause complications.

Our analysis of 751 cases of CSP reviewed until 2012 found that almost a third (30%) were misdiagnosed or diagnosed at a late gestational age, significantly contributing to a large number of treatment complications that could have been avoided by an early and correct diagnosis. Although an exact number cannot be quoted, it seems that, due to a higher awareness of the disease, among 1223 cases found in the literature published between 2012 and 2014, the number of misdiagnoses appeared to have dropped significantly.

Background

Due to the close and causal relationship between a previous CD and CSP, we have to discuss the gradual but steady increasing rate of CD in the USA and the rest of the world. In the USA, the rate of CD slowly increased from 5% in 1970 to

---

I. E. Timor-Tritsch (✉) · A. Monteagudo ·
T.-A. Bennett
Division of Obstetrical and Gynecological Ultrasound and Maternal Fetal Medicine, Department of Obstetrics and Gynecology, New York University School of Medicine, New York, NY, USA
e-mail: Ilan.timor@nyulangone.org

© The Author(s), under exclusive license to Springer Nature Switzerland AG 2023

J. S. Abramowicz, R. E. Longman (eds.), *First-Trimester Ultrasound*,
https://doi.org/10.1007/978-3-031-24133-8_18

32.9% in 2009 [2]. Recent national statistics by the Centers for Disease Control and Prevention report a leveling off of CD rate, which in 2012 reached 32.8% [3]. To our knowledge, no updated CDC communications to update the previous ones were published. Rates ranging from 35% to 80% were reported in other parts of the world [4], leading us to believe that the incidence of CSP is higher in those countries than in the USA. Expect an increase in incidence nationally and internationally mostly due to increased awareness and more accurate diagnosis.

Keeping in mind the causative connection between CD and its recognized consequences, such as the placenta previa and placenta accrete spectrum (PAS) in the last decade, many Ob/Gyn practitioners became increasingly exposed to the clinical picture of PAS. Most have rarely, if ever, faced a patient with a first- or early second-trimester CSP. The learning process was traumatic resulting in misdiagnosed patients with CSP as "aborting gestations," "ectopic pregnancies," and "cervical pregnancies." Also, obstetricians were confronted with diagnostic and management dilemmas. When "traditional" treatments, such as D&C and systemic methotrexate (MTX), were employed, practitioners experienced severe and almost unmanageable vaginal bleeding that, at times, led to hysterectomy. If "low-lying" pregnancies were left to continue, many resulted in second-trimester uterine ruptures and profuse internal or vaginal bleeding, causing loss of the pregnancy and requiring hysterectomy. Even in reviewing the literature, one could usually find reports of single or sporadic cases or a series of one to two dozen cases that would fit the clinical picture. It is clear that it was impossible to learn from the numerous, previously used treatments, "tested" on few patients (sometimes only one). The published review compiling 751 patients diagnosed with CSP [5] may have helped to shed light on the various treatments and their complications; however, to date, there is no universally recognized treatment protocol adopted by professional societies. Our chapter will discuss the pathogenesis, diagnosis, counseling, and management options to treat CSP based upon the evidence in the literature as well as our own clinical experience.

What Is a Cesarean Scar Pregnancy?

Cesarean scar pregnancy develops if a blastocyst implants *on* the uterine scar or *in* the dehiscence (otherwise known as a "niche") resulting from repair of the uterine incision at the previous CD. Implantation of the fertilized oocyte in the faulty anterior uterine wall will give rise to the CSP.

While the definition and diagnostic issues of CSP will be expanded on later, it may be useful to define the main features of it here:

- Cesarean scar pregnancy (CSP) is a potentially dangerous, man-made consequence of a previous cesarean delivery (CD).
- It is detected after a **previous cesarean delivery**.
- It features an empty uterine cavity and closed, empty endocervical canal.
- It is detected as a low/anterior gestational sac and/or placenta in close proximity (or **previa**) of the hysterotomy scar/niche with fetal or embryonic pole and/or yolk sac with/without heartbeats.
- It usually but not always demonstrates **abundant blood flow** around the gestational sac determined by color or power Doppler interrogation.
- An anteflexed/retroverted uterus strengthens the diagnosis.

Before engaging in the diagnosis of CSP, we also have to devote an additional paragraph to discuss the two ways an incision made at the time of the CD heals and appears after it was repaired. Normally, we expect that healing tissues generate a thick scar without leaving behind a defect. At times, a dehiscence or as it is usually referred a niche, with a certain depth and width, marks the area of the previous CD and can be seen with or without a saline infusion sonohysterography [6]. The niche can be triangular or rectangular and can be filled with fluid (Fig. 18.1a). The size of the niche on a sagittal section of the uterus may be misleading; therefore, the area should always be looked at in the transverse plane on which the real size of the dehiscence can be appreciated

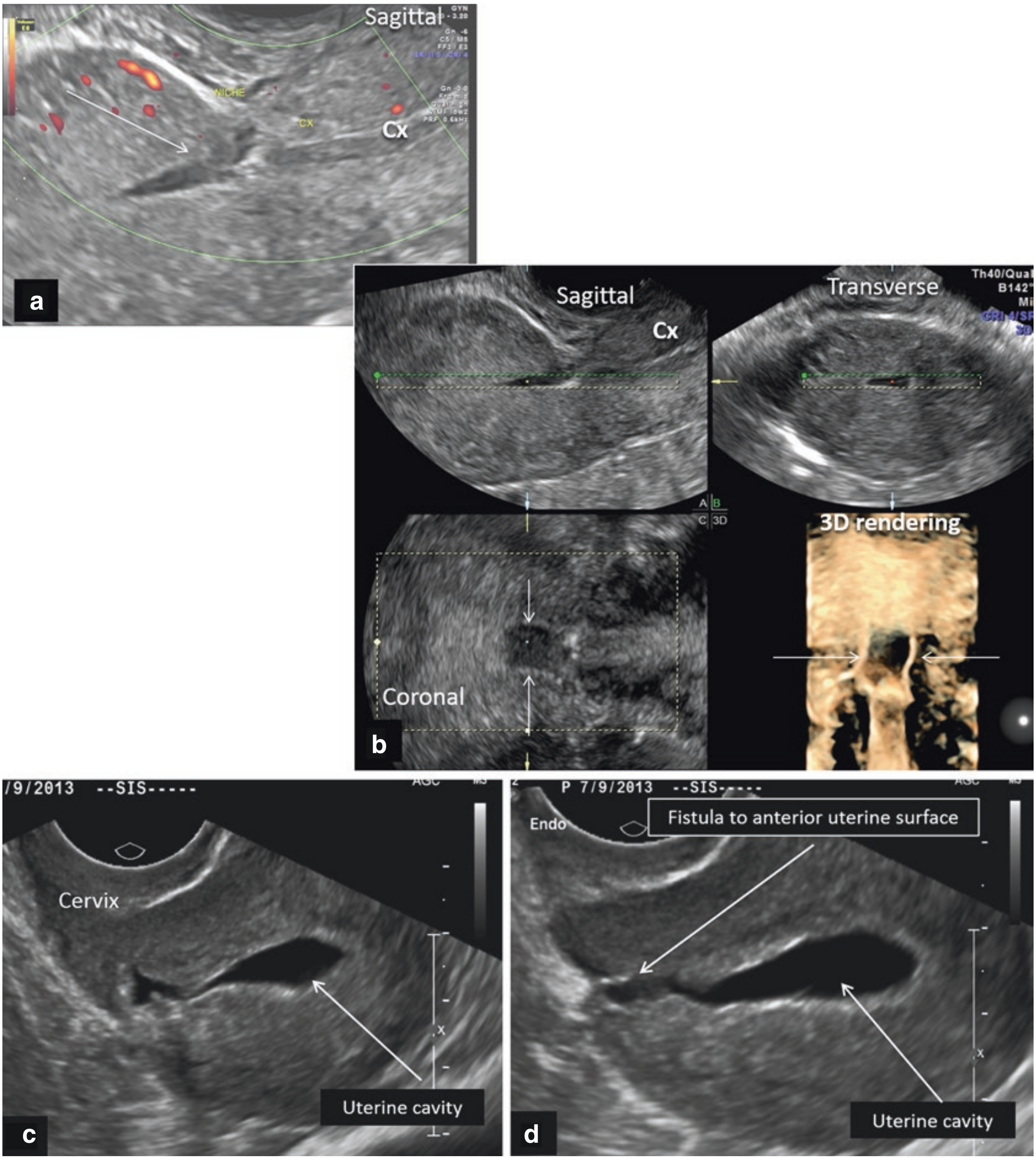
Sagittal
NICHE
CX
Cx
a
Sagittal
Cx
Transverse
3D rendering
Coronal
b
/9/2013 --SIS-----
Cervix
Uterine cavity
c
P 7/9/2013 --SIS-----
Endo
Fistula to anterior uterine surface
Uterine cavity
d

Fig. 18.1 Niche/defect left behind by the previous CD. (**a**) Sagittal image of the niche marked by an arrow (*Cx* cervix). (**b**) Three-dimensional orthogonal images of the uterus showing the niche (arrows). The width of the dehiscence should always be looked at on a transverse or coronal view since that is the real size of it. Unenhanced images. (**c**, **d**) At times, the niche/dehiscence extends all the way from the uterine cavity to the anterior surface of the uterus. Saline infusion sonographic images

(Fig. 18.1b). This is logical, since most primary cesarean incisions are performed from side to side, e.g., in the transverse plane. Bij deVaate et al. [7] published an extensive review analyzing 21 articles dealing with the prevalence, potential risk factors for development, and symptoms related to the presence of uterine niches following CD. The prevalence of a niche after a CD was found to vary between 56% and 84%. Several risk factors for the development of niches were

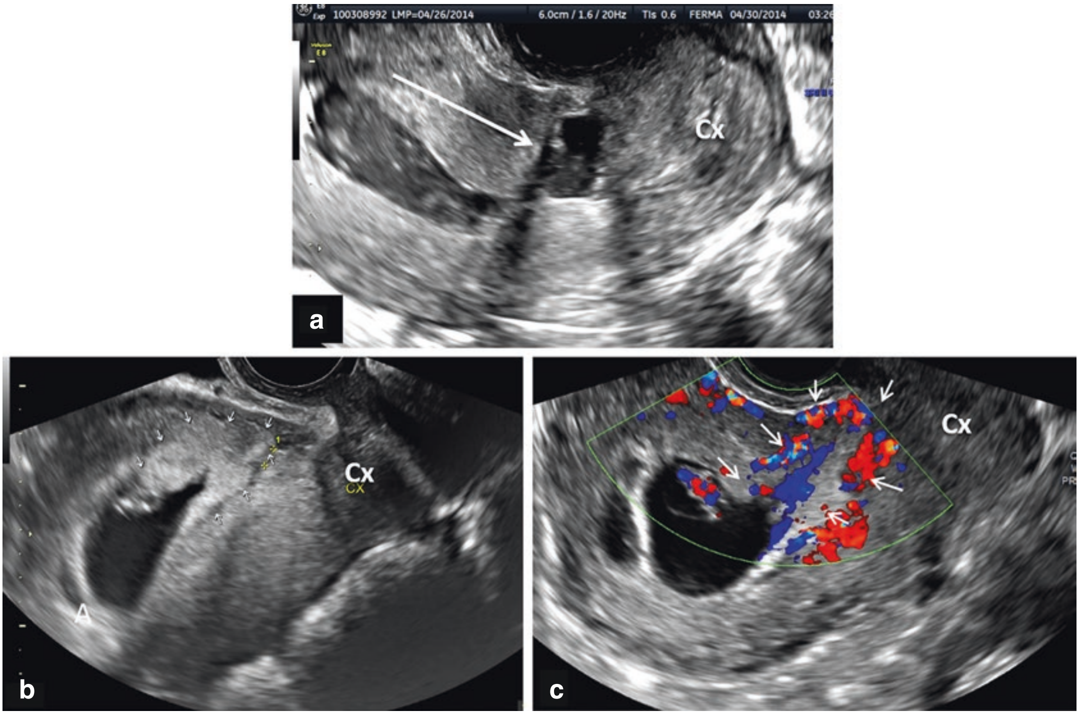

Fig. 18.2 Placental implantation into the niche of a previous CD. Sagittal images (*Cx* cervix). (**a**) Saline infusion sonohysterography of a uterus with a large niche. (**b**) Grayscale sagittal image of a CSP. Note the implantation of the placenta IN the niche outlined by small arrows. (**c**) Color Doppler image of the same CSP demonstrating the invasion of the placenta (outlined by small arrows) with its blood vessels into the myometrium

found: the technique of repair, location of the incision, wound healing, and probably number of layers included in the closure as well as multiple CDs and uterine retroflexion. The dehiscence left behind by the previous CD may be extensive and reaches the anterior uterine wall or the area below the bladder in the shape of a fistulous connection between the uterine cavity and the abovementioned areas (Fig. 18.1c, d).

At times, the niche is deep and wide (Fig. 18.2a), explaining the deep insertion of the tiny placenta with its rich blood supply (Fig. 18.2b, c). Since the prevalence of niches is relatively high, it can be expected that the possibility of such deep implantation is realistic; therefore, a careful scrutiny of the small placenta and its vessels should be performed in all first-trimester diagnoses of CSP.

Incidence/Risk Factor

Estimated incidence rates of CSP appear to be stable and range between 1/1800 and 1/2500 of all CDs performed [8–11]. Seow et al. [12] state that CSP was seen in 0.15% of all pregnancies with a history of a previous CD. The above numbers appear unrealistic; however, their true incidence is unknown due to the lack of population-based statistics (registries). As pointed out before, it seems that the actual rate did not increase in the last year since CD rates plateaued, and the increase in publications increased due to the actual awareness and its more accurate diagnosis.

The only risk factor for CSP is one or more [13] previous CDs.

It must be emphasized that "scar pregnancy" was described as associated with or caused by previous myomectomy [14], and also after in vitro fertilization [15]. In these two instances, the pathophysiology seems to be identical.

Pathogenesis of CSP

Later in this chapter, we will provide evidence that the histology of the tiny placental insertion or myometrial invasion of a CSP in the first trimester of the gestation is identical with the histologic findings of a PAS in the second and third trimesters of pregnancy. The previously and widely accepted explanation for the pathophysiology of PAS was that, in both diseases (CSP and PAS), intervening fibrinoid layer between the myometrium and the cytotrophoblastic shell in the placenta is naturally present between the endometrium in normally attached placentae when thinned or missing. This fibrin layer (fibrinoid material) is known by the name of Nitabuch layer. Previous uterine surgery or uterine interventions lead to *thin or absent decidua basalis in scarred areas, as well as the abovementioned protective layer* of the lower uterine segment. In CSP and in MAP, this membrane is missing and the placental villi attach itself and penetrate between the myometrial fibers into the depth of the uterine wall. These descriptions have prevailed for over 50 years and form the basis for diagnosis and grading of accreta placentation.

Other theories, such as the role of a low oxygen tension at the area of the scar providing a stimulus to help the invading cytotrophoblast [13, 16], as well as the in vitro studies of Kliman et al. [17] with trophoblast and EM explants, showing a strong propensity for attaching to exposed extracellular matrix and then to endometrial epithelial cells, are the most frequently quoted. Both theories support the observation that the more CDs a patient has, the higher the risk of placenta previa and placenta accrete.

While we duly mentioned the above explanation for the generation of CSP, we are also cognizant of the fact that there are **several theories** of the pathophysiological implantation **process** for the faulty placenta invasion. At this time, the relevant current hypothesis is the one by Eric Jauniaux, which theorizes that large cesarean scar defects in the lower uterine segment are associated with failure of normal decidualization and loss of the sub-decidual myometrium, and this secondary defect of the endometrium-myometrium interface leads to abnormally deep placental anchoring villi and trophoblast infiltration into the myometrium [18].

Diagnosis of Cesarean Scar Pregnancy

The two diagnostic modalities used are ultrasound and MRI; however, ultrasound is the best modality. Transvaginal sonography (TVS) presents an advantage over transabdominal ultrasound (TAS), since it has a higher resolution and can be placed in close proximity to the low, anterior gestational sac. MRI has been used for imaging and is expensive. In addition, it requires moving the patient to a radiology site. Also, MRI lacks the color Doppler flow that provides a high-resolution image, which is important in establishing a correct diagnosis. The authors of this chapter do not use or encourage the use of MRI in the diagnosis of cases suspected of CSP. The Society for Maternal Fetal Medicine also supports the use of transvaginal and/or transabdominal ultrasound to diagnose CSP [19, 20].

The diagnosis of CSP requires a high clinical index of suspicion. We reiterate that every woman with a history of a previous CD and a positive pregnancy test, presenting in the first trimester of the pregnancy, should be considered a "rule out CSP" until proven otherwise. Stirnemann et al. [21, 22] published studies to lay the basics for such screening if proven significant. Until that time, this should be strongly considered, since there is no downside to that first early scan. Godin et al. [23], Vial et al. [24], and Seow et al. [25] published similar sonographic criteria they used to define a CSP; however, other authors used additional characteristics, relying mostly on single cases.

Our diagnostic criteria of CSP [5, 26] took into consideration a history of previous CD, a positive pregnancy test, and the following sonographic criteria (Fig. 18.3):

- Endometrial and endocervical canal devoid of a gestational sac
- Placenta and/or a gestational sac embedded on or in the hysterotomy scar/niche
- In early gestations, a triangular gestational sac that fills a niche of the scar (Fig. 18.4)
- Thin or absent myometrial layer between the gestational sac and the bladder
- The presence of a chorionic sac, with or without embryonic/fetal pole and/or yolk sac and with or without heart activity
- The presence of a prominent and at times rich vascular pattern at or in the area of a CD scar. As a rule, detection of peri-trophoblastic blood flow, detected by the most sensitive Doppler settings around a low, anteriorly situated chorionic sac, in a patient with a previous CD, is a reliable sign of CSP.
- It is remarkable that, at very early stages of the pregnancy (4–5 weeks), the blood vessels tend to concentrate on the anterior side of the chorionic sac (Fig. 18.5) "marking" the site of the placental implantation.
- The usefulness of 3D ultrasound in the diagnosis is debated. However, it furnishes information regarding the exact location of the sac, its vascularity, and volume, the latter two in a

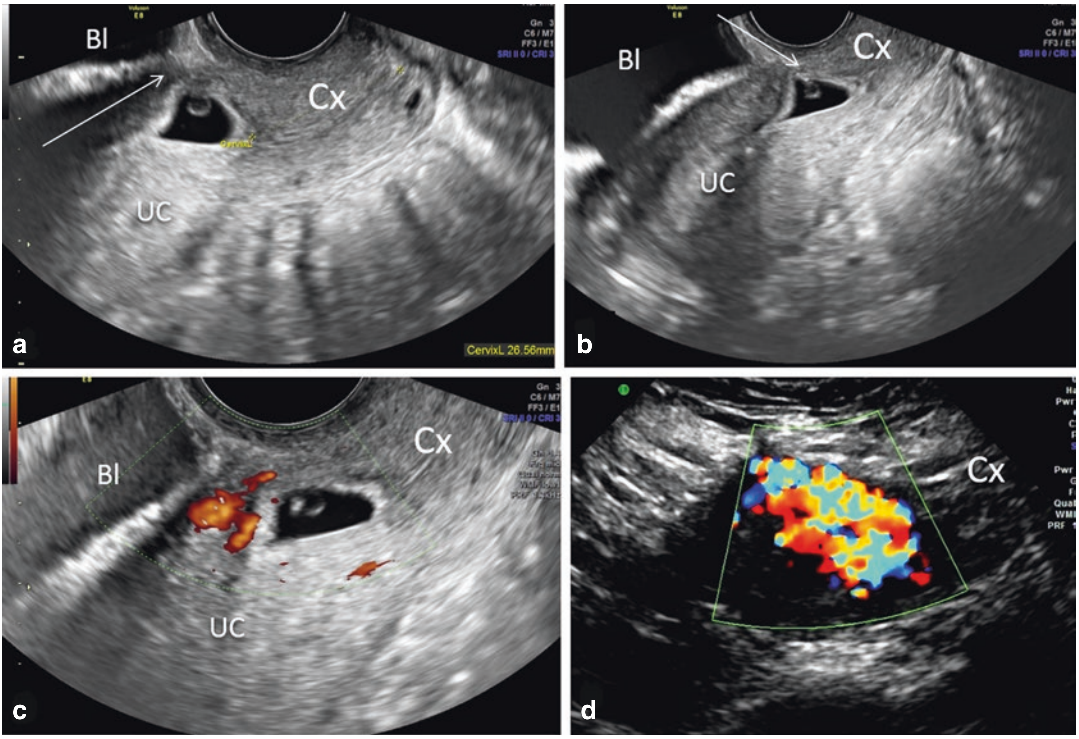

Fig. 18.3 Sonographic markers of CSP (*Cx* cervix, *Bl* bladder, *UC* uterine cavity). (**a**) Empty uterine cavity and cervical canal. Low anterior triangular gestational sac with yolk sac in close proximity to the bladder (long arrow). (**b**) Triangular gestational sac with close proximity to the bladder. (**c**) The developing vascularity between the sac and the bladder. (**d**) Arteriovenous malformation in a CSP that required UAE

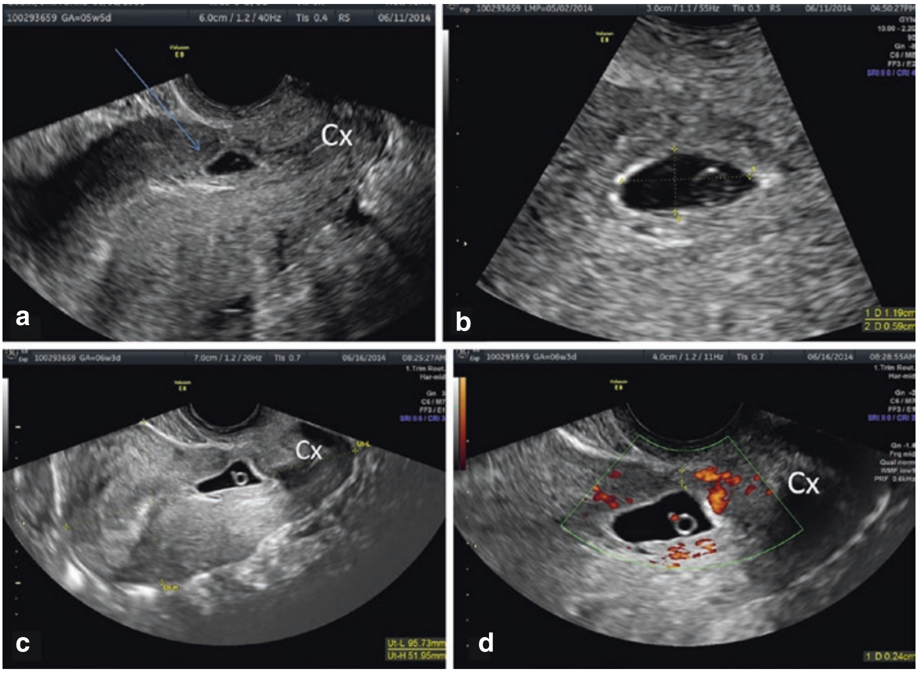
Cx
a
b
1 D 1.19cm
2 D 0.58cm
Cx
c
Ut-L 95.73mm
Ut-H 51.95mm
Cx
d
1 D 0.24cm

Fig. 18.4 Additional images of the shape of the early 4–6-week chorionic sac of the CSP (*Cx* cervix). (**a**) Flat sac. (**b**) Oval sac. (**c**) Triangular sac. (**d**) Square sac

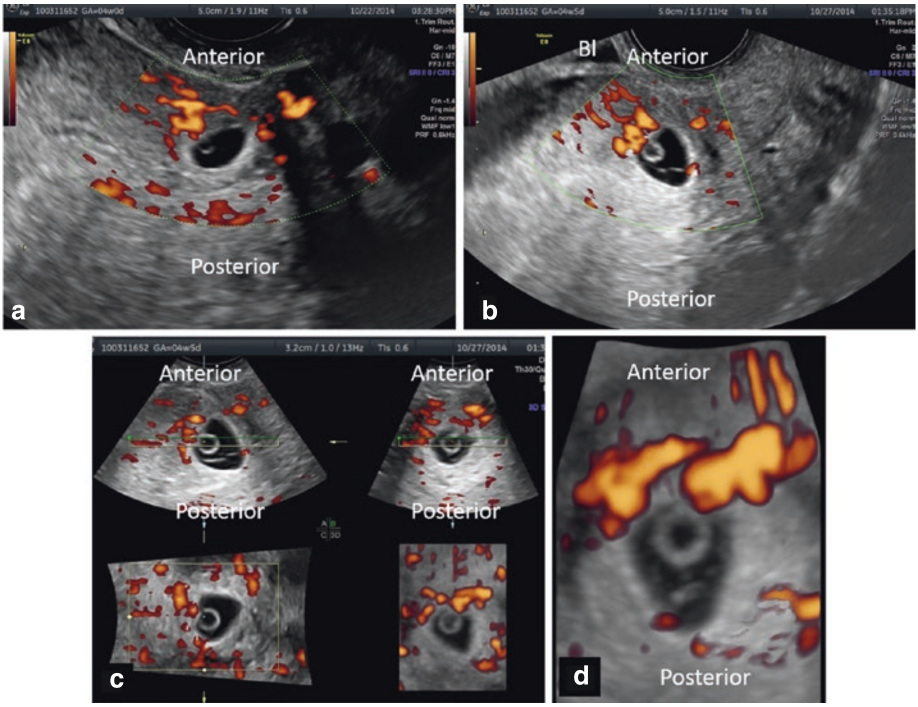
Anterior
Posterior
a
Bl
Anterior
Posterior
b
Anterior
Posterior
Anterior
Posterior
c
Anterior
Posterior
d

Fig. 18.5 The developing vascular grid of the early CSP. (**a**, **b**) 2D color Doppler of the vessels surrounding the chorionic sac. (**c**) Three-dimensional, orthogonal planes and 3D rendering (lower right picture) of the vascularity that start to concentrate on the anterior side of the sac, the future site of the placenta. We suspect that the future placenta will invade the myometrium in the anterior direction. (**d**) Thick-slice 3D rendering of the sac with its vessels clearly more prominent anteriorly

quantitative fashion (Fig. 18.6). We use the above measurements to follow the healing process of the treated cases or for the early warning signs of an impending enhanced myometrial vascularity (EMV) or also previously known as arteriovenous malformation (AVM) developing at the site of a conservatively treated or even an untreated, but spontaneously failing CSP [27, 28].

If an EMV (a.k.a. AVM) was suspected (at times, this may be the presenting sonographic picture), Doppler measurements of the blood velocity were measured and expressed by the peak systolic velocity (PSV) in cm/s. Velocities above 39 cm/s were considered for uterine artery embolization (UAE) by the interventional radiologist. This evaluation is best done when the region of interest of the Doppler interrogation is constricted to the questionable area, using the appropriate pulse repetition frequency and filter settings.

These are pathological, high-velocity, low-resistance “short circuits” of the bloodstream between an organ’s arterial and venous supply. Ultrasound presents a valuable tool for the diagnosis of AVM and guideline for their treatment [29]. Although uncommon, they may cause dangerous hemorrhages due to disrupted blood vessels, after miscarriage or uterine instrumentation [30]. The acquired form, seen in CSP, is usually traumatic, resulting from prior dilation and curettage (D&C), therapeutic abortion, uterine surgery, or direct uterine trauma. Their incidence is about 1% of CSPs. In our series of 60 CSPs, 5 patients had EMV [31].

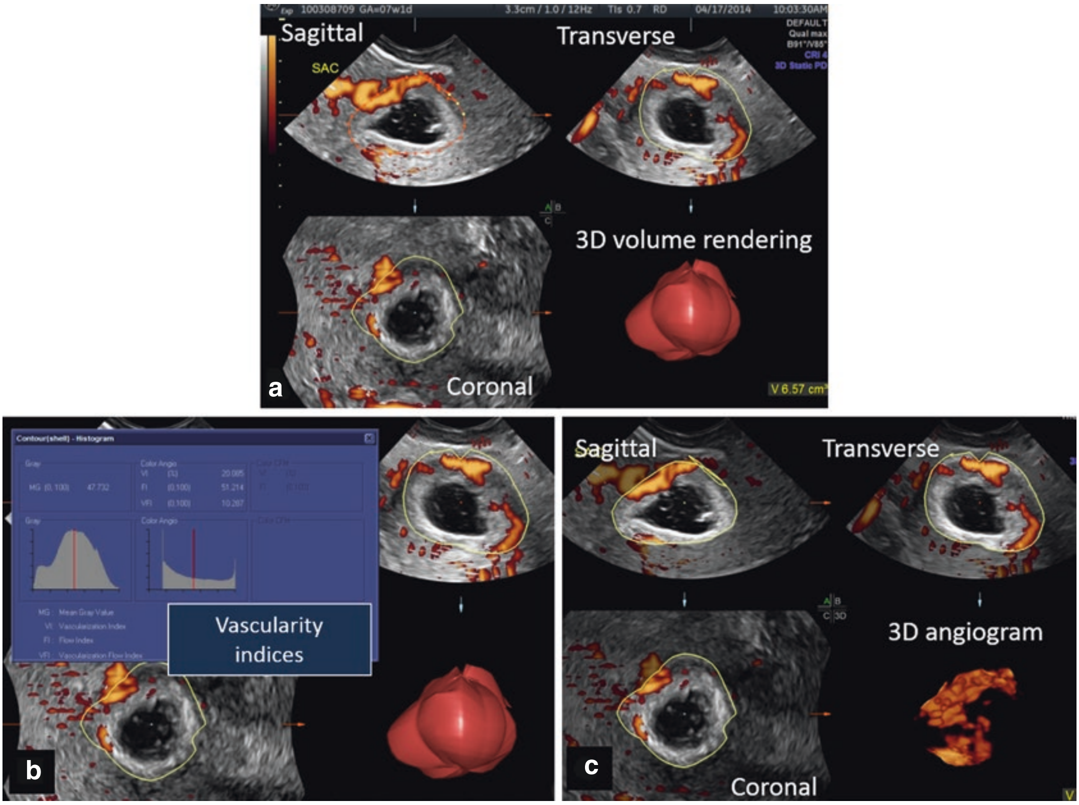

Fig. 18.6 The use of 3D ultrasound in the diagnosis and follow-up of treatment of CSP. (**a**) 3D orthogonal planes with power Doppler used in segmentation (marking the perimeter of the sac) to obtain the volume of it. (**b**) After the volume of the sac is obtained, a special algorithm is applied to compute and display the quantitative vessel content of the above volume. (**c**) Visual display of the three-dimensional vascular angiogram that can be used qualitatively for follow-up purposes after local injection of UAE treatments

Differential Diagnosis of CSP

There are two main differential diagnostic entities to consider: first, a **cervical pregnancy**, which is rare and has no history of a prior CDs, and second, a **miscarriage in progress**, which can be seen in the cervical canal or close to the internal os and "on its way out" having no heart activity. Also, under pressure on the cervix with the vaginal probe, the sac will slide back-and-forth, while a true CSP will stay fixed. It should be noted that misdiagnosis has, at times, severe consequences. The proof is in the literature: 107 of the 751 cases of CSP reviewed (13.6%) were missed or misdiagnosed leading to complications (e.g., hysterectomy and loss of fertility) [5]. Figure 18.7 demonstrates a simple method to distinguish between the two, abovementioned, differential diagnostic entities and a true CSP.

However, it is extremely important to realize that this simplified diagnostic aid is valid and reliable only while the gestational sac is small (e.g., 5–6 mm in diameter or 5–6 postmenstrual weeks) and remains "local," close to the niche or above the scar. In other words, the sac did not start to elongate and move/expand cranially to fill the uterine cavity. In this case, the sac will be found increasingly in the uterine cavity misleading the uninitiated observer to think that it is an intrauterine sac. In such cases, one should shift the attention from the sac and concentrate upon the blood vessels of the tiny placenta, which stay in their original site of implantation, thereby holding the most important diagnostic feature of CSP: the true site of placental implantation. Figures 18.2, 18.3, 18.4, and 18.5 clearly demonstrate the abovementioned diagnostic principle.

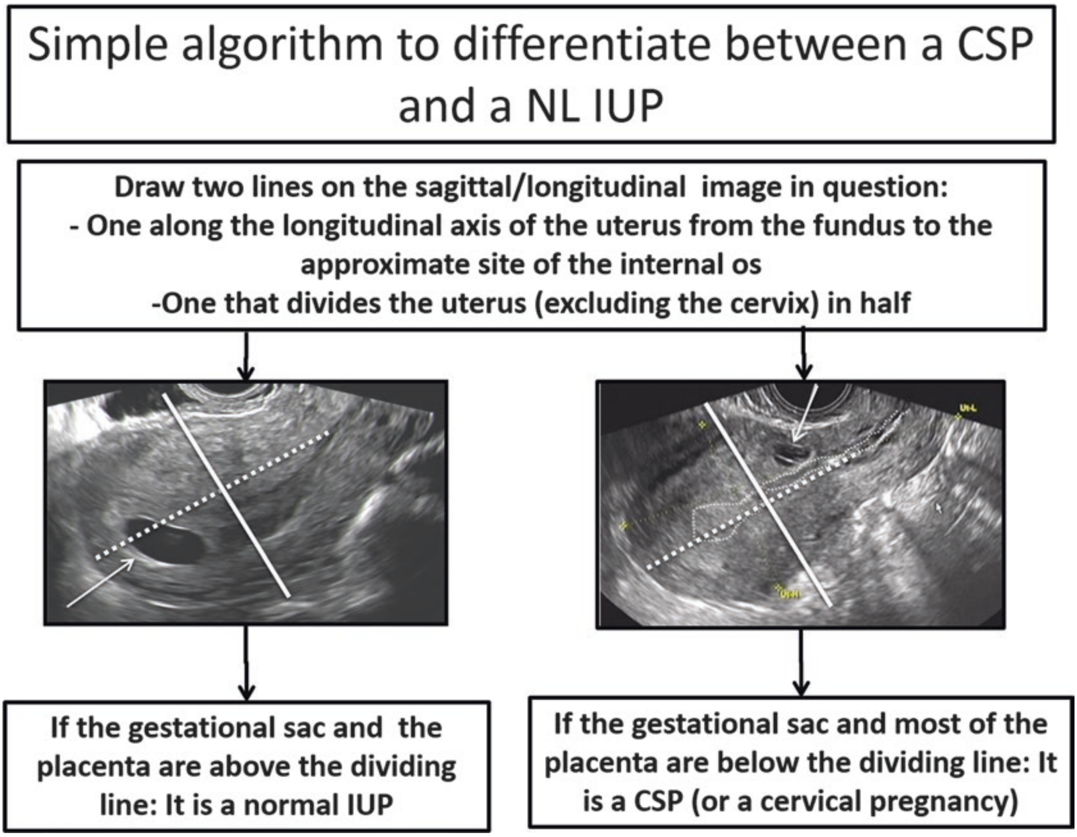

Simple algorithm to differentiate between a CSP and a NL IUP

Draw two lines on the sagittal/longitudinal image in question:
- One along the longitudinal axis of the uterus from the fundus to the approximate site of the internal os
-One that divides the uterus (excluding the cervix) in half

If the gestational sac and the placenta are above the dividing line: It is a normal IUP

If the gestational sac and most of the placenta are below the dividing line: It is a CSP (or a cervical pregnancy)

Fig. 18.7 The simple algorithm to differentiate between an IUP and a CSP (or cervical pregnancy)

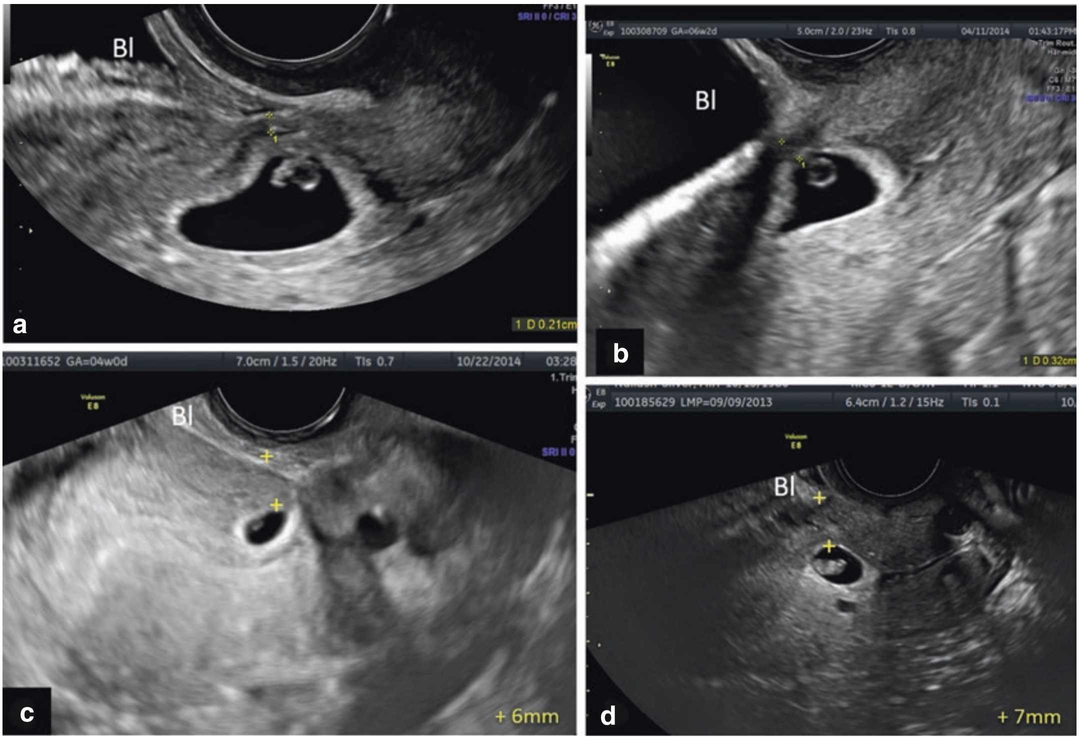

Fig. 18.8 The issue of distance between the anterior uterine surface and the gestational sac: "*in* the niche/scar" or "*on* the scar" (*Bl* bladder). (**a**, **b**) These two are examples of a close proximity of the sac to the bladder (2.1 mm and 3.2 mm, respectively). (**c**, **d**) Depicts two CSPs in which the sac is 6 and 7 mm remote from the bladder

Lately, clinicians and clinical researchers have started to pay attention to the exact location of placental implantation in the area of the scar/niche left behind by the previous CD. Vial et al. [24] suggested that there are two kinds of CSPs, based on the depth of implantation. The question is whether a deeply implanted chorionic sac *in* a niche or dehiscence, close to the bladder with very thin or no visible myometrium (Fig. 18.8a, b) recently termed type 2 CSP, will result in a worse outcome than if inserted *on* top of a scar, also called type 1 CSP, that has some thickness (Fig. 18.8c, d). Comstock et al. [32] and personal communication with Cali G. refer to "on-the-scar implantations" as "low-lying sacs" and assume that these are the CSPs that may proceed to third trimester giving rise to PAS. Deeply implanted in the niche, surrounded by myometrium, and seldom reach term is a "true" or type 2 scar pregnancy. We slightly differ about the latter form of CSP since we have witnessed the reaching delivery of a live offspring.

Rac et al. [33] studied 39 patients, of which 14 had histologically confirmed PAS. The smallest myometrial thickness measurement was one of the variables associated with invasion. More research is needed before the gestational-sac-to-bladder distance (Fig. 18.8) can become useful in counseling patients with CSP in the first trimester of pregnancy.

The Connection Between CSP and PAS

The connection or continuity between CSP and CSP has gradually become evident through clinical observation [34, 35]. We studied placental implantation in the early (second trimester) placenta accreta and in CSP, to find out if they represent different stages in the disease continuum leading to morbidly adherent placenta in the third trimester [36]. Two pathologists, blinded to the diagnosis, evaluated their histologic slides on the basis of these microscopic slides. They could not tell the difference between the two clinical entities and found that both had one thing in common: neither had intervening deciduae between the villi and the myometrium, consistent with the classic definition of morbidly adherent placenta. Therefore, our conclusion is that CSP and an early second-trimester placenta accreta are histopathologically identical and represent different stages in the disease continuum leading to PAS in the third trimester.

The next logical question is whether, left untreated, a CSP would result in a live-born offspring. We followed ten patients diagnosed with CSPs who opted to continue the pregnancy declining early termination [37]. The diagnosis of CSP was made before 10 weeks. All ten had sonographic signs of PAS by the second trimester. Nine of the ten patients delivered live-born neonates, between 32 and 37 weeks. One patient had progressive intractable vaginal bleeding, leading to hysterectomy, at 20 weeks. The other nine patients underwent hysterectomy at the CD. Blood loss ranged from 300 to 6000 mL. Histopathological diagnosis of all placentae was placenta percreta.

Above, we provided reliable data regarding two clinical issues: (a) CSP is a precursor of PAS, both sharing the same histopathology, and (b) pregnancies diagnosed as CSP in the first trimester may proceed to deliver live offspring, risking premature delivery and loss of uterus and fertility. This data can be used to counsel patients with CSP, to make an evidence-based and informed choice between first-trimester termination of an early pregnancy or continuation, risking premature delivery, and loss of uterus and fertility.

The societal recognition of the connection between CSP and PAS, in the USA, was the SMFM Consensus Statement published recently [20]. In this document, several PAS ultrasound markers have been described in the first trimester. Their prevalence and type of markers of PAS in the first trimester were shown to vary between *early first trimester* (6–9 weeks) and *later first trimester* (11–14 weeks). It also reinforces that implantation of a gestational sac in the lower uterine segment is one of the most common US markers for PAS in the first trimester. Finally, it draws attention to the fact that in high-risk women, a gestational sac implanted in close proximity to a uterine scar was identified in *82.4%* of women (95% CI, 85.8–95.7) with confirmed PAS.

PAS in the First Trimester?

PAS can exist in the first trimester of pregnancy. For beginners, Comstock et al. [32] described seven patients after sonographic examination at 10 weeks or earlier with placenta accreta, increta, and percreta, not only by their clinical course but, more importantly, by pathologic examination of the uterus. In six, at the time of the early ultrasound, the chorionic sac was located in the lower uterine segment, in the scar area of the previous CD. Two patients underwent D&C, at which time severe bleeding led to hysterectomy. The remaining four had sonographic findings typical of placenta accreta during subsequent scans but delivered at term. The author's conclusion suggested that, in a patient with a previous CD, a chorionic sac detected by a 10 week or less ultrasound, located in the lower uterine segment, suggests the possibility of placenta accreta. A similar article was published by Ballas et al. [34].

Using our material, Fig. 18.9 depicts the early sonographic markers of a MAP: placenta previa, focal loss of the clear space, and focally increased vascularity. The patient in this example delivered at 34 weeks and had placenta accreta. In ten patients, we reported [37] that the early sonographic markers of MAP could be detected at the end of the first and beginning of the second trimesters.

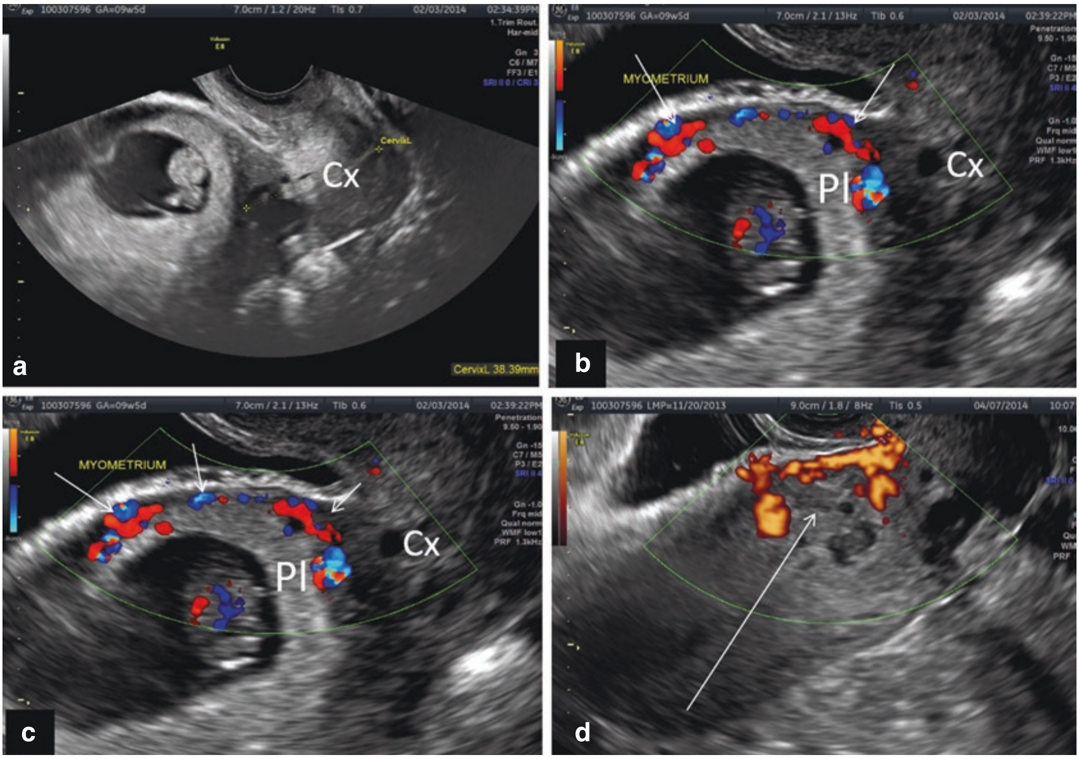

Fig. 18.9 CSP is a precursor of MAP. This is a 9 weeks and 5 days gestation (*Cx* cervix, *Pl* placenta). (**a**) Sagittal, grayscale image of a CSP with an anterior placenta previa. (**b**) Power Doppler reveals two areas of vessel proximity to the bladder with loss of the myometrium (arrows). (**c**) Another plane showing the same findings as in **b**. (**d**) A more lateral section concentrates on an area with clear vessel invasion of the myometrium (arrow)

Counseling Patients with a First-Trimester CSP

Prior to treatment and after the reliable diagnosis of CSP, one has to determine if fetal heartbeats are seen. If no yolk sac and/or no embryo and/or no heartbeats are seen, re-scan every 2–3 days. If, after a week, no heart activity, no yolk sac, and/or no embryo are detected, a sonography and biochemistry-based follow-up should be planned. Only after this time should the gestation be considered live or a pregnancy failure and the serum hCG should be followed until nonpregnant levels are reached. Some management protocols call for systemic administration of methotrexate (MTX), even with the absence of heartbeats for early drug effect. While such an approach is not contraindicated, the patient and the provider *must* be sure that under no circumstances is this a wanted pregnancy.

In the case of positive heart activity, counseling should enumerate the two main clinical management options to reach a decision as early as possible. The two options before further growth of the gestation are (a) termination or (b) continuation of the pregnancy. Our counseling of patients with a CSP diagnosed in the first trimester of pregnancy underwent a fundamental change. Several years ago, we would counsel toward termination of the pregnancy without delay. Recent studies on the natural history of the CSP, with the possibility of reaching term or near-term delivery of a live offspring, have changed our counseling [38, 39]. We provide the patient with evidence that this is possible and that the patient should understand that second- and third-trimester PAS may be complicated by severe hemorrhage and also necessitate hysterectomy. Management in the above case should be based on the patient's age, number of previous CDs, desired number of children, and expertise of the clinicians giving the care. If the patient decides to continue the pregnancy, bleeding precautions should be given. The management should be based upon serial ultrasounds, until a safe gestational age is reached. The SMFM guidelines detail the approach to CSP and discourage continuing the pregnancy unless proper, evidence-based consultation is well understood by the patient, a multidisciplinary team can be involved in the pregnancy management and the delivery, and blood products are available, since ultrasound cannot predict the blood loss at surgery [40].

Our general guidelines in counseling and managing the patient with a CSP are shown in Fig. 18.10.

Management of Cesarean Scar Pregnancy

Treatment regimens and their combinations can be classified as one of the following:

1. Major surgery (these require general anesthesia):
    (a) Laparotomy (hysterectomy or local excision)
    (b) Excision by laparoscopy, hysteroscopy, or transvaginal surgery
    (c) Dilatation of the cervix and sharp or blunt curetting
    (d) Suction aspiration without dilatation of the cervix
    (e) Excision performed by the vaginal route

The last two can be guided by continuous, real-time ultrasound.

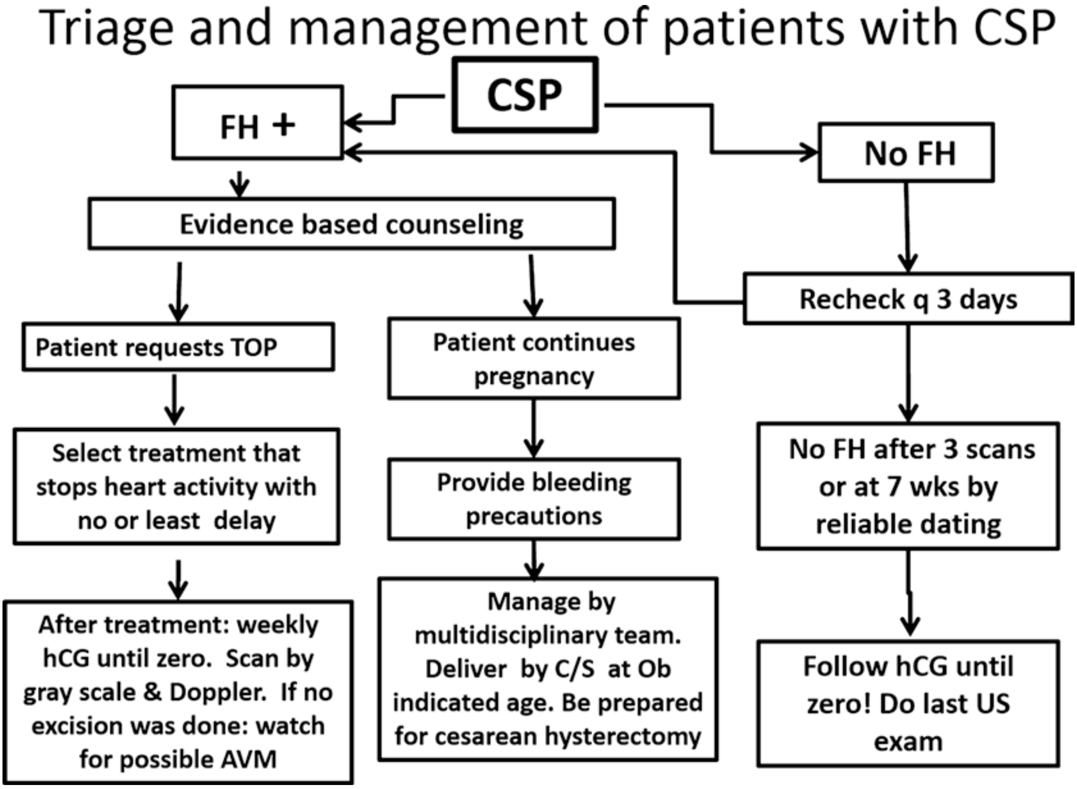
Triage and management of patients with CSP
CSP
FH +
No FH
Evidence based counseling
Recheck q 3 days
Patient requests TOP
Patient continues pregnancy
Select treatment that stops heart activity with no or least delay
Provide bleeding precautions
No FH after 3 scans or at 7 wks by reliable dating
After treatment: weekly hCG until zero. Scan by gray scale & Doppler. If no excision was done: watch for possible AVM
Manage by multidisciplinary team. Deliver by C/S at Ob indicated age. Be prepared for cesarean hysterectomy
Follow hCG until zero! Do last US exam

Fig. 18.10 Triage and management of CSP by the presence or absence of cardiac activity

2. Minimally invasive surgery (does not involve general anesthesia):
   (a) Local injection of MTX or KCl
   (b) Vasopressin locally was also used
3. Systemic medication
   (a) Single or repeated doses of methotrexate (MTX) and etoposide (some articles originating from China advocate intravenous use of MTX claiming reasonable success)
   (b) Uterine artery embolization (UAE)
4. Combination of the above treatments: A large number of articles report on combining treatments in a planned, simultaneous, or sequential fashion. Treatments are also changed, mostly after the first-line therapy failed. As a matter of fact, it is rare to find a recently (2012–2014) published case or case series in which the patients were managed *only* by one single treatment agent or protocol.
5. Adjuvant measures: Most recently, single Foley balloon and Cook cervical ripening double-balloon® placement and inflation to prevent and/or control bleeding, following or replacing local treatments such as aspiration, curettage, and local injection, have been used.
6. It is beneficial for the patient with CSP to be referred to a facility that provides evidence-based care as well as experienced in managing cases, in response to developing emergency situations [41]. Such centers should be able to provide operating rooms and interventional radiology procedures and have blood transfusion/blood products immediately available. The latter is important since bleeding complications are typical of this dangerous clinical entity.

Treatment Options Available for CSP

Based upon the in-depth and available literature, analyzing the different aspects of CSP, in 2012, there were about 33 published treatment modalities with their results and complications [5]. No preferred treatment became apparent; however, of the 751 patients, D&C (305), surgical excision (laparoscopic, hysteroscopic, and transvaginal) (261), UAE (142), MTX (92), and local, intragestational sac injection (86) were the most used.

Between 2012 and 2022, no less than 70 peer-reviewed articles on CSP were published. Not surprising is the fact that Chinese authors contributed to the overwhelming number of cases, describing their various and different treatment modalities and their combinations. This is due to their large population and over 40% CD rate. At least 36 primary or combination treatments were found; however, the number is not substantially different from the list of treatment approaches described in our review of 751 cases. No wonder one cannot draw a clear conclusion as to which treatment was the most effective, resulting in the least or no complications. This large number underlines the fact that, in 2015, there is no nationally/internationally agreed-upon or suggested management protocol published with a set of guidelines to manage CSP or early first-trimester placenta accreta. While the distribution of the various treatments and their rates of use are found in the tables of our previous review [5], the somewhat different distribution of treatment choices is detailed in Table 18.1.

Some of the general guidelines at counseling a patient diagnosed with CSP are the following:

We start with an evidence-based counseling and *consider the best management methods by gestational age (most published management-*

Table 18.1 Distribution of the different treatments applied for the cesarean scar pregnancies

Treatments: single or in combination	No. of patients	Percent of 1223 patients (%)
Dilatation and curettage	577	52.4
Uterine artery embolization	309	28.0
Methotrexate	236	21.4
Suction aspiration	81	12.0
Transvaginal excision	119	9.7
Laparoscopic excision	94	7.7
Hysteroscopic excision or guidance	63	5.2
Excision by laparotomy or straight TAH	15	1.2
High-frequency ultrasound	20	1.6

related articles do not take into consideration the gestational age at which the termination is suggested). We do take into consideration the CSP type and the practitioner's own experience with the treatment. ***We*** emphasize that CSP is a rare and dangerous clinical entity regardless of the management, and if TOP is desired, the patient should sign a detailed informed consent and her understanding of this. We emphasize that the decision of termination is time sensitive since the gestation grows every day along with its blood supply, which exposes the patient to a higher rate of possible complications. We stress and explain the importance of "early decision" to the patient without putting excess pressure on the patient, but we expect a decision one day after the diagnosis. We also emphasize that even the best treatment may endanger life. During the counseling, we also touch upon the usually pertinent question of patients: if expectant measurement is indeed an option to retain the pregnancy. We stress that while this is a possibility depending on the nature and the type of the CSP, however continuing the gestation may expose the patient to sever hemorrhage, uterine rupture, severe consequences of PAS, and even maternal mortality [38]. Despite the above, some CSPs may progress to/close to term; therefore, TOP should NOT be the only option offered. If continuation of CSP is entertained, we describe possible complications specific to PAS in each trimester. To remind the reader: the SMFM guidelines do not recommend expectant management.

Evaluating the global experience regarding the different treatment modalities of CSP, in addition to the one mentioned before [40], we include here the two detailed reviews on management, which also include their success and complication rates [42, 43].

Despite several treatments for CSP, our detailed discussion will be limited to the most used. A much more detailed analysis is found in our in-depth review [5], complete with their efficacy and complication rates. We now add the pertinent data resulting from the review of the 1223 cases published after 2012.

1. **Suction aspiration or D&C, alone or in combination**

   Based on our first review of treating 305 cases with D&C only or in combination with other means as a "first line" or a backup, therapy had a mean complication rate of about 62% (range, 29–86%) [5]. The main complication was unanticipated bleeding, forcing an emergency second- or third-line treatment that, almost always, was surgical. At times, hysterectomy became necessary. This option requires general anesthesia.

   There were some changes between the results of the two reviews. If D&C was used as a sole treatment, in 69 cases, 24 (34.7%) resulted in complication as opposed to first-line or secondary treatment combined with other treatments. Only 52 of 413 (12.2%) had complications. If UAE was combined with systemic MTX, it caused 35% complications, while combined with other means (e.g., suction evacuation or hysteroscopic excision among others), the rate was only 11.3%.

   As opposed to a spontaneous delivery or spontaneous abortion, where the uterine myometrial grid constricts the bleeding after placental separation, in CSP, the sharp curettage exposes vessels of the gestational sac leading to severe and sometimes unstoppable bleeding since there is less or no adequate muscle grid to contain the bleeding. A sharp curettage might injure the thin myometrium leading to bleeding or even perforation.

   If D&C or suction aspiration is still the preferred treatment, blood and blood products as well as a Foley balloon catheter should be readily available [44]. Foley balloon catheters or a cervical ripening Cook cervical ripening double-balloon catheter® [41] was successfully used to stop and tamponade possible bleeding [45, 46]. Cali et al. [47] successfully used the following sequential treatment approach in eight of their patients. At admission to the hospital, the patient undergoes UAE and, after 5 days, a gentle suction aspiration under continuous, real-time ultrasound is performed by immediate insertion and inflation of a Foley balloon catheter for bleeding prevention and control [44].

A number of recent articles advocate the safe and uncomplicated use of blunt sac aspiration; however, all were followed or preceded by other treatment methods [48]. Interestingly, no complications were seen in 81 suction aspirations in our review of the cases between 2012 and 2014. This probably is attributed to its blunt, as opposed to a sharp curetting at the time of D&C, and therefore, it is less prone to disrupt blood vessels.

2. **Uterine artery embolization, alone or in combination**

   This treatment requires general anesthesia. If used as a primary and only treatment, the complication rate among the 64 cases described in the review of 751 cases of CSP was 47%. It is difficult to evaluate the real complication rates, due to partial or incomplete data in the published articles. In another 78 cases, UAE was used in combination with other treatments. It seems that UAE is not the best first-line treatment, if administered alone as a single-agent therapy, since it allows the pregnancy, with its vascularity, to grow and increase. For this reason, Cali et al. [47] delayed suction aspiration in their patients with CSP for 5 days after UAE. Uterine artery embolization works better combined with other noninvasive and invasive (suction aspiration) treatments [49–51]. In our 60 cases of CSP, UAE was used as a secondary treatment in 4 patients with persistent vaginal bleeding or developing enhanced myometrial vascularity (EMV), also known as arteriovenous malformation (AVM). Embolization failed to stop the bleeding in one of the patients with EMV/AVM; therefore, hysterectomy was performed [31].

   If UAE fails, which may be the case, the clinician must contend with a larger gestation applying a secondary treatment. However, it is hard to evaluate its actual complication rates, since some articles have insufficient data to rely on. As stated previously, in our 60 cases of CSP, one of the patients required (and finally agreed to) AVM embolization to stop her continuing vaginal bleeding (as well as her high PSV on Doppler), 122 days after her initial local MTX injection (Fig. 18.11).

   In a recent article, we reported on a more serious kind/variant of EMV/AVM in terms of its difficult management (TIMOR-Tritsch IE insert enhanced) since all of the 13 patients in this series required one or more UAEs.

   Updating this treatment approach with the review of 1223 patients published after 2012, UAE was used alone or in combination in 309 cases with a mean complication rate of 28%, with its highest rate if combined with intra-arterial injection of MTX, at the time of the catheterization: 18 of 52 (34.6%).

   In a recent review of 142 patients treated with UAE, the authors concluded that the treatment of CSP patients with UAE can reduce the amount of intraoperative bleeding and the duration of vaginal bleeding, promote the improvement of patients' clinical symptoms, have less impact on the disruption of patients' sex hormone balance, reduce patients' surgical risks to a greater extent, preserve patients' normal fertility, and have better application [52].

3. **Excision by hysteroscopy and/or laparoscopy**

   Hysteroscopic and laparoscopic surgery requires general anesthesia. The overall complication rate for 108 cases managed by hysteroscopy was 13.8% [5]. However, no complications were noted if hysteroscopy was combined with transabdominal ultrasound guidance (9 cases were published). The rate of complications increased to 17% if hysteroscopy was combined with mifepristone. In the hands of an experienced clinician, guided by transabdominal ultrasound, hysteroscopy may be a reasonable way of treatment for CSP [48, 53–59]. The use of an inflatable balloon catheter, after treatment

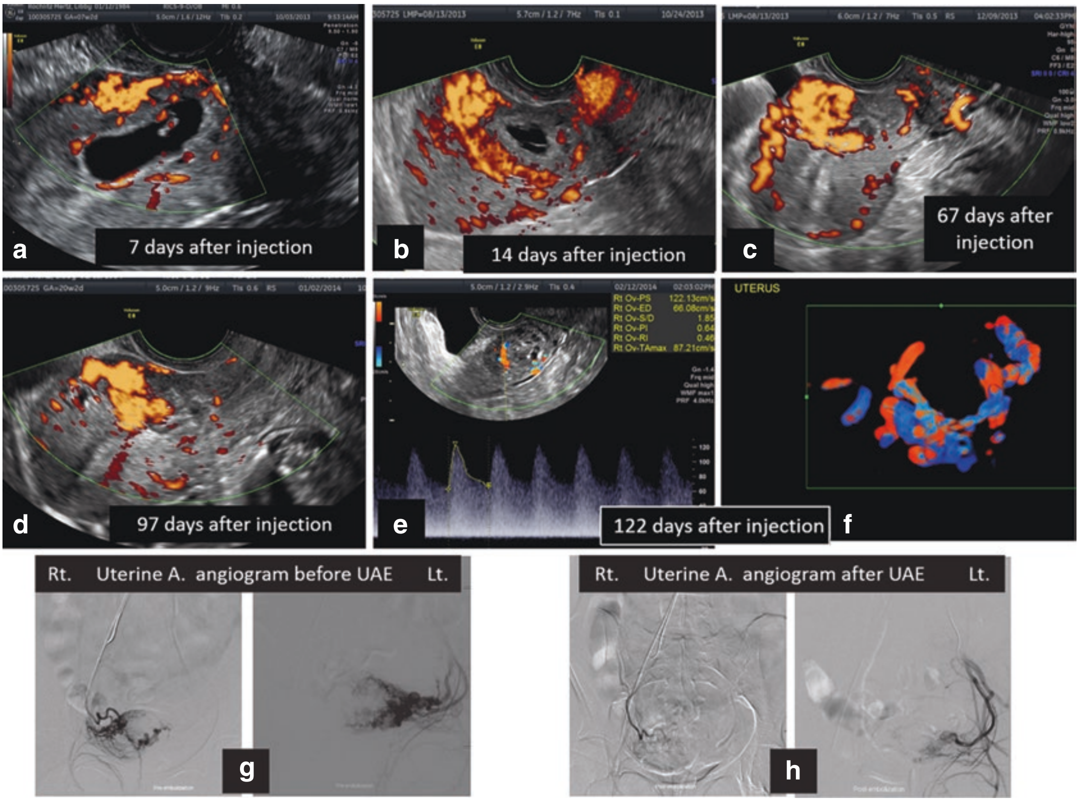

Fig. 18.11 Late development of an AVM after local intragestational injection of MTX with sonographic follow-up of the vascularization on days 7, 14, 67, 97, and 122 following the treatment (**a**–**f**). The patient refused an UAE after 4 weeks; however, the continuous vaginal spotting and slight bleeding finally led to the acceptance of the bilateral embolization of the uterine arteries, which was successful (**g**, **h**)

with hysteroscopic excision, may prevent (or treat) possible bleeding from the operative site.

Laparoscopic surgery, alone or in combination, was used to excise the site of the scar pregnancy and repair the anterior uterine wall. Fifty-four such cases were published up to 2012 in the reviewed literature, with complication rates between 20% and 30% [5]. Since 2012, there have been several other laparoscopically treated case reports [51, 60–64].

Robotic assisted laparoscopic removal of CSP was also published [65]. We speculate that the complicated, time-consuming, and probably costly robotic surgery involving dedicated staff and its availability only in selected medical centers make the use of this operative approach to CSP questionable, since it can be replaced with several office-based, simple, and less involved treatments.

One of the latest publications favors laparoscopic excision of the CSP combined with the site repair claiming that primary laparoscopic management is not only the most effective method with the lowest complication rates but also an approach that allows for simultaneous repair and revision of the cesarean scar defect. The authors demonstrate easily adaptable techniques for maintaining hemostasis, minimizing injury to normal myometrium, and creating multilayer closures that lead to successful revisions with minimal impact to subsequent fertility [66].

4. **Methotrexate**

One of the most frequently used therapies to treat CSP is undoubtedly methotrexate (MTX). It is administered in single or multiple, successive doses, intramuscularly, injected locally into the gestational sac, as intravenous slow drip, and finally injected into the umbilical artery at the time of a UAE. It was reported to be administered as a first-line or a secondary or backup medication, as a single agent and/or combined with any other conceivable treatment as an adjunct.

Systemic, "first-line," single-dose MTX is administered as an intramuscular, single injection. The usual protocol was 1 mg/kg of body weight or 50 mg/m^2 of body surface area. Its complication rate is 62.1% due to a required second-line treatment, when the fetal heartbeat fails to cease after several days [5]. Bodour et al. [67] challenged this result, which prompted a reevaluation of the reviewed material; however, after the more rigorous recounting of the cases, an even higher (66.1%) complication rate was found [68].

The reason for this, we suspect, may be caused by its slow action and the fact that the results may take days to be seen. We also suspect that it may not be able to stop cardiac activity and placental invasion. During these several days (or entire week), the gestational sac, the embryo or fetus, and its vascularity continue to grow, forcing a secondary treatment that must be able to handle a larger gestation with more abundant vascularization. The slow action of systemic MTX treatment is echoed, among others, in the series of Yin et al. [69]. It is true that there are also proponents of the use of systemic MTX as a single agent; however, it is impossible to attribute the cessation of the heart activity to the effect of MTX, since at least 10% of first-trimester intrauterine pregnancies undergo a spontaneous demise.

Based upon our recent review of 1223 cases of CSP, there were 236 cases in which MTX was administered as a single agent or in a combined fashion with other treatments, with a mean of 21.4% complications. Methotrexate used alone (as single or multidose) leads to 38% of the cases needing a secondary treatment [48, 70]. Combined with D&C (26 cases), another therapy with high complication rate, all needed a secondary treatment.

The guidelines of the Society of Maternal Fetal Medicine clearly discourage treating CSP using systemic MTX alone and encourage combining MTX with other treatment modalities [19].

Systemic, sequential, multidose use of MTX. The injected amounts of MTX are similar to the dose for the single-dose regimen. However, 2–3 intramuscular injections (1 mg/kg of body weight or 50 mg/m^2 of surface area) are given at an interval of 2 or 3 days over the course of a week. In this case, one should be aware of the cumulative, adverse effects of this drug on the liver and bone marrow, since the total amount is higher than that in the single-dose regimen. In fact, even multidose treatments have failed [71]. Some combine it with different doses of leucovorin, which protects against unwanted and adverse systemic effects (termed "rescue" regimen). Several articles expressed their authors' confidence in support of systemic multidose MTX treatment [72].

It is difficult to assess the complication rate associated with the above approach because it was often used in conjunction with or after "first-line" or even after "secondary" treatments [69]. It is clear that MTX can successfully be applied as an adjunct and combined with other mostly nonsurgical treatments. The drawback of both treatments is the long waiting time to observe their effect. If they fail to stop the heart and quickly lower the levels of hCG, a secondary treatment has to deal with a larger gestation and vascular supply.

While multidose MTX was reported to be useful in tearing CSP, it still had a failure rate of 13.4% in using it in 29 patients needing a secondary intervention by local, intragestational sac injection [73].

Intra-arterial or intravenous MTX treatment. Adopted and used in China—a total of 193 patients were treated using intravenous or intra-arterial administration of

MTX solution. The intra-arterial route is used at the time of UAE. Most intravascular treatments were combined with other methods such as suction aspiration laparoscopy, hysteroscopy, and D&C. Li et al. [74] treated 33 patients with CSP out of 13 patients treated with intravenous MTX. Three of the 13 required hysterectomy for profuse bleeding. Zhang et al. [75] have a series of 96 patients of which 33 had intravenous MTX treatment. Since most patients, however, were treated in combination with other methods, their outcome is unclear from the English abstract. Another method is to infuse MTX solution into the uterine artery at the time of UAE. An et al. [76] treated 22 patients with UAE and intra-arterial MTX infusion: 6 patients had severe hemorrhage, 12 had abdominal pain, and 4 hysterectomies were necessary. As opposed to this, Lan et al. [77] successfully used 50 mg MTX infused into the uterine artery at the time of UAE in 79 patients.

5. **Excision by hysteroscopic guidance alone or in combination**

   In our first review [5], hysteroscopic excision was used alone or with other treatments in 113 cases, with a mean complication rate of 18.4%, which is reasonably low in comparison to other treatment methods. General anesthesia is required for the procedure.

   In the literature published after 2012, we found 63 cases managed by this method alone or combined, usually, with laparoscopy [60, 75, 78–81].

6. **Excision by laparoscopic guidance**

   It is mostly used as the sole, standalone treatment, since it provides a final solution removing the gestational sac and the tiny placenta. General anesthesia is required. Fifteen of the 49 cases (30.6%) described in the literature published before 2013 involved complications, as opposed to the 94 cases published in or after 2012 [48, 51, 60, 61, 63, 64, 80, 81], which experienced only 7.7% in complications when hysteroscopy and laparoscopy were combined. The small numbers may not allow meaningful evaluation of the latter two approaches.

7. **Excision by laparotomy**

   Only a handful of articles were published. Fifteen patients undergoing excision of the gestational sac using this, relatively involved, surgery procedure, which is usually performed under general anesthesia [60, 81–83]. At times, elective laparotomy was the treatment of choice to perform hysterectomy, or it was used as a solution to treat bleeding complications [76, 84–87]. Figure 18.12a depicts the closed suture line after the excision of a CSP, while Fig. 18.12b shows the local results after 1 year.

8. **Transvaginal surgical excision**

   Scarce and mostly single case reports are in the literature. This procedure requires a skilled surgeon and is used electively in 119 patients with a relatively low (mean 9.7%) complication rate [88–91]. Li et al. [48] described this surgical approach, which elevates the bladder, excising the gestational sac after curetting and, finally, suturing the area. They managed 49 cases, reporting that, despite 18% minor complications, the procedure is easy and safe. Three patients had intrauterine pregnancies at 6 and 12 months postoperatively. One patient had a recurrent CSP and repeat transvaginal surgical excision. Another patient had an intrauterine pregnancy 5 months postoperatively; however, D&C was performed to prevent uterine rupture.

9. **Intragestational sac injection of methotrexate or potassium chloride, with continuous, real-time ultrasound guidance**

   No anesthesia is required. This approach (Fig. 18.13) had the fewest and least involved complications. In certain cases, we completed the local injection by an immediate placement of a Foley balloon catheter that, after inflation with several milliliters of saline solution, can be kept in place for several days to prevent vaginal bleeding (Fig. 18.14a–f). Of the 83 cases, only 9 (10.8%) involved complications. Cases per-

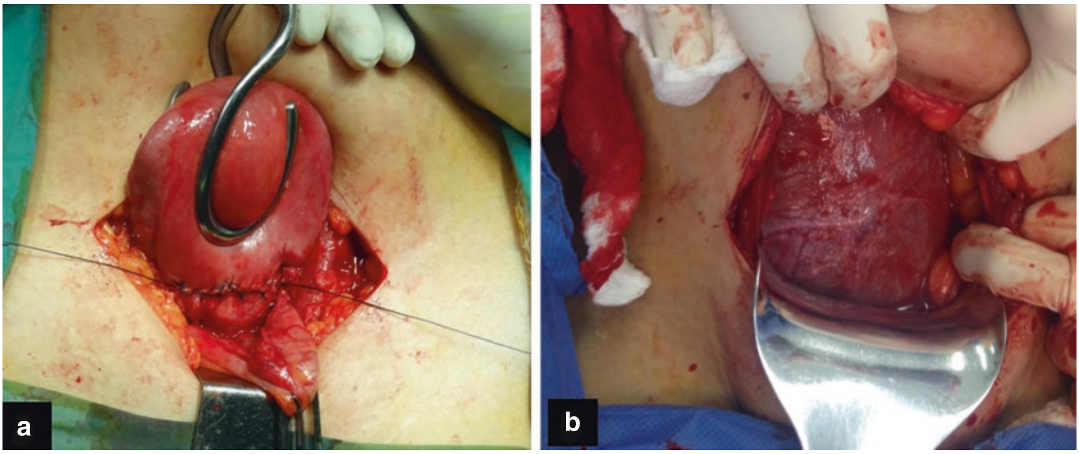

Fig. 18.12 Excision of a CSP sac and the resulting repair as well as a follow-up picture 1 year after a previously performed excision and repair. (Courtesy: Dr. Jose Palacios Jaraquemada, Argentina)

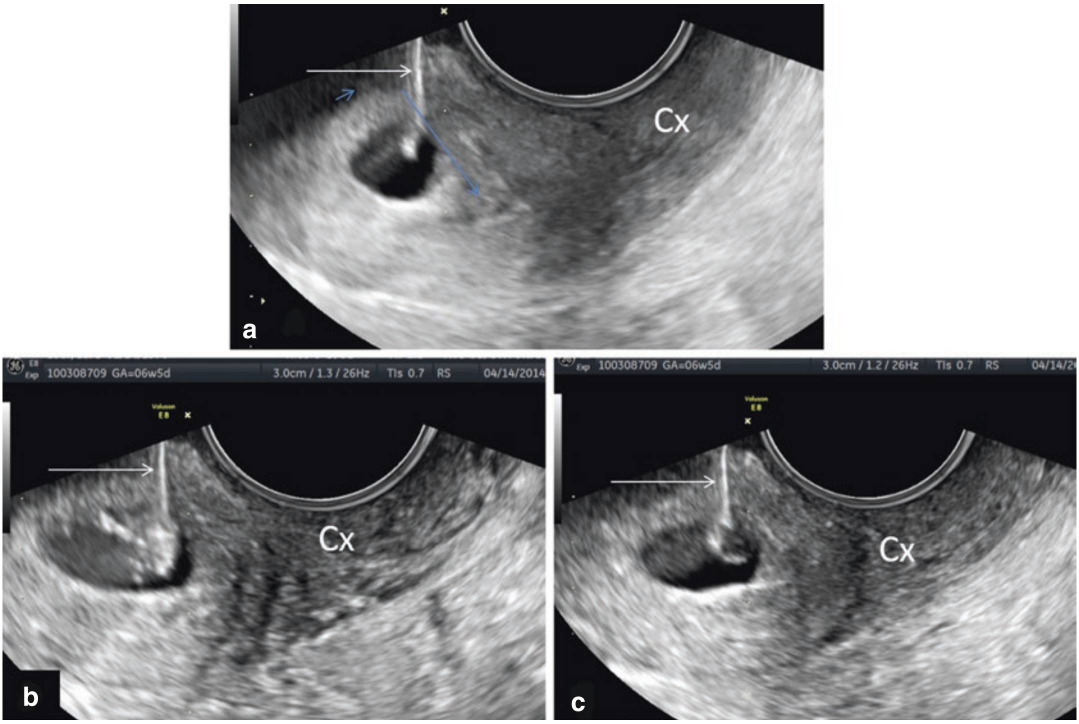
Cx
a
100308709 GA=06w5d
3.0cm / 1.3 / 26Hz
TIs 0.7
RS
04/14/2014
Voluson E8
Cx
b
100308709 GA=06w5d
3.0cm / 1.2 / 26Hz
TIs 0.7
RS
Voluson E8
Cx
c

Fig. 18.13 Transvaginal ultrasound-guided transvaginal, local injection of a CSP. The needle approach into the chorionic sac (**a**), insertion into the embryo (**b**), and targeting the yolk sac (**c**) trying to damage it with a rotation of the needle

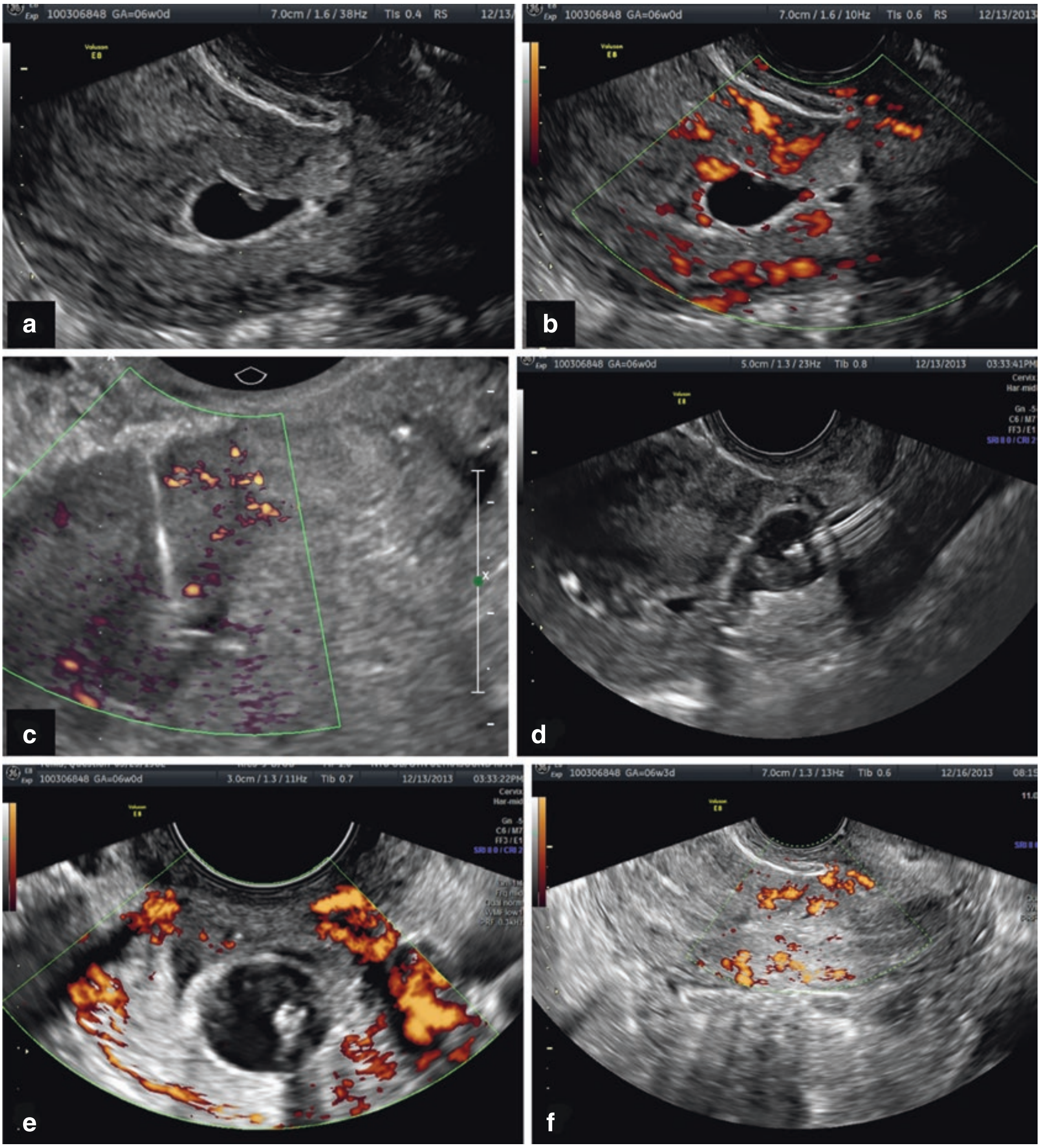
100306848 GA=06w0d
7.0cm / 1.6 / 38Hz
TIs 0.4
RS
a
100306848 GA=06w0d
7.0cm / 1.6 / 10Hz
TIs 0.6
RS
12/13/2013
b
c
100306848 GA=06w0d
5.0cm / 1.3 / 23Hz
Tib 0.8
12/13/2013
03:33:41PM
d
100306848 GA=06w0d
3.0cm / 1.3 / 11Hz
Tib 0.7
12/13/2013
03:33:22PM
e
100306848 GA=06w3d
7.0cm / 1.3 / 13Hz
Tib 0.6
12/16/2013
f

Fig. 18.14 Sequential images of treating a 5–6-week live CSP using local injection followed by insertion of a Foley balloon. (**a**) Sagittal image showing the gestational sac in an anteverted/anteflexed uterus. (**b**) The vascularization is evident. (**c**) The needle was inserted under transvaginal ultrasound guidance, and MTX was injected. (**d**) The inflated balloon in situ creating pressure on the surrounding tissues. (**e**) Transverse image of the inflated balloon with barely detectable blood vessels. (**f**) The area 3 days later after removal of the balloon. Minimal vascularity was seen, and the minimal vaginal bleeding stopped after 1 week

formed with transabdominal sonography guidance had a slightly higher complication rate (15%) than those using TVS guidance. Since 2012, several authors used this simple treatment in 53 patients.

Since the publication of our review, a handful of articles reported on the successful use of the local, intragestational sac injection of ethanol [80], MTX [71, 92–95], and KCl [70] in a total of 53 patients with a complication rate of 5.8%. Yin et al. [69] treated 20 of 34 patients with CSP by local, transvaginal ultrasound-guided intragestational sac injection of MTX, without complications. Yamaguchi et al. [95] treated 8 CSP cases, using intragestational injection of MTX, guided by TVS. Two of the patients needed additional local or systemic MTX injection. The time to hCG normalization was a mean of 78.5 days (range, 42–166 days). Four of the five patients went on and had pregnancies after the treatment and had uneventful parturition; however, another CSP was diagnosed in one patient. Pang et al. [93] successfully treated three patients with local, intragestational MTX injection. Some providers prefer the use of KCl for all their local injections in all types of ectopic pregnancies including CSP [96]. KCl is exclusively used to inject heterotopic pregnancies to enable the normal development of the intrauterine gestation.

Local, intragestational sac injections render a desired solution by stopping the heart activity, and it appears to be an effective and simple intervention for first-trimester CSP between 6 and 8–9 weeks and can be performed by TAS or TVS guidance. A single-balloon Foley or a double-balloon Cook catheter should be handy if bleeding is encountered. These treatments may be even more relevant for patients desiring future fertility.

In a recent publication, this treatment was used in 14 cases and the authors report that direct MTX injection into the gestational sac for NTEP treatment is safe and effective. The failure rate of 7% is considerably lower than what was previously reported for a failure of systemic MTX in similar cases (25%). Resolution of serum hCG after treatment can be quite prolonged even in uncomplicated cases [97]. No other larger series were found to add more information on this formally relatively widespread treatment.

10. **Shirodkar suture in the treatment of CSP**

    This was used by Jurkovic et al. [98], during the evacuation of a cesarean scar pregnancy, which is an effective method for securing hemostasis. In their view, it minimized the need for blood transfusion and ensured preservation of fertility.

11. **Foley single-balloon and Cook double-balloon catheters as an adjuvant to other treatments to prevent/control bleeding**

    A creative and relatively new approach to the treatment is inserting a Foley balloon catheter that is inflated at the site of the CSP, like the Bakri balloon in cases of obstetrical hemorrhage [45, 99–101]. We used this approach as an adjuvant to treatments of CSP [41, 44]. Even so, these approaches are almost always used in a planned fashion, in conjunction with another treatment or as backup, if bleeding occurs (Fig. 18.15a–h). Catheters may be kept in place for as long as 3–4 days, according to the individual case, provided that antibiotic coverage is prescribed. As stated above, this approach is almost always used in a pre-planned case of a patient who restarted bleeding 23 days after local injection of MTX, with a relatively large gestation of 9 weeks 3 days. Inflating the balloon to 20 mL controlled bleeding (Fig. 18.16).

12. **Recurrent CSP**

    Patients treated in the first trimester for CSP should be informed that such a gestation may not happen again in a future pregnancy since the risk is about 1% for reoccurrence. In the literature reviewed through 2012, seven recurrent cases of CSP were described [5]. Gupta et al. [102] provided an additional case, with a patient who had four consecutive CSPs within 2 years. Please note that this patient became pregnant with the fifth CSP, decided to continue the pregnancy, and at the time of this writing is 16 weeks pregnant.

    Two series are worth mentioning including relatively larger series with recurrence rates between 12% and 34% [103]. Forty-four studies (3598 women with CSP) were included. CSP recurred in 17.6% of women. Miscarriage, preterm birth, and placenta

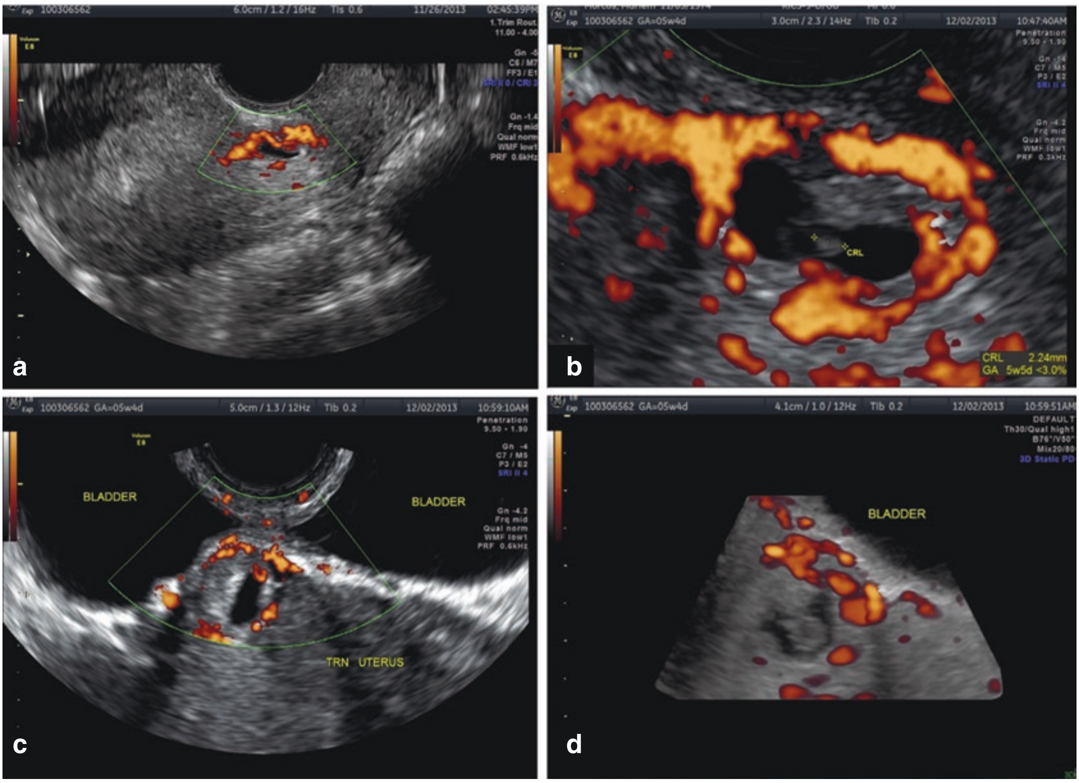

Fig. 18.15 Sequential, pictorial demonstration of the treatment of a 4-week 5-day CSP and use of a Foley balloon catheter. (**a**) The sagittal power Doppler image at 4 weeks 5 days. The patient selected to wait if systemic MTX would suffice as treatment. (**b**) At 5 weeks 4 days, embryonic heartbeats were seen. (**c**) A transverse section demonstrates the anterior placenta with its vessels between the sac and the bladder. (**d**) 3D Doppler angiography clearly shows the rich vascular web below the bladder. (**e**, **f**) After local, intragestational injection of MTX, a Foley balloon was inserted. The compressed sac is seen. (**g**, **h**) Two hours after balloon insertion, diminished blood flow was observed around the sac by Doppler interrogation

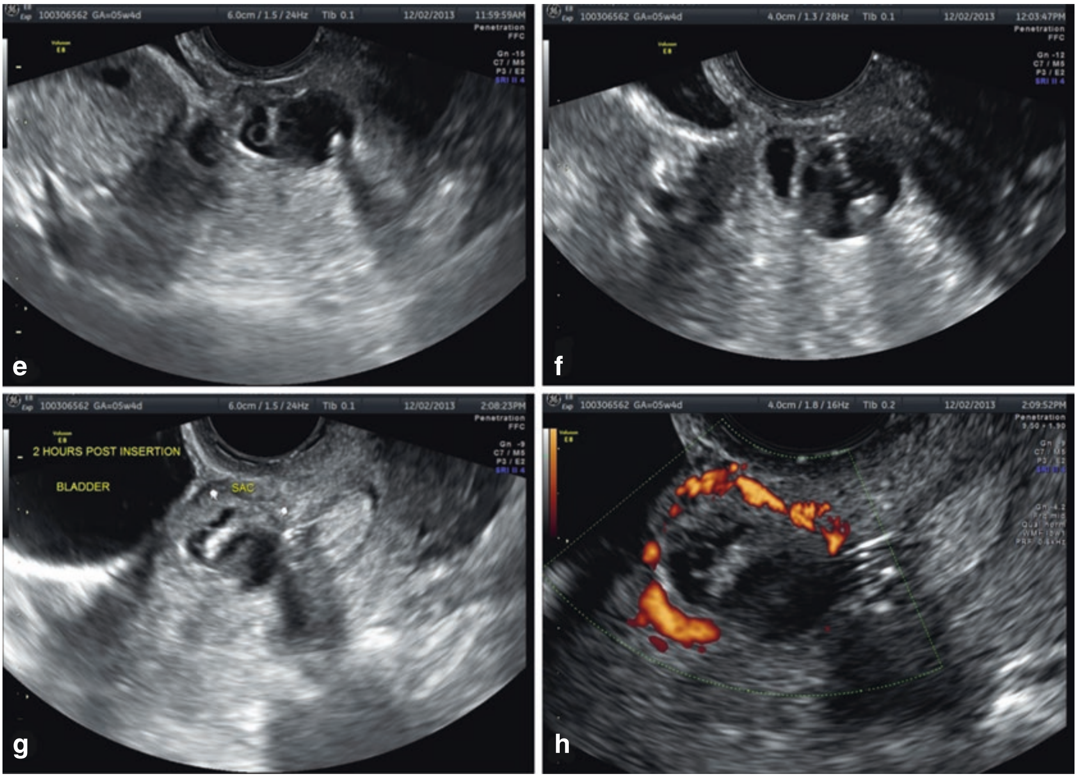

Fig. 18.15 (continued)

accreta spectrum disorders complicated 19.1% (65/341), 10.3% (25/243), and 4.0% of pregnancies, and 67.0% were uncomplicated. When stratifying the analysis according to the type of management, CSP recurred in 21% of women undergoing surgical and in 15.2% of those undergoing nonsurgical management. PAS disorders complicated 4.0% and 12.0% of cases, respectively.

13. **Multifetal CSP**

    Rare but possible, two gestational sacs with two embryos can be present as a twin CSP (Fig. 18.17). There was also a triplet CSP published. Their treatment, so far, was to terminate the pregnancies.

14. **Heterotopic CSP**

    Several heterotopic pregnancies were reported. In these cases, the intrauterine pregnancy can result in live offspring (Fig. 18.18). Several articles reported heterotopic IUP and CSP. The best review, however, containing detailed information is by Ugurlucan et al. [104]. Heterotopic CSP after CS may occur especially when a pregnancy follows assisted reproductive technology. These pregnancies are usually managed by selective injection of the scar pregnancy by local intragestational injection of KCl and laparoscopic excision [105, 106]. Fortunately, most intrauterine pregnancies can be preserved after treatment. A triplet heterotopic pregnancy was also reported by Hsieh et al. [107]. They reported a case of IVF-induced triplet heterotopic pregnancy of early gestational age that was diagnosed as early as 6 weeks' gestation. Treatment with embryo aspiration under vaginal ultrasonography for selective embryo reduction was given, and the concurrent intrauterine twin pregnancy was preserved successfully.

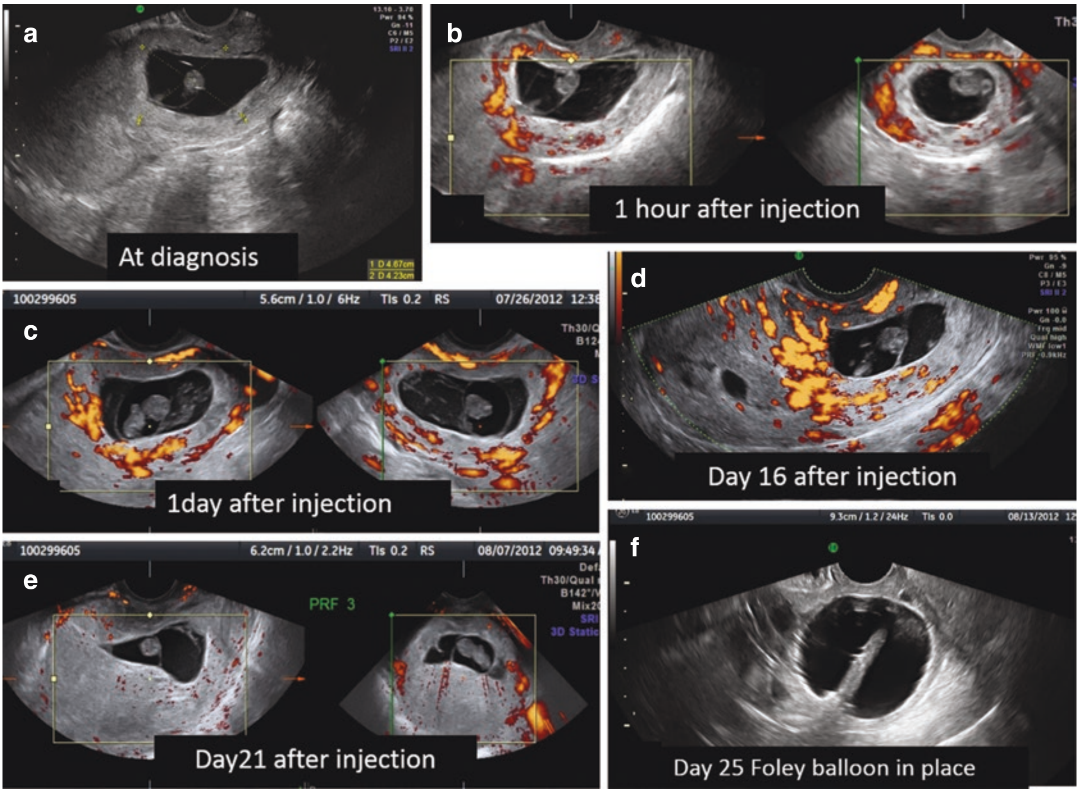
a
At diagnosis
1 D 4.47cm
2 D 4.23cm
b
1 hour after injection
100299605
5.6cm / 1.0 / 6Hz
Tls 0.2
RS
07/26/2012 12:38
c
1day after injection
d
Day 16 after injection
100299605
6.2cm / 1.0 / 2.2Hz
Tls 0.2
RS
08/07/2012 09:49:34
e
PRF 3
3D Static
Day21 after injection
100299605
9.3cm / 1.2 / 24Hz
Tls 0.0
08/13/2012
f
Day 25 Foley balloon in place

Fig. 18.16 The use of Foley balloon catheter in a patient with a relatively advanced CSP of 9+ weeks with a gestational sac of 4.4 × 4.3 cm treated by local intragestational injection of MTX and who started to bleed late, 25 days after treatment. (**a**–**e**) Sequential power Doppler ultrasound images from diagnosis and immediately after the local injection of MTX stopping the heartbeats and throughout days 1, 16, and 21 after treatment. No vaginal bleeding was reported; however, no real decrease of the sac size occurred and the small embryo was still visible in the sac. (**f**) On day 25, after the initial treatment, vaginal bleeding occurred, which was successfully treated by insertion of a Foley balloon catheter and inflated to about 4 cm diameter by about 20

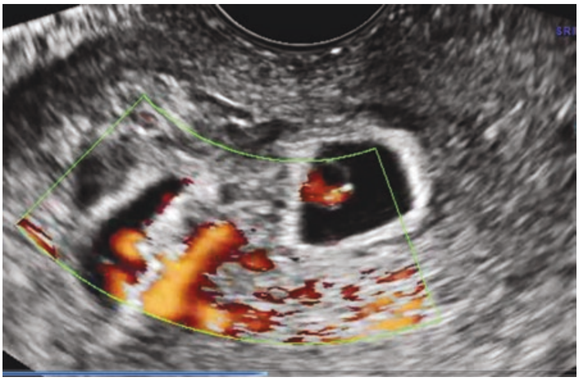

Fig. 18.17 Twin CSP in the scar with active heart activity in this 5-week 5-day pregnancy. Local, intragestational MTX was performed using one single needle insertion slightly adjusting the needle direction to reach both sacs

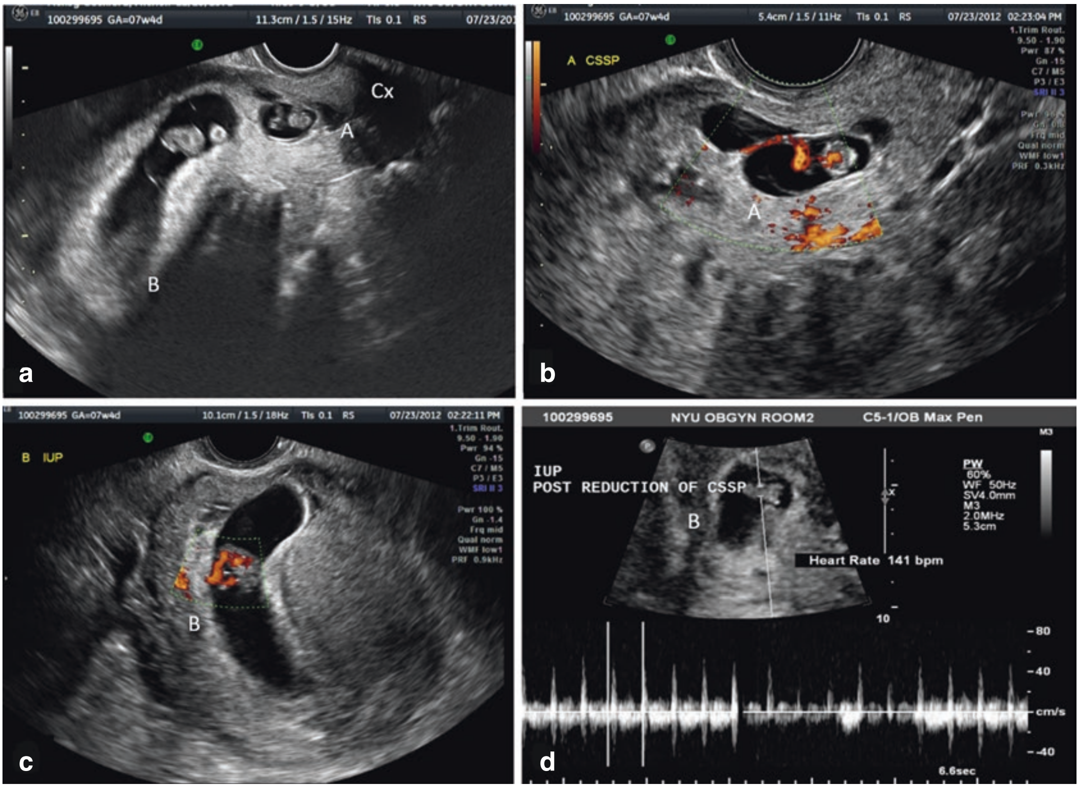
100299695 GA=07w4d
11.3cm / 1.5 / 15Hz
Cx
A
B
a
100299695 GA=07w4d
5.4cm / 1.5 / 11Hz
07/23/2012 02:23:04 PM
A CSSP
A
b
100299695 GA=07w4d
10.1cm / 1.5 / 18Hz
07/23/2012 02:22:11 PM
B IUP
B
c
100299695
NYU OBGYN ROOM2
C5-1/OB Max Pen
IUP
POST REDUCTION OF CSSP
B
Heart Rate 141 bpm
PW
60%
WF 50Hz
SV4.0mm
M3
2.0MHz
5.3cm
10
-80
-40
cm/s
-40
6.6sec
d

Fig. 18.18 Heterotopic CSP and IUP at 7 weeks and 4 days. (**a**) Panoramic sagittal view of the two sacs. Both embryos were alive. The intrauterine sac (**b**) is filling the available space in the uterine cavity (*Cx* cervix). (**b**) Image of the embryo (**a**) in the lower anterior sac. (**c**) Image of the intrauterine embryo (**b**) in the upper sac. (**d**) Proof of the heartbeats of the intrauterine embryo moments after the injection of scar pregnancy. The patient delivered at term a healthy neonate

Summary and Conclusion

Cesarean scar pregnancy (CSP) is ***not*** an ectopic pregnancy by definition. Contrary to ***real*** ectopic pregnancies, the CSP is in the uterine cavity and if not terminated (based upon the recently available literature) can result in a live offspring [108]. CSP is a relatively rare but dangerous and complication-ridden clinical entity, closely related to a consequence of cesarean deliveries (CD).

The best diagnostic tool for its detection, and at times for treatment, is transvaginal sonography. In addition, transabdominal and color Doppler and lately also microvascular color Doppler ultrasound provide satisfactory diagnostic information. The main differential diagnostic entities of a CSP are cervical pregnancy and a miscarriage in progress. Patients with CSP should be counseled based upon new, peer-reviewed evidence published in the latest literature. In addition, patients must be informed of the possible second- and third-trimester complications.

There is mounting evidence that every patient with previous CD should be screened for CSP, as soon as possible [39, 108]. Also, there has been evidence that first-trimester CSP and PAS share the same histologic picture, as CSP is a precursor of PAS. Most patients with a CSP diagnosed in the first trimester will by the third trimester have PAS. And a large number of repeat CD will have a very high risk of hysterectomy.

There is no single best treatment approach to terminate CSP with positive heart activity. Therefore, the procedure with the least complications should be considered and performed without delay. Single-dose systemic MTX injection is a lengthy and usually ineffective first-line therapy, delaying the final treatment. MTX, however, as an adjuvant to other treatments has a proven efficacy. Ultrasound-guided local, intragestational sac injection of MTX/KCl is simple and has low complication rates. Sharp curetting of the CSP site can cause severe bleeding. Uterine artery embolization (UAE) alone is less effective as a single, first-line treatment but has proven useful as an adjunct to other therapies and in cases of emergency due to sustained vaginal bleeding. Insertion and inflation of a Foley balloon or a Cook cervical ripening double-balloon catheter are effective to terminate a CSP or to prevent bleeding from the site of a CSP, or following local injection or endoscopic treatment of CSP. Attention should be given to the possibility of recurrent multifetal and heterotopic CSP.

To evaluate the present practices pertinent to diagnosing, counseling, and treating CSP, an international registry was created (www.CSP--registry.com). The aim of the registry was to investigate safety and efficacy of the different treatment options for termination of CSP from an international large registry and compare these findings with physician's views gained from the results of an international survey [109].

Teaching Points

- Diagnose a cesarean scar pregnancy by the diagnostic criteria and differentiate it from cervical pregnancy and/or a spontaneous abortion.
- Realize that there is a common histologic basis of cesarean scar pregnancy and morbidly adherent placenta (accreta, increta, and percreta).
- Construct a counseling and a management plan for the CSP taking into consideration patients' obstetrical goals and evidence-based management.

References

1. Timor-Tritsch IE. A cesarean scar pregnancy is not an ectopic pregnancy. Ultrasound Obstet Gynecol. 2022;59(4):424–7. https://doi.org/10.1002/uog.24877. Epub 2022 Mar 10. PMID: 35266211
2. Spong CY, Berghella V, Wenstrom KD, Mercer BM, Saade GR. Preventing the first cesarean delivery: summary of a joint Eunice Kennedy Shriver National Institute of Child Health and Human Development, Society for Maternal-Fetal Medicine, and American College of Obstetricians and Gynecologists Workshop. Obstet Gynecol. 2012;120(5):1181–93.
3. Hamilton BE, Hoyert DL, Martin JA, Strobino DM, Guyer B. Annual summary of vital statistics: 2010–2011. Pediatrics. 2013;131(3):548–58.
4. Arnold J. World cesarean rates: OECD countries 2012. http://www.cesareanrates.com/blog/2012/12/8/world-cesarean-rates-oecd-countries.html.
5. Timor-Tritsch IE, Monteagudo A. Unforeseen consequences of the increasing rate of cesarean deliveries: early placenta accreta and cesarean scar pregnancy. A review. Am J Obstet Gynecol. 2012;207(1):14–29.
6. Monteagudo A, Carreno C, Timor-Tritsch IE. Saline infusion sonohysterography in nonpregnant women with previous cesarean delivery: the “niche” in the scar. J Ultrasound Med. 2001;20(10):1105–15.
7. Bij de Vaate AJ, van der Voet LF, Naji O, Witmer M, Veersema S, Brolmann HA, et al. Prevalence, potential risk factors for development and symptoms related to the presence of uterine niches following Cesarean section: systematic review. Ultrasound Obstet Gynecol. 2014;43(4):372–82.
8. Jauniaux E, Jurkovic D. Placenta accreta: pathogenesis of a 20th century iatrogenic uterine disease. Placenta. 2012;33(4):244–51.
9. Jurkovic D, Hillaby K, Woelfer B, Lawrence A, Salim R, Elson CJ. Cesarean scar pregnancy. Ultrasound Obstet Gynecol. 2003;21(3):310.
10. Jurkovic D, Hillaby K, Woelfer B, Lawrence A, Salim R, Elson CJ. First-trimester diagnosis and management of pregnancies implanted into the lower uterine segment cesarean section scar. Ultrasound Obstet Gynecol. 2003;21(3):220–7.
11. Rotas MA, Haberman S, Levgur M. Cesarean scar ectopic pregnancies: etiology, diagnosis, and management. Obstet Gynecol. 2006;107(6):1373–81.
12. Seow KM, Hwang JL, Tsai YL, Huang LW, Lin YH, Hsieh BC. Subsequent pregnancy outcome after conservative treatment of a previous cesarean scar pregnancy. Acta Obstet Gynecol Scand. 2004;83(12):1167–72.
13. Norwitz ER. Defective implantation and placentation: laying the blueprint for pregnancy complications. Reprod Biomed Online. 2006;13(4):591–9.
14. Toro-Bejarano M, Mora R, Timor-Tritsch IE, Vernon J, Monteagudo A, D'Antonio F, Duncan K. Myomectomy

scar pregnancy – a serious, but scarcely reported entity: literature review and an instructive case. Case Rep Perinat Med. 2021;10(1):20210071. https://doi.org/10.1515/crpm-2021-0071.

15. Matsuzaki S, Nagase Y, Takiuchi T, Kakigano A, Mimura K, Lee M, Matsuzaki S, Ueda Y, Tomimatsu T, Endo M, Kimura T. Antenatal diagnosis of placenta accreta spectrum after in vitro fertilization-embryo transfer: a systematic review and meta-analysis. Sci Rep. 2021;11(1):9205. https://doi.org/10.1038/s41598-021-88551-7. PMID: 33911134; PMCID: PMC8080594
16. Rosen T. Placenta accreta and cesarean scar pregnancy: overlooked costs of the rising cesarean section rate. Clin Perinatol. 2008;35(3):519–29, x.
17. Kliman HJ, Feinberg RF, Haimowitz JE. Human trophoblast-endometrial interactions in an in vitro suspension culture system. Placenta. 1990;11(4):349–67.
18. Jauniaux E, Jurkovic D, Hussein AM, Burton GJ. New insights into the etiopathology of placenta accreta spectrum. Am J Obstet Gynecol. 2022; https://doi.org/10.1016/j.ajog.2022.02.038. Epub ahead of print. PMID: 35248577
19. Society for Maternal-Fetal Medicine (SMFM), Miller R, Timor-Tritsch IE, Gyamfi-Bannerman C. Society for Maternal-Fetal Medicine (SMFM) Consult Series #49: Cesarean scar pregnancy. Am J Obstet Gynecol. 2020;222(5):B2–B14. https://doi.org/10.1016/j.ajog.2020.01.030. Epub 2020 Jan 21. Erratum in: Am J Obstet Gynecol. 2020 Oct 6; PMID: 31972162
20. Shainker SA, Coleman B, Timor-Tritsch IE, Bhide A, Bromley B, Cahill AG, Gandhi M, Hecht JL, Johnson KM, Levine D, Mastrobattista J, Philips J, Platt LD, Shamshirsaz AA, Shipp TD, Silver RM, Simpson LL, Copel JA, Abuhamad A, Society for Maternal-Fetal Medicine. Special report of the Society for Maternal-Fetal Medicine Placenta Accreta Spectrum Ultrasound Marker Task Force: consensus on definition of markers and approach to the ultrasound examination in pregnancies at risk for placenta accreta spectrum. Am J Obstet Gynecol. 2021;224(1):B2–B14. https://doi.org/10.1016/j.ajog.2020.09.001. Erratum in: Am J Obstet Gynecol. 2021 Jul;225(1):91. PMID: 33386103
21. Stirnemann JJ, Chalouhi GE, Forner S, Saidji Y, Salomon LJ, Bernard JP, et al. First-trimester uterine scar assessment by transvaginal ultrasound. Am J Obstet Gynecol. 2011;205(6):551.e1–6.
22. Stirnemann JJ, Mousty E, Chalouhi G, Salomon LJ, Bernard JP, Ville Y. Screening for placenta accreta at 11–14 weeks of gestation. Am J Obstet Gynecol. 2011;205(6):547.e1–6.
23. Godin PA, Bassil S, Donnez J. An ectopic pregnancy developing in a previous caesarian section scar. Fertil Steril. 1997;67(2):398–400.
24. Vial Y, Petignat P, Hohlfeld P. Pregnancy in a cesarean scar. Ultrasound Obstet Gynecol. 2000;16(6):592–3.
25. Seow KM, Hwang JL, Tsai YL. Ultrasound diagnosis of a pregnancy in a cesarean section scar. Ultrasound Obstet Gynecol. 2001;18(5):547–9.
26. Timor-Tritsch IE, Monteagudo A, Santos R, Tsymbal T, Pineda G, Arslan AA. The diagnosis, treatment, and follow-up of cesarean scar pregnancy. Am J Obstet Gynecol. 2012;207(1):44.e1–e13.
27. Timor-Tritsch IE, Haynes MC, Monteagudo A, Khatib N, Kovács S. Ultrasound diagnosis and management of acquired uterine enhanced myometrial vascularity/arteriovenous malformations. Am J Obstet Gynecol. 2016;214(6):731.e1–731.e10. https://doi.org/10.1016/j.ajog.2015.12.024. Epub 2016 Feb 9. PMID: 26873276
28. Timor-Tritsch IE, McDermott WM, Monteagudo A, Calí G, Kreines F, Hernandez S, Stephenson C, Bryk H, D'Antonio F. Extreme enhanced myometrial vascularity following cesarean scar pregnancy: a new diagnostic entity. J Matern Fetal Neonatal Med. 2021;17:1–12. https://doi.org/10.1080/14767058.2021.1897564. Epub ahead of print. PMID: 33730990
29. Timmerman D, Wauters J, Van Calenbergh S, Van Schoubroeck D, Maleux G, Van Den Bosch T, et al. Color Doppler imaging is a valuable tool for the diagnosis and management of uterine vascular malformations. Ultrasound Obstet Gynecol. 2003;21(6):570–7.
30. Polat P, Suma S, Kantarcy M, Alper F, Levent A. Color Doppler US in the evaluation of uterine vascular abnormalities. Radiographics. 2002;22(1):47–53.
31. Timor-Tritsch IE, Khatib N, Monteagudo A, Ramos J, Berg R, Kovacs S. Cesarean scar pregnancy (CSP): experience of sixty cases. J Ultrasound Med. 2015;34(4):601–10.
32. Comstock CH, Lee W, Vettraino IM, Bronsteen RA. The early sonographic appearance of placenta accreta. J Ultrasound Med. 2003;22(1):19–23; quiz 4–6.
33. Rac M, Moschos E, Wells E, McIntire DD, Dashe JS, Twickler DM. Ultrasound (US) findings of placenta accreta in the first trimester. Ultrasound Obstet Gynecol. 2014;44(Suppl. 1):62–180.
34. Ballas J, Pretorius D, Hull AD, Resnik R, Ramos GA. Identifying sonographic markers for placenta accreta in the first trimester. J Ultrasound Med. 2012;31(11):1835–41.
35. Sinha P, Mishra M. Caesarean scar pregnancy: a precursor of placenta percreta/accreta. J Obstet Gynaecol. 2012;32(7):621–3.
36. Timor-Tritsch IE, Monteagudo A, Cali G, Palacios-Jaraquemada JM, Maymon R, Arslan AA, et al. Cesarean scar pregnancy and early placenta accreta share common histology. Ultrasound Obstet Gynecol. 2014;43(4):383–95.
37. Timor-Tritsch IE, Monteagudo A, Cali G, Vintzileos A, Viscarello R, Al-Khan A, et al. Cesarean scar pregnancy is a precursor of morbidly adherent placenta. Ultrasound Obstet Gynecol. 2014;44(3):346–53.

38. Timor-Tritsch IE, Monteagudo A, Calì G, D'Antonio F, Agten AK. Cesarean scar pregnancy: patient counseling and management. Obstet Gynecol Clin North Am. 2019;46(4):813–28. https://doi.org/10.1016/j.ogc.2019.07.010. PMID: 31677756
39. Timor-Tritsch I, Buca D, Di Mascio D, Cali G, D'Amico A, Monteagudo A, Tinari S, Morlando M, Nappi L, Greco P, Rizzo G, Liberati M, Jose-Palacios-Jaraquemada, D'Antonio F. Outcome of cesarean scar pregnancy according to gestational age at diagnosis: a systematic review and meta-analysis. Eur J Obstet Gynecol Reprod Biol. 2021;258:53–9. https://doi.org/10.1016/j.ejogrb.2020.11.036. Epub 2020 Nov 12. PMID: 33421811. PMID: 31677756
40. Miller R, Timor-Tritsch IE, Gyamfi-Bannerman C. Society for Maternal-Fetal Medicine (SMFM) Consult Series #49: Cesarean scar pregnancy. Am J Obstet Gynecol. 2020;222(5):B2–B14. https://doi.org/10.1016/j.ajog.2020.01.030. Epub 2020 Jan 21. Erratum in: Am J Obstet Gynecol. 2020 Oct 6: PMID: 31972162
41. Timor-Tritsch IE, Monteagudo A, Bennett TA, Foley C, Ramos J, Kaelin AA. A new minimally invasive treatment for cesarean scar pregnancy and cervical pregnancy. Am J Obstet Gynecol. 2016;215(3):351.e1–8. https://doi.org/10.1016/j.ajog.2016.03.010. Epub 2016 Mar 12. Erratum in: Am J Obstet Gynecol. 2020 Jun;222(6):618. PMID: 26979630
42. Maheux-Lacroix S, Li F, Bujold E, Nesbitt-Hawes E, Deans R, Abbott J. Cesarean scar pregnancies: a systematic review of treatment options. J Minim Invasive Gynecol. 2017;24(6):915–25. https://doi.org/10.1016/j.jmig.2017.05.019. Epub 2017 Jul 18. PMID: 28599886
43. Birch Petersen K, Hoffmann E, Rifbjerg Larsen C, Svarre NH. Cesarean scar pregnancy: a systematic review of treatment studies. Fertil Steril. 2016;105(4):958–67. https://doi.org/10.1016/j.fertnstert.2015.12.130. Epub 2016 Jan 18. PMID: 26794422
44. Timor-Tritsch IE, Cali G, Monteagudo A, Khatib N, Berg R, Forlani F, et al. The use of a Foley balloon catheter as an adjuvant therapy in preventing or managing bleeding during treatment for cesarean scar and cervical pregnancies. Ultrasound Obstet Gynecol. 2014;46:118–23.
45. Jiang T, Liu G, Huang L, Ma H, Zhang S. Methotrexate therapy followed by suction curettage followed by Foley tamponade for caesarean scar pregnancy. Eur J Obstet Gynecol Reprod Biol. 2011;156(2):209–11.
46. Yu XL, Zhang N, Zuo WL. Cesarean scar pregnancy: an analysis of 100 cases. Zhonghua Yi Xue Za Zhi. 2011;91(45):3186–9.
47. Cali G, Giambanco L, Puccio G, Forlani F. Morbidly adherent placenta: evaluation of ultrasound diagnostic criteria and differentiation of placenta accreta from percreta. Ultrasound Obstet Gynecol. 2013;41(4):406–12.
48. Li JB, Kong LZ, Fan L, Fu J, Chen SQ, Yao SZ. Transvaginal surgical management of cesarean scar pregnancy: analysis of 49 cases from one tertiary care center. Eur J Obstet Gynecol Reprod Biol. 2014;182C:102–6.
49. Cao S, Zhu L, Jin L, Gao J, Chen C. Uterine artery embolization in cesarean scar pregnancy: safe and effective intervention. Chin Med J. 2014;127(12):2322–6.
50. Gao L, Huang Z, Gao J, Mai H, Zhang Y, Wang X. Uterine artery embolization followed by dilation and curettage within 24 hours compared with systemic methotrexate for cesarean scar pregnancy. Int J Gynaecol Obstet. 2014;127(2):147–51.
51. Wu X, Xue X, Wu X, Lin R, Yuan Y, Wang Q, et al. Combined laparoscopy and hysteroscopy vs. uterine curettage in the uterine artery embolization-based management of cesarean scar pregnancy: a cohort study. Int J Clin Exp Med. 2014;7(9):2793–803.
52. Zhu W, Zhang X, Liu C, Liu Y, Xu W. Uterine artery embolization on serum β-HCG levels, fertility function and clinical efficacy in patients with cesarean uterine scar pregnancy. Front Surg. 2022;9:838879. https://doi.org/10.3389/fsurg.2022.838879. PMID: 35187063; PMCID: PMC8847222
53. Chang Y, Kay N, Chen YH, Chen HS, Tsai EM. Resectoscopic treatment of ectopic pregnancy in previous cesarean delivery scar defect with vasopressin injection. Fertil Steril. 2011;96(2):e80–2.
54. Chao A, Wang TH, Wang CJ, Lee CL, Chao AS. Hysteroscopic management of cesarean scar pregnancy after unsuccessful methotrexate treatment. J Minim Invasive Gynecol. 2005;12(4):374–6.
55. Chen ZY, Zhang XM, Xu H, Zhang J, Huang XF. Management of cesarean scar pregnancy by hysteroscopy combined with uterine artery embolism. Zhonghua Fu Chan Ke Za Zhi. 2011;46(8):591–4.
56. Deans R, Abbott J. Hysteroscopic management of cesarean scar ectopic pregnancy. Fertil Steril. 2010;93(6):1735–40.
57. Gubbini G, Centini G, Nascetti D, Marra E, Moncini I, Bruni L, et al. Surgical hysteroscopic treatment of cesarean-induced isthmocele in restoring fertility: prospective study. J Minim Invasive Gynecol. 2011;18(2):234–7.
58. Ozkan S, Caliskan E, Ozeren S, Corakci A, Cakiroglu Y, Coskun E. Three-dimensional ultrasonographic diagnosis and hysteroscopic management of a viable cesarean scar ectopic pregnancy. J Obstet Gynaecol Res. 2007;33(6):873–7.
59. Robinson JK, Dayal MB, Gindoff P, Frankfurter D. A novel surgical treatment for cesarean scar pregnancy: laparoscopically assisted operative hysteroscopy. Fertil Steril. 2009;92(4):1497.e13–6.
60. Wang G, Liu X, Bi F, Yin L, Sa R, Wang D, et al. Evaluation of the efficacy of laparoscopic resection for the management of exogenous cesarean scar pregnancy. Fertil Steril. 2014;101(5):1501–7.

61. He Y, Wu X, Zhu Q, Wu X, Feng L, Wu X, et al. Combined laparoscopy and hysteroscopy vs. uterine curettage in the uterine artery embolization-based management of cesarean scar pregnancy: a retrospective cohort study. BMC Womens Health. 2014;14:116.
62. Hudecek R, Ivanova Z, Smerdova M, Pankova S, Krajcovicova R. Effect of GnRH analogues pre-treatment on myomectomy outcomes in reproductive age women. Ceska Gynekol. 2012;77(2):109–17.
63. Jiang S, Zhao S. Laparoscopic surgery for ectopic pregnancy within a cesarean scar. Clin Exp Obstet Gynecol. 2013;40(3):440–4.
64. Wang YL, Weng SS, Huang WC, Su TH. Laparoscopic management of ectopic pregnancies in unusual locations. Taiwan J Obstet Gynecol. 2014;53(4):466–70.
65. Siedhoff MT, Schiff LD, Moulder JK, Toubia T, Ivester T. Robotic-assisted laparoscopic removal of cesarean scar ectopic and hysterotomy revision. Am J Obstet Gynecol. 2015;212(5):681.e1–4.
66. Yoon R, Sasaki K, Miller CE. Laparoscopic excision of cesarean scar pregnancy with scar revision. J Minim Invasive Gynecol. 2021;28(4):746–7. https://doi.org/10.1016/j.jmig.2020.06.017. Epub 2020 Jun 27. PMID: 32603870
67. Bodur S, Gun I, Guido R. What is the role of primary methotrexate treatment in scar ectopic pregnancy? Am J Obstet Gynecol. 2014;210(4):379–80.
68. Timor-Tritsch I, Monteagudo A. Correction: Unforeseen consequences of the increasing rate of cesarean deliveries: early placenta accreta and cesarean scar pregnancy. A review. Am J Obstet Gynecol. 2014;210(4):371–4.
69. Yin XH, Yang SZ, Wang ZQ, Jia HY, Shi M. Injection of MTX for the treatment of cesarean scar pregnancy: comparison between different methods. Int J Clin Exp Med. 2014;7(7):1867–72.
70. Uysal F, Uysal A. Spontaneous heterotopic cesarean scar pregnancy: conservative management by transvaginal sonographic guidance and successful pregnancy outcome. J Ultrasound Med. 2013;32(3):547–8.
71. Berhie SH, Molina RL, Davis MR, Anchan RM, Wang KC. Beware the scar: laparoscopic hysterectomy for 7-week cesarean delivery scar implantation pregnancy. Am J Obstet Gynecol. 2015;212(2):247.e1–2.
72. Kutuk MS, Uysal G, Dolanbay M, Ozgun MT. Successful medical treatment of cesarean scar ectopic pregnancies with systemic multidose methotrexate: single-center experience. J Obstet Gynaecol Res. 2014;40(6):1700–6.
73. Levin G, Zigron R, Dior UP, Gilad R, Shushan A, Benshushan A, Rottenstreich A. Conservative management of Caesarean scar pregnancies with systemic multidose methotrexate: predictors of treatment failure and reproductive outcomes. Reprod Biomed Online. 2019;39(5):827–34. https://doi.org/10.1016/j.rbmo.2019.05.015. Epub 2019 May 24. PMID: 31530445
74. Li C, Feng D, Jia C, Liu B, Zhan X. Transcatheter arterial chemoembolization versus systemic methotrexate for the management of cesarean scar pregnancy. Int J Gynaecol Obstet. 2011;113(3):178–82.
75. Zhang Y, Chen YS, Wang JJ, Lu ZY, Hua KQ. Analysis of 96 cases with cesarean scar pregnancy. Zhonghua Fu Chan Ke Za Zhi. 2010;45(9):664–8.
76. An X, Ming X, Li K, Wang J. The analysis of efficacy and failure factors of uterine artery methotrexate infusion and embolization in treatment of cesarean scar pregnancy. TheScientificWorldJOURNAL. 2013;2013:213603.
77. Lan W, Hu D, Li Z, Wang L, Yang W, Hu S. Bilateral uterine artery chemoembolization combined with dilation and curettage for treatment of cesarean scar pregnancy: a method for preserving the uterus. J Obstet Gynaecol Res. 2013;39(6):1153–8.
78. Fylstra DL. Cervical pregnancy: 13 cases treated with suction curettage and balloon tamponade. Am J Obstet Gynecol. 2014;210(6):581.e1–5.
79. Mollo A, Alviggi C, Conforti A, Insabato L, De Placido G. Intact removal of spontaneous twin ectopic caesarean scar pregnancy by office hysteroscopy: case report and literature review. Reprod Biomed Online. 2014;29(5):530–3.
80. Shao MJ, Hu MX, Xu XJ, Zhang L, Hu M. Management of caesarean scar pregnancies using an intrauterine or abdominal approach based on the myometrial thickness between the gestational mass and the bladder wall. Gynecol Obstet Investig. 2013;76(3):151–7.
81. Li Y, Xiang Y, Wan X, Feng F, Ren T. Clinical study on 39 cases with caesarean scar pregnancy with sonographic mass. Zhonghua Fu Chan Ke Za Zhi. 2014;49(1):10–3.
82. Abdelkader MA, Fouad R, Gebril AH, El Far MA, Elyassergi DF. Caesarean scar pregnancy: hysterotomy is rapid and safe management option. Arch Gynecol Obstet. 2014;290(2):381–3.
83. Kai K, Shimamoto K, Matsumoto H, Narahara H. Conservative surgical treatment for caesarean scar pregnancy. J Obstet Gynaecol. 2014;34(1):91–2.
84. Nankali A, Ataee M, Shahlazadeh H, Daeichin S. Surgical management of the cesarean scar ectopic pregnancy: a case report. Case Rep Obstet Gynecol. 2013;2013:525187.
85. Sorbi F, Sisti G, Pieralli A, Di Tommaso M, Livi L, Buccoliero AM, et al. Cervicoisthmic choriocarcinoma mimicking cesarean section scar ectopic pregnancy. J Res Med Sci. 2013;18(10):914–7.
86. Wozniak S, Pyra K, Kludka-Sternik M, Czuczwar P, Szkodziak P, Paszkowski T, et al. Uterine artery embolization using gelatin sponge particles performed due to massive vaginal bleeding caused by ectopic pregnancy within a cesarean scar: a case study. Ginekol Pol. 2013;84(11):966–9.
87. Zhang B, Jiang ZB, Huang MS, Guan SH, Zhu KS, Qian JS, et al. Uterine artery embolization combined with methotrexate in the treatment of cesarean scar pregnancy: results of a case series and review of the literature. J Vasc Interv Radiol. 2012;23(12):1582–8.

88. Shi J, Qin J, Wang W, Zhang H. Clinical study on 57 cases with caesarean scar pregnancy. Zhonghua Fu Chan Ke Za Zhi. 2014;49(1):18–21.
89. Wang DB, Chen YH, Zhang ZF, Chen P, Liu KR, Li Y, et al. Evaluation of the transvaginal resection of low-segment cesarean scar ectopic pregnancies. Fertil Steril. 2014;101(2):602–6.
90. Wang Z, Shan L, Xiong H. Transvaginal removal of ectopic pregnancy tissue and repair of uterine defect for cesarean scar pregnancy. Clin Exp Obstet Gynecol. 2013;40(4):546–7.
91. Le A, Shan L, Xiao T, Zhuo R, Xiong H, Wang Z. Transvaginal surgical treatment of cesarean scar ectopic pregnancy. Arch Gynecol Obstet. 2013;287(4):791–6.
92. Nguyen-Xuan HT, Lousquy R, Barranger E. Diagnosis, treatment, and follow-up of cesarean scar pregnancy. Gynecol Obstet Fertil. 2014;42(7–8):483–9.
93. Pang YP, Tan WC, Yong TT, Koh PK, Tan HK, Ho TH. Caesarean section scar pregnancy: a case series at a single tertiary centre. Singap Med J. 2012;53(10):638–42.
94. Seow KM, Wang PH, Huang LW, Hwang JL. Transvaginal sono-guided aspiration of gestational sac concurrent with a local methotrexate injection for the treatment of unruptured cesarean scar pregnancy. Arch Gynecol Obstet. 2013;288(2):361–6.
95. Yamaguchi M, Honda R, Uchino K, Tashiro H, Ohba T, Katabuchi H. Transvaginal methotrexate injection for the treatment of cesarean scar pregnancy: efficacy and subsequent fecundity. J Minim Invasive Gynecol. 2014;21(5):877–83.
96. Doubilet PM, Benson CB, Frates MC, Ginsburg E. Sonographically guided minimally invasive treatment of unusual ectopic pregnancies. J Ultrasound Med. 2004;23(3):359–70.
97. Gilbert SB, Alvero RJ, Roth L, Polotsky AJ. Direct methotrexate injection into the gestational sac for nontubal ectopic pregnancy: a review of efficacy and outcomes from a single institution. J Minim Invasive Gynecol. 2020;27(1):166–72. https://doi.org/10.1016/j.jmig.2019.03.016. Epub 2019 Mar 28. PMID: 30930212
98. Jurkovic D, Ben-Nagi J, Ofilli-Yebovi D, Sawyer E, Helmy S, Yazbek J. Efficacy of Shirodkar cervical suture in securing hemostasis following surgical evacuation of cesarean scar ectopic pregnancy. Ultrasound Obstet Gynecol. 2007;30(1):95–100.
99. Atilgan R, Celik A, Boztosun A, Ilter E, Yalta T, Ozercan R. Evaluation of cervical cytological abnormalities in Turkish population. Indian J Pathol Microbiol. 2012;55(1):52–5.
100. Tsui KH, Lin LT, Yu KJ, Chen SF, Chang WH, Yu S, et al. Double-balloon cervical ripening catheter works well as an intrauterine balloon tamponade in post-abortion massive hemorrhage. Taiwan J Obstet Gynecol. 2012;51(3):426–9.
101. Shao HJ, Ma JT, Yang XE, Xu LP, Yang CL. Diagnosis and treatment of cesarean scar pregnancy. Zhonghua Yi Xue Za Zhi. 2010;90(37):2616–9.
102. Gupta S, Pineda G, Rubin S, Timor-Tritsch IE. Four consecutive recurrent cesarean scar pregnancies in a single patient. J Ultrasound Med. 2013;32(10):1878–80.
103. Timor-Tritsch IE, Horwitz G, D'Antonio F, Monteagudo A, Bornstein E, Chervenak J, Messina L, Morlando M, Cali G. Recurrent cesarean scar pregnancy: case series and literature review. Ultrasound Obstet Gynecol. 2021;58(1):121–6. https://doi.org/10.1002/uog.23577. PMID: 33411387
104. Ugurlucan FG, Bastu E, Dogan M, Kalelioglu I, Alanya S, Has R. Management of cesarean heterotopic pregnancy with transvaginal ultrasound-guided potassium chloride injection and gestational sac aspiration, and review of the literature. J Minim Invasive Gynecol. 2012;19(5):671–3.
105. Demirel LC, Bodur H, Selam B, Lembet A, Ergin T. Laparoscopic management of heterotopic cesarean scar pregnancy with preservation of intrauterine gestation and delivery at term: case report. Fertil Steril. 2009;91(4):1293.e5–7.
106. Wang CJ, Tsai F, Chen C, Chao A. Hysteroscopic management of heterotopic cesarean scar pregnancy. Fertil Steril. 2010;94(4):1529.e15–8.
107. Hsieh BC, Hwang JL, Pan HS, Huang SC, Chen CY, Chen PH. Heterotopic caesarean scar pregnancy combined with intrauterine pregnancy successfully treated with embryo aspiration for selective embryo reduction: case report. Hum Reprod. 2004;19(2):285–7. https://doi.org/10.1093/humrep/deh080. PMID: 14747168
108. Timor-Tritsch IE. Cesarean scar pregnancy is not an ectopic pregnancy. Ultrasound Obstet Gynecol. 2022; https://doi.org/10.1002/uog.24877.
109. Agten AK, Monteagudo A, Timor-Tritsch IE, Thilaganathan B. Cesarean Scar Pregnancy Registry: an international research platform. Ultrasound Obstet Gynecol. 2020;55(4):438–40. https://doi.org/10.1002/uog.21952. PMID: 31840910

19

The First-Trimester Fetal Head and Brain

Ana Monteagudo and Ilan E. Timor-Tritsch

Introduction

Seek and you shall find. Matthew 7:7–11

Detection of fetal anomalies using ultrasound (US) has evolved as the US equipment and probes have evolved. The 18–20-week anatomy scan has been part of the routine imaging protocol for the pregnant patient for over 30 years; during this second-trimester scan, most anomalies are detected. However, many of them detected at the 18–20-week anatomy scan can already be visualized in the first trimester. Bromley et al. [1] reported a 41.4% detection rate of malformations at 11–13 6/7 weeks without even applying a dedicated scanning protocol; furthermore, they were able to diagnose as many as 71% of the lethal anomalies. In a prospective observational ultrasound study to determine the efficacy of diagnosing first-trimester anomalies, Becker and Wegner performed scans in 3094 consecutive fetuses between 11 and 13 6/7 weeks and found an 83.7% detection rate of major anomalies [2].

High-frequency transvaginal probes have been the mainstay of early fetal anatomical scanning due to their high frequencies and ability to place the transducer close to the developing fetus. The fact that this early scan has been dependent on a transvaginal imaging modality (at least our opinion) was the main reason why first- and early second-trimester fetal anatomical sonography has not gained popularity. Another reason may have been the inadequate understanding of early fetal developmental anatomy and embryology of some fetal anomalies. On the other hand, recent advances in new high-frequency transabdominal probes allow imaging of the first- and early second-trimester fetus and can therefore be used by operators not willing to engage in transvaginal scanning.

The first-trimester "nuchal scan" (nuchal translucency or NT scan) was introduced in the 1990s, and it was estimated that approximately 20% of the pregnancies were undergoing this US test in the USA. Nevertheless, recently, with the increased use and acceptance of NIPT or NIPS (noninvasive prenatal testing or screening), many centers are moving away from the performance of NT scan and moving towards performing an early fetal anatomy scan, which includes the structures of the "classical" NT scan.

The goal of this chapter is not to be a compendium of first-trimester fetal head-brain-spine normal structures and pathologies, but to motivate the reader to look beyond the nuchal translucency when scanning the first-trimester fetus.

A. Monteagudo (✉)
Carnegie Imaging for Women, Icahn School of Medicine at Mount Sinai, New York, NY, USA
e-mail: amonteagudo@mfmnyc.com

I. E. Timor-Tritsch
Grossman School of Medicine, New York, NY, USA

© The Author(s), under exclusive license to Springer Nature Switzerland AG 2023
J. S. Abramowicz, R. E. Longman (eds.), *First-Trimester Ultrasound*,
https://doi.org/10.1007/978-3-031-24133-8_19

What Normal and/or Abnormal Fetal Structures Can Be Reliability Detected at This Gestational Age?

In 1992, Timor-Tritsch et al. [3] described 97 low-risk patients scanned between 9 and 14 weeks using transvaginal sonography (TVS); the aim of the study was to assess at what gestational age fetal structures such as body contours, long bones, fingers, face, palate, feet, toes, and four-chamber view could consistently be imaged. The study revealed that by 13–14 weeks, all of the structures looked for could be consistently imaged (Table 19.1). Whitlow et al. [4] in 1998 performed a study to determine which was the optimal gestational age to measure the nuchal translucency and at the same time examine the fetal anatomy. They concluded that the best time is at 13 weeks of gestation. They realized that with increasing gestational age, the percentage of the cases in which anatomy could be evaluated increased from 75% at 11 weeks to 98% at 13 weeks. In addition, as gestational age increased, the need for TVS decreased from 42% at 11 weeks to 15% at 13 weeks.

In the USA, in contrast to most other countries in Europe, where ultrasounds are generally performed by dedicated physicians (sonologists), ultrasounds are carried out by sonographers (technicians). In 2004, Timor-Tritsch et al. [5] tested the ability of sonographers in the USA to perform fetal structural evaluation at 11–14 weeks. In their prospective cross-sectional study of 223 women between 11 and 13 6/7 weeks, the sonographers were asked to look for fetal structures of the head, neck, spine, heart, abdomen, chest, and extremities that targeted 37 fetal structures (Table 19.2). Cases were divided by gestational age into two groups: 11–12 weeks and 13–14 weeks. In this study, 11 structures of the head and neck were sought and similarly to other studies by 13–14 weeks greater than 80% were visualized, with rates almost reaching 100% for the calvarium, lateral ventricles, and choroid plexus. The authors concluded that anatomic survey of the fetus between 11 and 14 weeks can be performed by trained sonographers with good detection rates of most fetal structures.

Before proceeding to talking about societal guidelines pertaining to first-trimester US, it is important to make one critical point: ***Gestational age matters***! Not all structures sought during the second-trimester (18–22 weeks) scan are completely formed at 11–13 6/7 weeks, and not all

Table 19.1 List of embryonic/fetal structures and the gestational age at which they are always seen

Weeks	N	Ant & Post contours	Long bones	Fingers	Face Palate	Foot Toes	4 Chamber view
9	17	+	F&H ± T&R -	±	–	–	–
10	16	+	F&H ± T&R -	±	±	–	–
11	17	+	+	±	±	±	–
12	15	+	+	+	+	±	±
13	14	+	+	+	+	+	±
14	18	+	+	+	+	+	+

± : Threshold level (first seen)

+:

Discriminatory level (always seen)

Modified from [3]

F femur, *H* humerus, *T* tibia, *R* radius fetal structures “mature” at the same time or at the same gestational age. The fetal brain, the topic of this chapter, develops and continually changes during embryonic/fetal life as well as postnatally. Depending on the gestational age, structures may be deemed abnormal or pathologic, while in reality, they did not yet complete their development. For example, in the first trimester, a difference of 5–7 days in the gestational may lead to misdiagnosing a normally developing ventricular structure such as the rhombencephalon as ventriculomegaly or non-visualization of the falx as holoprosencephaly. Therefore, when performing a fetal anatomical survey, the American Institute of Ultrasound in Medicine (AIUM) [6] list of structures that constitutes a fetal anatomical scan at 18–20 weeks cannot be applied to the fetus at this early gestational age. In 2013, the International Society of Ultrasound in Obstetrics and Gynecology (ISUOG) published guidelines [7] as well as a list of suggested structures to be included in the first-trimester anatomical survey. More recently, in 2020, the AIUM published guidelines for the performance of the detailed first-trimester survey. This chapter reviews the anatomy of the fetal head emphasizing those structures that the AIUM considers part of the anatomy at 12–13 6/7 weeks [8].

Table 19.2 Percentage of structures seen at 11–12 weeks and 13–14 weeks by dedicated sonographers

Structure	11–12 weeks $n = 121$ (%)	13–14 weeks $n = 102$ (%)	*P* value
Head and neck			
Calvarium	120 (99)	100 (98)	NS
Intracranial anatomy	115 (95)	97 (95)	NS
Lateral ventricles	109 (99)	94 (92)	NS
Choroid plexus	118 (98)	97 (95)	NS
Cerebellum	63 (52)	70 (69)	0.01
Posterior fossa/ cisterna magna	67 (55)	73 (72)	0.01
Nuchal anatomy	115 (96)	95 (93)	NS
Lenses	106 (88)	91 (89)	NS
Profile	110 (91)	91 (89)	NS
Nose/lips	86 (71)	81 (79)	NS
Face	89 (74)	85 (83)	0.08
Spine			
Cervical	97 (80)	91 (89)	NS
Thoracic	98 (81)	89 (87)	NS
Lumbar	87 (72)	79 (77)	NS
Sacral	42 (35)	49(48)	NS
Heart			
Cardiac axis	86 (71)	75 (73)	NS
4-chamber view	33 (27)	42 (41)	0.03
RVOT	47 (39)	59 (58)	0.04
LVOT	45 (37)	62 (61)	0.0004
Aortic arch	22 (18)	31 (30)	0.03
Ductal arch	18 (15)	24 (24)	NS
Abdomen and chest			
Lungs	77 (64)	79 (77)	0.02
Diaphragm	65 (87)	94 (92)	NS
Ventral wall (cord insertion)	117 (97)	98 (96)	NS
Stomach	118 (98)	100 (98)	NS
Kidneys	97 (80)	93 (91)	0.02
Bladder	113 (03)	08 (06)	NS
Two vessels observed by the bladder	102 (84)	92 (90)	NS
Bowel	93 (77)	90 (88)	0.02
Genitalia	39 (32)	51 (50)	0.007
Extremities			
Humerus	118 (98)	98 (96)	NS
Radius/ulna	115 (95)	99 (97)	NS
Hand	118 (98)	100 (98)	NS
Fingers	104 (86)	92 (90)	NS
Femur	119 (98)	98 (96)	NS
Tibia/fibula	111 (92)	96 (94)	NS
Foot	117 (97)	95 (93)	NS

From [5]

Normal Fetal Head-Brain Anatomy

The first step in the evaluation of the anatomy of the head and brain is to perform biometry, which includes the biparietal diameter and head circumference. The fetal head or brain at 12–13 6/7 weeks can be imaged in the three “classical” planes, namely axial, sagittal, and coronal. However, at this gestational age, the axial and the sagittal planes are the most important as far as visualization of clinically useful anatomy and will be described in detail.

In the axial planes, evaluation of the fetal brain starts with the assessment of the cranium, which should be oval, intact, and echogenic or showing a normal degree of calcification. In the *axial transventricular plane*, the falx cerebri, a linear midline structure, divides the brain into the right and left hemispheres. The two sides of the falx cerebri with brightly echogenic choroid plexuses are seen within the ventricular cavity. The configuration of the falx cerebri with the paired choroid plexuses at its side has been likened to a butterfly, thus its name: the "butterfly sign." When absent, it is a powerful predictor of alobar holoprosencephaly [9]. The ventricular cavity is prominent, and in the normal setting, it contains sufficient amount of cerebrospinal fluid (CSF) to surround the choroid plexus. If the choroid plexus completely fills the ventricular cavity with minimal to no CSF seen around it, this can be an early clue to the presence of an open spina bifida and has been referred to in the literature as the "dry brain" [10]. The brain cortex at this gestational age is thin and is present just underneath the bony cranium (Fig. 19.1).

The second plane is the *axial transthalamic plane*, 1–2 mm inferior to the axial transventricular plane. In this plane, brightly echogenic choroid plexuses are seen anterior and lateral to the falx cerebri almost completely filling the anterior horns of the lateral ventricle. The additional structures seen in this plane are the thalami, the third ventricle, the cerebral peduncles, and the aqueduct of Sylvius. The thalami are paired structures located in the central aspect of the brain; the third ventricle is present in the midline. Sonographically, the third ventricle appears as an anechoic elliptical fluid-filled structure between the thalami. Posteriorly, the cerebral peduncles are seen flanking a rectangular anechoic fluid-filled structure, the aqueduct of Sylvius (Fig. 19.2a, b). The mesencephalon appears as a smooth rounded structure beyond the aqueduct of Sylvius. The arachnoid space is imaged between the mesencephalon and the occipital bone (Fig. 19.2c, d). An interesting feature has been described in cases of open spina bifida. This occurs when the mesencephalon changes its shape as the result of the reduced intracranial pressure. The end result is that the mesencephalon appears boxlike against the occipital bone and the normal subarachnoid space is no longer apparent, creating the appearance of the mesencephalon "crashing" against the occipital bone, hence the name "crash sign" [11].

The third plane is a small modification of the axial plane in which it is slightly tilted posterior to reveal the posterior fossa. It is called the *transcerebellar plane* and is 1–2 mm inferior to the transthalamic plane. Similarly to the transthalamic plane, a brightly echogenic choroid plexus is seen anterior and lateral to the falx cerebri almost completely filling the anterior horns of the

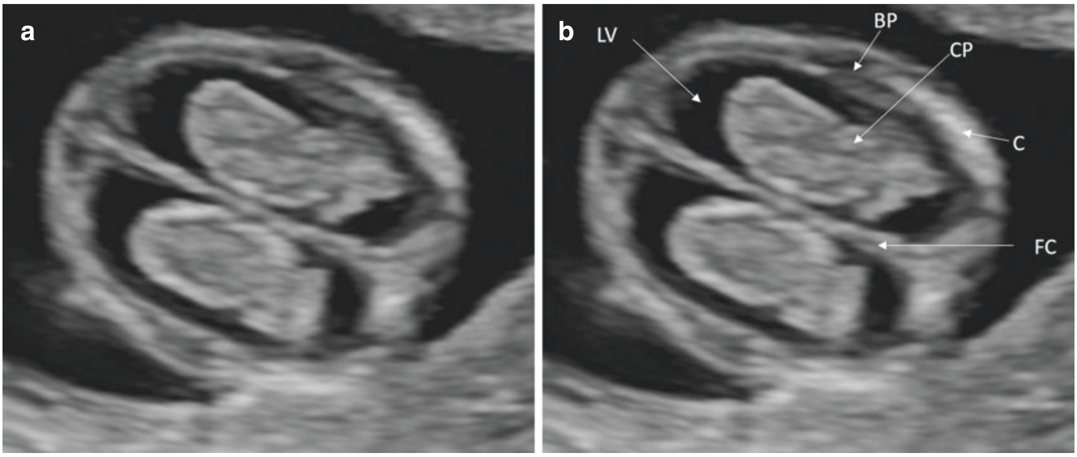

Fig. 19.1 Transventricular plane. (**a**) Displays the anatomic features of this plane, namely the intact cranium (c) surrounding the brain, the cavity of the lateral ventricle (LV); the echogenic choroid plexus (CP) is seen flanking the falx cerebri (FC). (**b**) The anatomic structures are labelled

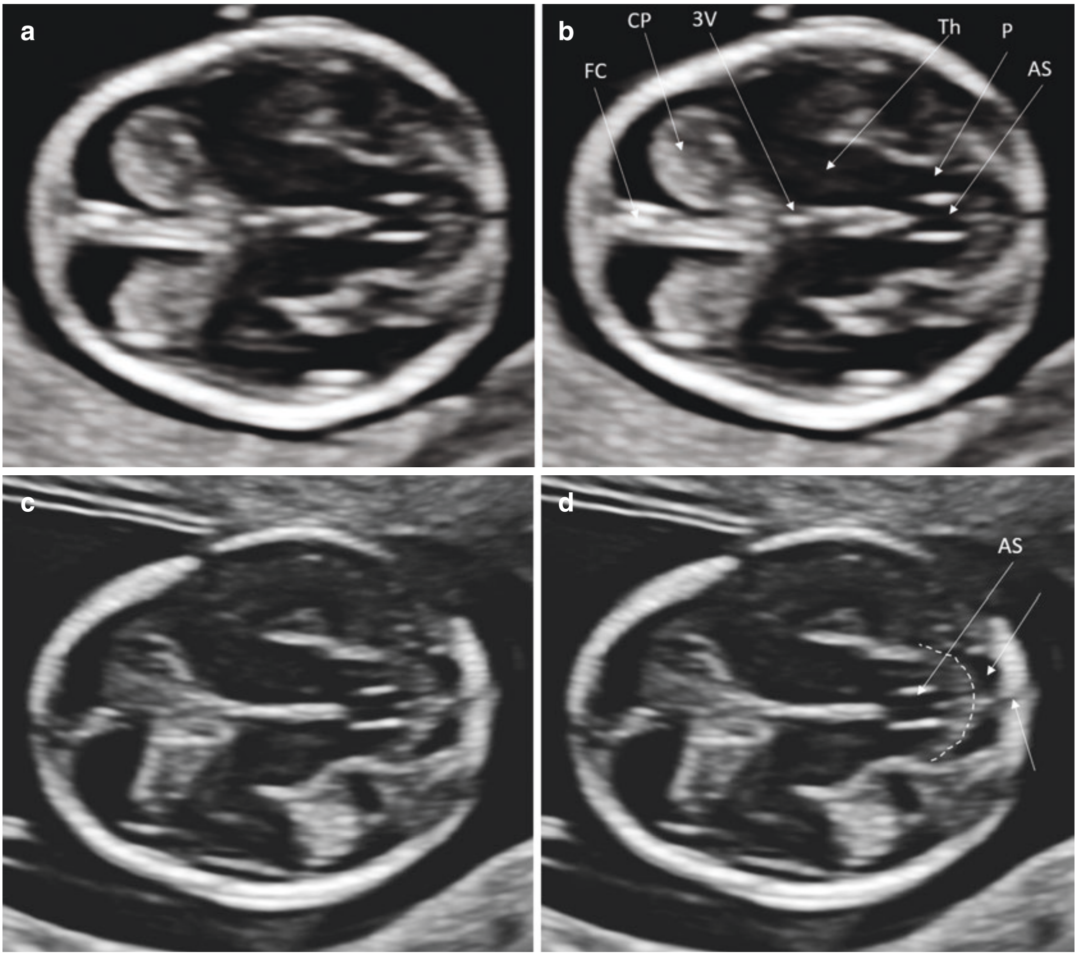

Fig. 19.2 Transthalamic plane. (**a**, **b**) In this plane, the falx cerebri (FC) falx cerebri (FC) is seen dividing the brain into the right and left hemispheres; the brightly echogenic choroid plexuses (CP) are almost filling the cavity of the lateral ventricle; the thalami (Th) are a paired structure in the center where the third ventricle (3V) is located; and moving posteriorly, the aqueduct of Sylvius (AS) has a rectangular shape... (**c**, **d**) The anatomic structures are at a slightly different angle (tilted posterior) than a, b. In this picture, the mesencephalon is outlined by the dashed line; between the occipital bone (OB) and the mesencephalon (dashed line), the subarachnoid (SA) space is seen

lateral ventricles. In this view, the thalami are seen extending to and eventually connecting to the cerebellar peduncles and ultimately joining the cerebellum. The cerebellum had an oval shape and beyond it is the fluid-filled cisterna magna (Fig. 19.3).

Turning the US probe 90° from the axial planes, the sagittal planes can be obtained. Many such planes can be generated by moving the transducer from side to side. Maybe the most important and revealing is the median plane or midsagittal plane. The median plane is a vital view during the evaluation of the brain at this gestational age. Most maternal-fetal-medicine specialists, as well as sonographers and sonologists, are familiar with this view, since this is the view in which the nuchal translucency (NT) is measured and the presence of the nasal bone is evaluated.

In the *median plane*, the brightly echogenic cranium should be seen surrounding the normal fetal brain structures. Evaluating the intracranial anatomy from the anterior to posterior, the following structures are seen: the brain parenchyma

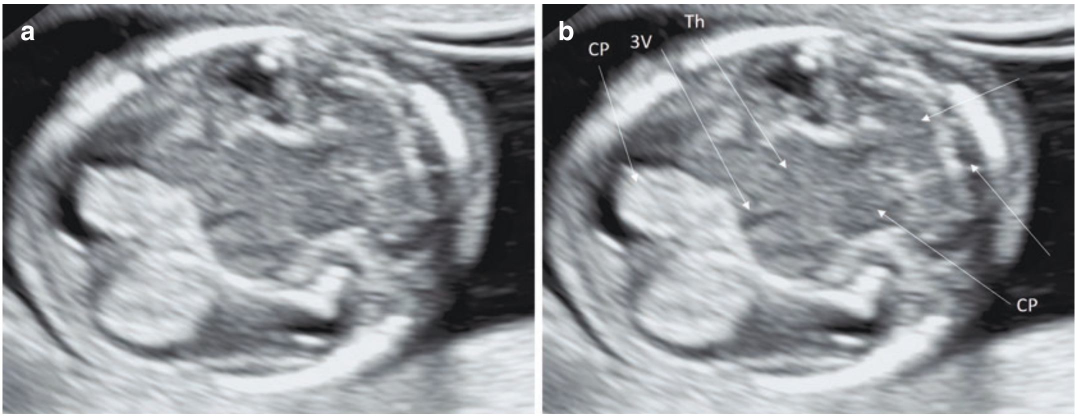

Fig. 19.3 Transcerebellar plane obtained by transvaginal sonography. (**a**) In this plane, the brightly echogenic choroid plexus (CP) is seen anteriorly within the anterior horns of the lateral ventricle; moving posteriorly, the paired thalami (Th) are seen in the center where an anechoic linear structure is seen; this represents the third ventricle (3V); moving posteriorly, the cerebral peduncles (CP) are seen reaching the cerebellum (c); the cisterna magna (CM) is seen between the cerebellum and the brightly echogenic cranium. (**b**) The anatomic structures are labelled

which is thin and just below the cranium, the anterior horns of the lateral ventricles which appear as prominent anechoic spaces, and the brightly echogenic choroid plexuses extending into the frontal horns. Slightly more posterior and below the choroid plexus, in the center of the brain, the thalamus is seen as a hypoechoic area extending into the midbrain and eventually into the brain stem (Fig. 19.4).

The posterior fossa at this gestational age appears to contain three anechoic areas, namely the brain stem, the fourth ventricle (also known as the intracranial translucency or IT), and the cisterna magna. The first and the widest is the brain stem (BS), while the fourth ventricle is posterior. The brightly echogenic choroid plexus (CP) of this ventricle is seen inferiorly, and slightly more posterior to the CP is the anechoic cerebello-peduncular cistern also known as the cisterna magna (CM) (Fig. 19.4). Posterior to the CM is the echogenic occipital bone. The fourth ventricle is slightly wider than the cisterna magna at this gestational age in this plane. Visualization of only one of these three anechoic spaces, mostly the brain stem, has been reported as a “clue” for the presence of open spina bifida. Other studies have reported screening for open spina bifida in the first trimester [10–12]. Lachman et al., in their initial report, described the diameter of the brain stem (BS) as well as that of the brain stem to occipital bone (BSOB) diameter in 30 fetuses with open spina bifida and in 1000 normal fetuses [12]. In the group of normal fetuses, the BS diameter and the BSOB diameter increased as the crown rump length (CRL) increased; therefore, their ratio decreased. In the group of fetuses with open spina bifida, the mean brain stem (BS) diameter is significantly increased while the mean BSOB diameter is significantly decreased; therefore, their ratio is increased. The BS/BSOB ratio >1 has been described as a consistent marker of open spina bifida at 11–13 6/7 weeks [13]. This is the result of posterior displacement of the brain stem and compression of the cisterna magna and fourth ventricle within the restricted space of the bony calvarium secondary to the open spina bifida.

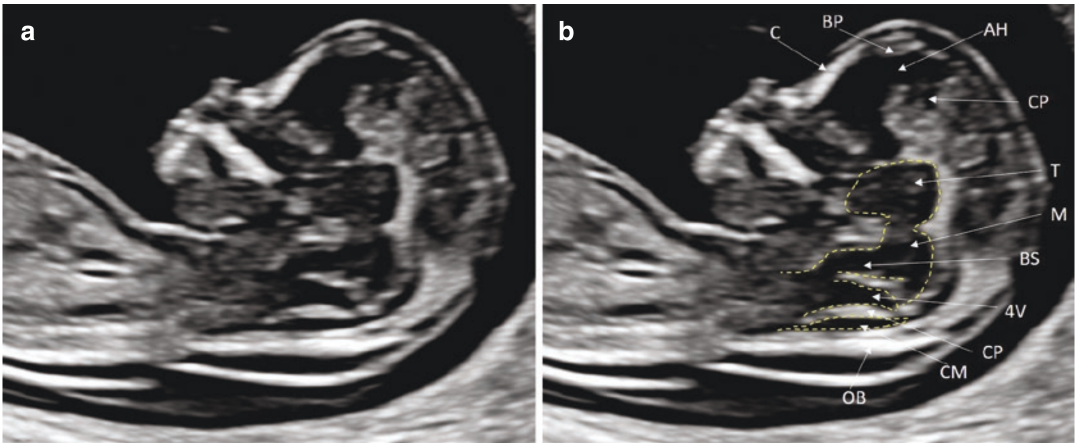

Fig. 19.4 Median (midsagittal) plane. (**a**) Starting anteriorly and moving posteriorly, the echogenic cranium (c) is seen surrounding the brain; the brain parenchyma (BP) is imaged as a thin layer just behind the cranium; the anterior horns (AH) of the lateral ventricles are prominent and the choroid plexus (CP) is seen extending into this cavity; moving posteriorly in the center of the brain is the anechoic thalamus (Th); this continues posteriorly as the mesencephalon (M) and eventually as the brain stem (BS); other structures seen in the posterior fossa are the anechoic fourth ventricle (4V), also known as the intracranial translucency; the choroid plexus (CP) of the fourth ventricle is imaged as a brightly echogenic linear structure between the fourth ventricle and the anechoic cisterna magna (CM); lastly, the occipital bone (OB) is seen as a brightly echogenic structure which is part of the cranium surrounding the brain. The dashed line outlines the thalamus, mesencephalon, brain stem, fourth ventricle, and cisterna magna. (**b**) The anatomic structures are labelled

Pathologies of the First-Trimester Fetal Brain

During the first trimester, there are few head-brain anomalies that lend themselves to prenatal diagnosis. These anomalies are typically severe and at times lethal. Brain anomalies that are easily diagnosed during the first trimester of the fetal brain will be discussed. Of note, when discussing the fetal brain, the face and spine need to be included.[1] Therefore, a few anomalies involving these two organs will be included in this text.

Neural Tube Defects

Exencephaly-Anencephaly Sequence

Brain anomalies that result from failure or abnormal closure of the anterior cranial neuropore at around 26–32 days postconception result in cerebral, spinal, or combined cerebral and spinal defects or dysraphia. Among these, exencephaly-anencephaly sequence, cephaloceles, and spina bifida are the most common defects with a reported prevalence of 1/1000 pregnancies [14].

The exencephaly-anencephaly sequence is a lethal malformation. In exencephaly, the typical sonographic feature is acrania, in which a relatively well-formed brain is seen without the covering of fetal cranium (Fig. 19.5). As the pregnancy continues, the exposed fetal brain begins to disintegrate eventually resulting in the typical sonographic features of anencephaly, in which the cranium is absent and the fetal orbits are prominent. Increasing the US gain, the amniotic fluid appears speckled as the result of the sloughing off of the exposed brain tissue (Fig. 19.6) [15]. Reported detection rates at 11–13 6/7 weeks are 100% [16, 17].

Cephalocele

Cephalocele is a cranial defect occurring along the bony sutures, through which brain and/or meninges or a combination of both herniates is thought to occur as a result of faulty cranial mesoderm development. Recent theories suggest

---

[1] See Chaps. 20 and 23.

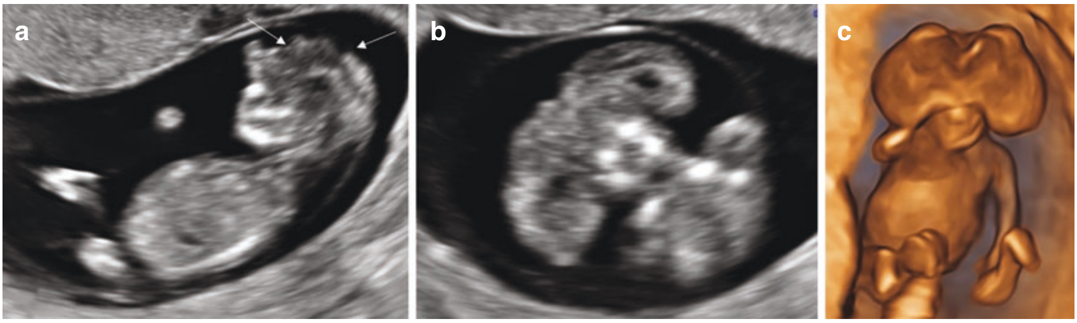

Fig. 19.5 Exencephaly-anencephaly sequence. (**a**) Sagittal view: the normal echogenic fetal calvarium encasing the brain is not seen; instead, the head appears "flat" and irregular. (**b**) Coronal view of the fetal head depicting a significant amount of brain tissue that has "fallen" to the side of the head since it is not confined by the calvarium. (**c**) 3D reconstruction of the fetus demonstrating exencephaly (arrow: abnormal head with absent calvarium)

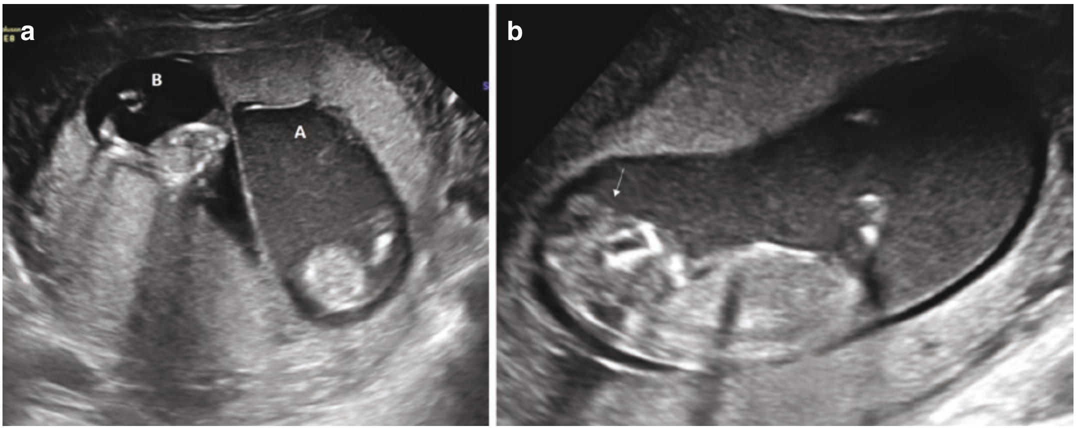

Fig. 19.6 Dichorionic-diamniotic twins with discordant brain anomaly. Twin A has exencephaly-anencephaly sequence, while B is normal. (**a**) The amniotic fluid of twin A contains low-level speckled fluid when compared to the anechoic amniotic fluid of twin B. (**b**) Twin A has the typical features of the exencephaly-anencephaly sequence; the head appears irregular and lacks the typical sonographic appearance of the smooth and regular echogenic calvarium (arrow)

that cephalocele is developmentally and genetically different from exencephaly-anencephaly sequence and should not be considered a neural tube defect [14]. Studies on posterior cephalocele occurring in fetuses with Meckel syndrome have found a relationship with ciliopathy syndromes [14]. Sonographic features are saclike structures posterior to the head in cases of posterior cephalocele or anterior by the fetal face in cases of an anterior cephalocele (Fig. 19.7). The size range of cephaloceles may be wide from very small to very large ones. They may contain only meninges (meningocele) or brain tissue (meningomyelocele). The larger the cephalocele, the more brain tissue it contains, and the worse is the prognosis for the fetus. Microcephaly may be seen in as many as 20–25% of the cases. Reported detection rates at 11–13 6/7 weeks are 100% [16].

Open Spina Bifida

The spine, similarly to the face, is part of the neuro-evaluation of the fetus. At 11–13 6/7 weeks, the fetal spine can be assessed in the sagittal, coronal, and axial planes in a similar fashion as it is routinely performed later during the second-trimester anatomical survey. In the second trimester, the diagnosis of open spina bifida relies on several sonographic markers: (1) the presence of bulges or irregularities of the spine; (2) two established and sensitive cranial findings: the "lemon" and "banana sign." *Open spina bifida* can be diagnosed at 11–13 6/7 weeks or earlier by observing a bulge or disruption of the bony spine and skin in the sagittal plane (Fig. 19.8a, b) [18, 19]. The sonographic detection of the "banana and lemon" sign has been reported in fetuses after the 12th week of pregnancy [18, 20]. In pregnancies 12 weeks or less, the cerebellum may just appear in a slightly convex shape, assuming the typical appearance of the "banana sign" which can be consistently demonstrated after the 12th week [20]. Recent research in this area has resulted in several additional cranial sonographic findings that have been developed specifically to screen fetuses at 11–13 6/7 weeks for open spina bifida. The signs include non-visualization of the intracranial translucency (IT) [10], increasing brain stem diameter to brain stem-to-occipital bone distance (BS/BSOB) [12], and a cisterna magna width <5th percentile [21] (Fig. 19.8c); the previously mentioned "crash sign" in which, due to the spinal defect, the mesencephalon at the level of the transthalamic plane becomes boxlike, the subarachnoid is no longer

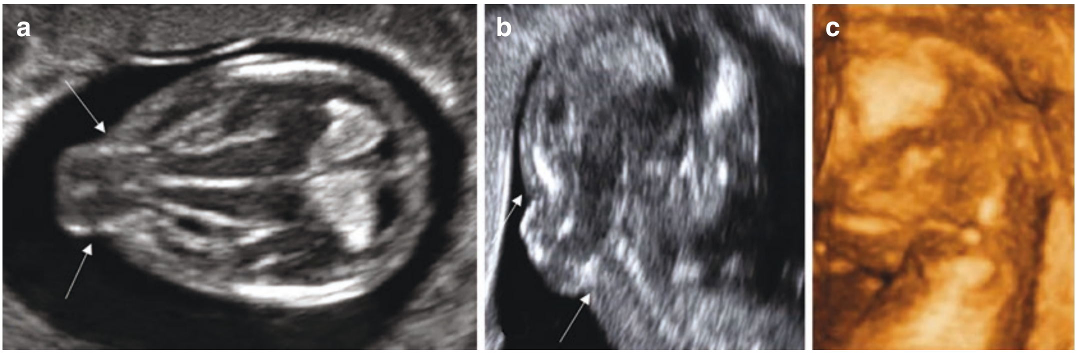

Fig. 19.7 Posterior cephalocele. (**a**) Axial section of the fetal head demonstrating the posterior cranial defect through which brain has herniated into the posterior cephalocele sac (arrows). (**b**) Sagittal view of the fetal head demonstrating the posterior cranial defect, the cephalocele sac with the brain and midbrain herniating into the sac (arrow). (**c**) 3D reconstruction of the cephalocele

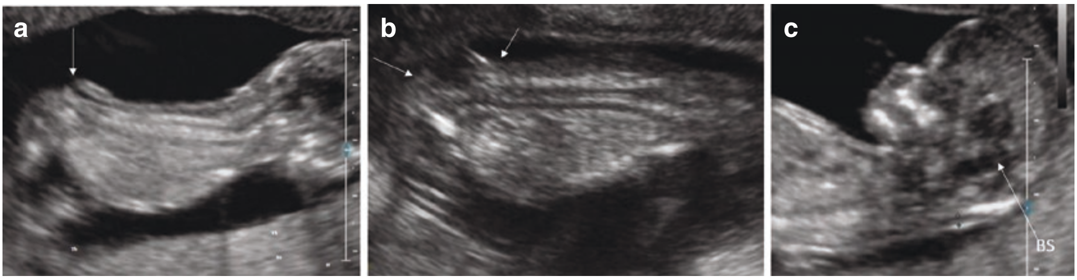

Fig. 19.8 Sagittal image of the fetal spine at 12 3/7 weeks with a lumbosacral open spina bifida. This finding was confirmed during subsequent studies as well as postnatally. (**a**) The lumbosacral spinal defect is seen at the arrow. (**b**) Sagittal view slightly off the midline demonstrating the myelomeningocele sac as well as the defect of the vertebral bodies (arrows). (**c**) Sagittal view of the fetal head demonstrating only one of the three spaces of the posterior fossa. The arrow points to the prominent brain stem (BS) with no visualization of the fourth ventricle (intracranial) translucency

seen and therefore the mesencephalon appears to "crash" into the occipital bone, comparable to a car crashing into a wall [11]; the mentioned "dry brain" sign, in which the choroid plexuses appear to almost completely fill the ventricular cavity in the axial transventricular plane [10]; and in the axial transthalamic plane, the biparietal diameter (BPD) measurement of <5th centile [22, 23] and biparietal-to-transverse abdominal diameter ratio of ≤1 (BPD/TA) [24]. Fetuses that "screen positive" for these new cranial sonographic markers should be referred to centers with expertise in scanning the early pregnancy. At present, there is limited data regarding the performance of these new cranial signs for the detection of open spina bifida.

Midline Developmental Anomalies

Holoprosencephaly

During normal fetal development, the falx cerebri, a midline structure that separates the single cavity of the forebrain into two hemispheres, should be seen after 9–10 weeks in all normal brains. Lack of visualization of the falx cerebri is consistent with holoprosencephaly (HPE). Holoprosencephaly (HPE) is a common malformation involving the forebrain, resulting from complete or incomplete failure of the forebrain to separate during the second to the third week postconception [25–27]. The prevalence of holoprosencephaly at 11–13 6/7 weeks has been reported as 1:1300 pregnancies, with approximately 66% having a chromosomal abnormality of which 86% have trisomy 13 and 4% trisomy 18 [28]. This anomaly has a spectrum ranging from the most severe alobar HPE to semilobar HPE and to lobar HPE and the least severe middle interhemispheric variant (MIHV). In approximately 80% of individuals affected with HPE [6], a craniofacial anomaly is also present [25]. The craniofacial anomalies range from cyclopia (single midline eye), synophthalmia (partial midline face fusion of the two eyes), and a proboscis (nasal appendage with a single nostril located above the eyes) [26]. During the first trimester, most of the diagnosed cases of HPE are alobar, although the semilobar type can also be appreciated, presenting a challenging task. Three-dimensional inversion rendering can be used to differentiate between a normal brain and HPE; this can be used as an additional tool in the diagnosis of HPE in the first trimester [29] (Fig. 19.9). Lobar HPE, which is a more subtle malformation and depends upon the appearance of the cava, is diagnosed at or after the 18–20-week anatomy scan. Most fetuses affected by HPE do not survive. Detection rates of 50–100% have been reported [16, 17].

In the normal first-trimester brain, as discussed above, the choroid plexuses are seen on each side of the midline falx; this configuration has been likened to a butterfly with the wings open [30], hence the "butterfly sign." Sepulveda and Wong [9] screened 11,068 live fetuses for HPE over a 9-year period using the "butterfly sign." Among this cohort, they diagnosed 11 cases of HPE, which demonstrated lack of visualization of the normal "butterfly sign." Detection rate of HPE using the absence of this sign was 100%. In addition, they noted that 40% had a biparietal diameter less than the 5th centile, which further aided in the diagnosis (Fig. 19.10).

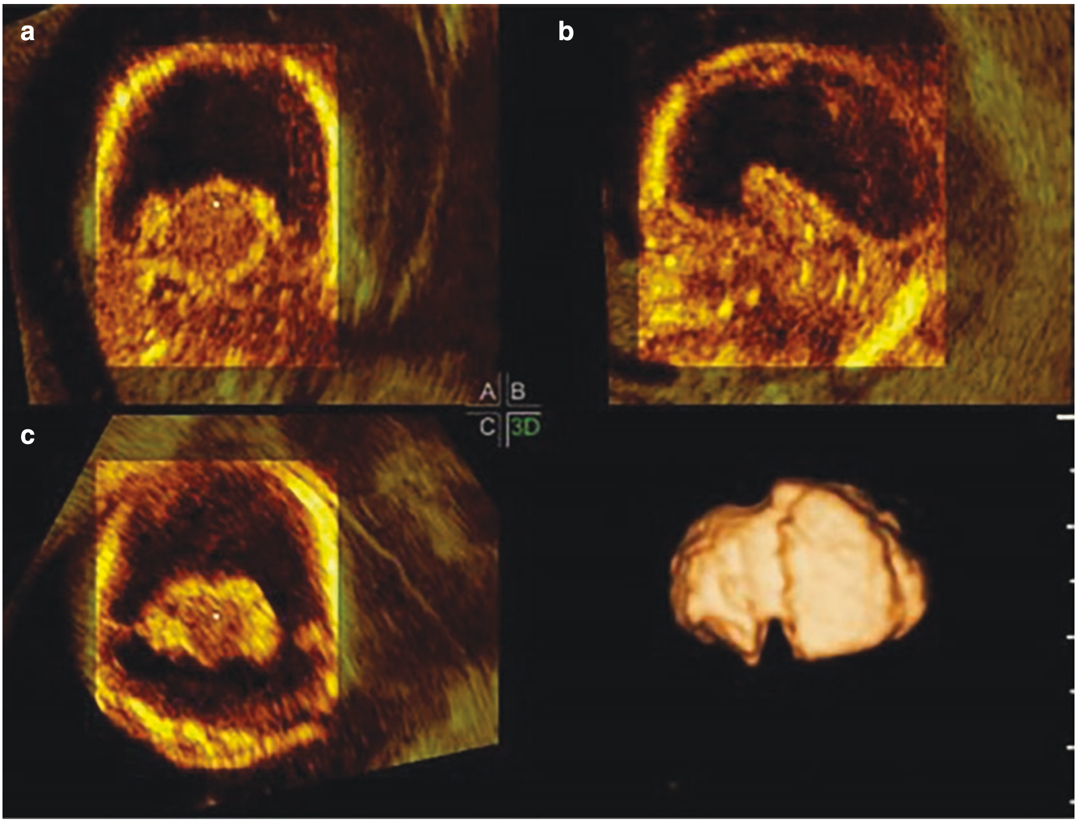

Fig. 19.9 The three orthogonal planes (axial, coronal, and sagittal) as well as the inversion mode are displayed from a 3D volume of a fetus with alobar holoprosencephaly. (**a**) Coronal section showing the single or "mono" ventricle; absence of midline structures and fused thalami. (**b**) Sagittal view of the fetus; the face is facing the left side of the picture; the head contains fluid. (**c**) Axial section showing similar features described in (**a**). (**d**) depicts the inverted 3D image of the fluid contained within the single brain ventricle

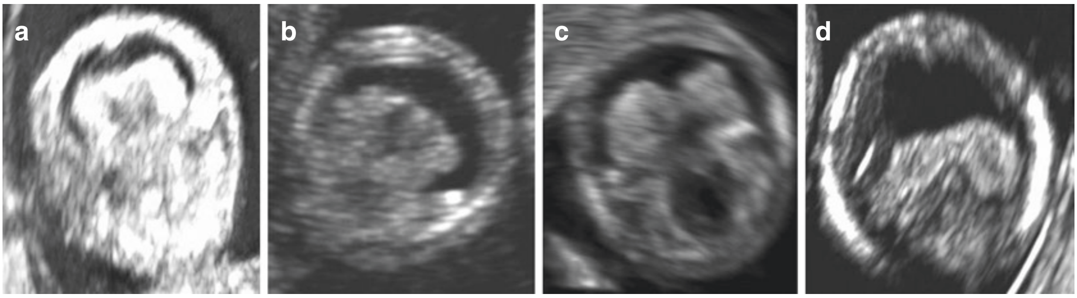

Fig. 19.10 A composite image of four cases of holoprosencephaly. (**a**) Fetus with HPE at 9 6/7 weeks; (**b**) fetus with HPE at 11 4/7 weeks; (**c**) fetus with HPE at 12 1/7 weeks; (**d**) fetus with HPE at 13 2/7 weeks. The common sonographic feature of all four fetuses with holoprosencephaly imaged in an axial view is the absent falx; single ventricular cavity; choroid plexus superior to the fused thalami; and absence of the normal "butterfly" appearance of the choroid plexus with the falx in the axial view

The Face[2]

Absent Nasal Bone, Cleft Lip ± Palate, Cataracts, Micrognathia

Evaluation of the face is part of the evaluation of the fetal brain, since the brain and facial anomalies may be present simultaneously, as is the case in holoprosencephaly. In the first trimester, similarly to the traditional second-trimester anatomical survey, a profile view of the face should be obtained. This may reveal an absent or hypoplastic nasal bone, a cleft lip and/or palate, micrognathia, or other anomalies.

Absent nasal bone is not considered a fetal malformation per se; however, it is a marker of fetal aneuploidy, specifically of the common trisomies (Fig. 19.11). The nasal bones are actually paired structures; there is a right and a left nasal bone, and there can be unilateral as well as bilateral absence or hypoplasia. Absent nasal bone is seen in 60% of fetuses with trisomy 21; its absence confers a likelihood ratio of 27.8 for Down syndrome. It is also found in 53% of trisomy 18 and in 45% of trisomy 13; furthermore, it can be seen in 2.5% of euploid fetuses [31]. Among euploid pregnancies, absent nasal bone is seen more frequently in African American women (5.8%) than in white women (2.6%) or Asian women (2.1%) [32]. In a recent publication among 57 fetuses with absent nasal bone and normal karyotype, three fetuses had an adverse outcome and in all additional sonographic abnormalities were seen [32].

Cleft lip and/or palate (CLP) is a common facial anomaly with a reported incidence of 1.7 per 1000 live births; however, ethnic and geographic variations exist [33]. In up to 80% of the cases, cleft lip is unilateral, typically affecting the left side, and most of the affected fetuses are male. However, isolated cleft palate is more commonly seen in females with a reported incidence of 1 in 2500 live births [33]. During development, a continuous upper lip is formed by 8 weeks when the medial nasal and maxillary processes fuse. Failure of fusion of the medial nasal and maxillary processes will result in a cleft lip affecting one or both sides. The palate develops from the primary and the secondary palate. Its development starts at 7 weeks but is not complete until 14th week. At 11–13 6/7 weeks, a sagittal, coronal, and axial view using 2D and 3D sonography can detect a CLP (Fig. 19.11). In cases of bilateral cleft lip and palate, a protuberance is seen anterior to the lips in the sagittal plane; in the axial plane, the cleft lip and palate can be seen as a deep indentation. Three-dimensional US, specifically 3D reconstruction of the face using the coronal plane, can help in evaluating the facial defects (Fig. 19.12d). Detection rates of CLP in the first trimester are low ranging from 5% to 50% [16, 17]. The retronasal triangle can be imaged using 2D or 3D sonography by obtaining an anterior coronal view of the fetal face. The apex of the retronasal triangle is made up of the two nasal bones, the sides are the frontal process of the maxilla, and the base of the triangle is the primary palate [34]. In cases of CLP, a defect can be imaged at the base of the triangle at the site of the palate. The retronasal triangle view likely can improve the detection and diagnostic rates of CLP; however, no large prospective studies looking at the efficacy of the retronasal triangle are available to date; furthermore, this view has recently been reported as a new way to evaluate the presence or the absence of the nasal bones [34–36] (Fig. 19.13). Three-dimensional US of the face can demonstrate that there are two nasal bones; therefore, it may, at times, reveal the absence of one of these small bones.

Cataracts. Their reported incidence is 1–6/10,000 births [37]. The fetal lens develops from the surface ectoderm before the sixth week of gestation [37]. Fetal cataracts may be the result of a very early in utero fetal infection, such as rubella, varicella, herpes, and CMV, or exposure to a toxin (anti-epileptic drugs such as carbamazepine), idiopathic or genetic. A genetic cause is seen in 30% of unilateral cases and in 50% of bilateral cases [37]; genetic causes include syndromes such as Walker-Warburg syndrome and karyotypic abnormalities such as trisomies 21, 18, and 13. The normal sonographic appearance

---

[2] See Chap. 20.

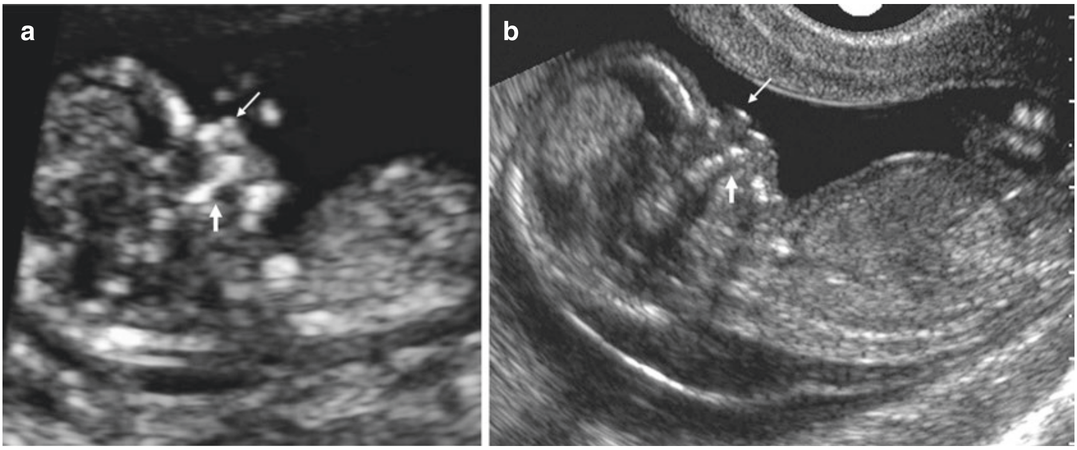

Fig. 19.11 Two fetuses are seen, one with a normal and the other with absent nasal bone and cystic hygroma. To image the nasal bone or its absence is important to obtain the correct sagittal scanning plane of the face which shows the tip of the nose (long arrow) and the palate (short arrow). (**a**) Fetus at 12 1/7 weeks with a normal-appearing nasal bone and palate. (**b**) Fetus with absent nasal bone and the palate shows the mandibular gap (arrow) suggestive of a cleft palate at 13 6/7 weeks

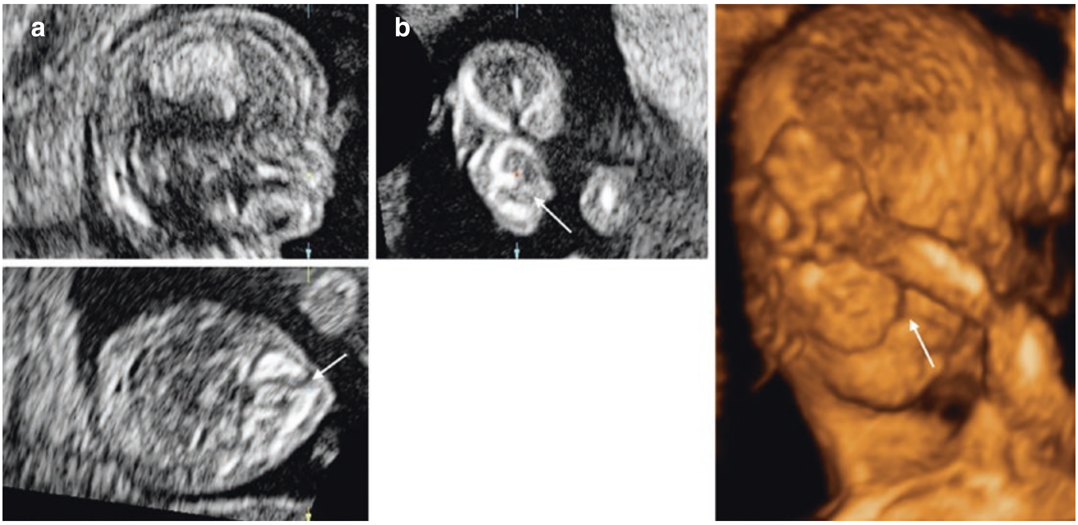

Fig. 19.12 Fetus with unilateral left-sided cleft lip and palate at 12 5/7 weeks. (**a**–**c**) display the 3D orthogonal planes of the same fetus. (**a**) A sagittal view of the face; (**b**) a coronal section showing the abnormal retronasal triangle with a gap at the area of the left side of the palate (arrow); (**c**) the axial section; arrow points to defect. (**d**) 3D reconstruction of the fetus with the unilateral cleft lip and palate (arrow)

of the fetal lens is that of a ring with an anechoic center and an outer echogenic rim (Fig. 19.14a). At times, the hyaloid artery can be seen as a linear structure between the posterior aspect of the lens and the optic disc; however, the hyaloid artery typically regresses before birth. In fetal cataracts, there is opacification of the anechoic center core of the lens; at times in conjunction with cataracts, there may be reduction in the size of the fetal eyes [38] (Fig. 19.14b).

The mandibular process forms the lower jaw, lip, and chin at around 8–12 weeks, with final fusion of all of the parts that will form the mandible, and completes by 13 weeks of pregnancy.

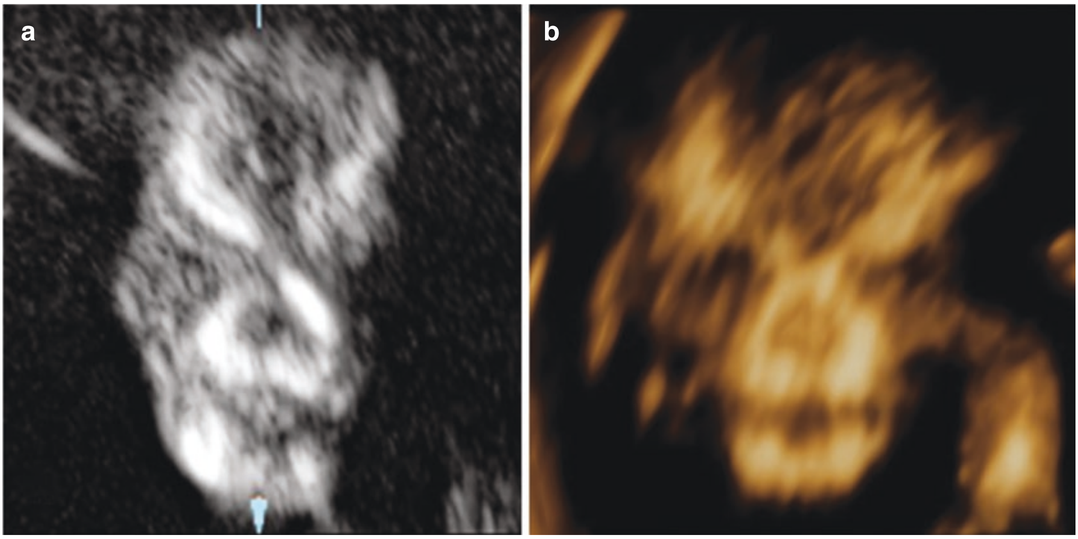

Fig. 19.13 The normal retronasal triangle is demonstrated. (**a**) using 2D; (**b**) using 3D thick slice

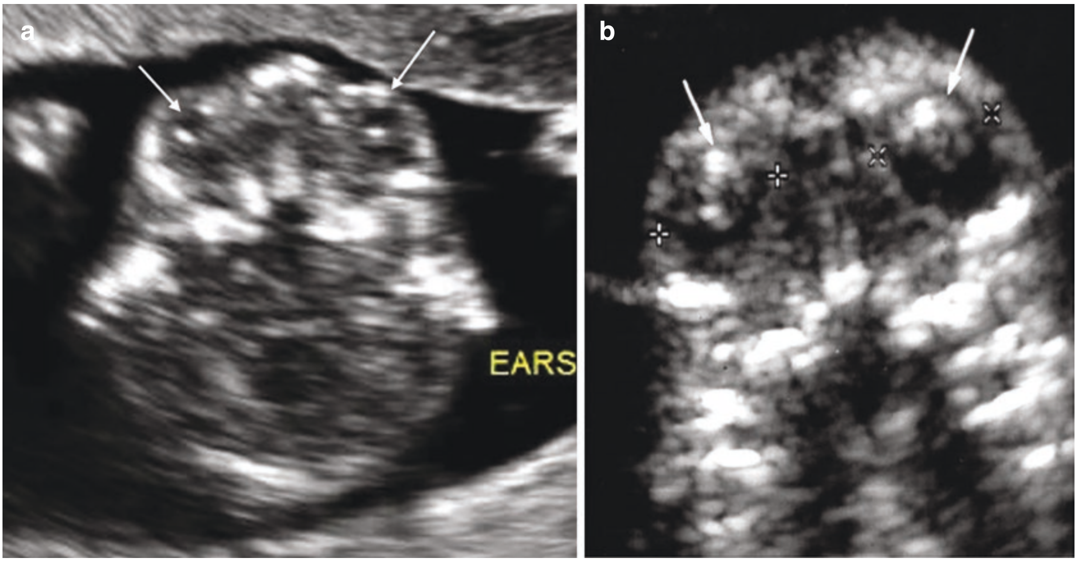

Fig. 19.14 Axial section of the fetal face at the level of the fetal orbits. (**a**) A fetus within normal lenses. The sonographic appearance of a normal lens is that of an echoic ring with a central sonolucency (arrows). (**b**) Axial section of a fetus with autosomal dominant cataracts at 12 5/7 weeks within the normal orbits; the ringlike appearance of the lens is lost and replaced by a ring filled with a central echogenic material, the cataract (arrows)

Normal development of the mandible can be disrupted as the result of genetic syndromes or environmental exposures [39]. *Micrognathia* is a common feature of over 100 genetic conditions such as Treacher Collins, Pierre Robin sequence, fetal akinesia syndrome, and chromosomal aneuploidy such as trisomies 18 and 13 as well as microdeletion syndromes [39, 40]. As stated by Paladini in 2010 [39], fetal micrognathia is almost always an ominous finding; therefore, when seen, a detailed workup is essential. Using 2D and 3D US, the normal fetal mandible can be

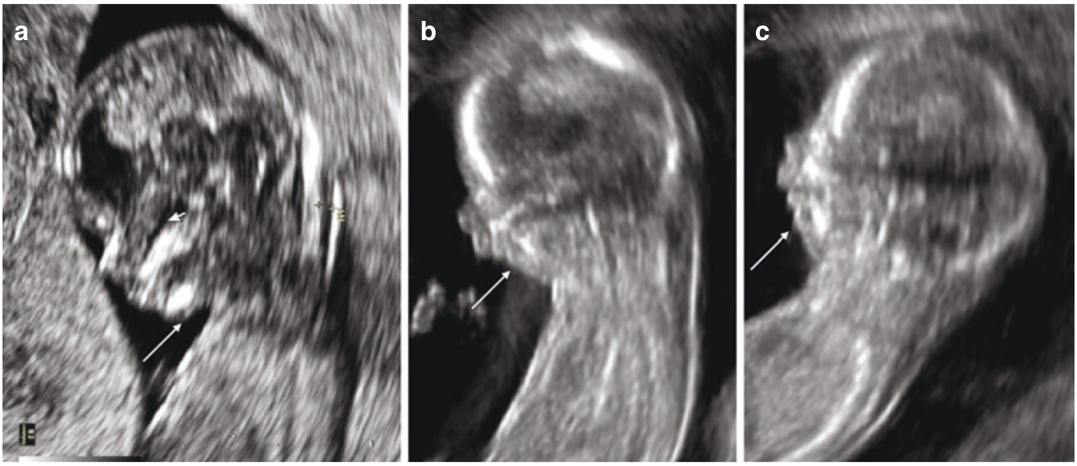

Fig. 19.15 Sagittal view of the fetal profile. (**a**) Normal fetal profile and mandible. (**b**, **c**) are slightly different views of the profile of a 13 6/7-week fetus with micrognathia (arrow) and a thick NT. The fetus was a carrier of an unbalanced deletion

imaged in the sagittal plane when obtaining the profile, in an axial view at the level of the mandible, or as part of the 3D image of the face (Fig. 19.15a). The diagnosis of micrognathia can rely on subjective or objective methods such as the jaw index and inferior facial angle. When applying these indexes to fetuses at 11–13 6/7 weeks, it is important to remember that they were developed based on fetuses at 18–20 weeks and have not been validated to be used at earlier gestational age [39, 40] (Fig. 19.15b, c).

Conclusion

In this chapter, the normal anatomy of the first-trimester fetal brain was reviewed using the axial planes as well as the median or midline sagittal plane. Illustrative pathologies were presented. In 2014, a consensus statement on fetal imaging was published [41]. This statement proceeded to say that "Offering first-trimester screening for aneuploidy assessment at 11 weeks to 13 6/7 weeks of gestation is recommended by the American College of Obstetricians and Gynecologists. If a late first trimester ultrasonography is performed for dating or nuchal translucency assessment, evaluation for early detection of severe fetal anomalies such as anencephaly and limb-body wall complex is reasonable. In some experienced centers, detection of other major fetal anomalies in the first trimester is possible" [41]. This statement brought to the forefront the fact that fetal anomalies can be detected in the first trimester.

The goal of this chapter was to further raise awareness and to promote the reality that first-trimester evaluation of the head, brain, and spine and detection of their anomalies are feasible and should be strongly considered even in the era of increasing use of noninvasive prenatal diagnosis. It is important to realize that a significant number of fetal anomalies can be reliably diagnosed. The most important information is that diagnosis of lethal and major anomalies has very high detection rates, and in some studies, this number is as high as 100% for anomalies such as exencephaly-anencephaly sequence, cephalocele, and holoprosencephaly. It is important to note that first-trimester detection of anomalies of the head, brain, and spine should become increasingly used in the realm of prenatal diagnosis and fetal ultrasound. "*Search for fetal anomalies and you shall find them.*"

Teaching Points

- Transabdominal and transvaginal grayscale sonography allows meaningful visualization of the normal fetal brain anatomy.
- The detection of fetal brain anomalies in the first trimester is possible.
- If targeted neuroscan is applied, detection rates of fetal brain anomalies are as high as 80%.

References

1. Bromley B, Shipp TD, Lyons J, Navathe RS, Groszmann Y, Benacerraf BR. Detection of fetal structural anomalies in a basic first-trimester screening program for aneuploidy. J Ultrasound Med. 2014;33(10):1737–45.
2. Becker R, Wegner RD. Detailed screening for fetal anomalies and cardiac defects at the 11–13-week scan. Ultrasound Obstet Gynecol. 2006;27(6):613–8.
3. Timor-Tritsch IE, Monteagudo A, Peisner DB. High-frequency transvaginal sonographic examination for the potential malformation assessment of the 9-week to 14-week fetus. J Clin Ultrasound. 1992;20(4):231–8.
4. Whitlow BJ, Economides DL. The optimal gestational age to examine fetal anatomy and measure nuchal translucency in the first trimester. Ultrasound Obstet Gynecol. 1998;11(4):258–61.
5. Timor-Tritsch IE, Bashiri A, Monteagudo A, Arslan AA. Qualified and trained sonographers in the US can perform early fetal anatomy scans between 11 and 14 weeks. Am J Obstet Gynecol. 2004;191(4):1247–52.
6. American Institute of Ultrasound in Medicine. AIUM practice guideline for the performance of obstetric ultrasound examinations. J Ultrasound Med. 2013;32(6):1083–101.
7. Salomon LJ, Alfirevic Z, Bilardo CM, Chalouhi GE, Ghi T, Kagan KO, et al. ISUOG practice guidelines: performance of first-trimester fetal ultrasound scan. Ultrasound Obstet Gynecol. 2013;41(1):102–13.
8. AIUM practice parameter for the performance of detailed diagnostic obstetric ultrasound examinations between 12 weeks 0 days and 13 weeks 6 days. J Ultrasound Med. 2021;40(5):E1–16.
9. Sepulveda W, Wong AE. First trimester screening for holoprosencephaly with choroid plexus morphology ('butterfly' sign) and biparietal diameter. Prenat Diagn. 2013;33(13):1233–7.
10. Chaoui R, Benoit B, Mitkowska-Wozniak H, Heling KS, Nicolaides KH. Assessment of intracranial translucency (IT) in the detection of spina bifida at the 11–13-week scan. Ultrasound Obstet Gynecol. 2009;34(3):249–52.
11. Ushakov F, Sacco A, Andreeva E, Tudorache S, Everett T, David AL, et al. Crash sign: new first-trimester sonographic marker of spina bifida. Ultrasound Obstet Gynecol. 2019;54(6):740–5.
12. Lachmann R, Chaoui R, Moratalla J, Picciarelli G, Nicolaides KH. Posterior brain in fetuses with open spina bifida at 11 to 13 weeks. Prenat Diagn. 2011;31(1):103–6.
13. Chaoui R, Benoit B, Entezami M, Frenzel W, Heling KS, Ladendorf B, et al. Ratio of fetal choroid plexus to head size: simple sonographic marker of open spina bifida at 11–13 weeks' gestation. Ultrasound Obstet Gynecol. 2020;55(1):81–6.
14. Copp AJ, Greene ND. Neural tube defects—disorders of neurulation and related embryonic processes. Wiley Interdiscip Rev Dev Biol. 2013;2(2):213–27.
15. Timor-Tritsch IE, Greenebaum E, Monteagudo A, Baxi L. Exencephaly-anencephaly sequence: proof by ultrasound imaging and amniotic fluid cytology. J Matern Fetal Med. 1996;5(4):182–5.
16. Rossi AC, Prefumo F. Accuracy of ultrasonography at 11–14 weeks of gestation for detection of fetal structural anomalies: a systematic review. Obstet Gynecol. 2013;122(6):1160–7.
17. Syngelaki A, Chelemen T, Dagklis T, Allan L, Nicolaides KH. Challenges in the diagnosis of fetal non-chromosomal abnormalities at 11–13 weeks. Prenat Diagn. 2011;31(1):90–102.
18. Bernard JP, Suarez B, Rambaud C, Muller F, Ville Y. Prenatal diagnosis of neural tube defect before 12 weeks' gestation: direct and indirect ultrasonographic semeiology. Ultrasound Obstet Gynecol. 1997;10(6):406–9.
19. Baxi L, Warren W, Collins MH, Timor-Tritsch IE. Early detection of caudal regression syndrome with transvaginal scanning. Obstet Gynecol. 1990;75(3 Pt 2):486–9.
20. Blumenfeld Z, Siegler E, Bronshtein M. The early diagnosis of neural tube defects. Prenat Diagn. 1993;13(9):863–71.
21. Garcia-Posada R, Eixarch E, Sanz M, Puerto B, Figueras F, Borrell A. Cisterna magna width at 11–13 weeks in the detection of posterior fossa anomalies. Ultrasound Obstet Gynecol. 2013;41(5):515–20.
22. Bernard JP, Cuckle HS, Stirnemann JJ, Salomon LJ, Ville Y. Screening for fetal spina bifida by ultrasound examination in the first trimester of pregnancy using fetal biparietal diameter. Am J Obstet Gynecol. 2012;207(4):306.e1–5.
23. Khalil A, Coates A, Papageorghiou A, Bhide A, Thilaganathan B. Biparietal diameter at 11–13 weeks' gestation in fetuses with open spina bifida. Ultrasound Obstet Gynecol. 2013;42(4):409–15.
24. Simon EG, Arthuis CJ, Haddad G, Bertrand P, Perrotin F. A biparietal/transverse abdominal diameter (BPD/TAD) ratio </=1: a potential hint for open spina bifida at 11–13 weeks scan. Ultrasound Obstet Gynecol. 2015;45(3):267–72.
25. Solomon BD, Gropman A, Muenke M. Holoprosencephaly overview. In: Pagon RA, Adam MP, Ardinger HH, Bird TD, Dolan CR, Fong

CT, et al., editors. GeneReviews(R). Seattle, WA, University of Washington; 1993.

26. Raam MS, Solomon BD, Muenke M. Holoprosencephaly: a guide to diagnosis and clinical management. Indian Pediatr. 2011;48(6):457–66.
27. Timor-Tritsch IE, Monteagudo A. Scanning techniques in obstetrics and gynecology. Clin Obstet Gynecol. 1996;39(1):167–74.
28. Kagan KO, Staboulidou I, Syngelaki A, Cruz J, Nicolaides KH. The 11–13-week scan: diagnosis and outcome of holoprosencephaly, exomphalos and megacystis. Ultrasound Obstet Gynecol. 2010;36(1):10–4.
29. Timor-Tritsch IE, Monteagudo A, Santos R. Three-dimensional inversion rendering in the first- and early second-trimester fetal brain: its use in holoprosencephaly. Ultrasound Obstet Gynecol. 2008;32(6):744–50.
30. Sepulveda W, Dezerega V, Be C. First-trimester sonographic diagnosis of holoprosencephaly: value of the “butterfly” sign. J Ultrasound Med. 2004;23(6):761–5; quiz 6–7.
31. Nicolaides KH. Screening for fetal aneuploidies at 11 to 13 weeks. Prenat Diagn. 2011;31(1):7–15.
32. Dukhovny S, Wilkins-Haug L, Shipp TD, Benson CB, Kaimal AJ, Reiss R. Absent fetal nasal bone: what does it mean for the euploid fetus? J Ultrasound Med. 2013;32(12):2131–4.
33. Mossey PA, Little J, Munger RG, Dixon MJ, Shaw WC. Cleft lip and palate. Lancet. 2009;374(9703):1773–85.
34. Martinez-Ten P, Adiego B, Perez-Pedregosa J, Illescas T, Wong AE, Sepulveda W. First-trimester assessment of the nasal bones using the retronasal triangle view: a 3-dimensional sonographic study. J Ultrasound Med. 2010;29(11):1555–61.
35. Sepulveda W, Wong AE, Martinez-Ten P, Perez-Pedregosa J. Retronasal triangle: a sonographic landmark for the screening of cleft palate in the first trimester. Ultrasound Obstet Gynecol. 2010;35(1):7–13.
36. Adiego B, Martinez-Ten P, Illescas T, Bermejo C, Sepulveda W. First-trimester assessment of nasal bone using retronasal triangle view: a prospective study. Ultrasound Obstet Gynecol. 2014;43(3):272–6.
37. Leonard A, Bernard P, Hiel AL, Hubinont C. Prenatal diagnosis of fetal cataract: case report and review of the literature. Fetal Diagn Ther. 2009;26(2):61–7.
38. Monteagudo A, Timor-Tritsch IE, Friedman AH, Santos R. Autosomal dominant cataracts of the fetus: early detection by transvaginal ultrasound. Ultrasound Obstet Gynecol. 1996;8(2):104–8.
39. Paladini D. Fetal micrognathia: almost always an ominous finding. Ultrasound Obstet Gynecol. 2010;35(4):377–84.
40. Rotten D, Levaillant JM, Martinez H, Ducou le Pointe H, Vicaut E. The fetal mandible: a 2D and 3D sonographic approach to the diagnosis of retrognathia and micrognathia. Ultrasound Obstet Gynecol. 2002;19(2):122–30.
41. Reddy UM, Abuhamad AZ, Levine D, Saade GR, Fetal Imaging Workshop Invited Participants. Fetal imaging: Executive summary of a Joint Eunice Kennedy Shriver National Institute of Child Health and Human Development, Society for Maternal-Fetal Medicine, American Institute of Ultrasound in Medicine, American College of Obstetricians and Gynecologists, American College of Radiology, Society for Pediatric Radiology, and Society of Radiologists in Ultrasound Fetal Imaging Workshop. Am J Obstet Gynecol. 2014;210(5):387–97.

20

Fetal Face and Neck

Henry O. Adekola, Sergiu Puiu,
and Jacques S. Abramowicz

Introduction

The fetal face develops from contributions of the various facial processes, which include the frontonasal, lateral nasal, medial nasal, maxillary, and mandibular processes [1, 2]. This development occurs between the fourth and eighth embryonic weeks by a series of coordinated and programmed events with primordial contributions from the head ectoderm and neural crest mesenchyme [1, 2]. Therefore, it should not be surprising that facial anomalies are usually associated with central nervous system anomalies.

Abnormalities in this fetal region can be and have been demonstrated in the first and early second trimesters [3–5]. In a systematic review of almost 80,000 fetuses evaluated for fetal anomalies between 11 and 14 weeks' gestational age, the highest detection rate was noted for neck abnormalities [3]. Facial and neck abnormalities are associated with lifelong morbidities and maybe the tip of the iceberg of major catastrophic and/or lethal syndromes. Diagnosis in the first and early second trimesters provides a wider spectrum of management options including prenatal genetic testing and counseling to the pregnant woman.

While two-dimensional (2D) ultrasound should still be the major imaging modality of the fetal face in the first trimester (and beyond), the transvaginal approach will, likely, be favored (Fig. 20.1). It is important to mention the role of 3-dimensional (3D) ultrasound. Most elements of the anatomy (orbits, nasal bone, ear, lips) can be demonstrated using both surface-rendering (Fig. 20.2 and Video 20.1) and multiplanar modes (Fig. 20.3), although bone is not completely mineralized (early in the first trimester), which renders their delineation more difficult. Multiplanar mode allows to obtain an exact coronal view, which is, generally, not obtainable with 2D ultrasound [6].

To delve completely into the anomalies of the face and neck, this chapter is divided into sections of the orbits, chin and mouth, nose, lips and palate, ears, as well as face and neck tumors. For more extensive description of normal fetal anatomy, see Chap. 8.

Supplementary Information The online version contains supplementary material available at https://doi.org/10.1007/978-3-031-24133-8_20.

H. O. Adekola (✉)
Department of Maternal-Fetal Medicine, Southern Illinois University, Springfield, IL, USA

S. Puiu
Department of Radiology and Imaging, "Nicolae Testemitanu" State University of Medicine and Pharmacy/Repromed Plus Hospital,
Chisinau, Republic of Moldova

J. S. Abramowicz
Department of Obstetrics and Gynecology, University of Chicago, Chicago, IL, USA
e-mail: jabramowicz@bsd.uchicago.edu

© The Author(s), under exclusive license to Springer Nature Switzerland AG 2023
J. S. Abramowicz, R. E. Longman (eds.), *First-Trimester Ultrasound*,
https://doi.org/10.1007/978-3-031-24133-8_20

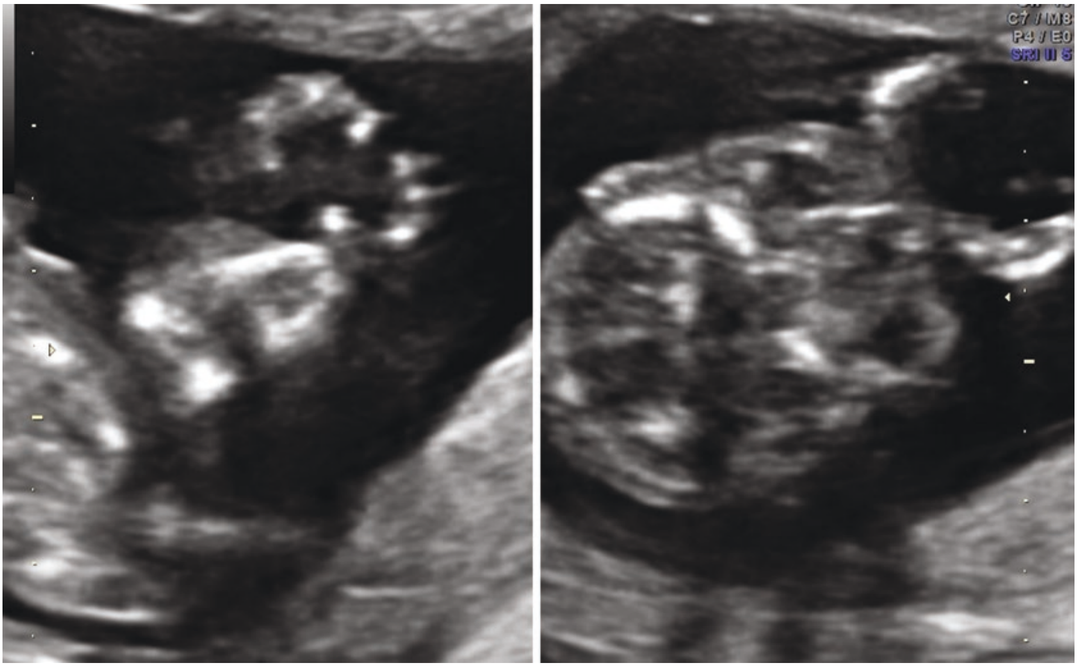

Fig. 20.1 Fetal face, 13 weeks. Left panel is coronal view with nasal bone, maxilla, and mandible (as well as radius-ulna in upper left). Right panel is oriented from bottom to up and demonstrates orbits, parts of the nasal bone, occipital bone, and some digits

Fig. 20.2 Fetal face, 13 weeks, 3D surface rendering. Facial features are distinguishable, although fetus seems to be covering his/her face

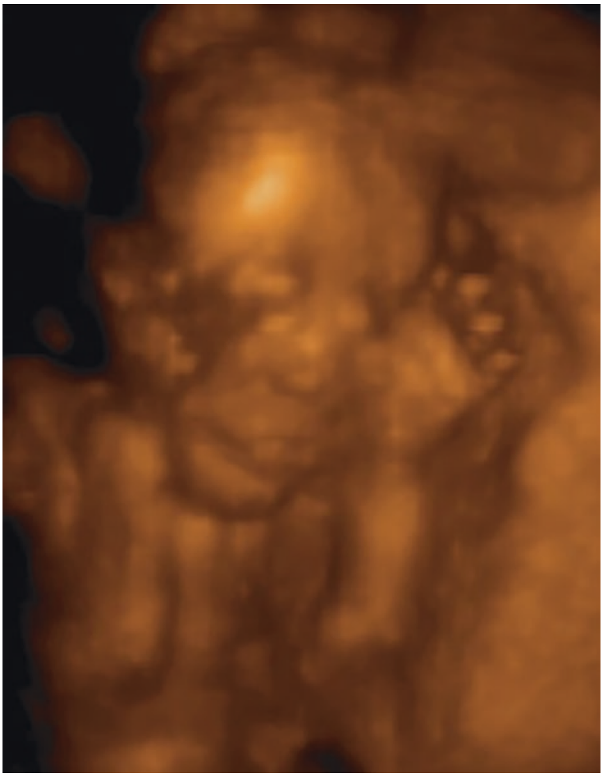

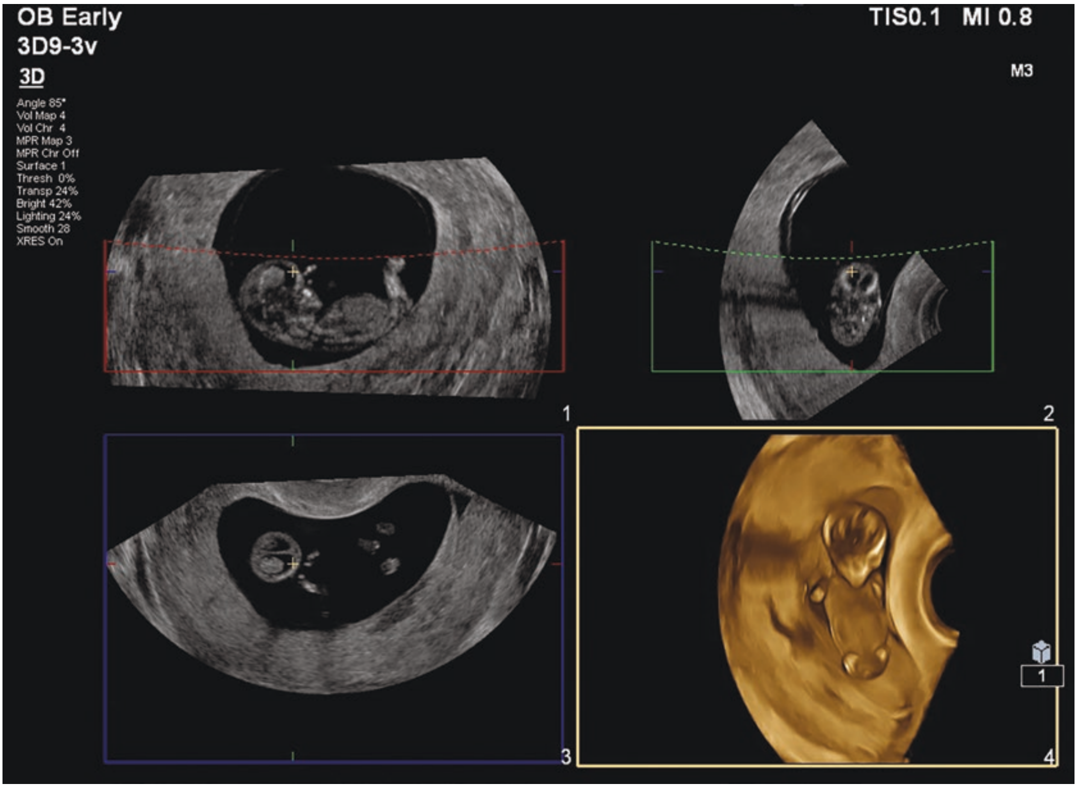
OB Early
3D9-3v
3D
Angle 85°
Vol Map 4
Vol Chr 4
MPR Map 3
MPR Chr Off
Surface 1
Thresh 0%
Transp 24%
Bright 42%
Lighting 24%
Smooth 28
XRES On
TIS0.1 MI 0.8
M3
1
2
3
4
1

Fig. 20.3 Fetal face, 11 weeks, multiplanar view. Upper left image is the acquisition plane; upper right is the coronal plane; lower left is the transverse plane. Lower left is the 3D rendering. It should be noted that in most machines, the upper right quadrant contains the transverse plane and the lower left the reconstructed coronal. Given the acquisition in the present case, the planes were rotated to obtain a profile view in the upper left quadrant, which is the most common acquisition plane

Orbits

Fetal orbits can clearly be visualized in the mid- to late first trimester by both 2D and 3D ultrasound (Fig. 20.1). The orbits appear as echolucent circles with the lens demonstrated as echogenic rings surrounding an anechoic area (Fig. 20.4). To assess the orbits, the coronal plane of the fetal head is the best approach (Fig. 20.5).

The most common abnormalities observed by ultrasound in the first and early second trimesters include hypertelorism, hypotelorism, anophthalmia/microphthalmia, and cataracts.

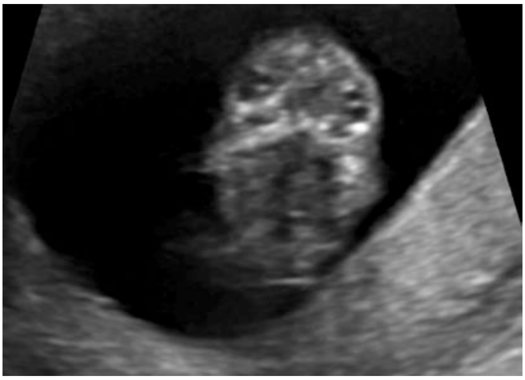

Fig. 20.4 Fetal orbits and lenses, 12 weeks

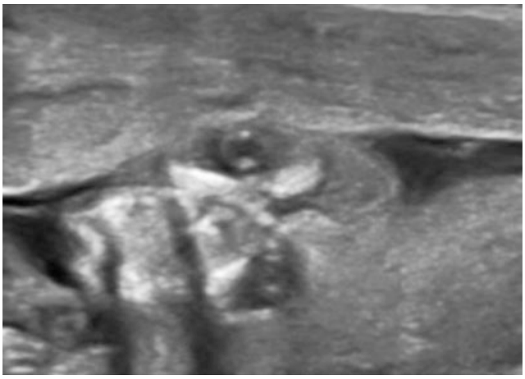

Fig. 20.5 Coronal view of fetal face, 14 weeks. Lenses are clearly demonstrated

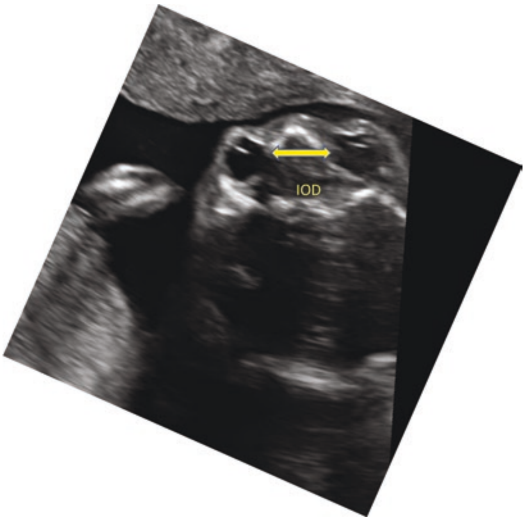

Fig. 20.6 Measurement of the interorbital distance (IOD). Normal measurement at 20 weeks

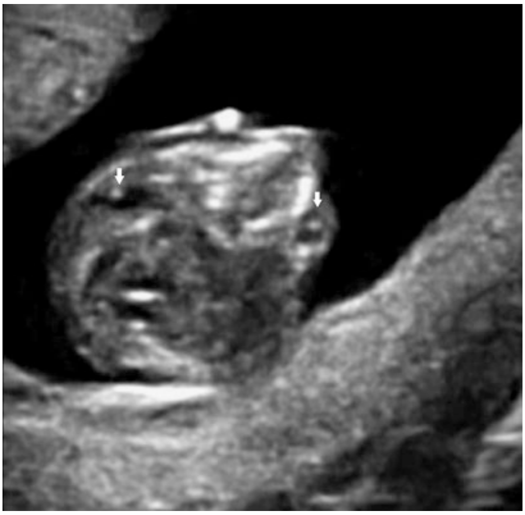

Fig. 20.7 Severe hypertelorism (arrows) in major face abnormality, 12 weeks

Hypertelorism

Hypertelorism, also called euryopia, is defined at interorbital distance of >95th percentile for gestational age [7–10]. From the early second trimester, the interorbital distance (IOD) should roughly be equal to the normal width for gestational age of a single orbit [7, 8] (Fig. 20.6).

During early human embryonic development, the eyes are laterally placed, similar to lower mammals, with migration towards the midline as pregnancy progresses. Several hypotheses have been proposed for hypertelorism and they include (1) primary arrest of midline progression of orbits; (2) secondary arrest due to presence of midline tumor; (3) abnormal growth of vectors of the skull bone, e.g., lesser wing of the sphenoid; and (4) maldevelopment of bones derived from the first branchial arches [11, 12]. It has also been ascribed to fetal trauma as it was observed as part of a myriad of anomalies in fetuses exposed to dilatation and curettage in the first trimester [13].

Hypertelorism is a rare condition, and its exact incidence is unknown. While this could be an isolated finding, its discovery should trigger detailed sonography including neurosonography as well as invasive prenatal testing (Fig. 20.7). This is because it has been associated with chromosomal aneuploidies like trisomy 18 (Edwards syndrome); 45,X (Turner syndrome); 22q11.2 deletion (DiGeorge syndrome); triploidy; tetrasomy 12p (Pallister-Killian syndrome); 4p deletion (Wolf-Hirschhorn syndrome); interstitial deletions of chromosomes 1, 13, and 17 [14, 15]; interstitial deletion of chromosome 13; and 9p duplication [16–20]. It has also been associated with genetic syndromes, including single-gene disorders such as craniosynostosis (including Apert, Carpenter, and Crouzon syndromes), frontonasal dysplasia, oculodentodigital dysplasia, and Neu-Laxova syndrome [9, 16, 21, 22]. While isolated hypertelorism may have good prognosis (with cosmetic and visual impairment), syndromic associations may have a poor prognosis with significant neurological maldevelopment. When isolated, there does not seem to be an increased recurrence risk.

Hypotelorism (Cyclopia)

This is defined as an interorbital distance <5th percentile for gestational age [7–11]. Rare, with an unknown incidence, it is almost always associated with cleavage anomalies of the fetal brain [21]. This may be due to the embryological relationship between the fetal forebrain (prosencephalon) and the facial midline area. Development of both areas is induced by the prechordal mesenchyme, which is the tissue situated between the prosencephalon and the stomodeum (roof of the primitive mouth) [11, 23]. Therefore, interruption of the development of the prechordal mesenchyme will lead to defective formation of the facial midline and brain cleavage. This may be severe enough, leading to failure of cleavage of the prosencephalon, and thus the prosencephalon remains a single cavity (holoprosencephaly) (Fig. 20.8), which includes some variations such as hypotelorism (Fig. 20.9a) and, if severe enough, a single optic cavity, also known as cyclopia (Fig. 20.9b) [11, 24–27]. Other anomalies and chromosomal aneuploidies associated with hypotelorism include trigonocephaly [28], microcephaly [11, 29], Meckel-Gruber syndrome [30, 31], maternal phenylketonuria [30, 31], and chromosomal aneuploidies like trisomy 13, trisomy 21, chromosomal 5p deletion, chromosomal 7p deletion, chromosome 7q11.23 deletion, and trisomy 4 mosaicism [10, 11, 30–33]. Thus, detection of hypotelorism should trigger detailed neurosonography, invasive prenatal testing, detailed history taking, and genetic counseling.

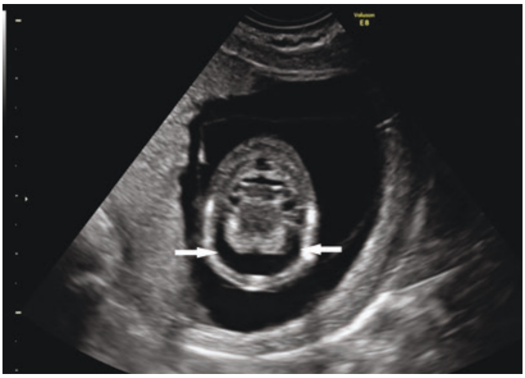

Fig. 20.8 Holoprosencephaly. Fused, single ventricle is demonstrated (arrows)

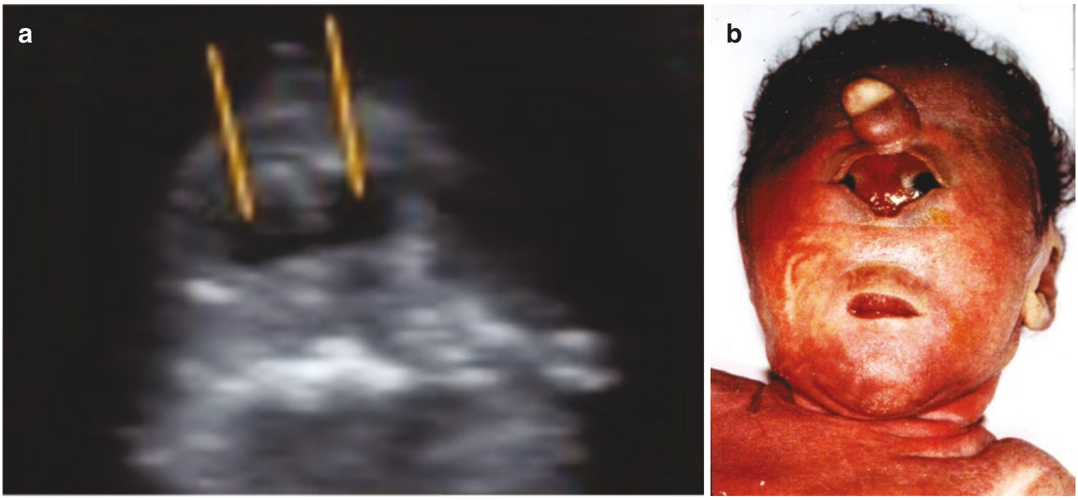

Fig. 20.9 (**a**) Hypotelorism. Orbits are marked by the two yellow arrows (Picture courtesy of Dr. Reem Abu-Rustum). (**b**) Single orbit (cyclopia), with two eye globes. A proboscis is also present (pathologic specimen, 15 weeks). See also Fig. 20.13

Microphthalmia/Anophthalmia

Microphthalmia is defined as a small malformed orbital globe, while anophthalmia is the absence of fetal orbital globe [34, 35]. Earlier works state that this distinction should be reserved until after evaluation by postnatal pathology [11], but improved ultrasound imaging modalities and fetal MRI may be able to differentiate these anomalies in the fetal period [36]. Both malformations can be unilateral, or bilateral, with a cumulative incidence of approximately 1 per 10,000 births [37–40].

Prenatal evaluation of the fetal eye including diagnosis of anomalies in the first and early second trimesters have been described [41] (Fig. 20.10). Sporadic fetal syndromes such as triploidy and trisomies 9 and 13 have been associated with microphthalmia/anophthalmia [34, 42, 43]. Other syndromes associated with this condition include Aicardi, Fraser, Fryns, Goldenhar, Gorlin, Lenz, Walker-Warburg, and fetal alcohol syndromes [11, 17, 43–48]. Non-syndromic conditions such as congenital viral infection (Rubella, Toxoplasmosis, Cytomegalovirus, and Parvovirus B19) and CHARGE syndrome have also been associated [34, 43].

As with all facial abnormalities, a detailed fetal imaging study including a neurosonogram should be performed and prenatal invasive testing should be offered. If pregnancy continuation is desired, a fetal MRI should be performed later in pregnancy.

Cataracts

Beneath each lens, placode is the optic vesicle. The lens placode is then separated from the surface ectoderm by mesenchymal tissue to form a hollow lens vesicle before the sixth week of gestation. The wall of this vesicle is lined by columnar cells. Cells of the deep wall and of the equatorial region increase in length and become the lens fibers. The future lenses of the eyes can be observed bilaterally from the beginning of the eighth week of pregnancy as areas of thickened ectoderm called the lens placodes [41]. Appearing as a hyperechogenic ring with a hypoechoic center within the fetal orbit, the normal fetal lens can be identified by ultrasound from ≥12 weeks' gestation [41, 49]. Congenital cataracts are characterized on ultrasound by homogeneous opacity of the lens, echogenic area in the expected position of the lens, and loss of the normal hypoechoic center of the lens (Fig. 20.11). It has an incidence of 1–6 per 10,000 births [50]. Fetal cataracts may be unilateral or bilateral.

Cataract development is linked to the embryological ocular development and may explain why

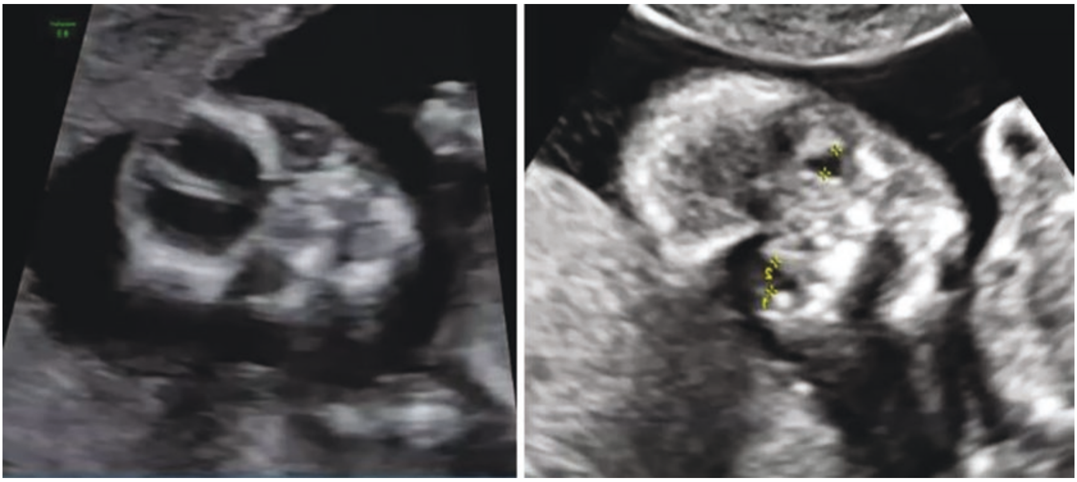

Fig. 20.10 Anophthalmia, 13 weeks. Left panel: normal face. The left lens is clearly visible. Right panel: anophthalmia. Orbits appear very small, and the lenses cannot be demonstrated

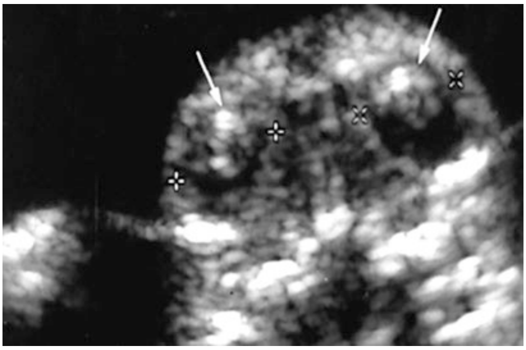

Fig. 20.11 Bilateral cataracts (arrows) in a 12 5/7-week fetus. (Modified from Monteagudo A, Timor-Tritsch IE, Friedman AH, Santos R. Autosomal dominant cataracts of the fetus: early detection by transvaginal ultrasound. Ultrasound Obstet Gynecol. 1996; 8:104–8)

cataract is not a feature of fetal infection occurring late in the first trimester. Therefore, a diagnosis of fetal cataract indicates a fetal infection occurring within the first 6 weeks of pregnancy, a genetic syndrome, or a metabolic disorder [51, 52].

Etiologies include genetic syndromes such as Walker-Warburg syndrome [53] and chondrodysplasia punctata [54] characterized by bilateral lesions; congenital infections such as toxoplasmosis [55, 56] rubella [52], cytomegalovirus [57], and Herpes simplex virus [57] that are usually associated with unilateral cataracts; and metabolic disorders like Zellweger syndrome [58] as well as Lowe's oculocerebrorenal syndrome [58, 59].

Nose

The fetal nose begins to form at the end of the fourth week with the appearance of the nasal (olfactory) placodes. The definitive fetal nose is formed with contributions from the frontonasal prominence, medial and lateral nasal processes, and maxillary process [1, 2]. The cartilaginous septum is derived from neural crest cells between the nasal cavities [1, 2, 60]. The nasal floor is formed by palatine shelves of the maxilla which at 10 weeks fuse with the inferior septum to form the secondary palate [1, 2, 60] (Fig. 20.12).

Fetal nose abnormalities include arrhinia, absent nasal bone, and proboscis.

Arrhinia

Arrhinia or congenital absence of the nose is a very rare anomaly. It is defined as total when the entire nose and olfactory bulbs are lacking and partial when at least one nostril and olfactory nerve are present [61].

It has been hypothesized that lack of development of the nose results from failure of the medial and lateral nasal processes to grow, but it is also possible that overgrowth and premature fusion of the nasal medial processes result in the formation of an atretic plate [62]. Arrhinia may also result from lack of resorption of the nasal epithelial plugs during the 13th to 15th weeks of gestation [62]. Another possible etiology may be related to abnormal migration of neural crest cells to this region, resulting in aberrant flow of the multiple mesodermal structures required to establish the nose and its cavities normally [62].

While arrhinia can be an isolated sonographic finding [63], it is commonly associated with other facial anomalies (hypertelorism, microphthalmia, low-set ears, high-arched palate, and cleft palate) [63, 64]. Other anomalies associated with arrhinia include holoprosencephaly [65], Treacher Collins syndrome [66], as well as fetal chromosomal anomalies such as mosaic trisomy 9 syndrome [67] and inversion of chromosome 9 [61].

Definitive prenatal diagnosis has mostly been reported in the mid-second trimester. However, recent improvement in ultrasound technology with 3D/4D ultrasound with high-definition (HD) live has provided fetal medicine/radiology specialists the ability to study the developing fetal face. This technology has enabled demonstration of fetal arrhinia (with cleft lip/palate) in the first trimester [68]. This is important as fetal arrhinia is associated with significant early neonatal morbidity [64].

Proboscis

Proboscis or rudimentary is a trunk-like appendage with either one or two openings with absence of the nose. This diagnosis is almost always asso-

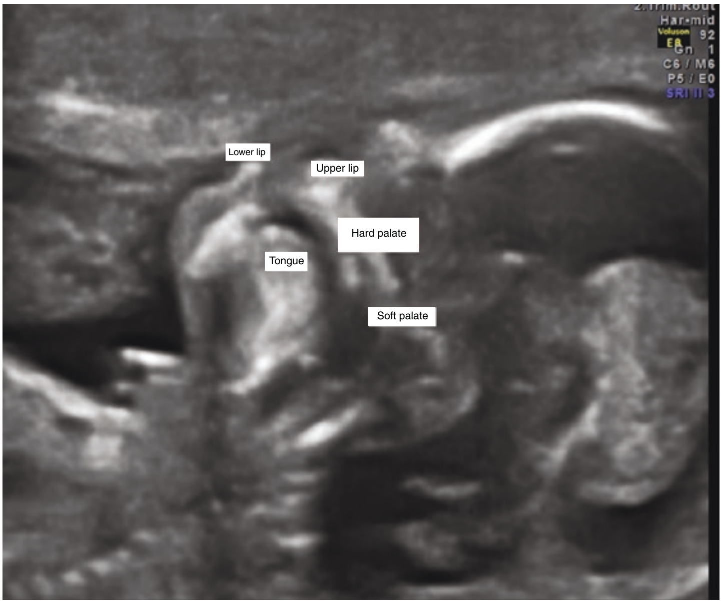

Fig. 20.12 Fetal profile 12 4/7 weeks (9 MHz probe). Hard and soft palates are demonstrated

ciated with cyclopia and holoprosencephaly [11, 23, 24, 26]. As previously described, it has been hypothesized as a primary disorder of the prechordal mesenchyme, which results in the abnormal induction of midfacial structures [11, 23]. This diagnosis can be made in the first trimester [27, 68] and should prompt invasive prenatal testing due to common association with trisomy 13 [33] (Fig. 20.13).

Absent Nasal Bone

The presence or absence of the nasal bone may be determined at the time of the 11- to 14-week ultrasound examination and used as part of the risk assessment for aneuploidy [69–71]. Ossification can be documented by ultrasound from about 10 to 11 weeks, at a CRL of 42 mm [72]. On ultrasound, with the transducer parallel to the nose long axis, two parallel echogenic lines should be clearly demonstrated, forming an "equal" sign: the nasal bone and the skin line overlying the nasal bridge (Fig. 20.14). When the nasal bone is absent, the skin line is demonstrated but not the second component of the "equal" sign on midsagittal view of the sonographic fetal profile (Fig. 20.15). Most common associated fetal aneuploidy is Down syndrome (trisomy 21) [69, 71]. It has also been reported in fetuses with trisomies 18 and 13, sex chromosome abnormali-

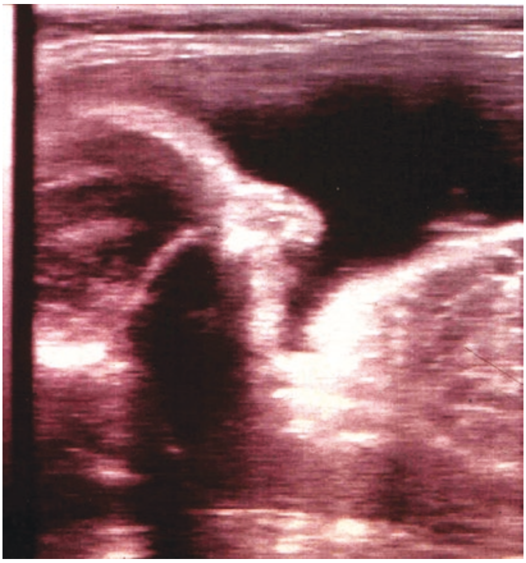

Fig. 20.13 Proboscis (old image, 15 weeks)

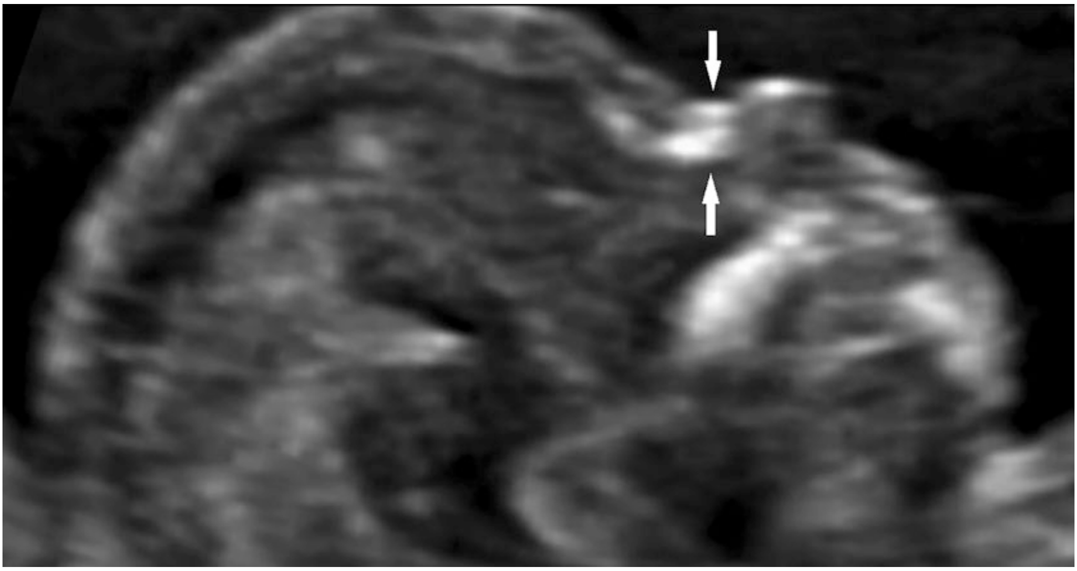

Fig. 20.14 Demonstration of the presence of the nasal bone. Note the "equal sign"

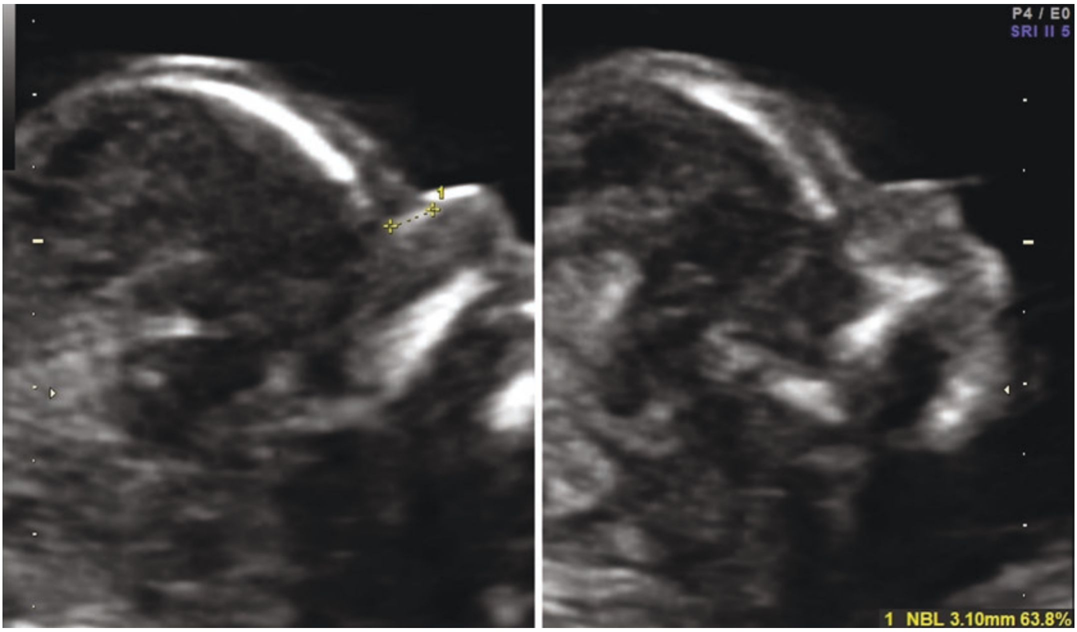
1
P4 / E0
SRI II 5
1 NBL 3.10mm 63.8%

Fig. 20.15 Absent nasal bone. Right panel, 12-week fetus. The "equal sign" is not visualized. Left panel: "equal sign" is observed

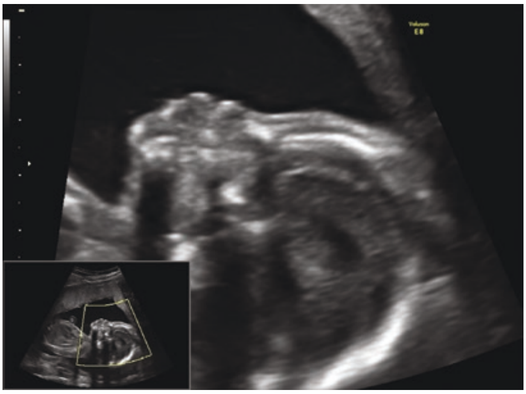

Fig. 20.16 Fetus with Binder phenotype (also known as maxillonasal dysostosis: flat profile (arrhinia) with abnormal position of the nasal bones and other facial bone anomalies). Notice virtually complete absence of the nose

ties, and other rarer aneuploidies [71]. Thus, this finding should prompt further aneuploidy screening and/or invasive prenatal testing. It should be noted that the nasal bone may be absent in various craniofacial anomalies, such as frontonasal dysplasia [73], Binder syndrome [74] (Fig. 20.16), or arrhinia [63]. It should also be noted that absent or short nasal bone is more common in populations of certain ethnic origin and may be a normal finding in up to 3% of fetuses [70].

Chin and Mouth

Micrognathia and Retrognathia

Both micrognathia and retrognathia are facial anomalies associated with maldevelopment or position of the fetal mandible. While the former is characterized by hypoplasia of the fetal mandible, the latter is characterized by abnormal position of the mandible in relation to the maxilla [75]. Fetal micrognathia is almost always associated with retrognathia, but the latter can be observed in isolation of the former [75, 76]. Micrognathia can be detected by first-trimester ultrasound [75, 77–80] and should prompt detailed ultrasound evaluation and possible invasive testing as this finding is usually the tip of the iceberg in a myriad of other fetal anomalies and fetal syndromes including Treacher Collins syndrome and Pierre Robin sequence trisomies 13 and 18 [76, 77]. Often the diagnosis may be made on a midsagittal view of the fetal profile where the upper lip appears prominent and the chin is receding (Fig. 20.17) and first-trimester diagnosis has been reported [81]. Rather than simple observation, however, various parameters and angles have been described to attempt an objective assessment of the chin position. The retronasal triangle (RNT) view is a 3D technique where a coronal plane of the face is obtained in which the primary palate and the frontal processes of the maxilla are visualized on the same plane. In fetuses with normal lower face anatomy, a gap is demonstrated between the right and left body of the mandible (the "mandibular gap") [82] (Fig. 20.18). Another parameter is the inferior facial angle (IFA), formed by the intersection of a line orthogonal to the vertical part of the forehead and a line through the tip of the chin and the upper lip. Normal value is 65° ± 16° (Fig. 20.19). An angle less than 49° is diagnostic of micrognathia, with a sensitivity and specificity of 100% and 99%, respectively [83]. This angle and the anteroposterior diameters of the mandible have been described in early pregnancy, at 11–13+6 weeks of gestation [84]. The frontal nasomental angle is the angle between a line drawn from the tip of the nose and frontal bone, intersecting the line from the nasal tip to the mentum (Fig. 20.20). Normal mean value is 147° ± 2.7°. Hence, the normal limit is 142° [85].

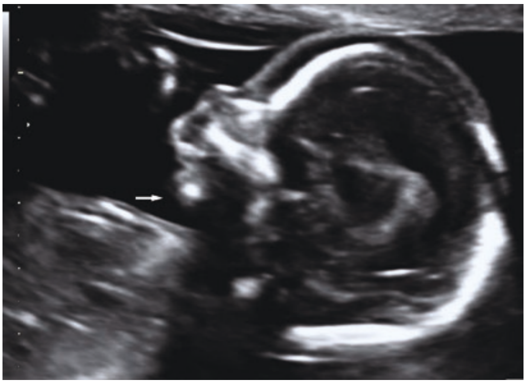

Fig. 20.17 Micrognathia. Fetal profile, 12 5/7 weeks. The arrow points to the receding chin

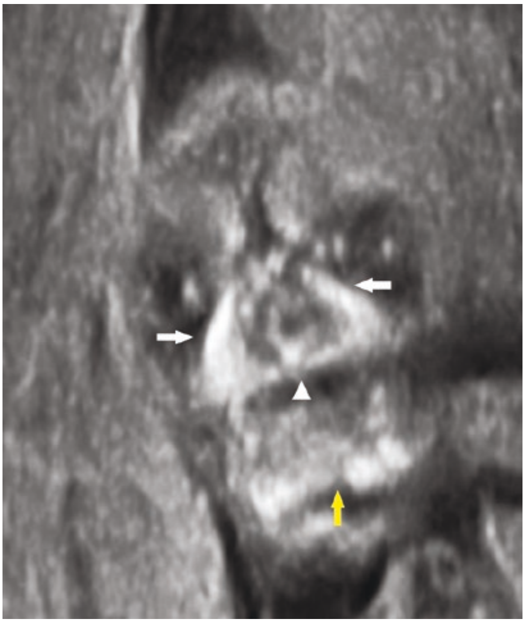

Fig. 20.18 View of the retronasal triangle, formed by the frontal processes of the maxilla (white arrows) and the primary palate (arrowhead). The (normal) mandibular gap is indicated by the yellow arrow. Fetus at 14 weeks

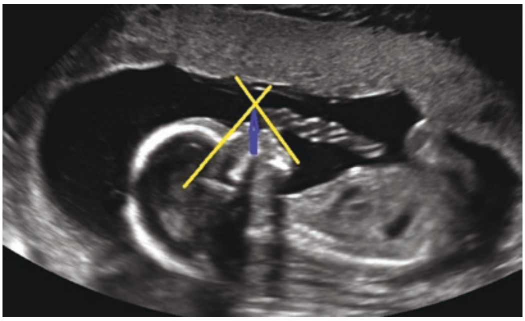

Fig. 20.19 Normal chin, 13 weeks. Measurement of the inferior facial angle (arrow), formed by the intersection of a line orthogonal to the vertical part of the forehead and a line through the tip of the chin and the upper lip

Other described facial markers are maxilla-nasion-mandible (MNM) angle, facial maxillary angle (FMA), and profile line (PL) distance [86]. The jaw index [85] is relatively easy to obtain by measuring the anteroposterior diameter of the fetal mandible, between the symphysis mentis and the middle of the line connecting the bases of the two rami, as a percentage of the BPD. It is independent of the gestational age, and a jaw index of less than 23 has a 100% sensitivity and 98.7% specificity and a jaw index of less than 21 has a 100% positive predictive value [85].

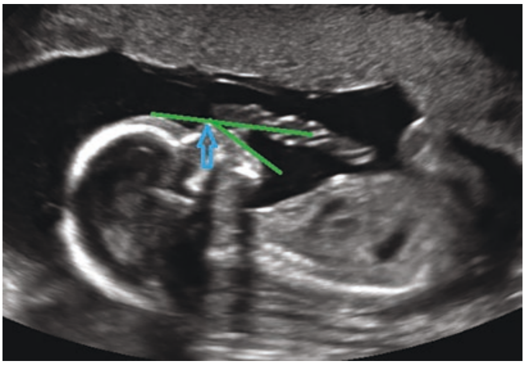

Fig. 20.20 Normal chin, 13 weeks. Measurement of the frontal nasomental angle (arrow) between a line drawn from the tip of the nose and frontal bone, intersecting the line from the nasal tip to the chin angle

Agnathia

Agnathia is an extremely rare anomaly with a reported incidence of less than 1 per 70,000 births [87]. In addition to being characterized by an absence of the mandible, it is almost always associated with ventromedial displacement of the external ear (otocephaly)—agnathia–otocephaly complex [11, 88]. The external ear migration from the fetal neck depends on the undisrupted development of the first branchial arch [11, 88, 89]. Current ultrasound technology with high-resolution transvaginal scanning and 3-dimensional (3D) ultrasound has enabled first-trimester diagnosis of this lethal anomaly [90, 91].

Macroglossia

In the neonate, macroglossia is defined as a resting tongue that protrudes beyond the alveolar ridge [92, 93]. Macroglossia can be classified as "true" in the presence of histologic abnormalities and "relative" when associated with an undeveloped jaw or oropharyngeal hypotonia [94].

Although the fetal tongue can be visualized (Fig. 20.12) and size estimated with created nomograms for first- and early second-trimester fetuses [95, 96], prenatal diagnosis of macroglossia at this time is limited to mid-second to early third-trimester fetuses [93, 97]. Commonest conditions that have been associated with prenatal macroglossia include Beckwith-Wiedemann syndrome and trisomy 21 [93, 97, 98].

Epignathus

Epignathus or oral teratoma is a rare congenital teratoma arising from the fetal hard palate. This tumor grows large enough to protrude through the mouth leading to facial distortion in addition to airway obstruction. Earliest report of this abnormality was in a 15-week fetus, initially mistaken to have an intracranial anomaly [99]. That case report highlighted the possibility of misdiagnosing this condition as a holoprosencephaly with proboscis if lesion is large enough to distort fetal features.

Lips and Palate

The fetal lips are demonstrated in a coronal plane, orienting the transducer up to demonstrate the upper lips and the nostrils (Fig. 20.21). The palate forms the roof of the mouth. It comprises two parts: the hard palate anteriorly and the soft palate posteriorly. A different classification is primary (lips, jaw, nasal bone) and secondary palate (hard and soft palates). The hard palate is horizontal behind the teeth line, and the soft palate curves downwards and backwards, ending in the uvula. The hard palate is easy to identify on midsagittal profile views (Fig. 20.22). In the same view, the soft palate can also be visualized by slightly angling the transducer. A transverse (axial) view, from inferior to superior, allows visualization of the palate but is, sometimes, difficult to obtain (Fig. 20.23). It can be accessed by getting a profile (median) view including the nasal bone and rotating the transducer 90°. Minimal tilt allows visualization of the anterior part of the maxilla as well as the primary palate (Figs. 20.12 and 20.23b). The use of 3D ultrasound has allowed major improvement in the visualization of the palate (Fig. 20.24) [100].

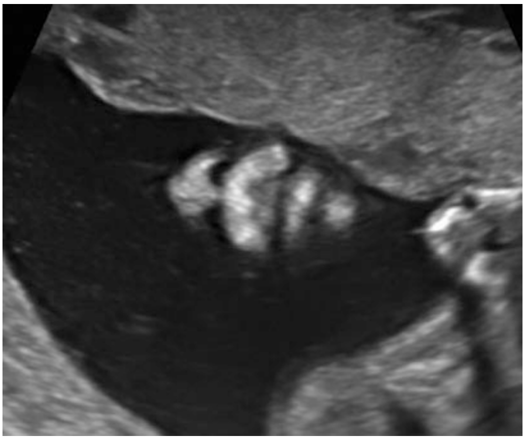

Fig. 20.21 Normal upper lips and nostrils, axial view, orienting up

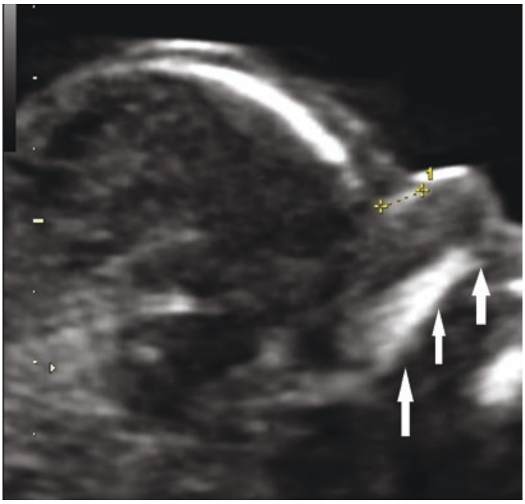

Fig. 20.22 Palate profile view, 13 weeks

Orofacial Cleft

This anomaly complicates 1 in 700 live births [101]. Commonly affecting individuals of Asian descent [101], the structures affected by lower facial clefts include the lip and nose, alveolus/premaxilla, and secondary palate.

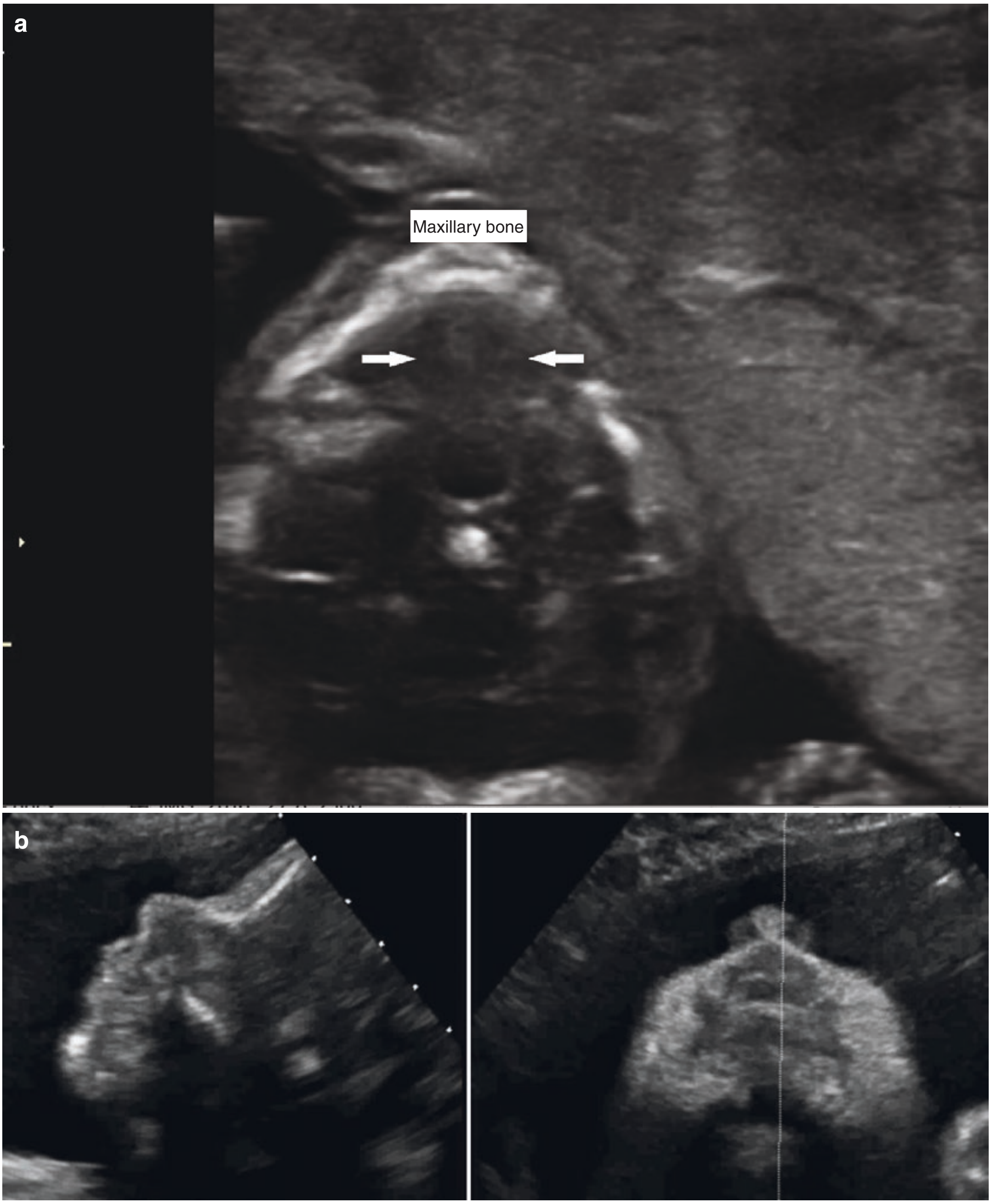

Fig. 20.23 Palate, 13 weeks. (**a**) The hard palate is visualized (arrows). The soft palate cannot be seen since it is almost vertical to the insonation beam. (**b**) With an x-Matrix probe, a transverse view (right), allowing view of the nostrils, upper lip, and hard palate, can more easily be obtained from a profile view (left)

Etiology of orofacial cleft is multifactorial with about approximately 50% of concordance observed in monozygotic twin gestations [102]. Environmental exposures to alcohol, cigarette smoking, retinoids, antiseizure medication (e.g., valproic acid, phenytoin, and oxazolidinones), organic solvents, and nutrient deficiency (folic acid) have been associated with

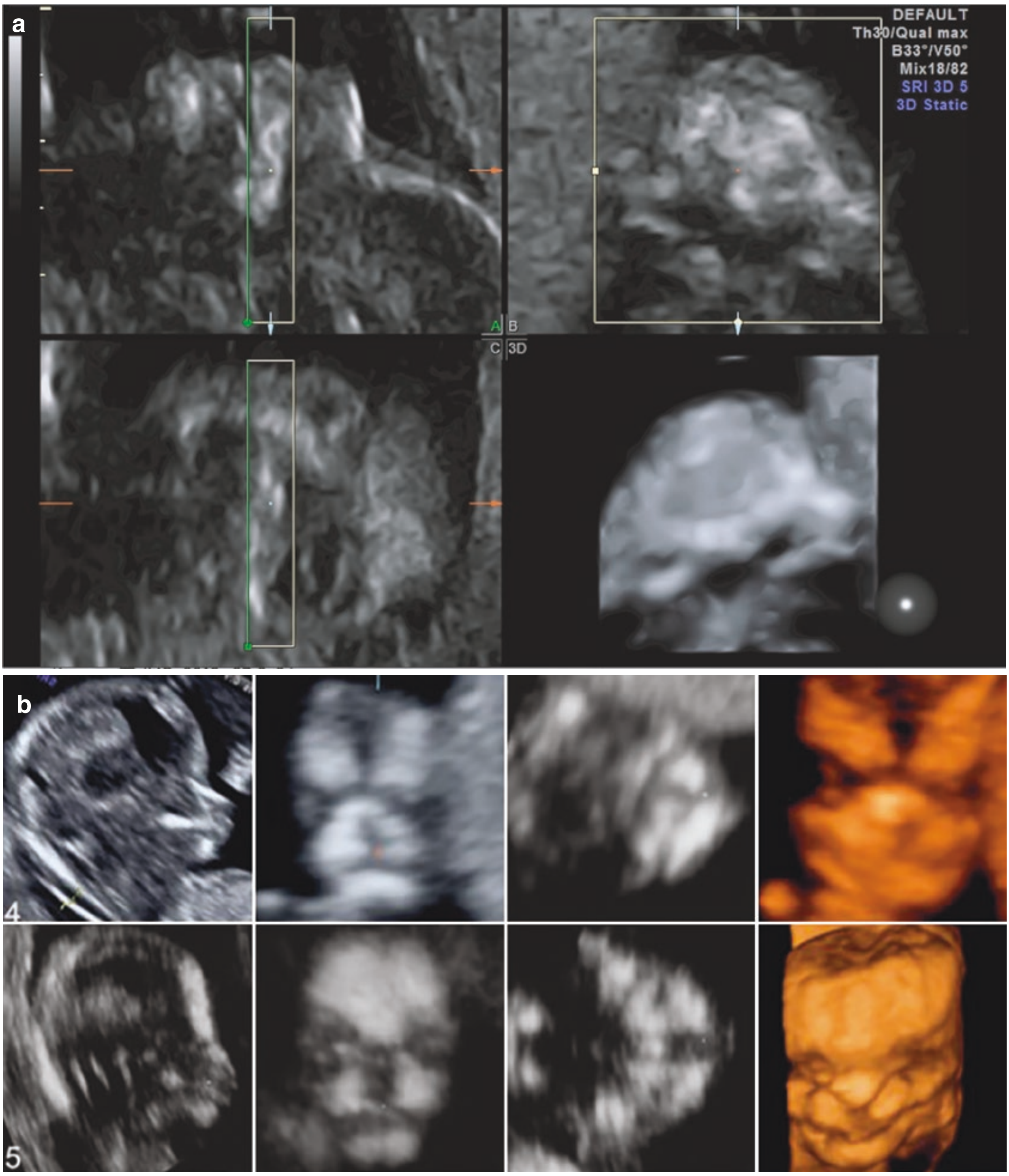

Fig. 20.24 Three-D diagnosis of cleft lip/palate. (**a**) With the fetal profile in the acquisition plane (upper left corner), a region of interest is defined around the lips and palate by the box. The green line is the viewing position (looking up from below the palate). Upper right is the transverse view, lower left the coronal, and lower right the reconstructed 3D volume. (**b**) Two cases of cleft palate (Modified from Martinez-Ten P, Adiego B, Illescas T, Bermejo C, Wong AE, Sepulveda W. First-trimester diagnosis of cleft lip and palate using three-dimensional ultrasound. Ultrasound Obstet Gynecol. 2012;40:40–6). Case 4: fetus at 13 1/7 weeks, unilateral cleft primary palate, and cleft secondary palate. No other anomalies, term delivery. Case 5: fetus at 13 2/7 weeks (one of monoamniotic dichorionic twins), median cleft of primary palate, cleft of secondary palate, holoprosencephaly, umbilical hernia, hydronephrosis, normal karyotype, termination of pregnancy. The clefts are marked on the images by the dot used in 3D for localization

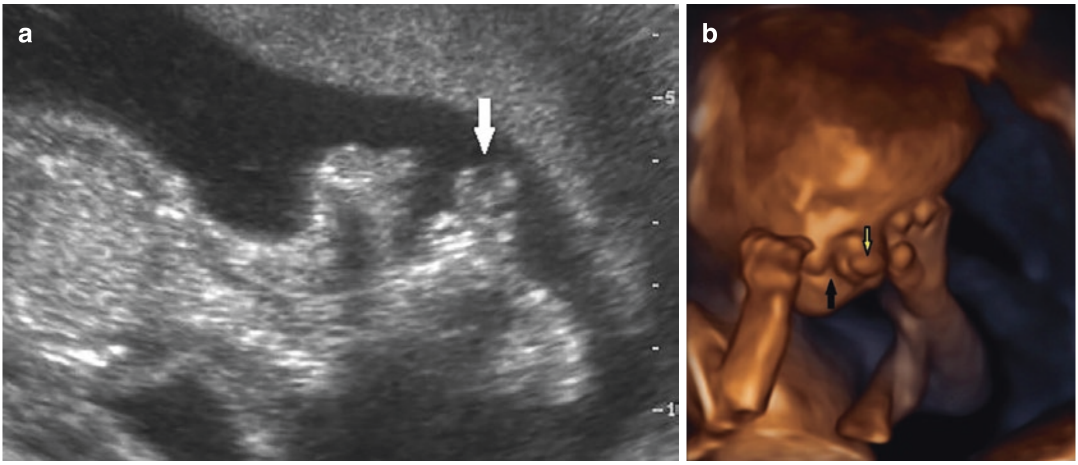

Fig. 20.25 Cleft lip, 13–14 weeks. (**a**) Prelabial protuberance (arrow), 2D, 14 weeks. (**b**) The protuberance is clearly visualized on this 3D reconstruction in different fetus, 13 weeks (yellow arrow)

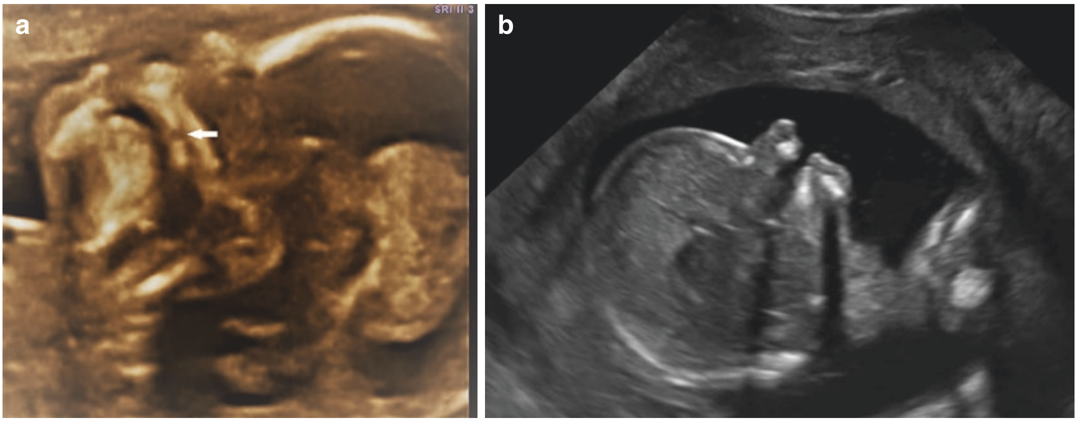

Fig. 20.26 Cleft palate. Both images at 13 weeks. (**a**) "Maxillary gap." A small gap is demonstrated (arrow). (**b**) Notice the complete absence of the palate (arrow). Compare with Figs. 20.12 and 20.22

this anomaly [103, 104]. Diagnosis of facial cleft can be made the first trimester and may be detected on standard midsagittal view of the fetal profile utilized to measure nuchal translucency. In this view, a premaxillary protrusion can be demonstrated [105] (Fig. 20.25). In addition, the presence of a maxillary gap of >1.5 mm at the 11–13-week ultrasound is associated with facial cleft [105, 106] (Fig. 20.26). Caution in diagnosing a cleft is recommended if this is the only sign, since at that time (11–13-week scan), some parts of the maxilla may still demonstrate minimal ossification. Targeted examination of the retronasal triangle in a coronal view is also utilized to demonstrate the presence of an orofacial cleft in the first trimester [107]. Various 3D techniques have been described for optimal visualization of the lips and palate: tomographic frontal view, reverse face, flipped face, and oblique face [108]. Orofacial clefts are classified as paramedian cleft (which is the commonest form) and median (midline) cleft (which is rare) [105].

Paramedian Orofacial Cleft

Paramedian orofacial cleft can be bilateral (64%) or unilateral (34%) [109]. Cleft lip with cleft palate, which is the most common type of orofacial

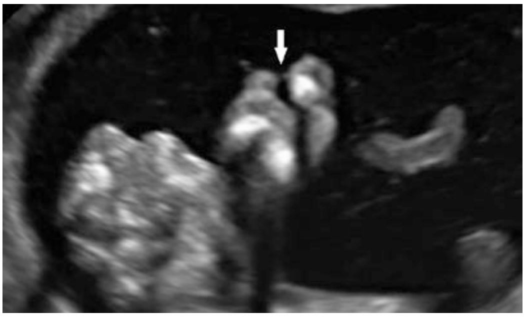

Fig. 20.27 Right paramedian cleft lip. 2D image (arrow). See Fig. 20.25b; cleft is indicated by black arrow

cleft, comprises 50% of cases [109]. Isolated cleft lip or cleft palate on the other hand comprises 25% [109] (Fig. 20.27). Paramedian orofacial cleft should prompt further ultrasound evaluation as greater than 10% of these fetuses will have associated anomalies [110], with these anomalies 2.5 times greater in fetuses with bilateral paramedian orofacial cleft compared to the former [110]. Fetal profile in addition to fetal orbits/lens, ears, and tongue position should also be evaluated for associated maldevelopment [105, 110].

Median Facial Cleft

This is very rare comprising less than 3% of orofacial cleft [109, 111]. This defect is in the median line of the face, extending to the nasal cavity and maxilla when defect is complete and affecting only the vermillion when incomplete. This defect is commonly associated with holoprosencephaly, which can be diagnosed during late first-trimester sonography [68, 105].

Ears

External Ear (Pinna/Auricle) Anomalies

By the end of the fourth week of development, the auricle develops from six mesenchymal proliferations/swellings known as hillocks derived from the first and second pharyngeal arches that surround the first pharyngeal cleft (which develops into the external auditory meatus) [2]. There are three auricular hillocks on each side of the external meatus that eventually fuse to form the auricle. The first three auricular hillocks emerge from the first pharyngeal arch, while the last three auricular hillocks arise from the second pharyngeal arch [2]. The external ears begin their embryological development in the lower neck region and gradually ascend posterolaterally to the level of the eyes as the mandible develops.

Evaluation of the fetal external ear as well as its anomalies in the first trimester can be difficult; however, high-resolution ultrasound as well as 3D/4D ultrasound (including HD live modalities) have improved our diagnostic abilities during this early gestational period [68, 90, 112] (Fig. 20.28a). Although external ear anomalies may be isolated, they are commonly associated with other major anomalies or may be part of a syndrome [113, 114]. Anomalies of the fetal external ear include anotia, microtia, macrotia, and melotia (low-set ears).

Anotia

This is complete absence of the external ear. There is no differentiation between the cheek and aural region with obliteration of the external auditory meatus. Anotia is caused by deficient formation of the hillocks that form the pinna and is usually associated with major malformations of the face (cleft lip/cleft palate) [115]. This anomaly has been reported in pregnancies resulting from consanguinity [116] as well as those exposed to the teratogens like retinoic acid and thalidomide [117, 118].

Microtia

This is used to describe a small pinna. In addition to abnormality of the external auditory meatus and hearing loss [119], it can be associated with cup-shaped (overfold) pinna [120].

Microtia is commonly associated with trisomies 13, 18, 21, and 22; fetal triploidy [121–123]; as well as exposure to teratogens (thalidomide, retinoic acid) [113, 117]. It can also rarely be an isolated finding in otherwise healthy individuals who inherit this in an autosomal dominant fashion [124].

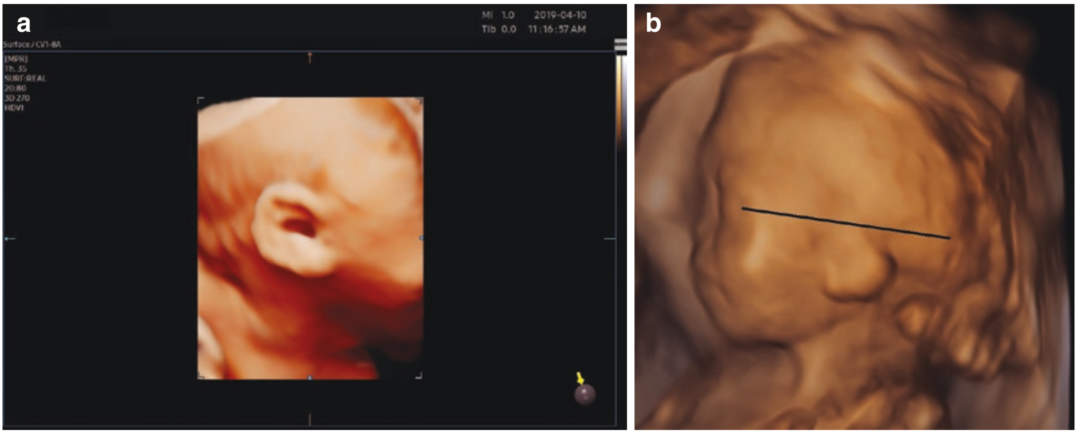

Fig. 20.28 Fetal ear. (**a**) 3D view of the fetal profile, 15 weeks. The left ear is visualized. (**b**) When drawing a horizontal line from the eye angle to the back of the head, the ear appears lower than expected (low-set ear) and malrotated in a fetus with Binder syndrome, 13 weeks

Macrotia (Large Ears)

Macrotia (also known as large pinna) is usually not associated with external ear shape or abnormal external auditory meatus [125]. It should be considered that isolated macrotia may represent a familial trend in an inherited and autosomal dominant fashion, albeit debatable. However, it may also be associated with fragile X syndrome [126], Marfan syndrome [127], cerebro-oculo-facial-skeletal syndrome (COFS) [128], and anophthalmia plus syndrome (bilateral anophthalmia and an abnormal ear with absent lobule) [129].

Melotia (Low-Set Ears)

This is diagnosed when the helix is attached to the cranium at a level below that of a horizontal plane with the corner of the orbit (Fig. 20.28b). This anomaly is commonly associated with fetal chromosomal aneuploidies (trisomies 13 and 18) in addition to major structural anomalies [130, 131] as well as genetic syndromes such as Apert, Crouzon, Noonan, and Treacher Collins syndromes [131]. It can also be associated with teratogens such as methotrexate and aminopterin [132].

Otocephaly

This has been addressed at a previous section of this text.

Tumors of the Face and Neck

Frontal Encephalocele

Frontal encephalocele may be detected during first-trimester dating ultrasound as well as ultrasound evaluation performed to obtain nuchal translucency. While most encephaloceles are occipital (Fig. 20.29), almost 10% of them were frontal in one large case series [133]. Both high-resolution transvaginal 2- and 3-dimension sonographic views were utilized to obtain this first-trimester diagnosis [133] (Fig. 20.30). Similar to other anomalies detected in the first trimester, a detailed ultrasound should be performed to determine the presence of other anomalies including facial cleft, abdominal wall defect, spine anomalies, and limb amputations [134, 135].

Cystic Hygroma

Cystic hygroma (referred to as lymphatic malformation in the pediatric literature) is commonly diagnosed at the 10–14-week ultrasound performed for pregnancy dating and/or as part of first-trimester fetal aneuploidy screen [136, 137]. It is a congenital abnormality of the vascular

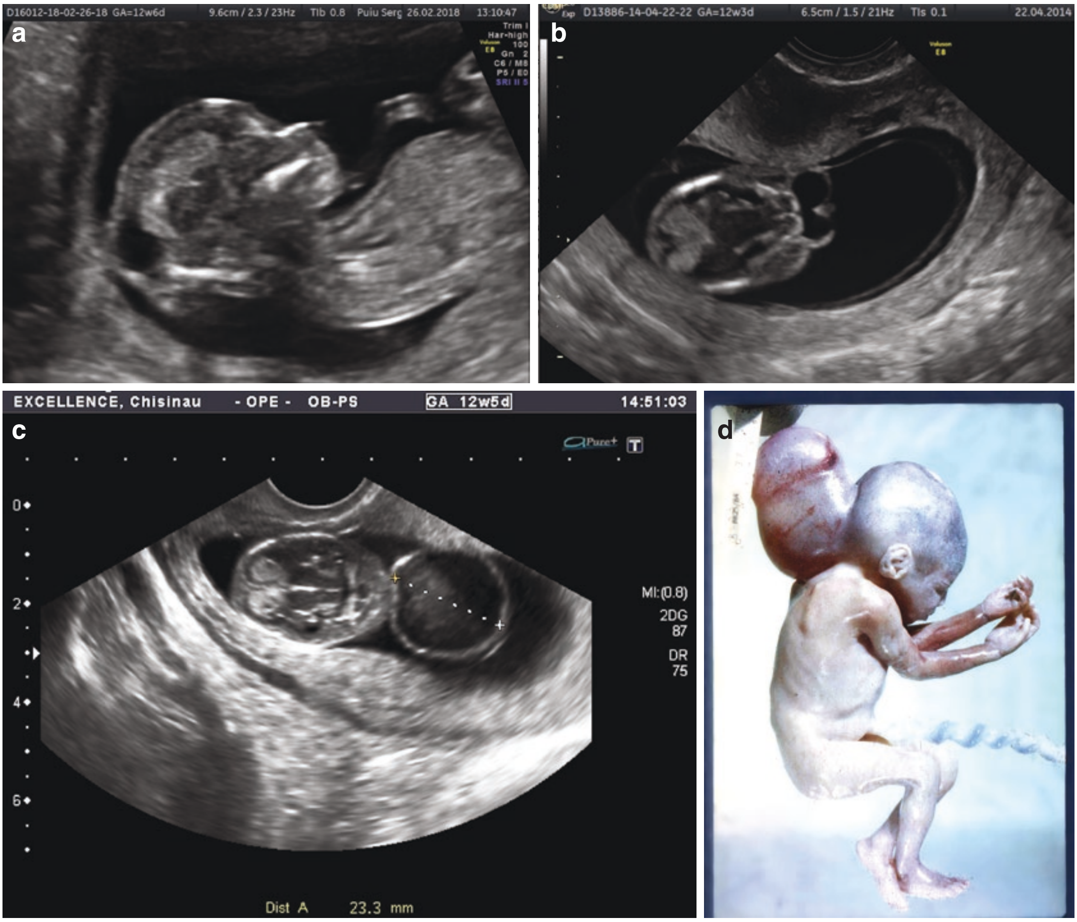
D16012-18-02-26-18 GA=12w6d 9.6cm / 2.3 / 23Hz TIb 0.8 Puiu Serg 26.02.2018 13:10:47
a
D13886-14-04-22-22 GA=12w3d 6.5cm / 1.5 / 21Hz TIs 0.1 22.04.2014
b
EXCELLENCE, Chisinau - OPE - OB-PS GA 12w5d 14:51:03
c
MI:(0.8)
2DG
87
DR
75
0
2
4
6
Dist A 23.3 mm
d

Fig. 20.29 Encephalocele. (**a**) Occipital encephalocele, 12 6/7 weeks; (**b**) occipital encephalocele, 12 3/7 weeks; (**c**) large occipital encephalocele, 12 5/7 weeks; (**d**) aborted fetus with large occipital encephalocele, 14 weeks

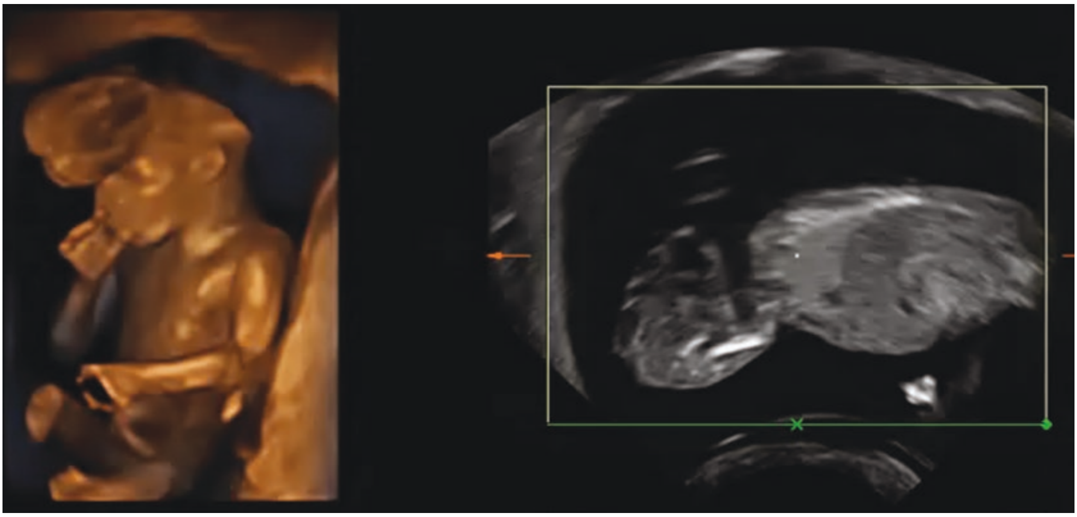

Fig. 20.30 Large frontal encephalocele, 12 weeks

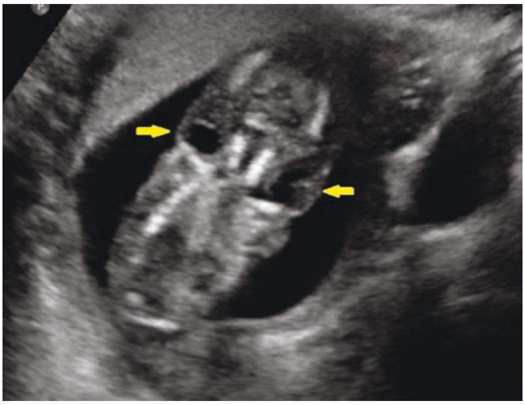

Fig. 20.31 Cystic hygroma of the neck: bilateral cystic structure in the fetal neck at 12 weeks (arrows)

lymphatic system, characterized by fluid-filled spaces, typically located at the fetal neck (Fig. 20.31). Cystic hygroma is commonly associated with fetal chromosomal aneuploidy in over 50% of cases [138, 139]. Even in eukaryotic fetuses, cystic hygroma is associated with a high risk of miscarriage and cardiopulmonary and skeletal abnormalities, in addition to disorders with a late postnatal onset such as Noonan syndrome [140–142]. Therefore, this finding should prompt invasive prenatal testing and if pregnancy is continued detailed fetal anatomy survey including a fetal echocardiogram.

Other Important Neck Masses and Tumors

Congenital masses/tumors may present as clear cystic masses (bronchogenic cyst), solid cystic masses (cervical teratoma), solid vascular mass (Hemangioma), and solid avascular mass (lymphangioma) [143]. These masses/tumors are relatively uncommon and slow growing and usually manifest with fetal symptomatology of neck extension/hyperextension and polyhydramnios after enlarging sufficiently [144]. This is probably the reason for diagnosis of these lesions in the late second and early third trimesters [144]. Furthermore, congenital goiters are also diagnosed beyond the first trimester [145], most likely due to initiation and completion of the fetal thyroid embryogenesis/organogenesis as well as functionality at the end of the first trimester [146, 147]. Hence, while these are important anomalies for the reader to be aware about, they are beyond the scope of this text.

Teaching Points

- The fetal face can be visualized by ultrasound from a GA of approximately 9 weeks.
- The transvaginal approach is, generally, preferred for detailed visualization.
- Clefts are the most common and micrognathia the second most common fetal facial anomalies.
- Many genetic disorders are characterized by facial structural or morphological anomalies.
- While performing a nuchal translucency scan, fetal profile, nose, eyes, and lips should be evaluated.

References

1. Som PM, Naidich TP. Illustrated review of the embryology and development of the facial region, Part 1: Early face and lateral nasal cavities. AJNR Am J Neuroradiol. 2013;34(12):2233–40.
2. Som PM, Naidich TP. Illustrated review of the embryology and development of the facial region, Part 2: Late development of the fetal face and changes in the face from the newborn to adulthood. AJNR Am J Neuroradiol. 2014;35(1):10–8.
3. Rossi AC, Prefumo F. Accuracy of ultrasonography at 11–14 weeks of gestation for detection of fetal structural anomalies: a systematic review. Obstet Gynecol. 2013;122(6):1160–7.
4. Karim JN, Roberts NW, Salomon LJ, Papageorghiou AT. Systematic review of first-trimester ultrasound screening for detection of fetal structural anomalies and factors that affect screening performance. Ultrasound Obstet Gynecol. 2017;50(4):429–41.
5. Salomon LJ, Alfirevic Z, Bilardo CM, Chalouhi GE, Ghi T, Kagan KO, et al. ISUOG practice guidelines: performance of first-trimester fetal ultrasound scan. Ultrasound Obstet Gynecol. 2013;41(1):102–13.
6. Merz E, Abramovicz J, Baba K, Blaas HG, Deng J, Gindes L, et al. 3D imaging of the fetal face - recommendations from the International 3D Focus Group. Ultraschall Med. 2012;33(2):175–82.
7. Jeanty P, Dramaix-Wilmet M, Van Gansbeke D, Van Regemorter N, Rodesch F. Fetal ocular biometry by ultrasound. Radiology. 1982;143(2):513–6.
8. Mayden KL, Tortora M, Berkowitz RL, Bracken M, Hobbins JC. Orbital diameters: a new parameter for

prenatal diagnosis and dating. Am J Obstet Gynecol. 1982;144(3):289–97.

9. Burns NS, Iyer RS, Robinson AJ, Chapman T. Diagnostic imaging of fetal and pediatric orbital abnormalities. AJR Am J Roentgenol. 2013;201(6):W797–808.
10. Trout T, Budorick NE, Pretorius DH, McGahan JP. Significance of orbital measurements in the fetus. J Ultrasound Med. 1994;13(12):937–43.
11. Roberto Romero GP, Jeanty P, Ghidini A, Hobbins J. Prenatal diagnosis of congenital anomalies: the face. Appleton and Lang; 2000.
12. Cohen MM Jr, Richieri-Costa A, Guion-Almeida ML, Saavedra D. Hypertelorism: interorbital growth, measurements, and pathogenetic considerations. Int J Oral Maxillofac Surg. 1995;24(6):387–95.
13. Holmes LB. Possible fetal effects of cervical dilation and uterine curettage during the first trimester of pregnancy. J Pediatr. 1995;126(1):131–4.
14. Park JP, Moeschler JB, Berg SZ, Bauer RM, Wurster-Hill DH. A unique de novo interstitial deletion del(17)(q21.3q23) in a phenotypically abnormal infant. Clin Genet. 1992;41(1):54–6.
15. Sarda P, Lefort G, Taviaux S, Humeau C, Rieu D. Interstitial deletion of chromosome 1 del (1) (q32 q42): case report and review of the literature. Clin Genet. 1992;41(1):25–7.
16. Ondeck CL, Pretorius D, McCaulley J, Kinori M, Maloney T, Hull A, et al. Ultrasonographic prenatal imaging of fetal ocular and orbital abnormalities. Surv Ophthalmol. 2018;63(6):745–53.
17. Benacerraf BR. Ultrasound diagnosis of fetal syndromes. 2nd ed. London: Churchill Livingstone; 2008.
18. Chrousos GA, Ross JL, Chrousos G, Chu FC, Kenigsberg D, Cutler G Jr, et al. Ocular findings in Turner syndrome. A prospective study. Ophthalmology. 1984;91(8):926–8.
19. Centerwall WR, Beatty-DeSana JW. The trisomy 9p syndrome. Pediatrics. 1975;56(5):748–55.
20. Dean JC, Simpson S, Couzin DA, Stephen GS. Interstitial deletion of chromosome 13: prognosis and adult phenotype. J Med Genet. 1991;28(8):533–5.
21. Society for Maternal-Fetal Medicine, Benacerraf BR, Bromley BS, Jelin AC. Hypertelorism. Am J Obstet Gynecol. 2019;221(5):B18–B9.
22. Judisch GF, Martin-Casals A, Hanson JW, Olin WH. Oculodentodigital dysplasia. Four new reports and a literature review. Arch Ophthalmol. 1979;97(5):878–84.
23. O'Rahilly RMF. The nervous system. New York: Wiley-Liss; 1994.
24. Cohen MM Jr, Jirasek JE, Guzman RT, Gorlin RJ, Peterson MQ. Holoprosencephaly and facial dysmorphia: nosology, etiology and pathogenesis. Birth Defects Orig Artic Ser. 1971;7(7):125–35.
25. Demyer W, Zeman W, Palmer CG. The face predicts the brain: diagnostic significance of median facial anomalies for holoprosencephaly (arhinencephaly). Pediatrics. 1964;34:256–63.
26. Pilu G, Romero R, Rizzo N, Jeanty P, Bovicelli L, Hobbins JC. Criteria for the prenatal diagnosis of holoprosencephaly. Am J Perinatol. 1987;4(1):41–9.
27. van Zalen-Sprock R, van Vugt JM, van der Harten HJ, Nieuwint AW, van Geijn HP. First trimester diagnosis of cyclopia and holoprosencephaly. J Ultrasound Med. 1995;14(8):631–3.
28. Dempsey RF, Monson LA, Maricevich RS, Truong TA, Olarunnipa S, Lam SK, et al. Nonsyndromic craniosynostosis. Clin Plast Surg. 2019;46(2):123–39.
29. Evans DG. Dominantly inherited microcephaly, hypotelorism and normal intelligence. Clin Genet. 1991;39(3):178–80.
30. Judisch GF, Kraft SP, Bartley JA, Jacoby CG. Orbital hypotelorism. An isolated autosomal dominant trait. Arch Ophthalmol. 1984;102(7):995–7.
31. Smith DW. Recognizable patterns of human malformation. 3rd ed. Philadelphia: WB Saunders Co; 1982. p. 619–20.
32. Gentile M, Volpe P, Cariola F, Di Carlo A, Marotta V, Buonadonna AL, et al. Prenatal diagnosis of chromosome 4 mosaicism: prognostic role of cytogenetic, molecular, and ultrasound/MRI characterization. Am J Med Genet A. 2005;136(1):66–70.
33. Twining P, Zuccollo J. The ultrasound markers of chromosomal disease: a retrospective study. Br J Radiol. 1993;66(785):408–14.
34. Society for Maternal-Fetal Medicine, Benacerraf BR, Bromley B, Jelin AC. Anophthalmia and microphthalmia. Am J Obstet Gynecol. 2019;221(5):B20–B1.
35. Ragge NK, Subak-Sharpe ID, Collin JR. A practical guide to the management of anophthalmia and microphthalmia. Eye (Lond). 2007;21(10):1290–300.
36. Araujo Junior E, Kawanami TE, Nardozza LM, Milani HJ, Oliveira PS, Moron AF. Prenatal diagnosis of bilateral anophthalmia by 3D "reverse face" view ultrasound and magnetic resonance imaging. Taiwan J Obstet Gynecol. 2012;51(4):616–9.
37. Shaw GM, Carmichael SL, Yang W, Harris JA, Finnell RH, Lammer EJ. Epidemiologic characteristics of anophthalmia and bilateral microphthalmia among 2.5 million births in California, 1989–1997. Am J Med Genet A. 2005;137(1):36–40.
38. Kallen B, Tornqvist K. The epidemiology of anophthalmia and microphthalmia in Sweden. Eur J Epidemiol. 2005;20(4):345–50.
39. Morrison D, FitzPatrick D, Hanson I, Williamson K, van Heyningen V, Fleck B, et al. National study of microphthalmia, anophthalmia, and coloboma (MAC) in Scotland: investigation of genetic aetiology. J Med Genet. 2002;39(1):16–22.
40. Busby A, Dolk H, Collin R, Jones RB, Winter R. Compiling a national register of babies born with anophthalmia/microphthalmia in England

1988–94. Arch Dis Child Fetal Neonatal Ed. 1998;79(3):F168–73.

41. Mashiach R, Vardimon D, Kaplan B, Shalev J, Meizner I. Early sonographic detection of recurrent fetal eye anomalies. Ultrasound Obstet Gynecol. 2004;24(6):640–3.
42. Allen JC, Venecia G, Opitz JM. Eye findings in the 13 trisomy syndrome. Eur J Pediatr. 1977;124(3):179–83.
43. Warburg M. Classification of microphthalmos and coloboma. J Med Genet. 1993;30(8):664–9.
44. Dobyns WB, Pagon RA, Armstrong D, Curry CJ, Greenberg F, Grix A, et al. Diagnostic criteria for Walker-Warburg syndrome. Am J Med Genet. 1989;32(2):195–210.
45. Pierson DM, Taboada E, Butler MG. Eye abnormalities in Fryns syndrome. Am J Med Genet A. 2004;125A(3):273–7.
46. Schauer GM, Dunn LK, Godmilow L, Eagle RC Jr, Knisely AS. Prenatal diagnosis of Fraser syndrome at 18.5 weeks gestation, with autopsy findings at 19 weeks. Am J Med Genet. 1990;37(4):583–91.
47. Paladini D, D'Armiento M, Ardovino I, Martinelli P. Prenatal diagnosis of the cerebro-oculo-facio-skeletal (COFS) syndrome. Ultrasound Obstet Gynecol. 2000;16(1):91–3.
48. Traboulsi EI, Lenz W, Gonzales-Ramos M, Siegel J, Macrae WG, Maumenee IH. The Lenz microphthalmia syndrome. Am J Ophthalmol. 1988;105(1):40–5.
49. Bronshtein M, Zimmer E, Gershoni-Baruch R, Yoffe N, Meyer H, Blumenfeld Z. First- and second-trimester diagnosis of fetal ocular defects and associated anomalies: report of eight cases. Obstet Gynecol. 1991;77(3):443–9.
50. Francis PJ, Berry V, Bhattacharya SS, Moore AT. The genetics of childhood cataract. J Med Genet. 2000;37(7):481–8.
51. Thut CJ, Rountree RB, Hwa M, Kingsley DM. A large-scale in situ screen provides molecular evidence for the induction of eye anterior segment structures by the developing lens. Dev Biol. 2001;231(1):63–76.
52. Karkinen-Jaaskelainen M, Saxen L, Vaheri A, Leinikki P. Rubella cataract in vitro: sensitive period of the developing human lens. J Exp Med. 1975;141(6):1238–48.
53. Vohra N, Ghidini A, Alvarez M, Lockwood C. Walker-Warburg syndrome: prenatal ultrasound findings. Prenat Diagn. 1993;13(7):575–9.
54. Basbug M, Serin IS, Ozcelik B, Gunes T, Akcakus M, Tayyar M. Prenatal ultrasonographic diagnosis of rhizomelic chondrodysplasia punctata by detection of rhizomelic shortening and bilateral cataracts. Fetal Diagn Ther. 2005;20(3):171–4.
55. Pedreira DA, Diniz EM, Schultz R, Faro LB, Zugaib M. Fetal cataract in congenital toxoplasmosis. Ultrasound Obstet Gynecol. 1999;13(4):266–7.
56. Arun V, Noble AG, Latkany P, Troia RN, Jalbrzikowski J, Kasza K, et al. Cataracts in congenital toxoplasmosis. J AAPOS. 2007;11(6):551–4.
57. Puder KS, Treadwell MC, Gonik B. Ultrasound characteristics of in utero infection. Infect Dis Obstet Gynecol. 1997;5(3):262–70.
58. Endres W, Schaub J, Stefani FH, Wirtz A, Zahn V. Cataract in a fetus at risk for oculo-cerebro-renal syndrome (Lowe). Klin Wochenschr. 1977;55(3):141–4.
59. Suchy SF, Lin T, Horwitz JA, O'Brien WE, Nussbaum RL. First report of prenatal biochemical diagnosis of Lowe syndrome. Prenat Diagn. 1998;18(11):1117–21.
60. Nishimura Y. Embryological study of nasal cavity development in human embryos with reference to congenital nostril atresia. Acta Anat (Basel). 1993;147(3):140–4.
61. Cohen D, Goitein KJ. Arhinia revisited. Rhinology. 1987;25(4):237–44.
62. Albernaz VS, Castillo M, Mukherji SK, Ihmeidan IH. Congenital arhinia. AJNR Am J Neuroradiol. 1996;17(7):1312–4.
63. Cusick W, Sullivan CA, Rojas B, Poole AE, Poole DA. Prenatal diagnosis of total arhinia. Ultrasound Obstet Gynecol. 2000;15(3):259–61.
64. Olsen OE, Gjelland K, Reigstad H, Rosendahl K. Congenital absence of the nose: a case report and literature review. Pediatr Radiol. 2001;31(4):225–32.
65. Takci S, Korkmaz A, Simsek-Kiper PO, Utine GE, Boduroglu K, Yurdakok M. Congenital partial arhinia: a rare malformation of the nose coexisting with holoprosencephaly. Turk J Pediatr. 2012;54(4):440–3.
66. Hansen M, Lucarelli MJ, Whiteman DA, Mulliken JB. Treacher Collins syndrome: phenotypic variability in a family including an infant with arhinia and uveal colobomas. Am J Med Genet. 1996;61(1):71–4.
67. Kaminker CP, Dain L, Lamas MA, Sanchez JM. Mosaic trisomy 9 syndrome with unusual phenotype. Am J Med Genet. 1985;22(2):237–41.
68. Pooh RK, Kurjak A. Novel application of three-dimensional HD live imaging in prenatal diagnosis from the first trimester. J Perinat Med. 2015;43(2):147–58.
69. Cicero S, Curcio P, Papageorghiou A, Sonek J, Nicolaides K. Absence of nasal bone in fetuses with trisomy 21 at 11–14 weeks of gestation: an observational study. Lancet. 2001;358(9294):1665–7.
70. Cicero S, Bindra R, Rembouskos G, Tripsanas C, Nicolaides KH. Fetal nasal bone length in chromosomally normal and abnormal fetuses at 11–14 weeks of gestation. J Matern Fetal Neonatal Med. 2002;11(6):400–2.
71. Kagan KO, Cicero S, Staboulidou I, Wright D, Nicolaides KH. Fetal nasal bone in screening for trisomies 21, 18 and 13 and Turner syndrome at 11–13 weeks of gestation. Ultrasound Obstet Gynecol. 2009;33(3):259–64.
72. Sonek JD, Cicero S, Neiger R, Nicolaides KH. Nasal bone assessment in prenatal screening for trisomy 21. Am J Obstet Gynecol. 2006;195(5):1219–30.

73. Sleurs E, Goncalves LF, Johnson A, Espinoza J, Devers P, Chaiworapongsa T, et al. First-trimester three-dimensional ultrasonographic findings in a fetus with frontonasal malformation. J Matern Fetal Neonatal Med. 2004;16(3):187–97.
74. Cook K, Prefumo F, Presti F, Homfray T, Campbell S. The prenatal diagnosis of Binder syndrome before 24 weeks of gestation: case report. Ultrasound Obstet Gynecol. 2000;16(6):578–81.
75. Society for Maternal-Fetal Medicine, Benacerraf BR, Bromley B, Jelin AC. Micrognathia. Am J Obstet Gynecol. 2019;221(5):B13–B5.
76. Paladini D. Fetal micrognathia: almost always an ominous finding. Ultrasound Obstet Gynecol. 2010;35(4):377–84.
77. Teoh M, Meagher S. First-trimester diagnosis of micrognathia as a presentation of Pierre Robin syndrome. Ultrasound Obstet Gynecol. 2003;21(6):616–8.
78. Xu BQ, Zhen L, Li DZ. First-trimester detection of micrognathia as a presentation of mandibulofacial dysostosis with microcephaly. J Obstet Gynaecol. 2021;41(5):821–3.
79. Zhen L, Yang YD, Xu LL, Cao Q, Li DZ. Fetal micrognathia in the first trimester: an ominous finding even after a normal array. Eur J Obstet Gynecol Reprod Biol. 2021;263:176–80.
80. Carvalho AP, Estevinho C, Coelho M, Rocha J, Marinho C, Rodrigues G. Abnormal fetal profile at first-trimester ultrasound scan complicated by severe polyhydramnios at the second half of pregnancy. J Med Ultrasound. 2021;29(1):65–7.
81. Galvao A, Inocêncio G, Rodrigues M. First trimester ultrasound detection of fetal micrognathia. Acta Obstet Ginecol Port. 2015;9(5):425–6.
82. Sepulveda W, Wong AE, Vinals F, Andreeva E, Adzehova N, Martinez-Ten P. Absent mandibular gap in the retronasal triangle view: a clue to the diagnosis of micrognathia in the first trimester. Ultrasound Obstet Gynecol. 2012;39(2):152–6.
83. Rotten D, Levaillant JM, Martinez H, Ducou le Pointe H, Vicaut E. The fetal mandible: a 2D and 3D sonographic approach to the diagnosis of retrognathia and micrognathia. Ultrasound Obstet Gynecol. 2002;19(2):122–30.
84. Li H, Zhu Z. Ultrasonographic study of fetal mandibular markers during the first trimester in a Chinese population. J Obstet Gynaecol Res. 2022;48(2):333–9.
85. Antonakopoulos N, Bhide A. Focus on prenatal detection of micrognathia. J Fetal Med. 2019;6:107–12.
86. Ji C, Jiang X, Yin L, Deng X, Yang Z, Pan Q, et al. Ultrasonographic study of fetal facial profile markers during the first trimester. BMC Pregnancy Childbirth. 2021;21(1):324.
87. Faye-Petersen O, David E, Rangwala N, Seaman JP, Hua Z, Heller DS. Otocephaly: report of five new cases and a literature review. Fetal Pediatr Pathol. 2006;25(5):277–96.
88. Johnston MC, Sulik KK. Some abnormal patterns of development in the craniofacial region. Birth Defects Orig Artic Ser. 1979;15(8):23–42.
89. Gekas J, Li B, Kamnasaran D. Current perspectives on the etiology of agnathia-otocephaly. Eur J Med Genet. 2010;53(6):358–66.
90. Rodriguez N, Casasbuenas A, Andreeva E, Odegova N, Wong AE, Sepulveda W. First-trimester diagnosis of agnathia-otocephaly complex: a series of 4 cases and review of the literature. J Ultrasound Med. 2019;38(3):805–9.
91. Huissoud C, La Mela Jumel A, Bisch C, Dijoud F, Pages O, Rudigoz RC. Take a look at the CHIN!—early diagnosis of isolated agnathia using two- and three-dimensional sonography. Fetal Diagn Ther. 2008;24(3):246–9.
92. Weiss LS, White JA. Macroglossia: a review. J La State Med Soc. 1990;142(8):13–6.
93. Weissman A, Mashiach S, Achiron R. Macroglossia: prenatal ultrasonographic diagnosis and proposed management. Prenat Diagn. 1995;15(1):66–9.
94. Vogel JE, Mulliken JB, Kaban LB. Macroglossia: a review of the condition and a new classification. Plast Reconstr Surg. 1986;78(6):715–23.
95. Achiron R, Ben Arie A, Gabbay U, Mashiach S, Rotstein Z, Lipitz S. Development of the fetal tongue between 14 and 26 weeks of gestation: in utero ultrasonographic measurements. Ultrasound Obstet Gynecol. 1997;9(1):39–41.
96. Bronshtein M, Zimmer EZ, Tzidony D, Hajos J, Jaeger M, Blazer S. Transvaginal sonographic measurement of fetal lingual width in early pregnancy. Prenat Diagn. 1998;18(6):577–80.
97. Eckmann-Scholz C, Jonat W. 3-D ultrasound imaging of a prenatally diagnosed Beckwith-Wiedemann syndrome. Arch Gynecol Obstet. 2011;284(4):1051–2.
98. Nicolaides KH, Salvesen DR, Snijders RJ, Gosden CM. Fetal facial defects: associated malformations and chromosomal abnormalities. Fetal Diagn Ther. 1993;8(1):1–9.
99. Gull I, Wolman I, Har-Toov J, Amster R, Schreiber L, Lessing JB, et al. Antenatal sonographic diagnosis of epignathus at 15 weeks of pregnancy. Ultrasound Obstet Gynecol. 1999;13(4):271–3.
100. Campbell S. Prenatal ultrasound examination of the secondary palate. Ultrasound Obstet Gynecol. 2007;29(2):124–7.
101. Dixon MJ, Marazita ML, Beaty TH, Murray JC. Cleft lip and palate: understanding genetic and environmental influences. Nat Rev Genet. 2011;12(3):167–78.
102. Grosen D, Bille C, Petersen I, Skytthe A, Hjelmborg J, Pedersen JK, et al. Risk of oral clefts in twins. Epidemiology. 2011;22(3):313–9.
103. Murray JC. Gene/environment causes of cleft lip and/or palate. Clin Genet. 2002;61(4):248–56.
104. Wyszynski DF, Beaty TH. Review of the role of potential teratogens in the origin of human nonsyndromic oral clefts. Teratology. 1996;53(5):309–17.

105. Society for Maternal-Fetal Medicine, Benacerraf BR, Bromley B, Jelin AC. Paramedian orofacial cleft. Am J Obstet Gynecol. 2019;221(5):B8–B12.
106. Chaoui R, Orosz G, Heling KS, Sarut-Lopez A, Nicolaides KH. Maxillary gap at 11–13 weeks' gestation: marker of cleft lip and palate. Ultrasound Obstet Gynecol. 2015;46(6):665–9.
107. Sepulveda W, Wong AE, Martinez-Ten P, Perez-Pedregosa J. Retronasal triangle: a sonographic landmark for the screening of cleft palate in the first trimester. Ultrasound Obstet Gynecol. 2010;35(1):7–13.
108. Martinez Ten P, Perez Pedregosa J, Santacruz B, Adiego B, Barron E, Sepulveda W. Three-dimensional ultrasound diagnosis of cleft palate: 'reverse face', 'flipped face' or 'oblique face'—which method is best? Ultrasound Obstet Gynecol. 2009;33(4):399–406.
109. Offerdal K, Jebens N, Syvertsen T, Blaas HG, Johansen OJ, Eik-Nes SH. Prenatal ultrasound detection of facial clefts: a prospective study of 49,314 deliveries in a non-selected population in Norway. Ultrasound Obstet Gynecol. 2008;31(6):639–46.
110. Gillham JC, Anand S, Bullen PJ. Antenatal detection of cleft lip with or without cleft palate: incidence of associated chromosomal and structural anomalies. Ultrasound Obstet Gynecol. 2009;34(4):410–5.
111. de Boutray M, Beziat JL, Yachouh J, Bigorre M, Gleizal A, Captier G. Median cleft of the upper lip: a new classification to guide treatment decisions. J Craniomaxillofac Surg. 2016;44(6):664–71.
112. Pooh RK. Prenatal diagnosis of low set ears with asymmetrical microtia in the first trimester. Donald School J Ultrasound Obstet Gynecol. 2016;10(2):111–2.
113. Melnick M, Myrianthopoulos NC, Paul NW. External ear malformations: epidemiology, genetics, and natural history. Birth Defects Orig Artic Ser. 1979;15(9):i–ix, 1–140.
114. Dudarewicz L, Kaluzewski B. Prenatal screening for fetal chromosomal abnormalities using ear length and shape as an ultrasound marker. Med Sci Monit. 2000;6(4):801–6.
115. Hartung B, Schweckendiek W. Malformations of the ear in cleft palate patients. J Maxillofac Surg. 1973;1(4):253–8.
116. Ellwood LC, Winter ST, Dar H. Familial microtia with meatal atresia in two sibships. J Med Genet. 1968;5(4):289–91.
117. Livingstone G. Congenital ear abnormalities due to thalidomide. Proc R Soc Med. 1965;58(7):493–7.
118. Mondal D, Shenoy RS, Mishra S. Retinoic acid embryopathy. Int J Appl Basic Med Res. 2017;7(4):264–5.
119. Ishimoto S, Ito K, Karino S, Takegoshi H, Kaga K, Yamasoba T. Hearing levels in patients with microtia: correlation with temporal bone malformation. Laryngoscope. 2007;117(3):461–5.
120. Aase JM. Microtia—clinical observations. Birth Defects Orig Artic Ser. 1980;16(4):289–97.
121. Alasti F, Van Camp G. Genetics of microtia and associated syndromes. J Med Genet. 2009;46(6):361–9.
122. Pont SJ, Robbins JM, Bird TM, Gibson JB, Cleves MA, Tilford JM, et al. Congenital malformations among liveborn infants with trisomies 18 and 13. Am J Med Genet A. 2006;140(16):1749–56.
123. Milic A, Blaser S, Robinson A, Viero S, Halliday W, Winsor E, et al. Prenatal detection of microtia by MRI in a fetus with trisomy 22. Pediatr Radiol. 2006;36(7):706–10.
124. Mastroiacovo P, Corchia C, Botto LD, Lanni R, Zampino G, Fusco D. Epidemiology and genetics of microtia-anotia: a registry based study on over one million births. J Med Genet. 1995;32(6):453–7.
125. Feingold M, Bossert WH. Normal values for selected physical parameters: an aid to syndrome delineation. Birth Defects Orig Artic Ser. 1974;10(13):1–16.
126. Heulens I, Suttie M, Postnov A, De Clerck N, Perrotta CS, Mattina T, et al. Craniofacial characteristics of fragile X syndrome in mouse and man. Eur J Hum Genet. 2013;21(8):816–23.
127. Child AH. Non-cardiac manifestations of Marfan syndrome. Ann Cardiothorac Surg. 2017;6(6):599–609.
128. Graham JM Jr, Anyane-Yeboa K, Raams A, Appeldoorn E, Kleijer WJ, Garritsen VH, et al. Cerebro-oculo-facio-skeletal syndrome with a nucleotide excision-repair defect and a mutated XPD gene, with prenatal diagnosis in a triplet pregnancy. Am J Hum Genet. 2001;69(2):291–300.
129. Fryns JP, Legius E, Moerman P, Vandenberghe K, Van den Berghe H. Apparently new "anophthalmia-plus" syndrome in sibs. Am J Med Genet. 1995;58(2):113–4.
130. Lehman CD, Nyberg DA, Winter TC III, Kapur RP, Resta RG, Luthy DA. Trisomy 13 syndrome: prenatal US findings in a review of 33 cases. Radiology. 1995;194(1):217–22.
131. Nunez-Castruita A, Lopez-Serna N. Low-set ears and associated anomalies in human foetuses. Int J Pediatr Otorhinolaryngol. 2018;104:126–33.
132. Del Campo M, Kosaki K, Bennett FC, Jones KL. Developmental delay in fetal aminopterin/methotrexate syndrome. Teratology. 1999;60(1):10–2.
133. Sepulveda W, Wong AE, Andreeva E, Odegova N, Martinez-Ten P, Meagher S. Sonographic spectrum of first-trimester fetal cephalocele: review of 35 cases. Ultrasound Obstet Gynecol. 2015;46(1):29–33.
134. Sepulveda W, Wong AE, Fauchon DE. Fetal spinal anomalies in a first-trimester sonographic screening program for aneuploidy. Prenat Diagn. 2011;31(1):107–14.
135. Daskalakis G, Sebire NJ, Jurkovic D, Snijders RJ, Nicolaides KH. Body stalk anomaly at 10–14 weeks of gestation. Ultrasound Obstet Gynecol. 1997;10(6):416–8.
136. Rottem S, Bronshtein M, Thaler I, Brandes JM. First trimester transvaginal sonographic diagnosis of fetal anomalies. Lancet. 1989;1(8635):444–5.
137. Bronshtein M, Rottem S, Yoffe N, Blumenfeld Z. First-trimester and early second-trimester diag-

nosis of nuchal cystic hygroma by transvaginal sonography: diverse prognosis of the septated from the nonseptated lesion. Am J Obstet Gynecol. 1989;161(1):78–82.

138. van Zalen-Sprock RM, van Vugt JM, van Geijn HP. First-trimester diagnosis of cystic hygroma—course and outcome. Am J Obstet Gynecol. 1992;167(1):94–8.
139. Economides DL, Whitlow BJ, Kadir R, Lazanakis M, Verdin SM. First trimester sonographic detection of chromosomal abnormalities in an unselected population. Br J Obstet Gynaecol. 1998;105(1):58–62.
140. Nicolaides KH, Heath V, Cicero S. Increased fetal nuchal translucency at 11–14 weeks. Prenat Diagn. 2002;22(4):308–15.
141. Senat MV, De Keersmaecker B, Audibert F, Montcharmont G, Frydman R, Ville Y. Pregnancy outcome in fetuses with increased nuchal translucency and normal karyotype. Prenat Diagn. 2002;22(5):345–9.
142. Graesslin O, Derniaux E, Alanio E, Gaillard D, Vitry F, Quereux C, et al. Characteristics and outcome of fetal cystic hygroma diagnosed in the first trimester. Acta Obstet Gynecol Scand. 2007;86(12):1442–6.
143. Rauff S, Kien TE. Ultrasound diagnosis of fetal neck masses: a case series. Case Rep Obstet Gynecol. 2013;2013:243590.
144. Sheikh F, Akinkuotu A, Olutoye OO, Pimpalwar S, Cassady CI, Fernandes CJ, et al. Prenatally diagnosed neck masses: long-term outcomes and quality of life. J Pediatr Surg. 2015;50(7):1210–3.
145. Mastrolia SA, Mandola A, Mazor M, Hershkovitz R, Mesner O, Beer-Weisel R, et al. Antenatal diagnosis and treatment of hypothyroid fetal goiter in an euthyroid mother: a case report and review of literature. J Matern Fetal Neonatal Med. 2015;28(18):2214–20.
146. Trueba SS, Auge J, Mattei G, Etchevers H, Martinovic J, Czernichow P, et al. PAX8, TITF1, and FOXE1 gene expression patterns during human development: new insights into human thyroid development and thyroid dysgenesis-associated malformations. J Clin Endocrinol Metab. 2005;90(1):455–62.
147. Kratzsch J, Pulzer F. Thyroid gland development and defects. Best Pract Res Clin Endocrinol Metab. 2008;22(1):57–75.

21

Fetal Gastrointestinal and Abdominal Wall Imaging

Desiree G. Fiorentino and Ryan E. Longman

Introduction

Recently, there has been increasing attention paid to the possibility of identifying sonographic findings characteristic of congenital anomalies in the first trimester. The nuchal translucency scan that is typically performed between 11 and 13 weeks and 6 days is a good opportunity to assess general fetal anatomy. Of the various components of the fetal gastrointestinal system and abdominal wall, many can be consistently visualized in the first trimester, particularly those that are fluid filled including the stomach. Others, like the fetal esophagus, are not routinely assessed in early gestation. Similarly, while there are many anatomic abnormalities that cannot be identified in early gestation, there exist several that can be reliably diagnosed in the first trimester, including fetal abdominal wall defects such as gastroschisis and omphalocele [1].

Embryology

In order to properly assess the fetal abdominal contents and integrity of the abdominal wall at less than 14 weeks, a general understanding of their embryonic origins is required (see also Chap. 5). The development of the fetal gastrointestinal tract (GI tract) begins in the fifth and sixth weeks of gestation and involves all three germ layers. The endoderm gives rise to the mucosal epithelium as well as the mucosal and submucosal glands; the mesoderm becomes the submucosal connective tissue, smooth muscle, and serosa; and the ectoderm further differentiates into the neural crest, which is the source of the peripheral nervous system including the nerves of the submucosal and myenteric plexuses that innervate the GI tract.

The initially hollow primitive gut tube forms when the embryonic disc folds to incorporate the dorsal aspect of the yolk sac into the embryo resulting in a cylinder of endodermal cells surrounded by mesoderm. As the tube develops, rapid proliferation of the endoderm leads to temporary occlusion of the tube. Subsequent recanalization normally occurs by week 8 of gestation, but errors of this process can occur anywhere along the tube (from esophagus to anus) resulting in stenosis or atresia.

Once the primitive gut tube is formed, further folding of the cranial, lateral, and caudal sections leads to the formation of the three divisions of the

D. G. Fiorentino (✉)
Division of Maternal-Fetal Medicine, Department of Obstetrics & Gynecology and Women's Health, Montefiore Medical Center/Albert Einstein College of Medicine, Bronx, NY, USA
e-mail: dfiorentin@montefiore.org

R. E. Longman
Department of Obstetrics and Gynecology, University of Chicago Pritzker School of Medicine, Chicago, IL, USA
e-mail: relongman@bsd.uchicago.edu

© The Author(s), under exclusive license to Springer Nature Switzerland AG 2023

J. S. Abramowicz, R. E. Longman (eds.), *First-Trimester Ultrasound*,
https://doi.org/10.1007/978-3-031-24133-8_21

GI tract: the foregut, midgut, and hindgut. The foregut receives its blood supply from the branches of the celiac artery and gives rise to the trachea and respiratory tract, esophagus, stomach, liver, gallbladder and bile ducts, dorsal and ventral pancreas, and upper duodenum. The midgut receives its blood supply from the branches of the superior mesenteric artery and gives rise to the lower duodenum, jejunum, ileum, cecum, ascending colon, and proximal two-thirds of transverse colon. The hindgut receives its blood supply from the branches of the inferior mesenteric artery and gives rise to the distal one-third of the transverse colon, descending colon, sigmoid colon, rectum, upper anal canal, and urogenital sinus [2].

Esophagus

The fetal esophagus is normally a collapsed structure that is not routinely assessed with ultrasonography. However, when specific efforts are made to visualize it, it can often be visualized in the first trimester. In a study of 102 fetuses at 11–14 weeks' gestation, the esophagus was identified in 88.2% using the bright echogenic transverse section of the esophagus in the area behind the heart as a reference point [3]. Once the transverse section of the esophagus is identified, the probe can then be rotated 90° to visualize the longitudinal section and trace its course. The descending thoracic aorta is another easily visualized anatomic landmark that can be used to identify the fetal esophagus as it will be found anterior to the aorta when in the longitudinal coronal plane.

Esophageal Atresia

Esophageal atresia is a multifactorial, sporadic condition characterized by an esophagus ending in a blind-ended pouch, with or without a coexisting tracheoesophageal fistula. It will not be discussed in great detail in this text as it is not easily diagnosed in the first trimester [1]. An absent fetal stomach and polyhydramnios are the typical findings of this entity in pregnancy and are not usually seen until the second or third trimester. This is partially because the fetus begins to swallow amniotic fluid around 16 weeks so that the fetal stomach is primarily filled with gastric secretions in the first trimester [4].

Stomach

The fluid-filled, and thus hypoechoic fetal, stomach is one of the earliest and most consistently sonographically identified components of the gastrointestinal system. At 11–14 weeks, the stomach and bladder should be the only hypoechoic fluid structures in the abdomen, making its identification on sagittal and axial scans easy [5]. In some fetuses, it can be visualized as a left-sided cavity in the upper abdomen as early as 8 weeks [6]. In a study of 1144 women with singleton pregnancies undergoing transabdominal and transvaginal ultrasound at 11–14 weeks, 99% of fetuses had an identifiable fetal stomach [7]. A small or absent stomach is most often a transient finding in an otherwise normal fetus, and as discussed above, esophageal atresia is not reliably diagnosed in the first trimester and cannot be excluded based on the presence of a fluid-filled stomach.

The reliable detection of the stomach in early gestation is an important component of the assessment of situs visceralis, and the International Society of Ultrasound in Obstetrics and Gynecology (ISUOG) recommends assessing the position of the stomach during the first-trimester fetal ultrasound scan [5]. In normal abdominal situs, the stomach occupies the left side of the abdomen on an axial view, with the liver and possibly the gallbladder (depending on gestational age) located on the right side.

Right-Sided Fetal Stomach

A right-sided fetal stomach can be seen in the first trimester and can be the first indication of heterotaxy or complex cardiac anomalies [1, 6]. Heterotaxy is an abnormal positioning of the thoracic and abdominal organs, usually with significant associated cardiac anomalies, and is caused by disruption of the left-right axis orientation during early development. Right-sided positioning of the fetal stomach can also be an early sign of primary ciliary dyskinesia with situs inversus totalis. Rarely, an isolated right-sided fetal stomach, also called dextrogastria, can occur [8]. Given the likelihood of associated anomalies, all fetuses with a right-sided stomach noted in early gestation should undergo a detailed assessment of other organ systems as well as a follow-up ultrasound and fetal echo.

Bowel, Liver, and Gallbladder

After approximately 12 weeks, the entire fetal bowel should be intra-abdominal. In the first trimester, the bowel lumen appears collapsed and there are not many distinct anatomic landmarks within the small or large intestines. The small bowel, with discrete bowel loops, becomes progressively more visible throughout the second trimester, and the colon is normally not visualized until the beginning of the third trimester. Nonetheless, there are anomalies of the bowel that can be recognized in early gestation.

The liver is the largest parenchymal organ in the gastrointestinal system. Further, it is proportionally larger in the fetus than in the child or the adult. In an axial plane of the upper abdomen, the normal liver occupies most of the right side of the fetus. In the sagittal and coronal planes, the liver is separated from the lungs by the diaphragm and appears less echogenic than both the lungs and bowel (Fig. 21.1). The fetal gallbladder is a teardrop-shaped hypoechoic structure in the right upper quadrant that can be visualized in about half of the fetuses at 13 weeks and almost all fetuses by 14 weeks [9]. An apparently absent gallbladder is usually a transient finding, and a follow-up ultrasound should be performed.

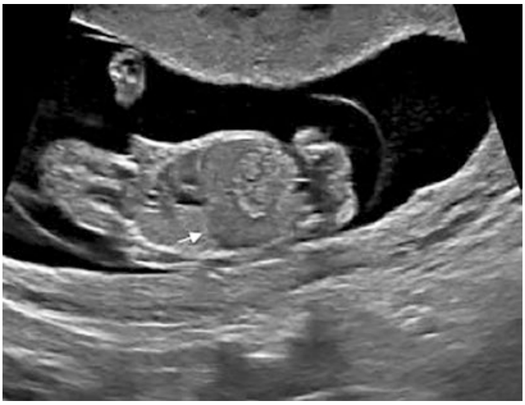

Fig. 21.1 Coronal view of a 12-week fetus showing the liver separated from the lungs by the diaphragm (arrow). The liver is hypoechoic when compared to lungs and bowel, and the bladder appears as an anechoic structure in the pelvis

Echogenic Bowel

Echogenic bowel, also called hyperechoic bowel, is a nonspecific finding characterized by the abnormal appearance of the bowel with echogenicity similar to surrounding bone. This can best be observed by decreasing the overall image gain until only bone is visible. If bowels are still observed, this is diagnostic of echogenic bowels. The frequency of the transducer used can affect the appearance of the bowel, and thus a suspicion of echogenic bowel should be confirmed with a low-frequency transducer (<5 MHz) and with machine harmonics turned off [10].

The etiology of echogenic bowel is thought to be excessively thick meconium resulting from decreased intestinal peristalsis or increased water resorption [11]. The differential diagnosis when echogenic bowel is seen is broad and includes aneuploidy in 10%, TORCH (toxoplasmosis, other agents, rubella, cytomegalovirus, herpes simplex) infections, cystic fibrosis, placental hemorrhage, ischemia, or simply a normal variant. Additionally, approximately half of the fetuses with echogenic bowel have other anomalies or fetal growth restriction and a detailed assessment of other organ systems is recommended [11].

Duodenal Atresia

Intestinal atresias are complete obstructions of the bowel lumen that produce a distended proximal GI tract. Most are difficult to appreciate until the second or third trimester when increased fetal swallowing of amniotic fluid may expose the obstruction and also cause polyhydramnios [1]. Duodenal atresia arises from failure of recanalization of the gut tube during intestinal development [2]. The characteristic prenatal ultrasound finding of duodenal atresia is the "double-bubble sign" created by a dilated stomach and proximal duodenum connected by a thin echolucent band. When detected prenatally, this entity is significantly associated with trisomy 21 in up to one-third of cases [12].

While several studies on the detection of fetal anomalies in the first trimester note that duodenal atresia was not picked up until the second trimester at the earliest, there have been individual reports of diagnosis in early gestation [1, 13–17]. As such, while duodenal atresia generally cannot, reliably, be detected during the first-trimester scan, rarely the characteristic double bubble may be seen in the upper abdomen and if located should prompt further evaluation.

Anorectal Atresia

Anorectal atresia is also often referred to as imperforate anus. In normal embryology, the hindgut ends in a pouch called the cloaca that is shared with the developing urogenital tract. A urorectal septum then divides the cloaca ventrally into the urogenital sinus and dorsally into the rectoanal canal. The portion of the cloaca adjacent to the ectoderm of the skin ultimately breaks down to create the anus. Failure of this anal membrane to rupture can lead to an imperforate anus [2]. This anomaly occurs more often in male fetuses and is associated with other malformations including renal abnormalities, skeletal lesions, esophageal atresia or tracheoesophageal fistula, and cardiac anomalies in 40% of cases [18]. It can also be seen as a part of VACTERL association or with aneuploidies.

The majority of anorectal atresias are not detected prenatally in any trimester. When they are identified, the findings vary throughout gestation. The most commonly identified first-trimester sign of an anorectal malformation is a dilated colon that presents as a tubular cystic mass in the lower abdomen and that is clearly delineated from the urinary bladder [18–20]. This cystic structure often resolves in the second trimester only to reappear in late gestation [21, 22]. The majority of published case series and case reports of first-trimester anorectal atresia were diagnosed between 11 and 14 weeks [18–20]. While an anorectal atresia can be difficult to diagnose in the first trimester, the reported incidence of colonic dilation in the first and third, but not second, trimesters indicates that it may be missed when a midtrimester scan is performed in the absence of a first-trimester scan. Additionally, a lower abdominal cystic mass that resolves in the second trimester should raise suspicion for a duodenal atresia and a third-trimester follow-up ultrasound should be performed.

Abdominal Cysts

In addition to intestinal obstructions, as discussed above, there are other potential etiologies for an abdominal cyst identified in a first-trimester fetus. As a group, abdominal cysts seen in early gestation are rare, but with the use of improving image resolution and transvaginal ultrasonography, their reported incidence is increasing [23]. Cysts can originate in the bowel, bladder, kidneys, ovary, mesentery, liver, or gallbladder/biliary system, but the origin of many first-trimester abdominal cysts is not identified. The majority of cysts are isolated findings, and spontaneous antenatal resolution occurs in up to 80% of cases [23–25]. Anechoic simple cysts that resolve in gestation are associated with euploid fetuses and have a good prognosis. Conversely, a cyst that does not resolve or that is associated with other abnormalities has a worse prognosis. Rarely, hepatic cysts and enteric duplication can also be visualized in the abdomen during the first trimester [15, 23, 26]. While expectant management and expectation of a good outcome are appropriate when an isolated anechoic abdominal cyst is seen in the first trimester, the association with anorectal atresia, as discussed above, and the occasional presence of associated anomalies suggest that follow-up ultrasonography and assessment of other organ systems are appropriate.

Abdominal Wall

Ultrasound of the fetal abdomen in the first trimester should always include evaluation of the abdominal wall. After 12 weeks, when physiologic midgut herniation (discussed below) has resolved, the normal insertion of the umbilical cord should also be documented [5]. At 12 weeks of gestation and beyond, an axial or parasagittal view of the abdomen should demonstrate an intact abdominal wall and normal cord insertion (Fig. 21.2). Color Doppler flow may aid with this visualization.

Beyond 12 weeks of gestation, ventral wall defects can reliably be seen with detection rates approaching 90–100% for omphalocele, gastroschisis, and limb body stalk anomaly in the first trimester [1, 13–15, 27].

Physiologic Midgut Herniation (Umbilical Hernia)

As early as 7–8 weeks of gestation, the bowel grows faster than the abdominal cavity. As a result of this elongation, the intestines temporarily move out of the limited space of the abdomen and herniate into the extraembryonic coelom of the umbilical cord [28]. By 7–8 weeks of gestation, this process can be sonographically visualized as a thickening of the umbilical cord at its insertion into the abdomen [6]. The umbilical hernia becomes most distinct by 9–10 weeks and can be seen as a hyperechogenic mass at the base of the umbilical cord (Fig. 21.3). During this herniation, the bowel rotates 90° counterclockwise (looking at the fetus). Midgut herniation should not measure more than 7 mm in maximum dimensions at any gestational age and should resolve by 10–11 weeks or by the time the fetus attains a crown-rump length of 45 mm [6, 29]. As the bowel returns to the abdomen, it rotates an additional 180° counterclockwise [28, 30]. Defects in rotation can lead to volvulus of the gut, possibly resulting in stenosis [2].

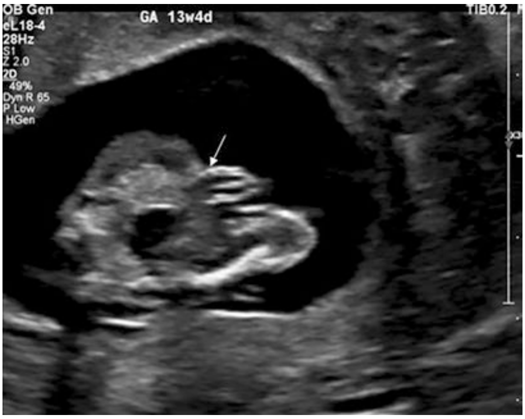

Fig. 21.2 Normal cord insertion (arrow) and an intact abdominal wall in a fetus at 13 weeks and 4 days gestation

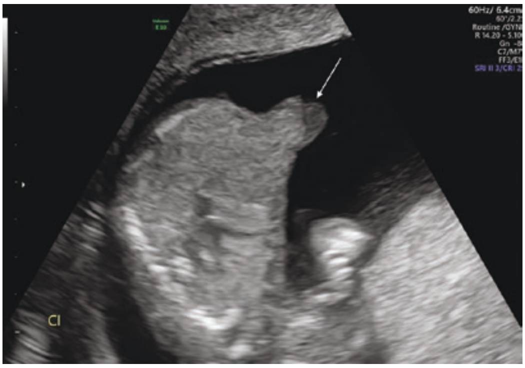

Fig. 21.3 Physiologic umbilical hernia at 10 weeks' gestation

Omphalocele

Omphalocele, also referred to as exomphalos, is a midline ventral wall defect with herniation of the abdominal viscera into the base of the umbilical cord. It is thought to arise from a defect in embryonic lateral wall fusion resulting in the persistent herniation of intestinal loops and possibly other abdominal viscera, in the umbilical cord, following physiologic midgut herniation [2]. Omphaloceles are covered by a membrane composed of amnion and peritoneum though this sac can, rarely, rupture prenatally. Sac contents typically include bowel but may also include liver, stomach, and bladder. The diagnosis of a small omphalocele cannot be definitively made before 12 weeks as physiologic midgut herniation has a similar appearance. Additionally, while the majority of physiologic umbilical hernias resolve by 11–12 weeks, isolated small omphaloceles containing bowel only have been described to resolve and may be thought of as representing delayed resolution of physiologic herniation [31]. It is important to note, however, that midgut herniation will never contain liver.

Up to 40% of fetuses with an omphalocele have chromosomal abnormalities with trisomy 18 being the most common followed by trisomy 13 and trisomy 21 [32, 33]. There is an inverse correlation between sac size and presence of aneuploidy with small omphaloceles with associated thickened nuchal translucencies having the highest rates of chromosomal abnormalities. Additionally, the rates of aneuploidy are higher at earlier gestational ages. Overall, up to 70% of omphaloceles are found with other malformations including cardiac defects, gastrointestinal atresias, renal anomalies, central nervous system malformations, and duplication cysts [34–36]. An omphalocele can also be a component of a genetic syndrome like Beckwith-Wiedemann, which is diagnosed in approximately 20% of isolated omphaloceles [37]. The prognosis of an omphalocele diagnosed in early gestation depends on the presence of other anomalies, syndromes, or aneuploidies.

Sonographically, omphaloceles are composed of exteriorized abdominal viscera covered by a thin membrane (Figs. 21.4, 21.5, and 21.6). The umbilical cord passes through the mass and inserts on the dome of the sac. Color Doppler may help confirm the cord attachment (Fig. 21.7). Ascites or Wharton jelly may be seen inside the sac.

Gastroschisis

Gastroschisis is a full-thickness paraumbilical defect allowing visceral herniation adjacent to an intact umbilical cord insertion site. Unlike omphalocele, gastroschisis is not covered by a

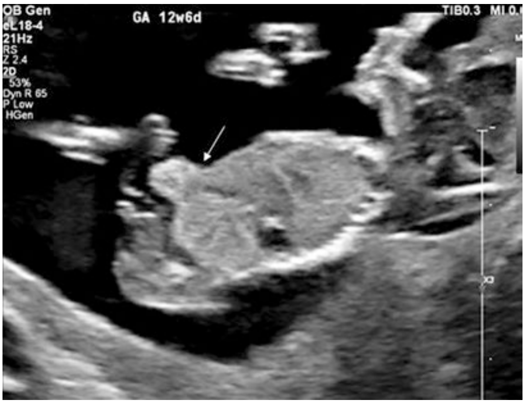

Fig. 21.4 Parasagittal view of a fetus at 12 weeks and 6 days with an omphalocele (arrow). Note the smooth appearance of the abdominal protrusion covered by membrane

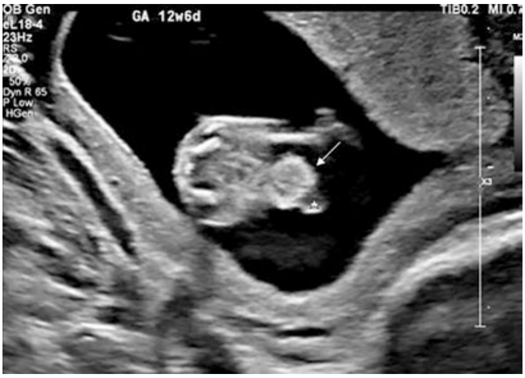

Fig. 21.5 Axial view of the same fetus in Fig. 21.4 again demonstrating the presence of an omphalocele (arrow). The umbilical cord can be seen inserting at the dome of the sac (star)

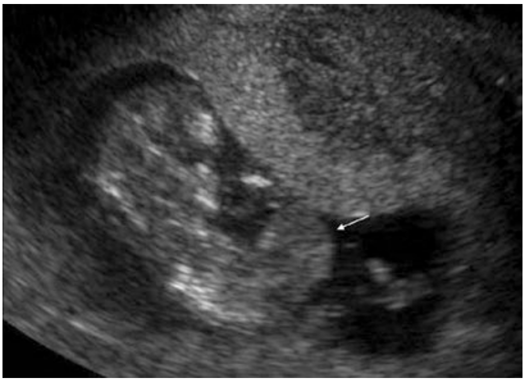

Fig. 21.6 Parasagittal view of two additional late first-trimester fetuses again demonstrating the smooth border of an omphalocele (arrow)

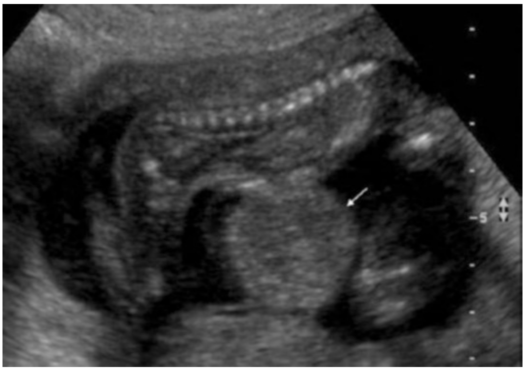

Fig. 21.6 (continued)

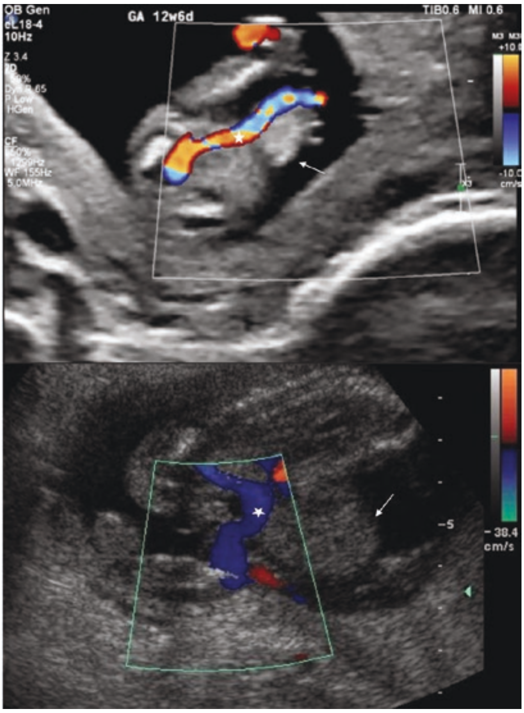

Fig. 21.7 Color Doppler demonstrates the location of the umbilical cord (star) in two fetuses with omphalocele (arrow) at 12 weeks and 6 days

membrane and typically does not involve the liver. Additionally, it is usually isolated and most often occurs in euploid fetuses. Risk factors for gastroschisis include young maternal age and smoking. The etiology is unclear and thought to be due to failure of embryonic mesenchyme to differentiate, leading to defective abdominal wall mesoderm, abnormal body wall folding, amnion rupture at the base of the umbilical ring during physiologic gut herniation, or vascular lesions involving the right umbilical vein or right vitelline artery [38]. The prevalence of gastroschisis is increasing worldwide [39].

On ultrasound, gastroschisis can be identified as multiple free loops of bowel with an irregular “cauliflower” appearance (Figs. 21.8, 21.9, and 21.10). The defect is almost always located to the right of an intact cord insertion site. Color Doppler interrogation of the umbilical cord vessels in relation to the herniation aids in distinguishing omphalocele, especially in the case of membrane rupture, from gastroschisis.

Limb-Body Stalk Anomaly

Limb-body stalk anomaly is also referred to as limb-body wall complex. It likely results from either early amnion rupture leading to the creation of fibrous bands that cause traumatic fetal lesions, improper folding of the germinal disc resulting in the persistence of the extraembryonic coelomic cavity, or vascular disruption in early embryonic development with failed ventral wall closure [40]. The three main types of malformations noted in this entity include body wall defects, limb deformities, and craniofacial abnormalities. This is a lethal anomaly, and early diagnosis is important for timely counseling.

The ultrasound findings of limb-body stalk anomalies are easy to visualize in the first trimester and include an abdominal wall defect with massive evisceration of abdominal contents, severe kyphoscoliosis, and a short umbilical cord [41, 42] (Fig. 21.11). Often, the cranial portion of the fetus is seen within the amniotic cavity and the caudal half is noted in the coelomic cavity [42, 43].

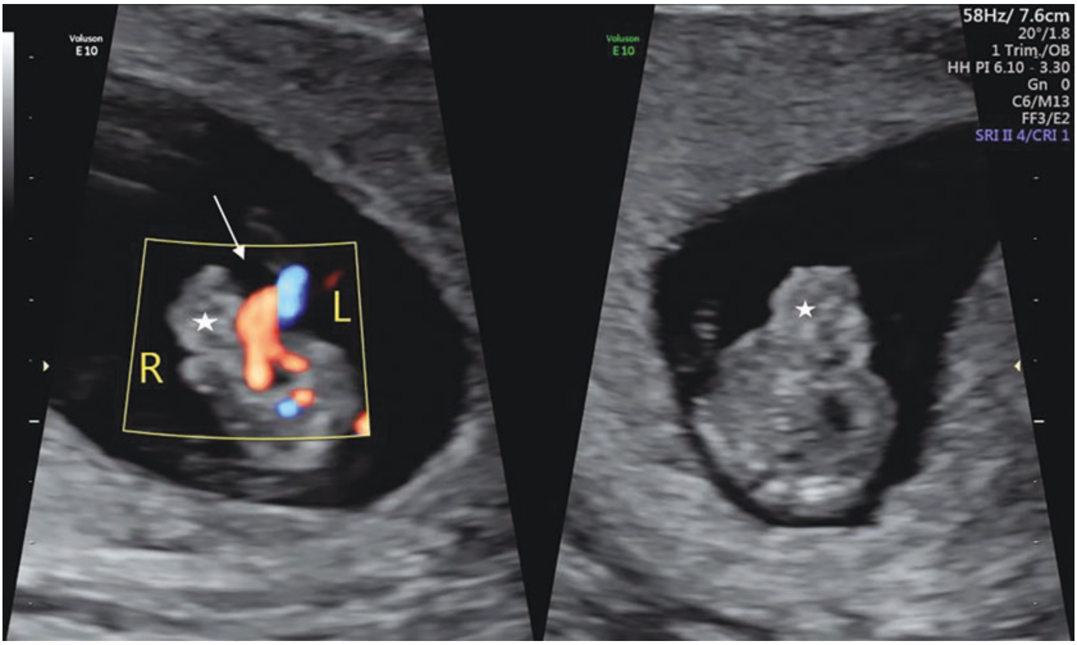
Voluson E10
R
L
Voluson E10
58Hz/ 7.6cm
20°/1.8
1 Trim./OB
HH PI 6.10 - 3.30
Gn 0
C6/M13
FF3/E2
SRI II 4/CRI 1

Fig. 21.8 Axial view of a fetus at 12 weeks' gestation demonstrating the irregular cauliflower appearance of bowel (star) floating freely in the amniotic fluid. Color Doppler shows an intact umbilical cord (arrow) insertion to the left of the abdominal wall defect

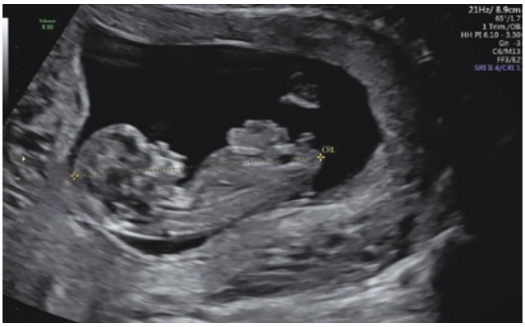
21Hz/ 8.9cm
65°/1.7
1 Trim./OB
HH PI 6.10 - 3.30
Gn -3
C6/M13
FF3/E2
SRI II 4/CRI 1
CRL

Fig. 21.9 Parasagittal view of a fetus at 12 weeks' gestation again demonstrating the irregular borders of a gastroschisis

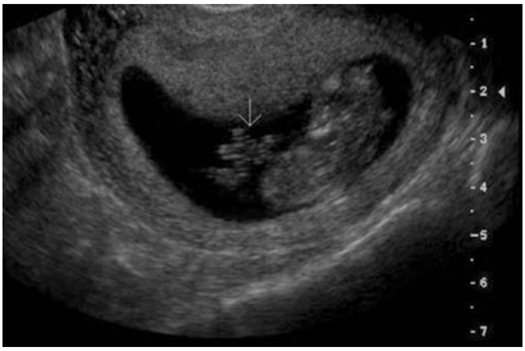

Fig. 21.10 A parasagittal view of a first-trimester embryo with gastroschisis. The arrow denotes the irregular borders characteristic of this anomaly

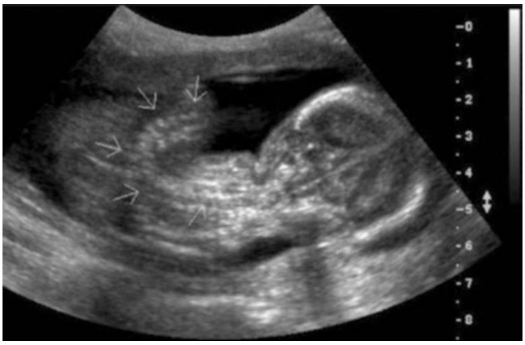

Fig. 21.11 Coronal view of a first-trimester fetus with limb-body stalk anomaly. The arrows trace the spine and demonstrate severe kyphoscoliosis

Conclusion

Through the use of axial, sagittal, and coronal imaging plus color Doppler flow, many components of the gastrointestinal system can be identified in the first trimester. An understanding of normal anatomy in early gestation coupled with knowledge of basic embryology allows for the detection of multiple major anomalies involving the fetal abdomen. Specifically, interruption of the ventral abdominal wall can reliably be identified in up to 90–100% of cases [1]. Any abnormalities noted on the first-trimester scan should prompt detailed assessment of other organ systems and a follow-up ultrasound in later gestation.

Teaching Points

- Through the use of axial, sagittal, and coronal imaging plus color Doppler flow, many components of the gastrointestinal system can be identified in the first trimester.
- The reliable detection of the stomach in early gestation is an important component of the assessment of situs visceralis.
- The frequency of the transducer used can affect the appearance of the bowel, and thus a suspicion of echogenic bowel should be confirmed with a low-frequency transducer (<5 MHz) and with machine harmonics turned off [10].
- A lower abdominal cystic mass that resolves in the second trimester should raise suspicion for a duodenal atresia, and a third-trimester follow-up ultrasound should be performed.
- Beyond 12 weeks of gestation, ventral wall defects can reliably be seen with detection rates approaching 90–100% for omphalocele, gastroschisis, and limb-body stalk anomaly in the first trimester [1, 13–15, 27].
- Midgut herniation should not measure more than 7 mm in maximum dimensions at any gestational age and should resolve by 12 weeks or by the time the fetus attains a crown-rump length of 45 mm [6, 29].
- Sonographically, omphaloceles are composed of exteriorized abdominal viscera covered by a thin membrane with the umbilical cord inserting into the dome of the sac.
- Gastroschisis is a full-thickness paraumbilical defect allowing visceral herniation adjacent to an intact umbilical cord insertion site.
- The ultrasound findings of limb-body stalk anomalies are easy to visualize in the first trimester and include an abdominal wall defect with massive evisceration of abdominal contents, severe kyphoscoliosis, and a short umbilical cord [41, 42].

References

1. Syngelaki A, Hammami A, Bower S, Zidere V, Akolekar R, Nicolaides KH. Diagnosis of fetal non-chromosomal abnormalities on routine ultrasound examination at 11–13 weeks' gestation. Ultrasound Obstet Gynecol. 2019;54(4):468–76.
2. Sadler TW. Langman's medical embryology. 14th ed. Philadelphia: Wolters Kluwer; 2019. 432 p
3. Venkatesh P. A simple and easy technique for imaging the fetal esophagus in the first, second, and third trimesters using the transverse section of the esophagus in the area behind the heart as a reference point. J Ultrasound Med. 2018;37(12):2863–72.
4. Pritchard J. Fetal swallowing and amniotic fluid volume. Obstet Gynecol. 1966;28:606–10.
5. Salomon LJ, Alfirevic Z, Bilardo CM, Chalouhi GE, Ghi T, Kagan KO, et al. ISUOG practice guidelines: performance of first-trimester fetal ultrasound scan. Ultrasound Obstet Gynecol. 2013;41(1):102–13.
6. Blaas HG, Eik-Nes SH, Kiserud T, Hellevik LR. Early development of the abdominal wall, stomach and heart from 7 to 12 weeks of gestation: a longitudinal ultrasound study. Ultrasound Obstet Gynecol. 1995;6(4):240–9.

7. Souka AP, Pilalis A, Kavalakis Y, Kosmas Y, Antsaklis P, Antsaklis A. Assessment of fetal anatomy at the 11–14-week ultrasound examination. Ultrasound Obstet Gynecol. 2004;24(7):730–4.
8. Versteegh HP, Adams SD, Boxall S, Burge DM, Stanton MP. Antenatally diagnosed right-sided stomach (dextrogastria): a rare rotational anomaly. J Pediatr Surg. 2016;51(2):236–9.
9. Bronshtein M, Weiner Z, Abramovici H, Filmar S, Erlik Y, Blumenfeld Z. Prenatal diagnosis of gall bladder anomalies—report of 17 cases. Prenat Diagn. 1993;13(9):851–61.
10. McNamara A, Levine D. Intraabdominal fetal echogenic masses: a practical guide to diagnosis and management. Radiographics. 2005;25(3):633–45.
11. Carroll SG, Maxwell DJ. The significance of echogenic areas in the fetal abdomen. Ultrasound Obstet Gynecol. 1996;7(4):293–8.
12. Hemming V, Rankin J. Small intestinal atresia in a defined population: occurrence, prenatal diagnosis and survival. Prenat Diagn. 2007;27(13):1205–11.
13. Bardi F, Smith E, Kuilman M, Snijders RJM, Bilardo CM. Early detection of structural anomalies in a primary care setting in the Netherlands. Fetal Diagn Ther. 2019;46(1):12–9.
14. Colosi E, Musone R, Filardi G, Fabbo A. First trimester fetal anatomy study and identification of major anomalies using 10 standardized scans. J Prenat Med. 2015;9(3–4):24–8.
15. Liao Y, Wen H, Ouyang S, Yuan Y, Bi J, Guan Y, et al. Routine first-trimester ultrasound screening using a standardized anatomical protocol. Am J Obstet Gynecol. 2021;224(4):396.e1–e15.
16. Petrikovsky BM. First-trimester diagnosis of duodenal atresia. Am J Obstet Gynecol. 1994;171(2):569–70.
17. Marquette GP, Skoll MA, Yong SL, Pugash D. First-trimester imaging of combined esophageal and duodenal atresia without a tracheoesophageal fistula. J Ultrasound Med. 2004;23(9):1232.
18. Lam YH, Shek T, Tang MH. Sonographic features of anal atresia at 12 weeks. Ultrasound Obstet Gynecol. 2002;19(5):523–4.
19. Wang Y, Dai X, Liu H, Li Y, Li L, Chen J. Anal atresia as the diagnostic clue in VACTERL association: a first-trimester case report. J Obstet Gynaecol Res. 2021;47(10):3702–6.
20. Ples L, Chicea R, Poenaru MO, Neacsu A, Sima RM, Micu R. Can anorectal atresia be diagnosed in the first trimester of pregnancy? A systematic literature review. Medicina (Kaunas). 2020;56(11):583.
21. Taipale P, Rovamo L, Hiilesmaa V. First-trimester diagnosis of imperforate anus. Ultrasound Obstet Gynecol. 2005;25(2):187–8.
22. Chen M, Meagher S, Simpson I, Lau TK. Sonographic features of anorectal atresia at 12 weeks. J Matern Fetal Neonatal Med. 2009;22(10):931–3.
23. Khalil A, Cooke PC, Mantovani E, Bhide A, Papageorghiou AT, Thilaganathan B. Outcome of first-trimester fetal abdominal cysts: cohort study and review of the literature. Ultrasound Obstet Gynecol. 2014;43(4):413–9.
24. Sepulveda W, Dickens K, Casasbuenas A, Gutierrez J, Dezerega V. Fetal abdominal cysts in the first trimester: prenatal detection and clinical significance. Ultrasound Obstet Gynecol. 2008;32(7):860–4.
25. Dhombres F, Friszer S, Castaing O, Bessis R, Jouannic JM. Fetal abdominal cysts at the first trimester scan. Gynecol Obstet Fertil. 2015;43(7–8):491–5.
26. Berg C, Baschat AA, Geipel A, Krapp M, Germer U, Smrcek JM, et al. First-trimester diagnosis of fetal hepatic cyst. Ultrasound Obstet Gynecol. 2002;19(3):287–9.
27. Kenkhuis MJA, Bakker M, Bardi F, Fontanella F, Bakker MK, Fleurke-Rozema JH, et al. Effectiveness of 12–13-week scan for early diagnosis of fetal congenital anomalies in the cell-free DNA era. Ultrasound Obstet Gynecol. 2018;51(4):463–9.
28. Ueda Y, Yamada S, Uwabe C, Kose K, Takakuwa T. Intestinal rotation and physiological umbilical herniation during the embryonic period. Anat Rec (Hoboken). 2016;299(2):197–206.
29. Bowerman RA. Sonography of fetal midgut herniation: normal size criteria and correlation with crown-rump length. J Ultrasound Med. 1993;12(5):251–4.
30. Soffers JH, Hikspoors JP, Mekonen HK, Koehler SE, Lamers WH. The growth pattern of the human intestine and its mesentery. BMC Dev Biol. 2015;15:31.
31. Khalil A, Arnaoutoglou C, Pacilli M, Szabo A, David AL, Pandya P. Outcome of fetal exomphalos diagnosed at 11–14 weeks of gestation. Ultrasound Obstet Gynecol. 2012;39(4):401–6.
32. Marshall J, Salemi JL, Tanner JP, Ramakrishnan R, Feldkamp ML, Marengo LK, et al. Prevalence, correlates, and outcomes of omphalocele in the United States, 1995–2005. Obstet Gynecol. 2015;126(2):284–93.
33. Brantberg A, Blaas HG, Haugen SE, Eik-Nes SH. Characteristics and outcome of 90 cases of fetal omphalocele. Ultrasound Obstet Gynecol. 2005;26(5):527–37.
34. Mann S, Blinman TA, Douglas Wilson R. Prenatal and postnatal management of omphalocele. Prenat Diagn. 2008;28(7):626–32.
35. Kagan KO, Staboulidou I, Syngelaki A, Cruz J, Nicolaides KH. The 11–13-week scan: diagnosis and outcome of holoprosencephaly, exomphalos and megacystis. Ultrasound Obstet Gynecol. 2010;36(1):10–4.
36. Groves R, Sunderajan L, Khan AR, Parikh D, Brain J, Samuel M. Congenital anomalies are commonly associated with exomphalos minor. J Pediatr Surg. 2006;41(2):358–61.
37. Wilkins-Haug L, Porter A, Hawley P, Benson CB. Isolated fetal omphalocele, Beckwith-Wiedemann syndrome, and assisted reproductive technologies. Birth Defects Res A Clin Mol Teratol. 2009;85(1):58–62.

38. Feldkamp ML, Carey JC, Sadler TW. Development of gastroschisis: review of hypotheses, a novel hypothesis, and implications for research. Am J Med Genet A. 2007;143A(7):639–52.
39. Castilla EE, Mastroiacovo P, Orioli IM. Gastroschisis: international epidemiology and public health perspectives. Am J Med Genet C Semin Med Genet. 2008;148C(3):162–79.
40. Russo R, D'Armiento M, Angrisani P, Vecchione R. Limb body wall complex: a critical review and a nosological proposal. Am J Med Genet. 1993;47(6):893–900.
41. Boitor-Borza D, Staicu A, Constantin R, Muresan D. First trimester sonographic diagnosis of limb-body wall defect associating both cephalic and thoraco-abdominal defects - a case report and literature update. Med Ultrason. 2022;24(2):245–7.
42. Daskalakis G, Sebire NJ, Jurkovic D, Snijders RJ, Nicolaides KH. Body stalk anomaly at 10–14 weeks of gestation. Ultrasound Obstet Gynecol. 1997;10(6):416–8.
43. Paul C, Zosmer N, Jurkovic D, Nicolaides K. A case of body stalk anomaly at 10 weeks of gestation. Ultrasound Obstet Gynecol. 2001;17(2):157–9.

22

First-Trimester Genitourinary Development and Anomalies

Yair J. Blumenfeld

Introduction

Fetal genitourinary (GU) anomalies (including various degrees of renal hydronephrosis and pyelectasis) are detected by prenatal ultrasound in up to 2% of pregnancies [1]. These congenital anomalies of the kidney and urinary tract (CAKUT) are the leading cause of pediatric nephropathy and can present in isolation or as part of a multiorgan syndrome [2]. While isolated second-trimester pyelectasis makes up the majority of these cases (found in approximately 1–2% of all pregnancies), in a large European registry of non-chromosomal congenital anomalies, renal anomalies comprised 13% of all isolated anomalies, the third most common group after cardiac and limb anomalies [3, 4].

Embryonic GU development involves several important first-trimester processes.[1] The initial development of the transient pronephros and mesonephros from approximately the fifth to seventh week of gestation is followed by development of the mesonephric duct (or Wolffian duct) [5]. The Wolffian duct develops a bud from its caudal end at approximately the seventh week of pregnancy, which grows dorsally and medially until it encounters the caudal end of the nephrogenic cord, also known as the "metanephric blastema," and induces the formation of the kidney, or metanephros [5]. Upon contact between the ureteral bud with the metanephric blastema, induction of the kidney begins as an interplay between the epithelial and mesenchymal tissues. This contact results in a series of branching divisions of the ureteral bud at its end, or ampulla. Early penetration of the metanephros and branching occurs by the 12th–14th weeks to form the renal pelvis and major calyces [5]. The gradual dilation and fusion of these early branches are thought to result from the pressure of urine excreted by the early formation of the renal working unites, or nephrons [5]. Perturbations in any aspect of this cascade (e.g., mutations of either metanephric or ureteric factors or disruption of other signaling) may cause inhibition of ureteric bud growth and renal hypoplasia or agenesis [6, 7]. Conversely, duplication or over-proliferation of structures can occur if there is a gain of function of the inductive factors.

While sonographic assessment of the GU tract is an important part of the second-trimester fetal anatomy survey, assessment of these organs is also recommended by most societal guidelines for first-trimester sonographic exams [8, 9]. According to the International Society of Ultrasound in Obstetrics and Gynecology (ISUOG), the fetal kidneys should be noted in their expected paraspinal location, as bean-shaped slightly echogenic

---

[1] See also Chap. 5.

Y. J. Blumenfeld (✉)
Department of Obstetrics & Gynecology,
Stanford University School of Medicine, Stanford,
CA, USA
e-mail: yairb@stanford.edu

© The Author(s), under exclusive license to Springer Nature Switzerland AG 2023
J. S. Abramowicz, R. E. Longman (eds.), *First-Trimester Ultrasound*,
https://doi.org/10.1007/978-3-031-24133-8_22

structures with typical hypoechoic central renal pelvis [8]. However, it is important to recognize that the ability to appropriately visualize the GU system in the first trimester by both abdominal and endovaginal views will vary by gestational age. In a study of 1288 women undergoing first-trimester ultrasound, the kidneys and bladder were appropriately seen in only 45% of cases at 10 weeks' gestation, but visualization improved with advancing gestational age, reaching 99% of cases by 13 weeks' gestation [10]. Fetal GU anomalies have been described in approximately 2% of first-trimester anatomy surveys if performed by endovaginal imaging, but some studies suggest that less than 10% of all GU anomalies will be detected in the first trimester, while the majority will be diagnosed in the second or third trimester [5, 11]. Therefore, most studies of fetal GU anomalies and societal guidelines for the management of GU anomalies are based on second- and third-trimester diagnoses. In this chapter, we review the existing literature on GU anomalies diagnosed in the first trimester, their sonographic findings, and associated genetic conditions.

Fetal Renal Size, Presence, and Location

First-trimester nomograms describing appropriate fetal kidney size have been reported, although size discrepancy in the first trimester is rare. The average anteroposterior and transverse renal diameter is approximately 4 mm at 12 weeks' gestation, and 6 mm by 14 weeks' gestation, while the longitudinal diameter of fetal kidneys is approximately 6 mm at 12 weeks' gestation and 9 mm at 14 weeks' gestation [12] (Fig. 22.1).

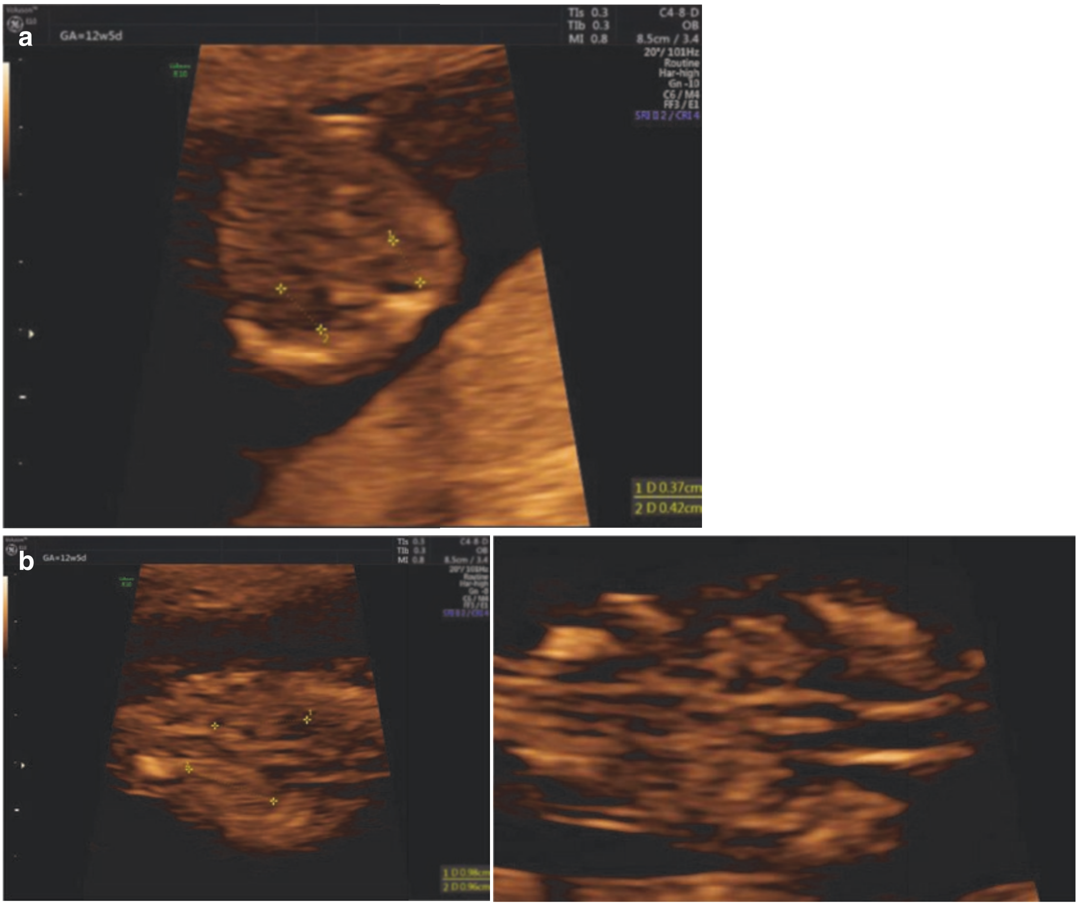

Fig. 22.1 First-trimester image of fetal kidneys in transverse (**a**) and coronal views (**b**)

More recently, a study by Brennan and colleagues provided charts detailing renal parenchymal thickness as a novel measurement to evaluate fetal kidney growth and potential function, but the earliest gestational age reported was 16 weeks' gestation [13]. More common than size discrepancy in the first trimester are abnormalities in renal sonographic appearance and location or complete absence of one or more kidneys altogether (renal agenesis).

Renal agenesis is caused by either complete failure of the kidneys to form or involution of a malformed kidney. Unilateral renal agenesis is more commonly found than bilateral renal agenesis, although both are rare, affecting approximately 1 in 1000–4000 pregnancies [14]. Only a minority of renal agenesis cases will be diagnosed in the first trimester, likely because the bulk of first-trimester amniotic fluid is not comprised of fetal urine, and even cases of bilateral renal agenesis can have normal first-trimester amniotic fluid level [11]. Approximately 30% of renal agenesis cases are associated with genetic syndromes or other structural birth defects, and a finding of an absent renal fossa/suspected renal agenesis should first prompt an evaluation for an ectopic renal location (rather than complete agenesis) including a pelvic kidney, cross-fused kidney, or horseshoe kidney [14] (Fig. 22.2). Three-dimension ultrasound has been shown to help with the diagnosis of ectopic kidneys, but usually this is performed after the first trimester [15].

Hydronephrosis/Pyelectasis

Dilation of the renal collecting system can be found in at least 2% of second- and third-trimester fetal surveys [1, 16]. A 2014 multidisciplinary update on the classification of fetal urinary tract dilation (UTD) provided definitions for both normal and abnormal dilation values and categorized dilation into three distinct severity categories (UTD 1, 2, and 3). However, the UTD definition cutoffs describe measurements after 16 weeks' gestation, with little guidance about first-trimester imaging or its implications [1]. In a study by Bronshtein and colleagues, among 35 urinary tract anomalies identified in the first trimester by endovaginal sonography, there were 27 (77%) cases of first-trimester "hydronephrosis," defined as a ureteropelvic junction dilation of 3 mm or greater [5]. Most significant cases of first-trimester hydronephrosis are usually in the setting of fetal lower urinary tract obstruction (LUTO) (Fig. 22.3).

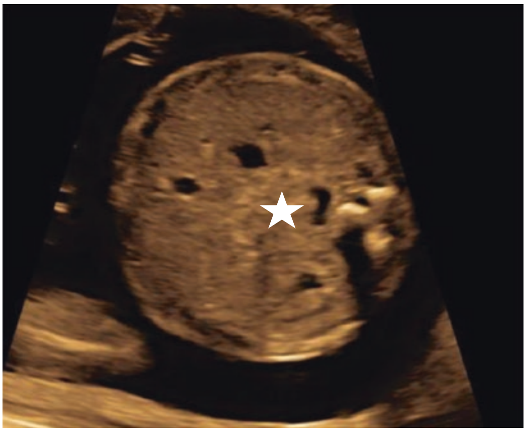

Fig. 22.2 Cross-fused fetal kidney. Note the inferior kidney in the appropriate renal fossa and the contralateral kidney in the midline, directly in front of the vertebral body (star)

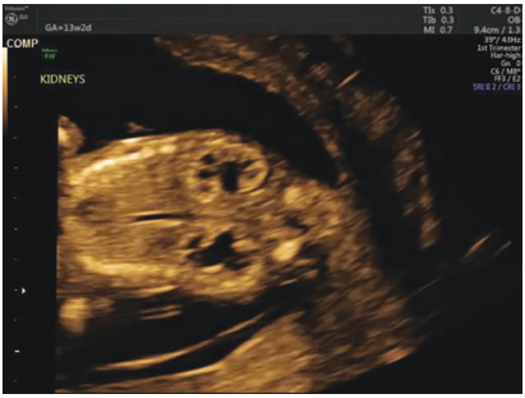

Fig. 22.3 Image of first-trimester hydronephrosis in the setting of fetal lower urinary tract obstruction (LUTO)

Cystic Renal Disease

Fetal cystic renal disease occurs in less than 1 in 3000 pregnancies [14]. The two most common renal cystic disorders are autosomal recessive polycystic kidney disease (ARPKD) and multicystic dysplastic kidneys (MCDK). In ARPKD, the cysts arise from the collecting ducts and are usually too small to delineate. ARPKD usually presents as large hyperechogenic kidneys with a smooth surface. Oligohydramnios can be present but usually in the late second or third trimester. MCDK is an anomaly that arises from a failed coordination of development of the metanephros and the branching ureteric bud, leading to multiple, non-communicating cysts of variable sizes [7] (Fig. 22.4). Most cases of cystic kidney disease will be diagnosed after the first trimester.

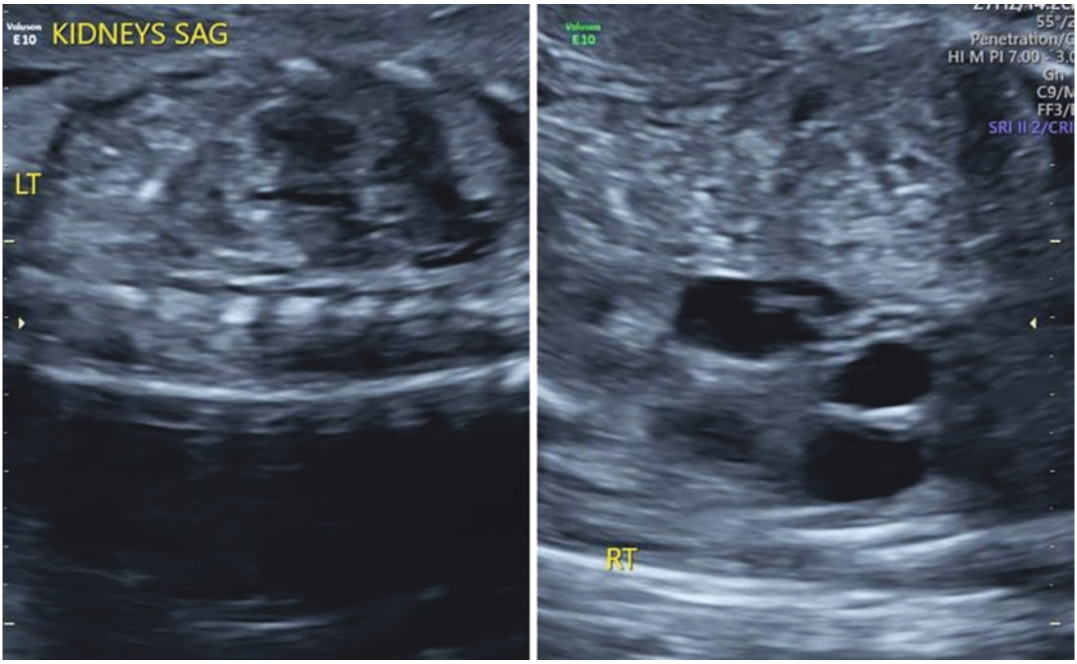

Fig. 22.4 Polycystic right-kidney disease in the sagittal plane

Fetal Bladder Abnormalities

Abnormalities of the fetal bladder can include an enlarged bladder (megacystis), absent bladder appearance, or bladder exstrophy. Megacystis, which is found in approximately 1 in 1500 pregnancies, can result from several mechanisms and is often associated with genetic anomalies and structural defects outside the GU system [17]. Megacystis is a diagnostic feature of fetal lower urinary tract obstruction (LUTO), which is characterized by megacystis and obstructive uropathy (Fig. 22.5). LUTO has several underlying etiologies including posterior (and, very rarely, anterior) urethral valves, urethral atresia or stenosis, prune belly syndrome, megacystis-microcolon hypoperistalsis syndrome, or cloacal anomalies [18]. An exact definition for megacystis size has not been universally accepted, but most case series define a first-trimester megacystis as a bladder size greater than 6–7 mm in diameter [18]. In a study of 541 cases of fetal megacystis, 223 (41%) were diagnosed before 18 weeks' gestation, and isolated LUTO was only found in 222 cases, the remainder associated with other genetic syndromes and with other structural anomalies [17]. In a study of 16 first-trimester megacystis cases (out of 5240 first-trimester scans, incidence 0.3%), only 2 were associated with oligohydramnios, all had a bladder size greater than 9 mm, 10 were associated with additional findings, and 4 had abnormal karyotype (2 cases of trisomy 13, 1 case of trisomy 18, and 1 case of trisomy 21) [19].

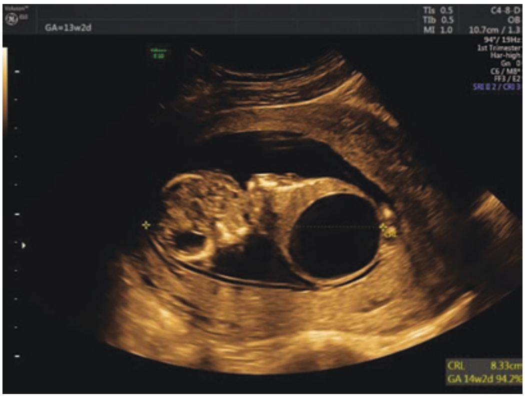

Fig. 22.5 First-trimester fetal megacystis in the setting of LUTO

Spontaneous resolution of first-trimester megacystis has been described in over 80 cases in the literature, with a 2.4% risk of chromosomal abnormalities in such cases and normal pediatric follow-up in 96.4% of cases [20]. Early (16-week) fetal cystoscopy in order to identify the underlying pathology of fetal megacystis, and potentially ablate posterior urethral valves using laser, has been described [21]. However, subsequent reports identified a risk of vesico-cutaneous fistulas in such procedures and additional studies identified the vesico-urethral angle as a particularly challenging location to navigate using existing fetoscopes [22, 23].

Abnormalities of the Fetal Genitalia

Abnormalities of the fetal external genitalia, for example hypospadias, are difficult to identify in the first trimester. Sonographic first-trimester determination of fetal gender can be performed by assessing the position of the genital tubercle in relation to the fetal spine [24, 25]. In a study by Youssef and colleagues, the first-trimester angle between the genital tubercle and an imaginary line passing tangentially through the fetal spine (the genital angle) was found to be different between male and female fetuses. Specifically, the average genital angle in males was significantly higher than that in females (51.2° vs. 18.9°) [24] (Fig. 22.6). When an angle greater than 30° is assigned a male gender, and an angle less than 10° is assigned a female gender, the accuracy of first-trimester male gender determination is 99–100% at 12–14 weeks, and for female gender determination is 91.5% at 12 weeks and 100% at 13 weeks [25].

Recently, the sonographic first-trimester anogenital distance has been described as a possible marker of distinguishing male from female fetal sex [26]. Disorders of sexual differentiation including hypospadias and clitoromegaly are rarely identified in the first trimester [27].

Congenital megalourethra results from the absence or hypoplasia of the corpus spongiosum

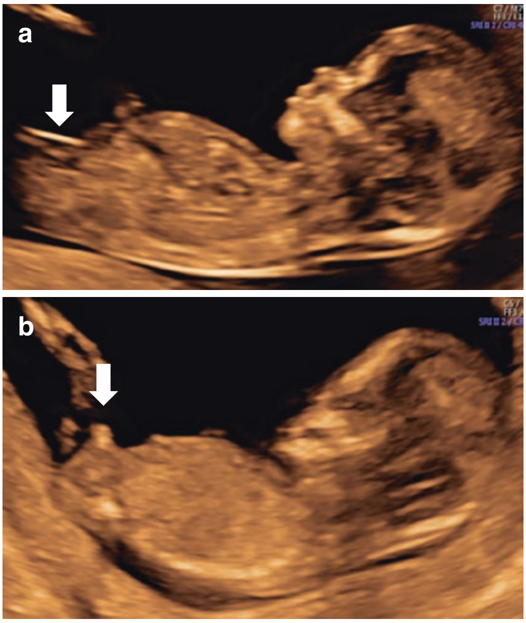

Fig. 22.6 First-trimester genital angle in the sagittal plane: female (**a**) and male (**b**)

or corpus cavernosum or is caused by anterior urethral valves. Sonographic findings in megalourethra include a cystic dilated anterior urethra and enlarged penis, and hydronephrosis is present in approximately 60% of cases [28]. In a meta-analysis of 50 megalourethra cases, only 1 was diagnosed in the first trimester [28]. In that cohort, 35 fetuses (70.0%) survived, and among the survivors, 41.9% of the neonates had renal impairment [28].

Genetic Evaluation

While CAKUT have multifactorial etiologies, there are several genetic etiologies that are important to evaluate during the workup of prenatally diagnosed GU anomalies.

Genetic disorders underlying fetal CAKUT cases include fetal aneuploidy (abnormal chromosome number such as in trisomy 21, or Down syndrome), which can be detected by prenatal karyotype, copy number variants (such as microdeletion/duplication syndromes) which can be detected by prenatal microarray testing, and single-gene disorders and single nucleotide polymorphisms which can be detected by single-gene sequencing panels or whole-exome and -genome testing. To date, dozens of genes and syndromes have been found to cause monogenic CAKUT, and copy number variations (CNVs) have been widely associated with CAKUT spectrum [29–31]. The implicated genes encode proteins in diverse developmental pathways, and inheritance modes of monogenic CAKUT include autosomal recessive (AR), autosomal dominant (AD), and X-linked (XL) [30].

The yield of these genetic tests will vary depending on the specific anomaly, the family history, and whether the finding is isolated or found in combination with other malformations. The American College of Obstetricians and Gynecologists (ACOG) and the Society for Maternal-Fetal Medicine recommend prenatal chromosomal microarray analysis for a patient with a fetus with one or more major structural abnormalities identified on ultrasonographic examination and who is undergoing invasive prenatal diagnosis [32, 33]. Copy number variants may be found in approximately 4–10% of children with CAKUT and in approximately 10% of prenatally diagnosed CAKUT cases, although the yield may be higher or lower depending on the specific anomaly [2, 34–36]. Among pediatric cases, whole-exome sequencing (WES) can reveal pathogenic variants in approximately 5–15% of all CAKUT cases [37]. A recent study of 163 cases of fetal CAKUT undergoing whole-exome sequencing found a 12.3% yield among those with a normal karyotype and microarray [37].

Conclusion

Fetal GU anomalies are commonly diagnosed in pregnancy, but only the minority will be identified in the first trimester. That said, adequate assessment of the fetal kidneys and bladder should be a mainstay of any first-trimester scan, and appropriate genetic evaluation is warranted in cases in which an abnormality is detected.

Teaching Points

- Evaluation of the fetal GU system, primarily the kidneys and bladder, is an integral part of the first-trimester scan.
- The sonographic yield of fetal GU anomalies increases with increasing gestational age, and most GU anomalies will not be detected in the first trimester.
- Suspected fetal lower urinary tract obstruction (LUTO) is a finding, not a diagnosis, and the differential diagnosis of first-trimester megacystis is broad.
- Extensive genetic evaluation by both microarray and single-gene disorder testing is warranted in the setting of a prenatally diagnosed GU anomalies.

References

1. Nguyen HT, Benson CB, Bromley B, et al. Multidisciplinary consensus on the classification of prenatal and postnatal urinary tract dilation (UTD classification system). J Pediatr Urol. 2014;10(6):982–98.
2. Groopman EE, Rasouly HM, Gharavi AG. Genomic medicine for kidney disease. Nat Rev Nephrol. 2018;14(2):83–104.
3. Calzolari E, Barisic I, Loane M, et al. Epidemiology of multiple congenital anomalies in Europe: a EUROCAT population-based registry study. Birth Defects Res A Clin Mol Teratol. 2014;100(4):270–6.
4. Carbone JF, Tuuli MG, Dicke JM, Macones GA, Odibo AO. Revisiting the risk for aneuploidy in fetuses with isolated pyelectasis. Prenat Diagn. 2011;31(6):566–70.
5. Bronshtein M, Yoffe N, Brandes JM, Blumenfeld Z. First and early second-trimester diagnosis of fetal urinary tract anomalies using transvaginal sonography. Prenat Diagn. 1990;10(10):653–66.
6. Dotsch J, Plank C, Amann K. Fetal programming of renal function. Pediatr Nephrol. 2012;27(4):513–20.
7. Vanderheyden T, Kumar S, Fisk NM. Fetal renal impairment. Semin Neonatol. 2003;8(4):279–89.
8. Salomon LJ, Alfirevic Z, Bilardo CM, et al. ISUOG practice guidelines: performance of first-trimester fetal ultrasound scan. Ultrasound Obstet Gynecol. 2013;41(1):102–13.
9. Mei JY, Afshar Y, Platt LD. First-trimester ultrasound. Obstet Gynecol Clin N Am. 2019;46(4):829–52.
10. Whitlow BJ, Economides DL. The optimal gestational age to examine fetal anatomy and measure nuchal translucency in the first trimester. Ultrasound Obstet Gynecol. 1998;11(4):258–61.
11. Syngelaki A, Hammami A, Bower S, Zidere V, Akolekar R, Nicolaides KH. Diagnosis of fetal non-chromosomal abnormalities on routine ultrasound examination at 11–13 weeks' gestation. Ultrasound Obstet Gynecol. 2019;54(4):468–76.
12. Bronshtein M, Kushnir O, Ben-Rafael Z, et al. Transvaginal sonographic measurement of fetal kidneys in the first trimester of pregnancy. J Clin Ultrasound. 1990;18(4):299–301.
13. Brennan S, Kandasamy Y, Rudd D, Schneider M, Watson D. Fetal kidney charts of a novel measurement of the renal parenchymal thickness to evaluate fetal kidney growth and potential function. Prenat Diagn. 2020;40(7):860–9.
14. Society for Maternal-Fetal Medicine. Electronic address pso, Norton ME, Cheng Y, et al. SMFM Fetal Anomalies Consult Series #4: genitourinary anomalies. Am J Obstet Gynecol. 2021;225(5):B2–B35.
15. Chang PL, Mrazek-Pugh B, Blumenfeld YJ. Prenatal diagnosis of cross-fused renal ectopia: does color Doppler and 3-dimensional sonography help? J Ultrasound Med. 2011;30(4):578–80.
16. Chapman T. Fetal genitourinary imaging. Pediatr Radiol. 2012;42(Suppl 1):S115–23.
17. Fontanella F, Maggio L, Verheij J, et al. Fetal megacystis: a lot more than LUTO. Ultrasound Obstet Gynecol. 2019;53(6):779–87.
18. Taghavi K, Sharpe C, Stringer MD. Fetal megacystis: a systematic review. J Pediatr Urol. 2017;13(1):7–15.
19. Favre R, Kohler M, Gasser B, Muller F, Nisand I. Early fetal megacystis between 11 and 15 weeks of gestation. Ultrasound Obstet Gynecol. 1999;14(6):402–6.
20. Girard N, Viaris de Lesegno B, Bussiere P, Egoroff C, Cordier AG, Benachi A. Prognosis of isolated first-trimester fetal megacystis with spontaneous resolution. Fetal Diagn Ther. 2017;42(4):271–7.
21. Ruano R, Yoshisaki CT, Salustiano EM, Giron AM, Srougi M, Zugaib M. Early fetal cystoscopy for first-trimester severe megacystis. Ultrasound Obstet Gynecol. 2011;37(6):696–701.
22. Vinit N, Gueneuc A, Bessieres B, et al. Fetal cystoscopy and vesicoamniotic shunting in lower urinary tract obstruction: long-term outcome and current technical limitations. Fetal Diagn Ther. 2020;47(1):74–83.
23. Sananes N, Favre R, Koh CJ, et al. Urological fistulas after fetal cystoscopic laser ablation of posterior urethral valves: surgical technical aspects. Ultrasound Obstet Gynecol. 2015;45(2):183–9.
24. Youssef A, Arcangeli T, Radico D, et al. Accuracy of fetal gender determination in the first trimester using three-dimensional ultrasound. Ultrasound Obstet Gynecol. 2011;37(5):557–61.
25. Efrat Z, Perri T, Ramati E, Tugendreich D, Meizner I. Fetal gender assignment by first-trimester ultrasound. Ultrasound Obstet Gynecol. 2006;27(6):619–21.
26. Arfi A, Cohen J, Canlorbe G, et al. First-trimester determination of fetal gender by ultrasound: measurement of the ano-genital distance. Eur J Obstet Gynecol Reprod Biol. 2016;203:177–81.
27. Pinhas-Hamiel O, Zalel Y, Smith E, et al. Prenatal diagnosis of sex differentiation disorders: the

role of fetal ultrasound. J Clin Endocrinol Metab. 2002;87(10):4547–53.

28. Moaddab A, Sananes N, Hernandez-Ruano S, et al. Prenatal diagnosis and perinatal outcomes of congenital megalourethra: a multicenter cohort study and systematic review of the literature. J Ultrasound Med. 2015;34(11):2057–64.
29. Sanna-Cherchi S, Westland R, Ghiggeri GM, Gharavi AG. Genetic basis of human congenital anomalies of the kidney and urinary tract. J Clin Invest. 2018;128(1):4–15.
30. Vivante A, Kohl S, Hwang DY, Dworschak GC, Hildebrandt F. Single-gene causes of congenital anomalies of the kidney and urinary tract (CAKUT) in humans. Pediatr Nephrol. 2014;29(4):695–704.
31. Saint-Faust M, Boubred F, Simeoni U. Renal development and neonatal adaptation. Am J Perinatol. 2014;31(9):773–80.
32. Committee Opinion No. 682 Summary: microarrays and next-generation sequencing technology: the use of advanced genetic diagnostic tools in obstetrics and gynecology. Obstet Gynecol. 2016;128(6):1462–3.
33. Society for Maternal-Fetal Medicine . Electronic address pso, Dugoff L, Norton ME, Kuller JA. The use of chromosomal microarray for prenatal diagnosis. Am J Obstet Gynecol. 2016;215(4):B2–9.
34. Southard AE, Edelmann LJ, Gelb BD. Role of copy number variants in structural birth defects. Pediatrics. 2012;129(4):755–63.
35. Singer A, Maya I, Frumkin A, et al. Is fetal isolated double renal collecting system an indication for chromosomal microarray? J Matern Fetal Neonatal Med. 2021;34(5):696–700.
36. Pinto EVF, Prochnow C, Kemppainen JL, et al. Genomics integration into nephrology practice. Kidney Med. 2021;3(5):785–98.
37. Lei TY, Fu F, Li R, et al. Whole-exome sequencing in the evaluation of fetal congenital anomalies of the kidney and urinary tract detected by ultrasonography. Prenat Diagn. 2020;40(10):1290–9.

23

Fetal Skeletal Anomalies

Carol B. Benson

Introduction

The skeletal system provides structure to the fetus and comprises the axial skeleton, made up of the spine, ribs, and cranium, and the appendicular skeleton, made up of the shoulders, pelvis, and extremities. The fetal skeleton starts to develop in the early first trimester and continues to form and grow throughout gestation. Beginning as early as 8 weeks' gestation, the fetal limb buds are visible sonographically. Over the course of the latter half of the first trimester, the skeletal system undergoes rapid growth and ossification. By the end of the first trimester, the diaphyses (shaft) of the long bones are easily visible sonographically, including the bones of the hands and feet. Thus, major abnormalities of the fetal skeleton can sometimes be identified on first-trimester ultrasound.

During routine first-trimester scans after 11 weeks' gestation, 30–40% of major skeletal anomalies can be identified [1, 2]. When detailed sonograms are performed, the detection rate of major skeletal anomalies climbs to 71% [3]. A list of components to be assessed during a first-trimester detailed obstetric ultrasound has been compiled by the American Institute of Ultrasound in Medicine and includes evaluation of the cranial bones, the face, the spine, and the extremities (Table 23.1) [4]. In the future, as ultrasound equipment and scanning skills improve and as more practitioners offer detailed obstetrical scans in the latter part of the first trimester, even more types of fetal skeletal anomalies will likely be detected.

Table 23.1 Skeletal system components detailed in first-trimester obstetric ultrasound[a]

Structures	Required	If indicated[b]
Fetal head		
Cranial bones (calvarium)	Yes	
Facial structures		
Nasal bone	Yes	
Profile	Yes	
Maxilla	Yes	
Mandible	Yes	
Orbits		If indicated
Fetal thorax		
Ribs		If indicated
Extremities		
Confirm four extremities	Yes	
3 long bones in each	Yes	
Presence of hands/feet	Yes	
Fingers/thumb/toes		If indicated
3D assessment of extremities		If indicated
Spine		
Vertebral elements/alignment	Yes	
Skin edge	Yes	
Scapula		If indicated

[a] Adapted from Ref. [4]

[b] Components that require evaluation only if clinically indicated or because of suspicious findings seen on the detailed scans

---

C. B. Benson (✉)
Department of Radiology, Brigham and Women's Hospital, Boston, MA, USA
e-mail: cbenson@bwh.harvard.edu

© The Author(s), under exclusive license to Springer Nature Switzerland AG 2023

J. S. Abramowicz, R. E. Longman (eds.), *First-Trimester Ultrasound*,
https://doi.org/10.1007/978-3-031-24133-8_23

This chapter discusses fetal anomalies of the skeletal system that can be diagnosed or suspected on first-trimester ultrasound. The value of adding three-dimensional (3D) ultrasound to the assessment will be described. In some cases of a skeletal anomaly, a definitive diagnosis may be made during the first trimester, but in many cases, an anomaly of the skeletal system may be suspected, and follow-up sonography in the second trimester should be recommended for further evaluation.

Skeletal Dysplasias

Skeletal dysplasias are a category of congenital abnormalities involving abnormal bone formation, development, and growth. Most conditions are genetic, and many can be diagnosed through molecular and genetic analysis of the fetus. Prenatal diagnosis of a skeletal dysplasia can rarely be made during the first trimester except in some severe lethal cases, most notably thanatophoric dysplasia [5, 6]. Many other types of severe skeletal dysplasia, however, cannot be diagnosed until the second trimester, while many nonlethal forms may not be apparent until the third trimester or after birth.

Thanatophoric dysplasia is characterized by extreme shortening of the long bones, particularly the humerus and femur, a narrow thorax, and an abnormally shaped cranium. Early diagnosis is made by identifying extremely short extremities, with disproportionate shortening of the long bones compared to the hands and feet (Fig. 23.1). Associated thickening of the nuchal translucency may also be seen.

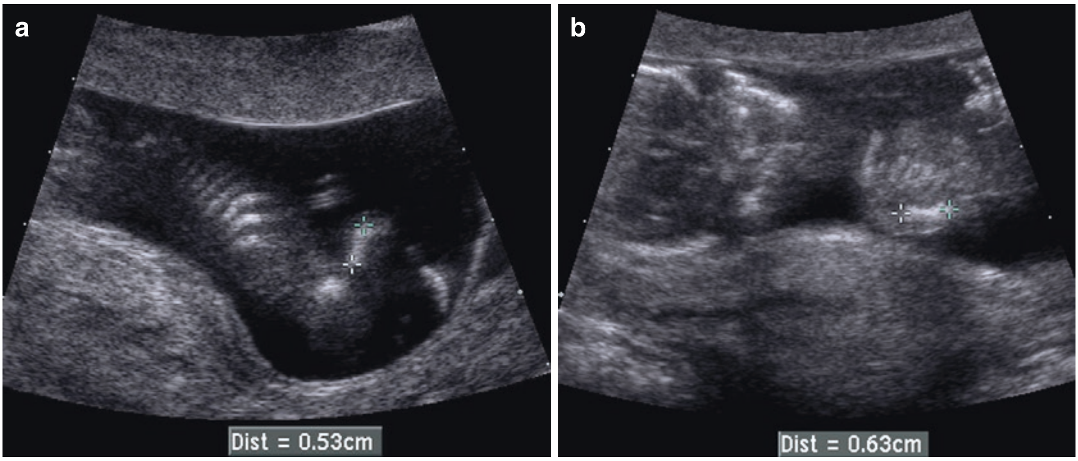

Fig. 23.1 Thanatophoric dysplasia at 13 weeks' gestation. (**a**) Image of femur length measurement (calipers) showing femur size extremely small for gestational age, measuring only 5.3 mm instead of the expected length of approximately 11 mm. (**b**) The humerus (calipers) also measures extremely small for gestational age. (**c**) Image of upper extremity (arrows) showing very small long bones of the upper arm and forearm compared to the size of the hand. (**d**) The nuchal translucency (calipers) is thickened to 3.4 mm in this fetus, a finding often seen in a fetus affected with askeletal dysplasia

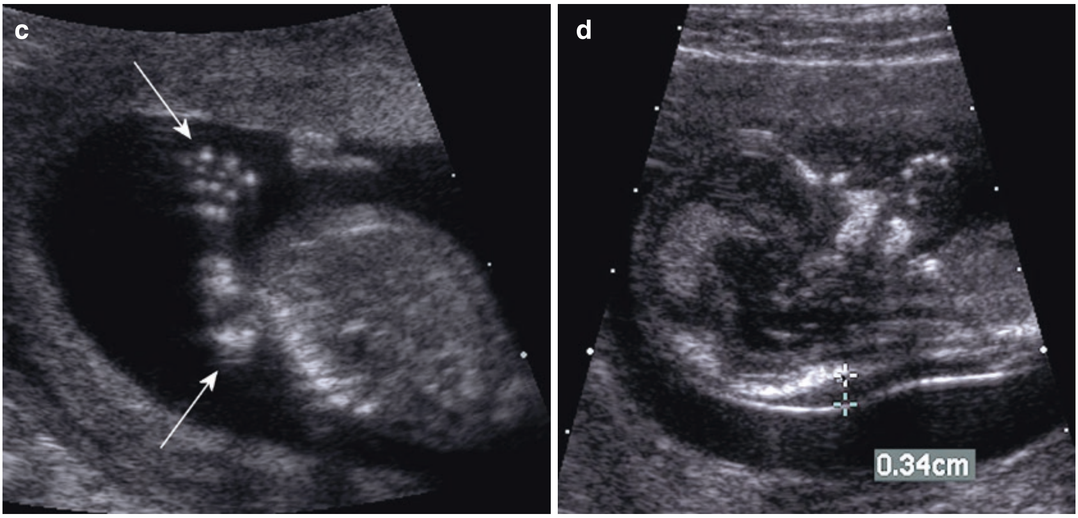

Fig. 23.1 (continued)

Arthrogryposis Multiplex Congenita

Congenital arthrogryposis multiplex congenita is a group of abnormalities characterized by severe joint contractures and limited fetal mobility because of a neurologic, muscular, or connective tissue disorder [7]. Genetic abnormalities or chromosomal anomalies, especially trisomy 18, may be diagnosed as the underlying cause in many cases. Sonographic findings include limited fetal motion, persistent flexion or hyperextension of joints, and abnormal posturing of the hands and feet. Hydrops may also be present [8]. The diagnosis of arthrogryposis is rarely made before the second or third trimester; however, in the first trimester, fetuses with arthrogryposis may have a thickened nuchal translucency, a clue to an underlying abnormality.

Findings of arthrogryposis in the first trimester may include thickened nuchal translucency and abnormal posturing of the hands and feet, such as in cases of trisomy 18 (Fig. 23.2). Three-dimensional ultrasound may provide valuable images for depicting the abnormal flexion, extension, and positioning of the extremities, particularly of the hands and feet.

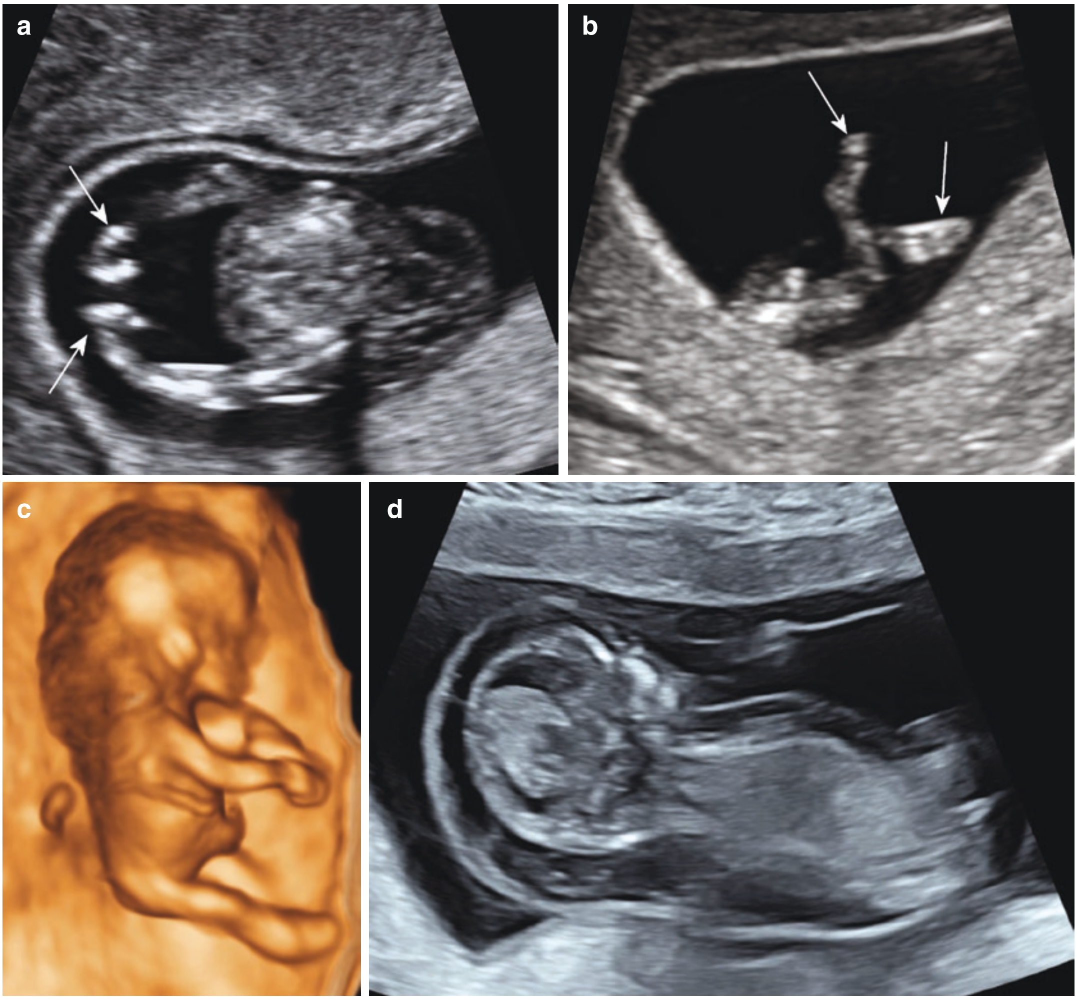

Fig. 23.2 Arthrogryposis from trisomy 18. (**a**) Image of upper extremities of 12-week fetus with trisomy 18 showing abnormal posturing of the hands (arrows), hyperflexed towards the forearms. (**b**) Image of another 12-week fetus with trisomy 18 demonstrating abnormal hyperextension of the feet at the ankles (arrows) from arthrogryposis. (**c**) 3D image of same fetus as (**a**) showing abnormal positioning of the arms, hands, legs, and feet, which persisted throughout the examination. (**d**) This fetus with trisomy 18 has a large cystic hygroma surrounding the neck, head, and trunk, a common finding in fetuses with this chromosomal abnormality

Cranial Anomalies

Anomalies involving the formation and configuration of the cranial bones, such as craniosynostosis, cannot be detected during the first trimester nor in most cases during the second trimester, because the cranial bones do not begin to fuse until the third trimester or after birth. Encephaloceles are defects in the cranium through which intracranial contents may protrude outside the skull. Such defects are typically diagnosed in the second trimester or later but can occasionally be diagnosed during the first trimester as an opening in the skull and a complex mass of tissue and fluid protruding across the defect and outside the skull (Fig. 23.3).

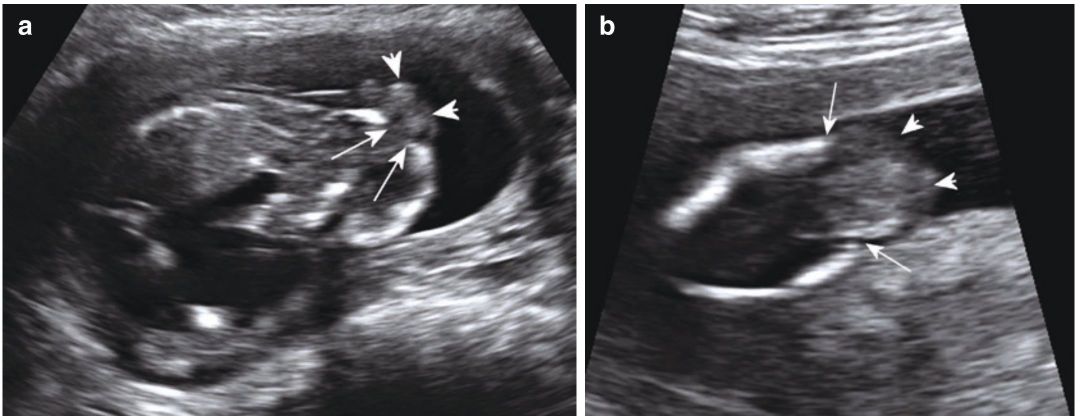

Fig. 23.3 Encephalocele. (**a**) Sagittal midline and (**b**) axial image of 13-week fetus showing defect in posterior skull (arrows) with tissue protruding outside the cranium into a sac (arrowheads)

Spinal Anomalies

The most common anomaly affecting the fetal spine is a neural tube defect, a meningomyelocele or meningocele. Other spinal anomalies include segmentation defects resulting in hemivertebrae and caudal regression abnormalities, including sacral agenesis. While most anomalies of the spine cannot be identified until the second or third trimester, some cases of meningomyelocele may be detected in the first trimester, appearing as disruption of the spine, most often in the lumbosacral region, with protrusion of a complex cystic and solid mass posteriorly, representing the dorsal sac of the neural tube defect (Fig. 23.4).

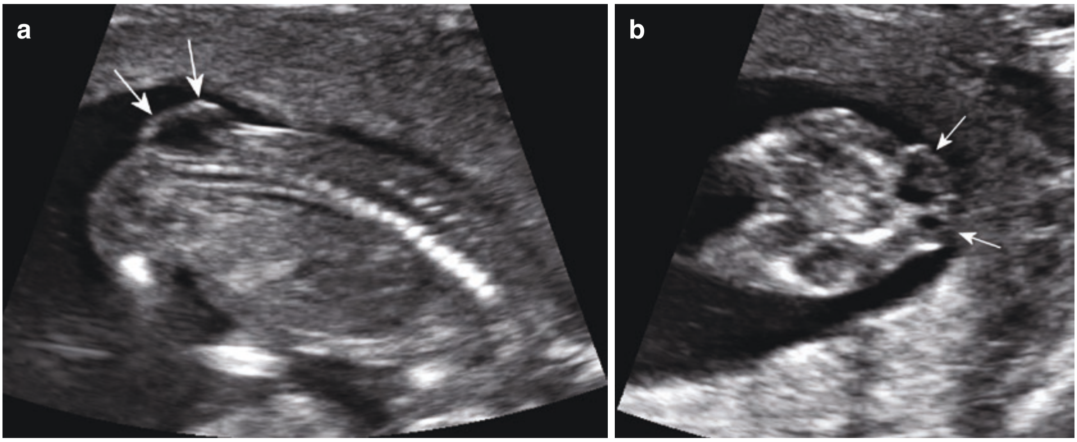

Fig. 23.4 Meningomyelocele. (**a**) Sagittal view of distal spine showing disruption of the spine and overlying skin by a protruding cystic mass (arrows). (**b**) Transverse view of the lower spine demonstrating widening of the spinal canal with a complex cystic mass extending posterior from the fetus (arrows), representing the dorsal sac of the meningomyelocele

Extremities

Polydactyly

Polydactyly is characterized by extra digits, fingers and/or toes. When present, careful assessment of the fetus is warranted as polydactyly may be a component of a syndrome, such as a skeletal dysplasia like short-rib polydactyly or trisomy 13 or Meckel-Gruber. Polydactyly may also be genetic, most often the isolated postaxial form, which is autosomal dominant [9]. The diagnosis may be made during first-trimester ultrasound by identifying an extra digit in the hand or foot (Fig. 23.5).

Clubfoot

Clubfoot or clubfeet, like polydactyly, may be an isolated anomaly, or the abnormality may be a component of a genetic syndrome, such as trisomy 18, or associated with other anomalies, such as meningomyelocele, or may be a result of a confined environment in utero, such as from severe oligohydramnios [9]. The sonographic diagnosis of clubfoot during the first trimester is made by identifying the bones of the foot oriented in parallel with the bones of the lower leg (Fig. 23.6).

Limb Reduction Defects

Absence of part of an extremity is termed a limb reduction defect. Defects may be as severe as missing an entire extremity or parts of multiple extremities, or may be less severe, with only a few digits from a hand or foot missing. The cause of the defect may be the result of amniotic bands or vascular disruption but may also be a component of a syndrome or the result of exposure to a teratogen [9, 10]. In the majority of cases, the reduction defect is isolated with only a single limb affected. In such cases, the upper extremity is affected more often than the lower, and an underlying genetic abnormality or associated anomalies are rarely found. When multiple reduction defects are present, additional nonskeletal anomalies are found in about half of the cases and an underlying etiology may be implicated [10].

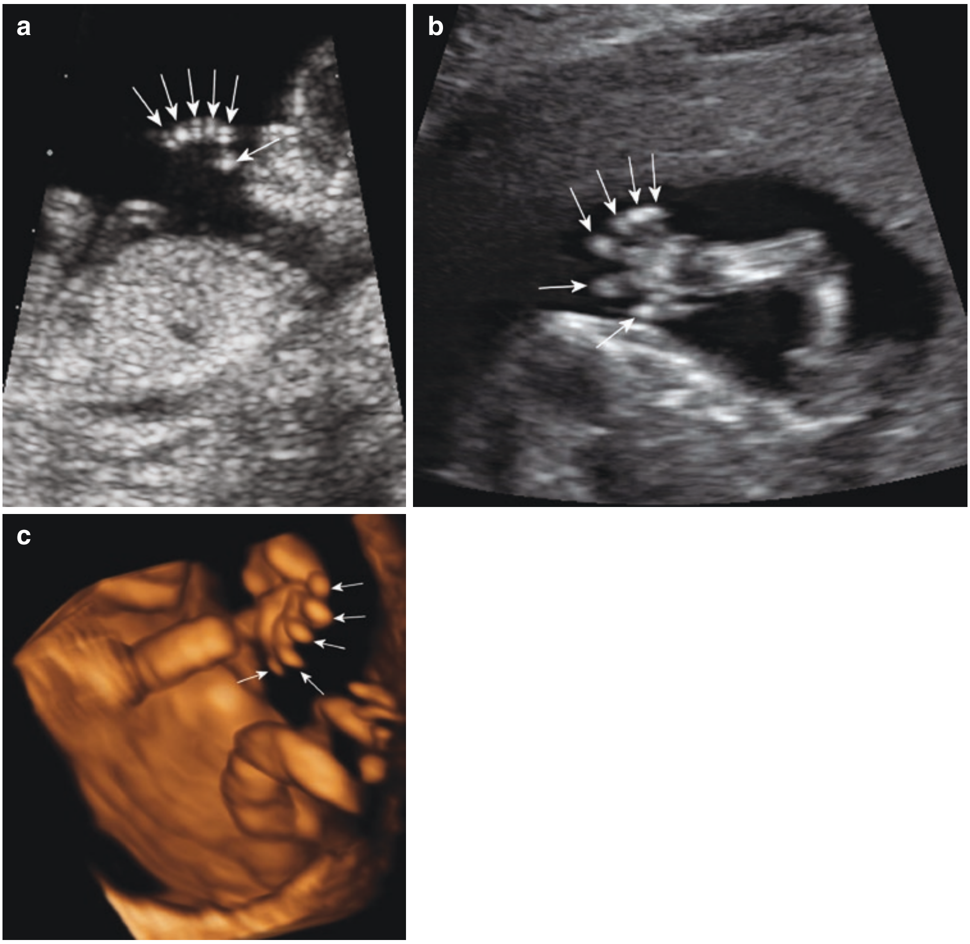

Fig. 23.5 Polydactyly. (**a**, **b**) Hands of two different fetuses, both 13 weeks' gestation and both with trisomy 13, showing postaxial polydactyly with 6 digits (arrows), including an extra digit next to the little finger. (**c**) 3D image of fingers of a hand with polydactyly showing 5 fingers (arrows) with postaxial polydactyly. The thumb is not visible on the image due to the fetal hand position

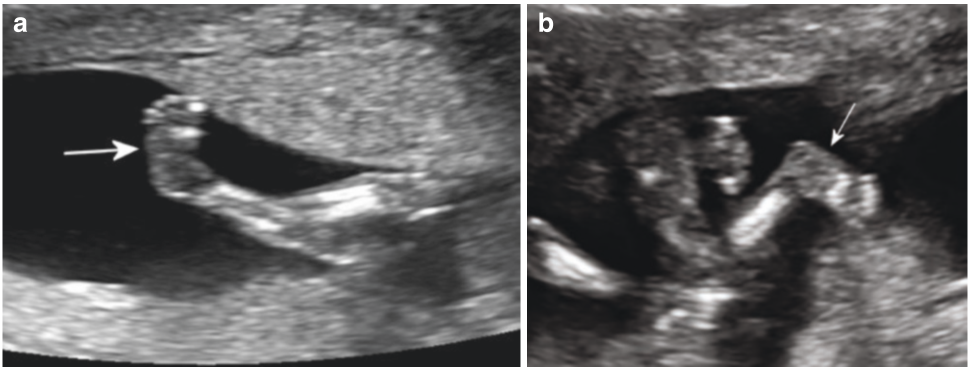

Fig. 23.6 Clubfoot. (**a**) Sonogram of foot in fetus with meningomyelocele showing associated clubfoot deformity. The bones of the foot (arrow) are aligned in parallel with the lower leg. (**b**) Image of clubfoot (arrow) in fetus with hereditary clubfoot showing the abnormal positioning of the foot with respect to the lower leg

Ectrodactyly or split hand/split foot syndrome, also called lobster claw hand, is characterized by a cleft in the central part of the hand and/or foot with absence of one or more fingers and/or toes. This anomaly may be the result of an isolated autosomal dominant or autosomal recessive genetic abnormality, or it may be seen as part of a syndrome that includes other fetal anomalies [11]. The sonographic diagnosis is made when a cleft is identified in a hand or foot accompanied by absence of one or more digits (Fig. 23.7).

Amniotic band sequence or amniotic band syndrome is a sporadic abnormality that results from disruption of the amnion early in pregnancy leading to fibrous bands entangling the fetus. The fibrous bands may cause limb amputation abnormalities from constriction or disruption of the extremity. Fibrous bands may disrupt the cranium or trunk [12]. The diagnosis of amniotic band sequence is made at ultrasound by identifying one or more limb reduction defects or unusual defects in the cranium or trunk. Fibrous bands can sometimes be seen crossing the gestational sac and attaching to the fetus (Fig. 23.8).

Terminal transverse limb deletions are those anomalies where the distal portion of an arm or leg is missing, but the proximal portion is normally formed. Many such defects likely result from amniotic bands even when fibrous bands are not seen at sonography. In the first trimester, the diagnosis of a terminal deletion is made by identifying the absence of part of the hand or foot, or absence of distal arm or leg (Fig. 23.9).

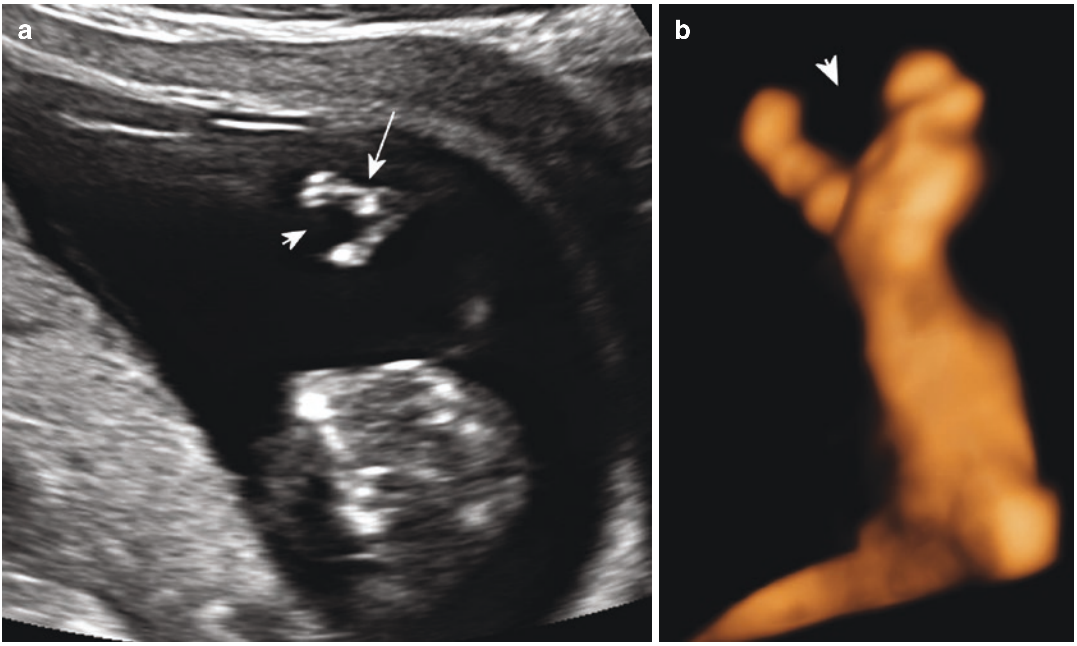

Fig. 23.7 Ectrodactyly, split hand/split foot syndrome at 13 weeks' gestation. (**a**) Image of left hand (arrow) with cleft (arrowhead) extending into the palm and missing digits in a fetus with clefts in both hands and both feet. (**b**) 3D sonogram of left hand showing large cleft (arrowhead) between thumb and remaining fingers of the hand. (**c**) 3D image of right upper extremity and face showing a similar cleft in the right hand. (**d**) 3D image of right foot showing a cleft (arrowhead) in the middle of the foot, similar to the clefts in the hands

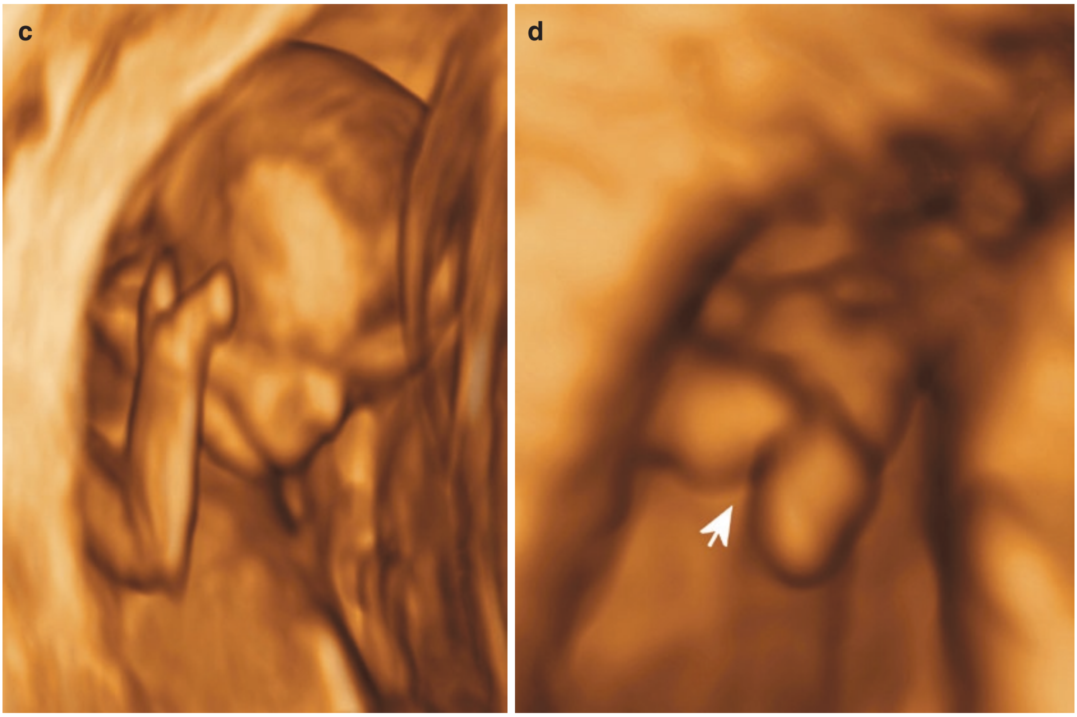

Fig. 23.7 (continued)

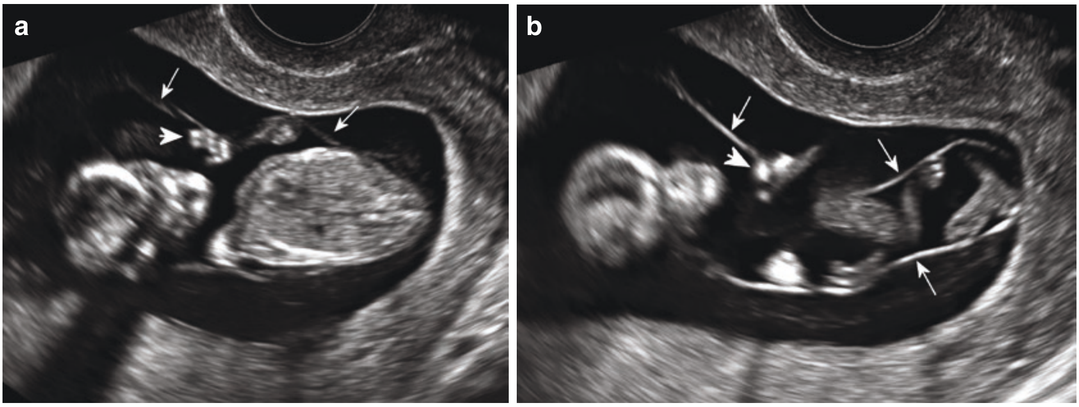

Fig. 23.8 Amniotic band sequence. (**a**, **b**) Fibrous bands (arrows) are seen crossing the gestational sac in this 12-week fetus. The bands are attached to and move with the hand (arrowhead). (**c**) Sonogram from a 13-week gestation showing multiple fibrous bands (arrows) crossing the gestational sac, entangling the fetus. (**d**) 3D sonogram of same fetus showing cleft in right hand (arrow) as a result of the bands

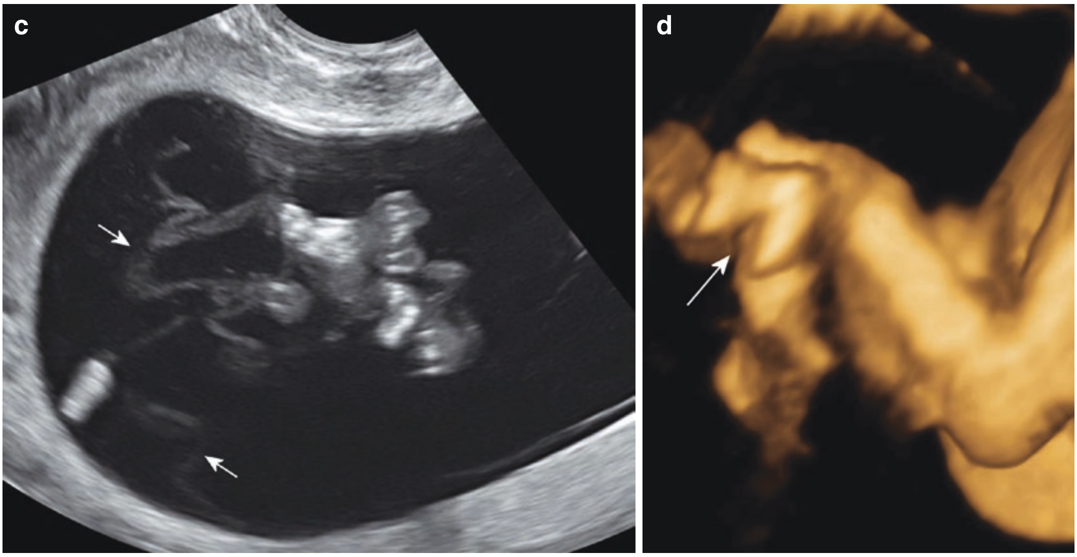

Fig. 23.8 (continued)

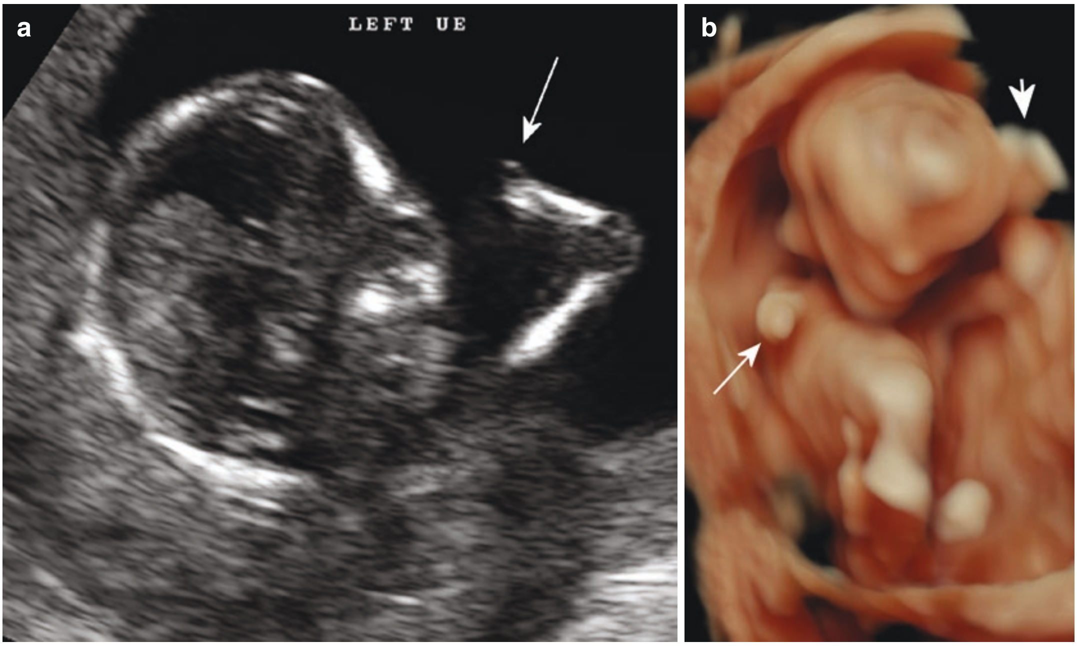

Fig. 23.9 Limb terminal deletion. (**a**) Sonogram of 13-week fetal left upper extremity showing termination of the extremity mid forearm (arrow) with absence of the distal forearm, wrist, and hand. (**b**) 3D sonogram of 12-week fetus in whom most of the right upper extremity is missing, with only a small nubbin of the upper arm (arrow) present. The left upper extremity is normal, with the hand (arrowhead) seen next to the ear. (**c**) 3D image of another 12-week fetus with terminal absence of all four extremities, with small segments of the upper arms (arrows) and nubbins in place of both legs (arrowheads)

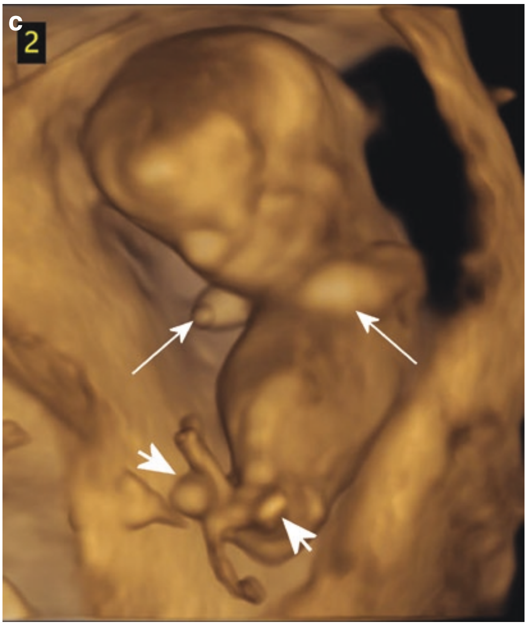

Fig. 23.9 (continued)

Summary

Detailed evaluation of the fetal skeletal system during first-trimester ultrasound, using both grayscale and 3D ultrasound, can facilitate the diagnosis of skeletal anomalies early in pregnancy. When a fetal skeletal abnormality is detected, careful assessment of the rest of the fetus is warranted to determine if the finding is isolated or if other anomalies are visible at this early stage of gestation. The patient can then be referred for counseling and testing, including maternal blood tests or chorionic villous sampling, to determine if the abnormality has a genetic component or to see if an underlying etiology can be determined. As ultrasound technology advances and the skills of operators and interpreting clinicians expand, fetal skeletal abnormalities will likely be detected more often during the first trimester than in the past.

Teaching Points

- The fetal skeleton starts to develop in the early first trimester and continues to form and grow throughout gestation.
- After 11 weeks' gestation, more than half of the major skeletal anomalies can be identified on detailed first-trimester scan using grayscale and 3D sonography.
- Prenatal diagnosis of a skeletal dysplasia can rarely be made during the first trimester except in some severe lethal cases, such as thanatophoric dysplasia.
- Anomalies of the upper and lower extremities, such as polydactyly, clubfoot, and limb reduction defects, are often apparent on first-trimester ultrasound and, when diagnosed, should prompt further assessment of the fetus for an underlying syndrome or chromosomal abnormality.

References

1. Bromley B, Shipp TD, Lyons J, Navathe RS, Groszmann Y, Benacerraf BR. Detection of fetal structural anomalies in a basic first-trimester screening program for aneuploidy. J Ultrasound Med. 2014;33:1737–45.
2. Syngelaki A, Hammami S, Bower V, Zidere R, Akolekar KH, Nicolaides A. Diagnosis of fetal non-chromosomal abnormalities on routine ultrasound examination at 11–13 weeks' gestation. Ultrasound Obstet Gynecol. 2019;54:468–76.
3. Vayna AM, Veduta A, Duta S, Panaitescu AM, Stoica S, Buinoiu N, Nedelea F, Peltecu G. Diagnosis of fetal structural anomalies at 11 to 14 weeks. J Ultrasound Med. 2018;37:2063–73.
4. Collaborative Subcommittee Task Force. AIUM practice parameter for the performance of detailed diagnostic obstetric ultrasound examinations between 12 weeks 0 days and 13 weeks 6 days. J Ultrasound Med. 2021;40:E1–E16.
5. Khalil A, Pajkrt E, Chitty LS. Early prenatal diagnosis of skeletal anomalies. Prenat Diagn. 2011;31:115–24.
6. Glanc P, Chitayat D. Approach to prenatal diagnosis of the lethal skeletal dysplasias. UpToDate. 2020; https://www.uptodate.com/contents/approach-to-prenatal-diagnosis-of-the-lethal-skeletal-dysplasias?search=skeletal%20dysplasia%20children&topicRef=13551&source=see_link
7. Bodzmer OA. Spinal muscular atrophy. UpToDate. 2021; https://www.uptodate.com/contents/spinal-muscular-atrophy?sectionName=Arthrogryposis%20multiplex%20congenita&search=arthrogryposis%20multiplex%20congenita&topicRef=6151&anchor=H-1989357564&source=see_link#H1989357564
8. Kalampokas E, Kalampokas T, Sofoudis C, Deligeoroglou E, Botsis D. Diagnosing arthrogryposis

multiplex congenita: a review. Obstet Gynecol. 2012;2012:264918.

9. Benacerraf BR. Ultrasound of fetal syndromes. 2nd ed. Philadelphia, PA: Elsevier; 2008.
10. Bergman JEH, Lohner K, van der Sluis CK, Rump P, de Walle HEK. Etiological diagnosis in limb reduction defects and the number of affected limbs: a population-based study in the northern Netherlands. Am J Med Genet. 2020;182A:2909–18.
11. Jindal G, Parmar VR, Gupta VK. Ectrodactyly/split hand feet malformation. Indian J Hum Genet. 2009;15:140–2.
12. Gandhi M, Rac WMF, McKinney J, for Society for Maternal-Fetal Medicine. Amniotic band sequence. Am J Obstet Gynecol. 2019;221:B5–6.

24

First-Trimester Ultrasound in Gestational Trophoblastic Disease

Kevin M. Elias, Neil S. Horowitz,
and Ross S. Berkowitz

Introduction

Gestational trophoblastic disease (GTD) is a series of conditions that arise from the trophoblastic epithelia of the placenta. The specific histologic subtypes of GTD are hydatidiform mole (complete or partial), invasive mole, choriocarcinoma, placental site trophoblastic tumor (PSTT), and epithelioid trophoblastic tumor (ETT). All types of GTD share a common tumor marker, human chorionic gonadotropin (hCG). Approximately 90% of cases of GTD are complete (CHM) or partial (PHM) hydatidiform moles, which are noninvasive, localized neoplasms resulting from an abnormal fertilization event [1–4]. CHM arise from fertilization of an empty egg and are usually diploid with a 46XX karyotype and androgenetic, while PHM are the result of fertilization of a normal ovum with two spermatozoa and thus have a triploid karyotype [5]. The remaining 10% of GTD include patients who develop malignancy following a nonmolar pregnancy [4]. Malignant forms of GTD are collectively referred to as gestational trophoblastic neoplasia (GTN).

The incidence of CHM ranges from 23 to 1299 cases per 100,000 pregnancies with wide variations reported between different regions of the world [6]. The main risk factors are maternal age over 35 and history of prior GTD. GTD often presents with abnormal bleeding and an elevated hCG. Prior to the wide accessibility of ultrasound in early pregnancy, classic findings of CHM on presentation included an enlarged uterus (size > dates), absent fetal heart tones, markedly elevated hCG for gestational age, pelvic pressure or pain, theca lutein cysts, vaginal bleeding and subsequent anemia, hyperemesis gravidarum, hyperthyroidism, and preeclampsia before 20 weeks [7]. PHM usually present as a missed abortion. Treatment for CHM and PHM includes uterine evacuation and post-evacuation monitoring of quantitative hCG. The majority of women will normalize their hCG after evacuation; however, approximately 15–20% of women with a CHM and 1–5% with PHM will have a plateau or rise in their hCG meeting the criteria for the diagnosis of postmolar GTN [3]. Treatment for GTN includes chemotherapy and occasionally surgical intervention.

Ultrasound plays an important role in managing patients with GTD, not only for the initial

---

K. M. Elias · N. S. Horowitz · R. S. Berkowitz (✉)
New England Trophoblastic Disease Center, Donald P. Goldstein M.D. Trophoblastic Tumor Registry, Brigham and Women's Hospital and Dana-Farber Cancer Institute, Dana Farber/Brigham and Women's Cancer Center, Division of Gynecologic Oncology and the Department of Obstetrics, Gynecology and Reproductive Biology, Harvard Medical School, Boston, MA, USA
e-mail: kelias@bwh.harvard.edu;
nhorowitz@mgh.harvard.edu;
rberkowitz@partners.org;
ross_berkowitz@dfci.harvard.edu

© The Author(s), under exclusive license to Springer Nature Switzerland AG 2023
J. S. Abramowicz, R. E. Longman (eds.), *First-Trimester Ultrasound*,
https://doi.org/10.1007/978-3-031-24133-8_24

diagnosis of molar pregnancy and GTN, but also in the evaluation of patients who present with recurrent or resistant disease and during long-term follow-up. Recent studies also demonstrate that it may be prognostic in identifying patients with GTN at risk for chemoresistance.

Ultrasound in the Diagnosis of Molar Pregnancy

Classic Sonographic Findings of Molar Pregnancy

Classic sonographic findings of a CHM include an enlarged uterus with complex heterogeneous material in the absence of a normal-appearing intrauterine gestation. Descriptions of CHM pregnancy include "snowstorm" appearance or a "cluster of grapes," which represent the enlarged hydropic villi [8, 9] (Fig. 24.1). A partial molar pregnancy, on the other hand, may show an enlarged placenta with multiple anechoic spaces along with fetal parts either representing a nonviable embryo or with stereotypical fetal anomalies (especially 3–4 syndactyly of the hands) and growth restriction as a result of triploidy [8, 10–13] (Fig. 24.2). Historically, only 30–47% of patients were diagnosed with a complete molar pregnancy in the first trimester. However, the increased use of ultrasound in early pregnancy has led to over 84% of diagnoses of CHM being made in the first trimester [14]. From 1994 to 2013, at the New England Trophoblastic Disease Center, the median gestational age at evacuation was 9 weeks for CHM and 12 weeks for PHM [15].

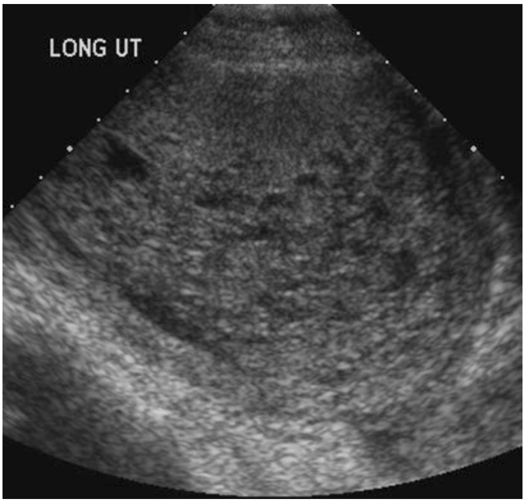

Fig. 24.1 Complete hydatidiform mole with classic diffuse vesicular changes. (*Figure provided by Dr. Carol B. Benson, Director of Ultrasound, Department of Radiology, Brigham & Women's Hospital and Professor of Radiology, Harvard Medical School, Boston, MA*)

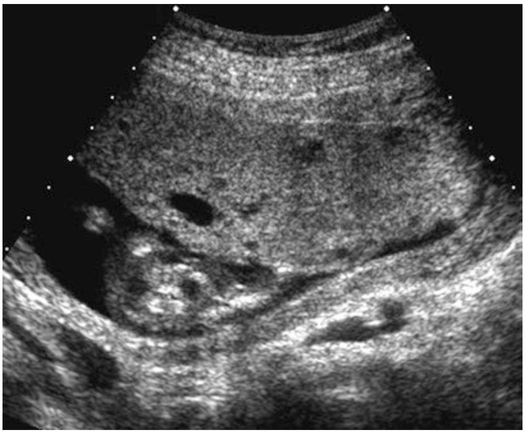

Fig. 24.2 Partial hydatidiform mole with focal vesicular changes and nonviable fetus. (*Figure provided by Dr. Carol B. Benson, Director of Ultrasound, Department of Radiology, Brigham & Women's Hospital and Professor of Radiology, Harvard Medical School, Boston, MA*)

Ultrasound Diagnosis of Early Molar Pregnancy

The classic sonographic appearance of CHM described above may be lacking in patients who present with bleeding early in the first trimester, making the sonographic diagnosis more difficult. The hydropic villi are smaller at earlier gestational ages, and the molar tissue may appear as a complex echogenic intrauterine mass with several anechoic or cystic spaces [7, 10] (Fig. 24.3). In early gestations, it may also be more difficult to differentiate PHM from CHM. One characteristic that may help to differentiate the two types of molar pregnancy is the presence of a gestational sac in PHM that either is empty or contains small fetal echoes surrounded by a large rim of

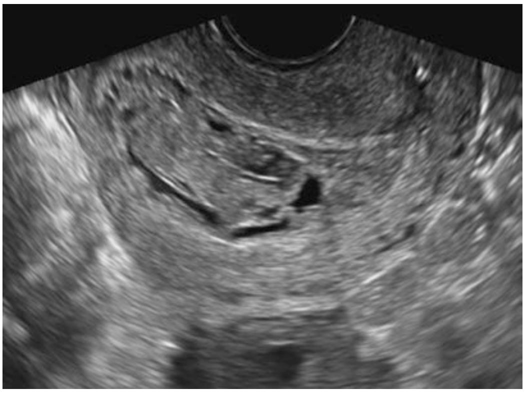

Fig. 24.3 First-trimester complete hydatidiform molar pregnancy with limited vesicular changes that are less prominent and best seen on transvaginal ultrasound images. (*Figure provided by Dr. Carol B. Benson, Director of Ultrasound, Department of Radiology, Brigham & Women's Hospital and Professor of Radiology, Harvard Medical School, Boston, MA*)

placental echoes with cystic spaces [16]. Additionally, the earlier the presentation, the more difficult it is to differentiate molar pregnancy from a hydropic nonmolar abortion. Ultrasonographic descriptions of early histologically confirmed molar pregnancies include an empty gestational sac or intrauterine anechoic fluid collection, fluid collection in association with an echogenic mass, thickened endometrium, and echogenic fluid-filled levels within the endometrium [17, 18].

Early molar pregnancy may also be confused with placental mesenchymal dysplasia (PMD) [19]. Like partial molar pregnancy, PMD may present with placentomegaly and grapelike vesicles, but in contrast to partial mole, the fetus in PMD has a normal karyotype and may be viable, although with severe fetal and/or maternal complications [20, 21]. Histologically, PMD differs from molar pregnancy by the absence of trophoblastic hyperplasia and carries no risk of developing into a malignancy [22]. PMD is commonly associated with Beckwith-Wiedemann syndrome [23].

Ultrasound can also be used to assess the volume of molar tissue present in the uterus, which has been shown to be a risk factor for GTN [24–27]. A 3-dimensional assessment of volume is felt by some experts to be superior to a single measurement. However, in one study, the size of the lesion measured sonographically was not predictive of the need for chemotherapy [25]. Although myometrial invasion can be assessed with ultrasound, MRI is often a better modality to demonstrate the presence of invasion of molar tissues into the uterine wall [26, 27].

Sensitivity of Ultrasound in Detecting Molar Pregnancy

Several investigators have examined the accuracy of ultrasound in the diagnosis of molar pregnancy. Fowler et al. published the largest study evaluating the role of ultrasound in the detection of molar pregnancy [28]. The authors reviewed 1053 consecutive cases of molar pregnancy with early ultrasound evaluation and found that the sensitivity for detecting either a CHM or a PHM was 44%. The mean gestational age at diagnosis was 10 weeks. They found that ultrasound was better at detecting CHM versus PHM (79% vs. 29%, $p < 0.0001$), and there was a false-positive rate of 10% whose final pathology demonstrated hydropic degeneration of nonmolar pregnancies. Other smaller reviews have shown sensitivity of ultrasound in detecting molar pregnancy to range from 34% to 57% [17, 18, 28, 29]. The sensitivity of ultrasound improves with increasing gestational age as the hydropic villi grow in size with advancing gestational age and are more easily seen by ultrasound. When analyzing ultrasound sensitivity by type of molar pregnancy, ultrasound is consistently more sensitive in detecting CHM (sensitivity range 58–95%) as compared to PHM (sensitivity range 17–29%) [7, 18, 28–31]. A recent cohort study examining ultrasound imaging in cases of missed miscarriage that subsequently had histologically confirmed hydatidiform moles again found that ultrasound predicted a higher number of CHM (95/128 (74.2%)) than PHM (68/167 (40.7%)) [32]. For all types of molar pregnancy, correlation with hCG is critical to the diagnosis [30].

Mimics of Molar Pregnancy

There are other conditions in early pregnancy that mimic the sonographic appearance of molar pregnancy such as hydropic degeneration of the placenta, missed abortion, blighted ovum, and retained products of conception. False-positive rates of ultrasound in molar pregnancy have been estimated anywhere from 4% to 10% [28, 33]. Hydropic changes of the placenta in other gestations can appear similar to the hydropic villi of molar disease but tend to be less homogeneously distributed [28, 34]. Although it can be difficult to differentiate an early partial molar pregnancy from other abnormalities of early pregnancy, the presence of an echogenic rim around the sac may be more indicative of a missed abortion or blighted ovum [16].

Color Doppler Ultrasound in Diagnosis of Molar Pregnancy

Color Doppler ultrasound allows the clinician to assess vascularity. In trophoblastic tissues, a high-velocity, low-resistance flow is consistent with increased vascularity. Thus, use of color Doppler imaging may help differentiate molar pregnancy from mimics such as missed abortion [10, 35].

Uterine Artery Doppler Measurement in Molar Pregnancy and Development of GTN

Several studies have shown that uterine artery-resistive indices correlate well with hCG levels and may therefore be helpful in the diagnosis and monitoring of treatment [36–41]. Yalcin et al. followed 21 patients with molar pregnancy with hCG and uterine artery Dopplers and found significant negative correlations with hCG and Doppler indices; that is, as the hCG declined demonstrating resolution of disease, the resistive indices rose [39]. In this study, the patients who ultimately developed postmolar GTN had significantly lower Doppler indices than those whose disease regressed spontaneously. Others have also demonstrated this inverse relationship of lower resistive indices indicating a greater risk of developing postmolar GTN [37, 38, 42–44]. One study of 25 patients with molar pregnancy undergoing surveillance with hCG and transvaginal ultrasound (TVUS) with Doppler also noted that surveillance with Doppler predicted GTN 1–3 weeks before routine hCG monitoring and that ultrasound findings tended to resolve about 8 weeks earlier than hCG normalization [40]. A prospective cohort study of 246 patients with a complete mole who were treated at three different trophoblastic disease centers in Brazil between 2013 and 2014 showed that a pre-evacuation pulsatility index ≤1.38 or post-evacuation pulsatility index ≤1.77 was significantly predictive of gestational trophoblastic neoplasia [45].

Ultrasound in the Diagnosis and Management of Ovarian Theca Lutein Cysts

Ovarian theca lutein cysts develop in 25–65% of complete molar pregnancies in association with markedly elevated hCG levels >100,000 mIU/mL. In a review of 386 patients with untreated hydatidiform mole, 102 patients (26.4%) had concurrent theca lutein cysts [46]. Theca lutein cysts appear sonographically to be anechoic, multi-loculated ovarian cysts [47] (Fig. 24.4). Mean cyst diameters are reported to be around 7 cm but can range in size from 3 to 20 cm [34, 47]. Typically, these cysts will be accompanied with the uterine sonographic findings detailed previously. Of note, theca lutein cysts are less likely to be seen in first-trimester complete or partial molar pregnancies where the hCG level is generally <100,000 mIU/mL [17]. The size of the theca lutein cysts has not been shown to correlate with persistent disease, although the presence of bilateral cysts is associated with an increased risk of GTN [46]. Serial ultrasound examination is useful to monitor the regression of theca lutein cysts, which tend to regress slowly over 2–4 months following molar evacuation as the

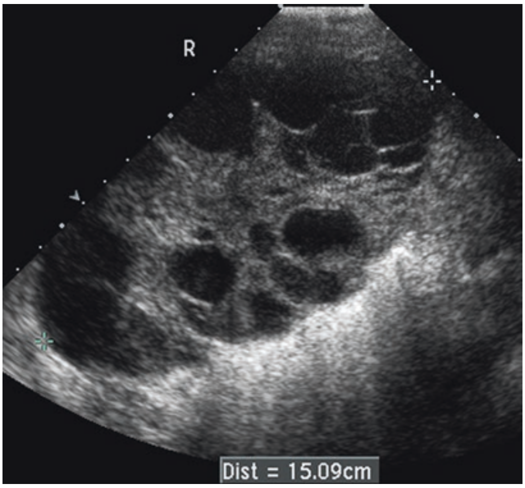

Fig. 24.4 Theca lutein cysts filling an ovary and appear as anechoic multi-loculated cystic structures. (*Figure provided by Dr. Carol B. Benson, Director of Ultrasound, Department of Radiology, Brigham & Women's Hospital and Professor of Radiology, Harvard Medical School, Boston, MA*)

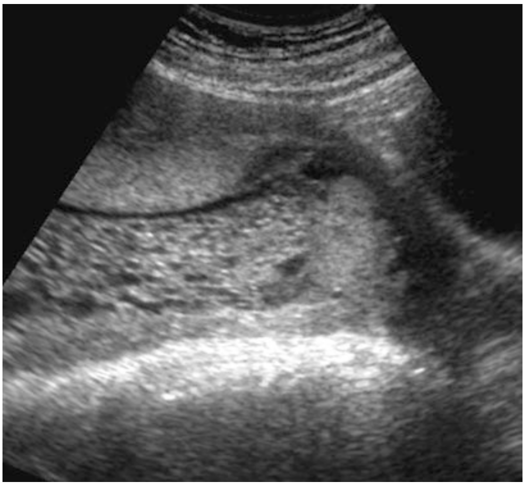

Fig. 24.5 Twin gestation with one normal placenta anteriorly and one complete molar pregnancy posteriorly demonstrating classic diffuse vesicular changes. (*Figure provided by Dr. Carol B. Benson, Director of Ultrasound, Department of Radiology, Brigham & Women's Hospital and Professor of Radiology, Harvard Medical School, Boston, MA*)

hCG level declines [48]. Although theca lutein cysts rarely rupture spontaneously or undergo torsion, in these cases, prompt laparoscopic intervention can be used effectively. The use of ultrasound guidance during percutaneous drainage of massively enlarged theca lutein cysts may also provide considerable relief of abdominal discomfort.

Ultrasound in the Diagnosis of Molar Pregnancies with a Coexistent Twin

Concurrent twin pregnancy with a hydatidiform mole and coexisting fetus is estimated to occur 1 in 22,000–100,000 pregnancies [49]. The diagnosis of a molar pregnancy with coexisting fetus is almost always made based on ultrasound findings and tends to be diagnosed at a later gestational age than a singleton CHM [50]. Ultrasound findings show a live fetus with either a single enlarged placenta with the classic cystic changes and increased echoes or two placentas, one normal and the other molar [51] (Fig. 24.5). Ultrasound is also critical in the ongoing management of these pregnancies to help ensure the well-being of the coexisting fetus. Of those pregnancies described in the literature that were continued after diagnosis of a twin molar gestation, more than half continued beyond the 28th week of gestation with almost 70% of children surviving [49]. However, these twin molar pregnancies are more likely to develop GTN as compared to singleton molar pregnancies [50]. In a series of 72 cases of complete molar pregnancy with coexisting normal fetus, the overall rate of GTN was 46%, and the rate of GTN was not significantly different between the group who chose to continue the pregnancy and those that interrupted the pregnancy at diagnosis [52].

Ultrasound in the Evacuation of Molar Pregnancy

The first step in the management of a molar pregnancy is uterine evacuation, typically with suction curettage [53]. Manual or electric vacuum suction techniques are equally efficacious [54]. The technique for uterine evacuation is similar to that used for spontaneous and induced abortions.

However, there is a greater concern for blood loss due to the increased vascularity of molar gestations. Intraoperative ultrasound may be a very useful tool during a suction curettage for molar pregnancy, particularly in cases with a large volume of intrauterine disease. When available, ultrasound should be used at the start of the procedure to examine the intrauterine disease and assess for pelvic extension. Ultrasound can be utilized to help prevent uterine perforation during the serial dilation of the cervix and placement of the suction curette. Finally, at the conclusion of the procedure, ultrasound allows the clinician to visualize the uterine cavity and confirm complete evacuation of molar tissues [53].

Ultrasound in the Diagnosis and Management of GTN

Ultrasound is the imaging modality of choice for the initial evaluation of the uterus and adnexa when a patient has been diagnosed with GTN. GTN includes invasive mole, choriocarcinoma, PSTT, and ETT. Choriocarcinoma arises from both cyto- and syncytiotrophoblasts and produces high levels of hCG. Choriocarcinoma is associated with early metastatic spread but is generally highly sensitive to chemotherapy. Unlike choriocarcinoma, PSTT and ETT arise from extravillous intermediate trophoblasts and produce low levels of hCG. Unfortunately, and importantly, both PSTT and ETT are relatively resistant to chemotherapy unlike the other types of GTN.

Ultrasound is not able to differentiate between types of GTN. Therefore, correlation with clinical history and hCG is critical. Betel et al. compared 17 cases of GTD to 14 cases of retained products of conception sonographically and found that GTD cases were more likely associated with a larger mass (>3.45 cm), thin endometrium (<12 mm), myometrial based mass, and vascular lakes [55]. Non-gestational conditions that have been described to mimic GTD sonographically include uterine leiomyomas and an adenomyomatous polyp [33, 56]. In addition to the increased vascularity, Doppler can also illustrate focal areas of increased flow within the myometrium in cases of invasive molar pregnancy and choriocarcinoma [57]. Measurement of uterine artery Doppler indices including the resistive index (RI) and the pulsatility index (PI) has been studied in GTN. RI and PI tend to be very low in GTN, and changes within these indices correlate with response to treatment and resolution of GTN over the course of follow-up with the indices increasing as the hCG levels decline [45, 57, 58]. Although ultrasound is not sufficient to make the diagnosis of a specific type of GTN, certain sonographic findings may be clues to the diagnosis:

- *Invasive molar pregnancy* may appear as an intrauterine mass(es) with anechoic areas and also often demonstrates focal areas of increased echogenicity within the myometrium or can appear as heterogeneous lesions containing fluid-filled cavities representing invasion (Fig. 24.6).
- *Choriocarcinoma* may appear as an enlarged uterus containing a semisolid heterogeneous echogenic mass with areas of necrosis and hemorrhage. Choriocarcinoma nodules are hypervascular showing increased vascularity on color Doppler. Choriocarcinoma can also be seen invading the myometrium or even out to the parametria.

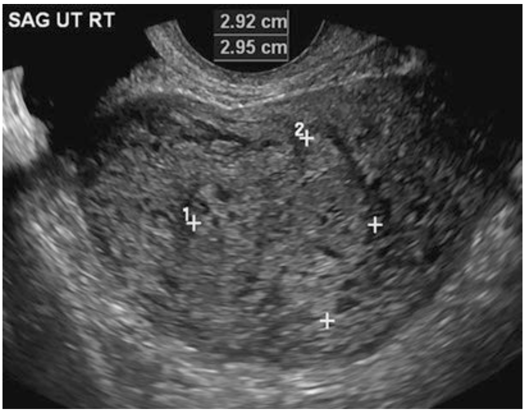

Fig. 24.6 Invasive complete molar pregnancy with intrauterine mass containing diffuse vesicular changes invading into the myometrium. (*Figure provided by Dr. Carol B. Benson, Director of Ultrasound, Department of Radiology, Brigham & Women's Hospital and Professor of Radiology, Harvard Medical School, Boston, MA*)

- *Placental site trophoblastic tumor* may also appear as small heterogeneous echogenic areas with fluid-filled cysts, but generally has less necrosis than choriocarcinoma. PSTT may also appear as a solid tumor with or without cystic spaces in the uterus or invading the myometrium. These masses can demonstrate a wide range of vascularity from a nonvascularized mass to a high degree of vascularity [59, 60].
- *Epithelioid trophoblastic tumor* appears early in the course of disease with irregular echolucent lacunae within the myometrium on transvaginal ultrasound, but later in the disease with a well-circumscribed solitary echogenic lesion in the fundal myometrium without blood flow [61].

Ultrasound to Assess Presence and Volume of Intrauterine Disease

Transvaginal ultrasound (TVUS) is the preferred technique to detect the presence of invasive GTN [37, 62, 63]. TVUS findings of GTN have been described as hypoechoic areas in the endometrium and intramyometrial nodules, clusters of high-amplitude echoes within the myometrium representing invasive tumor with echo-free areas representing hemorrhage, and multiple “serpiginous anechoic channels” throughout the central part of the uterus [62, 64, 65].

Ultrasound Evaluation for Postmolar GTN

Following diagnosis and evacuation of a CHM or PHM, serial hCG levels are used to determine the development of postmolar GTN. The diagnosis of postmolar GTN is made when hCG levels plateau for more than three consecutive weeks or rise for more than two consecutive weeks [66]. Once the diagnosis of GTN is made, ultrasound is one of the imaging tests used for identifying the location and extent of disease. The presence and size of any intrauterine tumor contribute to the prognostic risk score used to triage postmolar GTN patients to either single-agent or multiagent chemotherapy [66]. In one study of 33 patients with GTN, ultrasound findings were reviewed, and in 17/33 (51.5%) patients, the ultrasound demonstrated uterine disease that correlated 100% of the time with pathology from an endometrial curettage or hysterectomy. Of the 16/33 patients who did not have evidence of intrauterine disease on ultrasound, the endometrial curetting was positive for fragments of trophoblastic tumor in only 6/16 (37.5%) [67].

Color Doppler in Diagnosis of GTN

The vascular nature of GTN makes the use of color Doppler in conjunction with TVUS ideally suited for evaluating the presence and extent of intramyometrial disease. The use of Doppler can aid in the identification of myometrial invasion sonographically, a feature of GTN that was previously often only made histologically after hysterectomy. Doppler color flow mapping is seen as abnormal flow through the myometrium in cases of myometrial invasion [27, 36, 57, 62, 68]. TVUS with Doppler can identify small foci of resistant intrauterine disease and can be used to evaluate the depth of myometrial invasion, which may also be prognostic for resistant disease [37, 42]. Doppler can also be utilized to monitor and measure uterine artery blood flow, and a resistive index (RI) and pulsatility index (PI) can be calculated. In pregnancy, the resistance to blood flowing into the uterus drops dramatically with the development of uteroplacental blood vessels, and with the hypervascularity of GTD, the resistance is even less. In fact, resistive indices progressively decrease as one goes from a nonpregnant uterus to a normal pregnancy to molar pregnancy to invasive molar pregnancy and choriocarcinoma [35, 69–71]. Thus, in cases where the diagnosis is not clear, use of the color Doppler may demonstrate invasion into the myometrium and measurement of uterine artery pulsations may be low suggestive of a diagnosis of GTN.

Ultrasound in the Follow-Up of Molar Pregnancy and GTN

Use in Determining the Need for Surgical Intervention

Although the mainstay of treatment for GTN is chemotherapy, in select circumstances, surgical intervention is indicated [72]. Ultrasound has proven to be very useful in identifying patients who may benefit from surgery. First, patients presenting with bleeding from persistent intrauterine disease may benefit from either a repeat D&C, local resection, or hysterectomy. Second, patients undergoing chemotherapy whose hCG levels indicate chemoresistance may benefit from local resection or hysterectomy, particularly in those women where future fertility is no longer desired [73, 74]. Transvaginal ultrasound with color Doppler should be the first-line imaging modality to assess for intrauterine disease when there is concern for heavy vaginal bleeding or drug-resistant uterine tumor.

Uterine Artery Pulsatile Index as a Predictor of Chemotherapy Resistance in GTN

The association of lower uterine artery Doppler pulsatile indices and need for chemotherapy has been well established as described above. Thus, several investigators have queried whether the use of these resistive indices might be helpful in identifying patients at risk for chemotherapy resistance. Approximately, 30% of patients who are considered to have low-risk disease (FIGO risk scores <7) will become resistant to first-line single-agent chemotherapy and require subsequent alternative chemotherapy [75]. Among patients with FIGO risk scores of 5 or 6, 40% of patients develop resistance to single-agent treatments and require multiagent chemotherapy [76]. Several studies have demonstrated that Doppler indices can be predictive of chemotherapy resistance, as lower resistive indices suggest a greater risk of failure to single-agent chemotherapy and that multiagent chemotherapy should be used instead [42, 77]. Agarwal et al. investigated whether the uterine artery pulsatility index (UAPI) was a predictor of chemotherapy resistance [58]. Initially, they found in 164 patients that those with a UAPI <1 had 2.68 greater odds of developing methotrexate resistance as opposed to those with initial UAPI >1. A subsequent study by the same investigators showed that a UAPI <1 as compared to >1 was predictive of chemotherapy resistance (64.6% vs. 35.4%) in multivariate analyses. Patients with a FIGO score of 6 and UAPI < or = 1 had a 100% rate of single-agent methotrexate resistance [78]. A third study showed that UAPI values were significantly lower among methotrexate resistance patients and that coupling UAPI with the circulating angiogenic biomarker BMP-9 further improved the prediction accuracy [79]. Thus, there may be a role for measurement of the UAPI in addition to calculation of the FIGO risk score in patients requiring chemotherapy for GTN. This is currently being investigated in a prospective, multicenter, observational clinical trial [80].

GTN-Related Arteriovenous Malformations

The development of uterine arteriovenous malformations (AVM) is a well-known complication of GTN. Symptomatic AVM occurs in about 0.6% of cases [81]. The increased vascularity of the tumor may lead to the creation of abnormal communications between the uterine arteries and the myometrial veins [82]. AVMs can lead to significant life-threatening hemorrhage from the uterus making ultrasound critically important in making the diagnosis and subsequent management. While D&C is the treatment of choice for many conditions with heavy vaginal bleeding, in the case of AVM, this could severely exacerbate the bleeding, and other mechanisms for control of bleeding such as hysterectomy or arterial embolization are needed. In order to make the diagnosis sonographically, the Doppler mode is helpful. AVM will demonstrate pronounced vascularity on Doppler ultrasound. Pulse-wave Doppler will demonstrate elevated blood flow velocities in both systole and diastole in addition to "spectral broadening reflecting turbulence," low resistive index measurements (between 0.25 and 0.55), and mixing of arterial and venous waveforms [83]. Other investigators have described the hypervascularity of GTN-associated AVM as pale shades during both systole and diastole with a colored mosaic pattern representing the turbulent flow [84]. The AVM may persist long after treatment for GTN is completed. Management of symptomatic (i.e., bleeding) AVM can include selective uterine arterial embolization, although AVM with only mild bleeding may resolve with the use of progestins and tranexamic acid [81]. For more severe bleeding, however, embolization is indicated. One series of GTN-associated AVM reported in the literature described 19 cases with successful embolization in 18 of those patients, with 15/18 achieving success after one embolization with polyvinyl alcohol particles. The four remaining patients required two embolization procedures [85]. Successful subsequent normal-term pregnancy following embolization treatment for a GTN-associated AVM has been reported in this and another report [85, 86].

Ultrasound for the Evaluation of Subsequent Pregnancies

Vargas et al. reviewed 2432 subsequent pregnancies following complete and partial molar pregnancies and GTN [87]. They demonstrated that patients with a history of molar pregnancy and GTN have similar reproductive outcomes to the general population in subsequent pregnancies, except for observing a 1.7% incidence of repeat molar pregnancy. Successful pregnancies have even been described following advanced cases of GTN with extensive intrauterine disease that either caused uterine perforation or required localized resection of the uterus [88]. Therefore, patients should be reassured that following resolution of molar pregnancy and GTN, the vast majority of patients may achieve a normal pregnancy. Nonetheless, due to the increased risk of recurrent molar pregnancy, all patients should also undergo a first-trimester ultrasound to rule out repeat molar pregnancy in subsequent gestations.

Teaching Points

- The hydropic villi of complete molar pregnancy give the classic appearance of a "snowstorm" or "cluster of grapes" on ultrasound.
- The sensitivity of ultrasound in the diagnosis of molar pregnancy ranges from 34% to 57%, which increases dramatically when correlated with the level of hCG.
- Ultrasound is the first-line imaging modality used for the evaluation of the uterus and adnexa in the diagnosis of gestational trophoblastic disease.
- The use of transvaginal ultrasound and color Doppler allows for greater detection of myometrial invasion and persistent uterine disease.
- Uterine artery Doppler indices are significantly lower in GTN than in normal pregnancy.
- Uterine artery Doppler indices can be predictive of persistent disease and chemotherapy resistance.
- Patients with a history of GTD should undergo ultrasound evaluation during subsequent pregnancies to rule out recurrent molar pregnancy.

Acknowledgements The authors would like to acknowledge the contributions of Drs. Katharine Esselen and Donald P. Goldstein as prior co-authors to this chapter in the first edition. We would also like to recognize the support of the Donald P. Goldstein, MD, Trophoblastic Tumor Registry Endowment and the Dyett Family Trophoblastic Disease Research and Registry Endowment for support of the scholarly activities of the New England Trophoblastic Disease Center.

References

1. Berkowitz RS, Goldstein DP. Chorionic tumors. N Engl J Med. 1996;335(23):1740–8.
2. Lurain JR. Gestational trophoblastic disease II: classification and management of gestational trophoblastic neoplasia. Am J Obstet Gynecol. 2011;204(1):11–8.
3. Lurain JR. Gestational trophoblastic disease I: epidemiology, pathology, clinical presentation and

diagnosis of gestational trophoblastic disease, and management of hydatidiform mole. Am J Obstet Gynecol. 2010;203(6):531–9.

4. Seckl MJ, Sebire NJ, Berkowitz RS. Gestational trophoblastic disease. Lancet. 2010;376(9742):717–29.
5. Szulman AE, Surti U. The syndromes of hydatidiform mole. I. Cytogenetic and morphologic correlations. Am J Obstet Gynecol. 1978;131(6):665–71.
6. Berkowitz RS, Horowitz NS, Elias KM. Hydatidiform mole: epidemiology, clinical features, and diagnosis. In: Goff B, editor. UpToDate. Philadelphia, PA: Wolters Kluwer Health; 2021.
7. Benson CB, et al. Sonographic appearance of first trimester complete hydatidiform moles. Ultrasound Obstet Gynecol. 2000;16(2):188–91.
8. Albayram F, Hamper UM. First-trimester obstetric emergencies: spectrum of sonographic findings. J Clin Ultrasound. 2002;30(3):161–77.
9. Leopold GR. Diagnostic ultrasound in the detection of molar pregnancy. Radiology. 1971;98(1):171–6.
10. Dogra V, Paspulati RM, Bhatt S. First trimester bleeding evaluation. Ultrasound Q. 2005;21(2):69–85; quiz 149–50, 153–4.
11. Naumoff P, et al. Ultrasonography of partial hydatidiform mole. Radiology. 1981;140(2):467–70.
12. Fine C, et al. Sonographic diagnosis of partial hydatidiform mole. Obstet Gynecol. 1989;73(3 Pt 1):414–8.
13. Toufaily MH, et al. Triploidy: variation of phenotype. Am J Clin Pathol. 2016;145(1):86–95.
14. Soto-Wright V, et al. The changing clinical presentation of complete molar pregnancy. Obstet Gynecol. 1995;86(5):775–9.
15. Sun SY, et al. Clinical presentation of complete hydatidiform mole and partial hydatidiform mole at a regional trophoblastic disease center in the United States over the past 2 decades. Int J Gynecol Cancer. 2016;26(2):367–70.
16. Woo JS, et al. Sonographic appearances of the partial hydatidiform mole. J Ultrasound Med. 1983;2(6):261–4.
17. Lazarus E, et al. Sonographic appearance of early complete molar pregnancies. J Ultrasound Med. 1999;18(9):589–94; quiz 595–6.
18. Kirk E, et al. The accuracy of first trimester ultrasound in the diagnosis of hydatidiform mole. Ultrasound Obstet Gynecol. 2007;29(1):70–5.
19. Ulker V, et al. Placental mesenchymal dysplasia: a rare clinicopathologic entity confused with molar pregnancy. J Obstet Gynaecol. 2013;33(3):246–9.
20. Jimbo T, et al. Rare fetal complications associated with placental mesenchymal dysplasia: a report of two cases. J Obstet Gynaecol Res. 2015;41(2):304–8.
21. Guenot C, et al. Placental mesenchymal dysplasia: an underdiagnosed placental pathology with various clinical outcomes. Eur J Obstet Gynecol Reprod Biol. 2019;234:155–64.
22. Colpaert RM, et al. Diagnosis and management of placental mesenchymal disease. A review of the literature. Obstet Gynecol Surv. 2019;74(10):611–22.
23. H'Mida D, et al. Placental mesenchymal dysplasia with Beckwith-Wiedemann syndrome fetus in the context of biparental and androgenic cell lines. Placenta. 2008;29(5):454–60.
24. Allen SD, et al. Radiology of gestational trophoblastic neoplasia. Clin Radiol. 2006;61(4):301–13.
25. Seckin KD, et al. The impact of ultrasonographic lesion size and initial human chorionic gonadotropin values on treatment success in cases with complete hydatidiform mole. Eur Rev Med Pharmacol Sci. 2013;17(24):3381–4.
26. Green CL, et al. Gestational trophoblastic disease: a spectrum of radiologic diagnosis. Radiographics. 1996;16(6):1371–84.
27. Lim AK, et al. Pelvic imaging in gestational trophoblastic neoplasia. J Reprod Med. 2008;53(8):575–8.
28. Fowler DJ, et al. Routine pre-evacuation ultrasound diagnosis of hydatidiform mole: experience of more than 1000 cases from a regional referral center. Ultrasound Obstet Gynecol. 2006;27(1):56–60.
29. Sebire NJ. The diagnosis of gestational trophoblastic disease in early pregnancy: implications for screening, counseling and management. Ultrasound Obstet Gynecol. 2005;25(5):421–4.
30. Romero R, et al. New criteria for the diagnosis of gestational trophoblastic disease. Obstet Gynecol. 1985;66(4):553–8.
31. Kobayashi M. Use of diagnostic ultrasound in trophoblastic neoplasms and ovarian tumors. Cancer. 1976;38(1 Suppl):441–52.
32. Memtsa M, et al. Diagnosis and outcome of hydatidiform moles in missed-miscarriage: a cohort-study, systematic review and meta-analysis. Eur J Obstet Gynecol Reprod Biol. 2020;253:206–12.
33. Santos-Ramos R, Forney JP, Schwarz BE. Sonographic findings and clinical correlations in molar pregnancy. Obstet Gynecol. 1980;56(2):186–92.
34. Reid MH, McGahan JP, Oi R. Sonographic evaluation of hydatidiform mole and its look-alikes. AJR Am J Roentgenol. 1983;140(2):307–11.
35. Zhou Q, et al. Sonographic and Doppler imaging in the diagnosis and treatment of gestational trophoblastic disease: a 12-year experience. J Ultrasound Med. 2005;24(1):15–24.
36. Chau MT, et al. Perforation of the uterus by an invasive mole using color Doppler ultrasound: case report. Ultrasound Obstet Gynecol. 1993;3(1):51–3.
37. Carter J, et al. Persistent postmolar gestational trophoblastic disease: use of transvaginal sonography and colour flow Doppler. Aust N Z J Obstet Gynaecol. 1993;33(4):417–9.
38. Schulman H, et al. Umbilical velocity wave ratios in human pregnancy. Am J Obstet Gynecol. 1984;148(7):985–90.
39. Yalcin OT, Ozalp SS, Tanir HM. Assessment of gestational trophoblastic disease by Doppler ultrasonography. Eur J Obstet Gynecol Reprod Biol. 2002;103(1):83–7.

40. Zanetta G, et al. Detection of abnormal intrauterine vascularization by color Doppler imaging: a possible additional aid for the follow up of patients with gestational trophoblastic tumors. Ultrasound Obstet Gynecol. 1996;7(1):32–7.
41. Schneider DF, et al. Transvaginal ultrasound diagnosis and treatment follow-up of invasive gestational trophoblastic disease. J Clin Ultrasound. 1990;18(2):110–3.
42. Oguz S, et al. Doppler study of myometrium in invasive gestational trophoblastic disease. Int J Gynecol Cancer. 2004;14(5):972–9.
43. Gungor T, et al. Color Doppler ultrasonography in the earlier differentiation of benign molehydatidiforms from malignant gestational trophoblastic disease. Acta Obstet Gynecol Scand. 1998;77(8):860–2.
44. Abd El Aal DE, et al. Uterine artery Doppler blood flow in cases of hydatidiform mole and its correlation with beta-hCG. Eur J Obstet Gynecol Reprod Biol. 2003;111(2):129–34.
45. Asmar FTC, et al. Uterine artery Doppler flow velocimetry parameters for predicting gestational trophoblastic neoplasia after complete hydatidiform mole, a prospective cohort study. Clinics (Sao Paulo). 2017;72(5):284–8.
46. Montz FJ, Schlaerth JB, Morrow CP. The natural history of theca lutein cysts. Obstet Gynecol. 1988;72(2):247–51.
47. Chiang G, Levine D. Imaging of adnexal masses in pregnancy. J Ultrasound Med. 2004;23(6):805–19.
48. Long MG, et al. Ultrasonic morphology of the uterus and ovaries after treatment of invasive mole and gestational choriocarcinoma. Br J Radiol. 1990;63(756):942–5.
49. Vejerslev LO. Clinical management and diagnostic possibilities in hydatidiform mole with coexistent fetus. Obstet Gynecol Surv. 1991;46(9):577–88.
50. Steller MA, et al. Clinical features of multiple conception with partial or complete molar pregnancy and coexisting fetuses. J Reprod Med. 1994;39(3):147–54.
51. Bree RL, et al. Trophoblastic disease with coexistent fetus: a sonographic and clinical spectrum. J Clin Ultrasound. 1978;6(5):310–4.
52. Lin LH, et al. Multiple pregnancies with complete mole and coexisting normal fetus in North and South America: a retrospective multicenter cohort and literature review. Gynecol Oncol. 2017;145(1):88–95.
53. Berkowitz RS, Horowitz NS, Elias KM. Hydatidiform mole: treatment and follow-up. In: Goff B, editor. UpToDate. Philadelphia, PA: Wolters Kluwer Health; 2021.
54. Padron L, et al. Manual compared with electric vacuum aspiration for treatment of molar pregnancy. Obstet Gynecol. 2018;131(4):652–9.
55. Betel C, et al. Sonographic diagnosis of gestational trophoblastic disease and comparison with retained products of conception. J Ultrasound Med. 2006;25(8):985–93.
56. Furuhashi M, Miyabe Y, Oda H. Adenomyomatous polyp mimicking hydatidiform mole on ultrasonography. Arch Gynecol Obstet. 2000;263(4):198–200.
57. Lin LH, et al. Is Doppler ultrasound useful for evaluating gestational trophoblastic disease? Clinics (Sao Paulo). 2015;70(12):810–5.
58. Agarwal R, et al. Doppler ultrasonography of the uterine artery and the response to chemotherapy in patients with gestational trophoblastic tumors. Clin Cancer Res. 2002;8(5):1142–7.
59. Zhou Y, et al. Sonographic characteristics of placental site trophoblastic tumor. Ultrasound Obstet Gynecol. 2013;41(6):679–84.
60. Bajka M, et al. Transvaginal ultrasound of "placental-site trophoblastic tumor". Gynakol Geburtshilfliche Rundsch. 1995;35(1):38–41.
61. Okumura M, et al. Sonographic appearance of gestational trophoblastic disease evolving into epithelioid trophoblastic tumor. Ultrasound Obstet Gynecol. 2010;36(2):249–51.
62. Desai RK, Desberg AL. Diagnosis of gestational trophoblastic disease: value of endovaginal color flow Doppler sonography. AJR Am J Roentgenol. 1991;157(4):787–8.
63. Jauniaux E. Ultrasound diagnosis and follow-up of gestational trophoblastic disease. Ultrasound Obstet Gynecol. 1998;11(5):367–77.
64. Mangili G, et al. Transvaginal ultrasonography in persistent trophoblastic tumor. Am J Obstet Gynecol. 1993;169(5):1218–23.
65. Fleischer AC, et al. Sonographic patterns in trophoblastic diseases. Radiology. 1978;126(1):215–20.
66. Ngan HYS, et al. Update on the diagnosis and management of gestational trophoblastic disease. Int J Gynaecol Obstet. 2018;143(Suppl 2):79–85.
67. Berkowitz RS, et al. Pelvic ultrasonography and the management of gestational trophoblastic disease. Gynecol Oncol. 1983;15(3):403–12.
68. Aoki S, et al. Doppler color flow mapping of an invasive mole. Gynecol Obstet Investig. 1989;27(1):52–4.
69. Kurjak A, et al. Transvaginal color Doppler sonography in the assessment of pelvic tumor vascularity. Ultrasound Obstet Gynecol. 1993;3(2):137–54.
70. Long MG, et al. Preliminary Doppler studies on the uterine artery and myometrium in trophoblastic tumours requiring chemotherapy. Br J Obstet Gynaecol. 1990;97(8):686–9.
71. Long MG, et al. Doppler time velocity waveform studies of the uterine artery and uterus. Br J Obstet Gynaecol. 1989;96(5):588–93.
72. Braga A, et al. Treatment of high-risk gestational trophoblastic neoplasia and chemoresistance/relapsed disease. Best Pract Res Clin Obstet Gynaecol. 2021;74:81–96.
73. Clark RM, et al. The evolving role of hysterectomy in gestational trophoblastic neoplasia at the New England Trophoblastic Disease Center. J Reprod Med. 2010;55(5–6):194–8.

74. Berkowitz RS, Horowitz NS, Elias KM. Initial management of low-risk gestational trophoblastic neoplasia. In: Goff B, editor. UpToDate. Philadelphia, PA: Wolters Kluwer; 2021.
75. McNeish IA, et al. Low-risk persistent gestational trophoblastic disease: outcome after initial treatment with low-dose methotrexate and folinic acid from 1992 to 2000. J Clin Oncol. 2002;20(7):1838–44.
76. Braga A, et al. Predictors for single-agent resistance in FIGO score 5 or 6 gestational trophoblastic neoplasia: a multicentre, retrospective, cohort study. Lancet Oncol. 2021;22(8):1188–98.
77. Hsieh FJ, et al. Vascular patterns of gestational trophoblastic tumors by color Doppler ultrasound. Cancer. 1994;74(8):2361–5.
78. Agarwal R, et al. Uterine artery pulsatility index: a predictor of methotrexate resistance in gestational trophoblastic neoplasia. Br J Cancer. 2012;106(6):1089–94.
79. Harvey RA, et al. Uterine artery pulsatility index and serum BMP-9 predict resistance to methotrexate therapy in gestational trophoblastic neoplasia: a cohort study. Curr Probl Cancer. 2021;45(1):100622.
80. Verri D, et al. GestaTIonal TrophoblAstic NeoplasIa Ultrasound assessMent: TITANIUM study. Int J Gynecol Cancer. 2019;29(7):1216–20.
81. Braga A, Lima L, Parente RCM, Celeste RK, Rezende Filho J, Amim Junior J, Maesta I, Sun SY, Uberti E, Lin L, Madi JM, Viggiano M, Elias KM, Horowitz NS, Berkowitz RS. Management of symptomatic uterine arteriovenous malformations after gestational trophoblastic disease: the Brazilian experience and possible role for depot medroxyprogesterone acetate and tranexamic acid treatment. J Reprod Med. 2018;63(5–6):228–39.
82. Cura M, et al. Arteriovenous malformations of the uterus. Acta Radiol. 2009;50(7):823–9.
83. Clarke MJ, Mitchell PJ. Uterine arteriovenous malformation: a rare cause of uterine bleeding. Diagnosis and treatment. Australas Radiol. 2003;47(3):302–5.
84. Mungen E, et al. Color Doppler sonographic features of uterine arteriovenous malformations: report of two cases. Ultrasound Obstet Gynecol. 1997;10(3):215–9.
85. McGrath S, et al. Embolization of uterine arteriovenous malformations in patients with gestational trophoblastic tumors: a review of patients at Charing Cross Hospital, 2000–2009. J Reprod Med. 2012;57(7–8):319–24.
86. Garner EI, et al. Successful term pregnancy after selective arterial embolization of symptomatic arteriovenous malformation in the setting of gestational trophoblastic tumor. Gynecol Oncol. 2003;88(1):69–72.
87. Vargas R, et al. Subsequent pregnancy outcomes after complete and partial molar pregnancy, recurrent molar pregnancy, and gestational trophoblastic neoplasia: an update from the New England Trophoblastic Disease Center. J Reprod Med. 2014;59(5–6):188–94.
88. Behtash N, Ansari S, Sarvi F. Successful pregnancy after localized resection of perforated uterus in choriocarcinoma and a literature review. Int J Gynecol Cancer. 2006;16(Suppl 1):445–8.

25

Invasive Procedures in the First Trimester

Mark I. Evans, Jenifer Curtis, and Shara M. Evans

Introduction

Over 25 years ago, we published a paper entitled: "Integration of Genetics and Ultrasound in Prenatal Diagnosis: Just Looking Is Not Enough" [1]. Our thesis was, and it remains just as true today, that ultrasound visualization is an important part of prenatal diagnosis, but basically only covers half the story. In this 1996 study, we found that 42% of fetal genetic and congenital abnormalities were not detectable by ultrasound. There have been huge advances in both ultrasonographic and laboratory prenatal diagnostic capabilities, such that the ratio has not actually changed much. Thus, in this very comprehensive volume on first-trimester ultrasound, this chapter is the one dealing with the issue: "oh by the way, ultrasound can't do everything." Similarly, societies such as the International Society for Ultrasound in Obstetrics and Gynecology (ISUOG), not surprisingly, focus on ultrasound. They can sometimes lose the perspective that, in fact, ultrasound is just part of the evaluation. The opposite can be true for the American College of Medical Genetics and the International Society for Prenatal Diagnosis, in which the role of ultrasound in prenatal diagnosis is often underappreciated and underplayed.

The reality is that high-level competence in both technologies is essential for optimal fetal evaluation (which does not necessarily mean that it has to be the same person, although being "bilingual" in both techniques is very helpful). Prenatal diagnosis and reproductive choice are issues that go far beyond medicine, per se. The political fights over women's reproductive rights are clearly escalating particularly in the United States, with likely onerous restrictions on how far into pregnancy a woman will be able to legally terminate a pregnancy at least in many areas. As such, early accurate first-trimester diagnosis will become even more critical. Unfortunately, the disparities between those patients who have the resources to access technology and can travel to get services will increase and become even wider as time goes on.

As has been detailed extensively in other chapters in this volume, the use of ultrasound has become an integral component of modern management of all pregnancies. Contemporaneously with the development of ultrasound for prenatal diagnosis in the early 1970s came the beginnings of directly obtaining fetal tissue (amniotic fluid cells) in the late 1960s and 1970s. Without ultrasound guidance being available, most amniocen-

---

M. I. Evans (✉)
Fetal Medicine Foundation of America and
Comprehensive Genetics, PC, New York, NY, USA

Department of Obstetrics & Gynecology, Icahn
School of Medicine at Mt. Sinai, New York, NY, USA
e-mail: Evans@compregen.com

J. Curtis · S. M. Evans
Fetal Medicine Foundation of America and
Comprehensive Genetics, PC, New York, NY, USA

© The Author(s), under exclusive license to Springer Nature Switzerland AG 2023
J. S. Abramowicz, R. E. Longman (eds.), *First-Trimester Ultrasound*,
https://doi.org/10.1007/978-3-031-24133-8_25

teses were performed at 17+ weeks. This was to minimize the chance that the blindly inserted needle would hit something important. Accidental damage did occasionally occur [2].

Improvements in ultrasound led to better visualization which, in fact, also created the concept of parental bonding from viewing the fetal form on ultrasound [3]. Furthermore, there is also a psychological transition from a state of "I am pregnant" to "I am going to have a baby." These are very different emotional states and helped drive the desire to move prenatal diagnosis and screening from the second trimester to the first. Aneuploidy screening is covered elsewhere in the book (see Chap. 9), so we will concentrate here on diagnostic and therapeutic interventions.

In the late 1980s, we predicted that most diagnostic procedures would move into the first trimester in the 1990s [4]. For a variety of reasons, the transition did not universally occur. There was great variability in acceptance of that construct, which depended on a variety of factors and expected developments. Some depended upon the ability of providers and centers to accept and implement new technology, which has always had a wide spectrum of acceptance for new methods. Others depended upon patient's abilities to come for care earlier than usually, and finally there was the resistance of many physicians to change what had become their usual and customary care in the past couple of decades.

The transition was proceeding essentially on schedule at the most sophisticated centers, until the 1991 limb reduction defect scare was used to turn patients away from chorionic villus sampling (CVS) and to continue relying upon the established amniocentesis procedure, which was already performed by a much larger number of physicians. As such, those physicians then did not need to refer out patients to CVS centers.

First-trimester screening has become the norm for aneuploidy screening, so that most diagnostic procedures should be done in the first trimester as was documented in Denmark about 10 years ago. However, because of the widespread misperception that noninvasive prenatal testing (NIPT) can find everything that can be done on material from diagnostic procedures, many patients are foregoing the opportunity to get most complete information about their pregnancies. Paradoxically, despite better screening techniques, because of the lack of utilization of diagnostic screening, the overall percentage of "findable" abnormalities continues to go down—not up.

Chorionic Villus Sampling

More than four decades of experience have shown that CVS, in experienced hands, is both safe and effective [5, 6]. This is despite allegations in the early 1990s of increased risk of limb reduction defects [7, 8], which have been clearly disproven at the gestational age when CVS is almost always performed by objective data (although still disputed by some). CVS gained rapid acceptance, then decline, and now reacceptance in prenatal diagnosis. The current decline in procedure utilization from NIPT affects both CVS and amniocentesis. It is not a debate between the procedures.

In the 1980s, several US and European centers began performing CVS for prenatal diagnosis. Multiple single-institution and collaborative papers documented its accuracy and safety [9, 10]. Following the 1990 FDA approval of the Trophocan™ catheter (Concord/Portex; Keene, New Hampshire) for use in transcervical (TC) CVS, an increasing number of US physicians began offering the procedure. After the limb reduction defect (LRD) scare a couple of years later, Portex withdrew their catheter from the market [7, 8]. Today, the vast majority of TC procedures in the United States are performed using the "Cook" catheter.

As the procedure first came into routine clinical use in the late 1980s and 1990s, there were requirements at different levels to perform numerous procedures on non-continuing pregnancies to gain experience prior to clinical use. Other places had no guidelines or regulations. This led to wide and haphazard introduction. Similar confusion and poor performance were predicates to the Fetal Medicine Foundation's attempt to guide the introduction of nuchal translucency screening to improve quality control, which came several years later [11].

Indications

In practice, the most common indications for CVS are advanced maternal age, abnormal screening results for aneuploidy, or molecularly diagnosable genetic disorder. An understanding of the 1% background risk of abnormal microarrays for patients of all ages has not yet generally taken hold [12–16]. The recent advances in higher definition "molecular karyotyping" using array comparative genomic hybridization (aCGH), also known as microarrays (MCA), have shown that in patients with an ultrasound abnormality, the detection of pathologic copy number variants (CNVs) with duplications or deletions smaller than visible by traditional cytogenetic techniques is approximately 6–8% [12–16]. In pediatrics, for example, developments of aCGH have, over the 15 years, gained rapid acceptance and market share in pediatrics. The cytogenetic evaluation of dysmorphic children is now routinely done with aCGH rather than karyotype, because the yield is about twice as high [13]. As whole-exome sequencing and eventually whole-genome sequencing become established, it is likely that the tools for pediatric evaluation will follow that pathway as such studies are conducted when there is already clinical concern.

In prenatal patients with no abnormalities by history, ultrasound, or karyotype, the minimal yield of clearly pathological CNVs is at least 1% for all pregnancies, which is comparable to the aneuploidy risk of a 38-year-old [12–16]. This incidence is NOT age dependent and is greater than the 0.5% risk commonly quoted to 35-year-olds, which is the "American standard of care requirement." Thus, in our program, we routinely offer CVS and microarrays to all pregnant women. Multiple studies have confirmed these yields [12–16]. Over the past decade, since the introduction of microarrays, the incidence of variants of uncertain significance has reduced from 4% in the original publications to now down under 1%. Such follows the same course as for any new technology (e.g., choroid plexus cysts, single umbilical artery, and echogenic focus) when the first publications identified numerators, but subsequent studies were needed to work out the denominators of the incidence of conditions.

With the possible exception of those patients whose primary risk is for neural tube defects, any patient considered a candidate for amniocentesis could be offered CVS, if they are seen in the first trimester. CVS has the advantage of earlier diagnosis and shorter turnaround time for results allowing earlier intervention when chosen by the patient, and usually increasing privacy in reproductive choices.

Multiple Gestations

We routinely perform CVS on multiple pregnancies [17, 18]. It is considerably more difficult to perform than on singletons because a three-dimensional perspective and precise visualization of the needle or catheter are required because the pathway for aspiration of villi needs to avoid the other placentas. In very experienced hands, CVS is extremely accurate, although there is always a small percentage risk for cross contamination with adjacent placentas [17, 18]. In our experience, such cross contamination has not been a clinical problem. With 3% of all gestations in the United States now being multiples (as compared to 1/90 expectation for natural conceptions) and given that the infertility population on average is older than the average, a disproportionate number of multiple pregnancy patients are likely to want diagnostic procedures [18]. For our patients traveling considerable distances to see us, we routinely perform CVS; run FISH analysis for chromosomes 13, 18, 21, X, and Y overnight; and then typically perform fetal reductions (FR) as wanted the next day. We offer to run CMA on the remaining fetus(es). If there is an abnormality, they can return for a second FR on the abnormal fetus. Many of our patients starting with twins and/or who are local wait for the CMA results before performing the FR [17]. We have found this approach to be highly accurate that allows individualization of the approach to CVS and FR in one visit, rather than having to return 2–3 weeks later [18, 19]. Our usual approach for multiples considering FR is to test one more fetus than the parents are intending to keep. This virtually assures that there will be at least the intended number that are normal and can then give them a gender preference option in selected situations (described in detail later in this chapter) [20]. In the setting of a "vanishing twin," which may occur in up to 3% of pregnancies [21], studies suggest an increased risk of aneuploidy in the remaining placental tissue of the "vanished twin" [22]. Therefore, care must be taken during sampling if only the remaining twin is being evaluated.

Procedure

Genetic counseling is very important particularly as, in the past several years, there has been considerable complexity added to a patient's decisions with new technologies, such as cell-free DNA and enhanced molecular screening and diagnostic tests, and screening for preeclampsia now available.

We also counsel our patients that, for most of them (without significant history or ultrasound anomaly) in the middle 98%, it does not matter whether they have any procedure or not. The issue really is that "if they are going to be wrong, which way would they rather be wrong?" Would they rather take a small risk of having a baby with a significant problem or on the other extreme a small risk of having a complication because they wanted to know that? Patients have to also consider the implications of either extreme and decide "what do they fear the most," and we can minimize that at the expense of the other.

The next step is the ultrasound evaluation. First, fetal viability is confirmed. About 2% of patients are discovered to have a blighted ovum or an embryonic/fetal demise. This percentage was much higher 20 years ago when ultrasounds in the first trimester were less common [23]. Fetal size discrepancies should also be noted. The smaller-than-expected fetus, even in the first trimester, is at increased risk for aneuploidy [24, 25]. Such cases merit CVS for earlier diagnosis.

Placental evaluation is important in properly assessing patients for CVS as it determines whether the approach will be transcervical (TC) or transabdominal (TA). If the placenta is low lying and posterior, a TC approach is generally the most appropriate. Such cases may be attempted by novices under supervision. If the placenta is anterior and fundal, an abdominal approach is usually indicated. The cervical placental angle can often be maneuvered towards a vertical or horizontal configuration by judicious manipulation of bladder volume to make the desired approach easier (Fig. 25.1).

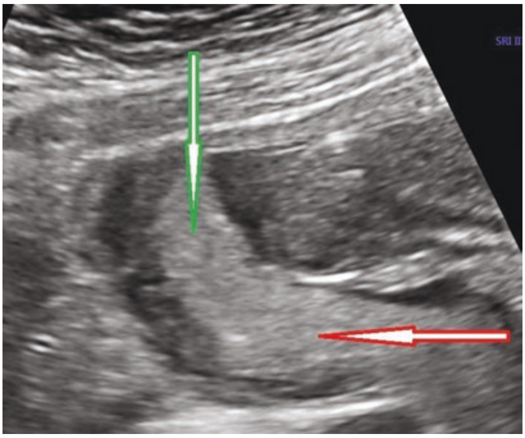

Fig. 25.1 Approaches to CVS: transcervical (red horizontal arrow) and transabdominal (green vertical arrow)

In our own experience, in singletons, we perform the TC approach in about 70% of cases. Less expert operators have a much higher proportion of TA cases because TA is usually technically easier for the inexperienced physician, as it is very comparable to doing an amniocentesis. The TC approach is more difficult and requires more experience for an operator to be competent and safe. Both approaches require a 3-dimensional (3-D) appreciation of the anatomy to be interpreted from 2-D ultrasound. We have found that there is a divide that generally cannot be overcome just by experience between those physicians and sonographers who are capable of thinking and acting in 3-D, and those who cannot.

We have also seen that operators who do not perform TC procedures use contortions of lifting the uterus vaginally to make it reachable abdominally. We think that this is very suboptimal and increases the risk of procedures when they are done by the wrong approach for the given location. We believe that a CVS operator must be proficient in both approaches for singletons, and it is absolutely essential in multiples.

Other factors must be considered before attempting CVS. At times, the patient gives a history of genital herpes simplex or a recent group B streptococcus (GBS) infection. Such cases should be individualized, and the small or theoretical risk of introducing an infection into the fetal-placental tissues should be discussed with the patient. TA-CVS or amniocentesis is usually offered when a significant risk of active GBS is present, as data are that uterine infection, in such cases, might occur almost entirely after TC aspiration [24, 26]. The choice of whether to perform TA-CVS or TC-CVS should be made according to the experienced operator's judgment, based on the previously described conditions and in accordance with the patient's bacterial/fungal cervical carrier status when known [17].

Safety

Over the past four decades, multiple reports from individual centers have demonstrated the safety and low rates of pregnancy loss following CVS [25, 26]. There is a large amount of literature, which will not be extensively reviewed here, from the 1980s and 1990s that has detailed the development of CVS as a clinical procedure and led to the United States Food and Drug Administration's removal of the restrictions on the use of the CVS catheter in 1989. The large majority of these projects did not find any increased risk of CVS over amniocentesis, but overall loss rates of both procedures were considerably higher than claimed by many operators of both procedures [25, 26].

Three studies in the past decade have been very important in our current understanding. The first was a meta-analysis published in 2007 by Mujezinovic and Alfirevic [5]. Because of the higher background rate of loss in the first trimester, CVS would be expected to have a higher overall loss rate. Yet it is impossible precisely to parse which losses are procedure related, as opposed to background. What they reported is that, in experienced centers, the loss rates within 2 weeks of the procedure, up to 24 weeks and at term, were essentially identical (Table 25.1).

Table 25.1 Amniocentesis and CVS loss rates

Loss before	Amniocentesis (%)	CVS (%)
14 days	0.6	0.7
24 weeks' gestation	0.9	1.0
Total	1.9	2.0

Mujezinovic and Alfirevic Obstet Gynecol [5]

The second study is the experience of the Danish first-trimester screening program, which over the past several years has maintained a very high detection rate for Down syndrome (>90%) while cutting their false-positive rates in half. As a consequence of first-trimester screening, the utilization of CVS in Denmark has been three times that of amniocentesis. Their data show that the procedure risk of CVS is as low as (and possibly even lower than) amniocentesis [27]. Furthermore, the incidence of late complications such as late demise was significantly lower in CVS patients than amniocentesis patients.

Lastly, Akolekar published a meta-analysis that demonstrated that overall procedure loss rates for CVS and amniocentesis were much lower than previously shown, and furthermore not different from each other—approximately 1/500 [6]. The primary confusion is the difference in background loss rates, which actually explains the vast majority of any differences between the two procedures.

Overall, we counsel our patients as to about a 1/1000 procedural risk of either CVS or amniocentesis in very experienced hands. Over the years, we quoted higher risks than we really believed were the case, but we wanted to be conservative. However, our own experience and the studies just described in the last paragraph convinced us to move the numbers. However, both procedures have considerably higher risks in inexperienced physicians or those who cannot visualize the anatomy in a 3-D manner as described above. As such, we believe that both CVS and amniocentesis should be performed preferably in "centers of excellence" by physicians, with experienced sonographers, who perform the procedure regularly—and not as an occasional item.

Complications of Chorionic Villous Sampling

Bleeding

Vaginal bleeding is seen in as many as 5–10% of patients sampled by TC but is less common after TA-CVS. Minimal spotting is more common and may occur in almost one-third of women sampled by the TC route [9, 28]. In most cases, the bleeding is self-limited, and the pregnancy outcome is excellent.

Infection

Since the initial development of TC-CVS, there has been concern that TC-CVS would introduce vaginal flora into the uterus. This possibility was confirmed by cultures that isolated bacteria from up to 30% of catheters used for CVS [29, 30]. In clinical practice, however, the incidence of post-CVS chorioamnionitis is extremely low [9, 10]. Infection following TA-CVS also occurs and has been demonstrated, at least in some cases, to be secondary to bowel flora introduced by inadvertent puncture by the sampling needle.

Rupture of Membranes

Gross rupture of the membranes, days to weeks after the procedure, is acknowledged as a rare post-CVS complication although in such late cases whether or not the complication is procedure related or just part of the background is very difficult to ascertain. Rupture can result from either mechanical or chemical injury to the chorion, allowing exposure of the amnion to subsequent damage or infection. One group reported a 0.3% incidence of delayed rupture of the membranes following CVS [31], a rate confirmed by Brambati et al. [32]. Unexplained, midtrimester oligohydramnios has also been suggested as being a rare complication of TC-CVS. In our experience and that of other very experienced groups, rupture is very rare.

Risk of Fetal Abnormalities Following Chorionic Villous Sampling

In the early 1990s, reports suggested that CVS may be associated with specific fetal malformations, particularly limb reduction defects (LRDs). Today, based on the published data, it appears safe to state that there is no increased risk for LRDs, or any other birth defect, when CVS is performed at >70 days of gestation [33–36].

The first suggestion of an increased risk for fetal abnormalities following CVS was reported by Firth et al. [7]. In a series of 539 CVS-exposed pregnancies, there were five infants with severe limb abnormalities in a cohort of 289 pregnancies sampled by TA-CVS at 55–66 days' gestation. Four of these infants had the unusual and very rare oromandibular-limb hypogenesis (OLH) syndrome, and the fifth had a terminal transverse LRD. OLH syndrome occurs in 1 per 175,000 live births [37], and LRDs normally occur in 1 per 1690 births [38]. Thus, the occurrence of these abnormalities in more than 1% of CVS-sampled cases raised a high level of suspicion. Subsequently, other groups reported the occurrence of LRDs and OLH following "early" CVS [39–44]. In 1992, a case-control study using the Italian Multi-Center Birth Defects Registry reported an odds ratio of 11.3 (95% CI 5.6–21.3) for transverse limb abnormalities following first-trimester CVS [39]. However, when stratified by gestational age at sampling, pregnancies sampled prior to 70 days had a 19.7% increased risk of transverse limb reduction defects, while patients sampled later did not demonstrate significantly increased risk. Other case-control studies, however, have not seen any association of CVS with LRDs [34, 35].

The risk for fetal malformations is real when CVS is done at an earlier gestation age, i.e., during the period of limb genesis at 6–7 weeks [7, 8, 41]. Brambati et al., practicing in Milan, had a large population at risk for β-thalassemia. Their population is also predominantly Catholic, for whom abortion at any gestational age is religiously proscribed. However, to assuage the guilt of wanting diagnosis, at-risk patients wanted it done as early in gestation as technically possible. For patients sampled at 6 and 7 weeks' gestation, they reported a 1.6% incidence of severe LRDs [41]. This rate decreased to 0.1% at 8–9 weeks. These data support the assumption that early gestational sampling and excessive placental trauma may be etiologic in the reported clusters of post-CVS LRDs.

In the United States, the population group most interested in early CVS has been the Orthodox Jewish community—known to be at high risk for Tay-Sachs and other Ashkenazi diseases. In the observant Jewish community, abortion is permitted, by religion, until 40 days postconception (7 weeks 5 days from LMP). Wapner and Evans have shown that, in very experienced centers, CVS can be safely and reliably performed, even at such very early gestational ages [33]. In a study they conducted, CVS was performed at less than 8 weeks' gestation. Of the 82 cases of early CVS, there was a single case of severe LRDs, a rate of 1.6%. While this risk is considerably higher than when done at the usual gestational age timeframe, we believe that in comparison to a 25% risk of lethal disorder and with proper genetic counseling, it could be a reasonable decision for couples to make. However, in the one case, despite the patient having had three previous early CVSs with signed consent forms acknowledging such a risk, they chose to sue the doctor stating that they did not "know." As a result of the legal exposure, virtually all centers that had been willing to do the procedure stopped performing it. Subsequently in many cases, the Orthodox rabbinate has quietly agreed to an exception to the 40-day rule for terminations in high-risk cases for which a diagnosis could not be made "in time."

The question whether CVS sampling after 10 weeks has the potential of causing more subtle defects, such as shortening of the distal phalanx or nail hypoplasia, was a major concern, debated thoroughly in the literature [43, 45]. The overall incidence of LRDs after CVS is estimated to be 1 in 1881 (ranging from 5.2 to 5.7 per 10,000), compared with 1 in 1642 (ranging from 4.8 to 5.97 per 10,000) in the general population [36, 45]; hence, there are no data to substantiate this concern. As noted, in most experienced centers performing CVS after 10 weeks, no increase in limb defects of any type has been observed [34, 36, 44–46].

Perinatal Complications

No increases in preterm labor, premature rupture of the membranes, small-for-gestational-age infants, maternal morbidity, or other obstetric complications have occurred in sampled patients [43]. Although the Canadian Collaborative Study showed an increased prenatal mortality in CVS sampled patients, with the greatest imbalance being beyond 28 weeks, no obvious recurrent event was identified [10]. To date, CVS is not considered to harbor additional prenatal complication as long as the procedure is performed by an experienced operator and after 10 weeks' gestation.

Long-Term Infant Development

Chinese investigators have evaluated long-term infant outcomes They evaluated 53 children from their initial placental biopsy experience of the 1970s. All were reported in good health, with normal development and school performance [47]. Schaap et al. [48] obtained long-term follow-up data after CVS and amniocentesis and found no significant differences for neonatal and pediatric morbidity. Based on their data, the authors concluded that TC-CVS performed around 10 weeks' gestation is not associated with an increased frequency of congenital malformations, compared with second-trimester amniocentesis.

Accuracy of CVS Cytogenetic Results

A major concern for all prenatal diagnostic procedures is the possibility of discordance between the prenatal cytogenetic diagnosis and the actual fetal karyotype/genotype. With CVS, these discrepancies can occur from either maternal tissue contamination or true biologic differences between the extraembryonic tissue (i.e., placenta) and the fetus. Fortunately, genetic evaluation of chorionic villi provides a high degree of success and accuracy [49]. In the late 1980s, the United States Collaborative Study revealed a 99.7% rate of successful cytogenetic diagnosis, with 1.1% of the patients requiring a second diagnostic test, such as amniocentesis or fetal blood analysis, to further interpret the results [49]. In our own experience, a follow-up amniocentesis is needed about 0.3% of the time.

Clinical errors or misinterpretation is rare, however, and the need for repeat testing continues to decrease, as more knowledge about the characteristics of chorionic villi is obtained. Multiple studies [26, 50] have demonstrated that CVS is associated with a low rate of maternal cell contamination or chromosomal abnormalities confined to the placenta, as will be described below. For example, tetraploidy on CVS FISH and culture is seen in about 0.5% of cases, but it is known to almost always be associated with a normal diploid fetus.

Maternal Cell Contamination (MCC)

Contamination of samples with a significant amount of maternal decidual tissue may lead to diagnostic errors, underlining the importance of preventing this occurrence [30, 50]. Generally, decidual contamination in CVS is almost always due to small sample size, which can make appropriate tissue selection difficult. In experienced centers, in which adequate quantities of tissue are available, this problem is rare, with clinically significant MCC occurring in less than 0.5% of CVS procedures. It is standard to separate maternal tissue from the sample. The chorionic "fronds" are distinguished from the maternal decidua under the microscope, making decidual removal by careful dissection possible.

In recent years, there has been much progress in the molecular techniques suitable for detection of MCC, allowing more accurate results in cases of molecular diagnoses, where MCC may jeopardize the validity of the test.

Confined Placental Mosaicism

True discrepancies between the karyotype of the villi and the direct fetal karyotype can occur, leading to either false-positive or false-negative clinical results. Although initially there was concern that this might invalidate CVS as a prenatal diagnostic tool, subsequent investigations have not only led to a clearer understanding of the clinical interpretation of villous tissue results, but also revealed new information about the etiology of pregnancy loss, possible causes of intrauterine growth restriction (IUGR), and biologic mechanisms for uniparental disomy and associated clinical syndromes.

A chromosomal aberration that does not involve the fetal cell lineage will produce a confined placental mosaicism (CPM), in which the trophoblast and perhaps the extraembryonic mesoderm may demonstrate aneuploid cells, but the fetus is euploid. Several mechanisms may apply in pregnancies where CVS mosaicism or non-mosaic feto-placental discrepancies are detected.

Mosaicism occurs in about 0.5% of all CVSs [51, 52], but it is confirmed in the fetus in only 10–40% of these cases. In contrast, amniocentesis mosaicism is observed in only 0.3% of cultures but, when found, is confirmed in the fetus in ~70% of cases [53, 54]. These feto-placental discrepancies are known to occur because the chorionic villi consist of a combination of extraembryonic tissue of different sources that become separated and distinct from those of the embryo in early developmental stages. Specifically, at the 32–64-celled blastocyst, only 3–4 blastomeres differentiate into the inner cell mass (ICM), which forms the embryo, mesenchymal core of the chorionic villi, amnion, yolk sac, and chorion, whereas the rest of the cells become the precursors of the extraembryonic tissues [55]. Furthermore, it appears that the placenta is more "tolerant" of abnormalities and remains viable as compared to the fetus, per se.

The probability of mosaic or non-mosaic trisomy in the fetus itself depends on the placental lineages in which the trisomic cell line was found. CVS culture represents the villous mesenchymal core and therefore reflects the chromosomal constitution of the fetus proper to a greater extent than the direct preparation, which represents the chorionic ectoderm, farther removed from the fetus. Thus, if a mosaic chromosomal aberration is detected on both direct preparation and long-term culture, it is more likely to represent a true mosaicism of the fetus [52]. Nevertheless, in gestations involving mosaic trisomic villous mesenchyme (with or without evidence of trisomy in direct cytotrophoblast examination), it is our usual policy to further examine the fetal karyotype by amniocentesis and perform a thorough fetal ultrasound scan in order to rule out fetal malformations.

Uniparental disomy (UPD) is another adverse outcome that may be associated with CPM. In

UPD, both chromosomes of a given pair are inherited from a single parent, rather than one from each. UPD results when the original trisomic embryo is "rescued" by the loss of the one extra chromosome. Because in the trisomic embryos two chromosomes come from one parent and one from the other, there is a theoretical 1 in 3 chance that the two remaining chromosomes originate from the same parent, leading to UPD. This may have clinical consequences if the chromosome involved harbors imprinted genes whose expression varies according to the parent of origin or if the two remaining chromosomes carry a mutant recessive gene, creating a homozygous state. In general, UPD has been reported for almost every chromosomal pair, although clinical consequences have been observed mainly in cases involving specific chromosomes (i.e., chromosomes 2, 6, 7, 10, 11, 14, 15, 16, 20) and depending on the parent of origin [53]. For instance, despite a relatively high frequency of CPM for trisomy 2 and trisomy 7, maternal UPD(2) and maternal UPD(7) have only been reported rarely [56–58].

A significant CPM involves chromosome 15 and is encountered in 27/100,000 samples [59]. This is associated with the risk for UPD(15), which may lead to well-recognized clinical syndromes. Chromosome 15 is known to carry genes that are subject to both paternal and maternal imprinting. Maternal UPD(15), resulting from the relatively more common maternally derived trisomy 15, causes the Prader-Willi syndrome. In contrast, paternal UPD(15) caused by rescue of the less common paternal trisomy 15 results in the less frequent Angelman syndrome.

In rare cases, CPM for trisomy 15 offers the important clue that UPD may be present in the "chromosomally normal" fetus, which may be at risk of having Prader-Willi/Angelman syndrome [60, 61]. For this reason, cases in which CVS reveals trisomy 15 (either complete or mosaic) should be evaluated for UPD if the amniotic fluid demonstrates an apparently euploid fetus [59].

Early Amniocentesis

Early amniocentesis is a procedure that has come and gone. It was developed in the early 1990s when several centers who did not have access to the FDA's Investigational Device Exemption to obtain CVS catheters felt "left out of the action" for advances in prenatal diagnosis. Nothing could stop them from taking amniocentesis needles off their shelves and using them for earlier amniocenteses.

Early amniocentesis is a first-trimester procedure, i.e., that was performed before 14 weeks of gestation (usually from 11+0 to 13+6) [62, 63]. Some series included procedures as early as 9+0 weeks. Traditional amniocentesis is usually performed after 15+0 weeks of gestation; invasive procedures between 14+0 and 14+6 are usually considered early and have been included in some series but not others [64]. Since 1987, various sized observational studies on EA reported rates of procedure-related fetal loss from 1.4% to 8.1% (Table 25.1). Early series concluded that EA was an appropriate technique for early diagnosis but was associated with an increased fetal loss rate [65, 66]. Assel et al. [67] compared EA with midtrimester amniocentesis and found a significant increased post-procedure fetal loss rate (1.8% vs. 0.4%) [68].

A prospective partially randomized study by Nicolaides et al. [69, 70] showed a higher rate of fetal loss after EA compared with CVS (4.9% vs. 2.1%), which was significant for pregnancies at 10–11 weeks, but it was not significant for the 12–13-week gestation period.

The CEMAT study compared EA between 11+0 and 12+6 weeks with standard amniocentesis (15+0 to 16+6). This multicenter randomized trial reporting on 1916 EA procedures showed an increased total pregnancy loss (pre-procedure and post-procedure losses including intrauterine and neonatal deaths) with the EA procedure (7.6% vs. 5.9; $P = 0.012$) [71].

Post-procedure Amniotic Fluid Leakage

Besides fetal loss, additional complications with EA have been reported as being directly related to those procedures. Leakage of amniotic fluid after EA is concerning because of the risk for infection, miscarriage, preterm labor/delivery, and fetal neonatal complications. The reported incidence varies from 0% to 4.6%. For example, the CEMAT study reported an increased rate of fluid leakage that was statistically significant before 22 weeks of gestation, when EA was compared with standard amniocentesis (3.5% vs. 1.7%) [71].

Many reports, however, have associated EA with congenital abnormalities. The lower limb extremities have increased susceptibility with temporary disturbances from a diminution in intra-amniotic volume [72]. Second-trimester procedures do not have any such association [73]. However, the CEMAT [71] trial and several others showed a significant increased rate of a foot anomaly (1.3% vs. 0.1%; $P = 001$) for EA from 11+0 week to 12+0. Tharmaratnam et al. [71] reported a rate of fixed flexion deformities of 1.6%. They showed a positive association with the amount of amniotic fluid removed and the rate of musculoskeletal deformities [74].

An international randomized trial of late first-trimester invasive prenatal diagnosis to assess the safety and accuracy of amniocentesis and TA-CVS performed at 11–14 weeks was reported in 2004 [47]. A fourfold increase in the rate of talipes equinovarus (club feet) was observed in cases where early amniocentesis was the technique used. The authors concluded that amniocentesis at, or before, 13 weeks carries an increased risk for this specific limb defect and an additional increase in early, unintended pregnancy loss. In another study, Alfirevic et al. [75] analyzed 14 randomized studies from the Cochrane Pregnancy and Childbirth Group Trials Registry and from the Cochrane Central Registry and Control Trials, in order to assess the safety and accuracy of the various invasive procedures employed for early prenatal diagnosis. Based on their results, they concluded that early amniocentesis was not a safe alternative to second-trimester amniocentesis because of increased pregnancy loss (relative risk 1.29) and higher rates of talipes equinovarus (relative risk 6.43). Early amniocentesis has been essentially completely abandoned as CVS is a clearly safer procedure in the first trimester and, arguably, at 14 weeks or more as well.

In conclusion, for first-trimester diagnosis, either TA-CVS or TC-CVS is the clinically appropriate method. We believe that utilization of both CVS methods is necessary to have the most complete, practical, and safe approach to first-trimester diagnosis. EA carries a significant risk for fetal loss and fetal malformations. We have not found a situation in about 20 years in which EA was the appropriate method for a patient.

Fetal Reduction

Fetal reduction (FR) has changed considerably over the nearly 35 years since we first published on the subject [18, 76]. These changes have taken place in medical technology outcomes, patient choices, and larger demographic and cultural shifts that are driving the pace and direction of change.

FR was developed as a way of managing pregnancies in which the risks to both mother and fetuses from carrying multiple embryos were extreme. Selective termination (as it was called then) of some of the fetuses to increase the viability of the remaining ones and reduce the risk of morbidity and mortality for the mother was a desperate approach to salvage the situation. As with numerous other technological changes, what began as a dominant concern with matters of life and death over time became accepted as being reasonable and generally supported. With much better management of ovulation induction and much rarer occurrence of high-order multiples, indications for FR have mostly morphed from crisis "life and death" into issues of quality of life and health [18]. FR has followed the generic pattern of the phases of development and diffusion of new technologies [77, 78].

FR was developed as a clinical procedure in the 1980s, when a small number of clinicians in both the United States and Europe attempted to reduce the usual and high adverse sequelae of multifetal pregnancies, by selectively terminating or reducing the number of fetuses to a more manageable number. The first European reports by Dumez and Oury [79], and the first American report by Evans et al. [76], followed by a further report by Berkowitz et al. [80], and later Wapner et al. [81], described a surgical approach to improve the outcome in such cases.

In the 1990s, multiple papers demonstrated that with triplets or more, FR provided clear improvement in reducing to twins. Numerous papers argued whether triplets had better outcomes "reduced" or not. Yaron et al. [82] compared triplets-to-twins data to unreduced triplets with two large cohorts of twins. The data showed substantial improvement of reduced twins as compared to triplets. Early collaborative series and others have suggested that pregnancy outcomes for cases starting at triplets or even quadruplets reduced to twins at about 12 weeks do fundamentally as well as starting as twins.

Overall, statistics on reductions improved noticeably over these decades to the point where FR is a routine procedure accepted as routine high-risk care and not one for which there is much interest in continuingly larger series [17, 18]. In the early 1990s, when half the cases were quadruplets or more, loss rates (up to 24 weeks) were 13%. Early premature deliveries were an additional 10%. Now, overall with decreasing starting numbers, better ultrasound, better understanding of zygosity, and a limited number of practitioners with extensive experience accounting for a high percentage of reductions, overall losses (i.e., including background) have decreased to about 2–3%. The key points are that counseling must be tailored to (1) specific starting and finishing numbers and (2) the experience of the operator.

With the rapid expansion of the availability of donor eggs, the number of "older women" seeking FR has increased dramatically. In our experience, about 15% of all patients we see seeking FR are now over 40 years of age, and nearly half of these are using donor eggs [17, 18]. It would appear that as advances in care have developed for achieving pregnancies and ways of moderating the risk of older women who wish to have children, more of them are electing to do so.

As a consequence of the shift to older patients, many of whom already had previous relationships and children, there is an increased desire by these patients to have only one further child. The number of experienced centers willing to do 2 to 1 FR is still limited, but we believe, based upon improvement of outcomes, that it can generally be justified. Twins to singletons currently constitute about 35% of the patients we see [17–19].

For patients who are "older," particularly those using their own eggs, the issue of genetic diagnosis has become progressively more salient. In 2009, about 60% of patients in the United States having ART cycles were over 35. Using the criteria of comparable risk to that of a 35-year-old, actually about 90% of IVF patients are at increased risk [17–19, 82, 83] (Table 25.2). However, as we have published, the incidence of abnormal microarrays is slightly over 1% for patients of all ages, which is comparable to the routine aneuploidy risks of a 38-year-old. Thus, we offer CVS and microarray to all patients both for singletons and multiples [14–16].

Unfortunately, most FR practitioners still make their decisions as to which fetuses to keep or reduce by ultrasound evaluation only. In the 1980s, we performed most of our procedures between 9 and 10 weeks with decisions based principally on basic ultrasound and fetal position [73]. For those patients for whom genetic assessment was appropriate, we initially had them undergo amniocentesis several weeks later back at their home center [84]. We eventually changed to doing CVS a week after reduction to twins,

Table 25.2 Genetic risks of aneuploidy for IVF patients

Factor	Risk	% of IVF cases
Advanced maternal age	>0.5%	60
Twins or more	Age 30 × 2 = Age 35	34
ICSI	1%	66
PGT-A	1% error rate	4

Percentages from the United States Centers for Disease Control and then to doing CVS the day before with FISH analysis overnight [18]. In the mid-1990s, we began to have a small but increasing percentage of patients reducing to a singleton; it, therefore, seemed prudent to know what we were keeping before committing to it. However, waiting for a full karyotype was and is problematic for both the time interval to get results, the inconvenience of having out of town patients (half our program) having to make two trips, and the fact that others reported a 1% mistake rate as to which was which under these circumstances [18]. As FISH technology became reliable, we began routinely to do procedures on two consecutive days [17, 18]. Over the last 20 years, the proportion of patients having CVS before FR has steadily risen from about 20% in 2000 to now about 85% of our patients [17, 18].

Our routine has been somewhat modified by microarrays. With twins, most of our local patients wish to wait for the full evaluation including microarray before reduction. For those coming from out of town for whom a second trip to see us is problematic, many still proceed following FISH but perform the microarray on the remaining fetuses. For patients with triplets or more, we commonly reduce to twins based upon the FISH and then continue to a singleton if they wish after the microarray results are reported [17, 18].

There have been many papers on the true risks of prenatal diagnosis with widely diverging statistics [14–18, 85–87]. We believe that, in multiples, the net effect in the most experienced hands is zero sum. Whatever risks there are of the diagnostic procedures, they are counterbalanced by the reduction of risk of loss by not, inadvertently, continuing a fetus with a serious problem who is more likely to have a spontaneous loss than a healthy one [17, 18].

An increasingly common scenario is the situation of monozygotic twins combined with one or more singletons [88–90]. Changes in IVF culture techniques, including increasing use of blastocyst transfers, have significantly increased the incidence of monozygotic twining. Single-embryo transfer has become the norm and replaced the easily treatable dichorionic/diamniotic twins with monochorionic twins for whom FR is much more problematic.

Dichorionic/triamniotic triplets (DCTA), for example, have far higher rates of pregnancy loss, TTTS, and complications of prematurity [88–90]. The risk of TTTS is >50%, and the risk of selective intrauterine growth restriction (IUGR) is about 20%. As such, our approach is that if the singleton is healthy (by US and CVS), the safest thing is to reduce the twins and keep the singleton. If the singleton is not healthy, then keeping the twins is acceptable. The one thing we cannot do is routinely reduce one of the two twins, as the risk of death or neurologic damage is as high as 12% [91]. Some papers have suggested radiofrequency ablation as a possible method for FR in monochorionic twins, but the incidence of loss and neurologic impairment of the survivor is elevated—reported as much as 10–12% of each [91, 92]. These numbers will likely improve over time, but just how low they can go is unclear.

In the vast majority of cases, the major risk factor in determining which fetuses to keep or reduce is a chromosomal risk. However, the same principles can be applied to Mendelian risks. For example, we have evaluated couple with triplets at 25% risk per fetus of disorders such as cystic fibrosis.

As part of the FISH results, we also obtain gender. Historically, we perceived a significant bias among those patients who were interested and who mostly expressed a preference for males [20]. These requests disproportionately came from patients of cultures that classically valued boys over girls. Because of such bias, we refused to let gender be a factor with the rare exception of genetic diseases with gender discordancy. Ironically, in X-linked disorders, it is the males at risk, making females the safer option.

Over the past 25 years, however, we noticed a shift to requests coming from all ethnic groups and a perceived equalization of gender preferences. In the early 2000s, our ethics consultant, John Fletcher, Ph.D., pushed us to re-evaluate, and we began to be willing to consider under the following approach [19, 20].

We prioritize FR decisions by the following:

1. Do we find a “problem”?
2. Are we “suspicious” about anything such as somewhat increased nuchal translucency

(>2 mm), smaller fetal size (such as more than ½ week), smaller gestational sac size, or placental concern?

3. If none of the above apply, then and only then we will consider gender preference.

Patients are told that we will have a non-gender disclosing "poker-faced" discussion with them when we get the results. They will then choose which of the four categories concerning gender they prefer. The groups are:

1. Those patients who want to know "everything."
2. Those who want to know "nothing."
3. Those who have no preference but want to know what they have kept (but not the reduced).
4. Those who, all things considered, do have a preference (but do not want to know the reduced fetus' or fetuses' genders) [18, 20].

We have published data that show that now, such requests come from patients of all ethnic backgrounds and cultures [20]. When patients do have a gender preference, there is an equal preference for females as males. For patients reducing to twins, the overwhelming preference is for one of each; for those reducing to a singleton, it is essentially a 50/50 split [20, 93, 94].

We have also been able to use our technology to extend services to groups of patients not previously well served. We have seen several gay male couples using surrogate carriers with egg donation when both partners fertilized the eggs. The couples desired FR for the usual clinical reasons, but they requested, if possible, to be left with twins—one fathered by each of them. We chose to consider this request in the same vein as gender preference: i.e., only if there are no higher clinical priorities. In several cases, we have been able to assess the pregnancies with CVS and ultrasound, document normal genetic results, perform paternity testing, and discover that one man genetically fathered two and the other had one. In such cases, we then reduced one of the twins fathered by the same man [95].

Over the past 30+ years, data from around the globe have shown that pregnancy outcomes are vastly improved by reducing the number of fetuses in multiples. All but the most conservative of commentators have long since accepted the efficacy of FR for triplets or more. The medical data now also show that reduction of twins to a singleton clearly improves outcomes. Thus, while we expect the vast majority of patients with twins to keep them, we believe that all patients with twins should be made aware of the possibility of FR. The issue then shifts to an ethical one that will never be universally accepted. We argue that from an autonomy and public health perspective, FR needs to be seen as a necessary, but hopefully increasingly rare, procedure.

Summary

Ultrasound is and will remain a very important part of prenatal diagnosis and screening. Increased capabilities of cell-free fetal DNA have created the impression for many that these blood tests can do "everything" that can be accomplished by CVS or amniocentesis specimens. There continues to be a huge misconception about the differences between screening and diagnostic tests in genetics and many other areas of obstetrics [96–98].

The reality is that every time there has been an advance in noninvasive methods, there has been a corresponding advance in the capabilities on direct fetal tissue. Whole-exome sequencing and whole-genome sequencing will work their way into routine practice over the next several years [99]. As long as there remains a gap between the comprehensiveness of what can be found by direct evaluation of fetal tissue and cell-free fetal DNA, procedures will still be required to determine almost half of genetic abnormalities [14–19]. At the same time, based on a patient's desires for privacy and the increasing possibility of the reemergence of significant restrictions on how far into pregnancy a woman may have reproductive choices, there is, and needs to be, an accelerated shift of definitive diagnoses into the first trimester. CVS, in experienced hands, is as safe as or even safer than amniocentesis and needs to become the mainstay of diagnostic procedures.

Teaching Points

- Ultrasound cannot do everything. The combination of high-quality ultrasound and diagnostic procedures performed by experienced operators is required for optimal genetic screening and diagnosis.
- Chorionic villus sampling is just as safe as amniocentesis in experienced hands.
- CVS specimens provide much more material than amniocentesis, allowing earlier procedures and faster turnaround time for diagnosis.
- Early amniocentesis (<15 weeks) should almost never be performed. It is considerably riskier than either CVS or traditional amniocentesis.
- Preimplantation genetic testing is useful for couples at high risk for Mendelian disorders. For chromosome disorders, it generally does not improve take-home baby rate for most couples.
- CVS or amniocentesis confirmation is still needed in PGT cases.
- CVS and FR together dramatically improve the outcome of healthy babies in multifetal pregnancies including twins.
- Genetic diagnosis before FR can provide secondary options for patients such as gender preference.

References

1. Evans MI, Hume RF, Johnson MP, Treadwell MC, Krivchenia E, Zador IE, Sokol RJ. Integration of genetics and ultrasound in prenatal diagnosis: just looking is not enough. Am J Obstet Gynecol. 1996;174(6):1926–30.
2. Evans MI, Johnson MP. Chorionic villous sampling. In: Evans MI, editor. Reproductive risks and prenatal diagnosis. Appleton & Lange: Norwalk; 1992. p. 175–84.
3. Fletcher JC, Evans MI. Maternal bonding in early fetal ultrasound examinations. NEJM. 1983;308:392–3.
4. Evans MI, Drugan A, Koppitch FC, Zador IE, Sacks AJ, Sokol RJ. Genetic diagnosis in the first trimester: the norm for the 90s. Am J Obstet Gynecol. 1989;160:1332–9.
5. Mujezinovic F, Alfirevic Z. Procedure related complications of amniocentesis and chorionic villus sampling. Obstet Gynecol. 2007;110:687–94.
6. Akolekar R, Beta J, Picciarelli G, Ogilvie C, D'Antonia F. Procedure related risk of miscarriage following amniocentesis and chorionic villus sampling: a systematic review and meta-analysis. Ultrasound Obstet Gynecol. 2015;45:16–26.
7. Firth HV, Boyd P, Chamberlain P, et al. Severe limb abnormalities after chorion villus sampling at 56–66 days' gestation. Lancet. 1991;337:726.
8. Firth HV, Boyd PA, Chamberlain PF, et al. Analysis of limb reduction defects in babies exposed to chorionic villus sampling. Lancet. 1994;343(8905):1069–71.
9. Rhoads GG, Jackson LG, Schlesselman SE, et al. The safety and efficacy of chorionic villus sampling for early prenatal diagnosis of cytogenetic abnormalities. N Engl J Med. 1989;320:609.
10. MRC working party on the evaluation of chorionic villus sampling: Medical Research Council European Trial of chorionic villus sampling. Lancet. 1991;337:1491.
11. Snijders RJM, Noble P, Sebire N, Souka A, Nicolaides KH. UK multicentre project on assessment of risk of trisomy 21 by maternal age and fetal nuchal-translucency thickness at 10–14 weeks of gestation. Lancet. 1998;352:343–6.
12. Wapner RJ, Martin CL, Levy B, Ballif BC, Eng CM, Zachary JM, et al. Chromosomal microarray versus karyotyping for prenatal diagnosis. N Engl J Med. 2012;367:2175–84.
13. Schaffer LG, Dabell PM, Fisher AJ, Coppinger J, Bancholz AM, Elison JW, et al. Experience with microarray based comparative genomic hybridization for prenatal diagnosis in over 5000 pregnancies. Prenat Diagn. 2012;32:976–85.
14. Evans MI, Wapner RJ, Berkowitz RL. Non invasive prenatal screening or advanced diagnostic testing: caveat emptor. Am J Obstet Gynecol. 2016;215:298–305.
15. Evans MI, Evans SM, Bennett TA, Wapner RJ. The price of abandoning diagnostic testing for cell free fetal DNA screening. Prenat Diagn. 2018;38:243–5.
16. Evans MI, Andriole S, Curtis J, Evans SM, Kessler AA, Rubenstein AF. The epidemic of abnormal copy number variants missed because of reliance upon reliance upon noninvasive prenatal screening. Prenat Diagn. 2018;38:730–4.
17. Rosner M, Pergament E, Andriole S, Gebb J, Dar P, Evans MI. Detection of genetic abnormalities using CVS and FISH prior to fetal reduction in sonographically normal appearing fetuses. Prenat Diagn. 2013;33:940–4.
18. Evans MI, Andriole SA, Britt DW. Fetal reduction – 25 years' experience. Fetal Diagn Ther. 2014;35:69–82.

19. Evans MI, Kaufman M, Urban AJ, Britt DW, Fletcher JC. Fetal reduction from twins to a singleton: a reasonable consideration. Obstet Gynecol. 2004;104:102–9.
20. Evans MI, Rosner M, Andriole S, Alkalay A, Gebb J, Britt DW. Evolution of gender preferences in multiple pregnancies. Prenat Diagn. 2013;33:935–9.
21. Landy HL, Weiner S, Carson SL. The "vanishing twin": ultrasonographic assessment of fetal disappearance in the first trimester. Am J Obstet Gynecol. 1986;155:14–9.
22. Rudnicki M, Vejerslev LO, Junge J. The vanishing twin: morphologic and cytogenetic evaluation of an ultrasonographic phenomenon. Gynecol Obstet Investig. 1991;31:141–5.
23. Johnson MP, Drugan A, Koppitch FC, Uhlmann WR, Evans MI. Postmortem CVS is a better method for cytogenetic evaluation of early fetal loss than culture of abortus material. Am J Obstet Gynecol. 1990;163:1505–10.
24. Drugan A, Johnson MP, Isada NB, Holzgreve W, Zador IE, Dombrowski MP, Sokol RJ, Hallak M, Evans MI. The smaller than expected first trimester fetus is at increased risk for chromosome anomalies. Am J Obstet Gynecol. 1992;167:1525–8.
25. Sorokin Y, Johnson MP, Uhlmann WR, Zador IE, Drugan A, Koppitch FC III, Moody J, Evans MI. Postmortem chorionic villus sampling: correlation of cytogenetic and ultrasound findings. Am J Med Genet. 1991;39:314–6.
26. Brun JL, Mangione R, Gangbo F, Guyon F, Taine L, Roux D, Maugey-Laulom B, Horovitz J, Saura R. Feasibility, accuracy and safety of chorionic villus sampling: a report of 10741 cases. Prenat Diagn. 2003;23(4):295–301.
27. Wulff CB, Gerds TA, Rode L, Ekelund CK, Petersen OB, Tabor A. Risk of fetal loss associated with invasive testing following combined first trimester screening for Down syndrome: a national cohort of 147,987 singleton pregnancies. Ultra Obstet Gynecol. 2016;47:48–4.
28. Jackson LG, Zachary JM, et al. Randomized comparison of transcervical and transabdominal chorionic villus sampling. N Engl J Med. 1992;327:594–8.
29. Brambati B, Varotti F. Infection and chorionic villus sampling. Lancet. 1985;2:609.
30. Scialli AR, Neugebauer DL, Fabro SE. Microbiology of the endocervix in patients undergoing chorionic villus sampling. In: Fracearo M, Simoni G, Brambati B, editors. First-trimester fetal diagnosis. New York: Springer; 1985. p. 69–73.
31. Hogge WA, Schonberg SA, Golbus MS. Chorionic villus sampling: experience of the first 1000 cases. Am J Obstet Gynecol. 1986;154:1249.
32. Brambati B, Tului L, Cislaghi C, Alberti E. First 10,000 chorionic villus samplings performed on singleton pregnancies by a single operator. Prenat Diagn. 1998;18(3):255–66.
33. Wapner RJ, Evans MI, Davis DO, Weinblatt V, Moyer S, Krivchenia EL, Jackson LG. Procedural risks versus theology: chorionic villus sampling for orthodox Jews at less than 8 weeks' gestation. Am J Obstet Gynecol. 2002;186:1133–6.
34. Wapner R, Jackson L, Evans MI, Johnson MP. Limb reduction defects are not increased following first-trimester chorionic villus sampling. Proceedings of the 16th annual meeting of the society of perinatal obstetricians, 1996 Feb, Kona, Hawaii, Kona The Society; 1996.
35. Froster UG, Jackson L. Limb defects and chorionic villus sampling: results from an international registry, 1992–94. Lancet. 1996;347:489–94.
36. Kuliev A, Jackson L, Froster U, Brambati B, Simpson JL, Verlinsky Y, Ginsberg N, Smidt-Jensen S, Zakut H. Chorionic villus sampling safety. Report of World Health Organization/EURO meeting in association with the Seventh International Conference on Early Prenatal Diagnosis of Genetic Diseases, Tel-Aviv, Israel, May 21, 1994. Am J Obstet Gynecol. 1996;174(3):807–11.
37. Hoyme F, Jones KL, Van Allen MI, et al. Vascular pathogenesis of transverse limb reduction defects. J Pediatr. 1982;101:839.
38. Foster-Iskenius U, Baird P. Limb reduction defects in over 1,000,000 consecutive live births. Teratology. 1989;39:127.
39. Mastroiacovo P, Botto LD, Cavalcanti DP. Limb anomalies following chorionic villus sampling: a registry based case control study. Am J Med Genet. 1992;6:856–63.
40. Dolk H, Bertrend F, Lechat MF. Chorionic villus sampling and limb abnormalities. The EUROCAT Working Group. Lancet. 1992;339:876.
41. Brambati B, Simoni G, Traui M. Genetic diagnosis by chorionic villus sampling before 8 gestational weeks: efficiency, reliability, and risks on 317 completed pregnancies. Prenat Diagn. 1992;12:784–9.
42. Hsieh FJ, Shvu MK, Sheu BC, et al. Limb defects after chorionic villus sampling. Obstet Gynecol. 1995;85(l):84.
43. Burton BK, Schultz CJ, Burd LI. Spectrum of limb disruption defects associated with chorionic villus sampling. Pediatrics. 1993;91(5):989–93.
44. Brent RL. Relationship between uterine vascular clamping, vascular disruption syndrome and cocaine teratology. Teratology. 1990;41:757.
45. WHO/PAHO consultation on CVS. Evaluation of chorionic villus sampling safety. Prenat Diagn. 1999;19(2):97–9.
46. Williams J, Medearis AL, Bear MD, et al. Chorionic villus sampling is associated with normal fetal growth. Am J Obstet Gynecol. 1987;157:708.
47. Angue H, Bingru Z, Hong W. Long-term follow-up results after aspiration of chorionic villi during early pregnancy. In: Fraccaro M, Simoni G, Brambati B, editors. First-trimester fetal diagnosis. New York: Springer-Verlag; 1985. p. 1.
48. Schaap AH, van der Pol HG, Boer K, Leschot NJ, Wolf H. Long-term follow-up of infants after transcervical

chorionic villus sampling and after amniocentesis to compare congenital abnormalities and health status. Prenat Diagn. 2002;22(7):598–604.

49. Ledbetter DH, Martin AO, Verlinsky Y, et al. Cytogenetic results of chorionic villus sampling: high success rate and diagnostic accuracy in the United States collaborative study. Am J Obstet Gynecol. 1990;162:495.
50. Philip J, Silver RK, Wilson RD, Thom EA, Zachary JM, Mohide P, Mahoney MJ, Simpson JL, Platt LD, Pergament E, Hershey D, Filkins K, Johnson A, Shulman LP, Bang J, MacGregor S, Smith JR, Shaw D, Wapner RJ, Jackson LG, NICHD EATA Trial Group. Late first-trimester invasive prenatal diagnosis: results of an international randomized trial. Obstet Gynecol. 2004;103(6):1164–73.
51. Ledbetter DH, Zachary JL, Simpson MS, et al. Cytogenetic results from the US collaborative study on CVS. Prenat Diagn. 1992;12(5):317.
52. Hahnemann JM, Vejerslev LO. European collaborative research on mosaicism in CVS (EUCROMIC)-fetal and extrafetal cell lineages in 192 gestations with CVS mosaicism involving single autosomal trisomy. Am J Hum Genet. 1997;60(4):917–27.
53. Bui T, Iselius L, Linsten J. European collaborative study on prenatal diagnosis: mosaicism, pseudomosaicism and single abnormal cells in amniotic fluid cell cultures. Prenat Diagn. 1984;4:145.
54. Hsu LYF, Perlis TE. United States survey on chromosome mosaicism and pseudomosaicism in prenatal diagnosis. Prenat Diagn. 1984;4:97.
55. Markert C, Petters R. Manufactured hexaparenteral mice show that adults are derived from three embryonic cells. Science. 1978;202:56.
56. Kotzot D. Abnormal phenotypes in uniparental disomy (UPD): fundamental aspects and a critical review with bibliography of UPD other than 15. Am J Med Genet. 1999;82(3):265–74.
57. Webb AL, Sturgiss S, Warwicker P, Robson SC, Goodship JA, Wolstenholme J. Maternal uniparental disomy for chromosome 2 in association with confined placental mosaicism for trisomy 2 and severe intrauterine growth retardation. Prenat Diagn. 1996;16:958–62.
58. Langolis S, Yong SL, Wilson RD, Kalousek DK. Prenatal and postnatal growth failure associated with maternal heterodisomy for chromosome 7. J Med Genet. 1995;32:871–5.
59. European Collaborative Research on Mosaicism in CVS (EUCROMIC). Trisomy 15 CPM: probable origins, pregnancy outcome and risk of fetal UPD. Prenat Diagn. 1998;18(1):35–44.
60. Cassidy SB, Lai LW, Erickson RP, et al. Trisomy 15 with loss of the paternal 15 as a cause of Prader-Willi syndrome due to maternal disomy. Am J Hum Genet. 1992;51:701.
61. Purvis-Smith SG, Saville T, Manass S, et al. Uniparental disomy 15 resulting from “correction” of an initial trisomy 15. Am J Hum Genet. 1992;50:1348.
62. Wilson RD. Early amniocentesis: a clinical review. Prenat Diagn. 1995;15:1259–73.
63. Penso CA, Frigoletto FD. Early amniocentesis. Semin Perinatol. 1990;14:465–70.
64. Wilson RD. Early amniocentesis: risk assessment. In: Evans MI, Johnson MP, Yaron YY, editors. Drugan AD: prenatal diagnosis. New York: McGraw Hill Publishing Co; 2006. p. P423–32.
65. Penso CA, Sanstrom MM, Garber MF, et al. Early amniocentesis: report of 407 cases with neonatal follow-up. Obstet Gynecol. 1990;76:1032–6.
66. Hanson FW, Tennant F, Hune S, et al. Early amniocentesis: outcome, risks, and technical problems at ≤12.8 weeks. Am J Obstet Gynecol. 1992;166:1707–11.
67. Assel BG, Lewis SM, Dickerman LH, et al. Single operator comparison of early and mid-second-trimester amniocentesis. Obstet Gynecol. 1992;79:940–4.
68. Shulman LP, Elias S, Phillips OP, et al. Amniocentesis performed at 14 weeks’ gestation or earlier: comparison with first-trimester transabdominal chorionic villus sampling. Obstet Gynecol. 1994;83:543–8.
69. Nicolaides K, de Lourdes Brizot M, Patel F, et al. Comparison of chorion villus sampling and early amniocentesis for karyotyping in 1,492 singleton pregnancies. Fetal Diagn Ther. 1996;11:9–15.
70. Nicolaides KH, deLourdes Brizot M, Patel F, et al. Comparison of chorionic villus sampling and amniocentesis for fetal karyotyping at 10–13 weeks’ gestation. Lancet. 1994;344:435–9.
71. The Canadian early and Mid-trimester Amniocentesis Trial (CEMAT) Group: randomized trial to assess safety and fetal outcome of early and mid-trimester amniocentesis. Lancet. 1998;351:242–7.
72. Eiben B, Hammons W, Nanson S, et al. On the complication risk of early amniocentesis versus standard amniocentesis. Fetal Diagn Ther. 1997;12:140–4.
73. Tabor A, Philip J, Madsen M, et al. Randomized controlled trial of genetic amniocentesis in 4,606 low risk women. Lancet. 1986;1:1287–93.
74. Tharmaratnam S, Sadex S, Steele EK, et al. Early amniocentesis: effect of removing a reduced volume of amniotic fluid on pregnancy outcome. Prenat Diagn. 1998;18:773–8.
75. Alfirevic Z, Sundberg K, Brigham S. Amniocentesis and chorionic villus sampling for prenatal diagnosis. Cochrane Database Syst Rev. 2003;9:CD003252.
76. Evans MI, Fletcher JC, Zador IE, Newton BW, Struyk CK, Quigg MH. Selective first trimester termination in octuplet and quadruplet pregnancies: clinical and ethical issues. Obstet Gynecol. 1988;71:289–96.
77. Cohen AB, Hanft RS. Technology in American Health Care: policy direction for effective evaluation and management. Ann Arbor: Univ Michigan Press; 2004.
78. Evans MI, Hanft RS. The introduction of new technologies. ACOG Clin Semin. 1997;2(5):1.
79. Berkowitz RL, Lynch L, Chitkara U, et al. Selective reduction of multiple pregnancies in the first trimester. N Engl J Med. 1988;318:1043.

80. Wapner RJ, Davis GH, Johnson A. Selective reduction of multifetal pregnancies. Lancet. 1990;335:90–3.
81. Yaron Y, Bryant-Greenwood PK, Dave N, et al. Multifetal pregnancy reduction (MFPR) of triplets to twins: comparison with non-reduced triplets and twins. Am J Obstet Gynecol. 1999;180:1268–71.
82. Balasch J, Gratacós E. Delayed childbearing: effects on fertility and the outcome of pregnancy. Curr Opin Obstet Gynecol. 2012;24(3):187–93.
83. Balasch J, Gratacós E. Delayed childbearing: effects on fertility and the outcome of pregnancy. Fetal Diagn Ther. 2011;29:263–73. https://doi.org/10.1159/000323142.
84. McLean LK, Evans MI, Carpenter RJ, Johnson MP, Goldberg JD. Genetic amniocentesis (AMN) following multifetal pregnancy reduction (MFPR) does not increase the risk of pregnancy loss. Prenat Diagn. 1998;18(2):186–8.
85. Wapner RJ, Johnson A, Davis G, Urban A, Morgan P, Jackson L. Prenatal diagnosis in twin gestations: a comparison between second-trimester amniocentesis and first-trimester chorionic villus sampling. Obstet Gynecol. 1993;82:49–56.
86. Brambati B, Tului L, Baldi M, Guercilena S. Genetic analysis prior to selective fetal reduction in multiple pregnancy: technical aspects and clinical outcome. Hum Reprod. 1995;10:818–25.
87. Tabor A, Alfirevic Z. Update on procedure-related risks for prenatal diagnosis techniques. Fetal Diagn Ther. 2010;27:1–7.
88. Pantos K, Kokkali G, Petroutsou K, Lekka K, Malligiannis P, Koratzis A. Monochorionic triplet and monoamniotic twin gestation after intracytoplasmic sperm injection and laser-assisted hatching. Fetal Diagn Ther. 2009;25:144–7.
89. Peeters SH, Evans MI, Slaghekke F, Klumper FJ, Middeldorp JM, Lopriore E, Oepkes D. Pregnancy complications for di-chorionic, tri-amniotic triplets: markedly increased over trichorionic and reduced cases. Am J Obstet Gynecol. 2014;210:S288.
90. Dziadosz M, Evans MI. Re-thinking single embryo transfer: increased risks of monozygotic twinning, a systematic review. Fetal Diagn Ther. 2017;42:81–91.
91. Gebb J, Dar P, Rosner M, Evans MI. Long term neurologic outcomes after common fetal interventions. Am J Obstet Gyneol. 2015;212(527):e1–9.
92. Wang H, Zhou Q, Wang X, Sang J, Chen P, Wang Y, Li L, Li H. Influence of indications on perinatal outcomes after radio frequency ablation in complicated monochorionic pregnancies: a retrospective cohort study. BMC Preg Child. 2021; https://doi.org/10.1186/s12884-020-03530-6.
93. Kalra SK, Milad MP, Klock SC, Grobman WA. Infertility patients and their partners: differences in the desire for twin gestations. Obstet Gynecol. 2003;102:152–5.
94. Evans MI, Evans SM, Curtis J, Britt DW. Fetal reduction and selective termination. In: Kilby M, Oepkes D, Johnson A, editors. Fetal therapy: scientific basis and clinical appraisal of clinical benefits. 2nd ed. Cambridge: Cambridge Univ Press; 2020.
95. Evans MI, Andriole S, Pergament E, Curtis J, Britt DW. Paternity balancing. Fetal Diagn Ther. 2013;34:135–9.
96. Evans MI, Evans SM. Prenatal testing or Screening? Matern Fetal Med. 2020;2:217–22.
97. Evans MI, Britt DW, Evans SM, Devoe LD. Changing perspectives of electronic fetal monitoring. Reprod Sci. 2022; https://doi.org/10.1007/s43032-021-00749-2.
98. Evans MI, Chen M, Britt DW. Understanding false negative in prenatal testing. Diagnostics. 2021;11:888. https://doi.org/10.3390/diagnostics11050888.
99. Lord J, McMullan DJ, Eberhardt RY, Rink G, Hamilton SJ, Quinlan-Jones E, Prigmore E, et al. Prenatal exome sequencing analysis in fetal structural anomalies detected by ultrasonography (PAGE): a cohort study. Lancet. 2019;393:747–57.

Sonography of Pelvic Masses Associated with Early Pregnancy

26

Catherine H. Phillips, Lavenia Carpenter,
Glynis Sacks, and Arthur C. Fleischer

Clinical Implications

First-trimester sonography allows for visualization of pelvic anatomy before the expanding uterus conceals neighboring structures. For the vast majority of young pregnant women, this study will be the first imaging exam of their pregnancy. Previously asymptomatic or minor pathology hidden to palpation reveals itself during sonography and impacts subsequent clinical decisions. Sonography is the test of choice for evaluation of pelvic masses in early pregnancy, the findings of which may require prompt treatment, alter the labor and delivery plan, or necessitate further imaging. The most recent joint guidelines on obstetrical sonography published by the American College of Radiology appropriately reflect the need for a comprehensive first-trimester sonogram that includes the "uterus, cervix, adnexa, and cul-de-sac region" along with the gestational sac contents [1]. This ensures that a comprehensive pelvic ultrasound exam is performed and enables nonspecific pelvic symptoms to be evaluated in real time.

Although most adnexal masses in pregnancy are benign [2, 3], they can cause significant complications despite their frequently benign cytology. The hormonal effects of pregnancy and increasing uterine girth can cause leiomyomata to enlarge, cysts to rupture, adnexal masses to undergo torsion, and cancers to grow. Early identification of abnormalities in the first trimester facilitates prompt medical intervention and surgical treatment, if necessary, during the second trimester when spontaneous abortion and preterm labor are lowest and surgical exposure remains adequate. Though smaller incidental masses with benign sonographic characteristics are amenable to observation [2], surgical intervention is typically pursued in those masses that are larger (usually >7 cm in diameter but a definitive cutoff has not been established), symptomatic, torse, and/or suspicious for malignancy. Sonography can be used to accurately differentiate between the architectural patterns of benign and malignant masses and to determine which would be associated with an increased risk of ovarian torsion [2, 4–7].

Techniques

Characterization of incidental findings on transabdominal obstetrical sonography, inability to visualize the adnexa or cervix, and examination of an obese patient may obligate further evalua-

---

C. H. Phillips (✉) · L. Carpenter · G. Sacks
A. C. Fleischer
Vanderbilt University Medical Center,
Nashville, TN, USA
e-mail: catherine.phillips@vumc.org;
lavenia.carpenter@vumc.org;
glynis.sacks@vumc.org; arthur.fleischer@vumc.org

© The Author(s), under exclusive license to Springer Nature Switzerland AG 2023
J. S. Abramowicz, R. E. Longman (eds.), *First-Trimester Ultrasound*,
https://doi.org/10.1007/978-3-031-24133-8_26

tion via a transvaginal approach [1, 4]. Transvaginal sonography is generally well tolerated by patients, avoids fetal radiation, and is less limited by subcutaneous tissue signal degradation. In addition, transvaginal sonography provides higher resolution imaging of pelvic pathology as it utilizes higher frequency transducers in closer proximity to pelvic anatomy compared to commonly used transabdominal probes.

Three-dimensional sonography has proven particularly beneficial in the imaging of uterus and adnexa. Transvaginal probes have been adapted to collect consecutive two-dimensional images throughout a region of interest while the probe is held stationary. This creates a user-independent imaging volume that can be manipulated and reconstructed into multiplanar reformats. The coronal plane is particularly useful for pelvic sonography as it adds diagnostic information about the fundal contour that is not only essential for characterization of uterine anomalies, but also not feasible with conventional two-dimensional transvaginal sonography.

Both two-dimensional and three-dimensional sonography can also include color Doppler interrogation. Doppler interrogation has been used to improve the sensitivity of ultrasound for diagnosing ovarian malignancy in nonpregnant patients. Evaluation of a pelvic mass in pregnancy is not complete without assessing internal Doppler flow, although physiologic hemodynamic changes of pregnancy can complicate analysis [8]. In general, disorganized vasculature with low-resistance and high-velocity flow is suspicious for more worrisome diagnoses [4]. Early in the first trimester, embryos are most susceptible to external teratogens, including thermal and mechanical energy generated by pulsed spectral Doppler, in particular [9]. To address this, the American Institute of Ultrasound in Medicine (AIUM) recommends against routine use of pulsed Doppler and for utilization of Doppler studies that include the embryo or fetus only when there is clear diagnostic benefit/risk advantage. Specifically, spectral Doppler should only be used when the TI and examination duration are kept low, with protocols involving TI values <1.0 representing minimal risk [10]. It should not be used routinely for determination of fetal heart rate.

Uterine Masses

Fibroids

Leiomyomas are benign smooth muscle tumors commonly referred to as "fibroids" and are the most prevalent gynecologic affliction of gravid and nongravid females, present in up to 70% of women by menopause [11]. They are commonly found incidentally on first-trimester sonography [5, 6]. On ultrasound, fibroids appear as round, well-defined myometrial based masses that are iso- or slightly hypo-echoic compared to the surrounding myometrium (Fig. 26.1) and demonstrate peripheral and mild internal vascularity on color Doppler sonography. They may contain shadowing calcifications and areas of cystic change when undergoing degeneration.

Fibroids are highly sensitive to estrogen, which can promote their growth and maturation in the first trimester. If fibroids outgrow their blood supply, they can undergo red/carneous degeneration, which results from hemorrhagic infarction secondary to venous thrombosis within

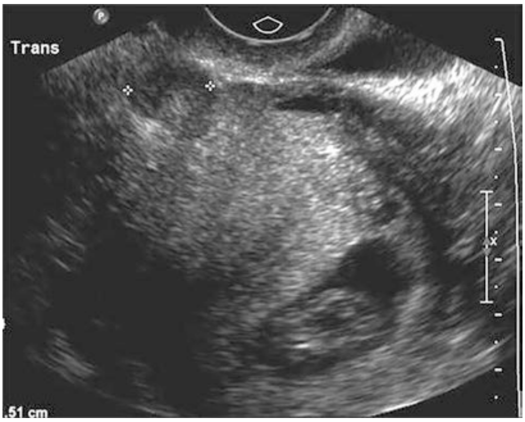

Fig. 26.1 Subserosal fibroid. Transvaginal grayscale transverse image of the uterus demonstrates a round heterogeneous mass, measuring 0.51 cm wide (+), projecting beyond the contour of the uterus. The gestational sac with embryo is noted within the uterus

the periphery of the tumor or rupture of intratumoral arteries. Although less common than red degeneration, hyaline, myxoid, and cystic fibroid degeneration are also possible during the first trimester. On ultrasound, degeneration would be marked by a change in fibroid echotexture and loss of peripheral vascularity. Patients will also frequently be symptomatic and present with focal or diffuse pain associated with the degenerative process.

It is important to utilize sonography in early pregnancy to identify those fibroids that could be clinically significant due to their size and location. Submucosal fibroids, for example, may increase the risk of early pregnancy loss. If first-trimester miscarriage is eluded, these submucosal masses can cause mass effect and disruption of placental implantation or compete with fetal growth and obstruct fetal and placental delivery if located within the lower uterine segment [6, 12]. Increased pressure above a low-lying fibroid during labor increases the risk of uterine rupture and fetal mortality. Despite these complications, prenatal intervention is uncommon and usually reserved for outside of pregnancy when the uterine, and commonly the fibroid, size has decreased.

Fibroids can present unexpected challenges for the medical imaging specialist, especially when they become large or are in challenging locations. For example, subserosal type fibroids pushed close to an ovary by the gravid uterus can be difficult to differentiate from a solid ovarian mass. Degenerative changes in such a fibroid may further complicate diagnosis. In such cases, color Doppler should be utilized to delineate blood flow that connects the uterus to the fibroid and exclude adnexal origin of the lesion. However, if ultrasound is inconclusive, further imaging with MRI may be required.

Adnexal Masses

Incidence of adnexal masses in pregnancy is less than 3%, with up to 6% of those masses being malignant [7, 13–15]. Given the high likelihood that an adnexal mass identified in pregnancy will be benign, the goal of ultrasound evaluation is to determine when conservative management is appropriate and when sonographic features are suspicious enough to warrant surgical intervention. Simple cysts of any size and classic-appearing benign cysts <5 cm are highly unlikely to be malignant lesions in menstruating females. Follow-up or further evaluation is recommended only when the size is greater than 5 cm. Reports have shown a high accuracy of ultrasound for the determination of malignant potential. Schmeler et al. and Kumari et al. reported correct diagnosis of malignancy in all pregnant patients studied presenting with incidental adnexal masses [7, 16].

Corpus Luteum

A retrospective review of sonography performed on over 18,000 pregnant patients identified a 2.3% prevalence of adnexal masses; the majority were small (<5 cm) simple cysts that were without complication during the pregnancies [17]. The majority of these cysts likely begin as corpora lutea: the most commonly encountered cystic adnexal mass during pregnancy [5]. Corpora lutea form after fertilization of an expulsed ovum from an ovarian follicle. They endure to produce progesterone and maintain the early pregnancy. Fluid filled with smooth, thick walls, they grow to a maximum diameter at the end of the first trimester. The decreasing functionality of the corpus luteum as the placenta assumes an endocrinologic role for the developing fetus is reflected sonographically by its decrease in size by the second trimester (Fig. 26.2a, b).

The lifetime of the corpus luteum in a pregnant woman is much longer than during a normal menstrual cycle due to its hormonal support of pregnancy. This longer life cycle makes complications such as rupture, torsion, and hemorrhage potentially more common in a pregnant patient (Fig. 26.3a, b).

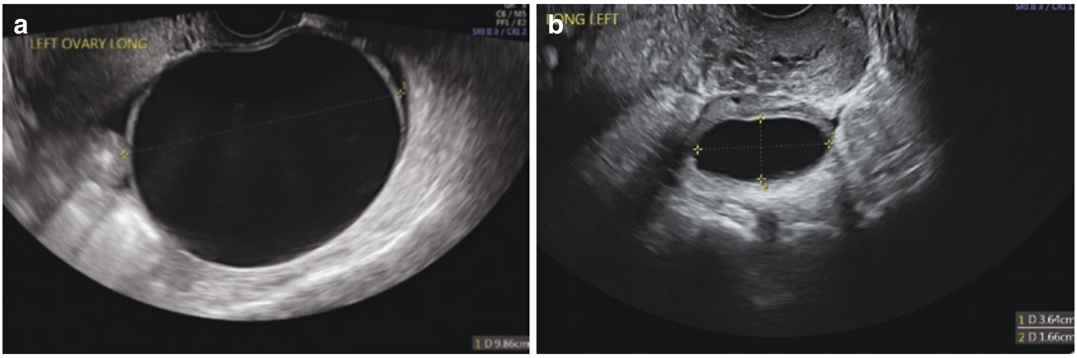

Fig. 26.2 Corpus luteum evolution during pregnancy. Grayscale transvaginal sagittal (**a**) views of the left ovary in a patient who was 7 weeks pregnant demonstrate a thick-walled predominantly anechoic cyst measuring 9.9 cm. The patient returned for her anatomy scan at 20 weeks' gestational age at which point grayscale transverse images of the ovary (**b**) demonstrate interval decrease in size of the left ovarian cyst, now measuring 3.6 cm

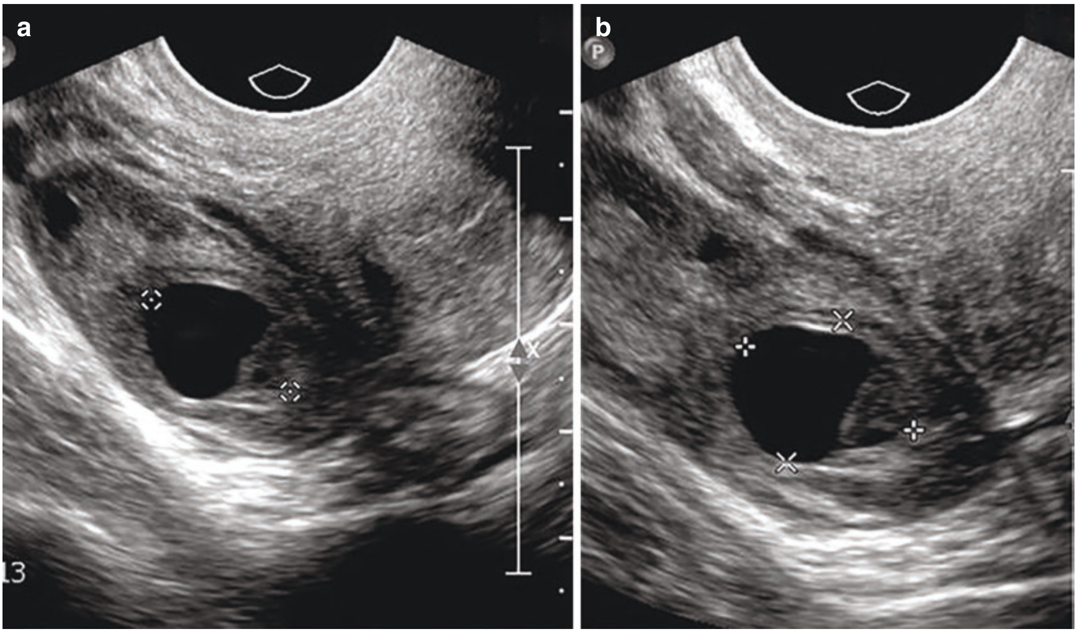

Fig. 26.3 Corpus luteum. Grayscale transvaginal transverse (**a**) and sagittal (**b**) images of the ovary demonstrate a predominantly anechoic cyst containing a thick wall and hypoechoic dependent debris, likely old blood products

Corpus Luteum Cysts

A persistent corpus luteum can seal externally within the ovary and continue to collect fluid within, forming a unilocular corpus luteum cyst. Because the cyst contains fluid, it is anechoic with posterior acoustic enhancement, though it may exhibit thin lacelike echogenic septa if it persists into the second trimester and is filled with blood [6]. The size of the cyst is a strong predictor of its ability to spontaneously regress, with almost all cysts <5 cm in diameter resolving completely without intervention [18]. The most recent guidelines (2010) for nongravid women from the Society of Radiologists in Ultrasound do not recommend follow-up sonography for simple cysts smaller than 5 cm, whereas yearly sonography of larger cysts should be considered, despite low malignant potential [19]. Standard scheduling of obstetric ultrasounds offers the opportunity to track the growth of corpus luteum cysts throughout pregnancy.

Both the corpus luteum and corpus luteum cyst have distinguishing dense peripheral “ring of fire” vascularity on color Doppler imaging (Fig. 26.4a–c). These vessels exhibit low resistance and high diastolic flow on spectral Doppler. There are typically little or no internal solid components. Ectopic or heterotopic pregnancies in the adnexa imitate corpus luteum cysts because they, too, are fed by a peripheral ring of vessels and can be seen directly adjacent to the ovary (Fig. 26.5a, b). The critical distinction is made by determining if the adnexal mass is para- or intraovarian. Ectopic pregnancies should move independently from the ovary with pressure applied by the examiner. This “sliding sign” is not visualized during examination of intraovarian corpus luteum cysts, which remain coordinated in movement with the ovary. In a retrospective study of 78 pelvic sonograms performed on women exhibiting symptoms consistent with ectopic pregnancy during the first trimester, the radiologists were able to correctly identify ectopics in 23 of 27 patients exhibiting the “sliding organ sign.” Although not a strong differentiator, ectopic pregnancies also tend to be more complex and echogenic than luteal cysts when compared to the ovarian parenchyma [20].

Corpus luteum cysts are usually asymptomatic, especially when they are relatively small in size, as opposed to ectopic pregnancies that will invariably become symptomatic. However, large cysts can rupture, undergo torsion, and bleed [18]. Intervention is imperative for ectopic pregnancies and considered for cysts and benign masses greater than 7 cm, but not recommended for small luteal cysts [19]. Surgical intervention is avoided when possible until progesterone support of the pregnancy has shifted from the corpus luteum to the placenta [21].

Hemorrhagic Corpus Luteum Cysts

The clinical presentation of a hemorrhagic corpus luteum cyst is characterized by more unilateral pain than its predecessors. The resolution of pain does not correlate with the resolution of the hemorrhagic cyst, which can evolve over subsequent months [22]. Sonographically, the acute phase of the hemorrhage will appear as very hyperechoic internal echoes within the cyst (Fig. 26.6a, b). As the blood settles, the cyst appears more heterogeneous with thin, fibrinous septations that are without color Doppler flow. The clot retracts to the

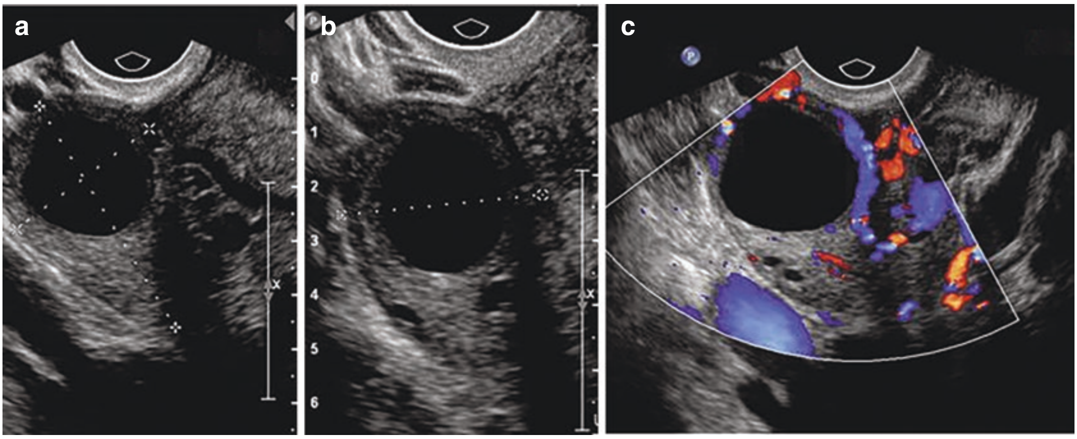

Fig. 26.4 Corpus luteum cyst of pregnancy. Transvaginal sagittal (**a**) and transverse (**b**) grayscale images of the ovary demonstrate an anechoic round structure with thin walls. Sagittal color Doppler image (**c**) demonstrates peripheral vascularity representing the “ring of fire”

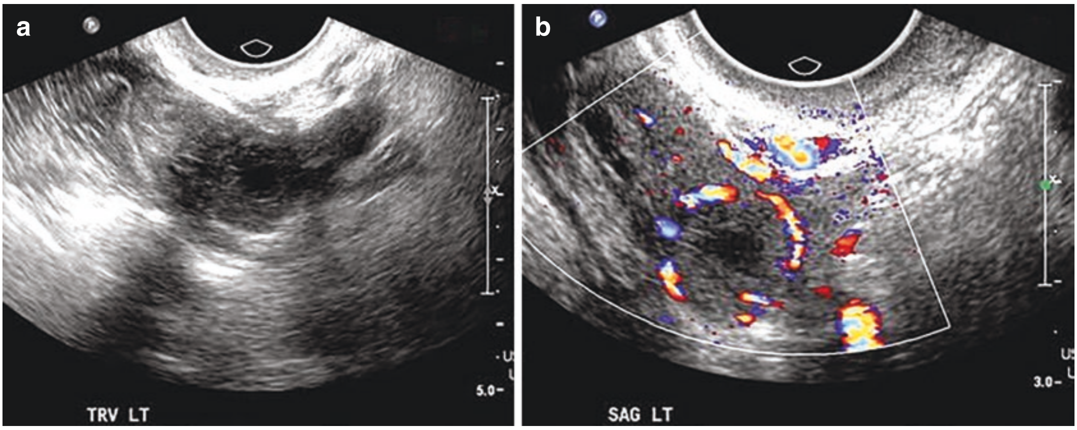

Fig. 26.5 Ectopic pregnancy. Transverse (**a**) image of the left adnexa demonstrates a tubular echogenic structure with thick echogenic ring and peripheral vascularity on sagittal color Doppler image (**b**)

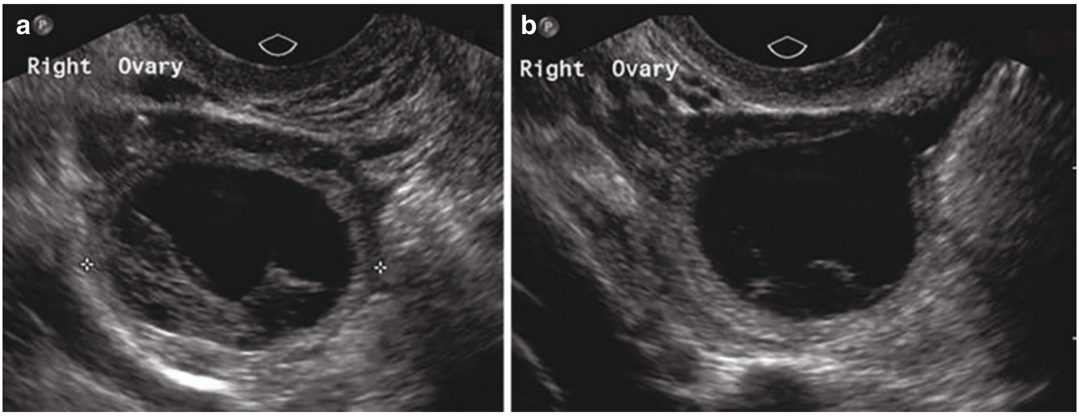

Fig. 26.6 Hemorrhagic corpus luteum cyst of pregnancy. Grayscale transvaginal transverse (**a**) and sagittal (**b**) images of the ovary show heterogeneous echogenic material within an otherwise anechoic cyst, representing hemorrhagic blood products within a corpus luteum cyst

walls of the cyst, appearing as a solid or reticular hyperechoic structure. Throughout this course, the cyst should always remain well defined with enhanced through-transmission owing to the predominant presence of non-bloody cystic fluid. If the cyst is not intact and the patient is symptomatic, a diagnosis of rupture is supported by the presence of free pelvic fluid.

Due to the lack of specificity observed in some hemorrhagic corpus luteum cysts, follow-up imaging may be appropriate. Growth requires continued surveillance. The presence of thick septations and nodular walls, especially when there is associated vascularity, is suspicious for neoplasia, and surgical intervention must be considered (Fig. 26.7a–c). Alternatively, magnetic resonance imaging may be helpful for further characterization, and its use may be limited without intravenous contrast which is usually deferred in pregnancy. By the second-trimester anatomy scan, true functional hemorrhagic cysts should have involuted.

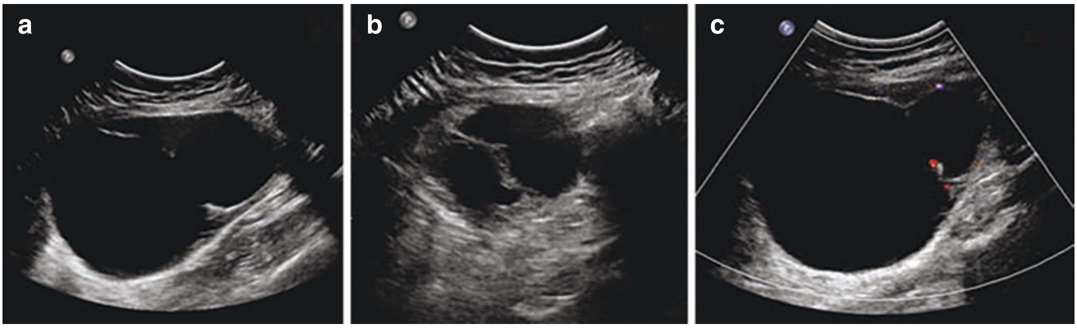

Fig. 26.7 Borderline mucinous tumor of the ovary. Transabdominal grayscale sagittal (**a**) and transverse (**b**) images of the ovary demonstrate a predominantly cystic mass with thick septations. Color Doppler imaging demonstrates blood flow within the septations (**c**)

Decidualized Endometriomas

Ultrasound has both high diagnostic sensitivity and specificity for endometriomas, which are most commonly seen as implants within the ovaries and adnexa. These cystic masses have a characteristic sonographic appearance with smooth inner wall, frequently with rim echogenic foci, and contain homogenous low-level echoes but not internal flow on Doppler (Fig. 26.8). The sonographic appearance of endometriomas can resemble a hemorrhagic corpus luteum cyst; however, the latter will involute by the second trimester and the former will persist. Just as the endometrium of the uterus decidualizes under the influence of progesterone during pregnancy, about 12% of ovarian endometriomas also undergo decidualization [23] (Fig. 26.9a–c). Their benign appearance transforms to closely mimic borderline ovarian tumors (Fig. 26.10a, b). They can rapidly develop solid intracystic papillary excrescences and irregular walls. The projections may be quite vascular and can exhibit low-resistance flow. Because ovarian endometriomas are more likely to undergo malignant transformation than extragonadal types, though uncommon in reproductive-age women with small endometriomas, the correct diagnosis is crucial and particularly complicated during pregnancy.

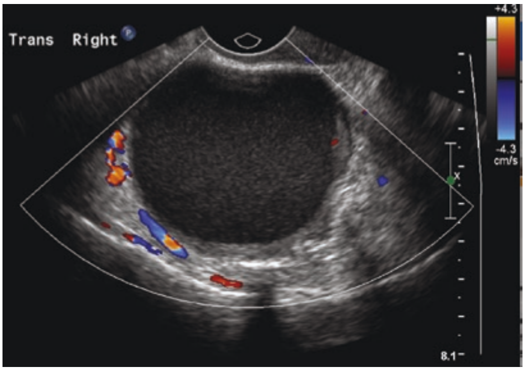

Fig. 26.8 Endometrioma. Transvaginal transverse image of the right ovary with color Doppler demonstrates a large thick-walled cyst containing diffuse low-level internal echoes and no internal flow on Doppler

Though the concerning features of decidualized endometriomas tend to resolve after delivery, most women elect for surgical removal while pregnant [24]. Ultrasound remains the modality of choice for initial characterization of ovarian masses in the hopes of distinguishing decidualized ovarian endometriomas from malignant tumors, though the task remains difficult. Endometriomas tend to become slightly smaller or remain stable in size throughout pregnancy, while cancerous lesions enlarge. Sonographic appearance of the wall of an endometrioma should be similar to that of the uterine endometrium. MRI does not add significant diagnostic benefit and is limited by avoidance of contrast but

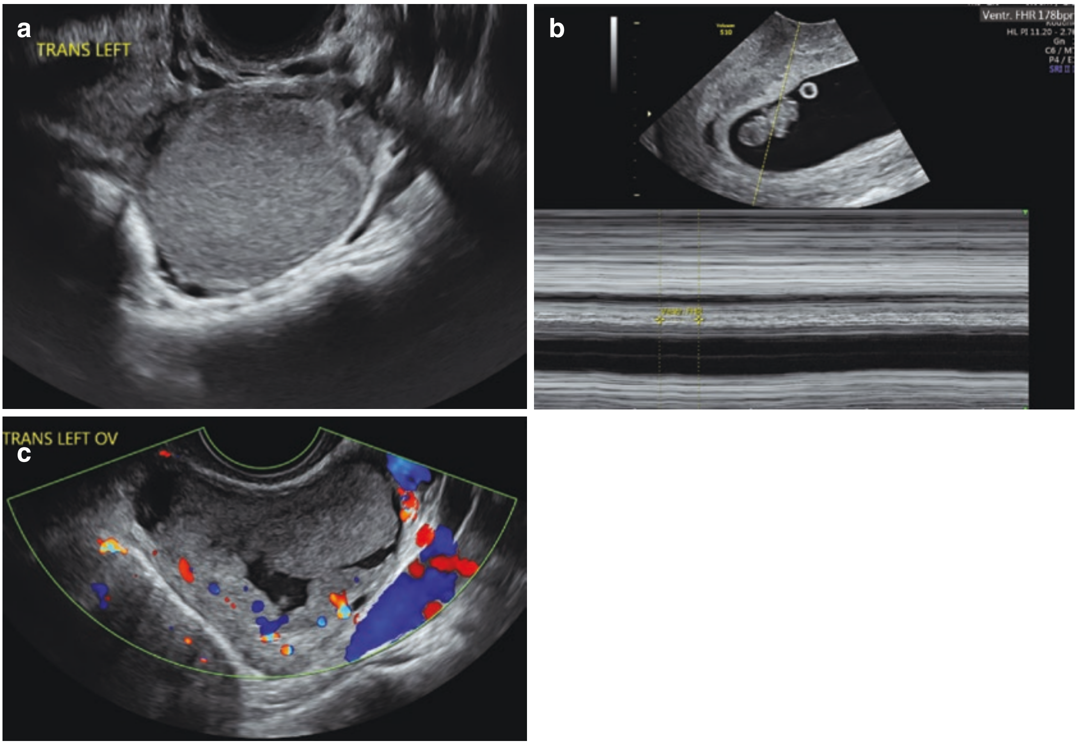
a
TRANS LEFT
b
Ventr. FHR 178bpm
c
TRANS LEFT OV

Fig. 26.9 Endometrioma of pregnancy with second-trimester decidualization. Transvaginal grayscale transverse image of the left ovary (**a**) demonstrating a thick-walled cyst with low-level internal echoes consistent with endometrioma. In the uterus was a single embryo with fetal heart rate corresponding to an 8w6d pregnancy (**b**). The patient returned at 26w0d, and the left ovary contained a complex cystic mass with irregular papillary projections that contained internal flow on Doppler (**c**), consistent with decidualized endometrioma

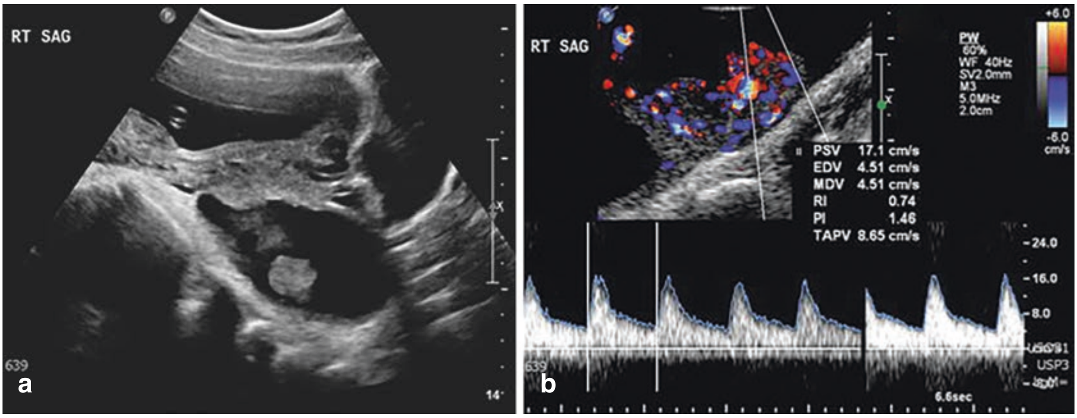
RT SAG
a
RT SAG
PW
60%
WF 40Hz
SV2.0mm
M3
5.0MHz
2.0cm
+6.0
-6.0
cm/s
PSV 17.1 cm/s
EDV 4.51 cm/s
MDV 4.51 cm/s
RI 0.74
PI 1.46
TAPV 8.65 cm/s
-24.0
-16.0
-8.0
USP3
6.6sec
b

Fig. 26.10 Decidualized ovarian endometrioma mimicking a borderline tumor. Sagittal image of the right adnexa (**a**) shows a cystic mass with internal irregular solid projections. Seventeen-week intrauterine pregnancy is noted. Color Doppler imaging demonstrates low-resistance vascularity within the papillary projections (**b**)

may assist in further comparison of endometrial tissues or ruling out a hemorrhagic corpus luteum cyst. Analysis of vascularity has not revealed consistent chronological, morphological, or flow differences. If surgical intervention is deferred, monthly sonographic follow-up is recommended [24].

Mature Teratomas

Although "dermoid cyst" is the term used most commonly, the correct medical nomenclature for these tumors is "mature teratoma." Sonography is a valuable modality for diagnosing benign ovarian mature teratomas. In a prospective study of 1066 sonograms of adnexal masses, radiologists correctly identified mature teratomas 86% of the time and never misdiagnosed them as malignant [25]. An older study of second- and third-trimester sonography of 131 adnexal lesions greater than 4 cm in diameter correctly identified 95% of the mature teratomas [2]. Advances in transvaginal ultrasound technology and changes in prenatal screening since publication of the latter study have led to improved early detection of smaller mature teratomas. This is important given that they are the most common complex pelvic mass identified during pregnancy and would otherwise go undiagnosed until much later in 10% of women with mature teratomas [5, 6].

Mature teratomas can exhibit a wide array of appearances. Nearly all mature teratomas are well-circumscribed complex heterogeneous echogenic masses arising from the ovary. They consist of well-differentiated tissues from multiple germ cell lineages (e.g., fat, calcifications, hair, and sebum), creating distinctive hyperechoic linear markings (lines and dots) within the mature teratoma (Fig. 26.11) and highly echogenic areas that strongly shadow ("tip of the iceberg sign") (Figs. 26.12a, b and 26.13a, b). This appearance may be mistaken for nearby gas-containing

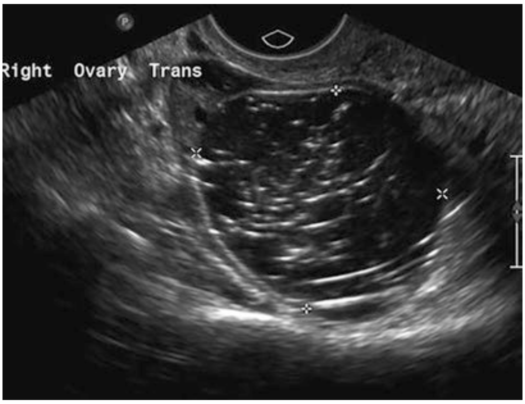

Fig. 26.11 Mature teratoma with hair. Transvaginal grayscale transverse image of the ovary demonstrates a heterogeneous round mass with punctate and linear echogenic foci, representing internal hair components

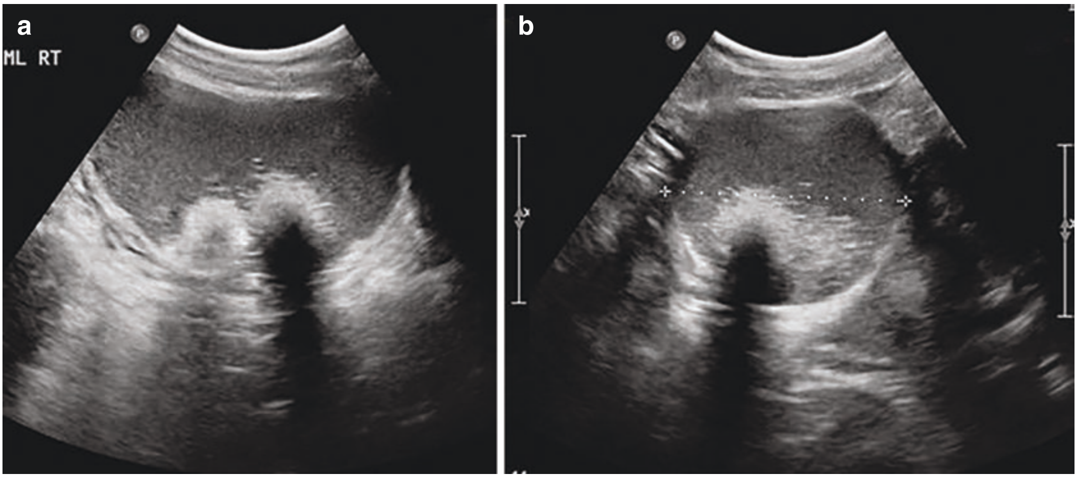

Fig. 26.12 Mature teratoma. Sagittal (**a**) and transverse (**b**) grayscale transabdominal images of the right ovary demonstrate a predominantly homogeneous echogenic mass with focal echogenic areas with posterior acoustic shadowing, representing internal calcifications

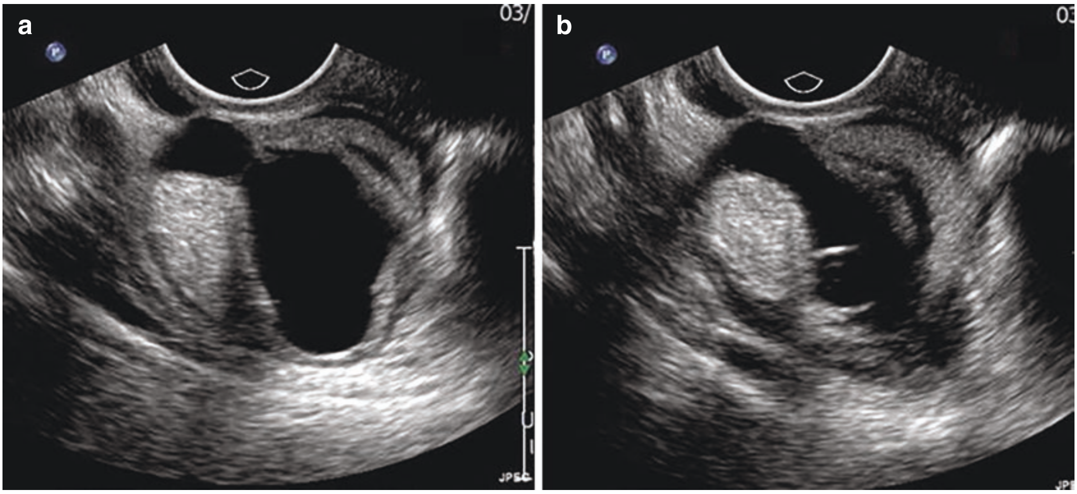

Fig. 26.13 Mature cystic teratoma and Brenner tumor. Grayscale transvaginal sagittal (**a**) and transverse (**b**) images of the ovary demonstrate a heterogeneous mass with mixed anechoic and solid echogenic components

bowel that only allows visualization of the surface closest to the transducer. Although less common, fat-fluid levels and balls of sebum are nearly pathognomonic for mature teratomas.

Benign cystic teratomas will not change in size under the influence of pregnancy but are well-known perpetrators of ovarian torsion in expectant mothers [6]. If the ovary does become torsed, it will typically exhibit limited venous outflow on color Doppler with free pelvic fluid from edema and vascular congestion. Upon scanning the adnexa, the main ovarian vessels may appear twisted, but some flow to the ovary from uterine collaterals can be present. Clinically, in the cases of intermittent torsion, the patient may experience repeated episodes of clinical improvement followed by pain as the torsion temporarily resolves and resumes, respectively, which may lead to the torsion not being captured sonographically if the patient is scanned during a period of detorsion. Pedunculated dermoid cysts are particularly prone to torsion and subsequent rupture, and patients can present with signs and symptoms of an acute abdomen [18]. If ruptured or torsed, surgical intervention is the management strategy of choice, as necrosis and peritonitis may develop. Otherwise, conservative observation for small mature teratomas is appropriate.

Ovarian Cancer

It is estimated that 1.2–6.8% of all persistent adnexal masses seen on prenatal sonography are malignant [4]. Epithelial ovarian tumors account for approximately 50% of all ovarian cancers detected in pregnancy with ovarian germ cell tumors making up 33% and stromal tumors, sarcomas, and metastatic lesions making up the remainder [26]. It is reassuring that the overall prevalence of adnexal masses in pregnancy is low, but the few cancers that exist are definite "do not miss" diagnoses. First-trimester sonography presents an opportunity for early detection of a cancer that is otherwise asymptomatic and, thus, might be diagnosed at advanced stages. As discussed, ultrasound has shown high accuracy for determination of malignant potential, although a benign mass may occasionally mimic a cancerous mass. If sonographic findings are indeterminant, MRI may add specificity, but will be limited due to the recommendation against the use of gadolinium contrast agents in pregnant patients.

Tumor markers associated with gynecologic cancers are physiologically elevated during pregnancy. Although CA-125 remains the best laboratory test for ovarian cancer in nongravid females, it is elevated in only half of the women with stage

I disease [4]. Healthy pregnant women can have elevated CA-125 levels (range 7–251 U/mL) that peak at an average of 55 U/mL (upper limit of normal 35 U/mL) during the first trimester [4, 27]. CEA, AFP, and beta-hCG levels increase during pregnancy as well. Given the variability of laboratory markers, imaging remains the best diagnostic tool for ovarian cancer in pregnancy.

The U.S. Department of Health and Human Services published a systemic review of 14 years of literature comparing the ability of multiple imaging modalities to differentiate benign from malignant adnexal masses. The report concluded "there is no evidence to support the superiority of any single modality" for this purpose, claiming that ultrasound, MRI, and CT are nearly equivalent while FDG-PET falls short [28]. However, since that time, there has been extensive work to develop specific sonographic criteria to describe and characterize adnexal lesions. Using the criteria proposed by the International Ovarian Tumor Analysis study remains superior to tumor markers and mathematical predictive models [29]. Additionally, the American College of Radiology Ovarian-Adnexal Reporting and Data System Ultrasound (O-RADS US) has been proven to provide a highly reliable framework for adnexal lesion malignancy risk stratification amongst radiologists, despite different subspecialty experience [30].

Sonographic evaluation of a malignant adnexal lesion starts by determining the origin of a suspicious mass. Intraovarian origin can be confirmed by probing with the transvaginal transducer and observing the absence of a cleavage plain between the mass and the ovary. Suspicion should be raised in the setting of large, complex cystic adnexal masses [17]. The presence of thick, irregular septations and mural nodules or papillary excrescences within a cystic mass are highly concerning. Serous cystadenocarcinoma exhibits more anechoic areas compared to their mucinous counterpart, but these lesions will not be unilocular [6, 18]. Careful evaluation of the entire cyst wall is very important because the borderline serous or mucinous cystadenocarcinoma may be almost completely unilocular, with the exception of one or more mural nodules that usually demonstrate associated vascularity by color Doppler (Fig. 26.14a–d).

Solid masses may represent metastasis, commonly from the GI tract (i.e., Krukenberg tumor), or primary solid tumors of the ovary. These have a wide range of sonographic appearances, though predominantly solid tumors with few cystic components generally represent the poorest prognoses. Solid tumors are divided into epithelial, germ cell, and sex cord/stromal types with distinct epidemiology aiding diagnosis. Epithelial ovarian tumors, including cystadenocarcinomas, are the most common ovarian cancers, largely affecting postmenopausal women. Germ cell tumors, including teratomas, tend to afflict younger women. Sex cord/stromal tumors (i.e., fibromas, thecomas, granulosa cell tumors) are sometimes associated with familial syndromes and appear in middle age.

Generally, malignant neoplasms demonstrate increased flow within solid components on color Doppler evaluation. Spectral Doppler may demonstrate low resistive and pulsatility indices, representing high blood flow to the tumor. Free fluid in the abdomen is likely indicative of maternal ascites from tumor spread. If surgical removal of a suspicious adnexal mass is indicated, laparoscopy and laparotomy are acceptable options. One meta-analysis comparing laparoscopic vs. open surgical management of adnexal masses in the second trimester demonstrated that laparoscopy was associated with better surgical outcomes, but longer operative times compared to laparotomy [26, 31]. When performed in the second or late first trimester, complication rates are low and most pregnancies will be delivered at term.

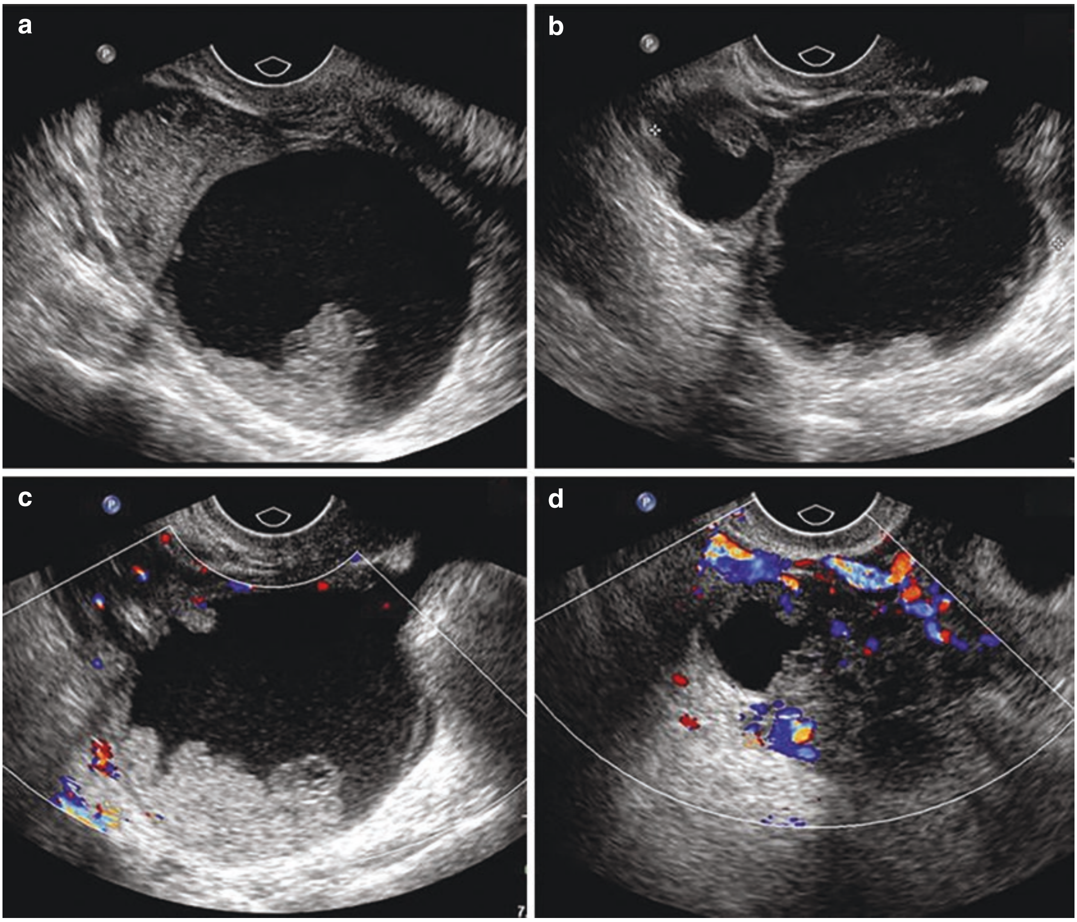

Fig. 26.14 Serous borderline tumor. Grayscale transvaginal sagittal (**a**) and transverse (**b**) images of the ovary demonstrate a large hypoechoic cystic mass with hyperechoic papillary projections. Color Doppler images (**c**, **d**) demonstrate mild vascularity within the papillary projections as well as a second lesion with moderate vascularity

Abdominal Mimickers

Appendicitis can present similarly to complicated right-sided adnexal masses due to its location near the right ovary. Classically, acute appendicitis presents with acute epigastric pain that shifts to the right lower quadrant and is associated with nausea, vomiting, and anorexia. Throughout pregnancy, the enlarging uterus forces the appendix slightly higher than McBurney's point (normally located one-third of the distance on an imaginary line from the right anterior superior iliac spine to the umbilicus), but this change is not significant during the first trimester. Pregnant women are also more likely to present with digestive or urinary complaints than nonpregnant women, which can mimic normal pregnancy symptoms.

CT is often utilized for diagnosis of acute appendicitis in nonpregnant women. However, in those who are pregnant and presenting with right-sided pain, sonography is the test of choice to avoid radiation. MRI can also be used as a problem-solving tool when ultrasound is indeterminate. On ultrasound, an inflamed appendix appears as a non-compressible dilated blind-ending tubular structure arising from the terminal cecum and measuring greater than 6 mm in transverse dimension. Echogenic surrounding fat is common due to peri-appendiceal inflammation. The appendix will be surrounded by a small amount of fluid in cases of rupture. Sometimes, a hyperechoic appendicolith is discovered occluding the appendiceal lumen.

If the appendix has ruptured, the wall will not be intact, allowing fluid (e.g., feces, pus) to collect at the opening. If it does not remain localized, the noxious fluid can irritate the uterus, resulting in higher rates of preterm labor and fetal loss. This is further exacerbated by delayed operative intervention in pregnant women. A sonographic workup for appendicitis must exclude ectopic/heterotopic pregnancies and ovarian torsion if the patient presents in the first trimester and abruption if presenting in the second or third trimester. Pyelonephritis, renal lithiasis, and round ligament pain are amongst differential diagnoses.

Pregnancy induces changes in the urinary system, including dilation of the ureters and collecting systems. Right pelvocaliectasis and ureterectasis are more prominent due to dextrorotation of the enlarging uterus, and hormonal influences on the smooth muscle of the ureter can also cause collecting system fullness bilaterally. Previously asymptomatic ectopic kidneys lying low in the pelvis can cause displaced “flank” pain from vesicoureteral reflux and ascending urinary tract infections. The pain can mimic an adnexal origin. Sonography will likely show hydronephrosis in a pelvic kidney located near an ovary, with infection confirmed by urinalysis.

Summary

A comprehensive sonographic examination of the pelvis in the first trimester allows an early opportunity to evaluate for adnexal pathology, which can be obscured later in pregnancy. Though most of the pathology discussed in this chapter is also encountered in nongravid females, the unique hormonal environment of pregnancy can instigate complications or cause otherwise benign-appearing masses to look suspicious. Sonography remains the imaging test of choice for examination of the adnexa and for distinguishing malignant from benign masses, affording the opportunity for early intervention when safest during the pregnancy. Its role during pregnancy surpasses tumor markers and can help clarify the physical exam, which is confounded by shifting anatomy. Ultrasound also allows characterization of uterine fibroids, which can cause failures in implantation, impede fetal growth, and complicate delivery. Sonography’s vital role during early pregnancy will continue to grow with technical advancements and continued utilization of three-dimensional images.

Teaching Points

- First-trimester sonography leads to earlier detection of small masses that would otherwise go undiagnosed until symptomatic or at an advanced stage. Early exams should cover a comprehensive inspection of the pelvis.
- Regularly scheduled obstetric sonography offers the opportunity to follow up and track first-trimester incidental findings for growth or complications.
- Though most pelvic masses identified in the first trimester are benign, malignancy is occasionally seen. Grayscale imaging in conjunction with color Doppler can help make the distinction between a benign and malignant adnexal mass.
- Fibroids are the most common gynecological masses in gravid and nongravid women. Both two- and three-dimensional sonography can be useful for localizing and measuring fibroids to determine if they will present challenges during pregnancy and labor.
- Sonography has high accuracy in the characterization of adnexal masses and determining their potential to undergo torsion. This can be very helpful during pregnancy, a time when cysts are more likely to rupture or hemorrhage and cystic or solid masses have more opportunity to be a fulcrum for ovarian torsion.
- Sonography remains superior to tumor markers for ovarian cancer detection during pregnancy.

References

1. AIUM-ACR-ACOG-SMFM-SRU practice parameter for the performance of standard diagnostic obstetric ultrasound examinations. J Ultrasound Med 2018;9999:1–12.
2. Bromley B, Benacerraf B. Adnexal masses during pregnancy: accuracy of sonographic diagnosis and outcome. J Ultrasound Med. 1997;16(7):447–52.
3. Smith LH, Dalrymple JL, Leiserowitz G, et al. Obstetrical deliveries associated with maternal malignancy in California 1992 through 1997. Am J Obstet Gynecol. 2001;184:1504–12.
4. American Congress of Obstetricians and Gynecologists. Practice Bulletin No. 174: Evaluation and management of adnexal masses. Obstet Gynecol. 2016;128(5):e320–226.
5. Elhalwagy H. Management of ovarian masses in pregnancy. Trends Urol Gynecol Sex Health. 2009;14(1):14–8.
6. Fleischer A, Manning F, Jeanty P, Romero R, editors. Sonography in obstetrics and gynecology: principles and practice. 6th ed. McGraw-Hill Professional: China; 2001.
7. Schmeler K, Mayo-Smith W, Peipert J, Weitzen S, Manuel M, Gordinier M. Adnexal masses in pregnancy: surgery compared with observation. Obstet Gynecol. 2005;105(5, Part 1):1098–103.
8. Wheeler TC, Fleischer AC. Complex adnexal mass in pregnancy: predictive value of color Doppler sonography. J Ultrasound Med. 1997;16(6):425–8.
9. Abramowicz J. Fetal Doppler: how to keep it safe? Clin Obstet Gynecol. 2010;53(4):842–50.
10. American Institute of Ultrasound in Medicine: Official Statements. Prudent use and safety of diagnostic ultrasound in pregnancy. 2021. http://www.aium.org/officialStatements/79.
11. Steart EA, Cookson CL, Gandolfo RA, Schulze-Rath R. Epidemiology of uterine fibroids: a systematic review. BJOG. 2017;124:1501–12.
12. Lee H, Norwitz E, Shaw J. Contemporary management of fibroids in pregnancy. Rev Obstet Gynecol. 2010;3(1):20–7.
13. Smith LH, Dalrymple JL, Leiserowitz GS, Danielsen B, Gilbert WM. Obstetrical deliveries associated with maternal malignancy in California, 1992 through 1997. Am J Obstet Gynecol. 2001;184(7):1504–12; discussion 1512–3.
14. Webb KE, Sakhel K, Chauhan SP, Abuhamad AZ. Adnexal mass during pregnancy: a review. Am J Perinatol. 2015;32(11):1010–6. https://doi.org/10.1055/s-0035-1549216. Epub 2015 May 22. PMID: 26007316
15. Aggarwal P, Kehoe S. Ovarian tumours in pregnancy: a literature review. Eur J Obstet Gynecol Reprod Biol. 2011;155(2):119–24.
16. Kumari I, Kaur S, Mohan H, Huria A. Adnexal masses in pregnancy: a 5-year review. Aust N Z J Obstet Gynaecol. 2006;46(1):52–4.
17. Bernhard L, Klebba P, Gray D, Mutch D. Predictors of persistence of adnexal masses in pregnancy. Obstet Gynecol. 1999;93(4):585–9.
18. Chiang G, Levine D. Imaging of adnexal masses in pregnancy. J Ultrasound Med. 2004;23(6):805–19.
19. Levine D, Brown D, Andreotti R, Benacerraf B, Benson C, Brewster W, et al. Management of asymptomatic ovarian and other adnexal cysts imaged at US: Society of Radiologists in Ultrasound Consensus Conference Statement. Radiology. 2010;256(3):943–54.
20. Blaivas M, Lyon M. Reliability of adnexal mass mobility in distinguishing possible ectopic pregnancy from corpus luteum cysts. J Ultrasound Med. 2005;24(5):599–603.
21. Ku CW, Shang X, Zhang VR, Allen JC, Tan NS, et al. Gestational age-specific normative values and determinants of serum progesterone through the first trimester of pregnancy. Sci Rep. 2021;11(1):4161.
22. Benacerraf B, Goldstein S, Groszmann Y. Corpus luteum and hemorrhagic cyst. In: Benacerraf B, Goldstein S, Groszmann Y, editors. Gynecologic ultrasound: a problem-based approach. 1st ed. Philadelphia: Saunders; 2014. p. 43.
23. Pateman K, Moro F, Mavrelos D, Foo X, Hoo W, Jurkovic D. Natural history of ovarian endometrioma in pregnancy. BMC Womens Health. 2014;14:128.
24. Groszmann Y, Howitt B, Bromley B, Feltmate C, Benacerraf B. Decidualized endometrioma masquerading as ovarian cancer in pregnancy. J Ultrasound Med. 2014;33(11):1909–15.
25. Sokalska A, Timmerman D, Testa A, Van Holsbeke C, Lissoni A, Leone F, Jurkovic D, Valentin L. Diagnostic accuracy of transvaginal ultrasound examination for assigning a specific diagnosis to adnexal masses. Ultrasound Obstet Gynecol. 2009;34(4):462–70.
26. Runowica CD, Brewer M. Adnexal masses in pregnancy. In: Godd B, Chakrabarti A, editors. UpToDate; 2021. https://www.uptodate.com/contents/adnexal-mass-in-pregnancy#H11.
27. Spitzer M, Kaushal N, Benjamin F. Maternal CA-125 levels in pregnancy and the puerperium. J Reprod Med. 1998;43(4):387–92.
28. Myers E, Bastian L, Havrilesky L, Kulasingam S, Terplan M, Cline K, et al. Evidence Report No. 130: Management of adnexal mass. 2006. http://archive.ahrq.gov/downloads/pub/evidence/pdf/adnexal/adnexal.pdf.
29. Timmerman D, Ameye L, Fischerova D, Epstein E, Melis G, Guerriero S, et al. Simple ultrasound rules to distinguish between benign and malignant adnexal masses before surgery: prospective validation by IOTA group. Br Med J. 2010;341:c6839.

30. Cao L, Wei M, Liu Y, Fu J, Zhang H, Huang J, Pei X, Zhou J. Validation of American College of Radiology Ovarian-Adnexal Reporting and Data System Ultrasound (O-RADS US): analysis on 1054 adnexal masses. Gynecol Oncol. 2021;162(1):107–12.
31. Ball E, Waters N, Cooper N, Talati C, Mallick R, Rabas S, Mukherjee A, Sri Ranjan Y, Thaha M, Doodia R, Keedwell R, Madhra M, Kuruba N, Malhas R, Gaughan E, Tompsett K, Gibson H, Wright H, Gnanachandran C, Hookaway T, Baker C, Murali K, Jurkovic D, Amso N, Clark J, Thangaratinam S, Chalhoub T, Kaloo P, Saridogan E. Evidence-based guideline on laparoscopy in pregnancy: commissioned by the British Society for Gynaecological Endoscopy (BSGE) Endorsed by the Royal College of Obstetricians & Gynaecologists (RCOG). Facts Views Vis Obgyn. 2019;11(1):5–25.

Index

A
Abdomen, 3DUS, 249–253
Abdominal cysts, 416
Abdominal pregnancy, 333, 334
Abdominal protrusion, 418
Abdominal wall, 132, 413
  abnormalities of fetal genitalia, 429
  bowel, liver, and gallbladder, 415, 416
  cystic renal disease, 428
  embryology, 413, 414
  esophagus, 414
  fetal bladder abnormalities, 429
  fetal renal size, presence and location, 426, 427
  gastroschisis, 418
  genetic evaluation, 430
  hydronephrosis/pyelectasis, 427
  limb-body stalk anomaly, 419
  omphalocele, 417
  physiologic midgut herniation, 417
  stomach, 414
Abdominal wall defect, 420
Aberrant Right Subclavian Artery (ARSA), 182–183
Abnormal-appearing fetus, 312
Abnormally positioned gestational sac, 298
Absent nasal bone, 382
Acardiac twins, 275
Acoustic output, 9, 10
Acrania-exencephaly-anencephaly sequence, 230, 239, 240
Active sonography, 48
Adenomyosis, 35
Adnexa, 40
Adnexal mass, 328, 477
Agnathia, 399
Alcohol, 79
American College of Obstetricians and Gynecologists (ACOG), 430
American institute of Ultrasound in Medicine (AIUM), 373
Aminopterin, 79
Amniocentesis, 278
Amnion, 301
Amnionicity, 232–235
  multiple gestations-multiple headaches, 265–268
Amniotic band sequence, 440, 441
Amniotic fluid, 420
Anembryonic pregnancy, 293
  with gestational sac, 154
Aneuploidy, 100, 139, 140
  biochemical and ultrasound screening for
    cell free DNA screening for, 142, 143
    cell free DNA testing, applications of, 146
    chromosome and genetic anomalies, first trimester ultrasound markers for, 141
    first trimester maternal serum biochemical screening, 141
    historical approaches, 140
    integrated and sequential screening, 142
    multiple gestations, aneuploidy screening in, 144, 145
    nuchal translucency ultrasound, 145, 146
    second-trimester maternal serum biochemical screening, 140, 141
    status of aneuploidy screening, 145
  screening, 144, 458
  tricuspid Doppler screening for, 207, 208
Angular pregnancies, 332, 333
Anomaly, 420
Anorectal atresia, 416
Anotia, 404
Anti-epileptic drugs (AEDs), 57
Antral follicle count (AFC), 36
Aorticopulmonary septum, 75
Appropriate for GA (AGA), 271
Arrhinia, 395
Arteriovenous malformations (AVM), 354, 452, 453
  late development of, 355
Arthrogryposis, 436
Arthrogryposis multiplex congenita, 435
Artificial Reproductive Technologies (ART), 1
As Low As Reasonable Achievable (ALARA), 176
Aspirin, 211, 212
Assisted reproductive technology (ART), 43, 261
  infertility, 47, 48
Atrial natriuretic peptide (ANP), 274
Atrial septum, 74

© The Editor(s) (if applicable) and The Author(s), under exclusive license to Springer Nature Switzerland AG 2023

J. S. Abramowicz, R. E. Longman (eds.), *First-Trimester Ultrasound*,
https://doi.org/10.1007/978-3-031-24133-8

Atrioventricular septum, 74
Automated volume count (AVC), 47
Axial transthalamic plane, 374

B
Bagel sign, 327
Beckwith-Wiedemann syndrome, 400
Benzodiazepines, 79, 80
Bicornuate uterus, 35
Bilaminar embryo, development of, 65
Biparietal diameter (BPD), 161, 166
Blood islands, 170
Body habitus, 151
Body mass index (BMI), 169
Body-stalk anomaly (BSA), 228, 229
Bone morphogenetic proteins (BMPs), 67
Brain natriuretic peptide (BNP), 274
Breathing movements, 202
Brenner tumor, 484
Bulbus cordis, 171

C
Carbamazepine, 57, 80
Carbon monoxide poisoning, 80
Cardiac axis, 181–182
Cardiac defects, 171
Cardiac development, 72, 170, 171
Cardiac diverticula, 178
Cardiac function, evaluation of, 190, 191
Cardiac scan, first trimester, 176
  alternatives for, 178, 179
  color Doppler, 178
  3-VV, 3-VTV and outflow tracts, 179, 180
Cataracts, 382
Cell-free DNA, 100, 104
Cell free DNA testing
  for aneuploidy, 142, 143
  applications of, 146
Cell signaling, 65
Central nervous system, 3DUS, 235
  acrania-exencephaly-anencephaly sequence, 239, 240
  axial view, 235, 237–239
  cervical spina bifida, 242–244
  holoprosencephaly, 239–241
  open spinal dysraphism, 241, 242
  sagittal view, 235, 236
Cephalocele, 377, 378
Cerebral hemispheres, 126
Cervical ectopic pregnancy, 296
Cervical pregnancy, 334, 335, 347
Cervical spina bifida (CEB), 242–244
Cesarean scar pregnancy (CSP), 213, 335, 339, 340
  algorithm, 347
  CSP sac, excision of, 358
  diagnosis, 340, 341, 343, 344, 346
  differential diagnosis of, 347, 348
  features, 340
  first trimester, counseling patients with, 350, 351
  incidence/risk factor, 342, 343
  management of, 351, 352
  and PAS, 348, 349
    in first trimester, 349
  pathogenesis of, 343
  sequential, pictorial demonstration of the treatment, 361
  sonographic markers of, 344
  transvaginal ultrasound guided transvaginal, 358
  treatment options for, 352, 353
    Foley single balloon and Cook double balloon catheters, 360, 361
    heterotopic, 362
    hysteroscopic and laparoscopic surgery, 354, 355
    hysteroscopic guidance, excision by, 357
    intragestational-sac injection, methotrexate/potassium chloride, 357, 360
    laparotomy, excision by, 357
    methotrexate, 355–357
    multifetal, 362
    recurrent CSP, 361, 362
    Shirodkar suture, 360
    suction aspiration/D&C, 353, 354
    transvaginal surgical excision, 357
    uterine artery embolization, 354
  triage and management of, 351
Chondrodysplasia punctata, 395
Choriocarcinoma, 450
Chorionic bump, 232, 233, 304, 305
Chorionic frondosum, 301, 302
  chorionic bump, 304
  hematoma, 304
  vaginal bleeding, 302, 304
  vascular pattern, 304, 306
Chorionic villus sampling
  complications of
    bleeding, 462
    infection, 462
    long-term infant development, 463
    perinatal complications, 463
    risk of fetal abnormalities, 462, 463
    rupture of membranes, 462
  confined placental mosaicism, 464, 465
  cytogenetic results, 463, 464
  early amniocentesis, 466
  indications, 459
  maternal cell contamination (MMC), 464
  multiple gestations, 459
  procedure, 460, 461
  safety, 461
Chorionicity, 117, 119, 232–235, 279
  multiple gestations-multiple headaches, 265–268
Choroid plexus (CP), 376
Chromosomal aneuploidies, 393
Cisterna magna (CM), 376
Cleft lip and palate (CLP), 242, 244, 245, 382
Clubfoot, 439
Cocaine, 80
Color Doppler, 178, 418, 419
Comparative genetic hybridization (CGH), 164

Complete hydatidiform mole (CHM), incidence of, 445
Completed abortion, 293
Concomitant mole, 272
Confined placental mosaicism (CPM), 143, 278, 464, 465
Congenital abnormalities, 146
Congenital anomalies, 227, 228, 278
  acrania-exencephaly-anencephaly sequence, 230
  body-stalk anomaly, 228, 229
  early pleural effusion, 231, 232
  fetal edema, 228, 229
  holoprosencephaly, 230, 231
Congenital anomalies of the kidney and urinary tract (CAKUT), 425
Congenital anomaly, 279
Congenital cataracts, 394
Congenital goiters, 407
Congenital heart defects (CHD), 55–57, 169
Congenital heart disease (CHD), 55, 58, 220, 279
  ductus venosus Doppler screening for, 204, 205
  tricuspid Doppler screening for, 207, 208
Congenital masses/tumors, 407
Congenital megalourethra, 429
Congenital uterine anomalies, 35
Conjoined twins, 275, 276
Contrast infusion sonography, for uterine cavity and tubal patency assessment, 43
Cook double balloon, 360
Cord entanglement, 276
Cornual pregnancy, 332
Corpus luteum, 477, 478
Corpus luteum cysts, 38, 478, 479
  of pregnancy, 479
Corticosteroids, 80
COVID-19, 85
Craniopagus, 276
Crown rump length (CRL), 95, 97, 154, 160, 264, 310
  fetal biometry, in early pregnancy, 159, 160, 162
  Pexsters, 161
  Robinson, 161
Cyst, 108
Cystic hygroma, 75, 163, 405, 407
Cystic renal disease, 428
Cysts of Morgagni, 40
Cytomegalovirus (CMV), 83

D
Decidualized ovarian endometrioma, 481–483
Deeply infiltrating endometriosis (DIE), 41
Dermoid cysts, 39
Diamniotic twins, 266
Diaphragm, development of, 69
Diastolic myocardial dysfunction, 274
Dichorionic-diamniotic (DCDA) pregnancy, 117
Dichorionic diamniotic membrane, 268
Dichorionic diamniotic twins, 265, 378
Dichorionic/triamniotic triplets (DCTA), 468
Diethylstilbestrol (DES), 80
Differential growth, multiple gestations-multiple headaches, 271
Discriminatory level, human chorionic gonadotropin, 322, 323
Discriminatory value, 152, 153
Documentation, 102
Doppler color flow mapping, 451
Doppler imaging technique, 212
  early first trimester, 213
  first trimester ultrasound markers, 213
  late first trimester, 214
Doppler insonation technique, 205
Doppler mode, 10
Doppler sonography, in early pregnancy
  aneuploidy and congenital heart disease, tricuspid Doppler screening for, 207, 208
  biophysical, biochemical and molecular screening, 208
  Doppler imaging technique, 212
    early first trimester, 213
    first trimester ultrasound markers, 213
    late first trimester, 214
  Doppler insonation technique, 205
  ductus venosus
    anatomy and hemodynamics, 197–199
    for congenital heart disease, 204, 205
    Doppler imaging technique for, 199
    ductus venosus Doppler waveforms, 199
    factors, 200, 203
    in first-trimester aneuploidy screen, 203, 204
  first trimester, uterine artery in, 208, 209
  placenta accreta spectrum, placental implantation site, 212
  tricuspid flow, Doppler investigation of, 205
  tricuspid flow pattern, 205, 206
  tricuspid regurgitation, 206, 207
  uterine artery, 209
  uterine artery Doppler, clinical applications of, 210–212
  uterine artery Doppler waveform, 209, 210
Doppler velocimetry, 10
Double ring sign, 158
Double sac sign (DSS), 110
Ductal arch, 178
Ductus venosus
  anatomy and hemodynamics, 197–199
  for congenital heart disease, 204, 205
  Doppler imaging technique for, 199
  ductus venosus Doppler waveforms, 199
  early fetal cardiac evaluation, markers for, 180
  factors, 200, 203
  in first-trimester aneuploidy screen, 203, 204
  reversal of flow in, 201
Ductus venosus A-wave, 204, 205
  velocity measurements, 202
Ductus venosus Doppler velocimetry, 273
Ductus venosus flow, 200
Ductus venosus pulsatility index for veins (PIV), 201
Ductus venosus S-wave velocity measurements, 202

Ductus venosus time-averaged maximum velocity (TAMXV), 203
Dynamic range, 27, 28

E
Early cardiac development, 73
Early cesarean scar pregnancy, developing vascular grid of, 345
Early fetal cardiac evaluation, indirect markers for
  Aberrant Right Subclavian Artery, 182
  cardiac axis, 181, 182
  heart-to-chest ratio, 183
  nuchal translucency and ductus venosus, 180
  tricuspid regurgitation, 180, 181
Early gestational sac, 152, 297
Early pregnancy, 95
  evaluation, 151
  first trimester of, 120
Early pregnancy failure, 154, 155
  amnion, 301
  chemical evidence of, 294
  embryo, 308–313
  first-trimester ultrasound, 293
  gestational sac, 295, 296, 298–301
  imaging of, 295
  placenta/chorionic frondosum, 301, 302, 304, 306
  recurrent pregnancy loss, 314
  retained products of conception, 313, 314
  risk factors, 293, 294
  ultrasound characteristics of, 294, 295
  yolk sac, 306, 307
Ebstein's anomaly, 74, 171, 181
Echogenic bowel, 415
Echogenic choroid plexus, 374
Ectopic, 339
Ectopic pregnancy (EP), 296, 319, 340, 480
  adnexal criteria for, 328
  adnexal findings in, 326
  ectopic pregnancy
    adnexal findings, 326
    endometrial thickness, 323
    intrauterine fluid, 323, 324
    work-up for, 328, 329
  endometrial findings in
    endometrial thickness, 323
    intrauterine fluid, 323, 324
  human chorionic gonadotropin dynamics, 321, 322
    discriminatory level, 322, 323
    threshold level, 322
  pregnancy, spontaneous resolution of, 330
  six strategies for, 329
  threshold level, ultrasound first, tubal rupture below, 329
  unusual
    abdominal pregnancies, 333, 334
    angular pregnancies, 332
    cervical pregnancy, 334, 335
    Cesarean scar pregnancies, 335
    cornual pregnancy, 332
    heterotopic pregnancy, 331
    interstitial pregnancy, 331, 332
    ovarian pregnancies, 332, 333
  work-up for, 328, 329
Ectrodactyly, 440
11-13+6 weeks of gestation, 171, 191
Embryo, 95, 108, 115, 155, 308
  anatomy, 310
  appearance, 309
  embryonic heart rate, 311–313
  embryonic motion, 308
  location, 308, 309
  size/growth rate, 309, 310
Embryo transfer, 47, 48
Embryonic cardiac activity (ECA), 116
Embryonic cavities, 69
Embryonic demise, 293
Embryonic heart bump, 311
Embryonic heart rate (EHR), 311–313
Empty amnion, 302
Encephaloceles, 436, 437
Endometrial glands, 35
Endometriomas, 39, 41, 481
Endometrium, 34, 324
Epignathus, 400
Epilepsy, 57
Epithelioid trophoblastic tumor, 451
Esophageal atresia, 414
Exencephaly-anencephaly sequence, 377, 378
Expanded amnion sign, 301
External insults, fetal susceptibility to, 7, 8
Extremities
  clubfoot, 438
  limb reduction defects, 438, 440

F
Face, 128
  cleft lip and palate, 242, 244, 245
  low-set ear, 242, 243, 245
  micrognathia, 245, 246
Facial maxillary angle (FMA), 399
Fetal alcohol syndrome (FAS), 57
Fetal anasarca, 312
Fetal anatomy, 95
Fetal anomalies, 53, 221, 222, 235, 371
Fetal biometry, in early pregnancy, 157
  biometric measurements, 166
  crown rump length, 159, 160, 162
  gestational sac, 157–159
  nasal bone, 165
  nuchal translucency, 162–165
  yolk sac, 159
Fetal bladder abnormalities, 429
Fetal brain, formation of, 68, 69
Fetal chromosome abnormalities, screening for, 139, 140
  cell free DNA screening for, 142, 143
  cell free DNA testing, applications of, 146
  chromosome and genetic anomalies, first trimester ultrasound markers for, 141

- first trimester maternal serum biochemical screening, 141
- historical approaches, 140
- integrated and sequential screening, 142
- multiple gestations, aneuploidy screening in, 144, 145
- nuchal translucency ultrasound, 145, 146
- second-trimester maternal serum biochemical screening, 140, 141
- status of aneuploidy screening, 145

Fetal circulatory pathways, 198
Fetal demise, 312
Fetal echocardiography, 56, 279
Fetal edema, in early pregnancy, 228, 229
Fetal face and neck
- absent nasal bone, 396, 398
- agnathia, 399
- arrhinia/congenital absence, 395
- cataracts, 394, 395
- cystic hygroma, 405
- epignathus, 400
- external ear (pinna/auricle) anomalies, 404
- fetal orbits, 391
- frontal encephalocele, 405
- hypertelorism, 392, 393
- hypotelorism (cyclopia), 393
- lips and palate, 400, 404
- macroglossia, 399
- micrognathia and retrognathia, 398
- microphthalmia/anophthalmia, 394
- proboscis/rudimentary, 395
- two-dimensional (2D) ultrasound, 389

Fetal face, development of, 69
Fetal gastrointestinal system, 132, 413
- abnormalities of fetal genitalia, 429
- bowel, liver, and gallbladder, 415, 416
- cystic renal disease, 428
- embryology, 413, 414
- esophagus, 414
- fetal bladder abnormalities, 429
- fetal renal size, presence and location, 426, 427
- gastroschisis, 418
- genetic evaluation, 430
- hydronephrosis/pyelectasis, 427
- limb-body stalk anomaly, 419
- omphalocele, 417
- physiologic midgut herniation, 417
- stomach, 414

Fetal genitalia, assessment of, 132, 134
Fetal heart, in early pregnancy, 130, 131, 169
- cardiac development, 170, 171
- cardiac function, evaluation of, 190, 191
- complementary ultrasound techniques, 189
  - 4D-spatio-temporal imaging correlation, 189, 190
- early fetal cardiac evaluation, indirect markers for
  - Aberrant Right Subclavian Artery, 182
  - cardiac axis, 181, 182
  - heart-to-chest ratio, 183
  - nuchal translucency and ductus venosus, 180
  - tricuspid regurgitation, 180, 181
- first trimester ultrasound, 169, 170
  - cardiac anomalies detection, 183–185
- first trimester, cardiac scan in, 176
  - alternatives for, 178, 179
  - color Doppler, 178
  - 3-VV, 3-VTV and outflow tracts, 179, 180
- high-risk population, 188, 189
- operator experience and route of ultrasound examination, 172
- optimal time, 172–174
- practical recommendations, 176
- precautions, 191
- safety, 191
- scan, 171

Fetal kidneys, 131
- in first trimester, 131, 132

Fetal pole, 158
Fetal reduction (FR)
- clinical procedure, 466
- dichorionic/triamniotic triplets (DCTA), 468
- FISH technology, 468
- IVF culture techniques, 468
- ultrasound evaluation, 467

Fetal skeleton, in first trimester, 132
Fetal susceptibility, 7, 8
Fibroids, 476, 477
FIGO risk scores, 452
First trimester anatomical assessment, 125, 126
- abdominal wall and umbilical cord, 132
- face, 128
- fetal brain, 126, 128
- fetal gastrointestinal tract, 132
- fetal genitalia, assessment of, 132, 134
- fetal heart, 130, 131
- fetal kidneys and urinary tract system, 131, 132
- fetal skeleton, 132
- spine, assessment of, 134
- thorax, 128

First-trimester embryology, 65
- aorticopulmonary septum, 75
- atrial septum, 74
- atrioventricular septum, 74
- bilaminar embryo, development of, 65
- cardiac development, 72
- cardiac septae formation and valvular development, 74
- early cardiac development, 73
- embryonic cavities and diaphragm, development of, 69
- embryonic weeks 3-4, 66, 67
- embryonic weeks 5-8, 69
- fetal brain, formation of, 68, 69
- fetal face, development of, 69
- gastrointestinal tract, development of, 70, 72
- lymphatic system, development of, 75
- neural tube, formation of, 67
- respiratory system, development of, 70
- urogenital system, development of, 72
- ventricular septum, 74, 75

First trimester fetal head and brain
  anatomy of, 373–376
  face, 382, 384
  gestational age, 372
  midline developmental anomalies, 380
  neural tube defects, 377, 378, 380
  Pathologies of, 377
First trimester of pregnancy, 95, 107, 108
  cardiac lesions, 56, 57
  early pregnancy dating, 120
  embryo, 115
  embryonic and fetal cardiac activity, 116
  gestational sac, 108–110
    gestational sac appearance and β-hCG, 113, 114
    mean sac diameter and viability, 111, 112
    measurement of, 110, 111
  guidelines for redating pregnancy, 162
  heterotopic pregnancy, 119
  multiple gestations and chorionicity, 117–119
  neural tube defects, screening for, 123, 124
  normal first trimester anatomical assessment, 125, 126
    abdominal wall and umbilical cord, 132
    face, 128
    fetal brain, 126, 128
    fetal gastrointestinal tract, 132
    fetal genitalia, assessment of, 132, 134
    fetal heart, 130, 131
    fetal kidneys and urinary tract system, 131, 132
    fetal skeleton, 132
    spine, assessment of, 134
    thorax, 128
  nuchal translucency evaluation, 121
    absent nasal bone, significance of, 123
    measurement, significance, 122
    nasal bone, assessment of, 122
  nuchal translucency evaluation measurement, criteria for, 121, 122
  ultrasound in, 1
  uterine artery in, 208, 209
  yolk sac, 114, 115
First-trimester pregnancy failure, 293
First trimester sonography
  abdominal mimickers, 486, 487
  adnexal masses, 477
  clinical implications, 475
  corpus luteum, 477
  corpus luteum cysts, 478, 479
  decidualized endometriomas, 481, 483
  hemorrhagic corpus luteum cyst, 479, 480
  mature teratomas, 483, 484
  ovarian cancer, 484, 485
  techniques, 475, 476
  uterine masses, fibroids, 476, 477
First-trimester ultrasound, 58, 169, 170, 433
  arthrogryposis multiplex congenital, 435
  cardiac anomalies detection, 183–185
  cranial anomalies, 436
  documentation, 102
  early pregnancy failure, 293
    amnion, 301
    chemical evidence of, 294
    embryo, 308–313
    gestational sac, 295, 296, 298–301
    imaging of, 295
    placenta/chorionic frondosum, 301, 302, 304, 306
    recurrent pregnancy loss, 314
    retained products of conception, 313, 314
    risk factors, 293, 294
    ultrasound characteristics of, 294, 295
    yolk sac, 306, 307
  equipment, 93, 94
  extremities (*see* Extremities)
  fetal anatomy, 98, 99
  fetal aneuploidy assessment, 100
  fetal number, 97
  gestational age, 97, 98
  guidelines and recommendations, 93
  indications, 94
  indications and timing, 95
  pre-eclampsia, 101, 102
  pregnancy location, 96
  quality assurance, 103
  safety, 94
  skeletal dysplasias, 434
  spinal anomalies, 437
  standard indications for, 51
  systematic review, 52
  training guidelines, 102
  transducers, 103
  viability, 95
First trimester uterine artery Doppler, 58
Foley balloon catheter, 363
Foley single balloon, CSP, 360, 361
Follicle maturation, 47
Follicular monitoring ultrasounds, 46, 47
Forebrain, 126
4D ultrasound, 134
4D-spatio-temporal imaging correlation, 189, 190
Frontal encephalocele, 405

G
Gain
  overall gain, 25
  time gain compensation, 25, 26
Gastrointestinal tract, development of, 70, 72
Gastroschisis, 72, 418, 420
Genetic abnormalities, 435
Genetic evaluation, 430
Genetic/structural anomaly, discordance for, 272
Gestational age, 94, 97
  estimation, 161
Gestational sac, 108–110, 152, 306
  fetal biometry, in early pregnancy, 157–159
  gestational sac appearance and β-hCG, 113, 114
  mean sac diameter and viability, 111, 112
  measurement of, 110, 111
  pregnancy failure, ultrasound evidence of, 295

- appearance, 295, 296, 298, 299
- location, 295
- prognosis of, 300, 301
- size/growth, 299, 300

Gestational trophoblastic disease (GTD), 445
- risk factors, 445
- ultrasound
  - arteriovenous malformations (AVM), 452, 453
  - Color Doppler in, 451
  - diagnosis and management of, 450
  - postmolar GTN, 451
  - surgical intervention, 452
  - TVUS findings, 451
  - uterine artery pulsatile index, 452

Group B streptococcus (GBS) infection, 461
Growth differentiation factor 9 (GDF9), 263
Growth restriction, multiple gestations-multiple headaches, 271
Guidelines, 93

H
Heart, 245, 247, 248
Heart-to-chest ratio, 183
Hematoma, 304
Hemorrhagic corpus luteum cyst, 479, 480
Hemorrhagic cysts, 38
Heterokaryotypia, 279
Heterotaxy, 187, 415
Heterotopic CSP, 362
Heterotopic pregnancy, 331
- first trimester of pregnancy, 119

High Resolution Episcopic Microscopy (HREM), 191
Higher order multiple gestations, 280, 282
High-pass filter, 199
High-risk population, fetal heart, in early pregnancy, 188, 189
Hindbrain, 126
Holoprosencephaly (HPE), 230, 231, 239–241, 380, 381
Human chorionic gonadotropin (hCG) discriminatory level, evidence against, 322
Human chorionic gonadotropin (hCG) dynamics, 321, 322
- discriminatory level, 322, 323
- threshold level, 322

Hydronephrosis/pyelectasis, 427
Hydrosalpinx, 40
Hypertelorism, 392, 393
Hypotelorism (cyclopia), 393
Hysterosalpingo-contrast-sonography (HyCoSy), 45
Hysterosalpingogram (HSG), 43, 45
Hysteroscopic and laparoscopic surgery, 354, 355
Hysteroscopic guidance, excision by, 357

I
Identical twins, 263
Iliac vessels, 37
Infections, 82, 83
Inferior facial angle (IFA), 398
Infertility
- advanced ultrasound techniques and reproductive pathology, 41
- in ART procedures, 47, 48
- baseline evaluation, 31
  - adnexa, 40
  - miscellaneous, 40
  - ovaries, 35, 37–40
  - uterus, 31, 34, 35
- follicular monitoring ultrasounds, 46, 47
- uterine cavity assessment and tubal patency assessment, contrast infusion sonography for, 43, 45

Intact cranium, 374
International Society of Ultrasound in obstetrics and Gynecology (ISUOG), 373, 414, 425
Interstitial pregnancy, 331
Interventricular septal defects, 188
Interventricular septum, 175
Intervillous vascular flow, 306
Intestinal atresias, 416
Intracranial translucency, 235, 241
Intradecidual sign (IDS), 110, 298, 299
Intragestational-sac injection, methotrexate/potassium chloride, 357, 360
Intramural fibroids, 32
Intraoperative ultrasound, 450
Intrauterine fluid, 324
Intrauterine pregnancy (IUP), 151, 347
Invasive molar pregnancy, 450
In vitro fertilization (IVF), 261
Ionizing radiation, 85
Iron deficiency anemia, 280
Irregular gestational sac, 298
Ischiopagus, 276
Ispilon sign, 281

J
Jaw index, 399

K
Knobology, 22

L
Lambda (λ) sign, 117, 267
Laparoscopic surgery, 355
Laparotomy excision, 357
Limb-body stalk anomaly, 419
Limb reduction defects, 438, 440
Limb terminal deletion, 442
Lithium, 80
Live born infants, rates of chromosome abnormalities in, 140
Low-set ear, 242, 244, 245
Lumbo-sacral spinal defect, 379
Lymphatic system, development of, 75

M
Macroglossia, 399
Macrotia, 405
Maternal cell contamination (MMC), 464
Maternal co-morbidities, 51, 53
  maternal conditions associated with congenital heart defects, 55–57
  maternal vascular disease, 57, 58
  obesity, 55
  pre-gestational diabetes, 53, 54
  systematic review, 52
Maternal metabolic diseases, 58
Maternal morbidity, 261
Maternal phenylketonuria, 393
Maternal pre-gestational diabetes, 53, 54
Maternal vascular disease, 57, 58
Mature cystic teratoma, 39, 484
Mature teratomas, 483, 484
Maxilla-nasion-mandible (MNM) angle, 399
MC twins, complications specific for, 272
  conjoined twins, 275, 276
  cord entanglement, 276
  twin anemia polycythemia syndrome, 274
  twin reversed arterial perfusion syndrome, 274, 275
  twin-to-twin transfusion syndrome, 272–274
Mean sac diameter (MSD), 110, 157, 158
Mechanical index (MI), 5
Meckel-Gruber syndrome, 393
Median facial cleft, 404
Melotia, 405
Meningomyelocele, 438
Mercury sulfide, 81
Metanephric blastema, 425
Methotrexate, 81, 152
  CSP, 355–357
Methyl mercury, 81
Microarray, 140
Microcephaly, 393
Micrognathia, 244–246, 384
Microphthalmia/anophthalmia, 394
Microtia, 404
Midbrain, 126
Miscarriage, 313, 314
Misoprostol, 81
Missed abortion, 293
Molar pregnancy
  classic sonographic findings, 446
  color Doppler ultrasound, 448
  evacuation, ultrasound in, 449
  mimics of, 448
  ovarian theca lutein cysts, 448, 449
  sensitivity of ultrasound, 447
  ultrasound diagnosis of, 446, 447
  uterine artery Doppler measurement in, 448
  with co-existent twin, 449
Monoamniotic twins, 266
  cord entanglement in, 277
Monochorionic diamniotic membrane, 268
Monochorionic-diamniotic (MCDA), 265
Monochorionicity, 261
Monozygocity, 279
Monozygotic twins, 263, 279
Multifetal CSP, 362
Multiple corpora lutei, 262
Multiple gestations, 261, 459
  aneuploidy screening in, 144, 145
  first trimester of pregnancy, 117–119
Multiple gestations-multiple headaches, 261
  chorionicity and amnionicity, diagnosis of, 265–268
  complications, 269
    complete hydatidiform mole and coexisting fetus, 272
    genetic/structural anomaly, discordance for, 272
    growth restriction and differential growth, 271
    vanishing twin, 269–271
  diagnosis, 263, 264
  embryology, 262, 263
  genetic and morphologic abnormalities, screening for, 277–280
  higher order multiple gestations, 280, 282
  maternal complications, 280
  MC twins, complications specific for, 272
    conjoined twins, 275, 276
    cord entanglement, 276
    twin anemia polycythemia syndrome, 274
    twin reversed arterial perfusion syndrome, 274, 275
    twin-to-twin transfusion syndrome, 272–274
  placentation, 264, 265
  twins, invasive diagnostic/therapeutic procedures in, 282
Multiple-gestation pregnancies, 94
Multiple pregnancies, chorionicity and amnionicity in, 232–234
Mycophenolate mofetil, 81
Myometrial invasion, 447

N
Nasal bone (NB), 165
  assessment of, 122
  fetal biometry, in early pregnancy, 165
  guidelines, for measurement, 165
Neural tube defects, screening for, 123, 124
Neural tube, formation of, 67
Neurosonography, 392
New England Trophoblastic Disease Center, 446
Non-invasive prenatal testing (NIPT), 169, 458
Non-invasive DNA screening (NIDS), 278
Non-ionizing radiation, 85
Non-viable pregnancy, 155
Normal cord insertion, 417
Nuchal translucency (NT), 22, 24, 99, 278, 375
  differential diagnosis for, 164
  early fetal cardiac evaluation, markers for, 180
  in era of cell free DNA screening, 145, 146
  evaluation, first trimester of pregnancy, 121
    measurement, criteria for, 121, 122
    measurement, significance, 122
    nasal bone, assessment of, 122

        nasal bone, significance of, 123
    fetal biometry, in early pregnancy, 162–165
    guidelines, measurement of, 164

O
Obesity, 55
Obstetric ultrasound, 102
Oculo-auriculo-vertebral (OAV), 245
Oligohydramnios, 428
Omphalocele, 70, 252, 311, 417, 418
Oocyte retrieval, 39–41, 46–48
Open spina bifida, 378–380
Open spinal dysraphism, 241, 242
Orofacial cleft, 400, 401, 403
Otocephaly, 405
Outflow tract relationship (OTR), 188
Output Display Standard (OSD), 4–6
Ovarian cancer, 484, 485
Ovarian pregnancy, 332, 333
Ovaries, 35, 37–40
Overall gain, 25
Ovum, ultrasound and, 6, 7

P
Paired angiogenic cords, 73
Parallel sequencing, 279
Paramedian orofacial cleft, 403, 404
Paratubal cysts, 40
Parvovirus B19, 83
Peak systolic velocity (PSV), 346
Pelvic adhesions, 41
Penicillamine, 81
Peritrophoblastic vascular flow, 306
Phenobarbital, 81
Phenylketonuria (PKU), 56
Phenytoin, 82
Physiologic gut herniation, 310
Physiologic umbilical hernia, 417
Pierre Robin sequence trisomies, 398
Placenta, 301, 302
    chorionic bump, 304
    hematoma, 304
    vaginal bleeding, 302, 304
    vascular pattern, 304, 306
Placenta accreta spectrum (PAS), 348, 349
    in first trimester, 349
    placental implantation site, 212
Placental mesenchymal dysplasia (PMD), 447
Placental site trophoblastic tumor, 451
Placentation, multiple gestations-multiple headaches, 264, 265
Pleural effusion, 231, 232
Polychlorinated biphenyls (PCB), 81
Polycystic right kidney disease, 428
Polydactyly, 439
Posterior cephalocele, 379
Preeclampsia, 209–211
    screening, 95
Pregnancy, 2, 5, 6
    drugs in, 78
    spontaneous resolution of, 330
    three-dimensional ultrasound
        chorionic bump, 232, 233
        multiple pregnancies, chorionicity and amnionicity in, 232–234
Pregnancy-associated plasma protein A (PAPP-A), 294
Pregnancy failure
    new rules regarding, 154, 155
    ultrasound findings diagnostic of, 155
    ultrasound findings suspicious for, 155
Pregnancy of unknown location (PUL), 153, 319–321
    ectopic pregnancy
        adnexal findings, 326
        work-up for, 328, 329
    ectopic pregnancy, endometrial findings in
        endometrial thickness, 323
        intrauterine fluid, 323, 324
    human chorionic gonadotropin dynamics, 321, 322
        discriminatory level, 322, 323
        threshold level, 322
    pregnancy, spontaneous resolution of, 330
    threshold level, ultrasound first, tubal rupture below, 329
Prenatal screening, 100
Proboscis, 395
Profile line (PL) distance, 399
Prominent rhombencephalon, 311
Pseudogestational sac, 108
Pulsatility index (PI), 450, 451
Pulse-repetition frequency (PRF), 3
Pyopagus, 276

Q
Quadruplet pregnancy, 281
Quality assurance, 103

R
Recurrent CSP, 361, 362
Recurrent pregnancy loss (RPL), 314
Renal agenesis, 427
Resistive index (RI), 450, 451
Respiratory system, development of, 70
Retained products of conception (RPOC), 313
    clinical evaluation, 313
    color Doppler mapping, 313, 314
Retronasal triangle (RNT), 398
Right sided fetal stomach, 415
Rotkitansky's nodule, 39
Rubella, 83

S
Safety, of ultrasound, 1
Saline infusion sonohysterography, 340
Second-trimester maternal serum biochemical screening, 140, 141

Serous borderline tumor, 486
Sexual differentiation, 429
Shear-wave elastography (SWE), 12
Shirodkar suture, 360
Skeletal dysplasias, 434
Small endometriomas, 39
Small for GA (SGA), 271
Smooth-walled anechoic sac, 325
Society for Maternal-Fetal Medicine, 430
Sonic hedgehog (Shh), 67
Sonoembryology, 222, 223
    4 to 5 weeks, 223
    5 to 6 weeks, 223, 224
    6 to 7 weeks, 224, 225
    7 to 8 weeks, 224, 226
    8 to 9 weeks, 224, 226
    9 to 10 weeks, 227
Sonography, 475
Sonography-based Automated Volume Count (SonoAVC), 47
Sonohysterogram (SHG), 43
Spatiotemporal image correlation (STIC) technology, 190, 220
Spina bifida, 241, 242
Spinal anomalies, 437
Spine, assessment of, 134
Stroma, 35
Structural abnormalities, 52
Structural anomalies, 279
Stuck twin, 274
Subchorionic hematomas (SCH), 302, 303
Subcornual implantation, 296
Submucosal fibroids, 32
Subserosal fibroid, 476
Suction aspiration, 353, 354
Systemic retinoids, 82

T
Teratogen, 77, 78
    drugs, 78–79
Teratogenic agents, 55
Teratogenic risk, perception of, 77, 78
Teratology, elements of
    alcohol, 79
    aminopterin, 79
    benzodiazepines, 79, 80
    carbamazepine, 80
    carbon monoxide poisoning, 80
    cocaine, 80
    corticosteroids, 80
    COVID-19, 85
    cytomegalovirus, 83
    diethylstilbestrol, 80
    infections, 82, 83
    lithium, 80
    methotrexate, 81
    methyl mercury, mercury sulfide, 81
    misoprostol, 81
    mycophenolate mofetil, 81
    parvovirus B19, 83
    penicillamine, 81
    phenobarbital, 81
    phenytoin, 82
    physical factors
        ionizing radiation, 85
        non-ionizing radiation, 85
        ultrasound, 85
    polychlorinated biphenyls, 81
    pregnancy, drugs in, 78
    rubella, 83
    systemic retinoids, 82
    teratogen, 78
        drugs, 78–79
    teratogenic risk, perception of, 77, 78
    thalidomide, 82
    Toxoplasma Gondii, 83, 84
    Treponema pallidum, 84
    valproic acid, 82
    varicella, 84
    warfarin, 82
    zika virus, 84
Terminal transverse limb deletions, 440
Thalidomide, 77, 82
Thanatophoric dysplasia, 434
Theca lutein cysts, 448, 449
Thermal index (TI), 5
Thoraco-abdominal wall defect, 312
Thoraco-omphalopagus, 276
Thorax, 128
    3DUS, 249–253
Threatened abortion, 293
Three-D acquisition, 11
Three-dimensional imaging, 29, 30
Three-dimensional ultrasound (3DUS), 11, 12, 134, 219, 435
    anatomical assessment, 222
    anomalies diagnosable during, 11-14 weeks scan, 235
        central nervous system, 235–244
        face, 242–246
        heart, 245, 247, 248
        thorax and abdomen, 249–253
        urinary tract, 249, 253, 254
    confidently imaged, 222
    congenital anomalies, 227, 228
        acrania-exencephaly-anencephaly sequence, 230
        body-stalk anomaly, 228, 229
        early pleural effusion, 231, 232
        fetal edema, 228, 229
        holoprosencephaly, 230, 231
    during early pregnancy, benefits of
        chorionic bump, 232, 233
        multiple pregnancies, chorionicity and amnionicity in, 232–234
    gestational age, 221, 222
    instrumentation, 219–221
    prenatal diagnosis, 219, 221, 222, 231, 241
    sonoembryology, 222, 223
        4 to 5 weeks, 223

        5 to 6 weeks, 223, 224
        6 to 7 weeks, 224, 225
        7 to 8 weeks, 224, 226
        8 to 9 weeks, 224, 226
        9 to 10 weeks, 227
Threshold level
    human chorionic gonadotropin, 322
    re-evaluation of, 322
Threshold value, 151, 153
Time Gain Compensation (TGC), 25, 26
Tissue harmonic imaging (THI), 28, 29
Toxoplasma Gondii, 83, 84
Training, 98
Transcerebellar plane, 374, 376
Transducer selection, 23
Transducers, 22
Transvaginal scanning, 371
Transvaginal sonography (TVS), 41, 151, 376
Transvaginal surgical excision, 357
Transvaginal ultrasound (TVUS), 448, 451, 452
Transventricular plane, 374
Treacher Collins syndrome, 398
Treponema pallidum, 84
Tricuspid flow
    Doppler imaging of, 206
    Doppler investigation of, 205
    pattern, 205, 206
Tricuspid regurgitation, 171, 179–181, 206, 207
Trigonocephaly, 393
Triplets, 281
Trisomy 21, 165, 278
T sign, 265, 267
Tubal patency, 45
Tubal ring, 327, 330
Turner syndrome, 162
Twin anemia-polycythemia syndrome (TAPS), 264, 274
Twin gestation, 449
Twin peak/lambda sign, 267
Twin pregnancy, velamentous insertion of cord in, 269
Twin reversed arterial perfusion (TRAP) syndrome, 274, 275
Twin-to-twin transfusion syndrome (TTTS), 272–274
    ductus venosus Doppler velocimetry, 273
    early signs of, 273
2D ultrasound, 46
2-dose protocol, 321

U
Ultrasound, 21, 51, 85, 445
    acoustic output, 9, 10
    bioeffects of, 2
        non-thermal effects, 3, 4
        thermal effects, 2, 3
    depth setting, 24
    and detrimental effects, 8, 9
    dynamic range, 27, 28
    in early gestation, 7
    external insults, fetal susceptibility to, 7, 8
    fetal exposure and safety statements, 12, 13
    in first trimester, 1
    focus, 26
    gain
        overall gain, 25
        time gain compensation, 25, 26
    infertility (*see* Infertility)
    knobology, 22
    medical applications, 3
    output display standard, 4–6
    and ovum, 6, 7
    for prenatal diagnosis, 457
    sector width, 25
    shear-wave elastography, 12
    subsequent pregnancies, 453
    systematic approach, 22
    3D/4D, 11, 12
    three-dimensional imaging, 29, 30
    tissue harmonic imaging, 28, 29
    tools, choosing, 21
    transducer selection and impact of frequency, 23
    types, 21
Umbilical cord, 132, 418, 419
Unilateral renal agenesis, 427
Unusual ectopic pregnancies
    abdominal pregnancies, 333, 334
    angular pregnancies, 332
    cervical pregnancy, 334, 335
    cesarean scar pregnancies, 335
    cornual pregnancy, 332
    heterotopic pregnancy, 331
    interstitial pregnancy, 331, 332
    ovarian pregnancies, 332, 333
Urinary bladder, 132
Urinary tract
    in first trimester, 131, 132
    3DUS, 249, 253, 254
Urogenital system, development of, 72
Uterine artery
    Doppler sonography, in early pregnancy, 209
    first trimester, 208, 209
Uterine artery Doppler, 209
    clinical applications of, 210–212
Uterine artery Doppler waveform, 209, 210
Uterine artery embolization (UAE), 346, 354, 365
Uterine artery pulsatility index (UAPI), 452
Uterine cavity, contrast infusion sonography for, 43, 45
Uterus, infertility, 31, 34, 35

V
Vaginal bleeding, 302, 304, 314
Valproic acid, 82
Vanishing twin, 270, 278
    multiple gestations-multiple headaches, 269–271
Varicella zoster virus, 84
Vascular flow, 314
Venetian blinds, 35
Ventricular septum, 74, 75
Viability, 95, 103

W
Walker-Warburg syndrome, 395
Warfarin, 82
Whole-exome sequencing (WES), 145, 430

Y
Yolk sac, 114, 115, 158, 159, 306, 308
  appearance, 306, 307
  fetal biometry, in early pregnancy, 159
  orientation of, 309

Z
Zika virus, 84
Zygocity, 261